UNIVERSITÉ DE STRASBOURG

Archives sédimentaires de la glaciation Ordovicien supérieur

le contexte, les faciès et architectures stratigraphiques associés

---

Synthèse des travaux en vue de l'obtention de l'**H**abilitation à **D**iriger les **R**echerches

Jean-François GHIENNE

8 décembre 2010

Institut de Physique du Globe de Strasbourg (UMR 7516 CNRS/ Université de Strasbourg)
Ecole et Observatoire des Sciences de la Terre
1, rue Blessig, 67084 Strasbourg Cedex, France
Tél.: 03 68 85 04 55, Fax: 03 68 85 04 02, *e-mail* : **ghienne@unistra.fr**

Liste des Publications

La déconvolution des signaux climatiques et tectoniques à partir du décryptage du message sédimentaire constitue le dénominateur commun de mes travaux de recherche. Des problématiques diverses ont ainsi été abordées par l'analyse des faciès de dépôt et des architectures stratigraphiques : forçage climatique des systèmes sédimentaires du Sahara au Quaternaire, structures de croissance générées par des cônes alluviaux sur plis de propagation, ou enregistrement sédimentaire de la glaciation Ordovicien supérieur. Les références utilisées pour construire ce mémoire de l'Habilitation à Diriger les Recherches ne concernent que cette dernière problématique. Elles apparaissent dans la liste ci-dessous *soulignées et en italique*. Les références soulignées intéressent cette même thématique, mais ne sont pas intégrées dans ce document (participation subalterne, ou publications directement issues du travail de thèse).

PUBLICATIONS rang A

acceptée (en révision)

Douillet G., **Ghienne** J.-F., Géraud Y., Abueladas A., Diraison M., Al-Zoubi A. (révision mineure) Late Ordovician tunnel valleys in southern Jordan. Special Publication of the Geological Society, London

2010

***Ghienne** J.-F., Monod, O., Kozlu, H., Dean, W.T.* – Cambrian-Ordovician depositional sequences in the Middle East : a perspective from Turkey. Earth Science Reviews, 1010, 101-146.

***Ghienne** J.-F., Girard F., Moreau J., Rubino J.-L.* – Late Ordovician climbing-dune cross-stratification: a signature of outburst floods in proglacial outwash environments? Sedimentology, 57, 1175-1198.

*Loi A., **Ghienne** J.-F., Dabard M.P., Paris F., Botquelen A., Christ N., Elaouad-Debbaj Z., Gorini A., Vidal M., Videt B., Destombes J.* – The Late Ordovician glacio-eustatic record from a high-latitude storm-dominated shelf succession: the Bou Ingarf section (Anti-Atlas, Southern Morocco). Palaeogeography Palaeoclimatology Palaeoecology, 296, 332-358.

Videt B., Paris F., Rubino J.-L., Boumendjel K., Dabard, M.-P., Loi A., **Ghienne** J.-F., Marante A., Gorini A. – Biostratigraphical calibration of the third-order Ordovician sequences on the northern Gondwana platform. Palaeogeography Palaeoclimatology Palaeoecology, 298, 359-375.

*Gutiérrez-Marco J.-C., **Ghienne** J.-F., Bernárdez E., Hacar M.P.* – Did the Late Ordovician African ice sheet reach Europe? Geology, 38, 279-282.

Bouchette F., Schuster M., **Ghienne** J.-F., Denamiel C., Roquin C., Moussa A., Marsaleix P., Duringer P. – Hydrodynamics in the Holocene Lake Mega-Chad. Quaternary Research, 73, 226-236.

2009

Schuster M., Duringer P., **Ghienne** J.-F., Roquin C., Sepulchre P., Moussa A., Lebatard A.-E., Mackaye H.T., Likius A., Vignaud V., Brunet M. – Chad Basin : Paleoenvironments of the Sahara since the Late Miocene. Comptes Rendus Geosciences, 341, 603-611.

Leleu S., **Ghienne** J.F., Manatschal G. – Alluvial fan development and morphotectonic evolution in response to contractional fault reactivation (Late Cretaceous-Palaeocene), Provence, France. Basin Research, 21, 157-187.

2008

*Le Heron D.P., Khoukhi Y., Paris F., **Ghienne** J.-F., Le Herissé A.* – Black shale, grey shale, fossils and glaciers : anatomy of the Upper Ordovician-Silurian succession in the Tazzeka Massif of eastern Morocco. Gondwana Research, 14, 483-496.

2007

***Ghienne** J.-F., Le Heron D., Moreau J., Denis M., Deynoux M.* – The Late Ordovician glacial sedimentary system of the North Gondwana platform. In : Hambrey, M., Christoffersen, P., Glasser, N., Janssen, P., Hubbard, B. and Siegert, M. (eds.) Glacial Sedimentary Processes and Products. Special Publication n°39, International Association of Sedimentologists, Blackwells, Oxford, pp. 295-319.

***Ghienne** J.-F., Boumendjel K., Paris F., Videt B., Racheboeuf P. and Ait Salem H.* – The Cambrian-Ordovician succession in the Ougarta Range (western Algeria, North Africa) and interference of the Late Ordovician glaciation on the development of the Lower Palaeozoic transgression on northern Gondwana. Bulletin of Geosciences, 82(3), 183-214. Doi 10.3140/bull.geosci.2007.03.183

Denis M., Buoncristiani J.-F., Konaté M., **Ghienne** J.-F., et Guiraud M. – Hirnantian glacial and deglacial record in SW Djado Basin (NE Niger). Geodinamica Acta, 20-3, 177-194.

Paris F., Le Hérissé A., Monod O., Kozlu H., **Ghienne** J.F., Dean W.T., Vecoli M., Günay Y. – Ordovician chitinozoans and acritarchs from southern and southeastern Turkey/Chitinozoaires et acritarches ordoviciens du sud et du sud-est de la Turquie. Revue de Micropaléontologie, 50, 81-107. doi:10.1016/j.revmic.2006.11.004

*Le Heron D., **Ghienne** J.-F., El Houicha M., Khoukhi Y., Rubino J.-L.* – Maximum extent of ice sheets in Morocco during the Late Ordovician glaciation. Palaeogeography Palaeoclimatology Palaeoecology, 245, 200-226. doi:10.1016/j.palaeo.2006.02.031

2006

Schuster M., Duringer P., **Ghienne** J.-F., Vignaud P., Mackaye H. T., Likius A., Brunet M. – The Age of the Sahara Desert, Science (Brevia), 311, p. 821.

2005

Leleu S., **Ghienne** J.F., Manatschal G. – Upper Cretaceous to Palaeocene basin-margin alluvial fans documenting interaction between tectonic and environmental processes (Provence, SE France). In: Alluvial Fans: Geomorphology, Sedimentology, Dynamics (Harvey A.M., Mather A.E. & Stokes M. Eds), Geological Society, London, Special Publications, 251, 217-239.

*Deynoux M., **Ghienne** J.F.* – Late Ordovician glacial pavements revisited – a reappraisal of the origin of striated surfaces. Reply. Terra Nova, 17, 488-491.

*Moreau J., **Ghienne** J.-F., Le Heron D., Rubino J.-L., Deynoux M.* – 440 Ma old ice stream in North Africa. Geology, 33, 753-756.

Schuster M, Roquin C., Brunet M., Caugy M., Duringer P., Fontugne M., Mackaye H.T., Vignaud P., **Ghienne** J.F. – Highlighting Holocene Lake Mega-Chad palaeoshorelines from space, Quaternary Science Review, 24, 1821-1827.

2004

*Deynoux M., **Ghienne** J.F.* – Late Ordovician glacial pavements revisited – a reappraisal of the origin of striated surfaces. Terra Nova, 16, 95-101.

2003

***Ghienne** J.F., Deynoux M., Manatschal G., Rubino J.L.* – Palaeovalleys and fault-controlled depocenters in the Late Ordovician glacial record of the Murzuq Basin (Central Libya), Comptes Rendus Geosciences, 335, 1091-1100.

Schuster, M., Duringer, Ph., **Ghienne**, J.F., Brunet, M., Vignaud, P. – Coastal conglomerates around the Hadjer el Khamis inselbergs (Chad): new evidence for Lake Mega-Chad high water level episodes. Earth Surf. Process. Landforms, 28, 1059-1069.

Monod O., Kozlu H., ***Ghienne*** *J-F., Dean W.T., Günay Y., Le Hérissé A., Paris F., Robardet M.* – Late Ordovician glaciation in Southern Turkey. Terra Nova, 15, 249-257.

Ghienne *J-F.,* – Late Ordovician sedimentary environments, glacial cycles, and post-glacial transgression in the Taoudeni Basin, West Africa. Palaeogeography Palaeoclimatology Palaeoecology, 189, 117-145. **Article classé comme " Top-50 most cited article" de la revue Palaeo-3 sur la période 2003-2007.**

2002

Lancaster N., Kocurek G., Singhvi A., Pandey V., Deynoux. M., **Ghienne** J.-F., Lô Khalidou – Late Pleistocene and Holocene dune activity and wind regimes in the western Sahara of Mauritania. Geology, 30, 991-994

Ghienne J.-F., Schuster M., Bernard A., Duringer P., Brunet M. – The Holocene giant Lake Chad revealed by Digital Elevation Models. Quaternary International, 87, 81-85.

2000

Ghienne *J.-F., Bartier D., Leone F., Loi A.* – Caractérisation des horizons manganésifères de l'Ordovicien supérieur de Sardaigne : relation avec la glaciation fini-Ordovicienne. Comptes Rendus de l'Académie des Sciences, Paris, 331, 257-264.

---------- thèse de doctorat ----------

1998

Paris F., Deynoux M., **Ghienne** J.-F. – Chitinozoaires de la limite Ordovicien-Silurien en Mauritanie. Comptes Rendus de l'Académie des Sciences, Paris, 326,499-504.

Underwood C., Deynoux M., **Ghienne** J.-F. – High palaeolatitude recovery of graptolites faunas after the Hirnantian (top Ordovician) extinction event. Palaeogeography Palaeoclimatology Palaeoecology, 142, 91-105.

Ghienne J.-F. et Deynoux M. – Large-scale channel fill structures in Late Ordovician glacial deposits in Mauritania, Western Africa. Sedimentary Geology, 119, 141-159.

Bennett M.R., Huddart D., Hambrey M.J., **Ghienne** J.-F. – Modification of braided outwash surfaces by aufeis: an exemple from Pedersenbreen, Svalbard. Zeit. Geomorph., 42, 1-20.

1996

Bennett M.R., Hambrey M.J., Huddart D., **Ghienne** J.-F. – The formation of a geometrical ridge network by the surge-type glacier Kongsvegen, Svalbard. Journal of Quaternary Research, 11, 437-449.

Bennett M.R., Huddart D., Hambrey M.J., **Ghienne** J.-F. – Moraine development at the high arctic valley glacier Pedersenbreen, Svalbard. Geog. Ann., 78a, 209-222.

1994

Ghienne J.-F., Deynoux M., Jeannette D. – Structures sédimentaires, discontinuités et caractères pétrophysiques des grès du Buntsandstein des Vosges du Nord, Trias de l'Est de la France. Comptes Rendus de l'Académie des Sciences, Paris, 319, 1351-1358.

PUBLICATIONS rang B et PROCEEDINGS

***Ghienne** J.-F. (2009)* Late Ordovician tunnel valleys. 71st EAGE Conference & Exhibition. Workshop 5 (Buried glacial valleys and recent advances in understanding groundwater and hydrocarbon reservoirs). Amsterdam, 8-11 juin 2009. Extended Abstract 4 pages http://earthdoc.eage.org/detail.php?pubid=32190 **(conférence invitée).**

Lahondère D., Le Metour J., Callec Y., Roger J., **Ghienne** J.-F., Gourvennec R. (2008) Notice explicative des cartes géologiques à 1/200 000 de la zone Centre de la Mauritanie. DMG, Ministère des Mines et de l'Industrie, Nouakchott, Rapport BRGM/RC-56742-FR, 398 pages.

Ghienne, J.-F., Rubino, J.-L., Moreau, J., Lafont, F., Khoja A. (2007) Sedimentary facies and architectures in the Late Ordovician glacial sediments of the Western Murzuq Basin. Excursion Guide, 3rd North African/Mediterranean Petroleum and Geosciences Conference & Exhibition (EAGE), Tripoli, Libya, 164 p.

Ghienne J.-F., Loi A., Paris, F. Rubino J.-L. (2008) Platform-scale correlation of North Gondwanan, Late Ordovician glacial cycles. Rend. Online Soc. Geol. Italia, 3, 429-430.

*Moreau J., Degermann L., **Ghienne** J.-F., Rubino J.-L. (2007)* Large-scale physiography of the Murzuq Basin shelf during Hirnantian ice-sheet final retreat and Silurian transgression: outcrops and seismic interpretations. 3rd North African/ Mediterranean Petroleum and Geosciences Conference & Exhibition (EAGE), 26 to 28 February 2007, Tripoli (Libya). Extended Abstract 4 pages

Joubert J.-B., Moreau J., **Ghienne** J.-F., and Rubino J.-L. (2007) FMI characterisation of Late Ordovician glacial facies and surfaces. 3rd North African/ Mediterranean Petroleum and Geosciences Conference & Exhibition (EAGE), 26 to 28 February 2007, Tripoli (Libya). Extended Abstract 4 pages

Paris F., K. Boumendjel K., Dabard M. P.,**Ghienne** J.-F., Loi A., Tang P.,Videt B., Achab A. (2007) Chitinozoan-based calibration of Early-Mid Ordovician transgressive events on northern Gondwana. Acta Paleotonlogica Sinica, 46, 370-375.

Rubino J.-L., Anfray R., Blanpied C., **Ghienne** J.-F., Manatschal G. (2003) Meander belt complex within the lower Mamuniyat Formation in western Al Qarqaf area, Libya. In: The geology of northwest Libya; Volume II, Sedimentary basins of Libya, second symposium (Salem M.J. & Oun Khaled M. eds), Symposium on the Sedimentary Basins of Libya. 2, 3-18.

Blanpied C., Deynoux M., **Ghienne** J.-F., Rubino J.-L. (2000) Late Ordovician glacially related depositional systems of the Gargaf Uplift (Libya) and comparisons with correlative deposits in the Taoudeni Basin (Mauritania). Geological Exploration in Murzuq Basin (M.A. Sola et D. Worsley Eds), Elsevier, 485-507.

Bano M., Duringer P., **Ghienne** J.-F., Schuster M. (1999) Ground penetrating radar of dry aeolian environment. 69th SEG Meeting, Extended Abstracts, 586-589.

COMMUNICATIONS

Schuster M., Bouchette F., **Ghienne** J.-F., Denamiel Cl., Roquin Cl., Moussa A., Duringer Ph. (2010). Le Lac Méga-Tchad : marqueurs morphosédimentaires et paléohydrodynamique. Colloque de restitution du projet SAHELP (ANR VULNERABILITE) « La vulnérabilité du Sahel et du Sahara: les leçons du passé », Maison des Sciences de l'eau, Montpellier, 10-11 Juin 2010. oral.

Schuster M., Duringer Ph., Moussa A., Roquin Cl., **Ghienne** J.-F. (2010) Du Chari au paléo-Chari : archives sédimentaires du tributaire principal du Lac Tchad. Colloque de restitution du projet /SAHELP (ANR VULNERABILITE) « /La vulnérabilité du Sahel et du Sahara: les leçons du passé », Maison des Sciences de l'eau, Montpellier, 10-11 Juin 2010 oral.

Bouchette F., Schuster M., **Ghienne** J.-F., Denamiel C., Roquin C., Moussa A., Duringer P. (2009) Hydrodynamique du lac Mega-Tchad à l'Holocène. 12ème Congrès Français de Sédimentologie (25-31 octobre), Livre des Résumés, *Publ. de l'Association des Sédimentologistes Français*, n° **64**, p. 49. oral

Ghienne J.-F. et Rubino J.-L. (2009) Archives sédimentaires de la glaciation Ordovicien supérieur: contexte, signatures stratigraphiques et réservoirs associés. 12ème Congrès Français de Sédimentologie (25-31 octobre), Livre des Résumés, *Publ. de l'Association des Sédimentologistes Français*, n° **64**, p. 149. **Présentation Invitée, 30 mn**.

Girard F., **Ghienne** J.-F., Moreau J., Du Bernard X., Rubino J.-L. (2009) Faciès et architecture d'une succession de fan proglaciaire (Ordovicien supérieur, Bassin de Murzuq occidental, SW libyen). 12ème Congrès Français de Sédimentologie (25-31 octobre), Livre des Résumés, *Publ. de l'Association des Sédimentologistes Français*, n° **64**, p. 153. oral

Girard F., **Ghienne** J.-F., Moreau J., Rubino J.-L. (2009) Architecture de chenaux fluvio-glaciaires à dynamique de crue (Ordovicien supérieur, Bassin de Murzuq occidental, SW libyen). 12ème Congrès Français de Sédimentologie (25-31 octobre), Livre des Résumés, *Publ. de l'Association des Sédimentologistes Français*, n° **64**, p. 152. poster

Loi A., **Ghienne** J.-F., Dabard M.P., Paris F., Vidal M., Destombes J. (2009) Analyse du signal eustatique de l'Ordovicien supérieur dans l'Anti-Atlas (sud Maroc). 12ème Congrès Français de Sédimentologie (25-31 octobre), Livre des Résumés, *Publ. de l'Association des Sédimentologistes Français*, n° **64**, p. 212. oral

Masini E., Mohn G., Manatschal G., **Ghienne** J.F., Lafont F. (2009) L'enregistrement tectono-sédimentaire des marges riftées profondes associé à l'amincissement crustal: éléments d'un analogue fossile alpin. 12ème Congrès Français de Sédimentologie (25-31 octobre), Livre des Résumés, *Publ. de l'Association des Sédimentologistes Français*, n° **64**, p. 222. oral

Moussa A., Duringer P., **Ghienne** J.-F., Schuster M., Brunet M., Vignaud P., Mackaye H.T., Likius A. (2009) Les séquences « dunes-lac » du Miocène tchadien : un exemple bien documenté de faciès éolo-lacustre. 12ème Congrès Français de Sédimentologie (25-31 octobre), Livre des Résumés, *Publ. de l'Association des Sédimentologistes Français*, n° **64**, p. 234. poster

Moussa A., Duringer P., Roquin C., Schuster M., **Ghienne** J.-F., Brunet M., Vignaud P., Mackaye H.T., Likius A. (2009) Architecture tri-dimensionnelle des barres fluviatiles du Chari : du satellite au terrain. 12ème Congrès Français de Sédimentologie (25-31 octobre), Livre des Résumés, *Publ. de l'Association des Sédimentologistes Français*, n° **64**, p. 235. oral

Rubino J.-L., **Ghienne** J.-F., Moreau J., Blanpied C., Girard F., Razin P., Haddadi N., Temple F., Douillet D. (2009) Variabilité du cortège transgressif post-glaciaire fini-ordovicien sur la bordure nord gondwanienne. 12ème Congrès Français de Sédimentologie (25-31 octobre), Livre des Résumés, *Publ. de l'Association des Sédimentologistes Français*, n° **64**, p. 288. oral

Schuster M., Duringer P., **Ghienne** J.-F., Roquin C., Bouchette F., Sepulchre P., Moussa A., Mackaye H.T., Likius A., Vignaud P., Brunet M. (2009) Le bassin du Lac Tchad d'hier à aujourd'hui : morceaux choisis. 12ème Congrès Français de Sédimentologie (25-31 octobre), Livre des Résumés, *Publ. de l'Association des Sédimentologistes Français*, n° **64**, p. 297. oral

Ghienne J.-F., Girard F., Moreau J., Rubino J.-L. (2009) Upper Ordovician fluvio-glacial architectures and facies suites, from outbursts to estuaries. Workshop « From River to Rock Record », 12-14 january 2009, Aberdeen, abstract book p.33. poster

Girard F., **Ghienne** J.-F., Moreau J., Rubino J.-L. (2009) Anatomy of Late Ordovician channels of a fluvio-glacial outburst-related delta plain. Workshop « From River to Rock Record », 12-14 january 2009, Aberdeen, abstract book p.39. poster

Douillet G. et **Ghienne** J.-F. (2009) Late Ordovician Jordanian tunnel valleys. 71st EAGE Conference & Exhibition. Workshop 5 (Buried glacial valleys and recent advances in understanding groundwater and hydrocarbon reservoirs). Amsterdam, 8-11 juin 2009. http://earthdoc.eage.org/detail.php?pubid=32188

Ghienne J.-F., Loi A., Paris, F. Rubino J.-L. (2008) Platform-scale correlation of North Gondwanan, Late Ordovician glacial cycles. 84 congresso Nazionale, Sassari, 15-17 septembre 2008. *Rend. Online Soc. Geol. Italia, 3*, 429-430. oral

F. Girard, J.-F. **Ghienne**, J. Moreau, J.-L. Rubino, Y. Boujazia (2008) Late Ordovician climbing dune assemblages, the signature of glacial outburst ?, 26th regional meeting of the International Association of Sedimentologists, Bochum, 1-3 septembre 2008, Schriftenreihe der Deutschen Gesellschaft für Geowissenschaften, 58, p. 110. poster

Ghienne J.-F., Loi A., Paris, F. Rubino J.-L. (2008) The Late Ordovician glacial record. Palaeozoic Climates, International Congress (meeting of the International Geoscience Programme IGCP 503 "Ordovician Palaeogeography and Palaeoclimate", Lille, 22-31 août, abstract volume p. 39 (http://sarv.gi.ee:igcp503/). **Présentation Invitée, 45 mn**

Paris F., Videt B., **Ghienne** J.-F., Tang P., de la Puente S. (2008) Factors susceptible to alter the original ∂13Corg signal in Early Papaeozoic marine sediments. Palaeozoic Climates, International Congress (meeting of the International Geoscience Programme IGCP 503 "Ordovician Palaeogeography and Palaeoclimate", Lille, 22-31 août, abstract volume p. 74 (http://sarv.gi.ee:igcp503/). oral

Paris F., K. Boumendjel K., Dabard M. P.,**Ghienne** J.-F., Loi A., Tang P.,Videt B., Achab A. (2007) Chitinozoan-based calibration of Early-Mid Ordovician transgressive events on northern Gondwana. 4th annual meeting of the IGCP 503 Project and Yangtze Conference, Nanjing, juin 2007. *Acta Paleotonlogica Sinica*, 46, 370-375. oral

Ghienne J.-F. et al. (26 participants du projet ECLIPSE), 2007, Glaciations et crises biologiques : exemple de l'épisode fini-ordovicien (archives sédimentaires, paléo-environnements et biodiversité, cycle du carbone), colloque de restitution du programme Insu Eclipse, 15-16 octobre, Paris. poster

Ghienne J.-F., Botquelen A., Dabard M.-P., Degermann L., Elaoud-Debbaj Z., El Houicha M., Khoukhy Y., Jati M., Le Heron D., Loi A., Paris F., Vidal F. (2007) The Hirnantian record in Morocco: preglacial/ glacial transition, glacial cycles and phases, and maximum extent of the ice-sheet in North Africa. IGCP Project 503 Regional Meeting and Field-trip, Saragosse, Espagne, 17-19 septembre 2007. oral

Boumendjel K., Aït Salem H., Paris F., **Ghienne** J.-F., Videt B., Zelouf K. (2007) Datation par les chitinozoaires des principaux épisodes transgressifs identifiés dans l'Ordovicien du Sahara Algérien. 6ème Séminaire de Géologie Pétrolière (SGP6), Sonatrach, Boumerdes, avril 2007.

Jammes S., Manatschal G., **Ghienne** J.-F., Schulmann K., Lavier L. (2006) Golfe de Gascogne-Pyrénées Occidentales : un laboratoire naturel pour étudier les structures d'amincissements et leurs rôles lors de la réactivation ? *Réunion des Sciences de la Terre, Société Géologique de France*, Dijon, 4-8 décembre 2006.

Moreau J., Degermann L., **Ghienne** J.-F., Rubino J.-L. (2006) Empreinte d'un fleuve de glace à l'échelle du Bassin de Murzuq (Libye), Caractérisation sur le terrain et en subsurface. *Réunion des Sciences de la Terre, Société Géologique de France*, Dijon, 4-8 décembre 2006. oral

Ghienne J.F. et participants du projet ECLIPSE "Glaciations et crises biologiques : exemple de l'épisode fini-ordovicien (archives sédimentaires, paléo-environnements et biodiversité, cycle du carbone)" (2005) Ampleur de la glaciation Hirnantienne (Ordovicien supérieur) : apport des archives sedimentaires, 10e *Congrès Français de Sédimentologie*, Giens, 11-13 octobre 2005, livre des résumés, Association des Sédimentologistes Français, vol. 51, p.143. oral

Moreau J., **Ghienne** J.-F., Deynoux M., Rubino J.L. (2005) Du fleuve de glace à la transgression post-glaciaire : grandeur et décadence des glaciers ordoviciens dans le bassin de Murzuq (Libye occidentale). 10e *Congrès Français de Sédimentologie*, Giens, 11-13 octobre 2005, livre des résumés, Association des Sédimentologistes Français, vol. 51, p. 220. oral

Schuster M., Tiercelin J.J., Duringer P., **Ghienne** J.F., Likius A., Mackaye H.-T., Roche H., Vignaud P., Brunet M. (2005) Nature et dynamique de systèmes sédimentaires continentaux d'Afrique au Mio-Plio-Quaternaire : exemples des séries à hominidés anciens des bassins du Turkana et du Tchad. 10e *Congrès Français de Sédimentologie*, Giens, 11-13 octobre 2005, livre des résumés, Association des Sédimentologistes Français, vol. 51, p. 277. oral

Duringer P , Schuster M., **Ghienne** J.F., Roquin C., Vignaud P., Mackaye H.-T., Brunet M. (2005) Huit arguments en faveur de l'existence du Méga-Lac Tchad (Holocène, sbassin du Tchad). 10e *Congrès Français de Sédimentologie*, Giens, 11-13 octobre 2005, livre des résumés, Association des Sédimentologistes Français, vol. 51, p.102. oral

Buoncristiani J.F., Guiraud M., **Ghienne** J.F., Denis M. (2005) Mise en évidence d'une dynamique d'ice stream sur la calotte fini-ordovicienne : exemple du Sahara central. 10e *Congrès Français de Sédimentologie*, Giens, 11-13 octobre 2005, livre des résumés, Association des Sédimentologistes Français, vol. 51, p.54. oral

Le Heron D.P., **Ghienne** J.F., Khoukhy Y., El Houicha M., Rubino J.L. (2005) La glaciation fini-ordovicienne en Méséta marocaine : extension maximale des fronts glaciaires, deltas de bordure de plate-forme et systèmes turbiditiques associés. 10e *Congrès Français de Sédimentologie*, Giens, 11-13 octobre 2005, livre des résumés, Association des Sédimentologistes Français, vol. 51, p. 189. poster

Ghienne J.F., Roquin C., Schuster M., Duringer Ph. (2005) Dynamique des systèmes sédimentaires littoraux du Méga-Lac Tchad holocène. 10e *Congrès Français de Sédimentologie*, Giens, 11-13 octobre 2005, livre des résumés, Association des Sédimentologistes Français, vol. 51, p.142. oral

Leleu S., **Ghienne** J-F., Manatschal G. (2005) Architecture et distribution de cônes alluviaux Campanien à Paléocène : Analyse morpho-tectonique d'un système compressif en Provence. 10e *Congrès Français de Sédimentologie*, Giens, 11-13 octobre 2005, livre des résumés, Association des Sédimentologistes Français, vol. 51, p. 192. oral

Ghienne J.-F., Le Heron D., Moreau J., Rubino J.-L,. Deynoux M. (2005) The Late Ordovician glacial sedimentary system of the north Gondwana platform. *International Association of Sedimentologists, Glacial Sedimentary Processes and Products*, 22-27 august 2005, University of Wales, Aberystwyth. **Présentation Invitée, 30 mn**

Moreau J., **Ghienne** J.-F., Rubino J.-L,. Deynoux M. (2005) The Late Ordovician deglaciation sequence in the Murzuq Basin (Libya). *International Association of Sedimentologists, Glacial Sedimentary Processes and Products*, 22-27 august 2005, University of Wales, Aberystwyth. oral

Denis M., Buoncristiani J.-F., **Ghienne** J.-F., Guiraud M. (2004) Enregistrement de la glaciation fini-ordovicienne dans le bassin du Djado (Niger). *Réunion des Sciences de la Terre, Société Géologique de France*, 20-25 septembre 2004. Oral

Moreau J., **Ghienne** J.-F. , Deynoux M., Rubino J.-L. (2004) Un courant de glace (ice stream) fini-Ordovicien en Libye. *Réunion des Sciences de la Terre, Société Géologique de France*, 20-25 septembre 2004, Strasbourg. Oral

Le Heron D.P., El Houicha M., Khoukhy Y., El Chellai H., **Ghienne** J.F. (2004) Defining the maximum extent of the Hirnantian ice sheet in Morocco. *International symposium on Early Palaeozoic Palaeogeography and Palaeoclimate, Erlangen, Erlanger geologische Abhandlungen*, Sonderband 5, 49. Oral.

Moreau J., **Ghienne** J.-F. , Deynoux M., Rubino J.-L. (2004) Ice-proximal sedimentary record of the Late Ordovician glacial cycles. *International symposium on Early Palaeozoic Palaeogeography and Palaeoclimate, Erlangen, Erlanger geologische Abhandlungen, Sonderband* 5, 55. Oral

Leleu S., Ghienne J-F., Manatschal G. (2004) Evolution of the European margin during Late Cretaceous, the case of the Provence (SE France). Réunion des Sciences de la Terre, Société Géologique de France, 20-25 septembre 2004, Strasbourg. Oral

Leleu S., **Ghienne** J-F., Manatschal G. (2004) Architecture et évolution de cônes alluviaux Campanien-Paléocène dans une structure de croissance compressive en Provence. *Colloque "Gérard Guieu", Marseille.*

Deynoux M., **Ghienne** J.F., Moreau J., Rubino J.L. (2004) Paléoglaciations : enregistrement, causes, effets. Colloque de Paléogéographie, Institut de France, Académie des sciences, Paris 8-9 Mars, livre des résumés.

Schuster M., Roquin C., Brunet M., Caugy M., Duringer Ph., Fontugne M., Mackaye H.T., Vignaud P., **Ghienne** J.F. (2004) Characterization of Lake Mega-Chad shorelines based on DEM and Landsat images: paleoenvironmental implications for Quaternary wet periods in Sahara. 20ème Colloque de Géologie Africaine, Orléans, juin 2004.

Rubino J.-L., **Ghienne** J.-F., Deynoux M., Moreau J. (2004) Les cycles glaciaires de l'Ashgillien supérieur du Nord Gondwana. Implications sur les faciès et la distribution des réservoirs. Cinquième Séminaire de Géologie Pétrolière Sgp5, Boumerdés (Algérie), 18-20 janvier 2004.

Leleu, S. **Ghienne**, J-F. and Manatschal, G. (2003) Architecture et évolution des cônes alluviaux Campanien-Paléocène dans une structure de croissance compressive en Provence. Réunion Soc. Geol. France, 6-7 novembre 2003, Paris.

Manatschal G., Leleu, S. **Ghienne**, J-F. (2003) Le Valaisan : océan ou bassin ? Implications pour l'évolution géodynamique du SE de la France au Crétacé. *Réunion Soc. Geol. France*, 6-7 novembre 2003, Paris.

Schuster M., **Ghienne** J.F., Duringer Ph., Likius A., Mackaye H.T., Brunet M., Vignaud P. (2003) Le méga-lac Tchad holocène : une évocaton de la *période bleue* du Sahara. *9ème Congrès Français de Sédimentologie* - Livre des résumés, Publ. ASF, Paris, n° 38, 468-469.

Moreau J., **Ghienne** J.-F., Deynoux M., Rubino J.-L. (2003) Architecture des sédiments glaciaires fini-ordoviciens du Bassin de Murzuq (Libye) : un complexe de vallées emboîtées. *9ème Congrès Français de Sédimentologie* - Livre des résumés, Publ. ASF, Paris, n° 38, 369-370.

Leleu, S. **Ghienne**, J-F. and Manatschal, G. (2003) Réponse sédimentaire de cônes alluviaux à une propagation de pli : exemple du Crétacé tardif-Paléocène de la Montagne Sainte-Victoire (Provence). *9ème Congrès Français de Sédimentologie* - Livre des résumés, Publ. ASF, Paris, n° 38, 300-301.

Schuster M., Duringer Ph., **Ghienne** J.F., Brunet M., Vignaud P., Likius A., Mackaye H.T. (2003) Toumai, Abel and mega-lake Chad : palaeontology, sedimentology and palaeoclimatology of central Sahara during the last 7 Ma (erg of Djurab, Chad) ; Results of the MPFT project. International Symposium, Archaeology of the Earliest Northeastern Africa (Poznan, 14-17 july 2003).

Leleu S., **Ghienne** J.-F., Manatschal G. (2003) Interaction between syntectonic alluvial fan deposits and climatically dominated flood-plain sedimentation: the example of a Late Cretaceous – Paleocene succession in Provence, SE France. *Alluvial Fans workshop*, Almeria, Espagne, 8-13 juin 2003.

Rubino J.-L., Deynoux M., **Ghienne** J.-F., Moreau J., Blanpied C., Laffont F., Andres-Calatrava R., Galeazzi S., Mynth T., Sommer F. (2003) Late Ordovician glaciation in northern Gondwana, Reappraisal and petroleum implications. *AAPG Hedberg Conference, Paleozoic and Triassic Petroleum Systems in North Africa,* February 17-20, 2003, Abstract Book.

Ghienne J.-F., Moreau J., Deynoux M., Rubino J.-L. (2003) Architecture of a Late Ordovician ice-proximal multistorey palaeovalley in the Murzuq Basin (Libya) : implication for sequence stratigraphy. *AAPG Hedberg Conference, Paleozoic and Triassic Petroleum Systems in North Africa,* February 17-20, 2003, Abstract Book (http://www.searchanddiscovery.net/documents/abstracts/hedberg2003algeria/allabstracts/Ghienne.pdf)

Deynoux M., **Ghienne** J.-F. (2003) New evidences on the specific character of the Late Ordovician striated surfaces and implication for ice-sheet dynamics. *AAPG Hedberg Conference, Paleozoic and Triassic Petroleum Systems in North Africa*, February 17-20, 2003, Abstract Book.

Duringer P., Schuster M., **Ghienne** J.F., Brunet P., Vignaud P. (2003) Evidence of the Holocene mega-lake in the Chad Basin: a synthesis. *French-Egyptian workshop on Earth and environmental sciences, Cairo University, Giza*, Egypt, February 17-19, 2003, Abstract Book p. 14.

Schuster M., **Ghienne** J.F., Duringer P., Brunet P., Vignaud P. (2002) Les épisodes de type "Méga-Lac Tchad": nouveaux travaux et perspectives. *Colloque CNRS ECLIPSE*, 21-22 octobre 2002, Paris, livre des Résumés.

Deynoux. M., **Ghienne** J.-F., Roquin C., Kocurek G., Lancaster N., Singhvi A., Lézine A.M., Libis A., Leprun J.-C., Lô K. (2002) Les systèmes quaternaires éoliens, lacustres et fluviatiles de Mauritanie occidentale: relations événementielles. *Colloque CNRS ECLIPSE*, 21-22 octobre 2002, Paris, livre des Résumés.

Leleu S., **Ghienne** J.-F., Manatschal G. (2002) Deconvolution of tectonic and climatic signals from syntectonic alluvial fan deposits in a foreland setting : the exemple of the Montagne Sainte Victoire. *Workshop Erosion and Orogeny, Annual Meeting of the Swiss Academy of Natural Sciences (Davos, septembre 2002),* livre des résumés p.8.

Ghienne J.-F., Monod O., Dean W.T., Kozlu H., Günay Y. ,Paris F, Le Herissé A. (2002) The Late Ordovician glaciomarine succession of Southern Turkey. *16th International Sedimentological Congress, juillet 2002, Rand Afrikaans University, Johannesbourg,* Abstract Volume p. 113.

Ghienne J.-F., Deynoux M., Rubino J.L., Blanpied C. (2002) Late Ordovician glacial valleys: the example of the Gargaf (Libya). *16th International Sedimentological Congress, juillet 2002, Rand Afrikaans University, Johannesbourg,* Abstract Volume p. 114-115.

Monod O., **Ghienne** J.-F., Dean W.T., Kozlu H., Gunay Y. Paris F., Le Hérissé A, Rickards, Cocks L.R.M. (2002) *Ordovician glaciation in Southern Turkey First International Symposium of the Faculty of Mines on Earth Sciences and Engineering*, 16-18 mai 2002, Istanbul.

Leleu, S. **Ghienne**, J-F. and Manatschal, G. (2001) Cônes alluviaux syntectoniques en situation d'avant-pays : Exemple de la Montagne Sainte-Victoire (Provence). *8ème Congrès Français de Sédimentologie* - Livre des résumés, Publ. ASF, Paris, n° 36, p. 217.

Schuster, M., Duringer Ph., **Ghienne**, J.F., Brunet, M., Vignaud, P., Mackaye, H.T. (2001) Les conglomérats côtiers du Lac Méga-Tchad autour des paléo-îles du Hadjer el Khamis. *8ème Congrès Français de Sédimentologie* - Livre des résumés, Publ. ASF, Paris, n° 36, p. 337-338.

Rubino J.-L., Anfray R., Blanpied C., **Ghienne** J.-F., Deynoux M., Manatschal G. (2001) Meander belt complexes in Latest Ordovician proglacial setting: Examples from the Mamuniyat Formation in Murzuk Basin. *Conference on fluvial Sedimentology, University of Nebraska, Lincoln, 6-10 août 2001, Abstract Volume.*

Leleu, S, **Ghienne**, J-F, & Manatschal G. (2001) Alluvial-tectonic relationships in a foreland setting: the example of the Montagne Sainte Victoire (Provence, France). *EUG XI, Journal of Conference Abstract*, 6, p.35.

Ghienne J-F., Kozlu H. Dean W. T., Günay Y., Monod O. (2001) Discovery of the northernmost evidence of an Ordovician glacier, Southern Turkey. *EUG XI, Journal of Conference Abstract*, 6, p.93.

Schuster M., Duringer P., **Ghienne** J.-F., Bernard A., Brunet M. Vignaud P. (2001) Lake Mega-Chad : Holocene extension and Pliocene palaeo-environmental implications. *EUG XI, Journal of Conference Abstract*, 6, p.56.

Deynoux M., **Ghienne** J.-F., Manatschal G., Rubino J.-L., Blanpied C., Khaeri T., Guillande R. (2000) Glacial valleys within the lower Mamuniyat unit in western Gargaf High. *Conference on the Geology of the Ghadamès Basin*, novembre 2000, Tripoli.

Ghienne J.-F., Manatschal G., Deynoux M. (2000) Syn-sedimentary, glacially-related deformation in the Mamuniyat Formation (Western Gargaf High). *Conference on the Geology of the Ghadamès Basin*, novembre 2000, Tripoli.

Rubino J.-L., Anfray R., Blanpied C., **Ghienne** J.-F., Manatschal G. (2000) Meander belt complex within the lower Mamuniyat Formation in the western Gargaf High. *Conference on the Geology of the Ghadamès Basin*, novembre. 2000, Tripoli.

Duringer Ph., **Ghienne** J.-F., Schuster M., Brunet M. et Vignaud P. (2000) Les séquences climatiques arides-humides des sites pliocènes à Australopithèques du Tchad: influences de la balance climatique équatoriale sur les oscillations du paléo-lac Tchad. *Les Hominidés et leurs environnements: Histoire et Interactions, Poitiers (Colloque international 18, 19 et 20 septembre 2000).*

Denys Ch., Schuster M., Duringer Ph., **Ghienne** J.-F., Brunet M. et Vignaud P. (2000) Approche taphonomique et sédimentologique des sites à Vertébrés du Pliocène tchadien: conditions et modalités de formation des gisements fossilifères. *Les Hominidés et leurs environnements: Histoire et Interactions, Poitiers (Colloque international 18, 19 et 20 septembre 2000).*

Ghienne J.-F., Duringer P., Schuster M., Bernard A. (2000) Un argument décisif pour l'existence du Méga-Lac Tchad : mise en évidence par altimétrie satellitaire d'une terrasse lacustre. *Les Hominidés et leurs environnements: Histoire et Interactions, Poitiers (Colloque international 18, 19 et 20 septembre 2000).*

Ghienne J.-F., Bano M., Duringer P., Ferry M., Schuster M. (1999) Nature et origine des surfaces de discontinuités imagées par géoradar au sein d'une dune éolienne active. *7ème congrès français de sédimentologie, Nancy, livre des résumés,* 169-170.

Bartier D., **Ghienne** J.-F., Leone F., Loi A. (1999) Etude minéralogique et géochimique des horizons à manganèse de l'Ordovicien supérieur de Sardaigne : relation avec la glaciation fini-ordovicienne. *7ème congrès français de sédimentologie, Nancy, livre des résumés,* 17-18.

Duringer P., **Ghienne** J.-F., Schuster M., Bano M., Brunet M., Vignaud P., Mackaye H.T. (1999) Nature et dynamique des milieux continentaux des sites pliocènes à Australopithèques du Tchad. *7ème congrès français de sédimentologie, Nancy, livre des résumés,* 137-138.

Schuster M., Duringer P., **Ghienne** J.-F., Bano M., Brunet M., Vignaud P., Andossa L. (1999) Dynamique transgressive et régressive des lacs de poche sahariens : exemple de lacs holocènes à diatomites du Tchad. *7ème congrès français de sédimentologie, Nancy, livre des résumés,* 275-276.

Ghienne J.-F. (1999) Modalités d'enregistrement d'une glaciation ancienne. Exemple de la glaciation fini-ordovicienne sur la plate-forme nord-gondwanienne en Afrique de l'Ouest. *7ème congrès français de sédimentologie, Nancy, livre des résumés,* 167-168.

Paris F., Robardet M., Dabard M.-P., Feist R., **Ghienne** J.-F., Guillocheau F., Le Hérissé A., Loi A., Melou M., Servais T., Shergold J., Vidal M., Vizcaino D. (1999) Ordovician sedimentary rocks of France. In: *P. Kraft and O. Fatka (Editors), Quo Vadis Ordovician?. 8th International Symposium on Ordovican System, Prague. Acta Universitatis Carolinae, Geologica, 43, 1/2:* 85-88.

---------- thèse de doctorat ----------

Blanpied C., Deynoux M., **Ghienne** J.-F., Rubino J.-L. (1998) Late Ordovician glaciation: depositionnal systems - a comparison from the Gargaf High (Libya) and the Taoudeni Basin (Mauritania). *The geological conference on exploration in Murzuq basin, 22-24 mars 1998, Sabha (Lybie).*

Paris F., **Ghienne** J.-F., Deynoux M. (1997) Découverte de chitinozoaires à la limite Ordovicien-Silurien dans le Sud-Est de la Mauritanie. *Réunion spéciale APF-SGF, De la biostratigraphie à la paléobiogéographie, Lyon, livre des résumés, Soc. Géol. France (Ed.)*, p 34.

Ghienne J.-F. et Deynoux M. (1997) Structures chenalisantes à grande échelle dans les dépôts glaciaires fini-ordoviciens de Mauritanie (Afrique de l'Ouest). *6ème congrès français de sédimentologie, Montpellier, livre des résumés,* 127-128.

Ghienne J.-F., Deynoux M., Jeannette D., Duringer P. (1993) Fluviatile sequential architecture and petrophysical associated characters in the Triasic Buntsandstein sandstones of the Vosges massif, Eastern France. *EUG VII, Terra Abstract, Abstract Suppl. 1 Terra Nova,* 5, p.737.

Archives sédimentaires de la glaciation Ordovicien supérieur

le contexte, les faciès et architectures stratigraphiques associés

---

Synthèse des travaux en vue de l'obtention de l'**H**abilitation à **D**iriger les **R**echerches

Jean-François GHIENNE

Sommaire

Dans ce document, les citations *en italique et soulignées* signalent les références sélectionnées pour constituer le mémoire de l'Habilitation à Diriger les Recherches, avec mention du chapitre dans lequel figure la publication. Les citations soulignées concernent des publications qui ne sont pas reproduites dans ce mémoire (participation subalterne, ou publications directement issues du travail de thèse).

Introduction

La falaise du Hodh ceinture le flan nord-oriental de l'Aouker, vaste dépression dunaire dans le sud-est mauritanien. Elle comprend une succession de grès essentiellement d'âge cambrien surmontée par la succession glaciaire fini-ordovicienne formant ici le ressaut sommital plus sombre (Deynoux, 1980 ; Ghienne, 2003, §6 ; Lahondère et al., 2008*). C'est l'équivalent vers l'ouest du Tassili Interne tel que défini par C. Kilian au Sahara central.*

Des glaciers au Sahara ? Il faut attendre 1960 pour que les géologues sahariens, issus du milieu académique ou travaillant pour l'exploration pétrolière, commencent à mettre en relation un ensemble de structures — restées jusque-là énigmatiques — avec un épisode climatique froid ordovicien mis en évidence quelque temps auparavant par les paléontologues étudiant les séries carbonatées intertropicales contemporaines (Spjeldnæs, 1961). Kilian, en 1922, avait subdivisé la succession stratigraphique du Paléozoïque inférieur du Sahara en deux ensembles : le Tassili Interne d'une part, essentiellement gréseux, qui englobe une succession cambrienne et ordovicienne, et qui ceinture les massifs de socle « précambriens » tel le bouclier du Hoggar ; le Tassili Externe d'autre part, avec les argiles gothlandiennes (i.e. siluriennes) à graptolites à sa base, puis de nouveau gréseux vers le haut (Silurien supérieur et Dévonien). Entre 1950 et 1960, une importante discordance de ravinement est identifiée dans la partie supérieure de l'équivalent du Tassili Interne. Mise en évidence en Mauritanie (Sougy, 1957), cette discordance sera par la suite reconnue jusqu'au Tchad, en passant par le Mali (Dars et al., 1957), l'Algérie (Borocco et Nyssen, 1959) et le Niger (Joulia, 1959). Elle sera parfois attribuée à une phase de déformation tectonique dite taconique, concept aujourd'hui abandonné. En 1962, l'équipe de l'Institut Français du Pétrole publie les premières photographies de surfaces striées avec le commentaire suivant : « (…) qui peuvent être attribuées à une action glaciaire » (Beuf et al., 1962). Ces structures sont maintenant interprétées classiquement comme les marqueurs de bandes de cisaillement intraformationnelles se développant au sein de sables sous-glaciaires (cf. section 3.1). Associés à des diamictites incluant des galets exotiques de socle que l'on découvrit à peu près simultanément en Libye (Freulon, 1959 ; Collomb, 1962), en Mauritanie (Sougy et Lécorché, 1963 ; Michoud et al., 1963) et en Algérie (Debyser et al., 1966), il devenait évident que le Sahara recélait un enregistrement sédimentaire glaciaire d'une exceptionnelle richesse. Il faudra attendre 1968 pour que ce repère stratigraphique essentiel soit également identifié dans l'Anti-Atlas marocain (Destombes, 1968a), époque à partir de laquelle la discordance de revinement d'extension continentale sera unanimement reconnue comme une surface d'érosion glaciaire (Debyser et al., 1966 ; Dia et al., 1969 ; Rognon, 1971). Dans le même temps, en Europe (Espagne, Bretagne, Allemagne), des faciès comparables seront désormais interprétés par Doré (synthèse *in* Robardet et Doré, 1988) comme des équivalents glaciomarins distaux de ces successions africaines plus proche du pôle Sud et des centres de glaciation ordoviciens.

Daté de l'Ordovicien supérieur, cet épisode climatique majeur est lié à la première des cinq grandes crises de la biodiversité que connut la Terre (Sepkoski, 1995 ; Servais et al., 2010). Il est d'autre part intimement lié à la constitution d'un système pétrolier très prolifique, avec des réservoirs à faciès glaciogéniques *s.l.* et une roche-mère postglaciaire dont la localisation est en grande partie contrôlée par les topographies résiduelles laissées par le retrait des glaciers. Essentiellement basée sur des observations de terrain, de l'échelle millimétrique à l'image satellite, mon activité de recherche depuis 15 années a pour l'essentiel consisté à examiner, caractériser et interpréter les éléments de ce système géologique à grande échelle que constitue le domaine de plate-forme cratonique dit nord-gondwanien (Afrique de l'Ouest, Magreb, plaque arabe, Turquie, Europe méridionale, voir carte page suivante) soumis à une glaciation d'envergure continentale à la fin de l'Ordovicien. Ces travaux s'inscrivent dans la suite des monographies régionales qui avaient fait progresser de manière significative nos connaissances sur ce système glaciaire (Beuf et al., 1971 ; Deynoux, 1980 ; Destombes et al., 1985 ; Massa, 1988 ; Vaslet, 1990). Avec la reprise de l'exploration pétrolière à la fin du 20ème siècle (Le Heron et Thusu, 2007), et l'intérêt croissant porté à tout ce qui touche à l'évolution des climats et de la biodiversité, l'étude de la période glaciaire (« icehouse mode ») de la fin de l'Ordovicien est devenue pluridisciplinaire associant à la sédimentologie la géologie pétrolière

(Davidson et al., 2000 ; Lüning et al., 2000 ; Le Heron et al., 2006, 2009), la paléontologie (Paris et al., 1995 ; Sheehan, 2001 ; Bourahrouh et al., 2004 ; Villas et al., 2006 ; Vecoli, 2008 ; Delabroye et Vecoli, 2010), l'études des signaux isotopiques (Saltzman et Young, 2005 ; Melchin et Holmden, 2006 ; Trotter et al., 2008 ; Ainsaar et al., 2010), et enfin les modèles (Armstrong et Coe, 1997 ; Brenchley et al., 2003 ; Achab et Paris, 2007 ; Page et al., 2007 ; Armstrong et al., 2009 ; Vandenbroucke et al., 2010) et simulations paléoclimatiques (Kump et al., 1999 ; Herrmann et al., 2004 ; Lefebvre et al., 2010).

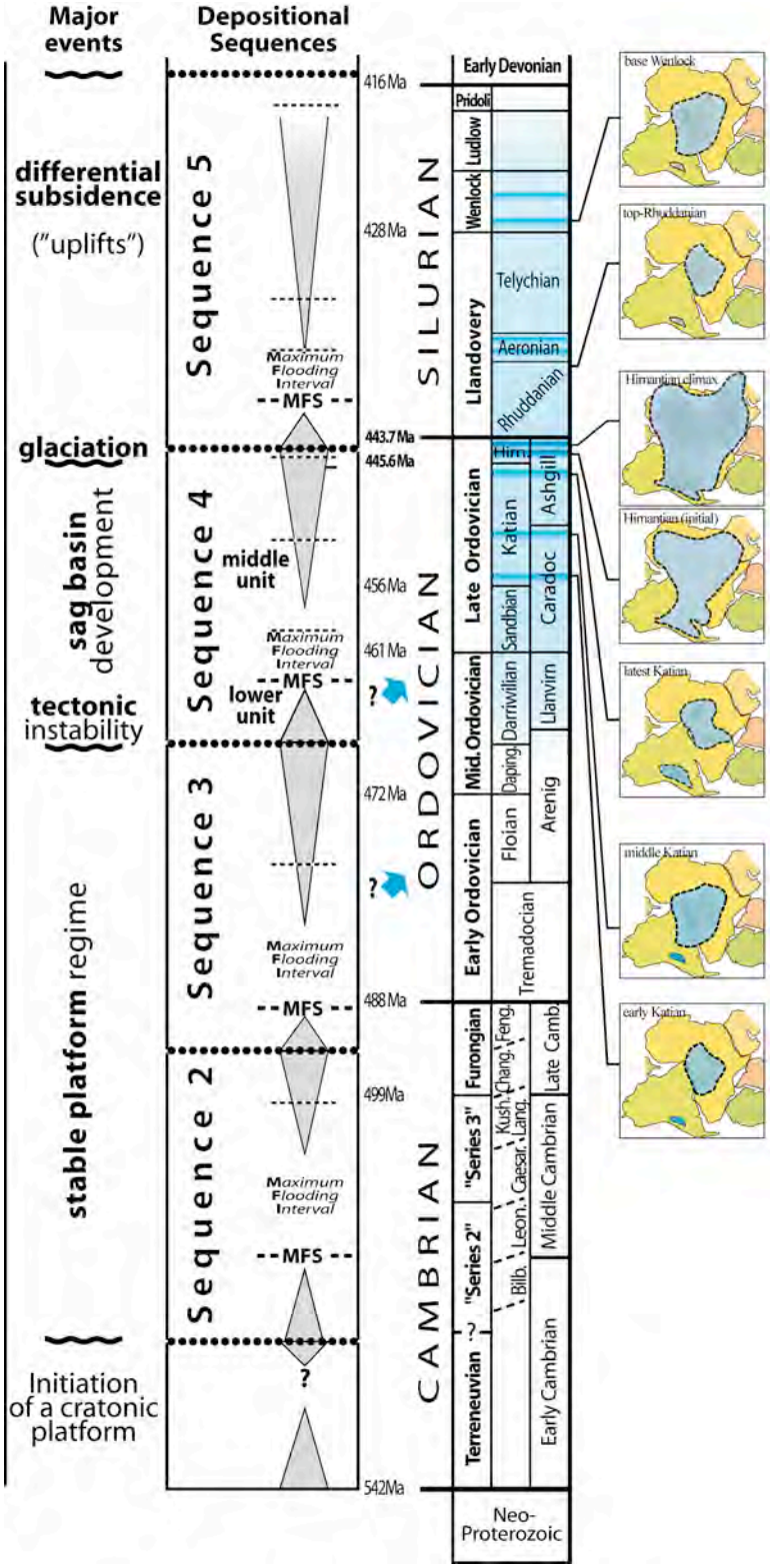

Charte stratigraphique pour la période Cambrien/ Ordovicien/ Silurien. La subdivision en séquences est déduite de l'analyse de la succession du Taurus (Turquie, Ghienne et al., 2010b, §1) mais elle est en grande partie extrapolable au domaine saharien (Ghienne et al., 2007a, §1).

L'initiation d'un mode climatique « icehouse » pourrait intervenir soit à la fin de l'Ordovicien moyen soit à l'Ordovicien inférieur (flèches bleues). Ce mode se termine dans le Silurien. Il s'étend donc sur une durée d'au moins 30 millions d'années. Une modulation climatique d'origine encore indéterminée (cycles de Milankovitch, séquestration du carbone organique… ?) est marquée par des phases de développement d'un ou plusieurs inlandsis (Loi et al., 2010, §2, lignes bleu foncé). Ce n'est que vers la fin de l'Ordovicien que les fronts glaciaires atteignent les bassins sédimentaires distribués autour du Gondwana. Ainsi, seuls les inlandsis de l'Hirnantien (maximum glaciaire) et peut-être celui de la fin du Katien, ont laissé un enregistrement sédimentaire glaciaire indubitable. Entre deux phases glaciaires, des hauts niveaux marins sont enregistrés, indiquant une couverture glaciaire très limitée. La permanence de cycles stratigraphiques à haute fréquence au cours de périodes interglaciaires suggère toutefois la persistance d'une calotte glaciaire au cœur du Gondwana. Phases glaciaires siluriennes d'après Lehnert et al., 2010).

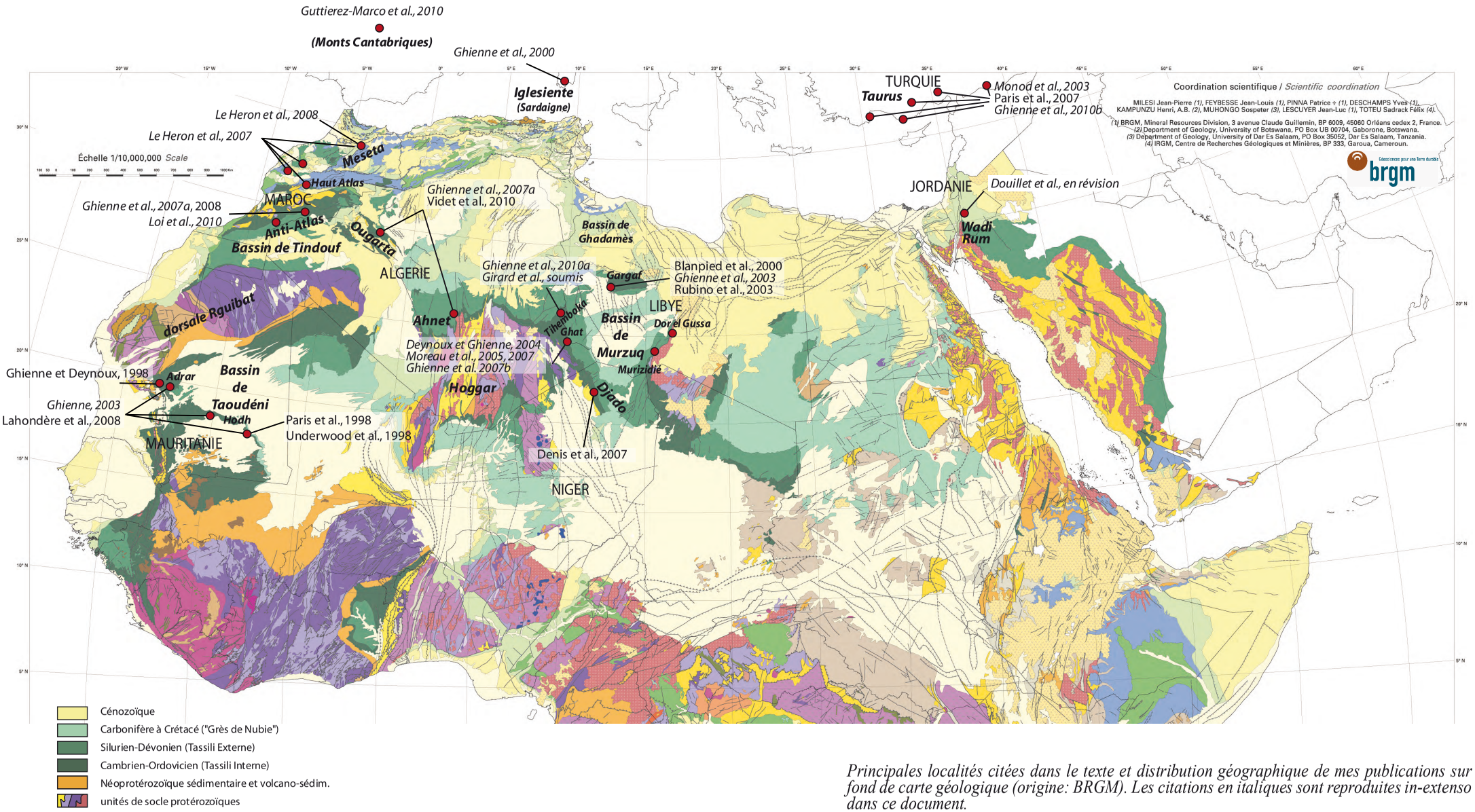

Principales localités citées dans le texte et distribution géographique de mes publications sur fond de carte géologique (origine: BRGM). Les citations en italiques sont reproduites in-extenso dans ce document.

Chapitre 1

1- La mise en place du décor: la plate-forme nord-gondwanienne

Le secteur du Wadi Rum (sud jordanien) illustre de manière spectaculaire la mise en place du décor nord-gondwanien. Sur un socle néoprotérozïque aplani (granites et dykes doléritiques), se dépose une épaisse série cambrienne (couleur ocre) à ordovicienne (Ordovicien inférieur à patine claire au toit des tours) essentiellement gréseuse. Si la sédimentation débute par des faciès continentaux (playas, arènes), des faciès marins bioturbés apparaissent dès la partie inférieure de la succession qui reste cependant dominée par des épandages de sables fluviatiles. Il faudra attendre la transgression de l'Ordovicien moyen (Darriwilian) pour qu'apparaissent des faciès marins francs à graptolites (Amireh et al., 2001). En Jordanie, les dépôts glaciaires — non visibles ici — reposent sur une couverture sédimentaire d'environ 1500 m d'épaisseur). Ils atteignent le socle autour du bouclier arabe à plus de 1000 km vers le sud. Les points blancs (véhicules 4x4) sur le sable à droite donnent l'échelle ; la dénivelée des affleurements dépasse 400 m.

Publications associées :

Ghienne J.-F., Boumendjel K., Paris F., Videt B., Racheboeuf P. and Ait Salem H. (2007a) The Cambrian-Ordovician succession in the Ougarta Range (western Algeria, North Africa) and interference of the Late Ordovician glaciation on the development of the Lower Palaeozoic transgression on northern Gondwana. Bulletin of Geosciences, 82(3), 183-214.

Ghienne J.-F., Monod, O., Kozlu, H., Dean, W.T. (2010b) Cambrian-Ordovician depositional sequences in the Middle East : a perspective from Turkey. Earth Science Reviews, 101, 101-146.

➔ Voir aussi :

Videt et al., 2010

Initialement axée sur l'enregistrement sédimentaire glaciaire, mon activité de recherche s'est plus récemment élargie aux successions préglaciaires d'âge cambro-ordovicien, c'est-à-dire précédant la glaciation fini-ordovicienne de plusieurs dizaines de millions d'années. En effet, une partie des problèmes posés par le « Glaciaire » ne peut être solutionnée que si l'évolution pré-glaciaire du domaine sédimentaire considéré est correctement appréhendée.

Bien connaître la dynamique d'un domaine sédimentaire particulier permet de mieux caractériser les changements qui lui sont imposés par la mise en route d'une glaciation. Il est également intéressant de pouvoir estimer l'ampleur d'une discordance de ravinement (érosion glaciaire ou surface d'émersion) à partir d'une succession stratigraphique. Des estimations relativement aisées sont possibles pour des paléovallées étroites, typiquement moins de 10 km, pour lesquelles les marges érosives, tronquant le substrat préglaciaire, sont bien individualisées (Ghienne et Deynoux, 1998 ; *Ghienne et al., 2003, §3)*. En revanche, dans le cas d'incisions régionales de largeur supérieure à 50 km, les marges de l'incision et sa géométrie d'ensemble ne sont généralement pas identifiables à l'affleurement, et difficilement repérables sur les lignes sismiques régionales. L'incision est alors à l'origine d'un hiatus stratigraphique dont l'amplitude ne peut être déterminée, sauf à supposer la parfaite géométrie tabulaire des strates de la succession préglaciaire sous-jacente. L'ampleur du hiatus stratigraphique est le résultat soit d'une érosion d'âge glaciaire, soit d'érosions d'âge préglaciaire et reprises par le contact basal glaciaire, soit de subsidences différentielles à l'échelle du bassin sédimentaire, soit enfin, d'une combinaison de ces trois situations.

L'analyse des successions préglaciaires a été menée en Mauritanie (Lahondère et al., 2008), en Algérie (*Ghienne et al., 2007b* ; Videt et al., 2010), en Libye, et en Turquie (*Ghienne et al., 2010b*). La Mauritanie permet de caractériser un domaine sédimentaire cratonique stable (Bassin de Taoudéni), relativement subsident au Cambrien, mais peu subsident à l'Ordovicien. Le chantier algérien a permis de reconstruire un profil de dépôt s'étendant sur environ 500 km de longueur, depuis l'Ahnet au sud en situation proximale, à l'Ougarta au nord avec extension jusqu'à l'Anti-Atlas marocain en situation distale, et continûment subsident sur toute la période considérée. En Libye, une série de discordances superposées a été caractérisée sur le revers oriental du Bassin de Murzuq, au droit d'un accident panafricain plusieurs fois ré-activé. En Turquie, une synthèse régionale a été proposée mettant en lumière des correspondances entre la stratigraphie du domaine stable (plaque Arabe) et celle de la plaque Turque. Les principaux résultats sont les suivants :

- Au droit des accidents de socle panafricain (en Ougarta, ancienne suture à l'est du Craton Ouest-Africain; en Libye, couloir de décrochement crustal), des déformations importantes mais localisées d'âge Ordovicien inférieur à Ordovicien moyen affectent la succession cambro-ordovicienne. Des soulèvements, qui se traduisent dans la stratigraphie par des surfaces d'érosion à l'échelle régionale, sont mis en évidence. Ailleurs, il s'agit de discordances angulaires, la surface d'érosion au toit du substratum basculé à plus de 20° étant scellée par l'Ordovicien moyen. En Turquie, le « Haut de Mardin », forme une vaste structure synclinale, érodée au cœur, et scellée par l'Ordovicien supérieur (Ghienne et al., 2010b, Fig. 5). L'apparition des boucliers (individualisation de la dorsale Rguibat, Mauritanie/ Algérie), ou de « pointements » de socle panafricain immédiatement sous la succession glaciaire (« horst » du Murizidié en Libye) est à mettre sur le compte de ses mouvements verticaux intra-Ordovicien. Si l'incision glaciaire vient à se surimposer à ces érosions antérieures, son ampleur peut être largement surestimée.

- En domaine stable, la discordance de ravinement glaciaire apparaît comme une discordance cartographique à l'échelle plurihectokilométrique. Dans le Bassin de Taoudéni en Mauritanie, elle atteint des horizons globalement de plus en plus anciens vers le S et l'E. Des épaisseurs de la succession glaciaire de même ordre de grandeur que les érosions, et des faciès siluriens sus-jacents peu profonds (ou passant très rapidement, en quelques mètres au-dessus de la limite d'action des vagues), suggèrent une ampleur de l'érosion glaciaire modérée, relativement uniforme à l'échelle du Bassin de Taoudéni, atteignant en moyenne quelques dizaines de mètres, hormis à l'axe des paléovallées. L'ampleur croissante vers le SE de la discordance de ravinement traduit moins des profondeurs croissantes d'érosion glaciaire qu'une diminution d'ensemble de l'épaisseur de la succession préglaciaire (non dépôt et/ ou érosions avant dépôt des faciès glaciaires), sans intervention d'une structuration tectonique préalable. Néanmoins, une discordance angulaire entre la succession glaciaire et son substratum est identifiée localement sur le pourtour du Bassin de Taoudéni, soit à l'échelle de l'affleurement au Tagant (Dia, 1969), soit à l'échelle cartographique au Zemmour (Deynoux, 1980). Ces discordances sont associées à la phase de déformation de l'Ordovicien moyen, qui, en dehors d'un signal à grande longueur d'onde, semble avoir épargné l'essentiel du domaine intracratonique que constitue le Bassin de Taoudéni.
- Les mouvements affectant la lithosphère à l'Ordovicien sont mis en relation avec les épisodes extensifs, ou plus probablement transtensifs, qui affectent la marge nord-gondwanienne depuis peut-être le Cambrien supérieur (*Ghienne et al., 2010b*). Ils aboutissent à une différentiation des aires de sédimentation sur la plate-forme avec l'individualisation de bassins (exemple Bassin de Prague) et de zones hautes, voire à la séparation de quelques blocs continentaux (Avalonia, Coks et Fortey, 2010 ; Hun superterrane de Stampfli et Borel, 2002) issu du bloc gondwanien et qui constitueront, avec ceux qui ne se détacheront plus tard au Dévonien, les noyaux des déformations varisques en Europe. Le plus souvent, un régime de subsidence succède à ces épisodes tectoniques dès l'Ordovicien supérieur. En domaine proximal, l'amortissement des différentiels de subsidence et des apports sédimentaires suffisent à lisser les topographies avant l'arrivée des glaciers. En domaine distal, la pérennisation de reliefs (épaules de rift ?) en association avec des apports sédimentaires déficitaires aboutissent à une plate-forme présentant sinon des reliefs émergés, au moins des topographies sous-marines (*Ghienne et al., 2000, §5*).
- En dépit d'une activité tectonique affectant essentiellement la marge continentale, la transgression cambro-ordovicienne conduit au premier ordre à l'ennoyage et au nivellement par les sédiments du domaine de plate-forme issu des collisions panafricaines néoprotérozoïques (Legrand, 1985 ; Fabre, 1988 ; Sharland et al., 2001 ; Fabre et Kazi-Tani, 2005 ; Eschard et al., 2005 ; *Ghienne et al., 2007a*, Fig. 10 ; *Ghienne et al., 2010b*, Fig. 4). Ce domaine sédimentaire subsident ne présentera pas de topographies héritées et les glaciers fini-ordoviciens pourront s'y étaler librement, circulant, sauf exception, au toit d'une pile sédimentaire ordovicienne, voire cambrienne pour ce qui concerne les domaines les plus proximaux ou ceux ayant été affectés par des réactivations localisées. Ainsi, les écoulements glaciaires, systématiquement orientés de manière centripète des hautes terres vers la marge continentale ne seront-ils pas confinés, au moins dans ce domaine nord-gondwanien, par des systèmes de rifts ou des zones orogéniques. A l'opposé de nombres d'inlandsis phanérozoïques (Eyles, 1993 ; 2008), celui de l'Ordovicien ne semble pas être physiquement en relation avec l'existence de rifts continentaux.

Enfin, l'analyse séquentielle de la succession Ordovicien supérieur dans son ensemble a permis de caractériser, par la mise en évidence de régressions forcées, l'existence d'épisodes glaciaires majeurs antérieurs à celui bien connu de l'extrême fin de l'Ordovicien (étage Hirnantien ; *Loi et al., 2010, §2*). Cet aspect est développé dans le chapitre suivant.

The Cambrian-Ordovician succession in the Ougarta Range (western Algeria, North Africa) and interference of the Late Ordovician glaciation on the development of the Lower Palaeozoic transgression on northern Gondwana

JEAN-FRANÇOIS GHIENNE, KHEIRA BOUMENDJEL, FLORENTIN PARIS, BLAISE VIDET, PATRICK RACHEBOEUF & HAMID AIT SALEM

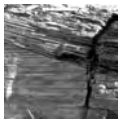

Depositional environments in the 1000–2000 m thick Cambrian-Ordovician succession range from inner-shelf siltstones to fluvial sandstones. Six transgressive-regressive (T-R), low-frequency (15–25 Ma) depositional sequences have been differentiated and correlated with both northern distal (Anti-Atlas, Morocco) and southern proximal (Ahnet, southern Algeria) areas. Sequence 1 ("Lower" Cambrian?) comprises fluvial deposits truncating volcanics and deformed Panafrican basement rocks. Marine strata appeared in Sequence 2 (lower and middle part of the "Middle" Cambrian) but fluvial conditions maintained to the South. Sequence 3 (upper "Middle" Cambrian) is erosionally truncated but further develops to the south, possibly comprising "Upper" Cambrian deposits. In Sequence 4 (Lower Ordovician), fluvial deposits are no longer present and inner-shelf siltstones reached southern Ougarta. Sequences 5 and 6, upper Lower-Middle Ordovician and Upper Ordovician, develop inner-shelf conditions throughout the study area at maximum flooding. Hirnantian glacial strata form a lowstand wedge in the upper part of the Sequence 6 regressive system tract. This succession designates a first-order transgression initiating in the Cambrian. It was temporarily perturbed just before its end by the Hirnantian glaciation. The related erosion led to a discontinuity, angular at basin scale, falsely suggesting a pre-glacial tectonic event. The post-glacial transgression, very fast relative to the Cambrian-Ordovician tempo, resulted in a drastic backstepping of the shorelines that shifted drastically to the south in the early Silurian. After deglaciation, the first-order inversion trend occurred between retrograding strata of the Cambrian-Ordovician succession and the prograding Siluro-Devonian wedge. This event marks in North Africa the maximum flooding of the Lower Palaeozoic megasequence. • Key words: Cambrian, Ordovician, North Gondwana, transgression, glaciation, sequence stratigraphy.

GHIENNE, J.-F., BOUMENDJEL, K., PARIS, F., VIDET, B., RACHEBOEUF, P. & SALEM, H.A. 2007. The Cambrian-Ordovician succession in the Ougarta Range (western Algeria, North Africa) and interference of the Late Ordovician glaciation on the development of the Lower Palaeozoic transgression on northern Gondwana. *Bulletin of Geosciences 82(3)*, 183–214 (14 figures). Czech Geological Survey, Prague. ISSN 1214-1119. Manuscript received June 25, 2007; accepted in revised form September 13, 2007; issued September 30, 2007. • DOI 10.3140/bull.geosci.2007.03.183

Jean-François Ghienne, Université Pasteur, CNRS, UMR 7517 Centre de Géochimie de la Surface, Ecole et Observatoire des Sciences de la Terre, 1 rue Blessig, 67084 Strasbourg Cedex, France; JeanFrancois.Ghienne@eost.u-strasbg.fr • Kheira Boumendjel, SONATRACH, Centre de Recherche et Développement, Av. du 1er novembre, 35000 Boumerdès, Algeria • Florentin Paris, Géosciences-Rennes, UMR 6118 du CNRS, Université de Rennes 1, 35042 Rennes-cedex, France; florentin.paris@univ-rennes1.fr • Blaise Videt, the same address as the previous author • Patrick Racheboeuf, UMR 6538 du CNRS, Université de Bretagne Occidentale, 29385 Brest-cedex, France • Hamid Ait Salem, SONATRACH, Centre de Recherche et Développement, Av. du 1er novembre, 35000 Boumerdès, Algeria

Stratigraphy aims to subdivide sedimentary successions into correlatable units corresponding ideally to time slices controlled by biostratigraphy. An extensive and thick sedimentary cover has been noted above the Proterozoic basement in the Sahara (Legrand 1985, Fabre 2005, Fabre & Kazi-Tani 2005), which extends to the east on the Arabian Plate (*e.g.*, Sharland *et al.* 2001). The first and still useful stratigraphical subdivision was made by Kilian (1922) who proposed to differentiate three units, from base to top: the Internal Tassili, later known as the Cambrian-Ordovician sandstones (*e.g.*, Fabre 1988); the intra-Tassilian trough or depression characterised by the graptolitic Silurian shales; the External Tassili, comprising the upper Silurian and Devonian shales and sandstones. This study concentrates on

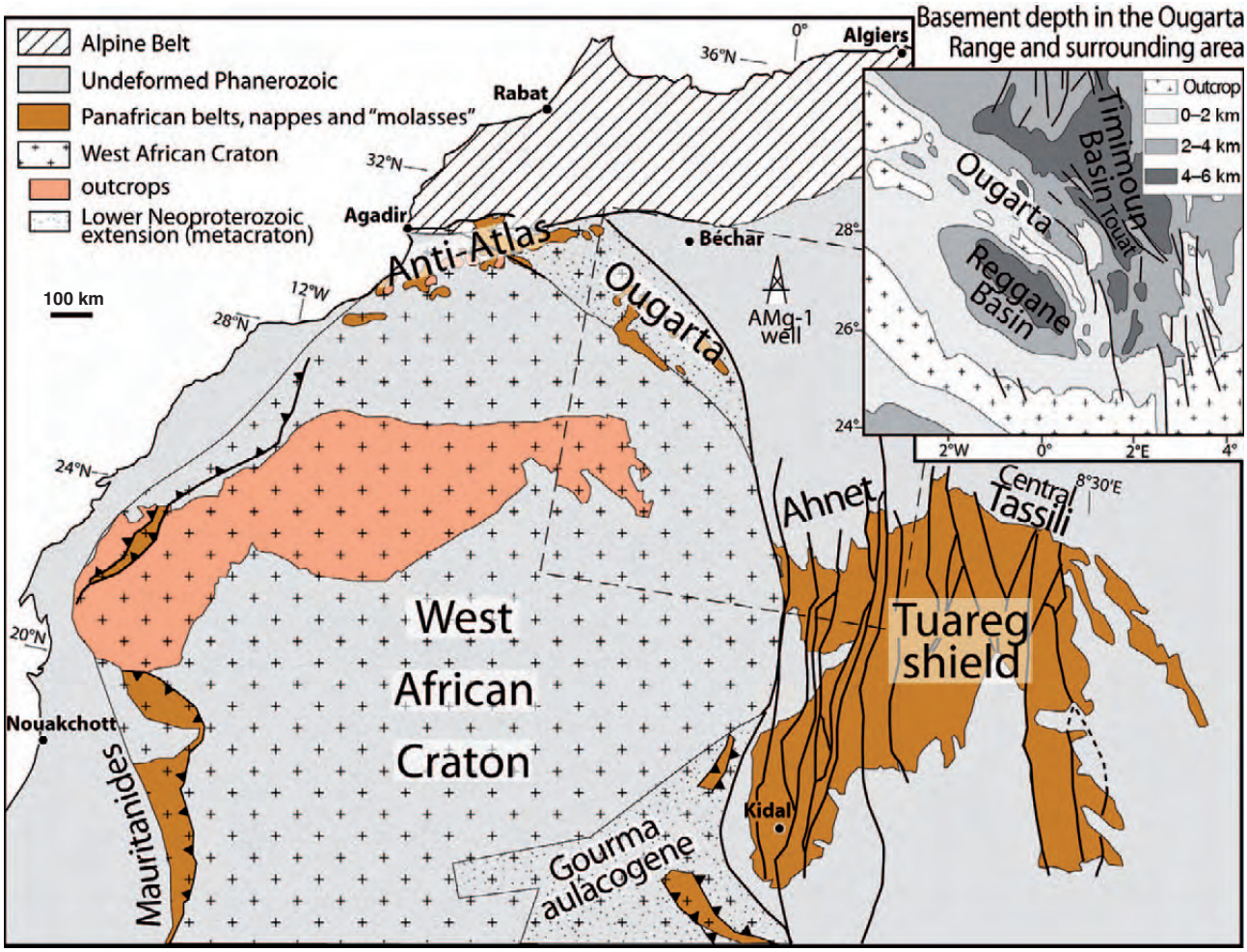

Figure 1. Map of northwestern Africa and location of the Ougarta Range on the northeastern margin of the West African Craton (modified from Ennih & Liégeois 2001). Basement depths around the Ougarta from Takherist (1990).

the Internal Tassili unit (Cambrian and Ordovician) typified by huge outcrops of quartz-rich sandstones that probably represent the most voluminous siliciclastic sequence ever deposited on continental crust (Burke & Kraus 2000, Avigad *et al.* 2005). Geological mapping and extensive work by petroleum geologists in parallel with the discovery of new faunas allowed the Cambrian and Ordovician succession to be further subdivided into four stratigraphic units (*e.g.*, units I to IV in Beuf *et al.* 1971), comprising a number of formations and members (Legrand 1974, 1985). The fourth unit corresponds to the latest Ordovician (Hirnantian), glacially related succession.

Cambrian and Ordovician strata constitute the lower part of the first-order Lower Gondwana Cycle (Cambrian to Middle Devonian) of Boote *et al.* (1998) and essentially correspond to the second Arabian Plate tectono-stratigraphic megasequence of Sharland *et al.* (2001). These strata were dominated over North Gondwana by fluvial to inner-shelf deposits. Correlative biostratigraphic data are relatively sparse with two exceptions: (1) the Anti-Atlas (southern Morocco, *e.g.*, Destombes *et al.* 1985, Elaouad-Debbaj 1988, Gutiérrez-Marco *et al.* 2003, Bourahrouh *et al.* 2004) and the Ougarta Range (western Algeria, *e.g.*, Fekirine & Abdallah 1998, Fabre & Kazi-Tani 2005), two areas that displayed abundant macrofaunas; (2) palynomorphs (chitinozoans, acritarchs) mainly from drill cores in sedimentary basins (Taugourdeau & de Jekhowsky 1960, Oulebsir & Paris 1995, Vecoli 1999, Vecoli & Le Hérissé 2004, Paris *et al.* 2007 and references therein). Correlation of these fossil-bearing strata with barren fluvial (or tidal) sandstones in more proximal, southern parts of the platform is still debated even though it is of prime importance in the understanding of the development of Palaeozoic sedimentary basins on the North African cratonic platform.

Therefore, this paper aims firstly to provide a basic sequence stratigraphic framework for the Cambrian-Ordovician succession of the Ougarta Range. Based on outcrop data, a profile nearly parallel to the proximal-to-distal vector will be examined, with in addition correlations pro-

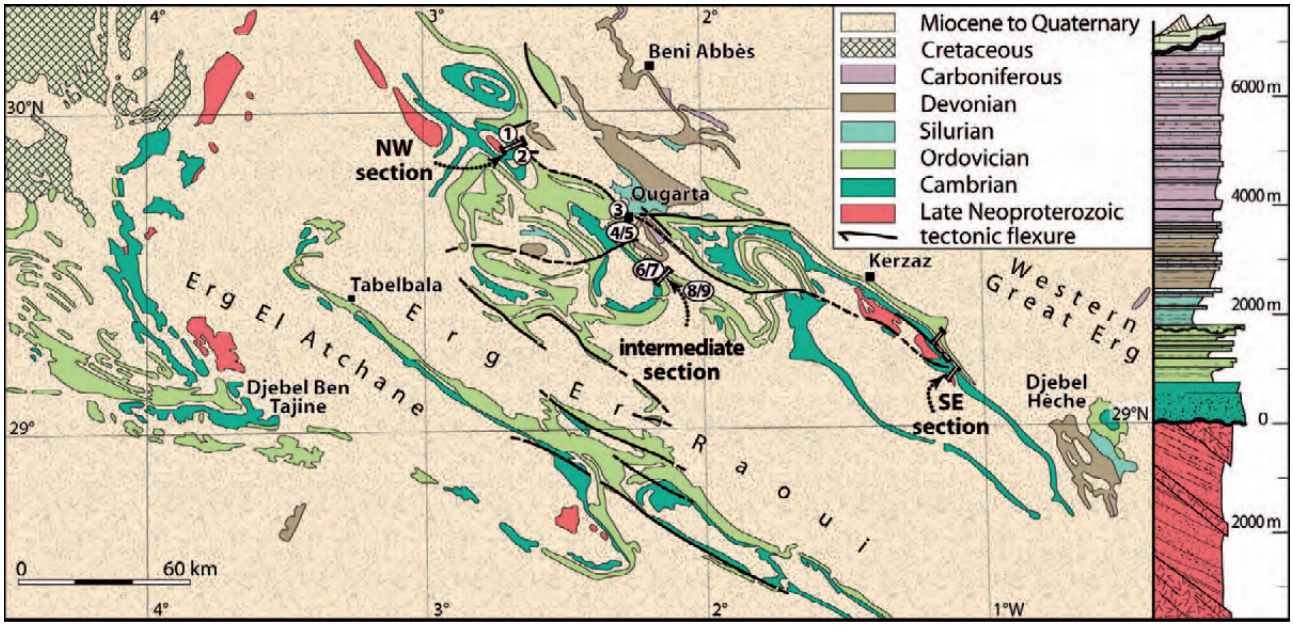

Figure 2. Geological sketch map of the Ougarta Range and synthetic log of the sedimentary succession. The three (NW, intermediate, SE) sections refer to logs in Fig. 4. Numbers (1–9) refer to logs illustrating the Late Ordovician glacial record in Fig. 6.

posed with the Anti-Atlas northward and the Ahnet area southward (*ca* 900 km from SE to NW, Fig. 1). A number of stratigraphic sequences will be illustrated and a depositional model comprising relationships in time and space from fluvial to inner-shelf deposits will be proposed in the context of the North African cratonic platform. Then, the progressive backstepping of the depositional edge upon the cratonic platform and the signature of intracratonic deformation will be discussed. Finally, the impact of the Late Ordovician glaciation on this otherwise well-organised succession will be examined.

Geological setting

During the Lower Palaeozoic, North Africa was part of a regionally continuous clastic-dominated North Gondwana platform. Fluvial successions in the SSE graded towards the NNW in storm-to-tide dominated successions. Multiphased Palaeozoic to Mesozoic tectonic uplifts have differentiated several intracratonic basins, the present geometry of which bears little relation to the much broader North Gondwana platform that had an off-shelf gradient towards the NNW during the whole of the Early Palaeozoic (Beuf *et al.* 1971, Boote *et al.* 1998, Carr 2002).

The Ougarta Range is one of these uplifts (Fig. 1), bounded by the Reggane Bassin to the West and the Timimoun Basin to the East (Takherist 1990). It corresponds to a folded domain, 120–180 km in width that trends NW-SE (Fig. 2). Here, thick Lower and Middle Palaeozoic strata overlying Neoproterozoic rocks have been deformed in response to the Variscan compressional event. Thick-skin (Donzeau 1971, 1983) *vs* thin-skin (Hervouet & Duee 1996) deformation models have been proposed. This domain, which links the Pan-African NW Hoggar towards the South (Fabre *et al.* 1988), to the Anti-Atlas towards the North (Burkhard *et al.* 2006; Fig. 1), acted repeatedly as an axis of preferential subsidence on the North Gondwana platform during the Lower Palaeozoic, as evidenced for instance by: (i) the preservation of a "Lower" Cambrian succession correlated with the Adoudounian strata of the Anti-Atlas (Destombes *et al.* 1985; Fabre 1988, 2005); (ii) an Early Ordovician flooding, resulting in the deposition of graptolite-bearing marine shales delineating an embayment corresponding broadly to the Ougarta domain outlines (Legrand 1985); (iii) an Ordovician to Devonian depocentre (Fabre & Kazi-Tani 2005). Donzeau (1974, 1983) interpreted the Ougarta as an aulacogene structure trending perpendicular to the North Gondwana margin.

It has been proposed recently that the Ougarta Range developed onto the northeastern margin of the West African Craton (Ennih & Liégeois 2001; Fig. 1). Here, the latest Neoproterozoic post-collisional development of transpressive and then progressively transtensive basins has resulted in first-order, metacratonic, crustal-scale structures. It is proposed that the Lower Palaeozoic depocentre developed on this relatively weaker domain, now integrated to the stable North Gondwana Platform. It has experienced structural inversion during the Variscan event, resulting likely in a thick-skinned uplift of the palaeo-margin of the West African Craton, as documented for instance

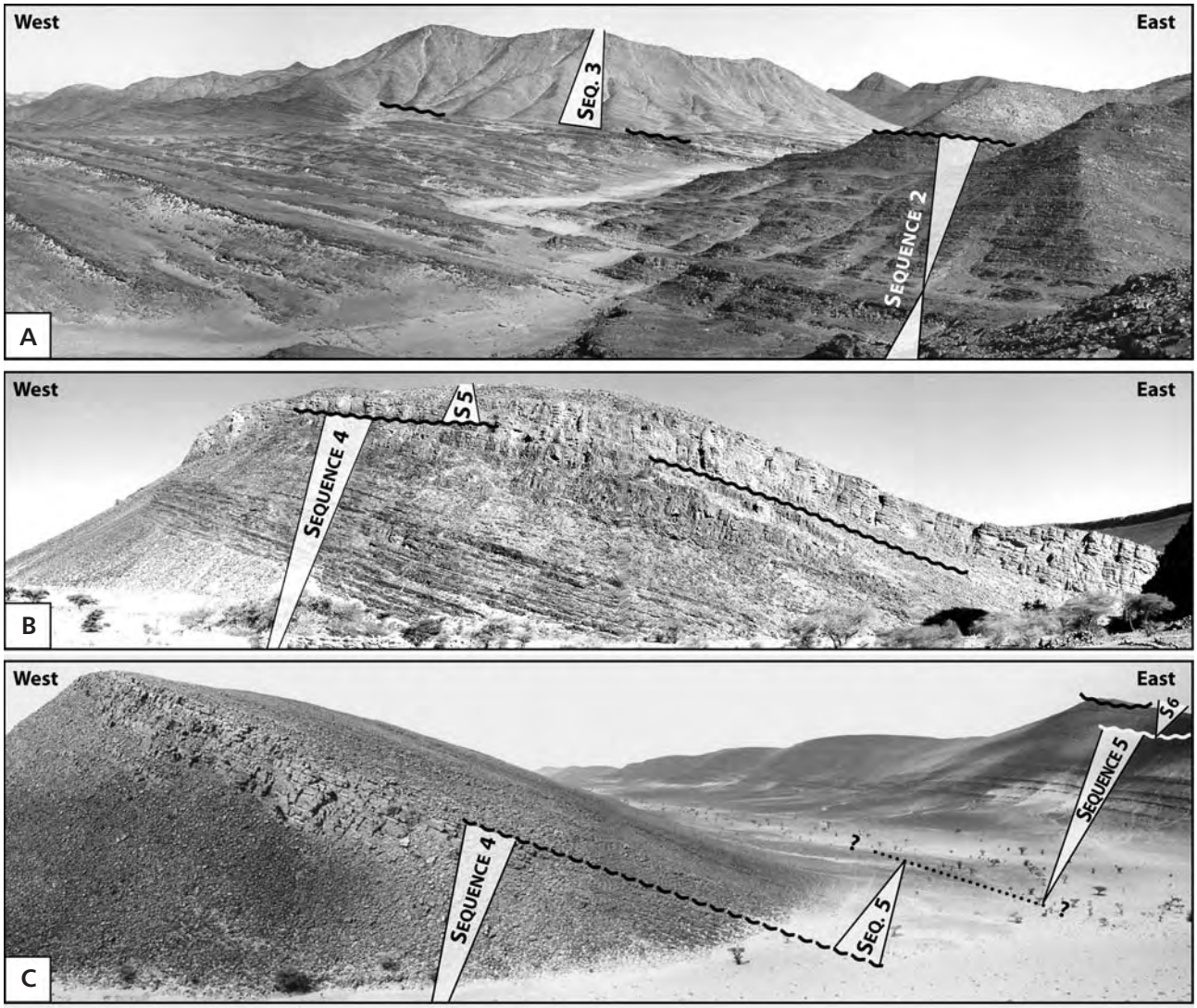

Figure 3 (first part). Exposures in the Ougarta Range. • A – Cambrian strata to the north of the Sebket el Melah (SE section). • B – Lower Ordovician strata in the Kheneg el Aatène (intermediate section). • C – Lower and Upper Ordovician strata in the Kheneg et Tlaïa (NW section).

in the adjacent Anti-Atlas (Donzeau 1974, Faik *et al.* 2001, Burkhard *et al.* 2006).

The Cambrian-Ordovician succession in the Ougarta Range

Pioneering works of Menchikoff (1933), Poueyto (1952), Arbey (1962) and Gomez Silva *et al.* (1963) proposed the lithostratigraphic nomenclature that is still currently used (Legrand 1985, Fekirine & Abdallah 1998; Figs 3, 4). The definition of lithostratigraphic units was based on both lithologies and observed bounding discontinuities.

Three sections, representative of the Cambrian-Ordovician succession in the Ougarta Range, have been logged (Figs 2–4). Two of them represent the depositional record at the extremities of a 150 km-long profile, which is oriented from the SE to the NW, *i.e.* in a direction roughly parallel to the palaeocurrent trend recognised both locally in braided fluvial deposits (dips of cross-strata) and regionally (Beuf *et al.* 1971). The SE sections (Sebkhet el Mellah and Foum Zeïdiya, Figs 3A, 4C) illustrates proximal depositional environments, whereas the NW section (Kheneg et Tlaïa, Figs 3C–E, 4A), located 150 km basinward, corresponds to a notably more distal area. In addition, the NW section also represents the sedimentary record of an almost continuously subsiding area characterised by the minor development of erosion surfaces and the development of an exceptionally thick Cambrian-Ordovician sequence. Conversely, the SE section illustrates a depositional record including well defined erosion surfaces. It is then also transitional with areas recognized to the South of the Ougarta

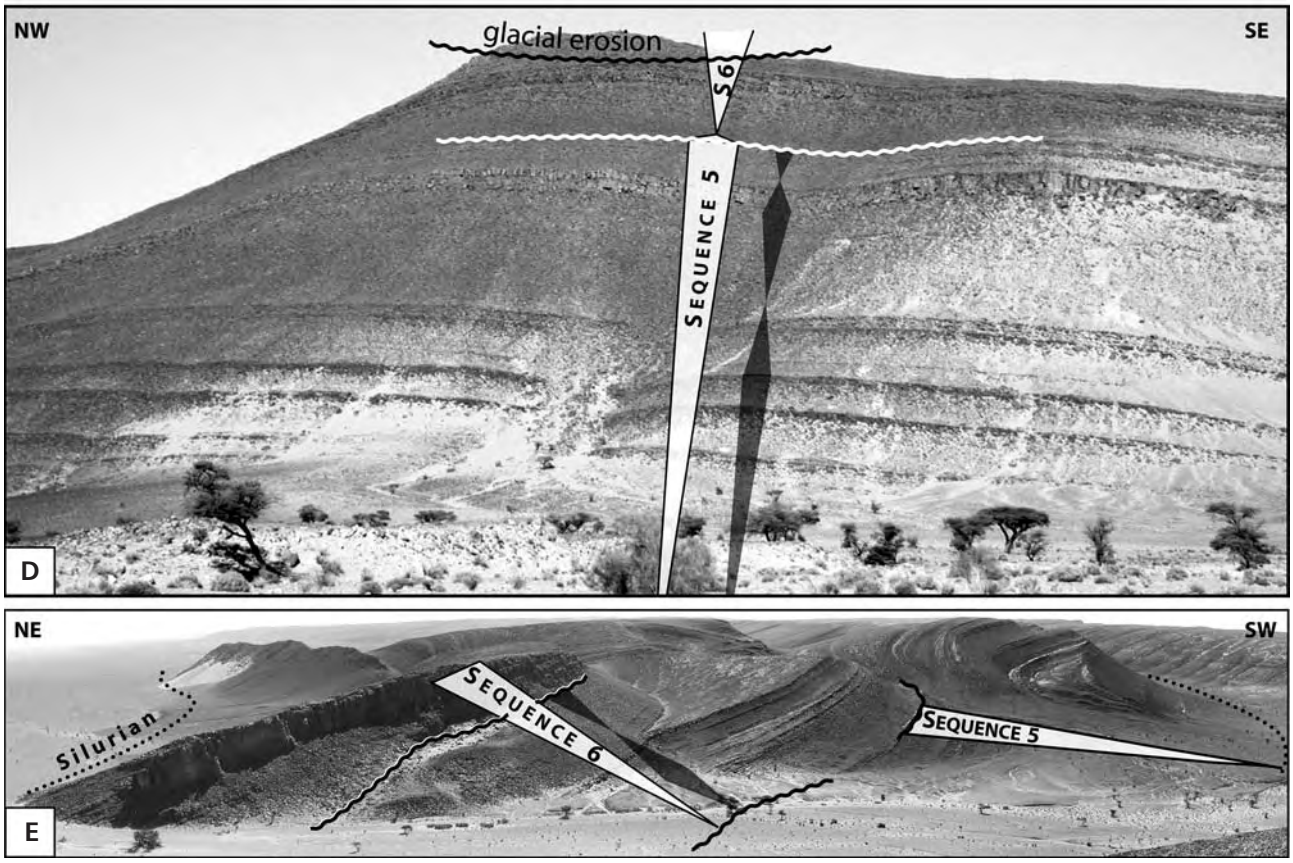

Figure 3 (second part). Exposures in the Ougarta Range. • D, E – Upper Ordovician strata in the Kheneg et Tlaïa (NW section).

where repeatedly uplifted blocks resulted in reduced Cambrian-Ordovician sections (*e.g.*, Djebel Hèche, Legrand 1985). An additional intermediate section shows facies and thickness changes for the Ordovician (Kheneg el Aatène, Figs 3B, 4B).

Pre-glacial depositional facies

The Cambrian-Ordovician strata in the Ougarta Range show a great variety in facies associations from fluvial coarse-grained sandstones to offshore fines, which are representative of the depositional environments on the North Gondwana Platform (*e.g.*, Beuf *et al.* 1971, Eschard *et al.* 2005). Seven depositional environments are basically recognized in the pre-glacial strata: braided fluvial, bioturbated sand-flat, mixed tidal and upper shoreface, upper shoreface, tidal ridges, storm-dominated shoreface and storm-dominated inner shelf deposits. Glacially related depositional environments, uppermost Ordovician in age, are described independently in a separate section.

Fluvial facies association. – The most common fluvial facies constitutes the main part of the Sebkhet el Mellah Fm. and is incidentally present in the Aïn Néchéa Fm. It is made up of coarse to very coarse arkoses or arkosic sandstones, comprising essentially 0.3–1 m thick, high-angle trough or planar cross-laminated bedsets (Fig. 5A). Sandstones are moderately sorted, with the exception of those underlining large-scale fining-upward successions that contain granules to gravels (NW section, 0–10 m; SE section, 420 and 505 m). Rip-up clasts are common; overturned beds rare. Cross-strata consistently dip towards the NW or NNW. Several metres-thick units are identified, some of them punctuated by thin (0.2–1 m thick) *Skolithos*-bearing sandstone beds. The latter horizons are typically better sorted, more indurated (less arkosic?), contain more rip-up clasts and show reactivation surfaces in well defined trough cross-strata.

The bulk of this association has a fluvial origin as supported by texture and sedimentary structures. The absence of both overbank deposits and channel structures suggests amalgamated braided-fluvial channel deposits, with very large width/depth channel ratios as known in a number of pre-vegetation braidplains (MacNaughton *et al.* 1997, Long 2004). In the Cambrian setting, intervening bioturbated and more mature horizons indicate episodic shallow-marine conditions, most probably corresponding to

tidal influences during high frequency transgressive events.

Subordinate coastal plain and estuarine environments have also been identified (NW section (390–410 m and 655 m). Very fine-grained, argillaceous and micaceous sandstones interfinger with dm-thick, cross-laminated, bioturbated (mainly *Skolithos*) sandstone beds with occasional liquefaction structures (overturned cross-strata, flame structures; Fig. 5B). An estuarine or coastal-plain environment with concomitant fluvial and marine influences is proposed for those deposits. At the 390 m level, they are characteristically underlain by braided fluvial sandstones and overlain by a sharp based, m-thick, cross-stratified bed deposited in an upper shoreface environment (wave ripples, large *Diplocraterion*).

Bioturbated sand-flat facies association. – Sand-flat deposits occur in thick, rather monotonous sandstone successions in the Aïn Néchéa Fm., specially in the SE section (540–580 m, 610–700 m) as well as in the Kheneg el Aatène Fm. in the intermediate section (330–380 m). In places, they are intensively bioturbated by *Skolithos* (5–100 cm in length) that may fully obliterate primary sedimentary structures ("piperocks"). The latter facies develop largely to the south, *e.g.*, in the Ahnet area (Banquette unit, see below). In the less bioturbated sandstones, low angle to sigmoidal trough cross-laminated bedsets with reactivation surfaces are preserved (Fig. 5C). Well defined cyclic successions, 3–5 in thickness, may develop in places. Thickening upward cross-laminated bed sets, which are progressively more and more bioturbated upwards (*Skolithos*, occasional *Rusophycus*), are truncated by a horizontally to subhorizontally laminated sandstone bed the top of which is burrowed by large *Diplocraterion.*

The texture, sedimentary structures and bioturbations indicate high-energy nearshore environments. Though most of the *Skolithos*-generated piperock are classically attributed to storm-dominated nearshores, tidal influences are suggested by frequent tidally-bundled, migrating bedforms (Nio & Yang 1991). The possibility that *Skolithos* burrows formed into previously deposited fluvial deposits or in mouth-bar sands cannot be rule out, at least locally. Sandstone beds with horizontal lamination and sparse *Diplocraterion* reflect episodic higher energy conditions and preservation of subordinate storm-related deposits. The bioturbated sand-flat facies reflects environments located between the shoreline and shoaling areas beyond which sedimentation was storm dominated.

Mixed tidal and shoreface facies association. – Mixed tidal and shoreface deposits are recognised in the Aïn Néchéa Fm. in the NW section, in the upper Foum Zeïdiya Fm. in the three sections (*e.g.*, 1620, 1700, 1790 m) and subordinate occurrences are present in the Bou M'haoud Fm. Those deposits form 0.5–10 m thick sandstone units that constitute the upper part of coarsening- and thickening-upward succession. In places, a poorly developed (< 1 m), thinning-upward trend is observed on top of it. Deposits are dominated by medium-grained, 0.2–1 m thick sandstone bed, either amalgamated or with intervening siltstones. They show a variety of primary sedimentary structures: isolated HCS and SCS beds; 0.2–0.5 m thick, low-angle tangential to sigmoidal, cross-laminated bed sets grading downward in bioturbated bottomsets and including reactivation surfaces underlain by a thin (< 2 mm) intercalation of fines or abundant 1–3 cm long rip-up clasts; low-angle to horizontally laminated sandstone beds; wave ripples with straight or polygonal crests; two-dimensional to linguloid current ripples. Those facies are moderately bioturbated, with *Skolithos* as the most common structures. *Daedalus* structures are relatively abundant in places in the Foum Zeïdiya Fm. (Lessertisseur 1971). Thin-bedded sandstones with pervasive mottling concealing primary sedimentary structures locally form < 1 m thick intervals. Thinning-upward beds in the topmost part of mixed tidal and shoreface successions are typified by small-scale HCS beds, wave ripples and may contain shell beds mainly made up of disarticulated to fragmented linguliformean brachiopods.

The facies interpretation is based on both the sedimentary structures and the stratigraphic position of these deposits. HCS-bearing facies represent open-marine environments. Sand waves, common *Skolithos* and *Daedalus* structures point to high-energy tidal-dominated environments, whereas fully bioturbated facies suggest low-energy restricted-marine environments. The association of open-marine, tidal-dominated and restricted-marine deposits through high-frequency cycles evidenced by the potential preservation of fine-grained sediments is interpreted as the amalgamation of sands deposited on both side of a shoaling area with minor preservation of upper shoreface deposits due to marine erosion. They represent transgressive facies, as supported by the stratigraphic occurrence of the mixed tidal and shoreface facies association on top of underlying storm-dominated facies and below overlying thinning-upward sandstones grading to inner shelf facies.

Figure 4. Sedimentary logs of the NW, intermediate and SE sections. Macrofauna relates to samples collected in February 2005. Location of section in Fig. 2.

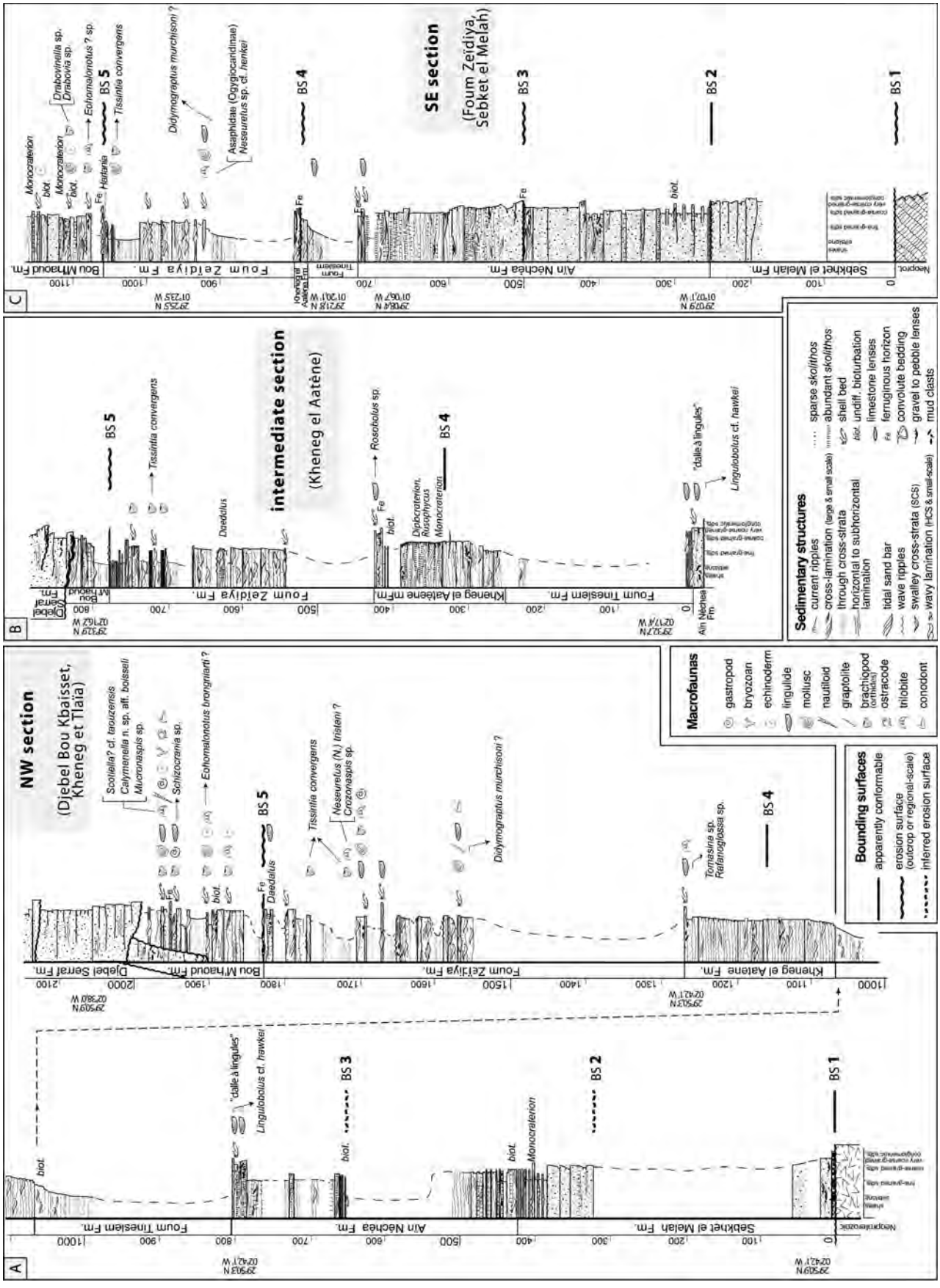
A
NW section
(Djebel Bou Kbaïsset, Kheneg et Tlaïa)
B
intermediate section
(Kheneg el Aatène)
C
SE section
(Foum Zeïdiya, Sebket el Melah)
Sebkhet el Melah Fm.
Aïn Nechéa Fm.
Foum Tinesiem Fm.
Foum Zeïdiya Fm.
Bou M'haoud Fm.
Djebel Serraf Fm.
Khéneg el Aatène Fm.
BS 1
BS 2
BS 3
BS 4
BS 5
Macrofaunas
gastropod
bryozoan
echinoderm
linguliide
mollusc
nautiloid
graptolite
brachiopod (orthida)
ostracode
trilobite
conodont
Bounding surfaces
apparently conformable
erosion surface (outcrop or regional-scale)
inferred erosion surface
Sedimentary structures
current ripples
cross-lamination (large & small scale)
through cross-strata
horizontal to subhorizontal lamination
tidal sand bar
wave ripples
swalley cross-strata (SCS)
wavy lamination (HCS & small-scale)
sparse skolithos
abundant skolithos
shell bed
undiff. bioturbation
limestone lenses
ferruginous horizon
convolute bedding
gravel to pebble lenses
mud clasts

Upper shoreface facies association. – Whereas thin upper shoreface deposits have already been reported within the bioturbated sand-flat facies association, an additional facies association is proposed here to describe fine-, medium- or coarse-grained sandstones that constitute 30 m-thick intervals within in the middle part of the Kheneg el Aatène Fm. in the NW (1170–1200 m) and intermediate (300–325 m) sections. They comprise amalgamated, m-thick, sandstone beds within which horizontal to low-angle laminations prevail. Those laminations locally show 1–4 cm thick, quartz-rich laminae, separated by black, < 1 mm thick horizons (Fig. 5D). Very coarse-grained lenses and lags of cm-long rip-up clasts have been observed. Isolated, erosion based, cross-bedded sandstone beds are also present, the topmost part of which comprises horizontal laminae truncating the underlying oblique laminae.

The predominance of horizontal to low-angle laminations, in association with thick laminae related to swash processes in the surf zone, the virtual absence of bioturbation and coarse-grained facies suggest a high-energy, most probably non-barred, upper shoreface environment. Cross-bedded sandstones were deposited in relation with longshore or wave-generated cross-shore currents (Clifton 1976).

Storm-dominated shoreface facies associations. – Two types of storm-dominated shoreface sandstones have been identified, an amalgamated and a non-amalgamated type. Amalgamated shoreface sandstones are present in the three sections within the lower part of the Kheneg el Aatène Fm. (NW section, 1060–1010 m) and in the upper part of the Foum Zeïdiya Fm. (1550–1575, 1600–1630 m). Here, the facies association that rest above conspicuous thickening-upward motifs comprising the innershelf facies association, is mainly made up of sorted fine to medium-grained sandstones. It is typified by large-scale, amalgamated HCS, micaceous sandstone beds, 0.4–0.8 m in thickness. Undulating laminae are ~2 m and locally up to 4 m in wavelength, 0.2–0.5 m in amplitude. The degree of amalgamation generally increases upwards where HCS beds grade in SCS beds. Bioturbation is virtually absent. Ovoidal, shell-rich limy concretions are frequent. These features, 1–2 m × 0.3–0.6 m, bear siltstone clasts and disarticulated faunas such as linguliformean brachiopods and occasional trilobites, bivalves, gastropods and graptolites.

Non-amalgamated shoreface sandstones have been identified in the uppermost Aïn Néchéa Fm. in the intermediate (0–10 m) and SE (720 m) sections, in the uppermost Kheneg el Aatène Fm. in the SE section (800 m) and in the Bou M'haoud Fm. in the NW section (> 1920 m). HCS beds, 0.2–0.5 m thick, with occasional wave ripples on top, are separated by siltstone interbeds. They form several metres-thick thinning upward successions. They are locally associated with low-angle laminated coarse-grained sandstones, conglomeratic lenses, or shell beds generally characterised by disarticulated to fragmented lingulids (uppermost Aïn Néchéa Fm.) or fragmented echinoderms (Bou M'haoud Fm.). In the NW section (1940 m), fossil-bearing lenses contain in addition trilobites, brachiopods, bryozoans, ostracodes, chitinozoans and scarce conodonts (Fig. 4).

The predominance of HCS in these sandstones definitely points to shoreface-dominated facies associations (Harms *et al.* 1982, Brenchley *et al.* 1986). The size of the HCS in both the amalgamated and non-amalgamated shoreface sandstones reflects high-energy storm-dominated environments, with preservation in respectively amalgamated low accommodation and high accommodation conditions. The former were deposited within long-term coarsening-upward (regressive) trends whereas the latter exhibit fining-upward (transgressive) trends. High accommodation allows wave ripples and fines to be preserved, while low accommodation results in amalgamation of event beds. SCS beds are here interpreted as the result of increasing amalgamation rates resulting in the systematic truncation of hummocks in shallower environments (Dumas & Arnott 2006). Ovoidal, shell-rich concretions most probably represent the infill by rip currents of storm-generated large-scale gutter casts. Early cementation that results in their pre-compaction ovoidal morphology, was favoured by the dissolution of the carbonate-rich shelly fauna.

Inner-shelf facies association. – The inner-shelf facies association forms thin (< 5 m) to thick (up to 250 m) successions that are generally poorly exposed. It comprises the whole of the Foum Tineslem Fm. and the lower part of the Foum Zeïdiya Fm. in the three sections. It has been identified in the Aïn Néchéa Fm. only in the topmost part of the soft talus in the NW section (640 m). This association comprises silty shales, micaceous siltstones and heterolithic facies. Heterolithic facies are fine-grained sandstone beds interstratified with siltstone interbeds. Silty shales and siltstones with rare sandstone beds typify lower and middle parts of inner-shelf succession. In the upper part of the thick inner-shelf successions a conspicuous coarsening- and thickening-upwards trend can be observed with the superimposition of successive 2–4 m thick, coarsening- and thickening-upwards smaller-scale successions. Sandstones initially appear within siltstones as flaser bedding, grading upwards in 1–4 cm thick rippled sandstone wavy beds with persistent orientations in cross-strata dips, followed by the development of 5–20 cm thick HCS beds, firstly lenticular and isolated with occasional wave reworking on top, then tabular and progressively amalgamated. Bioturbation is poorly expressed. Isolated lenticular shell beds with disarticulated brachiopods and scarce trilobites occur in places.

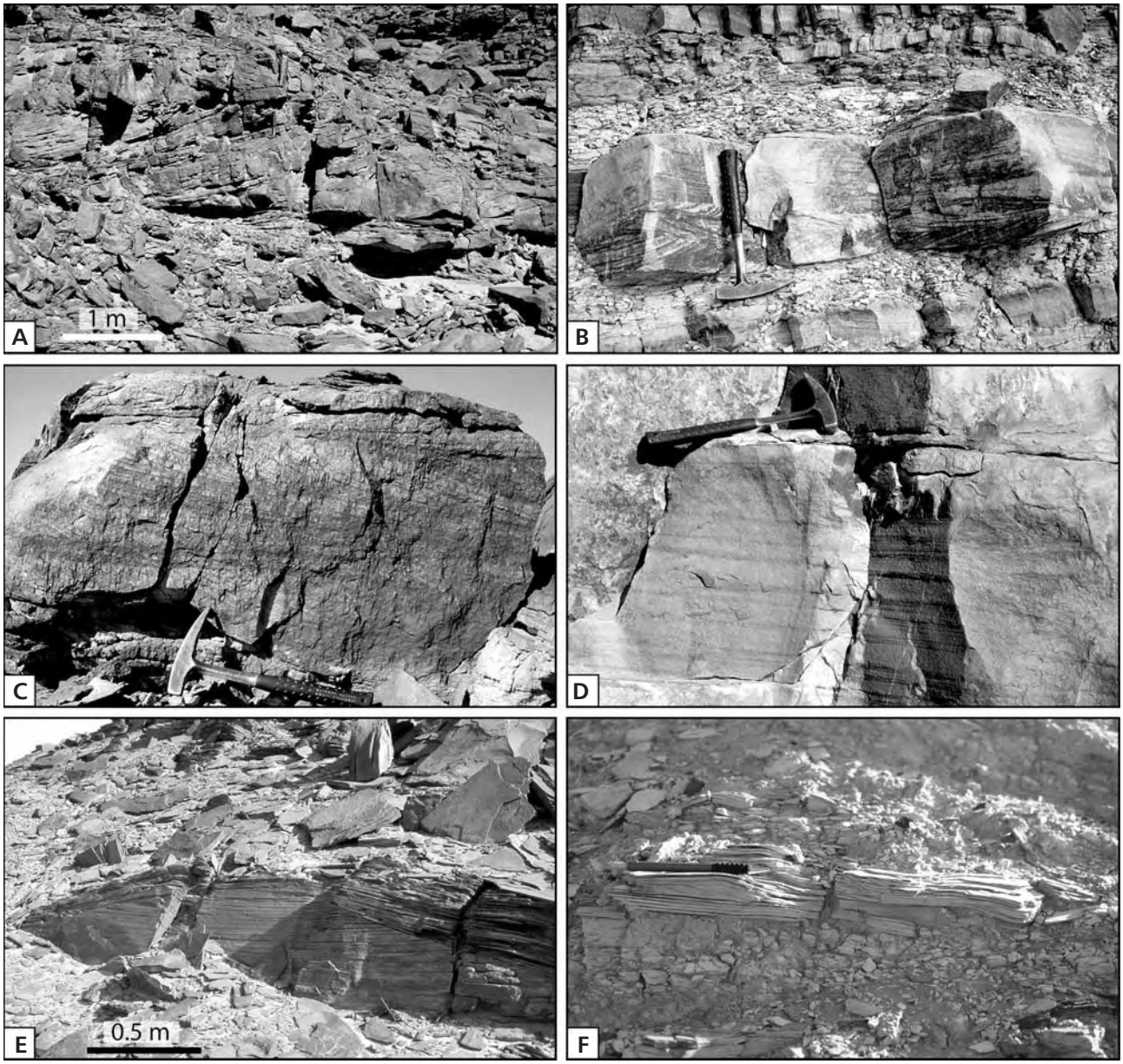

Figure 5. Sedimentary facies in the Cambrian-Ordovician succession of the Ougarta Range. • A – coarse-grained, cross-bedded sandstones (fluvial facies association; SE section, 450 m). • B – alternating argillaceous fine-grained sandstones and cross-bedded, bioturbated sandstone beds reflecting coastal plain to estuarine conditions (NW section, 655 m). • C – cross-bedded sandstones intensively bioturbated by *Skolithos* (bioturbated sand-flat facies association; SE section, 660 m). • D – horizontal to low-angle, thick laminations in medium to coarse-grained sandstones (upper shoreface facies association; intermediate section, 310 m). • E – large-scale hummocky cross-stratification (storm-dominated shoreface facies association; SE section, 780 m). • F – heterolithic deposits alternating siltstones and wavy to current-rippled sandstone beds (inner-shelf facies association; NW section, 1050 m).

Flasers and thin sandstone wavy beds characterised by consistent migrations of the foresets suggest distal tempestites deposited by low-density combined flows. Their association with relatively thick HCS beds reflects a storm-dominated inner-shelf. Muddy interbeds reflects post-storm deposition of fine material and/ or fair weather conditions.

Tidal ridges facies association. – The tidal ridges facies association characterises the Bou M'haoud Fm. in the SE section. It comprises 4–10 m thick, thickening- and coarsening upwards sandstone units showing a variety of facies. Their internal organisation is generally indistinct but two consistent patterns are: (i) erosion-based, 0.1–0.4 m thick, HCS to horizontally laminated beds prevailing in the fine- to medium-grained lower part, in association with wave ripples; (ii) medium to coarse-grained, 0.3–1 m thick trough-cross-bedded sandstones prevailing in the upper part. Sandstones are well to moderately sorted, even in

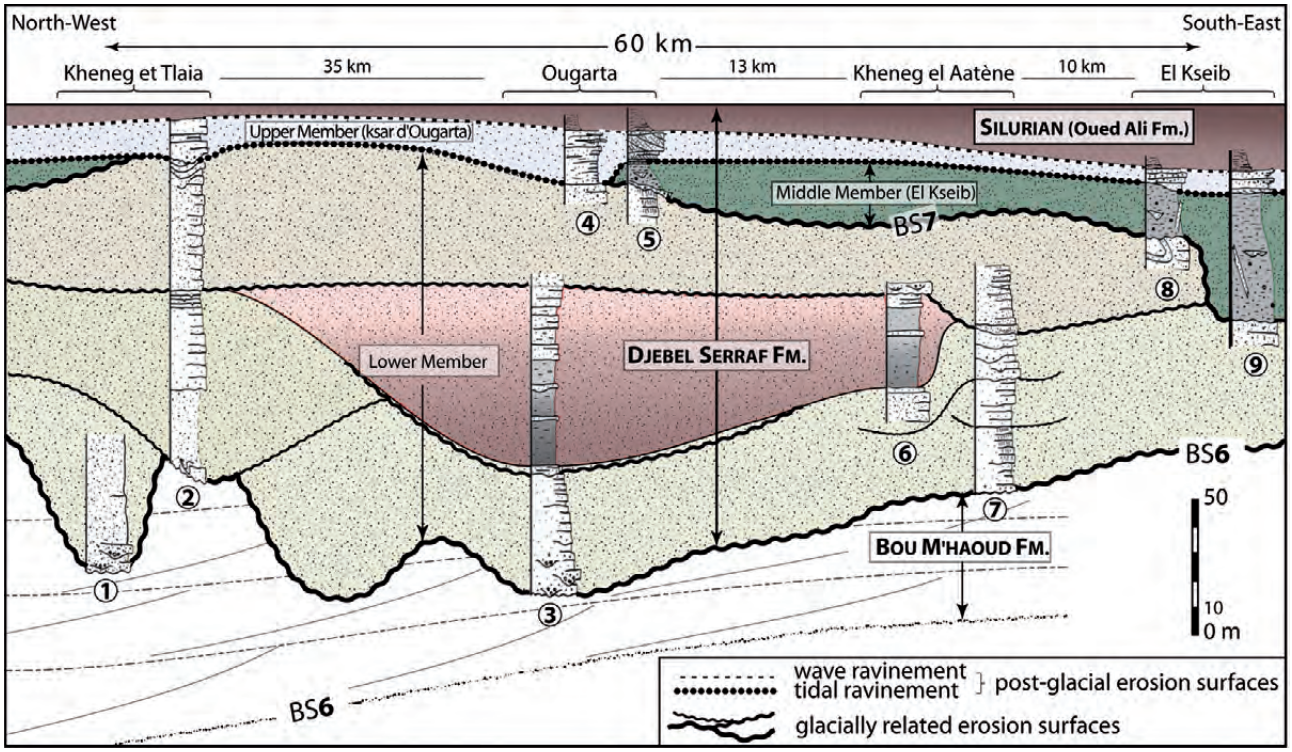

Figure 6. Correlation of nine cross-sections in the Djebel Serraf Fm. (location in Fig. 2), illustrating the internal stratigraphy of the Late Ordovician glacial record in the Ougarta Range, which is characterised by vertically superimposed erosion-based depositional units. See text for further details.

coarse-grained facies. *Skolithos* and shell beds (echinoderm and brachiopod fragments) are distributed in both facies.

Large-scale foresets, 6 m in height, have been observed in one outcrop that we have not had the opportunity to examine closely. However, we suggest that the facies patterns described above represent two depositional environments associated with large subtidal sandridges. Deposits in the lower part of the individual units show evidence of reworking either by wave or storm. They formed in inter-ridge areas or correspond to their bottomsets. Trough cross-bedded facies characterise migrating complexes driven by tidal currents. The frequent occurrence of coarse-grained sandstones that are usually absent from the shelf, shoreface or tidal environments may suggest that the tidal ridge facies association is associated with tidal-dominated delta environments.

The glacially related strata

Uppermost Ordovician, glacially related strata constitute the Djebel Serraf Fm., which is itself subdivided in three members (Arbey 1968, 1971, 1988; Legrand 1988). Deposition in the lower and middle members (the latter also known as the El Kseib Mb.) was influenced by glaciers while the upper member (also known as the Ksar d'Ougarta Mb.) is made up of post-glacial transgressive facies. The internal stratigraphy of the glacially related strata is rather intricate and only an outline of them is proposed in the following based on a reconstructed, regional-wide geological profile (Fig. 6).

Lower bounding surface. – The lower contact of the glacial deposits is an erosion surface truncating pre-glacial strata. This is a composite surface as internal erosion surfaces may locally cut through the whole of previously deposited glacial strata and amalgamate with older ones (Kheneg et Tlaïa area in Fig. 6). Erosion depth is unknown but a minimum value of 50 m is estimated, which corresponds to the residual thickness of pre-glacial strata between two adjacent incisions. From the NW towards the SE, the erosion affects progressively older strata. That does not imply more severe erosion toward the SE. A consistent depth of erosion into a Cambrian-Ordovician succession that progressively thin towards the SE would result in similar relationships.

Fluvio-deltaic facies association. – These deposits form the main part of the glacial record and comprise the lower member of the Djebel Serraf Fm. Erosion-based, several tens of metres thick units are laterally juxtaposed or vertically superimposed (Fig. 6). These units, which fill in several kilometres wide, up to 50 m deep palaeovalleys, are

made up of crudely stratified coarse-grained to argillaceous fine-grained sandstones. Erosion surfaces are locally underlain by conglomerate deposits (intraformational clasts). Horizontal to subhorizontal laminations are ubiquitous. Current ripples and vertical sheet dewatering structures are subordinate sedimentary structures. These units generally fine and thin upwards but one of those shows a 50 m-thick coarsening and thickening upward succession. Evidence for glacial influences is limited to the occurrence of poorly preserved intraformational glacial striae as described elsewhere in the Late Ordovician record (Deynoux & Ghienne 2004), and to large-scale (> 50 m) folded and subsequently truncated structures that are related to glacial loading processes (Le Heron *et al.* 2005).

These facies that are characterised by upper-flow regime conditions, and their overall large-scale architecture, characterise flood-dominated, sediment-laden stream-flow sediments deposited in proglacial fluvial environments (Ghienne 2003, Ghienne *et al.* in press). Delta systems and related coarsening- and thickening-up successions might have formed within glacially eroded and subsequently flooded depressions.

Glaciomarine facies association. – Glaciomarine deposits constitute the middle member (or El Kseib Mb. *sensu* Legrand 1988) of the Djebel Serraf Fm. It corresponds to rather thin (< 25 m thick) and lenticular sandy diamictite bodies including lonestones, sandstone dykes 0.1–1 m in thickness and small sandstone channel structures. Resting on a glacial erosion surface (Arbey 1968), these deposits reflect subaquatic outwash fan deposition (Powell 1990). They are ascribed to glaciomarine rather than glaciolacustrine facies as they bear abundant chitinozoans of Hirnantian age (*elongata* Biozone, Paris *et al.* 1995, 2007). Therefore, the glacial erosion surface at the base of this middle member also corresponds to a transgressive surface as it marks an abrupt and definitive change between underlying fluvio-deltaic deposits (lower member) and overlying marine deposits (middle and upper members).

Post-glacial facies association. – Post-glacial deposits comprise the bulk of the upper member of the Djebel Serraf Fm. (or Ksar d'Ougarta Member, *sensu* Legrand 1988) and constitute a widespread, erosion-based sandsheet that rests unconformably on underlying glacially-related strata (lower and middle Mbs.; Figs 6, 7A). This facies association is made up of medium- to coarse-grained, *Skolithos*-bearing, cross-bedded sandstones organised in large low-angle foresets similar to the tidal ridges facies association described in preglacial strata. Tidal ridges deposits are themselves truncated and overlain by coarse- to very coarse-grained sandstones that bears an abundant macrofauna (brachiopods, trilobites; Legrand 1988) and a few graptolites recalling *Normalograptus persculptus* (P. Štorch, written information in 2006). Coarse-grained sandstones then grade upward rapidly in less than 2 m in wavy heterolithic fine-grained sandstone beds and then siltstones and black shales, uppermost Ordovician and then lowermost Silurian in age.

These deposits are ascribed to a post-glacial transgressive wedge, initially developed in tidal environments devoid of glacial influences and related to post-glacial transgressive processes that lag the underlying coarse-grained glacially-related strata as proposed by Beuf *et al.* (1971) around the Tuareg Shield (*e.g.*, Ahnet area). Tidal deposits are themselves truncated by a wave ravinement surface sealed by shoreface to inner-shelf environments (Fig. 7A, B).

Sequence stratigraphic interpretation of the pre-glacial succession

The three sections present a conspicuous cyclic pattern that is well expressed in the NW section (Fig. 4). Here, up to 300 m thick fine-grained intervals highlight four 200–400 m thick sandstone units that progressively coarsen and then rapidly fine upward (Fig. 3). Sandstone units form geomorphological markers that can be correlated throughout the Ougarta Range. Six depositional sequences and associated bounding surfaces have been identified (Figs 4, 8). Bounding surfaces generally depart from lithostratigraphic boundaries but depositional cycles correspond mostly to the regional stages described by Legrand & Nabos (1962) and Legrand (1985). Higher frequency units are also recognizable.

Depositional units in the Ougarta Range

Three orders of depositional units have been delineated (Fig. 8). From the thicker to the thinner, they are: (i) depositional sequences; (ii) short-term sequences; (iii) genetic units.

Genetic units are 3–20 m in thickness, in places up to 50 m. Although further work is needed to ascertain their spatial continuity, the genetic units can apparently be correlated from the SE to the NW sections, at least those constituting the Foum Zeïdiya Fm. (Fig. 3D). They appear most often as coarsening and thickening upward assemblages, with a thin or absent fining and thinning interval in their uppermost part. No mappable erosion surface can be identified and they can be regarded as bounded by high-frequency maximum flooding surfaces. At smaller scale, genetic units internally comprise very high frequency cycles that are under the resolution of the sedimentary logs used in this paper. It is speculated that these smaller-scale units cannot be correlated over long distances as they should rep-

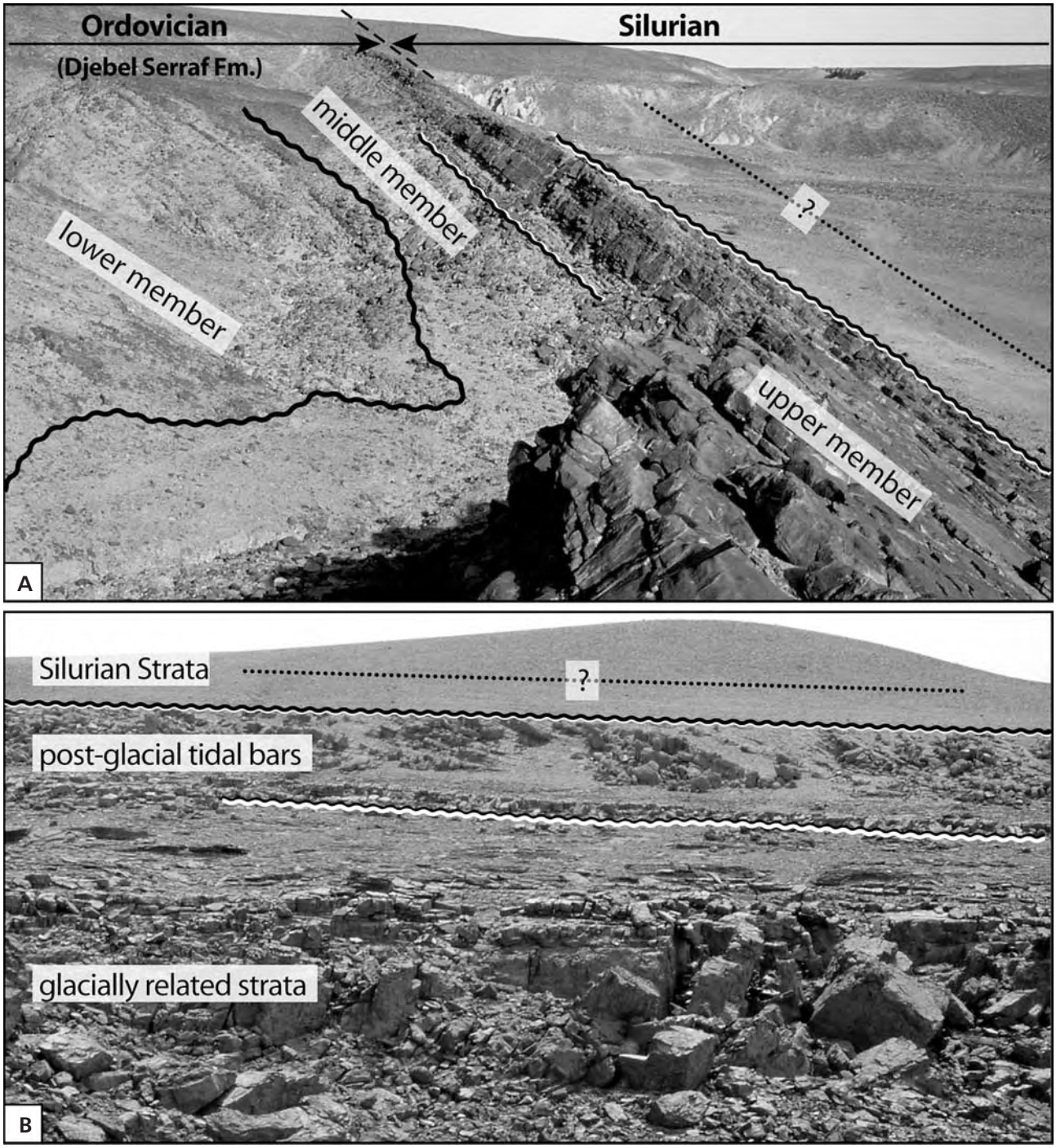

Figure 7. Stratigraphic relationship between glacially-related and post-glacial strata. Tidal deposits are bounded at their base and at their top by transgressive ravinement surfaces. • A – Ougarta Range (north to the Ksar d'Ougarta). • B – Ahnet area (Idjerrane High, southern Algeria).

resent the shoreface/ inner-shelf clinoforms that might not have exceeded ~10 km in length (*e.g.*, Hampson 2000).

Successive genetic units usually display consistent trends in thickness variations and facies composition. The stacking pattern of genetic units is then used to define informal short-term sequences that correspond to 100–200 m thick depositional units, the associated bounding surfaces of which are generally poorly defined (Fig. 3D, E). This approach is straightforward in the thick and well developed shallowing-upward portion of the depositional sequences, but less easy in the rather condensed deepening-upward portion of the depositional sequences. Short-term sequences are units, which can be correlated at least at the scale of the Ougarta Range and are also potentially useful

for long-range correlation. A short-term sequence may comprise a retrogradational and then progradational suite of genetic units. One of the two trends generally prevails and entirely retrogradational or progradational are also identified. In sand-dominated successions within which genetic units have not been properly logged (*e.g.*, Aïn Néchéa Fm. in the SE section), short-term sequence delineation is based on consistent basinward or landward shift of depositional facies.

Depositional sequences are 300–700 m thick units, the extent of which largely exceeds the Ougarta Range extending over the whole of the North African Platform and on its extension on the Arabian Plate (Sharland *et al.* 2001, 2004). Six depositional sequences have been distinguished (Figs 3, 8, 9) that are described in the following. They include several short-term sequences that are made up of a suite of genetic units. The delineation of depositional sequences is based on the recognition of transgressive and regressive trends. They then correspond to Transgressive-Regressive (T-R) sequences (Embry 1995, Catuneanu 2002) bounded by transgressive surfaces (or surfaces of maximum regression). T-R sequences predominate due to: (i) the overall shallow-marine setting within which highstand- and lowstand-system tracts are poorly differentiated; (ii) major maximum flooding surfaces virtually unidentifiable at outcrop as they are most often scree-covered; and (iii) the occurrence of significant transgressive erosion surfaces. T-R depositional sequences comprise an underlying transgressive system tract and an overlying regressive system tract (Fig. 8). The transgressive system tract of T-R depositional sequences comprises a lower, sand-dominated succession overlain by an upper, rapidly fining-up succession. The maximum flooding surface that ideally bound the transgressive and regressive system tracts has never been properly identified at outcrop as it is located within the poorly exposed soft talus of offshore facies (*e.g.*, Fig. 3C). The regressive system tracts are poorly expressed within Cambrian strata. In the Ordovician they consist generally in a thick coarsening-up succession, comprising shale-dominated sediments at the base and grading upwards in sand-dominated sediments (*e.g.*, Fig. 3B, D). They display progressively upwards more and more proximal short-term sequences. In some case, an additional stratigraphic surface can be identified that subdivides the regressive system tract into two packages assimilated as an underlying highstand and overlying lowstand wedges. Examples of correlative surfaces of a subaerial unconformity (end of sea level fall, *cf.* depositional sequence 4) and basal surfaces of forced regression (onset of sea level fall, *cf.* depositional sequence 5) have been evidenced in places.

In the following, depositional sequences identified in the Ougarta Range (Fig. 8) are described separately and integrated into a stratigraphic scheme at the platform scale through a correlation with the synthetic, Cambrian-Ordovician, basinward succession of the Anti-Atlas, and a coeval upstreamward succession fringing the Tuareg shield (Ahnet areas; Fig. 10). This correlation that is based both on the literature and on recently acquired field (Anti-Atlas, Ahnet) and biostratigraphic (Ougarta, AMg-1 well, *cf.* Fig. 9) data illustrates an almost 1000 km long depositional profile.

Depositional sequence 1: "Lower" Cambrian

Ougarta Range. – This sequence of fluvial deposits has not been studied in detail; its lower bounding surface (BS1) truncates the basement rocks. In the NW section, the Cambrian-Ordovician strata rest with an apparent conformity on rhyodacitic tuffs and lavas. The contact is underlain by a discontinuous, 0 to 0.2 m thick conglomerate bed overlain by a fining-upwards, arkosic, very-coarse to coarse-grained, cross-bedded sandstones. To the SW, BS1 cut through a > 4 km thick, steeply dipping folded succession of sandstones and volcanics (Fig. 2; Caby 1996). Conglomerates that contain fluvially reworked wind-shaped pebbles (dreikanters) have been documented (Arbey & Caby 1966).

The upper bounding surface (BS2) of depositional sequence 1 in the SE section separates the Sebkhet el Melah and Aïn Néchéa formations. A noticeable lithologic break is observed between underlying grey arkoses and overlying red arkosic sandstones. In addition, a prominent metre-thick silicification affects the topmost deposits. BS2 has not been observed in the NW section and so it is arbitrarily placed below arkosic sandstones that here constitute the upper part of the Sebkhet el Melah Fm., above a broadly fining-up succession of poorly outcropping fluvial deposits corresponding to the lower two-thirds of the formation.

Regional correlation. – The lower bounding surface of the Cambrian-Ordovician succession (BS1 in the Ougarta) corresponds to the major erosional unconformity that seals the Pan-African deformation. It is recognised around the Tuareg shield, where it is called the infra-Tassilian surface (Beuf *et al.* 1971, Fabre 2005) and truncates all the deformed, more or less metamorphosed Neoproterozoic to basal Cambrian rocks (sedimentary strata, volcanics, basement rocks) related to the Pan-African Orogeny and post-collisional collapse/strike-slip basins (Fig. 2). In outcrop, this is a flat surface but palaeorelief forms are known in places. This surface corresponds to a major fluvio-eolian by-pass (Beuf *et al.* 1971, Eschard *et al.* 2005) associated with a stratigraphic hiatus, increasing progressively from north to south. It is topped by marine uppermost Neoproterozoic – "Lower" Cambrian strata in Morocco (Destombes *et al.* 1985), whereas it is overlain by younger strata of "Upper"(?) Cambrian or Ordovician age in the Hoggar. Coeval intra-continental depositional systems have developed lo-

cally. The arkoses of the Sebkhet el Melah Fm., present in the whole of the Ougarta or in depocentres such as this related to the up to 1 km-thick Ben Tadjine conglomerates in southwestern Ougarta, are considered to be time-equivalent with processes that resulted in the infra-Tassilian surface to the south (Fabre *et al.* 1988). Hence, this depositional sequence is not present in the Ahnet area though coeval deposition might have been preserved in places (*e.g.*, Al Moungar conglomerates in the Tassili areas; Beuf *et al.* 1971, Fabre & Kazi-Tani 2005).

This depositional sequence most probably represents in the Ougarta a late transgressive to early highstand deposition. To the north, in the Anti-Atlas, the coeval succession would correspond to the uppermost part of the Western Anti-Atlas Group. However, the transgressive system tract is here fully developed including a thick carbonate-dominated succession (Upper Limestone Fm.). The lower Terminal Sandstones Fm. corresponds to the upper part of the regressive system tract (Landing *et al.* 2006).

Depositional sequence 2: "Middle" Cambrian

Ougarta Range. – The lithologic break and associated silicification possibly of pedogenetic origin (*e.g.*, Álvaro *et al.* 2003a) suggest that BS2 represents a stratigraphic hiatus across which sediment source and palaeoenvironments changed significantly. The second depositional sequence mainly comprises a transgressive system tract and an overlying subordinate regressive system tract. It seals BS2, which is interpreted as the amalgamation of a subaerial erosion surface with a transgressive surface.

The transgressive system tract is particularly well expressed in the NW section where a thick deepening-upward succession of fluvial to shallow-marine deposits is recorded (NW section, 300–550 m). In the SE section, marine influences develop progressively upward within an otherwise fluvial-dominated succession. The regressive system tract that has not been properly characterised is represented by fine-grained deposits in the NW section and by an uninterrupted, 80 m thick, fluvial unit in the SE section (Fig. 3A). The upper bounding surface (BS3) involves a subaerial erosion surface. It truncates underlying marine deposits and is overlain by estuarine deposits in the NW section while in the SE section, it is an undulating erosional surface with 1–2 m high palaeorelief forms underlain by a ferruginous granule lag including subangular quartz gravels.

Regional correlation. – The transgressive system tract of depositional sequence 2 correlates to the north with the lower "Middle" Cambrian transgressive strata constituting the upper part of the Terminal Sandstones (Tatelt Fm. of Landing *et al.* 2006; Fig. 10). In other part of the North Gondwana domain, deposition of carbonate successions, either thick as in Turkey (*e.g.*, Dean & Monod 1990, Dean 2005) or rather condensed as in Sardinia (*e.g.*, Pillola *et al.* 1998) is coeval with this worldwide transgression. This transgressive event marks the onset of the flooding of the continental platform in the Ougarta Range, which will occur only later to the south where BS2 should merge with BS1 to form together the Infra-Tassilian surface (*e.g.*, in the Ahnet area). On the Arabian Plate, the related maximum flooding surface most probably correlates to the Cm20 maximum flooding surface of Sharland *et al.* (2001).

The regressive system tract correlates with the large-scale progradation constituting the Internal Feijas Group overlain by the basal Tabanite Group of Destombes *et al.* (1985). It is suggested that BS3 in the Ougarta acted as a bypass surface, which fed in clastics the main part of the progradation to the north. Early regressive deposits of this sequence may have a time-equivalent fluvial counterpart to the south within the Ajjers Fm. of Beuf *et al.* (1971).

Depositional sequence 3: upper "Middle" Cambrian–"Upper" Cambrian?

Ougarta Range. – The third depositional sequence in the Ougarta is limited to a transgressive system tract constituting the upper half of the Aïn Néchéa Fm. In the SE section, it comprises a fining-up succession made up of red, subarkosic, unsorted, coarse- to very coarse-grained cross-bedded fluvial sandstones grading upward into white, quartz-rich sandstones of the bioturbated sand flat facies association characterised by the development of abundant *Skolithos* burrows (Fig. 8). To the NW, thin estuarine deposits underline a poorly differentiated 150 m-thick shallow-marine quartz-rich sandstones dominated by the mixed tidal and shoreface facies association. It correlates with sandstones, upper "Middle" Cambrian in age (Vecoli *et al.* 2007), which share a similar transgressive trend in the AMg-1 well (Fig. 9). A significant granulometric break is then used to locate the upper bounding surface of the sequence (BS4) that most probably corresponds to a tidal ravinement surface (see below). As in the AMg-1 well, the "Upper" Cambrian is most probably absent.

Figure 8. Facies and sequence stratigraphic interpretations in the Cambrian-Ordovician succession of the Ougarta Range. Key for sedimentary structures in Fig. 4. Delineation of Transgressive-Regressive depositional sequence is based on the recognition of transgressive surfaces. The latter merge in places with erosional surfaces. In a few cases (sequences 4, 5), the regressive system tract has been further informally subdivided based on the recognition of an internal stratigraphic surface (respectively, a correlative surface of a subaerial unconformity, and a basal surface of forced regression).

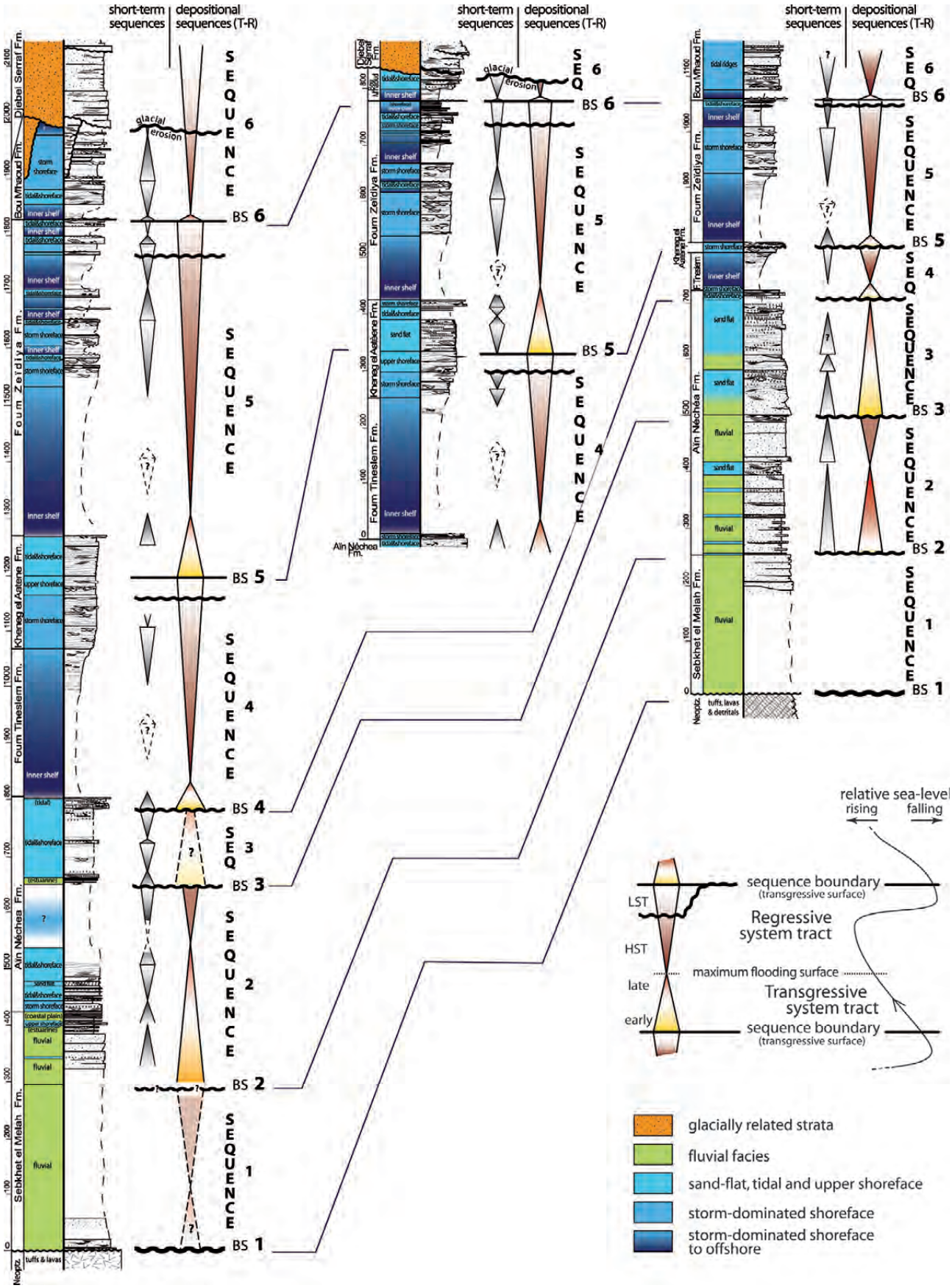
short-term sequences
depositional sequences (T-R)
SEQUENCE 6
SEQUENCE 5
SEQUENCE 4
SEQ 3
SEQUENCE 2
SEQUENCE 1
BS 6
BS 5
BS 4
BS 3
BS 2
BS 1
glacial erosion
Diebel Serrai Fm.
Bou Mhaoud Fm.
Foum Zeidiya Fm.
Khanag el Aatène Fm.
Foum Tineslem Fm.
Ain Néchea Fm.
Sebkhet el Melah Fm.
Neopz.
tuffs & lavas
relative sea-level
rising
falling
sequence boundary
(transgressive surface)
LST
Regressive
system tract
HST
maximum flooding surface
late
Transgressive
system tract
early
sequence boundary
(transgressive surface)
glacially related strata
fluvial facies
sand-flat, tidal and upper shoreface
storm-dominated shoreface
storm-dominated shoreface
to offshore

Regional correlation. – Strata coeval of the depositional sequence 3 biostratigraphically correlates to the Anti-Atlas with those constituting the middle to upper part of the Tabanite Group (Fig. 10). In the Central Anti-Atlas, *i.e.* in the axis of the Cambrian depocentre (Destombes *et al.* 1985), a 30 m-thick *Skolithos*-bearing sandstone unit is overlain by a 50-m thick succession dominated by offshore shales. These strata may represent respectively a transgressive system tract overlain by the lower part of a regressive assemblage. The later strata, "Upper" Cambrian in age (Destombes & Feist 1987), are truncated by coarse-grained sandstones underlining the Ordovician rocks. The absence (Ougarta) or poor development (Anti-Atlas) of the regressive system tract reflect uplift and subsequent erosion related to a poorly constrained "Upper" Cambrian tectonic event, which is identified in Morocco (Destombes *et al.* 1985, Destombes & Feist 1987, Burkhard *et al.* 2006), and in some places in Algeria (Legrand 1985, Crossley & McDougall 1998) and that may reflect distensive deformation affecting the continental margin further north (Ledru *et al.* 1994, Álvaro *et al.* 2003b). "Upper" Cambrian strata, however, were developed more largely farther to the east in other subsiding troughs of the North African platform (Albani *et al.* 1991, Vecoli *et al.* 1995, Vecoli 1999). On the Arabian Plate, the related maximum flooding surface most probably correlates to the Cm30 maximum flooding surface of Sharland *et al.* (2001). It is also suggested that depositional sequence 3 should be mostly represented to the south around the Tuareg Shield constituting the main part of the Ajjers Fm. of Beuf *et al.* (1971; equal to the Tin Taradjelli unit in the central Tassili type section of Eschard *et al.* 2005), an area which has not been affected by deformation at the continental margin.

Depositional sequence 4: Lower Ordovician

Ougarta Range. – The fourth depositional sequence comprises a thin, rapidly fining-upward transgressive system tract and an overlying rather thick regressive system tract. Its lower bounding surface (BS4) corresponding to a major granulometric break is sealed by a coarse-grained sandstone horizon forming the uppermost part of the Aïn Néchéa Fm. (*e.g.*, NW section, 790–800 m). It shows successively: (i) low-angle laminated to cross-bedded sandstones with *Skolithos* and disseminated fragments of linguliformean brachiopods; (ii) a sharp erosional contact overlain by several sandstone beds containing intraformational clasts and abundant disarticulated, non fragmented linguliformean brachiopods; (iii) in places, as in the NW section (795 m), a single 30 cm-thick shell-bed, observed at the very top of the Aïn Néchéa Fm. constituting a regional marker level (Gomez Silva *et al.* 1963, Legrand 1985), which laterally evolves into a several metre thick succession of unamalgamated sandstone beds of the storm-dominated shoreface facies association (*e.g.*, intermediate section, 0–10 m); (iv) argillaceous and glauconitic deposits constituting the base of the Foum Tineslem Fm. The lower bounding surface and overlying deposits are interpreted respectively as a tidal ravinement surface and tidal deposits. The later are truncated by a wave ravinement surface, and then, overlain by shoreface to inner-shelf deposits forming the lower Foum Tineslem Fm. This association points to a major transgressive event within the Cambrian-Ordovician succession formerly recognised by Legrand (1985). It is lower Tremadocian in age as dated by graptolites (Legrand 1966).

The regressive system tract comprises an up to 400 m thick, well defined coarsening- and thickening-upward succession of inner-shelf to shoreface deposits constituting the upper Foum Tineslem Fm. and the lower part of the Kheneg el Aatène Fm. (Fig. 3B). The thickness of the regressive system tract notably decreases to the SE where it is represented by a less than 100 m thick succession, even disappearing totally to the south (Gomez Silva *et al.* 1963, Legrand 1985, ORGM 2000; Fig. 8). It should be noted that this thin succession is not the result of erosion as it comprises a similar succession ending with storm-dominated shoreface deposit, which indicates condensed sedimentation (bypass) rather than post-depositional truncation.

The upper bounding surface of depositional sequence 4 has been placed in the NW section at the boundary between underlying reddish, subarkosic and micaceous shoreface

Figure 9. Dating of the Cambrian-Ordovician succession in the Ougarta Range. On the left, lithostratigraphic column and stratigraphic attributions based on macrofaunas for the Ordovician and on lithostratigraphic correlation with the Anti-Atlas for the Cambrian, according to Legrand (1985 and references therein). In the centre, new data used in this study: newly sampled macrofaunas for the Upper Ordovician (details in Fig. 4); chitinozoan distribution from the AMg-1 well (200 km NE of the Ougarta Range, *cf.* Fig. 1) for the Middle and Lower Ordovician (Paris *et al.* 2007); acritarch distribution from the AMg-1 borehole for the lowermost Ordovician and Cambrian (Vecoli *et al.* 2007). On the right, revised age attributions, correlation with global series (Webby *et al.* 2004 for the Ordovician), subdivision in seven transgressive-regressive depositional sequences as discussed in the text and illustrated in Fig. 8 and proposed correlation with the Sharland *et al.* (2001, 2004) chronostratigraphic charts using codes for maximum flooding surface on the Arabian Plate. Note that the definition of the Lower/Middle Ordovician boundary has changed since Legrand (1985; *cf.* Webby *et al.* 2004). The lower part of the Foum Tineslem Fm. has been attributed to the Tremadocian based on the recovery of a graptolite fauna (Legrand 1966) although the classical Tremadocian chitinozoan biozones have not been identified in well AMg-1. The upper Katian (lower Ashgill) is now formally identified in the Ougarta Range.

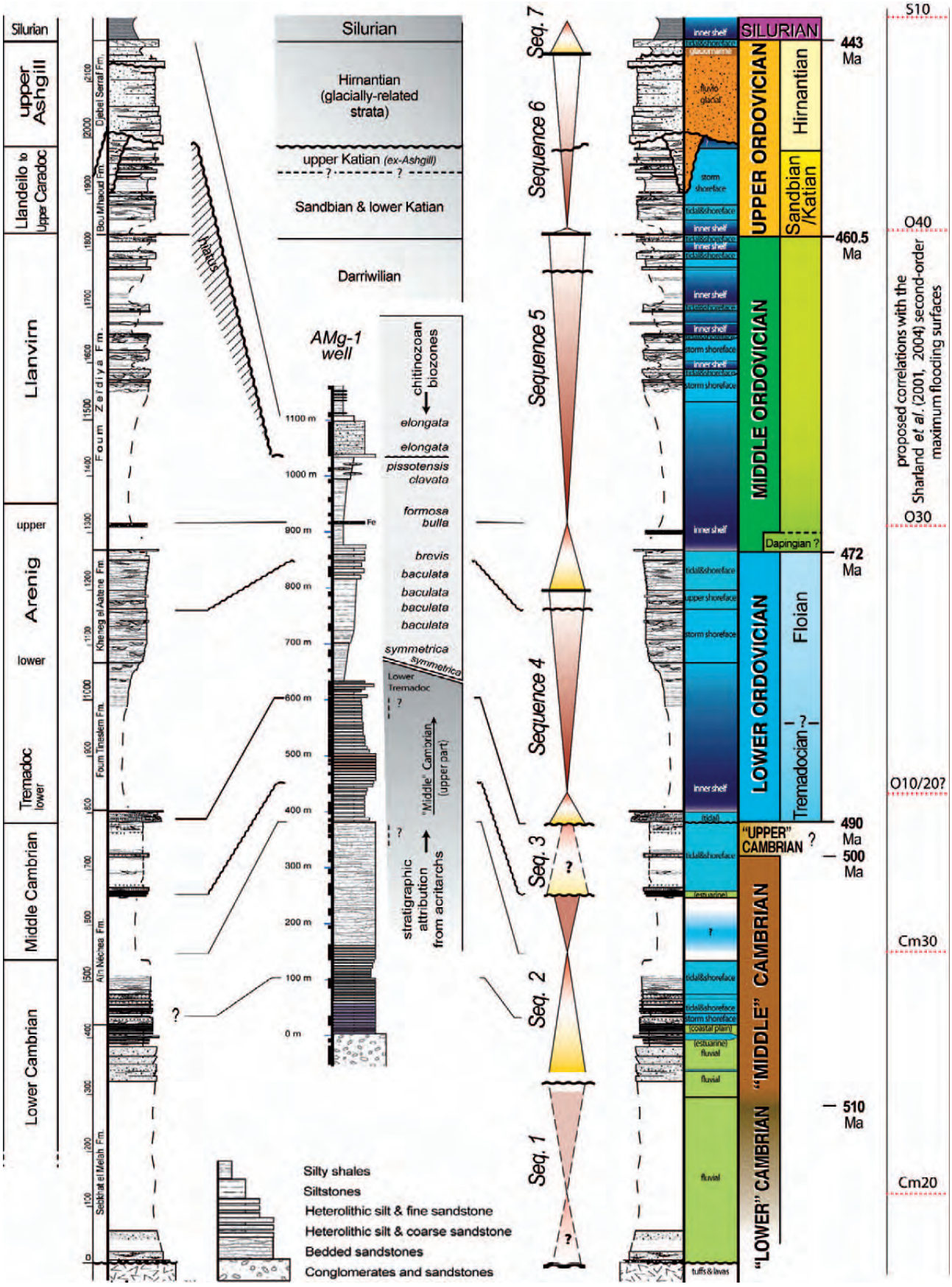
Silurian
upper Ashgill
Llandeilo to Upper Caradoc
Llanvirn
upper
Arenig
lower
Tremadoc
lower
Middle Cambrian
Lower Cambrian
Djebel Serraf Fm.
Bou Mheoud Fm.
Foum Zeidiya Fm.
Kheneg el Aatene Fm.
Foum Tineslem Fm.
Ain Nekrea Fm.
Sekrat el Melah Fm.
Silurian
Hirnantian (glacially-related strata)
upper Katian (ex-Ashgill)
Sandbian & lower Katian
Darriwilian
hiatus
AMg-1 well
chitinozoan biozones
elongata
elongata
pissotensis
clavata
formosa
bulla
brevis
baculata
baculata
baculata
symmetrica
symmetrica
Lower Tremadoc
"Middle" Cambrian (upper part)
stratigraphic attribution from acritarchs
1100 m
1000 m
900 m
800 m
700 m
600 m
500 m
400 m
300 m
200 m
100 m
0 m
Fe
Seq. 7
Sequence 6
Sequence 5
Sequence 4
Seq. 3
Seq. 2
Seq. 1
Silty shales
Siltstones
Heterolithic silt & fine sandstone
Heterolithic silt & coarse sandstone
Bedded sandstones
Conglomerates and sandstones
inner shelf
glaciomarine
fluvio glacial
storm shoreface
tidal&shoreface
upper shoreface
(estuarine)
(coastal plain)
fluvial
tuffs & lavas
SILURIAN
443 Ma
UPPER ORDOVICIAN
Hirnantian
Sandbian /Katian
460.5 Ma
MIDDLE ORDOVICIAN
Dapingian ?
472 Ma
LOWER ORDOVICIAN
Floian
Tremadocian ?
490 Ma
"UPPER" CAMBRIAN ?
500 Ma
"MIDDLE" CAMBRIAN
510 Ma
"LOWER" CAMBRIAN
S10
O40
O30
O10/20?
Cm30
Cm20
proposed correlations with the Sharland et al. (2001, 2004) second-order maximum flooding surfaces

sandstones and overlying white quartzitic tidal and shoreface sandstones. The occurrence of a ferruginous, conglomeratic and oolitic horizon that is reported in the literature within the Kheneg el Aatène Fm. (Gomez Silva *et al.* 1963, Fekirine & Abdallah 1998) is used to tentatively differentiate the correlative surface of a subaerial unconformity (Fig. 8). In the SE section, a thin (< 10 cm) conglomerate bed underlines a well defined truncation surface. Here the transgressive bounding surface is therefore superimposed onto a truncation surface. In the absence of fluvial deposits that might have been reworked during subsequent transgression, subaerial erosional processes cannot be ascertained. High frequency regressive and transgressive marine ravinement processes might have occurred with no emersion.

Regional correlation. – The transgressive system tract of the fourth depositional sequence is time-equivalent with an up to 100 m-thick argillaceous succession in the Anti-Atlas (lower Lower Fezouata shales; Fig. 10). To the south, the transgressive system tract finds a parallel with the uppermost part of the Ajjers Fm., especially where it comprises a fluvial-estuarine-sand flat succession (*e.g.*, the central Tassili type section, Eschard *et al.* 2005). On the Arabian Plate, Sharland *et al.* (2001) have identified two, Lower Ordovician, maximum flooding surfaces (O10, O20) that have not been distinguished from the Ougarta record. Either amalgamation may have occurred or one of these two events is less significant and only related to a short-term sequence. However, both events seem to be represented in the Anti-Atlas (Destombes *et al.* 1985).

Regressive deposits correspond in the Anti-Atlas to a thick succession including the upper Lower Fezouata shales (upper Tremadocian) and the Upper Fezouata shales (Floian, or lower Arenig) of Destombes *et al.* (1985) while to the south, they are either absent (*e.g.*, the Ahnet section, Fig. 10) or poorly developed. If present, they correspond to a thin prograding succession (unit of the Vire du Mouflon of Eschard *et al.* 2005). In subsurface of Algeria, the regressive system tract comprises the El Gassi shales and El Atchane sandstones (Fekirine & Abdallah 1998).

A time-equivalent erosional truncation, similar to the BS 4 in southeastern Ougarta, has also been identified in other places on the platform, *e.g.*, in the Nl-2 borehole with superimposed Lower and Middle Ordovician marine shales and no intervening evidence for fluvial deposition (Oulebsir & Paris 1995).

Depositional sequence 5: upper Lower Ordovician–Middle Ordovician

Ougarta Range. – Above bounding surface 5, the fifth depositional sequence comprises a transgressive system tract that progressively developed to the north where it corresponds the upper Kheneg el Aatène and lower Foum Zeïdiya fms. The subsequent regressive system tract constitutes the middle and upper Foum Zeïdiya Fm.

At its base, the transgressive system tract comprises relatively thick (60 m) deposits of the tidal and shoreface facies association (Fig. 3B). They are overlain by several sandstone beds containing intraformational clasts and abundant disarticulated, non fragmented linguliformean brachiopods similar to those of the basal part of depositional sequence 4. An overlying short-term sequence is capped by an oolitic ironstone horizon also including linguliformean brachiopods. This short-term sequence includes upper Arenig (lower Middle Ordovician, *i.e.* Dapingian) graptolites (Legrand 1964) and time-equivalent chitinozoans (*bulla* Biozone) are found within the ironstone horizon in the AMg-1 well (Benoît & Taugourdeau 1961). To the south, the transgressive system tract is limited to several, unamalgamated beds of the storm-dominated shoreface facies association here including conglomerate lenses.

The regressive system tract includes a well defined coarsening-upward succession of short-term sequences with alternating inner shelf and storm shoreface or tidal and shoreface facies associations (Fig. 3D). An abundant macrofauna designates this interval as an essentially Darriwilian succession (Figs 4, 9). The upper bounding surface corresponds to an erosional surface sealed with transgressive lag deposits (see below). However, some metres or tens of metres beneath the sequence boundary, an abrupt contact has been systematically noted that superimposes tidal or shoreface onto underlying inner shelf deposits (Fig. 8). This stratigraphic surface is tentatively interpreted as reflecting the onset of a major sea-level fall (as the basal surface) with overlying strata featuring a lowstand system tract.

Regional correlation. – The sand-dominated transgressive strata are correlated to the north with Floian strata (middle Arenig) of the Zini Sandstones in the western Anti-Atlas (Destombes *et al.* 1985) and with the Armorican Sandstone in Brittany (Paris 1990). Palynomorphs in adjacent areas (Oulebsir & Paris 1995) and in the AMg-1 well (Benoît

Figure 10. Regional correlation illustrating depositional sequence development to the north (Anti-Atlas, Morocco) and to the south (Ahnet, southern Algeria) of the Ougarta Range. The progressive disappearance of the fluvial facies through time, the thinning of the successive transgressive system tracts and the development of repetitive open marine conditions designate together the Cambrian to Ordovician succession as a first-order transgressive wedge in North Africa.

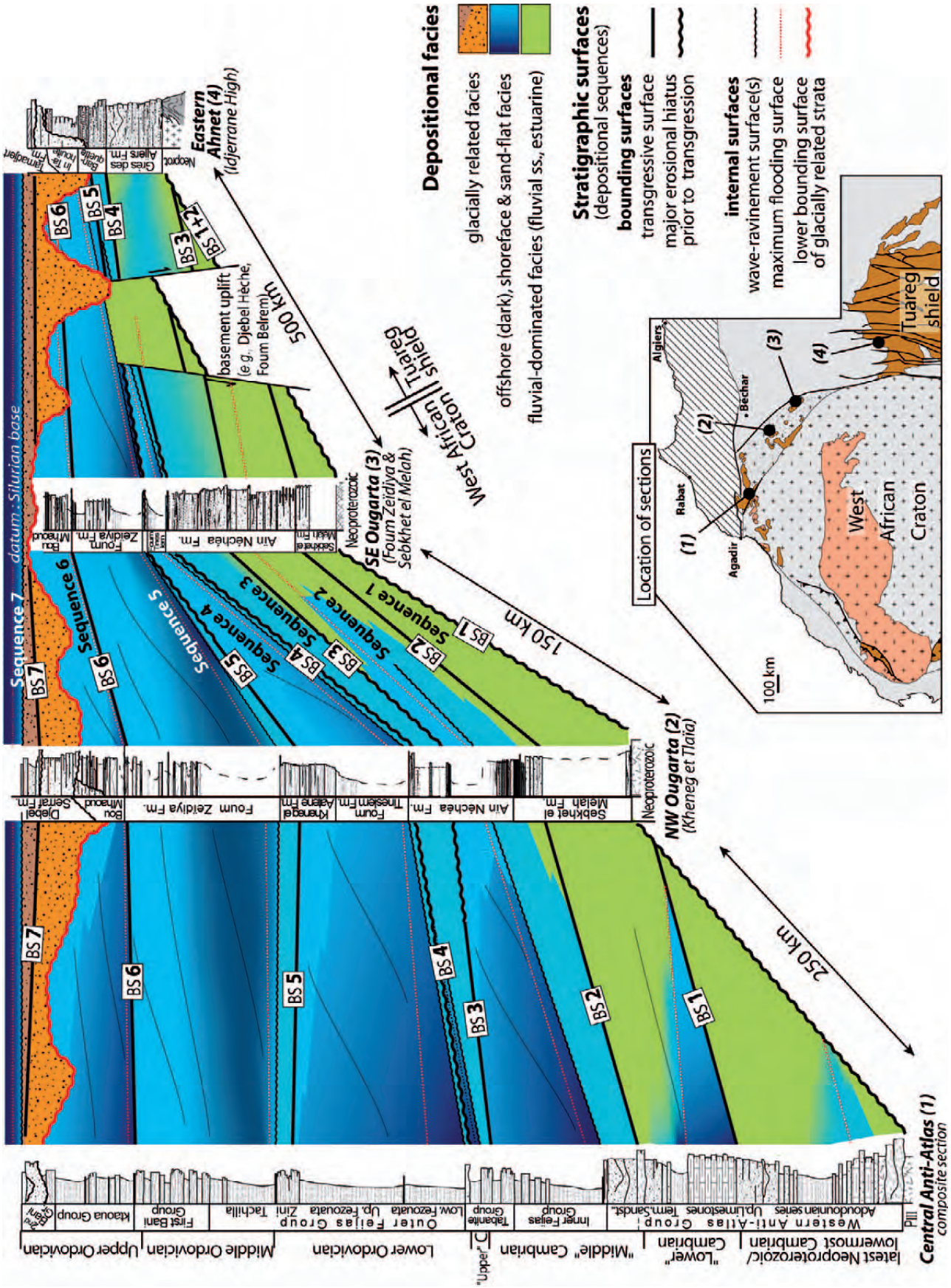
Depositional facies
glacially related facies
offshore (dark), shoreface & sand-flat facies
fluvial-dominated facies (fluvial ss., estuarine)
Stratigraphic surfaces
(depositional sequences)
bounding surfaces
transgressive surface
major erosional hiatus
prior to transgression
internal surfaces
wave-ravinement surface(s)
maximum flooding surface
lower bounding surface
of glacially related strata
Location of sections
Algiers
Béchar
Rabat
Agadir
(1)
(2)
(3)
(4)
West African Craton
Tuareg shield
100 km
Central Anti-Atlas (1)
composite section
NW Ougarta (2)
(Kheneg et Tlaïa)
SE Ougarta (3)
(Foum Zeidiya & Sebkhet el Melah)
Eastern Ahnet (4)
(Idjerrane High)
West African Craton
Tuareg shield
basement uplift
(e.g., Djebel Hèche, Foum Bel'rem)
250 km
150 km
500 km
datum : Silurian base
Sequence 7
Sequence 6
Sequence 5
Sequence 4
Sequence 3
Sequence 2
Sequence 1
BS 1
BS 2
BS 3
BS 4
BS 5
BS 6
BS 7
Latest Neoproterozoic/ lowermost Cambrian
"Lower" Cambrian
"Middle" Cambrian
Lower Ordovician
Middle Ordovician
Upper Ordovician
Western Anti-Atlas Group
Adoudounian series
Up. Limestones
Term. Sandst.
Inner Feïgas Group
Tabanite Group
Outer Feïgas Group
Low. Fezouata
Up. Fezouata
Zini
Tachilla
First Bani Group
Ktaoua Group
Sebkhet el Melah Fm.
Ain Nechéa Fm.
Foum Tinesfem Fm.
Khaneg el Aatane Fm.
Foum Zeidiya Fm.
Bou Mlaoud
Debeï Serrat Fm.
Neoproterozoic
Ain Nechéa Fm.
Sebkhet el Melah
Foum Zeidiya Fm.
Bou Mlaoud
Neoproterozoic
Gres des Ajjers Fm.
Tamadjert

& Taugourdeau 1961) show that the transgression began as early as the upper Floian (middle Arenig, *brevis* event of Paris *et al.* 2007) with another pulsation in the lowermost Darriwilian (uppermost Arenig, *bulla* event of Paris *et al.* 2007). This two-fold transgression is tentatively considered as parallel to the two short-term sequences identified in the Ougarta (intermediate section, 330–400 m), with severe condensation of deposits occurring during the Dapingian (upper Arenig), *e.g.*, in Brittany (Dabard *et al.* 2007) and illustrating in the Ougarta by shell beds and associated ironstones. Maximum flooding conditions occurred slightly later during the early Darriwilian and correspond to the *formosa* event of Paris *et al.* (2007). On the Arabian Plate, the related maximum flooding surface correlates to the O30 maximum flooding surface of Sharland *et al.* (2001).

To the south, the basal transgressive system tract forms a regionally widespread sandstone sheet known in subsurface as the Hamra Quartzites, or the Banquette unit in the Tassili, comprising mainly sand-flat *Skolithos*-rich deposits (Fig. 10). In places, this unit onlaps onto basement rocks (Beuf *et al.* 1971). In the Ahnet, tidal deposits comprise the maximum flooding thought more largely open marine conditions might have occurred coevally in more subsiding areas such as in the Tassili (Eschard *et al.* 2005).

Further south, regressive strata form mainly the shoreface-dominated In Tahouite Fm. (*e.g.*, Eschard *et al.* 2005). The regressive system tract correlates to the north with the Tachilla shales grading upwards into the sandstones of the First Bani Group (Destombes *et al.* 1985) of late Darriwilian age. If the identification of a basal sea-level fall surface in uppermost depositional sequence 5 is correct, the overlying strata can be considered as time-equivalent at least with the lower part of the First Bani Group. Strata of the upper First Bani Group, Late Darriwillian to early Sandbian, might represent late lowstand conditions not represented in the more proximal Ougarta Range.

Depositional sequence 6: Upper Ordovician

Ougarta Range. – The bounding surface 5 corresponds to the base of the Bou M'haoud Fm. (Gomez Silva *et al.* 1963). This flat surface is sharp at the outcrop scale (Fig. 11A) and erosional at the regional scale. To the south, it rests on progressively older and older genetic units of the underlying Foum Zeïdiya Fm. (compare Figs 4A–C). The erosion surface is underlain by ferruginous, coarse-grained to conglomeratic sandstones with occasional *Skolithos*. Sandstones are characterised by: (i) the occurrence of intraformational, rounded pebbles 3–25 cm in diameter (Fig. 11B); (ii) gravely, 40 cm-high asymmetric megaripples, 2.5 m in wavelength with pebble concentrations in their troughs (Fig. 11C); (iii) coarse-grained, 5–15 cm-high symmetric megaripples, 0.5 m in wavelength (Fig. 11D), with wave ripples in their troughs. Siltstones and shales rest abruptly above the coarse-grained sandstones. BS5 truncates and is overlain by marine deposits. Sedimentary structures in associated coarse-grained sandstones point to processes related to lag deposits in high-energy gravelly shoreface to offshore environments (*e.g.*, Leckie 1988, Hart & Plint 1989). The coarse-grained sandstone bed represents the only developed transgressive system tract, implying the transgression was non-accretionnary in the Ougarta Range (Helland-Hansen & Gjellberg 1994).

Above, stacked sandstone-dominated high frequency sedimentary cycles, and deep truncation by the overlying glacially related surface limits sequence stratigraphic interpretations (Fig. 3E). Pre-glacial strata, mostly Sandbian and early Katian (Caradoc and lower Ashgill) in age (Fig. 9) are ascribed to the lower part of a regressive system tract. The regressive system tract extends within the glacially-related strata (Figs 3D, E, 8, 9). The fluviodeltaic sandstones (lower member of the Djebel Serraf Fm.) that fill in palaeovalleys or depressions bounded by a subaerial to subglacial unconformity (Fig. 6) constitute a lowstand wedge at the top of the regressive system tract. The stratigraphic attribution of the glaciomarine and tidal deposits (respectively the middle and upper members of the Djebel Serraf Fm.) will be discussed latter. They are ascribed to the transgressive system tract of a seventh depositional sequence extending into the lower Silurian strata, with a subsequent regressive system tract represented by the Silurian-Early Devonian prograding wedge (Fig. 2).

Regional correlation. – The sixth depositional sequence has a poorly developed transgressive system tract, which may, however, be present to the south, *e.g.*, in the Ahnet, where time-equivalent strata might correspond to sand-flat deposits observed in zones of lesser glacial erosion. To the north in the Anti-Atlas, sedimentation is dominated by severe condensation (phosphatic and/ or ferruginous horizons). Alternatively, the regressive system tract mainly corresponds to the thick Ktaoua Group extending from the lower (but not lowermost) Sandbian to the Katian (lower Caradoc to pre-Hirnantian Ashgill; Destombes *et al.* 1985, Elaouad-Debbaj 1987, 1988; Bourahrouh *et al*. 2004). Southward, decreasing thickness of regressive strata in combination with potentially increasing glacial erosion together result in poor preservation of coeval strata, which are, however, locally preserved (Legrand 1985, Kichou-Braîk *et al.* 2006). On the Arabian Plate, the related maximum flooding surface most probably correlates to the O40 maximum flooding surface of Sharland *et al.* (2001).

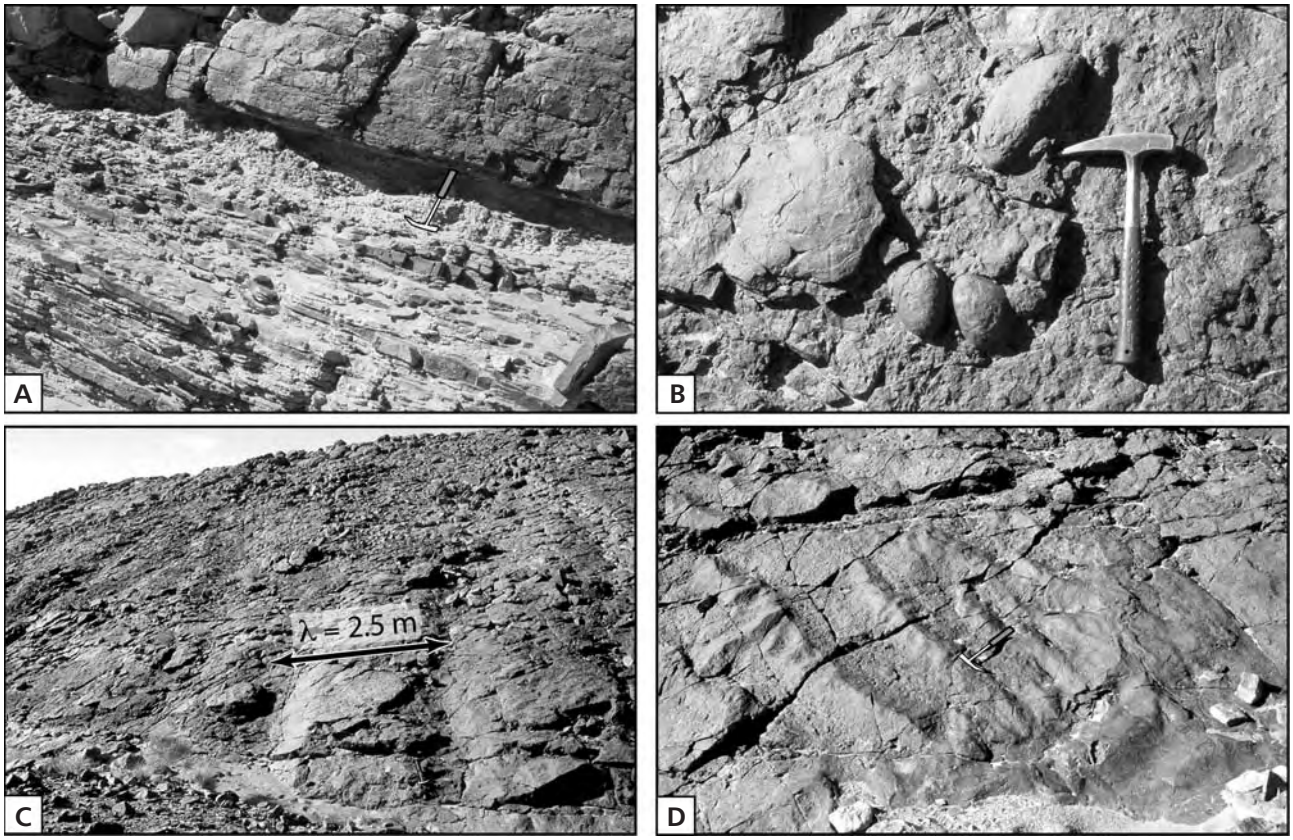

Figure 11. The ferruginous, coarse-grained to conglomeratic sandstone bed underlining the fifth bounding surface (BS5). • A – sharp-based contact on heterolithic, inner-shelf deposits. • B – intraformational rounded pebbles. • C – large-scale asymmetric current megaripples on bed top. • D – symmetric wave megaripples on bed top.

The erosion surface at the base of glacial deposits is traceable over the whole northern Gondwana. It has been recognised as a major erosional unconformity truncating Ordovician, Cambrian and locally basement rocks where the pre-glacial successions were thin and/or where deep glacial palaeovalleys were cut (Beuf *et al.* 1971, Ghienne & Deynoux 1998, Hirst *et al.* 2002, Eschard *et al.* 2005, Ghienne *et al.* in press). Glacial deposits of the Ougarta are correlated unambiguously with the Second Bani Group in the Anti-Atlas (Destombes 1968a, b, Destombes *et al.* 1985) and with the Felar-Felar Complex or Tamadjert Fm. in the Ahnet or the Tassili (Beuf *et al.* 1971, Legrand 1985, Eschard *et al.* 2005; Fig. 10). More precisely, the lower member of the Djebel Serraf Formation is suggested to be time-equivalent with the upper member of the Lower Second Bani Fm. of Destombes *et al.* (1985) or with the Lower Tichitt Group in Mauritania (Deynoux 1985, Ghienne 2003). These strata record in North Africa the first of two major Hirnantian glacial cycles (Sutcliffe *et al.* 2000, Štorch 2006, Ghienne *et al.* in press). The glacial maximum would be represented in the Ougarta Range by the glacial erosion surface at the base of the middle member of the Djebel Serraf Fm (El Kseib Mb., Fig. 6).

Time calibration

Age attributions based on both biostratigraphic data (Fig. 9) and regional correlation (Fig. 10) indicate that the depositional sequence durations are in the 15–20 Ma range (Fig. 9). The exact number of higher frequency units cannot be determined at outcrop due to poor exposures in fine-grained units and to amalgamation and/or condensation in the transgressive portion of depositional sequences. Three to five short-term sequences per depositional sequence are generally observed and a total number of 5 to 8 can thus be reasonably inferred (Fig. 8). Then, a short-term sequence lasted between 2 and 4 Ma. A minimum of four genetic units identified within each of the short-term sequence points to duration in the 0.2–1 Ma range. As a working hypothesis, it is here proposed that they represent 400 ka-long eccentricity cycles. Those are generally well expressed in the geological record (*e.g.*, Wade & Pälike 2004) and are considered as the most stable of the Earth's long-term astronomical frequencies (Laskar 1999). As a consequence, the short-term and depositional sequences may be assigned respectively to the third- and second-order sequences of the commonly used hierarchy (*e.g.*, Sharland *et al.* 2001). Whatever the exact duration of a high

frequency depositional cycles, they clearly represent orbitally controlled features.

Depositional sequence architecture at platform-scale

The Cambrian-Ordovician succession thins systematically towards the SE (sediment source area; Fig. 10). Finally, and dealing with non-decompacted thicknesses, 3000 to 5000 m of fluvial to shallow-marine sediments accumulated rather regularly for around a 100 Ma time interval in the Anti-Atlas, grading to 2000 m in NW Ougarta, while the coeval succession in SE Ougarta is 1000 m thick and usually < 500 m around the Tassili (Fig. 10). This accumulation reflects a globally greater subsidence rate towards the shelf edge.

Although the Ougarta Range only permits us to examine a 200 km-long "window" across each of the six depositional sequences, a stratigraphic architecture can be reconstructed at platform-scale (~ 500 km) for an idealised sequence (Fig. 12). With the exception of the glacially-related fluvio-deltaic deposits, the progressive disappearance of the fluvial facies and the development of open marine conditions from the lower to the upper segments of the NW and SE sections is noticeable. This change reflects a long-term and overall southeastward backstepping of the depositional environments from the Cambrian to the Ordovician (Beuf *et al.* 1971, Fabre & Kazi-Tani 2005). Therefore, the Ougarta "window" is progressively shifted basinward through time (Fig. 12). Assuming the pre-glacial depositional system did not change significantly, a model for a depositional sequence can be built between two end-members: (i) a proximal one, illustrated by a system tract succession in the lower part of the SE section; and (ii) a distal one, illustrated by a system tract succession in the middle part of the NW section.

A depositional sequence forms an up to 700 m-thick unit bounded by unconformities, which are generally best expressed towards the SE (Fig. 10). Transgressive system tracts mainly form an extensive, 100–300 m-thick, sand-dominated sheet-like unit. In the most proximal reaches of the platform, aggrading fluvial to marine sand-flat deposition occurred above the sequence boundary. Continentward backstepping onlaps are responsible for the progressively younger initiation of sediment deposition above the Infra-Tassilian surface. Intervening marine and bioturbated sand-flat deposits represent episodic high-frequency marine flooding (sequence 2). In the coastal portion of the platform, the transgressive system tracts most often comprise an extensively developed sand-dominated succession characterised by aggrading, *Skolithos*-rich, sand-flat or tidal and shoreface deposits (sequences 3, 5). In some proximal locations, subordinate estuarine facies are deposited and preserved (sequences 2, 3 in the NW section). Basinward (and subsequently), tide and shoreface erosion occurred, favouring the deposition of transgressive lags followed by sedimentary condensation (sequences 5, 6). Thick argillaceous sedimentation can, however, occur coevally in the deeper part of the basin below the storm wave base (*e.g.*, Tremadocian shales in the Anti-Atlas), which is likely related to regressive system tracts of short-term T-R sequences or high frequency sedimentary cycles.

In basinal areas, regressive system tracts form relatively thin (< 100 m) to thick (> 300 m) coarsening and thickening upwards heterolithic storm-dominated successions. In the more distal area, continuous sedimentation was generally maintained through a depositional cycle and boundaries are usually not observed in the regressive system tract, which may clearly differentiate highstand from lowstand conditions. In more proximal areas, truncation of regressive shoreface sand occurred, with potential amalgamation of stratigraphic erosion surfaces (subaerial, transgressive ravinements; BS5 in the SE section and BS6). Any fluvial deposit has usually been recognised in the topmost part of regressive system tracts, with the exception of glacially-related strata. Extensive shallow-marine sand flats separating the open shelf from fluvial environments and/or the removing of fluvial sediment during transgressions may explain this feature, independently or in combination. In the more proximal reaches of the platform, regressive system tract deposits basically comprise fining-upwards fluvial successions (depositional sequence 1). Such a trend probably records a lowering of fluvial energy with time in relation to decreasing topographic slope (*e.g.*, Catuneanu 2002). In addition, time-regressive fluvial strata reduced in thickness through time and then disappear as continental environments were progressively shifted southward during the Ordovician into a notably less subsiding area.

Discussion

Sequence hierarchy

To develop a system of sequence hierarchy needs a criterion that can be used to differentiate the relative significance of sequences and associated bounding surfaces. Either a system based on boundary frequency, which is equivalent to sequence duration or a system based on the magnitude of base level changes is generally proposed (*e.g.*, Catuneanu 2002 and references therein). For instance, Vail *et al.* (1991) proposed six orders of boundaries solely defined on boundary frequencies, with eustasy as the main driving factor in boundary generation. Whatever the system used, a primary requirement is that a sequence cannot contain a se-

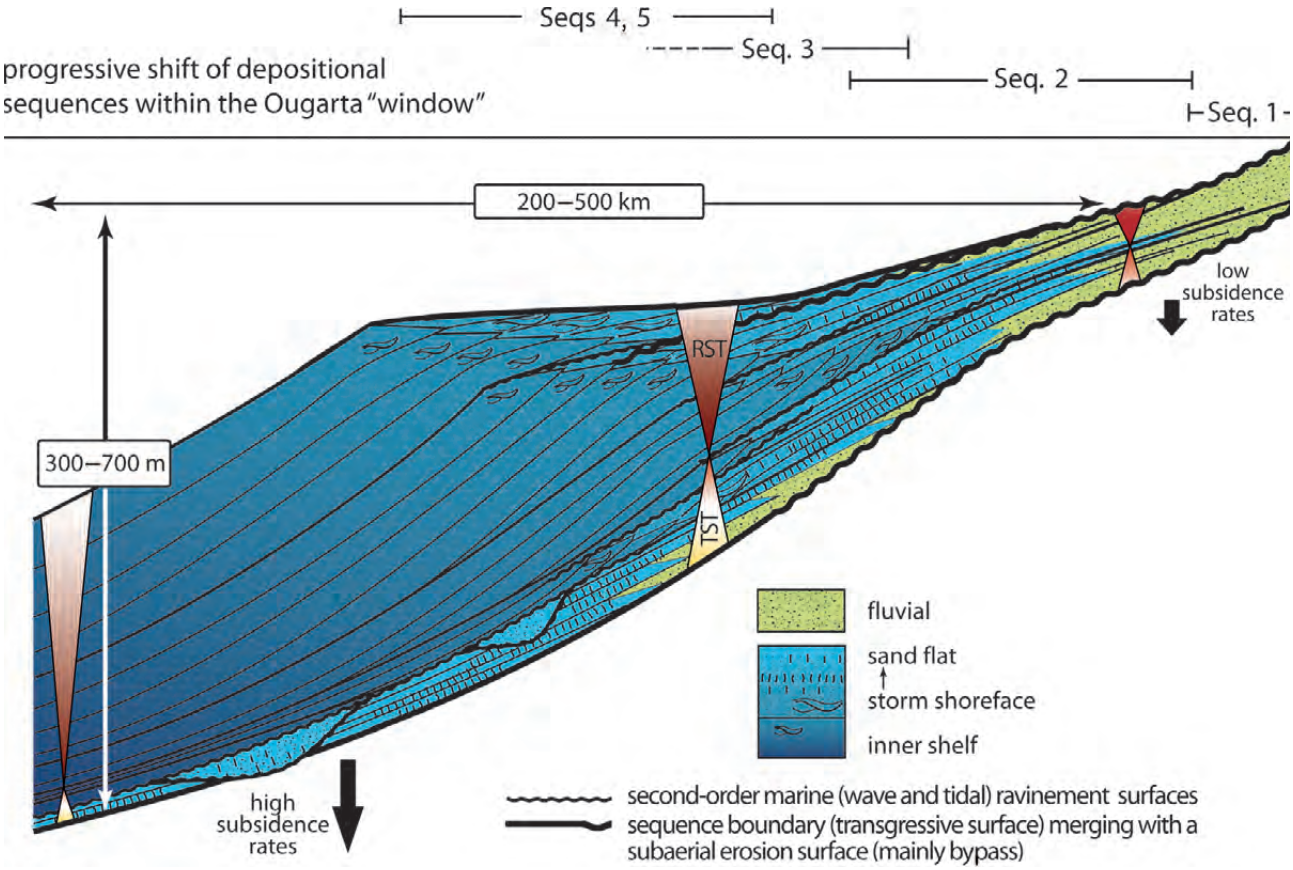

Figure 12. Reconstruction of a Cambrian or Ordovician T-R depositional sequence at the platform scale, assuming no major environmental change in the Ougarta Range through time. Bounding surfaces are transgressive surfaces. They merge to the south with essentially erosional surfaces. Subaerial erosion surfaces or basal surfaces of forced erosion are the most often poorly defined.

quence boundary with the same or lower order than its basal and highest boundary.

Embry (1995) considered that the main pitfall related to this approach using boundary frequency is the potential for subjectivity in picking surfaces of different orders in the sedimentary record. Alternatively, the system based on magnitude of base level changes uses physical attributes, such as the areal extent of the unconformable portion of the sequence boundary or the magnitude of base level rise. Such an approach, which suggests tectonics as the main driving factor for sequence generation can be applied with some success only if basin margins are well defined and preserved (Miall 1997). In addition, stratigraphic architecture is basically controlled by the interplay between sediment supply and rate of base-level change, rather than the magnitude of base level change. It follows that high rates of base level change (*e.g.*, a post-glacial transgression, a rotating block in an extensional setting) may generate prominent boundaries in the stratigraphic record while more continuous base level changes, even if of greater amplitudes, should develop more diffuse sequence boundaries.

Over the North African platform, where tectonic deformation is limited, where the extent of depositional areas can be up to several thousands of kilometres, the use of criteria related to the magnitude of base level changes will inevitably identify glacially related sea-level falls as the major driving factor for the generation of high-order (long term) sequence boundaries despite their short duration relative to long term, tectonically driven processes associated with potentially greater base level changes. This factor is particularly well expressed in the Taoudeni Basin sedimentary record. Here, the Neoproterozoic to Devonian sedimentary cover of the West African Craton has been subdivided by using unconformities intimately associated with the late Neoproterozoic and latest Ordovician glacial successions (Deynoux *et al.* 1985, 2006). In both cases, severe glacial erosion has emphasised an apparent "angular" unconformity at the basin scale caused by long-term, preglacial, syn-depositional downwarping of the cratonic basement (see below).

We are aware of the problem associated with subjectivity as pointed out by Embry (1995) but we suspect that glacially-related processes (base level fall of great amplitude, oversupplied sediment supply, high rate of base-level rise) may obscure our understanding of the sedimentary record. Hence, to unravel the interference of the Late Ordovician

glaciation on the Lower Palaeozoic stratigraphic succession, we need a sequence hierarchy independent of base level change, and that is why we have used and advocate a system based on frequency hierarchy to delineate depositional sequences.

Sequence specificities

Sequence boundaries correspond to erosional truncations that evolve basinward in essentially conformable surfaces with no demonstrable erosion. Whereas erosion confidently reflects local conditions where rate of sea-level fall exceeds subsidence rate, the contribution to erosion of subaerial processes relative to marine ones is unclear. In particular, shallow-marine facies bracket several erosion surfaces and any lowstand valleys have been identified. Moreover, any or minor fluvial deposits have been reported in the basal part of transgressive system tracts (Fig. 8). An additional feature of the depositional sequences is the considerable spatial extent of the sand-bodies, with minor variations in facies occurring over distances > 100 km.

Given that subsidence rates over the platform were of the same order as low-frequency sea-level fluctuation rates, *i.e.* several tens of metres per million years (*e.g.*, Haq *et al.* 1987), a transition from relative rise to relative fall occurred on the platform and migrated through time. During periods of long-term sea-level fall, the extent of areas experiencing base-level fall conditions progressively increased (*e.g.*, Catuneanu *et al.* 1998). These areas include logically proximal southern areas but also some so-called "basement highs" that are laterally adjacent to "depositional troughs". Both types of area correspond to zones of lesser subsidence favouring the erosion of previously deposited shoreface sands during high-frequency transgressions and regressions characterised by higher amplitude and rate of sea-level change. This cannibalization progressively feeds in clastics deeper and more subsiding portions of the platform. When the emersion occurred, erosion virtually ceased. Even in front of the established fluvial system, the subaerial unconformity should not have been incised and is mainly related to sediment bypass (Runkel *et al.* 1998, Posamentier 2001). Thus it can be speculated that erosion was preferentially associated with shoreface erosion processes rather than with fluvial incision. Long-term normal regression and continuous sedimentation was maintained in the areas with greater subsidence rates, where the effects of high-frequency erosional processes were minimum. This finally resulted in the formation of an extensive but fully diachronous regressive sand-sheet characterising sediment spreading through a long-term cycle in the context of this huge and very flat platform. If the shoreline was located in a sufficiently subsiding area, no long-term forced regression can have developed as aggrading conditions pertain throughout a full cycle of sea-level change.

Runkel *et al.* (1998) suggested that the formation of sandstone sheets reflected deposition of a continuous sediment supply of sand on a relatively stable, nearly flat basin of slow uniform subsidence during changes in sea level. Independently of possible true basement uplifts, architecture of depositional sequences in the Ougarta moreover suggests a general redistribution of the sediment during a period of low-frequency regressive system tract that might have a widespread geographic extent, displaying similar but diachronous facies successions with regressive and transgressive high-frequency wave reworking of the more shallow reaches of the platform (proximal areas and "basement highs"). Potential, if any, features related to subaerial processes were reworked during the subsequent transgression. The significance of aeolian processes acting on these surfaces is questioned (Fabre 1988). In particular, transgressive sand-rich lithologies may be ascribed to a generalised bypass of the finer-grained material or to the reworking of continental aeolian sand seas, the sand-dominated material of which is easily wave-reworked and spread over the platform in the form of huge sand flats.

Tectonics *vs.* eustasy

The Cambrian-Ordovician succession in the Ougarta Range records well organised, possibly periodic, stratigraphic cycles. The basin location, above a paleomargin of the stable West African Craton, which was reactivated during the later stages of the Pan-African orogeny (*cf.* Geological setting), probably favours a relatively regular subsiding pattern, more active than that characterising adjacent intracratonic domains (*e.g.*, the Taoudeni Basin), but less affected by tectonics than in recently cratonised areas (*e.g.*, the Tuareg shield, Fig. 1) where fault reactivations may have periodically and significantly altered the record of sea-level changes. A long-lasting subsidence pattern and a continuously rising eustatic sea level during the Ordovician as recognised worldwide (Ross & Ross 1992, Nielsen 2004, Haq & Al-Qahtani 2005) led to the progressive flooding of the cratonic platform (Fabre 1988, Fabre & Kazi-Tani 2005). Low frequency depositional sequences, the timing of which is more or less synchronous at least at the scale of the North Gondwana domain (*e.g.*, Sharland *et al.* 2001, Haq & Al-Qahtani 2005, Dabard *et al.* 2007), may record either second order tectono-eustatic cycles or deformation processes at the continent scale. Deformation processes involving the whole of the North African Platform may correspond to the response of the internal continental domain to rifting events occurring at the continental margin. For example, transgressive trends pointing out the lower part of depositional sequences may reflect extensio-

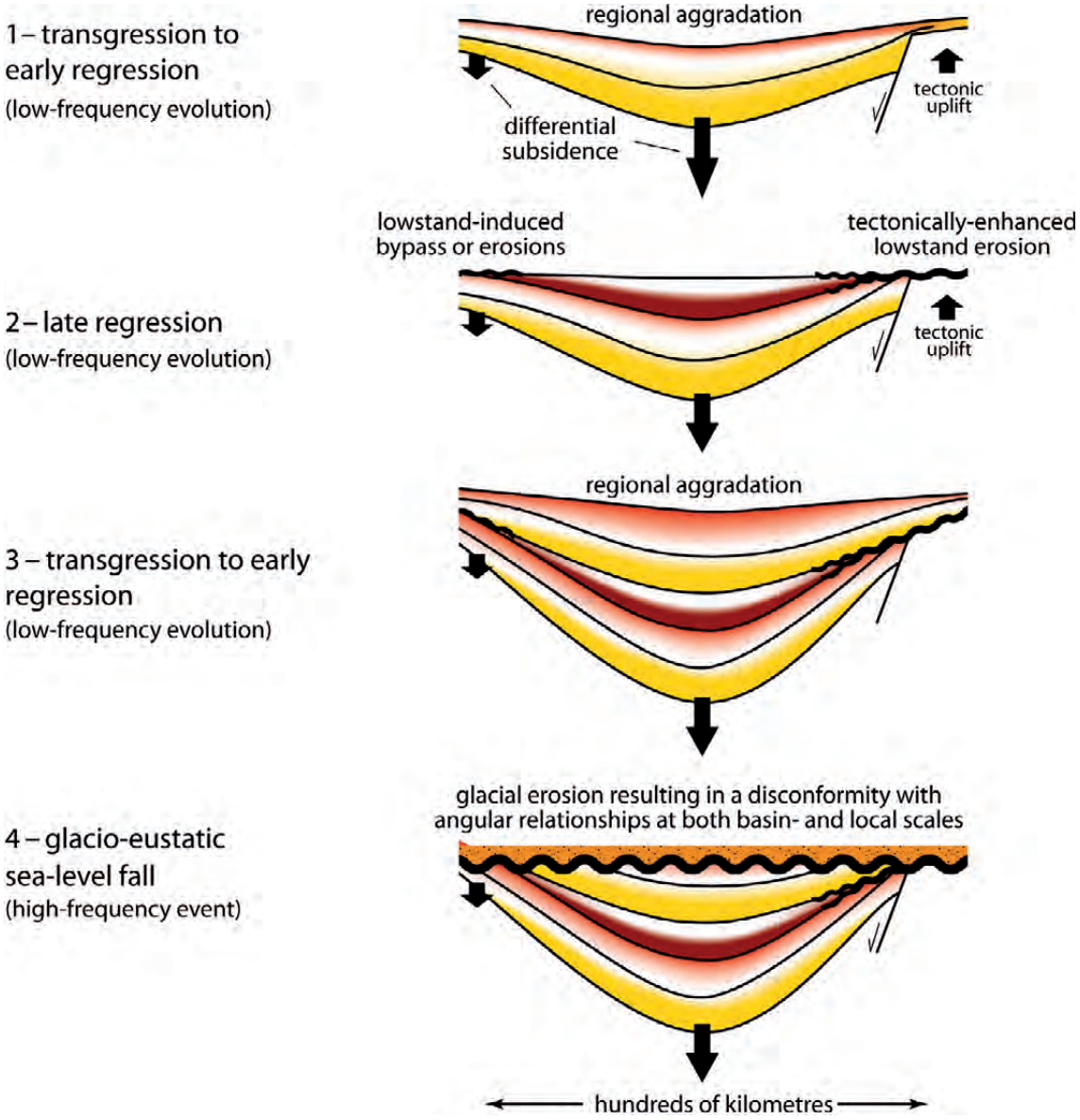

Figure 13. Sketch showing the generation of mappable angular unconformities. They do not represent unconformities related to short-lived tectonic phases but rather reflect large-scale geometries acquired on the long-term and highlighted by high-frequency eustatically-driven erosional truncations (see text for details).

nal tectonic events related to the separation of large continental blocks such as Avalonia (early Darriwilian: Prigmore *et al.* 1997) or the Hun Superterrane of Stampfli & Borel (2002) during the Upper Ordovician.

It is outside the scope of this paper to attempt to distinguish the eustatic and tectonic controls on Lower Palaeozoic depositional sequences. Here, because eroded thicknesses at each of the sequence boundaries are most probably limited to ten or tens of metres, we propose that the primary component for the development of depositional sequences in the Cambrian-Ordovician succession of the Ougarta Range is eustatic sea-level change. This is in agreement with the conclusions of Haq & Al-Qahtani (2005) who suggest from the Arabian record that during periods of tectonic quiescence, such as the Cambrian-Ordovician period, eustasy have been the significant controlling factor. That is illustrated in particular by essentially penecontemporaneous maximum flooding conditions from the Ougarta to the Arabian Plate (Sharland *et al.* 2001; Fig. 9). During periods of sea-level rise, accommodation related to sea-level change was cumulative with subsidence and thus attenuated the stratigraphic signature of potential tectonic uplift. Alternatively, during periods of sea-level fall, the long-term rate of sea-level fall durably exceeded rate of subsidence resulting in erosional unconformities and then amplifying the stratigraphic signature of

potential tectonic uplift. Mappable angular unconformities can appear in areas where differential subsidence rates existed prior to erosion (Fig. 13). They do not represent unconformities related to short-lived tectonic phases but large-scale geometries acquired on the long-term and highlighted by eustatically-driven erosional truncation corresponding to composite, amalgamated, subaerial or transgressive erosion surfaces during repeated high-frequency to short-term sea-level fluctuations. The more the amplitude of eustatic sea-level fall, the falsely greater the apparent tectonic event will appear (Fig. 13). Nevertheless, outside the Ougarta, localised but significant deformation events did occur close to Pan-African lineaments in response to stress at the continental margin. Such uplifts are well known in Algeria, where there might have resulted from the superimposition of Dapingian or early Darriwilian (*i.e.* Upper Arenig) strata on Tremadocian via an erosion surface (*e.g.*, Oulebsir & Paris 1995). In the Ahnet area, Beuf *et al.* (1971) have demonstrated that these uplifts were located above lithospheric structures prone to be reactivated.

A transgressive megasequence

From the Cambrian to Late Ordovician, successive depositional sequences show: (1) progressive disappearance of fluvial facies; (2) thinning of transgressive system tracts; and (3) development of repetitive open marine conditions from the lower part of sections onwards and from the NW to the SE Ougarta. These relationships that designate retrogradational architecture on the long term indicate that the Cambrian-Ordovician succession corresponds to a first-order transgressive system resulting in a step-by-step flooding of the North African Platform. This view do not support the Sharland *et al.* (2001) stratigraphic scheme, within which the Cambrian-Ordovician succession represents as a whole a single tectono-stratigraphic sequence.

The preservation of this thick transgressive system, though deposited in the context of a continuously rising eustatic sea level, implies in addition the progressive southeastward migration of the depositional edge from the Cambrian to the Ordovician. While a continuously subsiding platform occurred toward the north (*e.g.*, Anti-Atlas), subsidence was initiated in progressively more and more southern areas with differential subsidence patterns, contrasting depositional troughs and basement highs. Timing of this overall onlap relationship of Cambrian-Ordovician strata on the basement is supported by biostratigraphy and provenance studies. First, open marine conditions reached the most internal areas of the platform only during the Upper Ordovician. Near the Algeria-Mali boundary, *i.e.* 600 km south of the Ahnet area (right section in Fig. 10), Gatinski *et al.* (1966) documented the occurrence of biostratigraphically dated Upper Ordovician deposits bearing graptolites, trilobites and brachiopods above a thin (< 20 m) cross-stratified barren sandstone unit resting on the Neoproterozoic basement. Second, studies based on detrital zircons show that those of Pan-African age are predominant in Cambrian strata (matching the more arkosic nature of the sandstones) whereas they progressively disappear in parallel with the significant increase in proportion of zircons with older ages (> 1Ga). Therefore, the blanketing of the Pan-African sediment source is inferred and a many hundreds of kilometres southward migration of the source area is suggested (Avigad *et al.* 2003, Kolodner *et al.* 2006).

The Ordovician maximum flooding

If the Cambrian-Ordovician succession represents a transgressive system for the North Gondwana Lower Palaeozoic strata, what is the corresponding maximum flooding surface? (*i.e.* the stratigraphic surface marking in the long term the end of the shoreline transgression and separating retrograding to prograding strata).

It is generally recognised that higher eustatic sea levels were achieved during the Late, but not the latest, Ordovician (*e.g.*, Ross & Ross 1992, Nielsen 2004, Haq & Al-Qahtani 2005). The first-order maximum flooding surface (MFS) representing the culmination of the Cambrian-Ordovician shoreline transgression should have been Late Ordovician or older. Without the incidence of the Hirnantian glaciation, the Ordovician MFS should have been coincident with one of the second-order maximum flooding surfaces between the Middle and the Upper Ordovician, depending on relationships between rates of long-term sea-level rise and subsidence. Spatial variations in subsidence may induce stratigraphic sequence distortion with the onset of progradation delayed in the more subsiding area (Robin *et al.* 2005). In areas experiencing limited subsidence (~ 5–10 m/Ma, *e.g.*, the Taoudeni Basin in Mauritania or the Murzuq Basin in Libya), the Ordovician MFS might have occurred as early as the lower Middle Ordovician (early Darriwilian, *i.e. formosa* event *sensu* Paris *et al.* 2007 of early Llanvirn age), when rates of sea-level rise were greater, resulting in a general backstepping of the shorelines throughout the platform. In more subsiding areas such as the Ougarta (~ 10–20 m/Ma), or the Anti-Atlas (> 30 m/Ma), the Ordovician MFS may have been notably younger (Late Ordovician) and have been established when rate of sea-level rise had already noticeably declined. However, it must be born in mind that some restrictions to this oversimplified view such as long-term basinward migration of the shoreline from an internal and slowly subsiding area, which experienced sediment bypass or reworking, toward distal faster subsiding areas, most probably forced

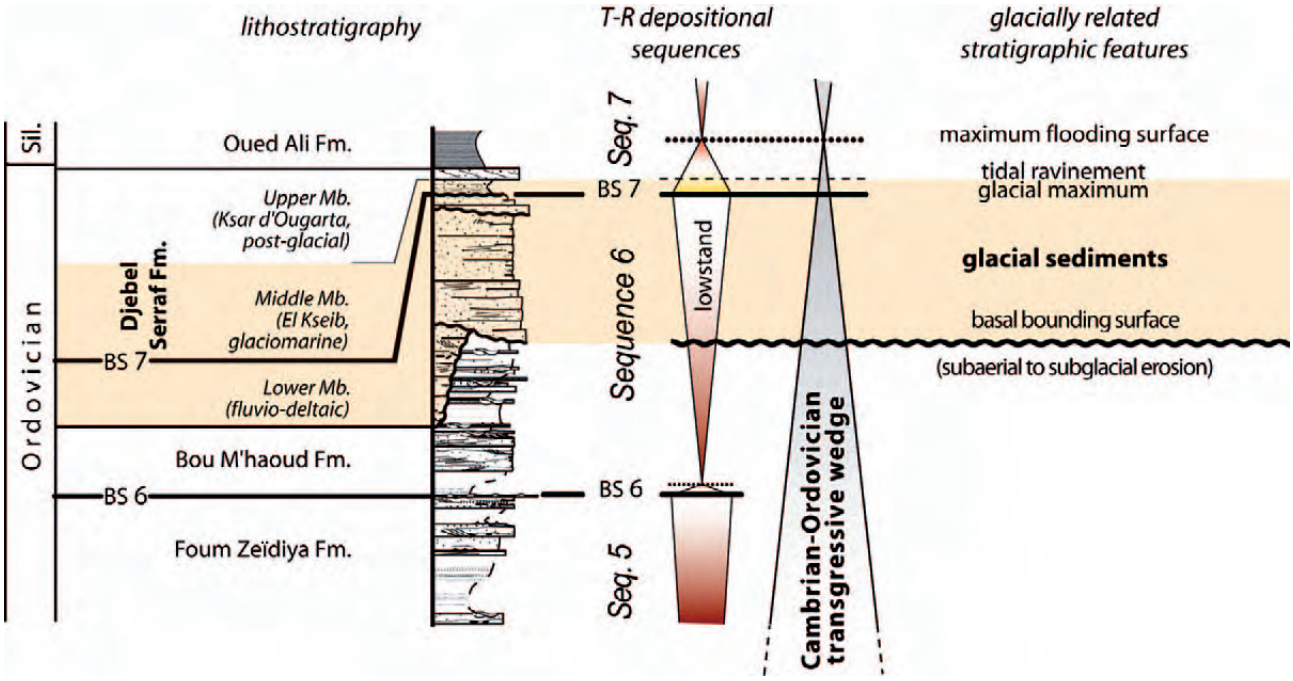

Figure 14. The Hirnantian glacial event in the context of the Cambrian-Ordovician transgression. Just before the end of this first-order, continent-wide transgression initiating in the Cambrian, the high-frequency Late Ordovician glaciation and especially the Hirnantian event only temporarily perturbed its overall backstepping trend.

the onset of progradation in the latter. Nevertheless, at the scale of a north Gondwana basinal area such as the Ougarta, these relationships may be used to explain some timing discrepancies between sedimentary basins.

The occurrence of the Hirnantian glaciation that mimics a major regressive trend, responsible for high-frequency sea-level fluctuations, with the development of extensive sand-dominated fluvio-deltaic strata has to be discussed in the context of the final stages of this Cambrian-Ordovician transgression (Fig. 14).

Significance of the Late Ordovician glacial event

The basal bounding surface of the glacially related strata is considered as an ideal allostratigraphic discontinuity (Fig. 14). It is well defined and synchronous (base of Hirnantian) at the geological time scale everywhere in North Gondwana (Ghienne *et al.* in press and references therein). Based on its prominent erosional character, this bounding surface is generally considered to be a major unconformity that includes a tectono-stratigraphic component and separating two major, long-term depositional sequences (Sharland *et al.* 2001, Carr 2002, Eschard *et al.* 2005). The overlying glacially related strata are sometimes regarded as an individual major depositional sequence (Fekirine & Abdallah 1998, Eschard *et al.* 2005). However, using a system of sequence hierarchy based on boundary frequency, we consider that this surface has no greater significance than that of other sequence boundaries documented in the underlying Cambrian-Ordovician succession. The surface can be ascribed to a subaerial (to subglacial) erosion underlining a lowstand wedge of an Exxon-type depositional sequence. Based on the restricted (0.5–2 Ma) time interval that corresponds to the Hirnantian glaciation (Brenchley *et al.* 1994, 2003; Paris *et al.* 1995; Sutcliffe *et al.* 2000; Ghienne *et al.* in press), we consider that glacially related strata cannot be assimilated alone into a depositional sequence but rather represent a short-term sequence or possibly at most a couple of genetic units.

Using transgressive surfaces for the delineation of T-R depositional sequences, a seventh bounding surface is naturally identified within the glacially related strata (Fig. 14). It corresponds to the glacial surface constituting the lower bounding surface of the glaciomarine deposits (middle member of the Djebel Serraf Fm.) above which a noticeable transgressive trend is expressed from glacial environments to non-glacial offshore shelf environments (Fig. 6). This surface most probably reflects the Hirnantian ice-maximum, which usually occurs in the upper half of the glacial wedge (Ghienne *et al.* in press), a correlation that makes sense with overlying strata deposited during an overall sea-level rise. Whereas the geometry of this surface essentially results from glacial erosion, its stratigraphic significance corresponds to a transgressive surface. It over-

lies fluvio-deltaic deposits at the top of the regressive system tract of the sixth depositional sequence and then forms the basal bounding surface of a seventh T-R depositional sequence.

Similar relationships, attributing the younger Hirnantian glacial strata to a transgressive system tract extending in the Silurian have also been described from the glacial record in Mauritania (Ghienne 2003). A maximum flooding surface can be pointed out for this seventh sequence in the lowermost Silurian (Lüning *et al.* 2000, surface S10 of Sharland *et al.* 2001), a time interval from which the shoreline renewed to migrate northward and even if deepening conditions were maintained northward by a low rate of offshore transport and locally by subsidence patterns. The seventh depositional sequence further includes the overlying Silurian strata, which correspond throughout North Gondwana to a well known prograding wedge (Bellini & Massa 1980, Lüning *et al.* 2000, Eschard *et al.* 2005) constituting its regressive system tract.

The Hirnantian glaciation has been responsible for: (i) considerable basal erosion, affecting the whole of the platform, with erosion depths in places greater than 300 m (Ghienne *et al.* in press, and references therein); (ii) the onset of continental conditions, either fluvial or subglacial, which arose quite instantaneously throughout the platform with sedimentation directly influenced by glaciers recognised from the Anti-Atlas to Southern Algeria; and (iii) very high rates of sea-level change, both within and at the end of the glaciation (post-glacial transgression). The glacial erosion, which was deeper and faster than all other preglacial erosion processes, led to a stratigraphic discontinuity along which latest Ordovician rests at first-order on progressively older strata toward the south (Fig. 10); Upper Ordovician to the north of the platform (*e.g.*, Destombes 1968a, b, Bourahrouh *et al.* 2004), then Middle and Lower Ordovician in intermediate areas (*e.g.*, Oulebsir & Paris 1995) and then Cambrian or basement rocks southwards (Beuf *et al.* 1971). The discontinuity, angular at the basin scale, truncates noticeably older basin-wide or localised syn-depositional deformation structures, falsely suggesting a major tectonic deformation event, sometimes related to the so-called Taconic unconformity, which would have occurred just prior to glaciation onset (*e.g.*, Crossley & McDougall 1998, Eschard *et al.* 2005). For example, in a number of areas located between the Ahnet and the Ougarta (figured by an oversimplified horst structure in Fig. 10), glacial strata rest on Lower Ordovician or Cambrian strata (Legrand 1985). This unconformable contact, highlighted by glacial erosion, is regarded as mainly reflecting deformation structures that affected deposition during the late Early Ordovician (Beuf *et al.* 1971; Fig. 13). In our scheme, there is no reason to attribute any tectono-stratigraphic value to the basal bounding surface of the glacially related strata.

The subsequent post-glacial transgression, which was very fast relative to the Cambrian-Ordovician tempo, resulted in a non-accretionary transgression (*e.g.*, Helland-Hansen & Gjellberg 1994) with a drastic southward backstepping of the shoreline during which post-glacial sedimentation dominated over the main part of the platform with in-situ wave or tidal reworking (Fig. 7; *e.g.*, Ghienne 2003, Moreau 2005). As a consequence, the combination of glacial erosion and post-glacial high rate of sea-level rise forced shorelines to shift drastically to the south. Early Silurian shorelines reach the south of the Koufra Basin (Libya-Chad boundary; Lüning *et al.* 2000), and were located south of the Djado area in Niger (Legrand 2003, Denis *et al.* 2007) or to the SE of the Hodh area in Mauritania (Paris *et al.* 1998, Ghienne 2003). From these southern locations, Silurian shorelines have then migrated throughout the platform to the NW (Bellini & Massa 1980, Lüning *et al.* 2000).

Conclusions

The Silurian flooding on the North Gondwana platform may be regarded as the end product of the Cambrian-Ordovician transgression, with specific features enhanced by the high-frequency Hirnantian glacial event. High sea levels of the Late Ordovician period were abruptly restored on the platform with latest Ordovician shorelines shifted southward relative to all other Late Ordovician shorelines. The global and virtually instantaneous nature of the Hirnantian glacial event has "synchronised" the stratigraphic architecture of the succession throughout the platform. At the end of the post-glacial transgression, a second-order maximum flooding occurred everywhere, whatever the local rate of subsidence, near the Ordovician-Silurian boundary or more probably within the earliest Silurian. This event, which also marks the first-order inversion trend between generally retrograding strata of the Cambrian-Ordovician succession and a prograding Siluro-Devonian wedge, corresponds to the maximum flooding of the Lower Palaeozoic transgressive-regressive megasequence in North Africa. Just before the end of this first-order, continent-wide transgression initiating in the Cambrian, the Late Ordovician glaciation, and especially the Hirnantian event, only temporarily perturbed its overall backstepping trend.

Acknowledgments

The authors are indebted to the SONATRACH (Algerian National Oil Company) for logistic and scientific support during fieldwork in the Algerian Sahara. One of us (B.V.) benefited from a post-doctoral grant from TOTAL S.A. The authors are grateful to J. Frýda, M. Mergl and P. Štorch (Czech Republic) as well as

E. Villas (Spain), M. Vidal and J. Vannier (France) for preliminary faunal identifications. They also thank O. Fatka, P. Kraft and O.E. Sutcliffe, for reviewing and greatly improving the manuscript. This is a contribution of EOST (Ecole et Observatoire des Sciences de la Terre) number 2007.501 – UMR 7517 to the ECLIPSE II (CNRS, France) and to IGCP 503 projects.

References

ALBANI, R., MASSA, D. & TONGIORGI, M. 1991. Palynostratigraphy (Acritarchs) of some Cambrian beds from the Rhadames (Ghadamis) Basin (Western Libya–Southern Tunisia). *Bolletino della Società Paleontologica Italiana 30, 255–280.*

ÁLVARO, J.J., VAN VLIET-LANOË, B., VENNIN, E. & BLANC-VALLERON, M.M. 2003a. "Lower" Cambrian paleosols from the Cantabrian Mountains (northern Spain): a comparison with Neogene-Quaternary analogues. *Sedimentary Geology 163*, 67–84.

ÁLVARO, J.J., GONZÁLEZ-GÓMEZ, C. & VIZCAÏNO, D. 2003b. Paleogeographic patterns of the Cambrian-Ordovician transition in the southern Montagne Noire (France): preliminary results. *Bulletin de la Société géologique de France 174/3*, 23–31.

ARBEY, F. 1962. Données nouvelles sur la sédimentation au Cambro-Ordovicien dans les Monts d'Ougarta (Saoura). *Comptes rendus de l'Académie des sciences, Paris 254*, 3726–3728.

ARBEY, F. 1968. Structures et dépôts glaciaires dans l'Ordovicien terminal des chaînes d'Ougarta (Sahara algérien). *Comptes rendus de l'Académie des sciences, Paris 268*, 76–78.

ARBEY, F. 1971. Glacio-tectonique et phénomènes périglaciaires dans les dépôts siluro-ordoviciens des monts d'Ougarta (Sahara algérien). *Comptes rendus de l'Académie des sciences, Paris 273*, 854–857.

ARBEY, F. 1988. *Diagénèses précoces et tardives: silicifications et roches silico-détritiques*. 521 pp. Thèse de doctorat d'état, Université de Paris-Sud, France.

ARBEY, F. & CABY, R. 1966. Présence de dreikanters à la base du Cambrien de la Sebkha el Melah; remarques sur la discordance du Paléozoïque et sur l'âge du soubassement dans la région des Monts d'Ougarta (Sahara algérien). *Comptes rendus sommaires de la Société géologique de France*, 63–64.

AVIGAD, D., KOLODNER, K., MCWILLIAMS, M., PERSING, H. & WEISSBROD, T. 2003. Origin of northern Gondwana Cambrian sandstone revealed by detrital zircon SHRIMP dating. *Geology 31*, 227–230.

AVIGAD, D., SANDLER, A., KOLODNER, K., STERN, R.J., MCWILLIAMS, M., MILLER, N. & BEYTH, M. 2005. Mass-production of Cambro-Ordovician quartz-rich sandstone as a consequence of chemical weathering of Pan-African terranes: environmental implications. *Earth and Planetary Science Letters 240*, 818–826.

BELLINI, E. & MASSA, D. 1980. A stratigraphic contribution to the Paleozoic of the Southern Basins of Libya, 1–56. *In* SALEM, M.J. & BUSWELL, M.T. (eds) *Geology of Libya I.* Academic Press, London.

BENOÎT, A. & TAUGOURDEAU, P. 1961. Sur quelques chitinozoaires de l'Ordovicien du Sahara. *Revue de l'Institut Français du Pétrole 16*, 1403–1421.

BEUF, S., BIJU-DUVAL, B., DE CHARPAL, O., ROGNON, P., GARIEL, O. & BENNACEF, A. 1971. *Les grès du Paleozoïque inférieur au Sahara.* 464 pp. Science et Technique du Pétrole 18, Paris.

BOOTE, D.R.D., CLARK-LOWES, D.D. & TRAUT, M.W. 1998. Paleozoic petroleum systems of North Africa, 7–68. *In* MACGREGOR, D.S., MOODY, R.T.J. & CLARK-LOWES, D.D. (eds) *Petroleum Geology of North Africa, Geological Society London Special Publication 132.*

BOURAHROUH, A., PARIS, F. & ELAOUAD-DEBBAJ, Z. 2004. Biostratigraphy, biodiversity and palaeoenvironments of the chitinozoans and associated palynomorphs from the Upper Ordovician of the Central Anti-Atlas, Morocco. *Palaeogeography, Palaeoclimatology, Palaeoecology 130*, 17–40.

BRENCHLEY, P.J., ROMANO, M. & GUTIÉRREZ-MARCO, J.C. 1986. Proximal and distal hummocky cross-stratification facies on a wide Ordovician shelf in Iberia, 241–255. *In* KNIGHT, R.J. & MCLEAN, J.R. (eds) *Shelf sands and sandstones. Memoir Canadian Society Petroleum Geologists II*.

BRENCHLEY, P.J., MARSHALL, J.D., CARDEN, G.A.F., ROBERTSON, D.B.R., LONG, D.G.F., MEIDLA, T., HINTS, L. & ANDERSON, T.F. 1994. Bathymetric and isotopic evidence for a short-lived Late Ordovician glaciation in a greenhouse period. *Geology 22*, 295–298.

BRENCHLEY, P.J., CARDEN, G.A., HINTS, L., KALJO, D., MARSHALL, J.D., MARTMA, T., MEIDLA, T. & NOLVAK, J. 2003. High-resolution stable isotope stratigraphy of Upper Ordovician sequences: Constraints on the timing of bioevents and environmental changes associated with mass extinction and glaciation. *Bulletin of the Geological Society of America 115*, 89–104.

BURKE, K. & KRAUS, J.U. 2000. Deposition of immense Cambro-Ordovician sandstone bodies, now exposed mainly in north Africa and Arabia, during the aftermath of the final assembly of Gondwana. *Geological Society of America Abstracts with Program 32(7)*, 249.

BURKHARD, M., CARITG, S., HELG, U., ROBERT-CHARRUE, C. & SOULAIMANI, A. 2006. Tectonics of the Anti-Atlas of Morocco. *Comptes Rendus Geosciences 338,* 11–24.

CABY, R. 1996. Rapport de mission de terrain dans le Grand Sud-Ouest Algérien. *Mémoires du Service géologique d'Algérie 8*, 49–51.

CARR, I.D. 2002. Second-order sequence stratigraphy of the Palaeozoic of North Africa. *Marine Petroleum Geology 25*, 259–280.

CATUNEANU, O. 2002. Sequence stratigraphy of clastic systems: concepts, merits, and pitfalls. *Journal of African Earth Science 35*, 1–43.

CATUNEANU, O., WILLIS, A.J. & MIALL, A.D. 1998. Temporal significance of sequence boundaries. *Sedimentary Geology 121*, 157–178.

CLIFTON, H.E. 1976. Wave-formed sedimentary structures – a conceptual model, 126–148. *In* DAVIS, R.A., JR. & ETHINGTON, R.L. (eds) *Beach and Nearshore Sedimentation. Society of Economic Paleontogists and Mineralogists, Special Publication 24.*

CROSSLEY, R. & MCDOUGALL, N. 1998. Lower Palaeozoic reservoirs of North Africa, 157–166. *In* MACGREGOR, D.S., MOODY, R.T.J. & CLARK-LOWES, D.D. (eds) *Petroleum Geology of North Africa. Geological Society London Special Publication 132*.

DABARD, M.P., LOI, A. & PARIS, F. 2007. Relationship between phosphogenesis and sequence architecture: sequence stratigraphy and biostratigraphy in the Middle Ordovician of the Armorican Massif (W France). *Palaeogeography, Palaeoclimatology, Palaeoecology 248*, 339–356.

DEAN, W.T. 2005. Trilobites from the Cal Tepe Formation (Cambrian), near Seydisehir, Central Taurides, south-western Turkey. *Turkish Journal of Earth Sciences 13*, 1–71.

DEAN, W.T. & MONOD, O. 1990. Revised stratigraphy and relationships of Lower Palaeozoic rocks, eastern Taurus Mountains, south central Turkey. *Geological Magazine 127*, 333–347.

DENIS, M., BUONCRISTIANI, J.-F., KONATÉ, M., GHIENNE, J.-F. & GUIRAUD, M. 2007. Hirnantian glacial and deglacial record in SW Djado Basin (NE Niger). *Geodinamica Acta 20(3)*, 177–194.

DESTOMBES, J. 1968a. Sur la présence d'une discordance générale de ravinement d'âge Ashgill supérieur dans l'Ordovicien terminal de l'Anti-Atlas (Maroc). *Comptes rendus de l'Académie des sciences, Paris 267 D,* 565–567.

DESTOMBES, J. 1968b. Sur la nature glaciaire des sédiments du groupe du 2^{e} Bani, Ashgill supérieur de l'Anti-Atlas, Maroc. *Comptes rendus de l'Académie des sciences, Paris 267 D,* 684–686.

DESTOMBES, J. & FEIST, R. 1987. Découverte du Cambrien supérieur en Afrique (Anti-Atlas, Maroc). *Comptes rendus de l'Académie des sciences, Paris 304*, 719–724.

DESTOMBES, J., HOLLART, H. & WILLEFERT, S. 1985. Lower Paleozoic rocks of Morocco, 291–325. *In* HOLLAND, C.H. (ed.) *Lower Paleozoic Rocks of northwest and west Central Africa*. John Wiley, New York.

DEYNOUX, M. 1985. Terrestrial or waterlain glacial diamictites? Three case studies from the Late Precambrian and Late Ordovician glacial drifts in West Africa. *Palaeogeography, Palaeoclimatology, Palaeoecology 51*, 97–141.

DEYNOUX, M., SOUGY, J. & TROMPETTE, R. 1985. Lower Paleozoic rocks of West Africa and the western part of Central Africa, 337–495. *In* HOLLAND, C.H. (ed.) *Lower Paleozoic Rocks of northwest and west Central Africa.* John Wiley, New-York.

DEYNOUX, M. & GHIENNE, J.-F. 2004. Late Ordovician glacial pavements revisited – a reappraisal of the origin of striated surfaces. *Terra Nova 16*, 95–101.

DEYNOUX, M., AFFATON, P., TROMPETTE, R. & VILLENEUVE, M. 2006. Pan-African tectonic evolution and glacial events registered in Neoproterozoic to Cambrian cratonic and foreland basins of West Africa. *Journal of African Earth Science 46*, 397–426.

DONZEAU, M. 1971. *Etude structurale dans le Paléozoïque des Monts d'Ougarta.* 100 pp. Thèse de doctorat, Faculté des Sciences, Orsay, France.

DONZEAU, M. 1974. L'Arc Anti-Atlas – Ougarta (Sahara nord-occidental, Algérie-Maroc). *Comptes rendus de l'Académie des sciences, Paris 278*, 417–420.

DONZEAU, M. 1983. Tectonique des monts d'Ougarta, 118–120. *In* FABRE, J. (ed.) *Afrique de l'Ouest, Introduction Géologique et termes stratigraphiques. Lexique stratigraphique international, Nouvelle série 1*. Pergamon Press, Oxford.

DUMAS, S. & ARNOTT, R.W.C. 2006. Origin of hummocky and swaley cross-stratification – The controlling influence of unidirectional current strength and aggradation rate. *Geology 34*, 1073–1076.

ELAOUAD-DEBBAJ, Z. 1987. *Acritarches et Chitinozoaires de l'Ordovicien du Maroc. Systématique, Biostratigraphie, corrélations*. 310 pp. Thèse de doctorat, Université de Rennes I (unpublished).

ELAOUAD-DEBBAJ, Z. 1988. Acritarches et chitinozoaires du Tremadoc de l'Anti Atlas central (Maroc). *Revue de micropaléontologie 31*, 85–128.

EMBRY, A.F. 1995. Sequence boundaries and sequences hierarchies: problems and proposals, 1–11. *In* STEEL, R.J., FELT, V.L., JOHANNESEN, E.P. & MATHIEU, C. (eds) *Sequence stratigraphy on the Northwest European Margin. Norwegian Petroleum Society, Special Publication 5.*

ENNIH, N. & LIÉGEOIS, J.-P. 2001. The Moroccan Anti-Atlas: the West African passive margin with limited Pan-African activity. *Precambrian Research 112*, 289–302.

ESCHARD, R., ABDALLAH, H., BRAIK, F. & DESAUBLIAUX, G. 2005. The Lower Paleozoic succession in the Tasilli outcrops, Algeria: sedimentology and sequence stratigraphy. *First Break 23*, 27–36.

FABRE, J. 1988. Les séries paléozoïques d'Afrique: une approche. *Journal of African Earth Science 7*, 1–40.

FABRE, J. 2005. Le Précambrien terminal – Cambrien: glaciation et enterrement d'une chaîne panafricaine, 117–144. *In* FABRE, J. (ed.) *Géologie du Sahara occidental et central. Tervuren African Geoscience Collection 108*. Musée Royal de l'Afrique Centrale, Tervuren.

FABRE, J. & KAZI-TANI, N. 2005. Ordovicien, Silurien, Devonien, Permo-Carbonifère, 147–360. *In* FABRE, J. (ed.) *Géologie du Sahara occidental et central. Tervuren African Geoscience Collection 108*. Musée Royal de l'Afrique Centrale, Tervuren.

FABRE, J., AIT-KACI, A., BOUIMA, T. & MOUSSINE-POUCHKINE, A. 1988. Le cycle molassique dans le rameau trans-saharien de la chaîne panafricaine. *Journal of African Earth Science 7*, 41–55.

FAIK, F., BELFOUL, M.A., BOUABDELLI, M. & HASSENFORDER, B. 2001. Les structures de la couverture Néoprotérozoïque terminal et Paléozoïque de la region de Tata, Anti-Atlas centre occidental, Maroc: deformation polyphasée, ou interactions socle/couverture pendant l'orogenèse hercynienne. *Journal of African Earth Science 32*, 765–776.

FEKIRINE, B. & ABDALLAH, H. 1998. Palaeozoic lithofacies correlatives and sequence Stratigraphy of the Sahara Platform, Algeria, 97–108. *In* MACGREGOR, D.S., MOODY, R.T.J. & CLARK-LOWES, D.D. (eds) *Petroleum Geology of North Africa. Geological Society London Special Publication 132*.

GATINSKI, G., KLOTCHKI, V.P., ROZMAN, K.S. & TROFIMOV, D.M. 1966. Nouvelles données sur la stratigraphie des dépôts paléozoïques du Sahara méridional. *Doklady Akademii nauk SSSR 170*, 1154–1157.

GHIENNE, J.-F. 2003. Late Ordovician sedimentary environments, glacial cycles, and post-glacial transgression in the Taoudeni Basin, West Africa. *Palaeogeography, Palaeoclimatology, Palaeoecology 189*, 117–145.

GHIENNE, J.-F. & DEYNOUX, M. 1998. Large-scale channel fill structures in Late Ordovician glacial deposits in Mauritania, western Sahara. *Sedimentary Geology 119*, 141–159.

GHIENNE, J.-F., LE HERON, D., MOREAU, J., DENIS, M. & DEYNOUX, M. In press. The Late Ordovician glacial sedimentary system of the North Gondwana platform. *In* HAMBREY, M., CHRISTOFFERSEN, P., GLASSER, N., JANSSEN, P., HUBBARD, B. & SIEGERT, M. (eds) *Glacial sedimentary processes and products. International Association of Sedimentologists, Special Publication 39*. Blackwells, Oxford.

GOMEZ SILVA, M., PACAUD, M. & WIEL, F. 1963. Contribution à l'étude du Cambro-Ordovician des chaînes d'Ougarta (Sahara algérien). *Bulletin de la Société géologique de France 7*, 134–141.

GUTIÉRREZ-MARCO, J.C., DESTOMBES, J., RÁBANO, I., ACEÑOLAZA, G.F., SARMIENTO, G.N. & SAN JOSÉ, M.A. 2003. El Ordovícico Medio del Anti-Atlas marroquí: paleobiodiversidad, actualización bioestratigráfica y correlación. *Geobios 36*, 151–177.

HAMPSON, G.J. 2000. Discontinuity surfaces, clinoforms, and facies architecture in a wave-dominated, shoreface-shelf parasequence. *Journal of Sedimentary Research 70*, 325–340.

HAQ, B.U. & AL-QAHTANI, A.M. 2005. Phanerozoic cycles of sea-level change on the Arabian Platform. *GeoArabia 10*, 127–160.

HAQ, B.U., HARDENBOL, J. & VAIL, P.R. 1987. Chronology of fluctuating seal levels since the Triassic. *Science 235*, 1156–1166.

HARMS, J.C., SOUTHARD, J.B. & WALKER, R.G. 1982. Structures and sequences in clastics rocks. *Society for Sedimentary Geology (SEPM) Short Course 9*, 1–253.

HART, B.S. & PLINT, A.G. 1989. Gravelly shoreface deposits; a comparaison of modern and ancient facies sequences. *Sedimentology 36*, 551–557.

HELLAND-HANSEN, W. & GJELLBERG, J.G. 1994. Conceptual basis and variability in sequence stratigraphy: a different perspective. *Sedimentary Geology 92*, 31–52.

HERVOUET, Y. & DUEE, G. 1996. Analyse morphostructurale par imagerie satellitaire et coupes structurales modélisées des monts d'Ougarta (Sahara occidental, Algérie): une chaîne hercynienne chevauchante à plis passifs. *Mémoires du Service géologique de l'Algérie 8,* 127–173.

HIRST, J.P.P., BENBAKIR, A., PAYNE, D.F. & WESTLAKE, I.R. 2002. Tunnel valleys and density flow processes in the upper Ordovician glacial succession, Illizi Basin, Algeria: influence on reservoir quality. *Marine Petroleum Geology 25*, 297–324.

KICHOU-BRAÏK, F., SAMAR, L., FEKIRINE, B. & LEGRAND, P. 2006. Découverte de graptolites d'âge Caradocien dans quelques sondages du Tinrhert (Sahara algérien). *Comptes Rendus Palevol 5(5)*, 675–683.

KILIAN, C. 1922. Aperçu général de la structure des Tassilis, des Ajjers. *Comptes rendus de l'Académie des sciences, Paris 175*, 825–827.

KOLODNER, K., AVIGAD, D., MCWILLIAMS, M., WOODEN, J.L., WEISSBROD, T. & FEINSTEIN, S. 2006. Provenance of north Gondwana Cambrian-Ordovician sandstone: U-Pb. SHRIMP dating of detrital zircons from Israel and Jordan. *Geological Magazine 143*, 367–391.

LANDING, E., GEYER, G. & HELDMAIER, W. 2006. Distinguishing eustatic and epeirogenic controls on Lower-"Middle" Cambrian boundary successions in West Gondwana (Morocco and Iberia). *Sedimentology 54*, 899–918.

LASKAR, J. 1999. The limits of Earth orbital calculations for geological time-scale use. *Philosophical Transactions of the Royal Society of London A 357*, 1735–1759.

LECKIE, D.A. 1988. Wave-formed, coarse-grained ripples and their relationship to hummocky cross-stratification. *Journal of Sedimentary Petrology 58*, 607–622.

LEDRU, P., AUTRAN, A. & SANTALLIER, D. 1994. Lithostratigraphy of Variscan terranes in the French Massif Central: a basis for paleogeographical reconstruction, 226–288. *In* KEPPIE, J.D. (ed.) *Pre-Mesozoic geology in France and related areas*. Springer, Berlin.

LE HERON, D.P., SUTCLIFFE, O.E., WHITTINGTON, R.J. & CRAIG, J. 2005. The origins of glacially related soft-sediment deformation structures in Upper Ordovician glaciogenic rocks: implication for ice sheet dynamics. *Palaeogeography, Palaeoclimatology, Palaeoecology 218*, 75–103.

LEGRAND, P. 1964. Un graptolite intéressant de l'Arénigien supérieur du Sahara algérien: Didymograptus v-fraactus wieli nov. subsp. *Comptes rendus sommaires de la Société géologique de France 9*, 360–363.

LEGRAND, P. 1966. Précisions biostratigraphiques sur l'Ordovicien inférieur et le Silurien des chaînes de l'Ougarta (Sahara algérien). *Comptes rendus sommaires de la Société géologique de France 97,* 243–245.

LEGRAND, P. 1974. Essai sur la paléogéographie de l'Ordovicien du Sahara algérien. *Compagnie Française des Pétroles, Notes et Mémoires 11*, 121–138.

LEGRAND, P. 1985. Lower Palaeozoic rocks of Algeria, 5–89. *In* HOLLAND, C.H. (ed.) *Lower Paleozoic Rocks of northwest and west Central Africa*. John Wiley, New York.

LEGRAND, P. 1988. The Ordovician-Silurian boundary in the Algerian Sahara, 139–143. *In* COCKS, L.R.M. & RICKARDS, R.B. (eds) A global analysis of the Ordovician-Silurian boundary. *Bulletin of the British Museum (Natural History), Geology 43*.

LEGRAND, P. 2003. Paléogeographie du Sahara algérien à l'Ordovicien terminal et au Silurien inférieur. *Bulletin de la Société géologique de France 174*, 19–32.

LEGRAND, P. & NABOS, G. 1962. Contribution à la stratigraphie du Cambro-Ordovicien dans le bassin saharien occidental. *Bulletin de la Société géologique de France 7*, 123–131.

LESSERTISSEUR, J. 1971. L'énigme du Daedalus (*Daedalus* Rouault, 1850). Ichnofossilia. *Bulletin du Muséum national d'histoire naturelle (Paris) 20*, 37–66.

LONG, D.G.F. 2004. Precambrian rivers, 660–663. *In* ERIKSSON, P.G., ALTERMANN, W., NELSON, D.R., MUELLER, W.U. & CATUNEANU, O. (eds) *The Precambrian Earth: Tempos and events (Developments in Precambrian geology) 12*. Elsevier, Amsterdam.

LÜNING, S., CRAIG, J., LOYDELL, D.K., ŠTORCH, P. & FITCHES, B. 2000. Lower Silurian 'hot shales' in North Africa and Arabia: regional distribution and depositional model. *Earth-Science Reviews 49*, 121–200.

MACNAUGHTON, R.B., DALRYMPLE, R.W. & NARBONNE, G.M. 1997. Early Cambrian braid-delta deposits, MacKenzie Mountains, north-western Canada. *Sedimentology 44*, 587–609.

MENCHIKOFF, N. 1933. La série primaire de la Saoura et des chaînes d'Ougarta. *Bulletin du Service de la Carte géologique d'Algérie 11*, 109–123.

MIALL, A.D. 1997. *The geology of stratigraphic sequences.* 433 pp. Springer-Verlag, Berlin.

MOREAU, J. 2005. *Architecture stratigraphique et dynamique des dépôts glaciaires ordoviciens du Bassin de Murzuk (Libye).* 192 pp. Thèse de doctorat, Université Louis Pasteur, Strasbourg, France (unpublished).

NIELSEN, A.T. 2004. Ordovician sea level changes: A Baltoscandian perspective, 83–94. *In* WEBBY, B.D., PARIS, F., DROSER, M. & PERCIVAL, I. (eds) *The Great Ordovician diversification event*. Columbia University Press, New York.

NIO, S.-D. & YANG, C.-S. 1991. Diagnostic attributes of clastic tidal deposits: a review, 3–28. *In* SMITH, D.G., REINSON, B., ZAITLIN, B.A. & RAHMANI, R.A. (eds) *Clastic tidal sedimentology. Canadian Society of Petroleum Geologists Memoir 16*.

ORGM (OFFICE NATIONAL DE LA RECHERCHE GÉOLOGIQUE) 2000. *Kerzaz. Carte géologique de l'Algérie à 1/200.000*. Service géologique de l'Algérie, Boumerdès.

OULEBSIR, L. & PARIS, F. 1995. Chitinozoaires ordoviciens du Sahara algérien: biostratigraphie et affinités paléogéographiques. *Review of Palaeobotany and Palynology 86*, 49–68.

PARIS, F. 1990. The Ordovician chitinozoan biozones of the Northern Gondwana Domain. *Review of Palaeobotany and Palynology 66,* 181–209.

PARIS, F., ELAOUAD-DEBBAJ, Z., JAGLIN, J.C., MASSA, D. & OULEBSIR, L. 1995. Chitinozoans and Late Ordovician glacial events on Gondwana, 171–176. *In* COOPER, D., DROSER, M.L. & FINNEY, S. (eds) *Ordovician Odyssey, Short papers for the seventh international symposium on the Ordovician System*. SEPM, Fullerton, California.

PARIS, F., DEYNOUX, M. & GHIENNE, J.-F. 1998. Chitinozoaires de la limite Ordovicien-Silurien en Mauritanie. *Comptes rendus de l'Académie des sciences, Paris 326*, 499–504.

PARIS, F., BOUMENDJEL, K., DABARD, M.P., GHIENNE, J.-F., LOI, A., TANG, P., VIDET, B. & ACHAB, A. 2007. Chitinozoan-based calibration of Early-Mid Ordovician transgressive events on northern Gondwana. *Acta Palaeontologica Sinica 46*, 370–375.

PILLOLA, G.L., LEONE, F. & LOI, A. 1998. The Cambrian and Early Ordovician of SW Sardinia. *Giornale di Geologia (Spec. Issue ECOS VII – Sardinia Guidebook) 60*, 25–38.

POSAMENTIER, H.W. 2001. Lowstand alluvial bypass systems: incised vs. unincised. *Bulletin American Association Petroleum Geologist 85*, 1771–1793.

POUEYTO, A. 1952. Rhyolites et Grès d'Ougarta, Terrains Gothlandiens, 25–47. *In* ALIMEN, H., LE MAÎTRE, D., MENCHIKOFF, N., PETTER, G. & POUEYTO, A. (eds) *Les Chaînes d'Ougarta et la Saoura, Monographies Régionales 15*. XIX Congrès Géologique International, Alger.

POWELL, R.D. 1990. Sedimentary processes at grounding line fans and their growth to ice-contact deltas, 53–77. *In* DOWDESWELL, J.A. & SCOURSE, J.D. (eds) *Glacimarine environments: processes and sediments*. *Geological Society London Special Publication* 53.

PRIGMORE, J.K., BUTLER, A.J. & WOODCOCK, N.H. 1997. Rifting during separation of Eastern Avalonia from Gondwana: evidence from subsidence analysis. *Geology 25*, 203–206.

ROBIN, C., ROUBY, D., GRANJEON, D., GUILLOCHEAU, F., ALLEMAND, P. & RAILLARD, S. 2005. Expression and modelling of stratigraphic sequence distortion. *Sedimentary Geology 178*, 159–186.

ROSS, J.R.P. & ROSS, C.A. 1992. Ordovician sea-level fluctuations, 327–336. *In* WEBBY, B.D. & LAURIE, J.R. (eds) *Global perspectives on Ordovician geology*. Balkema, Rotterdam.

RUNKEL, A.C., MCKAY, R.M. & PALMER, A.R. 1998. Origin of a classic cratonic sheet sandstone: stratigraphy across the Sauk II–Sauk III boundary in the Upper Mississippi Valley. *Geological Society of America Bulletin 110*, 188–210.

SHARLAND, P.R., ARCHER, R., CASEY, D.M., DAVIES, R.B., HALL, S.H., HEWARD, A.P., HORBURY, A.D. & SIMMONS, M.D. 2001. Arabian plate sequence stratigraphy. *GeoArabia Special Publication 2*, 1–371.

SHARLAND, P.R., CASEY, D.M., DAVIES, R.B., SIMMONS, M.D. & SUTCLIFFE, O.E. 2004. Arabian plate sequence stratigraphy – Revisions to SP 2. *GeoArabia 9*, 199–214 (chronostratigraphic chart available at http://www.stratigraphy.org/ga_charts.htm).

STAMPFLI, G.M. & BOREL, G.D. 2002. A tectonic model for the Paleozoic and Mesozoic constrained by dynamic plate boundaries and restored synthetic oceanic isochrones. *Earth Planetary Science Letters 196,* 17–33.

ŠTORCH, P. 2006. Facies development, depositional settings and sequence stratigraphy across the Ordovician-Silurian boundary: a new perspective from the Barrandian area of the Czech Republic. *Geological Journal 41*, 163–192.

SUTCLIFFE, O.E., DOWDESWELL, J.A., WHITTINGTON, R.J., THERON, J.N. & CRAIG, J. 2000. Calibrating the Late Ordovician glaciation and mass extinction by the eccentricity cycles of Earth's orbit. *Geology 28*, 967–970.

TAKHERIST, D. 1990. *Structure crustale, subsidence mesozoïque et flux de chaleur dans les bassins nord-sahariens (Algérie): apport de la gravimétrie et des données de puits*. 207 pp. Thèse de doctorat, Université de Montpellier (unpublished).

TAUGOURDEAU, P. & DE JEKHOWSKY, B. 1960. Répartition et description des Chitinozoaires siluro-dévoniens de quelques sondages de la C.R.E.P.S., de la C.F.P.A. et de la S.N. Repal au Sahara. *Revue de l'Institut Français du Pétrole 15*, 1199–1260.

VAIL, P.R., AUDEMARD, F., BOWMAN, S.A., EISNER, P.N. & PEREZ-CRUZ, C. 1991. The stratigraphic signatures of tectonics, eustasy and sedimentology – an overview, 617–659. *In* EINSELE, G., RICKEN, W. & SEILACHER, A. (eds) *Cycles and events in stratigraphy.* Springer-Verlag, Berlin.

VECOLI, M. 1999. Cambro-Ordovician palynostratigraphy (acritarches and prasinophytes) of the Hassi-R'Mel area and northern Rhadames Basin, North Africa. *Palaeontographia Italica 86*, 1–112.

VECOLI, M., ALBANI, R., GHOMARI, A., MASSA, D. & TONGIORGI, M. 1995. Précisions sur la limite Cambrien-Ordovicien au Sahara Algérien (Secteur de Hassi-R'mel). *Comptes rendus de l'Académie des sciences, Paris 320*, 515–522.

VECOLI, M. & LE HÉRISSÉ, A. 2004. Biostratigraphy, taxonomic diversity and patterns of morphological evolution of Ordovician acritarchs (organic-walled microphytoplankton) from the northern Gondwana margin in relation to palaeoclimatic and palaeogeographic changes. *Earth Science Reviews 67*, 267–311.

VECOLI, M., PARIS, F. & VIDET, B. 2007. "Middle" Cambrian non-marine organic walled microfossils from the Algerian Sahara and their implications for the debate on the nature and origin of cryptospores. *Geophysical Research Abstracts 9*. EGU General Assembly 2007, Vienna, Austria.

WADE, B.S. & PÄLIKE, H. 2004. Oligocene climate dynamics. *Paleoceanography 19(4)*, PA4019.

WEBBY, B.D., COOPER, R.A., BERGSTRÖM, S.M. & PARIS, F. 2004. Stratigraphic framework and time slices, 41–47. *In* WEBBY, B.D., PARIS, F., DROSER, M. & PERCIVAL, I. (eds) *The Great Ordovician diversification event*. Columbia University Press, New York.

Earth-Science Reviews 101 (2010) 101–146

Contents lists available at ScienceDirect

Earth-Science Reviews

journal homepage: www.elsevier.com/locate/earscirev

Cambrian–Ordovician depositional sequences in the Middle East: A perspective from Turkey

J.-F. Ghienne [a,*], O. Monod [b], H. Kozlu [c], W.T. Dean [d]

[a] Institut de Physique du Globe/Ecole et Observatoire des Sciences de la Terre, UMR7516 CNRS/Université de Strasbourg, 1 rue Blessig, 67084 Strasbourg Cedex, France
[b] 128 rue du Parc, 45000 Orléans, France
[c] TPAO, Exploration Department, 06520 Ankara, Turkey
[d] National Museum of Wales, Department of Geology, Cathays Park, CF103NP Cardiff, United Kingdom

ARTICLE INFO

Article history:
Received 1 July 2009
Accepted 18 April 2010
Available online 8 May 2010

Keywords:
Paleozoic
sequence stratigraphy
glaciation
Arabian Plate
Taurus Chain
Border Folds
Gondwana margin

ABSTRACT

In southern Turkey (Taurus Chain or Taurides) and southeastern Turkey (Border Folds of the Arabian Plate), nearly complete Cambrian to Ordovician successions are preserved. Four major sedimentary sequences are defined according to the main transgressive events and the subsequent shelf progradations. These sequences allow us to link the Turkish mostly distal Lower Palaeozoic detritals to the more proximal Arabian formations in spite of contrasting facies. The Lower Palaeozoic development is outlined through four successive steps defined in southern Turkey: (1) *initiation of a cratonic platform regime* (Terreneuvian, *i.e.* earliest Cambrian; Depositional Sequence 1), with fluviatile conglomerates and red-bed sediments associated with volcanics; (2) *development of a stable marine platform* (late Terreneuvian? to Early Ordovician; Depositional Sequences 2 and 3), including widespread but diachronous "middle Cambrian" Carbonates and subsequent storm-dominated, detritals; (3) *tectonic instability* (Middle Ordovician) leading to a new palaeogeography on the Gondwana platform with the differentiation of a sag basin (Bedinan–Qasim depocenter; lower part of Depositional Sequence 4); and (4) *glaciation* (latest Ordovician; upper part of Depositional Sequence 4) identified by glaciomarine deposits forming the Hirnantian glacial record.

This thick (>2000 m) detrital succession records a first-order, long-term, subsidence-driven Cambrian to Ordovician transgressive trend, and includes second-order sequences reflecting interactions between global eustasy and tectonic instability. On a larger scale, the identification of recurrent sequence stratigraphic features with similar trends in the Cambrian–Ordovician successions on the Arabian platform, implies that a former location of the Taurus domain cannot be situated in the (present day) Eastern Mediterranean area, but should lie directly north of the Arabian platform. This location places southern Turkey at the junction between the North African segment of the Gondwana siliciclastic shelf to the West (present-day coordinates), and the Eastern Arabian segment, in good agreement with mixed faunal signatures from both areas. Primary control of the tectonostratigraphic development of southern Turkey during the Lower Palaeozoic may be a forced evolution from arc/platform to rift/drift transitions ("cordilleran" model) that has migrated progressively eastwards from the Avalonian domain along the northern Gondwana margin to the Arabian domain, throughout the Lower Palaeozoic.

Contents

* Corresponding author.
E-mail address: ghienne@unistra.fr (J.-F. Ghienne).

0012-8252/$ – see front matter © 2010 Elsevier B.V. All rights reserved.
doi:10.1016/j.earscirev.2010.04.004

1. Introduction

Recent studies in Western Europe and the Eastern Mediterranean regions have emphasized the need for an accurate reconstruction of the North Gondwana margin and in particular of its Lower Palaeozoic development. Among the Cambrian to Ordovician cover sequences of northern Gondwana (e.g., Algeria–Morocco, Ghienne et al., 2007a), one of the best-preserved extends from northern Saudi Arabia to southern Turkey, where it exhibits relatively distal, Lower Palaeozoic successions in the Taurides. Such a geoprofile forms a continuous 1500 km long cross-section, in contrast to the coeval metamorphosed rocks resulting from the Variscan orogeny that are scattered in the western Mediterranean region.

This paper outlines Cambrian–Ordovician successions in southern Turkey (Figs. 1–3). It is based on the identification of four major Depositional Sequences, which unite most known related formations and other lithostratigraphic divisions. Since roughly equivalent sets of sedimentary units have also been identified on the Arabian platform (mostly in Oman, Saudi Arabia and Jordan, e.g., Husseini, 1990; Sharland et al., 2001; Haq and Al Qahtani, 2005; Guiraud et al., 2005; Molyneux et al., 2006; Schneider et al., 2007), precise links based on stratigraphic and sedimentological evidence may now be proposed between the Arabian and Turkish successions. The biostratigraphic framework is supported by up to date reassessments (Dean, 2005, 2006) and systematic palynomorph studies from both outcrop and subsurface samples (Paris et al., 2007b). Recently, a number of regional studies using conodonts (Göncüoğlu and Kozur, 1999; Şenel et al., 2000; Kozlu et al., 2002a,b; Sarmiento et al., 2003; Göncüoğlu et al., 2004) or ichnofossils (Erdoğan et al., 2004) have provided new biostratigraphic constraints. Rather than lengthy detailed facies descriptions, only diagnostic elements are presented here, in either the text or figures so as to substantiate our interpretations in terms of depositional environments and integration from the regional to the continental scale. Boundaries, content and background for regional correlations are given for each depositional sequence. A Lower Palaeozoic reconstruction of the Middle East is finally proposed, which illustrates the development of the North Gondwana platform from Cambrian to Ordovician in an area essentially free of Variscan tectonics.

2. Development of the lower Palaeozoic geology in Turkey

Following pioneer geological investigations in Turkey during the late 19th and early 20th centuries, the creation of the MTA Institute (Ankara, 1935) initiated the systematic geologic mapping of Turkey. In the mid-nineteen-fifties, Cambrian deposits were discovered, first

in the Border Folds near Mardin (Tolun and Ternek 1952; Ketin 1966), and in the Amanos Mountains (Dean and Krummenacher, 1961). Soon afterwards, Silurian, Ordovician and Cambrian formations were, in turn, identified in the Taurides (Yalçınlar, 1964; Monod, 1967; Haude 1975) and progressively extended (Özgül et al., 1973, Demirtaşlı, 1984) into the central and eastern Taurides (Wolfart, 1981). At the same time, the Turkish oil consortium (TPAO) was drilling exploratory wells through deeper horizons in eastern Turkey, and also identified several Palaeozoic successions in the subsurface. Thanks to Kellogg (1960) and Schmidt (1965), and stratigraphic dating by Dean (1967, 1972, 1982, 1983), the Derik–Mardin area has become the type-area for Cambrian–Ordovician formations in southeastern Turkey. Further east, in the Zap valley, a major tributary of the Tigris River, large exposures of Palaeozoic rocks (Cambrian to Permian) were recognized by Ketin (1979) and precisely dated (Janvier et al., 1984; Dean and Zhou, 1988; Higgs et al., 2002; Dean, 2006).

On a wider scale, a complete geological map of Turkey was published by MTA in the early sixties. More recently, the new map of Turkey (1/500,000 scale, Şenel, 2002) demonstrates vividly the high complexity of the geology of Turkey. In particular this map shows that the numerous Palaeozoic formations of the Taurides belong to various tectonic units, the lower ones considered as "autochthonous" or "para-autochthonous", and the higher units belonging to far-travelled allochthonous units (nappes) of exotic origin (Fig. 1). This study however basically focuses on essentially un-metamorphosed Lower Palaeozoic units of the Taurus Chain (or Taurides) running along southern Anatolia and those of the deformed margin of the Arabian Platform in southeastern Turkey (or Border Folds) (e.g., Şengör and Yılmaz, 1981).

Four major depositional sequences have been defined in the Cambrian–Ordovician successions of southern and southeastern Turkey, based on recognition of major transgressive events and subsequent shelf progradations. In spite of distinct facies, these four sequences allow reliable correlation between the Turkish and Arabian Lower Palaeozoic formations, for which a comprehensive sequence stratigraphic framework is available (Sharland et al., 2001).

In ascending order, we distinguish (Fig. 2):

(1) Depositional Sequence 1: earliest Cambrian (early Terreneuvian),
(2) Depositional Sequence 2: late Terreneuvian? to early Furongian, *sensu* Landing et al. (2007) and Babcock and Peng (2007) (*i.e.* early Cambrian to early Late Cambrian in the former terminology, e.g., Shergold and Geyer, 2003),
(3) Depositional Sequence 3: late Furongian to early Middle Ordovician, *sensu* Webby et al. (2004) and corresponding to Tremadocian, Floian and Dapingian stages (*i.e.* Late Cambrian to middle Arenig in the British regional terminology; see Bergström et al., 2009 for other regions),
(4) Depositional Sequence 4: late Middle to Upper Ordovician *sensu* Webby et al. (2004) and corresponding to Darriwilian, Sandbian, Katian and "early" Hirnantian stages (late Arenig to Hirnantian). The "upper" Hirnantian strata belong to the lowermost part of a fifth sequence, latest Ordovician to Silurian in age (not examined in this study).

Depositional sequences are defined on the basis of long-term transgressive and regressive trends in the sedimentary record, as shown by the vertical evolution of depositional environments and/or the stratal stacking pattern of higher frequency depositional units. They correspond basically to Transgressive–Regressive sequences *sensu* Embry (1995) (see also Catuneanu et al., 2009). The inversion point between a transgressive and a regressive system tract cannot always be pointed out unambiguously and a maximum flooding interval (MFI) may only be defined in places (Fig. 2; Molyneux et al., 2006).

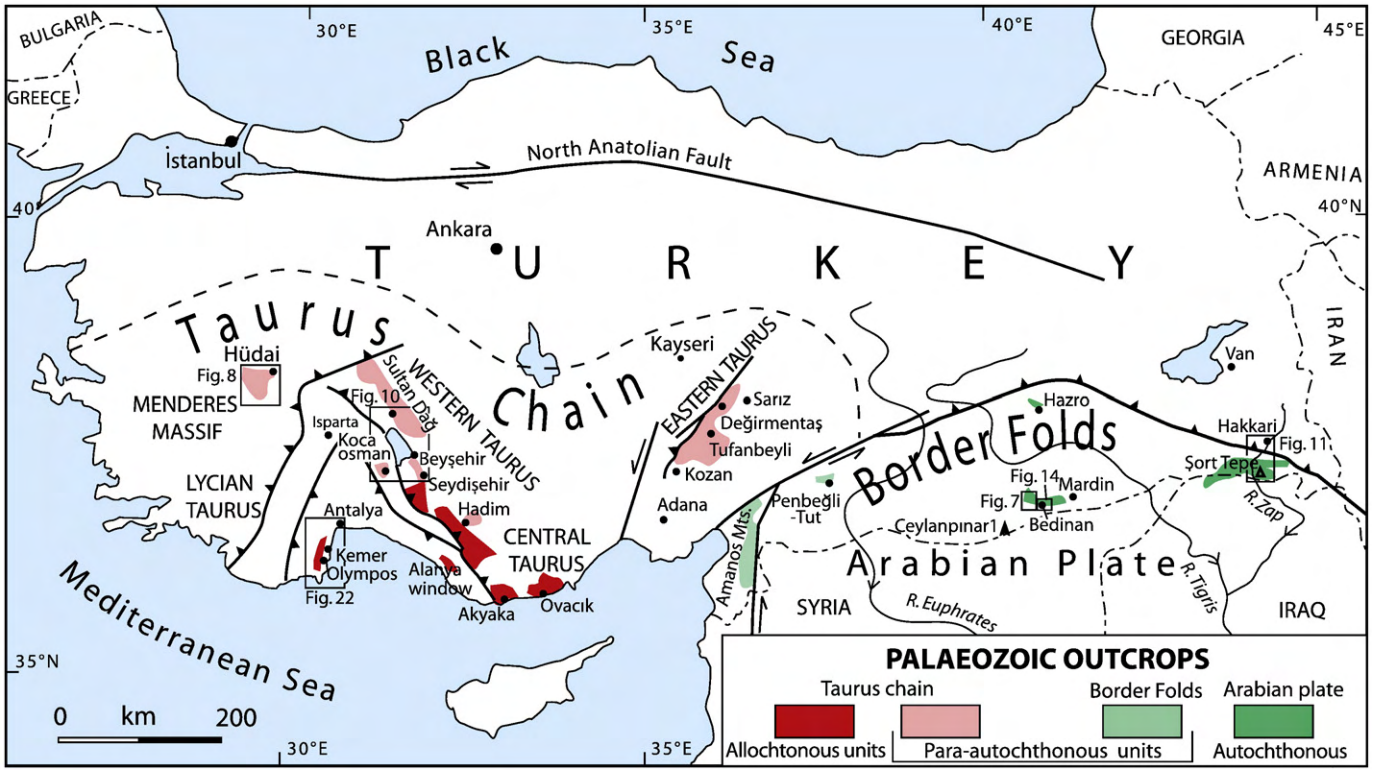

Fig. 1. Location of the main outcrops of the lower Palaeozoic formations discussed in the text. Main tectonic lines in the Taurus Chain and in the Border Folds, north of the Arabian platform. Dashed line indicates the approximate boundary of the Taurus Chain in southern Turkey.

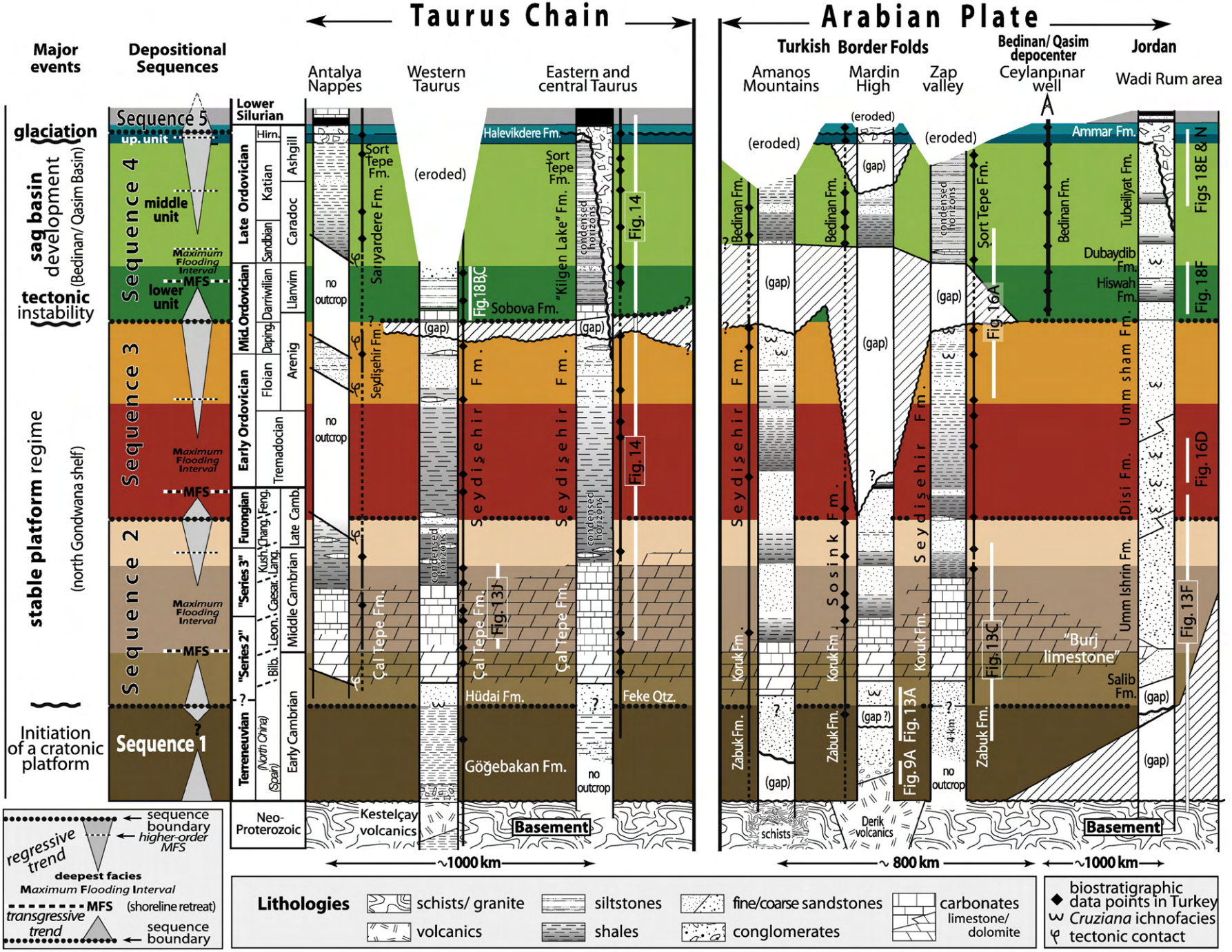
Taurus Chain
Arabian Plate
Major events
Depositional Sequences
glaciation
sag basin development (Bedinan/ Qasim Basin)
tectonic instability
stable platform regime (north Gondwana shelf)
Initiation of a cratonic platform
Sequence 5
Sequence 4
Sequence 3
Sequence 2
Sequence 1
up. unit
middle unit
lower unit
Maximum Flooding Interval
MFS
Lower Silurian
Late Ordovician
Mid. Ordovician
Early Ordovician
Hirn.
Katian
Sandbian
Darriwilian
Daping.
Floian
Tremadocian
Furongian
Ashgill
Caradoc
Llanvirn
Arenig
"Series 3"
"Series 2"
Terreneuvian
Late Camb.
Middle Cambrian
Early Cambrian
Kush.
Chang.
Feng.
Billa.
Leon.
Gaesa.
Lang.
(North China)
(Spain)
Antalya Nappes
Western Taurus
Eastern and central Taurus
Turkish Border Folds
Amanos Mountains
Mardin High
Zap valley
Bedinan/ Qasim depocenter
Ceylanpınar well
Jordan
Wadi Rum area
Sort Tepe Fm.
Sarıyardere Fm.
Seydişehir Fm.
Çal Tepe Fm.
Hüdai Fm.
Göğebakan Fm.
Halevikdere Fm.
"Kilgen Lake" Fm.
Sobova Fm.
Feke Qtz.
Kestelçay volcanics
Basement
Bedinan Fm.
Koruk Fm.
Sosink Fm.
Zabuk Fm.
Derik volcanics
schists
Ammar Fm.
Tubeiliyat Fm.
Dubaydib Fm.
Hiswah Fm.
Umm sham Fm.
Disi Fm.
Umm Ishrin Fm.
"Burj limestone"
Salib Fm.
no outcrop
condensed horizons
(eroded)
(gap)
(gap ?)
4 km
Fig. 14
Fig. 13J
Fig. 18BC
Fig. 16A
Fig. 13C
Fig. 13A
Fig. 9A
Figs 18E & N
Fig. 18F
Fig. 16D
Fig. 13F
~1000 km
~ 800 km
~1000 km
sequence boundary
higher-order MFS
regressive trend
deepest facies
Maximum Flooding Interval
MFS
(shoreline retreat)
transgressive trend
sequence boundary
Lithologies
schists/ granite
volcanics
siltstones
shales
fine/coarse sandstones
conglomerates
carbonates
limestone/ dolomite
biostratigraphic data points in Turkey
Cruziana ichnofacies
tectonic contact

The evolution of the Turkish Lower Palaeozoic sedimentary record is divided into four steps, which do not match with the depositional sequences but can be compared with other records from the Gondwana margin. From earliest to latest, the four steps are (Fig. 2, left column):

(1) Initiation of a cratonic platform regime (Terreneuvian, *i.e.* earliest Cambrian, Depositional Sequence 1);
(2) Development of a stable platform (Late Terreneuvian? to early Middle Ordovician, Depositional Sequences 2 and 3);
(3) Tectonic instability and differentiation of a sag basin (Middle to Late Ordovician, main part of Depositional Sequence 4);
(4) Glaciation (latest Ordovician, uppermost part of Depositional Sequence 4).

These four stages form the basic template of the present paper. Apart from the Cambrian carbonates, which represent a ubiquitous but diachronous transgressive event, the clastic sedimentary successions exhibit noticeably more distal facies in the Taurides than in the Border Folds. Thus, the Cambrian to Ordovician sedimentary records from both regions complement each other and unique cross-profiles can be reconstructed from the proximal areas (northwest Arabia) to the more distal ones (Taurides), through Jordan and southeastern Turkey (Border Folds). Figs. 4 and 5 show the first-order stratigraphic relationships as understood from a Turkish perspective. An overall continental onlap is inferred from Saudi Arabian and Jordanian records, which was coeval with the development of an extensive platform (early, but not the earliest, Cambrian up to the early Middle Ordovician) (Fig. 4). Related deposits include the widespread Çal Tepe and Koruk carbonate successions that correspond to a diachronous marker horizon encompassing "Series 2 and 3" of the Cambrian (*sensu* Babcock and Peng, 2007), and that will be informally referred to as "middle Cambrian" Carbonates in the following. After a mid-Ordovician tectonic re-organisation, an upper Ordovician sag basin was created, which trapped most of the detritals coming from Arabia, hence leaving a starved clastic sedimentation beyond (Eastern Taurus, Fig. 5).

3. Initiation of a cratonic platform regime (early Terreneuvian, Depositional Sequence 1)

The association of conglomerates and red-bed sediments with volcanics, the lack of biostratigraphic data and rapid lateral variations characterize the first depositional sequence, which is coeval with the ultimate Pan-African/Cadomian post-collisional events that affected northern Gondwana, prior to the onset of a cratonic platform regime.

3.1. Description of Depositional Sequence 1

3.1.1. Boundaries

To date, no satisfactorily dated Neoproterozoic strata are known in Turkey that could be compared with the Huqf supergroup in Oman (Le Guerroué et al., 2006; Allen, 2007) or time-equivalent strata in Iran (Stöcklin, 1968), which form the bulk of the first Arabian Plate tectonostratigraphic megasequence (AP1) of Sharland et al. (2001). Instead, deformed and slightly metamorphosed flysch-like siltstones with subordinate sandstones, grauwackes and cherty limestones, in places intruded by magmatic rocks emplaced close to the Proterozoic–Cambrian boundary, are recognised both in the Taurus (Sarıçiçek and Bozburun formations of Dumont, 1972; Gürsu et al., 2003; Sandıklı Basement Complex of Gürsu et al., 2004; Bozkaya et al., 2006; Emirgazi Fm. of Özgül et al., 1972; Kozlu and Göncüoğlu, 1997; Özgül and Kozlu, 2002; Bozkaya et al., 2002) and on the Arabian Plate (Ketin, 1966; Dean et al., 1997). Overlying this so-called "Infra-Cambrian" basement, two non-metamorphosed assemblages are distinguished (Figs. 6–8): (1) a lower assemblage, deposited in restricted, tectonically active basins (conglomerates and/or rapid lateral thickness changes, volcanism); and (2) an upper assemblage, dominated by sandstones without volcanics, that underlies the "middle Cambrian" Carbonates. Both assemblages are apparently paraconformable at the outcrop scale in the Mardin (Arabian Plate) and Sandıklı (Taurus) areas. However in the latter area, regional correlations (inset of Fig. 8) highlight a disconformity. Moreover, this surface is associated with drastic changes in sedimentation and subsidence patterns, substantiating a sequence boundary. The lower assemblage is ascribed to Depositional Sequence 1 (Terreneuvian), whereas the upper assemblage is integrated within Depositional Sequence 2.

3.1.2. Border Folds

In southeastern Turkey, Depositional Sequence 1 is best exposed in the Zap Valley and in the Mardin area. In the Zap valley (Cf. cross-profile in Fig. 11), it comprises a thick and poorly differentiated succession (>4000 m) of horizontally laminated to cross-bedded sandstones with occasional thin siltstone partings and common rip-up clasts. Occasional conglomeratic sandstones include gravel to pebbles of vein quartz, with other siltstone to sandstone lithologies. A few discrete dolomitic and stromatolitic beds, including wave ripples about 500 m below the top of the formation, indicate at least one shallow-marine ingression within this very thick and monotonous, fluvial to deltaic succession. In the upper part of this clastic succession, a distinct assemblage about 200 m thick, including large-scale lateral accretion surfaces is ascribed to the lower part of Depositional Sequence 2.

In the Mardin area, the basal detrital succession (lower part of Zabuk Fm.) (Fig. 6) was logged first by Kellogg (1960). It is much thinner (ca. 200 m) than in the Zap Valley and comprises mainly continental deposits. It rests on the "Derik volcanics" (Fig. 9A), a non-metamorphic succession of basaltic lavas and subordinate volcanoclastics, partly subaqueous (Göncüoğlu and Kozlu, 2000), the base of which is not exposed (Fig. 7). Overlying deposits include, in ascending order, conglomerates (Fig. 9B), a limestone horizon, and a 100 m red-bed type succession (Fig. 9C; see details in Fig. 6). No major unconformity exists between the underlying volcanic and overlying sedimentary rocks. Pseudo-angular relationships result from onlaps on local palaeoreliefs (Fig. 9A). This succession reflects a dry-land sedimentary system with alluvial-fan deposition fed initially by a local source near faulted basin margins, but evolving through time into playa environments with fan toes or fluvial overbanks fed by distant sources of micas and granitic pebbles.

3.1.3. Taurus Chain

Following the stratigraphic scheme of Bozkaya et al. (2006) (which, however, contradicts that proposed by Erdoğan et al., 2004; cf. also Güngör, 2006), a comprehensive "lower" Cambrian succession is recognised in the Western Taurus below the "middle Cambrian" Carbonates. North of Isparta, in the Sandıklı region, a thick (>1000 m) siliciclastic succession (see details in Fig. 8) overlies flysch-like and rhyolitic rocks of Neoproterozoic age (>543 Ma, Kröner and Şengör,

Fig. 2. Synthetic sketch of the lithologies and stratigraphic data of the Cambrian and Ordovician formations in the Taurus Chain and in the Arabian Plate. Colours indicate sequence stratigraphic correlations within Depositional Sequences 1 to 4 defined in southern Turkey. Note that sequence boundaries (dotted lines) do not match with stage boundaries. First order transgressive/regressive trends are separated by Maximum Flooding Surfaces (MFS, dashed lines), or Interval (MFI) in distal environments where MFS are not noticeable. Stratigraphic scales according to Shergold and Geyer (2003), Babcock and Peng (2007), Gozalo et al. (2007) for the Cambrian, Webby et al. (2004) and Bergström et al. (2009) for the Ordovician (Daping. : Dapingian ; Hirn.: Hirnantian). Spanish stages: Bilb: Bilbilian; Leon: Leonian; Caesar: Caesaraugustian; Lang: Languedocian. North China stages: Kush: Kushanian; Chang: Changshanian; Feng: Fengshanian.

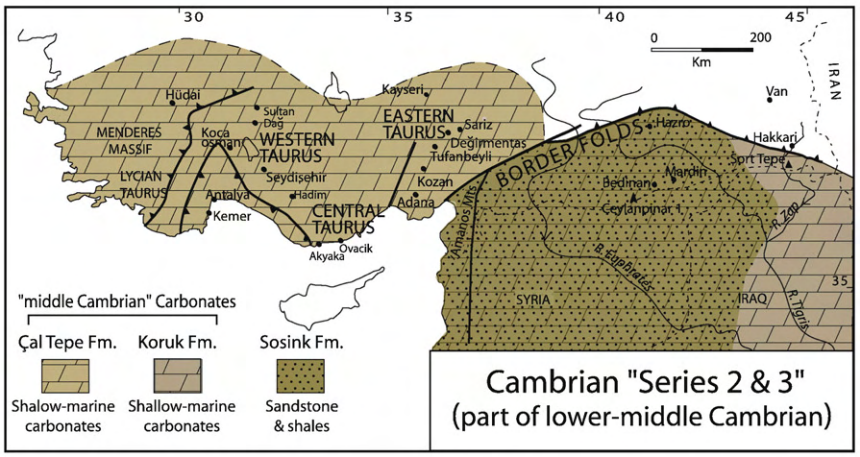
30
35
40
45
0
200
Km
IRAN
Van
Hüdai
Sultan Dağ
Kayseri
EASTERN TAURUS
Sariz
Değirmentas
Tufanbeyli
MENDERES MASSIF
Koca osman
WESTERN TAURUS
Seydişehir
Kozan
LYCIAN TAURUS
Antalya
Hadim
Adana
Kemer
CENTRAL TAURUS
Ovacik
Akyaka
BORDER FOLDS
Hazro
Hakkari
Sort Tepe
Mardin
Bedinan
Ceylanpinar 1
Amanos Mts
R. Euphrates
R. Zap
R. Tigris
SYRIA
IRAQ
35
"middle Cambrian" Carbonates
Çal Tepe Fm.
Koruk Fm.
Sosink Fm.
Shalow-marine carbonates
Shallow-marine carbonates
Sandstone & shales
Cambrian "Series 2 & 3"
(part of lower-middle Cambrian)

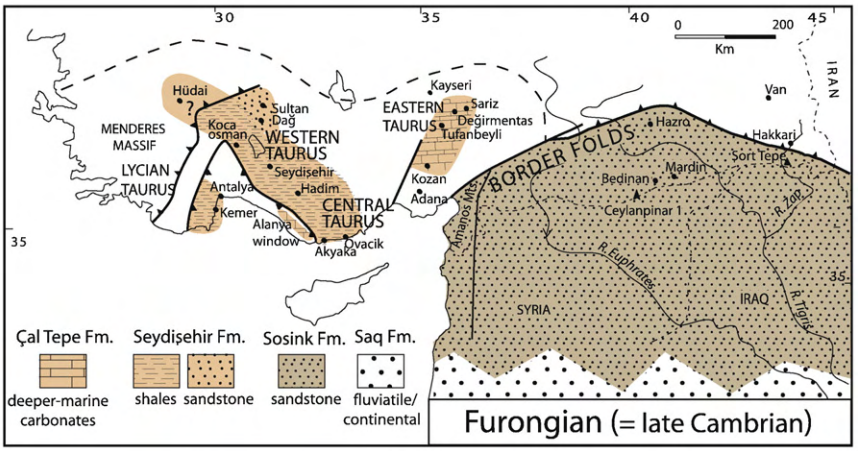
30
35
40
45
0
200
Km
IRAN
Van
Hüdai
Kayseri
Sultan Dağ
EASTERN TAURUS
Sariz
Değirmentas
Tufanbeyli
MENDERES MASSIF
Koca osman
WESTERN TAURUS
Seydişehir
Kozan
LYCIAN TAURUS
Antalya
Hadim
Adana
Kemer
Alanya window
CENTRAL TAURUS
Ovacik
Akyaka
BORDER FOLDS
Hazro
Hakkari
Sort Tepe
Mardin
Bedinan
Ceylanpinar 1
Amanos Mts
R. Euphrates
R. Zap
R. Tigris
SYRIA
IRAQ
35
Çal Tepe Fm.
Seydişehir Fm.
Sosink Fm.
Saq Fm.
deeper-marine carbonates
shales
sandstone
sandstone
fluviatile/ continental
Furongian (= late Cambrian)

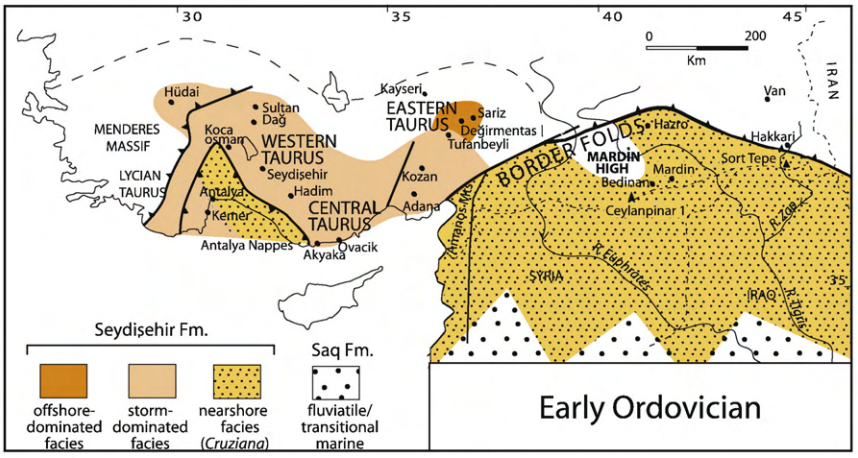
30
35
40
45
0
200
Km
IRAN
Van
Hüdai
Kayseri
Sultan Dağ
EASTERN TAURUS
Sariz
Değirmentas
Tufanbeyli
MENDERES MASSIF
Koca osman
WESTERN TAURUS
Seydişehir
Kozan
LYCIAN TAURUS
Antalya
Hadim
Adana
Kemer
CENTRAL TAURUS
Antalya Nappes
Ovacik
Akyaka
BORDER FOLDS
MARDIN HIGH
Hazro
Hakkari
Sort Tepe
Mardin
Bedinan
Ceylanpinar 1
Amanos Mts
R. Euphrates
R. Zap
R. Tigris
SYRIA
IRAQ
35
Seydişehir Fm.
Saq Fm.
offshore-dominated facies
storm-dominated facies
nearshore facies (Cruziana)
fluviatile/ transitional marine
Early Ordovician

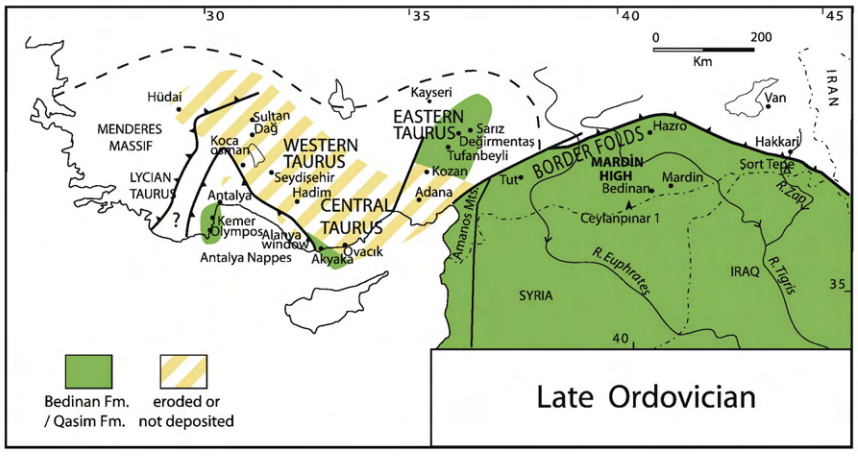
30
35
40
45
0
200
Km
IRAN
Van
Hüdai
Kayseri
Sultan Dağ
EASTERN TAURUS
Sariz
Değirmentas
Tufanbeyli
MENDERES MASSIF
Koca osman
WESTERN TAURUS
Seydişehir
Kozan
LYCIAN TAURUS
Antalya
Hadim
Adana
Kemer
Olympos
Alanya window
CENTRAL TAURUS
Antalya Nappes
Ovacik
Akyaka
BORDER FOLDS
Tut
MARDIN HIGH
Hazro
Hakkari
Sort Tepe
Mardin
Bedinan
Ceylanpinar 1
Amanos Mts
R. Euphrates
R. Zap
R. Tigris
SYRIA
IRAQ
35
40
Bedinan Fm. / Qasim Fm.
eroded or not deposited
Late Ordovician

1990; >541 Ma, Gürsu and Göncüoğlu, 2007). In the lower part of the succession, Depositional Sequence 1 is represented by the Göğebakan Formation. Overlying rhyolitic conglomerates (Fig. 9D) and basic pyroclastic rocks, arkosic beds and shales, the Göğebakan Fm. comprises mainly prodelta deposits (black siltstones, including thin low-density turbidites, Fig. 9E) but also includes spilitic dykes (Gürsu and Göncüoğlu, 2005). The upper part of the succession is ascribed to Depositional Sequence 2. In contrast to the relative uniformity in overlying Depositional Sequences 2 and 3, rapid lateral thickness changes are obvious (Fig. 8): 200–300 m thick to the NW (Orta Tepe section), 500–1000 m thick 10 km to the SW (Örenkaya section). Moreover, 60 km east of Isparta (Kocaosman section, Dumont, 1972), the complete absence of Depositional Sequence 1 is shown by the basal conglomerates of Depositional Sequence 2, which rest directly on the Sarıçiçek schists (Fig. 8).

In short, overlying a bi-modal volcanic event, Depositional Sequence 1 was deposited in differentiated basinal areas in the Taurides as well as in the Border Folds.

3.2. Regional correlations for Depositional Sequence 1 (Fig. 2)

A Terreneuvian age (*sensu* Landing et al., 2007) is attributed to Depositional Sequence 1 by (1) isotopic dating from the underlying volcanics (543–541 Ma), which shows that the onset of sedimentation in the Taurus occurred very close to the Neoproterozoic/Cambrian boundary; (2) this succession transitionally grades from the underlying volcanogenic suites into essentially siliciclastic suites; and (3) it is disconformably overlain by Depositional Sequence 2, possibly as old as late Terreneuvian.

The age of the volcanism conforms with granite protolith ages in the neighbouring Menderes Massif (Hetzel and Reichmann, 1996; Bozkurt and Oberhänsli, 2001; Gürsu and Göncüoğlu, 2005). In southeastern Turkey, Depositional Sequence 1 post-dates the Derik volcanics (Mardin area), both of which have their counterparts in Jordan, namely the Umm Ghaddah Fm. and the rhyolitic Aheimir Volcanic Suite (Amireh et al., 2007). Outside the related depocenters, coeval strata in southern Jordan are limited to very thin continental deposits (Fig. 9F).

As no significant unconformity separates the underlying volcanics from Lower Cambrian strata in the Taurus (Fig. 8), Depositional Sequence 1 and the underlying Neoproterozoic rocks may together belong to the same tectonostratigraphic cycle. The latter is time equivalent to the Ara Group of Oman (Allen, 2007), upper part of the first Arabian Plate megasequence (AP1) of Sharland et al. (2001). Both successions are characterized by intracontinental and/or subduction-related volcanism, basin partitioning, and dry climatic conditions (salt basins in Oman, red-bed succession in Turkey). Thick rift-basin successions (e.g. Zap Valley) and thin remnants outside the rift-basin (Mardin High) conform to the model of Sharland et al. (2001, their Fig. 3.8).

In southeastern Turkey, Depositional Sequence 1 and probably most of the underlying series, post-date the Neoproterozoic post-collisional sedimentary basins of the Middle East (Nehlig et al., 2002; Nadj transtensive system of Husseini, 1989, Cater and Tunbridge, 1992, Meert, 2003; Allen, 2007). The latter contain conglomeratic successions (e.g. Saramuj conglomerates in Jordan; Jarrar et al., 1991; Amireh et al., 2007; Zenifim Fm. and Eilat Conglomerates in southern Israel, Weissbrod and Sneh, 2002), the nature of which is very similar to those of the clearly younger Depositional Sequence 1. They differ, however, owing to latest Neoproterozoic deformations and metamorphism.

4. Development of a stable platform (late Terreneuvian, i.e. early Cambrian, to early Middle Ordovician, Depositional Sequences 2 and 3)

In contrast to Depositional Sequence 1, the second and third sequences are characterized by a uniform and widespread facies distribution, a reliable biostratigraphic framework based on trilobites and chitinozoans, and the lack of deformation or volcanism. They record two episodes of transgression and ensuing shelf progradations over a stable, cratonic platform. Depositional Sequence 2 includes the widespread but diachronous "middle Cambrian" dolomites and limestones (Çal Tepe and Koruk formations in the Taurides and southeastern Turkey respectively, Dean 2005, 2006), while storm-dominated, essentially carbonate-free, detrital deposits constitute Depositional Sequence 3 (Seydişehir Fm., Monod, 1967; Dean and Monod 1970; Özgül et al., 1972).

4.1. Description of Depositional Sequence 2

4.1.1. Boundaries

In the Mardin area (Arabian Plate), the upper assemblage of the Zabuk Fm., a 350 m thick sandstone-dominated succession is assigned to Depositional Sequence 2. Its lower boundary coincides with the sharp base of a fluvial sandstone sheet, which paraconformably (at the outcrop scale) overlies red-bed deposits of Depositional Sequence 1 (Figs. 6 and 13A). In the Taurides, at many localities, basal strata of Depositional Sequence 2 are missing owing to Alpine imbrications (e.g., Çal Tepe type-section, Fig. 10, Dean and Monod, 1970; Gutnic et al., 1979); however, in places, Depositional Sequence 2 overlies directly Neoproterozoic strata (Fig. 8, Kocaosman section, Dumont, 1972; Eastern Taurus, Göncüoğlu and Kozlu, 2000; Bozkaya et al., 2002), thus delineating a major stratigraphic break; at only two localities Depositional Sequence 2 overlies paraconformably the Terreneuvian clastic strata of Depositional Sequence 1 (Fig. 8, Sandıklı area, Bozkaya et al., 2006), as in the Mardin area case study.

Depositional Sequence 2 is overlain conformably by Depositional Sequence 3, and its upper boundary is thus poorly defined. Ideally, Depositional Sequence 2 ends with the most regressive Furongian (*i.e.* Upper Cambrian) strata, a criterion difficult to use, except at two localities, namely the Zap Valley (Fig. 11) and the Sultan Dağ in the Taurides (Fig. 10, Tülüce Tepe section, Fig. 12). In the Mardin region, this boundary is placed at the base of tidal sandstones, which may represent transgressive deposits below a marked flooding event within an otherwise tidal-dominated succession (Fig. 6). In more distal areas, the bounding surface occurs within a shale-dominated succession, and is not expressed (cf. Fig. 10).

4.1.2. Border Folds

In the Mardin region where it is best exposed, Depositional Sequence 2 comprises a three-fold succession, from base to top (Figs. 6 and 7): fluvial-dominated clastics (200–530 m), carbonates in the middle (530–765 m), and storm- to tidal-dominated clastics at the top (765–1160 m). The two former packages that essentially comprise a suite of deepening upwards deposits are attributed to the transgressive system tract, while the last forms the corresponding regressive system tract.

Basal clastics that rest abruptly on Depositional Sequence 1 form a fining- and thinning-upward succession, 160 m thick, grading from trough cross-bedded braided-stream sandstones, to meandering channel deposits (delta plain?) (Fig. 13A), and to tidally influenced mouth bar deposits that contain trace fossils (*Dimorphichnus*

Fig. 3. Four schematic maps of the present distribution of Cambrian to upper Ordovician formations in southern Turkey and in the adjacent countries. Contrasting facies on both sides of major tectonic lines imply that displacements of the Palaeozoic units occurred relative to the stable Arabian platform.

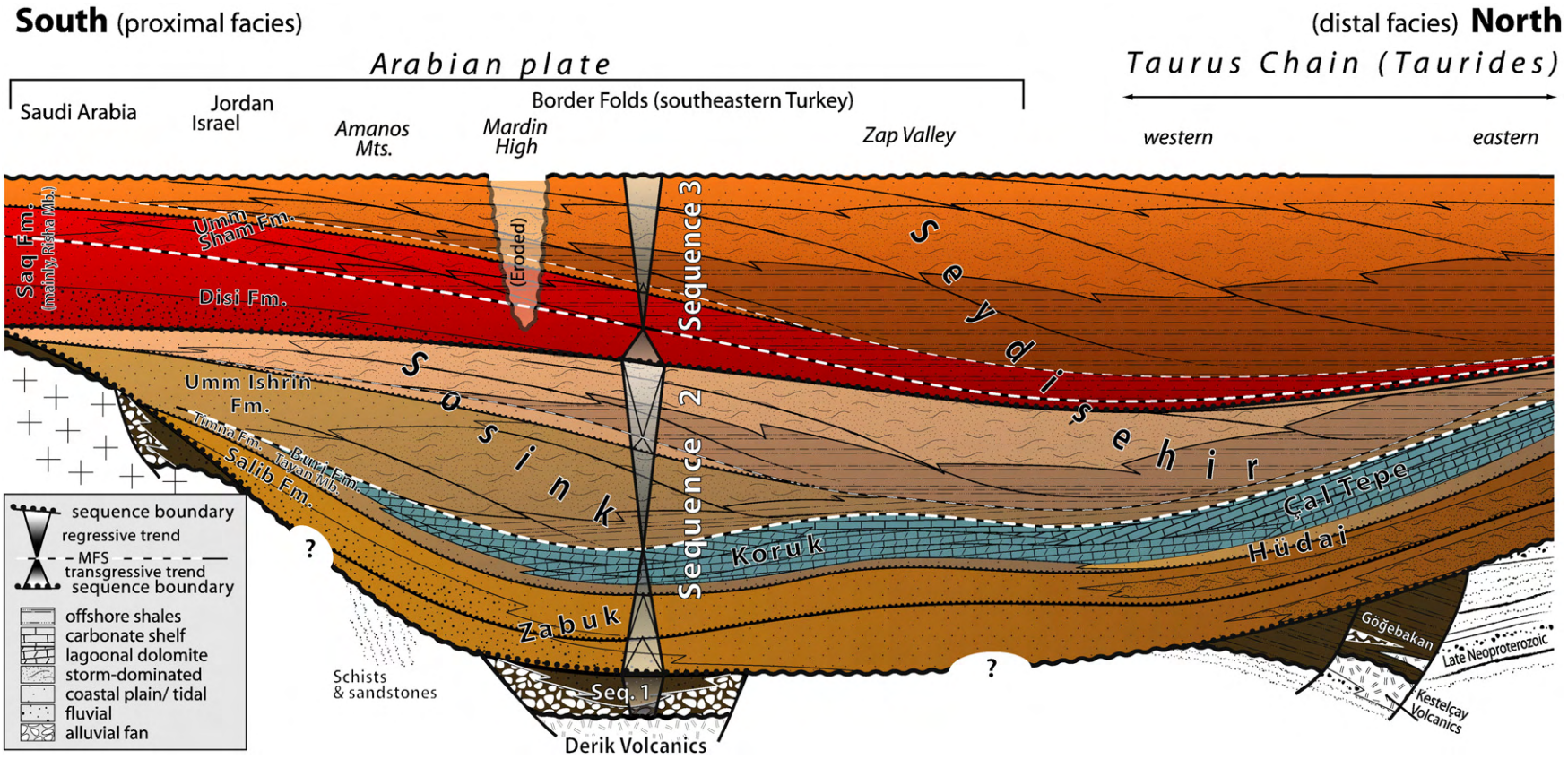

Fig. 4. Platform-scale architecture of Depositional Sequences 1 to 3 (Cambrian to early Middle Ordovician) showing progressive changes of detrital deposits from the Arabian Platform (proximal facies) to the Taurides (distal facies). Sequence 1 appears restricted to isolated, tectonically active basins; the maximum flooding surface of Sequence 2 (dashed line) takes place above the "middle Cambrian" Carbonates. Depositional Sequence 3 ends with regressive detritals of early Middle Ordovician age prograding northwards. "Mardin High" is a Middle Ordovician local uplift in the Border Folds, where most of Sequence 3 deposits have been eroded (cf. Figs. 2, 5 and 25). Dashed lines represent maximum flooding surfaces (MFS) in term of maximum shoreline retreats. Maximum Flooding Intervals (MFI, peak of deepest water) are shown in Fig. 2.

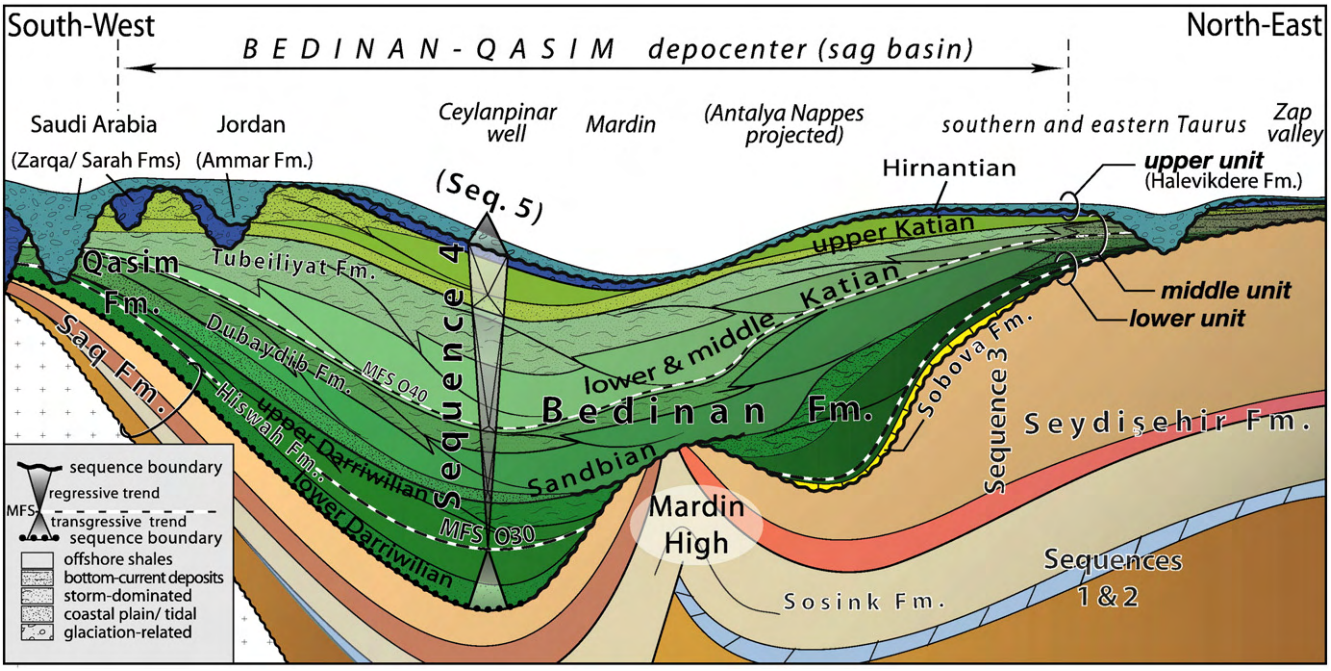

Fig. 5. Platform-scale architecture of Depositional Sequence 4 (late Middle Ordovician and Late Ordovician). Sequence 4 is informally subdivided into three units (lower, middle and upper units). Middle Ordovician tectonic instability is responsible for the Mardin High and related unconformities at the base of Sequence 4. At the top, the glacial deposits (Hirnantian) include a deeply incised erosion surface reaching the early Ordovician in the Taurides (Ovacık, Kozan) and the Cambrian in Saudi Arabia.

quadrifidus, Figs. 6 and 13B). Overlying coarse-grained sandstones form a monotonous fining-upward succession of fluvial to tidal sandstone. Marine influences are shown by trace fossils in this otherwise essentially continental succession. Palaeocurrent measurements indicate a source to the south or southwest (Arabian platform). This clastic succession is ascribed to two vertically superimposed third-order transgressive wedges at the base of Depositional Sequence 2 (Fig. 4). In the Zap Valley, Depositional Sequence 2 is poorly differentiated from Depositional Sequence 1 but, in the upper part of the succession, a ca. 200 m thick assemblage that includes distinctive cross-stratified sandstone organised in large-scale lateral accretion surfaces, indicates deposition in meandering channels of fluvial to tidal origin. They are attributed to the transgressive, fluvial-dominated clastics at the base of Depositional Sequence 2.

Carbonates of the Koruk Fm. and overlying offshore shales form a noticeably sheet-like unit, with limited thickness changes (75 m to 250 m) from the Amanos Mountains to the Zap Valley, 600 km apart (Dean and Monod, 1997; Dean, 2006) (Fig. 13C). Carbonate deposition commences with dolomites that contain occasional stromatolites. They are overlain by black to light-grey limestones, 10–50 m thick, grading from wackestone to grainstone including bioclastic, graded beds with abundant macrofauna (brachiopods, echinoderms and trilobites). Above, thinning-upwards red nodular limestone beds including clastic intercalations, and grading upwards into yellow-weathered shales typically constitute the upper part of this transgressive succession, and end the transgressive system tract of Depositional Sequence 2 (Figs. 4 and 5). Although most persistent in term of facies, this succession of lagoonal, reefal and offshore sediments is diachronous, as shown by the trilobite biozonation within the red nodular limestone, which ranges in age from the oldest (Amanos Mountains) to the middle (Zap Valley) Caesaraugustian (Cambrian "Series 3") (Dean and Krummenacher, 1961; Dean and Monod, 1990, 1997; Dean et al., 1981; Dean, 2006).

The regressive system tract of Depositional Sequence 2 is almost exclusively siliciclastic, except for a few calcareous bioclastic lenses. It is best exposed in the Zap Valley, where it comprises an overall coarsening- and thickening-upward (180 m) succession, within which the late Cambrian is well represented (Fig. 11; biostratigraphy based on the North China regional stages in Dean, 2006). This succession comprises storm-dominated offshore to shoreface sediments organised in a number of very high frequency cycles. In the Mardin area, (Figs. 6 and 7) the regressive system tract comprises a succession up to 660 m thick, with storm-dominated deposits at its base (Fig. 13D) and essentially dominated by tidal deposits upwards (Fig. 13E). The Languedocian age of its base (biostratigraphy according to the Spanish regional stages) is well established in the Mardin area (Dean, 1972, 1982; Erkmen and Bozdoğan, 1981) and in the Penbeğli–Tut inlier (Dean et al., 1997). In the upper part, frequent shell-beds yielded inarticulate brachiopods[1] (Fig. 6) suggesting a late Cambrian age. Correlation between the Zap Valley and the Mardin area (Fig. 4) suggests that the Languedocian regressive suite at the base of the regressive system tract of Depositional Sequence 2 (Fig. 6) is mostly condensed in the Zap Valley (Fig. 11). In the Mardin area, a major unconformity overlain by Upper Ordovician fine-grained sediments (Bedinan Fm.) truncates this succession at different levels, and the upper part of the regressive system tract (up to 500 m) is missing in places (Fig. 7B).

4.1.3. Taurus Chain

In the Taurus, Depositional Sequence 2 similarly comprises a three-fold succession: shallow-marine clastics at the base, carbonates in the middle, and clastics at the top. The succession differs from that of the Border Folds in its more distal depositional environments, especially at the base, as shown by shallow-marine deposits containing a highly diversified ichnofauna (Erdoğan et al., 2004) and a poorly developed, fine-grained, regressive system tract above.

In the Western Taurus, shallow-marine clastics that constitute the transgressive system tract of Depositional Sequence 2 comprise in ascending order the Celiloğlu and Hüdai formations (Dean and Özgül, 1994; Gürsu and Göncüoğlu, 2007), sometimes considered as two

[1] All footnotes refer to unpublished palaeontological data. *Westonia* cf. *urbiona* is common in *Lingula* shell-beds in the upper half of the Sosink Fm. (Figs. 6 and 7).

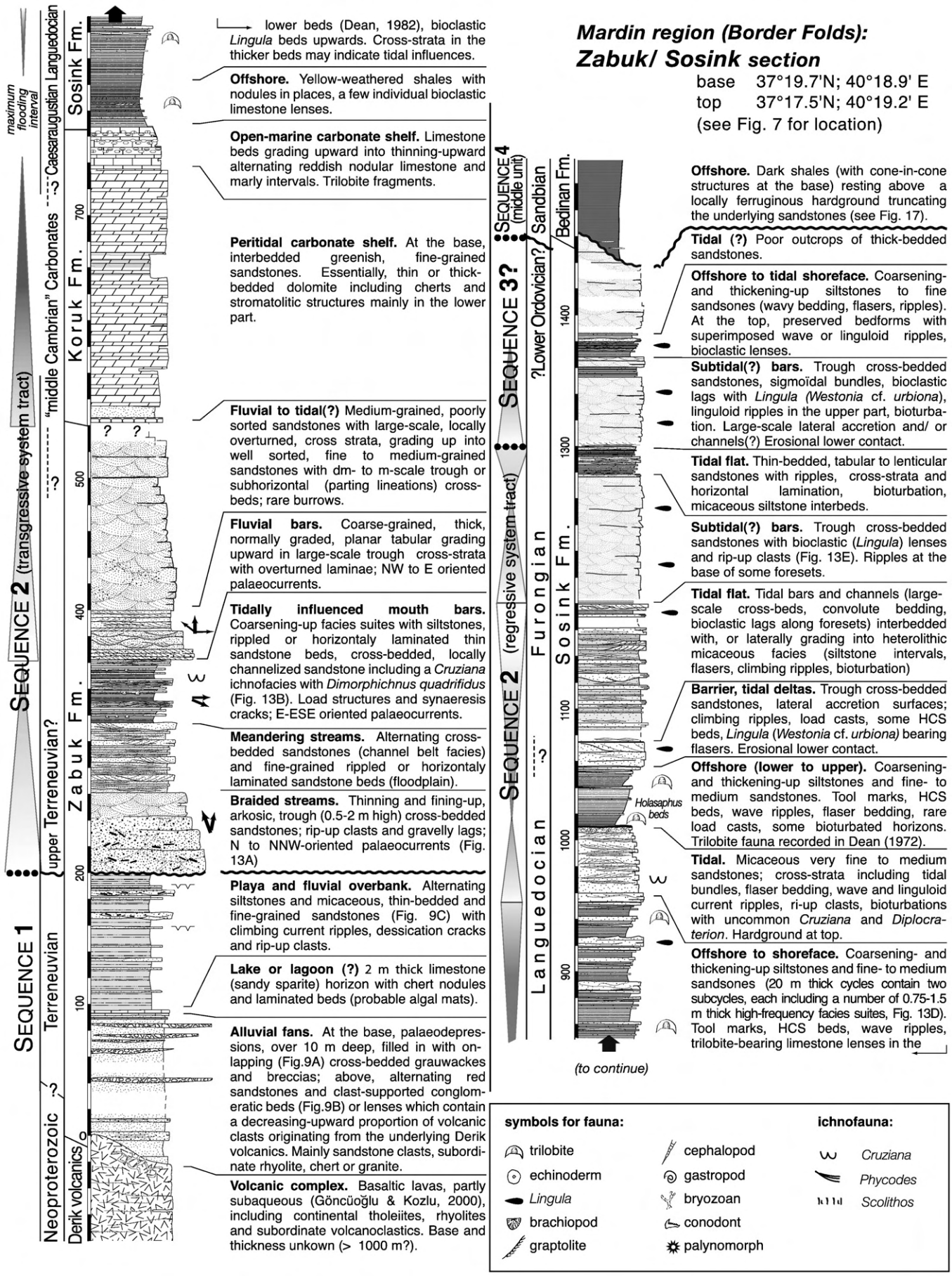
Mardin region (Border Folds):
Zabuk/ Sosink section
base 37°19.7'N; 40°18.9' E
top 37°17.5'N; 40°19.2' E
(see Fig. 7 for location)
SEQUENCE 1
SEQUENCE 2 (transgressive system tract)
maximum flooding interval
Neoproterozoic
Terreneuvian
upper Terreneuvian?
"middle Cambrian" Carbonates
Caesaraugustian Languedocian
Zabuk Fm.
Koruk Fm.
Sosink Fm.
Derik volcanics
SEQUENCE 2 (regressive system tract)
SEQUENCE 3?
SEQUENCE 4 (middle unit)
Languedocian
?Lower Ordovician?
Sandbian
Furongian
Sosink Fm.
Bedinan Fm.
Holasaphus beds
(to continue)
lower beds (Dean, 1982), bioclastic Lingula beds upwards. Cross-strata in the thicker beds may indicate tidal influences.
Offshore. Yellow-weathered shales with nodules in places, a few individual bioclastic limestone lenses.
Open-marine carbonate shelf. Limestone beds grading upward into thinning-upward alternating reddish nodular limestone and marly intervals. Trilobite fragments.
Peritidal carbonate shelf. At the base, interbedded greenish, fine-grained sandstones. Essentially, thin or thick-bedded dolomite including cherts and stromatolitic structures mainly in the lower part.
Fluvial to tidal(?) Medium-grained, poorly sorted sandstones with large-scale, locally overturned, cross strata, grading up into well sorted, fine to medium-grained sandstones with dm- to m-scale trough or subhorizontal (parting lineations) cross-beds; rare burrows.
Fluvial bars. Coarse-grained, thick, normally graded, planar tabular grading upward in large-scale trough cross-strata with overturned laminae; NW to E oriented palaeocurrents.
Tidally influenced mouth bars. Coarsening-up facies suites with siltstones, rippled or horizontaly laminated thin sandstone beds, cross-bedded, locally channelized sandstone including a Cruziana ichnofacies with Dimorphichnus quadrifidus (Fig. 13B). Load structures and synaeresis cracks; E-ESE oriented palaeocurrents.
Meandering streams. Alternating cross-bedded sandstones (channel belt facies) and fine-grained rippled or horizontaly laminated sandstone beds (floodplain).
Braided streams. Thinning and fining-up, arkosic, trough (0.5-2 m high) cross-bedded sandstones; rip-up clasts and gravelly lags; N to NNW-oriented palaeocurrents (Fig. 13A)
Playa and fluvial overbank. Alternating siltstones and micaceous, thin-bedded and fine-grained sandstones (Fig. 9C) with climbing current ripples, dessication cracks and rip-up clasts.
Lake or lagoon (?) 2 m thick limestone (sandy sparite) horizon with chert nodules and laminated beds (probable algal mats).
Alluvial fans. At the base, palaeodepressions, over 10 m deep, filled in with onlapping (Fig.9A) cross-bedded grauwackes and breccias; above, alternating red sandstones and clast-supported conglomeratic beds (Fig.9B) or lenses which contain a decreasing-upward proportion of volcanic clasts originating from the underlying Derik volcanics. Mainly sandstone clasts, subordinate rhyolite, chert or granite.
Volcanic complex. Basaltic lavas, partly subaqueous (Göncüoğlu & Kozlu, 2000), including continental tholeiites, rhyolites and subordinate volcanoclastics. Base and thickness unkown (> 1000 m?).
Offshore. Dark shales (with cone-in-cone structures at the base) resting above a locally ferruginous hardground truncating the underlying sandstones (see Fig. 17).
Tidal (?) Poor outcrops of thick-bedded sandstones.
Offshore to tidal shoreface. Coarsening- and thickening-up siltstones to fine sandsones (wavy bedding, flasers, ripples). At the top, preserved bedforms with superimposed wave or linguloid ripples, bioclastic lenses.
Subtidal(?) bars. Trough cross-bedded sandstones, sigmoïdal bundles, bioclastic lags with Lingula (Westonia cf. urbiona), linguloid ripples in the upper part, bioturbation. Large-scale lateral accretion and/ or channels(?) Erosional lower contact.
Tidal flat. Thin-bedded, tabular to lenticular sandstones with ripples, cross-strata and horizontal lamination, bioturbation, micaceous siltstone interbeds.
Subtidal(?) bars. Trough cross-bedded sandstones with bioclastic (Lingula) lenses and rip-up clasts (Fig. 13E). Ripples at the base of some foresets.
Tidal flat. Tidal bars and channels (large-scale cross-beds, convolute bedding, bioclastic lags along foresets) interbedded with, or laterally grading into heterolithic micaceous facies (siltstone intervals, flasers, climbing ripples, bioturbation)
Barrier, tidal deltas. Trough cross-bedded sandstones, lateral accretion surfaces; climbing ripples, load casts, some HCS beds, Lingula (Westonia cf. urbiona) bearing flasers. Erosional lower contact.
Offshore (lower to upper). Coarsening- and thickening-up siltstones and fine- to medium sandstones. Tool marks, HCS beds, wave ripples, flaser bedding, rare load casts, some bioturbated horizons. Trilobite fauna recorded in Dean (1972).
Tidal. Micaceous very fine to medium sandstones; cross-strata including tidal bundles, flaser bedding, wave and linguloid current ripples, ri-up clasts, bioturbations with uncommon Cruziana and Diplocraterion. Hardground at top.
Offshore to shoreface. Coarsening- and thickening-up siltstones and fine- to medium sandsones (20 m thick cycles contain two subcycles, each including a number of 0.75-1.5 m thick high-frequency facies suites, Fig. 13D). Tool marks, HCS beds, wave ripples, trilobite-bearing limestone lenses in the
symbols for fauna:
trilobite
echinoderm
Lingula
brachiopod
graptolite
cephalopod
gastropod
bryozoan
conodont
palynomorph
ichnofauna:
Cruziana
Phycodes
Scolithos

members of a single formation (Bozkaya et al., 2006); reported thicknesses are up to 600 m (Fig. 8). In the Sandıklı area, the Celiloğlu Fm. is made up of tidal-dominated deltaic sediments consisting of alternating shales, siltstones and sandstones with abundant trace fossils (Erdoğan et al., 2004). The overlying Hüdai Fm. (or "Hüdai Quartzite") comprises tidal sandstones (Fig. 13G) that have been recognized throughout the Taurides (Özgül et al., 1973, Göncüoğlu and Kozlu, 2000) and are, most often, conformably overlain by "middle Cambrian" Carbonates, with transitional facies (e.g., sandy dolomites) in places.

"Middle Cambrian" Carbonates that constitute the concluding part of the transgressive system tract form a conspicuous trilogy (dolomite/limestone/red nodular limestone), which can be traced all along the Taurus Chain, including the Antalya Nappes (Göncüoğlu and Kozur, 1999; Şenel et al., 2000). At the type-locality of the Çal Tepe Fm. near Seydişehir (Dean and Monod, 1970; Dean, 1972, 2005; Figs. 10 and 13J), above the unfossiliferous dolomites, limestone deposition starts in the Bilbilian (black limestone), extends into the Leonian to lower Caesaraugustian (light-grey limestone) and ends in the middle Caesaraugustian (red nodular limestone, Fig. 13H) (Dean, 2005; biostratigraphy according to the Spanish regional stages, *i.e.* middle Cambrian "Series 2" to the youngest "Series 3"). As in the Border Folds, the red nodular limestone facies also exhibits some diachronism, from Leonian (*Acadoparadoxides mureroensis* Biozone) in the western Taurides (Hüdai section, Dean and Özgül, 1994; Fig. 8), to Caesaraugustian in the Central Taurides (Seydişehir and Hadim sections, Dean, 2005; Fig. 10) with trilobites of the *Pardailhania* Biozone (ca. 7 Ma younger) and possibly as young as Furongian in the Eastern Taurus according to conodont data (Göncüoğlu et al., 2004). Deeper conditions are indicated by yellow-weathering shales, which frequently overlie the red nodular limestone facies. The shales contain several horizons with small calcareous or siliceous nodules (Fig. 13I), similar to those described by Loi and Dabard (2002) in other Palaeozoic successions. In the Hadim section, the yellow shales contain the zonal trilobite *Pardailhania hispida*, indicating the same age (middle Caesaraugustian) as the underlying red nodular limestones (Dean and Özgül, 1981; Dean, 2005).

In the Taurides, the regressive system tract (100–200 m?) of Depositional Sequence 2 is usually dominated by poorly differentiated, fine-grained detritals with subordinate, rippled sandstone beds. Thin isolated red nodular limestone lenses, less than 2 m thick, are occasionally present (Fig. 8). Languedocian strata are virtually unknown and only sporadic indications of Furongian deposits are suggested by conodonts (Hadim area, Özgül and Gedik, 1973; Alanya window, Göncüoğlu and Kozur, 1999; Sarız area, Göncüoğlu et al., 2004; Fig. 14) or by acritarchs (Sultan Dağ). Consequently, neither the Cambrian "Series 2"/Furongian boundary (formerly the Middle/Upper Cambrian boundary) nor the Cambrian/Ordovician boundary can be precisely located. Provisionally, the boundary between Depositional Sequences 2 and 3 is placed within a thin succession of Furongian sandstones, which exhibit the most regressive facies in the form of nearshore deposits (Fig. 12).

4.2. Description of Depositional Sequence 3

4.2.1. Boundaries

Depositional Sequence 3 rests conformably on Depositional Sequence 2, which explains why their contact has been unnoticed, as it is included within the Seydişehir Fm. This boundary has been discussed above (upper bounding surface of Depositional Sequence 2). By contrast, the upper boundary of Depositional Sequence 3 is a sharp lithologic break with a stratigraphic hiatus, separating sandstone-dominated deposits (upper part of Seydişehir Fm.) from much finer sediments (Bedinan Fm. or Şort Tepe Fm.). The disconformity is often underlined by a distinctive limestone unit (Sobova Fm. and related deposits).

4.2.2. Border Folds

Depositional Sequence 3 corresponds to the main part of the Seydişehir Fm., from the Amanos Mountains to the Zap Valley (Dean and Monod, 1990; Fig. 16A) and is also clearly identified in the subsurface (Bozdoğan and Erten, 1990). It is best exposed in the Zap Valley, where middle Furongian storm-dominated, essentially fine-grained strata can be ascribed to the transgressive system tract of Depositional Sequence 3 (Doğanlı section, Fig. 11).

Shortly after the maximum flooding interval, a short-term but distinctive regressive event is characterised by the unusual occurrence of amalgamated shoreface sandstone beds in an otherwise offshore-dominated succession (Fig. 11). From trilobite evidence, this event is dated as latest Cambrian (Dean, 2006) and is recorded a few tens of metres below the Cambrian/Ordovician boundary. The overlying coarsening-upward succession corresponds to the regressive system tract of Depositional Sequence 3 (Figs. 11 and 15). In the Zap Valley, biostratigraphic dating of this sequence is not available but, above the uppermost Cambrian strata (Dean, 2006), abundant trace fossils, of which *Cruziana furcifera* is most frequent, and acritarch assemblages (Martin, 1996) suggest an Early Ordovician age (undifferentiated Tremadocian and Floian). In the Amanos Mountains, Lower Ordovician detritals are dated using Tremadocian acritarchs in the lower part. Upwards, several superimposed, metres thick, high-frequency facies suites exhibit upper offshore deposits including *Cruziana* ichnofacies, and still higher, an increasing frequency of *Tigillites* beds clearly illustrates shallowing conditions up to nearshore environments in the upper part of the formation.

4.2.3. Taurus Chain

In the Taurides, Depositional Sequence 3 is represented mainly by a coarsening-upward detrital succession (>1000 m) that is usually strongly folded and imbricated by Alpine tectonics. But, an exceptional area in the eastern Taurus (Sarız–Saimbeyli region) offers several continuous, clearly exposed sections of Depositional Sequence 3 (Fig. 14), which correspond essentially to the Lower Ordovician Seydişehir Fm. (Monod, 1967; Dean and Monod 1970; Özgül et al., 1973).

At the base of Depositional Sequence 3, Furongian strata potentially represent a transgressive system tract, but are poorly identified, and condensed sedimentation probably prevails in most of the Taurides. Diagnostic trilobite evidence is difficult to establish (Dean, 2005) but some assemblages initially considered as Early Tremadoc by Shergold and Sdzuy (1984) are now re-interpreted as highest Furongian (Loi et al., 1996; Dean, 2006). A single section in the northwestern Sultan Dağ (Fig. 12, location Fig. 8) exhibits alternating shoreface sandstones, offshore silty shales, and red nodular limestone horizons containing diagnostic palynomorphs. In the lower part of this succession, a thin fining-up succession is attributed to the transgressive system tract of Depositional Sequence 3, up to offshore facies with nodules (cf. Loi and Dabard, 2002) ascribed to the maximum flooding interval. Just above, a

Fig. 6. The Cambrian succession in the Mardin region, Border Folds (location Figs. 1 and 7). Above the Derik Volcanics, continental deposits of Depositional Sequence 1 (lower Zabuk Fm.) are overlain by fluvial to tidal detritals (upper Zabuk Fm.). The latter, and lagoonal to shallow-marine "middle Cambrian" Carbonates (Koruk Fm.) form the transgressive system tract of Depositional Sequence 2. The MFI can be situated at the base of the Sosink Fm., the main part of which corresponds to the regressive system tract of Depositional Sequence 2. The uppermost part of the Sosink Fm. is ascribed to the transgressive system tract of Depositional Sequence 3 (lower Ordovician).

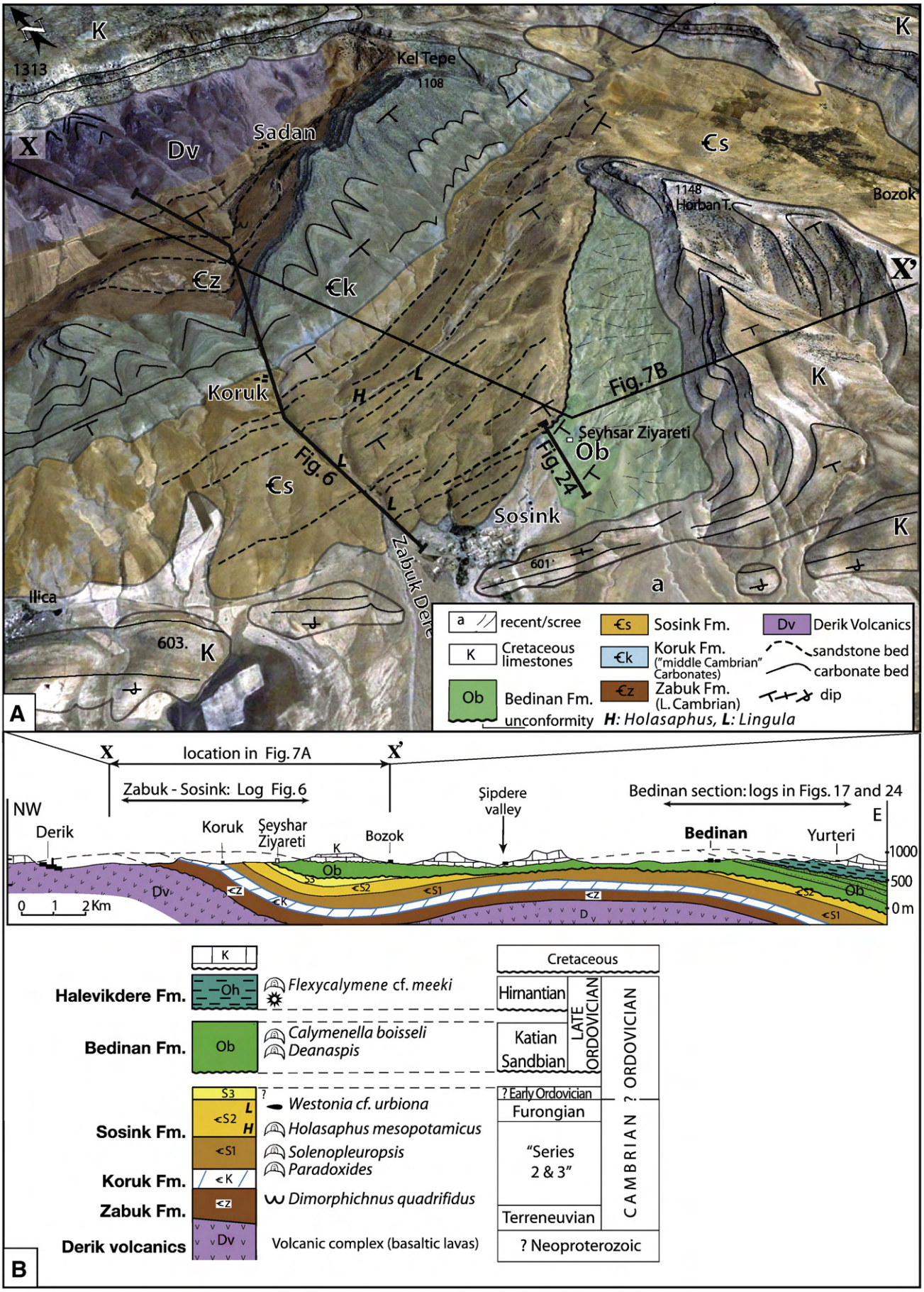
A
K
1313
Kel Tepe
1108
X
Dv
Sadan
Cs
1148
Horban T.
Bozok
X'
Cz
Ck
Koruk
H
L
Fig.7B
Seyhsar Ziyareti
Ob
Fig.6
Fig.24
Cs
Sosink
Zabuk Dere
601
a
Ilica
603.
recent/scree
Sosink Fm.
Derik Volcanics
Cretaceous limestones
Koruk Fm. ("middle Cambrian" Carbonates)
sandstone bed
carbonate bed
Bedinan Fm.
Zabuk Fm. (L. Cambrian)
dip
unconformity
H: Holasaphus, L: Lingula
location in Fig. 7A
Zabuk - Sosink: Log Fig. 6
Şipdere valley
Bedinan section: logs in Figs. 17 and 24
NW
E
Derik
Koruk
Şeyshar Ziyareti
Bozok
Bedinan
Yurteri
1000
500
0 m
0 1 2 Km
S3
S2
S1
B
Halevikdere Fm.
Bedinan Fm.
Sosink Fm.
Koruk Fm.
Zabuk Fm.
Derik volcanics
Oh
Flexycalymene cf. meeki
Calymenella boisseli
Deanaspis
Westonia cf. urbiona
Holasaphus mesopotamicus
Solenopleuropsis
Paradoxides
Dimorphichnus quadrifidus
Volcanic complex (basaltic lavas)
Cretaceous
Hirnantian
Katian
Sandbian
LATE ORDOVICIAN
? Early Ordovician
Furongian
"Series 2 & 3"
Terreneuvian
? Neoproterozoic
? ORDOVICIAN
CAMBRIAN

distinctive sharp-based assemblage of shoreface deposits (Fig. 12) may be correlated with a similar short-term regressive event at the Zap Valley section in the lowest part of the regressive system tract (see above and Fig. 11).

Depositional Sequence 3 most commonly comprises a fine-grained lower part, and a sandier upper part, which together constitute the regressive system tract. The lower part corresponds to thick (300–600 m) shale- to siltstone-dominated successions with subordinate sandstone beds and rare red limestone horizons, the age of which is mainly Tremadocian (Haude, 1975; Özgül et al., 1972; Göncüoğlu et al., 2004). Lithofacies and graptolites indicate inner to outer shelf, offshore depositional environments. The upper part (>500 m?), of Floian and early Middle Ordovician age (i.e. Arenig in the British regional terminology; Dean, 1971), is made up of alternating siltstones and sandstones, and has provided most of the recorded macrofossils (trilobites, cephalopods, brachiopods and gastropods, Dean and Monod, 1970; Monod, 1967). In the southern and western Taurides (Antalya Nappes, Sultan Dağ and Akyaka), the latter strata typically form a succession of storm-dominated, shallowing-upward facies suites, 5–10 m thick, comprising siltstones and sandstones (HCS, wave ripples, climbing ripples, cogenetic ripples and gutter casts; Fig. 16B and C). Bioturbation occurs frequently and is most often of *Phycodes* type, the *Cruziana* ichnofacies being very rare. Sandy, calcareous bioclastic lenses occur as reworked shell-beds in the upper half of the formation. Sarmiento et al. (1999) and Kozlu et al. (2002a,b) have reported a conodont fauna from a limestone lens in the upper part of the formation (Tekmen Member, Akyaka section, Central Taurus, Fig. 21). In spite of the absence of the zonal taxa, this horizon has been attributed to the Late Darriwilian, an age that is, however, in conflict with the overall stratigraphic scheme of Depositional Sequence 3.

In the eastern Taurus (Sarız–Saimbeyli area) the regressive system tract of Depositional Sequence 3 comprises three distinct coarsening, thickening-upwards units (from base to top: 300, 700 and 500 m thick), which represent three vertically superimposed individual prograding wedges overlain by thin tidal deposits (Fig. 14). When compared with those of the Central Taurides, the lithofacies of the upper half of Depositional Sequence 3 in the eastern Taurus can be distinguished by the occurrence of tidal markers and uncommon HCS beds, which suggest more proximal depositional environments.

4.3. Regional correlations of Depositional Sequences 2 and 3

4.3.1. Late Terreneuvian? to Cambrian "Series 3"

According to Erdoğan et al. (2004), trace fossils suggest a late Terreneuvian age for strata of the lower Depositional Sequence 2, but a younger age (Cambrian Series 2) cannot be excluded. The diachronism characterizing the "middle Cambrian" Carbonates in both the Taurides and Border Folds (Dean and Özgül, 1994) reflects a platform-scale sedimentary architecture (Fig. 4). Southern Turkey was entirely flooded during Cambrian "Series 2" as shown by the widespread deposition of carbonates devoid of any terrigenous fraction, which indicate a major retreat of the siliciclastic shorelines. The arrival of detritals — as shales within the red nodular limestones, and followed by shallowing-upward clastics — occurred as early as Cambrian "Series 2" in the Western Taurus and western Border Folds (Amanos) and proceeded northeastwards during Cambrian "Series 3". The deepest, condensed facies were deposited at the very end of Cambrian "Series 3" and extend into the Furongian in the eastern Taurus (Göncüoğlu et al., 2004). These relationships reflect an eastwards or northeastwards, proximal to distal, off-shelf gradient during the Cambrian "Series 3", both in the Taurides and in the Border Folds.

"Middle Cambrian" Carbonates forming the salient part of the transgressive system tract of Depositional Sequence 2 in Turkey provide a useful guideline for regional correlations (e.g., Gozalo et al., 2007). They form a continuous and well-developed horizon in the subsurface of Syria (Best et al., 1993; Brew et al., 1997) and at outcrop in Jordan (Burj Fm., Rushton and Powell, 1998; Elicki et al., 2002) and Israel (Soudry and Weissbrod, 1995). Southeastwards, the "middle Cambrian" Carbonates are not present along the margin of the Arabian Shield (Vaslet, 1987; McGillivray and Husseini, 1992) nor in Oman (Millson et al., 1996; Molyneux et al., 2006). In the latter area, the occurrence of time-equivalent strata is not known, and the Cambrian "Series 3" time interval is probably a stratigraphic hiatus. In Oman, strata of Cambrian "Series 2 and 3" may also be absent ("Angudan Unconformity") or if present, reflect continental conditions. To the west, the "middle Cambrian" carbonates can be followed tentatively as far as northeastern Egypt (Omara, 1972; Tawadros et al., 2001), although much thinner. In the subsurface of northwestern Egypt, only poorly defined dolomitized horizons are attributed to the "middle Cambrian" Carbonates (Andrawis et al., 1983; Keeley, 1989). To date, no Cambrian carbonates are known in northern Libya, although time-equivalent strata are entirely marine siliciclastics according to acritarch-based biostratigraphic data (Albani et al., 1991). By contrast, coeval Cambrian carbonates are widespread in more distal areas such as Sardinia (Pillola et al., 1998; Elicki, 2006), Spain (Gozalo et al., 2007), southern France (Montagne Noire: Álvaro et al., 1998) or northeastern Europe (Elicki, 2007b).

Platform-scale correlation of the siliciclastic deposits of Depositional Sequence 2 beneath and above the "middle" Cambrian Carbonates is more questionable. Correlation of the Turkish succession can be proposed with the Jordan succession, which also displays a full transgressive–regressive sequence (Bender, 1975; Amireh et al., 1994; Elicki et al., 2002; Elicki, 2007a; Schneider et al., 2007). An overall backstep of the clastics is identified, above which progradation resumed with *Cruziana*-bearing clastics, possibly as early as the highest part of Cambrian "Series 2". Although the facies of the formations are similar in southeastern Turkey and in Jordan, but more proximal in the latter, both successions are diachronous to a large extent. A tentative correlation may be proposed (Fig. 4):

(1) The early transgressive clastic deposits in Turkey (fluvial or deltaic base of Depositional Sequence 2) have probably no time-equivalent counterparts around the Arabo-Nubian Shield, such as in Jordan or central Saudi Arabia;
(2) Basal sandstones in Jordan (Salib Fm. of Amireh et al., 1994; Fig. 13F) should represent highstand conditions related to the fluvial-dominated (Border Folds) to tidal sandstones (Taurides) underlying the dolomites;
(3) Lagoonal dolomites (Cambrian "Series 2") in southeastern Turkey should be partly coeval with transgressive clastics in Jordan (in part, Tayan Mb. of Elicki, 2007a), but with open-marine limestone facies in the Taurides. They are absent further south (Fig. 13F);
(4) Maximum flooding conditions in term of shoreline retreat occurred within the Cambrian "Series 2" (Bilbilian of the

Fig. 7. (A) GoogleEarth view of the Mardin region, Border Folds. A continuous outcrop (log on Fig. 6) extends from the Derik Volcanics (Neoproterozoic), the Cambrian Depositional Sequences 1 and 2 (Zabuk, Koruk and Sosink Fms), to the overlying Late Ordovician Depositional Sequence 4 (Bedinan Fm.). Depositional Sequence 4 lies unconformably on Depositional Sequence 2. (B) Composite geological section from Derik to Bedinan. To the east, in its upper part, Depositional Sequence 4 comprises the Hirnantian glacial deposits (Halevikdere Fm., Fig. 24).

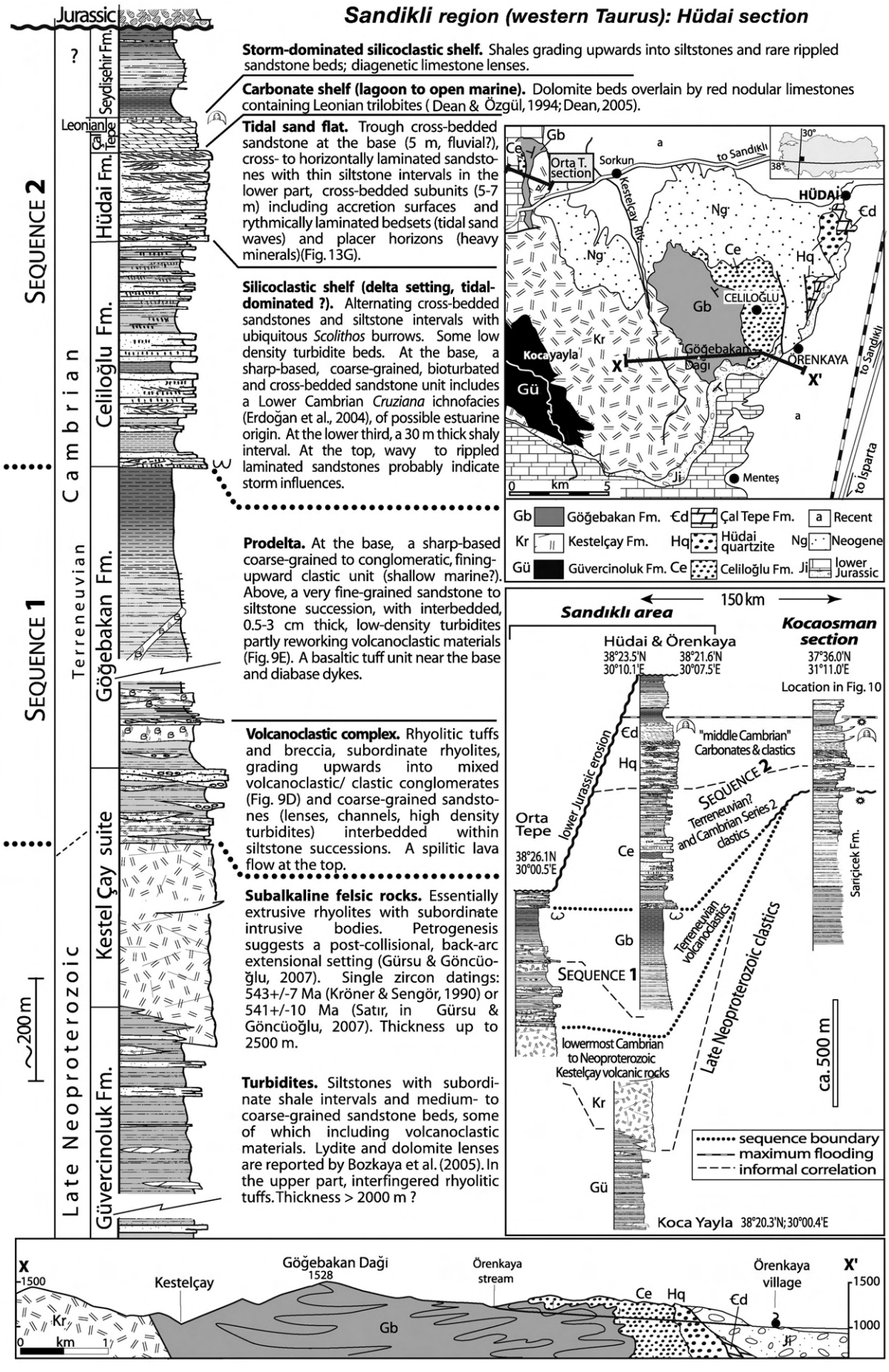
Sandikli region (western Taurus): Hüdai section
Jurassic
SEQUENCE 2
SEQUENCE 1
Cambrian
Terreneuvian
Late Neoproterozoic
Seydişehir Fm.
Çal Tepe
Leonian
Hüdai Fm.
Celiloğlu Fm.
Göğebakan Fm.
Kestel Çay suite
Güvercinoluk Fm.
~200 m
Storm-dominated siliciclastic shelf. Shales grading upwards into siltstones and rare rippled sandstone beds; diagenetic limestone lenses.
Carbonate shelf (lagoon to open marine). Dolomite beds overlain by red nodular limestones containing Leonian trilobites (Dean & Özgül, 1994; Dean, 2005).
Tidal sand flat. Trough cross-bedded sandstone at the base (5 m, fluvial?), cross- to horizontally laminated sandstones with thin siltstone intervals in the lower part, cross-bedded subunits (5-7 m) including accretion surfaces and rythmically laminated bedsets (tidal sand waves) and placer horizons (heavy minerals)(Fig. 13G).
Silicoclastic shelf (delta setting, tidal-dominated ?). Alternating cross-bedded sandstones and siltstone intervals with ubiquitous Scolithos burrows. Some low density turbidite beds. At the base, a sharp-based, coarse-grained, bioturbated and cross-bedded sandstone unit includes a Lower Cambrian Cruziana ichnofacies (Erdoğan et al., 2004), of possible estuarine origin. At the lower third, a 30 m thick shaly interval. At the top, wavy to rippled laminated sandstones probably indicate storm influences.
Prodelta. At the base, a sharp-based coarse-grained to conglomeratic, fining-upward clastic unit (shallow marine?). Above, a very fine-grained sandstone to siltstone succession, with interbedded, 0.5-3 cm thick, low-density turbidites partly reworking volcanoclastic materials (Fig. 9E). A basaltic tuff unit near the base and diabase dykes.
Volcanoclastic complex. Rhyolitic tuffs and breccia, subordinate rhyolites, grading upwards into mixed volcanoclastic/ clastic conglomerates (Fig. 9D) and coarse-grained sandstones (lenses, channels, high density turbidites) interbedded within siltstone successions. A spilitic lava flow at the top.
Subalkaline felsic rocks. Essentially extrusive rhyolites with subordinate intrusive bodies. Petrogenesis suggests a post-collisional, back-arc extensional setting (Gürsu & Göncüoğlu, 2007). Single zircon datings: 543+/-7 Ma (Kröner & Sengör, 1990) or 541+/-10 Ma (Satır, in Gürsu & Göncüoğlu, 2007). Thickness up to 2500 m.
Turbidites. Siltstones with subordinate shale intervals and medium- to coarse-grained sandstone beds, some of which including volcanoclastic materials. Lydite and dolomite lenses are reported by Bozkaya et al. (2005). In the upper part, interfingered rhyolitic tuffs. Thickness > 2000 m ?
Gb
Ce
Orta T. section
Sorkun
to Sandıklı
Kestelçay Rfy
HÜDAI
Ng
Cd
Hq
CELILOĞLU
Kr
Kocayayla
Göğebakan Dağı
ÖRENKAYA
X
X'
Gü
Ji
Menteş
0 km 5
to Sandıklı
to Isparta
Gb Göğebakan Fm.
Kr Kestelçay Fm.
Gü Güvercinoluk Fm.
Cd Çal Tepe Fm.
Hq Hüdai quartzite
Ce Celiloğlu Fm.
a Recent
Ng Neogene
Ji lower Jurassic
Sandıklı area
150 km
Kocaosman section
Hüdai & Örenkaya
38°23.5'N 30°10.1'E
38°21.6'N 30°07.5'E
37°36.0'N 31°11.0'E
Location in Fig. 10
"middle Cambrian" Carbonates & clastics
SEQUENCE 2
Terreneuvian? and Cambrian Series 2 clastics
lower Jurassic erosion
Orta Tepe
38°26.1N 30°00.5'E
Sarıçicek Fm.
Terreneuvian volcanoclastics
Late Neoproterozoic clastics
SEQUENCE 1
ca. 500 m
lowermost Cambrian to Neoproterozoic Kestelçay volcanic rocks
sequence boundary
maximum flooding
informal correlation
Koca Yayla 38°20.3'N; 30°00.4'E
X
X'
1500
1000
Kestelçay
Göğebakan Dağı
1528
Örenkaya stream
Örenkaya village
Kr
Gb
Ce
Hq
Cd
Ji
0 km 1

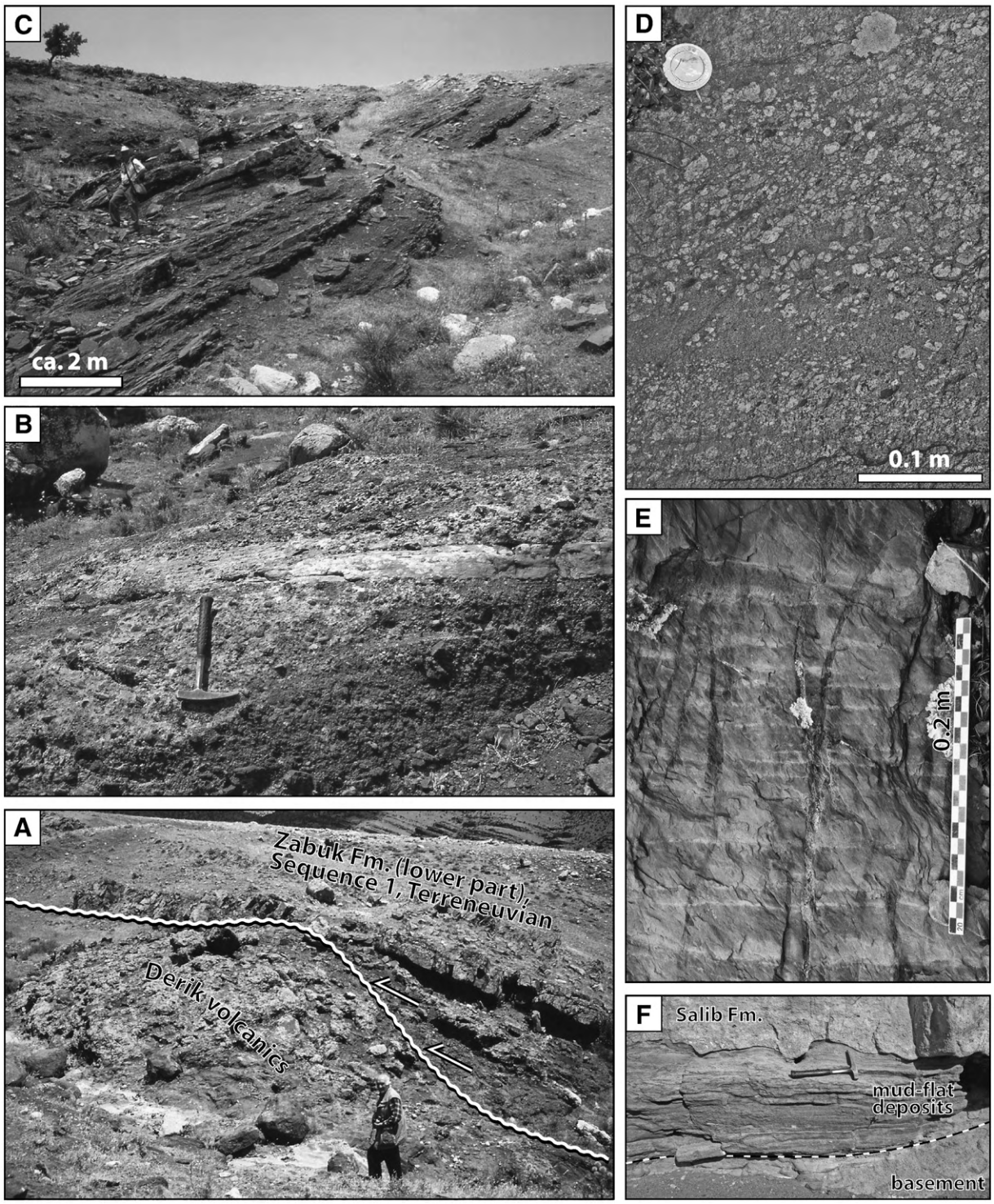

Fig. 9. Depositional Sequence 1 (Terreneuvian). (A–C) lower Zabuk Fm., Mardin region, Border Folds (cf. Fig. 6): (A) onlaps of cross-bedded grauwackes on the Derik volcanics (person for scale); (B) conglomerates and sandstones, alluvial-fan deposits (hammer for scale); (C) alternating sandstones and siltstones, playa to fluvial overbank deposits (red-bed deposits). (D–E) Göğebakan Fm., Sandıklı area, Western Taurus (cf. Fig. 8): (D) volcanoclastic (rhyolitic) conglomerates at the base; (E) succession of cm-scale low-density turbidites, prodelta deposits in the upper part; (F) in southern Jordan (Wadi Rum area), coeval strata correspond to thin and discontinuous, intracontinental mud-flat deposits.

Spanish regional terminology), as carbonate deposition ceased at that time in Jordan (Rushton and Powell, 1998) while deepening conditions continued in Turkey;

(5) In southern Turkey, maximum flooding in terms of peak of deepest water corresponds to the "middle" Cambrian red nodular limestone facies and associated condensed shaly

Fig. 8. The Cambrian succession (Depositional Sequences 1 and 2) in the Western Taurus. The most complete section is in the Sandıklı area (map), and exhibits more distal facies than the equivalent section in the Border Folds area (Fig. 6) on the Arabian platform. The lower boundary of Depositional Sequence 2 is a disconformity at the regional scale (lower right inset). Cross-section (XX′) is 8 km south of Hüdai, west of Örenkaya village. Kr: Kestelçay rhyolites; Gb: Göğebakan Fm.; Ce: Celiloğlu Fm.; Hq: Hüdai quartzites; Cd: Çal Tepe dolomite; Ji: Lower Jurassic conglomerates.

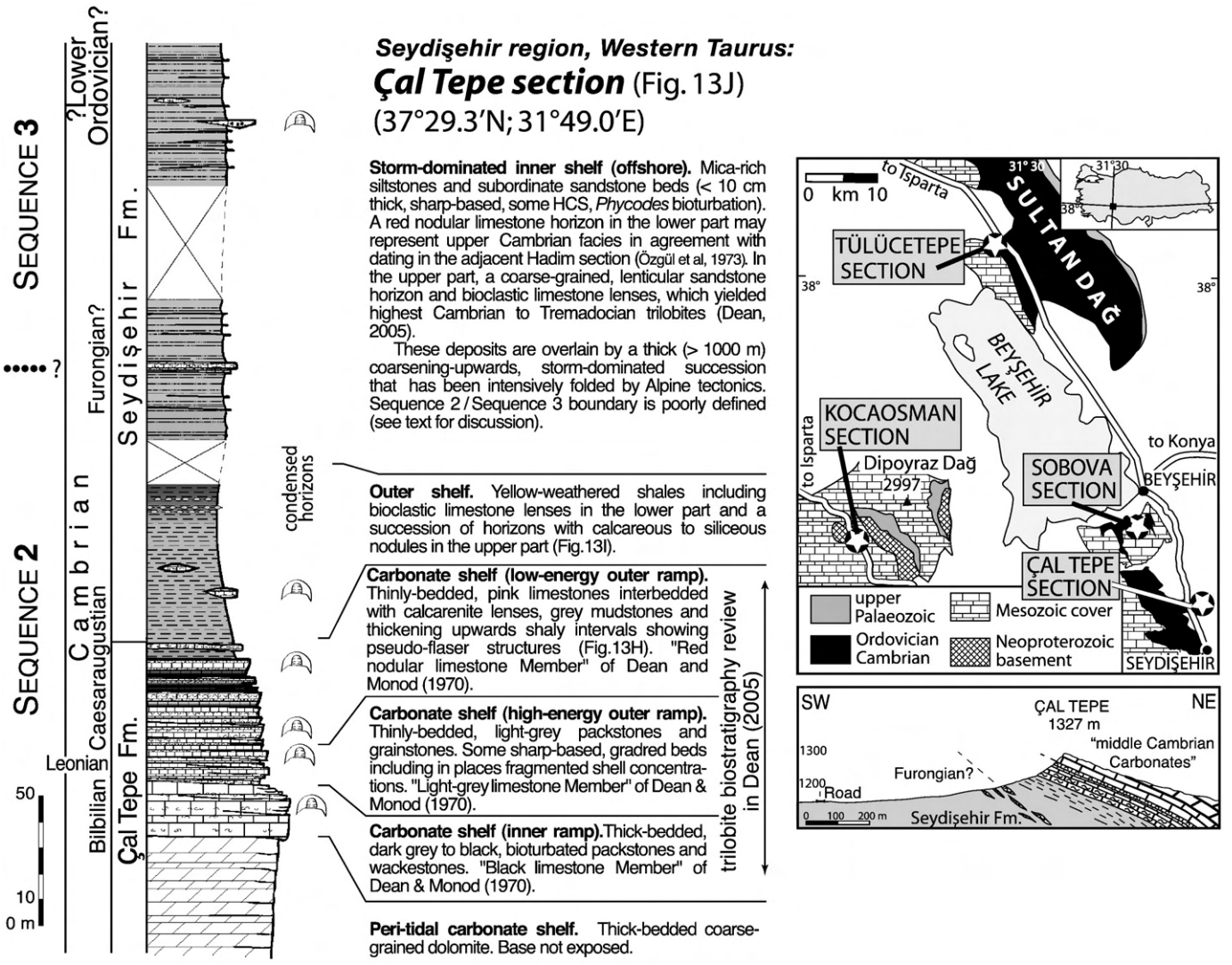

Fig. 10. The Cambrian succession at the Çal Tepe type-section and location of four Cambrian/Ordovician sections in the Western Taurus (map). The Çal Tepe section is overturned and shows the upper part of Depositional Sequence 2 and the lowest part of Depositional Sequence 3 within the Seydişehir Fm. In this distal, shale-dominated domain, the location of the sequence boundary cannot be precisely identified (cf. Fig. 13J). Cambrian biostratigraphy according to the Spanish regional stages (Dean, 2005).

deposits. In southern Jordan, coeval regressive deposits are the lowest part of Umm Ishrin Fm. (Fig. 13F). Similar deposits are also present in northeastern Saudi Arabia (Khursaniyah-81 well, Molyneux and Al-Hajri, 2000);

(6) Regressive, storm-dominated sandstones of the Cambrian "Series 3" in the Border Folds of Turkey (Sosink Fm.) should be time-equivalent to fluvial-dominated deposits in the proximal areas (Jordan, Umm Ishrin Fm.) and to condensed offshore shales in the more distal areas (Zap Valley and Taurides) (Fig. 4).

Sharland et al. (2001) defined their Cm20 Middle Cambrian maximum flooding surface as "the time of maximum distribution of relatively deep water sediments". According to our interpretation, the Cm20 maximum flooding surface corresponds to the peak of deepest water (upper part of Cambrian "Series 3"), and not to the maximum shoreline retreat (middle part of Cambrian "Series 2"). The time interval separating both events is ascribed to a maximum flooding interval (Fig. 2).

4.3.2. Furongian

Furongian strata (formerly Upper Cambrian) belong to the regressive system tract of Depositional Sequence 2, and extend into the lower part of Depositional Sequence 3 (Figs. 4 and 11). The eastward to northeastward offshelf gradient persisted during the Furongian as shown by lateral facies changes. In the Taurides, Furongian sandstones deposited to the west (Fig. 12) grade into shale-dominated horizons including carbonate beds to the east (Fig. 14). In the Border Folds, tidal sandstones predominate in the

Fig. 11. Map and section along the Zap Valley (Border Folds) and Cambrian to Lower Ordovician succession (Depositional Sequences 2 and 3) at Doğanlı village. The Yayla Tepe section (Dean, 2006) is located north of Samur Dağ Anticline (Fig. 13C). Star indicates dolomitic beds with stromatolites in the upper part of Zabuk Fm (>3000 m thick). Note that the Seydişehir Fm. includes the upper, regressive part of Sequence 2 (Furongian) and the lower, transgressive part of Sequence 3 (latest Furongian–Early Ordovician). Triangles highlight higher-frequency transgressive–regressive cycles. Stratal stacking pattern indicates the place of the sequence boundary.

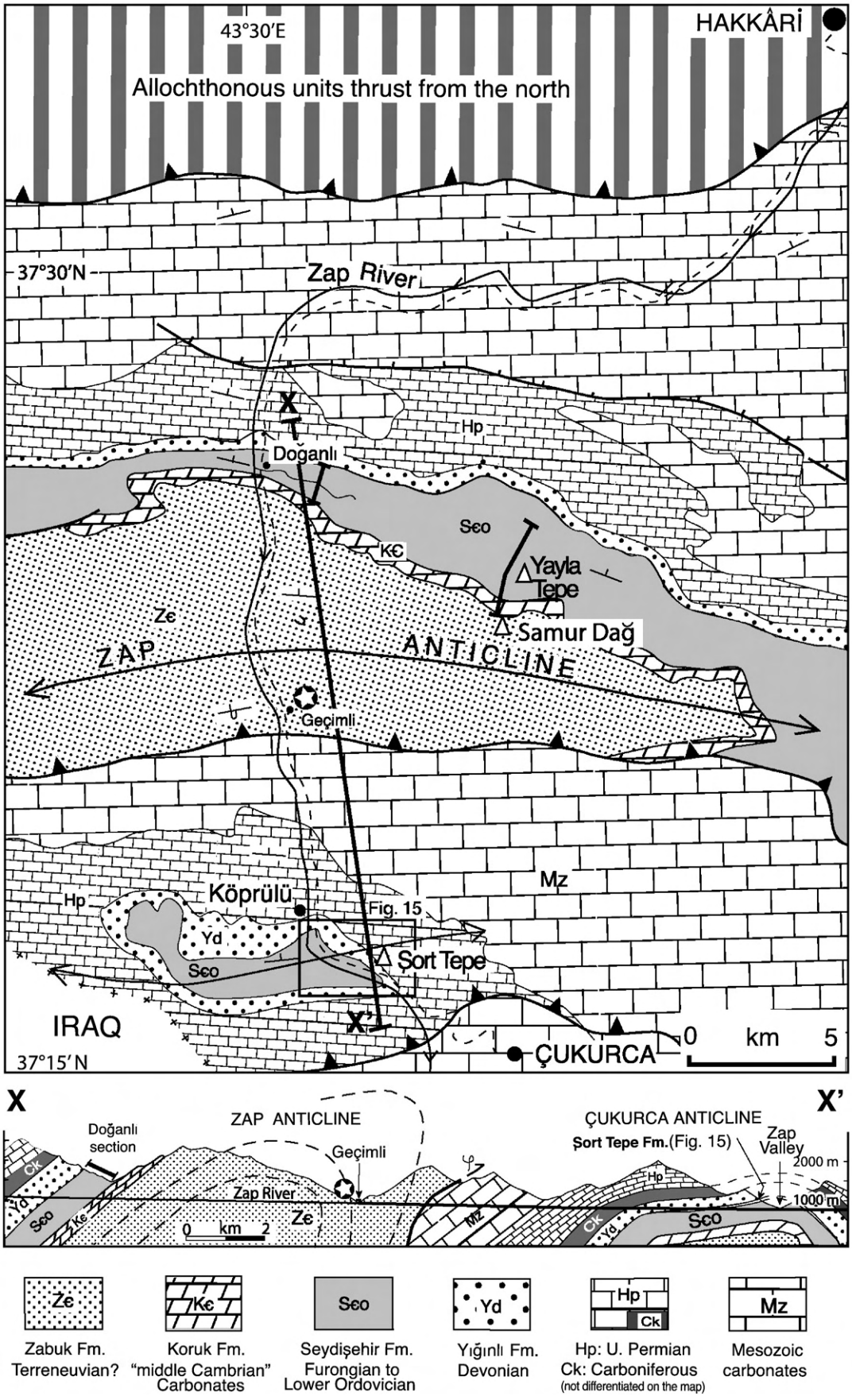
43°30′E
HAKKÂRİ
Allochthonous units thrust from the north
37°30′N
Zap River
X
Hp
Doğanlı
Sєo
Kє
Yayla Tepe
Samur Dağ
Zє
ZAP ANTICLINE
Geçimli
Mz
Köprülü
Hp
Fig. 15
Yd
Şort Tepe
Sєo
X'
IRAQ
37°15′N
ÇUKURCA
0 km 5
X
X'
ZAP ANTICLINE
ÇUKURCA ANTICLINE
Doğanlı section
Geçimli
Şort Tepe Fm.(Fig. 15)
Zap Valley
2000 m
1000 m
Ck
Hp
Yd
Sєo
Kє
Zap River
Zє
0 km 2
Mz
Zє
Zabuk Fm.
Terreneuvian?
Kє
Koruk Fm.
"middle Cambrian"
Carbonates
Sєo
Seydişehir Fm.
Furongian to
Lower Ordovician
Yd
Yığınlı Fm.
Devonian
Hp
Ck
Hp: U. Permian
Ck: Carboniferous
(not differentiated on the map)
Mz
Mesozoic
carbonates

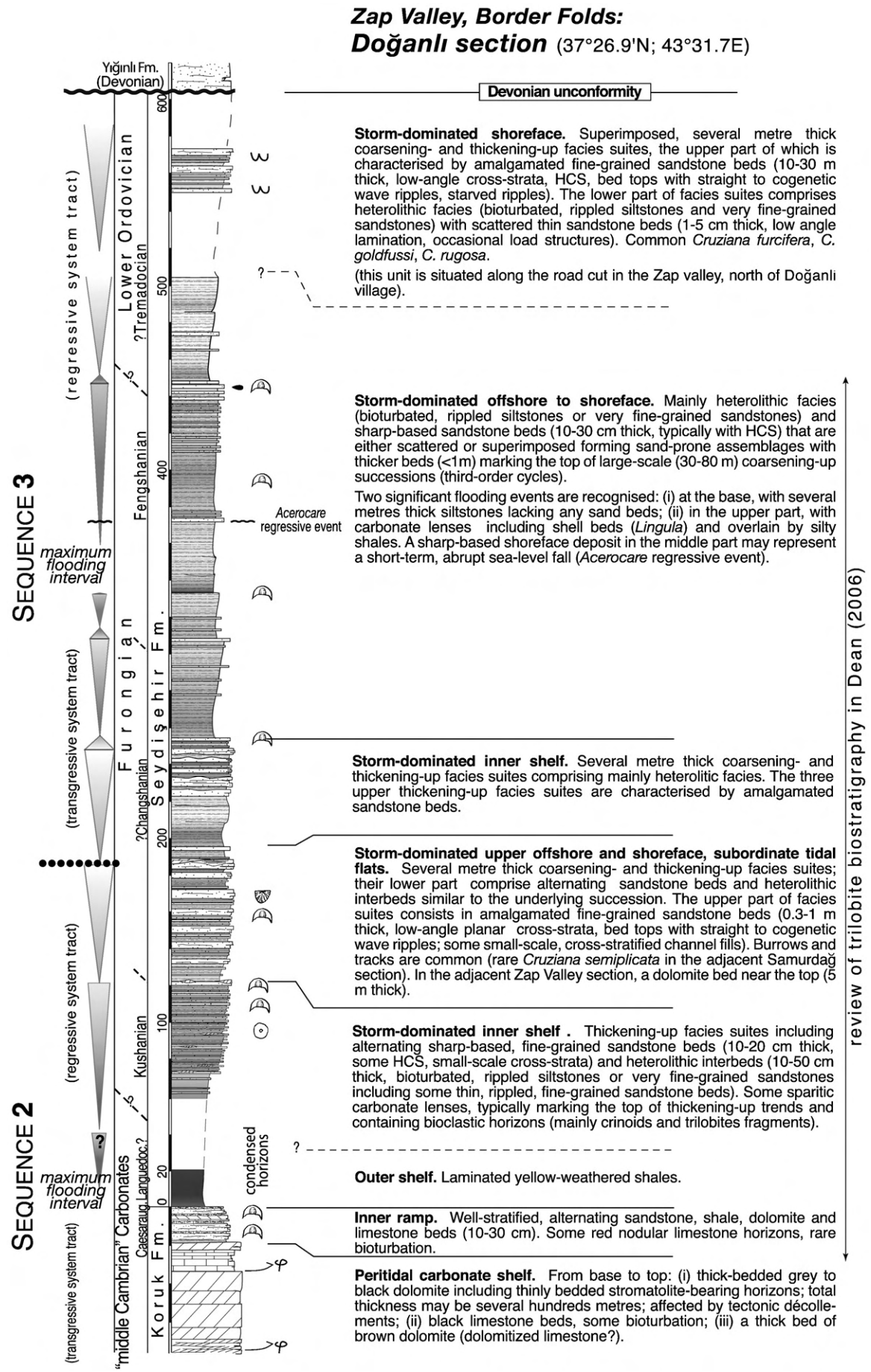

Fig. 11 *(continued).*

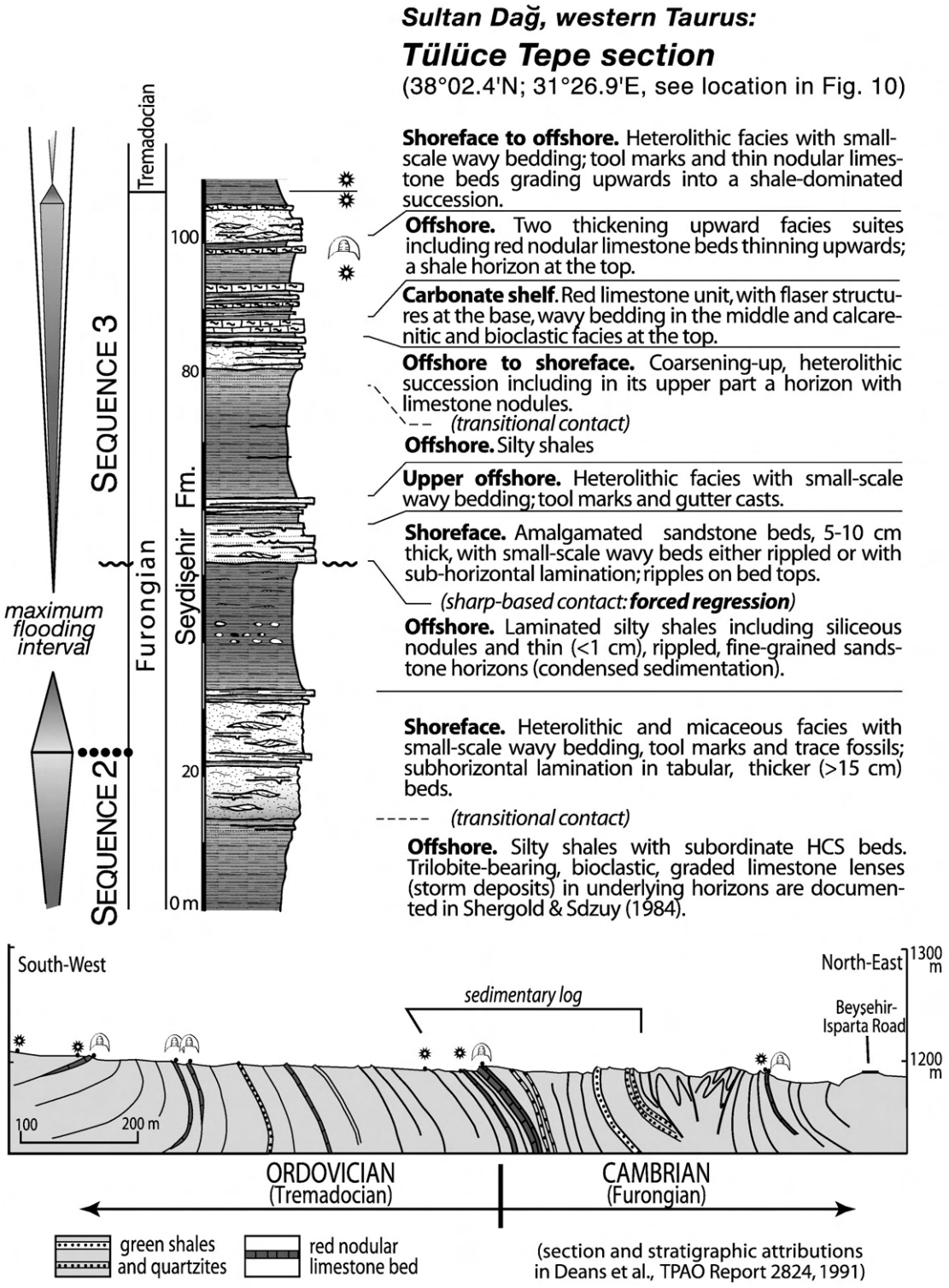

Fig. 12. The Cambrian/Ordovician boundary in the Western Taurus (Tülüce Tepe section, Sultan Dağ, location in Fig. 10). The sequence boundary between Depositional Sequences 2 and 3 is situated within the Seydişehir Fm. (Furongian = late Cambrian), at the base of shoreface deposits. Above, uppermost Cambrian strata reflect a transgressive trend (condensed horizons with nodules, occurrences of carbonate beds at MFI) followed by Tremadocian shales.

Mardin area while an offshore/shoreface-dominated succession prevails further east (Zap Valley, Fig. 11).

Furongian shallow-marine deposits in Turkey can be equated with fluvial-dominated strata in Jordan (Amireh et al., 1994, 2001). The fluvial succession of the upper Umm Ishrin Fm. should represent regressive strata of Depositional Sequence 2, and fluvial-dominated deposits including *Cruziana*-bearing tidal horizons (the lower part of the Disi Fm.) should correspond to transgressive strata of Depositional Sequence 3 (Figs. 2, 4 and 13F). Similarly, in northwestern Arabia, fluvial-dominated sandstones of the lower Saq Fm. (Risha Member of Vaslet, 1987) are regarded as mainly Furongian in age. In Oman, marine Furongian deposits overlie continental strata attributed to the Middle Cambrian (Millson et al., 1996). These marine shales represent the first marine-flooding

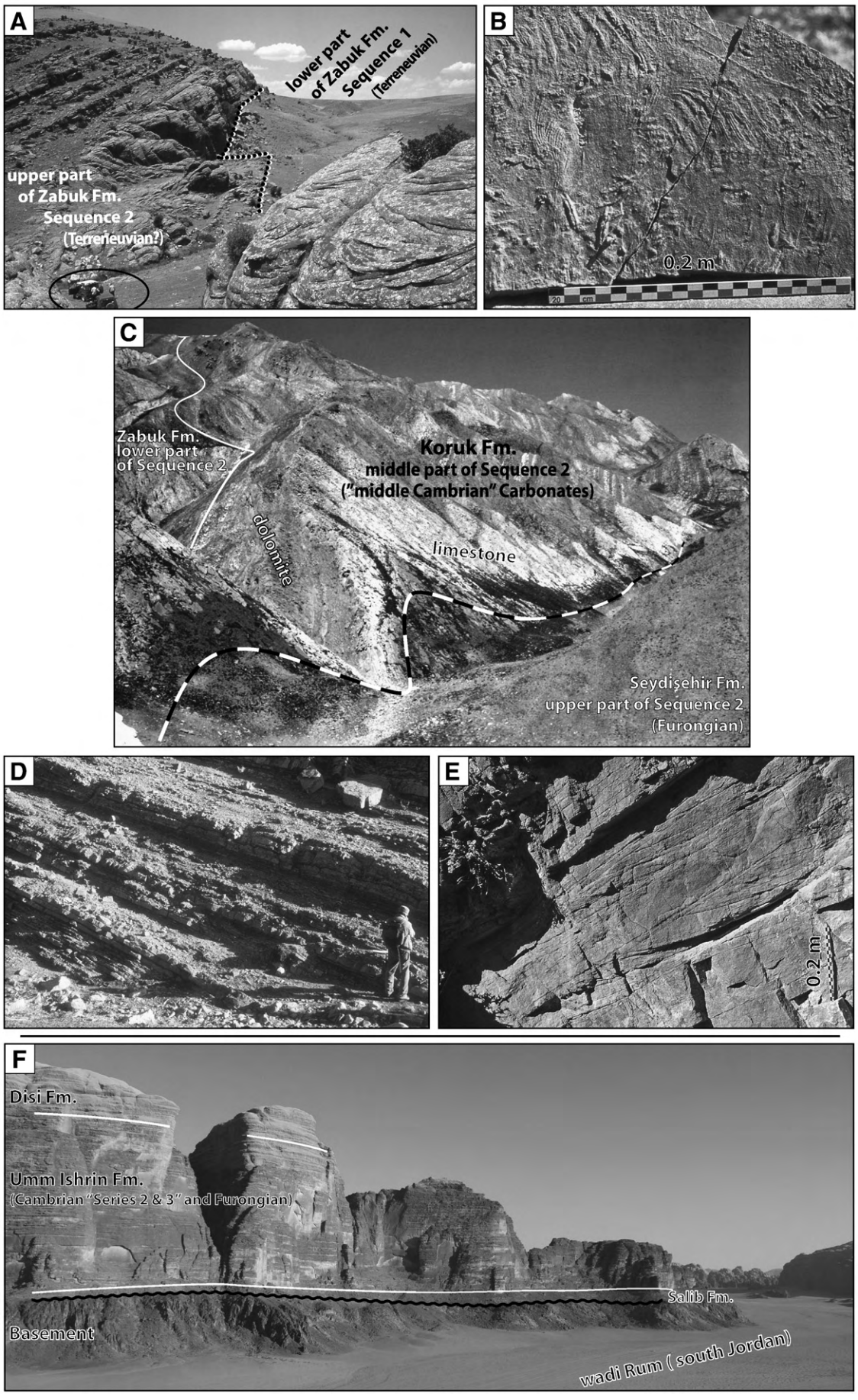
A
lower part
of Zabuk Fm.
Sequence 1
(Terreneuvian)
upper part
of Zabuk Fm.
Sequence 2
(Terreneuvian?)
B
0.2 m
C
Zabuk Fm.
lower part
of Sequence 2
Koruk Fm.
middle part of Sequence 2
("middle Cambrian" Carbonates)
dolomite
limestone
Seydişehir Fm.
upper part of Sequence 2
(Furongian)
D
E
0.2 m
F
Disi Fm.
Umm Ishrin Fm.
(Cambrian "Series 2 & 3" and Furongian)
Salib Fm.
Basement
wadi Rum (south Jordan)

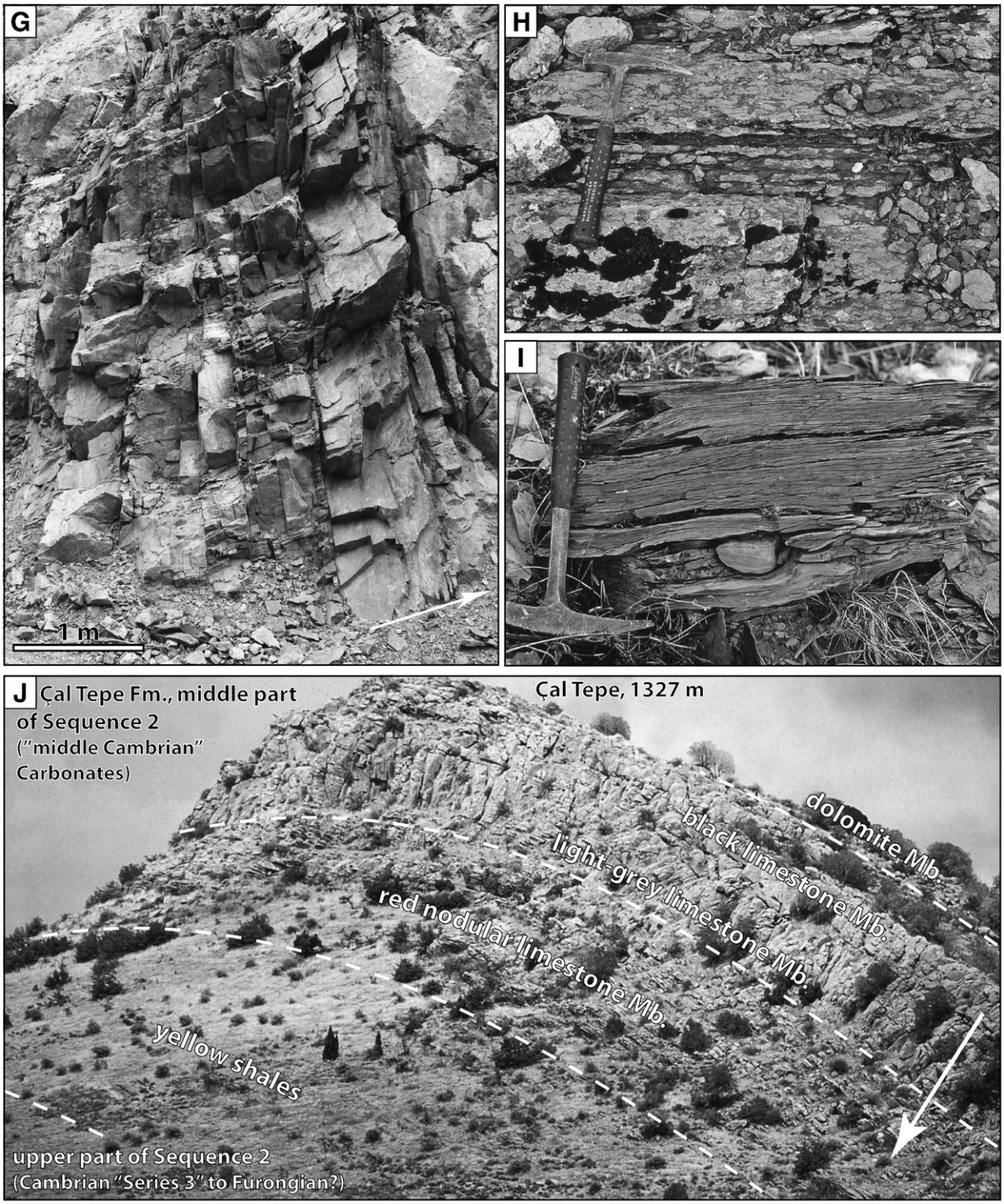

Fig. 13. Depositional Sequence 2. (A–B) upper Zabuk Fm., Mardin region, Border Folds (cf. Fig. 6): (A) the basal sharp-based contact (dotted line) of Depositional Sequence 2 on Depositional Sequence 1 is overlain by cross-bedded sandstones (main cliff in the lower part, braided streams; upper part, meandering streams; cars for scale in the lower left corner); (B) lower Cambrian trace fossils (*Dimorphichnus quadrifidus*), location on Fig. 7. (C) the Cambrian succession east of the Zap Valley (Samur Dağ area, eastern Border Folds, location on map Fig. 11, section in Dean, 2006). (D–E) Sosink Fm., Mardin region, Border Folds (cf. Fig. 6): (D) high-frequency facies cycles comprising storm-dominated deposits in the lower part of the formation (person for scale); (E) cross-bedded sandstones in the middle part of the formation (tidal sandbars). (F) in southern Jordan (Wadi Rum area), the coeval strata form a coarse-grained fluvial-dominated sandstone succession including the Salib (Cambrian "Series 2") and Umm Ishrin (Cambrian "Series 3" to Furongian) formations (cf. Fig. 2). (G) Sandıklı area, Western Taurus (cf. Fig. 8): cross-bedded sandstones (tidal sand bars with composite cross-stratification and lateral accretion surfaces) of the Hüdai Fm. (H–J) carbonate shelf to outer shelf facies in the Çal Tepe type-section, Seydişehir region, Western Taurus (cf. Fig. 10): (H) red nodular limestone in the upper part of the Çal Tepe Fm.; (I) yellow shales including nodules (condensed depositional environment); (J) general view of the overturned succession of the "middle Cambrian" Carbonates at Çal Tepe section (location Fig. 10) and of the base of the Seydişehir Fm ("yellow shales").

event, and define the Cm30 flooding interval (Sharland et al., 2001; Molyneux et al., 2006) that we tentatively correlate to the Furongian maximum flooding interval identified in the Zap Valley. These relationships imply a subsidence-driven continental onlap throughout the Cambrian (Fig. 4) from distal (Turkey, Terreneuvian?) to intermediate (Jordan, Cambrian "Series 2 and 3") and proximal areas

(Oman and Arabia, Furongian). The subsequent southward retreat of the clastic sources during the Furongian/ Early Ordovician regressive system tract resulted in fining-upward fluvial strata in the proximal areas (e.g., northwestern Arabia, Vaslet, 1987). A similar pattern arises from detrital zircon studies: Pan-African zircons predominate in the Cambrian strata but are progressively superseded by older (>1 Ga) zircons in younger strata. It reflects the blanketing of the Pan-African sources of the Arabo-Nubian Shield and a coeval southward migration of the detrital sources (Avigad et al. 2003; Kolodner et al. 2006).

Finally, we tentatively attribute the short-term but marked regressive event immediately beneath the Cambrian/Ordovician boundary (Figs. 11 and 12) to a global (glacio-?) eustatic sea-level fall. Its age may be equated with one of the best-known global hiatuses forming the Sauk II–Sauk III boundary in Laurentia, which associates a sea-level fall (e.g., Runkel et al., 1998), a global isotopic carbon excursion and mass extinctions (SPICE event of Saltzman et al., 2004; Zhu et al., 2004; Sial et al., 2008). It may be correlated with the *Acerocare* Regressive Event (Erdtmann, 1986), initially defined in Baltica, but later recognised in other parts of the north Gondwana shelf (Sardinia, Loi et al., 1996).

4.3.3. Lower Ordovician to early Middle Ordovician

In southern Turkey, Lower to early Middle Ordovician strata form the upper part of the regressive system tract of Depositional Sequence 3 in spite of a number of higher-frequency cycles, such as the conspicuous Tremadocian/earliest Floian cycle in the eastern Taurus (Fig. 14). A similar pattern is drawn from the Jordan record (Amireh et al., 2001; Schneider et al., 2007), where *Cruziana*-bearing intervals (upper Disi Fm., Umm Sahm Fm.) probably represent subordinate flooding events with fluvial facies as their regressive counterparts (Fig. 16D). Similar relationships are inferred from the Saq Sandstone in Saudi Arabia (Vaslet, 1987; McGillivray and Husseini, 1992). These superimposed high-frequency transgressive–regressive cycles may result in the far inland deposition of shale-prone facies, e.g. those with Tremadocian acritarchs reported in Jordan (Keegan et al., 1990) and northeastern Arabia (Molyneux and Al-Hajri, 2000). The Oman record is generally shown with two Tremadocian flooding events (Droste, 1997; MFS O10 and O20 of Sharland et al., 2001; Molyneux et al., 2006), which can be amalgamated distally, such as in Turkey. The sand-dominated Ghudun Fm. in Oman may be correlated with the well defined regressive wedge that constitutes the upper part of the Seydişehir Fm., essentially Floian in age (early Arenig in the British regional terminology).

A discrepancy may arise as concerns the place of the maximum flooding interval of Depositional Sequence 3: stratal stacking patterns suggest a maximum flooding surface of Furongian age (e.g., MFS Cm30 of Sharland et al., 2001, Figs. 2 and 11) whereas the deepest offshore facies are represented in eastern Turkey by Tremadocian fine-grained sediments within the regressive system tract (Fig. 14). The "Tremadocian flooding" recognized throughout northern Gondwana as far as southern Algeria results from a longer-term transgressive event that was initiated late in the Upper Cambrian (Haq and Schutter, 2008). It is relatively poorly evidenced in the distal setting of southern Turkey, in comparison with more proximal settings such as Oman or Algeria (Legrand, 1985; Fekirine and Abdallah, 1998; Vecoli, 2000; Carr, 2002; Eschard et al., 2005; Ghienne et al., 2007a; Galeazzi et al., 2010).

Contrasting with the prevailing uniform northeastward offshelf gradients in Depositional Sequence 2 and in most of Depositional Sequence 3, the upper part of the latter presents several inconsistencies. In the Taurides, the most proximal facies occur to the east with tide-influenced environments (Fig. 14), but offshore to shoreface conditions prevail to the west (Sultan Dağ). In the Border Folds, the Mardin succession reflects more proximal conditions than both the Amanos Mountains (to the west) and the Zap Valley (to the east), suggesting the presence of a palaeogeographic high. We infer that these local anomalous trends may announce the imminent onset of Middle Ordovician tectonic events.

5. Tectonic instability and differentiation of a sag basin (late Middle to Late Ordovician, Depositional Sequence 4)

A widespread but laterally differentiated, predominantly fine-grained succession characterizes Depositional Sequence 4. It is a thin to thick (20 m to over 1000 m) clastic wedge, resting unconformably on Depositional Sequences 3 and 2, and is topped by Upper Ordovician glacial deposits (Fig. 5). Related deposits (Figs. 15, 17 and 18) were identified long ago in the Border Folds (Bedinan Fm.: Kellogg, 1960, Dean, 1967; Dean and Monod, 1990; Steemans et al., 1996; Şort Tepe Fm.: Dean et al., 1981; Dean and Zhou, 1988). In the Taurides, only a few sections were assigned to time-equivalent deposits (Dean and Monod, 1990; Dean et al., 1999). Recently Depositional Sequence 4 was formally identified throughout southern Turkey (Figs. 18–22) thanks to the recovery of palynomorphs spanning the whole Middle to Late Ordovician (Paris et al., 2007b).

Contrasting with the extraordinarily widespread and long lasting stability of the northern part of the Gondwana platform from Cambrian to Early Ordovician, recurring instability is reflected through the succeeding deposits that form Depositional Sequence 4, and will lead to a new palaeogeographic organisation at platform scale (Fig. 5).

5.1. Boundaries

At outcrop, the lower boundary of Depositional Sequence 4 corresponds to a sharp lithologic break usually associated with a stratigraphic hiatus. In southeastern Turkey, Katian deposits rest on Lower Ordovician to Cambrian successions, with an up to 50 Ma hiatus. The unconformity is underlined by conglomerates in the Amanos Mountains. In the Mardin area, an angular unconformity is highlighted by a hardground and onlapping relationships at the outcrop scale (Figs. 6 and 7; Mardin High, Bozdoğan and Erten, 1990). A thin dolomitic horizon with Fe-oolithes underlines the unconformity in the Zap Valley (Fig. 15) (Dean and Zhou, 1988).

In the Taurides, this stratigraphic hiatus is identified all along the chain except in the Antalya Nappes (Kemer area) owing to tectonic imbrications. Lower Darriwilian to Upper Ordovician deposits onlap Depositional Sequence 3 (Fig. 5). The unconformity is usually underlined by a several metres thick limestone unit (Sobova Fm., Beyşehir area, Figs. 10 and 20, Dean, 1973; Kozan area, Fig. 19), which yielded Early Darriwilian conodonts (Sarmiento et al., 2003). Elsewhere, a sharp contact underlines the unconformity (Seydişehir area, Fig. 20; Anamur region, Fig. 21; Sarız region, Fig. 19; Dean and Monod, 1990).

By definition of a transgressive–regressive sequence, the upper bounding surface of Depositional Sequence 4 is situated on top of the maximum regressive facies, beneath the overlying transgressive strata, and thus matches the maximum glacio-eustatic sea-level fall of the Hirnantian glaciation. Where a glacial surface can be characterized, as in the northeastern Taurus (Monod et al., 2003) or in the Mardin High, the related unconformity is taken as the upper boundary of Depositional Sequence 4. The overlying, transgressive, glaciomarine facies suite forms the lowermost, transgressive part of a fifth sequence extending into the Silurian, which is beyond the aims of this paper. Where a glacial surface cannot be formally characterized, the boundary is placed on top of the coarsest glaciogenic deposits. Glaciation-related deposits are described together in Section 6.

5.2. Border Folds

Depositional Sequence 4 corresponds to a condensed succession in the Zap valley (Figs. 5 and 15) but exhibits an up to 700 m thick, coarsening- and thickening-upward clastic wedge, both in the Amanos Mountains (Dean and Monod, 1990) and in the Mardin area (Fig. 17). In

the latter, Upper Ordovician shales (Bedinan Fm.) rest unconformably upon strata of the Cambrian "Series 3" (Dean, 1983), after erosion of about 350 m of Furongian sandstones at the 10 km scale (Fig. 7b). This unconformity underlines the Mardin High (Bozdoğan and Erten, 1990), a regional tectonic uplift which occurred after the Cambrian but prior to the Sandbian (Early Caradoc). In the subsurface however, a few tens of kilometres south of the Mardin High (Ceylanpınar 1 well, Fig. 23), no significant stratigraphic hiatus exists in the succession, as shown by the continuous suite of palynomorphs ranging from early Darriwilian to Hirnantian reported by Paris et al. (2007b), including an Upper Ordovician succession up to 1100 m thick (Fig. 23).

On the Mardin High, deposition resumed in the Sandbian (Fig. 5), based on the occurrence of graptolites[2] and specific palynomorph assemblages (Paris et al., 2007b) (Fig. 17). Offshore facies rest directly upon the basal unconformity, but subsequent progressive deepening in the early Katian (middle Caradoc, Dean, 1967, 1983) is shown by the appearance of trinucleid trilobites (*Deanaspis*), within a biofacies that Zhou et al. (1998) consider indicating shallow outer-shelf conditions. The lower half of the Bedinan Fm. comprises essentially Sandbian to lower Katian storm-dominated fine-grained sediments (Fig. 17). The upper half is characterised by a suite of high-frequency, storm-dominated, offshore to shoreface cycles (Fig. 18D). Correlation between outcrop and subsurface logs indicates that this suite begins in the early Katian and reaches the middle Katian according to palynomorphs (Paris et al., 2007b) and trilobites (Dean, 1983). Uppermost strata of the Bedinan Fm. comprise 30 m thick cross-bedded sandstones probably tidal in origin, which are truncated by the glaciation-related deposits. In the subsurface, an additional, essentially shale-prone succession of upper Katian to Hirnantian age is identified beneath the glacial-related deposits (Paris et al., 2007b).

By contrast, in the Zap valley, Depositional Sequence 4 is restricted to an 8 m thick fine-grained succession, underlain by an oolitic brown-weathered dolomite bed (Fig. 15). The lowest two metres, including phosphatic nodules, may represent a residual, condensed transgressive wedge (cf. Dabard et al., 2007) of probable Darriwilian age (Paris et al., 2007b). The upper 6 m form a fining and then coarsening succession of Katian age. Related strata contain late Katian (Ashgill) trilobites (Dean and Zhou, 1988) together with middle Katian palynomorphs (Paris et al., 2007b), which may have been reworked. Devonian sandstones truncate this succession (Higgs et al., 2002).

5.3. Taurus Chain

Depositional Sequence 4 records major changes in both palaeogeography (tectonically controlled depocenters) and palaeoclimatic conditions (Hirnantian glaciation). For clarity, this sequence is subdivided into three units (lower, middle and upper), of Darriwilian, Sandbian–Katian, and Hirnantian age, respectively. The last, which contains the glacial deposits, is described in Section 6. Surprisingly, although the thickness of Depositional Sequence 4 rarely exceeds 100 m in the Taurides, the lower, middle and upper units can be consistently identified (Fig. 5), in spite of various facies differentiations in the Taurus Chain.

5.3.1. Lower unit

Wherever the lower unit of Depositional Sequence 4 is present in the Taurides, its base generally coincides with a sharp-based, 1 to 10 m thick carbonate horizon, resting in places on a ferruginous oolitic bed (Figs. 19 and 20). Internal facies changes and hardgrounds reveal a compound stratigraphy and probable gaps within this carbonate horizon, the age of which is early Darriwilian (late Arenig) in the Sobova Fm. stratotype (Dean and Monod, 1970; Dean 1973; Figs. 18B and 20) and in the Kozan region (Sarmiento et al., 2003; Fig. 20). Near Seydişehir, a thin (<20 m) fining-up, clastic wedge is locally intercalated between the underlying Seydişehir Fm. (Depositional Sequence 3) and the overlying limestone horizon; in this case, a basal, coarse-grained, transgressive lag truncates the Lower Ordovician sandstones (Figs. 18A and 20). Limestone horizons and hardgrounds indicate major shoreline backsteps and condensed sedimentation characterising a relatively high rate of sea-level rise. Like the "middle Cambrian" Carbonates, the Middle Ordovician limestone horizons reflect distal conditions with a starved, Gondwana-derived clastic supply.

Above the basal limestone horizon, the lower unit consists of a Late Darriwilian coarsening-upward detrital succession, a few metres to several tens of metres thick. Near Seydişehir, middle to late Darriwilian detritals (Paris et al., 2007b) were emplaced within a delta setting which prograded from NE to SW (on present-day coordinates), as shown by flute-casts and consistent current ripples (Figs. 18C and 20). Elsewhere, the coarsening-upward Darriwilian succession is much thinner. In the southeastern Taurides (Kozan area), it consists of siltstone a few metres thick, truncated by an intraformational conglomerate and/or overlying sandstones (Fig. 19). Regressive strata of this lower unit, either deltaic in origin or related to mass-flow deposition, suggest rapid, forced regression in the late (but not latest) Darriwilian.

5.3.2. Middle unit

The middle unit of Depositional Sequence 4 is best exposed in the eastern Taurides and comprises a regionally diachronous, 30 to 80 m thick, siltstone to fine-grained sandstone succession. In the eastern Taurus (Kilgen Lake section, north of Kozan, Fig. 19), it consists of graptolite-bearing siltstones and fine-grained sandstones. It is of latest Darriwilian (*Glyptograptus teretiusculus* zone) to Sandbian age according to graptolites[3] and to palynomorphs (Paris et al., 2007b). The highest beds include poorly preserved trilobites.[4] In the northeastern Taurides (Sarız region, Fig. 19), a siltstone-dominated succession, essentially late Katian in age (Early Ashgill, Dean and Monod, 1990) rests disconformably on Lower Ordovician strata. The large time interval (15 Ma) is represented by thin, condensed, poorly differentiated successions that include fine-grained sandstone deposited below storm-wave base and deep-water faunas (graptolites and cyclopygid trilobites) suggesting a non-subsiding outer shelf/upper slope depositional environment, dominated by shallow-water bottom-current sand deposits (e.g., Viana et al., 1998). This unusual facies is in good agreement with *in-situ* reworking as noted for palynomorph mixing (Paris et al., 2007b).

By contrast, coeval strata in the Antalya Nappes (Kemer unit, Marcoux, 1987; Janvier and Marcoux, 1977) comprise a thick (>500 m) fine-grained storm-dominated succession probably spanning the entire Late Ordovician, with well established upper Katian (Ashgill) strata (Dean et al., 1999; Paris et al., 2007b) (Fig. 22). This succession, characterized by high accumulation rates and abundant clastic supply, appears closer to those of the Arabian Plate than to those of (para-)autochthonous units in the Taurides (Fig. 3).

5.4. Regional correlations for Depositional Sequence 4

In the Middle to Upper Ordovician, a major transgressive event across the Northern Gondwana margin resulted in significant shoreline backsteps (e.g., Molyneux et al., 2006, their Fig. 2), flooding of large cratonic areas, and the onset of outer shelf conditions in areas of the Gondwana platform formerly dominated by continental environments (MFS O30 of Sharland et al., 2001; Haq and Al Qahtani, 2005; *Formosa* events of Paris et al., 2007a; Le Hérissé et al., 2007; Dabard et al., 2007; Ghienne et al., 2007a; "Late Llanvirn peak

[2] *Climacograptus orthoceratophilus*, indicating the lowest third of the Caradoc Series.

[3] *Climatograptus haljalensis*, *C. orthoceratophilus*, and the index species *Nemagraptus gracilis*.

[4] *Ulugtella* cf. *mediterranea*, *Placoparia* sp., *Selenopeltis* sp., and *Dionide* sp.

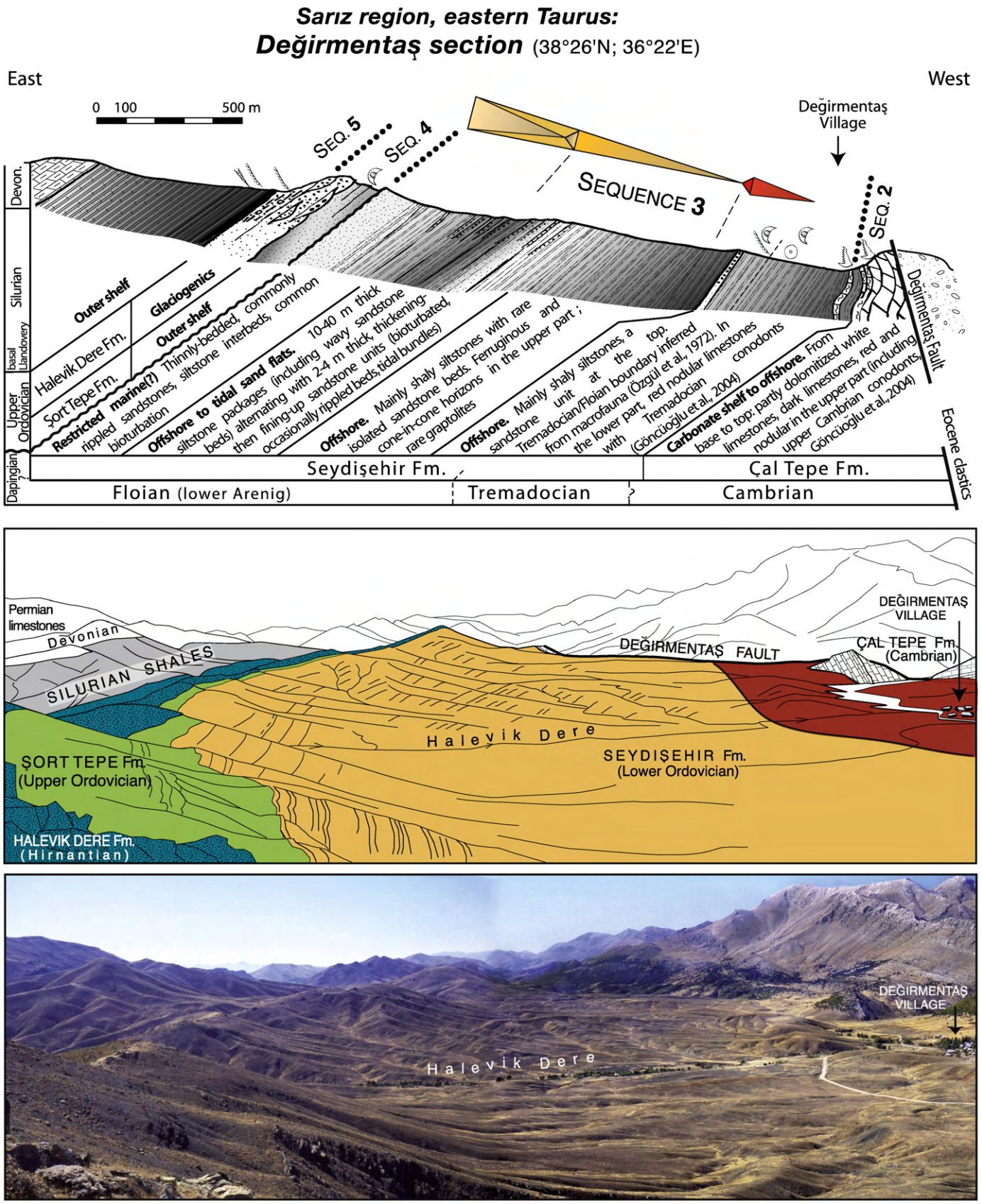

Fig. 14. Cross-profile and general view of the continuously exposed Cambrian to Silurian succession in the eastern Taurus (Sarız region, Fig. 1). See Fig. 19 for details within Depositional Sequence 4.

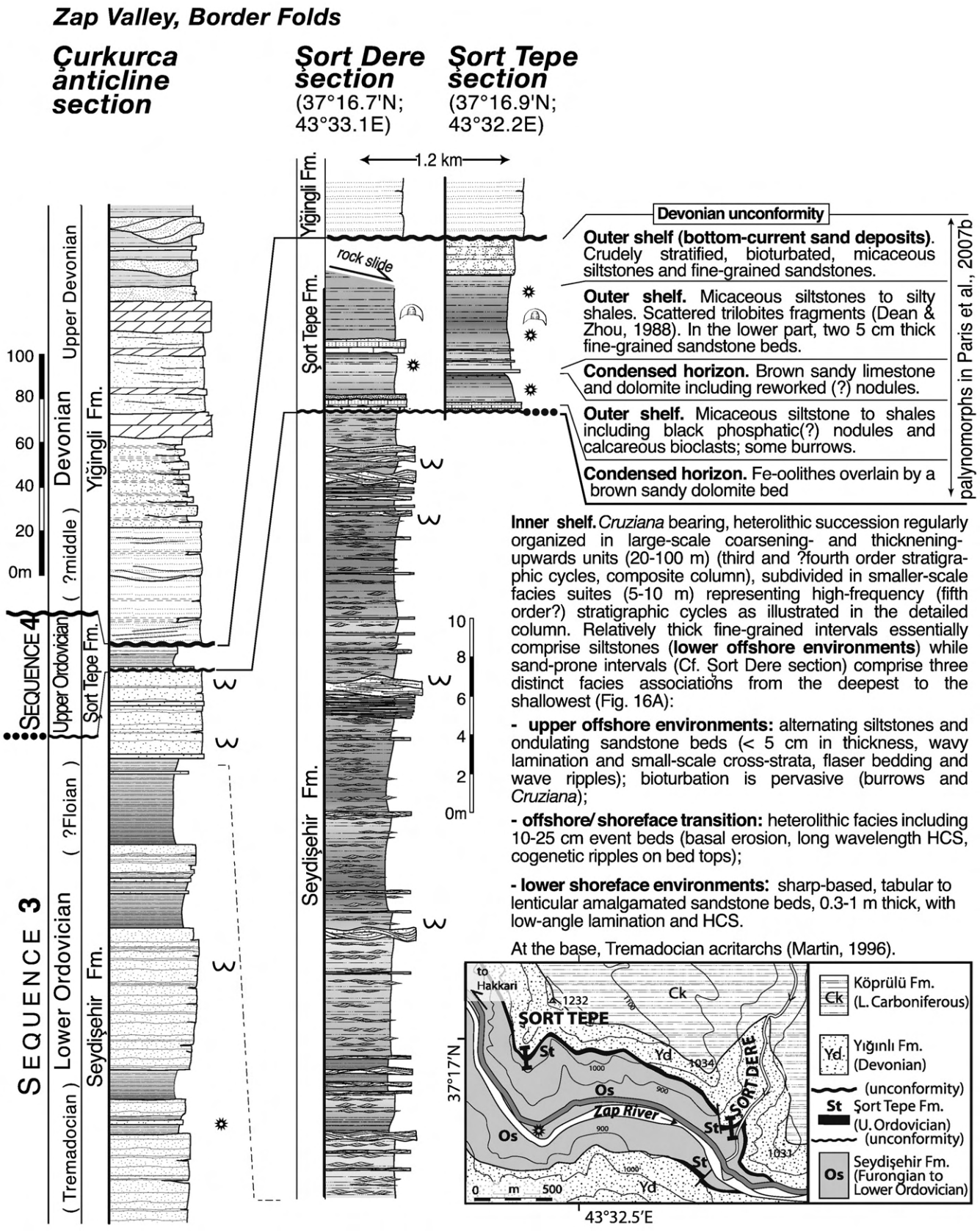

Fig. 15. The upper part of the Ordovician succession in the Çukurca anticline (Zap Valley, Border Folds) (cross section in Fig. 11; Şort Tepe view Fig. 16A). A sharp contact is noted between the Lower Ordovician Depositional Sequence 3 (Seydişehir Fm.) and the overlying, condensed Depositional Sequence 4. Hirnantian glacial strata are not present in this section owing to the Devonian unconformity (Higgs et al., 2002).

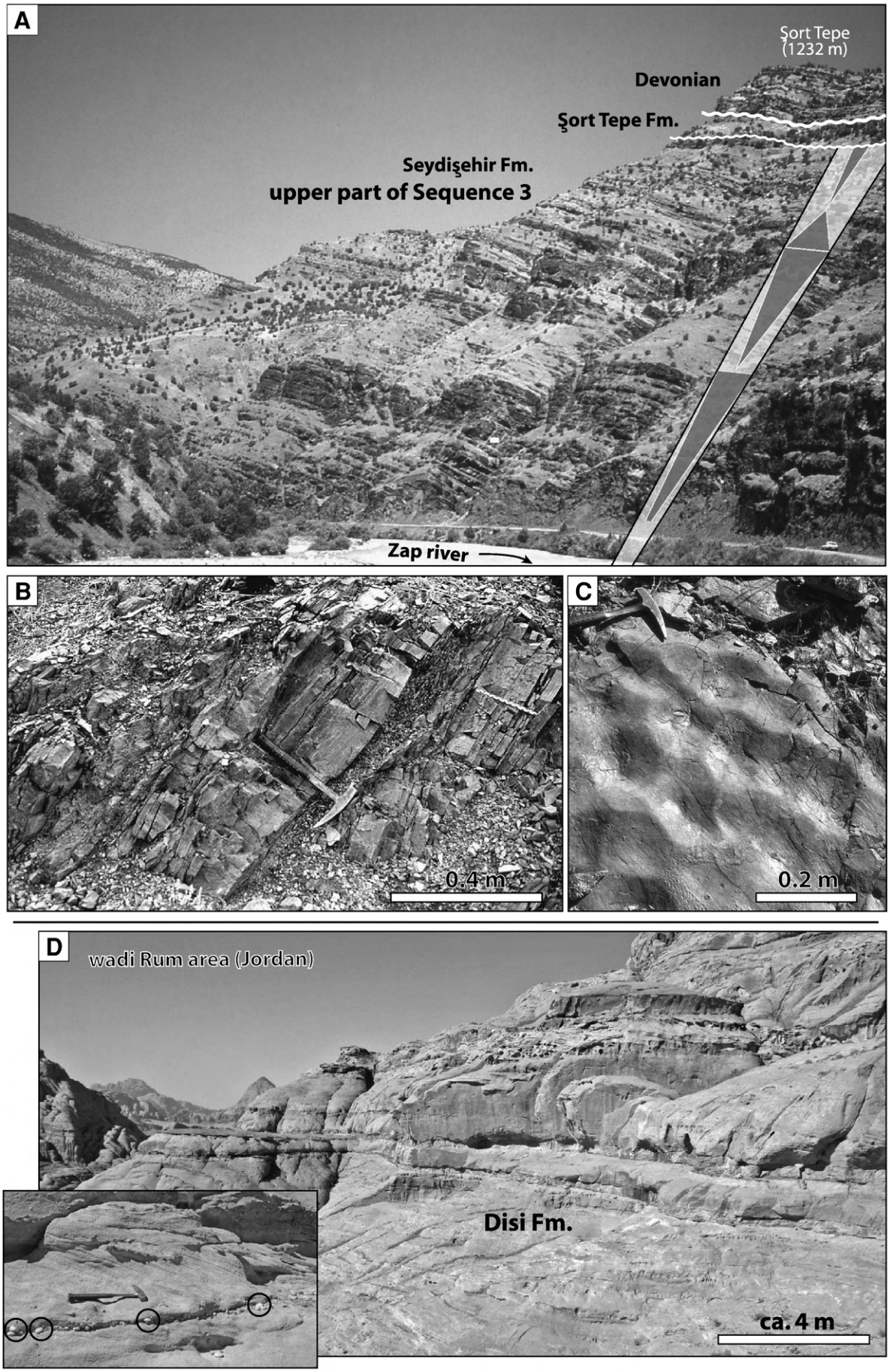
A
Şort Tepe
(1232 m)
Devonian
Şort Tepe Fm.
Seydişehir Fm.
upper part of Sequence 3
Zap river
B
0.4 m
C
0.2 m
D
wadi Rum area (Jordan)
Disi Fm.
ca. 4 m

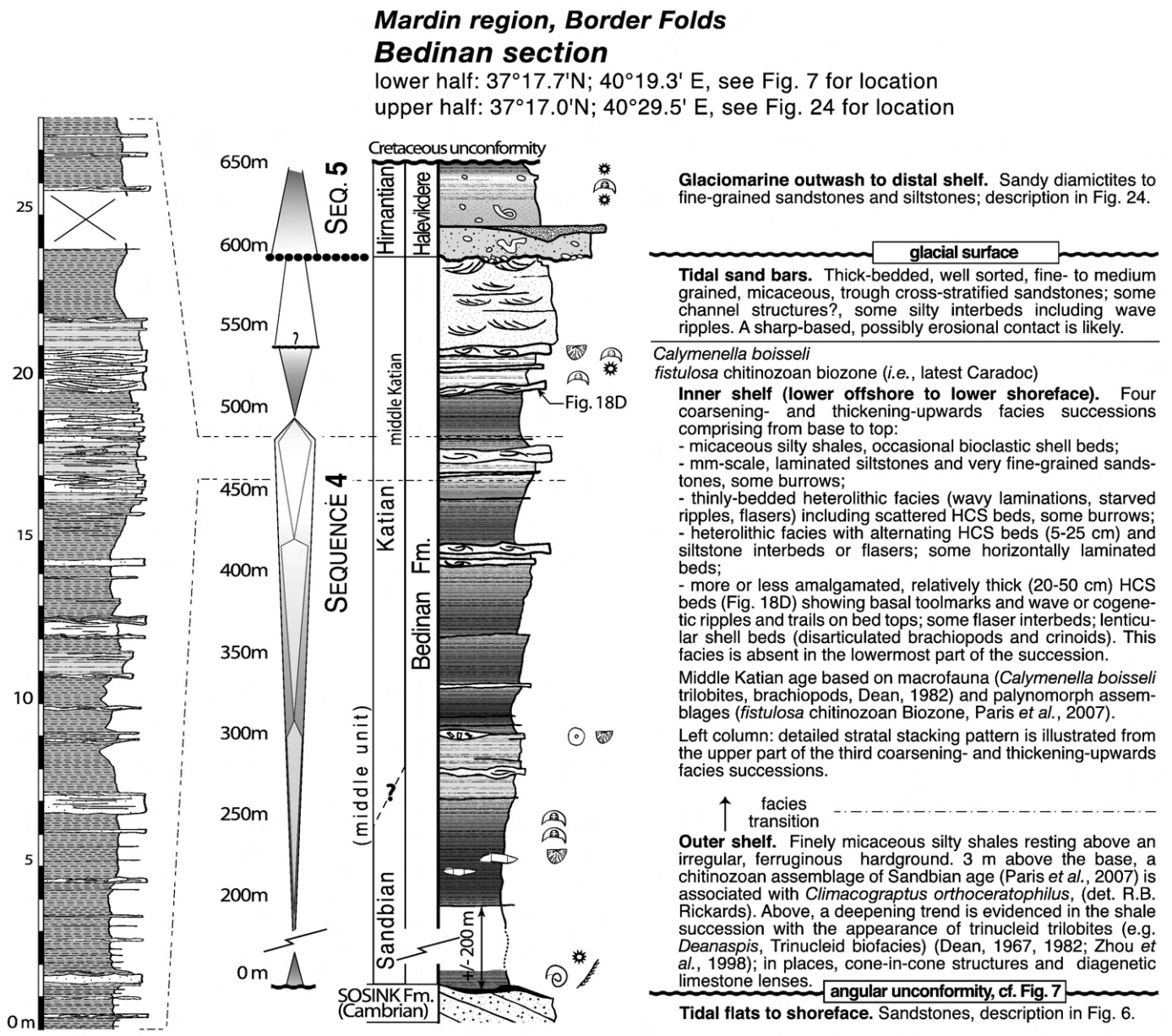

Fig. 17. The Upper Ordovician succession (middle and upper units of Depositional Sequence 4, Bedinan Fm.) in the Mardin High, Border Folds (Figs. 1 and 5). A glacial surface is present, which has truncated part of the underlying Bedinan Fm. (Katian). It contrasts with the nearby, more complete succession in the Ceylanpınar 1 well (Fig. 23).

transgression" of Galeazzi et al., 2010). The basal, major transgressive trend is emphasized by limestone beds at the base of an otherwise clastic Ordovician succession in southern Turkey, and is marked in Jordan by offshore shales with grapolitic faunas (Hiswa shales, Powell, 1989; Amireh et al., 2001; Figs. 5 and 18F). This event and higher-frequency subsequent transgressions with related shelf progradations resulted in Depositional Sequence 4 in southeastern Turkey, which corresponds essentially to the Qasim Fm. in central Saudi Arabia (Vaslet, 1987; El-Khayal and Romano, 1988; Paris et al., 2000; Şenalp and Al-Duaiji, 2001), and to the Khabour Fm. in Iraq (Al-Hadidy, 2007). Hence, we define a large-scale Bedinan–Qasim depocenter, or sag basin, including Depositional Sequence 4 in southern Turkey and coeval strata in the Middle East (Fig. 5).

5.4.1. Middle Ordovician

In the Taurides, the lower unit of Depositional Sequence 4 comprises a complete, high-frequency, transgressive–regressive cycle. Early Darriwilian transgressive conditions occur after a stratigraphic hiatus (Sobova Fm., Fig. 5). Where present, upper Darriwilian regressive strata are typified by the occurrence of

Fig. 16. Depositional Sequence 3. (A) Lower Ordovician Seydişehir Fm. (with higher-frequency cycles) unconformably overlain by Upper Ordovician Şort Tepe Fm. in the Zap Valley, eastern Border Folds (Fig. 15). (B–C) Storm-dominated facies (B: HCS beds and heterolithic facies, upper offshore; C: cogenetic ripples on bed tops, lower shoreface) characterizing Lower Ordovician depositional environments in the Western Taurus near Seydişehir. (D) in the Wadi Rum area (Jbal Burdah, southern Jordan), coeval strata form a thick, cross-bedded fluvial-dominated sandstone succession (the main part of the Disi and Umm Sham Fms, cf. Fig. 2) that includes m-thick, tidal-dominated, *Cruziana*-bearing, transgressive horizons (middle part of the picture). Fluvial strata include abundant quartz pebble lags (inset, lower left corner) which could be the source of the pebbles that were reworked and striated during the Hirnantian glaciation and are found now in the Mardin area (Halevikdere Fm., Fig. 18L) and in glacial strata of southern Jordan (Fig. 18M).

gravity-driven deposits. In the Border Folds, a significant but localized hiatus may occur (Bedinan Fm. resting on Sosink Fm. in the Mardin High; Figs. 5, 7 and 17). In adjacent areas, the continuous record of Depositional 4 highlights a clear tectonic differentiation of uplifting/subsiding areas during the Middle Ordovician (Paris et al., 2007b).

In more internal cratonic regions (Saudi Arabia), the related regressive event is not clearly expressed. In Jordan, it corresponds most likely to the lower Dubaydib Fm. (Amireh et al., 2001). The regressive trend and any related unconformity are not documented at outcrop around the Arabian Shield (Şenalp and Al-Duaiji, 2001) although a time-equivalent unconformity is figured in Oman (Droste, 1997; Molyneux et al. 2006). Regressive deposits are identified in the subsurface within the Hanadir Member of the Qasim Fm., immediately below a latest Middle Ordovician shaly interval (Al-Hajri and Owens, 2000) (Fig. 23). According to gamma-ray patterns (Al-Hajri and Owens, 2000; Şenalp and Al-Duaiji, 2001), this shaly interval is also documented in Iraq in the Akkas-1 reference well and suggests that K5 member of the Khabour Fm. (Al-Hadidy, 2007) may represent regressive Darriwilian deposits that constitute most of the lower unit in Turkish Depositional Sequence 4.

By contrast, in more western regions such as Morocco, a major (up to 500 m thick) regressive wedge was deposited at the end of the Middle Ordovician (First Bani Group of Destombes et al., 1985). There, subsequent transgression was delayed and occurred only in the early Sandbian (Gutierrez-Marco et al., 2003) while it occurred in Turkey as early as the late Darriwilian. Such discrepancies in sea-level change patterns are attributed to tectonic-driven events superimposed on the global-scale Middle Ordovician transgressive trend (Haq and Schutter, 2008).

5.4.2. Sandbian (early Caradoc of the British Series)

In the latest Middle Ordovician (*pissotensis* event of Paris et al., 2007a), transgressive conditions were renewed as shown in the southeastern Taurides (Fig. 19). Ensuing transgressive conditions during the Sandbian (deepening trend in the basal Bedinan Fm.), and succeeding regressive conditions in the late Sandbian are reflected by the basal Mardin High succession (Fig. 17) and adjacent Ceylanpınar 1 well (Fig. 23). Time-equivalent strata in the eastern Taurus (Fig. 19) and in the Zap Valley (Fig. 11) exhibit condensed successions deposited far from clastic sources. In Saudi Arabia, limited palynomorph data show the latest Middle Ordovician/earliest Late Ordovician transgressive trend to be located within the Hanadir Mb. of the Qasim Fm., and is reflected by a relatively thick shaly interval (Al-Hajri and Owens, 2000; Paris et al., 2000). This subordinate flooding event, which occurs within the maximum flooding interval of Depositional Sequence 4, is placed between MFS O30 and MFS O40 of Sharland et al. (2001) (Fig. 2). Regional correlations (Fig. 23) show that overlying regressive strata correspond to both the uppermost Hanadir Mb. and Kahfah Mb. of the Qasim Fm. in Saudi Arabia (Şenalp and Al-Duaiji, 2001) and constitute the main part of K4 and K3 members of the Khabour Fm. in the subsurface of Iraq (Al-Hadidy, 2007). In Jordan, it essentially corresponds to the upper Dubaydib Fm., which comprises nearshore facies (Amireh et al., 2001) deposited in more proximal conditions than those of the Border Folds.

5.4.3. Early Katian (late Caradoc of the British Series)

Overlying the regressive Sandbian strata, a major transgressive event usually represented by MFS O40 of Sharland et al. (2001) occurred in the early Katian (Fig. 5). On the Arabian plate, the age of maximum flooding conditions is however uncertain. Based on graptolites, an earliest Katian age is possible (El-Khayal, in Sharland et al., 2001; Şenalp and Al-Duaiji, 2001) but palynomorphs suggest a middle Katian age (*fistulosa* event of Paris et al., 2000, 2007a). This transgressive event is considered responsible for re-flooding of the northeastern Taurus (Sarız area), where coeval strata directly overlie Lower Ordovician strata (Fig. 19). Reworked palynomorphs, however, indicate the erosion of previously deposited Darriwilian strata prior to the onset of the Middle Katian deposits (Dean and Martin, 1992; Paris et al., 2007b). In the Border Folds, biostratigraphy both at outcrop and in the subsurface (Paris et al., 2007b) suggests that lower Katian strata are represented by the upper half of the Bedinan Fm. (Fig. 17), but locate the *fistulosa* Biozone in the higher levels, hence relatively high within an overall prograding wedge. Such relationships may indicate a lower Katian low-frequency transgressive–regressive event with maximum flooding conditions restricted to the lowest Katian. The deepest facies, favourable for palynomorph preservation, were deposited later (middle Katian = uppermost Caradoc) on the shelf, owing to a high-frequency, major transgression (*fistulosa* event of Paris et al., 2007a). This view of a high rate of sea-level rise agrees well with the major shoreline retreat shown in Oman during the deposition of the Hasirah Fm. (up to 500 km inland relative to the preceding transgressive event MFI O30, Molyneux et al., 2006). In Jordan, roughly coeval strata are the basal Tubeiliyat Sandstone Fm. (Powell, 1989; Amireh et al., 2001).

Middle Katian strata comprise a shale-dominated interval with a highly diagnostic gamma-ray blocky pattern between two sandstone packages, and can be confidently correlated with several published wells, from Saudi Arabia (Ra'an Mb. of Al-Hajri and Owens, 2000; Şenalp and Al-Duaiji, 2001) to the Iraqi wells (K3 member of the Khabour Fm., Akkas-1 well, Al-Hadidy, 2007) (Fig. 23). Significant thickening of the Middle Katian strata is evident, from the central part of the Arabian Plate (some tens of metres), to Syria (Best et al., 1993) and to southeastern Turkey (some hundreds of metres), while a more uniform thickness pattern typifies late Darriwillian to Sandbian deposits (Fig. 23). This is interpreted as a north-eastward migration of the Bedinan–Qasim depocenter through an overall displacement of the shelf profile within a subsiding sag basin trending NW–SE (Şenalp and Al-Duaiji, 2001). The deepest facies (*Zoophycos* ichnofacies) was deposited in northern Iraq (Sharland et al., 2001) while thinner successions are logged in southern Oman (Molyneux et al., 2006). Condensed, relatively deep-water sediments were deposited on the opposite side of the basin, as illustrated in the Zap Valley, within a virtually non-subsiding setting.

5.4.4. Late Katian (early Ashgill of the British Series)

Relatively thick late Katian (pre-Hirnantian Ashgill series in the British regional terminology) strata are recognized both in the Western Taurus and in the subsurface of the Mardin area (Fig. 23).

Fig. 18. Depositional Sequence 4. (A–C) Middle Ordovician (Darriwilian) Sobova Fm. in the Western Taurus (Beyşehir/Seydişehir region, location in Fig. 1): (A) a fining-up transgressive lag deposit underlines the basal unconformity (cf. Fig. 20) and includes coarse, rounded quartz grains (Q), *Lingula* fragments (Lf) and intraclasts (Ic); (B) a cystoid limestone bed from the lower member of the Sobova Fm. near Beyşehir (Fig. 10); (C) coarsening-upward, m-scale siltstone to sandstone facies suites including Bouma sequences (turbiditic environments) in the Tarasçı section (Fig. 20). (D) HCS beds (upper offshore environments) in the upper part of the Bedinan Fm. (middle Katian), Mardin region, Border Folds (Fig. 17). (E–F) In southern Jordan (Wadi Rum area, Wadi Hiswa): coeval strata form a mixed, tidal to storm-dominated, 350 m thick succession, from the Darriwilian Hiswa shales at the base, the upper Darriwilian–Sandbian Dubaydib Fm. in the middle, to the mainly Katian Tubeiliyat Fm. in the upper part. (G–K) In Turkey: Hirnantian glacial deposits of the Halevikdere Fm.: (G) A trilobite fragment in the glacial deposits: *Flexicalymene* n. sp. dorsal, left lateral, anterior and posterior view of the cranidium (scale bar: 5 mm; Bedinan section, Border Folds, Fig. 24); (H) a granite dropstone truncating glaciomarine outwash deposits (Ovacık section, Central Taurus, Fig. 21); (I) large-scale ball-and-pillow structures (sandstone) within a diamictite matrix (Kozan section, eastern Taurus, Fig. 19); (J) massive sandy diamictite including subangular sand grains, and mm- to cm-scale quartz and lithic clasts (Kemer section, Antalya Nappes, Fig. 22); (K) cross-bedded sandstone (tidal bars) in the upper part of the Hirnantian lower glacial cycle, recording a marked interglacial transgression (Kozan section, eastern Taurus, Fig. 19); (L) striated and facetted quartz pebbles from the Bedinan/Yurteri section (Mardin area, Border Folds, Fig. 24). Strikingly similar pebbles (M) can be collected in glacial strata of southern Jordan, most likely derived from the Lower Ordovician strata (cf. Fig. 16D). (N) in the Batn El Ghul area (Jbal Ahmar, southern Jordan), glacial strata (Ammar Fm., fluvial or deltaic sediments) are preserved in deeply (75–150 m) incised palaeovalleys truncating the Tubeiliyat Fm. (Katian).

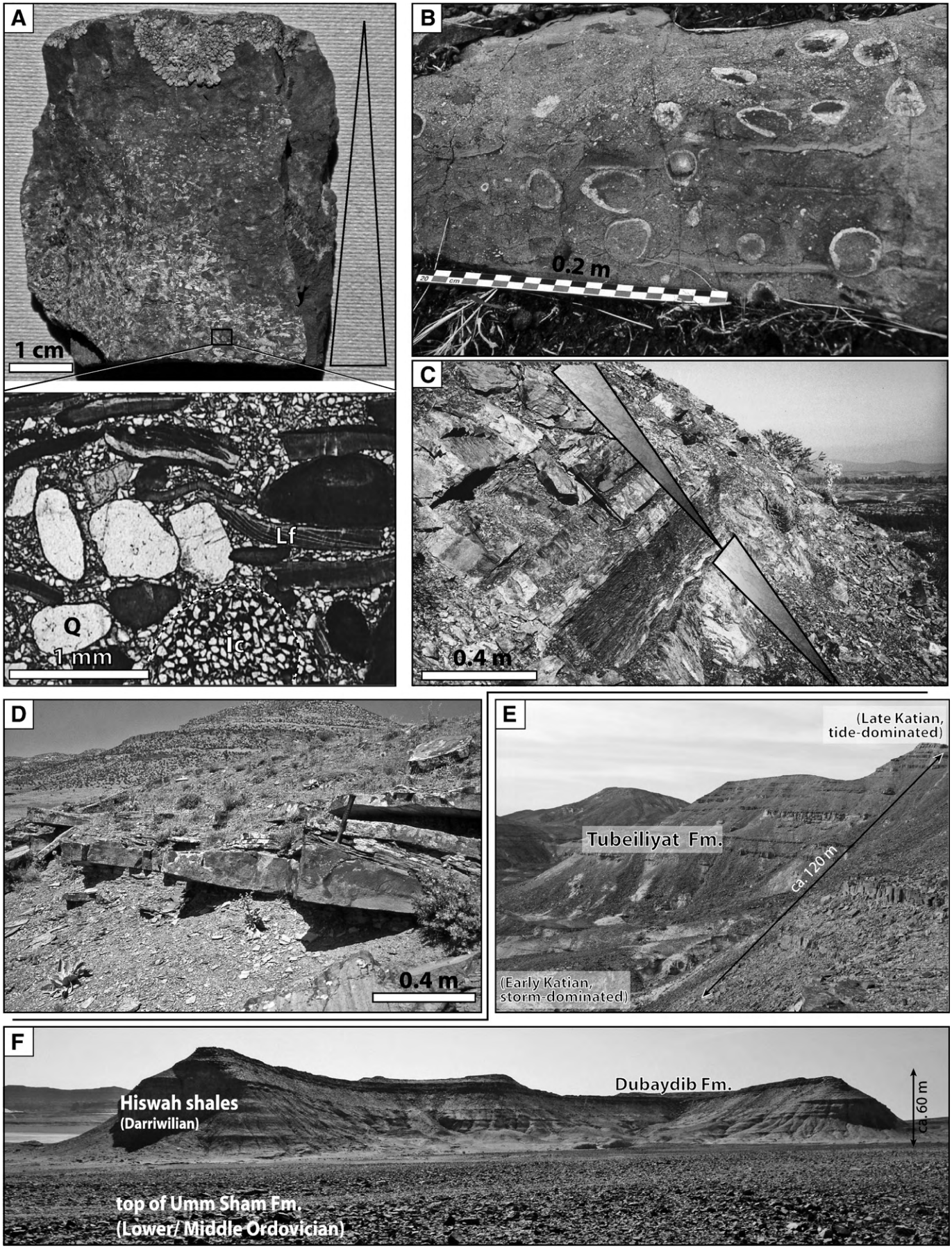
A
1 cm
Lf
Q
Ic
1 mm
B
0.2 m
C
0.4 m
D
0.4 m
E
(Late Katian,
tide-dominated)
Tubeiliyat Fm.
ca. 120 m
(Early Katian,
storm-dominated)
F
Hiswah shales
(Darriwilian)
Dubaydib Fm.
ca. 60 m
top of Umm Sham Fm.
(Lower/ Middle Ordovician)

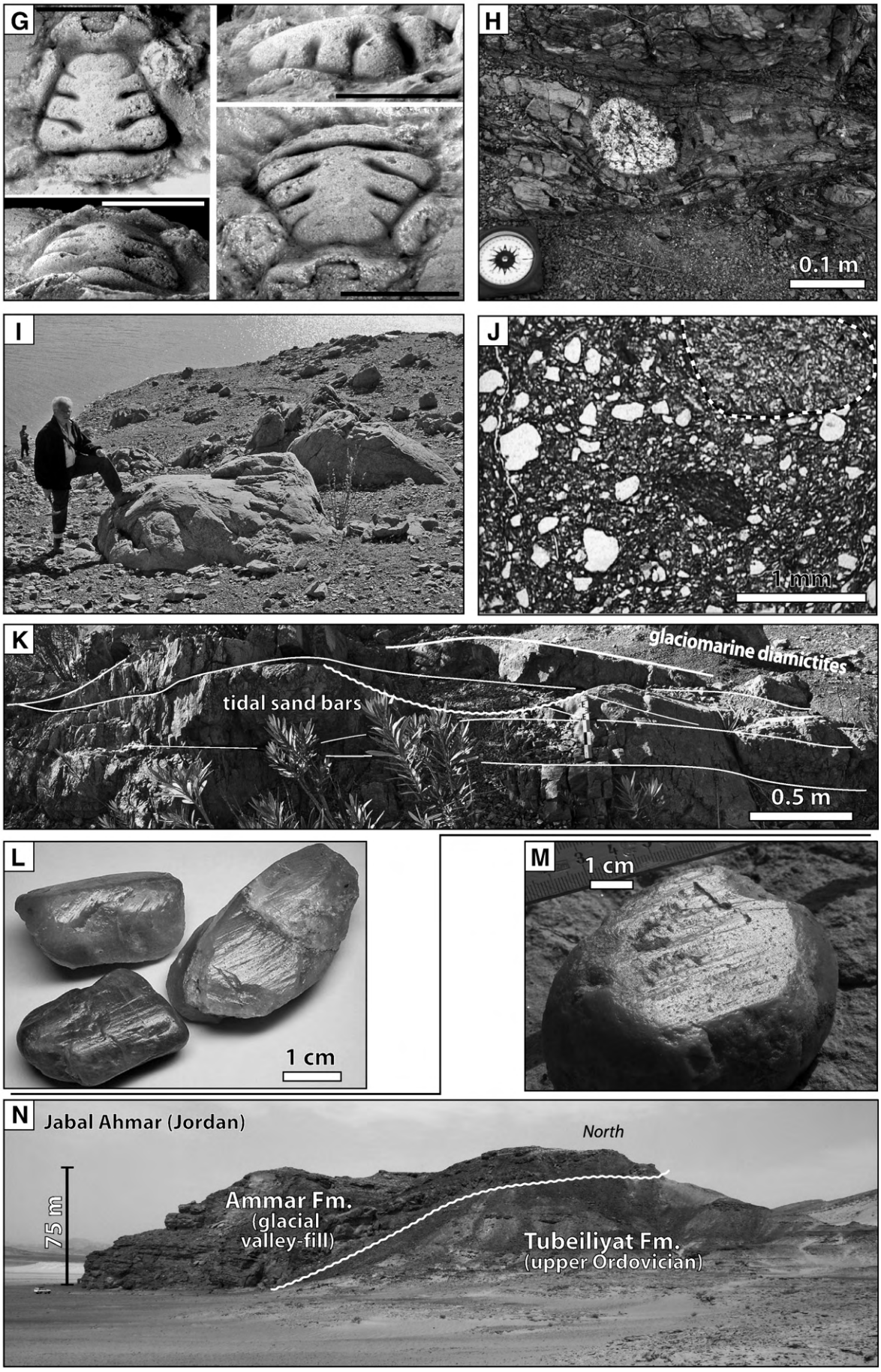
G
H
0.1 m
I
J
1 mm
K
glaciomarine diamictites
tidal sand bars
0.5 m
L
1 cm
M
1 cm
N
Jabal Ahmar (Jordan)
North
75 m
Ammar Fm.
(glacial
valley-fill)
Tubeiliyat Fm.
(upper Ordovician)

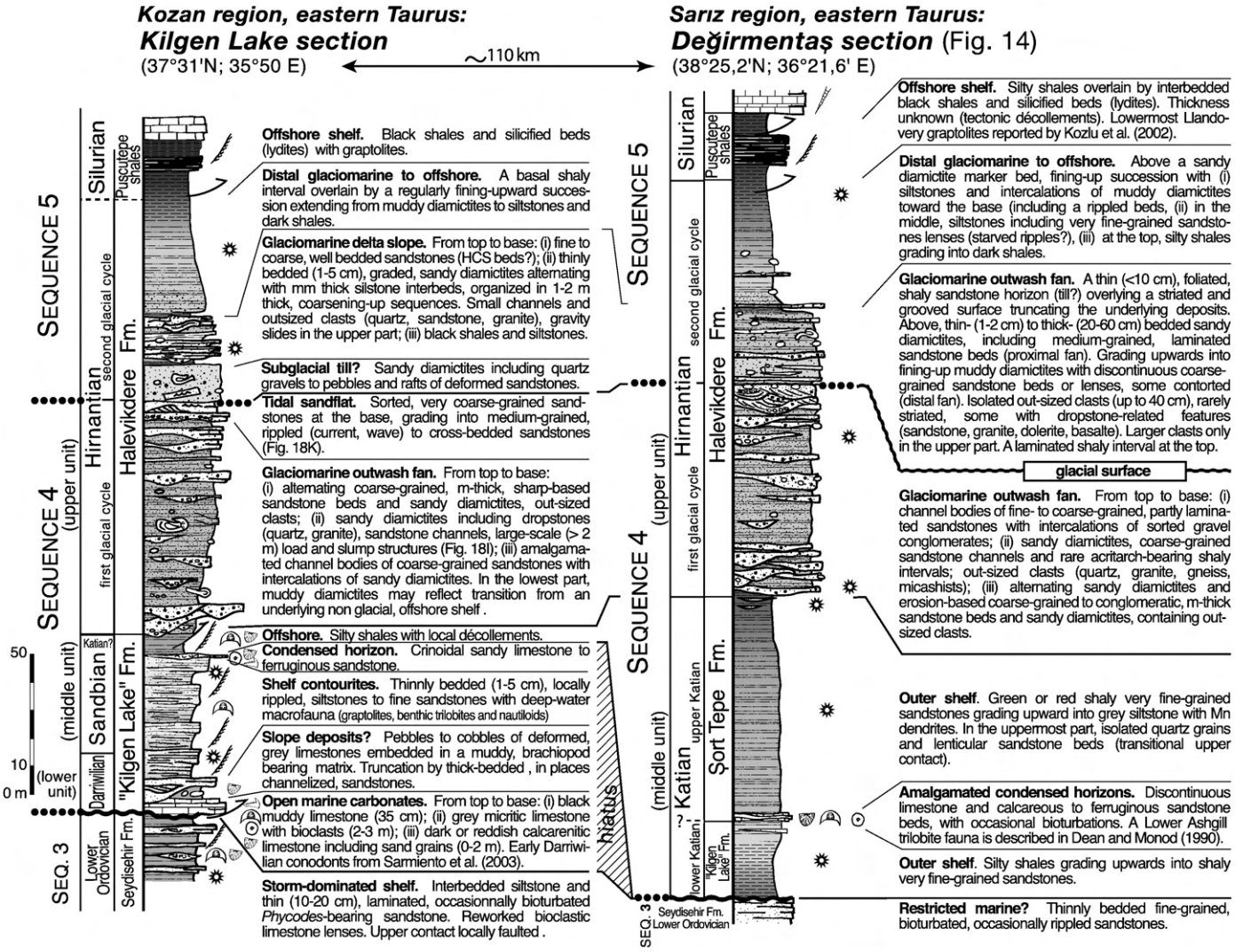

Fig. 19. The Middle to Upper Ordovician succession in the eastern Taurus (location in Fig. 1), showing the disconformable basal contact of Depositional Sequence 4 ("Kilgen Lake" Fm.) upon Depositional Sequence 3 (Seydişehir Fm.). In the Sarız region, the top of Depositional Sequence 4 is a glacial surface situated within the Halevikdere Fm. (Hirnantian). Darriwilian to Sandbian macrofossils are listed in footnotes 3 and 4 (Section 5.3.2).

By contrast, in the northeastern Taurus as well as in the Zap Valley, only a thin succession is identified. Late Katian strata are usually shale prone, except for the upper, sand-dominated part of the Bedinan Fm. in the Mardin High. Time-equivalent strata form essentially the Quwarah Mb. of the Qasim Fm. (Paris et al., 2000; Şenalp and Al-Duaiji, 2001) or the upper part of the mixed tidal- to storm-dominated Tubeiliyat Sandstone in Jordan (Amireh et al., 2001; Fig. 18E). In Saudi Arabia, Şenalp and Al-Duaiji (2001) recognized an erosional surface within the lower part of the Quwarah Mb., which they ascribe to the base of a tidal-dominated prograding wedge, similarly to the sharp-based sandy tidal deposits of the uppermost Bedinan Fm. on the Mardin High (Fig. 17). This also agrees with a number of sharp-based patterns inferred from subsurface gamma-ray logs in Saudi Arabia (Al-Hajri and Owens, 2000; Şenalp and Al-Duaiji, 2001) and in Iraq (Al-Hadidy, 2007) (Fig. 23). These coeval, sharp-based shallow-marine suites suggest that forced regression occurred in the latest Middle Katian, before transgressive conditions recommenced in the earliest Late Katian (early Ashgill). The latter are attributed to pre-Hirnantian glacio-eustatic events (Achab and Paris, 2007; Loi et al., in press). Related subaerial erosion surfaces in proximal reaches of the platform probably enhanced faunal reworking. It should be noted that no Late Katian reef-related carbonates have been recognized in southern Turkey, although these are well known further west in Spain, Morocco and Libya (Vennin et al., 1998; Villas et al., 2002; Bergström and Massa, 1991; Gutierrez-Marco et al., 2002). In the subsurface, the related unit may be traced throughout northern Libya but disappears towards Egypt (C. Blanpied, personal communication). To the authors' knowledge, this reef-related carbonate unit is not present in the Middle East.

6. Latest Ordovician: the Hirnantian glaciation (Depositional Sequence 4, upper unit)

The upper unit of Depositional Sequence 4 comprises essentially glaciation-related deposits. Together with the lowest part of a fifth latest Ordovician–Lower Silurian Depositional Sequence, they constitute the Hirnantian glacial record and have only recently been formally identified throughout Turkey (Fig. 5, Halevikdere Fm.; Monod et al., 2003).

6.1. Description

6.1.1. Boundaries

Glaciation-related deposits usually exhibit a sharp basal contact with conformable relationships (e.g. Antalya Nappes, Fig. 22) and no

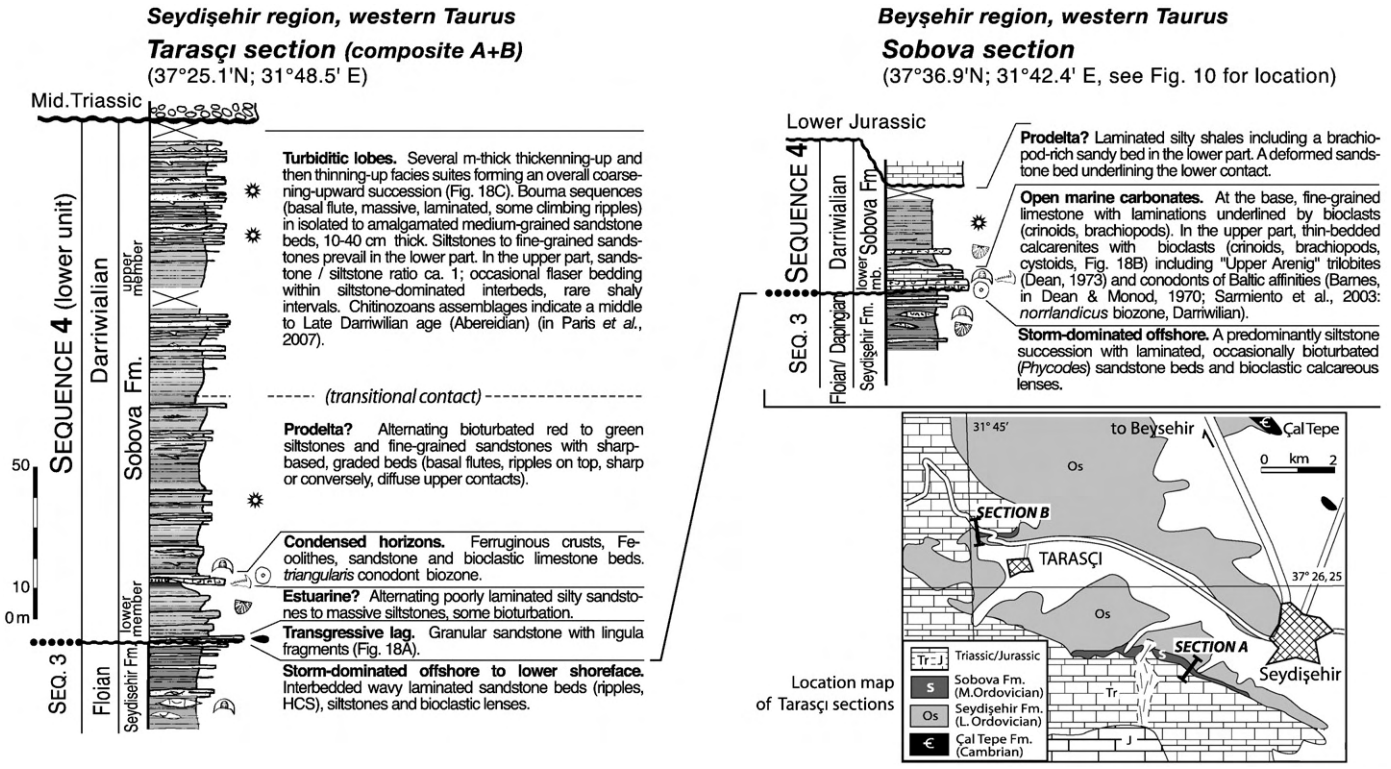

Fig. 20. Base of Depositional Sequence 4 (lower unit, Darriwilian; Sobova Fm.) in the Western Taurus (Seydişehir–Beyşehir region) (location in Figs. 1 and 10). Both sections show the transgression of the Sobova Fm. upon the lower Ordovician Seydişehir Fm.

(or minor) hiatus as testified in the northeastern Taurus (Paris et al., 2007b) (Fig. 19). Beneath the glacial deposits, the erosional contact locally reaches the Lower Ordovician rocks in the southern (Ovacık, Fig. 21) and southeastern Taurus (Kozan). In the latter area, the erosional unconformity can be followed at the 10 km scale with Upper Ordovician strata preserved in the immediate vicinity (Fig. 19). However, on the Mardin High (Border Folds), correlation with the subsurface shows the removal of Ordovician rocks about 200 m thick (Fig. 23).

6.1.2. Border Folds

In the Mardin High, glacial strata form a 75 m thick fining-upward conglomeratic unit (Monod et al., 2003) (Fig. 24). In places, the glacial succession overlies sandstone structures several metres long exhibiting small extensional "step fractures" interpreted as subglacial streamlined bedforms (Deynoux and Ghienne, 2004; Denis et al., in press). These are typical markers of a grounded ice-sheet, and a SE to NW ice-flow (Fig. 25) is indicated by their asymmetry. The overlying strata, made up of fining-up, transgressive, glaciomarine deposits, constitute the base of Depositional Sequence 5 (Fig. 24) and contain not only palynomorphs of Hirnantian age (Steemans et al., 1996; Paris et al., 2007b), but also brachiopod (orthids) fragments and rare trilobites[5] (Fig. 18G), the first to be found in any of the Turkish Hirnantian glacial deposits. Most of, if not all the Turkish specimens appear reworked from strata which are not yet known at outcrop in southeastern Turkey. No glaciation-related deposits have been formally identified in the Amanos Mountains, or in the Zap Valley where a deeply incised erosional unconformity allows Devonian sandstones to lie directly upon the truncated Upper Ordovician succession.

6.1.3. Taurus Chain

Where complete in the Taurides, Depositional Sequence 4 ends with an upper unit consisting of glaciation-related deposits dated as Hirnantian by palynomorph assemblages (Monod et al., 2003; Paris et al., 2007b). Glaciation-related strata have been identified from the northeastern to southern Taurides and in the Antalya Nappes, except in areas where the Palaeozoic succession is deeply truncated by Mesozoic or younger deposits, such as Western Taurus (Isparta, Sultan Dağ, Seydişehir and Hadim regions). The glacial deposits exhibit a fairly constant thickness (60–120 m) throughout the Taurides. Monod et al. (2003) detailed the succession in the southern and eastern Taurus where the strata comprise a basal, conglomeratic, proximal glaciomarine sandy wedge (Fig. 18H–J) overlain by thin tidal sandstones (Figs. 18K and 19). Its top is bounded by a striated glacial pavement in the northeastern Taurus, above which a fining-up, 40–80 m succession contains the full spectrum of recessional glaciomarine depositional environments. In the southern Central Taurus (Akyaka area, Fig. 21), relatively thin (<10 m) fluvio-glacial facies may replace the lower glaciomarine wedge. In only one section (5 km west from Ovacık, Fig. 21), the highest parts of the glacially related strata contain rare macrofauna, mainly brachiopod fragments.[6] In the Antalya Nappes, glacial strata show a conspicuous two-fold lithostratigraphy, with two sandy diamictite packages separated by non-glacial offshore shales (Fig. 22). In this glacial succession, the lower package represents the upper unit of Depositional Sequence 4 and the uppermost glaciomarine deposits record the glacial maximum and subsequent post-glacial transgression related to the retreating ice

[5] Trilobite fragments include not only *Colpocoryphe* sp. and dalmanitid fragments, but also *Flexicalymene* cf. *meeki* (Foerste 1910) known from the higher Ashgill of Scotland (Shirley, 1936) and from coeval carbonates in North America, where it is widespread.

[6] Among them, *Mirorthis* sp. known only from the Hirnantian in Morocco, China, Burma and Thailand; other fragments include *Dalmanella?* and undetermined orthids.

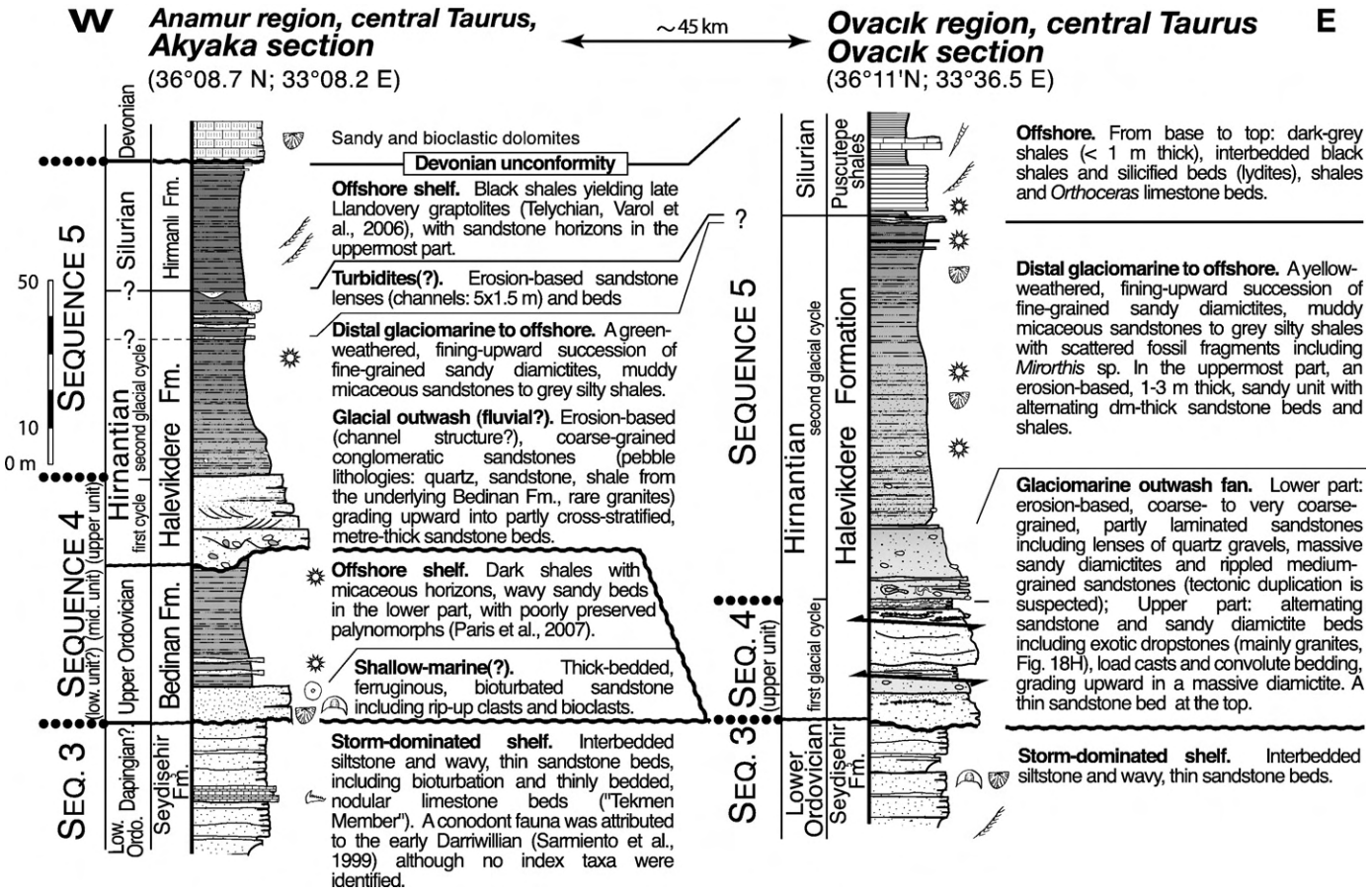

Fig. 21. The Upper Ordovician to lowermost Silurian succession (Depositional Sequence 4) in the Central Taurus (location in Fig. 1). A conspicuous erosion surface underlines the glaciation-related deposits. The upper part of the Halevikdere Fm. belongs to a second glacial cycle forming the base of a fifth Depositional Sequence that extends into the Silurian.

front, and hence constitute the base of the fifth sequence that continues with siliceous beds (lydites) and black shales of early Silurian age (Kozlu et al., 2002a,b; Varol et al., 2006) reflecting maximum flooding conditions.

6.2. Regional correlations

Despite faunal mixing due to glacial reworking of preglacial strata (Paris et al., 2007b; cf. also Miller and Al-Ruwaili, 2007 for Saudi Arabia), the glacial deposits are strictly Hirnantian in age and record a short-lived (<1 Ma) glacial event, which lasted less than the Hirnantian stage (Ghienne et al., 2007b). Compared with the pre-glacial strata, glaciation-related deposits show little variation in thickness throughout both Taurides and Border Folds. Basically, the twofold glaciation identified in North Africa (Sutcliffe et al., 2000; Ghienne et al., 2007b; Loi et al., in press) and more distal domains (Bohemia, Kosov Fm., Storch, 2006) is also present in Turkey. The intermediate transgressive episode is represented by offshore shales in the Kemer region (Fig. 22) and tidal sandbars in the Kozan area (Fig. 19). The maximum glacial advance is represented by the younger of the two glacial events: this is best illustrated by the glacial record in the Kemer area and is also illustrated in the Eastern Taurus by a striated glacial surface which underlies the upper glaciomarine succession, as in northern Morocco (Le Heron et al., 2007). The glacial maximum event is most probably coeval with the major glacial incision phase documented in central Saudi Arabia (Sarah Fm., Vaslet, 1990; Clark-Lowes, 2005). At that time, glaciers straddled southern Turkey as shown by glacial surfaces in both Taurides and Border Folds (Monod et al., 2003). The origin of these glaciers is questionable as they could either flow from isolated ice centres situated on elevated areas on the Gondwana margin (e.g., Moix et al., 2008), or derive from an ice lobe originating from the Gondwana continental ice-sheet. The Gondwanan origin of the ice lobe is favoured here, because of: (1) the rather uniform facies distribution at the 100 km scale, (2) the northwestward ice-flow direction recognized in the Mardin area, in good agreement with (3) the widespread ice-generated structures (striated pavements, palaeo-valleys) indicating a northward to northwestward-flowing ice-sheet in Jordan (Abed et al., 1993; Turner et al., 2005; Fig. 18 N) and northern Saudi Arabia where palaeovalleys up to 500 m deep have been identified within the Qasim depositional Basin (Vaslet, 1990; McGillivray and Husseini, 1992; Aoudeh and Al-Hajri, 1995 in Sharland et al., 2001; Clark-Lowes, 2005). In addition, strikingly similar striated and facetted quartz pebbles are found both in the Mardin area and southern Jordan (Fig. 18L and M), which are most likely derived from the proximal, Lower Ordovician successions (cf. Fig. 16D). Such an ice lobe could be responsible for local or regional erosion of the substrate in northern Syria, Irak and southeastern Turkey. In the Mardin region (Border Folds), the absence of pre-glacial Katian (i.e. Ashgill) strata, extensively represented in the neighbouring subsurface (Fig. 23) is considered as the result of a severe glacial erosion (~200 m). Erosion, however, is not systematic, as in the northeastern Taurus no stratigraphic hiatus is detectable.

The upper Hirnantian transgressive glaciomarine facies and the immediately overlying lydites and Early Silurian shales, which characterize the base of Depositional Sequence 5 in the Taurides,

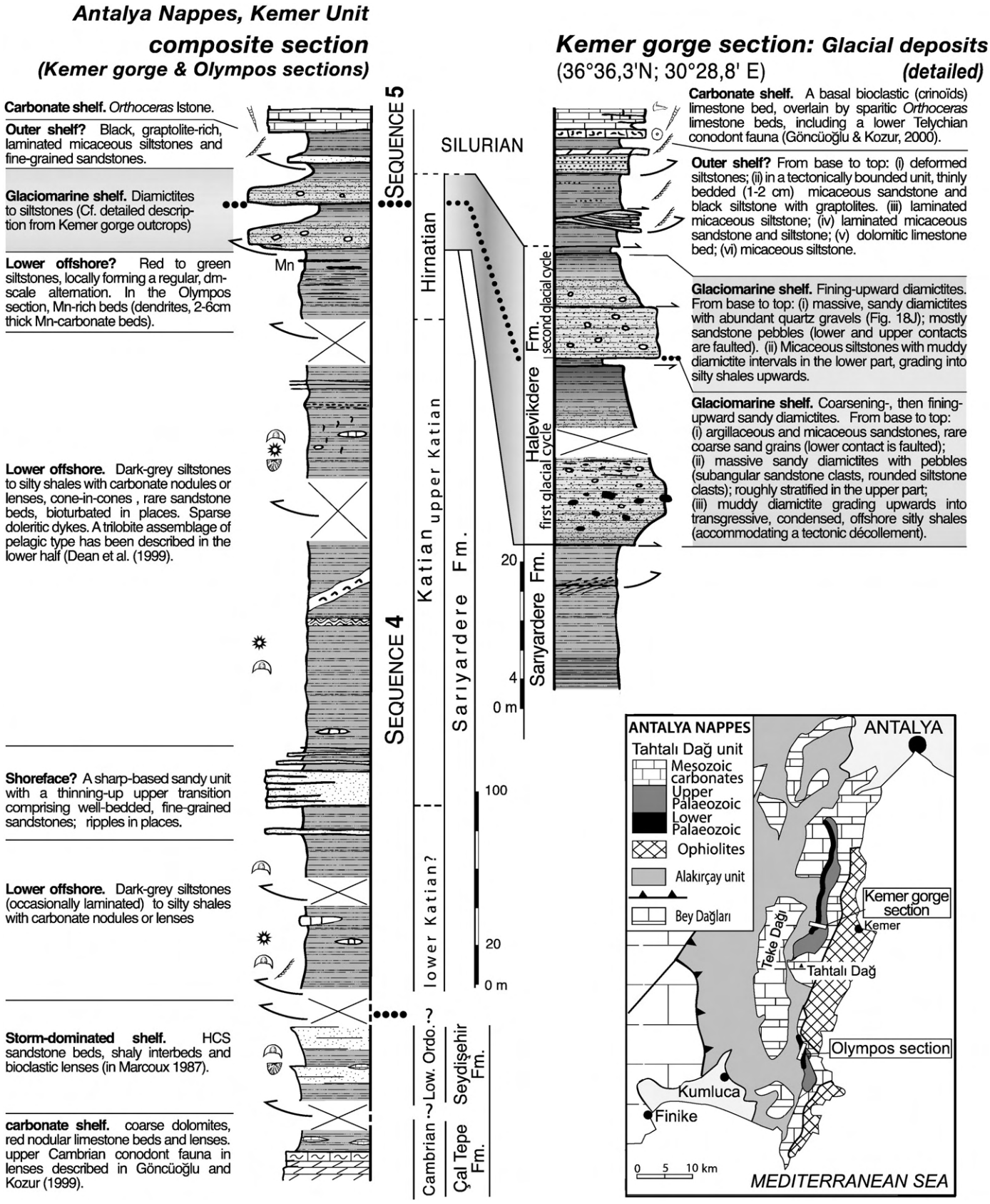

Fig. 22. The Upper Ordovician to lowermost Silurian succession (Depositional Sequence 4 and base of Sequence 5) in the Antalya Nappes. In the Kemer Gorge section (right), the glaciation-related deposits include two diamictite units (lower and upper glacial cycles) separated by condensed, offshore shales.

typify relatively distal regions of the North Gondwana shelf (such as northeast Morocco, Le Heron et al., 2007; France, southeast Brittany, Piçarra et al., 2002 or Barca et al., 1996; Bulgaria, Yanev et al., 2005 and NW Turkey, Sachanski et al., 2007), in areas that were not

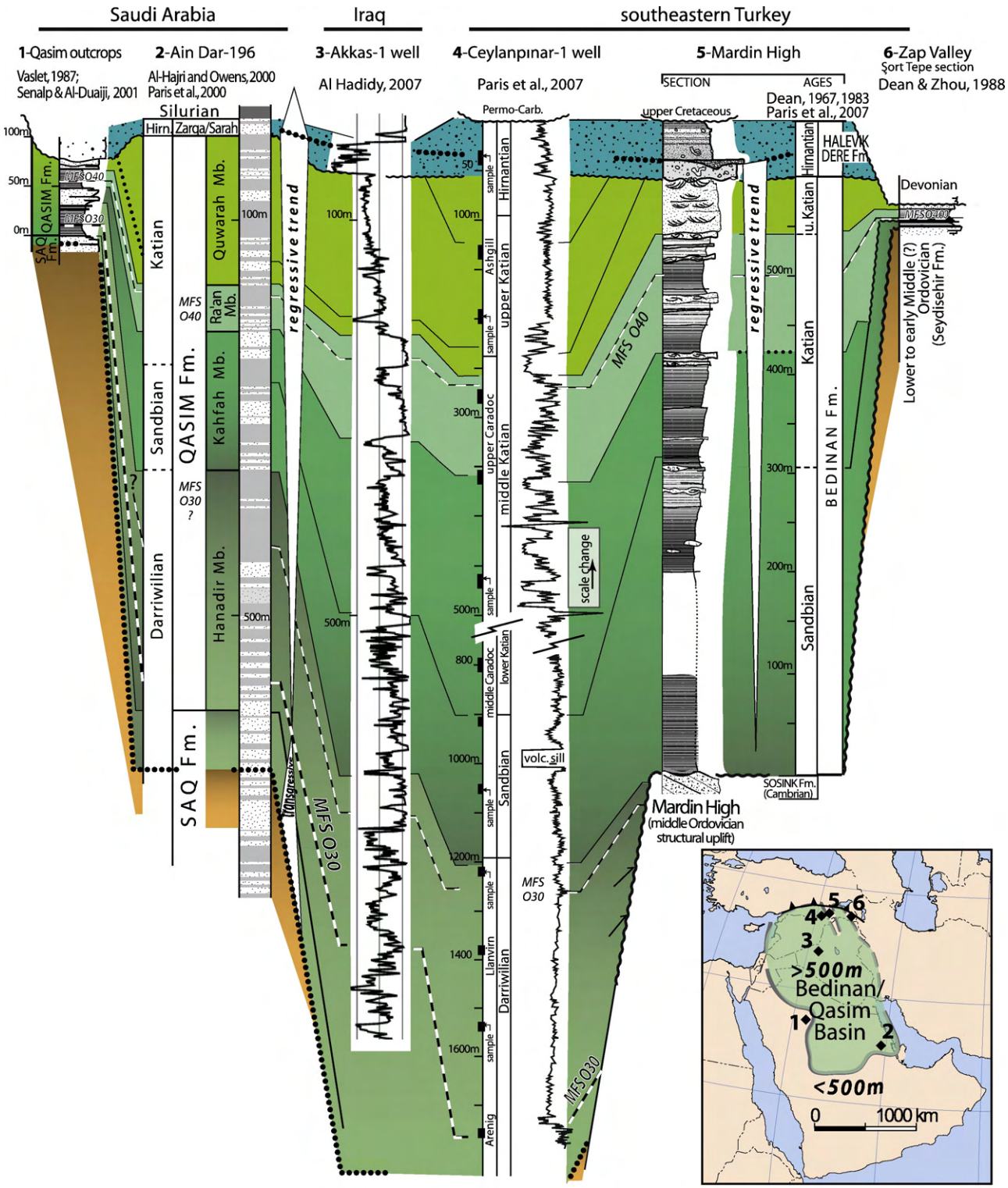

Fig. 23. Correlation scheme within the Middle to Upper Ordovician Bedinan–Qasim sag basin (Depositional Sequence 4) based on outcrop and well data from Saudi Arabia, Iraq and southeastern Turkey (Mardin High and Zap Valley, Border Folds). This figure illustrates the drastic thickness changes of Depositional Sequence 4 (Fig. 5), in contrast with the more uniform underlying Depositional Sequences 2 and 3 (Fig. 4). Location of Ceylanpınar 1 well in Fig. 1.

covered by ice. Hence, during the latest Ordovician, southern Turkey was attached to the Gondwana landmass as reflected by a locally grounded ice sheet, but in a distal position. Palaeoglacial reconstructions suggest that southern Turkey was situated at high to intermediate palaeolatitudes (higher than 45°) at the end of the Ordovician (Ghienne et al., 2007b).

7. The Turkish north Gondwanan connection: implications

7.1. Location of the Taurus domain relative to the Arabian Plate

While the Border Folds preserved an autochthonous sedimentary record that can readily be linked with the Arabian basins, the ties of

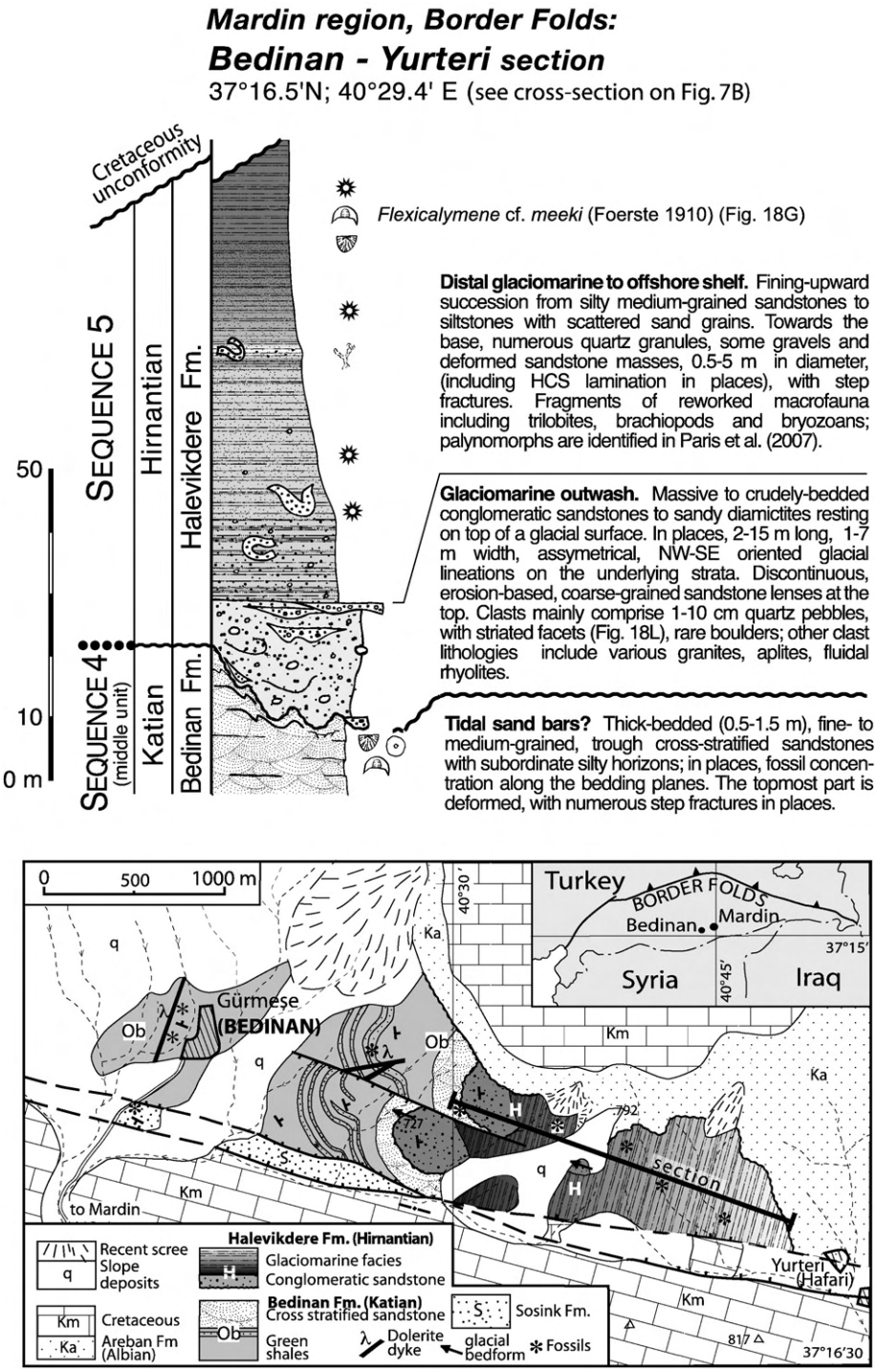

Fig. 24. The glaciation-related deposits in the Mardin region (Bedinan/Yurteri section, Border Folds). Upper Katian strata are absent owing to glacial erosion, in contrast to Ceylanpınar 1 well (Fig. 23). Glacial lineations are evidence for a grounded ice sheet in southeastern Turkey (Fig. 25).

the Taurides, which rifted away from Gondwana in Permo-Triassic times with other Cimmerian terranes (Şengör, 1990; Stampfli and Borel, 2002; Torsvik and Cocks, 2004; Ruban et al., 2007) are more elusive. To reconstruct the pre-rifting Eastern Mediterranean domain is beyond the scope of this contribution, but the Turkish Lower Palaeozoic record may provide some fundamental constraints. In a number of reconstructions, the Taurides domain is used to broadly "infill" the area of the present Eastern Mediterranean Sea (e.g., Keeley, 1989; Husseini, 1989; Stampfli and Borel, 2002; Fortey and Cocks, 2003; Monod et al, 2003; Garfunkel, 2004; Moix et al., 2008). However, this location is questionable as it involves inconsistencies on Lower Palaeozoic grounds (Fig. 2). We propose to situate the Taurides north of the Border Folds (Fig. 26) and discuss the resulting implications for Lower Palaeozoic reconstructions in the Middle East.

Fig. 25. Three tentative palaeogeographic reconstructions of the Taurus domain and of the Arabian platform during the Cambrian (A, development of a stable platform), Late Ordovician (B, differentiation of a sag basin) and Hirnantian (C, glaciation). See Section 7.1. for details.

Cambrian: stable platform

- **early Furongian** basinward extent of the shoreface/offshore transition; fluvial to coastal sandstones to the south
- **"middle Cambrian" carbonate** platform:
  - youngest age of the carbonates
  - landward maximum extent
  - fluvial to coastal sand-flats
- **lower** (left) and **upper Cambrian** (right) palaeocurrent trends
- area of non-deposition during the **lower part of the Cambrian**
- Arabian Shield
- present-day coastlines
- present-day Zagros thrust

some constraints outside Turkey

(1) Wajid Sandstones (Hussain, 2007); (2) palaeocurrents trends in the Saq Sandstones (Vaslet, 1987); (3) Lower/Middle carbonate strata in the Khursaniyah-81 well (Al Hajri & Owens, 2000); (4) carbonates southernmost extent (Rushton & Powell, 1998); (5) palaeocurrent trends in Jordan (Selley, 1972; Amireh et al., 1994); (6) Middle Cambrian strata in the Ghazalat Basin (Keeley, 1989); (7) Lower/ Middle carbonates in most of Syria (Best et al., 1993; Sharland et al., 2001).

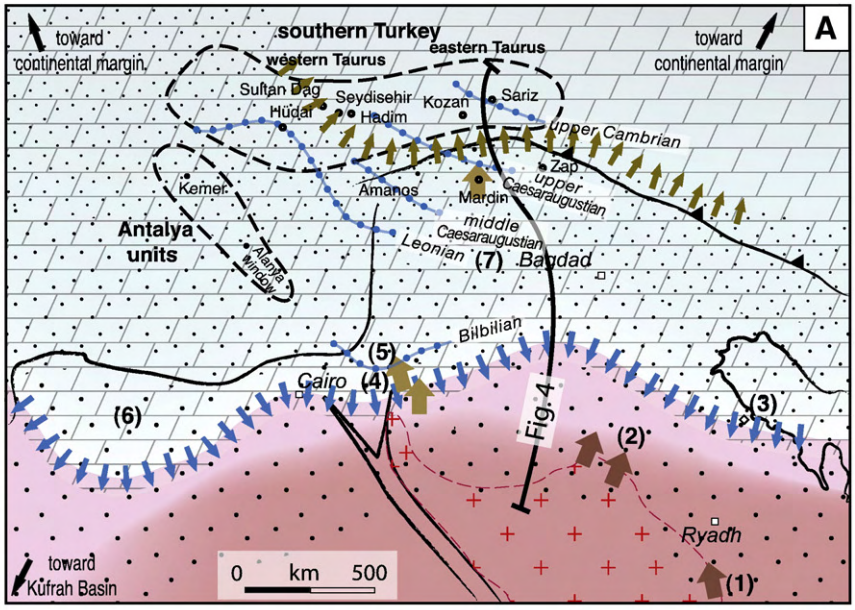

Late Ordovician: sag basin

- outer-shelf bottom-current deposits
- storm-dominated inner shelf (subordinate transgressive tidal deposits)
- landward maximum extent of open-marine conditions
- coastal to fluvial (poorly preserved)
- Palaeocurrents in fluvial deposits
- **Mid Ordovician** basement highs (Turkey)
- source area (non deposition)
- Arabian Shield
- present-day coastlines
- present-day Zagros thrust

some constraints outside Turkey

(1) marine flooding event in Oman (Molyneux et al., 2006); (2) Ain Dar-196 well (Al Hajri & Owens, 2000); (3) outcrop logs (a) and isopachs from subsurface data (b) (Senalp & Al-Duaiji, 2001); (4) Akkas-1 well from Iraq (Al-Hadidy, 2007) (cf. Fig. 22); (5) outcrop succession from southern Jordan (Amireh et al., 2001); (6) Interbedded fluvial and shallow-marine deposits (Semtner, 1993); (7) Silurian strata on laterized Panafrican basement in NW Sudan (Germann et al., 1993).

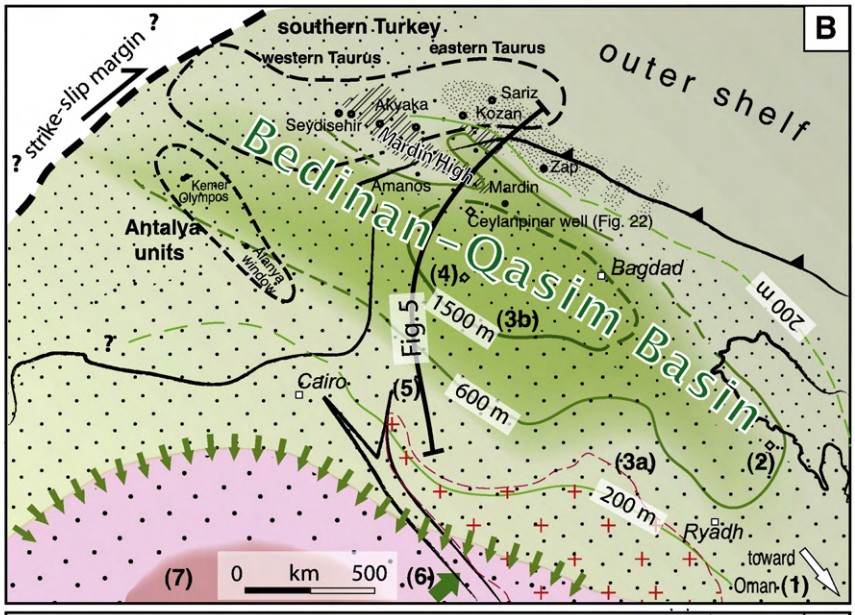

Hirnantian: glaciation

- North Gondwana ice sheet at the **Hirnantian glacial maximum**
- glacial valleys
- expected glacial fairways (ice stream)
- in Turkey: glaciomarine successions with dropstone including (red cross) or lacking (dots) exotic basement clasts
- ice-flow orientations in Turkey
- 600 m isopach in the Qasim Fm.
- 500 m isopach of the lower Silurian
- Arabian Shield
- present-day coastlines
- present-day Zagros thrust

some constraints outside Turkey

(1) glacial valleys from the Qasim area (Vaslet, 1990; Clark-Lowes, 2005); (2) glacial valleys from the subsurface (Aoudeh & Al-Hajri; 1995); (3) glacial valleys from Jordan (Powell et al., 1994; (4) ice stream originating from the Kufrah Basin (Le Heron & Craig, 2008); (5) isopach map of the Qusaiba Shales, reflecting depositional throughs (Jones & Stump, 1999 in Lüning et al., 2000).

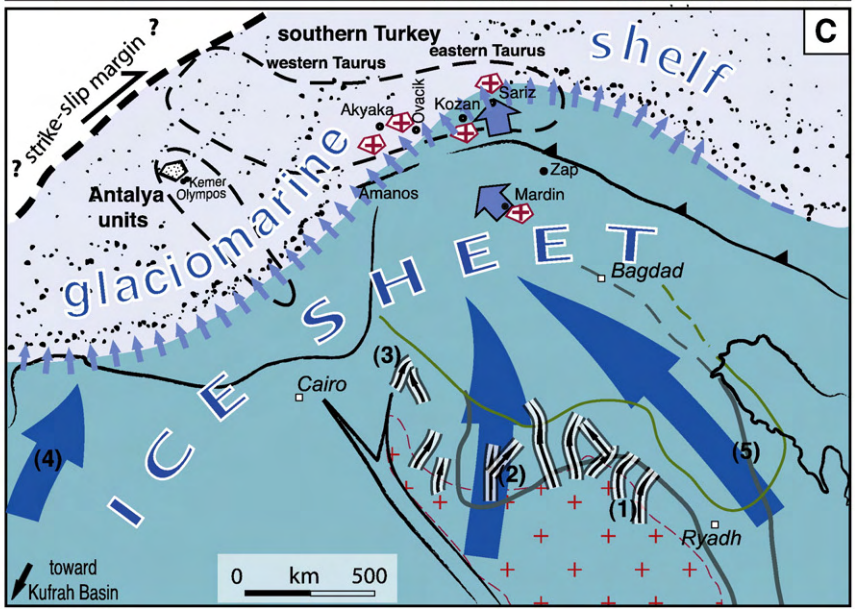

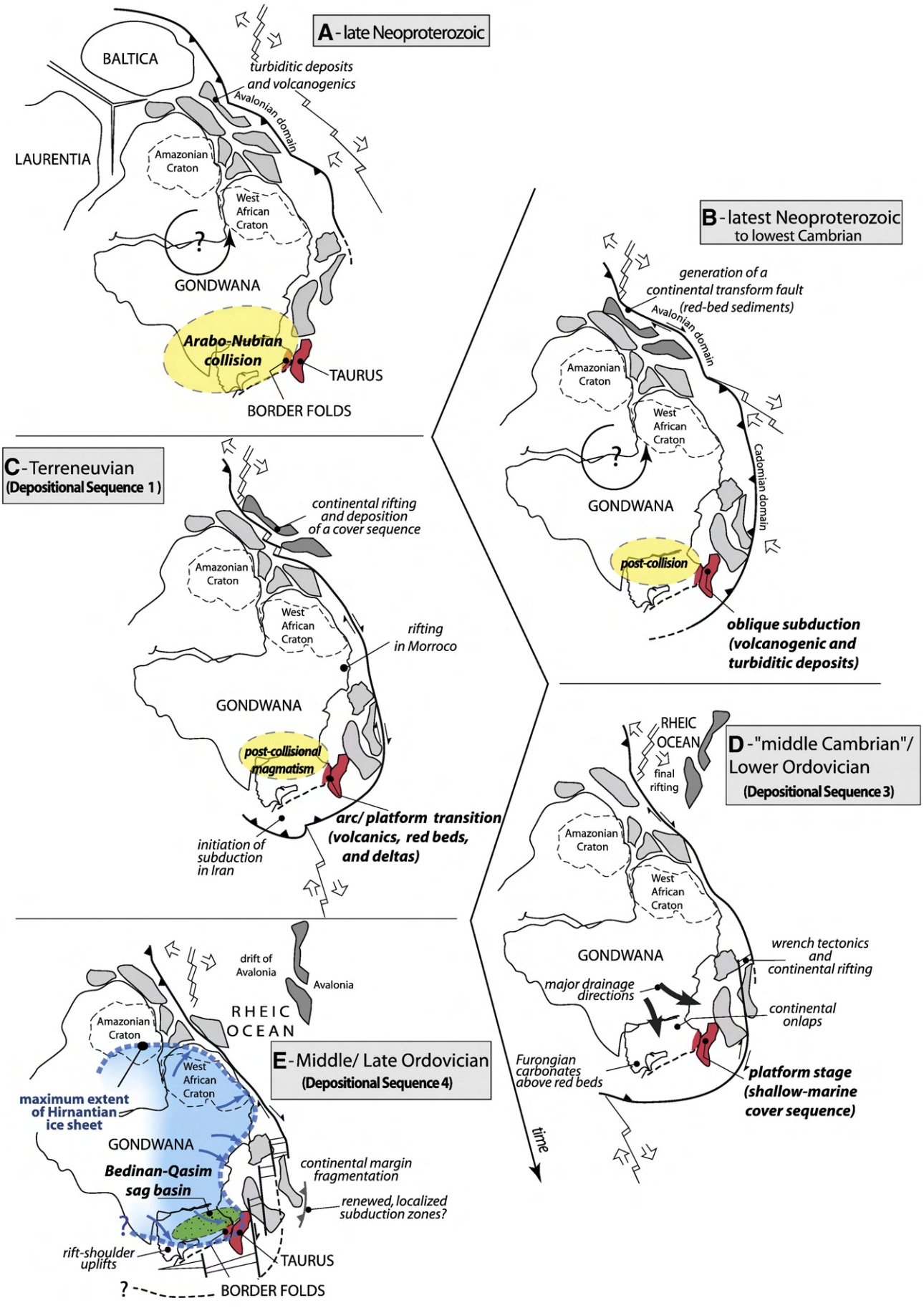
A - late Neoproterozoic
BALTICA
LAURENTIA
turbiditic deposits
and volcanogenics
Avalonian domain
Amazonian Craton
West African Craton
?
GONDWANA
Arabo-Nubian collision
TAURUS
BORDER FOLDS
B - latest Neoproterozoic
to lowest Cambrian
generation of a
continental transform fault
(red-bed sediments)
Avalonian domain
Amazonian Craton
West African Craton
?
GONDWANA
Cadomian domain
post-collision
oblique subduction
(volcanogenic and
turbiditic deposits)
C - Terreneuvian
(Depositional Sequence 1)
continental rifting
and deposition
of a cover sequence
Amazonian Craton
West African Craton
rifting
in Morroco
GONDWANA
post-collisional
magmatism
arc/ platform transition
(volcanics, red beds,
and deltas)
initiation of
subduction
in Iran
D - "middle Cambrian"/
Lower Ordovician
(Depositional Sequence 3)
RHEIC
OCEAN
final
rifting
Amazonian Craton
West African Craton
GONDWANA
wrench tectonics
and
continental rifting
major drainage
directions
continental
onlaps
Furongian
carbonates
above red beds
platform stage
(shallow-marine
cover sequence)
time
drift of
Avalonia
Avalonia
RHEIC
OCEAN
Amazonian Craton
West African Craton
E - Middle/ Late Ordovician
(Depositional Sequence 4)
maximum extent
of Hirnantian
ice sheet
GONDWANA
Bedinan-Qasim
sag basin
continental margin
fragmentation
renewed, localized
subduction zones?
rift-shoulder
uplifts
TAURUS
?
BORDER FOLDS

7.1.1. Cambrian reconstruction (Fig. 25A)

As already considered by several authors (Haude, 1975; Dean and Monod, 1997; Gozalo et al., 2007), the "middle Cambrian" Carbonates form a continuous belt, although the age of the red nodular facies exhibits noticeable differences from east to west, immediately before the carbonate/detrital turnover (Fig. 2). The latter indicates a north- to northeastward progradation of the overlying regressive clastic deposits upon the transgressive carbonates. The timing of this progradation is incompatible with a Taurus domain located within the Eastern Mediterranean but is easier to substantiate when placing it north of the Border Folds. In southern Europe, almost identical facies successions reflect the outstanding uniformity and the tectonic quiescence of the North Gondwana shelf during deposition of the "middle Cambrian" Carbonates (e.g., Elicki, 2007b). This stability persisted in southern Turkey during the Furongian and up to the early Middle Ordovician.

7.1.2. Middle/Late Ordovician reconstruction (Fig. 25B)

By contrast with the Cambrian to Lower Ordovician stability, Middle to Upper Ordovician Turkish successions exhibit regional differentiations. In the Border Folds, the Mardin High presents the same orientation as the larger-scale Bedinan–Qasim depocenter. This uplift may be extended into the Central Taurus where glacial deposits rest directly upon Lower Ordovician strata.

This reconstruction fits with the occurrence of coeval, unusual detrital facies (outer shelf bottom-current deposits) extending from the Zap Valley to the Eastern Taurus. In the western Border Folds, thick (Amanos, 700 m) to very thick (Ceylanpınar 1, >1500 m) Bedinan Fm. deposits are situated close to the Middle/Upper Ordovician depocenter, thus forming a large, elongated, SE–NW trending Bedinan–Qasim sag basin (Fig. 23). We assume that the isopach distribution reflects a basinal geometry, which comprises: a source area to the south (essentially the present-day Arabian Shield), a depocenter (Bedinan–Qasim sag basin), and a submarine swell to the north (Zap/Eastern Taurus area). If true, this geometry may account for the surprising identity between the Upper Ordovician succession in the Kemer area (Antalya units, Şenel et al., 1981) and that of the Arabian and Border Fold domain, providing that the original place of the Kemer area should be situated in a distal position. This basinal geometry is thought to have strongly influenced the pattern of ice flows during the Hirnantian.

The recent recovery of widespread Darriwilian strata and related outer shelf depositional conditions throughout the Taurus Chain does not support a large-scale "Sardinian–Taurian rise" as proposed by Hammann (1992) based on trilobite provincialism. Instead, localized and temporary uplifts may have occurred in Turkey.

7.1.3. Hirnantian reconstruction (Fig. 25C)

In southern Turkey, most of the Hirnantian successions reflect glacial settings that were situated close to the maximum ice front. In Arabia, glacial valleys are systematically perpendicular to the Upper Ordovician isopachs, and thus indicate that the distribution of the Hirnantian ice flows was controlled by the geometry of the former Bedinan–Qasim sag basin. By analogy with the organisation of the ice-sheet in North Africa (Moreau et al., 2005; Ghienne et al., 2007a,b; Le Heron and Craig, 2008), we suggest that large ice streams flowing northwestwards occupied the Bedinan–Qasim trough. In our reconstruction, the relatively thin and uniform Turkish glacial successions are situated aside from the main ice-stream pathway, in front of which much thicker glaciomarine deposits would be expected (e.g., Taylor et al., 2002; Le Heron et al., 2007). Most of the Turkish glacial successions reflect glaciomarine outwash deposits issued from the inter-stream areas, and contain exotic ice-rafted debris coming from the Arabo-Nubian shield through iceberg calving at the ice-stream fronts. By contrast, the non-erosional glaciomarine succession in the Kemer area (Antalya units) is devoid of exotic clasts (sandstones mainly), and this implies a more distal location.

During the latest Hirnantian, starved sedimentation in the Middle East reflects post-glacial southward backsteps of the shorelines. In the former Bedinan–Qasim sag basin however, persisting subsidence resulted in intra-shelf depressions that were filled subsequently by thick, partly turbiditic Lower Silurian deposits (Jones and Stump, 1999; Lüning et al., 2000). In the former outer swell area (Zap and Eastern Taurus), siliceous beds with condensed Lower Silurian succession reflect isolation from the continental clastic sources.

7.2. Tectonostratigraphic development

Basement/cover relationships are virtually unknown in southern Turkey except for the Menderes Massif, where, however, they were modified by post-Palaeozoic tectonics during the Miocene (Bozkurt and Oberhänsli, 2001). In the Turkish record, only limited clues concern the tectonic-driven events corresponding to Depositional Sequences 1 to 4.

Recently, magmatic and tectonic events related to an Avalonian/Cadomian system have been traced as far as eastern and southern Europe (Yiğitbaş et al., 2004; Buschmann et al., 2006; Carrigan et al., 2006; Bozkurt et al., 2008a; Okay et al., 2008a,b), suggesting that the "Pan-African" evolution identified in southwestern Turkey (Bozkurt and Oberhänsli, 2001; Candan et al., 2001; Bozkaya et al., 2006) may belong to this cordilleran-type subduction-related system (Gürsu et al., 2004). In southern Turkey, Lower Palaeozoic geodynamic events may be tentatively interpreted in the light of models based on adjacent domains where basement/cover relationships have been satisfactorily integrated, such as the Avalonian, Cadomian, Saxo-Thuringian/Bohemian and Oman/Iran study areas (Nance et al., 2002; Keppie et al., 2003; Linnemann et al., 2007; Pouclet et al., 2007; Allen, 2007; Nance and Linnemann, 2008).

7.2.1. A Cordilleran-type evolution for southern Turkey

A striking similarity appears in the tectonostratigraphic development of the Avalonian (Nance et al., 2002) and Turkish domains. Both share a similar succession of volcanoclastic turbidites, bimodal volcanics, red-bed type sediments, and an overall transgressive (fining-up), essentially siliciclastic succession including, in places, carbonates in its lower part. This succession is also recognized in northeastern Europe (Linnemann et al., 2007) and, partly, in Oman (Millson et al., 1996; Allen, 2007); a similar development has been inferred for a number of segments of the north Gondwana margin (e.g., Iberia, Sanchez-Garcia et al., 2003). However, if the successions are analogous, their development is diachronous along the Gondwana margin. We make use of a Cordilleran model based on the evolution of Avalonia (Nance et al., 2002; Keppie et al., 2003), assuming an eastward propagation of deformation/depositional zones during the latest Neoproterozoic to Early Palaeozoic time interval. This propagation, which ultimately resulted in the diachronous development of the Rheic Ocean to the north of Gondwana (Bozkurt et al., 2008b), may have occurred in response to either a steady, dextral relative motion between the Gondwana landmass (rotating counter-clockwise?) and an eastward?-shifting spreading centre ("proto-Tethys" of Stampfli and Borel, 2002), or to more discontinuous plate-tectonic rearrangements. Of course, this oversimplified model is unable to account for all the north Gondwana heterogeneities, but it may provide a first-order

Fig. 26. A tentative model of the tectonic evolution of the north Gondwana margin from the Avalonian domain to eastern Arabia (Oman). A similar, but fully diachronous sequence of events is depicted from the late Neoproterozoic to the Late Ordovician, assuming an eastward migration (present-day coordinates) of the deformation/depositional events (see Section 7.2. for details).

template for the uniform, but diachronous cover sequence of a 10,000 km long continental margin.

Following the events related to the Arabo-Nubian collision zone (Fig. 26A; Blasband et al., 2000; Meert, 2003; Allen, 2007), the Turkish record of a Cordilleran-type evolution would successively comprise:

(1) an oblique subduction stage with arc-related magmatism and volcanogenic turbiditic sedimentation (latest Neoproterozoic successions in southern Turkey) (Fig. 26B);
(2) an arc/platform transition with structural inversion and new intracontinental wrench-related basins (lowest Cambrian red-bed successions or delta settings of Depositional Sequence 1) (Fig. 26C);
(3) platform development with an extensive, correlative cover sequence of shallow-marine strata (upper Terreneuvian? or Cambrian "Series 2" to Lower Ordovician Depositional Sequences 2 and 3) (Fig. 26D);
(4) initial continental rifting following a shift of wrench tectonic inboard (Middle Ordovician tectonic instabilities) (Fig. 26E); and finally,
(5) rifting at the continental margin and development of a sag basin, essentially Late Ordovician in age, over the former cratonic platform (Depositional Sequence 4).

Similar but diachronous tectonostratigraphic events in Avalonia, Eastern Europe and the Oman/Iran study area are listed in Fig. 26. In the following, some details are given concerning the Turkish record of this five-fold succession of events. It should be noted that the Cordilleran-type model differs from other plate tectonic reconstructions which considered that southern Turkey either belonged to a stable Arabian passive margin (McGillivray and Husseini, 1992; Best et al., 1993; Konert et al., 2001; Sharland et al., 2001), or was situated in a back-arc setting (Tolluoğlu and Sümer, 1995; Gürsu and Göncüoğlu, 2005) throughout the Lower Palaeozoic.

7.2.2. Oblique subduction stage

The oblique subduction stage is represented in Turkey by the Neoproterozoic series of the Taurides (Kozlu and Göncüoğlu, 1997; Gürsu and Göncüoğlu, 2006), which comprise thick turbiditic to shallow-marine, siliciclastic to carbonate strata, conglomeratic in places, typically with numerous chert horizons and volcanogenic rocks (Fig. 26B). In places, these rocks have preserved indications of low-grade metamorphism that predates the deposition of Cambrian–Ordovician strata (Bozkaya et al., 2002). These successions probably record deposition in transtensional, volcanic arc basins. The subduction zone itself may be identified with the Istanbul–Zonguldak arc (Yiğitbaş et al., 2004; Gürsu and Göncüoğlu, 2005; Okay et al., 2008a). Meanwhile, in the Avalonian domain, red-bed type successions are deposited in continental basins related to wrench tectonics.

7.2.3. Arc/platform transition

Rhyolitic volcanism in bimodal suites is dated at 543–541 Ma (Kröner and Şengör, 1990; Bozkaya et al., 2006) in the Sandıklı basement complex of the Western Taurus (Fig. 8). At this point, deposition of the latest Neoproterozoic turbidites ended, whereas continental red-bed (Mardin area, Fig. 6) or deltaic successions (western Taurides, Fig. 8) began to accumulate in tectonically differentiated basins, Terreneuvian in age. This interval is considered as the arc/platform transition in southern Turkey (Fig. 26C). An associated structural inversion may be reflected by the coeval generation of disconformities, with a hiatus involving in places most of the earliest Cambrian, so that Depositional Sequence 2 rests directly on the Neoproterozoic succession. At that time, basal, transgressive strata of the cover sequence were deposited around Avalonia, whereas a transition from passive margin setting to a subduction zone occurred in the Oman/Iran area (Ramezani and Tucker, 2003; Allen, 2007). The arc/platform transition in Turkey is also coeval with latest post-collision magmatism in the Arabo-Nubian Shield (Beyth and Heimann, 1999; Blasband et al., 2000; Meert, 2003); the possibility of interference between the late post-collision extensional collapse or tectonic escape, and the inferred arc/platform transition cannot be excluded.

7.2.4. A platform development

Above the disconformable lower contact of Depositional Sequence 2, an uninterrupted subsidence pattern keeps pace at first order with sedimentation as shown by persistent shallow-marine environments. Neither regional uplift nor active subsidence leading to deep basinal conditions were present, which indicate a long period of tectonic stability (Fig. 26D). Contrasting with the differentiated Terreneuvian depocenters, the uniform facies of the "middle Cambrian" Carbonates and faunal mixing indicate the onset of a stable platform over the entire north Gondwana (Elicki, 2007b). Stable conditions persisted in southern Turkey from Cambrian "Series 2" to Early Ordovician. The ca. 2–2.5 km thick detritals deposited between 515 Ma (Bilbilian, middle part of Cambrian "Series 2") and 472 Ma (Early Ordovician) reflect the ongoing mean subsidence (i.e. about 50 m/Ma compacted sediment accumulation rate).

To the south, the overall Cambrian to Lower Ordovician succession onlaps the Neoproterozoic basement, from Turkey to the Arabian Shield (Taurides, Border Folds, Jordan, Saudi Arabia (Fig. 4), and reflects a subsidence-driven overstep of the depositional sequences. Basic estimates of the accumulation/subsidence rates using a backstripping method suggest the following scheme: the highest accumulation and subsidence rates (~100 m/Ma) coeval with the "middle Cambrian" Carbonates led to a significant shoreline retreat favouring carbonate deposition. Subsequently, a relatively high subsidence rate persisted, but reduced detrital supply resulted in condensed sedimentation (accumulation rate: 10 m to 30 m/Ma) in most of the Cambrian "Series 3". The reduced sediment supply may reflect a starved clastic input subsequent to a major shoreline retreat. Greater accumulation rates (40–70 m/Ma) during the Furongian and Early Ordovician reflect an increase of detrital supply subsequent to the shelf progradation from the south, despite lower tectonic subsidence rates (20–40 m/Ma). These decreasing, but significant subsidence rates conform with a thermal re-equilibration that followed the Terreneuvian arc/platform transition in southern Turkey.

A similar long-term, subsidence-driven sequence overstep is drawn in more westerly segments of the North Gondwana platform, e.g. western Algeria/southern Morocco (Fabre and Kazi-Tani, 2005; Ghienne et al., 2007a), but rifting events and the onset of the platform-scale subsidence occurred notably earlier there, in the Late Ediacaran/lowest Cambrian, as reflected by the Adoudounian carbonate series (Destombes et al., 1985; Soulaimani et al., 2004; Pouclet et al., 2007). We argue that their significance is similar to that of the Turkish "middle Cambrian" Carbonates. This view may in part question the latitude/temperature-dependent distribution of the Cambrian carbonates favoured by Courjault-Radé et al. (1992). In Oman, equivalent carbonates are much younger (Furongian and Changshanian according to Fortey, 1994; Molyneux et al., 2006) (Fig. 26D), a time interval corresponding to the return of a first-order regressive trend in southeastern Turkey (Figs. 4 and 11). The basal bounding surface of Depositional Sequence 2 is correlated with the pre-Siq unconformity in Saudi Arabia or with the Angudan unconformity in Oman (Loosveld et al., 1996; Sharland et al., 2001; Molyneux et al., 2006).

The eastward-propagating platform setting readily accounts for the distinct status of the Taurides from many other north Gondwana derived "terranes", where pervasive tectonic events have been identified throughout the Furongian and Early Ordovician (e.g., von Raumer et al., 2002; Silva and Pereira, 2004; Teipel et al., 2004;

Schulz et al., 2004). No tectonic event is evident during the Furongian either in Turkey or in Oman, a pattern that is apparently common in other more western (present-day coordinates) parts of Northern Gondwana where continental rifting occurred earlier (Fabre, 1988; Landing et al., 2006; Burkhard et al., 2006; Linnemann et al., 2007; Álvaro et al., 2007).

7.2.5. Initial continental rifting

Middle Ordovician tectonic activity on the Turkish platform is reflected by: (1) unconformity between Depositional Sequences 3 and 4; (2) regressive events in the Taurides associated with gravity-driven facies (turbidites, mass-flow deposits); and (3) resultant reworking of palynomorph assemblages. The most significant tectonic instability is therefore suspected during the Darriwilian, in both Taurides (gravity-driven facies) and Border Folds ("Mardin High" development). Although these clues alone are insufficient to infer continental rifting, time-equivalent magmatism outside the Taurides and ensuing initiation of a major sag basin (Bedinan–Qasim trough) are considered to support such an event. Interestingly, in Oman, coeval uplifts (the Al Huqf High) and hiatuses have been inferred from the Haima Supergroup (Droste, 1997; Sharland et al., 2001), as well as a Darriwilian mafic intrusion (Oterdoom et al., 1999). They are ascribed to rift shoulder uplifts. To the west, a late Early Ordovician to Middle Ordovician rifting event (Fig. 26E), formerly referred to as the "Sardic Phase", was identified by alluvial-fan deposition onto tilted blocks (Martini et al., 1991; Leone et al., 2002) and coeval granitoid intrusions (Laumonier et al., 2004; Helbing and Tiepolo, 2005). In Turkey, coeval granitic intrusions (Okay et al., 2008a) are probably linked to this Middle Ordovician continental rifting stage. This extensional phase generated inland deformations as far as southern Turkey and North Africa (Beuf et al., 1971; Echikh and Sola, 2000; Ghienne et al., 2007a; Galeazzi et al., 2010). These tectonic events may have induced localised, renewed, arc-related contractional deformation, as identified in several pre-Variscan basement units (Abati et al., 1999; von Raumer et al., 2002; Schulz et al., 2004). At the same time to the west, a rift/drift transition is present in the Avalonian to Cadomian domain (Prigmore et al., 1997; Nance et al., 2002), in relation with a fully developed Rheic Ocean (von Raumer and Stampfli, 2008; Bozkurt et al., 2008b; Murphy and Nance, 2008).

7.2.6. Rifting stage

The tectonostratigraphic pattern changed at the onset of the Late Ordovician with Sandbian to Katian strata recognized almost everywhere in southern Turkey, in spite of significant thickness changes (Fig. 23). The tectonic setting clearly differs from that of the Cambrian–Lower Ordovician platform, then characterized by poorly differentiated thickness changes at the 1000 km scale. By contrast, the Upper Ordovician succession marks the development of a long-wavelength depocenter (Bedinan–Qasim sag basin) forming a regularly and actively subsiding, NW–SE oriented, sag basin (Şenalp and Al-Duaiji, 2001) (Fig. 26E). Thin, more sandy successions overstepping the Arabian Shield (<300 m thick) in both Jordan and eastern Saudi Arabia (Al-Hajri and Owens, 2000) or Oman (Molyneux et al., 2006) roughly delineate the basin margins. The inferred drainage pattern around the basin flowed northwards in Jordan and northern Saudi Arabia, but to the northeast in central Saudi Arabia and Oman (Fig. 25B). The time-equivalent condensed succession (Şort Tepe Fm.) in the Zap Valley is interpreted as reflecting starved sedimentation on the northeastern margin of the Bedinan–Qasim sag basin (Fig. 23). The basin extended mainly from Saudi Arabia into Iraq and Syria, and into southeastern Turkey where the Darriwilian–Sandbian–Katian successions are amongst the thickest in the Middle East (up to 1500 m in the Ceylanpınar1 well). The status of the Taurides relative to this basin is discussed below.

The geometry of the Bedinan–Qasim sag basin conforms with a continental margin rim basin (Favre and Stampfli, 1992; Allen, 2007), developed about a thousand kilometres inboard of a continental edge, coeval with a drift phase and characterized by minimal amounts of stretching and relatively low accumulation rates (10 to 60 m/Ma). Coeval developments to the west include active fragmentation of the margin with creation of a network of seaways and limited formation of oceanic crust (Crowley et al., 2000; Cocks and Torsvik, 2002; Robardet, 2003; Linnemann et al., 2004). Further west, Avalonia was actively transferred toward lower palaeolatitudes (Cocks and Torsvik, 2002), and was docked against Laurentia at the end of the Ordovician. East of Turkey, in Iran, an initial continental rifting stage may be expected, which could have culminated in a Lower Silurian subsidence and volcanism phase (Stampfli, 2000).

Basin developments did not evolve significantly during the short-term Hirnantian glaciation. Drainage pattern was unchanged during the latest Ordovician, as shown by the orientations of the striated pavements and glacial palaeovalleys (Fig. 25C), which are roughly similar to the pre-glacial drainage pattern. Major unconformities beneath the glaciation-related strata were produced mainly by glacial erosion that truncated the pre-glacial deposits throughout the platform (e.g., Ghienne et al., 2007a).

The rift/drift transition ending with the transfer of terranes into the oceanic plate occurred later, most probably in the Late Silurian or Devonian (Ruban et al., 2007), and does not concern the Cambrian–Ordovician development of Turkey.

8. Conclusions

According to recent biostratigraphic data, a virtually continuous succession is preserved from Terreneuvian to latest Ordovician in southern Turkey (Taurus Chain and Border Folds). In spite of the Alpine deformations in the Taurides and, to a lesser extent, the Border Folds, four depositional sequences have been defined within the Cambrian and Ordovician formations of southern Turkey, and suggest new connections that concern the sediment sources, depositional facies and stratigraphic architecture of this segment of the Gondwana platform.

Based on the identification of recurrent sequence stratigraphic features, similar trends in the Cambrian–Ordovician successions have been pointed out in the Taurides and on the Arabian platform, and we tentatively connect the following regions: Western Taurus and Antalya Nappes with the western Border Folds (Amanos Mountains); Central and Southern Taurus with the central Border Folds (Mardin area); northeastern Taurus with the eastern Border Folds (Zap Valley). These side-by-side links suggest a former location of the Taurus domain north of the Arabian domain. This hypothesis has already been considered by several authors as a possible place for southern Turkey (cf. Göncüoğlu and Kozlu, 2000) and is strongly supported by the Cambrian–Ordovician sedimentary record.

This setting locates southern Turkey at the junction between two segments of the Gondwana platform: to the west (present-day coordinates), the African segment of the north Gondwana siliciclastic shelf; to the east, the Arabian segment of the north Gondwana margin (e.g., Guiraud et al., 2005). Both segments bear distinct drainage patterns during the Early Palaeozoic. As concerns the faunal content, southern Turkey has yielded mixed Cambrian faunal signatures reflecting influences from both margin segments, but also from Baltica especially during the Early Ordovician, in agreement with a northern position of southern Turkey.

Throughout the Early Palaeozoic, southern Turkey behaved basically as a stable depositional platform except for mild Middle Ordovician instability. This contrasts with the westerly North-Gondwana derived "terranes" which exhibit marked unconformities and magmatism. As a whole however, the primary control of the tectonostratigraphic development of southern Turkey during the Lower Palaeozoic remains the forced evolution from arc/platform to rift/drift transitions that moved progressively eastwards along the

Gondwana margin throughout the Lower Palaeozoic. We propose that the inferred stratigraphic architecture is representative of Lower Palaeozoic successions of the Middle East stable platform, and should be tested in the most distal domains of the former North Gondwana continental margin, in NW Turkey as well as in Variscan Europe.

Acknowledgments

J-F.G., O.M. and W.T.D. gratefully acknowledge TPAO's constant support and all facilities during fieldwork. J-F.G. and O.M. thank EOST-CNRS (Université de Strasbourg) and ISTO-CNRS (Orléans University) for financial support; W.T. Dean was supported by the National Museum of Wales, Cardiff, U.K. Part of our work was supported by the ECLIPSE 2 program of INSU. The authors are grateful to E. Kosun (Antalya University) for his help during fieldwork in the Antalya region. Petrological analyses on the Derik volcanics were performed by A. Pouclet (ISTO-Orléans). Many invaluable stratigraphic data were provided by F. Paris (Géosciences Rennes) and A. Le Herissé (Brest) for palynomorph assemblages; by R.B. Rickards (Cambridge University) for Ordovician graptolites; by L.R.M. Cocks (Natural History Museum, London) for articulate brachiopods; by L. Popov (Cardiff University) for lingulid brachiopods; and by A. Seilacher (Tübingen University) for trace fossils. The authors are greatly indebted to the late Francine Martin (Institut royal des Sciences naturelles de Belgique, Brussels) for acritarch determinations. Trilobite pictures were taken by Dr. L. McCobb (National Museum of Wales, Cardiff). The authors are grateful to Bryan Pratt and an anonymous referee for their careful and constructive review of the manuscript.

References

Abati, J., Dunning, G.R., Arenas, R., Díaz García, F., González Cuadra, P., Martínez Catalán, J.R., Andonaegui, P., 1999. Early Ordovician orogenic event in Galicia (NW Spain): evidence from U–Pb ages in the uppermost unit of the Ordenes Complex. Earth and Planetary Science Letters 165, 213–228.

Abed, A.M., Makhlouf, I.M., Amireh, B., Khalil, B., 1993. Upper Ordovician glacial deposits in southern Jordan. Episodes 16, 316–328.

Achab, A., Paris, F., 2007. The Ordovician chitinozoan biodiversification and its leading factors. Palaeogeography, Palaeoclimatology, Palaeoecology 245, 5–19.

Albani, R., Massa, D., Tongiorgi, M., 1991. Palynostratigraphy (Acritarchs) of some Cambrian beds from the Rhadames (Ghadamis) Basin (Western Libya–Southern Tunisia). Bolletino della Società Paleontologica Italiana 30, 255–280.

Al-Hadidy, A.H., 2007. Palaeozoic stratigraphic lexicon and hydrocarbon habitat of Iraq. GeoArabia 12, 63–130.

Al-Hajri, S., Owens, B., 2000. Sub-surface palynostratigraphy of the Palaeozoic of Saudi Arabia. In: Al-Hajri, S., Owens, B. (Eds.), Stratigraphic Palynology of the Palaeozoic of Saudi Arabia, GeoArabia Special Publication no. 1. Manama, Bahrain, pp. 10–17.

Allen, P.A., 2007. The Huqf supergroup of Oman: basin development and context for Neoproterozoic glaciation. Earth Science Reviews 84, 139–185.

Álvaro, J.J., Courjault-Radé, P., et al., 1998. Nouveau découpage stratigraphique des séries cambriennes des nappes de Pardailhan et du Minervois (versant sud de la Montagne Noire, France). Géologie de la France 2, 3–12.

Álvaro, J.J., Ferretti, A., González-Gómez, C., Serpagli, E., Tortello, M.F., Vecoli, M., Vizcaïno, D., 2007. A review of the Late Cambrian (Furongian) palaeogeography in the western Mediterranean region, NW Gondwana. Earth Science Reviews 85, 47–81.

Amireh, B.S., Schneider, W., Abed, A.M., 1994. Evolving fluvial-transitional-marine deposition through the Cambrian sequence of Jordan. Sedimentary Geology 89, 65–90.

Amireh, B.S., Schneider, W., Abed, A.M., 2001. Fluvial-shallow marine-glaciofluvial depositional environments of the Ordovician system in Jordan. Journal of Asian Earth Sciences 19, 45–60.

Amireh, B.S., Amaireh, M.Z., Abed, A.M., 2007. Tectono sedimentary evolution of the Umm Ghaddah Formation (late Ediacaran–early Cambrian) in Jordan. Journal of Asian Earth Sciences 33, 194–218.

Andrawis, S.F., Afify, F.E., El-Ahmeed, A.T., 1983. Lower Palaeozoic trilobites from subsurface rocks of the Western Desert, Egypt. Neues Jahrbuch für Geologie und Paläontologie Mitteilungen 2, 65–68.

Aoudeh, S.M., Al-Hajri, S.A., 1995. Regional Distribution and Chronostratigraphy of the Qusaiba Member of the Qalibah Formation in the Nafud Basin, Northwestern Saudi Arabia. In: GEO '94: The Middle East Geosciences – Selected Middle East Papers from the Middle East Geoscience Conference, V1. Gulf Petrolink, Bahrain.

Avigad, D., Kolodner, K., McWilliams, M., Persing, H., Weissbrod, T., 2003. Origin of northern Gondwana Cambrian sandstone revealed by detrital zircon SHRIMP dating. Geology 31, 227–230.

Babcock, L.E., Peng, S., 2007. Cambrian chronostratigraphy: current state and future plans. Palaeogeography, Palaeoclimatology, Palaeoecology 254, 62–66.

Barca, S., Durand-Delga, M., Rossi, P., Storch, P., 1996. Les micaschistes panafricains de Corse et leur couverture paléozoïque : leur interprétation au sein de l'orogène varisque sud-européen. (The Pan-African micaschists of Corsica (France) and their Palaeozoic cover: their place in the Variscan orogen of Southern Europe). Comptes Rendus de l'Académie des Sciences 322 (11), 981–986.

Bender, F., 1975. Geology of the Arabian Peninsula. Jordan: USGS Professional Paper 560-1, 1–36.

Bergström, S., Massa, D., 1991. Stratigraphic and biogeographic significance of Upper Ordovician conodonts from northwestern Libya. In: Salem, M.J., Busrewil, M.T., Ashour, A.M. (Eds.), The Geology of Libya, IV. Elsevier, Amsterdam, pp. 1323–1342.

Bergström, S.M., Chen, X., Gutierrez-Marco, J.C., Dronov, A., 2009. The new chronostratigraphic classification of the Ordovician System and its relations to major regional series and stages and the $\delta^{13}C$ chemostratigraphy. Lethaia 42, 97–107.

Best, J.A., Barazangi, M., Al-Saad, D., Sawaf, T., Gebran, A., 1993. Continental margin evolution of the northern Arabian platform in Syria. American Association of Petroleum Geologists Bulletin 77, 173–193.

Beuf, S., Biju-Duval, B., Charpal, P., Rognon, P., Gariel, O., Bennacef, A., 1971. Les grès du Paléozoïque inférieur au Sahara. Publication Institut français du Pétrole, vol. 18. 483 pp.

Beyth, M., Heimann, A., 1999. The youngest igneous event in the crystalline basement of the Arabian–Nubian Shield, Timna Igneous Complex. Israel Journal of Earth Sciences 48, 13–120.

Blasband, B., White, S., Brooijmans, P., De Boorder, H., Visser, W., 2000. Late Proterozoic extensional collapse in the Arabian–Nubian Shield. Journal of the Geological Society 157, 615–628.

Bozdoğan, N., Erten, T., 1990. Mardin yükselminin yaşı ve etkileri, GD Türkiye. Türkiye 8th Petrol Kongresi Bildirileri, pp. 207–227. in Turkish, English abstract.

Bozkaya, Ö., Yalçın, H., Göncüoğlu, C., 2002. Mineralogic and organic responses to stratigraphic irregularities: an example from the lower Paleozoic very low-grade metamorphic units of the Eastern Taurus autochthon Turkey. Schweiz. Mineralogisches und Petrographisches Mitteilungen 82, 355–373.

Bozkaya, Ö., Gürsu, S., Göncüoğlu, M.C., 2006. Textural and mineralogical evidence for a Cadomian tectothermal event in the Eastern Mediterranean (Sandıklı–Afyon area, western Taurides, Turkey). Gondwana Research 10, 301–315.

Bozkurt, E., Oberhänsli, R., 2001. Menderes Massif (Western Turkey): structural, metamorphic and magmatic evolution — a synthesis. International Journal of Earth Sciences 89, 728–744.

Bozkurt, E., Winchester, J.A., Yiğitbaş, E., Ottlet, C., 2008a. Proterozoic ophiolites and mafic–ultramafic complexes marginal to the Istanbul Block: an exotic terrane of Avalonia affinity in NW Turkey. Tectonophysics 461, 240–251.

Bozkurt, E., Pereira, M.F., Strachan, R., Quesada, C., 2008b. Evolution of the Rheic Ocean. Tectonophysics 461, 1–8.

Brew, G., Litak, R., Seber, D., Barazangi, M., Al-Imam, A., Sawaf, T., 1997. Basement depth and sedimentary velocity structure in the northern Arabian Platform, eastern Syria. Geophysical Journal International 128, 618–631.

Burkhard, M., Caritg, S., Helg, U., Robert, Ch., Charrue, Ch., Soulaimani, A., 2006. Tectonics of the Anti-Atlas of Morocco. Comptes Rendus Geoscience 338, 11–24.

Buschmann, B., Elicki, O., Jonas, P., 2006. The Cadomian unconformity in the Saxo-Thuringian Zone, Germany: palaeogeographic affinities of Ediacaran (terminal Neoproterozoic) and Cambrian strata. Precambrian Research 147, 387–403.

Candan, O., Dora, O.Ö., Oberhänsli, R., Çetinkaplan, M., Partzsch, J.H., Warkus, F.C., Dürr, S., 2001. Pan-African high-pressure metamorphism in the Precambrian basement of the Menderes Massif, western Anatolia, Turkey. International Journal of Earth Sciences 89 (4), 793–811.

Carr, I.D., 2002. Second-order sequence stratigraphy of the Palaeozoic of North Africa. Marine and Petroleum Geology 25, 259–280.

Carrigan, C.W., Mukasa, S.B., Haydoutov, I., Kolcheva, K., 2006. Neoproterozoic magmatism and Carboniferous high-grade metamorphism in the Sredna Gora Zone, Bulgaria: an extension of the Gondwana-derived Avalonian–Cadomian belt? Lithos 82, 125–147.

Cater, J.M., Tunbridge, I.P., 1992. Paleozoic tectonic history of the SE Turkey. Journal of Petroleum Geology 15, 35–50.

Catuneanu, O., Abreu, V., et al., 2009. Toward the standardization of sequence stratigraphy. Earth Science Reviews 92, 1–33.

Clark-Lowes, D.D., 2005. Arabian glacial deposits: recognition of palaeovalleys within the Upper Ordovician Sarah Formation, Al Qasim district, Saudi Arabia. Proceedings of the Geologists' Association 116, 331–347.

Cocks, L.R.M., Torsvik, T.H., 2002. Earth Geography from 500 to 400 million years ago: a faunal and palaeomagnetic review. Journal of the Geological Society of London 159, 631–644.

Courjault-Radé, P., Debrenne, F., Gandin, A., 1992. Palaeogeographic and geodynamic evolution of the Gondwana continental margins during the Cambrian. Terra Nova 4, 657–667.

Crowley, Q.G., Floyd, P.A., Winchester, J.A., Franke, W., Holland, J.G., 2000. Early Palaeozoic rift-related magmatism in Variscan Europe: fragmentation of the Armorican Terrane Assemblage. Terra Nova 12, 171–180.

Dabard, M.-P., Loi, A., Paris, F., 2007. Relationship between phosphogenesis and sequence architecture: sequence stratigraphy and biostratigraphy in the Middle Ordovician of the Armorican Massif (NW France). Palaeogeography, Palaeoclimatology, Palaeoecology 248, 339–356.

Dean, W.T., 1967. The correlation and trilobite fauna of the Bedinan Formation (Ordovician) in southeastern Turkey. Bulletin of the British Museum (Natural History) Geology 15, 81–123.

Dean, W.T., 1971. The Lower Palaeozoic stratigraphy and faunas of the Taurus Mountains near Beyşehir, Turkey. II. The trilobites of the Seydişehir Formation (Ordovician). Bulletin of the British Museum (Natural History) Geology 20, 1–24.

Dean, W.T., 1972. The trilobite genus *Holasaphus* Matthew, 1895 in the Middle Cambrian rocks of Nova Scotia and eastern Turkey. Canadian Journal of Earth Sciences 9 (3), 266–279.
Dean, W.T., 1973. The Lower Palaeozoic stratigraphy and faunas of the Taurus Mountains near Beyşehir, Turkey. III. The trilobites of the Sobova Formation (Lower Ordovician). Bulletin of the British Museum (Natural History) Geology 24, 279–348.
Dean, W.T., 1982. Middle Cambrian trilobites from the Sosink Formation, Derik–Mardin district, south-eastern Turkey. Bulletin of the British Museum (Natural History) Geology 36, 1–41.
Dean, W.T., 1983. Additional faunal data for the Bedinan Formation (Ordovician) of south-eastern Turkey. Special Papers in Palaeontology 30, 89–105.
Dean, W.T., 2005. Trilobites from the Çal Tepe Formation (Cambrian), near Seydişehir, Central Taurides, southwestern Turkey. Turkish Journal of Earth Sciences 13, 1–71.
Dean, W.T., 2006. Cambrian stratigraphy and trilobites of the Samur Dağ area, south of Hakkâri, southeasternTurkey. Turkish Journal of Earth Sciences 15, 225–257.
Dean, W.T., Krummenacher, R., 1961. Cambrian trilobites from the Amanos Mountains, Turkey. Palaeontology 4, 71–81.
Dean, W.T., Martin, F., 1992. Ordovician biostratigraphic correlation in southern Turkey. In: Webby, B.D., Laurie, J.R. (Eds.), Global Perspectives on Ordovician Geology. Balkema, Rotterdam, pp. 195–203.
Dean, W.T., Monod, O., 1970. The Lower Palaeozoic stratigraphy and faunas of the Taurus Mountains near Beyşehir, Turkey. I. Stratigraphy. Bulletin of the British Museum (Natural History) Geology 19, 411–426.
Dean, W.T., Özgül, N., 1981. Middle Cambrian Trilobite succession in the Çal Tepe Formation at Bağbaşı (Hadim-Konya), central Taurus, Turkey. Bulletin of the Mineral Research and Exploration Institute of Turkey 92, 1–6.
Dean, W.T., Monod, O., 1990. Revised stratigraphy and relationships of Lower Palaeozoic rocks, eastern Taurus Mountains, south central Turkey. Geological Magazine 127, 333–347.
Dean, W.T., Monod, O., 1997. Cambrian development of the Gondwanaland margin in southeastern Turkey. In: Göncüoğlu, M.C., Derman, A.S. (Eds.), Early Palaeozoic Evolution in NW Gondwana: Turkish Association of Petroleum Geologists, Special Publication, 3, pp. 61–74.
Dean, W.T., Özgül, N., 1994. Cambrian rocks and faunas, Hüdai area, Taurus Mountains, southwestern Turkey. Bulletin de l'Institut Royal des Sciences Naturelles de Belgique, Sciences de la Terre 64, 5–20.
Dean, W.T., Zhou, Z.Y., 1988. Upper Ordovician trilobites from the Zap Valley, South-east Turkey. Palaeontology 31, 621–649.
Dean, W.T., Monod, O., Perincek, D., 1981. Correlations of Cambrian and Ordovician rocks in southeastern Turkey. T.C. Petrol Işleri Genel Müdürlüğü Dergisi 25, 269–291.
Dean, W.T., Martin, F., Monod, O., Demir, O., Rickards, R.B., Bultynck, P., Bozdoğan, N., 1997. Lower Palaeozoic stratigraphy, Karadere–Zirze area, central Pontides, northern Turkey. In: Göncüoğlu, M.C., Derman, A.S. (Eds.), Early Palaeozoic Evolution in NW Gondwana: Turkish Association of Petroleum Geologists, Special Publication, vol. 3, pp. 32–38.
Dean, W.T., Uyeno, T.T., Rickards, R.B., 1999. Ordovician and Silurian stratigraphy and trilobites, Taurus Mountains near Kemer, southwestern Turkey. Geological Magazine 136, 373–393.
Demirtaşlı, E., 1984. Stratigraphy and tectonics of the area between Silifke and Anamur, Central Taurus Mountains. In: Tekeli, O., Göncüoğlu, M.C. (Eds.), Geology of the Taurus Belt, pp. 101–118.
Denis, M., Guiraud, M., Konaté, M., Buoncristiani, J.F., in press, Subglacial deformation and water-pressure cycles as a key for understanding ice stream dynamics: evidence from the Late Ordovician succession of the Djado Basin (Niger). International Journal of Earth Science. (doi:10.1007/s00531-009-0455-z).
Destombes, J., Hollard, H., Willefert, S., 1985. Lower Palaeozoic rocks of Morocco. In: Holland, C.H. (Ed.), Lower Palaeozoic Rocks of the World. 4. Lower Palaeozoic of North-Western and West-Central Africa. Wiley, New York, pp. 91–336.
Deynoux, M., Ghienne, J.-F., 2004. Late Ordovician glacial pavements revisited: a reappraisal of the origin of striated surfaces. Terra Nova 16, 95–101.
Droste, H.H.J., 1997. Stratigraphy of the Lower Paleozoic Haima Supergroup of Oman. GeoArabia 2, 419–472.
Dumont, J.F., 1972. Découverte d'un horizon Cambrien à Trilobites dans l'autochtone du Taurus de Pisidie, région d'Eğridir, Turquie. Comptes Rendus de l'Académie des Sciences, Paris 274, 2435–2438.
Echikh, K., Sola, M.A., 2000. Geology and hydrocarbon occurrences in the Murzuq Basin SW Libya. In: Sola, M.A., Worsley, D. (Eds.), Geological exploration of the Murzuq Basin. Elsevier, Amsterdam, pp. 397–416.
Elicki, O., 2006. Microbiofacies analysis of Cambrian offshore carbonates from Sardinia (Italy): environment, reconstruction and development of a drowning carbonate platform. Carnets de Géologie/Notebooks on Geology, Brest 2006 (01), 1–22.
Elicki, O., 2007a. Facies development during late Early–Middle Cambrian (Tayan Member, Burj Formation) transgression in the Dead Sea Rift valley, Jordan. Carnets de Géologie/Notebooks on Geology, Brest 2007 (07), 1–20.
Elicki, O., 2007b. Paleontological data from the Early Cambrian of Germany and paleobiogeographical implications for the configuration of central Perigondwana. In: Linnemann, U., Nance, R.D., Kraft, P., Zulauf, G. (Eds.), The Evolution of the Rheic Ocean: From Avalonian–Cadomian Active Margin to the Alleghanian–Variscan Collision: Geological Society of America, Special Paper, vol. 423, pp. 143–152.
Elicki, O., Schneider, J.W., Shinaq, R., 2002. Prominent facies from the Lower/Middle Cambrian of the Dead Sea area (Jordan) and their palaeodepositional significance. Bulletin de la Société géologique de France 173, 147–152.
El-Khayal, A.A., Romano, M., 1988. A revision of the upper part of the Saq Formation and Hanadir Shale (lower Ordovician) of Saudi Arabia. Geological Magazine 125, 161–174.
Embry, A.F., 1995. Sequence boundaries and sequences hierarchies: problems and proposals. In: Steel, R.J., Felt, V.L., Johannesen, E.P., Mathieu, C. (Eds.), Norwegian Petroleum Society, Special Publication, vol. 5, pp. 1–11.
Erdoğan, B., Uchman, A., Güngör, T., Özgül, N., 2004. Lithostratigraphy of the Lower Cambrian metaclastics and their age based on trace fossils in the Sandıklı region, southwestern Turkey. Geobios 37, 346–360.
Erdtmann, B.D., 1986. Early Ordovician eustatic cycles and their bearing on punctuations in early nematophorid (planktic) graptolite evolution. Lecture Notes in Earth Sciences 8, 139–156.
Erkmen, U., Bozdoğan, N., 1981. Cambrian acritarchs from the Sosink Formation in southeast Turkey. Revista Española de Micropaleontología 13, 47–60.
Eschard, R., Abdallah, H., Braik, F., Desaubliaux, G., 2005. The Lower Paleozoic succession in the Tasilli outcrops, Algeria: sedimentology and sequence stratigraphy. First Break 23, 27–36.
Fabre, J., 1988. Les séries paléozoïques d'Afrique: une approche. Journal of African Earth Sciences 7, 1–40.
Fabre, J., Kazi-Tani, N., 2005. Ordovicien, Silurien, Devonien, Permo-Carbonifère. In: Fabre, J. (Ed.), Géologie du Sahara occidental et central. Tervuren African Geoscience Collection 18. Musée Royal de l'Afrique Centrale, Tervuren, Belgique, pp. 147–360.
Favre, P., Stampfli, G.M., 1992. From rifting to passive margin: the example of the Red Sea, Central Atlantic and Alpine Tethys. Tectonophysics 215, 69–97.
Fekirine, B., Abdallah, H., 1998. Paleozoic lithofacies correlatives and sequence stratigraphy of the Saharan Platform, Algeria. In: MacGregor, D.S., Moody, R.T.J., Clark-Lowes, D.D. (Eds.), Petroleum Geology of North Africa: Geological Society, London, Special Publication, 132, pp. 97–108.
Fortey, R.A., 1994. Late Cambrian trilobites from the Sultanate of Oman. Neues Jahrbuch für Geologie und Paläontologie 194, 25–53.
Fortey, R.A., Cocks, L.R.M., 2003. Palaeontological evidence bearing on global Ordovician–Silurian continental reconstruction. Earth Science Reviews 61, 245–307.
Galeazzi, S., Point, O., Hadadi, N., Mather, J., Druesne, D., 2010. Regional geology and petroleum systems of the Illizi–Berkine area of the Algerian Saharan Platform: an overview. Marine and Petroleum Geology 27, 143–178.
Garfunkel, Z., 2004. Origin of the Eastern Mediterranean basin: a reevaluation. Tectonophysics 391, 11–34.
Ghienne, J.-F., Le Heron, D., Moreau, J., Denis, M., Deynoux, M., 2007a. The Late Ordovician glacial sedimentary system of the North Gondwana platform. In: Hambrey, M., Christoffersen, P., Glasser, N., Janssen, P., Hubbard, B., Siegert, M. (Eds.), Glacial Sedimentary Processes and Products: International Association of Sedimentologist Special Publication, 39, pp. 295–319.
Ghienne, J.-F., Le Heron, D., Moreau, J., Denis, M., Deynoux, M., 2007b. The Late Ordovician glacial sedimentary system of the North Gondwana platform. In: Hambrey, M., Christoffersen, P., Glasser, N., Janssen, P., Hubbard, B., Siegert, M. (Eds.), Glacial Sedimentary Processes and Products: International Association of Sedimentologist Special Publications, 39, pp. 295–319.
Göncüoğlu, M.C., Kozlu, H., 2000. Early Palaeozoic evolution of the NW Gondwana-land: data from southern Turkey and surrounding regions. Gondwana Research 3, 315–324.
Göncüoğlu, Y., Kozur, H.W., 1999. Upper Cambrian and Lower Ordovician conodonts from the Antalya Unit in the Alanya Tectonic Window, southern Turkey. Neues Jahrbuch für Geologie und Paläontologie Mitteilungen 10, 593–604.
Göncüoğlu, M.C., Göncüoğlu, Y., Kozlu, H., Kozur, H., 2004. Geological evolution of the Taurides during the Infra-Cambrian to Carboniferous period: a Gondwanan perspective based on new biostratigraphic findings. Geologica Carpatica 55, 433–447.
Gozalo, R., Liñán, E., Dies Álvarez, M.E., Gámez Vintaned, J.A., Mayoral, E., 2007. Lower–Middle Cambrian boundary in the Mediterranean subprovince. In: Linnemann, U., Nance, R.D., Kraft, P., Zulauf, G. (Eds.), The Evolution of the Rheic Ocean: From Avalonian–Cadomian Active Margin to the Alleghanian–Variscan Collision: Geological Society of America, Special Paper, 423, pp. 359–374.
Guiraud, R., Bosworth, W., Thierry, J., Delplanque, A., 2005. Phanerozoic geological evolution of Northern and Central Africa: an overview. Journal of African Earth Sciences 43, 83–143.
Güngör, T., 2006. Deformation of the lower Cambrian sequence in the Sandikli region (Afyon), central Turkey. Geodinamica Acta 19, 345–361.
Gürsu, S., Göncüoğlu, M.C., 2005. Early Cambrian back-arc volcanism in the western Taurides, Turkey: implications for rifting along the northern Gondwana margin. Geological Magazine 142, 617–631.
Gürsu, S., Göncüoğlu, M.C., 2006. Petrogenesis and tectonic setting of Cadomian felsic igneous rocks, Sandıklı area of the western Taurides, Turkey. International Journal of Earth Sciences 95, 741–757.
Gürsu, S., Göncüoğlu, M.C., 2007. Comments on "Deformation of the lower Cambrian sequence in the region (Afyon), central Turkey", by T. Güngör. Geodinamica Acta 20, 353–362.
Gürsu, S., Kozlu, H., Göncüoğlu, M.C., Turhan, N., 2003. Correlation of the basement rocks and Lower Paleozoic covers of the western parts of the western Taurides. Bulletin of the Turkish Association of Petroleum Geologists 15, 129–153 in Turkish, English abstract.
Gürsu, S., Göncüoğlu, M.C., Bayhan, H., 2004. Geology and Geochemistry of the Pre-early Cambrian rocks in the Sandıklı area: implications for the Pan-African evolution NW Gondwanaland. Gondwana Research 7, 923–935.
Gutierrez-Marco, J.C., Robardet, M., Rábano, I., Sarmiento, G.N., San José Lancha, M.A., Herranz Araújo, P., Pieren Pidal, A.P., 2002. Ordovician. In: Gibbons, W., Moreno, T. (Eds.), The Geology of Spain. The Geological Society, London, pp. 31–49.
Gutierrez-Marco, J.C., Destombes, J., Rabano, I., Acenolaza, G.F., Sarmiento, G.N., San José, M.A., 2003. The Middle Ordovician of the Moroccan Anti-Atlas: paleobiodiversity, biostratigraphic review and correlation. Geobios 36, 151–177.

Gutnic, M., Monod, O., Poisson, A., Dumont, J-F., 1976. Géologie des Taurides Occidentales (Turquie). Mémoires de la Société Géologique de France 137, 1–112.
Hammann, W., 1992. The Ordovician trilobites from the Iberian Chains in the province of Aragon, NE-Spain. I. The trilobites of the Cystoid Limestone (Ashgill Series). Beringeria, vol. 6. 219 pp.
Haq, B.U., Al Qahtani, A.M., 2005. Phanerozoic cycles of sea-level change on the Arabian Platform. GeoArabia 10, 127–160.
Haq, B.U., Schutter, S.R., 2008. A chronology of Paleozoic sea-level changes. Science 322, 64–68.
Haude, H., 1975. Stratigraphie und Tektonik des südlichen Sultan Dağ (SW Anatolien). Zeitschrift der Deutschen Geologischen Gesellschaft 123, 411–421.
Helbing, H., Tiepolo, M., 2005. Age determination of Ordovician magmatism in NE Sardinia and its bearing on Variscan basement evolution. Journal of the Geological Society 162, 689–700.
Hetzel, R., Reichmann, T., 1996. Intrusion age of Pan-African augen gneisses in the southern Menderes Massif and the age of cooling after Alpine ductile extensional deformation. Geological Magazine 133, 565–572.
Higgs, K.T., Finucane, D., Tunbridge, I.P., 2002. Late Devonian and early Carboniferous microfloras from the Hakkari Province of southeastern Turkey. Review of Palaeobotany and Palynology 118, 141–156.
Husseini, M.I., 1989. Tectonic and depositional of the late Precambrian–Cambrian Arabian and adjoining plates. American Association of Petroleum Geologists Bulletin 73, 1117–1131.
Husseini, M.I., 1990. The Cambro-Ordovician in Arabian and adjoining plates: a glacio-eustatic model. Journal of Petroleum Geology 13, 267–288.
Janvier, Ph., Marcoux, J., 1977. Les grès rouges de l'Armutgözlek Tepe : leur faune de Poissons (Antiarches, Arthrodires et Crossoptérygiens) d'âge dévonien supérieur (Nappes d'Antalya, Taurides occidentales — Turquie). Géologie Mediterranéenne 4, 183–188.
Janvier, Ph., Lethiers, F., Monod, O., Balkaş, Ö., 1984. Discovery of a vertebrate fauna at the Devonian–Carboniferous boundary in SE Turkey (Hakkâri Province). Journal of Petroleum Geology 7, 147–168.
Jarrar, G., Wachendorf, H., Zellmer, H., 1991. The Saramuj Conglomerate: evolution of a Pan-African molasse sequence from southwest Jordan. Neues Jahrbuch für Geologie und Paläontologie Mitteilungen 6, 335–356.
Jones, P.J., Stump, T.E., 1999. Depositional and tectonic setting of the Lower Silurian hydrocarbon source rock facies, central Saudi Arabia. American Association of Petroleum Geologists Bulletin 83, 314–332.
Keegan, J.B., Rasul, S.M., Shaheen, Y., 1990. Palynostratigraphy of the Lower Palaeozoic, Cambrian to Silurian sediments of Hashemite Kingdom of Jordan. Review of Palaeobotany and Palynology 66, 167–180.
Keeley, M.L., 1989. The Paleozoic history of the Western Desert of Egypt. Basin Research 2, 35–48.
Kellogg, H.E., 1960. The geology of the Derik–Mardin area, southeastern Turkey. Rep. Exploration Division, American Overseas Petroleum Ltd. TPAO Rep. 1367 (unpublished).
Keppie, J.D., Nance, R.D., Murphy, J.B., Dostal, J., 2003. Tethyan, Mediterranean, and Pacific analogues for the Neoproterozoic–Paleozoic birth and development of peri-Gondwanan terranes and their transfer to Laurentia and Laurussia. Tectonophysics 365, 195–219.
Ketin, I., 1966. Cambrian outcrops in southeastern Turkey and their comparison with the Cambrian of east Iran. Bulletin of the Mineral Resource and Exploration Institute (MTA, Ankara) 66, 77–89.
Ketin, I., 1979. The geological section of the area between Hakkari and Çukurca, along the Büyük Zap Suyu River. Turkish Geological Society, Altınlı Symposium, pp. 11–14. in Turkish.
Kolodner, K., Avigad, D., Mcwilliams, M., Wooden, J.L., Weissbrod, T., Feinstein, S., 2006. Provenance of north Gondwana Cambrian–Ordovician sandstone: U–Pb. SHRIMP dating of detrital zircons from Israel and Jordan. Geological Magazine 143, 367–391.
Konert, G., Al-Afifi, A.M., Al-Hajri, S.A., Droste, H.J., 2001. Paleozoic stratigraphy and hydrocarbon habitat of the Arabian Plate. GeoArabia 6, 407–442.
Kozlu, H., Göncüoğlu, M.C., 1997. Stratigraphy of the Infra-Cambrian rock-units in the Eastern Taurides and their correlation with similar units in southern Anatolia. In: Göncüoğlu, M.C., Derman, A.S. (Eds.), Early Palaeozoic Evolution in NW Gondwana: Turkish Association of Petroleum Geologists, Special Publication, 3, pp. 50–60.
Kozlu, H., Göncüoğlu, M.C., Sarmiento, G., Gül, M.A., 2002a. Mid-Ordovician (Late Darriwilian) conodonts from the Southern-Central Taurides, Turkey: geological implications. Turkish Journal of Earth Sciences 11, 113–126.
Kozlu, H., Günay, Y., Sachanski, V., 2002b. Stratigraphy and graptolite biostratigraphy of the Lower Silurian succession in SE Anatolia and the Taurus Belt. Turkish Petroleum Corporation Exploration Group Report, Ankara.
Kröner, A., Şengör, A.M.C., 1990. Archean and Proterozoic ancestry in Late Precambrian to Early Palaeozoic crustal elements of southern Turkey revealed by single-zircon dating. Geology 18, 1186–1190.
Landing, E., Geyer, G., Heldmaier, W., 2006. Distinguishing eustatic and epeirogenic controls on Lower–Middle Cambrian boundary successions in West Gondwana (Morocco and Iberia). Sedimentology 54, 899–918.
Landing, E., Peng, S., Babcock, L.E., Geyer, G., Moczydlowska-Vidal, M., 2007. Global standard names for the lowermost Cambrian series and stage. Episodes 30, 287–289.
Laumonier, B., Autran, A., Barbey, P., Cheilletz, A., Baudin, T., Cocherie, A., Guerrot, C., 2004. Conséquences de l'absence de socle cadomien sur l'âge et la signification des séries pré-varisques (anté-Ordovicien supérieur) du sud de la France (Pyrénées, Montagne Noire). Bulletin de la Société géologique de France 175, 643–655.
Le Guerroué, E., Allen, P.A., Cozzi, A., 2006. Chemostratigraphic and sedimentological framework of the largest negative carbon isotopic excursion in Earth history: the Neoproterozoic Shuram Formation (Nafun Group, Oman). Precambrian Research 146, 68–92.
Le Hérissé, A., Al-Ruwaili, M., Miller, M., Vecoli, M., 2007. Environmental changes reflected by palynomorphs in the early Middle Ordovician Hanadir Member of the Qasim Formation, Saudi Arabia. Rev. Micropal. 50, 3–16.
Le Heron, D., Craig, J., 2008. First order reconstruction of a Late Ordovician Saharan ice sheet. Journal of the Geological Society of London 165, 19–29.
Le Heron, D.P., Ghienne, J.-F., El Houicha, M., Khoukhi, Y., Rubino, J.-L., 2007. Maximum extent of ice sheets in Morocco during the Late Ordovician glaciation. Palaeogeography, Palaeoclimatology, Palaeoecology 245, 200–226.
Legrand, P., 1985. Lower Palaeozoic rocks of Algeria. In: Holland, C.H. (Ed.), Lower Palaeozoic of North-western and West Central Africa, pp. 5–89.
Leone, F., Ferretti, A., Hammann, W., Loi, A., Pillola, G.L., Serpagli, E., 2002. A general view of the Post-Sardic Ordovician sequence from SW Sardinia. Rendiconti della Società Paleontologica Italiana 1, 51–68.
Linnemann, U., McNaughton, N.J., Romer, R.L., Gehmlich, M., Drost, K., Tonk, C., 2004. West African provenance for Saxo-Thuringia (Bohemian Massif): did Armorica ever leave pre-Pangean Gondwana? — U/Pb-SHRIMP zircon evidence and the Nd-isotopic record. International Journal of Earth Sciences 93, 683–705.
Linnemann, U., Gerdes, A., Drost, K., Buschmann, B., 2007. The continuum between Cadomian orogenesis and opening of the Rheic Ocean: constraints from LA-ICP-MS U–Pb zircon dating and analysis of plate-tectonic setting (Saxo-Thuringian zone, northeastern Bohemian Massif, Germany. In: Linnemann, U., Nance, R.D., Kraft, P., Zulauf, G. (Eds.), The Evolution of the Rheic Ocean: From Avalonian–Cadomian Active Margin to the Alleghanian–Variscan Collision: Geological Society of America, Special Paper, vol. 423, pp. 61–96.
Loi, A., Dabard, M.-P., 2002. Controls of sea level fluctuations on the formation of Ordovician siliceous nodules in terrigenous offshore environments. Sedimentary Geology 151, 65–84.
Loi, A., Pillola, G.L., Leone, F., 1996. La limite Cambrien–Ordovicien dans le SW de la Sardaigne: relations avec des événements eustatiques globaux. Comptes Rendus de l'Académie des Sciences, Paris 323, 881–888.
Loi, A., Ghienne, J.-F., Dabard, M.P., Paris, F., Botquelen, A., Christ, N., Elaouad-Debbaj, Z., Gorini, A., Vidal, M., Videt, B., Destombes, J., in press. The Late Ordovician glacio-eustatic record from a high-latitude storm-dominated shelf succession: the Bou Ingarf section (Anti-Atlas, Southern Morocco). Palaeogeography Palaeoclimatology Palaeoecology. (doi:10.1016/j.palaeo.2010.01.018).
Loosveld, R.J.H., Bell, A., Terken, J.J.M., 1996. The tectonic evolution of interior Oman. GeoArabia 1, 28–50.
Lüning, S., Craig, J., Loydell, D.K., Storch, P., Fitches, B., 2000. Lower Silurian hot shales in North Africa and Arabia: regional distribution and depositional model. Earth Science Reviews 49, 121–200.
Marcoux, J., 1987. Histoire et topologie de la Néo-Téthys. Contribution à partir des exemples de la Turquie et de l'Himalaya-Tibet. PhD thesis (unpubl.) Université Paris 6, 660p.
Martin, F., 1996. Recognition of the acritarch-based "trifidum flora" (Ordovician) in the absence of the eponymous species. Bulletin de l'Institut Royal des Sciences naturelles de Belgique, Sciences de la Terre 66, 5–13.
Martini, I.P., Tongiorgi, M., Oggiano, G., Cocozza, T., 1991. Ordovician alluvial fan to marine shelf transition in SW Sardinia, western Mediterranean Sea: tectonically ("Sardic phase") influenced clastic sedimentation. Sedimentary Geology 72, 97–115.
McGillivray, J.G., Husseini, M.I., 1992. The Paleozoic petroleum geology of Central Arabia. American Association of Petroleum Geologists Bulletin 76, 1473–1490.
Meert, J.G., 2003. A synopsis of events related to the assembly of eastern Gondwana. Tectonophysics 362, 1–40.
Miller, M.A., Al-Ruwaili, M.H., 2007. Preliminary palynological investigation of Saudi Arabian Upper Ordovician glacial sediments. Revue de Micropaléontologie 50, 17–26.
Millson, J.A., Mercadier, C.G.L., Livera, S.E., Peters, J.M., 1996. The Lower Palaeozoic of Oman and its context in the evolution of a Gondwanan continental margin. Journal of the Geological Society 151, 213–230.
Moix, P., Beccaletto, L., Kozur, H.W., Hochard, C., Rosselet, F., Stampfli, G.M., 2008. A new classification of the Turkish terranes and sutures and its implication for the paleotectonic history of the region. Tectonophysics 451, 7–39.
Molyneux, S.G., Al-Hajri, S., 2000. Palynology of a problematic Lower Palaeozoic lithofacies in central Saudi Arabia. In: Al-Hajri, S., Owens, B. (Eds.), Stratigraphic Palynology of the Palaeozoic of Saudi Arabia, GeoArabia Special Publication no. 1. Manama, Barhein, pp. 18–41.
Molyneux, S., Osterloff, P., Penney, R., Spaak, P., 2006. Biostratigraphy of the Lower Palaeozoic Haima Supergroup, Oman; its application in sequence stratigraphy and hydrocarbon exploration. GeoArabia 11, 17–48.
Monod, O., 1967. Présence d'une faune ordovicienne dans les schistes de Seydişehir, à la base des calcaires du Taurus occidental. Bulletin of the Mineral Resource and Exploration Institute (MTA, Ankara) 69, 78–89.
Monod, O., Kozlu, H., Ghienne, J.-F., Dean, W.T., Günay, Y., Le Hérissé, A., Paris, F., Robardet, M., 2003. Late Ordovician glaciation in southern Turkey. Terra Nova 15, 249–257.
Moreau, J., Ghienne, J.-F., Le Heron, D., Rubino, J.-L., Deynoux, M., 2005. A 440 Ma old ice stream in North Africa. Geology 31, 753–756.
Murphy, J.B., Nance, R.D., 2008. The Pangea conundrum. Geology 36, 703–706.
Nance, R.D., Linnemann, U., 2008. The Rheic Ocean: origin, evolution and significance. GSA Today 18, 4–12.
Nance, R.D., Murphy, J.B., Keppie, J.D., 2002. A Cordilleran model for the evolution of Avalonia. Tectonophysics 352, 11–31.
Nehlig, P., Genna, A., Asfirane, F., 2002. A review of the Pan-African evolution of the Arabian Shield. GeoArabia 7, 103–124.
Okay, A.I., Satır, M., Shang, C.K., 2008a. Ordovician metagranitoid from the Anatolide–Tauride Block, northwest Turkey: geodynamic implications. Terra Nova 20, 280–288.

Okay, A.I., Bozkurt, E., Satır, M., Yiğitbaş, E., Crowley, Q.G., Shang, C.K., 2008b. Defining the southern margin of Avalonia in the Pontides: geochronological data from the Late Proterozoic and Ordovician granitoids from NW Turkey. Tectonophysics 461, 252–264.

Omara, S., 1972. An Early Cambrian outcrop in southwestern Sinai. Egypt: Neues Jahrbuch für Geologie und Paläontologie 5, 306–314.

Oterdoom, W.H., Worthing, M.A., Partington, M., 1999. Petrological and tectono-stratigraphic evidence for a Mid Ordovician rift pulse on the Arabian Peninsula. GeoArabia 4, 467–500.

Özgül, N., Gedik, I., 1973. New data on the stratigraphy and the conodont faunas of Çaltepe limestone and Seydişehir formation Lower Paleozoic of Central Taurus range. Bulletin. Geological Society of Turkey 16, 39–52.

Özgül, N., Kozlu, H., 2002. Kozan–Feke (Doğu Toroslar) yöresinin stratigrafisi ve yapısal konumu ile ilgili bulgular. Türkiye Petrol Jeologları Denergi Bülteni 14, 1–36 English abstract.

Özgül, N., Metin, S., Dean, W.T., 1972. Lower Palaeozoic stratigraphy and faunas of the eastern Taurus Mountains in the Tufanbeyli region, southern Turkey. Bulletin of the Mineral Resource and Exploration Institute (MTA, Ankara) 79, 9–16.

Özgül, N., Metin, S., Erdoğan, B., Goğer, E., Bingöl, I., Baydar, O., 1973b. Tufanbeyli dolayının Kambryien ve Tersiyer kayaları (Cambrian-Tertiary rocks of the Tufanbeyli region, eastern Taurus, Turkey). Bulletin of the Geological Society of Turkey 1, 82–100. (English abstract).

Paris, F., Verniers, J., Al-Hajri, S., 2000. Ordovician chitinozoans from Central Saudi Arabia. In: Al-Hajri, A., Owens, B. (Eds.), Stratigraphic Palynology of the Palaeozoic of Saudi Arabia: GeoArabia Special Publication, vol. 1, pp. 42–56. Manama, Barhein.

Paris, F., Le Hérissé, A., Monod, O., Kozlu, H., Ghienne, J.-F., Dean, W.T., Vecoli, M., Günay, Y., 2007a. Ordovician chitinozoans and acritarchs from southern and southeastern Turkey. Revue de Micropaléontologie 50, 81–107.

Paris, F., Boumendjel, K., Dabard, M.P.H., Ghienne, J.-F., Loi, A., Peng, T., Videt, B., Achab, A., 2007b. Chitinozoan-based calibration of Early–Mid Ordovician transgressive events on northern Gondwana. Acta Palaeontologica Sinica 46, 370–375.

Piçarra, J.M., Robardet, M., Bourahrouh, A., Paris, F., Pereira, Z., Le Menn, J., Gourvennec, R., Oliveira, T., Lardeux, H., 2002. Le passage Ordovicien–Silurien et la partie inférieure du Silurien (Sud-Est du Massif armoricain, France). Comptes Rendus Geosciences 334, 1177–1183.

Pillola, G.L., Leone, F., Loi, A., 1998. The Cambrian and Early Ordovician of SW Sardinia. Giornale di Geologia (Special Issue ECOS VII—Sardinia Guidebook), vol. 60, pp. 25–38.

Pouclet, A., Aarab, A., Fekkak, A., Benharref, M., 2007. Geodynamic evolutionof the northwestern Paleo-Gondwanan margin in the Morrocan Atlas at the Precambrian–Cambrian boundary. In: Linnemann, U., Nance, R.D., Kraft, P., Zulauf, G. (Eds.), The Evolution of the Rheic Ocean: From Avalonian–Cadomian Active Margin to Alleghanian–Variscan Collision: Geological Society of America, Special Paper, 421, pp. 27–60.

Powell, J.H., 1989. Stratigraphy and sedimentation of the Phanerozoic rocks of central and southern Jordan. Part A: Ram and Khrein groups. Natural Resources Authority Bulletin (Amman) 11, 1–72.

Prigmore, J.K., Butler, A.J., Woodcock, N.H., 1997. Rifting during separation of Eastern Avalonia from Gondwana: evidence from subsidence analysis. Geology 25, 203–206.

Ramezani, J., Tucker, R.D., 2003. The Saghand region, central Iran: U–Pb geochronology, petrogenesis and implications for Gondwana tectonics. American Journal of Science 301, 622–665.

Robardet, M., 2003. The Armorica 'microplate': fact or fiction? Critical review of the concept and contradictory palaeobiogeographical data. Palaeogeography, Palaeoclimatology, Palaeoecology 195, 125–148.

Ruban, D.A., Al-Husseini, M.I., Iwasaki, Y., 2007. Review of Middle East Paleozoic plate tectonics. GeoArabia 12, 35–56.

Runkel, A.C., McKay, R.M., Palmer, A.R., 1998. Origin of a classic cratonic sheet sandstone: stratigraphy across the Sauk II–Sauk III boundary in the Upper Mississippi Valley. GSA Bulletin 110, 188–210.

Rushton, A.W.A., Powell, J.H., 1998. A review of the stratigraphy and trilobite faunas from the Cambrian Burj Formation in Jordan. Bulletin of the British Museum (Natural History), London, (Geology) 54, 131–146.

Sachanski, V., Göncüoğlu, M.C., Gedik, I., Okuyucu, C., 2007. The Silurian of the Çatak and Karadere areas of the Zonguldak Terrane, NW Anatolia. Geologica Balcanica 36, 103–110.

Saltzman, M.R., Cowan, C.A., Runkel, A.C., Runnegar, B., Stewart, M.C., Palmer, A.R., 2004. The Late Cambrian SPICE ($\delta^{13}C$) event and the Sauk II–SAUK III regression: new evidence from Laurentian Basins in Utah, Iowa, and Newfoundland. Journal of Sedimentary Research 74, 366–377.

Sanchez-Garcia, T., Bellido, F., Quesada, C., 2003. Geodynamic setting and geochemical signatures of Cambrian–Ordovician rift-related igneous rocks (Ossa-Morena Zone, SW Iberia). Tectonophysics 365, 233–255.

Sarmiento, G.N., Gül, M.A., Kozlu, H., Göncüoğlu, M.C., 1999. Darriwilian conodonts from the Taurus Mountains, southern Turkey. 8th ISOS: Acta Universitatis Carolinae, Geologica, Praha, 41, pp. 37–40.

Sarmiento, G.N., Göncüoğlu, M.C., Göncüoğlu, Y., 2003. Early Darriwilian conodonts from the Sobova Formation in the Eastern and Western Taurides, Southern Turkey. In: Albanesi, G.L., Beresi, M.S., Peralta, S.H. (Eds.), Ordovician from the Andes, 17, pp. 143–144.

Schmidt, G.C., 1965. Proposed rock unit nomenclature, Petroleum District V, S.E. Turkey. Chart1, revised edition. Stratigraphic Committee, Turkish Association of Petroleum Geologists, Ankara. (unpublished).

Schneider, W., Amireh, B.S., Abed, A.M., 2007. Sequence analysis of the early Paleozoic sedimentary systems of Jordan. Zeitschrift der Deutschen Gesellschaft für Geowissen-schaften, Stuttgart 158, 225–247.

Schulz, B., Bombach, K., Pawlig, S., Braetz, H., 2004. Neoproterozoic to early-Palaeozoic magmatic evolution in the Gondwana-derived Austroalpine basement to the south of the Tauern Window, Eastern Alps. International Journal of Earth Sciences 91, 824–843.

Şenalp, M., Al-Duaiji, A.A., 2001. Qasim Formation: Ordovician storm and tide dominated shallow-marine siliciclastic sequences, Central Saudi Arabia. GeoArabia 6, 233–268.

Şenel, M., 2002. 1/500.000 Scale Geological Map of Turkey, Konya, Antalya, Adana, Hatay, Diyarbakır and Cizre Sheets. Mineral Resource and Exploration Institute (MTA), Ankara.

Şenel, M., Kengil, R., Ünverdi, M., Serdaroğlu, M., Gözler, M.Z., 1981. Teke Toroslarının güneydoğusunun jeolojisi. MTA Bulletin 95/96, 13–43 in Turkish, English abstract.

Şenel, M., Göncüoğlu, Y., Kozur, H.W., 2000. Conodont dated Cambrian rocks from the Tahtalidağ Nappe (Antalya Nappes) of the Kemer area, Western Taurides (Turkey). 2nd Croatian Geological Congress, Cavtat-Dubrovnik, April 2000, Proceedings, pp. 371–377.

Şengör, A.M.C., 1990. A new model for the Late Paleozoic–Mesozoic tectonic evolution of Iran and implications for Oman. The geology and tectonics of the Oman Region. Special Publication, Geological Society London 49, 797–831.

Şengör, A.M.C., Yılmaz, Y., 1981. Tethyan evolution of Turkey: a plate tectonic approach. Tectonophysics 75, 181–241.

Sharland, P.R., Archer, R., Casey, D.M., Davies, R.B., Hall, S.H., Heward, A.P., Horbury, A.D., Simmons, M.D., 2001. Arabian plate sequence stratigraphy. GeoArabia Special Publication 2, 1–371.

Shergold, J.H., Geyer, G., 2003. The subcommission on Cambrian stratigraphy: the status quo. Geologica Acta 1, 5–9.

Shergold, J.H., Sdzuy, K., 1984. Cambrian and early Tremadocian trilobites from Sultan Dağ, central Turkey. Senckenbergiana Lethaea 65, 51–135.

Shirley, J., 1936. Some British trilobites of the family Calymenidae. Quaterly Journal of the Geological Society London 92, 384–421.

Sial, A.N., Peralta, S., Ferreira, V.P., Toselli, A.J., Aceñolaza, F.G., Parada, M.A., Gaucher, C., Alonso, R.N., Pimentel, M.M., 2008. Upper Cambrian carbonate sequences of the Argentine Precordillera and the Steptoean C-Isotope positive excursion (SPICE). Gondwana Research 11, 437–452.

Silva, J.B., Pereira, M.F., 2004. Transcurrent continental tectonics model for the Ossa–Morena Zone Neoproterozoic–Paeozoic evolution, SW Iberian Massif, Portugal. International Journal of Earth Sciences 91, 886–896.

Soudry, D., Weissbrod, T., 1995. Morphogenesis and facies relationships of thrombolites and siliciclastic stromatolites in a Cambrian tidal sequence (Elat area, southern Israel). Palaeogeography, Palaeoclimatology, Palaeoecology 114, 339–355.

Soulaimani, A., Essaifi, A., Youbi, N., Hafi, A., 2004. Les marqueurs structuraux et magmatiques de l'extension crustale au Protérozoique terminal-Cambrien basal autour du massif de Kerdous (Anti-Atlas occidental, Maroc). Comptes Rendus Géosciences 336, 1433–1441.

Stampfli, G.M., 2000. Tethyan oceans. In: Bozkurt, E., Winchester, J.A., Piper, J.D.A. (Eds.), Tectonics and Magmatism in Turkey and Surrounding Area: Geological Society, London Special Publication, 173, pp. 1–23.

Stampfli, G.M., Borel, G., 2002. A plate tectonic model for the Paleozoic and Mesozoic constrained by dynamic plate boundaries and restored synthetic oceanic isochrones. Earth and Planetary Science Letters 196, 17–33.

Steemans, P., Le Hérissé, A., Bozdoğan, N., 1996. Ordovician and Silurian cryptospores and miospores from southeastern Turkey. Review of Palaeobotany and Palynology 91, 35–76.

Stöcklin, J., 1968. Structural history and tectonics of Iran: a review. American Association of Petroleum Geologists Bulletin 7, 1229–1258.

Storch, P., 2006. Facies development, depositional settings and sequence stratigraphy across the Ordovician–Silurian boundary: a new perspective from the Barrandian area of the Czech Republic. Geological Journal 41, 163–192.

Sutcliffe, O.E., Dowdeswell, J.A., Whittington, R.J., Theron, J.N., Craig, J., 2000. Calibrating the Late Ordovician glaciation and mass extinction by the eccentricity cycles of Earth's orbit. Geology 28, 967–970.

Tawadros, E., Rasul, S.M., Elzaroug, R., 2001. Petrography and palynology of quartzites in the Sirte Basin, central Libya. Journal of African Earth Sciences 32, 373–390.

Taylor, J., Dowdeswell, J.A., Kenyon, K.H., O'Cofaigh, C., 2002. Late Quaternary architecture of trough-mouth fans: debris flows and suspended sediments on the Norwegian margin. In: Dowdeswell, J.A., O'Cofaigh, C. (Eds.), Glacier-Influenced Sedimentation on High Latitude Continental Margins. Geological Society, London, Special Publication 203, pp. 55–77.

Teipel, U., Eichorn, R., Loth, G., Rohrmüller, J., Höll, R., Kennedy, A., 2004. U–Pb SHRIMP and Nd isotopic data from the western Bohemian Massif (Bayerischer Wald, Germany): implications for Upper Vendian and lower Ordovician magmatism. International Journal of Earth Sciences 91, 782–801.

Tolluoğlu, A., Sümer, E., 1995. An evolutionarty model on Early Paleozoic of Anatolian microcontinent, northern margin of Gondwana land. Geological Bulletin Turkey 38, 1–10.

Tolun, N., Ternek, Z., 1952. Notes géologiques sur la région de Mardin. Bulletin of the Geologic Society of Turkey 1, 15–19.

Torsvik, T.H., Cocks, L.R.M., 2004. Earth geography from 400 to 250 million years: a palaeomagnetic, faunal and facies review. Journal of the Geological Society of London 161, 555–572.

Turner, B.R., Makhlouf, I.M., Armstrong, H.A., 2005. Late Ordovician (Ashgillian) glacial deposits in southern Jordan. Sedimentary Geology 181, 73–91.

Varol, Ö.N., Demirel, I.H., Rickards, R.B., Günay, Y., 2006. Source rock characteristics and biostratigraphy of the Lower Silurian (Telychian) organic shales at Akyaka, Central Taurus region, Turkey. Marine and Petroleum Geology 23, 901–911.

Vaslet, D., 1987. The Paleozoic (Pre-Late Permian) of Central Arabia and correlations with neighbouring regions: D.G.M.R., Jeddah, Technical Record, B.R.G.M. TR 07-2, 167p.
Vaslet, D., 1990. Upper Ordovician glacial deposits in Saudi Arabia. Episodes 13, 147–161.
Vecoli, M., 2000. Palaeoenvironmental interpretation of microphytoplankton diversity trends in the Cambrian–Ordovician of the northern Sahara Platform. Palaeogeography, Palaeoclimatology, Palaeoecology 160, 329–346.
Vennin, E., Álvaro, J.J., Villas, E., 1998. High-latitude pelmatozoan–bryozoan mud-mounds from the late Ordovician northern Gondwana platform. Geological Journal 33, 121–140.
Viana, A.R., Faugères, J.-C., Stow, D.A.V., 1998. Bottom-current-controlled sand deposits — a review of modern shallow- to deep-water environments. Sedimentary Geology 115, 53–80.
Villas, E., Vennin, E., Alvaro, J.J., Hammann, W., Herrera, Z.A., Piovano, E., 2002. The late Ordovician carbonate sedimentation as a major triggering factor of the Hirnantian glaciation. Bulletin de la Société géologique de France 173, 569–578.
von Raumer, J.F., Stampfli, G.M., 2008. The birth of the Rheic Ocean — Early Palaeozoic subsidence patterns and subsequent tectonic plate scenarios. Tectonophysics 461, 9–20.
von Raumer, J.F., Stampfli, G.M., Borel, G., Bussy, F., 2002. The organization of pre-Variscan basement areas at the north-Gondwanan margin. International Journal of Earth Sciences 91, 35–52.
Webby, B.D., Paris, F., Droser, M.L., Percival, I.G., 2004. The Great Ordovician Biodiversification Event. Columbia Univ Press. 496pp.
Weissbrod, T., Sneh, A., 2002. Sedimentology and palaeogeography of the late Precambrian–Early Cambrian arkosic and conglomeratic facies in the northern margin of the Arabo-Nubian shield. Geological Survey opf Israel Bulletin 87, 1–44.
Wolfart, R., 1981. Lower Paleozoic rocks of the Middle East. In: Holland, C.H. (Ed.), Lower Paleozoic of the Middle East, Eastern and Southern Africa, and Antarctica, pp. 5–30.
Yalçınlar, I., 1964. Les couches du Paléozoique inférieur dans la Turquie méridionale. Publications de l'Institut de Géographie de l'Université d'Istanbul 39, 1–16.
Yanev, S., Lakova, I., Boncheva, I., Sachanski, V., 2005. The Moesian and Balkan Terranes in Bulgaria: Palaeozoic basin development, palaeogeography and tectonic evolution. Geologica Belgica 8, 185–192.
Yiğitbaş, E., Kerrich, R., Yılmaz, Y., Elmas, A., Xie, Q., 2004. Characteristics and geochemistry of Precambrian ophiolites and related volcanics from the Istanbul–Zonguldak Unit, Northwestern Anatolia, Turkey: following the missing chain of the Precambrian South European suture zone to the east. Precambrian Research 132, 179–206.
Zhou, Z.Y., Dean, W.T., Huilin, L., 1998. Early Ordovician Trilobites from Dali, West Yunnan, China, and their palaeogeographical significance. Palaeontology 41, 429–460.
Zhu, Mao-Yan, Zhang, Jun-Ming, Li, Guo-Xiang, Yang, Ai-Hua, 2004. Evolution of C isotopes in the Cambrian of China: implications for Cambrian subdivision and trilobite mass extinctions. Geobios 37, 287–301.

2- Le scénario : calendrier des événements glaciaires

L'Anti-Atlas marocain préserve une succession Paléozoïque inférieur très complète (Destombes et al., 1985). Entre Zagora et Tazzarine, le groupe du Premier Bani (fin de l'Ordovicien moyen) correspond à une épaisse succession à dominante gréseuse dont seul le toit est visible ici sur la droite. Les entablements du sommet, sur la gauche, appartiennent au groupe du Second Bani (Ordovicien terminal, Hirnantien). Entre les deux, la vaste cuesta à dominante argileuse recèle sur plus de 600 m un enregistrement des épisodes de bas niveau marin glacio-eustatique ayant ponctué l'Ordovicien supérieur (Loi et al., 2010 ; Fig. 14). Ils apparaissent dans le paysage sous la forme de ressauts gréseux.

Publication associée :

Loi A., Ghienne J.-F., Dabard M.P., Paris F., Botquelen A., Christ N., Elaouad-Debbaj Z., Gorini A., Vidal M., Videt B., Destombes J. (2010) The Late Ordovician glacio-eustatic record from a high-latitude storm-dominated shelf succession: the Bou Ingarf section (Anti-Atlas, Southern Morocco). Palaeogeography Palaeoclimatology Palaeoecology, 296, 332-358.

➔ Voir aussi :

Ghienne et al., 2007a (chapitre 6)

Ghienne et al., 2008

Depuis les années 1960, et jusque vers 1990, prédominait l'idée d'une glaciation longue couvrant l'essentiel de l'Ordovicien supérieur et du Silurien inférieur. C'est cette idée qui transparaissait dans les premières synthèses concernant cette glaciation (Hambrey, 1985) et qui avait permis la caractérisation par Frakes et al. (1992) d'un mode « *ice house* » pour cette période du Paléozoïque. Les travaux de P. Brenchley (Brenchley et al., 1994, 2003) ont ensuite associé la glaciation à une excursion isotopique majeure mais de courte durée et à une crise de la biodiversité sous la forme d'une double extinction en masse. Avec la généralisation concomitante de datations directes des dépôts glaciogéniques par le biais des palynomorphes (Paris et al., 1995), et plus rarement grâce aux macrofaunes associées (Sutcliffe et al., 2000 , 2001 ; Villas et al., 2006), s'est progressivement installée l'idée d'une glaciation de courte durée. Avec une durée de l'ordre du million d'années, la glaciation fini-ordovicienne se concevait dorénavant comme un accident climatique au sein d'une période globalement chaude. Cette vision des choses rejoignait les premières datations proposées par J. Destombes (1969b), pour qui le « Glaciaire ordovicien » était limité à l'Hirnantien, dernière subdivision de l'Ordovicien. De même, l'apparition de faciès glaciomarins sur la plate-forme distale était effectivement limitée à l'Hirnantien, comme dans la succession barandienne du Bassin de Prague (Storch, 1990). Par la suite, la plupart des travaux utilisèrent cette attribution d'âge par défaut (par exemple, *Ghienne, 2003, §6*) et les modélisations paléoclimatiques reprirent à leur compte ce concept d'accident climatique (Hermann et al., 2004; Lefebvre et al., 2010).

Les chantiers entrepris avaient tout d'abord confirmé cette vision d'une glaciation courte. Dans le sud-est du Bassin de Taoudéni, c'est-à-dire en position proximale, les associations de chitinozoaires (Paris et al., 1998) et de graptolites (Underwood et al., 1998) montraient que toute influence glaciogénique cessaient dès avant la fin de l'Ordovicien. En position distale, à la marge des fronts d'extension maximale des glaciers comme par exemple en Turquie, la biostratigraphie donnait également un âge tardi-ordovicien cantonné dans l'Hirnantien (*Monod et al., 2003, §4*; Paris et al., 2007). En Libye, l'altération météorique de la succession glaciaire n'est pas propice à la préservation des palynomorphes. Toutefois, plusieurs échantillons avaient également donné un âge fini-ordovicien, voire Hirnantien (biozone à *elongata*). Cela était de plus corroboré par la présence au sein des faciès glaciomarins d'une macrofaune remaniée (brachiopodes, trilobites) sous forme de galets lâchés dont l'âge était Ordovicien supérieur (Katien moyen, proche de l'ancienne limite Caradoc/ Ashgill, voir figure en Introduction ; *Ghienne et al., 2007b, §6* ; Guttierez-Marco, comm. pers.).

Cependant, plusieurs éléments laissaient planer un doute sur le concept d'une glaciation limitée à l'Hirnantien. En zone proximale, la base des formations glaciaires est azoïque, reposant sur des successions sous-jacentes beaucoup plus anciennes, elles-mêmes sans attribution stratigraphique précise. Un important hiatus stratigraphique est ainsi très mal contraint. D'autre part un faisceau d'arguments semblait montrer que la glaciation, ou au moins un refroidissement généralisé, précédait l'événement glaciaire Hirnantien : (i) aux basses latitudes, la mise en route d'upwellings suggérait que la glaciation avait débuté au cours de l'Ordovicien supérieur, bien avant l'Hirnantien (Pope et Steffen, 2003) ; (ii) au nord Niger (région du Djado), en zone très proximale, une succession à graptolites d'âge Hirnantien ou légèrement plus ancien scellait des horizons glaciaires (Legrand, 2003 ; Denis et al., 2007) ; (iii) en Amérique du Sud, des dépôts glaciaires siluriens étaient identifiés, indiquant la pérennisation de glaciers après le Silurien (Grahn et Caputo, 1992); enfin (iv), Saltzman et Young (2005) proposaient qu'une chute de niveau marin en association avec une excursion isotopique signait un premier cycle glaciaire quelque 10 millions d'années avant l'Hirnantien.

En 2004, je proposai dans le cadre du programme ECLIPSE II un projet de recherche sur 4 ans concernant la glaciation ordovicienne. L'un des enjeux majeurs de projet était d'établir le calendrier

des événements glaciaires de l'Ordovicien. Une analyse séquentielle haute résolution a été menée sur une coupe de l'Anti-Atlas marocain (coupe de Bou Ingarf) qui présentaient le double avantage d'avoir une biostratigraphie bien établie (Bourahrouh et al., 2004) et un enregistrement glaciaire bien identifiable. Les résultats maintenant publiés (Ghienne et al., 2008 ; *Loi et al., 2010*) apporte un éclairage nouveau sur ce problème de l'âge de la glaciation fini-ordovicienne qui se révèle être à la fois plus courte, et plus longue!, que l'Hirnantien (Page et al., 2007, Vandenbroucke et al., 2010). En effet, les conclusions de ces travaux sont les suivantes :

- Les 9 à 10 millions d'années précédant l'événement glaciaire hirnantien comprennent une succession de plate-forme silicoclastique dominée par les tempêtes. Le tempo de cette succession stratigraphique est dominé par l'empilement de cycles à très haute (<400ka), haute (400 ka) et basse (« 3ème ordre, 1,4-2,7 Ma) fréquences, dont les amplitudes souligne l'origine glacioeustatique.
- En particulier, ont été caractérisées trois régressions forcées d'une amplitude supérieure à 40 m. Ces épisodes régressifs, maintenant reconnus sur les (paléo-)plates-formes carbonatées intertropicales sous la forme de karsts (Calner et al. 2009), représentent des événements analogues à celui de l'Hirnantien, quoique de moindre ampleur. Les fronts glaciaires correspondant n'ont pas atteint les domaines de bassins sédimentaires, avec l'exception de l'épisode immédiatement pré-Hirnantien (*i.e.* Katien terminal) dont un enregistrement glaciaire est très possiblement présent au nord Niger. Les architectures sédimentaires résultantes (« *sharp-based shoreface* ») sont analogues à ce que sera la signature de l'événement hirnantien sur la plate-forme distale (cf. Chapitre 5).
- La glaciation dite hirnantienne ne correspond en fait qu'à une fraction de cet étage avec un Hirnantien inférieur dénué d'activité glaciaire, en accord avec la position de l'excursion isotopique détectée en Chine (Xu Chen et al., 2006). C'est à cet épisode qu'il faut rattacher l'essentiel des enregistrements glaciaires de l'Ordovicien, témoignant de fronts glaciaires ayant atteints les bassins sédimentaires distribués sur le pourtour du Gondwana occidental (Afrique/ Amérique du Sud).
- L'événement glaciaire hirnantien est lui-même subdivisé en deux cycles (stadial ?) séparés par une transgression dite intra-hirnantienne (interstadial ?), le second cycle correspondant au climax de la glaciation ordovicienne, ou plus exactement ordovico-silurienne (*Ghienne et al., 2007b, §6*). Chaque cycle (100 ou 400 ka ?) comprend aussi plusieurs phases d'avancée et retrait glaciaires de plus faible envergure (cf. section 6.4)

En résumé, une calotte polaire occupait les hautes latitudes gondwaniennes bien avant, et bien après, l'Hirnantien. Ses fluctuations sont à l'origine d'un signal glacioeustatique, dont les épisodes les plus marquants correspondent à des régressions forcées majeures globales. Un consensus apparaît donc qui réconcilie l'idée qu'avaient les « anciens » d'une glaciation longue, avec le concept plus récent d'accident climatique hirnantien. Un refroidissement (« *cool » ou « icehouse » mode*) au cours de l'Ordovicien, qui se prolongera dans le Silurien (Lehnert et al., 2010), a créé les conditions d'apparition et/ ou de développement de calotte(s) polaire(s) gondwanienne(s) que des fluctuations climatiques (contrôle orbital ?, instabilités climatiques ?) auront à plusieurs reprises amplifiées en véritables inlandsis. Le débat s'est maintenant déplacé vers la base de la succession stratigraphique avec la question suivante : quand donc a débuté la glaciation ordovicienne ? Des données thermométriques sur apatite de conodontes (Trotter et al., 2008), ainsi que la contraction des zones bioclimatiques déduites de la distribution du zooplancton (Vandenbroucke et al., 2009, 2010) semblent suggérer un refroidissement notable à l'Ordovicien moyen. Cependant, il n'est pas exclu que des glaciers aient occupé les hautes terres du Gondwana pendant tout le Paléozoïque inférieur et que l'existence d'une transition marquée d'un mode « *warm house* » sans glacier vers un mode « *ice house* » ne soit qu'une chimère.

Palaeogeography, Palaeoclimatology, Palaeoecology 296 (2010) 332–358

Contents lists available at ScienceDirect

Palaeogeography, Palaeoclimatology, Palaeoecology

journal homepage: www.elsevier.com/locate/palaeo

The Late Ordovician glacio-eustatic record from a high-latitude storm-dominated shelf succession: The Bou Ingarf section (Anti-Atlas, Southern Morocco)

A. Loi [a], J.-F. Ghienne [b,*], M.P. Dabard [c], F. Paris [c], A. Botquelen [d], N. Christ [b,1], Z. Elaouad-Debbaj [e], A. Gorini [a], M. Vidal [d], B. Videt [c], J. Destombes [f]

[a] Dipartimento di Scienze della Terra, Via Trentino, 51, 09127 Cagliari – Italy
[b] Institut de Physique du Globe de Strasbourg, UMR 7516 CNRS/Université de Strasbourg, 1 rue Blessig, 67084 Strasbourg Cedex – France
[c] Université de Rennes 1, UMR 6118 CNRS, Campus de Beaulieu, 35042 Rennes Cedex – France
[d] Université de Brest, UMR 6538 CNRS, 6 avenue Le Gorgeu – C.S. 93837, 29238 Brest Cedex 3 – France
[e] ENIM, Ecole Nationale de l'Industrie Minérale, B.P. 753, Rabat-Agdal – Morocco
[f] 19 rue de la Fon de Madran, 33600 Pessac – France

ARTICLE INFO

Article history:
Received 17 April 2009
Received in revised form 18 December 2009
Accepted 14 January 2010
Available online 21 January 2010

Keywords:
Katian
Hirnantian
Sea-level
Forced regression
Ice sheet
Sequence stratigraphy

ABSTRACT

Evidences of glaciation at the end of the Ordovician are widespread in western Gondwana. Some authors consider the glaciation was restricted to the Hirnantian time, but occurrences of glacial deposits in the Lower Silurian strata of South America indicate that the Gondwana glaciers did not completely disappear after the Hirnantian glaciation. In addition, numerous studies based on palaeoecology, sedimentology, sequence stratigraphy and stable isotopes have suggested that ice sheets formed as soon as the Early/Middle Katian. The objective of this work is to investigate the high-frequency eustatic signals in a stratigraphic succession corresponding to the Katian and the Hirnantian (~10 My comprising the uppermost part of the Ordovician). The studied section (Bou Ingarf section >600 m) is located in the Central Anti-Atlas, southern Morocco. It shows an almost continuous succession of siliciclastic platform deposits. The lower package, Katian to early Hirnantian in age, corresponds to a shelf succession, within which storm dynamics prevailed. The upper package, middle to upper Hirnantian in age, comprises a glaciation-related succession made up of a suite of coastal to flood-dominated fluvio-glacial deposits. The latter have essentially filled in large palaeochannels interpreted as subglacial tunnel valleys. From high-resolution facies and sequential analysis, a curve of variation of depositional environments was established at very high, high and low frequencies. Time calibration was performed based on a high-quality biostratigraphic control mainly derived from chitinozoan biozones through the whole succession. Assuming a constant tectonic subsidence and a bathymetric model (shoreface/upper offshore boundary: 30 m; upper offshore/lower offshore boundary: 120 m), changes in facies-based water depths are converted into an eustatic sea-level curve using a one-dimensional backstripping procedure. The eustatic sea-level curve shows that the stratigraphic succession is dominated by the stacking of sequences at very high- (<400 ka), high- (400 ka) and low- ("3rd order") frequencies that reflect eustatic variations controlled by ice-cap to ice-sheet growths throughout the Katian and Hirnantian. Three episodes of abrupt sea-level falls (>40 m) and coeval forced regressions were identified during the Katian. They represent glacial episodes of significant extent prior to the Hirnantian, but essentially lacking a glacial record. Strata reflecting the Hirnantian glaciation include two differentiated events and an intermediate but important transgression. The second Hirnantian glacial event, the only one associated with subglacial erosion in the Bou Ingarf area, corresponds to the Late Ordovician glacial climax characterised by a continental-scale ice sheet. Ice sheets permanently occupying the centre of the Gondwana landmass throughout the Late Ordovician may reconcile moderate Hirnantian eustatic sea-level fall amplitude (40–80 m) and palaeoglacial reconstructions that show a Hirnantian ice sheet covering the main part of western Gondwana.

1. Introduction

At the end of the Ordovician, evidences for an ice sheet are widespread over Gondwana. During the Hirnantian, a relatively short time interval (1–2 Ma, cf. Webby et al., 2004), glaciers reached Gondwana sedimentary basins resulting in an extensive glacial record

* Corresponding author.
E-mail addresses: alfloi@unica.it (A. Loi), ghienne@unistra.fr (J.-F. Ghienne), Marie-Pierre.Dabard@univ-rennes1.fr (M.P. Dabard), florentin.paris@univ-rennes1.fr (F. Paris).
[1] Present address: Ruhr-Universität Bochum, Institute for Geology, Mineralogy and Geophysics, Universitätsstrasse 150, D-44801 Bochum – Germany.

0031-0182/$ – see front matter © 2010 Elsevier B.V. All rights reserved.
doi:10.1016/j.palaeo.2010.01.018

(Deynoux et al., 1985; Vaslet, 1990; Sutcliffe et al., 2000; Schönian and Egenhoff, 2007; Ghienne et al., 2007a; Le Heron and Craig, 2008). Some authors (Brenchley et al., 1994; Sutcliffe et al., 2000; Brenchley et al., 2003) considered this time slice as corresponding entirely to the Late Ordovician glaciation itself though it can be alternatively regarded as the period of maximum extent of Gondwana glaciers at the end of the Ordovician (Ghienne, 2003; Pope and Steffen, 2003). Indeed, a Lower Silurian glacial record is well known in South America (Grahn and Caputo, 1992; Díaz-Martínez and Grahn, 2007 and references therein), indicating Gondwana glaciers did not fully disappear following the Hirnantian ice-sheet recession. Before the Hirnantian, no unambiguous glacial record has yet been documented. However several authors suggested pre-Hirnantian ice-sheet developments based on palaeoecology (Spjeldnæs, 1961; Ainsaar et al., 2004), sedimentary petrology and palaeoceanography (Hamoumi, 1988; Lavoie, 1995; Pope and Read, 1998; Hamoumi, 1999; Pope and Steffen, 2003), eustatic fluctuations (Loi, 1993; Leone et al., 1995; Bourahrouh et al., 2004; Saltzman and Young, 2005; Achab and Paris, 2007) or isotopic grounds (Ainsaar et al., 1999; Kaljo et al., 2004; Saltzman and Young, 2005). According to some authors, Ordovician ice sheets may have been initiated as early as the base of Katian (e.g., Pope and Read, 1998).

Hirnantian glaciation-related deposits are well exposed in the Central Anti-Atlas, southern Morocco (Destombes, 1968a,b, 1981; Destombes et al., 1985; Hamoumi, 1988; Sutcliffe et al., 2001; Bourahrouh et al., 2004; Le Heron, 2007). Here, they rest on top of a relatively thick (>400 m), storm-dominated shelf succession (Ktaoua Group of Destombes, 1971; Destombes et al., 1985; Destombes, 2006, Sandbian to Katian). The aim of this paper is to investigate in term of sequence stratigraphy a record of a Late Ordovician high-resolution sedimentary section. The Bou Ingarf section was selected owing to its well constrained biostratigraphic framework (Bourahrouh et al., 2004). In strata ranging from the early Katian to the early Hirnantian, facies interpretation and sequence analysis are combined with a backstripping procedure in order to propose an eustatic sea-level curve, which we regard as essentially reflecting glacio-eustasy up to the Hirnantian glacial maximum. During the Hirnantian glacial event, ice fronts reached the study area and northern Morocco (Le Heron et al., 2007). The interference of glacio-isostasy and the deposition of continental, fluvio-glacial strata do not allow a sea-level curve to be confidently proposed for this period. However, glacial advances and recessions can be delineated. The main inferences of the work are then discussed, specially the opportunity for worldwide correlations of Late Ordovician regressive/transgressive events.

2. Geological setting

The Anti-Atlas fold belt in southern Morocco exposes a very thick (up to 10 km) Palaeozoic succession. Located on the northern edge of the Tindouf intracratonic Basin (Fig. 1), this domain was part of the wider, stable, North Gondwana cratonic platform (Boote et al., 1998; Burkhard et al., 2006; Michard et al., 2008 and references therein). This geotectonic setting persisted during the main part of the Lower Palaeozoic, until the Anti-Atlas was strongly involved in inversion tectonic (Fig. 2) in the Late Carboniferous and Permian (Piqué and Michard, 1989).

Both palaeomagnetic (Smith, 1997; Evans, 2003) and palaeoenvironmental (Destombes et al., 1985; Hamoumi, 1988; Ghienne et al., 2007a) evidences indicate for the Anti-Atlas subpolar palaeolatitudes, between 50° and 70° S, during the Upper Ordovician (Fig. 1B). From the Middle Cambrian to the Silurian, siliciclastic deposition prevailed with alternating fluvial, shallow-marine and open-marine shelf environments. As everywhere in the regularly subsiding north Gondwana domain (Fig. 2), depositional sequences were controlled mainly by eustasy, with minor influences of the tectonic events that affected the Gondwana margin located to some several hundreds of kilometres to the north or north-west (Destombes et al., 1985; Sharland et al., 2001; Haq and Al-Qahtani, 2005; Burkhard et al., 2006; Ghienne et al., 2007b). However, in the Upper Ordovician, a NW–SE trending depositional trough developed in the Central Anti-Atlas extending southeastward into the Ougarta Range (NW Algeria). This trough experienced enhanced axial subsidence and depositional conditions that were deeper relative to those of adjoining areas (Legrand, 1974; Destombes et al., 1985). It likely corresponds to the reactivation of Neoproterozoic Panafrican fault trends (Ennih and Liégeois, 2001; Coward and Ries, 2003; Burkhard et al., 2006).

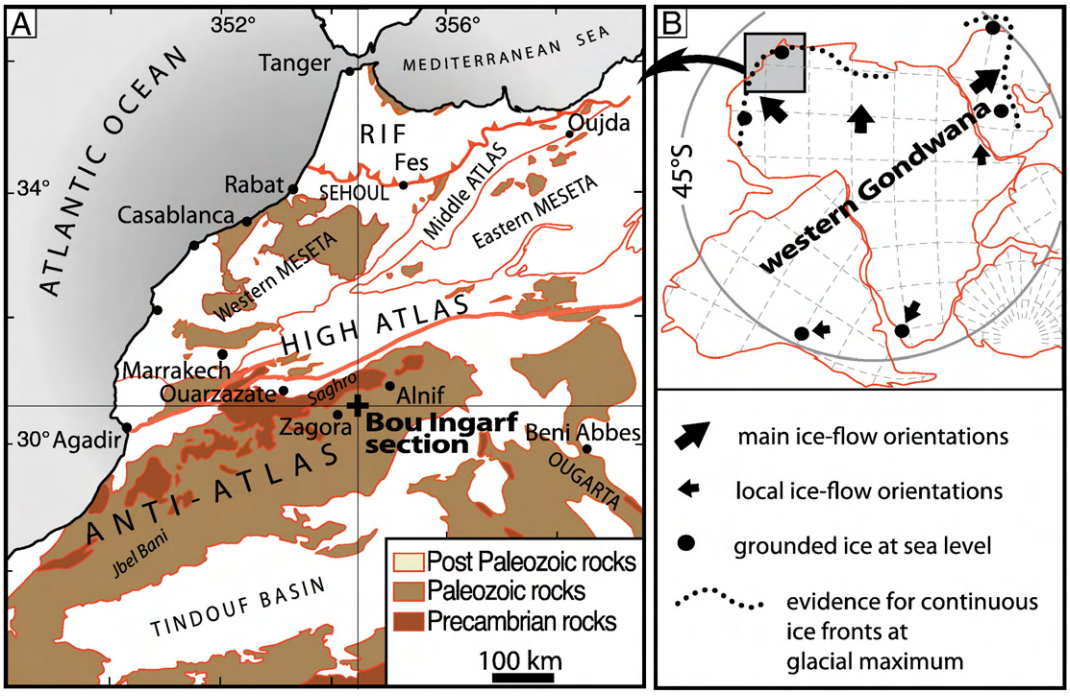

Fig. 1. (A) Location of the Bou Ingarf section, Anti-Atlas, southern Morocco (modified from Michard et al., 2008). (B) Palaeogeographic and palaeoglacial setting of the study area during the Hirnantian (modified from Ghienne et al., 2007a).

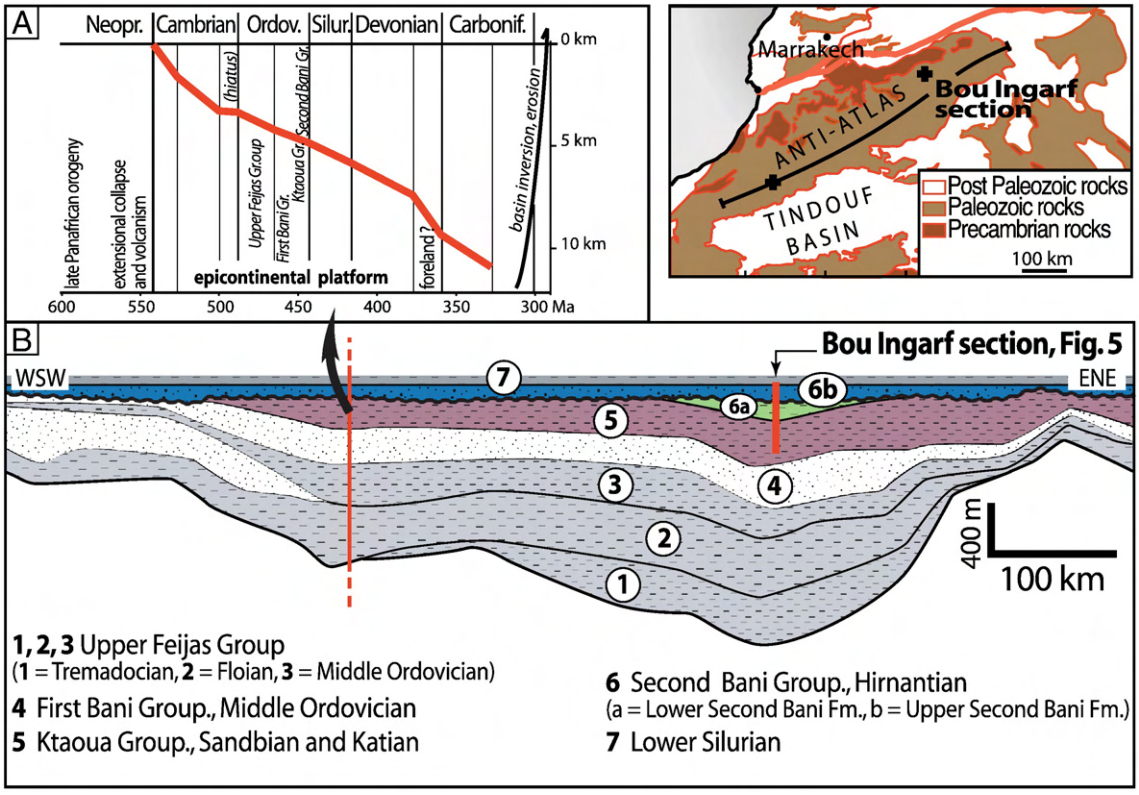

Fig. 2. Basin-scale stratigraphic setting. (A) Sediment accumulation curve without any corrections for the south-western Anti-Atlas, with indication of major tectonosedimentary events at the Gondwana margin (modified from Burkhard et al., 2006). At first order, constant accumulation rates are inferred from the Lower Ordovician to the Lower Devonian. (B) Geological cross-section showing thickness variations of Ordovician strata through the Anti-Atlas (location in map inset; modified from Destombes et al., 1985 and Michard et al., 2008).

The study area (Jbel Bou Ingarf, Figs. 1 and 3) is located between Zagora and Alnif, 100 km southeastward of Ouarzazate, in the most subsiding part of the Central Anti-Atlas trough (Fig. 2B). In this area, prior to the Hirnantian glacial event, exceptional accumulation rates in the 100–200 m/My range resulted in a very thick Late Ordovician succession characterised by continuous deposition and the absence or a poor development of erosional surfaces during lowstand events.

In the Central Anti-Atlas, the Middle–Late Ordovician lithostratigraphical scheme (Fig. 3) (Destombes, 1971, 1977, 1982, 1989; Destombes et al., 1985; Destombes, 2006) includes from base to top: (i) the latest Middle Ordovician to earliest Upper Ordovician First Bani Group (Guttierez-Marco et al., 2003); (ii) the Ktaoua Group, a shale-prone succession comprising the main part of the Upper Ordovician; (iii) the Hirnantian Second Bani Group, a sandstone-dominated succession (Figs. 3 and 4). Groups have been further subdivided into formations. The Ktaoua Group successively comprises the Sandbian to lower Katian Lower Ktaoua Fm., subdivided in three members (Assif bou Zeggarh, Middle Tiouririne and Amouguer Members), the middle Katian Upper Tiouririne Fm. and the upper Katian Upper Ktaoua Fm. Both the Lower and Upper Ktaoua formations are mostly composed of fine-grained, terrigenous facies including silty shales and subordinate sandstones and calcareous, phosphatic and/or ferruginous horizons that are most often highly fossiliferous. Conversely, storm-dominated sandstones and subordinate shales characterise the Upper Tiouririne Fm. The Second Bani Group is subdivided into two formations, the Lower and the Upper Second Bani Fms. It conformably overlies the Upper Ktaoua Fm. in the study area. The Lower Second Bani Fm. mainly comprises bioturbated sandstones while the Upper Second Bani Fm is dominated by fluvio-glacial medium to coarse-grained sandstones.

No stratigraphic hiatus was identified at the lower bounding surface of the Hirnantian Second Bani Group (Destombes, 1968a; Destombes et al., 1985; Bourahrouh et al., 2004) as confirmed by the lack of any erosional features at the outcrop scale. Only during the Hirnantian glacial maximum, when the Gondwana ice sheet reached northern Morocco (Rehamna inlier, Meseta, cf. Le Heron et al., 2007), did a glacial erosion surface develop within the Upper Second Bani Fm. Laterally, outside the Central Anti-Atlas trough, the lower bounding surface of the Second Bani Group corresponds to a glacially-related erosional unconformity (Destombes, 1968b; Destombes et al., 1985). In the latter areas, biostratigraphy identified the hiatus of the Upper Katian (Villas et al., 2006; Alvaro et al., 2007).

With the exception of the Upper Second Bani Fm., all these formations yield a rich macrofauna (Destombes et al., 1985) of trilobites (Destombes, 1966, 1972; Bruton, 2008), brachiopods (Havlicek, 1971; Guttierez-Marco et al., 2003; Villas et al., 2006), bivalves (Babin and Destombes, 1990) and echinoderms (Chauvel, 1966, 1977). The Hirnantia fauna was identified in the uppermost beds of the Upper Second Bani Fm. (Havlicek, 1971; Sutcliffe et al., 2001). In the study area, a diversified microfauna (acritarchs and chitinozoans) also is preserved (Elaouad-Debbaj, 1984, 1986, 1988; Bourahrouh et al., 2004 and unpublished data).

3. Methods of investigation

The Upper Ordovician succession is basically subdivided in two packages that have specific stratal stacking patterns. The lower package corresponds to a shelf succession (Ktaoua Group and lower part of the Lower Second Bani Fm.) and the upper package to a glaciation-related succession (Fig. 4). A sequence stratigraphic analysis was determined on the shelf succession. It is based on detailed logs (1:100 scale) performed on three adjacent sedimentary sections: the South Aït Ouazik section (lower Katian), the Bou Ingarf section (Katian to lower Hirnantian) and the Tizi Bou Ingarf section

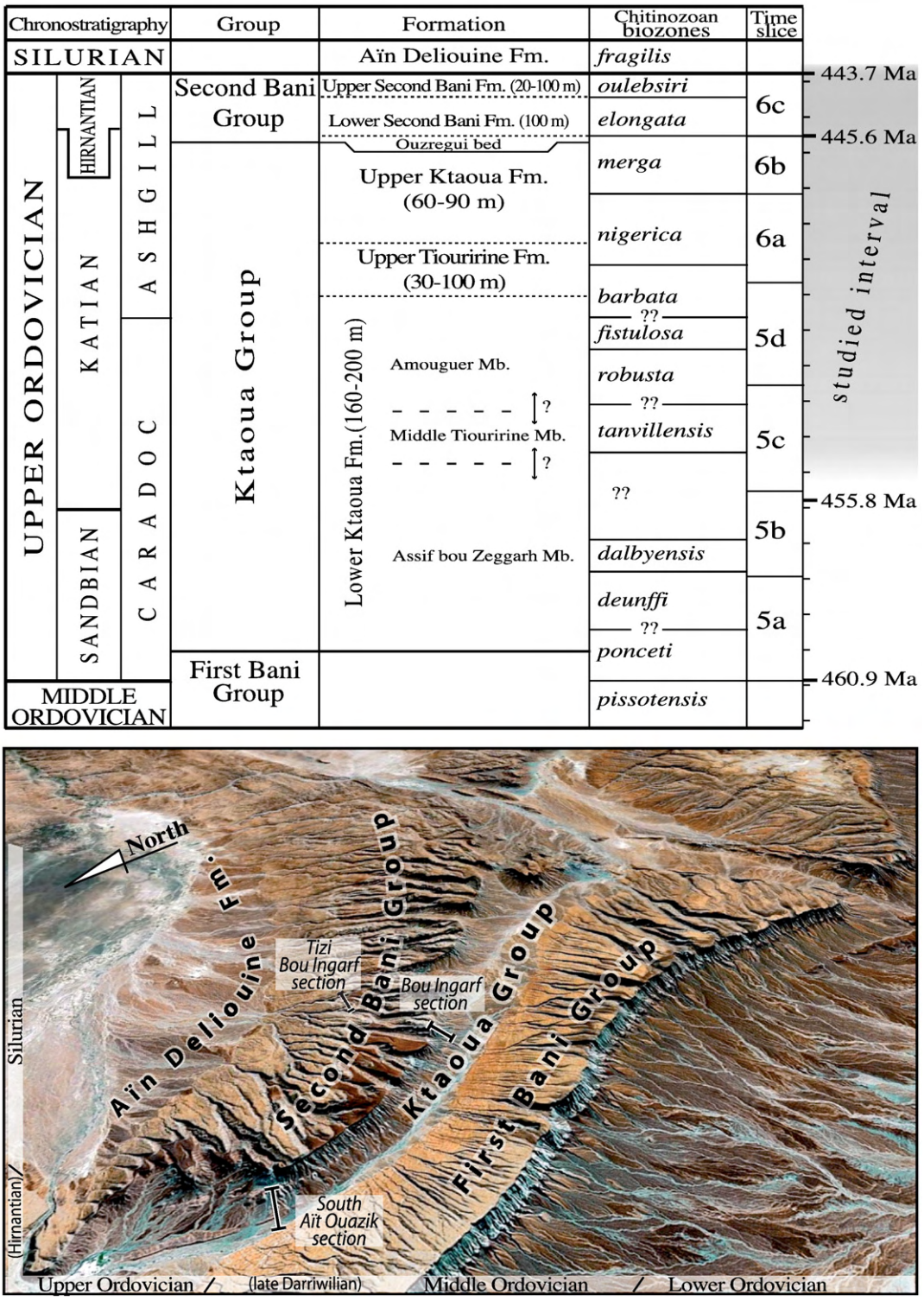

Fig. 3. Lithostratigraphic context of the studied interval compiled from Destombes et al. (1985), Paris (1990), Destombes (1977, 1982, 1989), Bourahrouh et al. (2004), Webby et al. (2004), Finney (2005), Chen et al. (2006) and Vandenbroucke et al. (2009). The base of *elongata* biozone is usually ascribed to the base of the Hirnantian but our study suggests the latter is slightly younger (cf. Fig. 5 and see Section 6.2. for a discussion). Main subdivisions and high-resolution logged sections used to produce the composite log in Fig. 5 are located on a 3D GoogleEarth view. View width in the foreground is ca. 20 km, in the background, ca. 45 km. Distance separating the Bou Ingarf and South Aït Ouazik sections is 7.5 km.

("middle" Hirnantian, up to the glacial erosion surface) (Fig. 3). A depositional model was established, based on facies analysis (composition, sedimentary structures, taphonomy). The sequence analysis is carried out following the integrated approach of genetic stratigraphy (Homewood et al., 1992, 1999). From the facies analysis and the interpretation of depositional environments, we can identify genetic units (*sensu* Homewood et al., 1992; Cross et al., 1993) and establish the stacking pattern of these units. Units of lower frequencies are defined after successive smoothings of the curve of genetic units.

The shelf succession is abruptly overlain by a sandstone-dominated glaciation-related succession corresponding to the upper Lower Second Bani and Upper Second Bani formations (Figs. 3 and 4). In contrast with the underlying shelf succession, the amalgamation of shallow-marine to fluvio-glacial sand bodies produced a more opaque

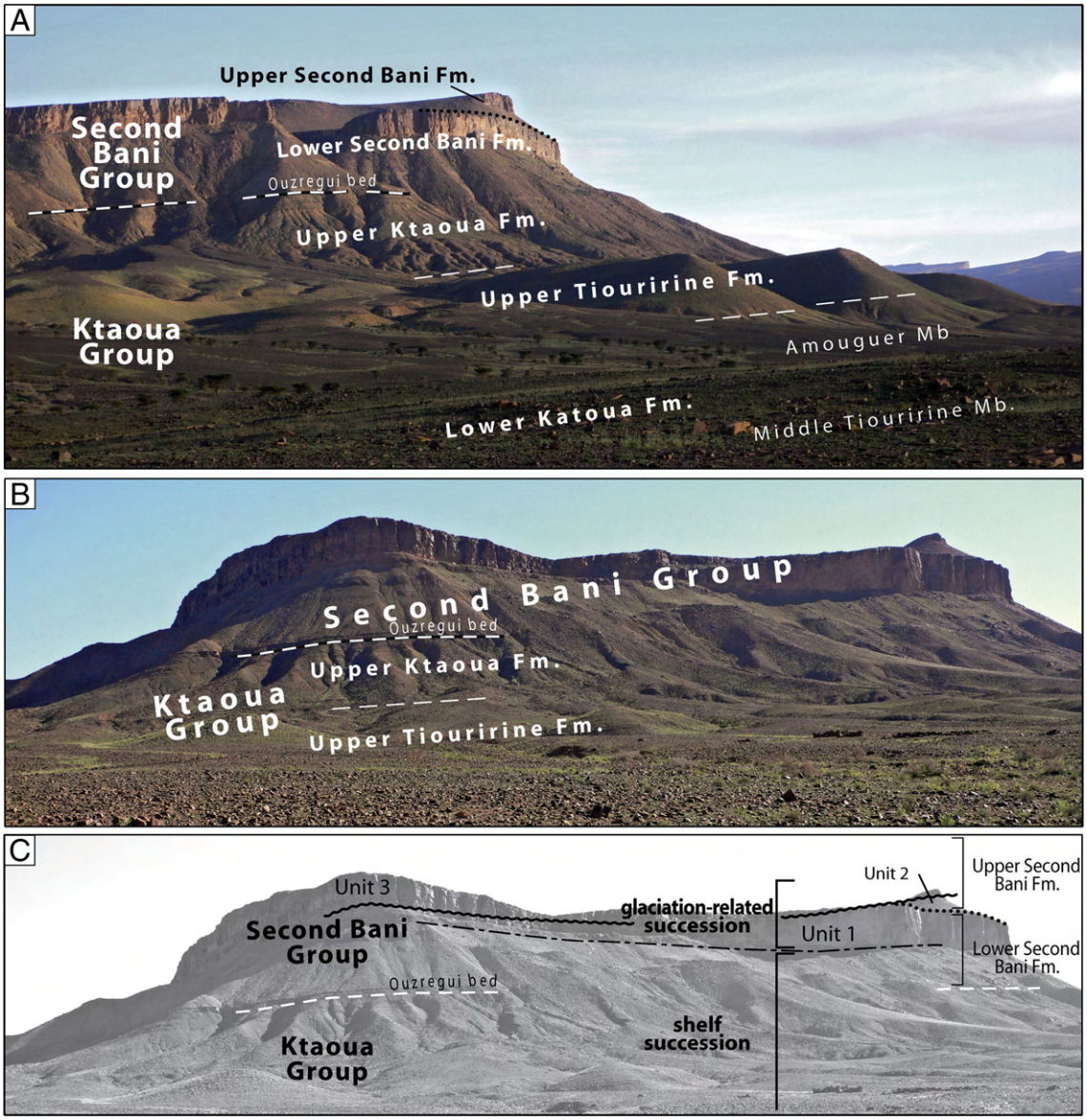

Fig. 4. General views of the sections (locations in Fig. 3). (A) South Aït Ouazik section with lithostratigraphic subdivisions according to Destombes et al. (1985) and Destombes (1977, 1982, 1989). (B) Bou Ingarf section with lithostratigraphic subdivisions according to Destombes et al. (1985). The boundary between the Ktaoua and Second Bani groups corresponds to a trilobite-rich condensed horizon (Ouzregui bed) and not to the sharp lithologic contact at the base of the above sandstones (cf. Fig. 5). (C) The same as in (B) with stratigraphic assemblages described in the text, including the shelf succession (upper part of Ktaoua Group and lower part of Second Bani Group, Cf. Figs. 3 and 5) and the overlying glaciation-related succession. The latter comprises four units (Cf. Figs. 9 and 12). A major erosional event occurred before Unit 3 deposition. Unit 4 is not shown. Codes for doted lines are given in Fig. 9.

stratigraphic record and previously established sedimentary tempos delineated in the underlying succession are no longer decipherable. In addition, severe intraformational erosion surfaces resulted in rapid lateral facies changes at the 100–500 m scale. Detailed geological mapping of a 5 km × 10 km area and a three-dimensional architectural analysis were then required in order to produce a synthetic profile.

A curve illustrating water-depth changes based on facies analysis is proposed (Fig. 5). A biostratigraphic framework (Bourahrouh et al., 2004) is established according to the chitinozoan biozones (Paris, 1990; Webby et al., 2004; Achab and Paris, 2007). The water-depth oscillations are then converted in a sea-level change using a backstripping algorithm considering a steady tectonic subsidence (see details in Section 6.4). This implies to establish a water-depth model. Two physical limits have been identified along the succession: the fair-weather wave base (FWWB), corresponding to the boundary between the shoreface and the upper offshore, and the storm wave base (SWB) corresponding to the boundary between the upper offshore (inner shelf zone) and the lower offshore (outer shelf zone) (e.g., Van Wagoner et al., 1990; Hampson and Storms, 2003). These boundaries related to the wave regime are controlled by numerous parameters (e.g., open/enclosed shelf, gradient, exposition to the winds, and storm energy), with a resulting great incertitude on their depth estimates. As sedimentary facies occurring in the studied succession suggest a high storm energy setting (shell beds, large-scale HCS), the fair-weather wave base and the storm wave base are estimated respectively to 30 m and 120 m, in agreement with both modern and ancient case studies (Hampson and Storms, 2003; Lasseur et al., 2009).

4. Shelf succession (Katian to lower part of Hirnantian)

Two types of facies are distinguished in the shelf succession: (i) the primary depositional shelf facies ("SH") that are associated with a substantial clastic input allowing almost continuous sediment

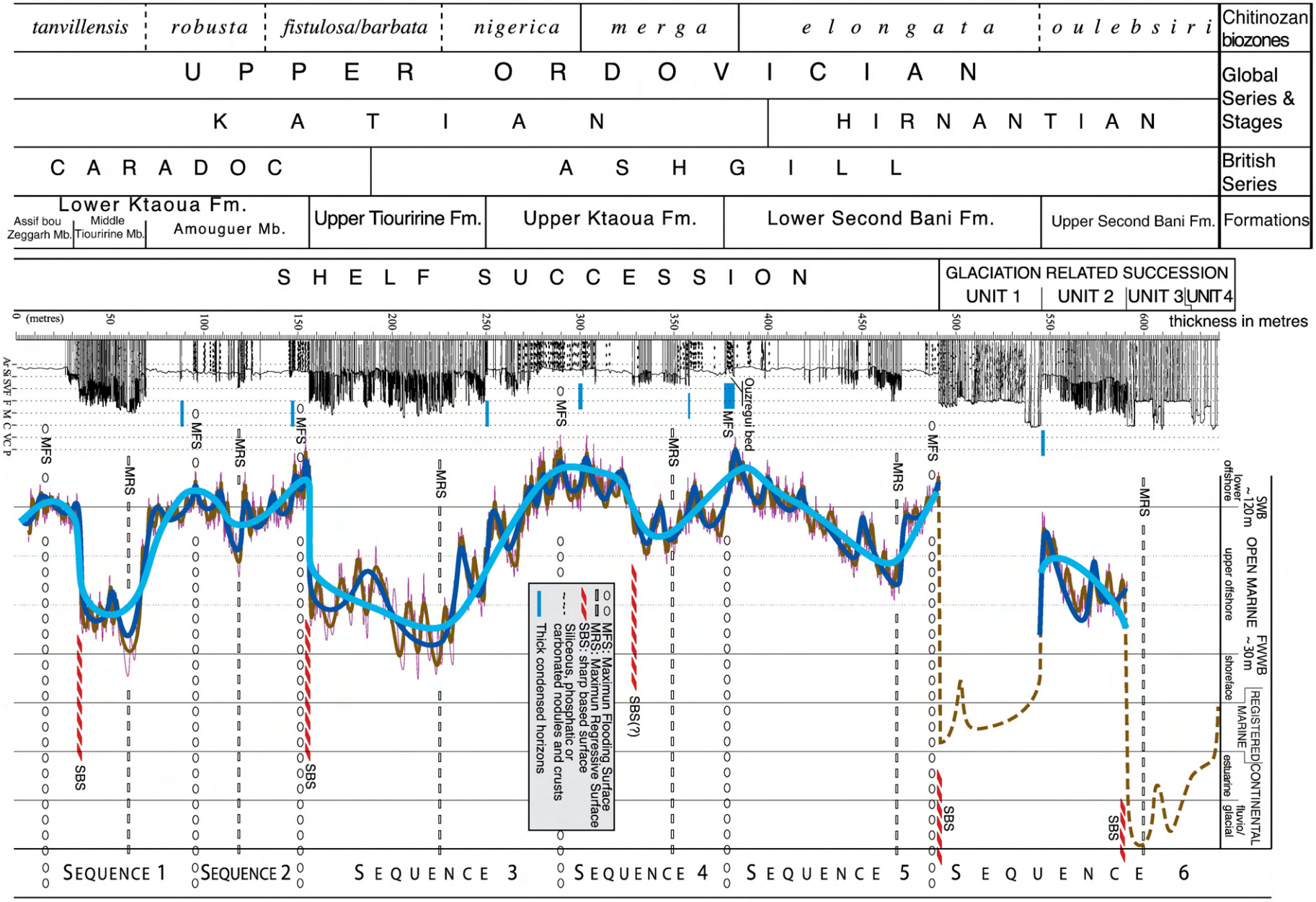

Fig. 5. The Bou Ingarf section compiled from three high-resolution sedimentary logs (locations in Fig. 3). Depositional environments are interpreted from facies analysis. Stratigraphic surfaces are based on a stacking pattern analysis (see text Section 4.3. and Fig.8 for details). Low-frequency sequences are bounded by maximum flooding surfaces (MFS). In such a one-dimensional representation, the internal architecture of Unit 3 cannot be evidenced (Cf. Fig. 12) and only its relative thickness is here relevant.

accumulation; (ii) the condensation facies ("SHc") that are associated with episodes of decreasing sediment supply. Their description is summarized in Table 1.

4.1. Primary depositional facies

4.1.1. Description

The SH/sm facies is a heterolithic facies (Fig. 6A) comprised of alternating fine- to medium-grained sandstone beds (5–30 cm thick) and clayey silty interbeds (up to several dm thick). The sandstone beds have hummocky cross stratification (HCS) with lateral (towards SE) and vertical accretion (Fig. 6B). The wavelengths of the HCS range from 1 m to several metres. The basal surfaces are planar or erosive with flute marks and pot marks. Cogenetic wave ripples rework some top surfaces. Bioturbation, mainly represented by *Planolites* and *Skolithos*, occurs occasionally.

The SH/ms facies is a heterolithic facies, which is composed of silty mudstones (Fig. 6C) containing coarse-grained silty laminae (1 to 3 cm thick) with intercalations of very fine-grained sandstone layers (several cm thick) and shell layers (1 mm to 1 cm thick). The sandstone intercalations have gently inclined lamination and HCS. The beds have a planar basal surface and a faintly wavy top surface. The shell layers are lenticular (<1 m of lateral extent). The bioclasts are scattered in a silty to fine- or medium-grained sandy matrix, parallel to the bedding plane and composed of a single coquina level. The taphonomic grade is homogeneous with a high degree of disarticulation and a moderate to high degree of fragmentation. Fossil taxa are always ecologically compatible with epibenthic suspension feeders (brachiopods, crinoids) and benthic trilobites with various feeding habits.

Finally, two clayey silty facies (SH/ml and SH/m) are composed of more or less dark silty mudstones containing lenticular shell layers (1 to several mm thick), similar to those of the SH/ms facies. The SH/ml facies (Fig. 6D) is characterised by the occurrence of silty laminae and the SH/m facies is devoid of any silty or sandy lamination.

4.1.2. Interpretation

Amongst the sedimentary structures observed in the primary depositional facies, the HCS, the cogenetic wave ripples and the silty laminae are related to storm wave action (Leckie and Walker, 1982; Aigner, 1985; Brenchley et al., 1986; Einsele, 1992; Dumas and Arnott, 2006). Their occurrence in the sedimentary record is primarily controlled by the position of the deposits along a shelf profile. According to facies models based on the sand/clay ratios and the sedimentary structures (Dott and Bourgeois, 1982; Aigner, 1985; Brenchley et al., 1986; Guillocheau and Hoffert, 1988; Johnson and Baldwin, 1996; Hampson and Storms, 2003), the above-described lithofacies range from the proximal (SH/sm), to the medial (SH/ms) and distal (SH/ml) parts of the upper offshore (Table 1).

The distribution and taphonomic grades of the coquina levels occurring in the SH/ms and SH/ml facies correspond to those of the type A-shellbeds described by Botquelen et al. (2004, 2006), which are related to storm wave accumulations on upper offshore environments. The SH/m facies that is devoid of any evidence of storm action, is interpreted as being deposited on the lower offshore.

4.2. Condensation facies

4.2.1. Description

The SHc/n facies is represented by siliceous (Si), phosphatic (P) or carbonated (Ca) nodules and crusts that underline bedding planes (Fig. 7A). The Si- and P-nodules have a rounded to more or less ovoid shape, with a size ranging from several mm to 5 cm. The P-nodules can be coalescent (Fig. 7B) forming crusts. The Ca-nodules are generally bigger (up to 20 cm) and some of them correspond to 1 m

Table 1
Description of the sedimentary facies and codes used in the text.

Facies codes	Lithologies and main sedimentary structures	Depositional environments
Shelf environments (SH)		
SH/sm	Alternations of fine- to medium-grained, 5–30 cm thick, sandstone beds with HCS and clayey silty beds; cogenetic waves ripples; *Planolites* and *Skolitos*.	Proximal part of a storm-dominated upper offshore
SH/ms	Laminated silty mudstones including discontinuous shell layers (mainly brachiopods) and very fine-grained sandy layers.	Medial part of a storm-dominated upper offshore
SH/ml	Dark, laminated silty mudstones; discontinuous shell layers (mainly brachiopods; absent in the glaciation-related succession).	Distal part of an upper offshore
SH/m	Dark silty mudstones devoid of any lamination.	Lower offshore
SHc/n	Nodules and crusts of siliceous (Si), phosphatic (P) or carbonated (Ca) compositions.	Condensed horizons (diagenetic processes) on upper and lower offshore
SHc/c	Amalgamated coquina levels (mainly brachiopods and trilobites), intercalated with thin terrigenous layers.	Condensed horizons (type B-shellbeds) on upper and lower offshore
Coastal environments (CO)		
CO/sb	Fine- to medium-grained muddy sandstone beds with pervasive bioturbation; some poorly bioturbated (*Skolitos*) sandstone beds.	Restricted marine environment
CO/sr	Medium-grained sandstone beds with 2D–3D current ripples; occasional wave ripples; megaripples with flaser bedding at bottomsets; *Planolites* and *Skolitos*.	Tidal-flat environment with sand bars
CO/s	Medium- to coarse-grained sandstone beds with gently inclined lamination; parting lineation, SCS and 3D-megaripples; current and wave ripples.	Barrier in a shoreface environment
CO/sm	Alternations of fine- to medium-grained sandstone beds and silty to very fine-grained sandstone beds; occasional HCS beds and bioturbation.	Open marine tidal flats to tide-dominated delta environments
Fluvio-glacial environments (FU)		
FU/sgm	Medium- to coarse-grained, lenticular sandstone beds (cut-and-fill structures); conglomeratic beds, some graded; rare mudstone interbeds; intraformational shear deformation structures.	Undifferentiated glacio-fluvial, at least in part subglacial
FU/sh	Medium-grained sheet-bedded sandstones with horizontal lamination, subordinate cross-lamination, climbing ripples, flutes.	Flood-dominated, proglacial, sheetflows
FU/sch	Medium-grained, amalgamated sandstone beds with horizontal to cross-lamination; sheet-like bodies or channel-levees assemblages.	Proglacial channel belt
FU/sx	Medium to coarse-grained, cross-stratified sandstone beds; lateral accretion surfaces; ripples; ice-crystal marks.	Meander bar complexes (possibly estuarine)

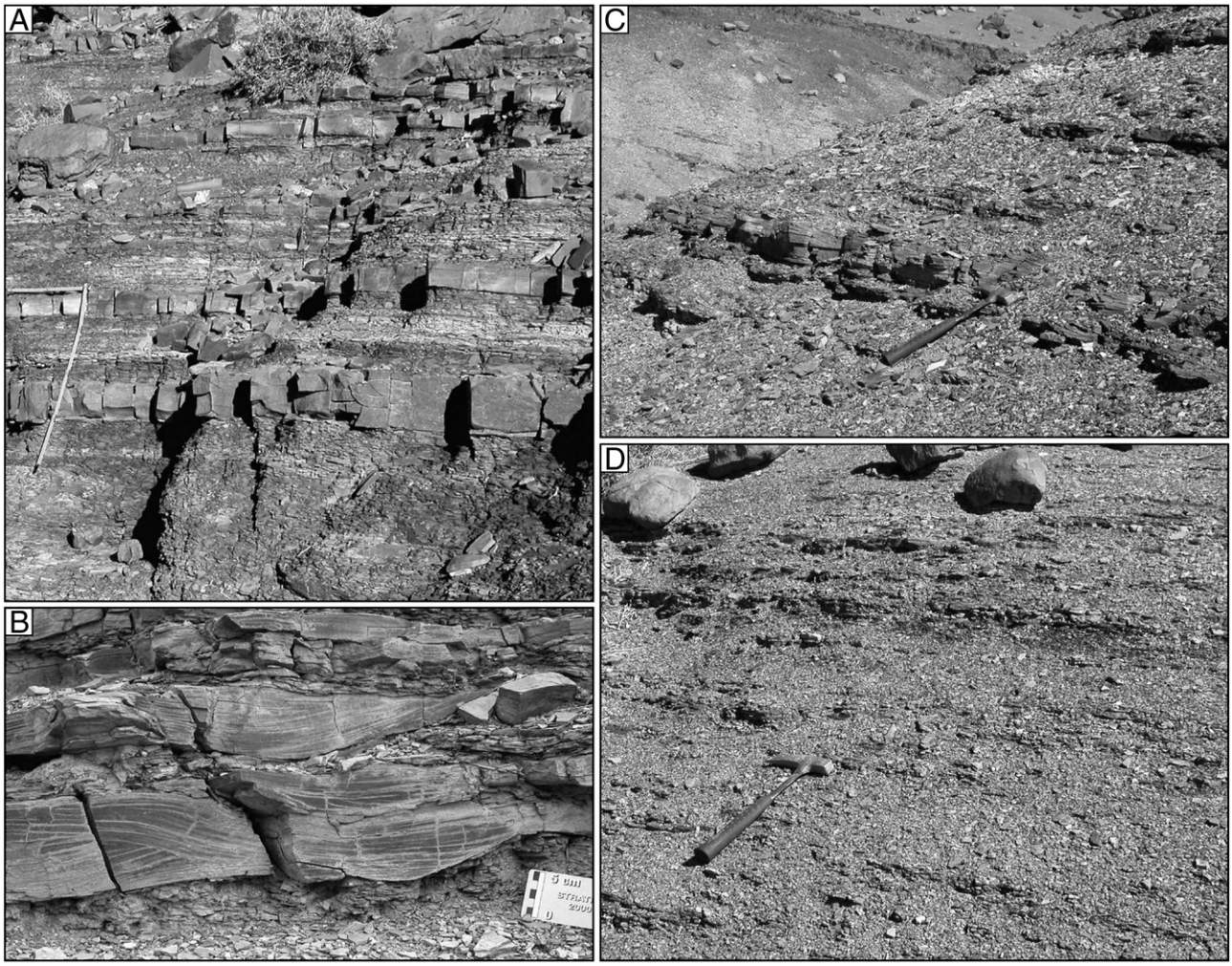

Fig. 6. Primary depositional facies of the shelf succession. (A) Alternations of sandstone beds with HCS and clayey silty interbeds (SH/sm), Upper Tiouririne Fm. (B) HCS in lateral and vertical acretion of the SH/sm facies, Upper Tiouririne Fm. (C) Intercalation of sandstone beds with HCS in the SH/ms facies, Upper Ktaoua Fm. (D) Silty laminae in the SH/ml facies, Upper Ktaoua Fm.

thick concretions that extend several metres laterally. The nodules and crusts are sometimes associated with shell accumulations. The SHc/n facies occurs within the SH/ms, SH/ml and SH/m primary depositional facies.

The SHc/c facies forms one to several centimetre thick shellbeds that are made up of superimposed individual coquina levels intercalated with thin terrigenous layers. Shells (brachiopods, bivalves, crinoids, cystoids, trilobites, and gastropods) are contained in a silty to sandy matrix (Fig. 7D) and are often densely packed with relative abundance of shells in section of 15 to 55% (volume shells). The shells are generally randomly oriented. The taphonomic grade is heterogeneous with variable degree of disarticulation and fragmentation. Bioturbation is pervasive and bioerosion is observed in some cases, mainly in the form of perforations. This facies can include P-, Si- and Ca-nodules and/or crusts. The SHc/c facies is present in all the primary depositional facies.

The association of SHc/n and SHc/c facies can form thick (up to 6 m) horizons (Fig. 7C) including terrigenous intercalations and subordinate Fe-oolitic horizons. In distal facies, one of them (here named "Ouzregui bed") located at the transition between Ktaoua and 2nd Bani Groups (Fig. 4), yield trilobites, gastropods, cephalopods, crinoids and rare bivalves. Among trilobites, exoskeletons are mostly articulated, or disarticulated but unbroken. In details, these taxa are not distributed in the overall interval, constituting different autochtonous associations (environmentally condensed assemblages, *sensu* Kidwell, 1998). These horizons that have a very large lateral extent (>10 km) correspond to marker beds at a regional scale.

4.2.2. Interpretation

Si-, P- and Ca-nodules are common in sedimentary successions and their formation is related to episodes of decreasing sediment supply (Loi et al., 1999; Loi and Dabard, 2002; Marshall-Neill and Ruffell, 2004; Bréhéret et al., 2004; Pope, 2004; Dabard et al., 2007). Such episodes lead to a relative stability of the sediment/water interface and a weak vertical migration of diagenetic fronts. Chemical reactions leading to the formation of various types of concretions can thus be observed. The shellbeds of the SHc/c facies have characteristics similar to those of type B-shellbeds described by Botquelen et al. (2004, 2006). They are interpreted as the amalgamation of several storm coquina layers in a context of low terrigenous inputs.

In terrigenous shelf environments, decreasing sediment supply is typically linked to episodes of sea-level rise. Coeval enhanced sediment storage in the coastal environments results in relative starvation in deeper segments of the shelf ("sediment volume partitioning", e.g., Cross and Lessenger, 1998). By comparison with similar, storm-dominated, North Gondwana platform successions (e.g., Loi and Dabard, 2002; Botquelen et al., 2004, 2006; Dabard et al., 2007), the SHc/n and SHc/c facies are interpreted as related to retrogradation phases of very high-, or high-frequency eustatic cycles. Thick condensed intervals resulting from the association of amalgamated SHc/n and SHc/c facies

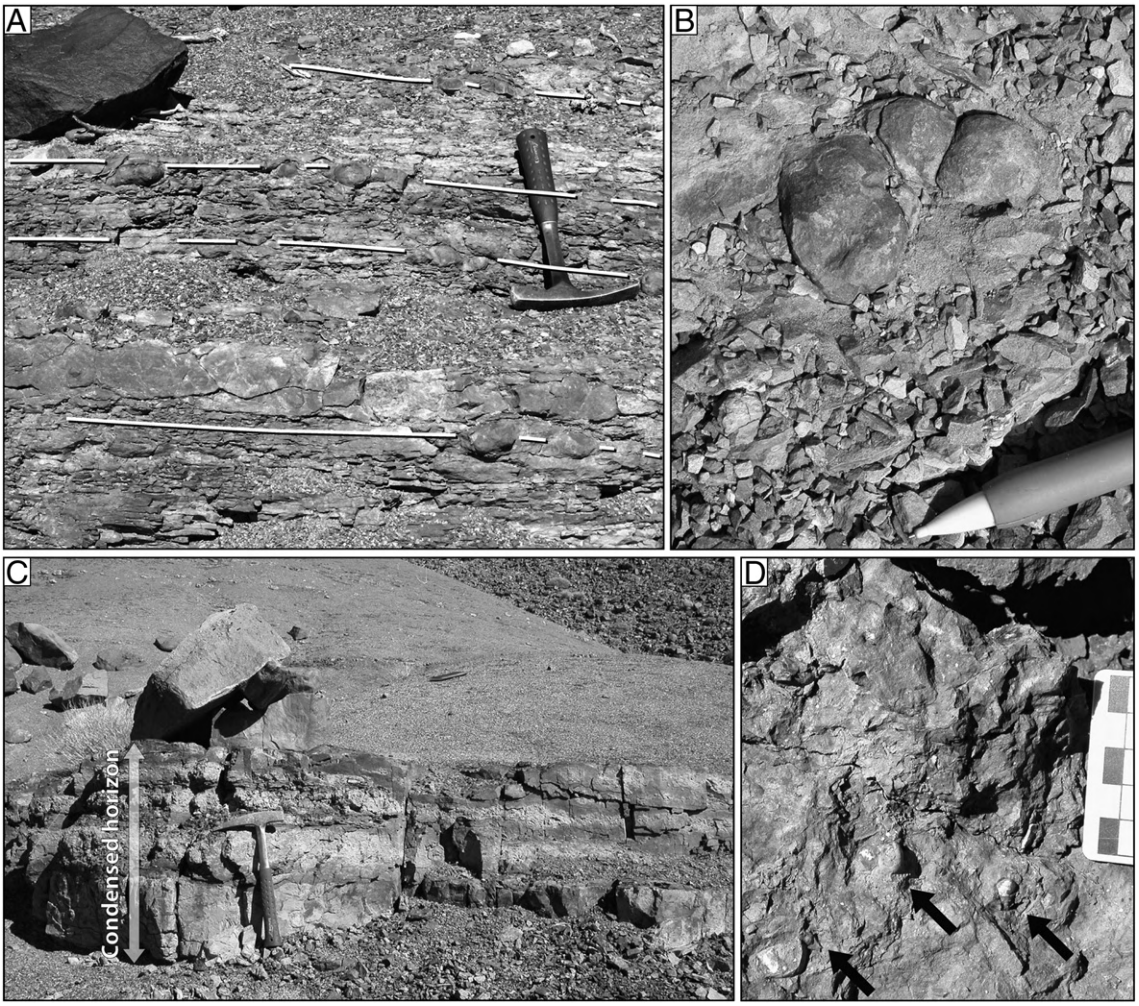

Fig. 7. Condensation facies at the base of the Upper Ktaoua Fm. (A) P-nodules aligned parallel to the bedding plane (white lines) in the SHc/n facies. (B) coalescent P-nodules (bedding plane view) in the SHc/n facies. (C) condensed horizon comprised of amalgamed beds of SHc/n (in white) and SHc/c (in grey) facies. (D) Details of SHc/c facies with trilobites (arrows).

document significant retrogradation phases related to lower-frequency cycles.

4.3. Sequence analysis

The sedimentary record results from the superposition of several orders of variations of relative sea level that are expressed by genetic units (stacking pattern). We repeatedly recognized a regular superposition of three orders of genetic units at high- to very high-frequencies. We advocate that such a striking organization reflects the relationships between the genetic units superposition and the Milankovitch orbital parameters (Guillocheau, 1991; Strasser et al., 1999; Loi and Dabard, 2002; Hillgärtner and Strasser, 2003; Dabard et al., 2007).

Based on high-resolution facies analysis, we identify very high-frequency (VHF) sequences (pink curve in Fig. 5). In heterolithic facies suites (SH/sm, SH/ms), they form one to several metres thick asymmetrical motifs (Fig. 8A). The progradation phase is expressed by relatively thick, coarsening-up and thickening-up strata reflecting a gradual, essentially shallowing-upward evolution of depositional areas. The beginning of the retrogradation phase is highlighted by various features: (i) the amalgamation of sedimentary structures (e.g., HCS amalgamation); (ii) the increase of bioturbation; (iii) the occurrence of condensation facies (i.e. SHc/n and SHc/c facies). The facies suites then reflect a rapid deepening-upward evolution as shown by the occurrence of overlying facies implying more distal environments. The sedimentary record during periods of shoreline progradation (highstand and sea-level fall) is thicker than during periods of shoreline retrogradation. This distortion basically reflects the sediment volume partitioning that occurs during an eustatic cycle (Cross, 1988; Guillocheau, 1991; Cross and Lessenger, 1998).

The relative homogeneity of fine-grained SH/ml and SH/m facies complicates the deciphering of the genetic units. However, they can be extrapolated from the sedimentary record considering the occurrence of the SHc/n or SHc/c condensation facies and the relative abundance of the silty laminae. In these facies suites, genetic units are several decimetres to 2–3 m thick. The progradation phase is expressed by an increase of the number of silty laminae (SH/ml facies) while the occurrence of nodules and/or crust and coquina beds characterise the retrogradation phase.

Lower frequencies sequences are identified from the smoothing of the genetic units curve (brown and dark blue curves in Fig. 5). High-frequency (HF) sequences (Fig. 8B) are one to several tens of metres thick. They are characterised by a larger environmental transition

Fig. 8. (A) Very high-frequency sequence in heterolithic SH/ms facies, Upper Tiouririne Fm. (B) High-frequency sequences (decametric thickness), Upper Tiouririne Fm. (C) Third-order sequence in the upper and lower offshore environments, Upper Ktaoua Fm. (D) Stacking pattern of genetic units and superposition of very high (VHF), high (HF′ and HF) and low (LF) frequencies sequences, Tiouririne Fm.

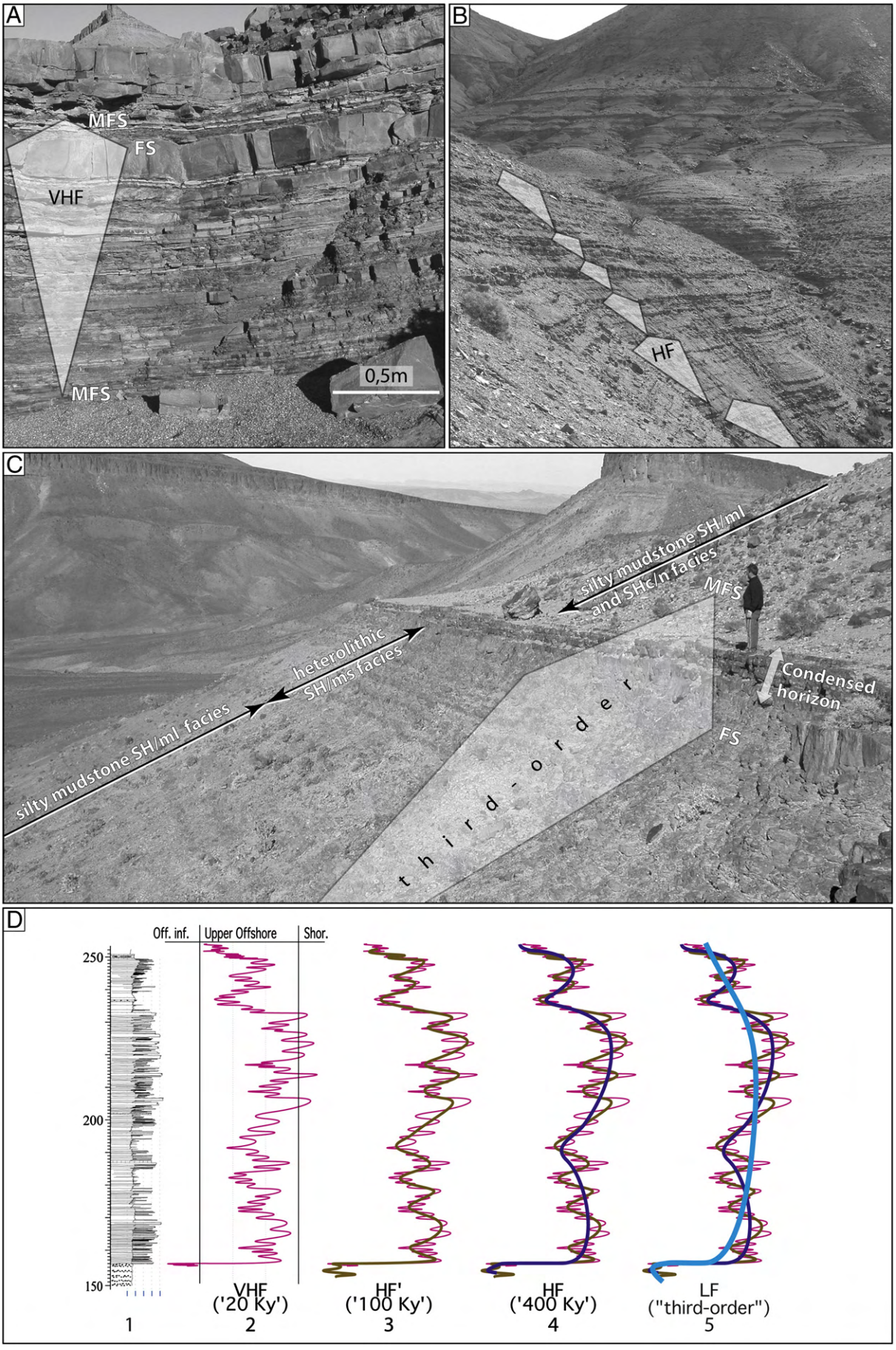
A
MFS
FS
VHF
MFS
0,5m
B
HF
C
silty mudstone SH/ml
and SHc/n facies
MFS
heterolithic
SH/ms facies
silty mudstone SH/ml facies
third-order
Condensed
horizon
FS
D
Off. inf.
Upper Offshore
Shor.
250
200
150
VHF
('20 Ky')
HF'
('100 Ky')
HF
('400 Ky')
LF
("third-order")
1
2
3
4
5

between deposits (Fig. 8B: from the proximal part of the upper offshore toward the lower offshore). Due to stratigraphic distorsion, the thickness of a VHF sequence is governed by the place it occupies within the HF signal (Guillocheau, 1991; Loi and Dabard, 2002). Then, in the retrogradation phase of HF sequences, the VHF sequences are generally thinner and the condensation beds are situated in close vertical proximity (see Dabard et al. (2007) for an another detailed case study).

Finally, lower-frequency sequences ("third-order") are extrapolated (Fig. 8C). In the latter sequences, the retrogradation phase is typically characterised by the stacking of VHF or HF genetic sequences containing condensed SHc/c and SHc/n facies or by regional-wide condensed horizons (Fig. 8C).

The successive steps used for sequence analysis are illustrated for a heterolithic facies suite in the Upper Tiouririne Formation (Fig. 8D; 150 to 250 m in the section, Fig. 5). A first smoothing of the VHF curve (curve 2 in Fig. 8D) gives evidence of HF′ cycles containing 4–5 VHF sequences (curve 3). Then, the smoothing of this curve produces in turn longer HF cycles (curve 4), each of them including about 3–4 HF′ sequences. These HF cycles correspond to the most conspicuous stratigraphic cycles throughout the shelf succession (dark blue curve in Figs. 5 and 8D). They are the reference for the time calibration (cf. Section 6). At last, a curve corresponding to low-frequency "third-order" cycles is performed (curve 5 in Fig. 8D, pale blue curve in Fig. 5).

5. Glaciation-related succession (upper part of Hirnantian)

The glaciation-related succession is subdivided into four units (Figs. 4 and 5) that essentially comprise specific facies suites (i.e. coastal "CO" and fluvial "FU" facies) distinct from those of the underlying shelf succession. Firstly, architecture and bounding surfaces are described. Secondly, additional facies not yet illustrated from the shelf succession (Section 4) are described and interpreted (Table 1). Finally, an outline of the Hirnantian glacial record in the Bou Ingarf area is proposed.

5.1. Architecture and bounding surfaces

The Unit 1 (upper part of the Lower Second Bani Fm., cf. Fig. 4C) constitutes a prominent, sharp-based, 40–50 m thick sandstone sheet of regional extent (Fig. 9). It rests sharply above fine-grained facies of the shelf succession (Figs. 9, 10A and E) without any apparent erosional contact. The upper bounding surface is placed at the top of a thick condensed horizon. In case of severe subsequent glacial erosion (cf. Unit 3), the main part of Unit 1 is missing (Fig. 9). Unit 1 comprises successively CO/sb, CO/sr and CO/s facies.

Unit 2 (lower part of the Upper Second Bani Fm.) constitutes a subdued fine-grained succession encased between Units 1 and 3. The erosion at base of Unit 3 largely altered its initial sheet-like geometry. The maximum residual thickness is 40 m but sometimes Unit 2 deposits are missing (Fig. 9). Unit 2 essentially comprises a coarsening-upward succession (SH/ml and CO/sm).

Unit 3 (middle part of the Upper Second Bani Fm) is erosion-based and its thickness shows great lateral variations ranging from few tens of metres (10–25 m) where basal erosion is minimal, up to 100 m where basal erosion is maximal (i.e. complete erosion of Unit 2 and part of Unit 1, Figs. 9 and 11E). In addition, Unit 3 contains internal erosion surfaces. Geological mapping indicates that individual erosion surfaces define channelled incisions corresponding to valleys that are several tens of metres deep and several hundreds of metres wide valleys. Three successively amalgamated valley systems have been distinguished within Unit 3 with NW–SE or NNE–SSW orientations. Erosional contacts are associated with conglomeratic facies (FU/sgm) and with deformation structures (large-scale folds affecting underlying deposits, intraformational striations or grooves, glacial lineations or other undifferentiated shear deformation structures). The bulk of palaeovalley infills are comprised of FU/sh and amalgamated FU/sch facies. The upper bounding surface of Unit 3 shows residual depositional palaeotopographies (channel-levees systems) filled in and sealed by Unit 4 sandstones.

Unit 4 (upper part of the Upper Second Bani Group) forms a sandstone sheet of regional extent. Its base is usually erosional, however, in places Unit 4 draped residual topographies at the top of Unit 3 (Fig. 9B), especially those corresponding to channel-levees highs and inter-channel, low-lying areas. Its upper bounding surface is a thick condensed horizon that covers the whole of the glaciation-related succession beneath the overlying Silurian strata (Fig. 12A). In its lower part, Unit 4 comprises the FU/sx facies and, in its upper part, the CO/s facies.

5.2. Coastal (CO) depositional facies

5.2.1. Description

The CO/sb facies (Fig. 10B) consists of 5–50 cm thick, fine- to medium-grained muddy sandstone beds with mm-scale silty interbeds. Pervasive bioturbation results in uneven bed surfaces and poorly developed to diffuse bedding. Several metres thick facies sequences produce a better expressed bedding pattern.

The CO/sr facies (Fig. 10C) is made up of one to several decimetres thick, medium-grained sandstone strata, including non-destructive bioturbation (*Skolithos* and *Planolites*), several mm-thick silty interbeds, current ripples and occasional wave ripples. Related successions include 10–50 cm thick, lenticular cross-stratified bedsets with poorly organised palaeocurrent trends (NW, SW, SE, and E). They have clay chips along foresets and flaser bedding occur at bottomsets. Several metres thick facies sequences are locally produced by variations in bed thicknesses.

The CO/s facies (Fig. 10F and G) comprise medium- to coarse-grained, amalgamated, thick sandstone beds including gently inclined lamination with parting lineations, swaley cross stratification (SCS) and lunate megaripples migrating to the NW. Clay chips are rare, silty interbeds absent. Strata comprising this facies are usually directly overlain by a nodular condensed horizon (SHc/n).

The CO/sm facies (Fig. 10D) comprises a dm-thick alternation of fine- to medium-grained sandstone beds, commonly pervasively bioturbated, and mica-rich silty to very-fine-grained interbeds. Non-bioturbated sandy beds with sharp base and top are characterised by HCS lamination.

5.2.2. Interpretation

The CO/sb, CO/sr and CO/s facies are superimposed in the Unit 1. The intense bioturbation observed in the CO/sb facies suggests regular sandy inputs forming thin depositional units in low-energy, restricted-marine environments. A notably higher-energy depositional environment is reflected by sedimentary structures observed in the CO/sr facies. The sheet-like geometries, ubiquitous current ripples but subordinate wave ripple, trails and burrows designate shallow-marine sand flats. Megaripples with mud chips represent tidal sand bars (e.g., Fenies and Tastet, 1998; Dalrymple and Choi, 2007). The coarser granulometry and the virtual absence of bioturbation indicate that the CO/s facies was developed in high-energy depositional environment. Parting lineation reflecting upper stage plane beds, SCS produced by the amalgamation of storm beds (Dumas and Arnott, 2006), and other cross-stratified bed sets indicate upper shoreface environments.

The CO/sm facies constitutes the upper part of Unit 2. HCS beds may represent storm deposits from the lower shoreface. However, the profusion of mica particles suggesting an active fluvial input through plume fallout processes and the dominance of bioturbated horizons similar to those observed in restricted-marine environments (CO/sb) suggest either a wave-influenced, open-coast tidal flat (e.g., Yang et al., 2005) or a tidal-dominated delta setting.

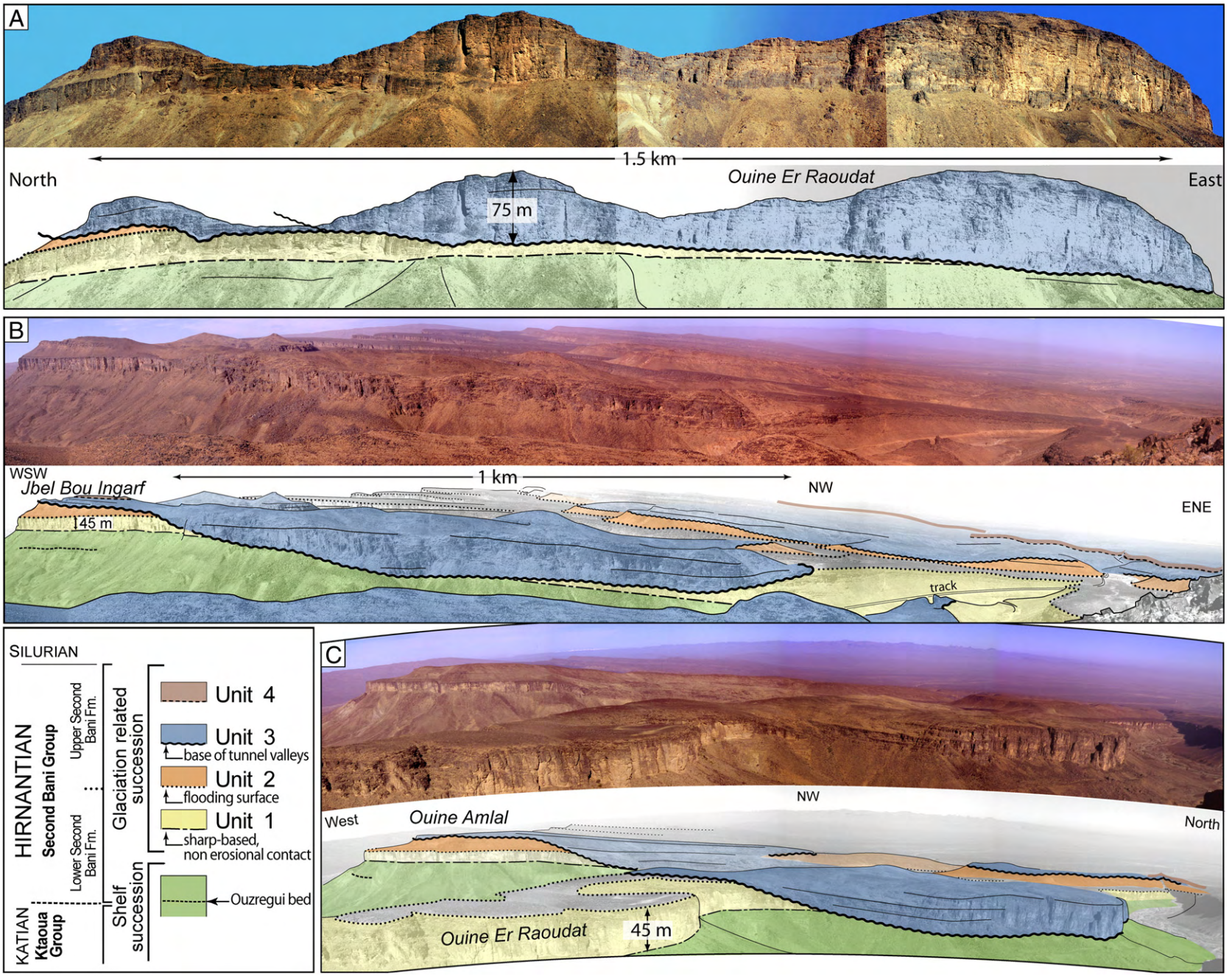

Fig. 9. Panoramic views in the Bou Ingarf area illustrating the stratigraphic architecture of the glaciation-related succession that essentially comprises a sheet-like Unit 1, a severely eroded Unit 2 and a channelled Unit 3. Unit 4 is poorly recorded here.

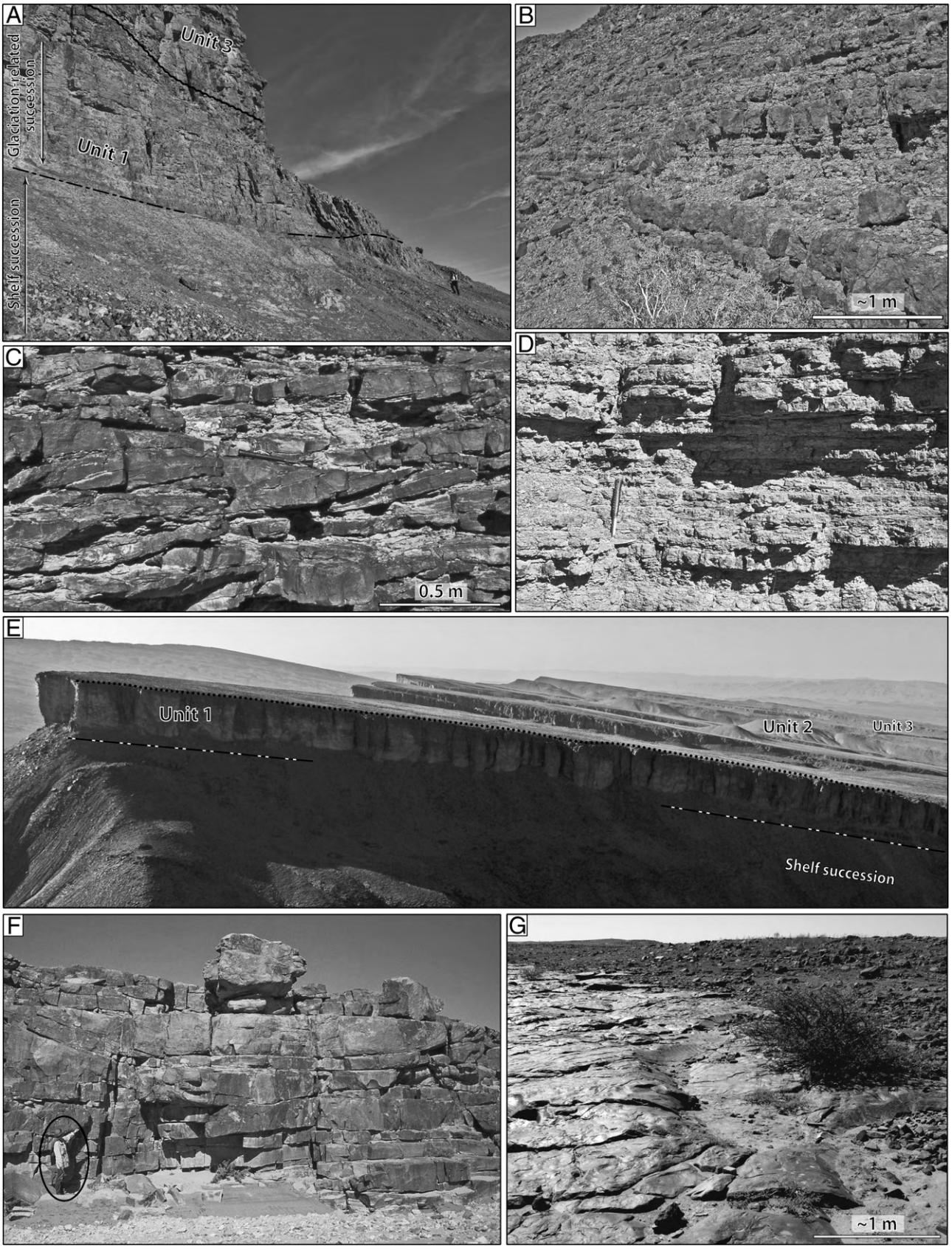

Fig. 10. Coastal facies and related stratigraphic surfaces of the glaciation-related succession (Units 1, 2 and 4). (A) The sharp-based contact between the shelf succession (SH/ms) and the glaciation-related succession (Unit 1, CO/sb) (persons for scale). (B) Pervasively bioturbated muddy sandstone beds (CO/sb, base of Unit 1; restricted-marine environments). (C) Cross-stratified sandstones beds (CO/sr, medial part of Unit 1; megaripples and flasers from tidal-flat environments). (D) thinly bedded, moderately bioturbated sandstones (CO/sm, upper part of Unit 2; tide-influenced sand-flats or delta setting). (E) The flooding surface at top of Unit 1 of the glaciation-related succession. It marks a major, intra-Hirnantian, transgressive event (Unit 1 thickness: ~45 m; see also Fig. 9). (F) Thick-bedded, cross-stratified sandstones (CO/s, upper part of Unit 4; barrier deposits in shoreface environments; person for scale). (G) preserved morphologies of megaripples with superimposed ripples in troughs (CO/s, top of Unit 4; shoreface environments).

5.3. Glacio-fluvial to estuarine (FU) depositional facies

5.3.1. Description

The FU/sgm facies (Fig. 11A, B and C) is restricted to the lower horizons of palaeovalley infills. It exhibits a rather chaotic stratification resulting from the amalgamation of cut-and-fill structures. Flute casts are abundant and intraformational deformation occurs as shear structures such as folds and striated surfaces. Individual strata comprise cross-stratified to graded sandstone beds. Matrix-supported conglomerate facies including intraclasts frequently occur within

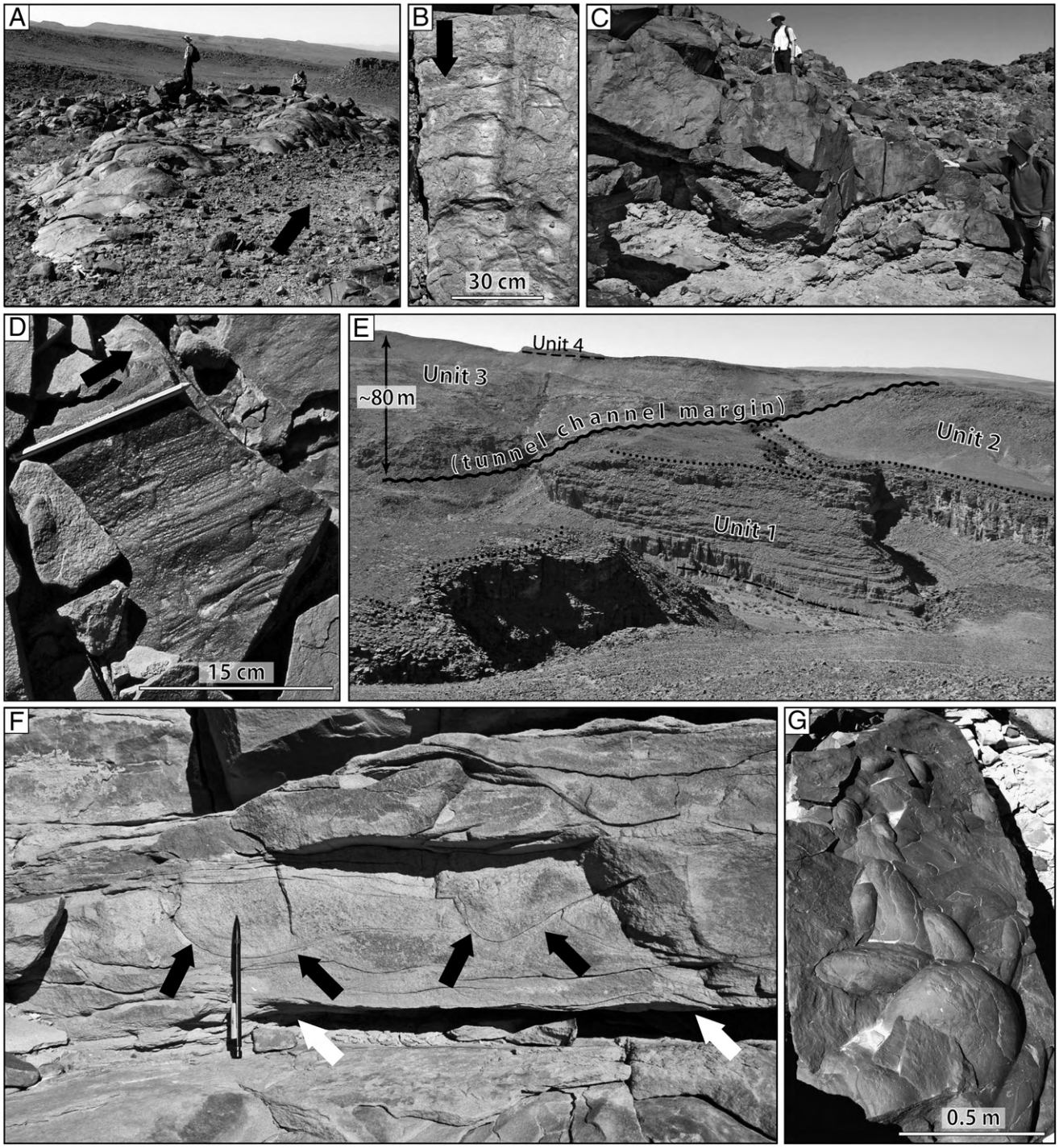

Fig. 11. Glacial deformation structures, fluvio-glacial facies and related sedimentary architecture (Unit 3). (A) A decametre-scale subglacial lineation within Unit 3, affecting FU/sgm facies and underlining an internal glacial erosion surface (person for scale; inferred ice flow indicating by the black arrow). (B) An irregular subglacial groove in FU/sgm facies (base of Unit 3; inferred ice flow indicating by the black arrow). (C) Cut-and-fill structures including conglomerate lenses (FU/sgm, Unit 3). (D) Intraformational striations (within FU/sh facies) indicating a subglacial, soft-sediment shear zone (inferred ice flow indicating by the black arrow). (E) Palaeovalley margin (tunnel valley; infill essentially with FU/sh flood-dominated fluvial deposits) truncating Units 2 and 1. (F, view in section) and (G, up-side-down) Scour marks within tabular sandstone beds indicate the higher-energy conditions did not occur at bed base (even surface, white arrows) but within it (black arrows); it suggests the lower part of the sandstone bed records waxing flow conditions (FU/sh; proglacial, flood-dominated fluvial environments). (H) stoss-erosional climbing ripples (FU/sh; Unit 3, flood-dominated fluvial deposits). (I) A 150 m wide channel-levee assemblage in the upper part of Unit 3 (FU/sch; proglacial channel belt). The overlying Unit 4 (essentially, FU/sx) thins above the channel-levee and thickens laterally (absence of erosional hiatus). (J) Large-scale lateral accretion surfaces in the lower part of Unit 4 (FU/sx; deposition in a possibly estuarine meandering channel belt). The overlying Co/s shoreface deposits are directly overlain by the Lower Silurian shales (geomorphic depression in the background). (K) Ice-crystal marks (FU/sx, Unit 4; estuarine environment).

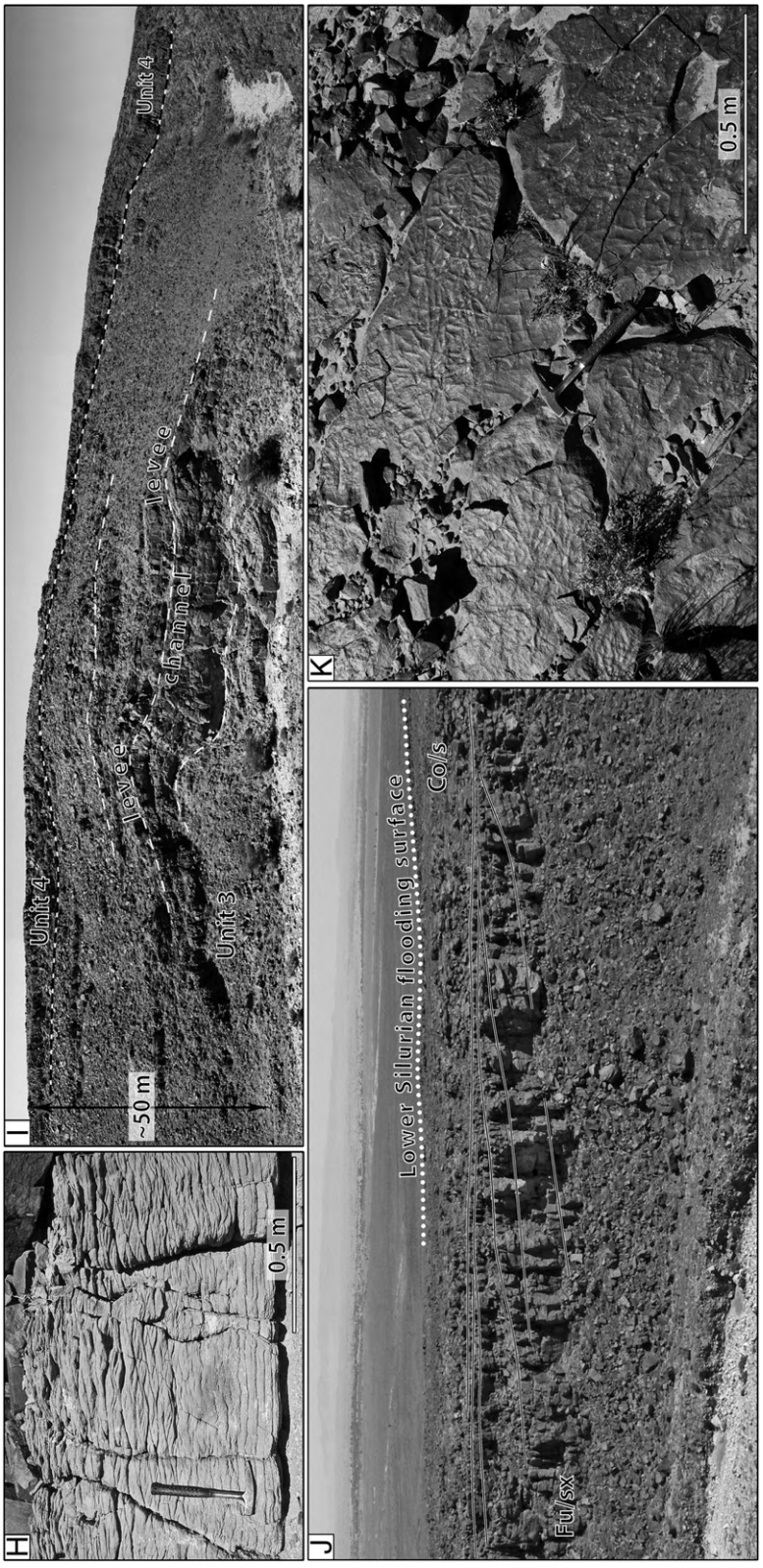

Fig. 11 (*continued*).

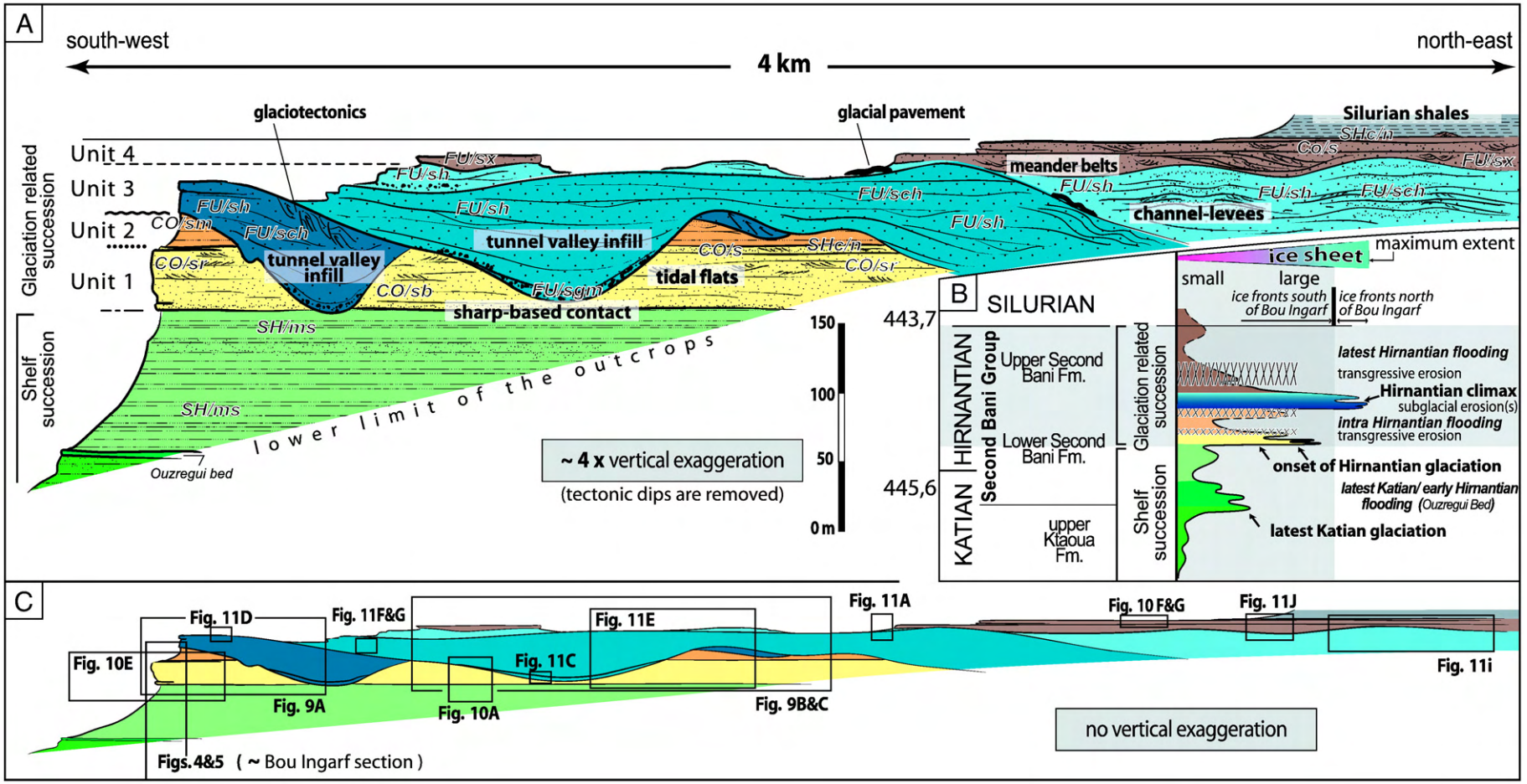

Fig. 12. Synthetic stratigraphic architecture of the glaciation-related succession in the Bou Ingarf area. (A) Stratigraphic architecture with vertical exaggeration and location of facies occurrences. (B) A simplified ice-sheet growth curve inferred from the Bou Ingarf record, with, in particular, the delineation of two Hirnantian glacial cycles and an intervening Hirnantian flooding. Erosion surfaces within the glaciation-related succession are either glacial or transgressive in origin. In this diagram, time axis is not linear and out-of-scale. (C) The same as in (A) with no vertical exaggeration and location of figures illustrating facies and stratigraphic architecture (Figs. 4, 5, 9, 10 and 11).

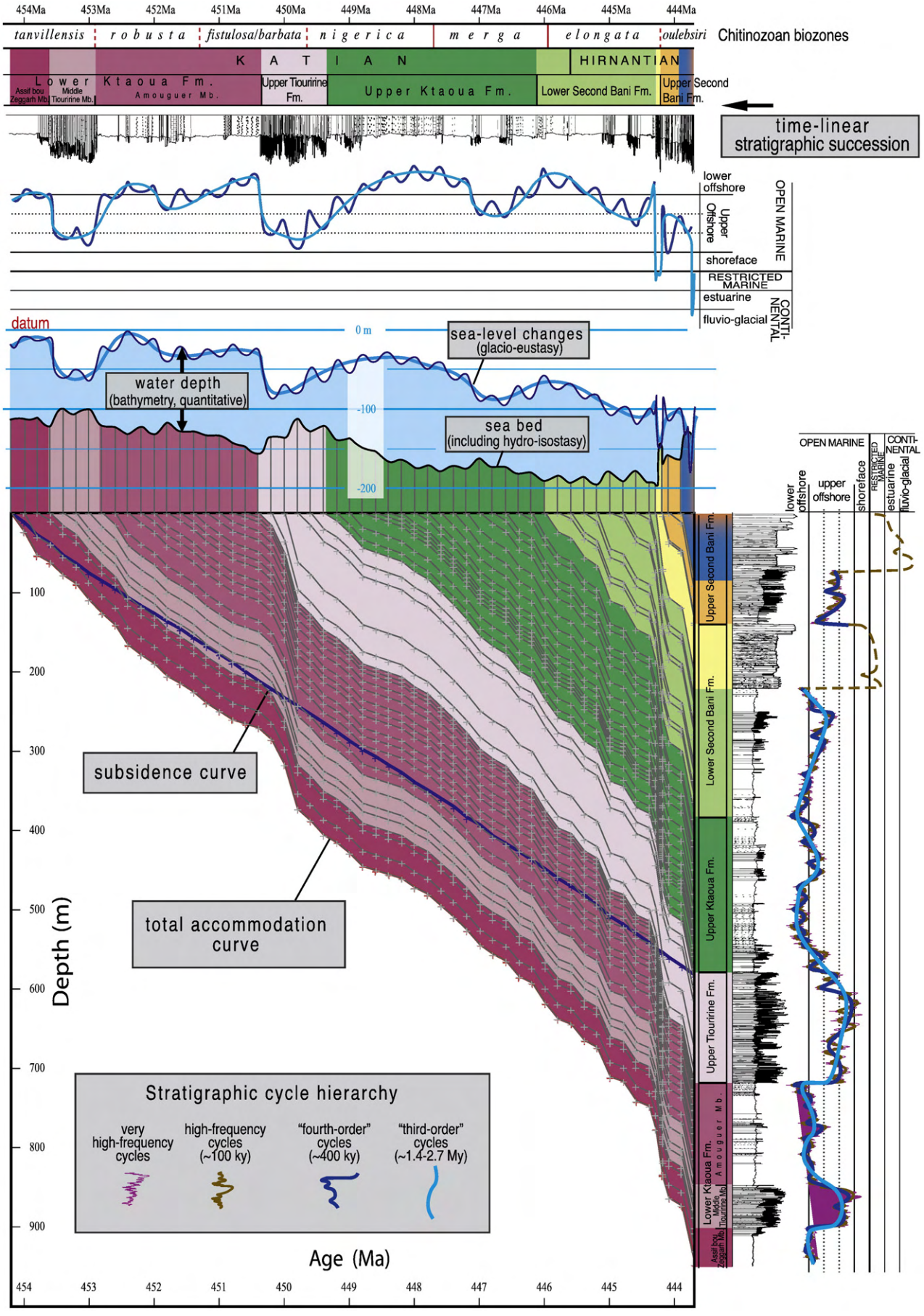
454Ma
453Ma
452Ma
451Ma
450Ma
449Ma
448Ma
447Ma
446Ma
445Ma
444Ma
tanvillensis
robusta
fistulosa/barbata
nigerica
merga
elongata
oulebsiri
Chitinozoan biozones
KATIAN
HIRNANTIAN
Lower Ktaoua Fm.
Assif bou Zeggarh Mb.
Middle Tiouririne Mb.
Amouguer Mb.
Upper Tiouririne Fm.
Upper Ktaoua Fm.
Lower Second Bani Fm.
Upper Second Bani Fm.
time-linear stratigraphic succession
lower offshore
upper offshore
shoreface
OPEN MARINE
RESTRICTED MARINE
estuarine
fluvio-glacial
CONTI-NENTAL
datum
0 m
-100
-200
sea-level changes (glacio-eustasy)
water depth (bathymetry, quantitative)
sea bed (including hydro-isostasy)
subsidence curve
total accommodation curve
Depth (m)
100
200
300
400
500
600
700
800
900
Upper Second Bani Fm.
Lower Second Bani Fm.
Upper Ktaoua Fm.
Upper Tiouririne Fm.
Lower Ktaoua Fm.
Amouguer Mb.
Middle Tiouririne Mb.
Assif bou Zeggarh Mb.
Stratigraphic cycle hierarchy
very high-frequency cycles
high-frequency cycles (~100 ky)
"fourth-order" cycles (~400 ky)
"third-order" cycles (~1.4-2.7 My)
Age (Ma)
454
453
452
451
450
449
448
447
446
445
444

sandstone beds. Clast-supported conglomerate beds also occur. Clast lithologies are representative from the underlying strata (sandstones and siltstones) with the exception of quartz gravels. Rarely, mud-dominated diamictites interbeds, 10–50 cm in thickness, also occur and include scattered sand grains and lonestones (gravel, pebble).

The FU/sh and FU/sch facies form the bulk of the palaeovalley infills and may form up to 80 m thick monotonous successions. The FU/sh facies (Fig. 11E, F, G and H) is comprised of medium-grained, slightly micaceous (0.25–1 m thick), sheet-like sandstone beds of wide lateral extent. They have abundant subhorizontal lamination with parting lineations. Gutter casts occur but are unexpectedly located within beds rather than at their base. Trough cross-strata, usually 1–2 m in width and stoss-depositional climbing ripples are subordinate depositional structures. Convolute bedding occurs in places.

Sandstone bodies comprising FU/sch facies are encased within successions dominated by FU/sh facies. They contain amalgamated, erosion-based, lenticular beds, 1–4 m in thickness, corresponding in places to channel structures. Internal lamination is poorly identifiable. Related sandstone bodies form either large-scale, erosion-based lenses (typically, 5×100 m), or vertically superimposed arrangements, several tens of metres in height and grading laterally in FU/sh facies.

The FU/sx facies (Fig. 11I, J and K) is comprised of medium- to coarse-grained sandstones including 5 to 10 m high sigmoidal geometries. In the lower part of this facies, thick (1–3 m) beds comprise the coarser grained, most often cross-stratified deposits including lags of rip-up intraclasts. To the top, the latter are truncated or prolonged laterally by tabular, thin (20–50 cm), sandstone beds with occasional wave ripples and ice-crystal marks.

5.3.2. Interpretation

The conglomeratic facies (FU/sgm) represents a combination of poorly sorted, high-energy, stream-flow and gravity-flow deposits, the source of which is in part the product of local incisions as shown the nature of intraclasts. Graded beds and diamictite intervals including lonestones may suggest subaqueous deposits. Intraformational deformations including shear structures within conglomeratic facies suites indicate the occurrence of subglacial soft-sediment shear zones (Deynoux and Ghienne, 2004) affecting glacio-fluvial deposits. Sheet-like sandy facies (FU/sh) corresponds to high-energy deposits from sheet flows. The occurrence of gutter casts within sandy sharp-based beds record the waxing- and then waning-flow conditions at the scale of individual beds. Climbing ripples indicate waning-flow events as well. A flood-dominated floodplain environment is inferred. The significant thickness of monotonous sheet-like sandstone facies and associated sedimentary structures indicates rapidly aggrading, sand-dominated floodplain deposits.

Amalgamated sandstone facies (FU/sch) represents channel belt deposits of an anastomosed fluvial channel network. In vertically stacked arrangement, they correspond to aggrading channel-levees systems (Adams et al., 2004) reflecting high floodplain aggradation rates (Malaske, 2001). Cross-bedded facies (FU/sx) including sigmoidal lateral accretion surfaces represents deposition within meander bar complexes. These fluvial or tidal-dominated meandering channels belonged to sub-emergent sandflats as indicated by the occurrence of wave ripples and ice-crystal marks (Hänzschel, 1935; Dionne, 1985).

5.4. An outline of the Hirnantian glacial record

The sharp contact between the distal part of the upper offshore deposits (SH/ml) of the shelf succession and the coastal deposits (CO/sb, CO/sr) of Unit 1 (Figs. 5 and 12A) indicates a severe forced regression. Its non-erosional character further suggests that emersion did not occur in the Bou Ingarf area and regressive conditions most likely maintained in the lowest beds of Unit 1. The 40–50 m thick overlying succession (Unit 1), comprising successively restricted-marine (CO/sb), tidal-dominated (CO/sr) and shoreface (CO/s) sediments, essentially records a tide-influenced aggradation and concomitant landward shoreline retreat within a transgressing barrier island-lagoon system (e.g., Plint, 1988; Reinson, 1992; Cattaneo and Steel, 2003). This trend includes poorly defined higher frequency events resulting in facies sequences possibly of autocyclic significance. At the top of Unit 1, transgressive conditions culminated with an abrupt facies shift from upper shoreface (CO/s) to distal part of the upper offshore environments (SH/ml). In details, the transition from shallow to deeper environments includes a wave ravinement surface that truncates shoreface deposits and is sealed by a thick condensed horizon (Fig. 5). Unit 1 then reflects a full glacio-eustatic regressive/transgressive cycle including a major downward shift characterising its base, high rates of aggradation in tide-influenced environments and, finally, a significant flooding event at its top (flooding surface in Fig. 9, Fig. 12B). The condensed horizon records the deepening event leading to the SH/ml facies deposition within Unit 2. The thickness of Unit 1 is fairly comparable with some Holocene estuarine successions recording the late post-glacial sea-level rise (e.g., Lericolais et al., 2001).

Unit 2 deposits represent a progressively shallowing-upward succession from shelf depositional environments to coastal environments. Subsequent to the aforementioned sea-level rise and associated increase in accommodation, it suggests essentially regressive conditions with normal progradation of a depositional profile possibly related to a delta setting. No glacio-eustatic forcing can be inferred from the Bou Ingarf sedimentary record for this sea-levell fall.

The severe erosion surface characterising the base of Unit 3 consists in superimposed palaeovalleys (Fig. 12). Geometries of the incisions, underlying folds interpreted as glaciotectonic deformation (Le Heron et al., 2005) and basal conglomeratic lags (FU/sgm), indicate bypass-dominated depositional systems related to tunnel valleys overdeepenings. Such valleys, which were cut under the ice by meltwater flows, are frequent along marginal segments of ice sheets straddling shallow-marine sedimentary platforms (e.g. the southern Scandinavian ice sheet: Van Dijke and Veldkamp, 1996; Huuse and Lykke-Andersen, 2000) and are relatively frequent in the Ordovician (Ghienne and Deynoux, 1998; Le Heron et al., 2004). As the bulk of the palaeovalley infills comprise aggradational, flood-dominated fluvial successions reflecting proglacial environments (FU/sh and FU/sch), high-frequency cycles are inferred. Though they relate to successive advances (tunnel valley erosion) and retreats (fluvio-glacial infills) of the ice fronts, they may represent an autocyclic signal. Accommodation space was provided by multiphased glacial erosion and no significant net aggradation occurred during deposition of Unit 3.

Unit 4 generally seals the topography inherited from the underlying fluvial channel-levee systems. It indicates a paraconformity without any severe basal erosion. Sand-flat deposits, composed of meandering channel structures (FU/sx), the upward switch into shoreface depositional settings (CO/s) and then condensed horizons conformably overlain by Silurian offshore shales indicate a transgressive estuarine setting. A basal tidal ravinement surface produced localised erosion surfaces. Its regional-wide distribution indicates the overall landward retreat of the depositional profile at the end of the Hirnantian glaciation. The post-glacial transgression culminated with a major condensation before sedimentation renewed with Silurian distal deposits.

To summarize, in the study area, the Hirnantian record highlights two high-amplitude regressive/transgressive cycles separated by an

Fig. 13. Results of the backstripping procedure. Assuming constant subsidence rates during the Late Ordovician, the water-depth curve and sediment accumulation trends are converted through a one-dimensional backstripping procedure into a sea-level curve. A time-linear stratigraphic succession was redrawn.

interglacial intra-Hirnantian flooding interval (Unit 2; Fig. 12B). Unit 1 reflects the earlier event corresponding to the onset of the Hirnantian glaciation. Neither emersion nor glacial erosion occurred at that time in the Bou Ingarf section. The stratigraphic record is essentially that of a glacio-eustatically driven, shallow-marine, transgressive facies suite. Truncating Unit 2 deposits, palaeovalley infills of Unit 3 reflect the later event, at time of the Hirnantian climax, when the ice sheet straddled the whole Anti-Atlas attaining more northern localities (Le Heron et al., 2007). Subglacial erosion repeatedly occurred producing tunnel valleys. The latest fluvio-glacial deposits likely represent lowstand to early time-transgressive conditions. Unit 4 represents transgressive deposits related to the deglaciation of the North Gondwana platform (Ghienne, 2003; Ghienne et al., 2007a) that occurred a short time before the Ordovician/Silurian boundary. This boundary is most likely comprised within condensed horizons at the transition between Unit 4 and overlying Early Silurian shale. This two-fold Hirnantian glaciation conforms to the North Gondwana glacial record (Storch, 1990; Sutcliffe et al., 2000; Storch, 2006), with a glacial maximum recognized during the second, later cycle (Brenchley et al., 2006; Ghienne et al., 2007a).

6. Toward a sea-level curve

6.1. Stratigraphic framework

A biostratigraphic framework based on chitinozoans was published in a previous work (Bourahrouh et al., 2004) for the upper two-thirds of the Bou Ingarf section. Five chitinozoan biozones are identified (*fistulosa*, *barbata*, *nigerica*, *merga*, and *elongata*) belonging to the upper Katian and Hirnantian (Fig. 3), i.e. the Ashgill in the British regional terminology (Paris, 1990; Webby et al., 2004). For this study, the Bou Ingarf section was newly sampled for palynological investigations, which confirm these former results (Fig. 5).

Trilobites from specific horizons provide additional information. The condensed fossiliferous horizon located at the transition between Ktaoua and Lower second Bani groups ("Ouzregui bed", Fig. 4; about 380 m in Fig. 5) yields *Flexicalymene ouzregui*, *Brongniartella platynota? marocana*, *Stenopareia* aff. *oblita* and trinucleids. Very similar trilobite species occur in the upper part of the Kraluv Dvur Formation in Bohemia, which is assigned to a late Rawtheyan age (Storch, 1990). The assemblage of the Bohemian succession is more diversified, as it contains taxa from deep environments (Proboscisambon assemblage) probably coupled with the stacking of assemblages by condensation (i.e. "Pernik bed", Brenchley and Storch 1989 and references therein). Taking strictly shelf fauna into account, the trilobite affinities are comparable with those of the Bou Ingarf section. In Bohemia, this fauna occurs just before the base of the Hirnantian according to the graptolite record (Storch, 2006). This is consistent with the immediately overlying base of chitinozoan *elongata* biozone (Fig. 5).

The middle and upper part of the Jbel Amouguer Member yield *Dalmanitina (D.) proaeva*, *Sokhretia?* aff. *solitaria*, *Flexicalymene tazarinensis*, *Eudolatites (E.)* aff. *angelini*, among others. These trilobite species are similar to some in the Zahorany (mainly) and Bohdalec formations from Bohemia (Vanek and Valicek 2001) whose ages are consistent with the chitinozoan *robusta* biozone (Villas et al., 2006).

The lower part of the studied section does not provide good stratigraphic marker horizons among trilobites but Destombes (1966) and Destombes et al. (1985) reported *Colpocoryphe grandis*, *Dalmanitina (D.) socialis* and *Marrolithus* sp. in the lower part of the Assif bou Zeggarh Member, a few metres above the top of the First Bani Group. These trilobites coexist with Sandbian chitinozoans (*deunffi* and *dalbyensis* biozones) in neighbouring localities (Elaouad-Debbaj, 1987). They are also recorded in Bohemia (Letna and Liben formations) and in the Armorican Massif where the uppermost part of the Postolonnec Formation and the lower part of the Kermeur Formation yield respectively Sandbian (*deunffi* and *dalbyensis* biozones) and early Katian chitinozoans (*tanvillensis* biozone; Paris, 1990; Dabard et al., 2007). These correlations are consistent with those proposed for this part of the section by Villas et al. (2006, Fig.3). Therefore, the top of Assif bou Zeggarh and the Middle Tiouririne members belong most likely to the early Katian.

6.2. Time calibration

Based on the chitinozoan biozones, the upper two-thirds of the Bou Ingarf section represent a 7 +/− 1 My time interval (Sadler and Cooper, 2004; Webby et al., 2004). On the HF curve (dark blue curve in Fig. 5) that is based on successive smoothings performed on the VHF curve (cf. Section 4.3), the same time interval corresponds to 18 +/− 2 genetic sequences. The uncertainties result from: (i) the fairly unprecise location of base of the former Ashgill Series within the strata yielding the *fistulosa/barbata* chitinozoan assemblages at Bou Ingarf; (ii) high-frequency genetic sequences, delineated in the Katian and early Hirnantian strata, cannot be delineated within the uppermost glacially-related wedge. Then, a genetic sequence ranges in duration from 0.3 My to 0.5 My, considering either the minimum (6 My/20 sequences) or maximum (8 My/16 sequences) ratios. Thus we postulate a genetic sequence is related to a 400 ky Milankovitch cycle. Considering a shorter period of 200 ky for the genetic sequence (resp. a longer period of 800 ky) implies an unsustainable duration of the Ashgill of 3.6 +/− 0.4 My (resp. 14.4 +/− 1.6). On the other hand, according to the HF curve, each biozone comprises four to six genetic sequences, which implies a mean biozone duration of 1.6 to 2.4 My. This time interval is in agreement with the stratigraphic framework of Webby et al. (2004; 1.5–2.5 My/biozone). Conversely, the duration of the overall Katian is estimated to 10.2 My (Finney, 2005). Taking into account that the base of our section is proposed to be early, not earliest, Katian age, the duration of the related time slice is fairly approximated to 22 genetic sequences representing 8.8 My.

In this study, genetic sequences are then ascribed to 400 ky eccentricity cycles. These cycles are considered as the most stable of the Earth's long-term astronomical frequencies (Laskar, 1999) and are generally well expressed in the geological record (e.g., Wade and Pälike, 2004). These long-term cycles are composed of two orders of higher frequency cycles delineated from the rock record (Figs. 5 and 8) likely represent ~100 ky and ~20 ky cycles (Laskar et al., 2004). Only a major change in absolute ages used by Sadler and Cooper (2004) would affect high-frequency cycle durations.

In order to propose a chronostratigraphic calibration, the duration of the glaciation-related package was estimated. The interval yielding the *elongata* and *oulebsiri* biozones, which is usually ascribed to the Hirnantian (Bourahrouh et al., 2004; Webby et al., 2004; Vandenbroucke et al., 2009), includes at least four HF genetic sequences beneath the first major sea-level fall (base of Unit 1) and up to two others occurring during the interglacial highstand (Unit 2) beneath the glacial erosion surface (base of Unit 3). Therefore, related strata represent at the minimum an about 2.4 My time slice ($4 \times 400 + 2 \times 400$ ky). In order to be in agreement with the recently proposed 1.9 My duration for the Hirnantian (Finney, 2005; Chen et al., 2006), such a duration requires: (i) a Katian/Hirnantian boundary located above the base of the *elongata* biozone, and (ii) Hirnantian sea-level lowstands of very short duration. We then ascribed each of the high-frequency Hirnantian glacial events to 100 ky events with higher frequencies potentially representing autocyclic signals. In addition, the base of the Hirnantian has to be comprised within the Lower Second Bani Fm. It has been placed arbitrarily at the first high-frequency maximum flooding event above the Ouzregui bed. Considering a Silurian/Ordovician boundary at 443.7 Ma, an astronomically calibrated chronostratigraphic framework is developed for the Bou Ingarf section (Fig. 13). Future studies that could demonstrate that the Hirnantian lower boundary is recorded substantially higher in the succession would required longer durations (up to 400 ky?) for Hirnantian sea-level lowstand assuming a fixed 1.9 My Hirnantian duration.

6.3. Stacking pattern and "third-order" sequences

A low-frequency curve (pale blue curve in Fig. 5) is constructed based on successive smoothings of the high-frequency signal. In the shelf succession, this curve represents a third-order curve, i.e. that records sea-level oscillations associated with an entire seaward shift of the depositional platform profile (e.g., Van Wagoner et al., 1988). Within the glaciation-related succession, two cycles are also delineated (from 480 to 640 m, Fig.5). However, these latter high-frequency oscillations record major change in depositional rates and setting associated with the Hirnantian glaciation and do not correspond to "third-order" cycles.

Two types of surfaces are identified. The third-order maximum flooding surfaces (MFS) indicate the turnaround from retrogradational to progradational stackings at the shoreline (Van Wagoner et al., 1990). However, only points of maximum depositional depth can be delineated based on a one-dimensional facies analysis in such a relatively distal setting. We propose a MFS location as being coincident with maximum rates of depth increase of the related HF genetic sequence, corresponding to a point slightly older than the maximum depth development. The turnaround from progradational to retrogradational stacking marks the maximum regressive surface (MRS) sensu Catuneanu et al. (2008). It corresponds to the shallower facies. The MFS and MRS are never abrupt in the study area (Fig. 5) and are preceded by an interval of nearly aggradational stacking. Using the MFS as sequence boundaries, six low-frequency sequences that we ascribed to third-order sequences are delineated (Fig. 5). Their duration ranges from 1.4 My to 2.7 My. The Hirnantian glaciation-related succession corresponds to the main part of the progradational stacking of the last sequence. Only the lower part of its retrogrational stacking is illustrated here (Unit 4), as it extends into the lower Silurian (see also Ghienne et al., 2007b).

Retrogradation phases are typically characterised by a gradual deepening-upward trend reflected by the progressive thinning of HF genetic sequences and the concentration and/or amalgamation of condensed facies (SHc/n and SHc/c). In contrast, within the progradational stackings, sharp-based surfaces (SBS) that reflect abrupt downward facies shifts are observed (i.e. 33 m, 156 m, 491 m and 590 m). The two older documented SBS (i.e. 33 m and 156 m, sequences 1 and 3) have superposed proximal facies of the upper offshore upon lower offshore facies. Strata between the SBS and the MRS represent a thick stacking of relatively shallow-water facies that should include strata coeval with forced regression (falling-stage system tract; Plint and Nummedal, 2000; Catuneanu et al., 2008). Around 328 m, the SBS superposed medial to distal facies of the upper offshore on lower offshore facies and has a less clear expression. The downward shift located ca. 491 m superposed restricted-marine to tidal deposits on upper and lower offshore facies whereas the downward shift ca. 590 m is the only one corresponding to an erosional surface. Whatever the water-depth attributed to individual depositional facies, the downward facies shifts record forced regression events on the shelf that can be correlated at least regionally across the basin (>400 km; Destombes, 1971; Destombes et al., 1985; Destombes, 2006). The overall tectonic quiescence throughout the depositional area, the regular ~3 My time interval between two successive facies downward shifts and the similar sheet-like stratigraphic signature of these events (Sahagian and Jones, 1993) all together strongly suggest that abrupt downward shifts represent glacio-eustatic sea-level falls occurring from the Katian (at least?) to the Hirnantian.

6.4. From water-depth change to sea-level oscillations: the backstripping procedure

Recent studies of Upper Ordovician strata conducted in low-latitude carbonate shelf (Holland and Patzkowsky, 1998; Nielsen, 2004; Long, 2007) have inferred abrupt eustatic changes, which were sometimes proposed to be related to pre-Hirnantian ice-sheet development (Saltzman and Young, 2005; Achab and Paris, 2007; Lodola et al., 2008; Desrochers et al., 2010-this issue). As noted by Holland and Patzkowsky (1998), sea-level fluctuations were estimated by many workers but most of the proposed curves simply reflect local water-depth changes. However, water-depth evolution presents a distorted view of sea-level evolution as it fails to account for tectonic, compaction and thickness of accumulated sediments. In the present study, we use one-dimensional backstripping to quantitatively convert the water-depth changes curve (Fig. 5) derived from facies analysis into a sea-level curve (Fig. 13). We are aware of the limitations of the method but results give compelling constraints on the development of pre-Hirnantian ice sheets. As any sea-level record is subject to local or regional tectonic effects, the eustatic estimate derived from backstripping the Bou Ingarf section must be nevertheless viewed as a testable template against which other records can be compared.

Backstripping progressively removes the effects of sediment accumulation and loading, including the effects of compaction and paleowater depth from tectonic subsidence. The backstripping algorithm we used has been developed by N. Cardozo, is freely available (http://homepage.mac.com/nfcd/work/programs.html), and is based on the Allen and Allen (1990) and Watts (2001) procedures. The time calibration is based on the HF (400 ky) curve obtained from facies analysis (cf. Section 6.2). A time-linear stratigraphic succession was drawn for the Bou Ingarf section (Fig. 13). The data processing (paleobathymetry, sediments thickness) was performed on the base of this 400 ky signal differentiating the rise and the fall periods (200 ky × 2). The quantification of paleowater-depth changes is performed using a facies-based analysis combining both depositional and condensation processes in storm-dominated clastic shelves (cf. Section 4.3). The amplitude estimates of glacio-eustatic changes are performed assuming quiescent tectonic and full isostatic compensation (intracratonic basin, Fig. 2).

To infer sea-level changes a model of tectonic subsidence is generally calculated, which is removed from the long-term accumulation trends (e.g., Kominz and Pekar, 2001). Considering the linear sediment accumulation curve that was calculated for the Anti-Atlas region through the whole Ordovician to the Devonian period (Burkhard et al., 2006) (Fig. 2), we regard the best approximation for tectonic subsidence has to be a constant subsidence rate throughout the 10 My studied time interval, even if possible tectonic influences were noted some 150 km to the east in the Tafilalt area (Destombes et al., 1985; El Maazouz and Hamoumi, 2007). Then, adjusting sea-level parameters of the backstripping procedure in order to produce a linear tectonic-subsidence curve (constant rate), a sea-level curve was derived from the time-calibrated sediment accumulation curve (Fig. 13).

Sensibility tests indicate that among parameters used in the backstripping procedure (time intervals, thicknesses of the post-Ordovician burial, compaction coefficients, palaeowater depth, degree of isostatic compensation) the critical issue is clearly the estimation of palaeowater depths in offshore facies. A fully developed error analysis (e.g., Kominz et al., 2008) is out of the scope of this paper and amplitudes of sea-level changes can be considered as only indicative. We perform sensibility tests that indicated amplitudes of sea-level changes most likely bracketed between one half and 1.5 the inferred amplitudes.

6.5. A Katian to Hirnantian sea-level curve

Firstly, the long-term trend obtained from backstripping illustrates a gradual sea-level fall throughout the Katian that is in good agreement with worldwide records (e.g., Haq and Schutter, 2008). Secondly, the amplitudes of sea-level change of the HF signal (400 ky) are variable. In most cases they are of about ten to a few tens of metres (10–30 m, Fig. 14). Based on a similar approach, but applied to a

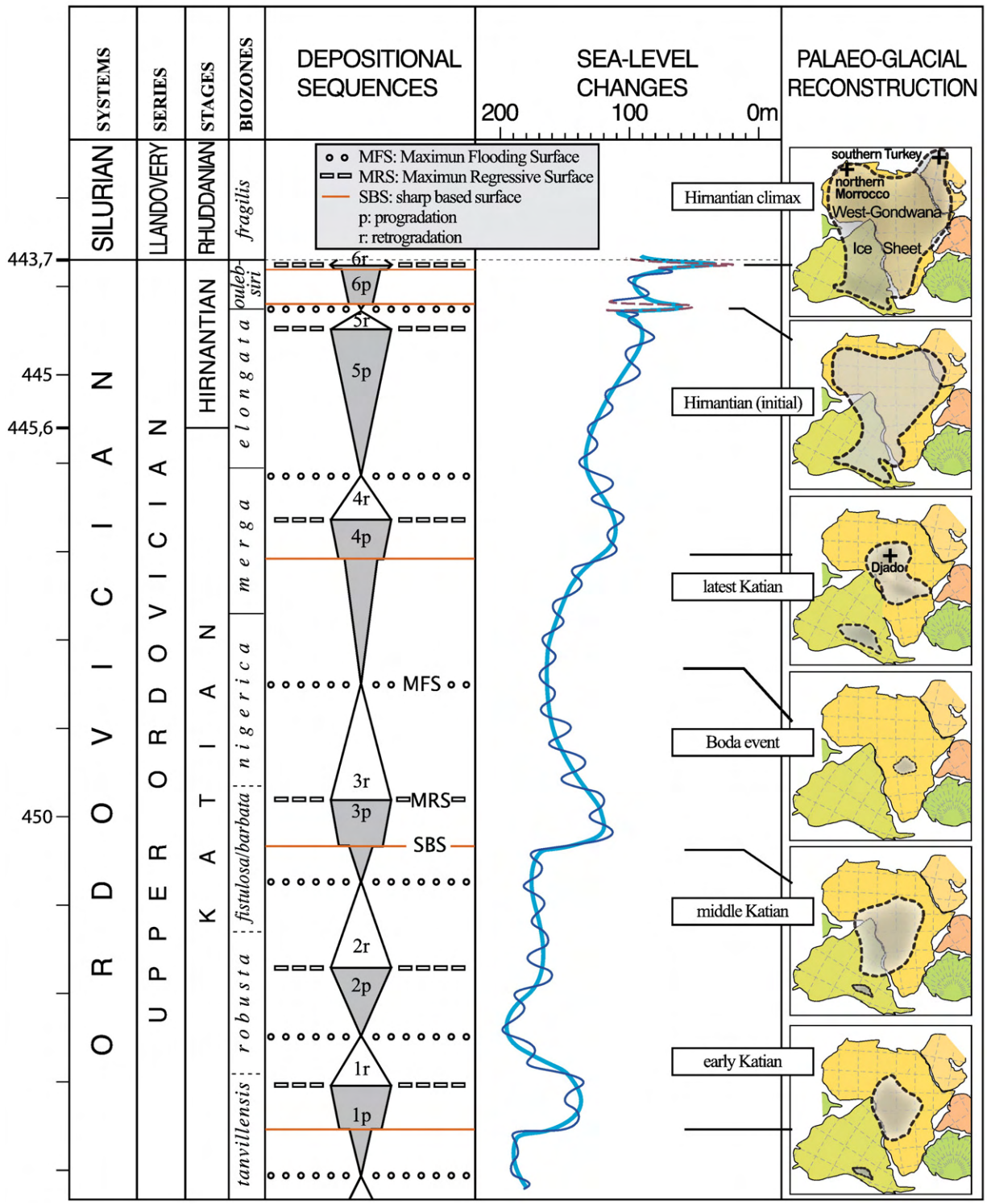

Fig. 14. Depositional sequences delineated in the Bou Ingarf section and eustatic sea-level change calculated from the backstripping procedure (Cf. Fig. 13). Informal palaeoglacial reconstructions are proposed for a selection of Late Ordovician key events.

carbonate shelf setting, Holland and Patzkowsky (1998) provided comparable amplitudes for short-term fluctuations. Amplitude changes of <10 m may be produced by a wide range of mechanisms, including changes in groundwater and lake levels, and changes in the ocean temperature (e.g., Revelle, 1990). However amplitudes greater than 10 m most likely point to a glacio-eustatic signal. Ice cap(s) likely cored in mountainous areas are thus inferred throughout the Late Ordovician.

Larger amplitudes of several tens of metres (>40 m) are repeatedly observed in the HF signal, in association with the sharp-based surfaces that highlight the third-order signal (Figs. 13 and 14; Table 2). These are thought to reflect an intensified glacio-eustatic signal linked with the growth of continental-scale ice sheets (Fig. 14). The sea-level falls associated with the growth of the Hirnantian ice sheet (590 m in Fig. 5) are estimated to at least 70 m. They are further discussed in Section 7.3.

Table 2
Sea-level fall estimates converted in ice-equivalent sea-level changes (see Section 7.2.) for the five major forced regression events related to a sharp-based surface in the stratigraphic record (Cf. Figs. 5 and 14). To compare, the present-day East Antarctica ice-sheet, the LGM Laurentide, the LGM Scandinavia/Barents ice sheet and the total ice cover at LGM correspond respectively to ~70 m, ~82 m, 14–18 m, 190–210 m of ice-equivalent sea-level changes.

Age	Position of the SBS in Fig. 5	Sequence nb. in Fig. 14	Sea-level fall estimate (min < **modelled** < max)	Ice-equivalent sea-level change (×1.48) (min < **modelled** < max)
Early Katian	33 m	1	25 < **50 m** < 75	37 < **74 m** < 111
Middle Katian	156 m	3	25 < **50 m** < 75	37 < **74 m** < 111
Latest Katian	330 m	4	15 < **30? m** < 45	22 < **44? m** < 67
Hirnantian (onset)	491 m	6	35 < **70 m** < 105	51 < **104 m** < 155
Hirnantian (climax) minimum amplitude	590 m	6	35 < at least **70 m** < 105	51 < at least **104 m** < 155
Hirnantian (climax) relative to preglacial[a]	_	_	50 < at least **100 m** < 150	74 < at least **148 m** < 222
Hirnantian (climax) relative to late Katian[b]	_	_	75 < less than **150 m** < 225	111 < less than **222 m** < 333

[a] Early Hirnantian datum immediately before sea-level fall.
[b] Late Katian datum, ~4 My before the onset of the Hirnantian glaciation, corresponding to the Boda event (see text). This estimate can be regarded as a maximum value because: (i) Late Katian ice cover was likely reduced at its minimum extent; (ii) the long-term change in ocean hypsometry (tectono-eustasy) may have accompanied any glacio-eustatic sea-level fall throughout the considered time interval.

However, in order to positively ascribe abrupt downward shifts to a glacio-eustatic signal, correlations with coeval events at the global scale are needed.

7. Implications and discussion

7.1. Global correlations of Katian events

The abrupt sea-level fall events (forced regression) and related SBS should preferentially be used for regional correlations rather than MFS as only the formers result from rapid and virtually synchronous, global events. In sufficiently deep shallow-marine settings (e.g., first and third sequences, Fig. 5), the abrupt sea-level fall is expressed by the SBS, across which shallow environments are superposed on largely deeper environments. In more proximal setting (e.g., 590 m in Fig. 5), the SBS takes the form of a subaerial to subglacial unconformity. On the contrary, the timing of the MFS depends on several basin-related parametres (sediment supply, subsidence rates). In addition, in relatively distal settings such as the Bou Ingarf section, the deepening- to shallowing-upward turnaround postdates (i.e. is younger than) the turnaround from retrogradational to progradational at the shoreline (Catuneanu et al., 1998). Then, maximum depositional depths are diachronous along a single shoreface/offshore profile and cannot be used to precisely locate a MFS that basically reflect trends at the shoreline.

Numerous other difficulties arise when correlating events across distinct palaeo-continents: (i) a time chart with sufficient precision (less than 1 Ma) for distinct palaeogeographic domains does not exist for the Ordovician, even if calibrations were recently proposed (Webby et al., 2004; Bergström et al., 2009); (ii) according to the shelf configuration, either the regressive or the transgressive signal can be poorly expressed explaining some controversy in the interpretation of the rock record (e.g., Tobin et al., 2005); (iii) most often, lithostratigraphic columns are used rather than time-linear stratigraphic succession, which lead to either the over- or under-estimate of event durations; (iv) lastly, the great number of events either eustatic (e.g., Nielsen, 2004) or isotopic (e.g., Kaljo et al., 2007) with a less than 2 My recurrence time do not facilitate correlations of global events. However, among stratigraphic anomalies already interpreted in the literature as representing major glacio-eustatic oscillations, some are potentially correlated to those we delineated in the Anti-Atlas. In the following, a non-exhaustive outline of correlatable events is given, the aim of which is only to stimulate future research.

The oldest abrupt sea-level fall we recognized occurred in the early (but not earliest) Katian at ca. 453.5 Ma (*tanvillensis* biozone). It belongs to Sequence 1 (Fig. 14) and is associated with the middle Tiouririne Member of the lithostratigraphy (Figs. 3 and 5). It may correspond to the high-amplitude regressive/transgressive event associated with the Guttenberg isotopic excursion (GICE) essentially identified in Laurentia (M3 event of Holland and Patzkowsky, 1998; Eureka Quartzite of Saltzman and Young, 2005) and in Baltoscandia (Ainsaar et al., 1999, 2004; "Solvang Lowstand Event" in Nielsen, 2004; Bergström et al., 2007; Calner et al., 2010).

The second abrupt sea-level fall occured in the middle Katian (most probably in the latest Caradoc in terms of the former British Series) at ca. 450.5 Ma (*fistulosa*/*barbata* biozones). It belongs to Sequence 3 (Fig. 14) and is associated with the Upper Tiouririne Fm. of the lithostratigraphy (Figs. 3 and 5). Post-glacial recovery occurred at ca. 449.5 Ma together with the onset of the chitinozoan *nigerica* biozone. This sea-level fall is tentatively correlated with the major regressive event reported in Baltoscandia by Calner et al. (2010-this issue). Although slightly older according to stratigraphic correlation charts (Webby et al., 2004), this regressive event is associated with a well defined palaeokarst interpreted by Calner et al. (2010-this issue) as the signature of a glacial event. In Laurentia, the significant transgressive C1 event evidenced by Holland and Patzkowsky (1998) may correspond to the post-glacial transgression. Elsewhere in North Gondwana, it likely corresponds to sharp-based sandstone units (e.g., the Maciurru Member in Sardinia; Loi, 1993; Leone et al., 1998, 2002).

The third sea-level fall occurred in the latest Katian (late Rawtheyian in the British stage terminology), but not the very latest Katian, at ca. 447 Ma (*merga* biozone; Sequence 4 in Fig. 14). This event, perhaps of moderate amplitude though deeper depositional environments provide imprecise estimates of water depths, was reported from the Anticosti carbonate succession (Desrochers et al., 2010-this issue), in the Avalonian domain (Wales: Brenchley et al., 2006; Scotland: Armstrong and Coe, 1997) and possibly in Baltoscandia by Nielsen (2004: Termi Lowstand Event?). Finally, it may correspond to the Punta Arenas Member, manganese-rich deposits of SW Sardinia (Loi, 1993; Ghienne et al., 2000).

Periods of high sea levels inferred from the Bou Ingarf section can also be correlated with global events. Studying the stratigraphic record of the Arabian Plate, Sharland et al. (2001) identified a mid Katian (i.e. Late Caradoc) second-order maximum flooding surface (MFS O40), which was redefined as a maximum flooding interval (MFI O40) by Molyneux et al. (2006). It corresponds to the *fistulosa* "transgressive event" of Paris et al. (2007). This time interval most likely corresponds to the 452.5–450.5 Ma interval that, in the proposed sea-level curve (Fig. 14), comprises two distinct maximum flooding intervals. It is worth noticing that even if the deeper but severely condensed facies are identified around 450.5 Ma, the back-stripping procedure clearly indicates that the highest sea levels occurred around 452.5 Ma (Figs. 5 and 14 to compare). It illustrates the difficulties encountered when (i) proposing a sea-level curve based simply on water-depth changes, (ii) looking for global correlations based on dataset that are not harmonized.

The 448–449 Ma time interval (*nigerica* biozone) corresponds to restored high sea levels after the second, 450.5 Ma, abrupt sea-level fall (*barbata*/*fistulosa* biozone). This episode resulted in a significant coastal onlap with transgressive, carbonate-prone strata deposited far in the

hinterland (e.g., the Ougarta Range, western Algeria, Ghienne et al., 2007b or bryozoan-bearing limestone in south-eastern Algeria, AMA-1 and Oued Ahara 101 borehole, unpublished data; southern Libya, Ghienne et al., 2007a). This transgression and following highstand period are temporally linked with the "mid-Ashgill" Boda event of Fortey and Cocks (2005). The latter represents a period of global warming (Boucot et al., 2003) characterised by the development of highly diversified faunal assemblages with migration towards higher palaeolatitude of species previously restricted to Laurentia and Baltica. Throughout the North Gondwana platform, it can be correlated with the unexpected growth of relatively high-latitude carbonate platforms (Hammann and Leone, 1997; Vennin et al., 1998; Buttler et al., 2007; Hammann and Leone, 2007). Though the deflection of a warm current may account for the sudden and massive immigration of a distinct benthic fauna (Hammann, 1992; Villas et al., 2002), rising sea levels penecontemporaneous with increasing temperatures indicate a glacio-eustatic forcing. Biodiversification and carbonate development were coeval with deposition of highly condensed, deepening facies in lower offshore conditions of the Bou Ingarf section. As high-frequency low amplitude cycles maintained during this time interval (Fig. 13), the relatively warm event was not able to melt the intra-continental Gondwana ice cap(s).

7.2. Ice-equivalent sea-level changes and pre-Hirnantian ice sheets

Glacio-eustatic estimates derived from backstripping can be converted in actual volume change from transferring ocean water to glacial ice. As a consequence of the water loading of the oceanic lithosphere (hydro-isostasy), the amplitude of ice-equivalent sea-level change (or Apparent Sea-Level of Pekar et al., 2002) exceeds the eustatic change. Assuming full compensation, these authors calculated an amplification factor up to ~1.48. Then, an early Katian (S1) and a middle Katian (S3) 50 m sea-level falls would approximately represent a 74 m (min 37 m – max 111 m) ice-equivalent sea-level change corresponding to an ice sheet comparable with the LGM Laurentides (Clark and Mix, 2002) or the present-day East Antarctic ice sheet (Huybrechts, 2002) (Table 2).

The most biostratigraphic dating of glaciomarine deposits, formerly regarded as Caradocian either in Algeria (Beuf et al., 1971) or in Libya (Bellini and Massa, 1980), are now generally considered as Hirnantian in age (Paris et al., 1995; Sutcliffe et al., 2000; Ghienne et al., 2007a). Presently, no glacial features are proven prior to the Hirnantian, with the possible exception of the Djado record in northern Niger (Denis et al., 2007a and b) (Fig. 14). This proximal area exhibits glacial features that pre-date a transgressive succession containing *N. ojsuensis* graptolites (Legrand, 1993; Denis et al., 2007a). This stratigraphic relationship suggests a latest Katian to earliest Hirnantian age (dicussion in Chen et al., 2006) for the related glacial strata. The latter may have record the late Katian glacial event inferred from the Bou Ingarf section in Sequence 5 (Figs. 5, 12B and 14). The ensuing post-glacial transgression leads in the Anti-Atlas to the extremely condensed horizon ("Ouzregui bed"). In constrast with Hirnantian ice sheets, Katian glaciers though of significant extent were restricted to the centre of the Gondwana landmass with basically no ice fronts straddling sedimentary basins. It results the absence of any glacial record (e.g., subglacial erosion, marine diamictites).

7.3. Timing and extent of Hirnantian ice sheets

This study indicates that the first major downward facies shift corresponding to the initial Hirnantian ice-sheet advance and forced regression occurred relatively high within the Hirnantian (Figs. 13 and 14), and not at its base as usually considered. This is in contrast with previous interpretations of the sedimentary record of low-latitude carbonate platforms (e.g., Brenchley et al., 2003; Kaljo et al., 2004), which suggests the onset of the Hirnantian glaciation is coincident with the base of the Hirnantian stage. However, most of the low-latitude records show time-equivalent, demonstrated or supposed, emersion surfaces. Therefore, associated hiatuses (see discussion in Kaljo et al., 2004 and Melchin and Holmden, 2006) may represent either the Hirnantian or the latest Katian sea-level falls while intervening deposits may principally reflect Hirnantian highstand periods. The most recent sequence stratigraphic interpretations of low-latitude carbonate platforms may be more consistent with the one proposed here (e.g., Desrochers et al., 2010-this issue).

Following the proposed time calibration, the older Hirnantian high-amplitude sea-level fall (base of Unit 1) occurred within the Hirnantian, at ca. 444.5. This event is correlated with the onset of the Hirnantian glacial event as currently documented in North Africa (Ghienne et al., 2007a and reference therein). The magnitude of related sea-level fall (base of Unit 1 in the Bou Ingarf section) is estimated to 70 m before high, "non-glacial" sea levels were mainly restored (Fig. 14). Maximum extent of the Gondwana ice sheet occurred shortly after, and would be bracketed, according to our chronostratigraphic framework, between 444 Ma and the end of the Hirnantian (443.7 Ma). An estimate of the younger Hirnantian sea-level fall (Unit 3) is virtually impossible as the whole area was glaciated, isostatically flexured and affected by glacial erosion as shown by glacial pavements and subglacial tunnel valleys (Destombes, 1968b; Ghienne et al., 2007a; Le Heron, 2007). The subsequent onset of fluvial deposition indicates continental conditions were maintained after the glacier retreated from the Bou Ingarf area. Any tentative estimate of the post-glacial sea-level rise then only represents eustatic sea-level rise after the fluvial plain was submerged and is therefore a minimum estimate.

The second, younger ice-sheet advance (related to Unit 3) was of greater extent relative to the first Hirnantian one as suggested by: (i) a more widespread palaeogeographic distribution of the glaciogenic features for the related ice-sheet advance with ice fronts that reached northern Morocco and Turkey (Monod et al., 2003; Le Heron et al., 2007; Ghienne et al., 2007a), (ii) estimates of Hirnantian sea-level change based on lower latitude settings (Storch, 1990, 2006; Brenchley et al. 2006). This pattern is well reflected in our sea-level curve. At least 70 m of sea-level fall characterises the younger Hirnantian event (Fig. 14). In addition, a minimum amplitude of 100 m would be calculated considering an early Hirnantian, pre-glaciation datum whereas a maximum amplitude of 150 m would be calculated considering the highest sea-level coeval with the Boda event (i.e. 4 My earlier) although this view neglects any tectono-eustatic trend in the curve (Table 2). Therefore, during the latest Ordovician glacial climax (in terms of ice-equivalent sea-level change that exceeds the eustatic change by ~1.48, see above), the latest Ordovician ice sheet may have stored a volume of ocean water equivalent to 222 m. The latter value is comparable with the entire ice cover at LGM, which has cumulated both the 118 m–130 m relative to present day and the water stored in ice today (~70 m), essentially within the East Antarctica Ice Sheet (Clark and Mix, 2002).

Even if considering minimal estimates (<100 m), a significant North Gondwana ice sheet existed (Young et al., 2004; Ghienne et al., 2007a; Le Heron and Dowdeswell, 2009). Greater estimates (>150 m) lead to a major continental-scale West Gondwana ice sheet with several ice domes distributed from North to South Africa (Vaslet, 1990; Sutcliffe et al., 2000; Ghienne et al., 2007a). The total volume of ocean water transferred to glacial ice has to include the volume of both pre-Hirnantian glaciers and that of polyphased Hirnantian ice-sheet growths. Then, the amplitude of estimated Hirnantian sea-level falls cannot be used straightforwardly for any palaeoglacial reconstructions. In the same manner, step-by-step post-glacial sea-level rises occurring from the latest Hirnantian to the Early Silurian (Ghienne et al., 2007a) are not really useful for this purpose.

8. Conclusion

The Bou Ingarf section (Anti-Atlas, southern Morocco) records a thick and virtually continuous, storm-dominated, siliciclastic

sedimentary record of Late Ordovician events. A calculated sea-level curve based on facies analysis and on a backstripping procedure indicates that the stratigraphic succession is dominated by the stacking of very high (<400 ky), high (400 ky) and low-frequency ("third-order": 1.4–2.7 Ma) sequences. We advocate that the three orders of sequences reflect glacio-eustasy throughout the Katian and the Hirnantian.

During the Katian, three major forced regressions and abrupt sea-level falls (>40 m), and ensuing sea-level rises are identified in the Bou Ingarf section. Such events are also recorded in other domains such as Baltoscandia and Laurentia. They likely represent glaciation episodes prior to the better known Hirnantian glaciation. Katian ice sheets did not reach sedimentary basins and the related glacial records are lacking, with the possible exception of the northern Niger succession that may preserve a latest Katian glacial record. The occurrences of pre-Hirnantian glacial events challenge the former views of an atypical short-term Hirnantian glaciation within a Lower Palaeozoic warm climatic mode. Considering the Mid Ordovician cooling phase recently evidenced from conodont thermometry (Trotter et al., 2008), and the occurrence of significant facies downward shifts throughout the Late Ordovician in both low- and high-palaeolatitude settings, the onset of ice-sheet growths noticeably occurred well before the Hirnantian glacial event (e.g., Pope and Read, 1998).

The Hirnantian glaciation itself is a mid to late Hirnantian event. It is best documented by the African record, with an excellent succession preserved in the Bou Ingarf section. It includes two distinct events, subordinate (autocyclic?) higher frequency cycles and an intermediate but important transgression. We propose the Hirnantian glacial event is time-equivalent with the facies change associated with the mid-Hirnantian development of the *Hirnantia* fauna in deep shelf settings such as the Hirnantian stratotype in China (Chen et al., 2006).

If a significant ice sheet permanently occupied the centre of the Gondwana landmass throughout the Late Ordovician, and most likely the Early Silurian, relatively moderate but time-restricted Hirnantian eustatic sea-level fall amplitude (40–80 m; ice-equivalent sea-level change in the 60–120 m range) may reconcile with palaeoglacial reconstructions of a major ice sheet at the glacial climax. The latter that should have resulted in an up to 220 m ice-equivalent sea-level change relative to Late Katian conditions and may have straddled the entire West Gondwana from Arabia to North and West Africa and part of South America and South Africa.

Acknowledgments

This work is a contribution to the ECLIPSE 2 programme (CNRS, France) and to IGCP Project no. 503. Constructive comments by reviewers Dr. M. Calner, M. Pope and A. Desrochers were greatly appreciated.

References

Achab, A., Paris, F., 2007. The Ordovician chitinozoan biodiversification and its leading factors. Palaeogeography, Palaeoclimatology, Palaeoecology 245, 5–19.
Adams, P.N., Slingerland, R.L., Smith, N.D., 2004. Variations in natural levee morphology in anastomosed channel flood plain complexes. Geomorphology 61, 127–142.
Aigner, T., 1985. Storm depositional systems. Lectures Notes Earth Sciences, vol. 3. Springer, Berlin. 174 pp.
Ainsaar, L., Meidla, T., Martma, T., 1999. Evidence for a wide-spread carbon isotopic event associated with late Middle Ordovician sedimentation and faunal changes in Estonia. Geological Magazine 136, 49–62.
Ainsaar, L., Meidla, T., Martma, T., 2004. The middle Caradoc facies and faunal turnover in the late Ordovician Baltoscandian palaeobasin. Palaeogeography, Palaeoclimatology, Palaeoecology 210, 119–133.
Allen, P.A., Allen, J.R., 1990. Basin Analysis, Principles and Applications. Blackwell Scientific Publications. 451 pp.
Alvaro, J.J., Vennin, E., Villas, E., Destombes, J., Vizcaïno, D., 2007. Pre-Hirnantian (latest Ordovician) benthic community assemblages: controls and replacements in a siliciclastic-dominated platform of the eastern Anti-Atlas, Morocco. Palaeogeography, Palaeoclimatology, Palaeoecology 245, 20–36.
Armstrong, H.A., Coe, A.L., 1997. Deep-sea sediments record the geophysiology of the late Ordovician glaciation. Journal Geological Society London 154, 929–934.
Babin, C., Destombes, J., 1990. Les Mollusques Bivalves et Rostroconches ordoviciens de l'Anti-Atlas marocain: intérêt paléogéographique de leur inventaire. Géologie Méditerranéenne 17, 243–261.
Bellini, E., Massa, D., 1980. A stratigraphic contribution to the Paleozoic of the southern basins of Libya. In: Salem, M.J., Busrewil, M.T. (Eds.), The Geology of Libya. Academic Press, London, pp. 3–56.
Bergström, S.M., Young, S., Schmitz, B., Saltzman, M.R., 2007. Upper Ordovician (Katian) $d^{13}C$ chemostratigraphy: a trans-Atlantic comparison. Acta Palaeontologica Sinica 46, 37–39 (suppl.).
Bergström, S.M., Chen, Xu., Gutierrez-Marco, J.C., Dronov, A., 2009. The new chronostratigraphic classification of the Ordovician System and its relations to major regional series and stages and the d ^{13}C chemostratigraphy. Lethaia 42, 97–107.
Beuf, S., Biju-Duval, B., De Charpal, O., Rognon, P., Gariel, O., Bennacef, A., 1971. Les grès du Paleozoïque inférieur au Sahara. Science et Technique du pétrole 18, Paris. 464 pp.
Boote, D.R.D., Clark-Lowes, D.D., Traut, M.W., 1998. Palaeozoic petroleum systems of North Africa. In: MacGregor, D.S., Moody, R.T.J., Clark-Lowes, D.D. (Eds.), Petroleum Geology of North Africa, Geological Society of London, Special Publication, vol. 132, pp. 7–68.
Botquelen, A., Loi, A., Gourvennec, R., Leone, F., Dabard, M.P., 2004. Formation et signification paléo-environnementale des concentrations coquillières: exemples de l'Ordovicien de Sardaigne et du Dévonien du Massif armoricain. Comptes Rendus Palevol 3, 353–360.
Botquelen, A., Gourvennec, R., Loi, A., Pillola, G.L., Leone, F., 2006. Replacements of benthic associations in a sequence stratigraphic framework, examples from Upper Ordivician of Sardinia and Lower Devonian of the Massif Armoricain. Palaeogeography, Palaeoclimatology, Palaeoecology 239, 286–310.
Boucot, A.J., Jia-yu, R., Chen, X., Scotese, C.R., 2003. Pre-Hirnantian Ashgill climatically warm event in the Mediterranean region. Lethaia 36, 119–132.
Bourahrouh, A., Paris, F., Elaouad-Debbaj, Z., 2004. Biostratigraphy, bodiversity and palaeoenvironments of the chitinozoans and associated palynomorphs from the Upper Ordovician of the Central Anti-Atlas, Morocco. Review of Palaeobotany and Palynology 130, 17–40.
Bréhéret, J.G., Hanzo, M., El Albani, A., Iatzoura, A., 2004. Impact de la vie benthique sur la genèse de nodules calcaires dans les black shales. Comptes Rendus Géosciences 336, 1355–1362.
Brenchley, P.J., Storch, P., 1989. Environmental changes in the Hirnantian (upper Ordovician) of the Prague Basin, Czechoslovakia. Geological Journal 24, 165–181.
Brenchley, P.J., Romano, M., Guttiérrez-Marco, J.C., 1986. Proximal and distal hummocky cross-stratified facies on a wide Ordovician shelf in Iberia. Shelf Sands and Sandstones: In: Knight, R.J., McLean, J.R. (Eds.), Canadian Society of Petroleum Geologists, vol. 2, pp. 241–255.
Brenchley, P.J., Marshall, J.D., Carden, C.A.F., Robertson, D.B.R., Long, D.G.F., Leidla, T., Hints, L., Anderson, T.F., 1994. Bathymetric and isotope evidence for a short-lived late Ordovician glaciation in a greenhouse period. Geology 22, 295–298.
Brenchley, P.J., Carden, G.A., Hints, L., Kaljo, D., Marshall, J.D., Martma, T., Meidla, T., Nolvak, J., 2003. High-resolution stable isotope stratigraphy of Upper Ordovician sequences: constrains on the timing of bioevents and environmental changes associated with mass extinction and glaciation. Bulletin of the Geological Society of America 115, 89–104.
Brenchley, P.J., Marshall, J.D., Harper, D.A.T., Buttler, C.J., Underwood, C.J., 2006. A late Ordovician (Hirnantian) karstic surface in a submarine channel, recording glacio-eustatic sea-level changes: Meifod, central Wales. Geological Journal 41, 1–22.
Bruton, D., 2008. A systematic revision of Selenopeltis (Trilobita: Odontopleuridae) with description of new material from the Ordovician Anti Atlas region, Morocco. Paläontologische Zeitschrift 82, 1–16.
Burkhard, M., Caritg, S., Helg, U., Robert, Ch., Charrue, Ch., Soulaimani, A., 2006. Tectonics of the Anti-Atlas of Morocco. Comptes Rendus Geoscience 338, 11–24.
Buttler, C., Cherns, L., Massa, D., 2007. Bryozoan mud-mounds from the Upper Ordovician Jifarah (Djeffara) Formation of Tripolitania, North-West Libya. Palaeontology 50, 479–494.
Calner, M., Lehnert, O., Joachimski, M., 2010. Carbonate mud mounds, conglomerates, and sea-level history in the Katian (Upper Ordovician) of central Sweden. Facies 56, 157–172.
Calner, M., Lehnert, O., Nõlvak, J., 2010. Palaeokarst evidence form widespread regression and subaerial exposure in the middle Katian (Upper Ordovician) of Baltoscandia: significance for global climate. Palaeogeography, Palaeoclimatology, Palaeoecology 296, 235–247 (this issue).
Cattaneo, A., Steel, R.J., 2003. Transgressive deposits: a review of their variability. Earth-Science Reviews 62, 187–228.
Catuneanu, O., Willis, A.J., Miall, A.D., 1998. Temporal significance of sequence boundaries. Sedimentary Geology 121, 157–178.
Catuneanu, O., Abreu, V., Bhattachary, J.P., Blum, M., Dalrymple, R.W., Eriksson, P.G., Fielding, C.R., Fisher, W.L., Galloway, W.E., Gibling, M.R., Giles, K.A., Holbrook, J.M., Jordan, R., Kendall, C.G., St, C., Macurda, B., Martinsen, O.J., Miall, A.D., Neal, J.E., Nummedal, D., Pomar, L., Posamentier, H.W., Pratt, B.R., Sarg, J.F., Shanley, K.W., Steel, R.J., Strasser, A., Tucker, M.E., Winker, C., 2008. Towards the standardization of sequence stratigraphy. Earth-Science Reviews 92, 1–33.
Chauvel, J., 1966. Echinodermes de l'Ordovicien du Maroc. Cahiers de Paléontologie 166, 1–120.
Chauvel, J., 1977. Note complémentaire sur les Cystoides Rhombiferes (Echinodermes) de l'Ordovicien marocain. Notes du Service Géologique du Maroc 38 (268), 115–139.
Chen, X., Rong, J., Fan, J., Zhan, R., Mitxhell, C.E., Harper, A.T., Melchin, M.J., Peng, P., Finney, S.C., Wang, X., 2006. The Global Boundary Stratotype Section and Point

(GSSP) for the base of the Hirnantian Stage (the uppermost of the Ordovician System). Episodes 29, 183–196.
Clark, P.U., Mix, A.C., 2002. Ice sheets and sea level of the Last Glacial Maximum. Quaternary Science Reviews 21, 1–7.
Coward, M.P., Ries, A.C., 2003. Tectonic development of North African basins. Petroleum Geology of Africa: New Themes and Developing Technologies: In: Arthur, T.J., MacGregor, D.S., Cameron, M.R. (Eds.), The Geological Society, London. Special Publication No. 207, pp. 61–83.
Cross, T.A., 1988. Controls on coal distribution in transgressive-regressive cycles. Sea-Level Change: An Integrated Approach: In: Wilgus, C.K., Hastings, B.S., Kendall, C.G., St., C., Posamentier, H.W., Ross, C.A., Van Wagoner, J.C. (Eds.), SEPM, Special Publication, vol. 42, pp. 371–380.
Cross, T.A., Lessenger, M.A., 1998. Sediment volume partitioning: rationale for stratigraphic model evaluation and high-resolution stratigraphic correlation. Sequence stratigraphy-Concepts and Applications: In: Gradstein, F.M., Sandvik, K.O., Milton, N.J. (Eds.), Norvegian Petroleum Society, Special Publication, vol. 8, pp. 171–195.
Cross, T.A., Baker, M.R., Chapin, M.A., Clark, M.S., Gardner, M.G., Hanson, M.S., Lessenger, M.A., Little, L.A., McDonough, K.J., Sonnenfeld, M.D., Valasek, D.W., Williams, M.R., Witter, D.A., 1993. Applications of high-resolution sequence stratigraphy to reservoir analysis. In: Eschard, R., Doligez, B. (Eds.), Reservoir characterization from outcrop investigations, Proceedings of the 7th Exploration and Production Research Conference. Paris Technip, pp. 11–33.
Dabard, M.P., Loi, A., Paris, F., 2007. Relationship between phosphogenesis and sequence architecture: sequence stratigraphy and biostratigraphy in the Middle Ordovician of the Armorican Massif (NW France). Palaeogeography, Palaeoclimatology, Palaeoecology 248, 339–356.
Dalrymple, R.W., Choi, K., 2007. Morphologic and facies trends through the fluvial-marine transition in tide-dominated depositional systems: a schematic framework for environmental and sequence-stratigraphic interpretation. Earth-Science Reviews 81, 135–174.
Denis, M., Buoncristiani, J.-F., Konaté, M., Ghienne, J.-F., Guiraud, M., 2007a. Hirnantian glacial and deglacial record in SW Djado Basin (NE Niger). Geodinamica Acta 20, 177–194.
Denis, M., Buoncristiani, J.-F., Konaté, M., Guiraud, M., 2007b. The origin and glaciodynamic significance of sandstone ridge networks from the Hirnantian glaciation of the Djado Basin (Niger). Sedimentology 54, 1225–1243.
Desrochers, A., Farley, C., Achab, A., Asselin, E., Riva, J.F., 2010. A far-field record of the end-Ordovician glaciation: The Ellis Bay Formation, Anticosti Island, Eastern Canada. Palaeogeography, Palaeoclimatology, Palaeoecology 296, 248–263 (this issue).
Destombes, J., 1966. Quelques Calymenina (trilobitae) de l'Ordovicien Moyen et Supérieur de l'Anti-Atlas (Maroc). Notes du Service Géologique du Maroc 26 (188), 33–44.
Destombes, J., 1968a. Sur la présence d'une discordance générale de ravinement d'âge Ashgill supérieur dans l'Ordovicien terminal de l'Anti-Atlas (Maroc). Comptes Rendus Académie des Sciences Paris 267, 565–567.
Destombes, J., 1968b. Sur la nature glaciaire des sédiments du groupe du 2^{e} Bani, Ashgill supérieur de l'Anti-Atlas, Maroc. Comptes Rendus Académie des Sciences Paris 267, 684–686.
Destombes, J., 1971. L'Ordovicien au Maroc. Essai de synthèse stratigraphique. Mémoires du Bureau de Recherche Géologique et Minière 73, 237–263.
Destombes, J., 1972. Les trilobites du sous-ordre des Phacopina de l'Ordovicien de l'Anti-Atlas (Maroc). Notes et Mémoires du Service Géologique du Maroc 240, 114p.
Destombes, J., 1977 (re-edited 2006). Carte géologique au 1/200000 de l'Anti-Atlas marocain. Paléozoïque inférieur: Cambrien moyen et supérieur – Ordovicien – base du Silurien. Feuille Jbel Saghro – Dadès, chapitre C. Notes et Mémoires du Service Géologique du Maroc 161, 41p.
Destombes, J., 1981. Hirnantian (Upper Ordovician) tillites on the north flank of the Tindouf basin, Anti-Atlas, Morocco. In: Hambrey, M.J., Harland, W.B. (Eds.), Earth's pre-Pleistocene glacial record. Cambridge University Press, pp. 84–88. Available on-line via www.aber.ac.uk/glaciology.
Destombes, J., 1982 (re-edited 2006). Carte géologique au 1/200000 de l'Anti-Atlas marocain. Paléozoïque inférieur: Cambrien moyen et supérieur – Ordovicien – base du Silurien. Feuille Bou Haiara - Zegdou, chapitre B. Notes et Mémoires du Service Géologique du Maroc 259, 30p.
Destombes, J., 1989 (re-edited 2006). Carte géologique au 1/200000 de l'Anti-Atlas marocain. Paléozoïque inférieur: Cambrien moyen et supérieur – Ordovicien – base du Silurien. Feuille Zagora – Coude du Dra, chapitre A. Notes et Mémoires du Service Géologique du Maroc 273, 54p.
Destombes, J., 2006. Carte géologique au 1/200000 de l'Anti-Atlas marocain. Paléozoïque inférieur: Cambrien moyen et supérieur – Ordovicien – base du Silurien. Sommaire général sur les mémoires explicatifs. Notes et Mémoires du Service Géologique du Maroc 515, 149p.
Destombes, J., Hollard, H., Willefert, S., 1985. Lower Palaeozoic rocks of Morocco. In: Holland, C.H. (Ed.), Lower Palaeozoic of North-western and West Central Africa. John Wiley, New-York, pp. 91–336.
Deynoux, M., Ghienne, J.F., 2004. Late Ordovician glacial pavements revisited — a reappraisal of the origin of striated surfaces. Terra Nova 16, 95–101.
Deynoux, M., Sougy, J., Trompette, R., 1985. Lower Paleozoic rocks of West Africa and the western part of Central Africa. In: Holland, C.H. (Ed.), Lower Paleozoic rocks of NW and W Central Africa. John Wiley, New-York, pp. 337–495.
Díaz-Martínez, E., Grahn, Y., 2007. Early Silurian glaciation along the western margin of Gondwana (Peru, Bolivia and northern Argentina): palaeogeographic and geodynamic setting. Palaeogeography, Palaeoclimatology, Palaeoecology 245, 62–81.
Dionne, J.-C., 1985. Formes, figures et faciès sédimentaires glaciels des estrans vaseux des régions froides. Palaeogeography, Palaeoclimatology, Palaeoecology 51, 415–451.
Dott, R.H., Bourgeois, J., 1982. Hummocky stratification: significance of its variable bedding sequences. Bulletin of the Geological Society of America 93, 663–680.
Dumas, S., Arnott, R.W.C., 2006. Origin of hummocky and swaley cross-stratification — the controlling influence of unidirectional current strength and aggradation rate. Geology 34, 1073–1076.
Einsele, G., 1992. Sedimentary Basins. Evolution, Facies and Sediment Budget. Springer-Verlag, Berlin. 628 pp.
El Maazouz, B., Hamoumi, N., 2007. Différenciation paléogéographique à l'Ordovicien supérieur dans le Tafilalt (Anti-Atlas oriental, Maroc) sous l'interaction de la glaciation et de la tectonique. Comptes Rendus Géosciences 339, 562–571.
Elaouad-Debbaj, Z., 1984. Chitinozoaires ashgilliens de l'Anti-Atlas (Maroc). Géobios 17, 45–68.
Elaouad-Debbaj, Z., 1986. Chitinozoaires de la Formation du Ktaoua inférieur, Ordovicien supérieur de l'Anti-Atlas, Maroc. Hercynica 2, 35–55.
Elaouad-Debbaj, Z., 1987. Acritarches et Chitinozoaires de l'Ordovicien du Maroc. Systématique, Biostratigraphie, corrélations. Doctoral Thesis of the University of Rennes I (unpublished).
Elaouad-Debbaj, Z., 1988. Acritarches de l'Ordovicien supérieur (Caradoc, Ashgill) de l'Anti-Atlas. Maroc. Revue Micropaléontologie 30, 232–248.
Ennih, N., Liégeois, J.P., 2001. The Moroccan Anti-Atlas: the West African craton passive margin limited Pan-African activity, Implications for the Northern limit of the craton. Precambrian Research 112, 289–302.
Evans, D.A.D., 2003. A fundamental Precambrian — Phanerozoic shift in earth's glacial style? Tectonophysics 375, 353–385.
Fenies, H., Tastet, J.-P., 1998. Facies and architecture of an estuarine tidal bar (the Trompeloup bar, Gironde Estuary, SW France). Marine Geology 150, 149–169.
Finney, S.C., 2005. Global series and stages for the Ordovician System: a progress report. Geologica Acta 3 (4), 309–316.
Fortey, R., Cocks, R., 2005. Late Ordovician global warming — the Boda event. Geology 35, 405–408.
Ghienne, J.F., 2003. Late Ordovician sedimentary environments, glacial cycles, and post-glacial transgression in the Taoudeni Basin, West Africa. Palaeogeography, Palaeoclimatology, Palaeoecology 189, 117–145.
Ghienne, J.-F., Deynoux, M., 1998. Large-scale channel fill structures in Late Ordovician glacial deposits in Mauritania, western Sahara. Sedimentary Geology 119, 141–159.
Ghienne, J.F., Bartier, D., Leone, F., Loi, A., 2000. Caractérisation des horizons manganésifères de l'Ordovicien supérieur de Sardaigne: relation avec la glaciation fini-ordovicienne. Comptes Rendus Académie des Sciences Paris 331, 257–264.
Ghienne, J.-F., Boumendjel, K., Paris, F., Videt, B., Racheboeuf, P., Ait Salem, H., 2007a. The Cambrian–Ordovician succession in the Ougarta Range (western Algeria, North Africa) and interference of the Late Ordovician glaciation on the development of the Lower Palaeozoic transgression on northern Gondwana. Bulletin of Geosciences 82 (3), 183–214.
Ghienne, J.-F., Le Heron, D., Moreau, J., Denis, M., Deynoux, M., 2007b. The Late Ordovician glacial sedimentary system of the North Gondwana platform. In: Hambrey, M., Christoffersen, P., Glasser, N., Janssen, P., Hubbard, B., Siegert, M. (Eds.), Glacial Sedimentary Processes and Products. Special Publication, vol. 39. International Association of Sedimentologists, Blackwells, Oxford, pp. 295–319.
Grahn, Y., Caputo, M.V., 1992. Early Silurian glaciations in Brazil. Palaeogeography, Palaeoclimatology, Palaeoecology 99, 9–15.
Guillocheau, F., 1991. Modalités d'empilement des séquences génétiques dans un bassin de plate-forme (Dévonien armoricain): nature et distorsion des différents ordres de séquences de dépôts emboîtées. Bulletin des Centres de Recherches Exploration-Production Elf-Aquitaine 15, 383–410.
Guillocheau, F., Hoffert, M., 1988. Zonation des dépôts de tempêtes en milieu de plate-forme: le modèle des plates-formes nord-gondwanienne et armoricaine à l'Ordovicien et au Dévonien. Comptes Rendus de l'Académie des Sciences Paris 309, 1047–1053.
Guttierez-Marco, J.C., Destombes, J., Rabano, I., Acenolaza, G.F., Sarmiento, G.N., San José, M.A., 2003. The Middle Ordovician of the Moroccan Anti-Atlas: paleobiodiversity, biostratigraphic review and correlation. Geobios 36, 151–177.
Hammann, W., 1992. The Ordovician trilobites from the Iberian Chains in the province of Aragon, NE-Spain. I. The trilobites of the Cystoid Limestone (Ashgill Series). Beringeria 6, 219.
Hammann, W., Leone, F., 1997. Trilobites of the 'post-Sardic' (Upper Ordovician) sequence of southern Sardinia. Part 1. Beringeria 20, 217.
Hammann, W., Leone, F., 2007. Trilobites of the 'post-Sardic' (Upper Ordovician) sequence of southern Sardinia. Part II. Beringeria 38, 160.
Hamoumi, N., 1988. La plate-forme ordovicienne du Maroc: dynamique des ensembles sédimentaires. Thèse de Doctorat d'Etat, University Louis Pasteur, Strasbourg (unpublished).
Hamoumi, N., 1999. Upper Ordovician glaciation spreading and its sedimentary record in Moroccan North Gondwana margin. Acta Universitatis Carolinae, Geologica 43, 111–114.
Hampson, G.J., Storms, J.E.A., 2003. Geomorphological and sequence stratigraphic variability in wave-dominated, shoreface-shelf parasequences. Sedimentology 50, 667–701.
Hänzschel, W., 1935. Rezente Eiskristalle in meerischen Sedimenten und fossile Eiskristallspuren. Senckenbergiana 17, 151–177.
Haq, B.U., Al-Qahtani, A.M., 2005. Phanerozoic cycles of sea-level change on the Arabian Platform. GeoArabia 10 (2), 127–160.
Haq, B.U., Schutter, S.R., 2008. A chronology of Paleozoic sea-level changes. Science 322, 64–68.

Havlicek, V., 1971. Brachiopodes de l'Ordovicien du Maroc. Notes du Service Géologique du Maroc 230, 1–135.
Hillgärtner, H., Strasser, A., 2003. Quantification of high-frequency sea-level fluctuations in shallow-water carbonates: an example from the Berriasian–Valanginian (French Jura). Palaeogeography, Palaeoclimatology, Palaeoecology 200, 43–63.
Holland, S.M., Patzkowsky, M.E., 1998. Sequence stratigraphy and relative sea-level history of the Middle and Upper Ordovician of the Nashville Dome, Tennessee. Journal of Sedimentary Research 68, 684–699.
Homewood, P.W., Guillocheau, F., Eschard, R., Cross, T.A., 1992. Corrélation Haute Résolution et Stratigraphie Génétique: une approche intégrée. Bulletin des Centres de Recherches Exploration-Production Elf-Aquitaine 16, 357–381.
Homewood, P.W., Mauriaud, P., Lafont, F., 1999. Best practices in Sequence Stratigraphy for explorationists and reservoir engineers. Centres de Recherches Exploration-Production Elf-Aquitaine, Memoir 25, 81.
Huuse, M., Lykke-Andersen, H., 2000. Overdeepened Quaternary valleys in the eastern Danish North Sea: morphology and origin. Quaternary Science Reviews 19, 1233–1253.
Huybrechts, P., 2002. Sea-level changes at the LGM from ice-dynamic reconstructions of the Greenland and Antarctic ice sheets during the glacial cycles. Quaternary Science Reviews 21, 203–231.
Johnson, H.D., Baldwin, C.T., 1996. Shallow clastic seas. In: Reading, H.G. (Ed.), Sedimentary Environments: Process, Facies and Stratigraphy. Blackwell Science, Oxford, pp. 232–280.
Kaljo, D., Hints, L., Martma, T., Nolvak, J., Oraspold, A., 2004. Late Ordovician carbon isotope trend in Estonia, its significance in stratigraphy and environmental analysis. Palaeogeography, Palaeoclimatology, Palaeoecology 210, 165–185.
Kaljo, D., Martma, T., Saadre, T., 2007. Post-Hunnebergian Ordovician carbon isotope trend in Baltoscandia, its environmental implications and some similarities with that of Nevada. Palaeogeography, Palaeoclimatology, Palaeoecology 245, 138–155.
Kidwell, S.M., 1998. Time-averaging in the marine fossil record: overview of strategies and uncertainties. Geobios 30, 977–995.
Kominz, M.A., Pekar, S.F., 2001. Oligocene eustasy from two-dimensional sequence stratigraphic backstripping. Geological Society of America Bulletin 113, 291–304.
Kominz, M.A., Browning, J.V., Miller, K.G., Sugarman, P.J., Mizintseva, S., Scotese, C.R., 2008. Late Cretaceous to Miocene sea-level estimates from the New Jersey and Delaware coastal plain coreholes: an error analysis. Basin Research 20, 211–226.
Laskar, J., 1999. The limits of Earth orbital calculations for geological time-scale use. Philosophical Transactions Royal Society. London A 357, 1735–1759.
Laskar, J., Rotubel, P., Joutel, F., Gastineau, M., Correia, A.C.M., Levrard, B., 2004. A long term numerical solution for the insolation quantities of the Earth. Astronomo and Astrophysics 428, 261–285.
Lasseur, E., Guillocheau, F., Robin, C., Hanot, K., Vaslet, D., Coueffe, R., Neraudeau, D., 2009. A relative water-depth model for the Normandy Chalk (Cenomanian–Middle Coniacian, Paris Basin, France) based on facies patterns of metre-scale cycles. Sedimentary Geology 213, 1–26.
Lavoie, D., 1995. Late Ordovician high-energy temperate-water carbonate ramp, southern Quebec, Canada: implications for Late Ordovician oceanography. Sedimentology 42, 95–116.
Le Heron, D., 2007. Late Ordovician glacial record of the Anti-Atlas, Morocco. Sedimentary Geology 201, 93–110.
Le Heron, D.P., Craig, J., 2008. First-order reconstructions of a Late Ordovician Saharan ice sheet. Journal of the Geological Society 165, 19–29.
Le Heron, D., Dowdeswell, J.A., 2009. Calculating ice volumes and ice flux to constrain the dimensions of a 440 Ma North African ice sheet. Journal of the Geological Society, London 166, 277–281.
Le Heron, D., Sutcliffe, O., Bourgig, K., Craig, J., Visentin, C., Whittington, R., 2004. Sedimentary architecture of Upper Ordovician tunnel valleys, Gargaf Arch, Libya: implications for the genesis of a hydrocarbon reservoir. GeoArabia 9, 137–160.
Le Heron, D.P., Sutcliffe, O.E., Whittington, R.J., Craig, J., 2005. The origins of glacially related soft-sediment deformation structures in Upper Ordovician glaciogenic rocks: implication for ice sheet dynamics. Palaeogeography, Palaeoclimatology, Palaeoecology 218, 75–103.
Le Heron, D.P., Ghienne, J.-F., El Houicha, M., Khoukhi, Y., Rubino, J.-L., 2007. Maximum extent of ice sheets in Morocco during the Late Ordovician glaciation. Palaeogeography, Palaeoclimatology, Palaeoecology 245, 200–226.
Leckie, D.A., Walker, R.G., 1982. Storm- and tide-dominated shorelines in Cretaceous Moosebar–Lower Gates interval-outcrop equivalents of deep basin gas trap in western Canada. Bulletin of the American Association Petroleum Geology 66, 138–157.
Legrand, P., 1974. Essai sur la paléogéographie de l'Ordovicien du Sahara algérien. Compagnie Française des Pétroles, Notes et Mémoires 11, 121–138.
Legrand, P., 1993. Graptolites d'âge ashgillien dans la région de Chirfa (Djado, République du Niger). Bulletin des Centres de Recherches Exploration-Production Elf-Aquitaine 17, 435–442.
Leone, F., Loi, A., Pillola, G.L., 1995. The post-Sardic Ordovician sequence in south-western Sardinia. 6th Paleobenthos International Symposium: Rend. Sem. Fac. Sc. Univ. Cagliari, suppl., vol. 65, pp. 81–106.
Leone, F., Ferretti, A., Hammann, W., Loi, A., Pillola, G.L., Serpagli, E., 1998. Outline of the post-Sardic Ordovician sequence in South-western Sardinia. Giorn. Geologia, ser.3a 60, Spec. Issue, pp. 39–56.
Leone, F., Ferretti, A., Hammann, W., Loi, A., Pillola, G.L., Serpagli, E., 2002. A general view on the post-Sardic Ordovician sequence from SW Sardinia. Rendiconti della Società Paleontologica Italiana 1, 51–68.
Lericolais, G., Berné, S., Féniès, H., 2001. Seaward pinching out and internal stratigraphy of the Gironde incised valley on the shelf (Bay of Biscay). Marine Geology 175, 183–197.
Lodola, D., Kemp, D., Simmons, M.D., 2008. Links between sea-level and palaeoclimates in the Palaeozoic. Abstract volume of the IGCP503 International Congress, Palaeozoic Climates, Lille, august 2008. 60 pp.
Loi, A., 1993. Sedimentological-petrographical study and paleogeographical approach of the Upper Ordovician of the central southern Sardinia. European Journal of Mineralogy "Plinius" 9, 81–86.
Loi, A., Dabard, M.P., 2002. Controls of sea level fluctuations on the formation of Ordovician siliceous nodules in terrigenous offshore environments. Sedimentary Geology 153, 65–84.
Loi, A., Dabard, M.P., Chauvel, J.J., Le Hérissé, A., Pleiber, G., Cotten, J., 1999. Les nodules silico-alumineux: une expression de la condensation sédimentaire sur une plate-forme distale. Comptes Rendus Académie des Sciences Paris 328, 599–605.
Long, D.G.F., 2007. Tempestite frequency curves: a key to Late Ordovician and Early Silurian subsidence, sea-level change, and orbital forcing in the Anticosti foreland basin, Quebec, Canada. Canadian Journal of Earth Sciences 44, 413–431.
Malaske, B., 2001. Anastomosing rivers: a review of their classification, origin and sedimentary products. Earth-Science Reviews 53, 149–196.
Marshall-Neill, G., Ruffell, A., 2004. Authigenic phosphate nodules (Late Cretaceous, northern Ireland) as condensed succession microarchives. Cretaceous Research 25, 439–452.
Melchin, M.J., Holmden, C., 2006. Carbon isotope chemostratigraphy in Arctic Canada: sea-level forcing of carbonate platform weathering and implications for Hirnantian global correlation. Palaeogeography, Palaeoclimatology, Palaeoecology 234, 186–200.
Michard, A., Hoepffner, C., Soulaimani, A., Baidder, L., 2008. The variscan belt. Continental Evolution: The Geology of Morocco. : In: Michard, A., Saddiqi, O., Chalouan, A., Frizon de Lamotte, D. (Eds.), Lecture Notes in Earth Sciences, vol. 126. Springer, pp. 65–132.
Molyneux, S., Osterloff, P., Penney, R., Spaak, P., 2006. Biostratigraphy of the Lower Palaeozoic Haima Supergroup, Oman; its application in sequence stratigraphy and hydrocarbon exploration. GeoArabia 11, 17–48.
Monod, O., Kozlu, H., Ghienne, J.-F., Dean, W.T., Günay, Y., Le Hérissé, A., Paris, F., Robardet, M., 2003. Late Ordovician glaciation in southern Turkey. Terra Nova 15, 249–257.
Nielsen, A.T., 2004. Ordovician sea level changes: a Baltoscandian perspective. In: Webby, B.D., Paris, F., Droser, M., Percival, I. (Eds.), The Great Ordovician Diversification Event. Columbia University Press, New York, pp. 84–93.
Paris, F., 1990. The Ordovician chitinozoan biozones of the northern Gondwana Domain. Review of Palaeobotany and Palynology 66, 181–209.
Paris, F., Elaouad-Debbaj, Z., Jaglin, J.C., Massa, D., Oulebsir, L., 1995. Chitinozoans and Late Ordovician Glacial Events on Gondwana: In: Cooper, C., Droser, M., Finney, S. (Eds.), 7th, ISOS, Society of Economic Paleontologists and Mineralogists (SEPM) publication, Las Vegas, pp. 171–176.
Paris, F., Boumendjel, K., Dabard, M.P., Ghienne, J.-F., Loi, A., Tang, P., Videt, B., Achab, A., 2007. Chitinozoan-based calibration of Early-Mid Ordovician transgressive events on northern Gondwana. Acta Paleotonlogica Sinica 46, 370–375.
Pekar, S.F., Christie-Blick, N., Kominz, M.A., Miller, K.G., 2002. Calibration between glacial eustasy and oxygen isotopic data for the early icehouse world of the Oligocene. Geology 30, 903–906.
Piqué, A., Michard, A., 1989. Moroccan Hercynides, a synopsis. The Paleozoic sedimentary and tectonic evolution at the northern margin of West Africa. American Journal Earth Science 289, 286–330.
Plint, A.G., 1988. Sharp-based shoreface sequences and "offshore bars" in the Cardium Formation of Alberta; their relationship to relative changes in sea level. Sea Level Changes — An Integrated Approach. : In: Wilgus, C.K., Hastings, B.S., Kendall, C.G., St., C., Posamentier, H.W., Ross, C.A., Van Wagoner, J.C. (Eds.), Special Publication, vol. 42. Society of Economic Paleontologists and Mineralogists (SEPM), pp. 357–370.
Plint, A.G., Nummedal, D., 2000. The falling stage systems tract: recognition and importance in sequence stratigraphic analysis. Sedimentary Response to Forced Regression. In: Hunt, D., Gawthorpe, R.L. (Eds.), Special Publication, vol. 172. Geological Society of London, pp. 1–17.
Pope, M.C., 2004. Cherty carbonate facies of the Montoya Group, southern New Mexico and western Texas and its regional correlatives: a record of Late Ordovician paleoceanography on southern Laurentia. Palaeogeography, Palaeoclimatology, Palaeoecology 210, 367–384.
Pope, M.C., Read, J.F., 1998. Ordovician meter-scale cycles: implications for climatic and eustatic fluctuations in the central Appalachians during a global greenhouse, non glacial to glacial transition. Palaeogeography, Palaeoclimatology, Palaeoecology 138, 27–42.
Pope, M.C., Steffen, J.B., 2003. Widespread, prolongated late Middle to Late Ordovician upwelling in North America: a proxy record of glaciation? Geology 31, 63–66.
Reinson, G.E., 1992. Transgressive barrier island and estuarine systems. In: Walker, R.G., James, N.P. (Eds.), Facies Models — Response to Sea Level Change. Geological Association of Canada Publications, pp. 179–194.
Revelle, R.E., 1990. Sea Level Change. National Research Council, Studies in Geophysics, Washington, National Academy Press. 234 pp.
Sadler, M., Cooper, R.A., 2004. Calibration of the Ordovician timescale. In: Webby, B.D., Paris, F., Droser, M., Percival, I. (Eds.), The Great Ordovician Diversification Event. Columbia University Press, New York, pp. 48–51.
Sahagian, D.L., Jones, M., 1993. Quantified Middle Jurassic trough Paleogene eustatic variations based on Russian platform stratigraphy: stage level resolution. Geological Society of America Bulletin 105, 1109–1118.
Saltzman, M.R., Young, S.A., 2005. Long-lived glaciation in the Late Ordovician? Isotopic and sequence-stratigraphic evidence from western Laurentia. Bulletin of the Geological Society of America 33, 109–112.
Schönian, F., Egenhoff, S.O., 2007. A Late Ordovician ice sheet in South America: evidence from the Cancañiri tillites, southern Bolivia. The Evolution of the Rheic Ocean: In: Linnemann, U., Nance, R.D., Kraft, P., Zulauf, G. (Eds.), Geological Society of America, Special Paper, vol. 423, pp. 525–548.
Sharland, P.R., Archer, R., Casey, D.M., Davies, R.B., Hall, S.H., Heward, A.P., Horbury, A.D., Simmons, M.D., 2001. Arabian Plate sequence stratigraphy. GeoArabia Spec. Publ., vol. 2. 371 pp.

Smith, A.G., 1997. Estimates of the Earth's spin (geographic) axis relative to Gondwana from glacial sediments and paleomagnetism. Earth-Science Reviews 42, 161–169.
Spjeldnæs, N., 1961. Ordovician climatic zones. Norsk Geologisk Tidsskrift 41, 45–77.
Storch, P., 1990. Upper Ordovician-lower Silurian sequences of the Bohemian Massif, central Europe. Geological Magazine 127, 225–239.
Storch, P., 2006. Facies development, depositional settings and sequence stratigraphy across the Ordovician–Silurian boundary: a new perspective from the Barrandian area of the Czech Republic. Geological Journal 41, 163–192.
Strasser, A., Pittet, B., Hillgärtner, H., Pasquier, J.-B., 1999. Depositional sequences in shallow carbonate-dominated sedimentary systems: concepts and definitions. Sedimentary Geology 128, 201–221.
Sutcliffe, O.E., Dowdeswell, J.A., Whittington, R.J., Theron, J.N., Craig, J., 2000. Calibrating the Late Ordovician glaciation and mass extinction by the eccentricity cycles of the Earth's orbit. Geology 23, 967–970.
Sutcliffe, O.E., Harper, D.A.T., Aït Salem, A., Whittington, R.J., Craig, J., 2001. The development of an atypical Hirnantian brachiopod fauna and the onset of glaciation in the Late Ordovician of Gondwana. Transactions of the Royal Society of Edinburgh. Earth Sciences 92, 1–14.
Tobin, K.J., Bergström, S.M., De La Garza, P., 2005. A mid-Caradocian (453 Ma) drawdown in atmospheric pCO_2 without ice sheet development ? Palaeogeography, Palaeoclimatology, Palaeoecology 226, 187–204.
Trotter, J.A., Williams, I.S., Barnes, C.R., Lécuyer, C., Nicoll, R.S., 2008. Did ccooling oceans trigger Ordovician biodiversification? Evidence from conodont thermometry. Science 321, 550–554.
Van Dijke, J.J., Veldkamp, A., 1996. Climate-controlled glacial erosion in the unconsolidated sediments of northwestern Europe, based on a genetic model for tunnel valley formation. Earth Surface Processes and Landforms 21, 327–340.
Van Wagoner, J.C., Posamentier, H.W., Mitchum, R.M., Vail, P.R., Sarg, J.F., Loutit, T.S., Hardenbol, J., 1988. An overview of sequence stratigraphy and key definitions. Sea Level Changes — An Integrated Approach. : In: Wilgus, C.K., Hastings, B.S., Kendall, C.G., St, C., Posamentier, H.W., Ross, C.A., Van Wagoner, J.C. (Eds.), Special Publication, vol. 42. Society of Economic Paleontologists and Mineralogists (SEPM, pp. 39–45.
Van Wagoner, J.C., Mitchum Jr., R.M., Campion, K.M., Rahmanian, V.D., 1990. Siliciclastic sequence stratigraphy in well logs, core, and outcrops: concepts for high-resolution correlation of time and facies. American Association of Petroleum Geologists Methods in Exploration Series, vol. 7. 55 pp.
Vandenbroucke, T.R.A., Gabbott, S.E., Paris, F., Aldridge, R.J., Theron, J.N., 2009. Chitinozoans and the age of the Soom Shale, an Ordovician black shale Lagerstätte, South Africa. Journal of Micropalaeontology 28, 53–66.
Vanek, J., Valicek, J., 2001. New index of the genera, subgenera, and species of Barrandian trilobites. Part A–B (Cambrian and Ordovician). Palaeontologia Bohemiae 7, 1–49.
Vaslet, D., 1990. Upper Ordovician glacial deposits in Saudi Arabia. Episodes 13, 147–167.
Vennin, E., Álvaro, J.J., Villas, E., 1998. High-latitude pelmatozoan–bryozoan mud-mounds from the late Ordovician northern Gondwana platform. Geological Journal 33, 121–140.
Villas, E., Vennin, E., Alvaro, J.J., Hammann, W., Herrera, Z.A., Piovano, E.L., 2002. The Late Ordovician carbonate sedimentation as a major triggering factor of the Hirnantian glaciation. Bulletin de la Société Géologique de France 173, 269–278.
Villas, E., Vizcaïno, D., Álvaro, J.J., Destombes, J., Vennin, E., 2006. Biostratigraphic control of the latest-Ordovician glaciogenic unconformity in Alnif (Eastern Anti-Atlas, Morocco), based on brachiopods. Geobios 39, 727–737.
Wade, B.S., Pälike, H., 2004. Oligocene climate dynamics. Paleoceanography 19 (4), PA4019.
Watts, A.B., 2001. Isostasy and Flexure of the Lithosphere. Cambridge University Press. 458 pp.
Webby, B.D., Cooper, R.A., Bergström, S.M., Paris, F., 2004. Stratigraphic framework and time slices. In: Webby, B.D., Paris, F., Droser, M., Percival, I. (Eds.), The Great Ordovician Diversification Event. Columbia University Press, New York, pp. 41–47.
Yang, B.C., Dalrymple, R.W., Chun, S.S., 2005. Sedimentation on a wave-dominated, open-coast tidal flat, south-western Korea: summer tidal flat — winter shoreface. Sedimentology 52, 235–252.
Young, G.M., Minter, W.E.L., Theron, J.N., 2004. Geochemistry and palaeogeography of upper Ordovician glaciogenic sedimentary rocks in the Table Mountain Group, South Africa. Palaeogeography, Palaeoclimatology, Palaeoecology 214, 323–345.

3- Spécificités de l'enregistrement sédimentaire glaciaire fini-ordovicien

Galets et blocs facettés et striés sont parmi les meilleurs indicateurs d'une sédimentation d'origine glaciaire. De haut en bas : galets de quartz, région de Mardin (sud-est de le Turquie, 5 à 7 cm) ; bloc de grès-quartzite, falaise du Hodh (Mauritanie) ; galet de quartz montrant de plus des cupules d'arrachement en croissant (Jordanie, 8 cm).

Publications associées

3.1 Zones de cisaillement sous-glaciaires

Deynoux M., Ghienne J.F. (2004) Late Ordovician glacial pavements revisited – a reappraisal of the origin of striated surfaces. Terra Nova, 16, 95-101.

Deynoux M., Ghienne J.F. (2005) Late Ordovician glacial pavements revisited – a reappraisal of the origin of striated surfaces. Reply. Terra Nova, 17, 488-491.

Moreau J., Ghienne J.-F., Le Heron D., Rubino J.-L., Deynoux M. (2005) 440 Ma ice stream in North Africa

➔ Voir aussi : *Ghienne et al., 2007b* (Chapitre 6) ; Denis et al., 2007

3.2 Vallées en tunnel

Ghienne J.F., Deynoux M., Manatschal G., Rubino J.L. (2003) - Palaeovalleys and fault-controlled depocenters in the Late Ordovician glacial record of the Murzuq Basin (Central Libya), C.R. *Geosciences,* 335, 1091-1100.

Ghienne J.-F. (2009) Late Ordovician tunnel valleys. 71st EAGE Conference & Exhibition. Workshop 5 (Buried glacial valleys and recent advances in understanding groundwater and hydrocarbon reservoirs). Amsterdam, 8-11 juin 2009. Extended Abstract http://earthdoc.eage.org/detail.php?pubid=32190 (conférence invitée)

Douillet G., Ghienne J.-F., Géraud Y., Abueladas A., Diraison M., Al-Zoubi A. (révision mineure) Late Ordovician tunnel valleys in southern Jordan. Special Publication of the Geological Society, London

➔ Voir aussi : Lahondère et al., 2008; *Guttierez-Marco et al., 2010* (Chapitre 4) ; *Loi et al., 2010* (Chapitre 2) ;

3.3 Environnements fluvioglaciaires à dynamique de crues

Ghienne J.-F., Girard F., Moreau J., Rubino J.-L. (2010) Late Ordovician climbing-dune cross-stratification: a signature of outburst floods in proglacial outwash environments? Sedimentology, 57, 1175-1198.

Girard F., Ghienne J.-F., Rubino J.L. (soumis) Channelized sandstone bodies (« Cordons ») in the Tassili n'Ajjer (Algeria & Libya) : snapshots of a Late Ordovician proglacial outwash plain. Special Publication of the Geological Society, London

➔ Voir aussi : Rubino et al., 2003

3.4 Evolution sédimentaire fini- à post-glaciaire

Moreau J., Degermann L., Ghienne J.-F., Rubino J.-L. (2007) Large-scale physiography of the Murzuq Basin shelf during Hirnantian ice-sheet final retreat and Silurian transgression: outcrops and seismic interpretations. 3rd North African/ Mediterranean Petroleum and Geosciences Conference & Exhibition (EAGE extended abstract), 26 to 28 February 2007, Tripoli (Libya).

➔ Voir aussi : *Ghienne, 2003* (Chapitre 6) ; *Ghienne et al., 2007 a et b* (Chapitres 1 et 6) ; Lahondère et al., 2008

Du Protérozoïque au Quaternaire, l'enregistrement sédimentaire d'une glaciation inclut typiquement des planchers striés, des faciès conglomératiques ou de diamictites, la présence de déformations glaciotectoniques (du mm au km), la présence de galets d'origine exotique, facettés et, dans le meilleur des cas, striés (Benn et Evans, 1998). Dans le Paléozoïque nord-gondwanien, certains faciès de dépôt sont tout à fait caractéristiques de la glaciation et totalement absents des successions pré- et postglaciaires. Il s'agit par exemple des « argiles microconglomératiques à blocaux », correspondant en fait le plus souvent à des diamictites sableuses pauvres en galets issus d'une variété d'environnements de dépôt glaciomarins. De même, les faciès à mégarides chevauchantes en régime supercritique sont la signature de régimes de crues proglaciaires ou jökulhlaups (Roberts, 2005 ; Snorrason et al., 2002 ; *Ghienne et al., 2010a*). La seule présence de l'un ou l'autre de ces faciès permet presque à coup sûr d'attribuer une origine glaciogénique *s.l.* à la succession sédimentaire qui les renferme. Tout épisode glaciaire se marque également dans l'enregistrement sédimentaire par des discordances de ravinement à l'échelle des bassins sédimentaires, soit par érosion glaciaire, soit par émersion lors des épisodes de bas niveaux marin glacio-eustatique. Plus généralement, l'amplification des flux sédimentaires (érosion, transport par les eaux de fontes ; Dowdeswell et al., 2002 ; Eyles, 2006) et le déport des sources de sédiments vers l'aval par suite de la migration des fronts glaciaires aboutissent à un cortège de structures sédimentaires qui ne sont pas en elles-mêmes indicatrices d'environnements glaciaires mais qui traduisent une dynamisation d'ensemble du système sédimentaire. Les dynamiques de crue à dimension catastrophique ou l'existence de surpressions fluides généralisées dans les bassins sédimentaires en sont deux exemples. Cette dynamisation affecte non seulement les domaines proglaciaires, mais aussi les domaines océaniques (upwellings) et atmosphérique (contraction des zones bioclimatiques) dont les évolutions sont inscrites dans les messages sédimentaires et bio-géochimiques des plates-formes carbonatées des basses latitudes. Dans les domaines relativement distaux de la plate-forme, et isolés des fronts glaciaires, le maximum glaciaire hirnantien se marque en revanche essentiellement par la mise en place d'environnements de dépôts peu profonds similaires à ceux identifiés dans la succession pré-hirnantienne lors des épisodes de bas niveau marin glacio-eustatiques.

3.1. Zones de cisaillement sous-glaciaires

Au sud de la ville de Ghat à la frontière algéro-libyenne, la photographie aérienne ou l'image satellitaire (ici d'après GoogleEarth, 12x20 km) révèle au toit du Tassili Interne (Cambrien-Ordovicien à gauche), et exhumées sous le Tassili Externe (Silurien-Dévonien, à droite), des alignements de linéations glaciaires à grande échelle témoignant d'un paléo-fleuve de glace ou ice stream (*Moreau et al., 2005*). *Apparaissant ici à peu près au centre de la figure, on peut en observer la courbure, arrivant du sud et se dirigeant initialement N10 avant d'obliquer vers le NNW.*

Les stries glaciaires sont fréquentes dans les grès fini-ordoviciens. Elles peuvent avoir quatre origines distinctes : (i) planchers glaciaires développés à l'interface glace/ substrat ; (ii) bandes de cisaillement affectant une pile de sédiments sous-glaciaires (Boulton, 1996 ; Eyles et Boyce, 1998 ; Evans et al., 2006 ; Piotrowski et al., 2006); (iii); zones de cisaillement en relation avec des glissements gravitaires ; (iv) stries glacielles produites par la dérive de glaces flottantes imprimant leur marque au fond des rivières ou sur les estrans, ou plus au large s'il s'agit d'iceberg. La première interprétation était la plus souvent retenue. L'existence de structures caractérisant des déformations sur matériel meuble a ensuite conduit Woodworth-Lynas et Dowdeswell (1994) à proposer que les surfaces striées ordoviciennes relevaient de processus glaciels. Depuis le début des années 2000 s'est cependant imposé le modèle des bandes de cisaillement intraformationnelles déformant la pile sédimentaire non consolidée sur quelques décimètres à plusieurs mètres sous l'interface glace/ sédiment (*Deynoux et Ghienne, 2004* ; Le Heron et al., 2005 ; Denis et al., 2007 ; Denis et al., 2010). Cette dernière est elle aussi porteuse de stries, mais généralement moins bien exprimées et moins bien préservées que les stries intraformationnelles (*Deynoux et Ghienne, 2005*). Les stries intraformationnelles possèdent des profils en V caractéristiques qui les distinguent des autres types (photo ci-contre).

Le modèle des bandes de cisaillement intraformationnelles implique que la majeure partie du substrat sur lequel circulaient les glaciers ordoviciens était un sédiment, sable ou silt argileux, et non une roche consolidée. Si cela paraît assez intuitif pour des sédiments de l'épisode glaciaire lui-même ou pour des sédiments immédiatement pré-glaciaires, cette remarque est également localement valable pour des zones plus internes où des surfaces striées sont identifiées dans des couches cambriennes, restées à l'état de sédiment pendant plus de 40 millions d'années. Cette observation est à mettre en parallèle avec la quasi-absence de galets de grès et la sur-représentation des sables dans les dépôts glaciaires. Cela suggère que l'essentiel du substrat était constitué de sables.

Les stries ne constituent pas le seul type de linéation glaciaire. On rencontre aussi des cannelures, plus larges, des plis d'entraînement ou plis en fourreaux affectant tout type de lithologie, des pélites aux grès très grossiers, des moutonnements d'envergure plurimétrique et plus ou moins allongé dans le sens de l'écoulement glaciaire (pseudo roches moutonnées, photographie ci-contre), et des linéations à grande échelle (*Moreau et al., 2005* ; *Ghienne et al., 2007b, §6, fig. 4* ; Denis et al., 2010). Ces dernières correspondent aux MSGL (« *mega-scale glacial lineation* ») caractérisées dans le Quaternaire (Canals et al., 2002 ; Andreassen et al., 2007; Ottesen et al., 2008). Dans les exemples ordoviciens, les linéations à grandes échelles

correspondent à des structures taillées dans un noyau de sédiment sous-jacent qui apparaît peu ou non déformé, si ce n'est par quelques surfaces striées intraformationnelles (*Ghienne et Deynoux, 2005*). Ces linéations sont moulées par une carapace de grès intensément déformées présentant le plus souvent des figures de liquéfaction voire de fluidilisation (Denis et al., 2010) et qui représentaient la véritable semelle de glissement du glacier au toit des sédiments. Ces linéations sont larges de un à plusieurs mètres, pour des longueurs de la dizaine de mètres au kilomètre (photographie ci-contre). Facilement repérables sur photographie aérienne, elles apparaissent maintenant sur les images satellitaires couvrant de vastes surfaces exhumées par l'érosion et constituant de véritables surfaces glaciaires fossiles. Un ordre de grandeur au-dessus, un dernier type de linéation glaciaire est constitué par un motif de tôle ondulée présentant des longueurs d'ondes plurikilométriques et des amplitudes verticales de plusieurs dizaines de mètres (< 100 m). Leur cœur est constitué soit de sédiments glaciaires des cycles ou phases glaciaires antérieurs, soit de sédiments préglaciaires. Les linéations de type MSGL leur sont le plus souvent imposées (*Moreau et al., 2005, fig. 4*). Recoupées ensuite par des directions d'écoulement glaciaire sécantes, ces structures prennent la forme de buttes témoins identifiables tant en sismique qu'à l'affleurement (cf. chapitre 6).

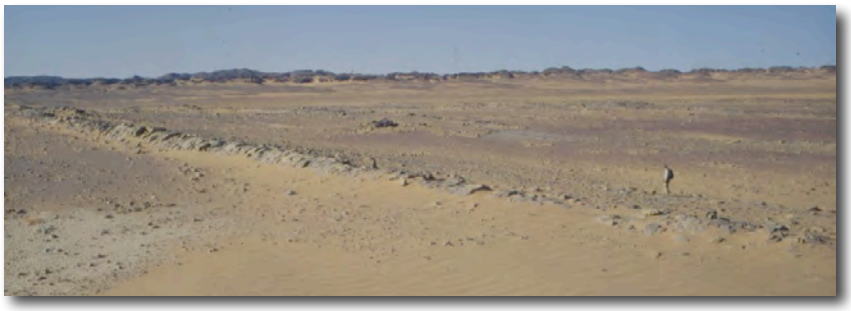

La formation des linéations glaciaires, de l'échelle métrique à l'échelle kilométrique est quasi systématiquement associée à des figures de surpressions fluides, qui en-dehors des classiques liquéfactions, sont à l'origine de tout un cortège de structures d'injection. Injections sableuses quand il s'agit de conduits verticaux cylindriques (diamètre : 5 cm à 2 m), ou des dykes (épaisseur 0,1-1 m) ; injection de fluide en régime turbulent et chargés en sable quand il s'agit de flûtes inversées ou de pseudo-dykes. Ces derniers peuvent former des réseaux polygonaux sur des surfaces de plusieurs km^2 (Denis et al., 2007b) ou être associés aux vallées en tunnel (cf. section 3.2).

L'allongement des linéations à grande échelle, leur distribution cartographique sur des extensions atteignant la centaine de kilomètres, et leur association quasi-systématique avec des processus de surpression fluide affectant la pile sédimentaire sous-glaciaire permettent de les mettre en relation avec des vitesses élevées de l'écoulement glaciaire (*Moreau et al., 2005* ; Denis et al., 2007, 2010 ; *Ghienne et al., 2007b* ; Le Heron et Craig, 2008). Ces lieux d'écoulement préférentiels des glaces drainent les inlandsis et constituent des fleuves de glaces ou « *ice streams* » (Stokes et Clark, 2001 ; Bennett, 2003 ; Stokes et al., 2007; Ó Cofaigh et al., 2010). Les recherches sur les équivalents sub-actuels ont montré que le mécanisme fondamental initiant ces fleuves de glaces était associé à l'existence de surpressions fluides au sein de bassins sédimentaires sous-jacents (Peters et al., 2006), ce que corroborent effectivement l'enregistrement sédimentaire ordovicien.

Une question est fréquemment posée par les personnes habituées des enregistrements sédimentaires glaciaires quaternaires ou permo-carbonifères : où sont les tillites ? Des diamictites sableuses dans le Hodh en Mauritanie ont été interprétées comme des tillites par Deynoux (1980, 1985). Une interprétation alternative a été proposée (*Ghienne, 2003, §6*) qui en fait des coulées de débris remaniant et mixant les dépôts en domaine proglaciaire et comblant des dépressions laissées libres par le retrait glaciaire. En Algérie, les faciès de « moraines de fond » de Beuf et al. (1971)

semblent correspondre en fait à des conglomérats à la base de chenaux ou de vallées en tunnel (cf. section 3.2). A l'est du Bassin de Murzuq, une véritable tillite reposant sur un plancher strié a cependant été identifiée. Plus généralement, des horizons de tillite sont identifiés dans les domaines marginaux d'extension des fronts glaciaires. Il s'agit de niveaux de diamictite sableuse, épais de quelques décimètres, à galets striés orientés, et présentant parfois une foliation. De tels faciès ont été observés en Turquie (*Monod et al., 2003, §4*), en Afrique du Sud (*Deynoux et Ghienne, 2005*) et au Maroc dans les Rehamna au nord du Haut Atlas (*Le Heron et al., 2007, §4*). Dans les domaines proximaux, la dynamique sous-glaciaire était dominée par des processus érosifs. Dans les domaines périphériques, le domaine sous-glaciaire constituait un environnement de dépôt participant au cisaillement en base de glacier (Boulton, 1990, 2006).

doi: 10.1111/j.1365-3121.2004.00536.x

Late Ordovician glacial pavements revisited: a reappraisal of the origin of striated surfaces

Max Deynoux and Jean-François Ghienne

Ecole et Observatoire des Sciences de la Terre, Centre de Géochimie de la surface, CNRS-UMR 7517, 1 rue Blessig, 67084 – Strasbourg, France

ABSTRACT

The recognition of ice-related unconformities is of prime importance when dealing with the sequential architecture of pre-Pleistocene glacial successions. Late Ordovician striated surfaces strikingly preserved in North Gondwana were long considered as abrasion surfaces at the sole of a grounded glacier overriding unlithified sediments, or having resulted from the scouring action of drifting icebergs. Field observations from Mauritania and Libya show that these striated surfaces require an alternative interpretation, which can be applied to similar surfaces described elsewhere, such as in Permo-Carboniferous or Neoproterozoic glacial sequences. A new model is proposed that involves superimposed concurrent décollement planes within a subglacial brittle shear zone in unlithified sand beds. Shear zones in subglacial sediments are well known in Quaternary deposits but, to date, it has not been demonstrated that they may form striated surfaces occurring at continent scale with orientations consistent with palaeo ice-flow reconstructions based on larger-scale indicators.

Terra Nova, 16, 95–101, 2004

Introduction

Striated pavements are glacial features generally observed on hard rock surfaces. They are commonly superimposed on larger landforms such as roches moutonnées, and result from subglacial abrasion by debris-laden ice. In the pre-Quaternary geological record, such striated pavements, overlain by diamictite (tillite) horizons, provide convincing evidence of former glaciations. However, a number of striated surfaces appear to have been formed on unlithified deposits (outwash sandstones or diamictites), questioning their mode of formation, preservation potential and palaeoenvironmental significance. Such soft-sediment striated surfaces are generally interpreted to have been formed by the mechanical action of ice in three different ways: (1) by subglacial erosion of a debris-rich glacier sliding over frozen or compacted sediments (e.g. Westgate, 1968); (2) by scouring and plastic deformation beneath a nearly buoyant moving glacier at its grounding zone (e.g. Visser, 1990); and (3) by the scouring action of drifting icebergs (e.g. Rocha-Campos *et al.*, 1994), sea ice (e.g. Héquette *et al.*, 1995), or shore, estuarine or river ice (e.g. Collinson, 1971; Dionne, 1985). Observations on impressive striated surfaces within Late Ordovician glacial deposits in Mauritania (Deynoux, 1980; Ghienne, 1998) and Libya (M. Deynoux *et al.*, work in progress), and comparison with structures already described in Algeria (Beuf *et al.*, 1971) and Saudi Arabia (Vaslet, 1990; Senalp and Al-Laboun, 2000) (Fig. 1), allow us to propose a fourth process based on the existence of décollement planes in subglacial unlithified deforming beds.

Correspondence: Max Deynoux, Ecole et Observatoire des Sciences de la Terre, Centre de Géochimie de la surface, CNRS-UMR 7517, 1 rue Blessig, 67084 – Strasbourg, France. Tel.: +33 3 90 24 04 42; fax: +33 3 88 36 72 35; e-mail: mdeynoux@illite.u-strasbg.fr

Geological setting

In the three studied areas, the Hodh in the Taoudeni Basin of Mauritania, and the Gargaf and Ghat areas in the Murzuq Basin of Libya, the Late Ordovician glacial drift forms discontinuous outcrops filling up to 150-m-deep broad palaeodepressions or N–S- to WNW–ESE-orientated palaeovalleys cut into Cambro-Ordovician sandstones.

In the Hodh area, the glacial deposits consist of a lower continental succession onlapped by an upper marine succession (Deynoux, 1980, 1985; Ghienne, 1998, 2003) (Fig. 2). The continental succession is made up of cross-bedded sandstones forming 0–100-m-thick erosion-based bodies overlain by 0–50-m-thick poorly exposed horizons made up of unstratified argillaceous microconglomeratic sandstones with polymict striated pebbles to boulders. The striated surfaces occur in the upper part of the sandstones that were deposited by glaciofluvial streams in an outwash plain. Intercalated argillaceous deposits are either subglacial tillites or proglacial tillite-reworking debris flows.

In the Gargaf area, the glacial drift is made up of a succession of three stratigraphic units (Fig. 2). The lower unit forms a coarsening-up sequence comprising storm-dominated shelf to shoreface deposits with glaciomarine influence. The middle unit is made up of fluvial sandstones with fine- to coarse-grained meander belt and flood-related deposits. The upper unit consists of an imbrication of coarsening-up depositional systems, including several fluvial-dominated to wave-influenced coarsening-upward deltaic deposits. The middle and upper units are separated by an erosional glacial and transgressive surface, which displays the striations.

In the Ghat area, the sedimentary succession is roughly similar (Fig. 2). The striated surfaces occur in association with low-relief erosional surfaces atop cross-bedded fluvial sandstones. These surfaces display drumlin-like alignments, up to 10 m wide and several kilometres long, identifiable on aerial and satellite images with a constant NNW–SSE trend (Fig. 3). They are onlapped by coarsening-up delta-like

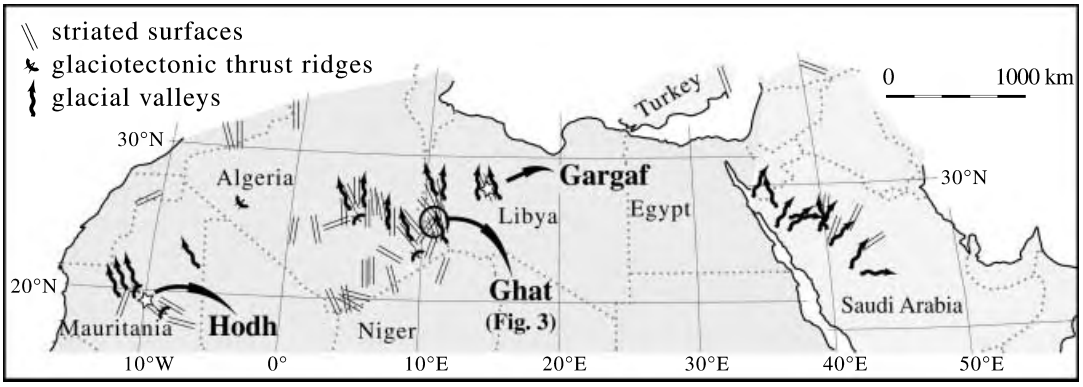

Fig. 1 Large-scale distribution of the main Late Ordovician palaeo-ice flow indicators on the northern Gondwana platform.

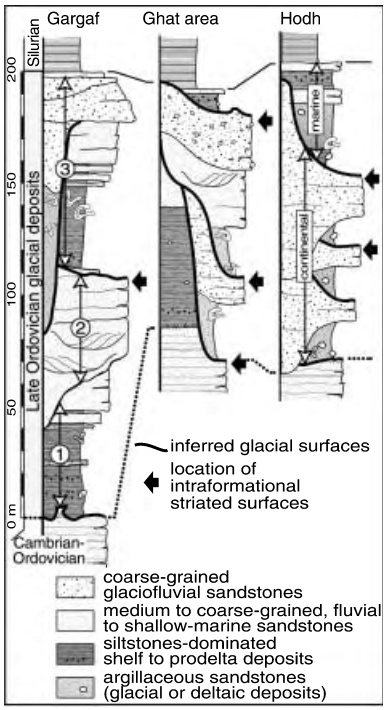

Fig. 2 Synthetic logs of the glacial successions with location of the striated surfaces.

successions, starting with microconglomeratic, argillaceous sandstones including lonestones.

Characteristics of the striated pavements

Stratigraphic occurrence

At the regional scale, the striated surfaces are found at the transition between glaciofluvial sandstones and overlying mudstones to argillaceous sandstones, which display evidence of glacial input (diamictites interpreted as subglacial tillite or tillite-reworked debris flow, or dropstone-bearing shelf to prodeltaic deposits). However, at the outcrop scale, the striated surfaces are generally not found precisely at the interface between these two contrasting lithologies. In many examples, they are observed in the upper part of the fluvial sandstones, over flat horizontal to slightly undulating surfaces (Fig. 4a). These surfaces are laterally overlain by dismantled patches decimetres to a few metres thick of chaotic structureless to highly deformed sandstones that were called 'grès bousculés' by Deynoux (1980) in Mauritania. These disturbed sandstones are petrographically similar to the underlying fluvial sandstones. They comprise decimetre- to metre-scale folded structures (including unrooted sheath folds), rare intraformational sheared clasts or sandstone masses, and dewatering structures such as pipes (Fig. 4b) and vertical sand sheets. In the Ghat area the 'grès bousculés' form the above-mentioned drumlin-like alignments (Fig. 3).

Additional striated surfaces, with similar characteristics and orientations, can be found at different superimposed horizons within apparently undeformed fluvial sandstones, up to several metres below the uppermost striated surface (Fig. 4c). In the Ghat area, several vertically superimposed surfaces were observed with strictly parallel striations within a 20-m-thick cross-stratified, sandstone succession. In these intraformational occurrences, it is possible to observe that the base of the overlying sandstone bed shows exactly the negative counterpart of the underlying striations.

Detailed features of the striated surfaces

Striae are no more than a few millimetres deep, but can be traced over several metres in length. They are straight features with in a few cases local individual gentle curvature. They consist of the juxtaposition of parallel ridges and troughs (Fig. 4e). In cross-section, ridges, a few millimetres to 1 cm in width, are flat, bumpy or sharp, whereas troughs are generally narrower and sharper with often a V-shaped symmetric profile. They are commonly superimposed on large and shallow grooves (Fig. 4a).

Associated structures

Sandstones beneath a striated surface very often show small-scale extensional step fractures (Biju-Duval *et al.*, 1974). Primary sedimentary laminations are displaced. Step fractures immediately below striated surfaces are characterized by a uniform orientation that is perpendicular to the striae direction and these fractures do not interrupt the striated surface (Fig. 4d). Most fractures dip up-glacier. In rare finer-grained and silty intercalations, small-scale sheath folds and extensional crenulation cleavages were observed several metres below the 'grès bousculés'. Relatively rare features also occur on the striated surfaces. They were observed on the uppermost surfaces overlain by the 'grès bousculés'. They consist of thin sand flows

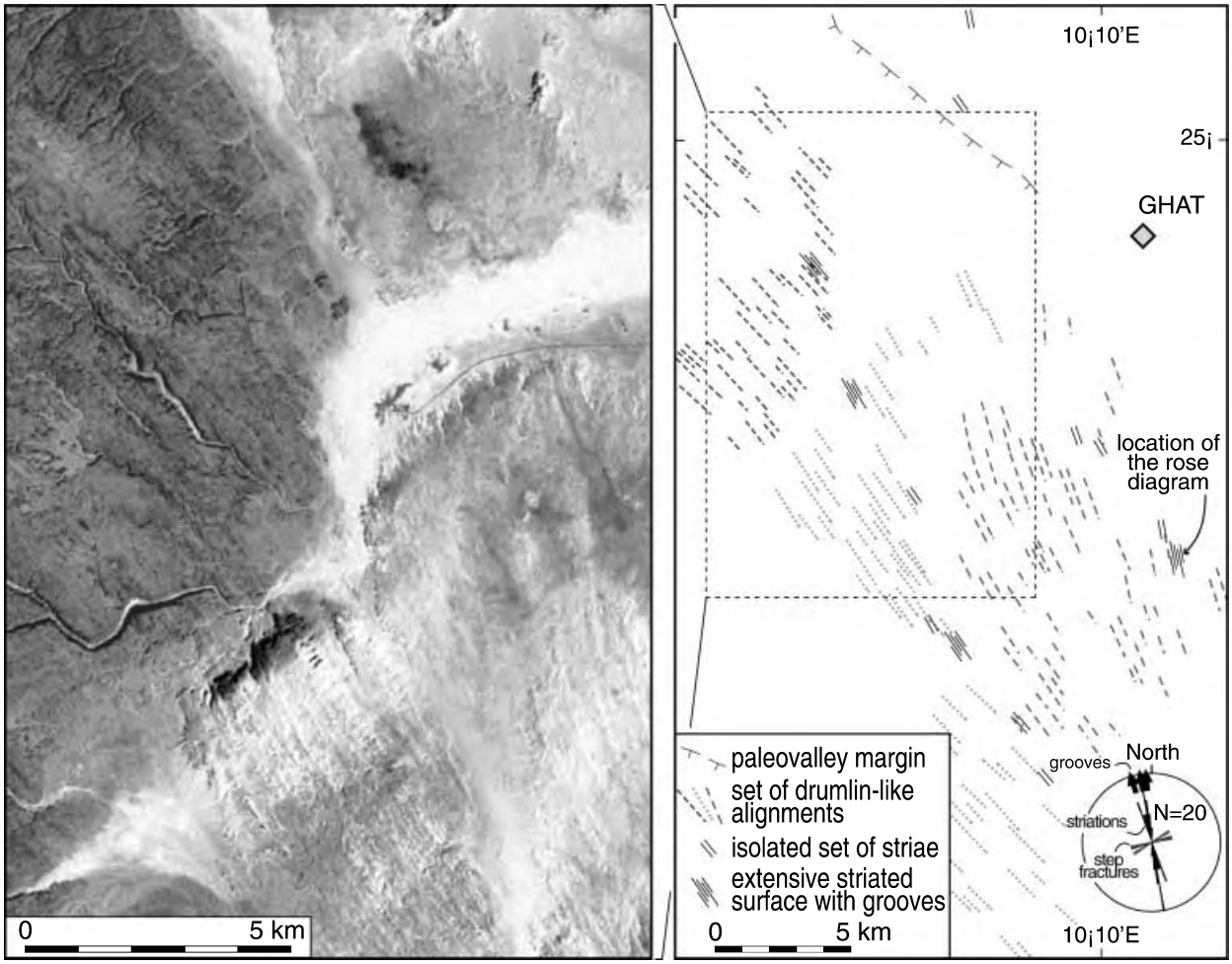

Fig. 3 Sketch map from a Landsat satellite image of the drumlin-like alignments in the Ghat area. The rose diagram refers to striae and step fracture orientations measured on superposed striated surfaces in a 5-m-thick exposure of glaciofluvial sandstones (same location as for Fig. 4c). Satellite image from Nasa Geocover Website (zulu.ssc.nasa.gov/mrsid/).

covering the striations (Fig. 4a), or filling small orthogonal trough-dissecting ridges and connecting troughs on the striated surfaces. Short gouges with lateral ridges and plough marks at their downstream head, inscribing the striated surfaces, were also observed (Fig. 4f).

Orientation

At a regional scale, the striae orientation, as well as indicators of the sense of movement (crescent-shaped fractures, ploughed grooves), is consistent with larger-scale ice-flow indicators such as glaciotectonic thrust ridges, glacial valleys and streamlined subglacial bedforms. They are also consistent with palaeocurrents measured in the glaciofluvial sandstones. At the continental scale (Fig. 1), this homogeneity of orientation supports the palaeogeographical reconstruction of an ice sheet flowing from the south over the North Gondwana platform (Beuf *et al.*, 1971; Deynoux, 1980, 1985; Vaslet, 1990; Ghienne, 1998, 2003).

Interpretation

Striated surfaces are intraformational structures, as shown by their superimposition with their negative counterparts, that occur at various horizons within proglacial outwash sandstones. Because most of the previously described Late Ordovician striated pavements were observed on the present-day exposed upper part of the sandstones, a subglacial abrasion process has usually been proposed (e.g. Beuf *et al.*, 1971; Senalp and Al-Laboun, 2000). However, accurate observations show that, in fact, these uppermost exposures are generally laterally overlain by the 'grès bousculés' that are easily dismantled due to their disturbed and chaotic nature. Accordingly, an origin by subglacial abrasion would imply a purely sandy till origin for the 'grès bousculé'. Their disturbed aspect may fit with such an interpretation, but this cannot be applied to the undisturbed intervening sandstones between the underlying striated surfaces. The superposition of several striated surfaces within the same sandstone succession would represent repetitive glacial advances or repetitive uplift of a nearly buoyant tidewater glacier. However, the

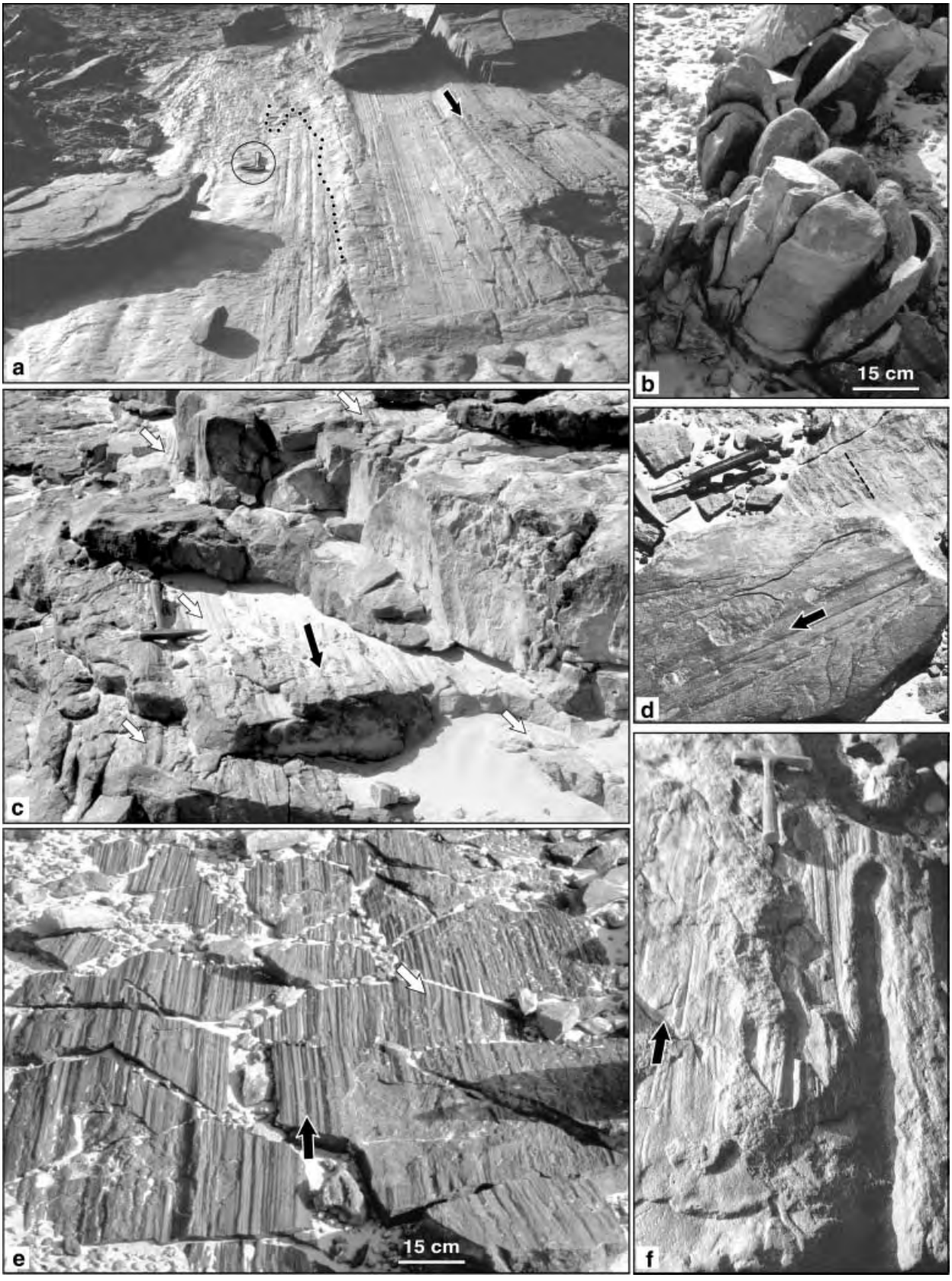

Fig. 4 Examples of striated surfaces; black arrows indicate the palaeo-ice flow orientation. (a) Striations superimposed on large and shallow grooves in the Ghat area. In the background behind the circled hammer, the striae are covered by a thin sand sheet (dotted line) flowing from the lateral ridge of a groove. (b) Sandstone pipes in the Gargaf area, reflecting fluidization and water-escape within the 'grès bousculé'. (c) Five superimposed striated surfaces (white arrows) in a less than 2-m-thick cross-bedded glaciofluvial sandstone in the Ghat area. (d) Step fractures (parallel to the dashed line) perpendicular to the immediately overlying striae. (e) Typical view of a striated surface in the Gargaf area. Note the bumpy and V-shaped aspect of, respectively, the ridges and intervening troughs, and the local gentle curvatures (white arrow). (f) Gouge with lateral ridges and frontal plough mark scribing a striated surface in the Hodh area. Hammer for scale.

V-shaped profile of individual striae cannot be explained either by sand-sized or clast-sized erosional in-ice tools. Sand grain settlement in a standing water body or even sand deposition from meltwater flow over frozen pavement might also be envisaged. Both scenarios do not fit with the fluvial and homogeneous nature of the intervening sandstones and would not favour preservation of perfect striated pavements. Scouring by free-floating glacial ice masses was alternatively proposed by Woodworth-Lynas and Dowdeswell (1994) for the Late Ordovician striated and grooved surfaces reported by Beuf *et al.* (1971) in Algeria and by Vaslet (1990) in Arabia. In addition to the absence of specific characteristics, the intraformational character of the striations, their constant regional orientation and the fluvial nature of the associated sediments do not support this interpretation.

The intraformational character of the striations, and their association with folds, step fractures and plough marks strongly suggest that they were produced within a shear zone affecting unlithified sediment several metres thick. The striated surfaces correspond to brittle shear planes in granular material (Mandl *et al.*, 1977; Passchier and Trouw, 1996). Associated step fractures are interpreted as Riedel shears within which fractures dipping up-glacier are more common. Structures indicative of ductile deformation (*sensu* Van der Wateren *et al.*, 2000) are poorly developed and are mainly represented by fold structures in the 'grès bousculés'.

Shear zones in subglacial or proglacial deformable sediments are well known in Quaternary deposits (e.g. Hart and Boulton, 1991; Van der Wateren, 1995; Boulton, 1996a; Van der Wateren *et al.*, 2000). Deformed beds occur when a glacier moves over unlithified sediments, within which a high pore-water pressure is generated. This leads to a coupling between the ice sheet and the underlying sediment. The Ordovician striated surfaces exist almost everywhere within a 700-km-wide area behind the inferred maximum ice-front position. Their distribution and usual association with drumlin-like alignments suggest formation within a subglacial peripheral zone of the ice-sheet of the order of 1000 km in width.

In most of the subglacial deformation models, strain rates decrease gradually with depth. Although the lower contact of the shear zone does not generally correspond to a sharp discontinuity above the underlying undeformed substratum, this contact corresponds to a sliding décollement surface in several Quaternary examples (Boulton, 1987; Hart and Boulton, 1991; Boulton and Dobbie, 1993; Van der Wateren, 1995). Superposed striated surfaces in the Ordovician examples could be interpreted either as successive basal décollement planes occurring at different depths depending on pore-water pressure and basal shear stress, or as simultaneous shear planes within a brittle shear zone. The absence of subsequent deformation in association with the striated surfaces in the deeper horizons supports the latter interpretation. Finally, Late Ordovician superposed striated surfaces are interpreted as concurrent intraformational décollement surfaces, within a subglacial brittle shear zone in unlithified deforming sand beds (Fig. 5).

Field observations have shown that Ordovician subglacial shear zones

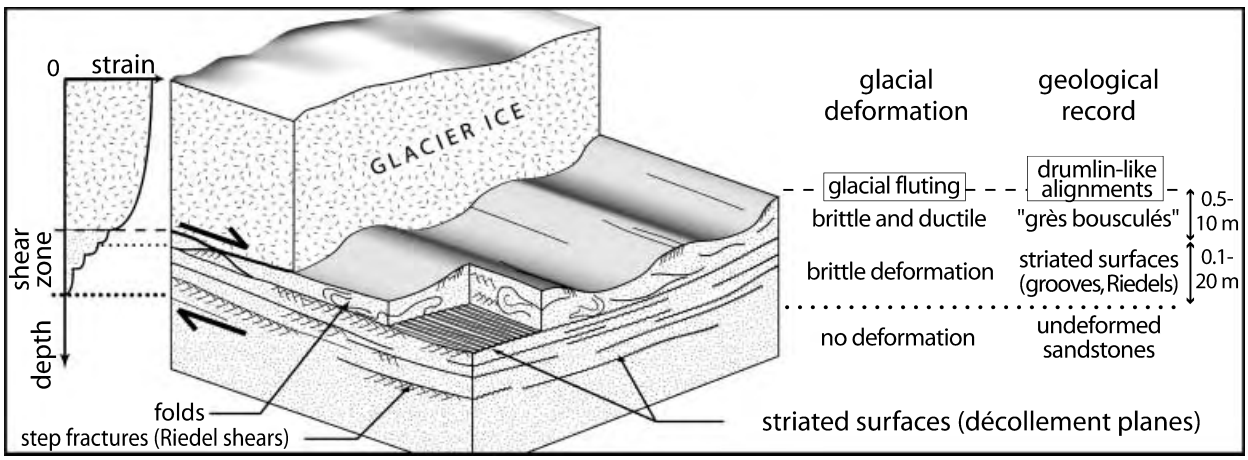

Fig. 5 Interpretative sketch for the origin of the striated surfaces and associated structures.

are made up of two superimposed deformation zones. In the lower one, which includes the striated décollement planes, Riedel shears (step fractures) and discrete small-scale sheath folds affecting only finer-grained intercalations, brittle deformation predominates in compacted fairly well-drained (or frozen?) sands. The upper deformation zone, which corresponds to the 'grès bousculés', is characterized by pervasive deformation including large-scale unrooted sheath folds and drumlin-like alignments. Here, the combination of higher shear stress with pore-water overpressure may explain a more ductile style of deformation. If the amount and nature of strain is sufficient to disorganize the geometric relationships between the sediment grains, at least part of the 'grès bousculés' can be considered as a deformation till (Elson, 1957; Boulton, 1996b). This is compatible with the formation of drumlin-like alignments (Boulton, 1987, 1996a).

The presence within the 'grès bousculés' of folded Riedel shears and rare intraformational clasts (some made up of pieces of striated surfaces), capable of scribing gouges with plough marks, indicates that the lower limit of this relatively more ductile horizon was able to cut down into the underlying brittle shear zone. A comparable process was described as excavational deformation by Hart and Boulton (1991) and as subglacial erosion beneath extensional ice flows in (Boulton 1996a) model. The application of the latter model to the Ordovician setting might suggest that the striated surfaces were possibly formed up-ice from the glacial equilibrium line.

The appearance of non-deformed to poorly deformed water-escape structures at the upper part of the sandstones and generally in association with the 'grès bousculés', as well as the development of well-preserved liquefaction structures (convolute bedding, incipient sand flows dissecting the striations), suggests that intraformational liquefaction and dewatering represent final processes in the evolution of the shear zone. Some observed channels, which cut into the 'grès bousculés' and underlying striated sandstones, might represent a late subglacial drainage system. It is suggested that dewatering in the underlying sediments occurred during ice-front retreat, leading to locking of the deformation, and finally to fossilization of the subglacial shear zone. Dewatering may be related either to compressional ice flows replacing extensional ice flows during the concomitant retreats of both the ice-front and the glacial equilibrium line, or to other conditions resulting in a more efficient subglacial drainage during ice-sheet recession.

Conclusions

Most of the striated surfaces observed in the Late Ordovician glacial drift in northern Gondwana, and probably some of those in pre-Pleistocene glaciations elsewhere, correspond to décollement surfaces in subglacial unlithified deforming beds. The intraformational character of the décollement surfaces favours their preservation, whereas actual glacial pavements and typical subglacial deposits (diamictites) have a low preservation potential when exposed to subsequent fluvial erosion or to the ravinement by waves during post-glacial transgression.

Even if striated surfaces are not true glacial pavements, they can be used to confirm the existence of an overriding glacier, and to define its palaeo-flow trend. The recognition of subglacial soft sediment deformation in Late Ordovician ice-sheet dynamics has inferences for the former ice-sheet characteristics such as its thermal regime, ice thickness and subsequent isostasic effect, terrestrial or marine setting, erosive and depositional behaviour. Accordingly, this new interpretation of the Late Ordovician striated surfaces offers novel perspectives that will encourage a new approach to the glaciofluvial sandstones and associated structures in pre-Pleistocene glaciations.

References

Beuf, S., Biju-Duval, B., De Charpal, O., Rognon, P., Gariel, O. and Bennacef, A., 1971 *Les grès du Paléozoïque inférieur au Sahara*. editions Technip, Paris.

Biju-Duval, B., Deynoux, M. and Rognon, P., 1974. Essai d'interprétation des 'fractures en gradins 'observées dans les formations glaciaires précambriennes et ordoviciennes du Sahara. *Rev. Géogr. Phys. Géol. Dynamique, Paris*, **16**, 503–512.

Boulton, G.S., 1987. A theory of drumlin formation by subglacial deformation. In: *Drumlin Symposium* (J. Menzies and J. Rose, eds), pp. 25–80. Balkema, Rotterdam.

Boulton, G.S., 1996a. Theory of glacial erosion, transport and deposition as a consequence of subglacial sediment deformation. *J. Glaciol.*, **42**, 43–62.

Boulton, G.S., 1996b. The origin of till sequences by subglacial sediment deformation beneath mid-latitude ice-sheets. *Ann. Glaciol.*, **22**, 75–84.

Boulton, G.S. and Dobbie, K.E., 1993. Consolidation of sediments by glaciers: relations between sediment geotechnics, soft-bed glacier dynamics and subglacial ground-water flow. *J. Glaciol.*, **39**, 26–44.

Collinson, J.D., 1971. Some effects of ice on a river bed. *J. Sedim. Petrol.*, **41**, 557–564.

Deynoux, M., 1980. Les formations glaciaires du Précambrien terminal et de la fin de l'Ordovicien en Afrique de l'ouest. Deux exemples de glaciation d'inlandsis sur une plate-forme stable. *Travaux Lab. Sci. Terre, St. Jérome, Marseille*, **B17**.

Deynoux, M., 1985. Terrestrial or water-lain glacial diamictites? Three case studies from the Late Precambrian and Late Ordovician glacial drifts in West Africa. *Palaeogeogr. Palaeoclimatol. Palaeoecol.*, **51**, 97–141.

Dionne, J.-C., 1985. Formes, figures et facies sédimentaires glaciels des estrans vaseux des régions froides. *Palaeogeogr. Palaeoclimatol. Palaeoecol.*, **51**, 415–451.

Elson, J.A., 1957. Origin of washboard moraines. *Geol. Soc. Am. Bull.*, **68**.

Ghienne, J.-F., 1998 Modalités d'enregistrement d'une glaciation ancienne; exemple de la glaciation fini-ordovicienne sur la plate-forme nord-gondwanienne en Afrique de l'Ouest. Doctoral Dissertation, Université Louis Pasteur, Strasbourg.

Ghienne, J.-F., 2003. Late Ordovician sedimentary environments, glacial cycles, and post-glacial transgression in the Taoudeni Basin, West Africa. *Palaeogeogr. Palaeoclimatol. Palaeoecol.*, **189**, 117–145.

Hart, J.K. and Boulton, G.S., 1991. The interrelation of glaciotectonic and glaciodepositional processes within the glacial environment. *Quat. Sci. Rev.*, **10**, 335–350.

Héquette, A., Desrosiers, M. and Barnes, P.W., 1995. Sea ice scouring on the inner shelf of the southeastern Canadian Beaufort Sea. *Mar. Geol.*, **128**, 201–219.

Mandl, G., de Jong, L.N.J. and Maltha, A., 1977. Shear zones in granular material. *Rock Mechanics*, **9**, 95–144.

Passchier, C.W. and Trouw, R.A.J., 1996 *Microtectonics*. Springer Verlag, Berlin.

Rocha-Campos, A.C., Dos Santos, P.R. and Canuto, J.R., 1994. Ice scouring in Late Paleozoic rhythmites, Parana Basin, Brazil. In: *Earth's Glacial Record* (M. Deynoux, J.M.G. Miller, E.W. Domack, N. Eyles, I.J. Fairchild and G.M. Young, eds), pp. 234–240. Cambridge University Press, Cambridge.

Senalp, M. and Al-Laboun, A., 2000. New evidence of the Late Ordovician Glaciation in Central Saudi Arabia. *Saudi Aramco J. Technol.*, 11–40.

Van der Wateren, F.M., 1995. Structural geology and sedimentology of push moraines. Processes of soft sediment deformation on a glacial environment and the distribution of glaciotectonic styles. *Mededelingen Rijks Geologishe Dienst, Haarlem*, **54**.

Van der Wateren, F.M., Kluiving, S.J. and Bartek, L.R., 2000. Kinematic indicators of subglacial shearing. In: *Deformation of Glacial Materials* (A. Maltman, B. Hubbard and M. J. Hambrey, eds). *Geol. Soc. London, Spec. Publ.*, **176**, 259–278.

Vaslet, D., 1990. Upper Ordovician glacial deposits in Saudi Arabia. *Episodes*, **13**, 147–161.

Visser, J.N.J., 1990. Glacial bedforms at the base of the Permo-Carboniferous Dwyka formation along the western margin of the Karoo Basin, South Africa. *Sedimentology*, **37**, 231–245.

Westgate, J.A., 1968. Linear sole markings in Pleistocene till. *Geol. Mag.*, **105**, 501–505.

Woodworth-Lynas, C.M.T. and Dowdeswell, J.A., 1994. Soft-sediment striated surfaces and massive diamicton facies produced by floating ice. In: *Earth's Glacial Record* (M. Deynoux, *et al.*, eds), pp. 241–259. Cambridge University Press, Cambridge.

Received 23 December 2003; revised version accepted 16 February 2004

doi: 10.1111/j.1365-3121.2005.00640.x

Reply

Late Ordovician glacial pavements revisited: a reappraisal of the origin of striated surfaces

Max Deynoux and Jean-François Ghienne

Ecole et Observatoire des Sciences de la Terre, Centre de Géochimie de la surface, CNRS-UMR 7517, 1 rue Blessig, 67084 Strasbourg, France

Introduction

The aim of our paper was to propose a well-argued genetic model for the formation of a widespread type of subglacial, intraformational striated surface, which has been repeatedly observed in the pre-Pleistocene glacial record (e.g. Ghienne, 1998; Lopez-Gamundi and Martinez, 2000; Senalp and Al-Laboun, 2000; Sutcliffe *et al*., 2000) but never fully described and discussed. We thank Sutcliffe *et al*. for their comments that will allow us to specify some points and to depict some additional aspects, which may promote further developments.

The formation of intraformational striated surfaces

Sutcliffe *et al*. claim that ductile deformation is closely associated with the intraformational striated surfaces, implying that these structures were formed in ductile sediments. We agree that abundant folding (overturned cross-strata, drag folds, sheath folds, etc.) and loading structures are locally preserved in association with intraformational striated surfaces. However, most of these structures are generally considered as resulting from the loss of strength in overpressured sands and subsequent laminar (viscous) shear, as in the case of liquefaction structures. We only regard the occurrence of sheath folds as factual evidence for the ductile deformation of planar structures. However, if 'ductile' deformation structures occurred in close spatial association with striated surfaces, this does not imply that striated surfaces formed contemporaneously with 'ductile' deformation structures within the same horizon beneath the ice sheet. The intraformational décollement planes, which correspond to a relative displacement between two horizons, are associated with Riedel structures typically observed in fault zones. Striated surfaces record brittle failure in sands and this interpretation is in agreement with the fact that striated surfaces are generally not directly associated with folding deformation as shown by the undeformed primary sedimentary structures preserved just above and/or below the surfaces.

While we could consider that the formation of slickensides in granular material (e.g. Mandl *et al*., 1977) might be an analogue for the formation of intraformational subglacial striae, we cannot follow the proposition that 'striations may reflect the intense ductile deformation of planar structures'. The morphology of the striae (V-shaped, linear, parallel, etc.) is not related to the primary sedimentary structures occurring in sheared sandstones, which can display massive, rippled or horizontally laminated, or even cross-laminated beds. The morphology of the striae is similarly not dependent on the granulometry of the sandstones (fine to coarse), suggesting that abrasion is a negligible process in the formation of striated surfaces (except if an intraclast occurs). Another argument against the ductile origin of striated surfaces is the general observation that décollement planes are never refolded (except in case of deformation related to a subsequent glacial event), a condition which is unlikely to occur in a ductile setting.

Correspondence: Dr Max Deynoux, Directeur de Recherche Emérite, Ecole et Observatoire des Sciences de la Terre (EOST), Centre de Géochimie de la Surface, UMR 7517, 1, rue Blessig, 67084 Strasbourg Cedex, France. Tel.: +33 3 90 24 04 42; fax: +33 3 90 24 04 02; e-mail: mdeynoux@illite.u-strasbg.fr

Temporal relationship between 'ductile' deformation and striated surfaces

The understanding of associated striated surfaces and 'ductile' deformation is not straightforward and the data given by Sutcliffe *et al*. in their comments cannot afford the distinction between the four following propositions:

1. Folding and loading represent a former, totally disconnected mode of deformation of the subglacial sediment layer, which is overprinted afterwards by striated surfaces (see the South African example below);
2. Folding and loading reflects a dilative behaviour in overpressured sands immediately before the formation of the striated surfaces. A more compact grain-to-grain framework results, which is subsequently deformed under brittle conditions (e.g. Murray, 1994);
3. Folding and loading occurred simultaneously in close association with the striated surfaces in the same subglacial horizon (preferred model of the authors' comment);
4. Folding and loading structures occurred simultaneously but in different horizons in a contemporaneous deforming subglacial sediment layer, the boundary between the two modes of deformation migrating vertically through time (our preferred model).

As proposed in Deynoux and Ghienne (2004), and in agreement with the comment, 'subglacial shear zone are probably characterized by the heterogeneous distribution of strain with sporadic discontinuous deformation and regular changes in the position of a transition from ductile to brittle sediments'. Our model (Fig. 5 of Deynoux and Ghienne, 2004)

represents a subglacial shear zone in a homogeneous succession of sand beneath an ice sheet. Clearly, this is an oversimplification when several layers of sediments with distinct rheology are usually encountered. As expected, folding is classically observed in silty horizons beneath or between sand-dominated horizons displaying décollement planes. However, at the first order, we maintained that the subglacial shear zone can be subdivided in an upper part with abundant deformation structures (our 'brittle and ductile' horizon, or 'grès bousculés') and a lower part essentially characterized by striated surfaces (our 'brittle' horizon). This model parallels observations in modern glacial setting in which the upper part of the deformation zone was dilated and prone to viscous deformation in contrast to deeper parts that appear to have deformed along discrete planes (Boulton and Dent, 1974). Because the displacement is transferred across the deformation zone by a combination of continuous and discontinuous strain, the subglacial deformation zone corresponds strictly speaking to a brittle–ductile shear zone (e.g. Van der Wateren *et al.*, 2000).

A South African case study

In their comment, Sutcliffe *et al.* frequently referred to South African examples; we would also like to refer to observations made by one of us (JFG) near Clanwilliam (Pakhuis Pass, Western Cape Fold Belt). Here, an outstanding exposure shows a suite of soft-sediment deformations overlain by a glaciomarine succession (Fig. 1).

Deformation in the lowermost levels is ascribed to extensive loading and folding (Blignault, 1981). This deformation can be interpreted either as resulting from earlier subglacial conditions or corresponding to conditions of dilative deformation immediately prior to the formation of the striated surface. The former hypothesis is preferred because 'ductile' deformation structures are one order greater in size than those relative to the formation of the striated surfaces and streamlined bedforms. This first stage of deformation is interpreted as reflecting full glacial conditions with relatively slow flowing ice.

Streamlined bedforms, striated surfaces and associated deformations are interpreted as a subglacial soft-sediment shear zone totally consistent with our proposed model and most probably developed under fast flowing ice as shown by the high elongation ratio of the streamlined bedforms. Step fractures dipping up-ice (Fig. 1d; Biju-Duval *et al.*, 1974) post-date the formation of the striated surface and reflect later shearing within the shear zone. The stratigraphic location and the clast fabric of the diamictite horizon suggest a terrestrial tillite. Deposition of the tillite may either be concurrent or post-date the deformation stage in the marginal subglacial zone. The succession from the lowermost, folded soft-sediments, up to the tillite and the overlying glaciomarine sequence is interpreted as a comprehensive record of a deglaciation sequence, first characterized by deformation events and continued by deposition events.

Recognition of different types of subglacial décollement planes in soft sediments

It is well known that several décollement surfaces may occur between the clean ice and the underlying undeformed sediments (e.g. Murray, 1994; Hart, 1998). The genetic model proposed in Deynoux and Ghienne (2004) is only valid for striated surfaces deeply sited in subglacial soft-sediment deforming layers. Other types of décollement plane also exist overlying extensive ductile deformations, an association that may explain some misinterpretations. Based on Late Ordovician examples, three types of décollement surfaces are recognized in subglacial soft-sediment shear zones. They were successively identified from base to top in the South African example (Fig. 1h).

The type 1 surface, which corresponds to our genetic model, was a truly intraformational, fully striated décollement plane. It usually occurs in inner segments of the subglacial zone (Mauritania, Algeria, Libya, Saudi Arabia). Both the hangingwall and the footwall are characterized by a strictly identical sandy lithology. This is clearly different from the conventional subglacial abrasion process.

The type 2 surface, occasionally striated, formed the boundary between a subglacial tillite and underlying soft sediments (e.g. Ehlers and Stephan, 1979). Such surfaces, capped by loose lithologies (the tillite), are poorly preserved but were identified in the ice-marginal setting of the Late Ordovician glacial record in Turkey (Fig. 4b of Monod *et al.*, 2003), Morocco (D. Le Heron and J.-F. Ghienne, unpublished data) and South Africa (Fig. 1e). Here, abrasion is a significant process as shown by the granule-size striae, furrows and ploughing structures due to the scratching effect of the overlying heterogeneous material. If the lithology of the tillite is roughly similar to the underlying sandstone, this type of surface would be difficult to distinguish from type 1. Type 2 surfaces are in places true intraformational décollement plane but may also locally corresponds to a type 3 surface fossilized by subsequent subglacial deposition.

The type 3 surface corresponded to the interface between the moving debris-rich basal ice and the underlying deforming sediments, a till or previously deposited soft sediments. This latter type of surface, which is usually overlain by glaciomarine muddy facies, is frequent and fully fluted and striated in numerous Carboniferous examples. In the Late Ordovician glacial record, these surfaces generally correspond to reworked (wave-reworked?) smooth surfaces. The type 3 surface most probably represents the main subglacial décollement plane (e.g. Hart, 1998). Types 2 and 3 merge laterally when tillite deposition does not occurred locally or regionally.

Unfrozen subglacial sands during the Late Ordovician glaciation

Sutcliffe *et al.* claim that the transition between frozen and unfrozen sediments possibly localizes the formation of the striated surfaces (type 1). Abundant liquefaction to fluidization structures in association with the occurrence of open channels are preserved in the subglacial deforming zone. Although we are not able to determine precisely the timing of their formation, we proposed (and maintain as a working hypothesis) that fluid escape directly follow the deformation stage occurring in unfrozen,

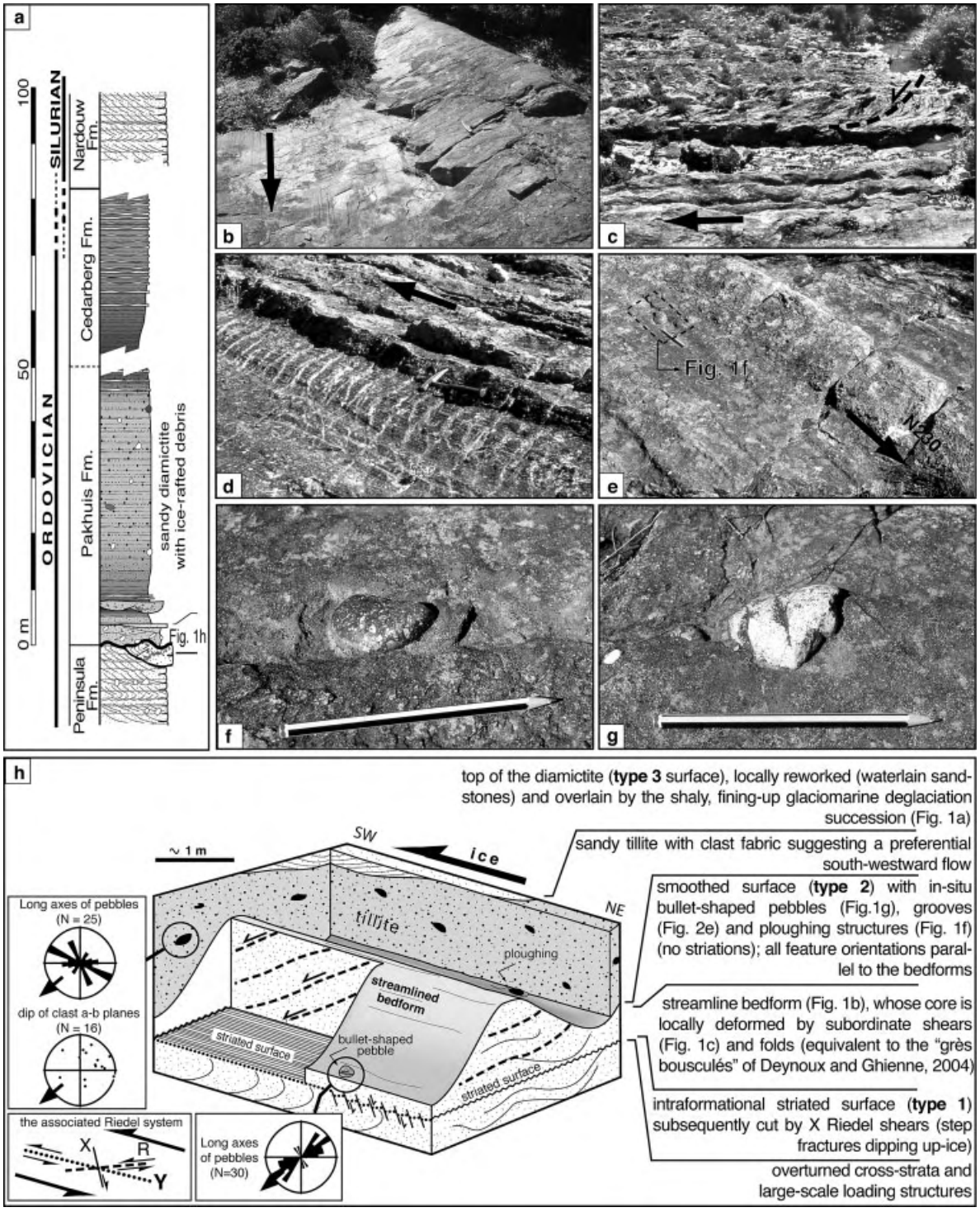

Fig. 1 The subglacial shear zone in Pakhuis Pass (Western Cape Fold Belt, South Africa); black arrows or pencil tips indicate the palaeo-ice flow orientation. (a) Sedimentary cross-section with relative position of the shear zone, the tillite and the glaciomarine succession. (b) Streamlined bedform and underlying striated surface (type 1) (hammer for scale). (c) Secondary R Riedel shears in the core of a weathered, 1 m high streamlined bedform. (d) Weathered streamlined bedform but well preserved underlying striated décollement surface (type 1), subsequently cut by step fractures (X Riedel shears) (hammer for scale). (e) Pebble ploughed in large-scale grooves at the interface (surface type 2) between streamlined bedforms and the tillite (pencil for scale). (f) Ploughing structure (location in Fig. 1e, pencil for scale). (g) Bullet-shaped clast with fractured lee side (pencil for scale). (h) Sketch showing the spatial relationship between deformation structures, clast fabrics and the three types of décollement planes. Temporal relationships are interpreted in the text.

overpressured subglacial sands (see Deynoux and Ghienne, 2004).

Rather than the transition between frozen and unfrozen sand, we suggest that granulometric transitions are of prime importance in the localization of the intraformational striated surfaces. In a sandstone succession, the finer horizons (typically fine-grained rippled sandstones) preferentially localize the striated surfaces. This observation suggests striated surfaces formed in horizons with fluid overpressure. Liquefaction and a contrasting behaviour between well drained sediments and sediments with fluid overpressure together suggest that subglacial deformation mainly occurs in unfrozen but water-saturated sediments.

Conclusion

Even if we recognize some necessary shortcuts in our genetic model for the formation of intraformational striated surfaces, we regard the alternative model proposed by Sutcliffe *et al.* as non-valid. The occurrence of fold structures and others indicators for 'ductile' deformation does not invalidate our model but emphasizes the complexity of subglacial shear zones in space and time. Discrepancies between the two models are so large that the model of Deynoux and Ghienne (2004) does clearly not 'represent a development of an older interpretation proposed by Sutcliffe *et al.* (2000)' as claimed in the comment. It proposed some improvements to a model previously initiated in Ghienne (1998).

References

Biju-Duval, B., Deynoux, M. and Rognon, P., 1974. Essai d'interprétation des 'fractures en gradins' observées dans les formations glaciaires précambriennes et ordoviciennes du Sahara. *Rev. Géogr. Phys. Géol. Dynam. (Paris)*, **16**, 503–512.

Blignault, H.J., 1981. Ice sheet deformation in the Table Mountain Group, Western Cape. *Annale Univ. van Stellenbosch Series A1 (Geology)*, **3**, 1–66.

Boulton, G.S. and Dent, D.L., 1974. The nature and rates of post-depositional changes in recently deposited till from south-east Iceland. *Geogr. Ann.*, **56A**, 121–134.

Deynoux, M. and Ghienne, J.-F., 2004. Late Ordovician glacial pavements revisited: a reappraisal of the origin of striated surfaces. *Terra Nova*, **16**, 95–101.

Ehlers, J and Stephan, H.-J., 1979. Forms at the base of till strata as indicators of ice movement. *J. Glaciol.*, **22**, 345–355.

Ghienne, J.-F., 1998. *Modalités d'enregistrement d'une glaciation ancienne; exemple de la glaciation fini-ordovicienne sur la plate-forme nord-gondwanienne en Afrique de l'Ouest*. Unpublished Doctoral Dissertation, Université Louis Pasteur, Strasbourg, 407 pp.

Hart, J.K., 1998. The deforming bed/debris-rich basal ice continuum and its implications for the formation of glacial landforms (flutes) and sediments (melt-out till). *Quatern. Sci. Rev.*, **17**, 737–754.

Lopez-Gamundi, O. and Martinez, M., 2000. Evidence of glacial abrasion in the Calingasta-Uspallata and western Paganzo basins, mid Carboniferous of western Argentina. *Palaeogeogr. Palaeoclimatol. Palaeoecol.*, **159**, 145–165.

Mandl, G., de Jong, L.N.J. and Maltha, A., 1977. Shear zones in granular material. *Rock Mech.*, **9**, 95–144.

Monod, O., Kozlu, H., Ghienne, J-F., Dean, W.T., Günay, Y., Le Hérissé, A., Paris, F. and Robardet, M., 2003. Late Ordovician glaciation in Southern Turkey. *Terra Nova*, **15**, 249–257.

Murray, T., 1994. Glacial deformation. In: *The Geological Deformation of Sediments* (A. Maltman, ed.), pp. 74–93, Chapman & Hall, London.

Senalp, M. and Al-Laboun, A., 2000. New evidence of the Late Ordovician Glaciation in Central Saudi Arabia. *Saudi Aramco J. Technol.*, **Spring**, 11–40.

Sutcliffe, O.E., Dowdeswell, J.A., Whittington, R.J., Theron, J.N. and Craig, J., 2000. Calibrating the Late Ordovician glaciation and mass extinction by the eccentricity cycles of Earths orbit. *Geology*, **28**, 967–970.

Van der Wateren, F.M., Kluiving, S. J. and Bartek, L.R., 2000. Kinematic indicators of subglacial shearing. In: *Deformation of Glacial Materials* (A. Maltman, B. Hubbard and M.J. Hambrey, eds). *Geol. Soc. London Spec. Publ.*, **176**, pp. 259–278.

Received 11 January 2005; revised version accepted 18 May 2005

440 Ma ice stream in North Africa

Julien Moreau*
Jean-François Ghienne
Ecole et Observatoire des Sciences de la Terre, Centre de Géochimie de la Surface, 1 rue Blessig, 67084 Strasbourg cedex, France
Daniel Paul Le Heron CASP, Department of Earth Sciences, 181A Huntingdon Road, Cambridge CB3 0DH, UK
Jean-Loup Rubino Centre Scientifique et Technique Jean Feger (CSTJF), Total, Avenue Laribeau, 64018 Pau, France
Max Deynoux Ecole et Observatoire des Sciences de la Terre, Centre de Géochimie de la Surface, 1 rue Blessig, 67084 Strasbourg cedex, France

ABSTRACT

Landsat images, ASTER digital elevation models, aerial photographs, and field investigations in the western Murzuq Basin (Libya) and the adjacent Tassili N'Ajjers (Algeria) provide paleogeomorphological evidence for the existence of a Late Ordovician ice stream at least 200 km long and 80 km wide. This includes mega-scale glacial lineations, an associated subglacial meltwater drainage system, and ice-front features. This first comprehensive description of a pre-Cenozoic ice stream may help to identify other examples in the Proterozoic to Paleozoic glacial record. Reconstruction of the extent and behavior of former ice sheets, and reservoir prospect analysis in glacially related successions, have to take into account the potential occurrence of ice streams.

INTRODUCTION

Ice streams are the most dynamic components of contemporary ice sheets. Their location and temporal evolution are of critical importance in the reconstruction of Pleistocene ice masses (Bennett, 2003; Clark and Stokes, 2003). Pre-Tertiary ice sheets were of magnitudes comparable to those of the Cenozoic (Crowell, 1999; Ghienne, 2003). Thus, the occurrence of paleo-ice streams should be expected. However, while a limited number of Paleozoic ice streams have been described previously (Visser et al., 1997), relatively low quality exposure means that they have been located using widely separated ice flow indicators and facies distributions. In contrast, the Sahara affords excellent exposures of Upper Ordovician strata that are suitable for geomorphological analysis. In this paper we describe key geomorphological evidence for an ancient ice stream based on criteria developed for Pleistocene glaciation. Subglacial bedforms at the 0.1 to >10 km scale, in association with a meltwater drainage system, are interpreted in terms of firm paleogeomorphological evidence for the occurrence of a 440 Ma ice stream.

LOCATION AND GEOLOGIC SETTING

During the Late Ordovician, ice masses repeatedly covered most of the western Gondwana platform. An ice sheet flowing northward from the continental interior extended continuously from Mauritania to Arabia (Ghienne, 2003). Between the Hoggar Massif and the Murzuq-Djado Basin, Late Ordovician glacial deposits crop out continuously over 700 km (Fig. 1). The orientation of these outcrops (NNW-SSE) is roughly parallel to the local ice-flow orientation inferred from abundant striated surfaces and streamlined bedforms (Beuf et al., 1971; Deynoux and Ghienne, 2004). The study area focuses on a 200-km-long segment of this outcrop located near the town of Ghat on the western rim of the Murzuq Basin (eastern Tassili N'Ajjer, Algeria, and Wadi Tannezuft area, Libya; Fig. 1). Here, four major crosscutting glacial erosion surfaces (GESs) (Fig. 2) record four successive glacial advances. A fifth GES (last re-advance subordinate to the fourth GES) is recognized in the south. Across the region, each surface defines the lower boundary of a deglaciation sequence deposited during ice sheet recession and culminating in an interglacial period (Ghienne, 2003). This study focuses on the geomorphology of the fourth and fifth GESs.

METHODOLOGY

Subglacial bedforms have been characterized at various scales from field study and Landsat image interpretation (panchromatic images archived in the Global Land Cover Facility: http://glcf.umiacs.umd.edu/) and supplemented by aerial photograph analysis. An orthorectified ASTER digital elevation model (20 × 40 km) has been exploited in GOCAD in order to characterize the three-dimensional geometry of the successive GESs in the vicinity of Ghat.

Glacial Lineations

The distribution of subglacial bedforms was mapped out from the above data sources (Fig. 3A). Lineations are parallel to the intraformational glacial striae examined at outcrop and are hence parallel to ice flow (Deynoux and Ghienne, 2004). A flow set (Stokes and Clark, 2003) of abundant glacial lineations of common orientation is identified on both the fourth and fifth GESs (in black, Fig. 3A). Subglacial bedforms become more scattered, less uniformly oriented, and generally shorter westward of a well-defined boundary (Fig. 3A) that corresponds to the flow set margin. Silurian and younger deposits conceal its eastern margin. Therefore, the flow set is 200 km in length and at least 80 km in width (Fig. 3A).

Studied GESs comprise superimposed mega-scale glacial lineations (MSGLs) that have distinct length to width (i.e., elongation) ratios and amplitudes (Table 1); elongation ratios increase as amplitude decreases. Attenuated drumlins, only present in the fifth GES, show small elongation ratios relative to amplitude (Table 1). At the largest scale, GESs are corrugated by kilometer-wide elongate ridges that separate straight valley-like depressions (Table 1; Figs. 2, 3A, and 3C).

The different types of bedforms (large and narrow MSGLs, attenuated drumlins and ridges) are erosion features that cut into earlier glaciogenic sediments. Lineations are generally cored by deformed gla-

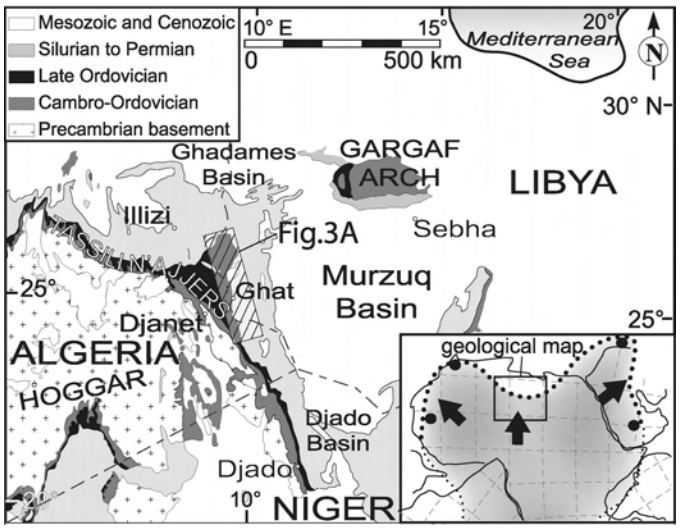

Figure 1. Geological sketch map of Murzuq Basin, with location of Figure 3A (study area). Inset map shows maximum extent of Ordovician ice sheet (dotted line), with data control points (large dots) and main ice-flow orientations (arrows).

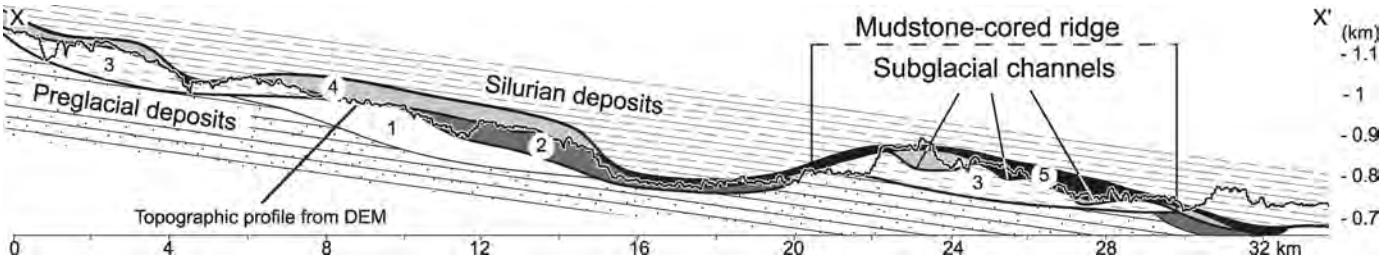

Figure 2. Geological cross section in Ghat area (location in Fig. 3B). Cross section traverses ridge (largest scale subglacial bedform) and subglacial channels. Fourth glacial erosion surface (GES, major glacial advance) underlies fourth depositional glacial sequence. Fifth GES, preserving full glacial paleotopography, results from local re-advance in context of overall retreat. DEM—digital elevation model.

ciofluvial sand (now consolidated sandstones; Deynoux and Ghienne, 2004). However, ridges are preferentially cut into a 60–80-m-thick succession of mud-dominated deltaic facies.

Distribution of Lineations, Meltwater Channels, and Ice-Front Features

Within the flow set, regional variability in the nature, size, and shape of the subglacial bedforms is observed. South of Ghat (50–100 km), the flow set is sinuous. Convergent flow patterns are evident in places where large and narrow MSGLs plunge into the flow set (Fig. 3D).

In the Ghat area, parallel ridges and superimposed large and narrow MSGLs show a dense assemblage of high elongation ratio (>10) lineations (Figs. 3A, 3B). They are locally overprinted by fanning and attenuated drumlins (Fig. 3A) of the fifth GES. Moreover, anastomosing networks of subglacial channels are observed cutting into mudstone-cored ridges (Figs. 2, 3B).

Farther north (50–100 km from Ghat), ridges are shorter. Large and narrow MSGLs are rarely observed (Fig. 3A). Here, mudstone-cored ridges are truncated by large subglacial channels interpreted as tunnel valleys (Ghienne and Deynoux, 1998; Le Heron et al., 2004).

Glaciotectonic folds and thrusts occur at the latitude of Ghat and northward (Fig. 3A). One example, 20 km NW of Ghat, is of particular interest because it defines the maximum extent the ice sheet reached during the fifth glacial advance (Fig. 3A). Southward, fanning attenuated drumlins are observed and northward, abundant sandstone channels spread out, representing a coeval proglacial fluvial network (Fig. 2B).

Evidence for a Late Ordovician Ice Stream

Subglacial streamlined bedforms are widely recognized in the Late Ordovician glacial record of the Sahara (Beuf et al., 1971; Le Heron et al., 2005) and are interpreted as indicating fast-flowing ice. Independently, small (4–10 km in width) ice streams have been inferred from the occurrence of glacial valleys. However, similar structures are now best reinterpreted as tunnel valleys (Hirst et al., 2002). In the study area, MSGLs with high elongation ratios (from 10 to 100) are directly analogous to Pleistocene subglacial bedforms (references in Table 1). They indicate the very high ice velocities that characterize fast-flowing ice streams (e.g., Clark, 1993). Using criteria developed by Clark and Stokes (2003) to recognize an ice stream footprint, we observe the following features in common with Pleistocene ice streams: (1) the flow set has distinctive dimensions (>200 km in length, >80 km in width); (2) MSGLs are concentrated within the flow set (Fig. 3A); (3) the western (observed) margin of the flow set is sharply defined, <1.5 km in width, and includes convergent flow patterns (Fig. 3D); and (4) deformable bed conditions are present throughout the study area (Deynoux and Ghienne, 2004).

South of Ghat, the sinuous flow set with large and superimposed narrow MSGLs (Figs. 3A, 3D) is compared favorably to the bundle structure imaged by Canals et al. (2000). Subglacial channels joining northward into tunnel valleys are comparable to the meltwater drainage systems identified below former Antarctic ice streams (Lowe and Anderson, 2002; O'Cofaigh et al., 2002).

Temporal Evolution of the Late Ordovician Ice Stream

Crosscutting relationships of subglacial bedforms allow the multiphased evolution of the ice stream to be reconstructed. The largest scale ridges and the development of large MSGLs (1, Fig. 4) probably occurred at the ice maximum. These features were then overprinted conformably by further narrow MSGLs (2, Fig. 4). The extreme elongation ratio of the narrow MSGLs indicates that the highest ice velocities were reached during this phase, possibly by a surge. This stage is probably synchronous with relatively deep marine ice fronts in the Ghadames Basin (Fig. 1). This phase was followed by a meltwater incision phase (3, Fig. 4), concomitant with active ice front recession. Minor re-advance (forming the fifth GES) molded discordant attenuated drumlins (4, Fig. 4). Both the fan-shaped distribution of attenuated drumlins (4, Fig. 4), which reflect dispersive flow and lower ice velocity (Clark and Stokes, 2003), and close association with proglacial fluvial channels indicate a continental ice sheet terminus. These changes are interpreted as the transition from a marine terminating, ''rubber-stamped'' paleo-ice stream (phases 1–3) to one that became terrestrially terminating and ''smudged'' (phase 4; Clark and Stokes, 2003).

This chronology, in particular incision of the lineations by subglacial meltwater, is comparable to sequences of events determined from seafloor imagery of Antarctic sediments (Anderson et al., 2002; O'Cofaigh et al., 2002). The final phase, whereby a continental to very shallow marine ice front develops, resembles the behavior of ice sheets during the Last Glacial Maximum in the Northern Hemisphere (e.g., Boulton et al., 2001). In the study area, a warm-based ice sheet is inferred from the occurrence of an ice stream, in agreement with subglacial deformation of water-saturated sands (Deynoux and Ghienne, 2004). However, thermal conditions beyond the flow set are less well known and transitions between warm and cold-based ice are expected to have occurred (Le Heron et al., 2005).

Figure 3. Ice-stream–generated features. A: Geomorphological map shows subglacial bedforms that are 0.1 to >10 km in length; their consistent orientation and close comparison to Pleistocene subglacial bedforms suggest that eolian and/or tectonic origin can be discounted. Parallel mega-scale glacial lineations (MSGLs) are concentrated within flow set but are more scattered to west. From south to north, three assemblages of subglacial bedforms are recognized: (1) 50–100 km south of Ghat, MSGLs are sinuous and parallel; (2) in Ghat area, ridges and MSGLs are well developed, and often overprinted by attenuated drumlins and subglacial channels (cf. B); (3) 50–100 km north of Ghat, lineations are rare; ridges are shorter and cut by sinuous, ~5-km-wide, 50–150-m-deep incisions interpreted as tunnel valleys. Ice-front–related features (tens-of-meters-high glaciotectonic folds and thrusts, 0.2–1-km-wide proglacial channels) are also shown.

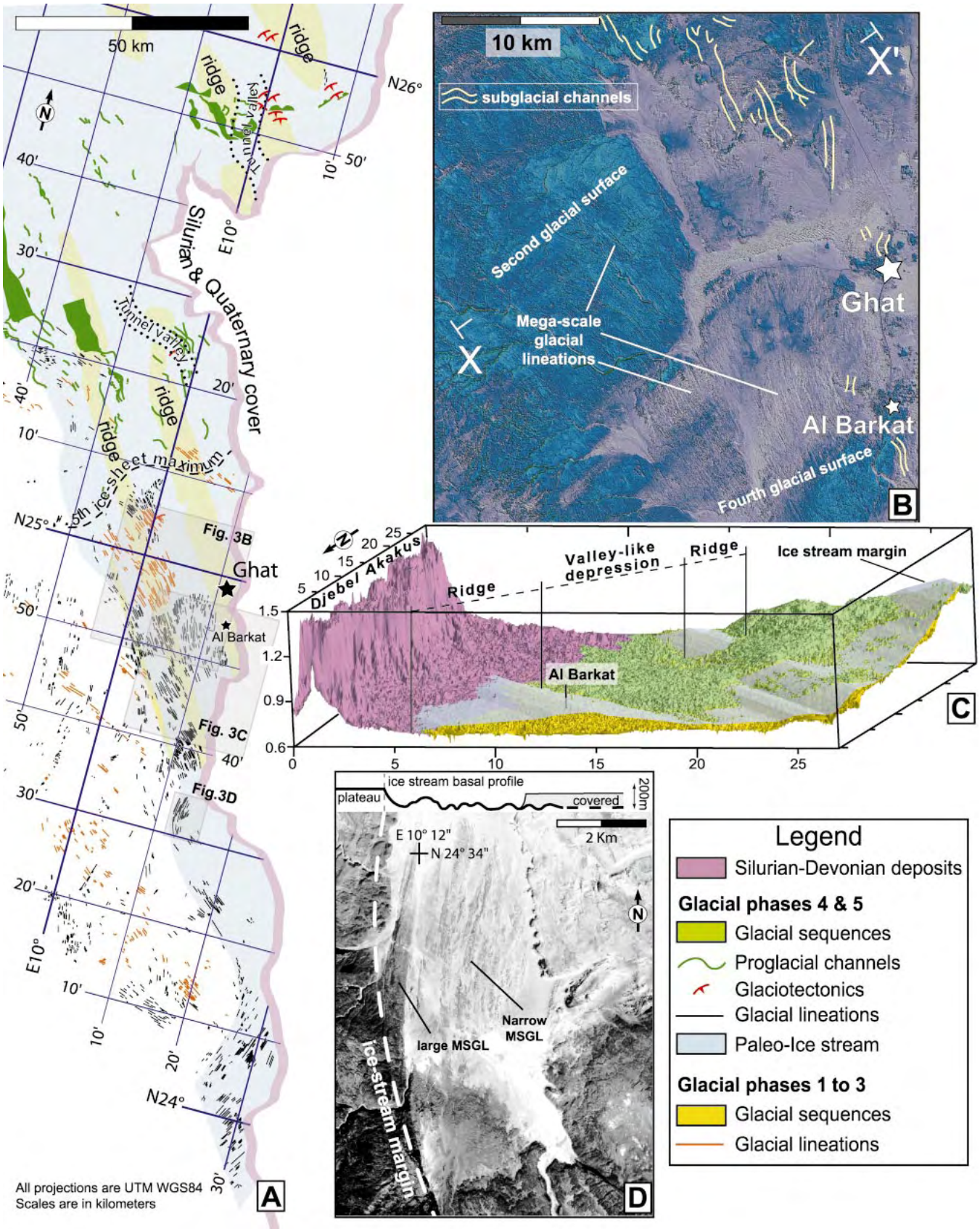

B: Landsat data (location in A) showing MSGLs on second and fourth glacial erosion surfaces (GESs, bottom left corner of image) and network of sinuous channels cutting into ridge (right of image), interpreted as subglacial meltwater drainage system. Channels are 0.4–1 km wide, 40–60 m deep, locally overdeepened with striated floors, and are filled with sandstone and/or exotic clast–bearing sandy diamictite. C: Three-dimensional reconstruction (GOCAD) of flow set surface near its western margin (location in A), showing two ridges separated by valley-like depression. D: Western margin of ice stream showing convergence of large and narrow MSGLs into flow set (location in A). Inset shows topographic profile of fourth GES (thick line); to east, latter is covered by latest glacially related deposits.

TABLE 1. CLASSIFICATION OF THE SUBGLACIAL STREAMLINED BEDFORMS ACCORDING TO SHAPE CRITERIA, AND ANALOGY IN THE PLEISTOCENE

Streamlined bedforms	Amplitude (m)	Width (km)	Length (km)	Elongation ratio (W/L)	References to Pleistocene analogs
Ridges	50/120	3/15	>50	4/>10	Canals et al. (2000)
MSGL					
Large	10/30	0.2/0.8	>5	5/20	Anderson et al. (2002); Canals et al. (2000); Clark (1993); Evans el al. (2004);
Narrow	1/20	00.1/0.05	1/5	≫20	O'Cofaigh et al. (2002); Sejrup et al. (2003); Stokes and Clark (2003)
Attenuated drumlins	1/20	0.001/0.05	0.01/0.2	4/10	Clark (1993)

Note: W/L—width/length; MSGL—mega-scale glacial lineations

CONCLUSION AND PERSPECTIVES

Outstanding three-dimensional exposures allow geomorphological criteria developed from Pleistocene studies to be applied successfully to a Late Ordovician case study. We consider that attenuated subglacial bedforms concentrated in a flow set with distinctive size, boundaries, and landforms provide firm evidence for an Ordovician ice stream. In the absence of proven topographic or tectonic control, the flow set appears to be related to a ''pure'' ice stream (Bennett, 2003). What controlled its location? MSGLs have been recognized in the study area on several vertically stacked glacial erosion surfaces separated by complete deglaciation sequences (Figs. 3A, 3B). This observation indicates that ice streams developed repeatedly in the same place and suggests that a determining factor should exist. As a working hypothesis, we propose that the Ghadames Basin was a preglacial embayment north of the study area. Rather than a simple topographic focus of the initial ice-flow lines, the occurrence of muddier, easily deformable subglacial sediments and/or a calving pull process in relatively deeper water (Stokes and Clark, 2004) could have accelerated the ice flow, triggering fast-flowing ice and localizing the ice streams.

The recognition of ice streams is crucial for reconstructing the dynamics of the Late Ordovician ice sheets. Furthermore, this study may help recognition of ice stream footprints both elsewhere in the Late Ordovician record and in other ancient ice age records. This discovery is particularly noteworthy for petroleum geologists, since Late Ordovician glaciogenic rocks are major north African reservoirs: ice streams may induce preferential basin-scale erosion, focus sediment delivery, and influence reservoir architecture. Other time-equivalent ice streams await discovery.

ACKNOWLEDGMENTS

We thank Total for funding this study and for their technical and scientific support, and the National Oil Company of Libya for the opportunity to work in such an exceptional field area. We also thank Claude Roquin of Centre National de la Recherche Scientifique, Strasbourg, for assistance with the remote sensing imagery, and Mike Hambrey, Chris Clark, and Chris Stokes for insightful and constructive reviews.

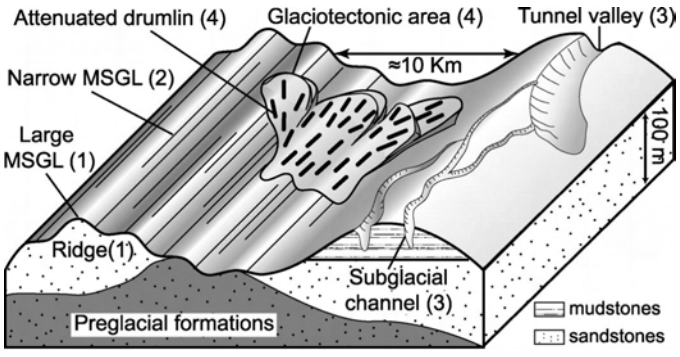

Figure 4. Spatial and temporal relationship between ridges, mega-scale glacial lineations (MSGLs), attenuated drumlins, and meltwater drainage system. Numbers refer to sequence of events proposed in text.

REFERENCES CITED

Anderson, J.B., Shipp, S.S., Lowe, A.L., Wellner, J.S., and Mosola, A.B., 2002, The Antarctic Ice Sheet during the Last Glacial Maximum and its subsequent retreat history: A review: Quaternary Science Reviews, v. 21, p. 49–70.

Bennett, M.R., 2003, Ice streams as the arteries of an ice sheet: Their mechanics, stability and significance: Earth-Science Reviews, v. 61, p. 309–339.

Beuf, S., Biju-Duval, B., de Charpal, O., Rognon, P., Gariel, O., and Bennacef, A., 1971, Les grès du Paléozoïque Inférieur au Sahara: Sédimentation et discontinuités, évolution structurale d'un craton: Paris, Technip, 464 p.

Boulton, G.S., Dongelmans, P., Punkari, M., and Broadgate, M., 2001, Palaeoglaciology of an ice sheet through a glacial cycle: The European ice sheet through the Weichselian: Quaternary Science Reviews, v. 20, p. 591–625.

Canals, M., Urgeles, R., and Calafat, A.M., 2000, Deep sea-floor evidence of past ice streams off the Antarctic Peninsula: Geology, v. 28, p. 31–34.

Clark, C.D., 1993, Mega-scale glacial lineations and cross-cutting ice flow landforms: Earth Surface Processes and Landforms, p. 1–29.

Clark, C.D., and Stokes, C.R., 2003, Palaeo-ice stream landsystem, *in* Evans, D.J.A., ed., Glacial landsystems: London, Arnold, p. 202–227.

Crowell, J.C., 1999, Pre-Mesozoic ice ages: Their bearing on understanding the climate system: Geological Society of America Memoir 192, p. 1–112.

Deynoux, M., and Ghienne, J.-F., 2004, Late Ordovician glacial pavements revisited: A reappraisal of the origin of striated surfaces: Terra Nova, v. 16, p. 95–101.

Evans, J., Dowdeswell Julian, A., and O'Cofaigh, C., 2004, Late Quaternary submarine bedforms and ice-sheet flow in Gerlache Strait and on the adjacent continental shelf, Antarctic Peninsula: Journal of Quaternary Science, v. 19, p. 397–407.

Ghienne, J.F., 2003, Late Ordovician sedimentary environments, glacial cycles, and post-glacial transgression in the Taoudeni Basin, West Africa: Palaeogeography, Palaeoclimatology, Palaeoecology, v. 189, p. 117–145.

Ghienne, J.F., and Deynoux, M., 1998, Large-scale channel fill structures in Late Ordovician glacial deposits in Mauritania, Western Sahara: Sedimentary Geology, v. 119, p. 141–159.

Hirst, J.P.P., Benbakir, A., Payne, D.F., and Westlake, I.R., 2002, Tunnel valleys and density flow processes in the Upper Ordovician glacial succession, Illizi Basin, Algeria: Influence on reservoir quality, *in* Carr, I.D., and Redfern, J., eds., A synthesis of current understanding of the structural evolution of North Africa: Beaconsfield, UK, Scientific Press.

Le Heron, D.P., Sutcliffe, O., Bourgig, K., Craig, J., Visentin, C., and Whittington, R., 2004, Sedimentary architecture of Upper Ordovician tunnel valleys, Gargaf Arch, Libya: Implication for the genesis of a hydrocarbon reservoir: Geoarabia, v. 9, p. 137–159.

Le Heron, D.P., Sutcliffe, O.E., Whittington, R.J., and Craig, J., 2005, The origins of glacially related soft-sediment deformation structures in Upper Ordovician glaciogenic rocks: Implication for ice-sheet dynamics: Palaeogeography, Palaeoclimatology, Palaeoecology, v. 218, p. 75–103.

Lowe, A.L., and Anderson, J.B., 2002, Reconstruction of the West Antarctic ice sheet in Pine Island Bay during the Last Glacial Maximum and its subsequent retreat history: Quaternary Science Reviews, v. 21, p. 1879–1897.

O'Cofaigh, C., Pudsey, C.J., Dowdeswell Julian, A., and Morris, P., 2002, Evolution of subglacial bedforms along a paleo-ice stream, Antarctic Peninsula continental shelf: Geophysical Research Letters, v. 29, p. 4.

Sejrup, H.P., Larsen, E., Haflidason, H., Berstad, I.M., Hjelstuen, B.O., Jonsdottir, H.E., King, E.L., Landvik, J., Longva, O., Nygard, A., Ottesen, D., Raunholm, S., Rise, L., and Stalsberg, K., 2003, Configuration, history and impact of the Norwegian Channel Ice Stream: Boreas, v. 32, p. 18–36.

Stokes, C.R., and Clark, C.D., 2003, Laurentide ice streaming on the Canadian Shield: A conflict with the soft-bedded ice stream paradigm?: Geology, v. 31, p. 347–350.

Stokes, C.R., and Clark, C.D., 2004, Evolution of late glacial ice-marginal lakes on the northwestern Canadian Shield and their influence on the location of the Dubawnt Lake palaeo-ice stream: Palaeogeography, Palaeoclimatology, Palaeoecology, v. 215, p. 155–171.

Visser, J.N.J., van Niekerk, B.N., and van der Merwe, S.W., 1997, Sediment transport of the late Palaeozoic glacial Dwyka Group in the southwestern Karoo Basin: South African Journal of Geology, v. 100, p. 223–236.

Manuscript received 12 April 2005
Revised manuscript received 24 May 2005
Manuscript accepted 24 May 2005

Printed in USA

3.2. Vallées en tunnel

*Sur la marge occidentale de l'Adrar de Mauritanie, l'oued Hanouk entaille profondément les grès cambro-ordoviciens fournissant, à l'échelle sismique, une section naturelle de vallée-tunnel fini-ordovicienne (*Ghienne et Deynoux, 1998*). La discordance de ravinement résultante avait été parfaitement caractérisée dès 1962 par T. Monod (croquis en encart). Les faciès bien stratifié (en vert, et sur le devant de la photographie) sont recoupés par la vallée dont le remplissage (en orangé, partie centrale) repose en biseau d'aggradation sur la discordance (bien visible à gauche, dans l'ombre sur la droite). La hauteur des affleurements avoisine 200 m.*

Un des éléments glaciogéniques les plus marquants du paysage fini-ordovicien est l'existence de réseaux de paléovallées (Beuf et al., 1971). A leur approche, la discordance de ravinement basale des formations glaciaires y est très accentuée. Le plus souvent, leur échelle plurikilométrique permet de les identifier sur les images satellitaires où elles apparaissent comme de grands cordons sableux en topographie inversée (voir image interprétée ci-dessous, Mauritanie). Ces vallées avaient été identifiées au Sahara avant même que l'on ne parle de glaciation fini-ordovienne (Monod, 1954). Plusieurs dizaines d'exemples sont maintenant connus de la Mauritanie (Trompette, 1973, Deynoux, 1980) à la plaque Arabe (Vaslet , 1990 ; Powell et al. 1994). En Arabie, ainsi qu'en Algérie, ces paléovallées, parfois profondes de plus 400 m ont localement tronqué la totalité de la succession cambro-ordovicienne, atteignant le socle (Beuf et al., 1971 ; McGillivray et Husseyni, 1992). Par analogie avec les vallées creusées sur la plate-forme européenne lors des épisodes glaciaires quaternaires, *Ghienne et Deynoux (1998)* ont proposé que certaines de ces paléovallées correspondent à des vallées en tunnel, structures creusées pour l'essentiel dans les sédiments sous-glaciaires par les eaux de fonte sous pression circulant en base de glacier. Il ne s'agit pas de vallée glaciaire *stricto sensu* dans le sens où ce n'est pas un creusement par la glace qui en est à l'origine ; de même, il ne s'agit pas d'eskers, remplissage de conduits sous-glaciaires creusés aux dépens de la masse de glace. Quelques eskers ordoviciens sont cependant également identifiés, bien que d'envergure limitée avec des largeurs n'excédant pas la dizaine de mètres.

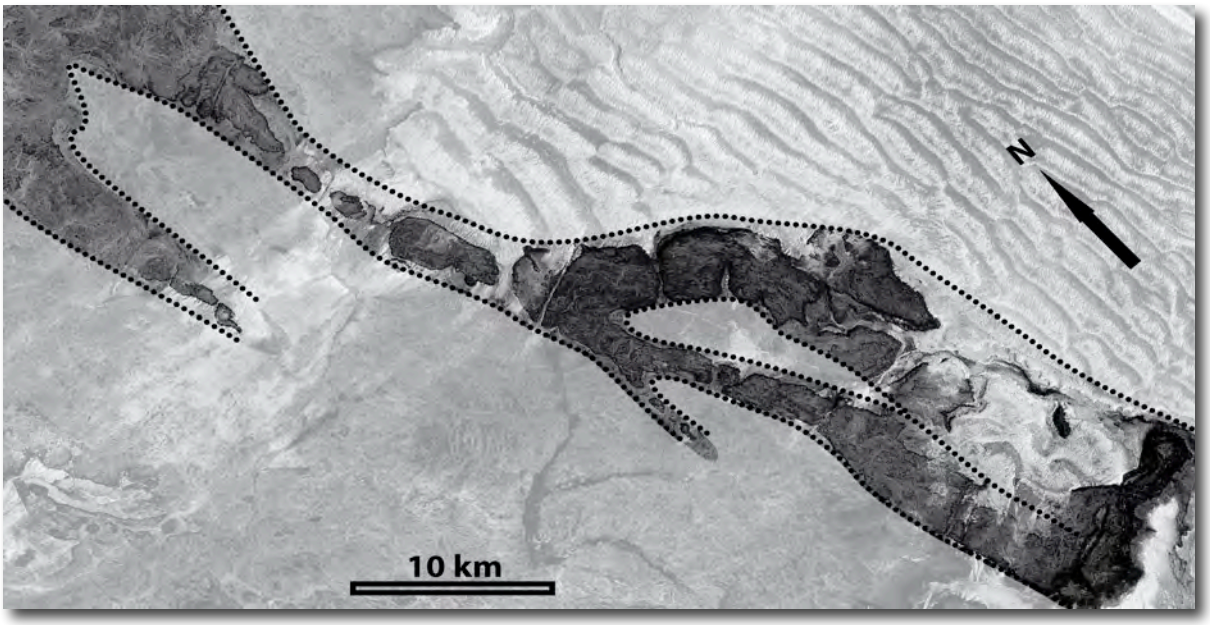

Cette interprétation de vallées en tunnel a été reprise ensuite par Hirst et al. (2002) pour des exemples algériens, puis par *Ghienne et al. (2003)* et Le Heron et al. (2004) pour un exemple de Libye situé sur le môle du Gargaf. Des analogues permo-carbonifères ont été identifiés en Australie (Eyles et De Broekert, 2001), mais, pour ces glaciations, les vallées en tunnel semblent avoir été plus rares (ou plus rarement préservées ?). Le Heron et al. (2004) ont établi un modèle de remplissage détaillé de vallée en tunnel, en environnements proglaciaires fluviatiles à turbiditiques. Des structures de taille légèrement inférieure ont été caractérisées dans des domaines plus distaux, tels le Maroc, où elles correspondent plutôt à des gros chenaux de quelques centaines de mètres de largeur pour quelques dizaines de mètres de profondeur (*Loi et al., 2010, §2, fig. 9 B&C*). Ici aussi, le remplissage a lieu en domaine proglaciaire après le retrait des fronts glaciaires. Enfin, et plus surprenant, des vallées en

tunnel ont été identifiées en Espagne, dans les Monts Cantabriques (*Guttierez-Marco et al., 2010, §5*). Elles constituent aujourd'hui le seul indice d'une présence glaciaire sur le domaine européen à l'Ordovicien supérieur. En Jordanie, le réseau de vallées en tunnel, encaissé dans la succession préglaciaire, constitue le seul enregistrement sédimentaire de la glaciation qui ait échappé aux ravinements transgressifs postglaciaires (*Douillet et al., en révision*). Les vallées en tunnel constituent dans certains cas des réservoirs à hydrocarbures (Le Heron et al., 2009).

Ces nombreux exemples permettent de dresser le portrait des vallées en tunnel ordoviciennes (*Ghienne, 2009*):

- Il existe un continuum depuis les grandes vallées — avec largeurs atteignant 5 km —, jusqu'aux chenaux, de largeur pluridécamétrique. Les vallées en tunnel sont légèrement sinueuses, leur orientation générale étant parallèle aux écoulements glaciaires régionaux.
- En section, l'inclinaison des berges est comprise entre 10 et 35° avec un fond plat (Ghienne et Deynoux, 1998). Les rapports largeur/ hauteur sont compris entre 5 (chenaux) et 50 pour les plus grandes vallées (Lahondère et al., 2008).
- Les chenaux et vallées en tunnel sont caractérisés par l'existence d'une banquette gréseuse tapissant le fond de l'incision et drapant la partie basse des berges. Le contact entre l'encaissant et cette banquette est soit franc, soit diffus dans le cas où les sédiments de l'encaissant ont été déstabilisés (*Douillet et al., en révision*). Cette banquette contient typiquement des faciès conglomératiques et/ ou des structures érosives en base de banc (flûtes, classiques ou inversées ; gouttières d'érosion ; structures de type *cut-and-fill*)(Ghienne et Deynoux, 1998 ; *Loi et al., 2010, §2*). Elle peut être connectée à des dykes gréseux injectés dans l'encaissant, lui-même parfois affecté par de la glaciotectonique. Une ou plusieurs bandes de cisaillement intraformationelles en affectent le toit, attestant ainsi de l'environnement sous-glaciaire (Lahondère et al., 2008 ; *Guttierez-Marco et al., 2010*).
- Le remplissage des chenaux et vallées en tunnel repose en biseau d'aggradation sur la banquette ou les marges de l'incision (*Ghienne et al., 2003* ; *Douillet et al., en révision ; figure ci-contre, wadi Taharamet, Libye*). Le plus souvent intégralement gréseux, et constitué dans ce cas de faciès à dynamique de crue en bancs érosifs amalgamés (Ghienne et Deynoux, 1998; Lahondère et al., 2008 ; *Loi et al., 2010, §2*), le remplissage par des successions deltaïques argilo-gréseuses granocroissantes intervient aussi quelquefois mais uniquement dans les cas d'incisions profondes (Le Heron et al., 2004 ; *Douillet et al., en révision*). Un cas unique de remplissage par des faciès glaciomarin à galets lâchés a été observé.

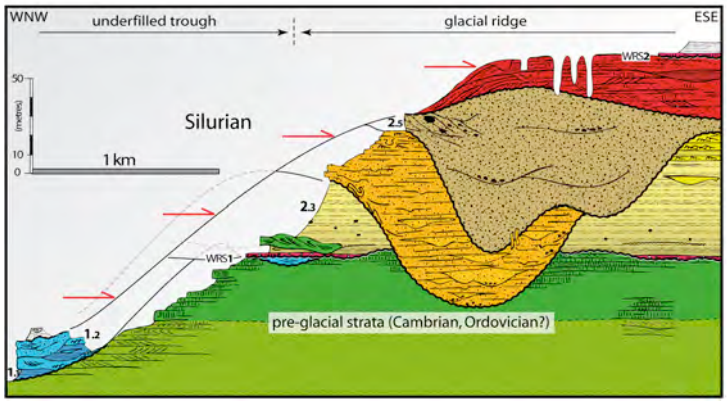

Les vallées en tunnel caractérisent les domaines de marges glaciaires, avec des exutoires marquant les fronts glaciaires des périodes de retrait. Ce sont les analogues des structures quaternaires identifiées en subsurface en Mer du Nord, au Danemark, en Hollande ou en Allemagne (Huuse et Lykke-Andersen, 2000 ; Jorgensen et Sandersen, 2006 ; Lonergan et al., 2006 ; Lutz et al., 2009), avec lesquelles elles partagent le contexte de plate-forme sédimentaire, l'organisation en réseau, la nature du remplissage (Le Heron et al., 2009),… ainsi qu'une série de questionnements : processus de l'incision ? calendrier du remplissage ? relations entre phases glaciaires et générations de vallées en tunnel ? …

Available online at www.sciencedirect.com
SCIENCE DIRECT®
C. R. Geoscience 335 (2003) 1091–1100
COMPTES RENDUS GEOSCIENCE

Stratigraphy

Palaeovalleys and fault-controlled depocentres in the Late-Ordovician glacial record of the Murzuq Basin (central Libya)

Jean-François Ghienne [a,*], Max Deynoux [a], Giänreto Manatschal [a], Jean-Loup Rubino [b]

[a] *École et observatoire des sciences de la Terre, Centre de géochimie de la surface, CNRS–UMR 7517, 1, rue Blessig, 67084 Strasbourg cedex, France*
[b] *CSTJF, av. Larribau, 64018 Pau cedex, France*

Received 10 July 2003; accepted 22 September 2003

Presented by Jean Dercourt

Abstract

In the Gargaf area, the stratigraphic architecture of the Late-Ordovician glacial drift results from successive glacial erosion events, with the location of the main glacial valleys partly controlled by inherited Panafrican structural trends, and by the existence of glacio-isostatically induced fault-related depocentres. Four laterally discontinuous, depositional units correspond to the filling of palaeovalleys. Each of the corresponding basal bounding surfaces was incised during a major ice front advance, reaching at least the northern Gargaf (> 28°S). The bulk of the glacial record is made up of fluvial to shallow-marine sediments deposited in relatively distal glacial environments. Each unit, which recorded a glacial-interglacial climatic cycle, can be used for correlation throughout the Murzuq Basin and even at the scale of the North Gondwana platform. ***To cite this article: J.-F. Ghienne et al., C. R. Geoscience 335 (2003).***

Résumé

Paléovallées et dépocentres sur failles dans les séries glaciaires fini-ordoviciennes du bassin de Murzuq (Libye centrale). Dans la région du Gargaf, l'architecture stratigraphique de dépôts glaciaires fini-ordoviciens résulte d'érosions glaciaires successives, avec localisation des vallées glaciaires en partie guidée par les accidents structuraux hérités de l'orogenèse panafricaine, et par l'existence de dépocentres liés à la réactivation de failles lors de processus glacio-isostatiques. Quatre unités de dépôt latéralement discontinues forment le remplissage des paléovallées. Chaque surface basale d'érosion représente une avancée majeure des fronts glaciaires, atteignant au moins le Nord du Gargaf (> 28°S). Les sédiments glaciaires, comprennent essentiellement des dépôts fluviatiles ou marins peu profonds, déposés dans des environnements relativement distaux par rapport aux fronts glaciaires. Chaque unité, enregistrant un cycle climatique glaciaire-interglaciaire, peut être corrélée sur l'ensemble du Bassin de Murzuq, voire même à l'échelle de la plate-forme nord-gondwanienne. ***Pour citer cet article : J.-F. Ghienne et al., C. R. Geoscience 335 (2003).***

* Corresponding author.
E-mail address: ghienne@illite.u-strasbg.fr (J.-F. Ghienne).

1631-0713/$ – see front matter
doi:10.1016/j.crte.2003.09.010

Keywords: Libya; Ordovician; glaciation; palaeovalley

Mots-clés : Libye ; Ordovicien ; glaciation ; paléovallée

Version française abrégée

1. Introduction

À la fin de l'Ordovicien, la plate-forme nord-gondwanienne est à plusieurs reprises couverte par des glaciers [1–3,6,7,18]. En Libye, dans le bassin de Murzuq, les dépôts résultants sont globalement subdivisés en une formation inférieure argileuse (Melaz Shuqran) et une formation supérieure gréseuse (Mamunyiat) [12,14]. Dans le détail, une telle subdivision lithostratigraphique ne peut être maintenue [15]. Ainsi, des levés dans la région du Gargaf [4,5] montrent : (1) que les sédiments glaciaires se subdivisent en plusieurs unités de dépôt limitées par des surfaces d'érosion liées à la formation de paléovallées ; (2) que chaque unité comprend généralement une succession à dominante argileuse à la base et à dominante sableuse au sommet ; (3) qu'il existe une relation entre des directions structurales anciennes, l'orientation des paléovallées et l'existence de dépocentres associés à des failles actives pendant la glaciation.

2. Paléovallées glaciaires

Au sein de la succession glaciaire de la région du Gargaf, quatre unités de dépôt verticalement superposées et latéralement juxtaposées sont définies (Fig. 1a et b). L'unité 1 surmonte une surface basale érosive, régionalement plane mais localement irrégulière, recoupant différents horizons préglaciaires localement très déformés. La surface basale de l'unité 2 dessine des paléovallées de plusieurs kilomètres de large, latéralement limitées par des zones faillées ou déformées (Fig. 1a, profils A30–41, C14–35 et C39–51). La surface basale de l'unité 3 dessine des paléovallées comparables à celle de l'unité 2 (profil C8–30). L'unité 4 comble des vallées beaucoup plus étroites (3–5 km) et encaissées (> 150 m) (profils B9–14, C3–7 et C9–14 ; Figs. 1c–d et 2a).

L'origine glaciaire des surfaces d'érosion marquant la base des unités de dépôt peut être déterminée par les structures associées ou par la nature des sédiments sus-jacents. La surface de base de l'unité 1 est associée à des déformations importantes affectant les sédiments préglaciaires et elle est directement recouverte par des grès argileux microconglomératiques à rares galets exotiques striés. Des surfaces striées, fractures en gradin, plis, roches moutonnées, chenaux sous-glaciaires (Fig. 2b) marquent la surface de base de l'unité 3. Bien que la morphologie des surfaces basales des unités 2 et 4 soit caractéristique d'une érosion glaciaire, la mise en place de faciès de haute énergie dans le remplissage sus-jacent en a oblitéré les structures glaciogéniques. Toutes ces vallées ont été creusées dans des sédiments apparemment peu lithifiés, comme le suggère l'abondance des déformations et des figures d'échappement d'eau affectant les sédiments tant glaciaires que préglaciaires.

3. Les unités de dépôt

Mis à part les quelques galets striés d'origine exotique dispersés dans des grès argileux microconglomératiques et les structures d'érosion et de déformation sous-glaciaires associées aux limites d'unités, les indices purement glaciaires sont rares. Cependant, la complexité de la sédimentation essentiellement (glacio-)marine et fluviatile est caractéristique de l'environnement glaciaire : variations latérales de faciès rapides, nombreuses surfaces d'érosion internes, structures chenalisantes et paléovallées, structures indiquant de fortes décharges sédimentaires.

L'unité 1 (30–70 m), essentiellement argileuse à la base, avec quelques rares galets striés isolés et intercalations gréseuses à litage oblique en mamelons, passe vers le haut à des bancs gréseux à laminations planes ou ondulées et rides de vagues. Cette succession est interprétée comme le passage d'une sédimentation glacio-marine distale à des dépôts sableux de plate-forme marine dominée par les tempêtes.

L'unité 2 (< 70 m), constituée essentiellement de grès fins à grossiers, montre de très fortes variations latérales de faciès, avec notamment des bancs tabulaires à laminations planes, structures d'échappement d'eau et intercalations silto-gréseuses finement lami-

nées passant à des unités amalgamées faites de mégarides chevauchantes. L'existence de surfaces d'accrétion latérale de 5 à 20 m de hauteur (Fig. 2c), recoupées par des structures en chenaux et la marque en photographie aérienne de ceintures de méandre parfaitement préservées (Fig. 1e), permettent d'interpréter les dépôts de l'unité 2 comme le résultat de l'agradation d'un système fluviatile méandriforme [17]. Les bancs tabulaires et les mégarides chevauchantes représentent, dans ce schéma, des dépôts de débordement de chenaux liés à des phénomènes de crues proglaciaires.

L'unité 3 est constituée par la juxtaposition de successions grano-croissantes débutant par des faciès argileux à figures de tempêtes, en *onlap* sur des structures de déformation sous-glaciaires, ou sur un mince niveau gréseux basal bioturbé et remanié par la houle. Ces dépôts argileux passent vers le haut à des faciès gréseux où alternent bancs à laminations planes et lits plus fins à rides. Des corps chenalisants de largeur hectométrique existent localement. Cette unité est interprétée comme le résultat de la progradation de lobes deltaïques succédant à un épisode transgressif consécutif à un retrait glaciaire.

Le comblement des paléovallées de l'unité 4 (Fig. 1d) débute par un grès grossier, localement fortement déformé, qui moule les flancs raides de la vallée (Fig. 2a). Au-dessus reposent successivement en *onlap* des grès fins argileux massifs à figures d'échappement d'eau et plissements gravitaires, puis des bancs de grès granoclassés, et finalement des grès grossiers à litages obliques formant de grandes structures chenalisantes sinueuses amalgamées. L'encaissement des vallées, dont les flancs sont moulés par des grès grossiers à la base, et la succession grano-croissante susjacente, suggèrent une érosion et un remplissage initial par des eaux de fonte sous-glaciaires d'un système de vallées en tunnel [8,10,13], colmaté ensuite par la progradation d'un cône sub-aquatique proglaciaire évoluant vers un environnement fluviatile.

4. Dépocentres et failles associées

À l'échelle régionale, l'orientation des paléovallées et la localisation de dépocentres apparaissent liées aux grands linéaments structuraux NNW–SSE et nord–sud héritées du socle (Fig. 1c). Les dépocentres, identifiés dans les unités 2 et 3, correspondent à des zones d'accumulation à subsidence différentielle et d'extension kilométrique. Un premier type de dépocentres, caractérisé par un remplissage très grossier, montre un épaississement au droit de failles affectant les sédiments de l'unité 1 et le substratum préglaciaire, mais scellées par l'unité 3 (Fig. 1a, profils A10–11, B16 et C14). Des brèches intraformationelles ainsi que des volcans de sable jalonnent leur bordure faillée. Un second type de dépocentre montre des géométries en *onlap* et en *roll-over* au sein de l'unité 3 (profil C30, Fig. 2d). Bien que de tels dépocentres puissent résulter d'instabilités gravitaires sur des fronts de delta ou sur les bordures de la vallée [9], la plupart de ceux-ci sont alignés le long d'accidents affectant l'ensemble de la couverture sédimentaire (Fig. 1d).

Des déplacements verticaux n'excédant pas 50 m et une distribution spatiale en relation avec des structures linéamentaires suggèrent, pour l'origine de ces dépocentres, un rejeu en régime extensif d'accidents panafricains provoqués par l'interaction entre le champ de contraintes régional et des contraintes flexurales d'origine glacio-isostasique [11].

5. Conclusion

L'architecture sédimentaire des dépôts glaciaires (sensu lato) est contrôlée par la répétition de périodes d'érosion glaciaire et par la formation de dépocentres liés à la réactivation par glacio-isostasie d'un réseau de failles préexistant. Cela se traduit par des unités sédimentaires discontinues et juxtaposées remplissant des paléovallées et paléodépressions. Chaque surface basale d'érosion représente une avancée majeure des fronts glaciaires sur la plate-forme, atteignant au moins le Nord du Gargaf ($> 28°S$). L'évolution de la morphologie de ces surfaces d'érosion glaciaire, depuis une surface à peu près plane jusqu'à des vallées fortement encaissées peut être interprétée, dans un schéma de retrait glaciaire généralisé, comme le reflet d'un changement de la position relative du Gargaf par rapport à la limite septentrionale de chaque maximum glaciaire. La transition d'origine climatique ou zonale entre un glacier à base froide et un glacier à base tempérée [16] pourrait expliquer notamment l'évolution vers une importante production d'eau de fonte sous-glaciaire entraînant la formation de vallées en tunnel avant le dépôt de l'unité 4. L'orientation des paléovallées, parallèle aux grandes failles de direction

nord–sud ou NNW–SSE et les déformations synsédimentaires le long de leurs flancs, suggèrent que les zones de faiblesse structurale et/ou que la distribution des dépocentres a/ont pu servir de guide à l'érosion glaciaire après le dépôt de l'unité 1.

L'enregistrement glaciaire, comprenant essentiellement des dépôts fluviatiles à marins peu profonds, reflète des environnements relativement distaux par rapport aux fronts glaciaires. Ils succèdent à des phases importantes de retrait des fronts glaciaires vers le sud et correspondent à la mise en place de conditions régionales interglaciaires. Chaque unité a été déposée pendant un temps assez court correspondant à une fraction d'un cycle climatique glaciaire-interglaciaire. Ces unités forment donc des unités allostratigraphiques qui sont corrélables sur l'ensemble du Bassin de Murzuq et au-delà sur la plate-forme nord-gondwanienne [7]. L'architecture stratigraphique est celle d'un système caractérisé par de fréquentes « cannibalisations ». Une accommodation sédimentaire peu importante pendant la durée de la glaciation contraste avec les fortes accommodations régnant lors du dépôt de chaque unité de dépôt correspondant au remplissage d'une paléovallée.

1. Introduction

During the Latest Ordovician, the western Gondwana was located in southern high latitudes. It was covered by an extensive ice sheet centred in Central Africa, the front of which fluctuated throughout present-day West and North Africa, and Arabia [1–3,6,7,18]. In Libya, the Late Ordovician glacial record of the Murzuq Basin is generally subdivided into basin-wide lithostratigraphic units: the lower mud-dominated Melaz Shuqran Formation and the upper sand-dominated Mamuniyat Formation [12,14]. However, detailed regional studies do not support this subdivision [15]. In the Gargaf area in the northern part of the basin, field work based on aerial photographs and geological mapping [4,5] shows that: (1) the glaciation-related successions can be subdivided into several depositional units bounded by unconformities related to the formation of glacial palaeovalleys, (2) each depositional unit comprises a coarsening-up succession grading from mud-dominated into sand-dominated deposits, and (3) relationships exist between the inherited regional structural trends and the location of the main valleys, glacial depocentres, and syn-glacial fault-controlled structures.

2. Glacial palaeovalleys

Four depositional units, which are vertically superimposed as well as laterally juxtaposed, have been defined within the Upper Ordovician glacial deposits in western Gargaf (Fig. 1a and b). A fifth transgressive unit, not described in this paper, was deposited during late-glacial time before the deposition of the Silurian shales.

Unit 1 is of large lateral extension and rests on a relatively flat surface at regional-scale. Although this basal surface is rarely visible, landscape observation and mapping clearly show that the contact is erosional, as indicated by local shallow and wide depressions cut into different horizons of the Lower to Middle Ordovician sandstones that are in place highly deformed below the surface. The lower bounding surface of Unit 2 coincides with wide palaeovalleys up to 20 km in width, 100 m in depth and more than 60 km in length. These palaeovalleys are laterally bounded by faulted and/or folded zones affecting both the pre- and syn-glacial deposits (Fig. 1a, profiles A30–41, C14–35 and C39–51). Unit 3 rests on Unit 2, Unit 1, or locally on the pre-glacial sandstones (Hawaz Formation). Its lower bounding surface forms palaeovalleys similar in extension to those of Unit 2 (profile C8–30) and is associated with well preserved subglacial deformation structures. Unit 4 corresponds to the filling of narrow palaeovalleys up to 150 m in depth and less than 5 km in width, deeply incised in the previous units and pre-glacial sandstones (profiles B9–14, C3–7 and C9–14) (Figs. 1c–d and 2a).

The glacial origin of the bounding surfaces can be asserted from the associated structure and/or from the nature of the overlying deposits. Direct evidence of glacial erosion exists for the basal surfaces of Units 1 and 3. In occasional exposures of bounding surface 1, preglacial sandstones are highly deformed and overlain by glaciomarine microconglomeratic argillaceous sandstones including rare striated exotic pebbles. Intraformational deformation structures including striated 'décollement' planes, Riedel shear step fractures, folds, 'roches moutonnées', or

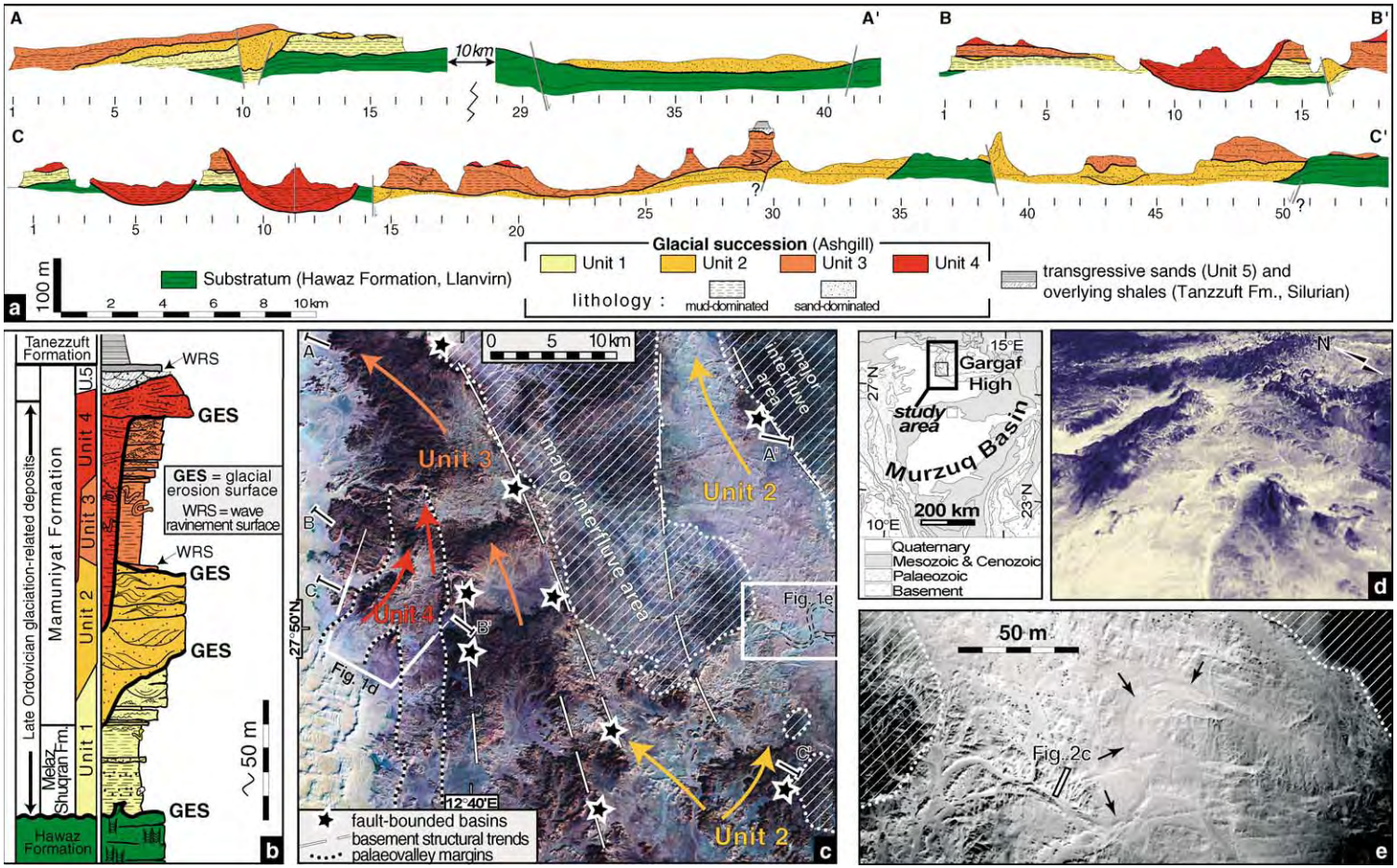

Fig. 1. (**a**) Selected cross-profiles showing the stratigraphic architecture of the Late Ordovician glacial record in the Gargaf area. (**b**) Synthetic log of the glaciation-related units with location of the main glacial erosion surfaces. (**c**) Satellite image (available at http://zulu.scc.nasa.gov/mrsid/mrsid.pl), of part of the western Gargaf area with location of the cross-profiles in (**a**), outlines of the palaeovalleys of Units 2, 3, and 4, and the distribution of the fault-controlled depocentres relative to the regional structural trend and to palaeovalleys. (**d**) 3D view of the confluence of two palaeovalleys in Unit 4 (location and scale in Fig. 1c). (**e**) Aerial photograph of a meander belt complex in Unit 2 (location in Fig. 1c).

Fig. 1. (**a**) Profils 2D illustrant l'architecture stratigraphique de la succession glaciaire fini-ordovicienne dans la région du Gargaf. (**b**) Log synthétique des unités « glaciaires » avec localisation des principales surfaces d'érosion. (**c**) Vue satellitaire partielle (disponible à http://zulu.scc.nasa.gov/mrsid/mrsid.pl) de la partie occidentale du Gargaf, avec la position des profils 2D de (**a**), le tracé des paléovallées des unités 2, 3 et 4, et la distribution spatiale des dépocentres sur failles par rapport aux structures linéamentaires et aux paléovallées. (**d**) Vue en 3D, montrant la confluence de deux paléovallées de l'unité 4 (localisation et échelle, Fig. 1c). (**e**) Photographie aérienne d'un complexe de méandres dans les dépôts de l'unité 2 (localisation sur la Fig. 1c).

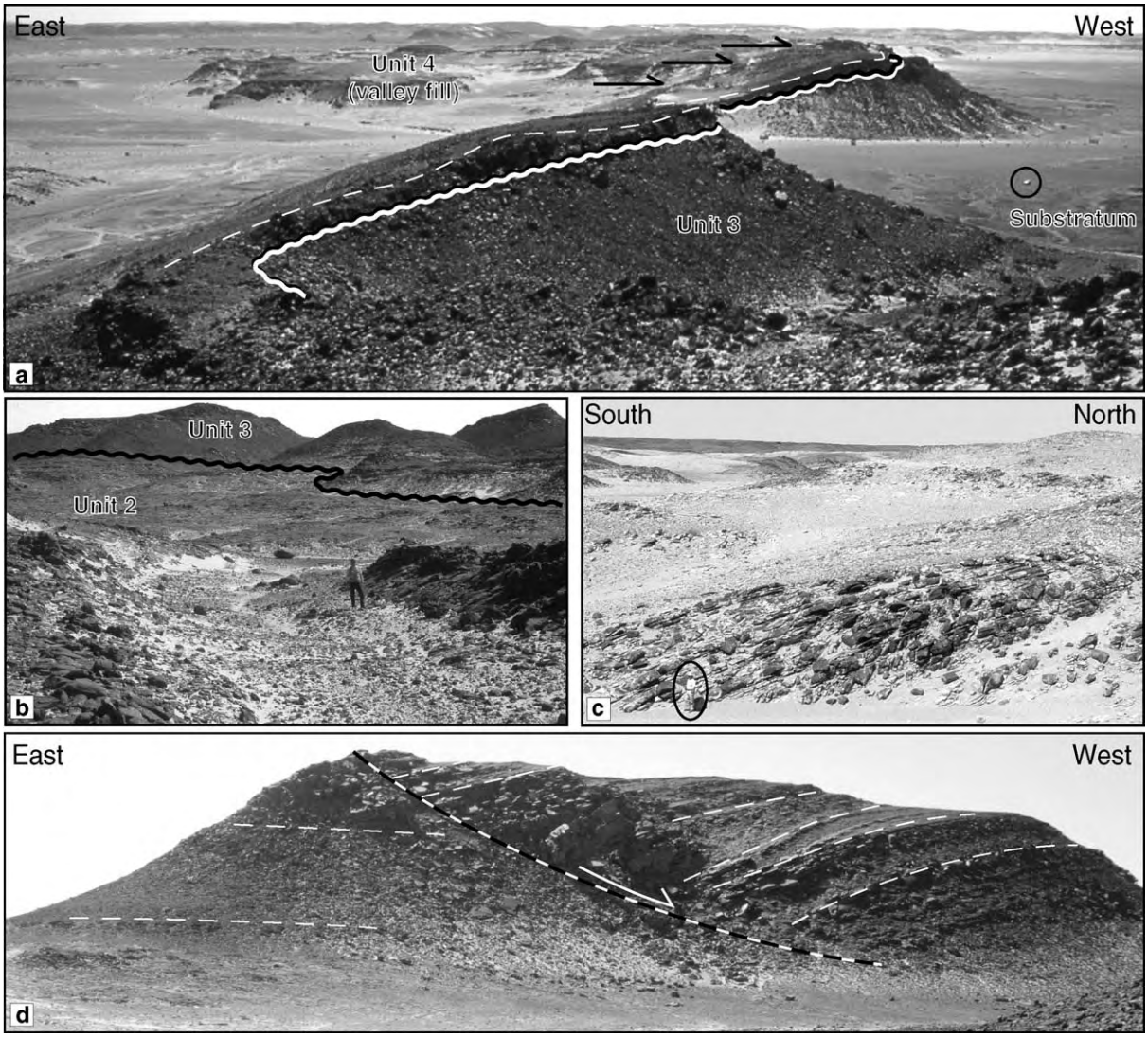

Fig. 2. (**a**) Western margin of a north–south-oriented palaeovalley of Unit 4; the bulk of the valley fills onlaps (black arrows) onto sandstone beds (dashed line) that drape the erosional surface (wavy line) (circled car for scale). (**b**) Glacial erosional surface at the base of Unit 3 deposits, along which intraformational striated surfaces (not shown) were found within the upper part of Unit 2 deposits; person for scale, standing within a subglacial channel. (**c**) Epsilon-cross-stratification within Unit 2, of laterally accreted meander-bar deposits (encircled person for scale, location of the profile in Fig. 1e). (**d**) Roll-over structure within a Unit-3 depocentre (cliff height: 70 m).

Fig. 2. (**a**) Bordure occidentale d'une paléovallée d'orientation méridienne appartenant à l'unité 4 ; l'essentiel du remplissage repose en *onlap* (flèches noires) sur des grès (ligne tiretée) moulant la surface d'érosion (ligne ondulée) (véhicule cerclé pour échelle). (**b**) Surface d'érosion glaciaire à la base de l'unité 3, le long de laquelle ont été trouvées des surfaces striées intraformationelles au sein des grès de l'unité 2 ; personnage pour échelle, au milieu d'un chenal sous-glaciaire. (**c**) Structures d'accrétion latérale d'une barre de méandre au sein de l'unité 2, reflétant la construction d'une barre de méandre (personnage cerclé pour échelle, localisation du cliché sur Fig. 1e). (**d**) Structure en *roll-over* au sein d'un dépocentre structural de l'unité 3 (hauteur de la colline : 70 m).

subglacial channels (Fig. 2b) point to subglacial shearing and erosion along the lower bounding surface of Unit 3. No direct evidence of glacial erosion was found along bounding surfaces of Units 2 and 4. However, in both cases the surfaces are overlain by high-energy shallow marine or fluvial sandstones, which

may have eroded the pre-existing glaciogenic features.

All palaeovalleys were most probably incised within unlithified sand or mud, as suggested by abundant soft-sediment deformation structures affecting both glacial and preglacial deposits.

3. Depositional units

Within the depositional units direct evidence of glacial processes is inferred from occasional striated exotic dropstones and subglacial deformation structures associated with bounding surfaces. In addition, the bulk of the sedimentary record, which corresponds to fluvial and shallow-marine depositional environments, is characteristic of glacial conditions as shown by the complex nature of the facies associations, internal unconformities, deformation structures, large-scale channels, palaeovalleys and evidence of high-sediment discharge and dump sedimentation.

3.1. Description

Unit 1 is made up of a basal mud-dominated succession (30–70 m) overlain by a coarsening-up sand-dominated succession (10–15 m). The mud-dominated succession consists of massive, microconglomeratic argillaceous sandstones including rare exotic striated pebbles, sharply overlain by laminated silty shales. The latter comprises lenticular or laterally extensive beds of fine-grained sandstones with wave or current ripples and small-scale hummocky cross stratifications. Slump and load structures were also observed. The sand-dominated succession rests upon the mud-dominated one with either an erosive or progressive contact. It is made up of well-sorted medium-grained sandstone beds with horizontal to wavy laminations, and graded beds passing upward into fine-grained wave-rippled sandstones.

Unit 2 (< 70 m) is made up of fine- to coarse-grained sandstones, characterized by rapid (kilometre-scale) lateral facies changes whose relationship is generally difficult to trace and interpret. Extensive, several-metre thick, medium- to coarse-grained sandstone sheets, with horizontal to subhorizontal laminations, vertical sheet-dewatering structures, and intervening fine-grained laminated sandstones, pass laterally into amalgamated cosets of 2D or 3D climbing megaripples. Another facies assemblage consists of 5–20 m high large-scale epsilon cross-stratifications (Fig. 2c), coarse-grained channel structures, and fine-grained sandy plugs with current ripples and convolute bedding. A kilometre-scale meandering belt with chute channels can be observed in aerial photographs (Fig. 1e).

Unit 3 is made up of a juxtaposition of delta-like coarsening-up systems, locally affected by syn-sedimentary deformation. The lowermost part of Unit 3 generally consists of laminated mudstones onlapping either the subglacial features preserved on the lower bounding surface, or a decimetre to metre-thick bioturbated and wave-rippled basal sandstone bed. Upwards, micaceous siltstones, with fine-grained sandstone intercalations including waves and polygonal ripples, grade into coarsening-up sandstones. The latter typically display flat laminations in the thicker beds, and wave or current ripples in the intervening thinner beds. Climbing ripples are commonly observed. Isolated, 100 m wide channel structures also occur in places eroding the underlying sediments.

Unit 4 consists of an overall coarsening-up sequence. The incision is initially draped by unsorted coarse-grained sandstones, locally highly deformed, that mould the valley sides, and which are later onlapped by the bulk of the valley infill (Fig. 2a). This infill consists from base to top of: (1) fine-grained muddy sandstones including slump structures, turbidite-like sandstone beds along the valley sides, and conspicuous dewatering structures, (2) an erosion-based succession made up of laterally extensive medium-grained, graded, sandstone beds with abundant dewatering structures, (3) laterally and vertically stacked large-scale sinuous channel structures made up of cross-laminated coarse-grained sandstones. The valley fill is sharply capped by coarse- to very coarse-grained sandstones, which overflow the valley sides and rest on Unit 3 deposits outside the valleys (Fig. 1a, profiles B1–5, C15–20).

3.2. Interpretation

The sediments of Unit 1 are interpreted as distal glacio-marine deposits in front of retreating marine ice fronts, passing upwards into storm-dominated prograding shelf deposits. The valley infill in Unit 2

resulted from the aggradation of sinuous to meandering fluvial systems [17]. This is confirmed by well preserved meander belt structures including variously oriented slightly dipping lateral accretion surfaces, well-bedded overbank deposits and fine-grained sandy plugs. The climbing megaripples, which are characteristic of Unit 2, represent highly concentrated sediment-laden stream-flow deposits, possibly related to outburst events resulting in outflows outside the sinuous channels. The characteristics of the lower bounding surface of Unit 3 suggest both a glacial environment and a transgressive event, and the valley fill deposits record the various stages of the progradation of deltaic lobes, from storm-dominated pro-delta up to the shoreface or fluvial environments. The depth and narrowness of the palaeovalleys of Unit 4, and the presence of the initial valley fill moulding the erosional topography, rather suggest erosion and first infill by sub-ice meltwater flows in tunnel valleys later infilled by proglacial prograding subaquatic fan to delta deposits [8,10,13]. A fluvial braidplain is inferred for the upper part of Unit 4.

4. Fault-controlled depocentres

Small-scale soft-sediment deformation structures are common and distributed throughout the study area. They are either due to subglacial shearing or triggered by local gravity-driven instabilities due to high-rate of sediment supply (e.g., delta sequences in Unit 3). They are not considered as directly related to tectonic events. At a larger-scale, palaeovalleys and local wedge-shaped fault-bounded depocentres are parallel and clearly linked with NNW–SSE and north–south striking faults, which correspond to regional Panafrican tectonic trends in the underlying basement (Fig. 1c).

The local fault-bounded depocentres observed in Units 2 and 3, are up to 50 m thick, 500 m to 2 km wide, and can be traced over several kilometres parallel to the axis of the palaeovalleys.

A first type of fault-bounded depocentre was observed in Unit 2. It is characterized by a medium- to very coarse-grained infill, and shows a significant thickening into the footwall (Fig. 1a, profiles A10–11, B16 and C14). Underlying sediments of Unit 1 are faulted and offset. Overlying deposits belonging to Unit 3 locally seal the fault system. The occurrence of intraformational breccias located at the fault-bounded side of the depocentres suggests the existence of small transient palaeorelief forms. The presence of sand-volcanoes close to the faults indicates overpressure during the infill of the depocentres. Although gravitational processes could be envisaged for the formation of these depocentres, their alignment along the main lineaments (Fig. 1c), and the fact that the pre-glacial substratum is involved in the deformation, strongly suggest a tectonic origin.

A second type of fault-bounded depocentre shows onlap and rollover geometries within well bedded Unit 3 sediments (Fig. 1a, profile C30, Fig. 2d). Faults were not observed cutting across pre-glacial rocks, and a gravity-driven mechanism due to slope instability in delta setting or along valley sides [e.g., [9] appears as the probable triggering mechanism. However, a number of these depocentres are aligned along structural trends as well (Fig. 1c).

Fault-bounded depocentres related to the first type were active during a time range starting after deposition of Unit 1. As they are filled by fluvial sandstones and sealed by sediments belonging to Unit 3, they coincide with the deposition of Unit 2. Depocentres related to the second type were active during the deposition of Unit 3.

The small amount of vertical displacement, which does not generally exceed 50 m, the spatial association with pre-existing lineament orientation of Panafrican origin, as well as the lack of a consistent vergence of the faults bounding the depocentres, suggest that this deformation, occurring during the Late Ordovician glaciation is more likely associated with the reactivation of pre-existing structures during deglaciation events rather than associated to a large-scale tectonic event. The interaction of a crustal stress field with flexural stresses due to ice-sheet loading or to the subsequent removal of ice load results in low-strain either extensional or wrench tectonics [11]. It should be noted that these faults were also reactivated later during the so-called Hercynian event.

5. Conclusion

The architecture of the glacial succession is controlled primarily by successive glacial erosion events

resulting in laterally discontinuous and juxtaposed sedimentary units filling palaeodepressions and palaeovalleys. Each of the corresponding basal bounding surfaces represents a major ice-front advance throughout the north Gondwana platform, reaching at least the northern Gargaf (> 28°N). The progressive evolution of the shape of the bounding surfaces from a relatively flat regionally extensive surface, to well-defined wide and shallow palaeovalleys, and to narrow and deeply incised palaeovalleys may reflect a change in the position of the Gargaf area relative to the successive maximum northern extension of the ice fronts in an overall glacial retreat. Climatically controlled or subglacial zonal changes [16] from cold-based to warm-based glacier conditions may also explain this evolution and particularly the intense meltwater production during the latest glacial advance resulting in the formation of tunnel valleys. Palaeovalley orientations parallel to the north–south or NNW–SSE striking faults and syn-sedimentary deformation along palaeovalley margins could also suggest that structural weaknesses and/or the distribution of fault-bounded basins may have acted as guides for the glacial erosion processes starting after the deposition of Unit 1. The relationships between regional structural trends inherited from Panafrican lineaments and syn-glacial faults and associated small-scale depocentres suggest glacio-isostatically induced fault reactivation. The latter took part in the complex architecture of the Upper Ordovician deposits of the Gargaf area.

Although sedimentary units are bounded by erosional surfaces of glacial origin, the bulk of the sedimentary succession is made up of fluvial to shallow-marine sediments reflecting pro- to distal glacial environments related to either retreating marine ice-front evolution or interglacial conditions (ice front shifted southward). Each of the sedimentary units was deposited during a short time interval corresponding to a fraction of a climatically controlled glacial cycle. They correspond to allostratigraphic units that should be correlated within the Murzuq Basin and outside throughout the north Gondwana platform [7]. The stratigraphic architecture suggests a low-accommodation depositional system, within which several "cannibalisation" events have occurred through repetitive glacial erosion events. Low-accommodation conditions throughout the whole glaciation contrast with high accommodation conditions that characterise the filling of glacially eroded palaeovalleys by relatively thick (up to 100 m) sedimentary units.

Acknowledgements

This work was supported by Repsol Exploration Murzuq SA and partners (Total, OMV, Norsk-Hydro). We thank Géoscience Consultant (Bagneux, France) for providing the 3D view of Fig. 1d.

References

[1] S. Beuf, B. Biju-Duval, O. De Charpal, P. Rognon, O. Gariel, A. Bennacef, Les grès du Paléozoïque inférieur au Sahara, in: Science et Technique du Pétrole, Vol. 18, Institut Français du Pétrole, Éditions Technip, 1971.

[2] M. Deynoux, Les formations glaciaires du Précambrien terminal et de la fin de l'Ordovicien en Afrique de l'Ouest. Deux exemples de glaciation d'inlandsis sur une plate-forme stable, Trav. Lab. Sci. Terre Saint-Jerôme Marseille (B) 17 (1980).

[3] M. Deynoux, Terrestrial or waterlain glacial diamictites? Three case studies from the Late Precambrian and Late Ordovician glacial drifts in West Africa, Palaeogeogr. Palaeoclimatol. Palaeoecol. 51 (1985) 97–141.

[4] M. Deynoux, Contribution to the stratigraphy and sedimentology of the Upper Ordovician 'glacial' formations of the Murzuq Basin, Libya, unpublished report, 1998.

[5] M. Deynoux, J.-F. Ghienne, G. Manatschal, Stratigraphy and sedimentology of the Upper Ordovician glacially-related deposits of the Western Gargaf High, Fezzan, Northern Libya (Explanatory booklet of the Geological Map), unpublished report, 2000.

[6] J.-F. Ghienne, Modalités de l'enregistrement d'une glaciation ancienne. Exemple de la glaciation fini-ordovicienne sur la plate-forme nord-Gondwanienne en Afrique de l'Ouest, thèse, université Louis-Pasteur, Strasbourg,1998.

[7] J.-F. Ghienne, Late Ordovician sedimentary environments, glacial cycles, and post-glacial transgression in the Taoudeni Basin, West Africa, Palaeogeogr. Palaeoclimatol. Palaeoecol. 189 (2003) 117–145.

[8] J.-F. Ghienne, M. Deynoux, Large-scale channel fill structures in Late Ordovician glacial deposits in Mauritania, Western Africa, Sediment. Geol. 119 (1998) 141–159.

[9] T. Glover, K. Adamson, R. Whittington, B. Fitches, J. Craig, Evidence for soft-sediment deformation – the Duwaysah Slide of the Gargaf Arch, central Libya, in: M.A. Sola, D. Worsley (Eds.), Geological Exploration in Murzuq Basin, Elsevier Science, 2000, pp. 417–430.

[10] J.P.P. Hirst, A. Benbakir, D.F. Payne, I.R. Westlake, Tunnel valleys and density flow processes in the Upper Ordovician glacial succession, Illizi Basin, Algeria: influence on quality reservoir, J. Pet. Geol. 25 (2002) 297–324.

[11] A.C. Johnston, The effect of large ice sheets on earthquake genesis, in: S. Gregersen, P.W. Basham (Eds.), Earthquakes at North-Atlantic Passive Margins: Neotectonics and Postglacial Rebound, in: NATO ASI Series, Series C, Vol. 266, 1989, pp. 581–600.

[12] E. Klitzsch, Lower Palaeozoic rocks of Libya, Egypt, and Sudan, in: C.H. Holland (Ed.), Lower Palaeozoic of the Middle East, Eastern and Southern Africa, and Antarctica, John Wiley & Sons, 1981, pp. 131–163.

[13] D. LeHeron, O.E. Sutcliffe, K. Bourgig, J. Craig, C. Visentin, R. Whittington, Sedimentary architecture of Upper Ordovician tunnel valleys, Gargaf Arch, Libya: implications for the genesis of a hydrocarbon reservoir, GeoArabia (accepted).

[14] D. Massa, Paléozoïque de Libye occidentale. Stratigraphie et Paléogéographie, thèse d'État, université de Nice, 1988.

[15] N. McDougall, M. Martin, Facies models and sequence stratigraphy of Upper Ordovician outcrops in the Murzuq Basin, SW Libya, in: M.A. Sola, D. Worsley (Eds.), Geological Exploration in Murzuq Basin, Elsevier Science, 2000, pp. 223–236.

[16] J. Menzies, W.W. Shilts, Subglacial environments, in: J. Menzies (Ed.), Past Glacial Environments, Butterworth-Heinemann Ltd., Oxford, UK, 1996, pp. 15–136.

[17] J.-L. Rubino, R. Anfray, C. Blanpied, M. Thu, J.-F. Ghienne, M. Deynoux, G. Manatschal, Meander belt complexes in Latest Ordovician proglacial setting; examples from the Mamuniyat Formation in Murzuk Basin (SE Libya), in: 8^{e} Congrès français de sédimentologie, livre des résumés, Vol. 36, Association des sédimentologistes français, 2001, p. 315.

[18] D. Vaslet, Upper Ordovician glacial deposits in Saudi Arabia, Episodes 13 (1990) 147–161.

Late Ordovician tunnel valleys

Jean-François Ghienne

Institut de Physique du Globe de Strasbourg, Ecole et Observatoire des Sciences de la Terre, UMR 7516 CNRS/ Strasbourg University, 1, rue Blessig, 67084 Strasbourg cedex, France.

e-mail: ghienne@unistra.fr

Introduction

Overdeepened incisions forming tunnel valleys are remarkable geomorphic elements, which provide valuable information on past subglacial hydrological regimes and may constitute attractive reservoir targets. Geometries and distribution of Quaternary tunnel valleys have been intensively illustrated based on geophysics, while the glacial record of pre-Pleistocene glaciation offers exposures of analogous structures, from which the internal architecture and sedimentary infill can be easily delineated.

The Late Ordovician glacial record (~ 444 Ma) preserved the elements of subglacial tunnel drainage networks in the form of a spectrum of palaeovalleys (km-scale) to palaeochannels (10-100's m scale) (Ghienne and Deynoux, 1998; Hirst et al., 2002; Le Heron et al., 2004, 2009; Denis et al., 2007). A database that comprises more than 30 elements taken from Mauritania, Morocco, Algeria, Libya, Niger and Jordan is used to exemplify the specificities of these pre-Pleistocene tunnel drainage networks.

Palaeoglacial setting

The Late Ordovician palaeoglacial setting is that of a continental-scale ice-sheet, with several phases of ice-front advances and recessions. Continuous ice fronts are inferred from Mauritania to Saudi Arabia at time of the glacial maximum (Fig. 1; Ghienne et al., 2007a). Ice-flow orientations are to the WNW to NNW in Mauritania, essentially to the NNW to N in Algeria and Libya, and to the NE in Saudi Arabia. Ice-stream pathways and correlative inter-stream areas have been described at the 100's km scale (Moreau et al., 2005; Ghienne et al., 2007a; Le Heron and Craig, 2008).

Throughout this huge domain, the Late Ordovician ice sheet mainly straddled a poorly to non-consolidated substrate made up of fluvial to shallow-marine siliciclastics. To the South, sand prevailed whereas to the North, argillaceous fine-grained sediments constitute the main part of the preglacial stratigraphic succession (Ghienne et al., 2007b).

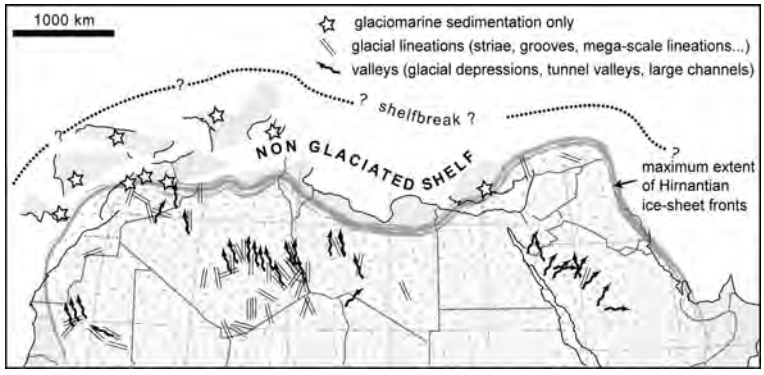

Figure 1: *Paleoglacial setting of Late Ordovician tunnel drainage networks at the Hirnantian glacial maximum (from Ghienne et al., 2007a).*

Cross-section and map-view of Late Ordovician tunnel networks

Large valleys may extent more than 50 km while channels are of limited extent (< 5 km). Tunnel valley generally form low sinuosity structures and confluence or difluence are observed in some cases (Fig. 2). Incision depths range from 200 m (deepest valleys) to less than 30 m (channels) (Fig. 3). Widths range from 5 km to 10 m. The cross-sectional morphology of the deep valleys is usually relatively steep sided (10-35°) with flat bottoms. Dealing with channels, vertical margins are occasionally observed. Although width/ depth ratios range from 50 (wide valleys) to less than 5 (channels), a continuum is observed between the two types of end-members. Palaeovalleys orientations are most often parallel to the main ice-flow orientations (Fig. 1).

***Figure 2**: Map view of Late Ordovician tunnel valleys. The Jordan example constitutes a network of small tunnel valleys showing internal cross-cutting relationships.*

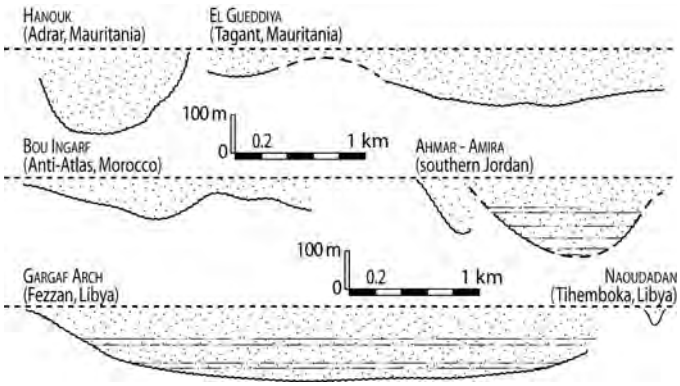

***Figure 3**: Cross-sections of tunnel valleys from the Late Ordovician glacial record, with vertical exaggeration. A siltstone to sandstone succession of deltaic origin fills in the palaeovalleys of Amira and from the Gargaf Arch. Other structures are filled by fluvio-glacial sandstones.*

Internal architecture and sedimentary infill

Tunnel networks are incised in pre-glacial or syn-glaciation sand to shale successions. The infill of both valleys and channels is characteristically composed of two distinct units. The lower one drapes the incision surface and represents a concave-up sediment body of limited thickness (1-30 m). It corresponds to either a chaotic unit (mixture in various proportion of deformed and/ or slumped pre-incision sediments, coarse-grained to conglomeratic glacio-fluvial sandstones, lag deposits and other undifferentiated ice-contact deposits) or a medium- to coarse-grained sandstone package including subglacial shear zones (striated surfaces, fluidilized sediments). Sand injection in the form of dykes or sills is usually observed within this chaotic unit or within the underlying pre-incision host sediment succession. In addition, glaciotectonic deformation (thrust and fold) may affect the pre-incision sediment succession. Resulting structures are truncated by the erosional surface (Fig. 4).

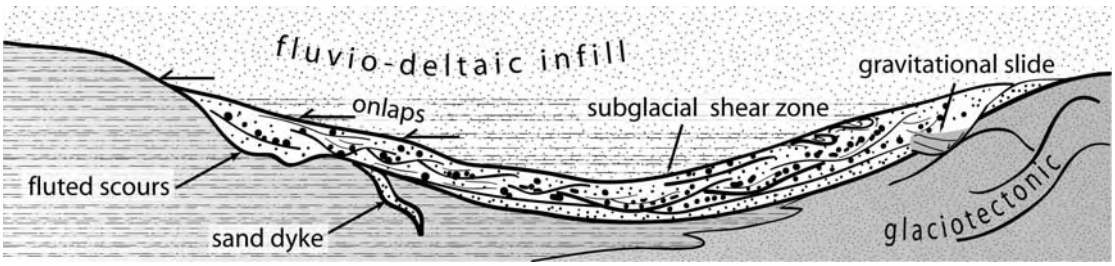

***Figure 4**: Main architectural elements of a tunnel valley or channel based on the Late Ordovician glacial record. At the first-order, the main infill that is made up of fluvio-deltaic deposits onlaps a lower concave-up unit related to subglacial processes. This scheme is out of scale.*

The second unit comprises the main infill of the valley or the channel. It onlaps the lower one. The bulk of the infill of the largest valleys is made up of either medium- to coarse-grained, flood-dominated, fluvio-glacial sandstones or coarsening- and thickening upward siltstone to sandstone successions of deltaic origin, including turbidite deposits. In channels, fluvio-glacial sandstones are usually observed. A single dropstone-bearing, subaquatic infill (glaciomarine?, subglacial lake?) has been observed.

The lower chaotic unit is though to reflect a subglacial package linked with meltwater drainage and incision processes while the main, upper unit represent fluvio-deltaic successions deposited after an ice front recession (Fig. 4). Fluvio-glacial infills either overfilled or underfilled the valleys and channels. In the case of underfilling, a latter re-incision is common.

Conclusion

Tunnel valleys seem to have been preferentially incised in inter-stream areas (zones of relative ice/ sediment coupling) while tunnel channels are essentially represented at the top of giga-scale glacial lineations formed within ice-stream pathways. The two categories of structures would then reflect distinct hydrological regimes. Dealing with a particular tunnel valley network, both the cross-sections and the distance in-between two adjacent valleys (e.g. 5 km for the Jordan network, ~40 km for a Mauritanian network) are similar. This statement that suggests the system was adjusted to a specific subglacial meltwater regime may help to extrapolate the spatial distribution and sizes of tunnel valleys in sedimentary basins from restricted datasets.

References

Denis, M., Buoncristiani, J.-F., Konaté, M. and Guiraud, M. [2007] The origin and glaciodynamic significance of sandstone ridge networks from the Hirnantian glaciation of the Djado Basin (Niger). *Sedimentology*, **54**, 1225-1243.

Ghienne, J.-F. and Deynoux, M. Large-scale channel fill structures in Late Ordovician glacial deposits in Mauritania, western Sahara. *Sediment. Geol.*, **119**, 141-159.

Ghienne, J.-F., Le Heron, D., Moreau, J., Denis, M., Deynoux, M. [2007a] The Late Ordovician glacial sedimentary system of the North Gondwana platform *in Glacial Sedimentary Processes and Products, (Eds.* Hambrey, M., Christoffersen, P., Glasser, N., Janssen, P., Hubbard, B. and Siegert, M. (eds.) Special Publication n°39, International Association of Sedimentologists, Blackwells, Oxford, pp. 295-319.

Ghienne, J.-F., Boumendjel, K., Paris, F., Videt, B., Racheboeuf, P. & Ait Salem, H. [2007b] The Cambrian-Ordovician succession in the Ougarta Range (western Algeria, North Africa) and interference of the Late Ordovician glaciation on the development of the Lower Palaeozoic transgression on northern Gondwana. Bulletin of Geosciences, **82(3)**, 183-214

Hirst, J.P.P., Benbakir, A., Payne, D.F. and Westlake, I.R. [2002] Tunnel Valleys and Density Flow Processes in the upper Ordovician glacial succession, Illizi Basin, Algeria: influence on reservoir quality. *Mar. Petrol. Geol.* **25**, 297-324.

Le Heron, D., Sutcliffe, O.E., Bourgig, K., Craig, J., Visentin, C. and Whittington, R. [2004] Sedimentary Architecture of Upper Ordovician Tunnel Valleys, Gargaf Arch, Libya: Implications for the Genesis of a Hydrocarbon Reservoir. *GeoArabia* **9**, 137-160.

Le Heron, D. and Craig, J. [2008] First-order reconstructions of a Late Ordovician Saharan ice sheet. *J. Geol. Soc.*, **165**, 19-29.

Le Heron, D., Craig, J. and Etienne, J.L. [2009] Ancient glaciations and hydrocarbon accumulations in North Africa and the Middle East. *Earth-Science Reviews*, **93**, 47-76.

Moreau J., Ghienne J.-F., Le Heron D., Rubino J.-L., Deynoux M. [2005] 440 Ma old ice stream in North Africa. *Geology,* **33***, 753-756.*

Late Ordovician tunnel valleys in southern Jordan

G. Douillet[1], J.-F. Ghienne[1]*, Y. Géraud[1], A. Abueladas[2] , M. Diraison[1] and A. Al-Zoubi[2]

[1] Ecole et Observatoire des Sciences de la Terre, Institut de Physique du Globe de Strasbourg, UMR 7516 CNRS – Université de Strasbourg, 1 rue Blessig, 67084 Strasbourg, France ()
[2] Surveying and Geomatics Engineering Department, Faculty of Engineering, Al-Balqa' Applied University, Al-Salt 19117, Jordan

*Corresponding author (e-mail: ghienne@unistra.fr)

Running title: Ordovician tunnel valleys in Jordan

Abstract: 170 words
Core Text: 5202 words
Reference list: 1900 words (68 items)
Figure captions: 587 words
Total: 7867 words

Abstract: The Upper Ordovician glacial record of southern Jordan (Ammar Fm.) essentially consists in palaeovalley infills and of a subordinate time-transgressive fluvial to shallow-marine succession overstepping both the palaeovalleys and interfluve areas. Valley size (60-160 m in depth, 1-3 km in width), steep (20-50°) margins, internal organisation and depositional facies point to tunnel valleys. The latter are infilled by either fluvioglacial sandstones or fluviodeltaic coarsening-upward successions including fine-grained clayey sediments. Re-occupation of previous valleys is evidenced in places. At least three generations of tunnel valleys are inferred from cross-cutting relationships, although they most probably only reflect temporary standstills and minor re-advances related to the overall recession succeeding to the main glacial advance corresponding in Saudi Arabia to the Sarah Fm. Petrophysical measurements indicate the higher permeabilities are located in the glacially related strata (1.5-3 Darcy in fluvioglacial infills), with a somewhat reduced porosity (22-28) relative to the preglacial sandstones owing to a higher clay content likely of diagenetic origin. Sandstone amalgamation however gives a high reservoir quality to fluvioglacial sandstones. (END OF ABSTRACT)

Article soumis en juin 2010 aux *Special Publications of the Geological Society London,* volume "Glaciogenic reservoirs", accepté avec révision mineure (octobre 2010)

Subglacial overdeepened incisions of tunnel valley networks are remarkable geomorphic elements with high preservation potential at geological time scale. They provide valuable information on past subglacial hydrological regimes (Piotrowski, 1997; Eyles 2006) and may constitute attractive hydrocarbon and water reservoir targets (Hirst *et al.* 2002; Sandersen & Jorgensen, 2003; Le Heron *et al.* 2004, 2009; BURVAL working group, 2009; Moscariello *et al.* 2009). The geometry and distribution of Quaternary tunnel valleys have been intensively illustrated based on geophysics especially in northern Europe (Huuse & Lykke-Andersen 2000; Praeg 2003; Kluiving et al. 2003; Jorgensen et al. 2003; Lonergan *et al.* 2006; Bosch et al. 2009; Lutz et al. 2009), while the glacial record of pre-Pleistocene glaciation offers exposures of analogous structures, from which the internal architecture and sedimentary infill can be more easily delineated. Tunnel valleys have been reported from Carboniferous-Permian successions (Eyles & de Broekert, 2001) but are more frequently reported based on the Upper Ordovician glacial record. Hirnantian (~ 444 Ma) glacial advances on the Gondwana shelf throughout the Arabian and North African regions resulted in tunnel valley incisions and related infilling successions (Ghienne *et al.* 2007; Le Heron *et al.* 2009). In North Africa, they are documented in Mauritania (Ghienne & Deynoux 1998), Morocco (Le Heron, 2007; Loi *et al.* 2010), Algeria (Hirst *et al.* 2000) and Libya (Ghienne *et al.* 2003; Le Heron *et al.* 2004). Tunnel valleys in Spain (Guttiérez-Marco *et al.* 2010) are associated with the maximum glacial extent (Fig. 1). In southern Jordan, Abed *et al.* (1993) and Powell *et al.* (1994) have documented glacial valleys in the Batn al Ghul area, which we re-interpret in the present contribution as tunnel valleys. Their stratigraphic context, spatial distribution and infilling architecture are described. Inferences for palaeoglacial reconstructions and hydrocarbon reservoir characterisation are outlined.

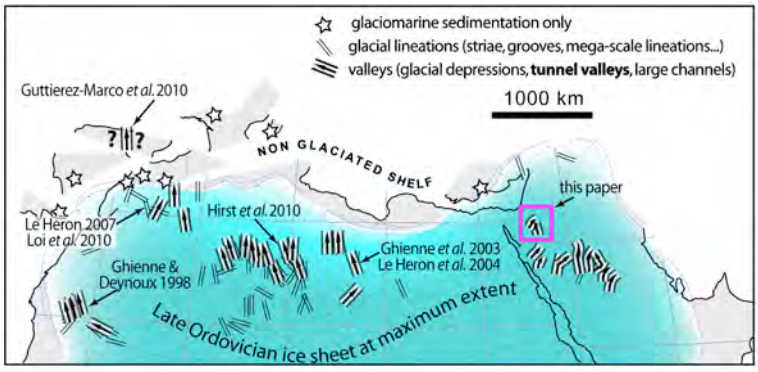

Fig. 1. Reconstruction of the North Gondwana platform at the Hirnantian glacial maximum, with location of the study area in southern Jordan. Main contributions interpretating tunnel valleys from the Upper Ordovician glacial record are plotted

Stratigraphic context

The Batn al Ghul study area is located 35 km east of Wadi Ram, halfway between Ma'an and al Mudawwara (Fig. 2). Here, Lower Palaeozoic strata mainly comprise a thick wedge (> 1200 m) of fluvial to shallow-marine sandstones with subordinate fine-grained intervals (Bender, 1974; Powell, 1989; Khalil, 1994; Schneider *et al.* 2007). The Lower Cambrian to Early/Middle Ordovician Ram Group is made up of fluvial sandstones with occasional tidal intercalations (Amireh *et al.* 1994). The Middle to Upper Ordovician strata (lower part of the Khreim Group), including the graptolitic Darriwilian Hiswa Shales at the base, comprise a shallow-marine, intensively bioturbated succession with alternating tide- or storm-dominated intervals (Makhlouf, 2002; Masri, 1998; Sharland *et al.* 2001; Amireh *et al.* 2001; Armstrong *et al.* 2005). Upper Ordovician pre-glacial strata (*i.e.* Katian) are essentially represented by the Tubeiliyat Fm. Related strata, 200 m thick, were initially ascribed to a member of the Upper Ordovician to Silurian Mudawwara Fm. (e.g. Abed *et al.* 1993; Amireh *et al.* 2001) but have been subsequently referred to as an independent formation (Armstrong *et al.* 2005). In spite of the lack of biostratigraphic data, sequential analysis and comparison with better-constrained successions (*e.g.*, Morocco: Loi *et al.* 2010) suggest that the youngest Katian strata may be present beneath Hirnantian strata in interfluve areas.

The Tubeiliyat Fm. is locally deeply truncated by glacial palaeovalleys, the infill of which corresponds to the lower part of the Ammar Fm. (Abed *et al.* 1993; Powell *et al.* 1994; Amireh *et al.* 2001; Armstrong *et al.* 2005; Turner *et al.* 2005). At the top of the Ammar Fm., a transgressive trend is usually recorded by an up to 15 m thick fining-upward sheet-like succession that most often oversteps

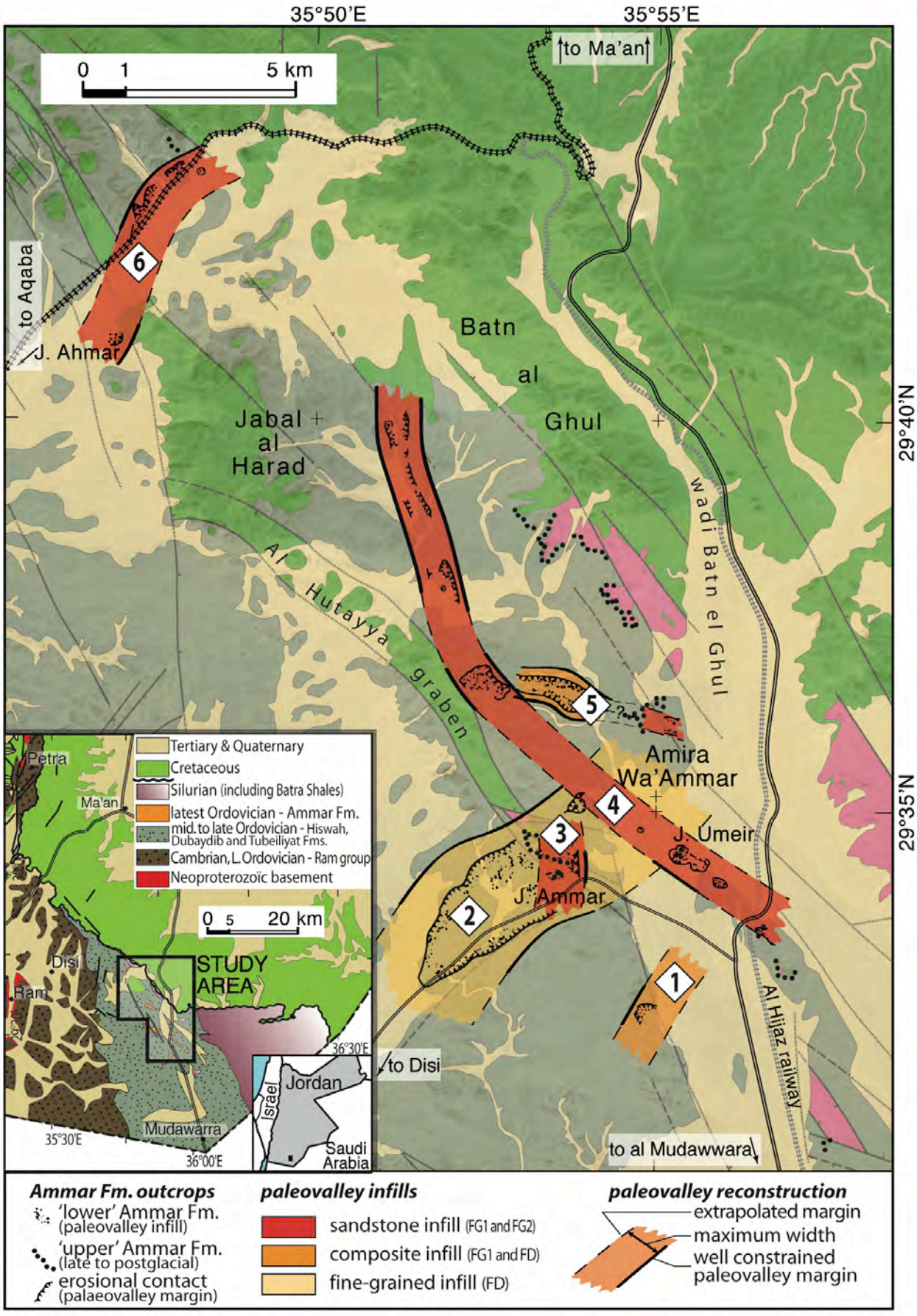

Fig. 2. Geological map of southern Jordan with location of the Ammar Fm. outcrops and extrapolated tunnel valley paths (geological contour lines from Masri, 1998). Palaeovalley numbering (1-6) in diamond shapes (cf. Fig. 3)

palaeovalleys and interfluves (Tr in Figs 3 & 4). It commences with cross-stratified sandstones and conglomeratic lags — some of which with striated and facetted quartz pebbles (Abed *et al.* 1993) — and ends with medium- to fine-grained, brachiopod-bearing storm-dominated deposits. In places, only a thin (< 1 m) transgressive lag is identified, which truncates glaciogenics or rests directly upon the pre-glacial Tubeiliyat Fm. In the uppermost Ammar Fm., an 8 m thick, storm-dominated, shallowing-upward shoreface succession is preserved beneath the overlying graptolitic offshore shales of the Batra Fm ("Hot Shales" of Lüning *et al.* 2000). The age and the significance of the latter is questionable. The occurrence in the uppermost Ammar Fm. of a complete post-glacial high-frequency cycle, which includes facies associations identical to those of the preglacial Tubeiliyat Fm., would however suggests an Early Silurian age for the lowest Batra Fm. (Lüning *et al.* 2005; Loydell *et al.* 2009) rather than a latest Ordovician age (Armstrong *et al.* 2005, 2009). Glaciogenics are exposed in a restricted area (10 x 20 km) where they have been preserved from both Cretaceous and Recent erosion in the form of residual hills. In places, the original architecture is altered by post-Cretaceous faulting most probably reactivating a Nadj-related fault system (N140/160; e.g. the al Hutayya graben; Masri, 1998; Turner *et al.* 2005).

Palaeovalleys

Powell *et al.* (1994) have basically mapped two glacial palaeovalleys. Recent fieldwork has allowed us to delineate a network of six cross-cutting palaeovalleys (Fig. 2). They are successively described from south to north (Palaeovalleys 1 to 6) (Fig. 3). Incision depths are estimated considering the youngest preserved strata of the Tubeiliyat Fm. at the valley thalwegs. Palaeovalleys widths are only indicative and are given after extrapolation up to the contact between the Ammar and Batra formations, taking into account the dips of the palaeovalley margins.

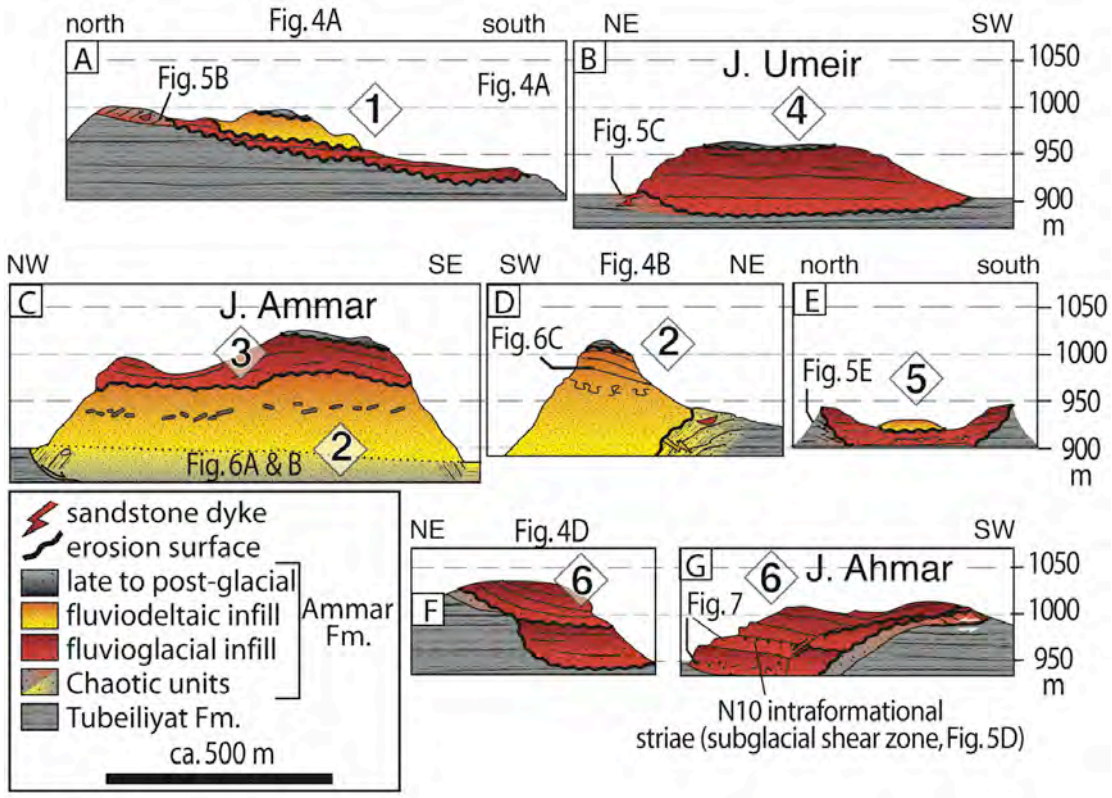

Fig. 3. Sketchy palaeovalley cross-sections. Numbers refer to Fig. 2. Locations of photographs are given (Figs 4, 5, 6 and 7)

Palaeovalley 1

No outcrop of the Ammar Fm. was previously known in this area (Figs. 3A & 4A). An erosion surface truncates 50 m of the middle Tubeiliyat Fm. but the total depth of the incision may be estimated to a hundred metres. The initial width was ca. 1 km with a margin dipping up to 25°. Valley orientation was SSW-NNE. Overlying a gravely sandstone lag, the lower palaeovalley infill corresponds to a medium- to coarse-grained sandstone succession, 10-20 m thick, with mainly with subhorizontal laminations. Higher along the valley margin, the coarse-sandstones are lacking. Instead, a chaotic unit including a

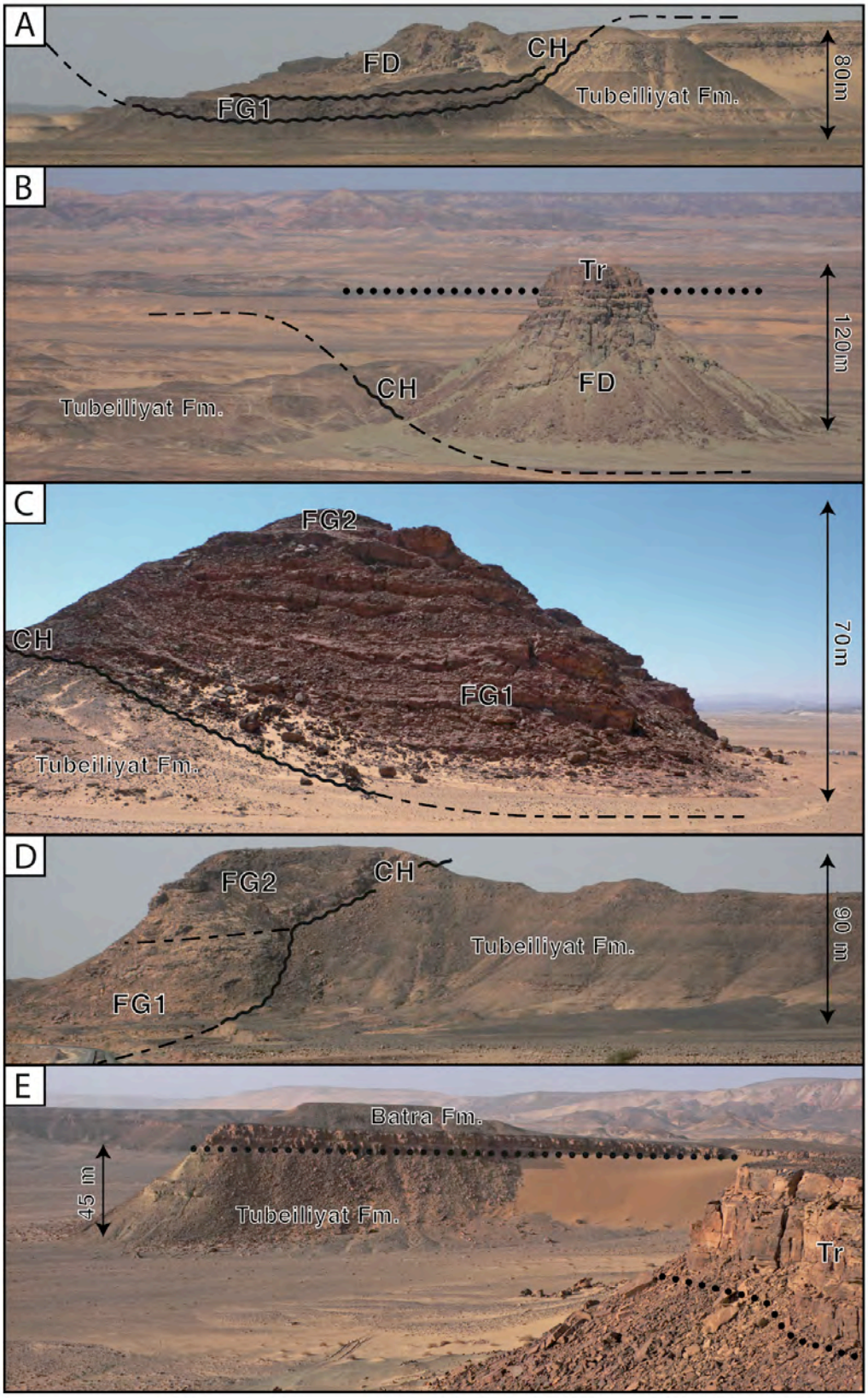

Fig. 4. Stratigraphic architectures in the Upper Ordovician Ammar Fm.: (A) Palaeovalley 1, with re-occupation of a former valley. The composite infill include a basal sand-dominated succession, truncated and overlain by a coarsening-upwartd succession; (B) Palaeovalley 2, residual hill made up of a coarsening-upward infill overlain by late to postglacial transgressive deposits; (C) Palaeovalley 6 (Jbal Ahmar) with 5-15 m thick, erosion-based, fining-upward sandstone facies sequences onlapping the valley margin; (D) Palaeovalley 6, with evidence for a valley re-occupation within a sandstone-dominated succession. The second incision phase resulted in a much wider and shallower erosion surface; (E) the sheet-like transgressive succession resting directly upon the preglacial Tubeiliyat Fm. in interfluve areas; CH: basal chaotic unit; FG1: fisrt fluvioglacial infill; FD: fluviodeltaic infill; FG2: second fluvioglacial infill; Tr: transgressive unit (see Fig. 8 for inferred stratigraphic relationships)

megablock (15 m) of Tubeiliyat sandstone underlines the contact (CH in Fig. 4A). The contact is in places characterized by striations and grooves perpendicular to the valley orientation and dipping toward the valley axis (Fig. 5B). Both the basal sandstones and the chaotic units are overlain with onlap relationships by a coarsening-upward, 35 m thick succession. In its lower part, poorly stratified very fine- to fine-grained argillaceous sandstones include undulating to subhorizontal laminations and dm-scale cut-and-fill structures. Upwards, thick-bedded medium-grained sandstones include gravely lags and assemblages of stoss-erosional climbing ripples.

Palaeovalley 2

Outcrops belonging to Palaeovalley 2 are distributed along a SW-NE oriented, 2-3 km wide and 8 km long belt dominated by subdued topographies with the exception of three prominent residual conical hills (Amira Wa'Ammar area, Fig.1). Palaeovalley 2 is the largest incision with a depth estimated to 160 m and an initial width estimated to 3 km (Figs 3 A & B and 4B). Margins are discontinuously preserved for both its northern and southern edges, with a basal chaotic unit systematically underlying them. It comprises megablocks originating from the Tubeiliyat Fm. mixed with coarse-grained to conglomeratic sandstones. The latter correspond either to isolated lenses, cut-and-fill structures, or in places, to sand intrusions. They include striated (mainly quartz) or exotic (mainly granite) pebbles (Fig. 5A). Megablocks, usually 1-10 m in length but occasionally up to 100 m, are either folded or fractured (small-scale extensional fault networks). Contact of the chaotic unit upon the undeformed strata of the Tubeiliyat Fm. is locally unclear and possibly due to the progressive bending of the pre-glacial strata toward the valley axis.

The chaotic unit is onlapped by a coarsening-upward succession, the base of which is not visible. Its top is locally truncated by the Palaeovalley 3 incision or overlapped by a transgressive unit. A maximum thickness of 80 m is exposed. In its lower part, poorly stratified fine-grained sandstones usually present a yellow-weathered onion splitting. The original laminations are altered by liquefaction processes that resulted in dm-scale folding, ball-and-pillow structures, horizontal sheet-dewatering structures and sand pipes related to small-scale sand volcanoes (Fig. 6B). However cm-scale alternating fine-grained argillaceous/ very-fine-grained sandstone layers are identified in places, as well as stoss-depositional climbing ripples (Fig. 6A). The middle palaeovalley infill is made up of poorly stratified very fine to fine-grained sandstones. The latter transitionally grade upwards into thick (1-3 m), erosion-based, fine- to medium-grained sandstone beds and fine-grained interbeds, with metre-scale load and flame structures and abundant 5-50 cm long rip-up clasts (Fig. 6C). Poorly defined ripples or subhorizontal laminations are locally discernible. Upwards, fine-grained interbeds as well as load structures progressively disappear while vertical sheet dewatering structures become more abundant.

The related incision was previously recognized by Abed *et al.* (1993) and Armstrong *et al.* (2005) but was questioned by Turner *et al.* (2005) who interpreted the basal yellow-weathered fine-grained sandstones as a disturbed Tubeiliyat facies involving earthquake related liquefaction processes (seismites). However, the large-scale coarsening-upward trend, the recognition of primary sedimentary structures that do not occur within the Tubeiliyat Fm. and the onlapping relationships upon a chaotic unit including exotic clasts demonstrate that these strata belong to a palaeovalley infill (Ammar Fm.). A petrography that is very similar to the adjacent Tubeiliyat Fm. (*Abed et al.* 1993) proves that infill is made up of eroded and then re-deposited material derived from the Tubeiliyat Fm.

Palaeovalley 3

A single outcrop corresponds to the Palaeovalley 3 infill (Fig. 3B) but the related incision event has long been recognized as it is clearly identifiable in the upper Jbal Ammar (Abed *et al.* 1993; Powell *et al.* 1994; Armstrong *et al.* 2005). The geometry of the erosion surface points to an approximately S-N orientated palaeovalley. The contact is underlined by a laminated, conglomeratic, gravely sandstone lag including quartz pebbles and intraformational clasts. It truncates decametric load and flame structures disturbing the underlying Palaeovalley 2 infill sediments. In addition, the contact is affected by small-scale extensional faults. Above, a coarse- and then medium-grained fining-upwards succession displays subhorizontal laminations and cut-and-fill structures at the base and through cross-bedding in the upper part. The latter is truncated by the late to post-glacial sandstone succession that oversteps laterally the palaeovalley infills.

Palaeovalley 4

Outcrops of Palaeovalley 4 can be followed almost continuously for 7 km, east of the Jbal al Harad, in a NNW-SSE orientation (Fig. 1). The incision depth and initial width are poorly constrained but should not exceed 70 m and 1 km respectively. This valley was mapped by Powell *et al.* (1994), who extended its length with an incision that we now ascribe to Palaeovalley 5. Based on a curvature of axis of the

valley to the SE and similar infilling successions, we suggest that it can be prolonged 7 km further southeastwards, as shown by discontinuous but aligned outcrops (lower palaeovalley of Turner *et al.* 2005). Among these is the Jbal Umeir, where both margins of a palaeovalley are preserved (Fig. 3D).

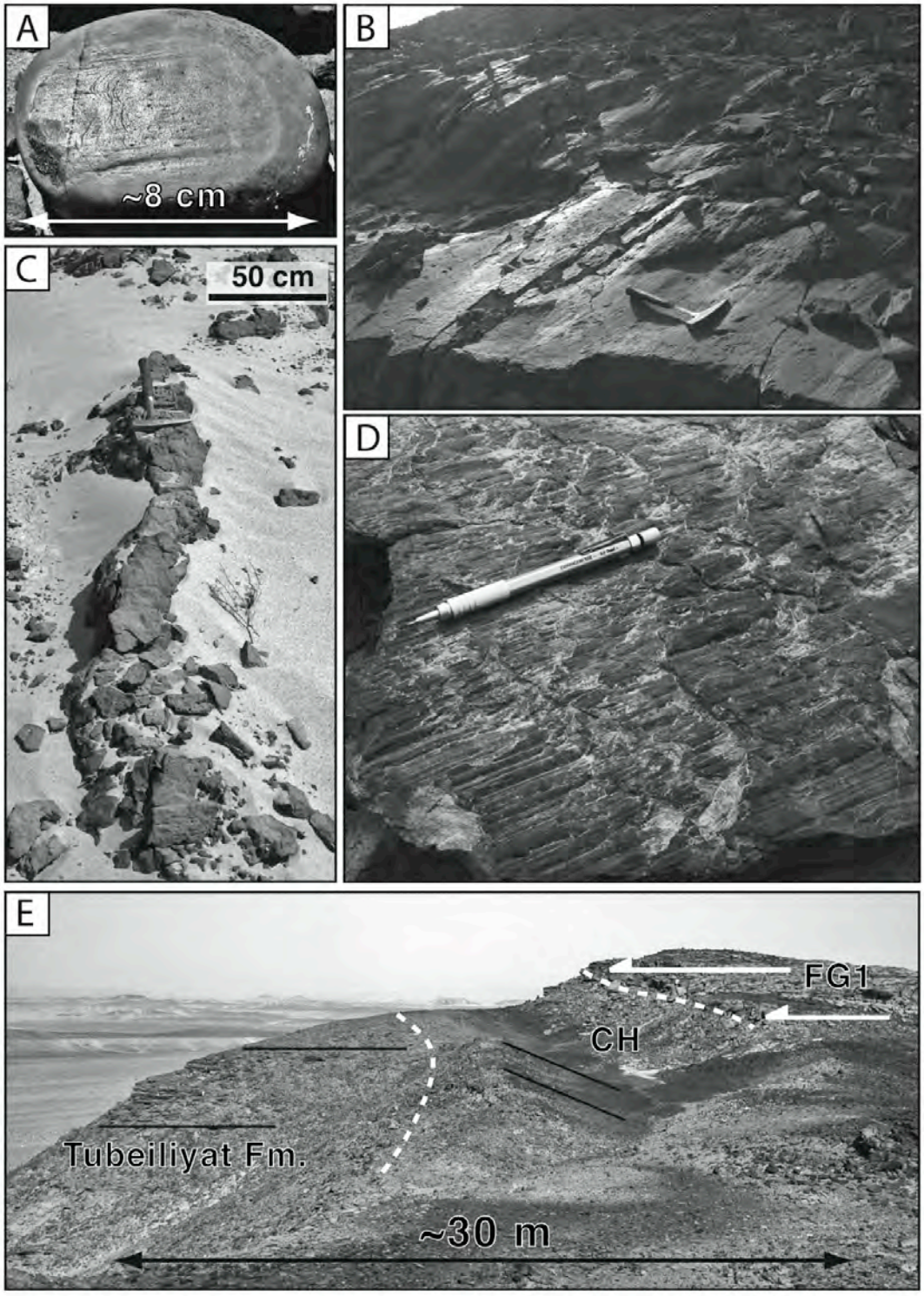

Fig. 5. Glacial Structures: (A) Striated and facetted quartz pebble with crescentic marks. (B) Grooves, and poorly defined striae along Palaeovalley 1 margin and dipping toward valley axis; (C) Sandstone dyke at the base of the Jbal Umeir; (D) intraformational striae on bedding planes (orientation N10) at Jbal Ahmar; (E) the chaotic unit (CH) underlining Palaeovalley 5 margin: undisturbed Tubeiliyat strata on the left, disturbed Tubeiliyat strata dipping toward the valley axis in the middle, onlapping sandstones (fluvioglacial infill) on the right

The dips of the palaeovalley margins are steep and locally reach up to 50°. Though the main palaeovalley infill usually rests directly upon truncated pre-glacial strata, poor outcrops of a 10 m thick basal chaotic unit are identified in places. The chaotic unit includes scoured surfaces highlighted by gravel lags, coarse-grained, often cross-stratified, sandstone masses embedded in siltstones or fine-grained sandstones and 5-50 cm thick sandstone dykes (Fig. 5C).

The paleovalley infill is made up of medium-grained sandstones including 10 m thick facies sequences associating thin-bedded successions and erosion-based, lenticular thick beds. Sandstones are dominated by horizontal to subhorizontal laminations with parting lineations. Thick beds correspond either to 0.5-3 m thick, channelized sandstone bodies or to 5-10 m thick packages of amalgamated sandstones with poorly defined boundaries. Gutter casts and climbing ripples are frequently associated with the thin sandstone beds. Small rip-up clasts and load structures are occasional. In the Jbal Umeir, Turner *et al.* (2005) claimed to have identified a glacial surface with striations and grooves. We interpret the latter structures as artefacts and consider that this surface may be only the result of scour processes by turbulent water flows. The valley infill is truncated by a 20 m thick fining-upwards successions, with very coarse-grained cross-bedded sandstone at the base, coarse- to medium-grained cross-bedded or horizontally laminated sandstones in the middle and medium-grained sandstones including ripples, HCS-like cross-strata, bioturbations and brachiopods moulds at the top.

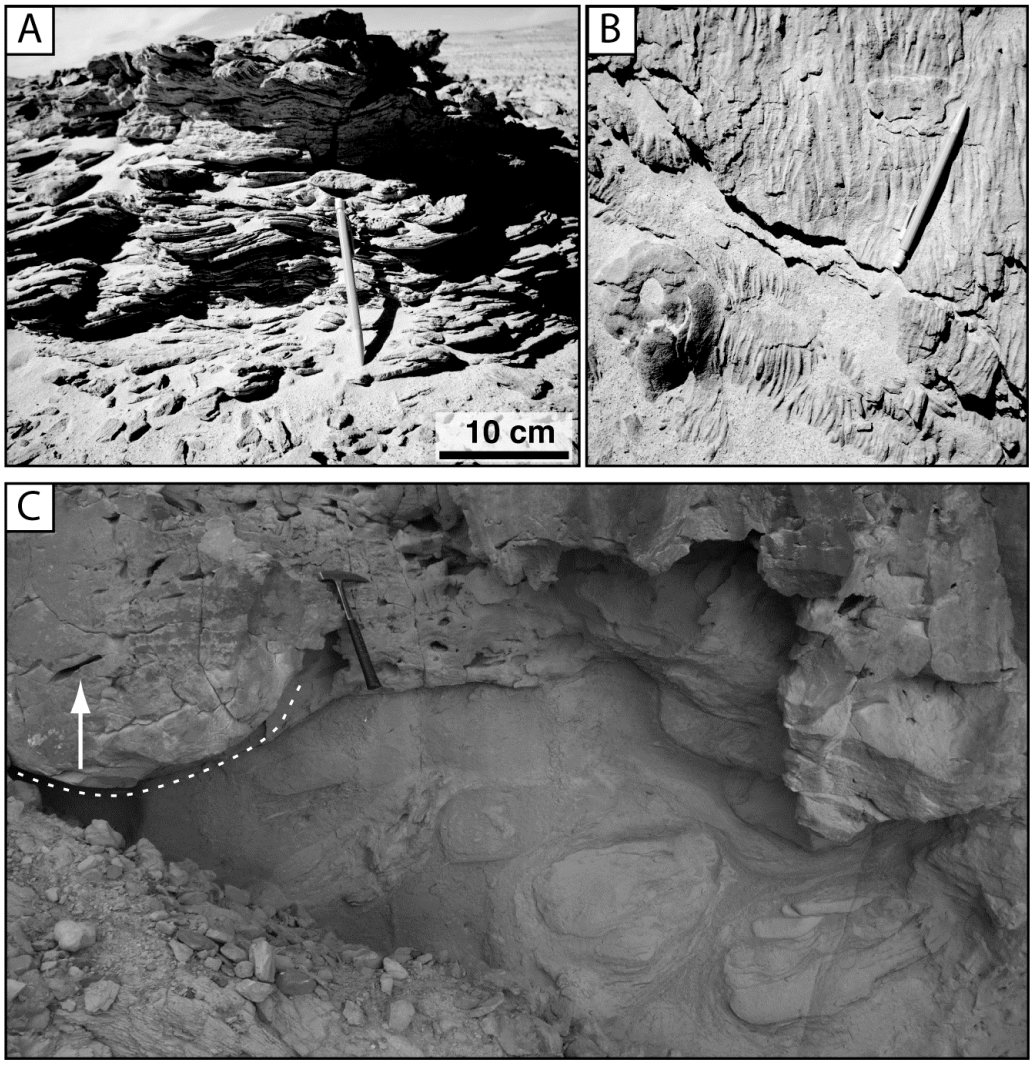

Fig. 6. Deltaic deposits: (A) Stoss-depositional climbing ripples; (B) Vertical sheet-dewatering structures and dm-scale sand volcano in the lower part of Palaeovalley 2 infill (pencil for scale); (C) Sharp-based sandstone bed including large rip-up clasts (white arrow, upper part) and load structures (lower part) in the upper part of Palaeovalley 2 infill (30 cm long hammer for scale)

Palaeovalley 5

Paleovalley 5 is described based on a 1.5 km long outcrop preserving both margins. The paleovalley orientation runs ESE-WNW, and includes a well-defined bend. Extrapolated width is ca.1 km and minimum incision depth is 60m (Fig. 3E). The southern margin is noticeably erosional with dips at 35°, truncating sharply the Tubeiliyat Fm. In contrast, the northern margin comprises a basal chaotic unit including tilted blocks or folded beds dipping toward the valley axis and representing disturbed strata from the Tubeiliyat Fm (Fig. 5E). The basal chaotic unit is onlapped by 0.5-5 m thick sandstone beds representing an initial, lower infilling succession (10-15 m), which is truncated in turn by a succeeding, upper infilling succession. The contact is underlined by amalgamated intraformational conglomerate beds that include quartz gravels and pebbles, some of which are striated. In places, sandstones of the lower initial infill are intensively deformed and affected by dense arrays of small-extensional fractures. The upper palaeovalley infill is a coarsening-upward succession with fine-grained argillaceous sandstones including stoss-depositional climbing ripples at its base. Size and infill type are similar to those of palaeovalley 1 and we suspect that the two outcrops are remnants of a single palaeovalley.

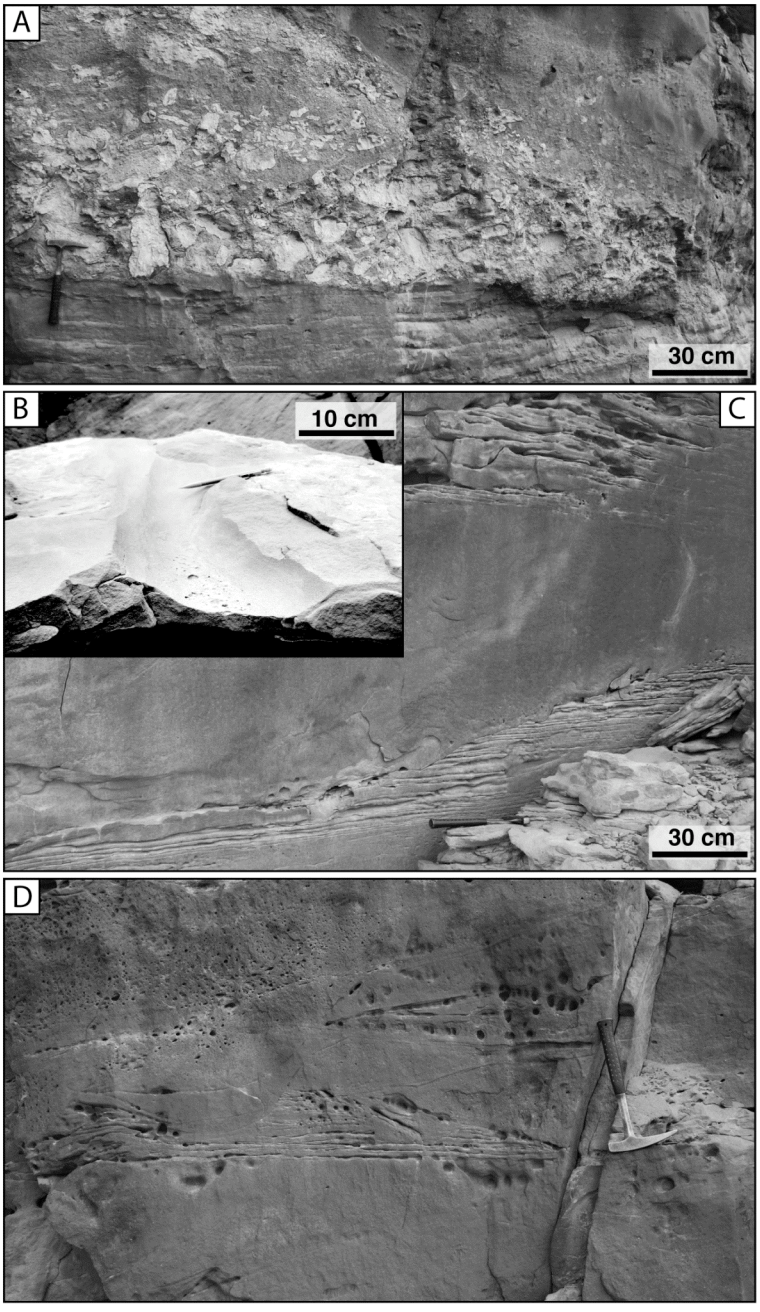

Fig. 7. Fluvioglacial deposits (Palaeovalley 6). (A) Intraformational conglomerates with pebbles and cobbles derived from the Tubeiliyat Fm. in the lower part of the fluvioglacial succession (30 cm long hammer for scale); (B) Imprint of a gutter in thin-bedded deposits, including a basal lag of small rip-up clasts; (C) a channelized sandstone body truncating and overlain by thin-bedded, horizontally laminated sandstones; (D) Cut-and-fill structures within a channelized sandstone body (30 cm long hammer for scale)

A clear truncation of the Tubeiliyat Fm. and onlaps relationships permitted an early recognition of Palaeovalley 6 in the northern part of the study area (Abed *et al.* 1993; Powell *et al.* 1994). Remnants of the Palaeovalley 6 infill are distributed along a 5 km long, SSW-NNE oriented strip, including the Jbal Ahmar that preserves a palaeovalley margin to the southeast (Figs 3 F & 4C). Along with the deep truncation at the northwest margin in a separated outcrop (Figs 2, 3G & 4D), a width of 1.5 km at least and an incision depth of 120 m may be estimated. Associated with the steep (>20°) slope of the SE margin is a basal chaotic unit. The latter includes disturbed pre-glacial Tubeiliyat sandstone beds dipping outward from the valley and associated with listric faults, as well as amalgamated intraformational conglomerate beds. In the northern outcrops, the chaotic unit is only visible near the palaeovalley bottom, where it consists in a 10-50 cm thick, coarse-grained, crudely cross-stratified sandstone bed. The latter rests directly upon the surface, and a conglomeratic lag including striated quartz pebbles lies on top of it.

In the Jbal Ahmar, the 70 m thick infill succession is made up of superimposed, erosion-based, 5-15 m thick, fining-upward facies sequences, the stack of which forms an overall fining-upward succession (Abed *et al.* 1993). Facies sequences thin towards the palaeovalley margins, resulting in well-defined onlap relationships (Fig. 4C). Coarse-grained deposits typically highlight internal erosion surfaces at the base of each of the facies sequences. In the lower part of the succession (its base is unknown), intraformational conglomerates include pebbles and cobbles derived from the Tubeiliyat Fm. (Fig. 7A) as well as quartz gravels but exotic lithologies are scarce (only one quartzite pebble was found). Upwards, intraformational lags or gravely sandstones underline the base of the facies sequences. These includes thin-bedded successions and erosion-based, lenticular thick beds. Thick beds correspond to 0.5-3 m thick, channelized sandstone bodies (Fig. 7C), consisting in cross-stratified or subhorizontally laminated sandstones, with in places cut-and-fill structures (Fig. 7D). Climbing-dune cross-stratification (CDCS of Ghienne *et al.* 2010a) is present in places. Thin-bedded successions are composed of medium-grained sandstones organized in 4-15 cm thick, sheet-like beds with prevailing horizontal laminations (Fig. 7C), basal gutter casts (Fig. 7B), poorly defined ripples and occasional very coarse-grained sandstone lenses. In the northern outcrops, the geometry of the basal erosion surface indicates re-incision of the initial paleovalley infill by a wider but shallower paleovalley (Fig. 4E). We suspect that this re-incision event may be related with a horizon bearing intraformational striae on the bedding planes (orientation N10) at the base of the upper third of the Jbal Ahmar succession (Fig. 5D). They identify a subglacial soft-sediment shear zone (Deynoux & Ghienne, 2004; Le Heron *et al.* 2005; Denis *et al.* 2007), related to a formerly overlying glacial surface (ice/ sediment interface) that has not been preserved in the stratigraphic record.

The tunnel valley interpretation

Geometry

The Upper Ordovician palaeovalley structures from Jordan are interpreted here as tunnel valleys with their subsequent infill. The overall glacial context is proven by recurrent horizons including striated pebbles (Fig. 5A). Depth, width, steep margins, low width to depth ratio and low sinuosity are altogether indicative of tunnel valleys when compared width the Quaternary tunnel drainage networks truncating continental to shallow-marine successions of the Neogene sedimentary platforms in Northern Europe. In particular, their external geometry can be easily compared with Danish tunnel valleys (Sandersen & Jorgensen, 2006). They also compare with other Upper Ordovician palaeovalleys referred to as tunnel valleys (Fig., 1; e.g. Ghienne & Deynoux 1998; Hirst *et al.* 2002; Le Heron *et al.* 2004, 2009), though the Jordan examples exhibit smaller dimensions in general. The geometry, subglacial depositional facies and deformation structures characterizing the chaotic unit present in the lower palaeovalley infills are also regarded as essential features (see below).

Depositional environments and timing of palaeovalley infills

Three facies associations corresponding to three distinct depositional environments can be delineated in the valley infills: subglacial, fluvial, and deltaic. In the basal chaotic units, partly cross-stratified, coarse to conglomeratic deposits include striated pebbles and are intimately associated with deformation structures affecting sediment masses derived from the pre-glacial strata. The former are ascribed to facies deposited by meltwater flows, while the latter are regarded as the result of the instability of the steep valley margins. They involve either rotational gravity gliding (listric faults and stratal dips oriented outward, grooved décollement planes, Fig. 5G), folded collapsing structures (stratal dips oriented toward valley axis, Fig. 5E), or formation of large blocks detached from their parent strata. Sand intrusions in the form of sandstone dykes indicate the development of elevated hydrostatic pressures. The location of chaotic units relative to the valley margins, i.e. not only restricted to valley thalwegs but also moulding upwards the valley sides, is not compatible with a proglacial,

subaerial or subaqueous depositional package. Basal chaotic units are therefore interpreted as subglacial complexes, mixing glacio-fluvial deposits and deformation structures. They are penecontemporaneous with processes that lead to valley incision, associating erosion by meltwater flows, at least temporally overpressured, and gravitational instabilities that may have involved glacial loading (Le Heron *et al.* 2004) and/ or retrogressive landslide-type deformation along steep valley margins. Basal chaotic units have been described from both Late Ordovician (Ghienne & Deynoux 1998; Le Heron *et al.* 2004; Loi *et al.* 2010) and Pleistocene tunnel valleys (e.g. Boulton & Hindmarsh, 1987; Huuse & Lykke-Andersen, 2000; Kluiving *et al.* 2003; Lutz *et al.* 2009).

Sandstone-dominated successions were deposited by turbulent flows mainly under upper-flow regime conditions generating localized scours, channel incisions and plugs, upper-stage plane beds, cut-and-fill structures, all features that bear strong similarities with successions interpreted as deposited by ephemeral sheet-flood braided streams (Tunbridge, 1981; Olsen, 1989; Dam & Andreasen, 1990; Neef *et al.* 1996). If the latter usually characterize arid environments, ablation-related floods in proglacial braided settings also result in ephemeral sheet flows (Maizels, 2002; Carriwick & Russell, 2007). We interpret sandstone-dominated succession as fluvio-glacial deposits (FG in Figs 4 & 8). Braided channel belts aggraded, resulting in the infill of the palaeovalleys. In a few cases, conglomerates within the basal part of the infills (Fig. 7A) may be related to the reworking of a subaerial landslide by stream flows after ice-front recession. Fining-upward trends are ascribed to sediment sources moving away as ice-front retreated further inland.

Fine-grained successions characterized by more or less laminated argillaceous lithologies, common climbing ripples assemblages, water-escape and load structures are ascribed to distal delta-front environments, with alternating plume-fallout and bedload deposition from underflows in an overall fluviodeltaic environment (FD in Figs 4 & 8). The lack of dropstones or of gravity-flow deposits indicates the lack of marine or lacustrine ice fronts and the development of outwash plains in between the ice fronts and the shorelines. A relatively thin fining-upward trend was noted in the lower part of the deltaic deposits infilling Palaeovalley 2 (FD(l) in Fig. 8). It may reflect a delta-front to prodelta succession representing a preserved initial infill related to a recessing ice-front. However, an overall coarsening-upward trend is most often observed (FD(u) in Fig. 8) as highlighted by the succeeding deposition of sharp-based thick sandstone beds interpreted as mouth-bar deposits (Fielding et al. 2005; Schoemaker *et al.* 2010). Because the transition from distal to proximal delta-front is usually abrupt and heavily loaded, and considering the absence of fluvial successions at the top of the prograding successions, we suggest that delta progradation occurred essentially during an ice-front advance phase rather than through a normal regressive evolution during a late to post-glacial stage. In this case, paleovalley infill occurred after, and independently from, the ice advance phase related to the previous incision. It is not known whether fluviodeltaic systems were confined between palaeovalley margins or unconfined and overstepping inter-valley areas, wherefrom they would have been eroded later (subsequent glacial erosion or post-glacial transgressive ravinement surfaces).

Considering both fluvioglacial and fluviodeltaic infilling successions, it appears that the tunnel valleys remained essentially underfilled immediately after the ice had retreated from the study area. Their infill occurred either just after, during a further ice-front recession (fluvial successions) or later, during a renewed ice-sheet advance (delta successions). The lack of clear offshore or lacustrine muds at the base of the prograding successions does not however conform to the view of a water-body occupying palaeovalleys during long-lasting interglacials and suggests high-frequency fluctuating ice-sheet margins instead.

Stratigraphic units and correlations

The European Quaternary tunnel valleys were formed in the subglacial, ice-sheet marginal zone and most probably reflect recessional ice margins (Van Dijke & Veldkamp 1996; Krohn *et al.* 2009; Sandersen *et al.* 2009). In the Late Ordovician, successive generations of tunnel valley incision and subsequent infills may either reflect orbitally controlled, relatively low-frequency cycles of major glacial advance/ retreat or, alternatively, higher frequency pulsations affecting ice-sheet balance fluxes. Dealing with the Late Ordovician case study in Jordan, stratigraphic relationships of successive glacial sequences have not been preserved in inter-valley areas. Consequently, the six described palaeovalley infills described herecould potentially be the result of six distinct generations of isolated tunnel valleys reflecting ice-sheet advance/ retreat cycles or, alternatively, could represent an intricate network of essentially coeval valleys within a single cycle.

However, an improved scenario may be proposed. Re-occupation of Palaeovalleys 1 and 4 is suggested by (i) a composite infill, which comprises an initial fluvioglacial infill (FG1), (ii) evidence for a re-incision event and (iii) a subsequent final deltaic infill (FD, Figs 3 & 4). In Palaeovalley 6, a polyphased evolution is suggested as well by the geometry of the basal erosion surface that includes a

knick point (Fig. 4E) possibly in relation with a subglacial shear zone (Fig. 5D) that bound to vertically superimposed fluvioglacial infilling succession (FG1 & FG2, Figs 3 & 4). Re-occupations of tunnel valleys by successive low-frequency glacial cycles is frequent in Quaternary case studies owing to the underfilling of a former palaeovalley, post-depositional compaction processes due to sediment and/ or glacial overburden, or preferential meltwater drainage paths in sand-dominated valley infills (Piotrowski 1994; Huuse & Lykke-Andersen 2000; Jorgensen & Sandersen 2006, Smith *et al.* 2009; Lutz *et al.* 2009). Assuming that a fluvioglacial infill cannot be strictly coeval with a nearby deltaic succession in such a restricted study area (10 x 20 km), and considering similarities in infilling successions and stratigraphic cross-cutting relationships, we suggest a three-fold scenario that minimizes the number of recorded ice advance/ retreat phases in southern Jordan (Fig. 8). An early ice-sheet advance and subsequent retreat could be related to the incision and to the lower infill of Palaeovalleys 1, 5 and 6 through fluvioglacial aggradation (FG1). A second ice-sheet advance would be related to re-occupation of Palaeovalley 1 and 5 and incision of Palaeovalley 2. Ice-sheet retreat is only associated with a relatively thin delta-front to prodelta succession at the base of the latter palaeovalley. A third ice-sheet advance from the south to the north (N10 orientated intraformational striae) lead first to the final infilling of Palaeovalley 1, 2 and 4 (FD), and then to (i) the incision of Palaeovalleys 3 and 5 that cut obliquely previous tunnel valley infills, (ii) re-occupation of Palaeovalley 6 and (iii) to the subsequent fluvioglacial overfilling (FG2) during an ice-sheet retreat that was possibly the last one in Jordan. In this scenario, two tunnel valley generations are most often preserved at any particular location (Fig. 3). As a result, in a three dimensional view, a dense network of palaeovalleys is preserved (Fig. 1) that is very similar to Quaternary case studies (e.g. Huuse & Lykke-Andersen, 2000; Jorgensen & Sandersen 2006; Lonergan *et al.* 2006).

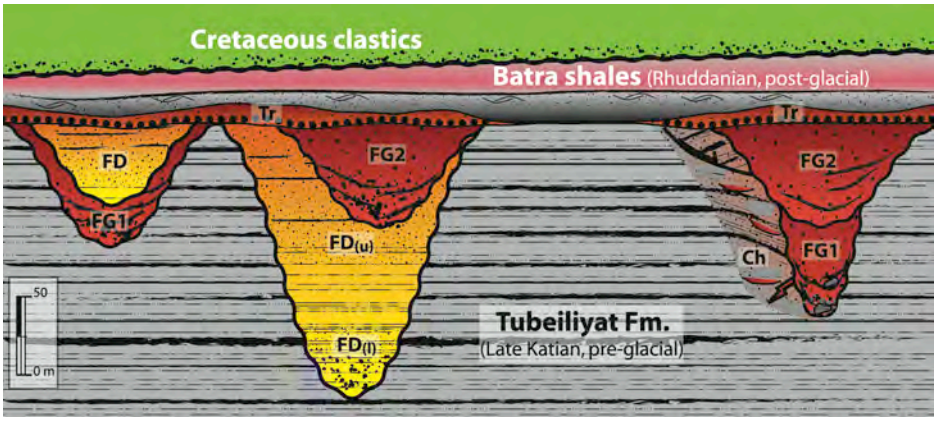

Fig. 8. Synthetic stratigraphy. Same color code as in Fig. 3. A minimum a three glacial advance/ retreat phases is inferred from cross-cutting relationships in the palaeovalley network (first incision and initial fluvioglacial infill, FG1; second incision and lower deltaic infilling, FD(l) ; progradation and upper deltaic infill, FD(u), incision and subsequent fluvioglacial infill, FG2. A transgressive succession (Tr) with variable thickness oversteps valley infills and interfluve areas. In the study area, the Cretaceous unconformity cuts into the basal Silurian strata

Correlations with the polyphase glacial development in Saudi Arabia can be proposed although in a most speculative way. In Saudi Arabia outcrops, which have preserved a more proximal glacial record, two main glacial cycles lead to deep palaeovalley incisions and subsequent infills (Fig. 1; respectively the Zarqa and Sarah Fm.; Vaslet, 1990; McGillivray & Husseini, 1992; Sharland *et al.* 2001; Clark-Lowes 2005). A late glacial advance occurred, as evidenced by subglacial deformations in the overlying Hawban Member (Miller & Al-Ruwaili, 2007). A rapid interpretation would consider that the three phases from the Jordan record can be correlated with those of Saudi Arabia. However, the three ice-sheet advances recorded to the south, may not necessarily have reached southern Jordan. To the north indeed, the ice-sheet reached southern Turkey only once, during the Hirnantian glacial maximum (Ghienne *et al.* 2010b). Presently, we suspect that the tunnel valleys in Jordan were formed beneath the outermost part of an ice sheet during temporary standstills and minor re-advances related to the overall recession succeeding to the second and main glacial advance in Saudi Arabia. We consider that the palaeovalleys and the related infills comprising the lower Ammar Fm. are essentially correlative to the Sarah Fm. Neither the underlying Zarqa Fm. nor the overlying Hawban Mb. of Saudi Arabia would be related to tunnel valley incision events in Jordan. Our scenario is fundamentally

different from the one proposed by Turner et al. (2005), who consider that the Zarqa and Sarah glacial advances resulted respectively in glacial erosion of fault-bounded depressions and in lowstand incised valleys.

Are tunnel valleys in southern Jordan reservoir analogues?

Preglacial shallow-marine sandstones (Tubeiliyat Fm.), sandstone-dominated palaeovalley infills (lower Ammar Fm., fluvioglacial) and post-glacial transgressive facies (upper Ammar Fm., shallow-marine) have been sampled for a preliminary petrophysical study. Porosity and permeability are determined using mercury injection tests, probe permeameter and nitrogen permeameter measurements (Swanson, 1981 ; Pittman, 1992 ; Nabawy *et al.* 2009).

Mercury injection tests were performed on 0.003 and 220MPa injection pressure range corresponding to 300 to 0.003 µm diameter range. Probe permeability was determined on surface sample under low injecting pressure, and nitrogen injections were performed under 7 bars confining pressure and 2 bars of head pressure. Samples location and porosity and permeability values are plotted on a schematic representation of a paleovalley (Fig. 9).

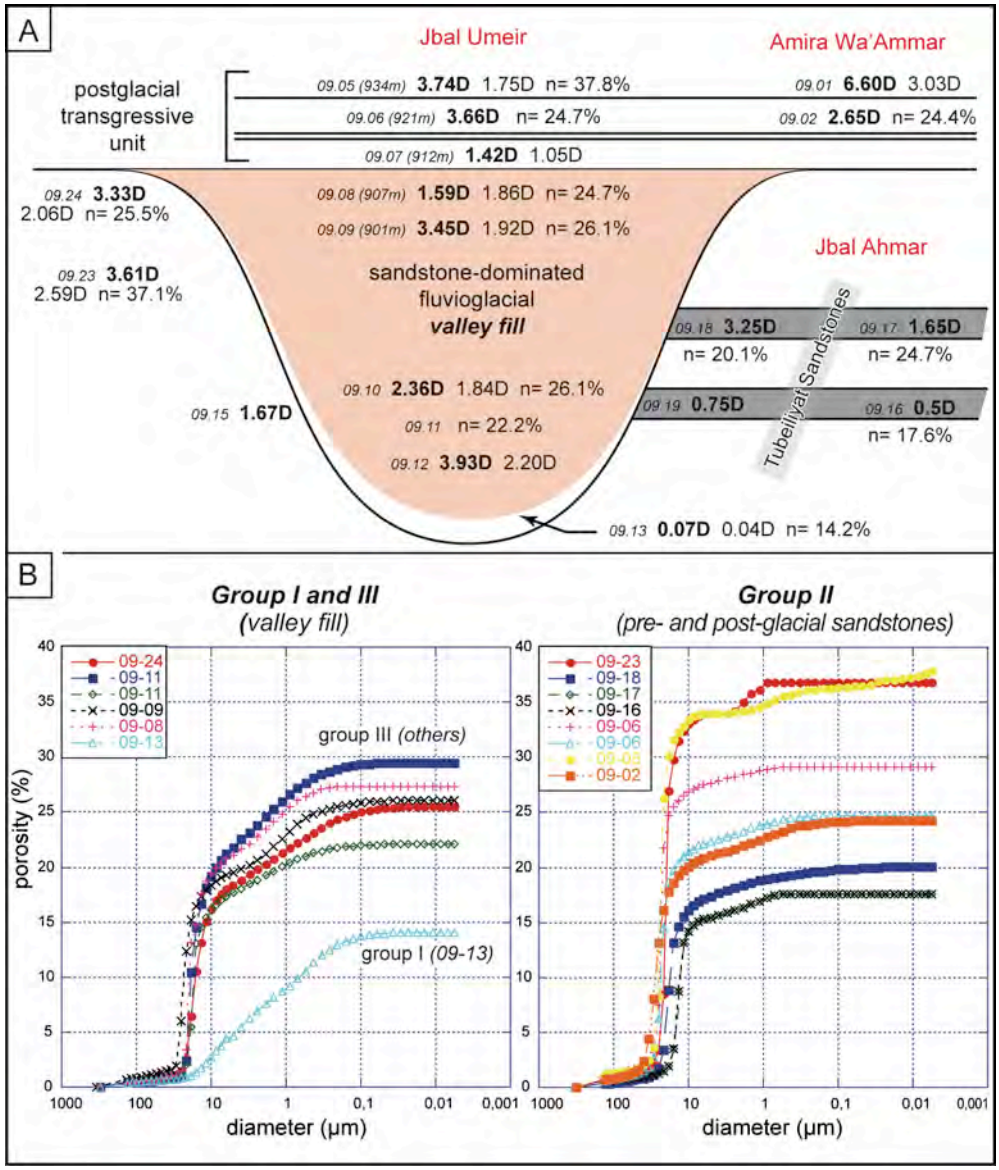

Fig.9. Petrophysical results. (A) Schematic representation of the preglacial, palaeovalley infill and postglacial sediments with porosity and permeability data. For each sample, values in bold, in regular font and 'n' correspond respectively to permeability (Darcy) parallel to primary sedimentary laminations, permeability (Darcy) orthogonal to laminations and porosity (in %); (B) Results from mercury injection tests: three groups are delineated (see text for details)

Using porosity distribution *vs.* threshold, three porosity groups are described. First, the group of the sample 09-13, representing a clayey sandstone horizon associated with a basal chaotic unit. Porosity is homogeneously distributed between 20 and 0,05 µm. This distribution is clearly controlled by an high clay content. The second group is comprised of samples 09-02, -05, -06, -16, -17, -18, -23, corresponding to the preglacial (Tubeiliyat Fm.) and postglacial (upper Ammar Fm.) successions. Thresholds between 40 and 10 µm control more than 90% of the pore volume. The porosity ranges between 22 and 37%. This distribution is representative of the intergranular space of a well sorted sandstone, as typically expected for shallow-marine depositional depsoits. The third group is formed by samples from the fluvioglacial infill of palaeovalleys (lower Ammar Fm.), 09-08, -09, -11 and by one sample (09-24) located on the upper part of the preglacial substrate but close to the palaeovalley. In the third group, two sets of thresholds control the access to the porosity. First, and as in the previous group, thresholds range from 40 to 10 µm and second, thresholds range from 10 to 0.15 µm, with porosity distributed between 22 and 28%. The first set represents the intergranular space while the second set could be induced by clay particles inside this intergranular space. Though possibly representing a partial filling-up of pores during the burial history as proposed by Dubernard & Carrio-Schaffhauser (2003) for similar features in the Nubian sandstones, A SEM analysis would be necessary to define the origin of these clays.

Flowing tests show a slightly greater permeability (1.5-3 Darcy) and good connectivity within the fluvioglacial palaeovalley infill, relative to the laterally adjacent Tubeiliyat Sandstones (0.5-3 Darcy) that include, in addition, clayed films and shaly intervals. However, the highest permeability values (2-4 Darcy) are found in the transgressive postglacial sandstones.

Both the porosity and permeability measurements indicate that reservoir quality is primarily controlled by depositional fabric as also inferred from other case studies of Upper Ordovician tunnel valleys (Hirst *et al.* 2002 ; Le Heron *et al.* 2004). High permeability and good connectivity within the sandstone bodies design fluvioglacial palaeovalley infills as structures with an intrinsic high reservoir quality and/ or as preferential drain for diagenetic fluids. Low porosity and permeability in the basal chaotic units may act as discontinuous lateral seals, disconnecting palaeovalley bodies from the preglacial strata. In contrast, the highest porosity and permeability values characterize the postglacial succession that is fully connected with the palaeovalley infills (Fig. 8).

Conclusion

The Upper Ordovician glacial record in southern Jordan is dominated by fluvioglacial to fluviodeltaic successions (Ammar Fm.), which correspond to the infill of tunnel valleys, typically 0.5-1 km in width and 50-150 m in depth. Altogether they are tentatively correlated with glacial advance/ retreat cycle related to the Sarah Fm. of Saudi Arabia. Fluvioglacial infills made up of amalgamated sandstone throughout resulted in significant sandstone bodies. The latter are encased in more heterogeneous, tide- to storm-dominated preglacial successions. They are sealed by the Lower Silurian source rock (*Hot Shales* of the Batra Fm.). Regarding the Ordovician/ Silurian play in nearby basinal areas, great permeability (1.5-3 Darcy) and good connectivity within fluvioglacial sandstone bodies design sand-dominated palaeovalley infills as large-scale heterogeneities within the Palaeozoic succession. As they may behave as significant reservoir or draining structures, they have to be integrated in water and hydrocarbon flow models.

Acknowledgments

The authors gratefully acknowledge TOTAL for financial support and the Al-Balqa' Applied University for facilities during fieldwork. The authors are grateful to XX for … their careful and constructive review of the manuscript.

References

ABED, A.M., MAKHLOUF, I.M., AMIREH, B.S. & KHALIL, B. 1993. Upper Ordovician glacial deposits in southern Jordan. *Episodes,* **16**, 316-328.

AMIREH, B.S., SCHNEIDER, W. & ABED, A.M. 1994. Evolving fluvial-transitional-marine deposition through the Cambrian sequence of Jordan. *Sedimentary Geology,* **89**, 65-90.

AMIREH, B.S., SCHNEIDER, W. & ABED, A.M. 2001. Fluvial-shallow marine-glaciofluvial depositional environments of the Ordovician system in Jordan. *Journal of Asian Earth Sciences,* **19**, 45-60.

ARMSTRONG, H.A., TURNER, B.R., MAKHLOUF, I.M., WILLIAMS, M., ABDUL-FATTAH ABU SALAH & AHMAD AL SMADI, 2005. Sequence stratigraphy and depositional environment of an Upper Ordovician (Hirnantian), peri-glacial petroleum source rock. *Palaeogeography, Palaeoclimatology, Palaeoecology,* **220**, 273-289.

ARMSTRONG H.A., ABBOTT, G., TURNER, B.R., MAKHLOUF, I. M., MUHAMMAD, A.B., PEDENTCHOUK, N. & PETERS, H. 2009. Black shale

deposition in an Upper Ordovician – Silurian permanently stratified, peri-glacial basin, southern Jordan. *Palaeogeography, Palaeoclimatology, Palaeoecology*, **273**, 368-377.

BENDER, F. 1974. *Geology of Jordan; Contributions to the Regional Geology of the Earth.* Gebrüder Borntraeger, Berlin, Germany. 196 pp.

BOSCH, J.H.A., BAKKER, M.A.J, GUNNINK, J.L. & PAAP, B.F. 2009. Airborne electromagnetic measuremnts as basis for a 3D geological model of an Elsterian incision. *Zeitschrift der Deutschen Gesellschaft für Geowissen-schaften, Stuttgart,* **160**, 249-258.

BOULTON, G.S. & HINDMARSH, R.C.A. 1987. Sediment deformation beneath glaciers: Rheology and geological consequences. *Journal of Geophysical Research,* **92**, 9059-9082.

BURVAL WORKING GROUP, 2009. Buried Quaternary valleys — a geophysical approach. *Zeitschrift der Deutschen Gesellschaft für Geowissen-schaften, Stuttgart,* **160**, 237-247.

CARRIVICK, J.L. & RUSSELL, A.J. 2007. Glacifluvial landforms of deposition. *In:* Elias, S.A. (eds) *Encyclopedia of Quaternary Science*. Elsevier, B.V., Amsterdam, **2**, 909-919.

CLARKE LOWES, D.D. 2005. Arabian glacial deposits: recognition of palaeovalleys within the Upper Ordovician Sarah Formation, Al Qasim district, Saudi Arabia. *Proceedings of the Geologists' Association*, **116**, 331-347.

DAM, G. & ANDREASEN, F. 1990. High-energy ephemeral stream deltas; an example from the Upper Silurian Holmestrand Formation of the Oslo region, Norway. *Sedimentary Geology*, **66**, 197-225.

DENIS, M., BUONCRISTIANI, J.-F., KONATÉ, M., GHIENNE, J.-F. & GUIRAUD, M. 2007. Hirnantian glacial and deglacial record in SW Djado Basin (NE Niger). *Geodynamica Acta*, **20**, 177-195.

DEYNOUX, M. AND GHIENNE, J.-F. 2004. Late Ordovician glacial pavements revisited – a reappraisal of the origin of striated surfaces.*Terra Nova*, **16**, 95-101.

DU BERNARD, X. & CARRIO-SCHAFFHAUSER, E. 2003. Kaolinitic meniscus bridges as an indicator of early diagenesis in Nubian sandstones, Sinai, Egypt: *Sedimentology*, **50**, 1221-1229.

EYLES, N. 2006. The role of meltwater in glacial processes. *Sedimentary Geology,* **190**, 257-268.

EYLES, N. & DE BROEKERT, P. 2001. Glacial tunnel valleys in the Eastern Goldfields of Western Australia cut below the Late Paleozoic Pilbara ice sheet. *Palaeogeography, Palaeoclimatology, Palaeoecology*, **171**, 29-40.

FIELDING, C.R., TRUEMAN, J.D. & ALEXANDER, J. 2005. Sharp-based, flood-dominated mouth bars sands from the Burdekin River Delta of northeastern Autralia : extending the Spectrum of mouth-bar facies, geometry, and stacking patterns. *Journal of Sedimentary Research*, **75**, 55-66.

GHIENNE, J.-F. & DEYNOUX, M. 1998. Large-scale channel fill structures in Late Ordovician glacial deposits in Mauritania, western Sahara. *Sedimentary Geology*, **119**, 141-159.

GHIENNE, J.-F., DEYNOUX, M., MANATSCHAL, G. & RUBINO, J.-L. 2003. Palaeovalleys and fault-controlled depocentres in the Late-Ordovician glacial record of the Murzuq Basin (central Libya). *Comptes Rendus Geoscience,* **335**, 1091-1100.

GHIENNE, J.-F., LE HERON, D., MOREAU, J., DENIS, M. & DEYNOUX, M. 2007. The Late Ordovician glacial sedimentary system of the North Gondwana platform. *In:* HAMBREY, M., CHRISTOFFERSEN, P., GLASSER, N., JANSSEN, P., HUBBARD, B. & SIEGERT, M. (eds) Glacial Sedimentary Processes and Products. *Internal Association of Sedimentologists, Special Publication*, **39**, 295-319.

GHIENNE, J.-F., GIRARD F., MOREAU, J., RUBINO, J.-L. 2010a (in press). Late Ordovician climbing-dune cross-stratification: a signature of outburst floods in proglacial outwash environments? *Sedimentology*, DOI: 10.1111/j.1365-3091.2009.01142.x.

GHIENNE**,** J.-F., MONOD, O., KOZLU, H., DEAN, W.T. 2010b (in press) Cambrian-Ordovician depositional sequences in the Middle East : a perspective from Turkey. *Earth Science Reviews*. http://dx.doi.org/10.1016/j.earscirev.2010.04.004

GUTIÉRREZ-MARCO, J.-C., GHIENNE, J.-F., BERNÁRDEZ & E., HACAR, M.P. 2010. Did the Late Ordovician African ice sheet reach Europe? *Geology*, **38**, 279-82.

Hirst, J.P.P., Benbakir, A., Payne, D.F. & Westlake, I.R. 2002. Tunnel Valleys and Density Flow Processes in the upper Ordovician glacial succession, Illizi Basin, Algeria: influence on reservoir quality. *Marine Petroleum Geology*, **25**, 297-324.

HUUSE, M. & LYKKE-ANDERSEN, H. 2000. Overdeepened Quaternary valleys in the eastern Danish North Sea: morphology and origin. *Quaternary Science Reviews,* **19**, 1233-1253.

JØRGENSEN, F. & SANDERSEN, P.B.E. 2006. Buried and open tunnel valleys in Denmark – erosion beneath multiple ice sheets. *Quaternary Science Reviews*, **25**, 1339-1363.

JØRGENSEN, F., LYKKE-ANDERSEN, H., SANDERSEN, P., AUKEN, E. & NØRMARK, E. 2003. Geophysical investigations of buried Quaternary valleys in Denmark: An integrated application of transient electromagnetic soundings, reflection seismic surveys and exploratory drillings. *Journal of Applied Geophysics*, **53**, 215-228.

KHALIL, B. 1994. *The Geology of Ad Disa area (Qannassiva).* Natural Resources Authority of the Hashemite Kingdom of Jordan, Geology Directorate, Amman.

KLUIVING, S.J., BOSCH, J.H.A., EBBING, J.H.J., MESDAG, C.S. & WESTERHOFF, R.S. 2003. Onshore and offshore seismic and lithostratigraphic analysis of a deeply incised Quaternary buried valley system in the Northern Netherlands. *Journal of Applied Geophysics,* **53**, 249-271.

KROHN, C. F., LARSEN, N. K., KRONBORG, C., NIELSEN, O. B. & KNUDSEN, K. L. 2009. Litho- and chronostratigraphy of the Late Weichselian in

Vendsyssel, northern Denmark, with special emphasis on tunnel-valley infill in relation to a receding ice margin. *Boreas*, **38**, 811-833.

LE HERON, D. P. 2007. Late Ordovician glacial record of the Anti-Atlas, Morocco. *Sedimentary Geology*, **201**, 93-110

Le HERON, D., SUTCLIFFE, O.E., BOURGIG, K., CRAIG, J., VISENTIN, C. & WHITTINGTON, R. 2004. Sedimentary Architecture of Upper Ordovician Tunnel Valleys, Gargaf Arch, Libya: Implications for the Genesis of a Hydrocarbon Reservoir. *GeoArabia,* **9**, 137-160.

LE HERON, D.P., SUTCLIFFE, O.E., WHITTINGTON, R.J. & CRAIG, J. 2005. The origins of glacially related soft-sediment deformation structures in Upper Ordovician glaciogenic rocks: implication for ice sheet dynamics. *Palaeogeography, Palaeoclimatology, Palaeoecology*, **218**, 75-103.

LE HERON, D.P., CRAIG, J. & ETIENNE, J.L. 2009. Ancient glaciations and hydrocarbon accumulations in North Africa and the Middle East. *Earth-Science Reviews*, **93**, 47-76.

LOI, A., GHIENNE, J.-F., DABARD, M.P., PARIS, F., BOTQUELEN, A., CHRIST, N., ELAOUAD-DEBBAJ, Z., GORINI, A., VIDAL, M., VIDET, B. &DESTOMBES J. 2010 (in press). The Late Ordovician glacio-eustatic record from a high-latitude storm-dominated shelf succession: the Bou Ingarf section (Anti-Atlas, Southern Morocco). *Palaeogeography, Palaeoclimatology, Palaeoecology*.

LONERGAN, L., MAIDMENT, S. C. R. & COLLIER, J. S. 2006. Pleistocene subglacial tunnel valleys in the central North Sea basin: 3-D morphology and evolution. *Journal of Quaternary Science,* **21**, 891-903.

LOYDELL, D.K., BUTCHER, A., FRYDA, J., LÜNING, S. & FOWLER, M. 2009. Lower Silurian « Hot Shales in Jordan : a new depositional model. *Journal of Petroleum Geology*, **32**, 261-270.

LÜNING, S., CRAIG, J., LOYDELL, D.K., STORCH, P. & FITCHES, B. 2000. Lower Silurian hot shales in North Africa and Arabia: regional distribution and depositional model. *Earth Science Reviews,* **49**, 121-200.

LÜNING, S., SHAHIN, Y. M., LOYDELL, D., AL-RABI, H. T., MASRI, A., TARAWNEH, B. & KOLONIC S. 2005. Anatomy of a world class source rock: Distribution and depositional model of Silurian organic-rich shales in Jordan and implications for hydrocarbon potential. *American Association of Petroleum Geologists, Bulletin*, **89**, 1397-1427.

LUTZ, R., KALKA, S., GAEDICKE, C. REINHARDT, L. & WINSEMANN, J. 2009. Pleistocene tunnel valleys in the German North Sea : spatial distribution and morphology. *Zeitschrift der Deutschen Gesellschaft für Geowissen-schaften, Stuttgart,* **160**, 225-235.

MAKHLOUF, I. 2002. Sea-Level Fluctuations and Storm-Wave Influence on Ordovician Shelf Sediments, Jordan. *Littoral 2002, The Changing Coast. EUROCOAST / EUCC, Porto – Portugal Ed. EUROCOAST – Portugal, ISBN* 972-8558-09-0

MAIZELS, J. 2002. Sediments and landforms of modern proglacial terrestrial environments. *In:* MENZIES, J. (eds) *Modern and past glacial environments*. Butterworth-Heinemann, oxford, 279-316.

MASRI, A. 1998. Geological map of Batn al Ghul (Jabal al Harad). Natural Resources Authority of the Hashemite Kingdom of Jordan, Geology Directorate, Amman (scale 1 :50,000).

MCGILLIVRAY, J.G. & HUSSEINI, M.I. 1992. The Palaeozoic petroleum geology of Central Arabia: *American Association of Petroleum Geologists, Bulletin,* **76**, 1473-1490.

MILLER, M.A. & AL-RUWAILI, M.H. 2007. Preliminary palynological investigation of Saudi Arabian Upper Ordovician glacial sediments. *Revue de Micropaléontologie,* **50**, 17-26.

MOSCARIELLO, A., BOSCH, A., EHLERS, J. & JANSZEN A. 2009. Buried glacial valley workshop challenges geoscientists and engineers to work together. *First Break,* **27**, 5-6.

NABAWY, B., GERAUD, Y., ROCHETTE, P. & BUR, N. (2009).-Pore-throat characterization in highly porous and permeabe sandstone. *American Association of Petroleum Geologists, Bulletin*, **93**, 719-739.

NEEF, G., BOTTRILL, R.S. & COHEN, D.R. 1996. Mid and Late Devonian arenites deposited by sheet-flood, braided streams and rivers in the northern Barrier Ranges, far western New South Wales, Australia. *Sedimentary Geology*, **103**, 39-61.

OLSEN, H. 1989. Sandstone-body structures and ephemeral stream processes in the Dinosaur Canyon Member, Moenave Formation (Lower Jurassic), Utah, USA. *Sedimentary Geology*, **61**, 207-221.

PIOTROWSKI, J.A. 1994. Tunnel-valley formation in NW Germany – geology, mechanisms of formation and subglacial bed conditions for the Bornhöved tunnel valley. *Sedimentary Geology*, **89**, 107-141.

PIOTROWSKI, J.A. 1997. Subglacial hydrology in northwestern Germany during the last glaciation: groundwater flow, tunnel valleys, and hydrological cycles. *Quaternary Science Reviews*, **16**, 169-185.

PITTMAN, E. D. 1992. Relationship of porosity and permeability to various parameters derived from mercury injectioncapillary pressure curves for sandstone: *American Association of Petroleum Geologists, Bulletin*, **76**, 191-198.

POWELL, J.H. 1989. Stratigraphy and sedimentation of the Phanerozoic rocks of central and southern Jordan. Part A : Ram and Khreim groups. *Natural Resources Authority Bulletin (Amman)*, **11**, 1-72.http://dx.doi.org/10.1016/S0277-3791(96)00046-7

POWELL, R.D., KHALIL MOH'D, B. & MASRI, A. 1994. Late Ordovician-Early Silurian glaciofluvial deposits preserved in palaeovalleys in South Jordan. *Sedimentary Geology,* **89**, 303-314.

PRAEG, D. 2003. Seismic imaging of mid-Pleistocene tunnel-valleys in the North Sea Basin – high resolution from low frequencies. *Journal of Applied Geophysics*, **53**, 273-298.

SANDERSEN, P.B.E. & JØRGENSEN, F., 2003. Buried Quaternary valleys in the western part of Denmark—occurrence and inferred implications for

groundwater resources and vulnerability. *Journal of Applied Geophysics,* **53**, 229-248.

SANDERSEN, P.B.E. & JØRGENSEN, F. 2006. Buried and open tunnel valleys in Denmark—erosion beneath multiple ice sheets. *Quaternary Science Reviews*, **25**, 1339-1363.

SANDERSEN, P. B. E., JØRGENSEN, F., LARSEN, N. K., WESTERGAARD, J. H. & AUKEN, E. 2009. Rapid tunnel-valley formation beneath the receding Late Weichselian ice sheet in Vendsyssel, Denmark. *Boreas*, **38**, 834-851.

SCHNEIDER, W., AMIREH, B.S. & ABED, A.M. 2007. Sequence analysis of the early Paleozoic sedimentary systems of Jordan. *Zeitschrift der Deutschen Gesellschaft für Geowissen-schaften, Stuttgart*, **158,** 225-247.

SCHOMACKER, E.R., KJEMPERUD, A.V., NYSTUEN, J.P. & JARHEN, J.S. 2010. Recognition and significance of sharp-based mouth-bar deposits in the Eocene Green River Formation, Uinta Basin, Utah. *Sedimentology,* **57**, 1069-1087.

SHARLAND, P.R., ARCHER, R., CASEY, D.M., DAVIES, R.B., HALL, S.H., HEWARD, A.P., HORBURY, A.D. & SIMMONS, M.D. 2001. Arabian Plate Sequence Stratigraphy. *GeoArabia Special Publication*, **2**, 1-371.

SMITH, J.A., HILLENBRAND C.-D., LARTER R.D., GRAHAM, A.G.C. & KUHN, G. 2009. The sediment infil of subglacial meltwater channels on the West antarctic continental shelf. *Quaternary Research*, **71**, 190-200.

SWANSON, B. F. 1981. A simple correlation between permeabilities and mercury capillary pressures: Journal of Petroleum Technology, **33**, 2498-2504.

TUNBRIDGE, I.P. 1981. Sandy high-energy flood sedimentation – some criteria for recognition, with an example from the Devonian of S. W. England. *Sedimentary Geology,* **28**, 79-95.

TURNER, B.R., MAKHLOUF, I.M. & ARMSTRONG, H.A. 2005. Late Ordovician (Ashgillian) glacial deposits in southern Jordan. *Sedimentary Geology*, **181**, 73-91.

VAN DIJKE, J.J. & VELDKAMP, A. 1996. Climate-controlled glacial erosion in the unconsolidated sediments of northwestern Europe, based on a genetic model for tunnel valley formation. Earth Surface Processes and Landforms, **21**, 327-340.

VASLET, D. 1990. Upper Ordovician glacial deposits in Saudi Arabia. *Episodes,* **13**, 147–167.

3.3. Environnements fluvio-glaciaires à dynamique de crues

Les faciès à mégarides chevauchantes (climbing-dune cross-stratification, ou « grès à rides » de Beuf et al., 1971) sont très fréquents au toit du Tassili Interne en Algérie et en Libye. Ils forment des successions plurimétriques ininterrompues interprétées comme le résultat de débâcles catastrophiques proglaciaires à l'origine d'écoulement à forte charge sableuse transportée en suspension (Ghienne et al., 2010a).

En dehors des dépôts glaciaires *sensu stricto* (till, faciès glaciomarins, cônes juxtaglaciaires), les successions fini-ordoviciennes comprennent un spectre d'environnements de dépôt étendu du fluviatile aux turbidites (*Ghienne, 2003, §6* ; Le Heron et al., 2006 ; *Ghienne et al., 2007b, §6*). En ce qui concerne les successions fluviatiles, des architectures résultant de réseaux en tresse ont été identifiées en Mauritanie (*Ghienne, 2003, §6*). Des architectures de réseaux méandriformes, possiblement à la transition de domaines estuariens, sont présents en Libye (Rubino et al., 2003). Cependant, à l'échelle de la plate-forme, deux éléments dominent dans l'enregistrement sédimentaire fluvio-glaciaire : les nappes gréseuses à mégarides chevauchantes, et les structures chenalisantes dites « en cordon » (Beuf et al., 1971). Elles sont toutes deux associées à des régimes de crues, dynamique fluviale caractéristique des contextes fluvio-glaciaires (Marren, 2005 ; Russell et al., 2005 ; Duller et al., 2008).

- Le faciès à mégarides chevauchantes est caractéristique de l'enregistrement sédimentaire fini-ordovicien dans lequel il une des signatures de l'environnement proglaciaire. Il est très représenté de la Mauritanie (*Ghienne, 2003, §6*) à la Libye (*Ghienne et al., 2003, §3* ; Le Heron et al., 2006), mais semble moins fréquent plus au nord. Au Maroc, il n'est connu qu'en de rares endroits. Il a de longue date intrigué les sédimentologistes (« grès à rides » d'origine nivéo-éolienne de Beuf et al., 1971) et a suscité diverses interprétations. La plus communément répandue est celle de dépôts sableux en régime d'antidunes (Hirst et al., 2002). Cependant, les morphologies de mégarides, et les architectures associées ont permis de proposer que cette structure sédimentaire traduit la migration de trains de dunes dans un régime hydrodynamique inférieur (*Ghienne et al., 2010a*), analogue à plus grande échelle des assemblages de rides chevauchantes. La formation de mégarides chevauchantes résulte de la combinaison d'écoulements catastrophiques et d'une limitation du stock sédimentaire transporté à la classe granulométrique des sables. Un écoulement stratifié à forte charge sableuse en suspension apparaît alors, avec une charge de fond réduite en proportion. La décélération de ces écoulements, par expansion du flot dans des systèmes de barres d'embouchures sableuses, ou dans toutes situations induisant des cellules à écoulements secondaires (courants de retour, confluences), entraîne un transfert rapide de cette charge sableuse en suspension vers le fond. Ce processus permet l'aggradation, et ainsi la préservation, des pentes amont de mégarides, condition nécessaire pour la génération de trains de mégarides en assemblages chevauchants. Bien que rarement identifiée dans les enregistrements quaternaires, cette structure sédimentaire y est possiblement plus fréquente qu'il n'y paraît (Wisemann et al., 2010).

- Les structures chenalisantes « en cordon » apparaissent en *topset* de successions deltaïques proglaciaires épaisses d'une centaine de mètres: elles appartiennent donc à un système sédimentaire de type plaine deltaïque (*Ghienne et al., 2007a*, *Girard et al., soumis*). Elles alimentent, via des barres d'embouchures, des clinoformes de pente de delta à angle faible (<1°), construit à partir de la migration de lobes progradants. L'architecture stratigraphique d'un tel système a été établie à partir de la succession fini-ordovicienne de l'ouest du bassin de Murzuq, en Libye (« fan de la Tihemboka », thèse F. Girard, en cours). La succession de dépôts de la plaine deltaïque atteint 50 m d'épaisseur en amont (au Sud, vers le front glaciaire) pour diminuer progressivement vers le Nord. Ce système fluvio-glaciaire non-confiné génère une architecture de chenaux particulière, donnant à l'affleurement une juxtaposition de cordons gréseux subparallèles apparaissant en topographie inverse. L'image satellite haute résolution révèle au moins 3 générations de ceintures de chenaux plus ou moins sinueuses. Cette organisation pourrait suggérer une stabilisation des berges par des sables gelés, au moins de manière saisonnière. L'écoulement fluvio-glaciaire est orienté vers le NW. Ces ceintures de chenaux s'intègrent dans une architecture

traduisant une aggrado-progradation du système forcée par la répétition d'évènements de crues/ décrues. En période de crue, une phase d'érosion et de transit est déduite de la préservation de dépôts de vannage conglomératique à galets mous en base de chenaux ; elle est contemporaine de l'alimentation des clinoformes gréseux sur la pente de delta et des débordements de part et d'autre des ceintures de chenaux actives. En période de décrue, la décélération des écoulements provoque une phase d'aggradation généralisée sur la plaine deltaïque, avec des dépôts en rétrogradation depuis les zones distales (embouchure) vers les zones proximales. Des levées à grès fins à rides et laminations planes sont construites en zone distale, puis intervient finalement le comblement sableux du chenal par des assemblages de mégarides 3D en régime chevauchant. Entre deux crues glaciaires, l'essentiel des dépôts est cantonné aux barres d'embouchures deltaïques et, en aval, aux dépôts par décantation. Cette aggrado-progradation aboutit à l'émergence du continuum barres d'embouchure/ chenal à levées/ chenal de la plaine deltaïque, dont le résultat est la construction d'un corps sableux composite ou « cordon ». Si, en carte, la morphologie de ces cordons est chenalisante, la succession verticale des faciès en interne est contrôlée par la migration du système vers l'aval.

Etant issus d'une multitude de sources échelonnées le long des fronts glaciaires, ces systèmes fluvioglaciaires ne correspondent pas à proprement parler à des systèmes distributaires et ne rentrent pas dans les classifications conventionnelles de dépôts fluviatiles (Gibling, 2006). Ils forment une bande de ceintures de chenaux étroite de quelques dizaines de kilomètres entre le front glaciaire et le littoral, mais s'étendant d'est en ouest sur plusieurs centaines de kilomètres aboutissant à un système de type sandur non confiné. La zone juxtaglaciaire, qui met en connexion ce réseau de chenaux et les sources sous-glaciaires, est en cours d'étude. Elle correspond au débouché des systèmes en tunnel mentionnés plus haut (cf. section 3.2).

SEDIMENTOLOGY the journal of the International Association of Sedimentologists

Sedimentology (2010) **57,** 1175–1198 doi: 10.1111/j.1365-3091.2009.01142.x

Late Ordovician climbing-dune cross-stratification: a signature of outburst floods in proglacial outwash environments?

JEAN-FRANÇOIS GHIENNE*, FLAVIA GIRARD*, JULIEN MOREAU*[1] and JEAN-LOUP RUBINO†

**Ecole et Observatoire des Sciences de la Terre, Institut de Physique du Globe de Strasbourg, UMR 7516 CNRS – Université de Strasbourg, 1 rue Blessig, 67084 Strasbourg, France (E-mail: ghienne@unistra.fr)*

†CSTJF, Total, Avenue Laribeau, 64018 Pau, France

ABSTRACT

Climbing dune-scale cross-statification is described from Late Ordovician paraglacial successions of the Murzuq Basin (SW Libya). This depositional facies is comprised of medium-grained to coarse-grained sandstones that typically involve 0·3 to 1 m high, 3 to 5 m in wavelength, asymmetrical laminations. Most often stoss-depositional structures have been generated, with preservation of the topographies of formative bedforms. Climbing-dune cross-stratification related to the migration of lower-flow regime dune trains is thus identified. Related architecture and facies sequences are described from two case studies: (i) erosion-based sandstone sheets; and (ii) a deeply incised channel. The former characterized the distal outwash plain and the fluvial/subaqueous transition of related deltaic wedges, while the latter formed in an ice-proximal segment of the outwash plain. In erosion-based sand sheets, climbing-dune cross-stratification results from unconfined mouth-bar deposition related to expanding, sediment-laden flows entering a water body. Within incised channels, climbing-dune cross-stratification formed over eddy-related side bars reflecting deposition under recirculating flow conditions generated at channel bends. Associated facies sequences record glacier outburst floods that occurred during early stages of deglaciation and were temporally and spatially linked with subglacial drainage events involving tunnel valleys. The primary control on the formation of climbing-dune cross-stratification is a combination between high-magnitude flows and sediment supply limitations, which lead to the generation of sediment-charged stream flows characterized by a significant, relatively coarse-grained, sand-sized suspension-load concentration, with a virtual absence of very coarse to gravelly bedload. The high rate of coarse-grained sand fallout in sediment-laden flows following flow expansion throughout mouth bars or in eddy-related side bars resulted in high rates of transfer of sands from suspension to the bed, net deposition on bedform stoss-sides and generation of widespread climbing-dune cross-stratification. The later structure has no equivalent in the glacial record, either in the ancient or in the Quaternary literature, but analogues are recognized in some flood-dominated depositional systems of foreland basins.

Keywords Bedforms, fluvioglacial, jökulhlaup, megaripples, meltwater, Murzuq Basin, sediment concentration, suspended load.

INTRODUCTION

Features that characterize glacier outburst deposits in distal outwash plains and river-mouth environments (e.g. Maizels, 1993; McLeod *et al.*, 1999; Duller *et al.*, 2008) remain incompletely understood, except that they usually correspond to net aggradational events (e.g. Church, 1972;

[1]Present address: Geology and Petroleum Geology Department, King's College, Aberdeen AB24 3UE, UK.

Smith *et al.*, 2006). When deciphering the sedimentary record, there is in addition potentially significant overlap between processes and products of very large 'normal' rivers, and those of high-magnitude, low-frequency events (Marren, 2005). Much recent research has focused on the impact of glacier outbursts in the ice-proximal proglacial zone (1 to 10 km from the ice front; Russell *et al.*, 2005, and references therein) and most of the criteria listed for distinguishing high-magnitude discharge regimes in the paraglacial sedimentary record (Marren, 2005) cannot be used if dealing with distal outwash plains. To examine non-glacial flood-dominated systems could also be informative but, as observed by Mutti *et al.* (1996) and Fielding (2006), most of the flood-related depositional facies have been largely overlooked in previous literature and, therefore, require further studies both in terms of description and interpretation. This study proposes such a contribution.

Dune-scale, aggrading, undulated laminations are one of the most striking and conspicuous depositional structures in the Upper Ordovician paraglacial successions of West and North Africa (Beuf *et al.*, 1971; their figs 259 to 264; Protic, 1984; Abugares & Ramaekers, 1993; El-Hawat *et al.*, 2000; McDougall & Martin, 2000; Hirst *et al.*, 2002; Ghienne, 2003; Le Heron *et al.*, 2004, 2006; Eschard *et al.*, 2005; Ghienne *et al.*, 2007b). In most cases, they represent climbing-dune cross-stratification (CDCS). Whatever their interpretation, as CDCS is absent in pre-glacial and post-glacial successions, they typify the paraglacial sedimentary record. Based on exposure data from the Western Murzuq Basin/Tassili n'Ajjer area (southern Libya to Algeria boundary; Fig. 1A and C), this paper aims firstly at documenting occurrences of CDCS.

If structures produced by climbing ripples are common in a variety of glaciofluvial to deep-water environments, the occurrence of dune-scale climbing cross-stratification is, in contrast, unusual in the sedimentary record. Such structures have been reported in glacigenic subaqueous fans (Gorrell & Shaw, 1991; Russell & Arnott, 2003; Russell *et al.*, 2007b), in flood-dominated fluvio-deltaic successions (Mutti *et al.*, 1996) and in turbidites (Roep & Fortuin, 1996; Amy & Talling, 2006). Mutti *et al.* (2003) proposed a comprehensive model of flood-generated hyperpycnal flows within which CDCS characterizes facies sequences from turbiditic systems adjacent to feeder deltas. Climbing-dune cross-stratification is also known in base-surge deposits from hydrovolcanic settings (Cagnoli & Ulrych, 2001). Considering that: (i) Late Ordovician CDCS is related closely to a paraglacial context; (ii) CDCS probably represents a rather unusual, high-energy depositional setting (Le Heron *et al.*, 2006; Ghienne *et al.*, 2007b); and that (iii) high-magnitude flood deposits form a significant part of recent outburst-prone proglacial sedimentary systems (e.g. Maizels, 1993; Russell & Knudsen, 1999a; Russell *et al.*, 2005; Smith *et al.*, 2006; Duller *et al.*, 2008; Marren *et al.*, 2009), a genetic link between this remarkable sedimentary structure and glacier outbursts (or *jökulhlaups* in Icelandic) has to be investigated. In the *Discussion* section, it is advocated that widespread deposition of CDCS typifies high-magnitude flood events and constitutes firm evidence for glacier outburst in the case of paraglacial sedimentary records. Finally, specific flow conditions responsible for CDCS will be outlined.

GEOLOGICAL, PALAEOGLACIAL AND DEPOSITIONAL SETTINGS

The Murzuq Basin and the Late Ordovician glaciation

Throughout the Palaeozoic to Cenozoic evolution of West and North Africa, tectonic uplifts in the intra-plate domain created several intracratonic basins, the present geometry of which bears little relation to the broader North Gondwana platform that had an off-shelf gradient towards the NNW during the early Palaeozoic (Beuf *et al.*, 1971; Boote *et al.*, 1998; Coward & Ries, 2003). In the Murzuq Basin (Western Libya, Fig. 1A), as elsewhere on the platform, the Lower Palaeozoic succession is comprised of a Cambrian to Ordovician transgressive sedimentary package (fluvial to shallow-marine), an uppermost Ordovician erosion-based glacigenic unit and a Silurian to Lower Devonian regressive package (inner shelf to fluvial) (Bellini & Massa, 1980; Eschard *et al.*, 2005; Ghienne *et al.*, 2007a) (Fig. 1B).

In the latest Ordovician (Hirnantian stage, < 2 Ma in duration), a continental-scale ice sheet extended over present-day West and North Africa, as well as Arabia, possibly reaching South Africa (Ghienne *et al.*, 2007b). In the Murzuq Basin, successive ice-front advance and retreat cycles resulted in up to five erosion-based, vertically superimposed and laterally juxtaposed, glacial depositional sequences (Fig. 1D). These sequences essentially include paraglacial succes-

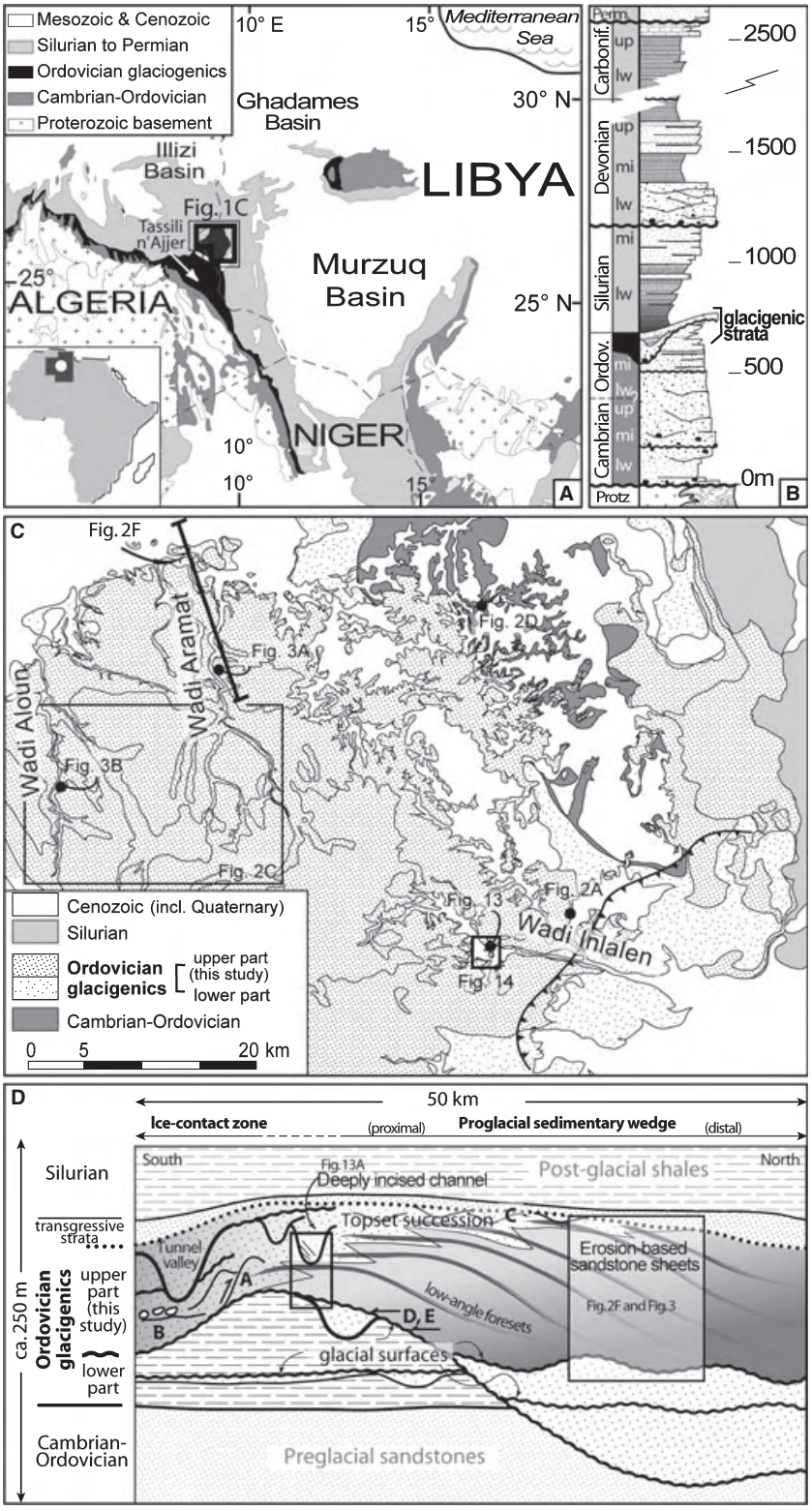

Fig. 1. Geological setting. (A) Location of the study area in western Libya (western Murzuq Basin) and eastern Algeria (Tassili n'Ajjer area). (B) Synthetic Palaeozoic succession in the Murzuq Basin; climbing-dune cross-stratification specifically occurs in the Late Ordovician glacigenics and is absent from pre-glacial and post-glacial strata. (C) Geological map of the area of the Wadis Inlalen, Aramat and Aloun, with location of the main features illustrated in figures, which belong to the upper part of the glacigenic strata; the black line with triangles gives the inferred position of the ice-sheet front at the time of the deposition of the studied sedimentary wedge; the downstream termination of the sedimentary wedge is at *ca* 50 km to the north (cf. Fig. 2F). (D) Stratigraphic framework of climbing-dune cross-stratification case studies described in the text: downstream of an ice-contact zone ('A' glaciotectonic deformation, see Fig. 2A; 'B' outsized clasts, see Fig. 2B; tunnel valleys), the fluvio-deltaic sedimentary wedge includes CDCS in relatively distal erosion-based sandstone sheets (first case study, Figs 2F and 3), in the intermediate distributary channel network ('C' see Fig. 2C, not described here; cf. Beuf *et al.*, 1971) and in proximal deeply incised channels (second case study, Fig. 13). The sedimentary wedge onlaps onto a glacial surface ('D, E', see Fig. 2D & E).

sions with a range of fluvial, deltaic and shallow-marine deposits passing distally into turbidites (Le Heron *et al.*, 2006; Ghienne *et al.*, 2007b) and reflecting deglacial to interglacial contexts. Each of the depositional sequences fills palaeovalleys, glacial troughs or depressions, some of them representing former ice-stream pathways (Ghienne *et al.*, 2003, 2007b; Moreau, 2005; Moreau

et al., 2005; Buoncristiani *et al.*, 2007; Le Heron & Craig, 2008). Glacial striations and mega-scale lineations, tunnel valleys and palaeocurrents document a relatively uniform pattern of palaeoflows at the scale of the glaciated platform (Beuf *et al.*, 1971; Ghienne *et al.*, 2007b; Le Heron & Craig, 2008). In the Murzuq Basin, glacier and fluvial palaeoflows range in direction from the NW to the NNE.

Palaeoglacial and depositional setting

Facies sequences including CDCS described in this paper belong to a 50 to 150 m thick succession, which onlaps a subglacial erosional palaeolandscape (Figs 1D, 2D and F). To the south, an ice-front margin (Fig. 1C) and ice-contact environments are inferred from the occurrence of a glaciotectonic fold-and-thrust belt (Moreau, 2005; Ghienne *et al.*, 2007b; Fig. 2A), tunnel channels indicating the connection with a subglacial drainage network (Moreau *et al.*, 2005), possible kettle hole structures and recurrent depositional facies indicative of upper-flow regime conditions, as suggested by distinctive structures in very coarse to coarse-grained sandstones similar to those described in the literature (e.g. Fielding, 2006; Duller *et al.*, 2008). The latter locally include outsized (0·5 to 1·5 m) rip-up sandstone clasts (Fig. 2B; e.g. Russell & Marren, 1999; Russell *et al.*, 2005; their fig. 7.11) that are considered by Marren (2005) as one of the criteria for the recognition of high-magnitude flood deposits. Northwards of this ice-proximal zone, and in stratigraphic connection with it, a sand-dominated, coarsening-upward sedimentary wedge is preserved, which progressively fines to the north (Fig. 1D). This stratigraphic architecture then indicates that sediment aggradation occurred concomitantly with a complex ice-sheet margin evolution, and work is in progress to define high-resolution sequence stratigraphic correlations between the ice-proximal zone and the related proglacial sedimentary wedge.

Downstream of the ice-contact zone, the sedimentary wedge involves a topset/foreset/bottomset architecture (Fig. 1D). Topset successions are made up of medium to coarse-grained sandstones, including subordinate intraformational conglomerates; they are characterized by the occurrence of a distributary channel network evident as 10 to 30 m thick, 0·1 to 1 km wide cross-stratified sandstone ribbons (Figs 2C and 3A; 'cordon' structures of Beuf *et al.*, 1971; Eschard *et al.*, 2005) hosted in rippled to horizontally laminated sandstones. In the southern proximal region, the topset succession is up to 60 m thick. The wedge progressively thins and eventually pinches out downstream to the north (Fig. 2F). The estimated dip of the depositional surface of the topset succession is in the 0·5 to 2 m km^{-1} range (< 0·15°). The topset/foreset transition is particularly well-exposed to the north of the study area (Wadi Aramat, Figs 1 and 3A). Here, visual bed-to-bed correlation at the 10 km scale allows the architecture of the prograding wedge to be delineated (Fig. 2F). Foresets are characterized by medium to coarse-grained erosion-based sandstone sheets, 2 to 12 m in thickness, which alternate with relatively thick (5 to 25 m) fine-grained intervals comprising silty shales to muddy fine-grained sandstones (Fig. 3). Foresets have maximum dip angles of 5 to 15 m km^{-1} (i.e. < 1), and are typically 40 to 60 m in height. Bottomset deposits are characterized by 2 to 10 m thick medium-grained rippled or structureless sandstone beds, alternating with thinner (0 to 5 m) fine-grained intervals. The succession is truncated by erosional transgressive surfaces. Bioturbated tidal sandstones, a wave ravinement surface and overlying offshore fine-grained sediments overlie the topset succession.

The sedimentary wedge is interpreted as a deltaic succession, which includes outwash plain/delta-plain topsets, delta-front foresets and lobe-related bottomsets. The geometry of the low-angle delta-front foresets is highlighted by the erosion-based sandstone sheets. The latter represent event beds (see below) deposited within a finer-grained regime of background sedimentation dominated by plume fallout origin. The lack of any ice-rafted debris in fallout deposits indicates that no glaciomarine ice front occurred at the time of delta development, at least within the study area. Then, successions including CDCS belong to an aggrading sandur-type proglacial fluvio-deltaic setting and were deposited between a continental ice-front to the south and a water body to the north. Ice-contact fluvioglacial depositional environments, aggradational topsets and related down-current delta development most probably relate to a period of ice-front advance (e.g. Marren, 2005; Smith *et al.*, 2006). However, as the succession onlaps onto the last basin-wide glacial surface and is overlain by post-glacial shallow-marine deposits, deposition of the sedimentary wedge that includes the CDCS described below is thought to have occurred during an ice-front stillstand or short-lived re-advance within

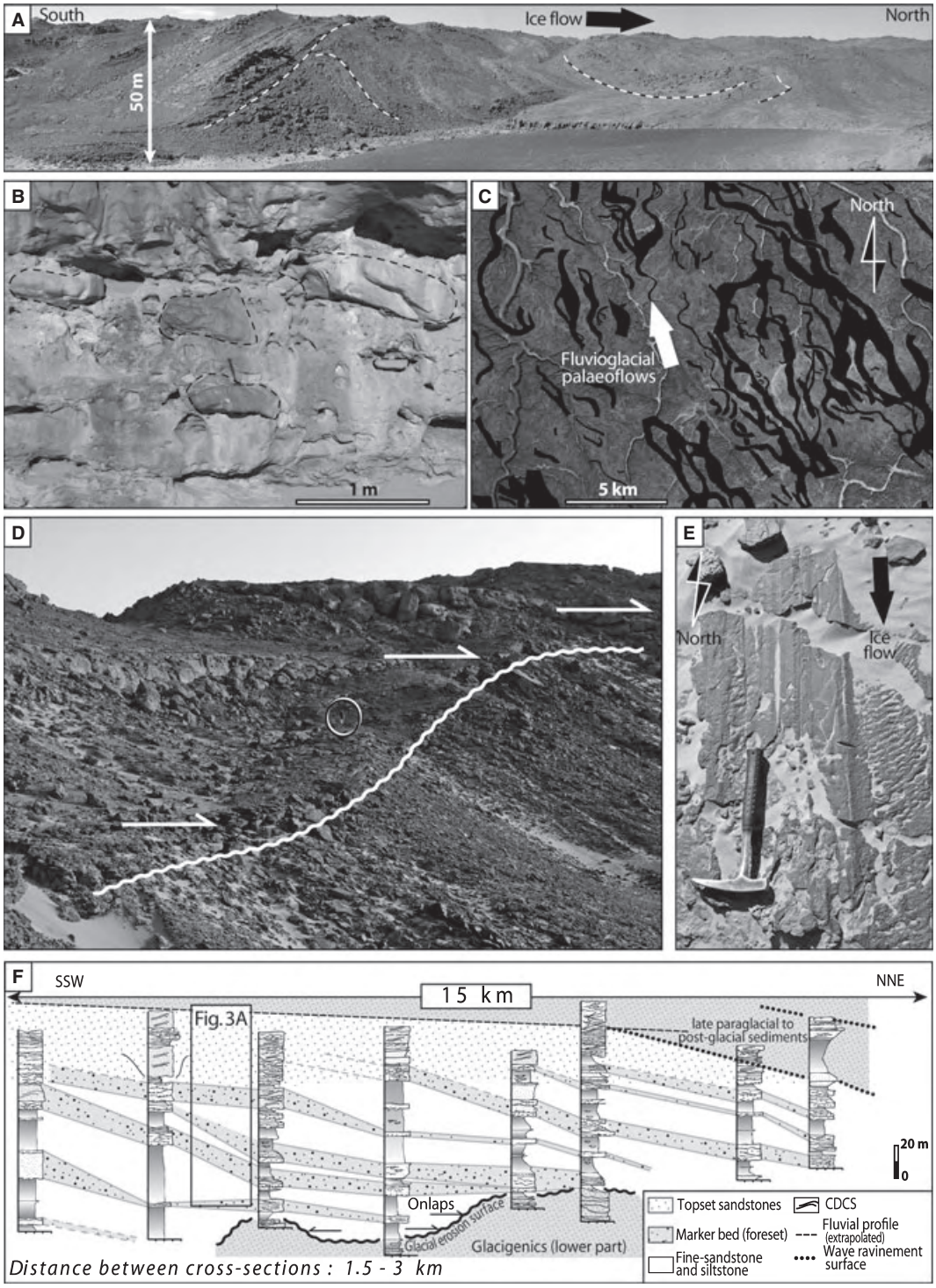

Fig. 2. Palaeoglacial setting. (A and B) Ice-contact features including a glaciotectonic fold-and-thrust belt (A) and outsized rip-up sandstone clasts (B), locations in Fig. 1D. (C) Mapping on a Spot satellite image of the distributary channel network from the topset succession. (D) Onlap relationships highlighting the glacial erosion surface (white undulated line) that separates the proglacial sedimentary wedge containing CDCS (upper left) and the underlying lower glaciogenics (lower right; location in Fig. 1C). Person for scale (circled) is *ca* 1·8 m tall. (E) Subglacial, soft-sediment shear zone including striae and grooves at the base of the studied sedimentary wedge. Hammer for scale is 33 cm long. (F) Sedimentary logs and correlation along a 15 km long profile, using erosion-based sandstone sheets that are uninterrupted from the topset to foreset successions; the coarsening-upward succession onlaps onto a glacial palaeorelief form (see also Figs 1D and 2D); the downstream termination of the topset succession has been reworked during an ensuing transgression (wave-ravinement surface) (Wadi Aramat, profile location in Fig. 1C).

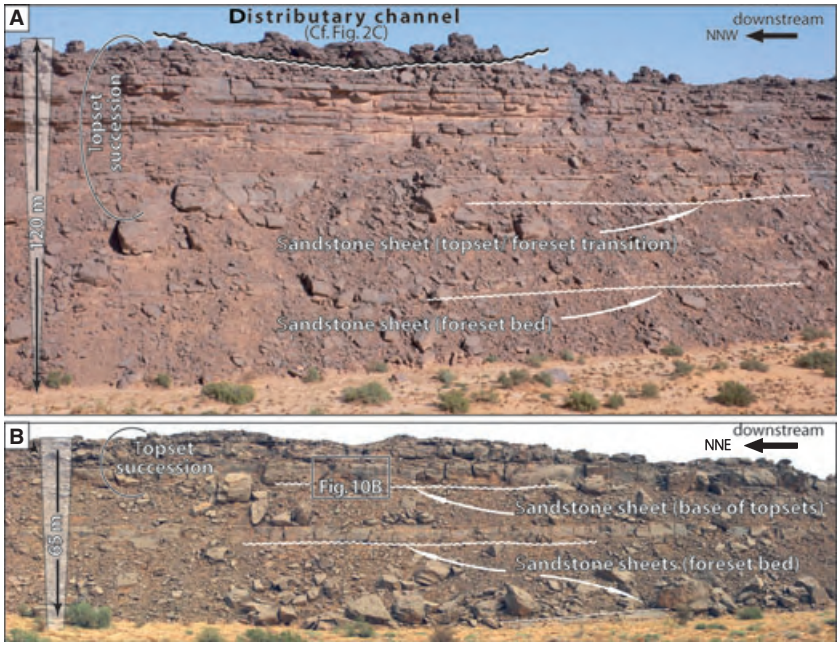

Fig. 3. Outcrop photographs showing the coarsening-upward succession including CDCS with stratigraphic position of erosion-based sandstone sheets at the base of the topset succession and at the transition with, or within, the foreset succession [(A) in the Wadi Aramat, (B) in the Wadi Aloun, locations in Fig. 1C; close-up view in Fig. 10B].

an overall ice-sheet recession period (cf. Ghienne *et al.*, 2007b).

AN OVERVIEW OF CLIMBING DUNE-SCALE CROSS-STATIFICATION FROM ORDOVICIAN GLACIGENICS

The structure of Late Ordovician climbing dune-scale cross-stratification is documented below. Related architectures and associated facies sequences will be described based on two case studies in the following sections.

Description

In most cases, climbing dune-scale cross-stratification is characterized by aggrading, undulated laminations that are distinctively asymmetrical. The stoss and lee-sides of formative bedforms can easily be recognized (Fig. 4A). Two types of structures are described in this study. A first type corresponds to regularly aggrading laminations that have almost constant angles of climb (Figs 4B and 5C), and within which the stoss-depositional structure is the most frequent. Successions several metres thick are typically observed without any internal erosion or reactivation surfaces. Stoss-erosional (Fig. 5A and B) as well as vertically aggrading (draped lamination; Fig. 5C and D) structures are also documented. The axes of trough geometries are oriented perpendicular to the palaeoflow as indicated by the stoss/lee-side asymmetry (Fig. 4C). In the case of stoss-depositional structure that implies the full preservation of the original geometry of bedform trains, topographies of formative bedforms can be described directly. Bedform crests are rounded, lee sides are tangential. Bedforms typically have 0·2 to 1 m amplitudes (height) and 1·5 to 3 m wavelengths (spacing), with lower values most often related to vertically aggrading laminations (Fig. 5C). Crest orientation is constant at the outcrop scale (Fig. 6). Dune-form index values (height to spacing ratio) are in the 0·04 to 0·15 range. Amplitudes up to 3 m high have also been documented (Fig. 5B) but require good outcrop conditions for recognition. Greater amplitudes are rare. A second type of structure with an intricate cross-stratified pattern and cross-set differentiations includes steep (up to 70°) cut-and-fill structures (Fig. 7). In places, an upward transition can be observed from aggrading laminations of the first type to structures of the second type (see case studies).

Other subordinate structures correspond to almost symmetrical, vertically aggrading laminations or to amalgamated shallow swales and hummocks without any bedform shapes distinctively preserved. Less common are compound climbing structures with a superimposed, centimetre-scale ripple cross-lamination. The latter are similar to structures described by Stanley (1974).

Aggrading laminations are observed in medium to coarse-grained sandstones (Fig. 8). In places, differential weathering (Fig. 9A) highlights changes in granulometry or grain packing modes

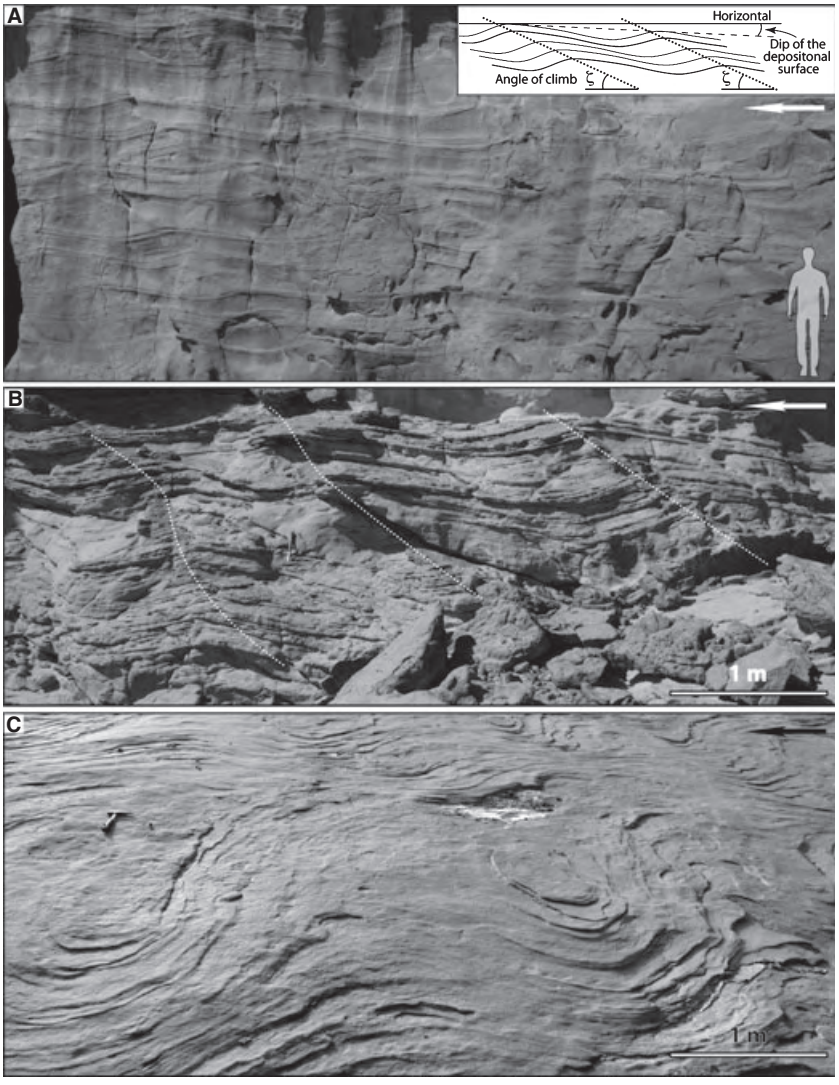

Fig. 4. Regularly aggrading, climbing cross-stratification with a stoss-depositional structure (two-dimensional CDCS). (A) Scale has been omitted intentionally, enhancing the similarity with ripple-drift cross-lamination (Wadi Inlalen); in the inset, angular relationships between the horizontal, angle of climb (ζ) and inclined depositional surfaces. (B) Detailed view, with minor variation in the angle of climb (white dotted lines). (C) Oblique plan view, showing aggrading trough geometries perpendicular to palaeoflows oriented from right to left.

differentiating stoss-sides from lee-sides (e.g. Kleinhans, 2004), the brink point zone or laminations generated by distinct angles of climb. A rhythmic pattern in sandstone lamination is evidenced locally, with a decimetre to metre-scale vertical spacing (Fig. 9B, see also Fig. 14B and D and Beuf *et al.*, 1971, their fig. 259).

Interpretation

A single, undulated, asymmetrical lamination represents an individual train of dunes. The aggrading structure then offers a unique opportunity to visualize directly ancient dune-scale streambed topographies, which usually are obliterated by trough-related erosional surfaces at the origin of the cross-sets characterizing most of the sedimentary records of dune-scale migrating bedforms (e.g. Bridge, 1997). Except for the size, the above-described structure is similar to the climbing-ripple cross-lamination or ripple-drift cross-lamination (Jopling & Walker, 1968; Allen, 1970, 1973; Hunter, 1977; Ashley *et al.*, 1982; Rubin, 1987). Spatially and/or temporally decelerating sediment-laden flows are an ideal situation for deposition of climbing lamination (cf. non-uniform versus unsteady flow case studies of Allen, 1970). The stoss-depositional structure indicates high rates of sediment deposition relative to the bedload sediment transport rate according to the following simple relation $\tan\zeta = MH/2j_b$, in which ζ is the angle of climb (inset of Fig. 4A), M the rate of sediment deposition normal to the bed, H the dune height and j_b the bedload sediment transport rate (Allen, 1970). Net deposition on bedform stoss-sides generally is interpreted as the result of high suspended-load fallout rates, and correlative high suspended-load

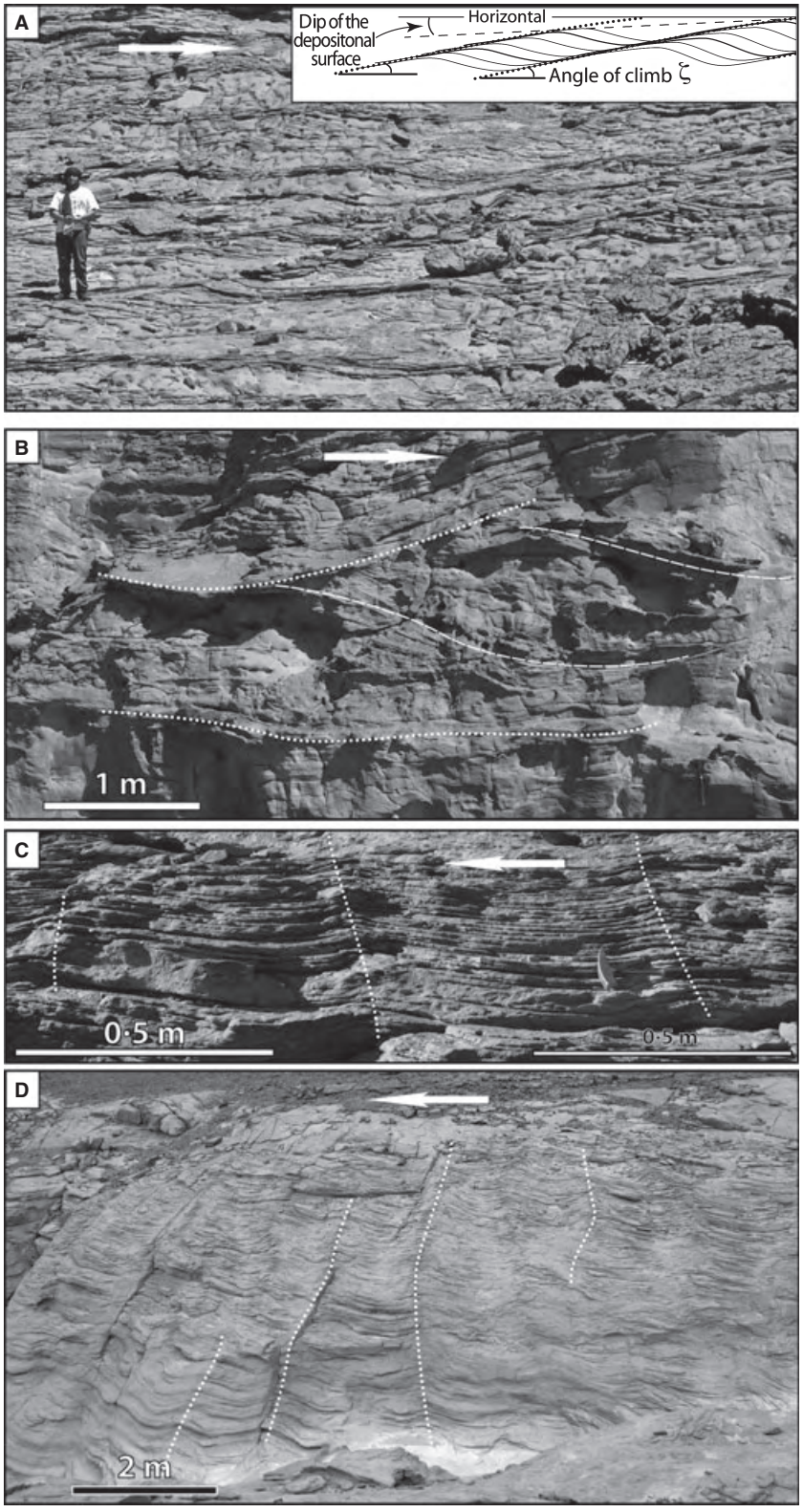

Fig. 5. Other structures comprising regularly aggrading, climbing cross-stratification (two-dimensional CDCS). (A) and (B) Stoss-erosional structure of either: (A) small-scale climbing-dune cross-stratification; or (B) medium-scale climbing-dune cross-stratification (Wadi Inlalen). Person for scale in (A) is *ca* 1·8 m tall. (C) and (D) Vertically aggrading cross-stratification, which has lesser bedform amplitudes and minor variations in the angle of climb.

concentrations (Ashley *et al.*, 1982; Rubin, 1987). However, in order to maintain turbulence in the flow-boundary zone and then tractive bedforms, either ripples or dunes, it should be noted that relatively high, but nonetheless limited, suspended-load sedimentation would have to occur to avoid direct fallout deposition and the suppression of any lamination indicative of traction

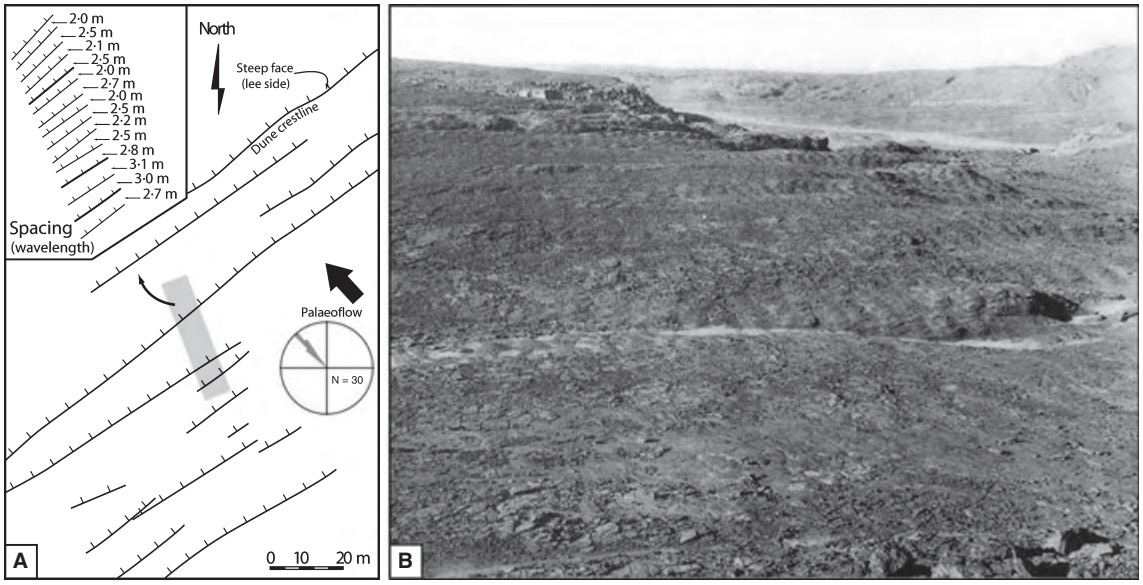

Fig. 6. Regularly aggrading, climbing cross-stratification (two-dimensional CDCS) in the Tassili N'Ajjer, Algeria (modified from Beuf *et al.*, 1962). (A) Involved bedforms have straight crestlines with minor orientation changes at the outcrop scale; in the inset, detail of the spacing between successive crests of a single train of dunes. (B) Aerial oblique photograph showing the outstanding uniformity of this depositional facies; the width in the foreground is *ca* 100 m.

processes (e.g. Allen & Leeder, 1980; Lowe, 1988; Arnott & Hand, 1989; Sumner *et al.*, 2008). Only sediment-laden stream flows and not hyperconcentrated flows are dealt with here.

Regularly aggrading, dune-scale laminations (first type) involved two-dimensional (2D, linear crest, cf. Fig. 6) climbing bedforms, generated by tractional and unidirectional flows and migrating under lower-flow regime conditions. Ordinary wavelength variability along a single dune train (inset of Fig. 6A) results in the subordinate vertical changes in the angles of climbs. More intricate patterns including cut-and-fill structures (second type) have geometries that indicate concomitant erosion and deposition processes (Fig. 7); they are ascribed to the aggradation of three-dimensional (3D, lobate or lunate crests) dunes. The onset of localized but rather deep erosion surfaces is ascribed to the development of turbulence and related trough topographies, which are associated with stronger flow separation and reattachment resulting in greater dune trough-scour depths (Leclair, 2002). Structures resulting from aggrading dunes, either 2D or 3D, are referred to as climbing-dune cross-stratification (CDCS). Climbing-dune cross-statification with 1 to 3 m spacing designates trains of small subaqueous dunes in the classification recommended by Ashley (1990), whereas bedforms with up to 10 m spacing correspond to medium dunes. However, in terms of morphology, they may alternatively be ascribed to 'mega-ripples', a class of small dunes that have dune-form indexes typically greater than 0·05 (Ashley, 1990; cf. also Idier *et al.*, 2004; Best *et al.*, 2007; 'small' dunes of Carling *et al.*, 2000, their fig. 6).

Symmetrical, vertically aggrading laminations and shallow swales and hummocks are more enigmatic. The latter may, in places, represent 2D/3D transitional structures that involve lower-flow regime dunes with slightly sinuous crestlines (e.g. Allen & Underhill, 1989). However, symmetrical bedforms probably represent structures related to the dune/plane-bed transition or other upper-flow regime bedforms (Simons & Richardson, 1966; Allen & Leeder, 1980; Saunderson & Lockett, 1983). Antidune facies cannot be ruled out in considering formation processes of aggrading laminations (Rust & Gibling, 1990; Hirst *et al.*, 2002; Fielding, 2006; Hornung *et al.*, 2007; Duller *et al.*, 2008) but are distinct from CDCS as defined in the present study, which are basically generated by lower-flow regime dunes.

In most natural sand-dominated systems, flow conditions in the dune-stability field are characterized by low suspended-load concentrations relative to their transport capacity; this results in low aggradation depositional environments characterized by a traction-dominated flow-boundary zone and angle of climbing less than 1° (Bridge,

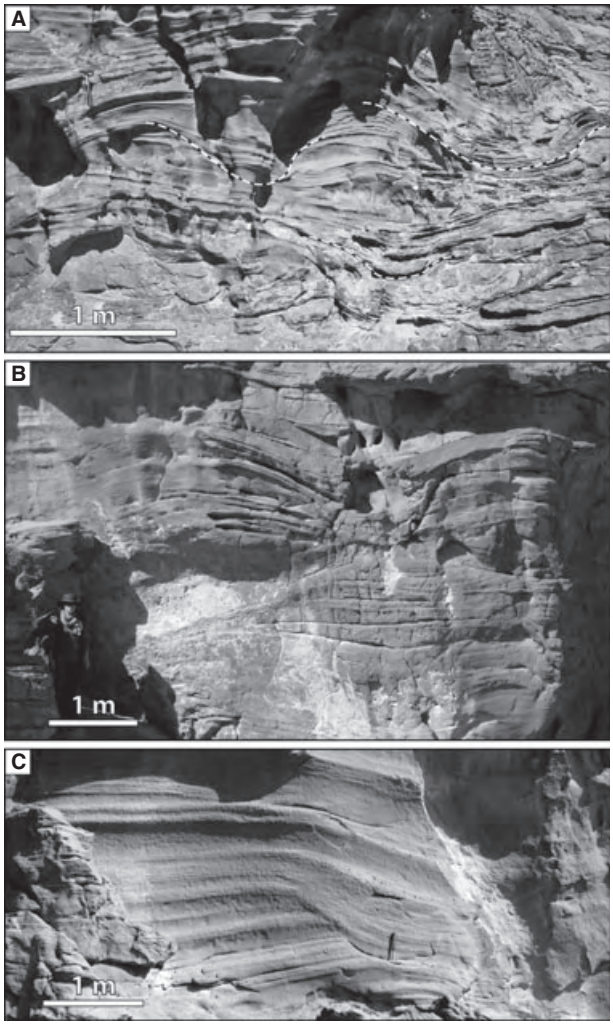

Fig. 7. Aggrading climbing-dune cross-stratification including erosional surfaces (three-dimensional CDCS, Wadi Inlalen). (A) and (B) Intricate assemblages of climbing bedforms with steep-sided cut-and-fill structures [enhanced by white dots in (A)]. (C) Detailed view of a cut-and-fill structure demonstrating concomitant erosion and deposition during the aggradation of the laminations. Flows are mainly transverse to the photographs.

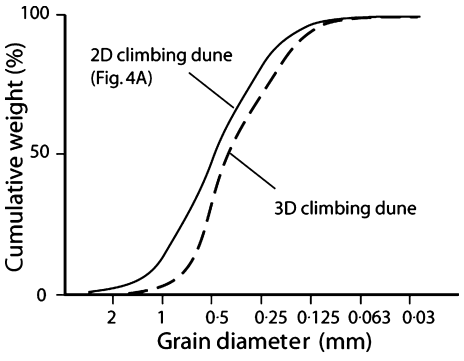

Main statistical results	Mean	Median	Sorting $(Q75/Q25)^{1/2}$
2D climbing dune	612 µm	486 µm	1·63
3D climbing dune	411 µm	359 µm	1·56

Fig. 8. Grain-size distribution based on thin section analysis for climbing-dune cross-stratified sandstones (one sample from a 2D bedform, and one another from a 3D bedform).

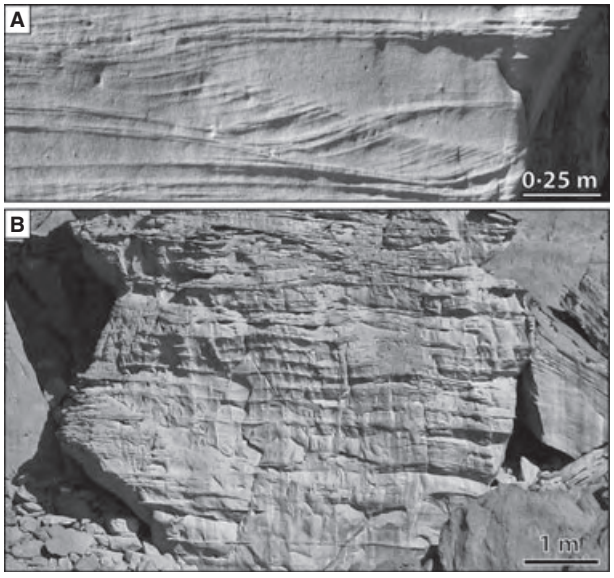

Fig. 9. Granulometry or grain packing changes as highlighted by differential weathering. (A) The brink point zone or individual laminations generated by dunes with distinct angles of climb are locally evidenced. (B) A rhythmic pattern in sandstone lamination as evidenced by differential weathering (Wadi Inlalen).

1997; Carling *et al.*, 2000; Jerolmack & Mohrig, 2005). In such settings, the coarse-grained sand-sized sediment is essentially entrained through grain-by-grain bed erosion and an effective cross-set differentiation occurs. At higher suspended-load concentrations and fallout rates the contribution of direct sediment fallout with net gain of sediment from the flow is increased relative to traction-related processes. Climbing dune-scale cross-statification or climbing-ripple cross-stratification with no cross-set differentation can occur (Jerolmack & Mohrig, 2005). The depositional flow boundary zone derived a significant part of its particles from sediment fallout. As relatively high suspended-load concentrations frequently occurred and were maintained within fine-grained sand-sized systems, the climbing ripple cross-stratification is a common sedimentary structure. Alternatively, as far as the lower-flow regime is concerned, sustained and relatively high suspended-load concentra-

tion of coarser-grained sediment necessitates flow conditions that most frequently carry a concurrent and significant proportion of very coarse to gravelly sediment load. The resulting bedload-dominated sediment transport does not allow climbing structures to be formed. It will be argued in the *Discussion* that sediment supply limitation combined with sustained high-magnitude flows originates in such conditions, which may explain why the CDCS is unusual in the sedimentary record.

Within the proglacial depositional wedge, CDCS is identified in three types of lithosomes (Fig. 1D): (i) deeply incised (> 20 m) sandstone channels at the transition between the ice-proximal depositional zone and the topsets; (ii) sandstone plugs from the distributary channel network (Fig. 2C); and (iii) extensive, erosion-based sandstone sheets at the topset/foreset transition (Figs 2F and 3). A forthcoming contribution (cf. Girard *et al.*, 2009) will specifically deal with the sedimentary architecture and development of the topset distributary channel network that contains a wealth of additional depositional facies that are outside the scope of the present study. In the following, facies sequences including CDCS from distal erosion-based sandstone sheets (first case study) and from a relatively ice-proximal, deeply incised channel (second case study) are documented in greater detail.

CLIMBING-DUNE CROSS-STRATIFICATION IN SANDSTONE SHEETS

Description

Observations are from distinct sandstone sheets located in the Wadis Aramat and Aloun (Figs 1, 3 and 10). Sandstone sheets are erosion-based bodies that typically belong to the topset/foreset transition at the downstream end of the proglacial outwash plain (Fig. 2F); their onset is in the lower part of the topset succession. These sheets continue, without any significant facies change, into the upper part of the foreset succession, where they correspond to low-angle clinoforms that rest sharply on muddy fine-grained sandstones or siltstones (Fig. 3). Sandstone sheets are typically comprised of medium to coarse-grained sandstones; they are 3 to 12 m thick (Fig. 10), have an along strike development of several kilometres and a 10 to 30 km lateral extent. These sheets may thin or thicken laterally, in relation to an undulose basal erosion surface.

Erosion-based sandstone sheets are comprised of a relatively thin, discontinuous, lower unit, overlain by an upper unit that constitutes the main body of the sheet (Fig. 11A). The basal erosion surface is characterized by 0·5 to 2 m wide scour marks. If preserved (Fig. 10A), the lower unit is dominated by crudely defined, horizontal, subhorizontal or undulose laminae in medium to coarse-grained sandstones. Syn-depositional deformation structures include large-scale load and flame structures and occasional vertical sheet-dewatering structures. The lower bounding surface of the overlying upper unit truncates sandstones of the lower unit or, if the latter was eroded entirely, corresponds to the basal erosion surface of the sandstone sheet. Associated scours include isolated rip-up clasts or intraformational conglomerates. The conglomerates are matrix-supported with a maximum clast size of 50 cm and a matrix of coarse sand. Clast composition is derived from the underlying substrate. At localities where erosion-based sandstone sheets are characterized predominantly by CDCS, low-angle to horizontal sandstone laminations were firstly deposited above the conglomerates. A transition with the overlying CDCS may occur locally with the development of isolated slip faces within otherwise horizontally laminated sandstones (Figs 10D and 11A). Climbing dune-scale cross-statification most commonly involves 2D dunes (Fig. 10B) with tabular depositional geometries reflecting horizontal depositional surfaces (Fig. 10B).

Stoss-depositional to draped lamination is the most common structure and cross-set differentiation is usually not possible owing to ubiquitous vertical facies transitions (Figs 10 and 11). A rather constant angle of climb is noted over several metres thick successions. In places, an upward transition from stoss-erosional to stoss-depositional CDCS and then draped lamination is documented (Fig. 10C). In addition, Beuf *et al.* (1971) and Hirst *et al.* (2002) described a facies transition from symmetrical climbing bedforms grading up into asymmetrical climbing dunes. In the uppermost part of the sandstone sheets (top of the upper unit), three types of facies evolution are recognized: (i) most commonly, CDCS ends abruptly; a smooth horizontal surface on top of the sandstone sheet truncates all the underlying structures (Fig. 11C); (ii) CDCS involving 3D bedforms occurs above climbing 2D bedforms, before being truncated as well by a smooth

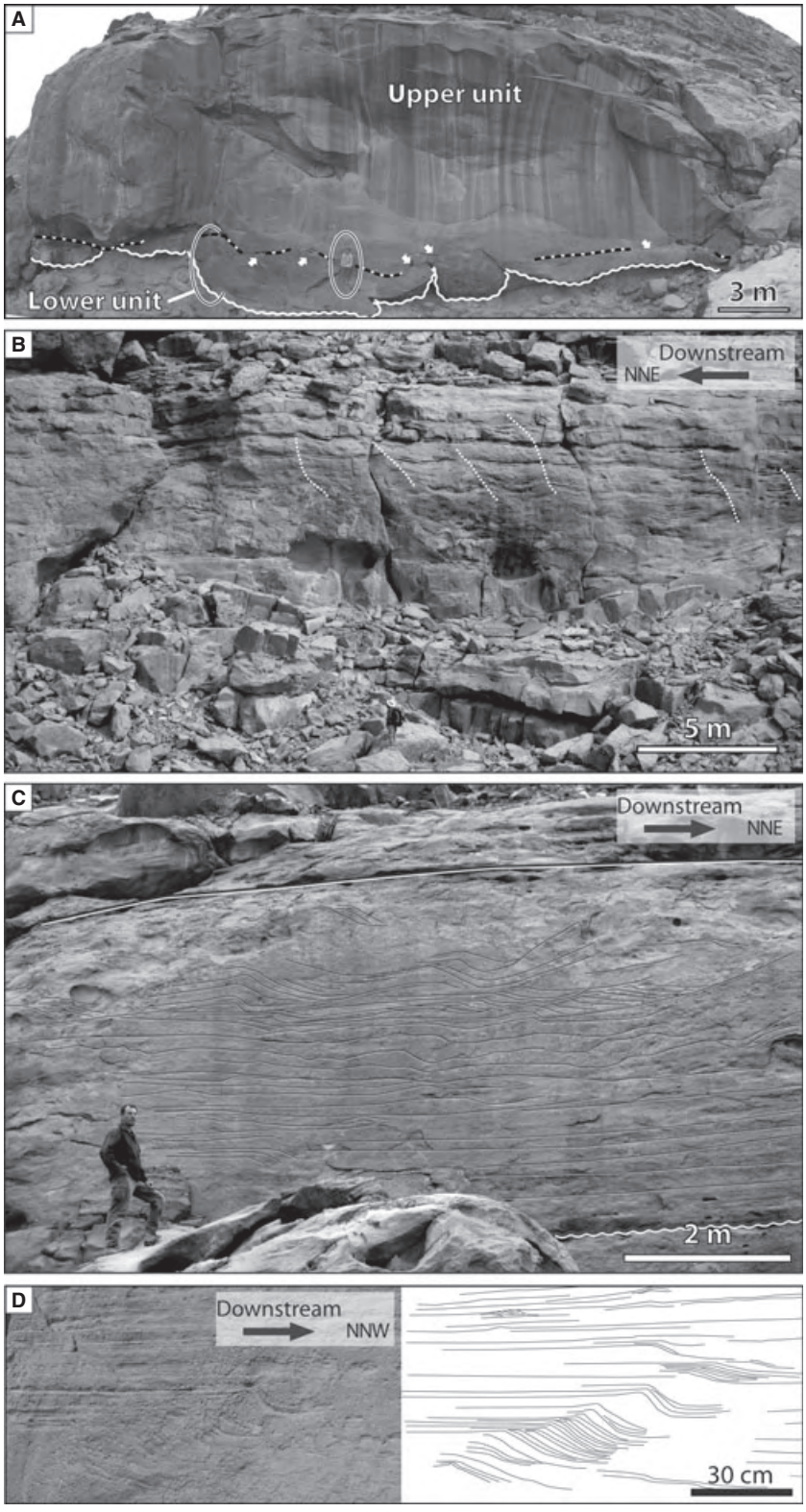

Fig. 10. Erosion-based sandstone sheets (cf. also Fig. 3). (A) A cross-section within a sandstone sheet showing the scoured and loaded basal erosion surface (undulated white line) and the subsequent erosion surface (black and white dots) associated with intraformational conglomerates (Cong) and large rip-up clasts indicated by white arrows; the lower unit is bounded by these two erosional surfaces while the overlying sandstones correspond to the upper unit that constitutes the bulk of the sandstone sheet. Note the sharp top of the upper unit in the upper right corner of the photograph. (B) A detailed view of the sandstone sheet illustrated in Fig. 3B, including uniformly aggrading climbing-dune cross-stratification (two-dimensional CDCS) forming the bulk of at least the two upper thirds of the sandstone body (flow towards the left, Wadi Aloun); no break in sedimentation is recognized, indicating that a sandstone sheet represents a single depositional event. (C) Upward transition from poorly defined cross-stratification or flat beds grading into stoss-erosional and then stoss-depositional CDCS evidencing waning-flow conditions (flow towards the right, Wadi Aramat). (D) Isolated slip faces (incipient bedform) within horizontally laminated sandstones at the base of a sandstone sheet (northern Wadi Aramat).

surface (Fig. 11B); and (iii) poorly defined ripple cross-lamination is superimposed on both stoss and lee-sides of dunes forming compound structures (Fig. 11A). In this case, the top surface of the sandstone sheet has an undulose surface with 1 to 3 m high relief, which is overlain by cross-stratified sandstone beds filling in residual depressions.

Palaeoflows as indicated by the angle of climb are very uniform at the outcrop scale (Fig. 6). The

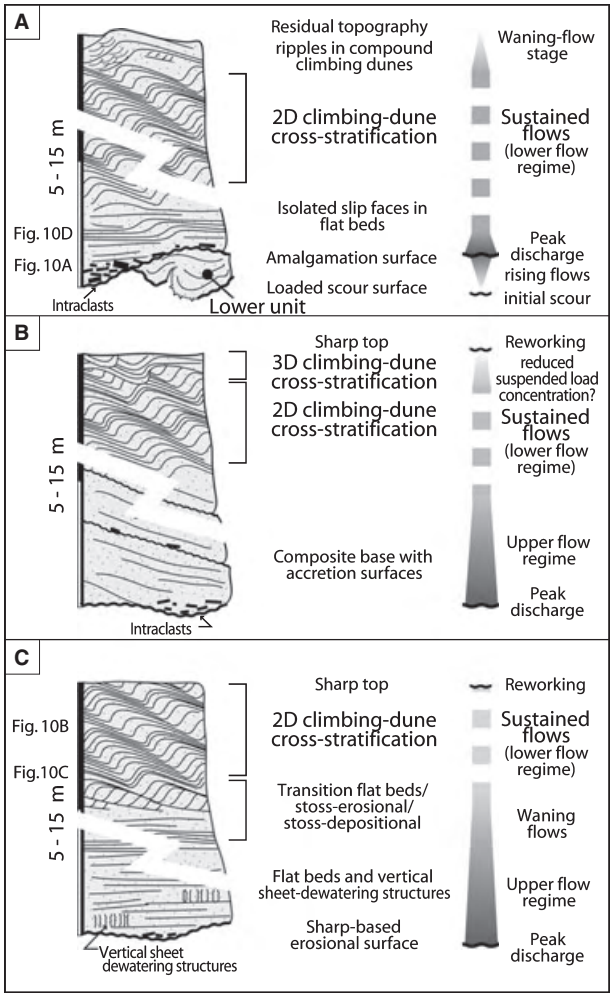

Fig. 11. Context of climbing-dune cross-stratification within facies sequences related to sandstone sheets. Vertical evolution figured in the lower parts does necessarily imply vertical evolution in the upper parts [i.e. upper evolution depicted in (A) may follow a lower evolution as in (B)]. Laminations are out of scale. See text for detail.

comprehensive study of Beuf *et al.* (1962; cf. also Beuf *et al.*, 1971, their fig. 264) indicates consistent WNW to NNE-ward orientations at the regional scale (100 km).

Interpretation

Geometries

As shown by the stratigraphic location of erosion-based sandstone sheets within the proglacial sedimentary wedge (Figs 1D, 2F and 3), related depositional processes occurred near a fluvial/subaqueous transition zone, i.e. in relation to river outflows. Such a location and the sheet-like geometry reflecting unconfined to poorly confined flows suggest a plane-jet model (Wright, 1977; Hoyal *et al.*, 2003). The upstream spatial distribution of distributary channels (Fig. 2C) and the 10 to 30 km lateral extent of individual sandstone sheets together suggest a line of distinct point-source river outflows rather than a single, major point-source (e.g. Gomez *et al.*, 2000). As the sheet geometry of the sandbody is established within the topset succession, it is inferred that channel outflows (i.e. the confined/unconfined transition, or development region in the plane-jet model) occurred in shallow areas. Inundated distal outwash plains with damming of the meltwaters behind barrier systems (e.g. Ward *et al.*, 1976) or restricted marine domains such as wide lagoons most probably provided a suitable depositional context for the erosion-based sandstone sheets and related CDCS (Fig. 12).

Facies sequences

Both overlying, and overlain by sharp contacts marked by scours, the lower unit of erosion-based sandstone sheets represents initial depositional conditions with predominant upper-flow regime sedimentary structures. Because the deepest scours (Fig. 11A) and largest rip-up clasts are associated with the upper contact, the peak discharge and the main episode of erosion are thought to temporally follow the deposition of

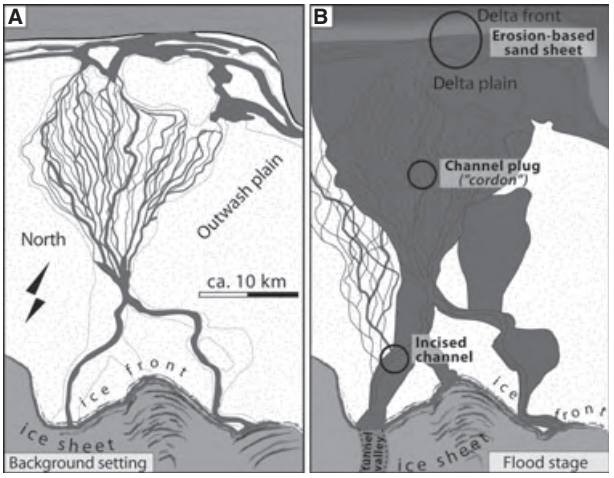

Fig. 12. Proglacial landsystem with locations of CDCS deposition. (A) Background setting (i.e. pre-outburst setting) with channel incisions and development of a sandur-type braidplain. (B) Flood stage with CDCS deposition in: (i) eddy-related side-bar in incised channels (cf. second case study); (ii) unconfined mouth bars producing erosion-based sandstone sheets at the fluvial/subaqueous transition (cf. first case study); and (iii) channel plugs throughout the distributary channel network; a connection with the subglacial drainage network, essentially tunnel valleys, is inferred.

basal sandstones constituting the lower unit of the sandstone sheets. Large-scale syn-depositional load, flame and sheet dewatering structures indicate sudden sandstone deposition. Such a sequence of events is compatible with a model of rising flow stage sedimentation (Maizels, 1993; Mulder *et al.*, 1998; Russell & Knudsen, 2002; Mutti *et al.*, 2003).

In the main body of the sandstone sheet (upper unit), the occurrence of widely distributed CDCS indicates at least temporary quasi-uniform sustained flows and predominant lower-flow regime conditions. Vertical facies transitions indicate that sandstone sheets represent event beds in spite of their thickness. Based on occurrences of isolated slip faces in horizontally laminated sandstone or of aggrading symmetrical laminations, which are interpreted, respectively, as incipient bedforms reflecting the plane bed/dune transition of upper-flow regime bedforms (see above), earlier higher-energy flow conditions may have developed prior to CDCS deposition.

Waning-stage flow conditions in erosion-based sandstone sheets are interpreted from (Fig. 11): (i) the occurrence of basal erosion surfaces and related conglomerates; (ii) basal facies indicating higher energy (upper flow?) conditions prior to lower-flow regime deposition dominated by CDCS; (iii) stoss-erosional to stoss-depositional facies sequences similar to well-known structures in climbing ripple successions (Jopling & Walker, 1968; Allen, 1970); and (iv) final stage processes that include bedload-dominated transport and deposition by ripples over dune morphologies inherited from previous flow conditions. The occasional upward occurrence of CDCS involving 3D bedforms is problematic. It is suggested that, in the context of waning-flow conditions, a decreasing suspended-load concentration is responsible for such a transition, indicating the later development of more turbulent flow conditions (cf. Discussion section). The sharp abandonment surface (Fig. 11) is thought to reflect winnowing processes during falling stage to post-flood conditions, resulting in the development of an erosion surface in places and transport/deposition by 'normal' (i.e. low-aggradation) dunes elsewhere.

Depositional model

Sandstone sheets represent very thick (3 to 12 m) and extensive event beds implying a significant sand mobilization and demonstrating that CDCS can be ascribed to flood-related depositional facies. The facies sequence basically records waning-flow conditions and poorly confined flows across a distal outwash plain/subaqueous transition (Fig. 12). Relatively uniform (at the outcrop scale) but unsteady conditions are inferred. Subsequent to peak discharge (scours at the base of the upper unit), regularly aggrading CDCS involving 2D bedforms (Fig. 11B) indicates minor vertical or longitudinal changes in spacing or height of dunes, suggesting the temporary development of sustained sediment-laden flows (Fig. 11). As far as the plane-jet model is concerned, sustained suspended-load fallout rate can occur in the relatively distal, extensive area corresponding to the zone of established flow rather than in the proximity of the zone of flow establishment (Hoyal *et al.*, 2003; Russell & Arnott, 2003). In shallow flooded distal outwash plains or lagoons, the preservation of thick sandstone sheets (up to 12 m) implies the absence of significant reworking by later lower meltwater disharges and suggests basal erosion and/or an ensuing, flood-related to post-flood, significant aggradation of the fluvio-deltaic succession (Smith *et al.*, 2006).

Erosion-based sandstone sheets correspond to laterally extensive mouth bars deposited over the distal outwash plain by sediment-laden flows exiting the proglacial distributary channel network; they are comparable with mouth bars generated by sediment-laden river outflows of flood-dominated deltas (Mutti *et al.*, 1996, 2003) but, dealing with Late Ordovician examples, the flow expansion occurred earlier, i.e. upstream, within the fluvial-dominated delta-plain or in lagoons rather than in deeper water bodies. This specificity is responsible for distinct sheet-like architecture and related facies sequences. Continuation of sandstone sheets and of CDCS deposition in the upper part of foreset successions further suggests that river-charged outflows are maintained beyond the onset of subaqueous environments. Any expected flow transformation into a turbidity current (hyperpycnal flows; Duringer *et al.*, 1991; McLeod *et al.*, 1999; Mulder *et al.*, 2003; Mutti *et al.*, 2003) may have occurred at a point of the low-angle clinoforms located downstream of the deposition of CDCS.

CLIMBING-DUNE CROSS-STRATIFICATION IN A DEEPLY INCISED CHANNEL

Description

The second case study is from a channelled sandstone body in the Wadi Inlalen (Figs 1 and

13). Incision depth is 25 m, channel orientation is SSW to NNE and channel width is 500 m, including a 200 m wide, relatively flat, channel bottom. Erosional margins, with dips up to 20°, are identified in several places (Fig. 14A). The channel infill is composed of two units (lower and upper units; Fig. 14B and C).

The lower unit, 0 to 12 m in thickness, is a laterally discontinuous fining-upward succession. At the base, and then highlighting the channel incision surface, are intraformational conglomerates with a coarse-grained sandy matrix. Matrix-supported or clast-supported conglomerates occur, which contain 2 to 15 cm long rip-up intraclasts derived from the underlying beds. In the matrix-supported arrangement, diffusely graded sand laminae are recognized in places. Overlying the conglomerates is a succession of coarse to very coarse-grained sandstones with large-scale CDCS including up to 4 m high low-angle foresets, 10 to 30 m in wavelength (Fig. 13C). Both the moderately developed clast fabrics and foreset orientations indicate palaeoflows towards the SW.

The upper unit is 5 to 20 m thick and has an erosional lower bounding surface (Fig. 13D). It consists of medium to coarse-grained sandstones including stoss-depositional CDCS. At the 100 m scale, trains of preserved bedforms highlight inclined depositional surfaces dipping up to 10° (Figs 4A, 13B and D). It should be noted that depositional surfaces are clearly distinct, with largely lesser dips, from surfaces that reflect the angle of climb of successive bedform trains (inset of Fig. 4A; see also discussion in Hunter, 1977). Bedform migrations are transverse to depositional dips. In one location (location 1 in Fig. 14, corresponding to Fig. 13), NNE dipping surfaces have superimposed bedforms migrating southeastwards (Fig. 13B). In another location 2 km to

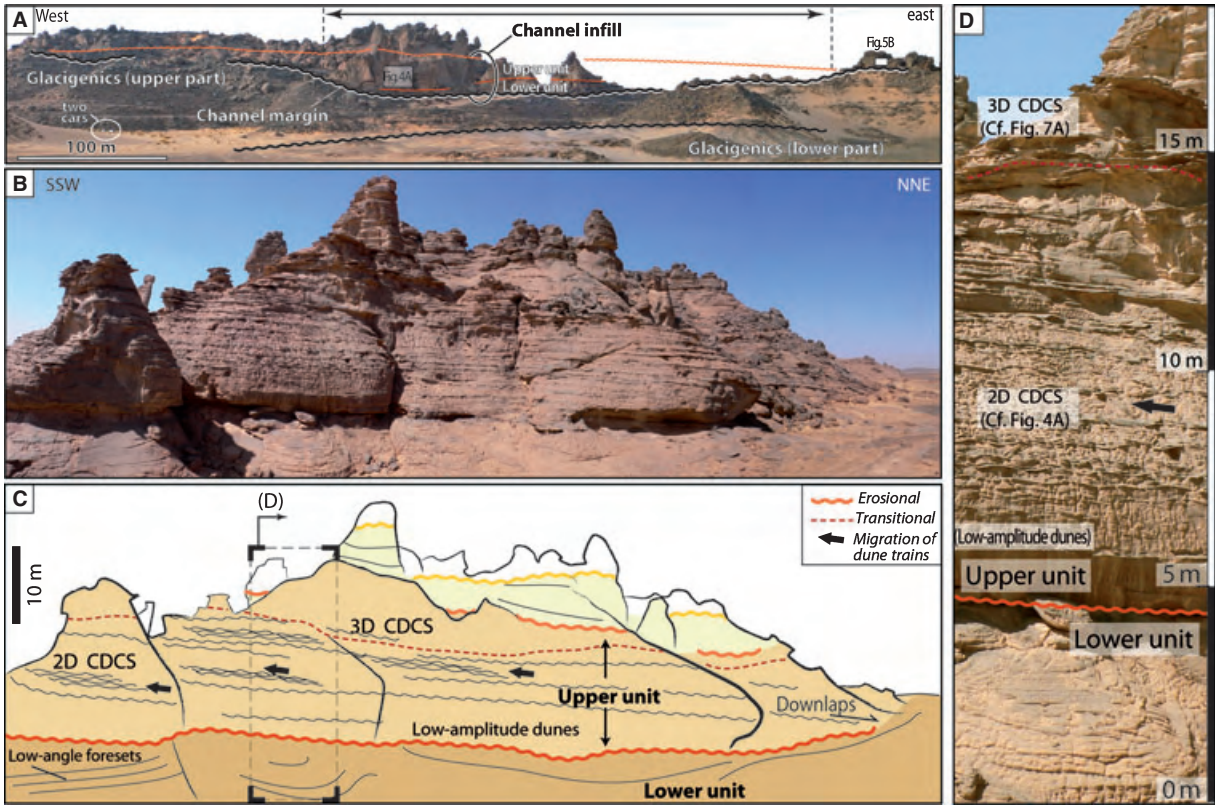

Fig. 13. Sedimentary infill of a deeply incised channel in the Wadi Inlalen (location in Fig. 1C and D). (A) Panoramic view from the south (location in Fig. 14A). (B) and (C) General view and interpretative line drawing showing the two erosion-based depositional units and downlap geometries in the upper unit (no tectonic dips); accretion surfaces dipping towards the right are superimposed with CDCS involving bedforms migrating towards the left. (D) Cross-section illustrating a sedimentary log of the channel infill (detailed view, location in C); it shows large-scale cross-stratification in the lower unit and, in the upper unit, a transition from low-amplitude dunes at the base, two-dimensional CDCS in the middle (see also Fig. 4A), and three-dimensional CDCS to the top (see also Fig. 7A) (vertical scaling is approximate).

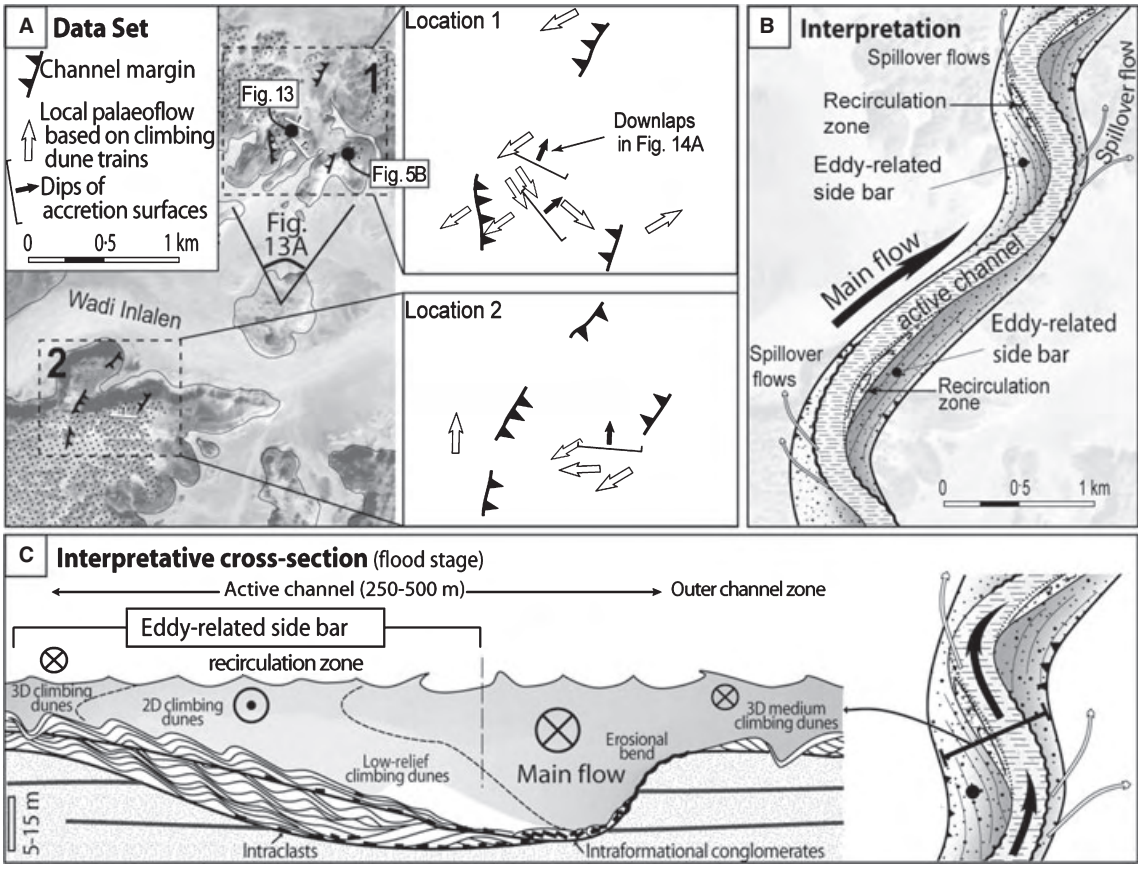

Fig. 14. Palaeoflow orientations and interpreted depositional geometries in a deeply incised channel (Wadi Inlalen, location in Fig. 1C). (A) The data set superimposed on a SPOT satellite image for scaling; note the transverse to opposite orientations of bedform migrations and distinct dips of accretion surfaces in zones 1 and 2. (B) Proposed reconstruction of the channel geometry and of inferred eddy-related side bars; during flood stages, both the channel and adjacent areas were flooded. (C) Conceptual cross-profile (laminations are out of scale) showing CDCS deposition in the recirculation zone of eddy-related side bars with bedform migration essentially upcurrent relative to the channel system; the vertical facies evolution (Fig. 13D) represents non-uniform rather than temporal variations in flow conditions over an accreting bar surface.

the south, NW-dipping depositional surfaces have superimposed bedforms migrating southwestwards (location 2 in Fig. 14).

From base to top, a section across the upper unit shows the following vertical evolution (Fig. 13D): (i) poorly developed bedforms (< 0·15 m in height); (ii) a regularly climbing, stoss-depositional structure involving 2D bedforms, 0·3 to 0·5 m in height, with constant angles of climb; (iii) stoss-depositional structures involving 3D bedforms with a greater (0·5 to 1·2 m) vertical development (Fig. 7A). An amplification in heights of the formative bedforms is then observed from low-amplitude dunes at the base, 2D dunes in the middle and higher 3D dunes upwards. The vertical facies transition is also identified laterally considering that low-amplitude dunes, 2D and 3D dunes developed successively along a single, inclined depositional surface, respectively, from its inner part (close to channel axis) to its middle and then outer part. It contrasts with tabular geometries related to erosion-based sandstone sheets.

The channel infill is overstepped by sandstones representing later deposition above the former channel and adjacent outer channel areas (Fig. 13A); they contain CDCS (e.g. Fig. 5B) and large-scale low-angle foresets, which together indicate north to NE-oriented palaeoflows (Fig. 14A). Variability in palaeoflows relative to the regional trend is then noticed. Palaeoflow indications that conform to the outwash plain setting with an ice front to the south and a delta development to the north are: (i) the channel orientation (SSW/NNE); (ii) the in-channel sedimentary accretion related to inclined depositional surfaces (NW or NNE); and (iii) palaeoflows in deposits that immediately seal the channel

infill (north to NE). Palaeoflow indications that are contradictory to the depositional setting are: (i) orientation of large-scale foresets and clast imbrication in the lower unit of the channel infill; and (ii) the migration of 2D climbing bedforms along accretion surfaces (SE and SW) in the upper unit. A model is proposed below which explains such an intricate flow pattern at the 100 m scale.

Interpretation

Geometries

The second case study relates to a fluvial channel developed within a relatively proximal, proglacial, outwash plain setting (Fig. 1D). The spatial distribution of gentle, kilometre-scale channel bends evidenced by erosional margins indicates a slightly sinuous, but non-meandering channel axis. Climbing dune-scale cross-statification mainly developed in the upper unit of the channel infill (Fig. 13). Here, the overall depositional geometry that implies dunes migrating up along accretion surfaces indicates bar-edification processes. In the context of a NNE-ward flowing channel, as suggested by regional trends in palaeoflow, such a geometry suggests a sinuous channel that developed reverse flows and channelward eddy accretions at channel bends (Fig. 14B). A reverse circulation in the flow separation zone of asymmetrical channel junctions, which lead to bedforms migrating upstream on the flow-confluence barform (Bristow *et al.*, 1993), has not been investigated because no evidence for confluences was observed.

Facies sequence

In both the lower and upper units, CDCS overlie facies indicative of higher-energy flow conditions. Intraformational conglomerates of the lower unit, which seal the channel erosion surface, include diffusely graded laminae that probably reflect deposition by supercritical flows (Brennand & Shaw, 1996; Russell *et al.*, 2007b; Duller *et al.*, 2008). In the upper unit, immediately succeeding to an erosional stage but preceding lower-flow conditions generating well-developed dunes, low-amplitude dunes represent transitional bedforms developed in the dune stability field but under a relatively high rate of suspended-load fallout. In the middle part of the upper unit, two-dimensional CDCS with angles of climb showing minor changes through time and space (Figs 4A, 13B and D) indicate steady flows. The upward transition to CDCS involving 3D bedforms indicates the onset of turbulent flow conditions in the upper parts of the accreting bar surface.

Depositional model

Depositional geometries indicate that the vertical facies sequence can be interpreted in terms of spatial variability in non-uniform fluid flow conditions above a downstream-accreting bar surface from the inner to outer segments (Fig. 14C): (i) erosion, close to the flow-separation zone and channel axis; (ii) low-amplitude dunes along the inner segment of the individual depositional surface; (iii) deposition of CDCS involving 2D bedforms along the intermediate segment; and (iv) transition to CDCS with 3D bedforms within the outer segment. It is proposed here that lower-flow regime conditions generating climbing dunes arise in relatively protected depositional zones where significant settling of a relatively coarse-grained suspended load and high preservation potential occurred. The suspended load was mobilized from the essentially non-depositional channel axis and was transferred continuously to the adjacent trains of dunes enhancing sand-bed aggradation within reverse flow conditions. By analogy with CDCS in erosion-based sandstone sheets, it is inferred that the transition to 3D bedforms occupying the upper levels of the accretion surfaces reflects progressively decreasing suspended-load concentrations allowing turbulence development.

In contrast to CDCS in sandstone sheets, relatively steady but essentially non-uniform flows are inferred here. In the channel infill, CDCS is related to a type of eddy-related side bar characterized by superimposed bedforms migrating up inclined accretion surfaces that dip channelwards (Fig. 14B and C). Such bars formed at the margins of sinuous (but not meandering) channels and should have alternated with zones of bank erosion at the channel bends. Eddy bar landforms commonly characterize fluvioglacial systems (Marren, 2005; Carrivick & Russell, 2007). However, eddy bars from the case study are distinct from expansion or pendant bars that are most often associated with gravelly depositional systems. These bars are also distinct from eddy-accretion processes described in Nanson & Page (1983) and Burge & Smith (1999) but have similarities with reattachment-bar processes, described in Rubin *et al.* (1990), which commonly produce rippled successions with upstream climbing structures. Such a depositional pattern is representative of flood conditions, where high stream powers favour flow separations at bends of

sinuous channels. Climbing dune-scale cross-statification that only relates to secondary flows cannot be used to reconstruct any palaeoflow conditions occurring in the channel axis, a zone that was characterized chiefly by bypass or erosion. This depositional model seems to have been poorly documented in the literature, although smaller-scale analogues are commonly observed in flood deposits of modern Sahara wadis (Fig. 15).

DISCUSSION

Climbing dune-scale cross-statification, i.e. aggrading lamination produced by lower-flow regime climbing dunes, developed in a variety of contexts throughout sand-rich, virtually unconfined, proglacial outwash plains (Fig. 12). Two case studies have illustrated associated facies sequences, with CDCS formed and preserved in laterally extensive mouth-bar environments (sandstone sheet) and eddy-related side bars (incised channel) (Fig. 12). They are regarded as two end-members with, on the one hand, relatively uniform (at least at the outcrop scale, for example, Fig. 6) but essentially unsteady flow conditions related to waning flows in mouth-bar environments and, on the other hand, relatively steady but essentially non-uniform flow conditions related to side bars. Climbing dune-scale cross-statification has been reported only with limited development in recent proglacial environments (Gorrell & Shaw, 1991; Russell & Arnott, 2003; Russell *et al.*, 2007b). Climbing-dune development in these examples reflects either spatially (abrupt flow expansion) or temporally (flow pulsation) transient flow conditions related to subaqueous hydraulic jumps debouching from subglacial tunnels. In the following, relationships with glacier outburst are discussed, as well as the specific flow conditions that resulted in the recurrent and widespread (kilometre-scale) deposition of CDCS that characterizes Late Ordovician glacigenics.

Relationship with glacier outburst flood

Architectures, facies sequences and sand volumes indicate that CDCS is a flood-related structure. According to Marren (2005), and considering erosion-based sandstone sheets, the preservation of waxing-stage deposits, strongly uniform palaeoflows and laterally extensive basal

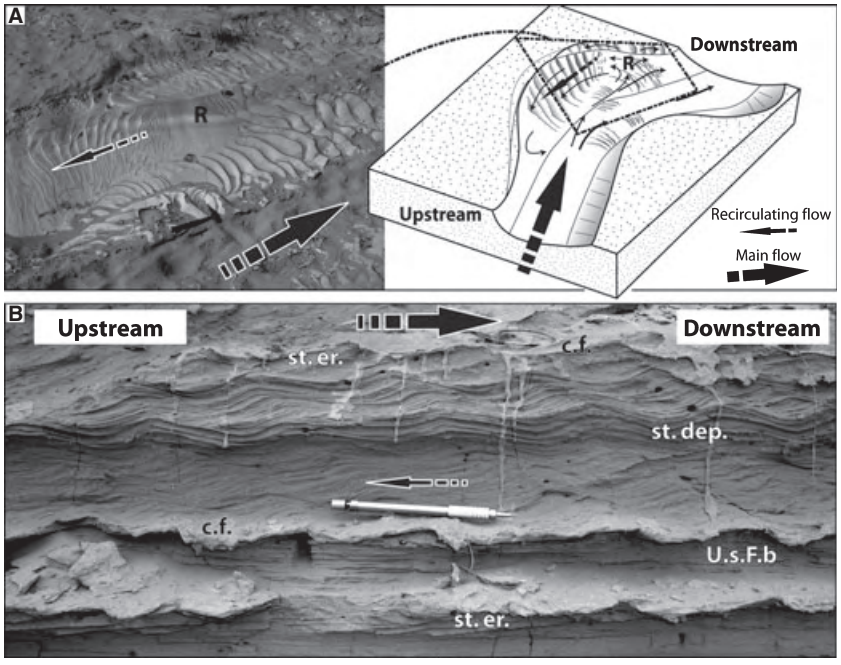

Fig. 15. Present-day reversed flows in Saharan wadis. (A) Development of a recirculation zone and related reversed flow downstream of a metre-scale bend as evidenced by ripple train migrations; 'R' locates the reattachment point (hammer for scale is 33 cm long). (B) In related depositional successions, stoss-depositional climbing-ripple cross-stratification indicating upcurrent migrations prevails, while downstream flow orientations are primarily reflected by subordinate upper-stage flat beds 'U.s.F.b', poorly developed stoss-erosional climbing assemblages 'st.er.' or waning-flow ripples that are draped by a 2 to 5 mm thick clay layer 'c.f.' (pen for scale is 15 cm long).

erosion surfaces typify high-magnitude low-frequency events. In the proglacial context, such events are potentially ascribed to glacier outbursts. Other criteria identifying glacier outburst deposits, such as large rip-up clasts, ice-block features, hyperconcentrated or debris flow deposits and large-scale gravel foresets are not recognized in association with CDCS; however, they specifically characterize proximal outwash plains and/or flows that carry a significant gravel load. Besides, some of these criteria have been recognized in the ice-proximal depositional zone (see above) but are basically not applicable to the relatively distal, sand-dominated Late Ordovician context. However, as proposed below, the present authors argue that dramatic volumes of mobilized sand, the palaeoglacial context and the record of pulsating flow conditions designate processes related to glacier outbursts.

Firstly, considering sandstone sheets, an up to 12 m thick sand pile was being deposited without any internal erosion or reactivation surface (Figs 10B and 11). It demonstrates that a single depositional event commonly mobilized one cubic kilometre (L = 20 km × l = 5 km × H = 0·01 km) of sand neglecting clastics trapped downstream in the lower part of the foresets and upstream in distributary channels. The one cubic kilometre of sand (*ca* $1{\cdot}75 \times 10^{12}$ kg, assuming dry, unconsolidated sand with a density of 1750 kg m^{-3}) is equal to sediment volume estimated for the 1918 jökulhlaup on Myrdalssandur (Maizels, 1993; Duller *et al.*, 2008) and is comparable with the total mass of suspended sediment that was carried during recent Icelandic jökulhlaups. Snorrason *et al.* (2002) inferred $0{\cdot}25 \times 10^{12}$ kg of suspended sediment finer than 0·2 mm in 1996 and $0{\cdot}05 \times 10^{12}$ kg of suspended sediment finer than 2 mm in the 1972 jökulhlaup. As explained by the authors, these values are underestimated and ignore bedload transport (see also Roberts, 2005); they are in the range of total mass of sand mobilized during individual Late Ordovician events.

Secondly, at the Ordovician time scale, deposition of CDCS characterized a deglaciation stage rather than full glacial conditions (Ghienne *et al.*, 2007b). Such a context enhances meltwater volumes, sediment availability and outburst frequency (Evans & Clague, 1994; Marren, 2005; his fig. 4). The drainage of subglacial lakes, which constitute recurrent features even in the absence of sub-ice volcanism (e.g. Siegert *et al.*, 1996; Björnsson, 2002; Alley *et al.*, 2006; Peters *et al.*, 2007), periodically transfers great quantities of sediments from the subglacial environment towards the proglacial outwashes. Related high-magnitude flood events are associated with incisions of tunnel channels (e.g. Roberts, 2005; Russell *et al.*, 2007a), which are also a common feature of the Late Ordovician glacial record (Ghienne & Deynoux, 1998; Hirst *et al.*, 2002; Le Heron *et al.*, 2004, 2009; Moreau *et al.*, 2005).

Thirdly, CDCS in eddy-related side bars preserved rhythms that take the form of subtle changes in the angle of climb (Fig. 9B) that are interpreted as the signature of pulsating, suspended-load fallout rates. Rhythmically bedded sands are well-known from outburst-related successions at the transition from suspension to traction deposition (O'Connor, 1993; Smith, 1993; Russell & Knudsen, 1999b). As described above, such a spatial transition also characterizes the eddy-related side bar sedimentation, co-existing with essentially non-depositional flows at the adjacent channel axis. Russell & Knudsen (1999b) estimated that each rhythmite represents the record of flood pulses in the order of seconds or minutes in duration. The periodic breaking of large, in-phase waves in more proximal segments of the flood route dominated by supercritical flows may affect distant downcurrent flow conditions and be responsible for such a rhythmic pattern. Rhythmically bedded sands in proglacial settings are potentially thought to represent a distinctive feature of outburst flood deposits.

Flow conditions for CDCS development

If climbing dunes characterize high-magnitude flood events, why are CDCS not more common in the geological record? It is argued here that the primary control on the formation of CDCS is a combination between high-magnitude flows and sediment supply limitations. The Late Ordovician glacial record is specifically dominated by sandstones, with virtually no conglomerates and a subordinate amount of fine-grained, clay-rich material (Ghienne *et al.*, 2007b). It reflects both the lack of a glaciated mountainous area providing coarse supraglacial material, and the nature of the subglacial eroded substrate that was essentially made up of the thick Cambrian-Ordovician sandstones (500 to 2000 m; see above). In Northern Niger, i.e. up to 600 km straight up-ice (Fig. 1), Late Ordovician ice moved on sands and sandstones (Denis *et al.*, 2007, 2009). The eroded substrate was not able to provide any quantities either of coarse extra-clasts (gravels to cobbles), or of fine-grained material. No bedrock

lithology has been eroded by glaciers up-ice from the study area, except possibly for a very restricted area. As a consequence, meltwater flows essentially transport sand-sized sediments.

The transport capacity of Late Ordovician meltwater floods was then dedicated to the sand fraction. Great volumes of sand were carried as suspended load, even though a tractive flow-boundary zone was maintained explaining the generation of dunes. As far as concentrated, high-magnitude turbulent flows carrying only sand are concerned, only minor, or no, bedload deposition occurs when entering mouth-bar environments or all other zones of jet-related flow establishment. Bypassing of the sand-sized material occurs and, in contrast to gravel-rich depositional systems (e.g. Mutti *et al.*, 2003), initially high sandy suspended-load concentration pertains downstream in the zone of established flow with no or minor sediment dilution. Turbulent sand-dominated initial outflows are then transformed in sediment-laden stream flows that are characterized by unusually high suspended-load concentrations and related sediment-induced flow stratification (Wright & Parker, 2004). Such stratified flows that experienced reduced vertical turbulent flux of mass and momentum have reduced suspended-load transport capacity with respect to an unstratified flow of equal flow rate (McLean, 1992; Bennett, 1995; García, 2007). Resulting greater rates of suspended-load fallout to the flow-boundary zone enhance deposition by aggradation of the bed and CDCS development. The present authors suggest that horizontal laminations, including incipient bedforms (Fig. 10D) to low-amplitude dunes (Fig. 13D), reflect severely stratified flow conditions with high fallout rates and dramatically reduced flow turbulences. Strikingly uniform bedforms with linear crestlines (Figs 4 and 6) would be ascribed to less severe stratified flow conditions but with reduced flow turbulences favouring the stability of 2D bedforms. Finally, rather than reflecting higher-energy conditions (Ashley, 1990), 3D bedforms (Fig. 7) are interpreted as transitional structures associated with spatially (eddy bars) or temporally (sandstone sheets) decreasing suspended-load concentration and sediment-induced stratification. Renewed flow separations and reattachments resulted in the greater dune trough-scour depths (Leclair, 2002) that characterized CDCS involving 3D bedforms. Facies sequences including CDCS then involve declining and concurrent suspended-load fallout rate and flow intensity, the trajectory of which cannot be resolved on the usual stability-field diagrams that basically ignore the effects of suspended-load sedimentation (Lowe, 1988; Sumner *et al.*, 2008).

It should be noticed that flows that had the ability to transport gravel to cobble-sized material but that actually transported and deposited a predominant sand-grade component are also documented from some Icelandic sandar case studies. Antidune facies that prevail in related deposits (e.g. Duller *et al.*, 2008) could however suggest that they may represent more proximal flow conditions. Similar deposits may thus be expected in upstream segments of Late Ordovician outwash plains. Alternatively, conditions for widespread (i.e. kilometre-scale) CDCS deposition may have occurred in downstream segments of ancient distal outwash plains of Icelandic sandar systems. According to the depositional model inferred from the Late Ordovician, conditions for CDCS deposition may have occurred preferentially in Iceland when the sandar corresponded to truly unconfined depositional systems in front of advancing ice fronts, i.e. prior to recent meltwater channel entrenchments related to ice-front retreats (e.g. Gomez *et al.*, 2000; Magilligan *et al.*, 2002).

CONCLUSION

Specific conditions, including sediment supply limitations, characterized the Late Ordovician outwash plains. High-magnitude events identified as glacier outbursts remobilized great volumes of sand that were transported essentially as suspended load. Downcurrent, related sediment-laden stream flows had high sand-sized suspended-load concentration but were sufficiently dilute to generate tractive bedforms. High fallout rates resulting in sustained sand-bed aggradation resulted in a succession including climbing-dune cross-stratification (CDCS). Flow conditions were characterized by a sediment-induced stratification partly inhibiting dune-related turbulences. Such flows, and related occurrences of CDCS, may have been overlooked in the sedimentary record but the present authors rather suspect that they actually are rare, because, in contrast to the Late Ordovician context, most flood-dominated depositional systems have mixed sediment load (gravel/sand/fines) generating dilute sand-sized suspension load unable to produce CDCS. Besides, dune-generating sand-dominated depositional systems usually have low sand-sized suspended-load concentrations resulting in a

low aggradation rate and significant cross-set differentiation. Sediment supply limitations are not restricted to the glacial environment and CDCS is also reported from non-glacial flood-dominated settings, within which high discharge events remobilized great volumes of sand in drainage basins of foreland systems (e.g. Mutti *et al.*, 1996). Sediment nature and concentration, and not the glacial setting, represent the main forcing factor for the generation of CDCS during flood events. However, as far as paraglacial depositional environments are concerned, CDCS is regarded here as a distinctive criterion for glacier outburst deposits.

ACKNOWLEDGEMENTS

The authors are grateful to J. Winsemann, P. Marren and H. Russell and an anonymous reviewer for their constructive comments that enhanced the paper. This paper is a contribution to the Eclipse II (CNRS, France) and IGCP503 projects. Field work was funded by Total.

REFERENCES

Abugares, Y. and **Ramaekers, P.** (1993) . *Short Notes and Guidebook on the Palaeozoic Geology of the Ghat Area, SW Libya*. Earth Science Society of Libya, Tripoli, 84 pp.

Allen, J.R.L. (1970) A quantitative model of climbing ripples and their cross-laminated deposits. *Sedimentology*, **14,** 5–26.

Allen, J.R.L. (1973) A classification of climbing ripple cross-lamination. *J. Geol. Soc. London*, **129,** 537–541.

Allen, J.R.L. and **Leeder, M.R.** (1980) Criteria for the instability of upper-stage plane beds. *Sedimentology*, **27,** 209–217.

Allen, P.A. and **Underhill, J.R.** (1989) Swaley cross-stratification produced by unidirectional flows, Bencliff Grit (Upper Jurassic), Dorset, UK. *J. Geol. Soc. London*, **146,** 241–252.

Alley, R.B., Dupont, T.K., Parizek, B.R., Anandakrishnan, S., Lawson, D.E., Larson, G.J. and **Evenson, E.B.** (2006) Outburst flooding and the initiation of ice-stream surges in response to climatic cooling: a hypothesis. *Geomorphology*, **75,** 76–89.

Amy, L. and **Talling, P.J.** (2006a) Anatomy of turbidites and linked debrites based on long distance (120 × 30 km) bed correlation, Marnoso Arenacea Formation, Northern Apennines, Italy. *Sedimentology*, **53,** 161–212.

Arnott, R.W.C. and **Hand, B.M.** (1989) Bedforms, primary structures and grain fabric in the presence of suspended sediment rain. *J. Sed. Petrol.*, **59,** 1062–1069.

Ashley, G.M. (1990) Classification of large scale subaqueous bedforms: a new look at an old problem. *J. Sed. Petrol.*, **60,** 160–172.

Ashley, G.M., Southard, J.B. and **Boothryod, J.C.** (1982) Deposition of climbing ripple beds: a flume simulation. *Sedimentology*, **29,** 67–79.

Bellini, E. and **Massa, D.** (1980) A stratigraphic contribution to the Paleozoic of the Southern Basins of Libya. In: *The Geology of Libya*, Vol. I (Eds M.J. Salem and M.T. Bursrevil), pp. 1–56. Academic Press, London.

Bennett, J.P. (1995) Algorithm for resistance to flow and transport in sand-bed channels. *J. Hydraul. Eng.*, **121,** 578–590.

Best, J.L., Ashworth, P.J., Sarker, M.H. and **Roden, J.E.** (2007) The Brahmaputra-Jamuna River, Bangladesh. In: *Large Rivers, Geomorphology and Management* (Ed. A. Gupta), pp. 395–433. Wiley & Sons, Chichester, UK.

Beuf, S., De Charpal, O., Debyser, J., Gariel, O. and **Montadert, L.** (1962) *Recherche sédimentologique; Le Cambro-Ordovicien du Tassili des Ajjers (Résultats de la mission 1961–1962)*. Institut Français du Pétrole, unpublished report 7700-A.

Beuf, S., Biju-Duval, B., De Charpal, O., Rognon, P., Gariel, O. and **Bennacef, A.** (1971) *Les grès du Paléozoïque inférieur au Sahara*. ''Science et Technique du pétrole'', 18, Paris, 464 pp.

Björnsson, H. (2002) Subglacial lakes in Iceland. *Glob. Planet. Change*, **35,** 255–271.

Boote, D.R.D., Clark-Lowes, D.D. and **Traut, M.W.** (1998) Paleozoic petroleum systems of North Africa. In: *Petroleum Geology of North Africa* (Eds D.S. Macgregor, R.T.J. Moody and D.D. Clark-Lowes), *Geol. Soc. London Spec. Publ.*, **132,** 7–68.

Brennand, T.A. and **Shaw, J.** (1996) The Harricana glaciofluvial complex, Abitibi region, Quebec: its genesis and implications for meltwater regine and ice-sheet dynamics. *Sed. Geol.*, **102,** 221–262.

Bridge, J.S. (1997) Thickness of sets of cross strata and planar strata as a function of formative bed-wave geometry and migration, and aggradation rate. *Geology*, **25,** 971–974.

Bristow, C.S., Best, J.L. and **Roy, A.G.** (1993) Morphology and facies models of chanel confluences. In: *Alluvial Sedimentation* (Eds M. Marzo and C. Puigdefabregas), *Int. Assoc. Sedimentol. Spec. Publ.*, **17,** 91–100.

Buoncristiani, J.F., Guiraud, M. and **Denis, M.** (2007) Ordovician paleo ice stream glacial landsystem. *Houille Blanche*, **3,** 79–85.

Burge, L.M. and **Smith, D.G.** (1999) Confined meandering river eddy accretions: sedimentology, channel geometry and depositional processes. In: *Fluvial Sedimentology VI* (Eds N.D. Smith and J. Rogers), *Int. Assoc. Sedimentol. Spec. Publ.*, **28,** 113–130.

Cagnoli, B. and **Ulrych, T.J.** (2001) Ground penetrating radar images of unexposed climbing dune-forms in the Ubehebe hydrovolcanic field (Death Valley, California). *J. Volcan. Geoth. Res.*, **109,** 270–298.

Carling, P.A., Gölz, E., Orr, H.G. and **Radecki-Pawlik, A.** (2000) The morphodynamic of fluvial sand dunes in the River Rhine, near Mainz, Germany. I. Sedimentology and morphology. *Sedimentology*, **47,** 227–252.

Carrivick, J.L. and **Russell, A.J.**, 2007. Glacifluvial landforms of deposition. In: *Encyclopedia of Quaternary Science*, Vol. 2 (Ed. S.A. Elias), pp. 909–919. Elsevier, B.V., Amsterdam.

Church, M. (1972) Baffin Island sandurs: a study of Arctic fluvial processes. *Bull. Geol. Surv. Can.*, **216,** 208.

Coward, M.P. and **Ries, A.C.** (2003) Tectonic development of North African basins. In: *Petroleum Geology of Africa: New Themes and Developing Technologies* (Eds T.J. Arthur and D.S. MacGregor), *Geol. Soc. London, Spec. Publ.*, **207,** 61–83.

Denis, M., Buoncristiani, J.-F., Konaté, M., Ghienne, J.-F. and **Guiraud, M.** (2007) Hirnantian glacial and deglacial record in SW Djado Basin (NE Niger). *Geodin. Acta*, **20,** 177–194.

Denis, M., Guiraud, M., Konaté, M. and **Buoncristiani, J.-F.** (2009) Subglacial deformation and water-pressure cycles as a key for understanding ice stream dynamics: evidence from the Late Ordovician succession of the Djado Basin (Niger). *Int. J. Earth Sci.*, in press.

Duller, R.A., Mountney, N.P., Russell, A.J. and **Cassidy, N.C.** (2008) Architectural analysis of a volcanoclastic jökulhlaup deposit, southern Iceland: sedimentary evidence for supercritical flow. *Sedimentology*, **55,** 939–964.

Duringer, P., Paicheler, J.C. and **Schneider, J.L.** (1991) Un courant d'eau continu peut-il générer des turbidites? Résultats d'expérimentation analogiques (Can a continuous water flow generate turbidites? Results from analogue experiments) *Mar. Geol.*, **99,** 231–246.

El-Hawat, A.S., Bezan, A., Obeidi, A. and **Barghati, H.** (2000) The Upper Ordovician – Lower Silurian Succession of Western Libya: sequence stratigraphy and Glacioeustatic-Tectonic scenario. In: *The Geology of Northwest Libya* (Eds M.J. Salem and K.M. Oun) *Sed. Basins Libya – Sec. Symp.*, **1,** 65–78. Earth Science Society of Libya.

Eschard, R., Abdallah, H., Braik, F. and **Desaubliaux, G.** (2005) The Lower Paleozoic succession in the Tasilli outcrops, Algeria: sedimentology and sequence Stratigraphy. *First Break*, **23,** 27–36.

Evans, S.G. and **Clague, J.J.** (1994) Recent climatic and catastrophic geomorphic processes in mountain environments. *Geomorphology*, **10,** 107–128.

Fielding, C.R. (2006) Upper flow regime sheets, lenses and scour fills: extending the range of architectural elements for fluvial sediment bodies. *Sed. Geol.*, **190,** 227–240.

García, M.H. (2007) Sediment transport and morphodynamics. In: *Sedimentation Engineering: Processes, Management, Modelling and Practice* (Ed. M.H. García), *ASCE Manuals Rep. Eng. Pract.*, **110,** 21–164.

Ghienne, J.-F. (2003) Late Ordovician sedimentary environments, glacial cycles, and post-glacial transgression in the Taoudeni Basin, West Africa. *Palaeogeogr. Palaeoclimatol. Palaeoecol.* **189,** 117–145.

Ghienne, J.-F. and **Deynoux, M.** (1998) Large scale channel fill structures in Late Ordovician glacial deposits in Mauritania, western Sahara. *Sed. Geol.*, **119,** 141–159.

Ghienne, J.-F., Deynoux, M., Manatschal, G. and **Rubino, J.L.** (2003) Palaeovalleys and fault-controlled depocenters in the Late Ordovician glacial record of the Murzuq Basin (Central Libya). *CR Geosci.*, **335,** 1091–1100.

Ghienne, J.-F., Boumendjel, K., Paris, F., Videt, B., Racheboeuf, P. and **Ait Salem, H.** (2007a) The Cambrian-Ordovician succession in the Ougarta Range (western Algeria, North Africa) and interference of the Late Ordovician glaciation on the development of the Lower Palaeozoic transgression on northern Gondwana. *Bull. Geosci.*, **82,** 183–214.

Ghienne, J.-F., Le Heron, D., Moreau, J., Denis, M. and **Deynoux, M.** (2007b) The Late Ordovician glacial sedimentary system of the North Gondwana platform. In: *Glacial Sedimentary Processes and Products* (Eds M. Hambrey, P. Christoffersen, N. Glasser, P. Janssen, B. Hubbard and M. Siegert), *Int. Assoc. Sedimentol. Spec. Publ.*, **39,** 295–319.

Girard, F., Ghienne, J.-F., Moreau, J. and **Rubino, J.-L.** (2009) *Anatomy of a Late Ordovician Channel Network into a Fluvioglacial Outburst-Related Delta Plain. From River to Rock Record.* Abstract book, p. 39. University of Aberdeen, Aberdeen.

Gomez, B., Smith, L.C., Magilligan, F.J., Mertes, L.A.K. and **Smith, N.D.** (2000) Glacier outburst floods and outwash plain development: Skeidarársandur, Iceland. *Terra Nova*, **12,** 126–131.

Gorrell, G. and **Shaw, J.** (1991) Deposition in an esker, bead and fan complex, Lanark, Ontario, Canada. *Sed. Geol.*, **72,** 285–314.

Hirst, J.P.P., Benbakir, A., Payne, D.F. and **Westlake, I.R.** (2002) Tunnel Valleys and Density Flow Processes in the upper Ordovician glacial succession, Illizi Basin, Algeria: influence on reservoir quality. *Mar. Petrol. Geol.*, **25,** 297–324.

Hornung, J.J., Asprion, U. and **Winsemann, J.** (2007) Jet-efflux deposits of a subaqueous ice-contact fan, glacial Lake Rinteln, northwestern Germany. *Sed. Geol.*, **193,** 167–192.

Hoyal, D.C.J.D., Van Wagoner, J.C., Adair, N.L., Deffenbaugh, M., Li, D., Sun, T., Huh, C. and **Giffin, D.E.** (2003) Sedimentation from jets: a depositional model for clastic deposits of all scales and environments. *Am. Ass. Petr. Geol., Search and Discovery*, Online Article #40082.

Hunter, R.E. (1977) Terminology of cross-stratified sedimentary layers and climbing-ripple structures. *J. Sed. Petrol.*, **47,** 697–706.

Idier, D., Astruc, D. and **Hulscher, S.J.M.H.** (2004) Influence of bed roughness on dune and megaripple generation. *Geophys. Res. Lett.*, **31,** L13214.

Jerolmack, D.J. and **Mohrig, D.** (2005) Frozen dynamics of migrating bedforms. *Geology*, **33,** 57–60.

Jopling, A.V. and **Walker, R.G.** (1968) Morphology and origin of ripple-drift cross-lamination, with examples from the Pleistocene of Massachusetts. *J. Sed. Petrol.*, **38,** 971–984.

Kleinhans, M.G. (2004) Sorting in grain flows at the lee side of dunes. *Earth-Sci. Rev.*, **65,** 75–102.

Le Heron, D.P. and **Craig, J.** (2008) First-order reconstructions of a Late Ordovician Saharan ice sheet. *J. Geol. Soc. London*, **165,** 19–29.

Le Heron, D., Sutcliffe, O.E., Bourgig, K., Craig, J., Visentin, C. and **Whittington, R.** (2004) Sedimentary architecture of Upper Ordovician Tunnel Valleys, Gargaf Arch, Libya: implications for the genesis of a hydrocarbon reservoir. *GeoArabia*, **9,** 137–160.

Le Heron, D.P., Craig, J., Sutcliffe, O. and **Whittington, R.** (2006) Late Ordovician glaciogenic reservoir heterogeneity: an example from the Murzuq Basin, Libya. *Mar. Petrol. Geol.*, **23,** 655–677.

Le Heron, D., Craig, J. and **Etienne, J.L.** (2009) Ancient glaciations and hydrocarbon accumulations in North Africa and the Middle East. *Earth-Sci. Rev.*, **93,** 47–76.

Leclair, S.F. (2002) Preservation of cross-strata due to the migration of subaqueous dunes: an experimental investigation. *Sedimentology*, **49,** 1157–1180.

Lowe, D.R. (1988) Suspended-load fallout rate as an independent variable in the analysis of current structures. *Sedimentology*, **35,** 765–776.

Magilligan, F.J., Gomez, B., Mertes, L.A.K., Smith, L.C., Smith, N.D., Finnegan, D. and **Garvin, J.B.** (2002) Geomorphic effectiveness, sandur development, and the pattern of landscape response during jökulhlaups: Skeidarársandur, southeastern Iceland. *Geomorphology*, **44,** 95–113.

Maizels, J.K. (1993) Lithofacies vaiations within sandur deposits: the role of runoff regime, flow dynamics and sediment supply characteristics. *Sed. Geol.*, **85,** 299–325.

Marren, P.M. (2005) Magnitude and frequency in proglacial rivers: a geomorphological and sedimentological perspective. *Earth-Sci. Rev.*, **70,** 203–251.

Marren, P.M., Russell, A.J. and **Rushmer, E.L.** (2009) Sedimentology of a sandur former by multiple jökulhlaups, Kverkfjöll, Iceland. *Sed. Geol.*, **213,** 77–88.

McDougall, N. and **Martin, M.** (2000) Facies models and sequence stratigraphy of Upper Ordovician outcrops in the Murzuq Basin, SW Libya. In: *Geological Exploration in Murzuq Basin* (Eds M.A. Sola and D. Worsley), pp. 223–236. Elsevier Science, Amsterdam.

McLean, S.R. (1992) On the calculation of suspended load for noncohesive sediments. *J. Geophys. Res.*, **97,** 5759–5770.

McLeod, P., Carey, S. and **Sparks, S.** (1999) Behaviour of particle-laden flows into the ocean: experiemtal simulation and geological implications. *Sedimentology*, **46,** 523–536.

Moreau, J. (2005) Architecture stratigraphique et dynamique des dépôts glaciaires ordoviciens du Bassin de Murzuk (Libye). Unpublished PhD Thesis, Université Louis Pasteur, Strasbourg, France.

Moreau, J., Ghienne, J.-F., Le Heron, D., Rubino, J.-L. and **Deynoux, M.** (2005) A 440 Ma old ice stream in North Africa. *Geology*, **33,** 753–756.

Mulder, T., Syvitski, J.P.M. and **Skene, K.I.** (1998) Modeling of erosion and deposition by turbidity currents generated at river mouths. *J. Sed. Res.*, **68,** 124–137.

Mulder, T., Syvitski, J.P.M., Migean, S., Faugères, J.-C. and **Savoye, B.** (2003) Marine hyperpycnal flows: initiation, behavior and related deposits. A review. *Mar. Petrol. Geol.*, **20,** 861–882.

Mutti, E., Davoli, G., Tinterri, R. and **Zavala, C.** (1996) The importance of ancient fluvio-deltaic systems dominated by catastrophic flooding in tectonically active basins. *Sci. Geol. Mem.*, **48,** 233–291.

Mutti, E., Tinteri, R., Benevelli, G., di Biase, D. and **Cavanna, G.** (2003) Deltaic, mixed and turbidite sedimentation of ancient foreland basins. *Mar. Petrol. Geol.*, **20,** 733–755.

Nanson, G. and **Page, K.** (1983) Lateral accretion of fine-grained concave benches on meandering rivers. *Int. Assoc. Sedimentol. Spec. Publ.*, **6,** 133–143.

O'Connor, J.E. (1993) Hydrology, hydrolics, and geomorphology of the Bonneville flood. *Geol. Soc. Am. Spec. Pap.*, **274,** 83.

Peters, L.E., Anandakrisnan, S., Alley, R.B. and **Smith, A.M.** (2007) Extensive storage of basal meltwater in the onset region of a major West Antarctic ice stream. *Geology*, **35,** 251–254.

Protic, D. (1984) *Geological Map of Libya, 1:250 000, Sheet Tikíúmit, NG 32-7*. Industrial Research Center, Tripoli.

Roberts, M.J. (2005) Jökulhlaups: a reassessment of floodwater flow through glaciers. *Rev. Geophys.*, **43,** 1–21.

Roep, T.B. and **Fortuin, A.R.** (1996) A submarine slide scar and channel filled with slide blocks and megarippled Globigerina sands of possible contourite origin from the Pliocene of Sumba, Indonesia. *Sed. Geol.*, **103,** 145–160.

Rubin, D.M. (1987) Cross-bedding, bedforms and paleocurrents. *Concepts in Sedimentology and Paleontology*, Vol. 1, SEPM, Tulsa, OK, 187 p.

Rubin, D.M., Schmidt, J.C. and **Moore, J.N.** (1990) Origin, structure, and evolution of a reattachment bar, Colorado River, Grand Canyon, Arizona. *J. Sed. Res.*, **60,** 982–991.

Russell, H.A.J. and **Arnott, R.W.C.** (2003) Hydraulic-jump and hyperconcentrated-flow deposits of a glacigenic subaqueous fan: Oak Ridges Moraine, Southern Ontario, Canada. *J. Sed. Petrol.*, **73,** 887–905.

Russell, A.J. and **Knudsen, Ó.** (1999a) Controls on the sedimentoly of the November 1996 jökulhlaup deposits, Skeidarársandur, Iceland. In: *Fluvial Sedimentology VI* (Eds N.D. Smith and J. Rogers), *Int. Assoc. Sedimentol. Spec. Publ.*, **28,** 315–329.

Russell, A.J. and **Knudsen, Ó.** (1999b) An ice-contact rhythmite (turbidite) succession deposited during the November 1996 catastrophic outburst flood (jökulhlaup), Skeidarársandur, Iceland. *Sed. Geol.*, **127,** 1–10.

Russell, A.J. and **Knudsen, Ó.** (2002) The effects of glacier-outburst flood flow dynamics on ice-contact deposits: November 1996 jökulhlaup, Skeidarársandur, Iceland. In: *Flood and Megaflood Processes and Deposits: Recent and Ancient Examples* (Eds I.P. Martini, V.R. Baker and G. Garzón), *Int. Assoc. Sedimentol. Spec. Publ.*, **32,** 67–83.

Russell, A.J. and **Marren, P.M.** (1999) Proglacial fluvial sedimentary sequences in Greenland and Iceland: a case study from active proglacial environments subject to jökulhlaups. In: *The Description and Analysis of Quaternary Stratigraphic Field Sections* (Eds A.P. Jones, M.E. Tucker and J.K. Hart), *Quatern. Res. Assoc. Tech. Guide*, **7,** 171–208.

Russell, A.J., Fay, H., Marren, P.M., Tweed, F.S. and **Knudsen, Ó.** (2005) Icelandic jökulhlaup impacts. In: *Iceland—Modern Processes and Past Environments* (Eds C. Caseldine, A. Russell, J. Hardardóttir and Ó. Knudsen), *Dev. Quatern. Sci.*, **5,** 153–203.

Russell, A.J., Gregory, A.R., Large, A.R.G., Fleisher, P.J. and **Harris, T.D.** (2007a) Tunnel channel formation during the November 1996 jökulhlaup, Skeidarárjökull, Iceland. *Ann. Glaciol.*, **45,** 95–103.

Russell, H.A.J., Sharpe, D.R. and **Bajc, A.F.** (2007b) Sedimentary signatures of the Waterloo Moraine, Ontario, Canada. In: *Glacial Sedimentary Processes and Products* (Eds M. Hambrey, P. Christoffersen, N. Glasser, P. Janssen, B. Hubbard and M. Siegert), *Int. Assoc. Sedimentol. Spec. Publ.*, **39,** 85–108.

Rust, B.R. and **Gibling, M.R.** (1990) Three-dimensional antidunes as HCS mimics in a fluvial sandstone: the Pennsylvanian South Bar Formation near Sydney, Nova Scotia. *J. Sed. Petrol.*, **60,** 540–548.

Saunderson, H.C. and **Lockett, F.P.** (1983) Flume experiments on bedforms and structures a the dune—plane bed transition. *Int. Assoc. Sedimentol. Spec. Publ.*, **6,** 49–58.

Siegert, M.J., Dowdeswell, J.A., Gorman, M.R. and **McIntyre, N.F.** (1996) An inventory of Antarctic sub-glacial lakes. *Antarctic Sci.*, **8,** 281–286.

Simons, D.B. and **Richardson, E.V.** (1966) Resistance to flow in alluvial channels. *U.S. Geol. Surv. Prof. Pap.*, **422J,** 61.

Smith, G.A. (1993) Missoula flood dynamics and magnitudes inferred from sedimentology of slack-water deposits on the Columbia Plateau, Washington. *Geol. Soc. Am. Bull.*, **105,** 77–100.

Smith, L.C., Sheng, Y., Magilligan, F.J., Smith, N.D., Gomez, B., Mertes, L.A.K., Krabill, W.B. and **Garvin, J.B.** (2006) Geomorphic impact and rapid subsequent recovery from the 1996 Skeidarársandur jökulhlaup, Iceland, measured with multi-year airbone lidar. *Geomorphology*, **75,** 65–75.

Snorrason, Á., Jónsson, P., Sigurdsson, O., Pálsson, S., Árnasson, S., Vikingsson, S. and **Kaldal, I.** (2002) November 1996 jökulhlaup on Skeidarársandur outwash plain, Iceland. In: *Flood and Megaflood Processes and Deposits: Recent and Ancient Examples* (Eds I.P. Martini, V.R. Baker and G. Garzón), *Int. Assoc. Sedimentol. Spec. Publ.*, **32,** 55–65.

Stanley, K.O. (1974) Morphology and hydraulic significance of climbing ripples with superimposed micro-ripple-drift cross-lamination in Lower Quaternary lake silts, Nebraska. *J. Sed. Petrol.*, **44,** 472–483.

Sumner, E.J., Amy, L.A. and **Talling, P.J.** (2008) Deposit structure and processes of sand deposition from decelerating sediment suspension. *J. Sed. Res.*, **78,** 529–547.

Ward, L.G., Stephen, M.F. and **Nummedal, D.** (1976) Hydraulics and morphology of glacial outwash distributaries, Skeidarársandur, Iceland. *J. Sed. Petrol.*, **46,** 770–777.

Wright, L.D. (1977) Sediment transport and deposition at river mouths: a synthesis. *Geol. Soc. Am. Bull.*, **88,** 857–868.

Wright, S. and **Parker, G.** (2004) Flow resistance and suspended load in sand-bed rivers: simplified stratification model. *J. Hydraul. Eng.*, **130,** 796–805.

Manuscript received 20 February 2009; revision accepted 4 December 2009

Channelized sandstone bodies ("Cordons") in the Tassili N'Ajjer (Algeria & Libya): snapshots of a Late Ordovician proglacial outwash plain

F. Girard[1]*, J.-F. Ghienne[1], J.-L. Rubino[2]

[1] Ecole et Observatoire des Sciences de la Terre, Institut de Physique du Globe de Strasbourg, UMR 7516 CNRS – Université de Strasbourg, 1 rue Blessig, 67084 Strasbourg, France
[2] Total S.A., CSTJF, Avenue Larribau 64018 Pau Cedex, France
*Corresponding author (e-mail: flavia.girard@eost.u-strasbg.fr)

Running Title

Late Ordovician proglacial channels

Number of words

Total words (abstract-text-table and figure captions-references): 9276

Text words (without abstract): 5909

References words: 2416

Figures words: 759

Table:17

Abstract: The architecture, distribution and development of channelized sandstone bodies are described from Late Ordovician paraglacial successions of the Tassili N'Ajjer (SE Algeria and SW Libya) based on satellite images and field data (sedimentary logs, photomosaics). Sandstone bodies forming ribbons at outcrop ("Cordons" structures of the literature) typify a fluvioglacial outwash plain deposited in between a continental ice front and a delta-front zone. Channelized sandstone bodies are straight to sinuous, their widths are in the 60-600 m range, thicknesses in the 5-30 m range and they have a mean W/T ratio of 16.5. They develop within an aggrado-prograding sand-dominated topset succession including at its distal end terminal distributary channel and mouth-bar environments. Architecture of channel bodies and related depositional facies, which includes climbing-dune cross-stratification, indicate that channelized sandstone bodies represent plugs of isolated channels in relation with high-magnitude flood events (glacier outbursts). The plugs fossilized networks of both braided channels and interlaced anastomosed channels, offering outburst-related snapshots of an unconfined proglacial outwash braidplain constituted by the amalgamation of adjacent, elongated outwash fans.
(End of Abstract)

Article soumis en juin 2010 aux *Special Publications of the Geological Society London,* volume "Glaciogenic reservoirs"

To identify former fluvial systems based on their stratigraphical record, either from their internal organization (Miall, 1996) and/ or from the geometry of resulting sediment bodies (Friend, 1983; Gibling, 2006) is not straightforward. Despite a considerable research has been conducted on modern (Boothroyd & Nummedal 1978; Maizel 1993, 1997; Gomez *et al.* 2000; Magilligan *et al.* 2002; Carrivick & Russell 2007; Duller *et al.* 2008) and Pleistocene (Church 1972; Dawson & Bryant 1987; Krzyszkowski 2002; Winsemann 2009; Zielinski & Van Loon 2002, 2003) sandur-type plains, fluvial channel bodies of proglacial outwash plains has received much less attention than braided or meandering end-member rivers. If successions of proglacial outwash plain deposits may have a number of similarities with that of some non-glacial braided channel belts, distal alluvial fans, or megafans, erosional and depositional processes are been here largely impacted by low-frequency, high-magnitude floods (glacial outburst or jökulhlaup) generated by the catastrophic drainage of subglacial ice-dammed lakes (e.g. Björnsson 2002; Snorrason *et al*. 2002; Russell *et al.* 2005; Marren 2005; Peters *et al.* 2007; Russell 2009). However, only few accounts have dealt with channel responses to extreme fluctuations in runoff and sediment inputs upon the distal proglacial drainage system, though channel networks on proglacial outwash plain are used as prototypes of braided river systems (e.g. Zielinski & Van Loon, 2002, 2003; Marren, 2004 and references therein).

The Late Ordovician (Hirnantian) glaciation was responsible for the deposition of a thick sand-dominated wedge (Eschard *et al.* 2005; Le Heron *et al*. 2006; Ghienne *et al.* 2007a). Related successions frequently constitute valuable hydrocarbon reservoirs that contain large volumes of recoverable hydrocarbon reserves, especially regarding North African and Arabian case studies (e.g. Hirst *et al.* 2002; Le Heron *et al.* 2006, 2009; Galeazzi *et al*. 2010). The present contribution provides a detailed analysis of fluvioglacial channel networks, the heterogeneity of which may have in part controlled fluid flows though the glaciogenic succession. Based on cross-profiles and satellite images, it successively explores related sedimentary facies and the external geometry of channelized sandstone bodies that are usually exposed in three dimensions providing an outstanding record of ancient proglacial outwash drainage networks. Considering that high-magnitude flood events have been recently inferred based on the occurrence of unusual sedimentary structures in the related depositional successions (Ghienne *et al.* 2010), the role of outburst-related processes on the fluvioglacial architecture is then discussed. Finally, relationships with other non-glacial potential analogues are outlined.

Context

Geological setting

The Tassili N'Ajjer plateau is comprised of Cambrian to Ordovician sandstone strata deposited upon the Hoggar Shield at the southern edge of the Illizi Basin (SE Algerian) and at the western edge of the Murzuq Basin (SW Libya) (Fig. 1). Throughout its Palaeozoic to Cenozoic evolution, the corresponding area was a stable intra-plate domain, with tectonic uplifts individualizing several intracratonic basins, the present geometry of which bear little relation to the broader North Gondwana platform that had an off-shelf gradient toward the NNW throughout the early Palaeozoic (Beuf *et al*. 1971; Coward & Ries 2003; Fabre & Kazi-Tani 2005; Galeazzi *et al*. 2010). Structural highs, such as the Tihemboka High that trends SSW-NNE separating the Illizi and Murzuq basins, were recurrently active during the Palaeozoic. At the first order, the Lower Palaeozoic succession consists in a Cambrian to Ordovician transgressive sedimentary package (fluvial to shallow-marine succession), an uppermost Ordovician, erosion-based, glacially-related unit, and a Silurian to Lower Devonian regressive package (inner shelf to fluvial) (Bellini & Massa 1980; Eschard *et al*. 2005; Ghienne *et al*. 2007b).

In the latest Ordovician (Hirnantian stage, < 2Ma in duration), a continental-scale ice sheet extended present-day West and North Africa, as well as Arabia, possibly joining South Africa (Ghienne *et al*. 2007b). In places, high-frequency ice-front advance and retreat cycles resulted in up to five erosion-based, vertically superimposed and laterally juxtaposed, glacial depositional sequences. They essentially comprise proglacial to interglacial successions with a range of fluvial, deltaic and shallow-marine deposits passing distally into turbiditic deposits (Ghienne 2003; Le Heron *et al.* 2006; Ghienne *et al.* 2007a). Each of the depositional sequences fill in palaeovalleys, glacial troughs or depressions, some of which representing former ice-stream pathways (Moreau *et al*. 2005; Ghienne *et al*. 2007b; Le Heron & Craig 2008). Glacial striations and mega-scale lineations, tunnel valleys and fluvioglacial palaeocurrents document together a relatively uniform pattern of palaeoflows at the scale of the glaciated platform.

Depositional setting

Channels described in this contribution fit in a late glacial evolution, subsequent to the Hirnantian glacial maximum (Ghienne *et al*. 2007a; Loi *et al.* 2010). They characterize the upper part of a 50-150 m thick succession, which onlaps a subglacial erosional palaeolandscape (Fig. 2). To the South, an ice-front margin and ice-contact environments are inferred from the occurrence of a glaciotectonic fold-and-thrust belt and tunnel channels indicating the connection with a subglacial drainage network (Fig. 2). Northward of this ice-proximal zone (50-75 km apart), and in stratigraphic connection with it, a sand-dominated, coarsening-upward sedimentary wedge is preserved. It involves a topset/ foreset/ bottomset architecture (Fig. 2). Topsets are

essentially made up of medium- to coarse-grained sandstones, and include the investigated channels evidenced by km-scale sandstone ribbons corresponding to inverted topographies (Fig. 3) ("Cordon" structures of Beuf *et al*. 1971; Hirst *et al*. 2002). In the southern proximal region, the topset succession is up to 60 m thick. It progressively thins and eventually pinches out downstream to the North (Fig. 2). Occasional bioturbation including *Arenicolites* occurs in some topset deposits. Climbing dune cross-stratification (CDCS), interpreted as the result of glacial outburst events, also characterize topset successions and their transition with upper foresets (Ghienne *et al*. 2010). Foresets are characterized by medium to coarse-grained erosion-based sandstone sheets, 2-12 m in thickness, which alternate with relatively thick (5-25 m) fine-grained intervals comprising silty shales to muddy fine-grained sandstones. Foresets have maximum dip angles of 5-10 m/km (*i.e.* <1°), and are typically 40-60 m in height. Bottomset deposits are made up of 2-10 m thick medium-grained rippled or structureless sandstone beds, alternating with thinner (0-10 m) argilaceous fine-grained intervals. Upper horizons in the topset succession are in places intensively disturbed, with folds and thrusts affecting an up to 15 m thick sandstone pile. Post-glacial erosional transgressive surfaces (wave, tide) and related bioturbated sandstones truncate the upper part of the topset succession.

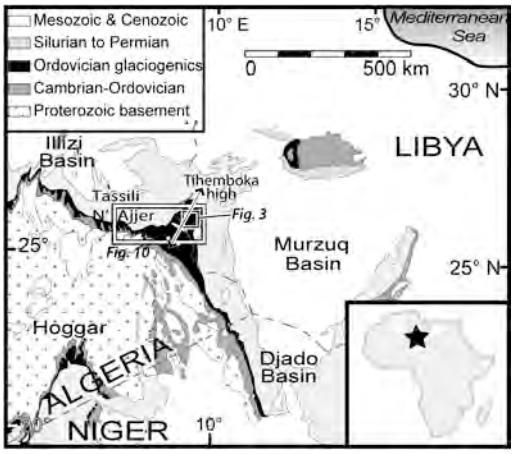

Fig. 1. Geological sketch map with location of the study area in western Libya (western Murzuq Basin) and eastern Algeria (Tassili N'Ajjer Plateau). The Tihemboka structural high separates the Murzuq and Illizi basins

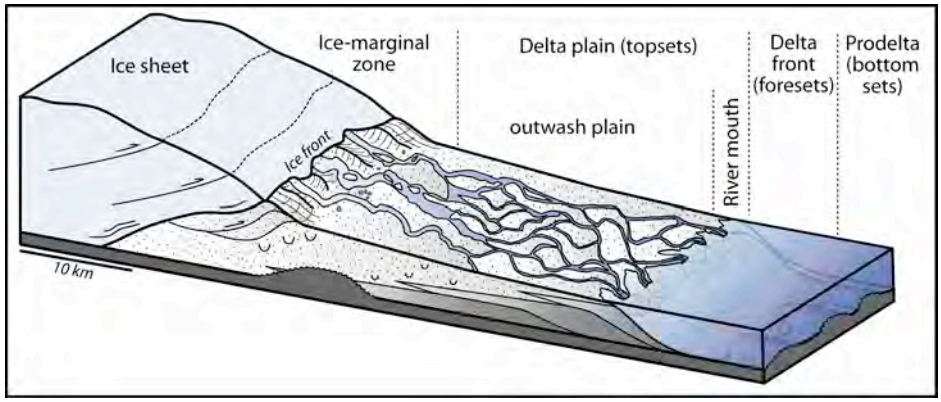

Fig. 2. Depositional setting of the channelized sandstone bodies. Channel networks develop in a topset succession between an ice-marginal zone to the south and river mouths to the north. The related sediment wedge onlaps a glacial surface including palaeotopographies

The sedimentary wedge is interpreted to reflect a fluviodeltaic progradation, which includes outwash plain/ delta-plain topsets, delta-front foresets and lobe-related bottomsets (Ghienne *et al*. 2010) (Fig. 2). The thick (40-60 m) topset succession to the south, pinching out to the north, allows a slope gradient of the palaeo-depositional surface to be estimated in the 0.5-2 m/km range. The shallow-marine coastal setting is indicated by bioturbation. The lack of any ice-rafted debris in fallout deposits indicates that no glaciomarine ice front occurred at the time of delta development, at least within the study area. Then, successions including channel bodies belong to an aggrading sandur-type proglacial fluvio-deltaic setting and were deposited between a continental ice-front to the south and a sea to the north. Ice-contact fluvioglacial depositional environments, aggradational topsets and related down-current delta development most probably relate to a period of ice-front advance (*e.g*., Maizels 1997; Marren 2002, 2005; Russell *et al*. 2005; Smith *et al*. 2006). As the succession onlaps onto the last basin-wide glacial surface and is overlain by post-glacial shallow-marine deposits, deposition is thought either to have occurred during an ice-front stillstand or short-lived re-advance (glacial surge?) within an overall ice-sheet recession period, or to be associated to the ultimate advance of the Hirnantian

ice sheet across the study area. In the latter case, the associated glacial surface would correspond to the poorly defined glaciotectonic deformation that is evidenced beneath transgressive surfaces and related deposits.

Methods

Channel bodies have been studied at the outcrop scale based on detailed sections and profiles in a restricted area (4x5 km) in southwest Libya (Fig. 3) (wadi Aramat, Tihemboka area), and at regional scale based on their spatial distribution as seen on satellite images extending from southeast Algeria to southwest Libya (Tassili N'Ajjer, 250x100 km). Internal architecture and facies successions in sandstone bodies were investigated along walls of wadi canyons up to 50 m in height cutting Late Ordovician channel bodies transversally to palaeoflow orientations (Figs 3, 4, 5, 6 & 7). Measured cross sections were logged at a scale of 1:100, noting grain size, bed thickness, bed contacts and geometry, sedimentary structures and palaeocurrent directions. Eight depositional Facies (F1 to F8, numbers increasing with grain size) have been described and interpreted (Table 1 & Fig. 8). High-resolution Spot, Alos and Google Earth™ satellite images were used to unravel external geometries and trends in orientation, and to map the distribution of about 300 channel bodies. In the case of channel bodies outcropping as inverted topographies, channel-body thicknesses were derived from the SRTM30 Digital Elevation Model incuded in the GoogleEarth™ software.

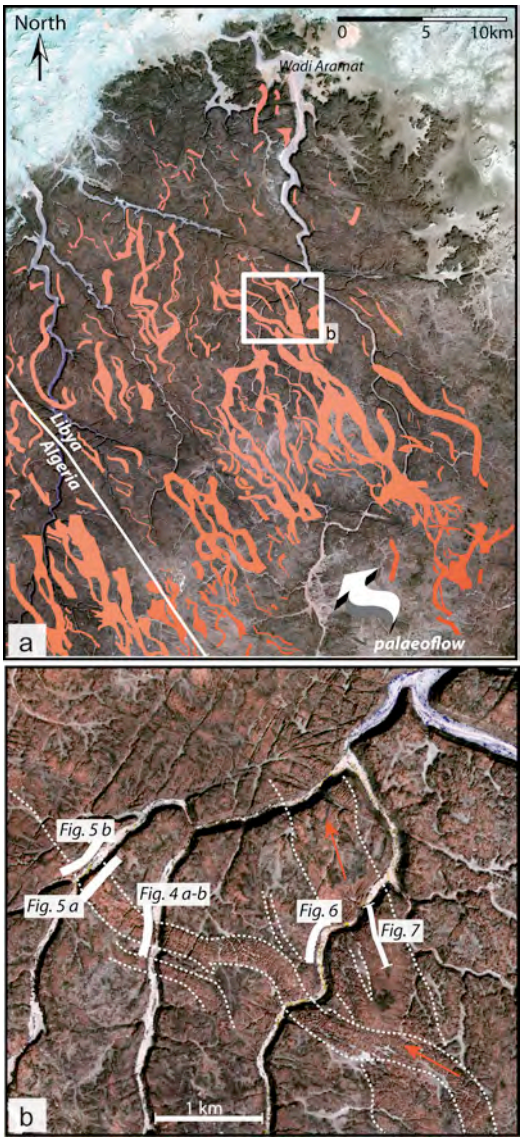

Fig. 3. (a) Mapping of channelized sandstone bodies forming sandstone ribbons ("Cordon" structures) in southwest Libya, Tihemboka area (Spot image, palaeoflow toward the NNW); (b) Detailed view in the Wadi Aramat area with location of studied outcrops and photomosaics

Outcrop-scale channel architecture

In the Wadi Aramat area, natural sections of large-scale channel bodies are provided by canyon downcuttings with kilometric spacing (Figs 3, 4, 5, 6 & 7). Small-scale individual channel bodies (Fig. 6) are in addition connected to the larger ones. Channel bodies are amalgamated with underlying more sheet-like sandstone bodies. Their superimposition results in 25-40 m thick compound sandstone bodies, those encompass deposits from three vertically superimposed units (from base to top: Lower, Transitional and Upper units). Though only the latter unit includes channelized sandstone bodies and is ascribed to fluvial depositional environments, the whole succession is described and interpreted in order to show the stratigraphic architecture of a prograding mouth-bar/ fluvial channel system in the topsets of a proglacial fluviodeltaic wedge.

Lower unit description (Figs 4, 5, 6 & 7)

The Lower unit basically includes very thick sandstone beds alternating with successions of thinner sandstone beds. The former are 4-10 m thick, several kilometres wide, tabular, medium-grained sandstone bodies, with a flat, erosional base showing uncommon flute casts but frequent large-scale load and flame structures. They can be prolonged basinward into the foreset succession and correspond to the erosion-based sandstone sheets of Ghienne *et al*. (2010). Thick sandstone beds are entirely laminated, including mainly crudely defined ripple lamination (F4) or horizontal to subhorizontal laminations (F3) grading upwards into two-dimensional CDCS (F5; Climbing-Dune Cross-Stratification, Ghienne *et al*. 2010). Vertical sheet-dewatering structures are usually present at bed tops.

Intervening successions include sharp-based, thin (0.3-1.5 m thick), medium-grained sandstone beds and some relatively rare <0.5 m finer grained interbeds. Lower bed contacts display dm-scale gutter casts and frequent load casts. Horizontally to subhorizontally laminated medium-grained sandstone (F3) predominates. Bed tops are associated with either ripple trains locally developing into stoss-depositional climbing ripples

Facies (units)	Lithology	Main sedimentary structures.	Bed or bedset thickness	Interpretation
F1 (Lu, Tu, Uu)	Siltstone to fine-grained sandstone	No structure, or faintly laminated.	5 cm-1m	Prevailing suspension fall-out deposits, some bedload deposition from low-density underflows.
F2 (Lu, Tu, Uu)	Fine-grained sandstone (well sorted)	Current-ripple lamination, stoss-depositional climbing-ripple cross-stratification, pebble lags, dm-scale load structures, 3D ripple bedforms on bed tops in Uu.	10 cm-1m	Traction deposition from decelerating and/ or expanding turbulent flows, with significant suspension fall-out in case of aggrading bedforms, lower-flow regime conditions.
F3 (Lu, Tu, Uu)	Fine to medium-grained sandstone (moderately sorted)	Horizontal lamination with partling lineations (Fig. 8b); occasionnally, small-scale subhorizontal to concave-up laminations in the lower part of sandstone beds (Fig. 8j). Load structures. Rare Arenicolites-type bioturbation in Tu (Fig. 8a) and sheet dewatering structures in Lu and Tu (Fig. 8f).	5 cm-2 m	Traction deposition from quasi-steady turbulent flow in upper-flow regime conditions. Occasional antidune deposits (Langford & Bracken 1987; Alexander et al. 2001), upper plane beds otherwise.
F4 (Lu, Tu)	Medium-grained sandstone (poorly sorted)	Crude ripple cross-stratification (1-2 cm deep scours, faint lamination throughout, occasionally superimposed on larger scale bedforms, Fig. 8c), vertical sheet dewatering structures (sheets are 10 to 50 cm in height, 0.3-5 cm in width).	1-7 m	Reworking by low-energy currents of sand-dominated plume fall-out, re-deposition as tractive bedload layers (quasi-steady lower-flow regime condition without sustained bedload transport). High rate of deposition. Water escape processes.
F5 (Lu, Tu, Uu)	Medium-grained sandstone (moderately sorted)	Two-, occasionnaly three-dimensional (Uu) climbing-dunes cross-stratification, stoss-depositional to vertically aggrading (CDCS, wavelength < 5m, Fig. 8h).	1-10 m	Turbulent deposition from sustained decelerating and/ or expanding turbulent flows, with high sand-sized suspension-load concentration (Ghienne et al. 2010), lower-flow regime conditions.
F6 (Tu)	Medium-grained sandstone (moderately sorted)	Vertically aggrading, low relief, symmetrical and undulated lamination, episodic crestal jumps (wavelenght < 1m, Fig. 8e).	5 cm-1m	Traction deposition from quasi-steady turbulent flows in upper-flow regime conditions (stationary antidunes in underflows, Spinewine et al. 2009).
F7 (Uu)	Medium to coarse-grained sandstone (poorly sorted)	Horizontal to subhorizontal , thick (5-15 cm) laminations, representing large-scale undulated bedforms (up to 40 m in wavelenght, 0.5-2 m in height, Fig. 8g & i).	1-10m	Traction deposition from turbulent flows in upper-flow regime conditions and high sand-sized suspension load, at the transition from upper-plane beds to migrating and/or stationary antidunes (Fielding 2006; Duller et al. 2008).
F8 (Tu, Uu)	Intraformational conglomerates with a medium- to very coarse-grained sandstone matrix	Sandstone and siltstone clasts, massive or crude cross-stratification in places, dm- to m-scale gutter casts and load structures (Fig. 8d).	1 cm-1m	Bypass and cut-and-fill processes by turbulent flows, with prevailing upper-flow regime conditions.

Table 1 - *Lithofacies classification; Lu, Tu & Uu = Lower, Transitional & Upper units*

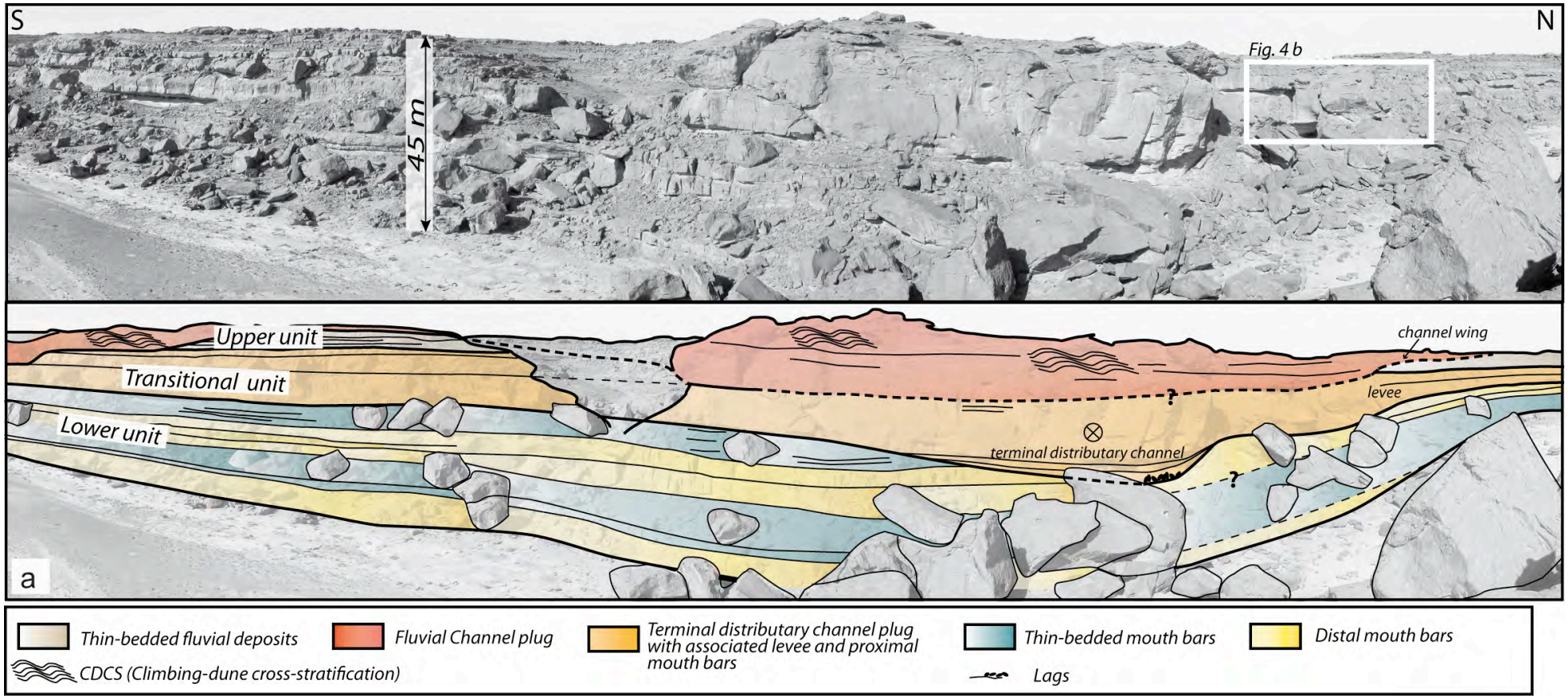
S
N
45 m
Fig. 4 b
Upper unit
Transitional unit
Lower unit
channel wing
levee
terminal distributary channel
?
?
a
Thin-bedded fluvial deposits
Fluvial Channel plug
Terminal distributary channel plug with associated levee and proximal mouth bars
Thin-bedded mouth bars
Distal mouth bars
CDCS (Climbing-dune cross-stratification)
Lags

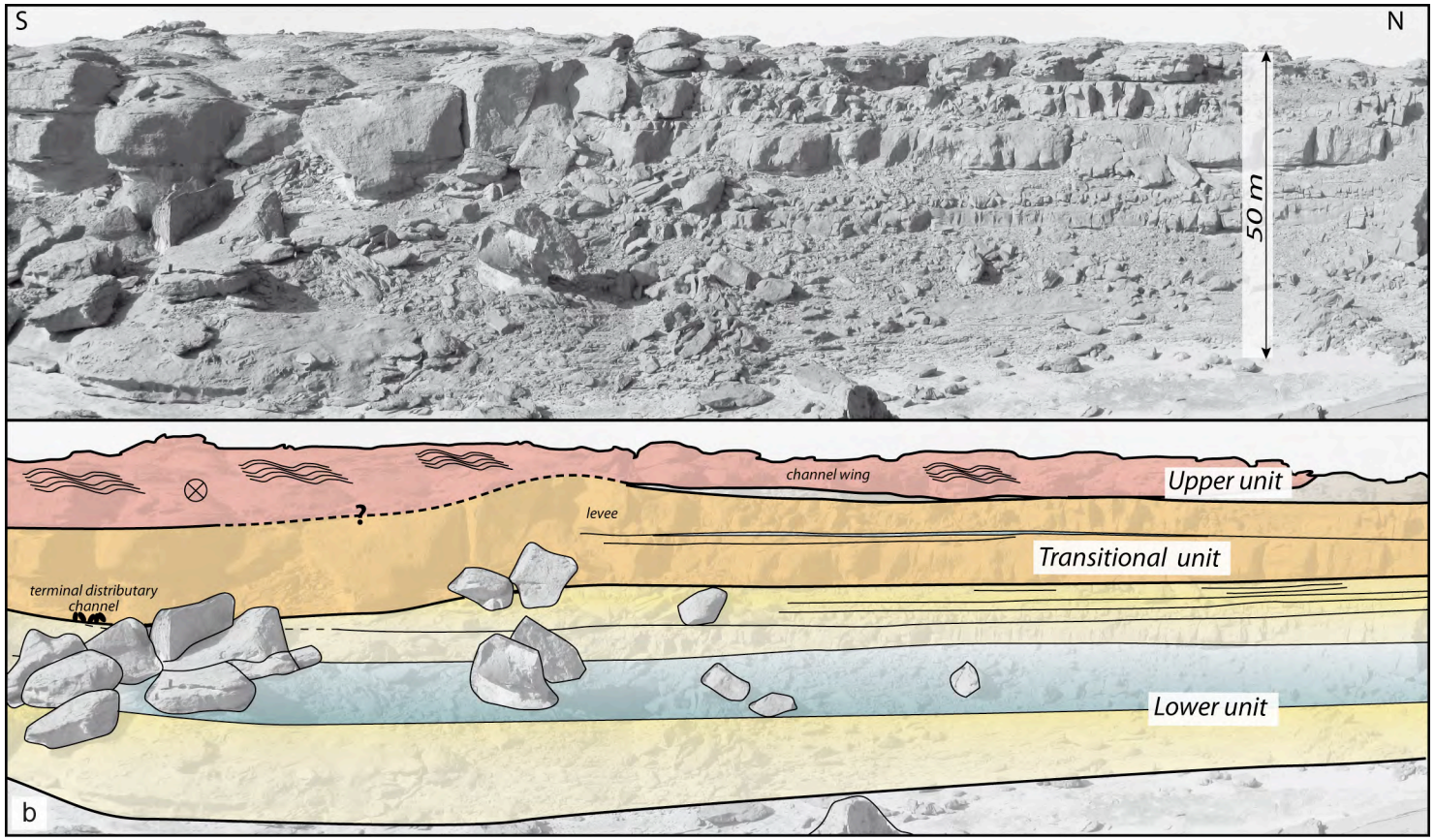

Fig. 4. Photomosaics showing relationships between architectures (line drawings) and related depositional environments (colour ranges) in the Lower, Transitional and Upper units (see Fig. 3 for location); (b) is a detail of (a), showing the levee architecture associated with the Transitional unit

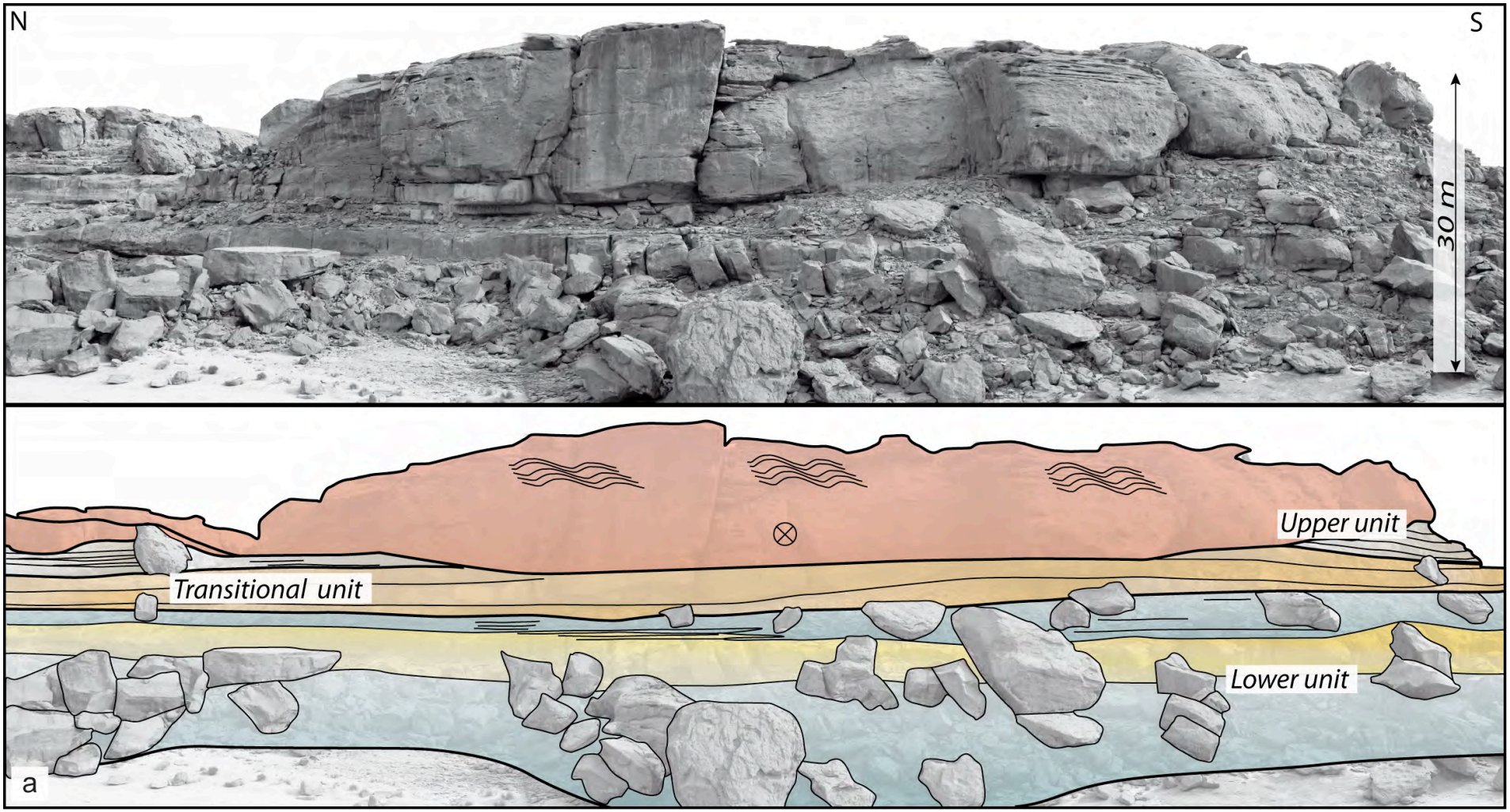
N
S
30 m
Upper unit
Transitional unit
Lower unit
a

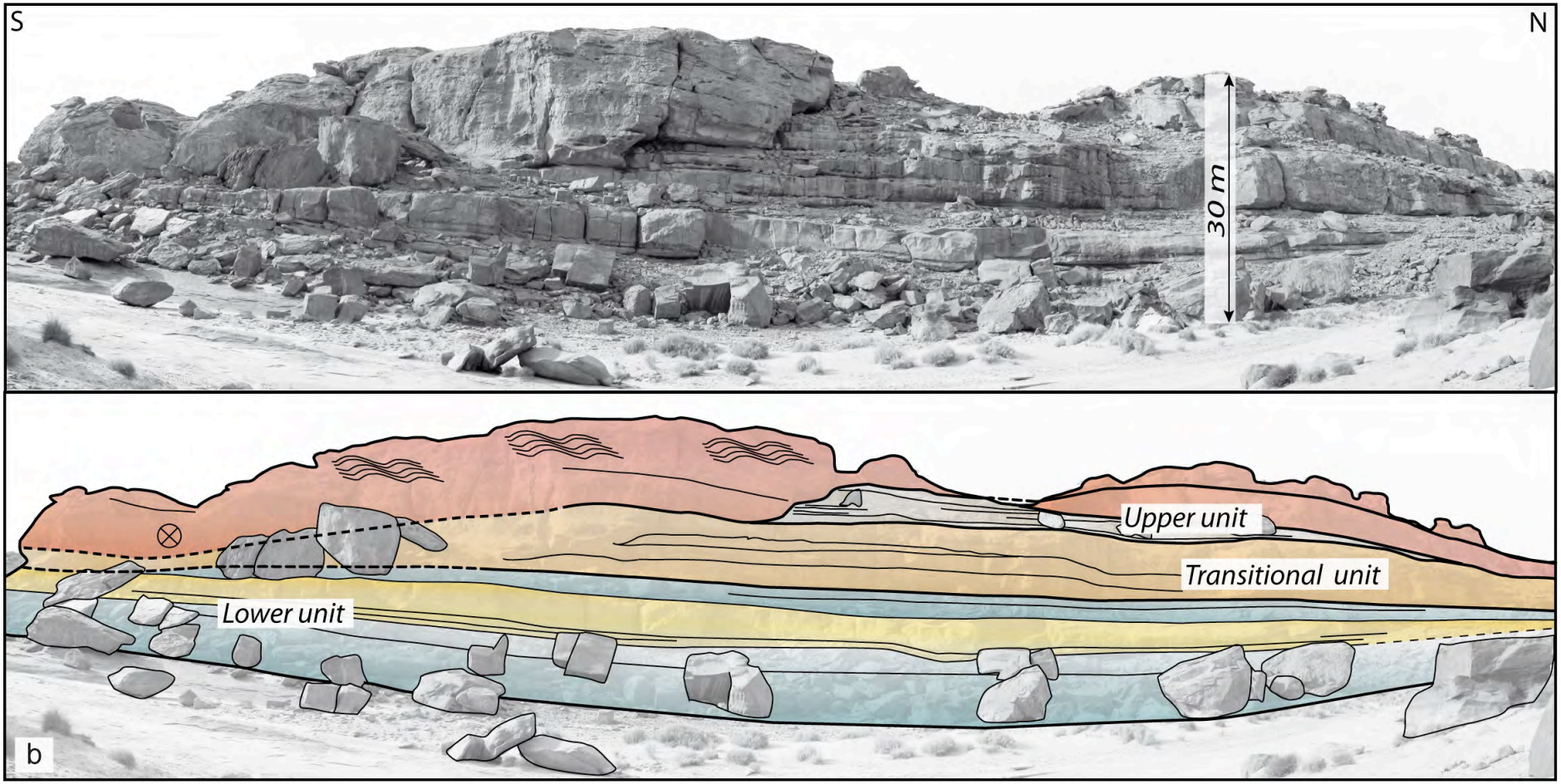

Fig. 5. Photomosaics showing relationships between architectures (line drawings) and related depositional environments (colour ranges) in the Lower, Transitional and Upper units within the same compound sandstone bodies as in Fig. 4, but 1 km further downstream. (a) and (b) illustrate the same structure as seen on the opposite sides of the wadi (see Fig. 3)

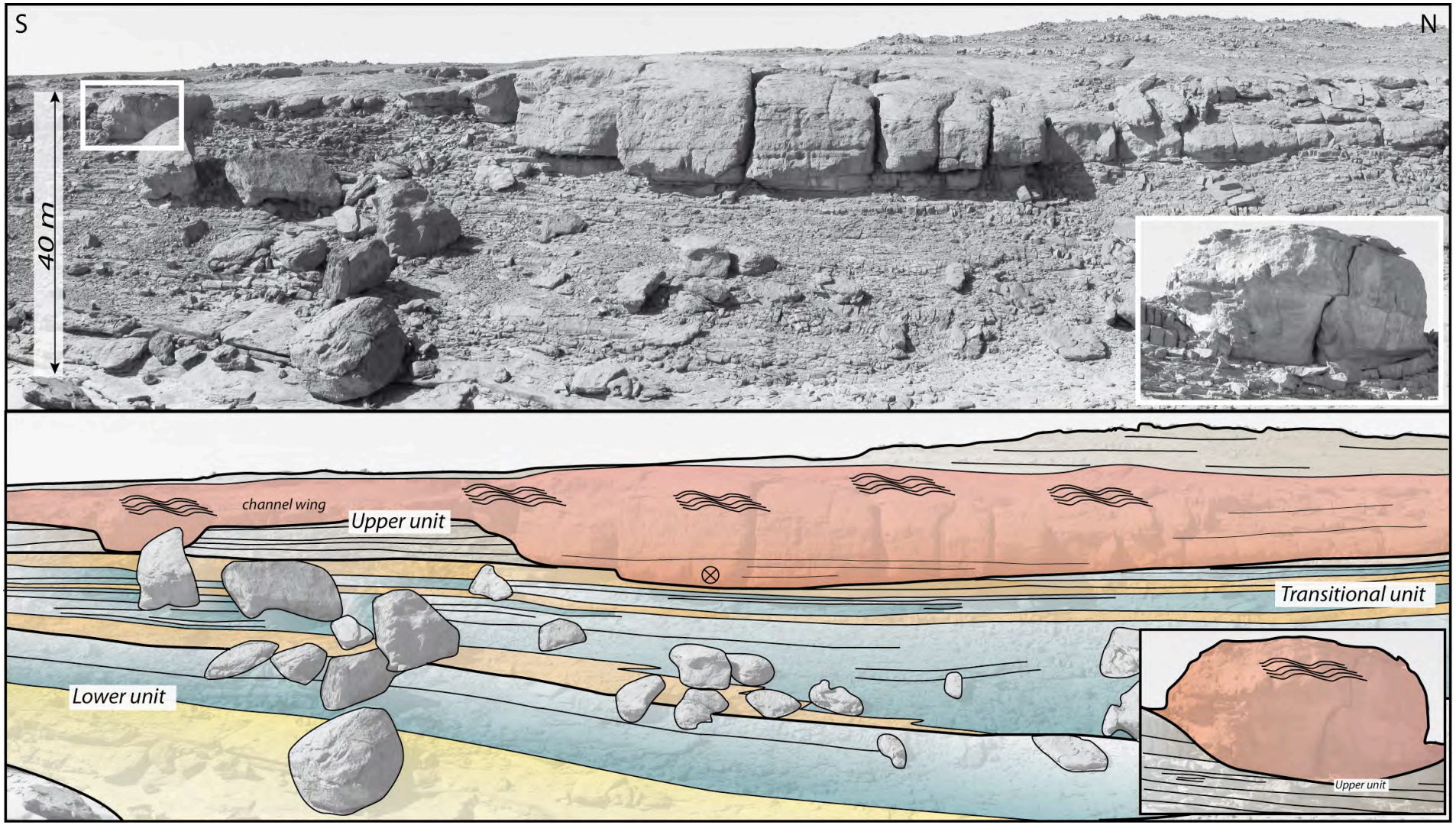

Fig. 6. Photomosaics showing relationships between architectures (line drawings) and related depositional environments (colour ranges) in the Lower, Transitional and Upper units within another compound sandstone body (see Fig. 3 for outcrop location sections and Fig. 4a for colour ranges). Inset: detail of an adjacent small-scale channelized sandstone body

assemblages (F2) or lags of small (< 5 cm) rip-up clasts. Sandstone beds are usually stacked but interbeds of very fine-grained sandstones to siltstones (F1) are present in places, suggesting occasional fining-upward trends at bed/interbed scale. Vertical sheet-dewatering structures are ubiquitous (Fig. 8f). In some rare places, tracks and vertical U-shape burrows can be found, some of which of the type *Arenicolites* (Fig. 8 a).

Transitional unit description

The Transitional unit typically consists in several metres thick, tabular, erosion-based medium-grained sandstone bodies. Vertical stacking forms a distinctive set of 2 to 4, but more generally 3, amalgamated bodies (Fig. 7). They together constitute a 5-15 m thick sandstone sheet that has a several kilometres lateral extent (Figs 4, 5 & 6). The latter interdigitates laterally with thinner bedded successions comparable to those of the Lower unit (Fig. 6). Regarding the lowest tabular sandstone body, a basal, poorly differentiated shallow scour may exist, with 1-5 m incision depths and up to 100 m in width. The scour is preferentially positioned in the axis of overlying channelized sandstone bodies of the Upper unit (Figs 4a & b) and is generally associated with metre to several metre-wide gutter casts, uncommon flute casts and lags of 1-10 cm long rip-up clasts and/ or intraformational conglomerate lenses (F8) (Fig. 8d). At the lower bounding surface of the Transitional unit, scouring results in places in the amalgamation of the tabular sandstone bodies with the underlying erosion-based sandstone sheets of the Lower unit. At its upper bounding surface, and approaching the axis of an overlying channelized sandstone body, thick, tabular bodies of the Transitional unit locally thicken, resulting in convex-up geometries and clinoform-like structures in views transverse to palaeoflows (Figs 4a & b).

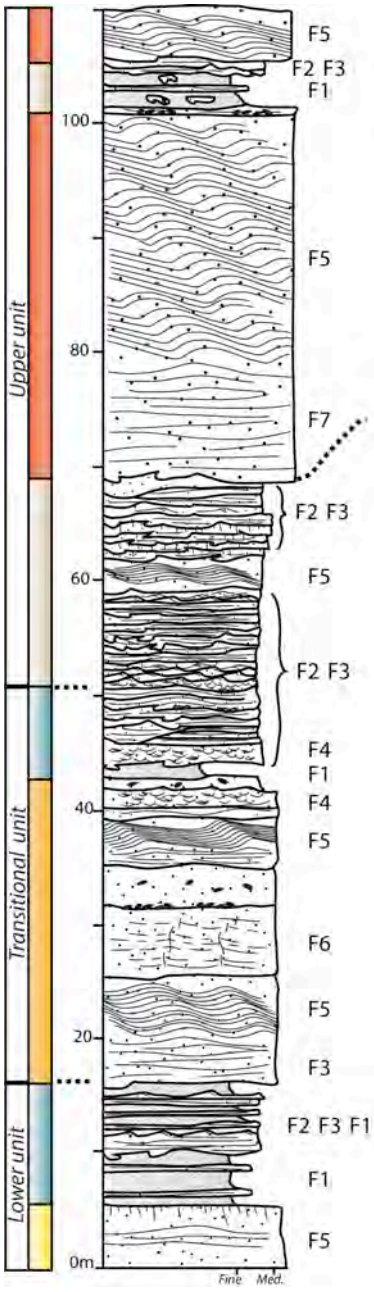

Facies associations are similar to those of the Lower unit, especially regarding thin-bedded successions. Thick tabular sandstone bodies of the Transitional unit may however differ with less represented two-dimensional CDCS (F5) and the occurrence of a distinct climbing cross-stratification that involve undulated, low-relief almost symmetric bedforms (F6, Fig. 8e). Away from shallow scours, amalgamation of the thick sandstone bodies may decrease with intervening stoss-depositional climbing ripple assemblages (F2) and rare fine-grained intervals (F1) preserved in interbeds. Both thick and thin sandstone beds show vertical sheet-dewatering structures.

Fig. 7. Sedimentary log illustrating depositional pattern in the Lower, Transitional and Upper units (see Fig. 3 for location and Fig. 4a for colour ranges). Facies code are given in Table 1

Upper unit description

The Upper unit comprises channelized bodies corresponding to sandstone ribbons at outcrop, either large-scale (Figs 4, 5 & 6) or small-scale features (Fig. 6), and inter-channel thin-bedded deposits. Its lower contact is conformable where thin-bedded deposits are present in the lower part of the unit, but erosional truncations with locally steep margins (up to 30°) may occur in the axis of some large-scale channel bodies. Large-scale channel bodies form a package of amalgamated sandstones while inter-channel thin-bedded deposits correspond to well-stratified successions. The latter comprises tabular, 0.5-2 m thick, erosion-based sandstone beds including mainly horizontal lamination (F3) associated with ripple cross-stratification (F2; Fig. 8b). Lags of small (< 5 cm) rip-up clasts on top of the beds are frequent (Fig. 7). In contrast with similar depositional facies from the underlying units, they are virtually devoid of any dewatering features.

A poor bedset differentiation characterizes sandstones of large-scale channel bodies. Deposits at the channel axis correspond to a finning-upward sandstone suite. At the base, it comprises several metre thick bedsets with large (> 10 m) bedform wavelengths resulting in poorly defined undulated to low-angle laminations (F7) (Fig. 8g & i). In its upper part, 2D and 3D CDCS (F5) predominates (Fig. 8h). The width of the large-scale channel body is typically in the 100-300 m range. The contacts between inter-channel deposits and large-scale

channel bodies are essentially erosional. Channel-body wings, also characterized by CDCS deposition, overstep inter-channel deposits and may in places connect with small-scale, less than 30 m wide, laterally adjacent channel bodies. The basal scour of the latter, 2-10 m in depth, is either slightly concave-up or have more incised gutter-type geometries in association with intraformational conglomerates (F8). Both large-scale and small-scale channel bodies are sealed by well-stratified thin-bedded sandstone successions. As they include other subsequent channel bodies, they are similarly ascribed to inter-channel successions. Satellite images of the study area reveal that up to 3 generations of channel bodies with intervening inter-channel successions are locally superimposed (Fig. 3).

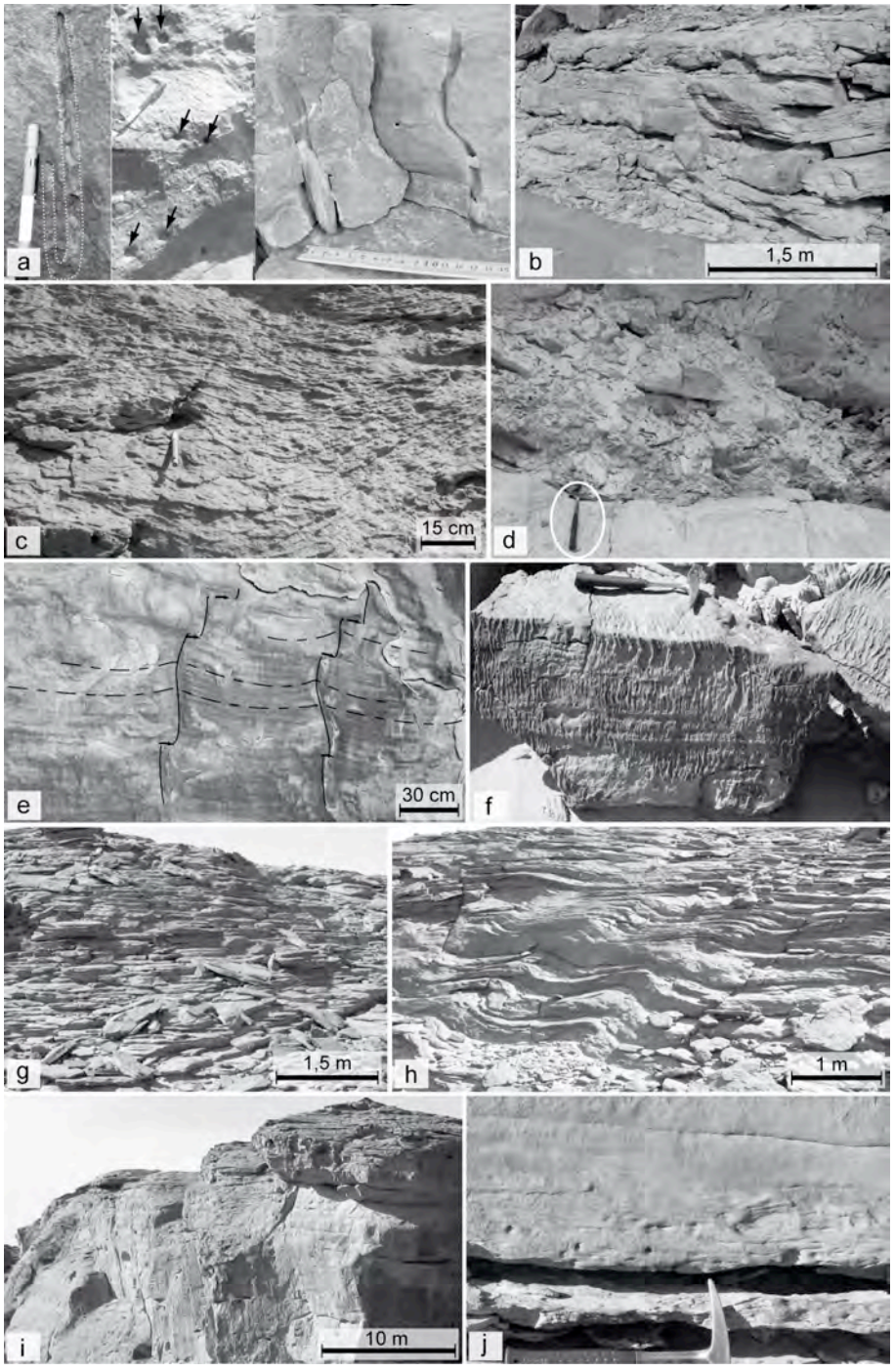

Fig. 8. Depositional Facies from the Wadi Aramat area (Tihemboka High, western Libya); (a) Pairs of vertical or U-shaped, *Arenicolites*-type burrows in thin-bedded mouth bars (F3, Lower Unit); (b) Thin-bedded sandstone with prevailing F3 facies in the Upper unit (inter-channel area); (c) Crude ripple cross-stratification in proximal mouth bars (F4, Transitional unit); (d) Intraformational conglomerates in the basal part of terminal distributary channel (F8, Transitional unit); (e) Vertically aggrading, low relief, symmetrical and undulated lamination (dotted lines), with episodic crestal jumps (arrows), interpreted as climbing stationary antidunes in proximal mouth bars (F6, Transitional unit); (f) Vertical sheet-dewatering structures in thin-bedded mouth bars (F3, Lower unit); (g) Horizontal to subhorizontal, thick laminations, representing large-scale undulated bedforms in lower part of channel plug (F7, Upper unit); (h) Two-dimensional, stoss-depositional to vertically aggrading, climbing-dune cross-stratification (CDCS), in the upper part of a large-scale channelized sandstone body (F5, Upper unit); (i) General view of horizontal to subhorizontal, laminations representing large-scale undulated bedforms (F7, Upper unit); (j) Small-scale subhorizontal to concave-up laminations interpreted as antidune deposits in proximal mouth-bar deposits (F3, Transitional unit)

Compound sandstone bodies

Successive amalgamation of sheet-like sandstone bodies (Lower and Transitional units) and channelized sandstone bodies (Upper unit) results in compound sandstone bodies that do not correspond to stratigraphic units but favours the preservation of channelized sandstone bodies as inverted topographies (Fig. 3). Boundaries with laterally adjacent deposits are either erosional or diffuse (Fig. 5a & b). In the former case, they correspond to a

true stratigraphic surface even if polyphased, while in the latter case, they look like erosional margins but are in fact of diagenetic origin or correspond to fractures. For instance, sandstone beds constituting the sheet-like Transitional unit go beyond the looking like channel margin and amalgamate with sandstones constituting the sandstone bodies, and in particular those of the channelized sandstone body (Figs 4, 5, 6 & 7). If the ribbon geometry essentially reflects the plan-view shape of the channelized sandstone bodies of the Upper unit, the compound sandstone body cross-section incorporates a thicker sediment pile partly crosscutting stratigraphic architectures (Fig. 9).

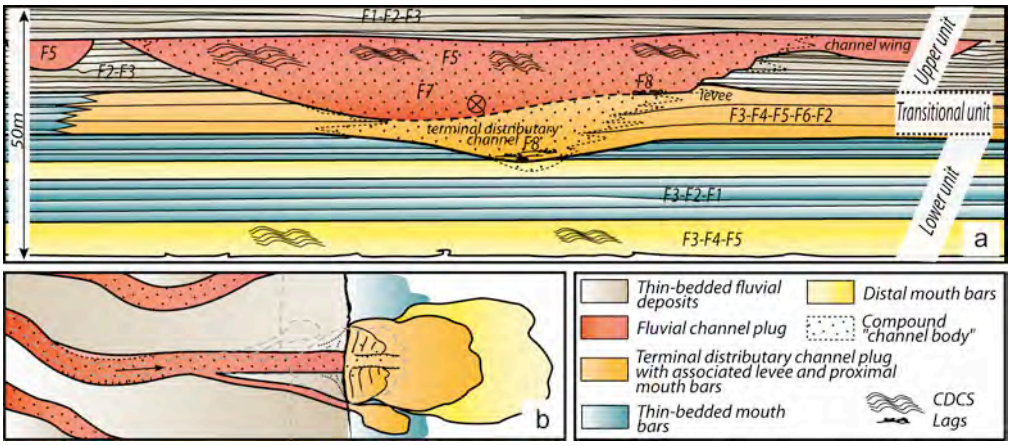

Fig. 9. Synthetic architectural (a) and depositional (b) models illustrating the location of channelized sandstone bodies at the top of a prograding mouth-bar system built from river jet effluxes. Facies codes are given in Table 1. Channelized sandstone bodies represent plugs of fluvioglacial channels passing downstream in subaqueous terminal distributary channels

Interpretation

In the context of a prograding deltaic wedge, compound sandstone bodies that result from the vertical stacking of sheet-like units with channelized bodies in their upper part, are related to aggrado-prograding mouth-bar/ channel systems (Figs. 4, 5, 6, 7, & 9). The above-described units reflect successive stages through time and space of the development of river mouths during delta advance. The *Arenicolites*-type burrows testifying shallow-marine environments are associated with the Transitional unit, in good agreement with other occurrence of this bioturbation in restricted-marine environments such as mouth bars, tidal flats or bay-head deltas (Droser *et al*. 1994; Buatois *et al*. 2002; Gerard & Bromley 2008). We tentatively situate the subaerial/ subaqueous boundary at the stratigraphic contact between the transitional essentially sheet-like unit and the Upper unit that include channelized bodies. This position coincides with infrequent argillaceous interbeds upwards and with the disappearance of vertical sheet dewatering structures in the sedimentary record.

Geometries and facies in the Lower unit indicate unconfined sand-dominated deposition from turbulent flows with both lower (F2, F4, F5) and upper (F3, F6) flow regime conditions. In particular climbing-dune cross-stratification (CDCS) reflects high sand-sized suspension-load concentration (Ghienne *et al*. 2010). At the scale of a thick sandstone bed, the basal erosion surface and the fining- and waning-upward trends are interpreted as reflecting expanding turbulent jets in front of terminal distributary channel mouths (Fig. 9b) (Sutter 1994; Edmonds & Slingerland 2007; Schomacker *et al*. 2010) and rapid sedimentation in distal mouth bar environments of a shallow water delta during the falling stage of a single short-duration high-energy discharge event (Mellere *et al*. 2002; Mutti *et al*. 2003; Fielding *et al*. 2005). The downstream connection with the "erosion-based sandstone sheet" case study of Ghienne *et al*. (2010), and occurrences of CDCS demonstrate a flood dynamics involving highly concentrated sediment-laden flows. High depositional rates are in agreement with ubiquitous post-depositional water escape structures (Lowe 1975). Thinner beds in intervening successions reflect similar but minor flood events deposited under waning turbulent flows. They are interpreted as thin-bedded mouth bars.

As well, the sheet-like architecture of the Transitional unit reflects essentially unconfined sediment-laden flows even if confined flows were in places associated with basal scours. Basal erosion and intraformational conglomerates (F8) indicates bypass processes in a channelized area interpreted as a subaqueous terminal distributary channel (Plink-Björklund *et al.* 2001; Mellere *et al*. 2002; Olariu & Bhattacharya 2006) scoured by turbulent jet flow (Hoyal *et al*. 2003) (Figs 4 & 9). The clinoform-like

geometries of sandstone bodies near channel axis are interpreted as related to subaqueous levee architecture that grade laterally and distally into proximal mouth bars (Figs 4 & 9) deposited as a result of the expanding jet flow (Fielding *et al*. 2005; Edmonds & Slingerland 2007; Schomacker *et al*. 2010). The whole depositional dynamic is fundamentally similar to that prevailing in the Lower unit but a more proximal location resulted in complete amalgamation of flood-related mouth-bar deposits in the form of vertically stacked, thick, tabular beds. Aggrading antidunes (F6) reflect shallower environments but still characterized by a high sand-sized suspension-load concentration related to high-magnitude floods. Laterally, thinner-bedded mouth-bar successions reflect lateral deceleration of expanding flows and/ or similar but minor flood events deposited under waning turbulent flows.

In the Upper unit, well stratified thin-bedded fluvial deposits are dominated by upper stage plane beds, with occasional ripples, lags of small rip-up clast, basal gutter casts, load structures (F3 and F2), all features that have strong similarities with successions interpreted as deposited by ephemeral sheet-flood braided streams (Tunbridge 1981; Olsen 1989; Delucca & Eriksson 1989; Dam & Andreasen 1990; Neef *et al.* 1996; Brierley 1996). If the latter usually characterize arid environments, ablation-related floods in proglacial braidplain settings also result in ephemeral sheet flows (Maizels 2002; Carriwick & Russell 2007; Gomez *et al*. 2000). The channel bodies, both of the large- and small-scale types, are devoid of accretion surfaces and are interpreted as sandy channel plugs. Infilling facies typically comprise a waning-flow sequences with from base to top: scour-related surface, ubiquitous upper flow regime condition in the lower part (F7) and lower flow regime conditions but with high-concentration sand-sized suspended load in the upper part (F5). Ubiquitous CDCS in the upper part of channel plugs attest their relationships with high-magnitude glacial floods (Ghienne *et al.* 2010). Channel plugs encompassing an axial scour infill and adjacent wings suggest a flood-related channel widening and subsequent net aggradation of the depositional surface after the outburst event. Finally the whole depositional system is considered as an outwash braidplain, which recorded two distinct and alternating depositional regimes: 'normal' sedimentation upon sandy braidplain driven by ablation-related floods and outburst events resulting in channel plugging. Both the regimes are also recorded downstream in mouth-bar environments (see above). The lack of argilaceous deposits is inherent both to their poor preservation potential in pre-vegetation braided systems (Davies & Gibling 2010) and to the Late Ordovician sand-dominated system (Ghienne *et al*. 2010). Poor development of cross-stratified facies indicates that the background sedimentary record was dominated by ephemeral ablation-related processes rather than by deposits typifying perennial sand-dominated rivers (e.g. Cant & Walker 1975, 1978; Miall, 1996).

Regional-scale channel distribution

Channels in map view

Channel body distribution based on satellite images give an outstanding impression of the proglacial delta plain organisation (Fig. 10). The area under examination consists in a 50 km wide, 250 km long stripe in the Tassili N'Ajjer across the Algeria/ Libya boundary. It comprises more than 340 sinuous to straight sandstone ribbons, termed "Cordons" by Beuf *et al*. (1971), which most often correspond to up to 10 km long channel bodies similar to those studied in the Upper unit of the Wadi Aramat exposures. The longer bodies can be continuously track on up to 16 km lengths. Both the large- and small-scale types are recognized (Fig. 11). Within the topset succession, the present-day erosional surface intersects strata almost randomly and the map therefore does not represent an actual distribution of time-equivalent channels. For example, only few channels are mapped in area where the present-day surface mostly intersects late- to post-glacial shallow-marine deposits. Alternatively, in other places, channels are over-represented relative to inter-channel areas owing to the outcropping mode with preferential preservation of channel bodies as inverted topographies. In addition, detection of channel bodies varies with the type of satellite images. In the Tihemboka High area for which a high-quality Spot image was available (2.5 m of spatial resolution), it results in a denser distribution of sandstone ribbons. Nevertheless the channel body distribution faithfully reflects the proglacial palaeo-channel networks and statistics can be performed.

Channel-body orientations have been analysed in two distinct areas with very similar patterns (Fig. 10) allowing data to be mixed together (Fig. 12a). Orientations of channel bodies, longer than 0.5 km, range from 286°N to 28°N, with a mean at 294°N. Two thirds of the channel bodies are oriented toward the north-northwest (320-360°N). No variation is apparent when comparing proximal (southern) and distal (northern) contexts. However, in the western part of the mapped area (Fig. 10), a distinct set of wider channel bodies is pointed out, which we suspect to belong to another glacial sequence. Channel bodies then appear basically parallel to each others, corresponding to linear drainage networks throughout the area. In addition, a number of channel

bifurcations have been mapped. A confluence may arise at the km-scale, which mimics braid-bar morphologies. Some of the large-scale channel bodies have neither confluence nor bifurcation along of their entire exposed length. Channel bodies are straight with sinuosity (length of channel thalweg/ length of segment) less than 1.05 or faintly sinuous (1.1-1.5), and rare sinuous examples (1.2-1.35) are recognised (e.g. Fig. 11).

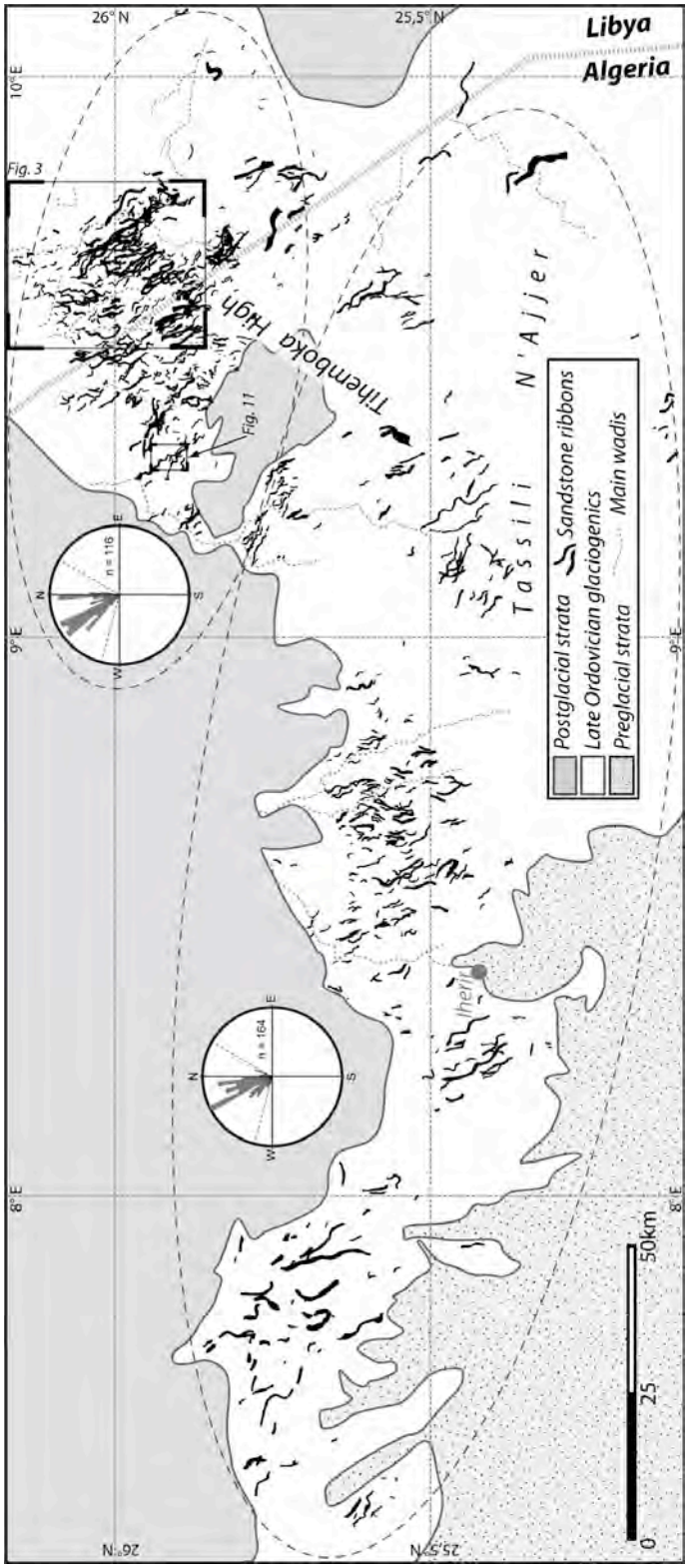

Fig. 10. Distribution of the channelized sandstone bodies ("Cordon" structures) throughout the Tassili N'Ajjer Plateau. Ranges of channel-body orientations of ribbons longer than 0.5 km are given for two distinct areas (envelope with dotted lines)

Channel body architecture

Channel body widths (340 samples) and thicknesses (available for 224 bodies) have been systematically estimated based on measurements of residual inverted topographies. Sandstone ribbons have basically consistent width and sharp boundaries. However, in rare places on high-resolution satellite images (Fig. 11), a more intricate organisation is revealed. Indeed, large-scale channel bodies comprise a sinuous, narrow and uninterrupted main ribbon twisting in between almond-shape to crescentic bodies occupying concave bends. In addition, scroll bars (lateral accretion) have been suspected but correspond only to subordinate features. Therefore, on low-resolution images or on degraded exposures where the internal architecture is not highlighted, measured widths of sandstone ribbons may correspond either to that of the narrow central ribbon or to that of a larger scale ribbon amalgamating the narrow ribbon and adjacent bodies (inset of Fig. 11). Sandstone ribbon widths vary in the 40-630 m range, two thirds of them being in the 60-160 m range (Fig. 12b). The Width/Frequency bar chart illustrates a roughly unimodal distribution that shows a peak at channel width of 100 m and a median at ca. 125 m (Fig. 12c). Measured thicknesses (224 measurements) correspond to minimum values, as thalweg incision depths are unknown. The channel bodies are 3 to 30 m thick in good agreement with field studies (see above, and Beuf *et al*. 1971). The Width/Thickness Frequency bar chart (Fig. 12d) indicates W/T ratios in the 5-42 range, half of the W/T being in the 10-17 ranges. A polymodal distribution might be proposed, but significance of distinct groups (e.g. 10-14, 15-20 and 22-27?) has not been elucidated.

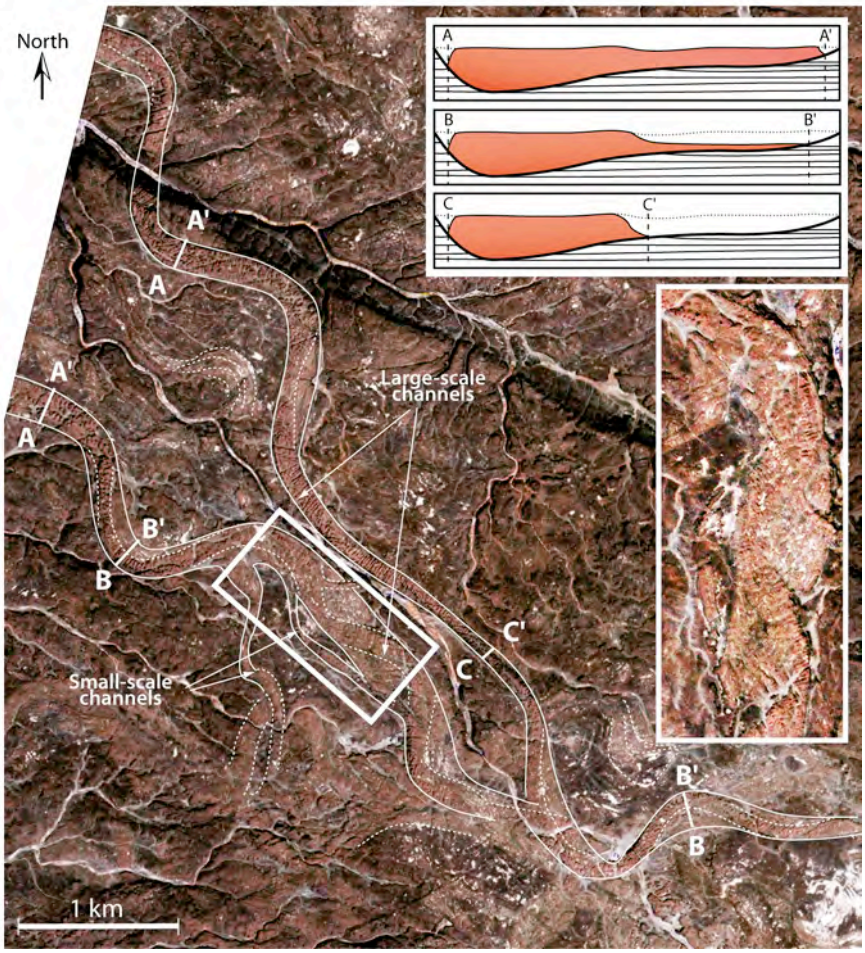

Fig. 11. Details of channelized sandstone bodies in the Algerian part of the Tihemboka High (Spot image), with a zoom (white rectangle) on a particular segment of an anastomosed sinuous channel. Internal geometries and different orders of channels are identifiable. The width of a sandstone ribbon depends on preservation: bankfull (A-A'), intermediate (B-B') and low-stage (C-C') cross-sections are evidenced

Interpretation

To interpret the figure 10 is not straightforward. For instance, in the context of a progradation, and assuming an ice front more or less stabilised to the south (see the Geological Setting section), it is unclear whether the picture is essentially representative of the entire 50 km long, last channel networks extending from a proglacial zone to the south to river mouths to the north, or of the juxtaposition of diachronous final segments of a prograding river-mouth system progressively shifted basinward through time. Another limitation arises considering channel body bifurcations. The latter may represent either channel diffluences within a distributary system (Olariu & Batthacharya 2006; North & Warwick 2007), bifurcations of braided channels (Rust 1978; Bristow & Best 1993; Ashworth *et al*. 2000), or channel avulsions and/or independent division and junction within an anastomosing network (Nanson & Knighton, 1996; Bristow 1996; Makaske 2001; Twidale 2004). Only bifurcations of small-scale channel bodies from larger-scale bodies can be definitely ascribed to true channel diffluences. Anyway, channel-body bifurcations do not represent a fundamental feature of the studied channel-body networks. More significant elements are (i) parallel channel bodies, with an averaged orientation that matches other regional-scale glacial and fluvial palaeoflow trends (Beuf et al., 1971; Ghienne *et al*. 2007a), (ii) almost constant width along an individual body and (iii) low sinuosities. Constant widths indicate that channel bodies generally do not include features related to lateral channel migration and constitute plug infills in agreement with the interpretations based on outcrop sections. Scroll bars remain subordinate geometries and true meandering system are absent (satellite image, cross-section) although they are recognizable in other glacial sequences (e.g. Rubino *et al*. 2003). It suggests that sinuous channel bodies from the Tassili N'Ajjer do not correspond to meandering channel plugs. However, geometries of large-scale channel bodies in detailed plane view attest in places that the differentiation of channels and of alternate bar-type sand-bodies can occur (Fig. 11). We however suggest that they correspond to the plugs of respectively low-stage and bankfull channel cross-profiles, with variable preservation conditions (insets in Fig. 11). A former bar geometry is inferred in underlying deposits, which should have existed before the channel plugging phase. Considering the size of the channels bodies typically in the 60-600 m range (low-stage and bankfull sections undifferentiated), and genetic links between large- and small-scale bodies, they are thus best interpreted as plugs of braided channels with interlaced anastomosed sinuous channels.

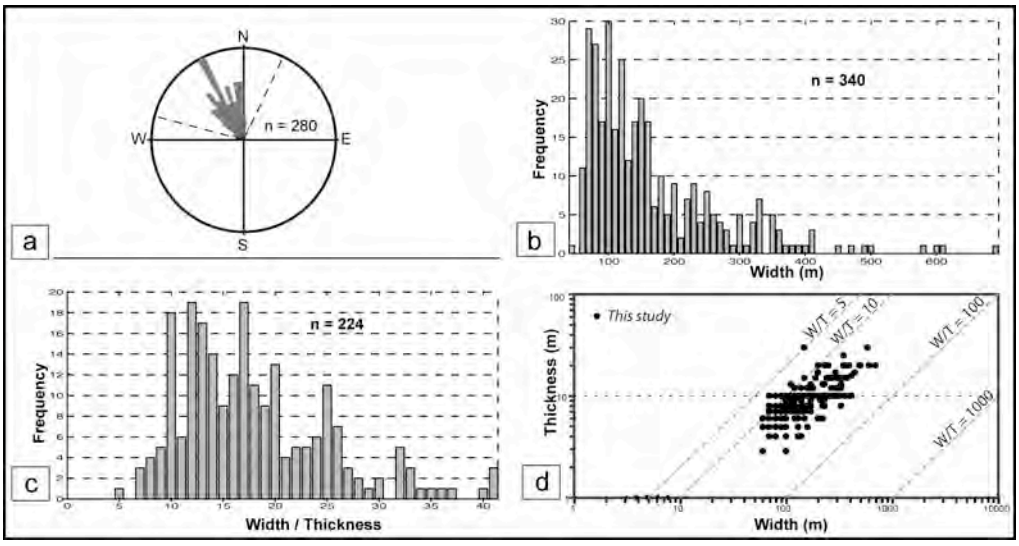

Fig. 12. Orientation trend (a) and widths (b) of channelized sandstone bodies (undifferentiated bankfull and low-stage cross-sections). (c) Frequency plot of the Width to Thickness ratio for ribbons mapped in Fig. 10; Width vs. thickness plot for 224 ribbons, with a W/T mean value of 16.5

Channels transferred meltwater and sediments from the ice-marginal zone to the river mouths, along a less than 50 km long proglacial plain. In a particular zone (e.g. the Tihemboka High, Fig. 10), no lateral differentiation or hierarchy is apparent indicating a line source of sediment input points in front of the ice sheet. If trunk channels existed upstream, as suggested by the occurrence of deeply incised channels in relation with the proglacial zone (Ghienne *et al*. 2010), they should have been numerous and quite uniformly distributed through time and space (Russell *et al*. 2005). Nearby sediment input points did not allowed individual fan to grow up but instead favoured the development of many proglacial, adjacent and parallel elongated fans, the juxtaposition of which lead to a virtually planar and unconfined outwash plain (Fig. 13). Such a uniform distributary network also implies a line source at river mouths, which characterizes proglacial delta setting (Nemec & Steel 1988; Orton & Reading 1993). This is supported by the absence of clear distributary patterns within the preserved channel networks even though some of them represent features close to the river mouth as indicated by the stratigraphic architecture of the succession within which they are encased.

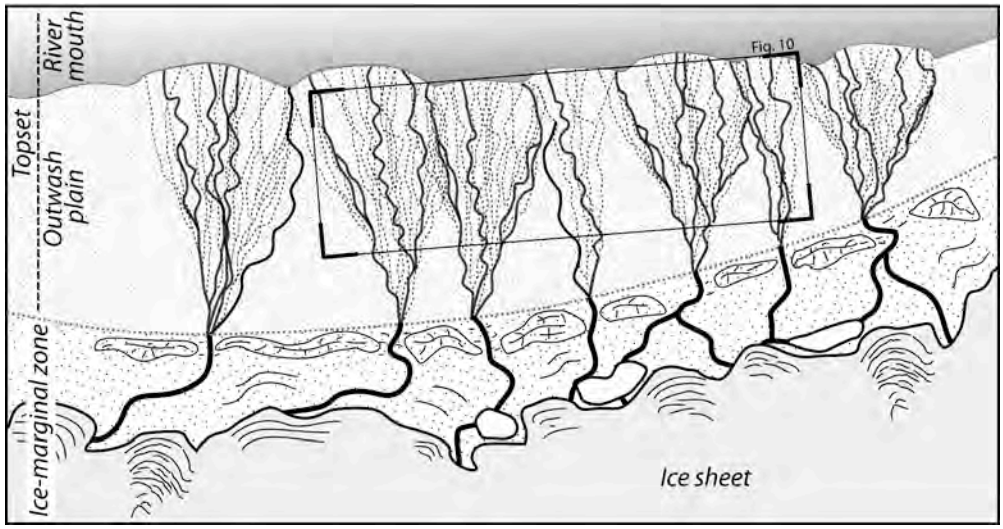

Fig. 13. Reconstructed map view of the studied Late Ordovician proglacial outwash braidplain that consists in unconfined fluvioglacial channel networks of adjacent elongated fans, including subordinate interlaced anastomosed sinuous channels. Sediment input points rapidly shifting through time and space in the ice-marginal zone results in a uniform distribution of the meltwater and sediment discharges upon the outwash plain and related braidplain deltas

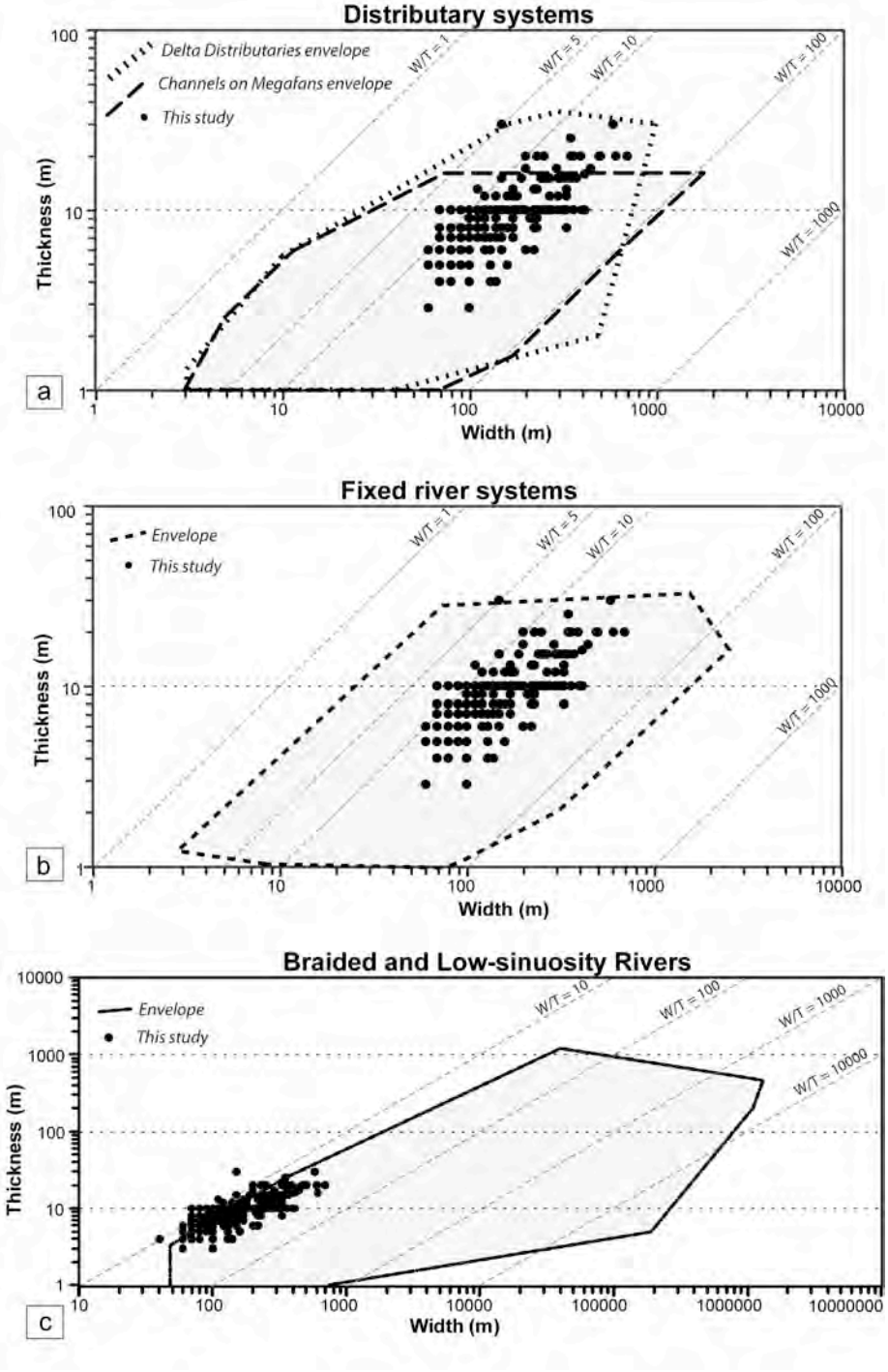

Fig. 14. Width : Thickness plots and associated envelopes for (a) distributary systems, (b) fixed river systems and (c) braided and low sinuosity rivers (from Gibing 2006), compared by the data set of the present study

This proglacial outwash setting with moderate slope gradient (2 m/km) and migrating sediments input points (glacial outlets) may fundamentally differ from other better known unconfined systems, such as higher gradient aprons with a coarser sediment load and lesser water discharge, or low-gradient sand-dominated channel belts on megafans (Hartley *et al*. 2010). Best analogues are probably coastal Icelandic sandur plains (Maizels 1997, 2002; Marren 2002, 2005), including interlaced anastomosed channels in addition of the features representative of the braidplain setting (Twidale 2004).

A last important point is to note that there is no significant difference in orientation trend of channel bodies comparing the one of the Tihemboka High and the more western area. Therefore, this tectonic element though recurrently effective during the Lower Palaeozoic (Beuf *et al*. 1971), had no interference on the latest Ordovician depositional surface, indicating it was either inactive or with uplift rates largely lesser than outwash plain aggradation rates.

Discussion

Although unconfined braided fluvial systems featured pre-vegetation settings (e.g. Davies & Gibling 2010), pre- and postglacial sandstone-dominated fluvial successions in Algeria and Libya that are respectively Cambrian and Lower Devonian in age, lack of any well defined channel bodies outcropping in the form sandstone ribbons (Beuf *et al*. 1971; Eschard *et al*. 2005; Ghienne *et al*. 2007b). Instead, they are characterized by extensive cross-stratified sandstone-sheets typically interpreted as braided stream deposits (e.g. Allen 1983; Gibling, 2006). Hence, specific conditions may have arisen in the Late Ordovician paraglacial context in order to explain profusion of ribbon-type channel bodies. We identified two potential dissimilarities that may have make different paraglacial and non-glacial fluvial systems upon the North Gondwana platform: frozen outwash plains and the occurrence of high-magnitude outburst events. Frozen sands enhancing bank stability (Syvitski 1986) can be suspected throughout the outwash plain. A consequence would have been the development of relatively deep channels as suggested by relatively low W/T ratios of channel bodies. However, it is thought that frozen sands and bank stability should have resulted preferentially in meandering channel belts (*cf.* modern Siberian case studies, Sidorchuck *et al.* 2001). The outburst-related scheme is preferred because Late Ordovician sandstone ribbons are closely associated with deposition of climbing-dune cross-stratification (CDCS) that typify high-magnitude flood events related to glacier outbursts or jökulhlaups in sand-dominated systems (Ghienne *et al*. 2010).

In case of braided channel belts, large-scale and small-scale channel bodies correspond to plugs of second and third-orders channels respectively. Dealing with subordinate interlaced anastomosed channels, plugs relate either to low-stage or bankfull channel cross-sections. Distinct modes of channel plugging can have occurred separately or in combination through time and space. Indeed, plugs may have infilled abandoned channels, generating localised flow expansions enhancing sand deposition from widespread, outwash-scale outburst-related sheet flows. Plugging stages may have also involved autocyclic processes alternating, during a flood peak, scour episodes with channel infilling stages as experimented by Sheets *et al.* (2007) and Van Dijk *et al*. (2009). Plugging phase could alternatively occur during waning-stage flow conditions of outburst events, within an overall backstepping of the place of deposition from distal mouth-bar environments to the outwash channels (Hopkins 1985; Mulder *et al*. 1998; Olariu & Bhattacharya 2006; Van Dijk *et al*. 2009). Whatever the plugging mode or combination of modes, the plugs fossilized the channel networks offering outburst-related snapshots of the outwash-braidplain organisation. However, first-order channel belt boundaries are not identified and it is unknown if they correspond to either separate km-scale wide features or contiguous channel belts forming a virtually continuous braidplain throughout the whole outwash surface. Inter-channel successions interpreted as braid bars represent mostly the ablation-related background sedimentation that continuously aggraded over the whole outwash plain, and interrupted by recurring outburst events. Flood hardened or giant gravel bars that characterise outburst-dominated sandur plains (Marren 2005) are not present owing to the absence of coarse material in the Late Ordovician glacial system.

Channel plugs are most probably diachronous across the Tassili N'Ajjer, considering that a single outburst resulting from the catastrophic drainage of subglacial meltwater storages should have only affect a restricted, 10-50(?) km wide portion of the outwash plain. Partial or complete plugging of the channels subsequent to an outburst event probably promoted avulsions and redistribution of the channels and/ or of the uncharacterised first-order channel belts across the outwash plain.

Plug-related channel bodies imply that W/T ratios of channel bodies essentially reflect W/T ratio of channels. Except for channels only just scoured during the outburst event, we can expect a flood-related alteration of W/T ratios of pre-flood sinuous channels. In particular, widening and/ or deepening of the pre-flood channel cross section may occur during major flood events (Bristow 1996). As the channel bodies have thicknesses comprised in 5 to 30 m, a mean width of 120-130 m, and a mean W/T of 16-17 (Fig. 12), they are included in the narrow ribbons to broad sheets categories according to the classification of Gibling (2006). The Late Ordovician data set has been plotted in W/T graphs and is compared with the envelopes of three categories proposed by Gibling (2006): distributary systems, fixed river systems, and braided and low-sinuosity rivers (Fig. 14 a, b & c). Our data set best fits with the two former categories although it as been related to a system analogue to the latter. Unsurprisingly, as the Late Ordovician channel bodies correspond to plugs, their W/T ratio does not fit the bodies representing long-lived evolutions including significant lateral migrations that usually characterize braided river systems. They probably resemble the fixed river and distributary systems because the latter are more frequently, at geological time scale, affected by avulsion, a process that "freeze" segments of the channel network, similarly with the snapshots related to the outburst-related plug events over the Late Ordovician outwash plain.

Conclusion

Large-scale stratigraphic architecture of proglacial outwash plains are intimately controlled by ice-front evolution, with for instance aggradation phases related to glacial advances. Sedimentation over the outwash plains have in addition a number of specificities directly linked to the proglacial setting that is responsible for the

alternation of high-frequency/ low-magnitude events with low-frequency/ high magnitude events, within systems dominated by high meltwater and sediment discharges. Numerous subglacial outlets, either penecontemporaneous or diachronous but rapidly shifting through time within the ice-marginal zone, result in a distributary pattern that occur essentially upstream the outwash plain. Such outwash plain is comprised of a succession of juxtaposed elongated fans, which forced each together to flow basinward with limited possibilities for developing apparent lobate geometries. It resulted a somewhat planar outwash plain and, downstream, braidplain-delta patterns. The occurrence of glacial outbursts in the Late Ordovician, which were able to plug the pre-flood channel networks, active as well as inactive channels, or new scours, offers snapshots of the outwash channel distribution in the form of an extensive array of sandstone ribbons that are presently exposed as inverted topographies in the Tassili N'Ajjer area.

References

ALEXANDER, J., BRIDGE, J.S., CHEEL, R.J. & LECLAIR, S.F. 2001. Bedforms and associated sedimentary structures formed under supercritical water flows over aggrading sand beds. *Sedimentology*, **48**, 133-152.

ALLEN, J.R.L. 1983. Studies in fluviatile sedimentation: bars, bar-complexes and sandstone sheets (low-sinuosity braided streams) in the Brownstones (L. Devonian), Welsh Borders. *Sedimentary Geology*, **33**, 237-293.

ASHWORTH, P.J., BEST, J.L., RODEN, J.E., BRISTOW, C.S. & KLAASSEN, G.J. 2000. Morphological evolution and dynamics of a large, sand braid-bar, Jamuna River, Bangladesh. *Sedimentology*, **47**, 533-555.

BELLINI, E. & MASSA, D. 1980. A stratigraphic contribution to the Paleozoic of the Southern Basins of Libya. *In:* SALEM, M.J. & BURSREVIL, M.T. (eds) *The Geology of Libya, Vol. I*, Academic Press, London, 1-56.

BEUF, S., BIJU-DUVAL, B., DE CHARPAL, O., ROGNON, P., GARIEL, O. & BENNACEF, A. 1971. *Les grès du Paléozoique inférieur au Sahara.* ''Science et Technique du pétrole'', 18, Paris, 464 pp.

BJÖRNSSON, H. 2002. Subglacial lakes in Iceland. *Global Planete Change*, **35**, 255-271.

BOOTHROYD, J. C. & NUMMEDAL, D. 1978. Proglacial braided outwash: a model for humid alluvial-fan deposits. *Canadian Society of Petroleum Geologists Memoir,* **5**, 641-668.

BRIERLEY, G.J. 1996. Channel Morphology and Element Assemblages: A Constructivist Approach to Facies Modelling. *In:* CARLING, P.A. & DAWSON, M.R. (eds) *Advances in Fluvial Dynamics and Stratigraphy*. 263-298.

BRISTOW, C.S. & BEST, J.L. 1993. Braided rivers: perspectives and problems. *In:* BEST, J.L. & BRISTOW, C.S. (eds) *Braided Rivers*. Special Publication Geological Society, **75**, 1-11.

BRISTOW, C. 1996. Reconstructing Fluvial Channel Morphology from Sedimentary Sequences. *In:* CARLING, P.A. & DAWSON, M.R. (eds) *Advances in Fluvial Dynamics and Stratigraphy*. 350-371.

BUATOIS, L.A., MANGÁNO, M.G., ALISSA, A. & CARR, T.R. 2002. Sequence stratigraphic and sedimentologic significance of biogenic structures from a late Paleozoic marginal- to open-marine reservoir, Morrow Sandstone, subsurface of southwest Kansas, USA. *Sedimentary Geology*, **152**, 99-132.

CANT, D.J. & WALKER, R.G. 1975. Development of a braided-fluvial facies model for the Devonian Battery Point Sandstone, Québec. *Canadian Journal of Earth Science*, **13**, 102-119.

CANT, D.J. & WALKER, R.G. 1978. Fluvial processes and facies sequences in the sandy braided South Saskatchewan River, Canada. *Sedimentology*, **25**, 625-648.

CARRIVICK, J.L. & RUSSELL, A.J. 2007. Glacifluvial landforms of deposition. *In:* ELIAS, S.A. (eds) *Encyclopedia of Quaternary Science*. Elsevier, B.V., Amsterdam, **2**, 909-919.

CHURCH, M. 1972. Baffin Island sandurs: a study of Arctic fluvial processes. *Geological Survey of Canada Bulletin,* **216**, 208 pp.

COWARD, M.P. & RIES, A.C. 2003. Tectonic development of North African basins. *In:* ARTHUR, T.J. & MACGREGOR, D.S. (eds) *Petroleum Geology of Africa: New Themes and Developing Technologies*. Geological Society, London, Special Publications, **207**, 61-83.

DAM, G. & ANDREASEN, F. 1990. High-energy ephemeral stream deltas: An example from the upper Silurian Holmestrand Formation of the Oslo Region, Norway. *Sedimentary Geology,* **66**, 197-225.

DAVIES, N.S. & GIBLING, M.R. 2010. Cambrian to Devonian evolution of alluvial systems: The sedimentological impact of the earliest land plants. *Earth-Science Reviews*, **98**, 171-200.

DAWSON, M.R. & BRYANT, I.D. 1987. Three-dimensional facies geometry in Pleistocene outwash sediments, Worcestershire, U.K. *The Society of Economic Paleontologists and Mineralogists*, **39**,191-196.

DELUCCA, J.L. & ERIKSSON, K.A. 1989. Controls on synchronous ephemeral- and perennial-river sedimentation in the middle sandstone member of the Triassic Chinle Formation, northeastern New Mexico, U.S.A. *Sedimentary Geology*, **61**, 155-175.

DROSER, M.L., HUGUES, N.C. & JELL, P.A. 1994. Infaunal communities and tiering in Early Palaeozoic nearshore clastic environments: trace-fossil evidence from the Cambro- Ordovician of New South Wales. *Lethaia*, **27**, 273-283.

DULLER, R.A., MOUNTNEY, N.P., RUSSELL, A.J. & CASSIDY, N.C. 2008. Architectural analysis of a volcaniclastic jökulhlaup deposit, southern Iceland: sedimentary evidence for supercritical flow. *Sedimentology,* **55**, 939-964.

EDMONDS, D. A. & SLINGERLAND, R. L. 2007. Mechanics of river mouth bar formation: Implications for the morphodynamics of delta distributary networks, *Journal of Geophysical Research*, **112**, F02034, doi:10.1029/2006JF000574.

ESCHARD, R., ABDALLAH, H., BRAIK, F. & DESAUBLIAUX, G. 2005. The Lower Paleozoic succession in the Tasilli outcrops, Algeria: sedimentology and sequence Stratigraphy. *First Break*, **23**, 27-36.

FABRE, J. & KAZI-TANI, N. 2005. Ordovicien, Silurien, Devonien, Permo-Carbonifère. *In* FABRE, J. (eds) *Géologie du Sahara occidental et central*. Tervuren African Geoscience Collection 108. Musée Royal de l'Afrique Centrale, Tervuren. 147-360.

FIELDING, C.R., TRUEMAN, J.D. & ALEXANDER, J. 2005. Sharp-based, flood-dominated mouth bars sands from the Burdekin River Delta of northeastern Autralia : extending the Spectrum of mouth-bar facies, geometry, and stacking patterns. *Journal of Sedimentary Research*, **75**, 55-66.

FIELDING, C.R. 2006. Upper flow regime sheets, lenses and scour fills: Extending the range of architectural elements for fluvial sediment bodies. *Sedimentary Geology*, **190**, 227-240.

FRIEND, P.F. 1983. Towards the field classification of alluvial architecture or sequence. *In :* COLLINSON, J.D. & LEWIN, J. (eds) *Modern and Ancient Fluvial Systems*. International Association of Sedimentologists, Special Publication, **6**, 345-354.

GALEAZZI, S., POINT, O., HADDADI, N., MATHER, J. & DRUESNE, D. 2010. Regional geology and petroleum systems of the Illizi–Berkine area of the Algerian Saharan Platform: An overview. *Marine and Petroleum Geology*, **27**, 143-178.

GERARD, J.R.F. & BROMLEY, R.G. 2008. *Ichnofabrics in clastic sediments : application to sedimentological core study, a practical guide,* Gerard J.R.F. (eds), 100 pp.

GHIENNE, J.-F. 2003. Late Ordovician sedimentary environments, glacial cycles, and post-glacial transgression in the Taoudeni Basin, West Africa. *Palaeogeography, Palaeoclimatology, Palaeoecology,* **189**, 117-145.

GHIENNE, J.-F., BOUMENDJEL, K., PARIS, F., VIDET, B., RACHEBOEUF, P. & AIT SALEM, H. 2007a. The Cambrian-Ordovician succession in the Ougarta Range (western Algeria, North Africa) and interference of the Late Ordovician glaciatio on the development of the Lower Palaeozoic transgression on northern Gondwana. *Bulletin of Geosciences*, **82**, 183-214.

GHIENNE, J.-F., LE HERON, D., MOREAU, J., DENIS, M. & DEYNOUX, M. 2007b. The Late Ordovician glacial sedimentary system of the North Gondwana platform. *In:* HAMBREY, M., CHRISTOFFERSEN, P., GLASSER, N., JANSSEN, P., HUBBARD, B. & SIEGERT, M. (eds) *Glacial Sedimentary Processes and Products*. Internal Association of Sedimentologists, Special Publication, **39**, 295-319.

GHIENNE, J.-F., GIRARD, F., MOREAU, J. & RUBINO, J.-L. (2010) Late Ordovician climbing-dune cross-stratification: a signature of outburst bloods in proglacial outwash environments?. *Sedimentology*, DOI: 10.1111/j.1365-3091.2009.01142.x.

GIBLING, M.R. 2006. Width and thickness of fluvial channel bodies and valley fills in the geological record: a literature compilation and classification. *Journal of Sedimentary Research*, **76**, 731-770.

GOMEZ, B., SMITH, L.C., MAGILLIGAN, F.J., MERTES, L.A.K. & SMITH, N.D. 2000. Glacier outburst floods and outwash plain development: Skeidarársandur, Iceland. *Terra Nova*, **12**, 126-131.

HARTLEY, A.J., WEISSMAN, G.S., NICHOLS, G.J. & WARWICK, G.L. 2010. Large distributive fluvial systems: characteristics, distribution, and controls on development. *Journal of Sedimentary Research*, **80**, 167-183.

HIRST, J.P.P., BENBAKIR, A., PAYNE, D.F. AND WESTLAKE, I.R. 2002. Tunnel Valleys and Density Flow Processes in the upper Ordovician glacial succession, Illizi Basin, Algeria: influence on reservoir quality. *Marine Petroleum Geology*, **25**, 297-324.

HOPKINS, J.C. 1985. Channel-fill deposits formed by aggradation in deeply scoured, superimposed distributaries of the Lower Kootenai Formation (Cretaceous). *Journal of Sedimentary Petrology*, **55**, 42-52.

HOYAL, D.C.J.D., VAN WAGONER, J.C., ADAIR, N.L., DEFFENBAUGH, M., LI, D., SUN, T., HUH, C. & GIFFIN, D.E. 2003. Sedimentation from jets: a depositional model for clastic deposits of all scales and environments. *American Association of Petroleum Geologists*, Search and Discovery, Online Article #40082.

KRZYSZKOWSKI, D. 2002. Sedimentary successions in ice-marginal fans of the Late Saalian glaciation, southwestern Poland. *Sedimentary Geology*, **149**, 93-109.

LANGFORD, R. & BRACKEN, B. 1987. Medano Creek, Colorado, a model for upper-flow-regime fluvial deposition. *Journal of Sedimentary Petrology*, **57**, 863-870.

LE HERON, D.P., CRAIG, J., SUTCLIFFE, O. & WHITTINGTON, R. 2006. Late Ordovician glaciogenic reservoir heterogeneity: an example from the Murzuq Basin, Libya. *Marine and Petroleum Geol*ogy, **23**, 655-677.

LE HERON, D.P. & CRAIG, J. 2008. First order reconstructions of a Late Ordovician Saharan ice sheet. *Journal of the Geological Society, London*, **165**, 19-29.

LE HERON, D., CRAIG, J. & ETIENNE, J.L. 2009. Ancient glaciations and hydrocarbon accumulations in North Africa and the Middle East. *Earth-Science Reviews*, **93**, 47-76.

LOI, A., GHIENNE, J.-F., DABARD, M.P. , PARIS, F. , BOTQUELEN, A., CHRIST, N., ELAOUAD-DEBBAJ, Z., GORINI, A., VIDAL, M., VIDET, B. & DESTOMBES, J. 2010. The Late Ordovician glacio-eustatic record from a high-latitude storm-dominated shelf succession: The Bou Ingarf section (Anti-Atlas, Southern Morocco). *Palaeogeography, Palaeoclimatolog,y Palaeoecol*ogy, in press, doi:10.1016/j.palaeo.2010.01.018.

LOWE, D.R. 1975. Water escape structures in coarse-grained sediments. *Sedimentology*, **22**, 157-204.

MAGILLIGAN, F.J., GOMEZ, B., MERTES, L.A.K., SMITH, L.C., SMITH, N.D., FINNEGAN, D. & GARVIN, J.B. 2002. Geomorphic effectiveness, sandur development, and the pattern of landscape response during jökulhlaups: Skeidarársandur, southeastern Iceland. *Geomorphology*, **44**, 95–113.

MAIZELS, J.K. 1993. Lithofacies variations within sandur deposits: the role of runoff regime, flow dynamics and sediment supply characteristics. *Sedimentary Geology*, **85**, 299-325.

MAIZELS, J.K., 1997. Jökulhlaup deposits in proglacial areas. *Quaternary Science Reviews*, **16**, 793-819.

MAIZELS, J. 2002. Sediments and landforms of modern proglacial terrestrial environments. *In:* MENZIES, J. (eds) *Modern and past glacial environments*. Butterworth-Heinemann, oxford, 279-316.

MAKASKE, B. 2001. Anastomosing rivers: a review of their classification, origin and sedimentary products. *Earth-Science Reviews*, **53**, 149-196.

MARREN, P.M. 2002. Fluvial–lacustrine interaction on Skeidarársandur, Iceland: implications for sandur evolution. *Sedimentary Geology*, **149**, 43-58.

MARREN, P.M. 2004. Present-day sandurs are not representative of the geological record. *Sedimentary Geology*, **164**, 335-340.

MARREN, P.M. 2005. Magnitude and frequency in proglacial rivers: a geomorphological and sedimentological perspective. *Earth-Science Reviews*, **70**, 203-251.

MELLERE, D., PLINK-BJÖRKLUND, P. & STEEL, R.J. 2002. Anatomy of shelf deltas at the edge of a prograding Eocene shelf margin, Spitsbergen. *Sedimentology*, **49**, 1181-1206.

MIALL, A.D. 1996. *The Geology of Fluvial Deposits*. New York, Springer-Verlag, 582 p.

MOREAU, J., GHIENNE, J.-F., LE HERON, D., RUBINO, J.-L. & DEYNOUX, M. 2005. A 440 Ma old ice stream in North Africa. *Geology*, **33**, 753-756.

MULDER, T., SYVITSKI, J.P.M. & SKENE, K.I. 1998. Modelling of erosion and deposition by turbidity currents generated at river mouths. *Journal of Sedimentary Research*, **68**, 124-137.

MUTTI, E., TINTERI, R., BENEVELLI, G., DI BIASE, D. & CAVANNA, G. 2003. Deltaic, mixed and turbidite sedimentation of ancient foreland basins. *Marine and Petroleum Geology*, **20**, 733-755.

NANSON, G.C. & KNIGHTON, A.D. 1996. Anabranching rivers: their cause, character and classification. *Earth Surface Processes and Landforms,* **21**, 217-239.

NEEF, G., BOTRILL, R.S. & COHEN, D.R. 1996. Mid and Late Devonian arenites deposited by sheet-flood, braided streams and rivers in the northern Barrier Ranges, far western New South Wales, Australia. *Sedimentary Geology*, **103**, 39-61.

NEMEC, W. & STEEL, R.J. 1988. What is a fan delta and how do we recognize it?. In: NEMEC, W. & STEEL, R.J. (eds) Fan Deltas: Sedimentology and Tectonic Settings. Blackie and Son, 3-22.

NORTH, C.P. & WARWICK, G.L. 2007. Fluvial fans: myths, misconceptions, and the end of the terminal-fan model. *Journal of Sedimentary Research*, **77**, 693-701.

OLARIU, C. & BHATTACHARYA, J.P. 2006. Terminal distributary channels and delta front architecture of river-dominated delta systems. *Journal of Sedimentary Research*, **76**, 212-233.

OLSEN, H. 1989. Sandstone-body structures and ephemeral stream processes in the Dinosaur Canyon Member, Moenave Formation (Lower Jurassic), Utah, U.S.A. *Sedimentary Geology*, **61**, 207-221.

ORTON, G.J. & READING, H.G. 1993. Variability of deltaic processes in terms of sediment supply, with particular emphasis on grain size. *Sedimentology*, **40**, 475-512.

PETERS, L.E., ANANDAKRISNAN, S., ALLEY, R.B. & SMITH, A.M. 2007. Extensive storage of basal meltwater in the onset region of a major West Antarctic ice stream. *Geology*, **35**, 251–254.

PLINK-BJÖRKLUND, P., MELLERE, D. & STEEL, R. J. 2001. Turbidite variability and architecture of sand-prone, deep-water slopes: Eocene clinoforms in the central basin, Spitsbergen. *Journal of Sedimentary Research*, **71**, 895-912.

RUBINO, J.-L., ANFRAY, R., BLANPIED, C., GHIENNE, J.-F. & MANATSCHAL, G. 2003. Meander belt complex within the lower Mamuniyat Formation in western Al Qarqaf area, Libya. *In:* SALEM, M.J. & OUN KHALED, M. (eds) *The geology of northwest Libya; Volume II, Sedimentary basins of Libya, second symposium*. Symposium on the Sedimentary Basins of Libya, **2**, 3-18.

RUSSELL, A.J., FAY, H., MARREN, P.M., TWEED, F.S. & KNUDSEN, O´. 2005. Icelandic jökulhlaup impacts. *In:* CASELDINE, C., RUSSELL, A., HARDARDOTTIR, J. & KNUDSEN, O´. (eds) *Iceland— Modern Processes and Past Environments*. Development in quaternary Science, **5**, 153-203.

RUSSELL, A.J. 2009. Jökulhlaup (ice-dammed lake outburst flood) impact within a valley-confined sandur subject to backwater conditions, Kangerlussuaq, West Greenland. *Sedimentary Geology*, **215**, 33-49.

RUST, B.R. 1978. A classification of alluvial channel systems. *In:* MIALL, A.D. (eds) *Fluvial Sedimentology*. Canadian Society of Petroleum Geologists Memoir, **5**, 187-198.

SCHOMACKER, E.R., KJEMPERUD, A.V., NYSTUEN, J.P. & JARHEN, J.S. 2010. Recognition and significance of sharp-based mouth-bar deposits in the Eocene Green River Formation, Uinta Basin, Utah. *Sedimentology,* **57**, 1069-1087.

SHEETS, B.A., PAOLA, C. & KELBERER, J.M. 2007. Creation and preservation of channel-form sand bodies in an experimental alluvial system. *In:* NICHOLS, G.J., WILLIAMS, E. & PAOLA, C. (eds) *Sedimentary Processes, Environments and Basins*. Special Publication 38, International Association of Sedimentologists Oxford, Blackwell, 555-567.

SIDORCHUK, A., BORISOVA, O. & PANIN, A. 2001. Fluvial response to the Late Valdai/Holocene environmental change on the East European Plain. *Global and Planetary Change*, **28**, 303-318.

SMITH, L.C., SHENG, Y., MAGILLIGAN, F.J., SMITH, N.D., GOMEZ, B., MERTES, L.A.K., KRABILL, W.B. & GARVIN, J.B. 2006. Geomorphic impact and rapid subsequent recovery from the 1996 Skeidarársandur jökulhlaup, Iceland, measured with multi-year airbone lidar. *Geomorphology*, **75**, 65-75.

SNORRASON, Á., JÓNSSON, P., SIGURDSSON, O., PÁLSSON, S., ÁRNASSON, S., VIKINGSSON, S. & KALDAL, I. 2002. November 1996 jökulhlaup on Skeidarársandur outwash plain, Iceland. *In :* MARTINI, I.P., BAKER, V.R. & GARZÓN, G. (eds) *Flood and megaflood processes and deposits: recent and ancient examples*. Special Publication of International Association of Sedimentologists, **32**, 55-65.

SPINEWINE, B., SEQUEIROS, O.E., GARCIA M.H., BEAUBOUEF, R.T., SUN T., SAVOYE B. & PARKER G. 2009. Experiments on wedge-shaped deep-sea sedimentary deposits in minibasins and/or on channel levees emplaced by turbidity currents. Part II: Morphodynamic evolution of the wedge and of the associated bedforms. *Journal of Sedimentary Research*, **79**, 608-628.

SUTTER, J.R. 1994. Deltaic coasts. *In:* CARTER, R.W.G. & WOODROFFE, C.D. (eds) *Coastal evolution: Late Quaternary shoreline morphodynamics*. Cambridge university, 87-120.

SYVITSKI, J.P.M. 1986. Estuaries, deltas and fjords of eastern Canada. *Geoscience Canada*, **13**, 91-100.

TUNBRIDGE, I.P. 1981. Sandy high-energy flood sedimentation – some criteria for recognition, with an example from the Devonian of S. W. England. *Sedimentary Geology,* **28**, 79-95.

TWIDALE, C.R. 2004. River patterns and their meaning. *Earth-Science Reviews*, **67**, 159-218.

VAN DIJK, M., POSTMA, G. & KLEINHANS, M.G. 2009. Autocyclic behaviour of fan deltas: an analogue experimental study. *Sedimentology*, **56**, 1569-1589.

WINSEMANN, J., HORNUNG, J.J., MEINSEN, J., ASPRION, U., POLOM, U., BRANDES, C., BUBMANN, M. & WEBER, C. 2009. Anatomy of a subaqueous ice-contact fan and delta complex, Middle Pleistocene, North-west Germany. *Sedimentology*, **56**, 1041-1076.

ZIELINSKI, T. & VAN LOON, A. J. 2002. Present-day sandurs are not representative of the geological record. *Sedimentary Geology,* **152**, 1-5.

ZIELINSKI, T. & VAN LOON, A. J. 2003. Pleistocene sandur deposits represent braidplains, not alluvial fans. *Boreas*, **32**, 590-611.

3.4. Evolution sédimentaire fini- à post-glaciaire

Au nord de Ghat (sud-ouest de la Libye), la transgression postglaciaire a envahi un domaine constellé de topographies glaciaires résiduelles. Un remaniement en domaine tidal a coiffé les reliefs de faciès gréseux (premier et second plans) tandis qu'une sédimentation argileuse (base des argiles du Tanezzuft) occupaient les dépressions (3ème plan). La sédimentation argileuse n'atteindra les paléoreliefs que plusieurs millions d'années après la déglaciation hirnantienne, soit au Llandovery moyen. Une longue période de progradation de la plate-forme silicoclastique silurienne s'en suivra, culminant avec les grès de l'Acacus (arrière-plan, derrière les dunes) (Klitzsch, 1981 ; Massa, 1988 ; Storch et Massa, 2006 ; Moreau et al., 2007).

Le retrait glaciaire généralisé sur la plate-forme nord-gondwanienne intervient au cours de la partie supérieure de l'Hirnantien (Paris et al., 1998 ; *Ghienne et al., 2007b, §6*). A la transition Ordovicien/ Silurien, les bassins sédimentaires de ce domaine peuvent être considérés comme libres de glace, même si une calotte glaciaire reste active plus au sud, comme en témoigne l'enregistrement sédimentaire sud-américain. Cette disparition des glaciers est organisée en une série d'avancées/ retraits glaciaires, ces derniers de plus en plus marqués. Associées à cette période de déglaciation, des structures thermokarstiques ont été préservées au sein d'environnements fluviatiles à estuariens. Elles trahissent le réchauffement climatique en cours à la fin de l'Hirnantien. Les dépôts ultérieurs constituent un système transgressif avec quelques spécificités (*Moreau et al., 2007*): présence d'une topographie héritée relativement accidentée, installation d'un vaste système à dominante tidale (*Ghienne, 2003, §6* ; Eschard et al., 2005 ; *Ghienne et al., 2007a, Fig. 7, §1*), submersion définitive de la plate-forme au Silurien inférieur et dépôts des argiles à graptolites riches en matière organique dans les dépressions résiduelles. Cette dernière spécificité est partagée avec la plupart des séries transgressives postglaciaire (par exemple, Lang et al., 1991 ; Isbell et al., 2010).

- La présence d'un permafrost ordovicien a été suspectée depuis les travaux de Beuf et al. (1971) en Algérie. Ces auteurs ont décrit des pingos fossiles, structures de diamètre kilométrique qui ont également été identifiées en Arabie Saoudite (Vaslet, 1990). Elles suggèrent l'existence, au moins localement, d'un permafrost continu. Un autre type de structure circulaire mais de moindre envergure (pluridéca- à plurihectométriques), a été mis en évidence au sein des dépôts fluviatiles fini- à post glaciaires de l'Anti-Atlas (stage Master2, A. Nutz). Contrairement aux pingos, souvent isolés ou à distances les uns des autres, ces structures sont juxtaposées. Il s'agit de dépressions au sein desquelles s'infléchissent et s'épaississent les bancs gréseux démontrant ainsi le caractère syn-sédimentaire de leur formation (cf. image ci-dessous). Au centre de chacune d'elles, les bancs gréseux présents de part et d'autres sont absents. L'analyse de l'architecture stratigraphique au

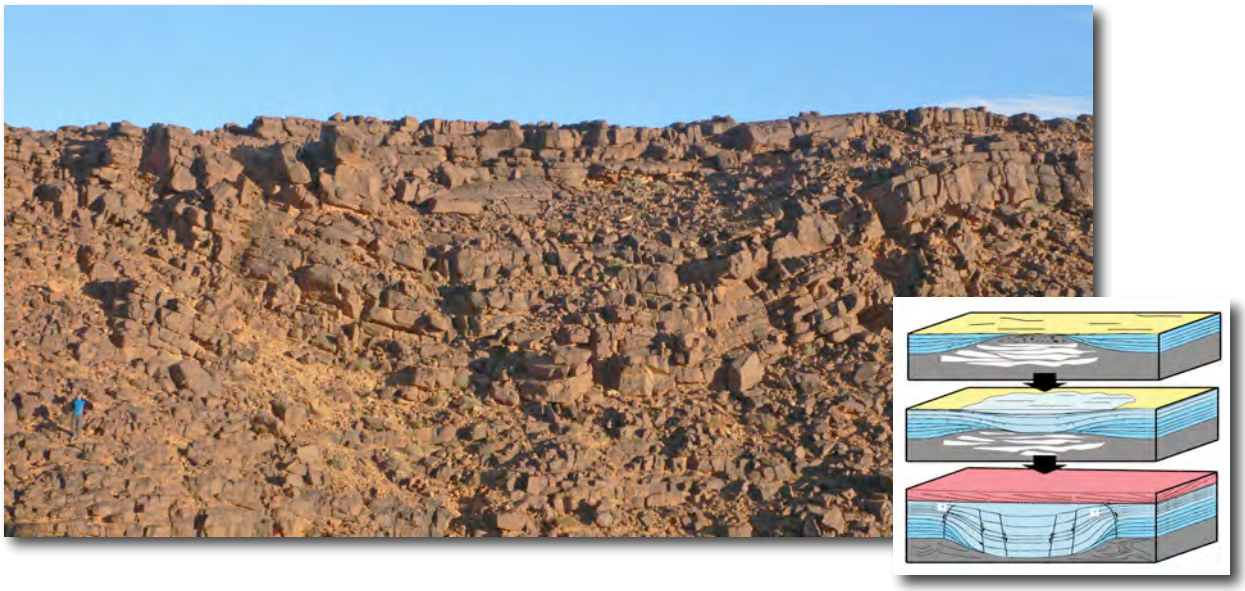

contact de la structure indique qu'il s'agit plutôt d'une lacune sédimentaire de non-dépôt que d'une érosion. Le remplissage de ces structures montre la présence de nombreuses rides de clapot suggérant la formation d'étendue d'eau libre très peu profonde. Des empreintes de cristaux de glaces s'y sont préférentiellement formées. Ces structures circulaires sont interprétées comme des cicatrices de lithalsas (ou palses minérales), lentilles de glace générant un permafrost discontinu. Pendant une phase d'aggradation de la plaine alluviale, la croissance des lentilles de glace a

conduit à une mosaïque de dépôts gréseux et de buttes cryogéniques à cœur de glace de ségrégation. La fusion de ces lentilles a ensuite constitué comme un ensemble de mini-bassins sédimentaires affectée par une « subsidence ». Ces structures sont pour l'essentiel scellées par les derniers dépôts fluviatiles. Elles sont interprétées comme la signature d'une récurrence de climat froid au sein de la séquence de déglaciation et pourraient être contemporaines d'une phase de ré-avancée glaciaire dans les domaines les plus proximaux.

- Les glaciers en retrait ont laissé sur la plate-forme une physiographie complexe au sein de laquelle on peut distinguer des zones « hautes » et des zones dépressives (*Ghienne et al., 2007b, §7* ; *Moreau et al., 2007*). Le caractère « haut » des premières s'entend en relatif par rapport aux secondes, les dénivelées pouvant atteindre la centaine de mètres. Les zones dépressives sont restées hors du champ des dépôts sédimentaires fini-glaciaires. Il s'agit le plus souvent soit de zones ayant subit une érosion glaciaire, ensuite inondées par la dynamique transgressive, et laissées libres de dépôt par un retrait rapide des fronts glaciaires, soit des zones les plus distales de la plate-forme qui ne verront le retour d'une sédimentation active que plusieurs millions d'années après la déglaciation. Les parties « hautes » de la plate-forme correspondent soit à des zones ayant subit une moindre érosion glaciaire, soit à des zones qui ont été le siège d'une sédimentation active avec par exemple la progradation des systèmes fluvio-deltaïque à dynamique de crue décrit précédemment (cf. section 3.3 et figure ci-contre). La juxtaposition des zones dépressives et des zones « hautes » produit une physiographie en damier, la taille des cases variant de l'échelle régionale (l'Adrar de Mauritanie est une zone « haute », *Ghienne, 2003, §6*), à l'échelle plurikilométrique. En particulier, la présence des linéations glaciaires à grande échelle des domaines de fleuve de glace, plus ou moins ennoyés par les dépôts glaciaires, sont à l'origine de mosaïques beaucoup plus serrées (Ghienne et al., 2007b, §6, fig. 9B).

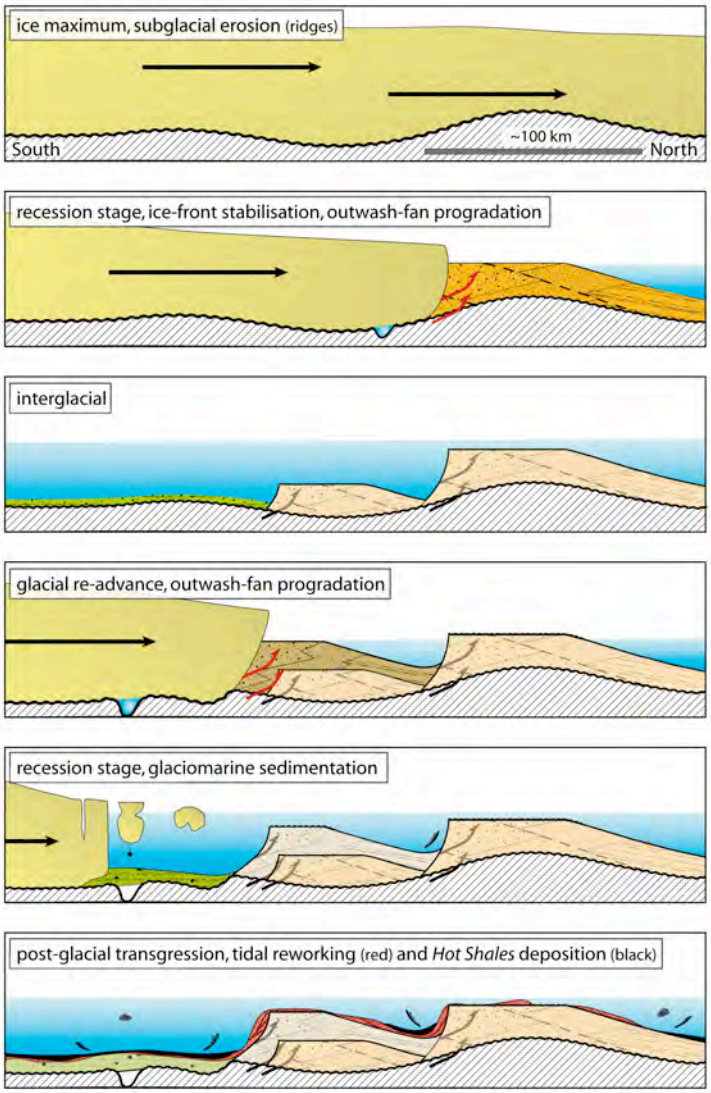

- Sur les zones « hautes » s'installent des systèmes à dynamique de marées au sein desquels la bioturbation ré-apparaît ainsi que de rares faunes peu diversifiées à bivalves ou brachiopodes (faunes à *Hirnantia*). Le contact entre les sédiments glaciogéniques sous-jacents et les faciès tidaux correspond systématiquement à une surface d'érosion assimilée à une surface de ravinement tidal transgressif (Hwang et Heller, 2002). Le vannage par les courants de marée remanie et transporte les sables glaciaires via des systèmes

de mégarides ou de grandes barres tidales (*Ghienne et al., 2007a, §1*) analogues de celles aujourd'hui présentent en Mer du Nord (Dronkers, 2005). Ce transport d'effectue vers les zones dépressives, soit vers le continent (vers le sud), soit vers le large (vers le nord), soit latéralement et avec une composante de dérive littorale assez systématiquement orientée de l'ouest vers l'est. Des systèmes de clinoformes tidaux établissent localement une transition entre les zones « hautes » et les zones dépressives (en rouge sur figure page précédente). Dans les zones dépressives situées le plus souvent sous la limite d'action des vagues de tempêtes, s'accumulent les sédiments les plus fins, présentant parfois quelques récurrences glaciomarines distales, possiblement alimentées en éléments lâchés par de la glace de mer dérivante. La transgression postglaciaire se poursuivant, une aggradation des faciès tidaux est enregistrée sur les zones « hautes » tandis qu'un niveau de condensation intensément bioturbé se développe dans les parties basses.

- Une nouvelle étape dans la transgression postglaciaire conduit à la submersion des zones « hautes » qui passent alors en domaine de *shoreface* puis d'*offshore*, avec formation d'une surface de ravinement transgressive par les vagues (*Ghienne, 2003, Fig. 11, §6*; *Ghienne et al., 2007a, §1*; *Douillet et al., en révision*). Une surface de condensation pendant l'intervalle de temps correspondant au Silurien le plus basal (Rhuddanien inférieur) s'y développe alors que la progradation depuis le sud de la plate-forme silicoclastique silurienne a débuté (Bellini et Massa, 1980; Storch et Massa, 2006). Les apports sédimentaires corrélatifs permettent le piégeage d'une importante quantité de matière organique plus spécifiquement dans les zones protégées de l'action des vagues, c'est-à-dire soit en profondeur, soit dans des baies abritées dont la topographie est héritée du retrait glaciaire. La progradation au littoral s'accentuant, avec montée lente mais continue du niveau marin relatif, les zones dépressives les plus proximales se trouvent alors progressivement comblées et les zones « hautes » deviennent, avec un retard dépendant de leur développement vertical — mais le plus souvent à l'Aéronien —, le siège d'une sédimentation argileuse cette fois relativement pauvre en matière organique (meilleure oxygénation ?, moindre production ?). Une roche-mère plus tardive est également identifiée dans les zones plus distales de la plate-forme, dont la mise en place semble indépendante de l'évolution postglaciaire hirnantienne et possiblement liée à une dynamique d'upwelling lors du maximum d'inondation Silurien inférieur. Ces deux horizons riches en matière organique constitueront les futures roches-mères du système pétrolier Ordovicien/ Silurien (Lüning et al., 2000, 2005; Fello et al., 2007). A ce schéma d'ensemble, il semblerait que se superposent quelques rejeux tectoniques avec soulèvements localisés, érosion, et mise en place d'une séquence transgressive d'âge télychien, soit plus de 15 millions d'années après la fin de la glaciation ordovicienne. L'étude de la distribution de ces anomalies à l'échelle de la plate-forme est en cours.

Large-scale physiography of the Murzuq Basin shelf during Hirnantian ice-sheet final retreat and Silurian transgression: outcrops and seismic interpretations

Moreau J., Degermann L., Ghienne J.-F., Rubino J.-L. (2007)

3rd North African/ Mediterranean Petroleum and Geosciences Conference & Exhibition (EAGE extended abstract), 26 to 28 February 2007, Tripoli (Libya).

Depositional architecture of Lower Palaeozoic rocks into the Murzuq Basin is strongly influenced by the Hirnantian glaciation. This study aims to integrate outcrop and subsurface data at the basin scale. A major objective is to identify in the subsurface ice-stream imprints and to compare them with structures known at outcrop in the Ghat-Tikiumit area that has been unambiguously shaped ice-stream activity (Moreau et al. 2005). The Late Ordovician ice sheet came repeatedly across the studied area four to five times (depending the palaeolatitude, Ghienne et al. 2006) and left behind sediments mainly recording waning and interglacial stages. The successive glacial advances and retreats generated glacial depositional sequences bounded by erosional subglacial surfaces. The fourth glacial erosion surface is the major and most extensive one. It merges southward with the fifth and last glacial surface. An overall trend of southward glacial retreat through the Murzuq Basin can be traced along these surfaces. This trend is emphasized by the presence of recessive ice fronts. These ice fronts are characterized by outwash deposits, which are in places intensively deformed by large-scale glaciotectonic folds and thrusts.

The fourth glacial phase comprises a succession of southward, stepwise backstepping, depositional assemblages (Figure 1), each comprising from base to top (AG4, figure 2): ice-contact submarine outwash-fan deposits (channels, mass flows) deposited during rapid ice front recession; prograding fan-delta deposits (outburst facies with 3D or 2D climbing dunes grading downstream in sandy turbidites) with subordinate proglacial fluvial facies. The latter stage reflects a temporary stabilization of the ice front (glaciotectonic), before a new rapid recession stage releasing accommodation space for the deposition of a succeeding assemblage. When the maximum ice retreat of the fourth phase is reached, a large fluvial plain aggraded over the whole area (SG4).

Following a significant glacial re-advance, the fifth glacial sequence is deposited above a well identified erosion surface (AG5, figure 1 and 3). At the maximum ice extent, a continental ice front occurred underlined by glaciotectonic structures and tunnel-valley mouth. To the north (downstream), a low sinuosity fluvial braid-plain developed and graded into a delta and turbiditic system (figure 2). The ultimate and rapid ice retreat has left a residual palaeotopography south of this last ice front. This palaeorelief, up to 200 m in relief, have been subsequently flooded by the postglacial transgression (Figure 3). Over the higher areas, tidal reworking of the glacial deposits has built migrating tidal ridges (AT2, figure 1 and 2). Bioturbated ebb tidal deltas (foreset with 10° dip) prograded along the slope of the former subglacial ridges. Downward, in the bottom parts of the glacial valleys constituting in sheltered area, they graded into laminated siltstones and shales with granule lags (figure 3). Finally, the development of the post-glacial transgression totally flooded even the higher areas. This stage interrupted the tidal activity and permitted the deposition of Lower Silurian "Hot Shale" into the glacial depressions that have been kept underfilled.

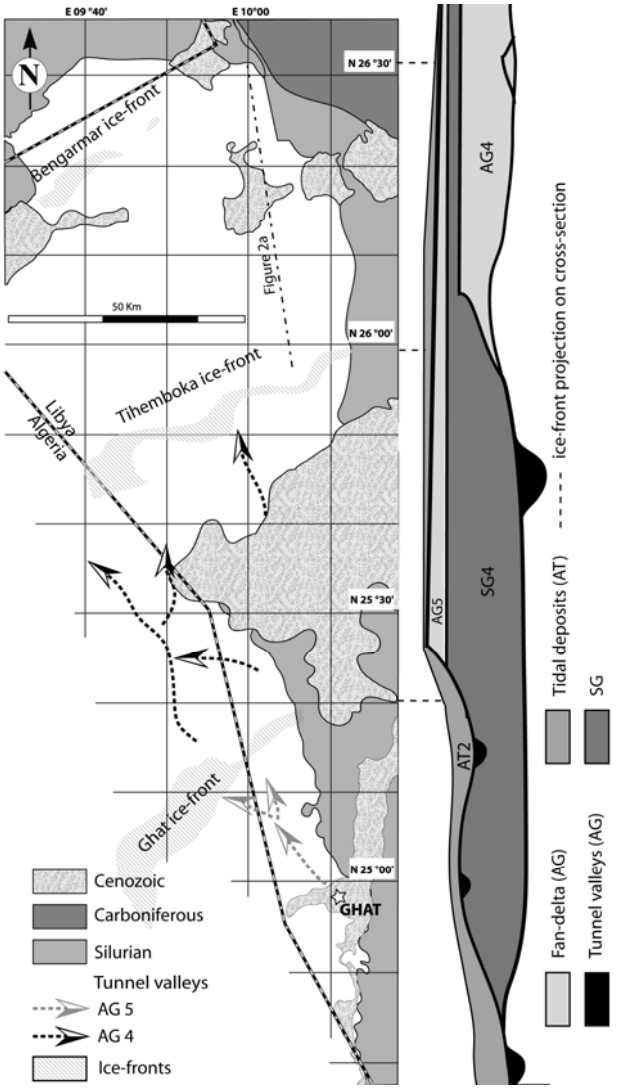

Figure 1: Ghat-Tikiumit area location map and North-South cross-section illustrating ice-sheet retreat features that are exposed in the western Murzuq Basin, location figure 4.

The architecture illustrated in the Ghat-Tikiumit outcrops (figure 3) serves as a guideline to identify ice fronts in the subsurface. The Ordovician-Silurian surface boundary reflects most of the post-glacial physiography in the Murzuq Basin. The initial geometry of this surface, that is known to have a characteristic response on seismic profiles, can be restored *via* flattening using a continuous reflector considered horizontal at time of deposition. An upper Silurian reflector has been used in this study. In addition, the regional mapping of associated depositional architectures has been undertaken. First, regional and lateral (E-W) onlap terminations of the Silurian deposits on glacial morphologies highlight an eastern ice-stream margin (figure 4). Such an ice-stream margin corresponds to about 100-200 ms of Silurian thickness variation in a few kilometers. As the western margin of this ice stream is known at outcrop (Fig. 3), a large ice stream, ca. 350 km in width, is mapped in the Murzuq Basin (figure 4). Second, the mapping of the Silurian base at a smaller scale (5 to 70 km) shows subordinate elongated highs corresponding to large-scale subglacial ridges and erosional troughs (Moreau et al. 2005) and sinuous km-large channels interpreted as tunnel valleys. Third, ovoid to circular high areas are interpreted as fan-delta depocenters (figure 4). These flat-topped structures display downlap structures at their base. Silurian reflectors onlap onto the southern steep erosion surface of these fan-delta bodies, which corresponded to palaeo ice-fronts (figure 4). Some 50-100ms high fold and thrust structures are observed in places. Silurian reflectors are conformable on the top of the structure and backlaps are observed on the northern slope of the fan-delta bodies.

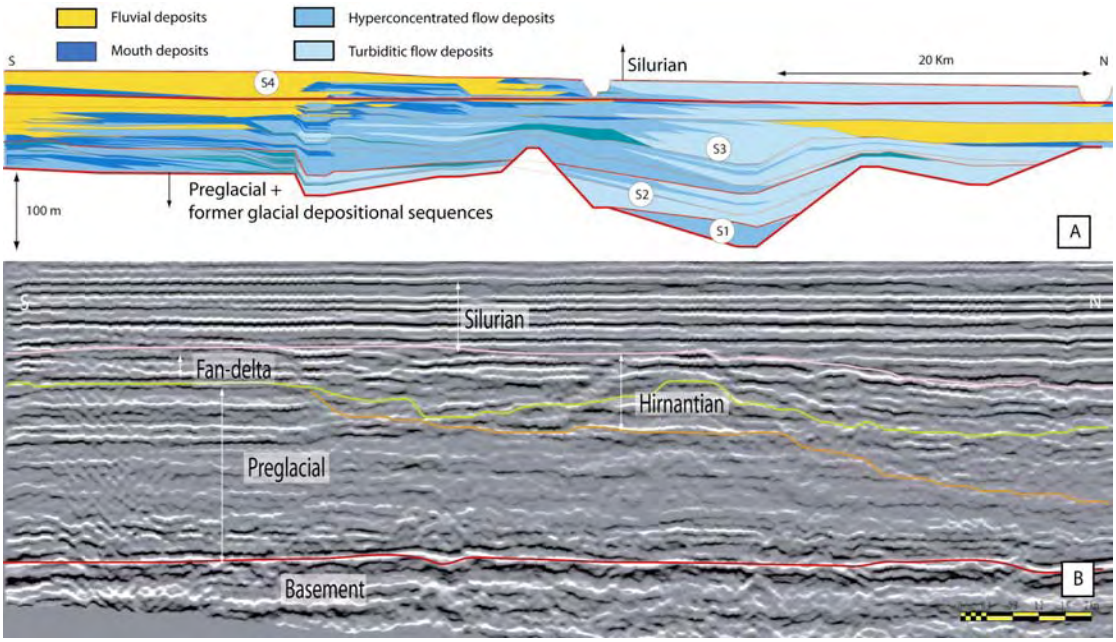

Figure 2: comparison between two proglacial fan-delta systems directly associated with ice fronts to the south. A. Outcrop data: fan-delta associated to the Tihemboka ice front, location figure 1. B Subsurface analogue: fan-delta on a north-south trending seismic line (flattened and filtered). In red, the top basement; in orange the erosional base of the glacial Hirnantian succession; in yellow-green, the AG4 glacial erosion surface; in violet, the base of Silurian deposits. Size and structures of this fan-delta are comparable with the architecture observed in the Tihemboka area.

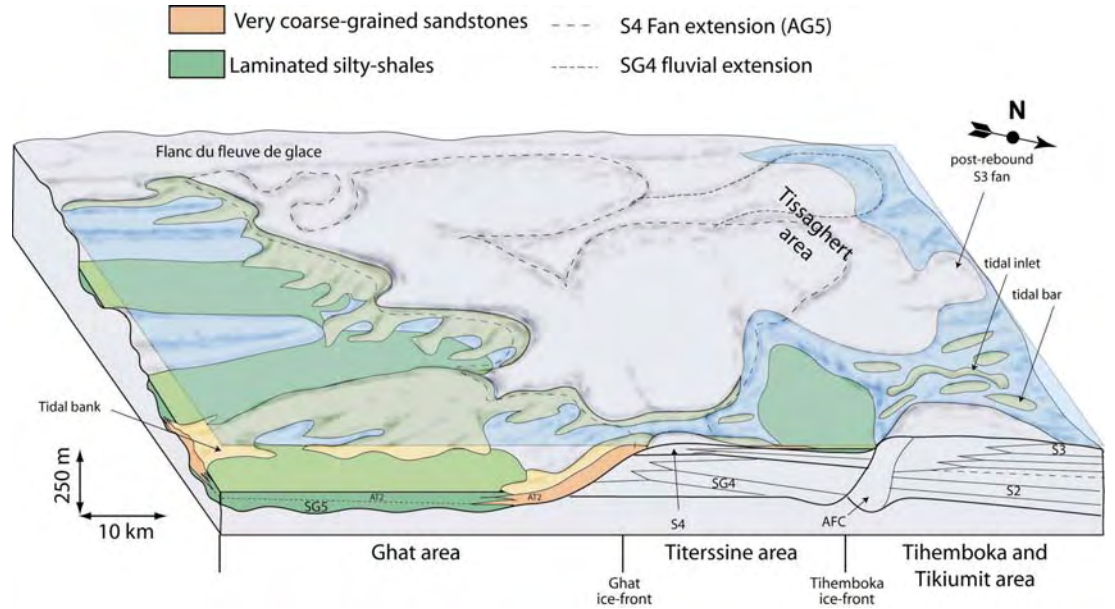

Figure 3: 3D reconstruction of the physiography during postglacial transgression and associated development of AT2 tidal unit as observed in the Ghat-Tihemboka exposures, location figure 4.

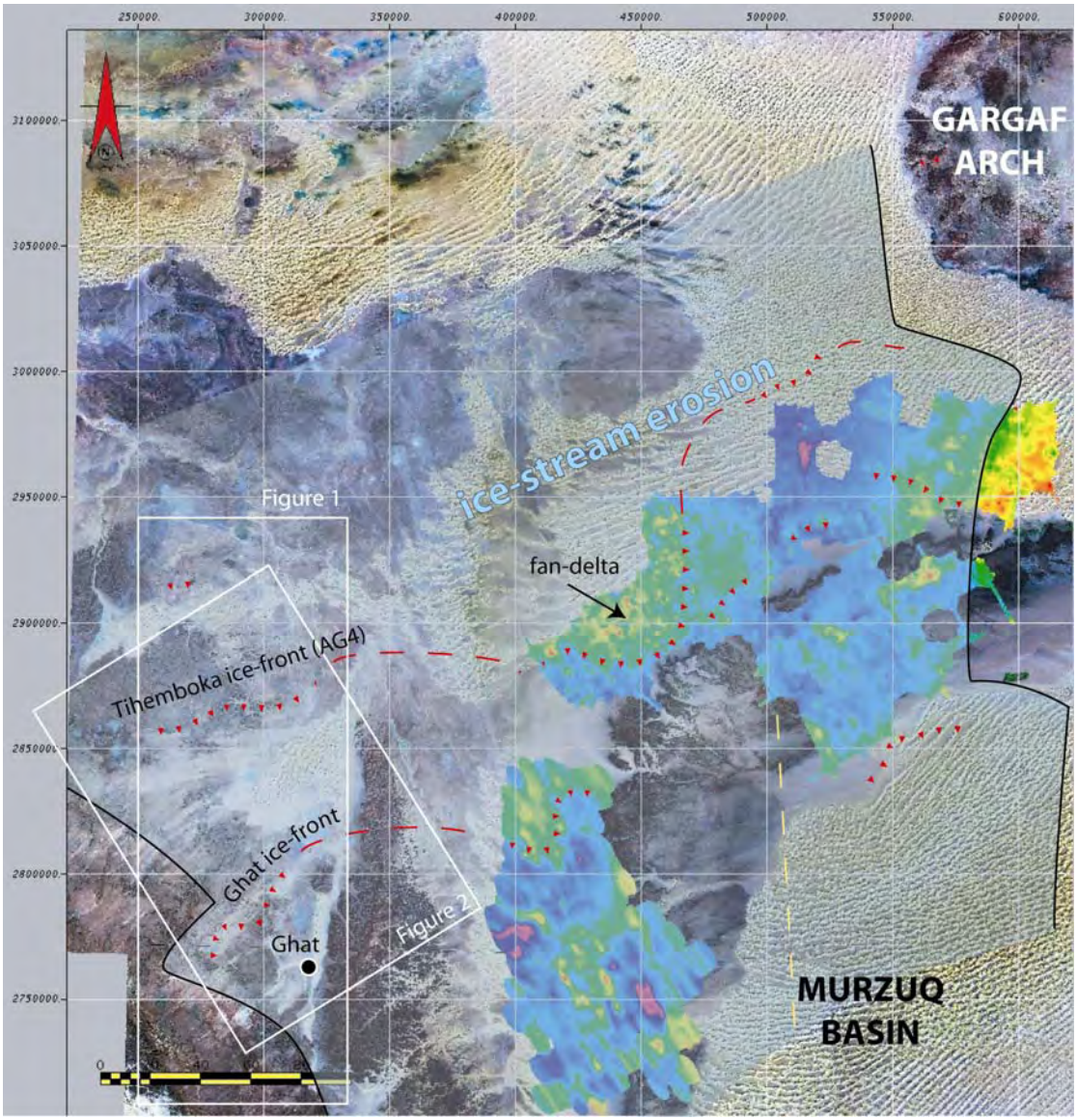

Figure 4: Late Ordovician glacially derived physiography from outcrop and subsurface analysis. Shaded area corresponds to ice-stream pathway (major erosion) during Hirnantian maximum. Red lines with triangles correspond to identified ice-fronts. Red dashed lines are proposed correlations between exposures and ice-front structures interpreted from subsurface data. The colored maps show physiography of base Silurian surface from seismic interpretation (yellow and green: higher area; blue and purple: lower areas). Landsat images come from Global Land Cover Facility: http://glcf.umiacs.umd.edu/.

This comparison between the outcrop and subsurface datasets allows the large-scale physiography of the Late Ordovician glaciated shelf to be reconstructed during final ice-sheet retreat and subsequent Silurian transgression. Features of ice-front and associated fan deltas in exposed areas are comparable to seismic interpretations within the Murzuq Basin. This work gives keys for Ordovician large-scale reservoir location and sedimentological heterogeneities. As Silurian "Hot Shale" occur in sheltered areas during Silurian transgression, the mapping of the major underfilled erosion (ice streams) is a key-point for the understanding of the Ordovician-Silurian play.

Ghienne J.-F., Le Heron D., Moreau J., Denis M., Deynoux M. [2006], in press, The Late Ordovician glacial sedimentary system of the North Gondwana platform. In : Hambrey, M., Christoffersen, P., Glasser, N., Janssen, P., Hubbard, B. and Siegert, M. (eds.) *Glacial Sedimentary Processes and Products.* Special Publication, International Association of Sedimentologists, Blackwells, Oxford.
Moreau, J., Ghienne, J.-F., Le Heron, D. P., Rubino, J.-L., Deynoux, M. [2005] 440 Ma ice stream in North Africa, Geology 33, 753-756.

4- Le maximum glaciaire ordovicien: des glaciers, jusqu'où?

Les surfaces glaciaires fini-ordovicienne d'Afrique (Beuf et al., 1971) et d'Arabie (Vaslet, 1990) sont connues de longue date. Des indices convaincants de surfaces d'érosion glaciaire ont récemment été découvert en Turquie (Monod et al., 2003). Dans les Monts Cantabriques au nord de l'Espagne, des vallées glaciaires ont maintenant été mises en évidence (Guttierez-Marco et al., 2010). Une telle vallée se devine dans la photographie ci-dessus au niveau du vallon central tapissé de bruyère (les pendages sont subverticaux).

Publications associées

Monod O., Kozlu H., Ghienne J-F., Dean W.T., Günay Y., Le Hérissé A., Paris F., Robardet M. (2003) Late Ordovician glaciation in Southern Turkey. Terra Nova, 15, 249-257.

Le Heron D., Ghienne J.-F., El Houicha M., Khoukhi Y., Rubino J.-L. (2007) Maximum extent of ice sheets in Morocco during the Late Ordovician glaciation. Palaeogeogr. Palaeoclimat. Palaeoecol., 245, 200-226.

Gutiérrez-Marco J.-C., Ghienne J.-F., Bernárdez E., Hacar M.P. (2010) Did the Late Ordovician African ice sheet reach Europe? Geology, 38, 279-282.

➔ Voir aussi

Ghienne et al., 2007b (Chapitre 6)

Ghienne et al., 2010b (Chapitre 1)

Loi et al., 2010 (Chapitre 2)

Si le Sahara et ses confins restent le domaine de prédilection pour l'analyse de l'enregistrement glaciaire fini-ordovicien, il est maintenant clair que l'inlandsis en a dépassé les limites. L'étude des zones périphériques, où chaque avancée glaciaire ne se marque pas nécessairement par une surface d'érosion, a été entreprise dans le double but de : (i) caractériser l'extension maximale des glaciers, (ii) établir la transition avec la plate-forme distale jamais englacée (cf. chapitre 5). Ainsi, des surfaces glaciaires ont-elles été identifiées en Turquie, sur la Meseta marocaine et même en Espagne.

- En Turquie, des faciès conglomératiques à la transition Ordovicien/ Silurien étaient connus depuis longtemps mais attribués à un conglomérat de base de la transgression silurienne. La mise en évidence de faciès glaciomarins nous a conduit à faire la revue systématique des affleurements présentant ces faciès, depuis les Nappes d'Antalya à l'ouest, sur la plaque Turque (Taurus occidental, central et oriental), et jusqu'à la région de Mardin sur la plaque Arabe (*Monod et al., 2003* ; *Ghienne et al., 2010b, §1*). Partout ont été retrouvés des faciès typiquement glaciaires avec des cortèges glaciomarins plus ou moins éloignés des fronts glaciaires. L'enregistrement sédimentaire des Nappes d'Antalya est le plus distal et met clairement en évidence deux cycles glaciaires attribués à l'Hirnantien (cf. chapitre 2 et section 6.4). La succession du Taurus oriental est beaucoup plus proximale. Il y a abondance de galets et blocs exotiques lâchés. Un fragment de surface glaciaire sous la forme d'une surface striée surmontée d'une tillite d'une vingtaine de centimètres d'épaisseur a été identifié. Sur la plaque Arabe, dans le secteur de Mardin, ce sont des linéations sous-glaciaires en pseudo drumlins qui ont été découvertes. Dans les deux cas, la surface glaciaire est positionnée à la base de la succession glaciomarine qui enregistrera la déglaciation fini-hirnantienne et passera en transition au Silurien. Elles indiquent ainsi que les glaciers ordoviciens ont atteint le niveau marin en Turquie lors du dernier cycle glaciaire.
- Au Maroc, la présence de l'inlandsis ordovicien était connue ou supposée en différents points de l'Anti-Atlas (Destombes et al., 1985 ; Michard et al., 2008) mais des faciès glaciomarins étaient réputés s'étendre tant au Haut Atlas (Ouanaimi, 1998) que dans l'ensemble du domaine de la Meseta (Huvelin, 1977). Une revue quasi systématique de ces affleurements en collaboration avec les collègues marocains des universités d'Oujda et de El Jadida nous a permis de confirmer que certaines zones n'avaient pas été atteintes par l'inlandsis ordovicien (Haut Atlas oriental, Tazzeka, Massif Central marocain). En revanche, des surfaces glaciaires ont été identifiées dans le Haut-Atlas, sous la forme de drumlins, et jusque dans les Rehamna, où une surface striée et une tillite métrique sus-jacentes ont été mises en évidence (*Le Heron et al., 2007*). Cette surface glaciaire est positionnée à la base de la séquence glaciomarine terminale de l'Ordovicien : elle est ainsi considérée comme synchrone de la surface glaciaire du Taurus oriental.
- En Espagne, où des faciès glaciomarins et deltaïques assez proximaux sont présents (Guttierez-Marco et al., 2002 ; Alvaro et Van Vliet Lanoë, 2009), avec de plus une surface d'érosion à la base de la succession, la présence de l'inlandsis est suspectée de longue date. Elle n'a cependant jamais été démontrée formellement. Dans les Monts Cantabriques, au nord de la péninsule, une série d'incisions à remplissage à cachet glaciaire a été découverte par les géologues étudiant le tracé d'un tunnel autoroutier. Il s'avère que ces incisions présentent toutes les caractéristiques de vallées en tunnel (largeur, profondeur, banquette à la base, remplissage proglaciaire, cf. section 3.3) (*Guttierez-Marco et al., 2010*). Les profondeurs d'incision et les remplissages peuvent localement dépasser 200 m d'envergure verticale. Ces vallées, totalement comblées ou sous-remplies selon les cas, sont scellées par les faciès transgressifs postglaciaires. Elles démontrent que des glaciers étaient présents à l'Ordovicien sur l'actuelle Europe et leur mise en évidence ouvre la voie à de nouvelles investigations.

Les surfaces glaciaires décrites ci-dessus sont associées au second cycle glaciaire de l'Hirnantien. Cette contemporanéité ne peut pas être confirmée par la biostratigraphie, qui n'a plus, à cette échelle, la résolution temporelle nécessaire. Ces surfaces sont cependant considérées comme synchrones par suite de leur relation stratigraphique avec les successions de déglaciation et de transgression postglaciaire sus-jacentes. Elles représentent autant de jalons marquant les fronts glaciaires du maximum hirnantien. Il en est de même des successions glaciaires d'Afrique du Sud (Vandenbroucke et al., 2009b) et d'Argentine (Sanchez et al., 1991). L'ensemble des régions gondwaniennes où les glaciers ont atteint le niveau marin est circonscrit dans un petit cercle assimilable, à l'Ordovicien, au 45ème parallèle de latitude sud, extension comparable au dernier maximum glaciaire (LGM) du Pléistocène (*Ghienne et al., 2007a, §6*). Cependant, il n'y a aucune garantie que ces différents points appartenaient à une même masse glaciaire. Pour Moix et al. (2008), les glaciers ordoviciens de Turquie ne seraient pas la prolongation de l'inlandsis nord-gondwanien mais des calottes glaciaires adossées à des épaules de rifts. La même interprétation pourrait être proposée pour l'Espagne. Mais l'enregistrement stratigraphique dans ces régions est à peu près continu de l'Ordovicien moyen au Silurien et aucune zone de reliefs n'a été détectée. On ne peut en revanche exclure l'existence de calottes périphériques incorporées à l'inlandsis gondwanien au moment du maximum glaciaire.

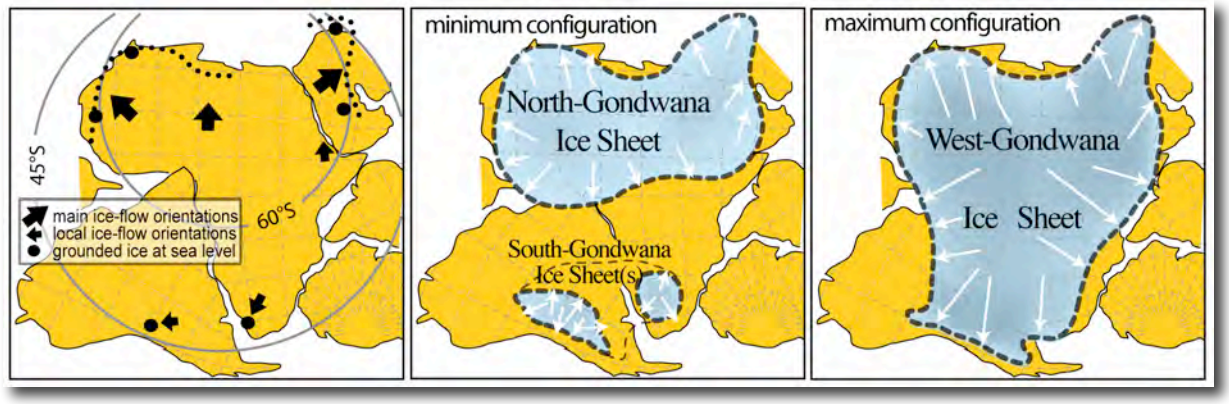

Autre question en débat : quelle était l'extension spatiale de cet inlandsis présent sur le nord-Gondwana ? Si une continuité des fronts glaciaires semble assurée de l'Arabie à la Mauritanie, la jonction avec les fronts sud-américain et sud-africain est plus problématique. Deux reconstructions, l'une dite minimaliste, l'autre maximaliste, sont proposées (*Ghienne et al., 2007a, §6* ; figure ci-dessus). Une extension minimaliste envisage un inlandsis nord-gondwanien qui englobait l'actuelle Afrique de l'Ouest, Afrique du Nord et l'Arabie et débordant au sud vers l'Afrique Centrale (Young et al., 2004 ; Le Heron et Dowdeswell, 2009). Les glaciers méridionaux correspondraient dans ce cas à des calottes adossées à des reliefs gondwaniens tels qu'un massif proto-andin (Diaz-Martinez et Grahn, 2007). L'extension maximaliste enserre l'ensemble de ces domaines, aboutissant au concept d'un vaste inlandsis installé sur l'ensemble du Gondwana occidental, inlandsis qui serait la plus importante masse de glace constituée durant le Phanérozoïque. La validation de l'une au l'autre de ces hypothèses par une estimation des chutes de niveau marin (100-150 m dans un cas, 200-250 m dans l'autre) se heurte à de nombreux problèmes tels que : estimation des paléobathymétries, importance des compensations isostatiques, volumes de glaces pérennes présents sur le continent dès avant et après l'épisode Hirnantien (*Loi et al., 2010, §2*). Enfin, maximum d'extension glaciaire ne signifie pas nécessairement volume maximum de glace. Le maximum hirnantien pourrait ne représenter qu'un épisode signant la fin de glaciation et pendant lequel un régime thermique moins sévère en base de glacier aurait permis l'étalement de l'inlandsis sur des surfaces plus étendues que celles couvertes par un inlandsis à base essentiellement froide, plus épais et donc plus volumineux.

doi: 10.1046/j.1365-3121.2003.00495.x

Late Ordovician glaciation in southern Turkey

O. Monod,[1] H. Kozlu,[2] J.-F. Ghienne,[3] W. T. Dean,[4] Y. Günay,[2] A. Le Hérissé,[5] F. Paris[6] & M. Robardet[6]

[1]*ISTO-CNRS, Université d'Orléans, 45067-Orléans, France;* [2]*TPAO, Exploration Group, M. Kemal Mah., 06520 Ankara, Turkey;* [3]*EOST, CNRS-CGS, 1 rue Blessig, 67084-Strasbourg, France;* [4]*Department of Geology, National Museum of Wales, Cardiff CF1 3NP, UK;* [5]*UBO, Dépt. Sc. de la Terre, 6 Av. Le Gorgeu, 29285 Brest, France;* [6]*UMR Géosciences, University Rennes I, 35042-Rennes, France*

ABSTRACT

We present a new survey of several Palaeozoic sections in both the Taurus range and the Border Folds that documents typical glacial features including a glacial pavement and striated dropstones (Halevikdere Formation) and demonstrates the former presence of an ice sheet in southern and south-eastern Turkey. Evidence for the late Ashgill (Hirnantian) age of this episode is provided by macro- and microfossils found within the glacial formation. The extension of ice-related deposits into the northernmost part of the Arabian Platform (Mardin region) implies a much wider distribution of the Ordovician ice sheet than was previously believed, and strongly suggests that southern Turkey lay close to Egypt during the Lower Palaeozoic.

Terra Nova, 15, 249–257, 2003

Introduction

Since the late 1960s, recognition of the extent of the Late Ordovician ice sheet in western Gondwana has increased progressively (e.g. Ghienne, 2003, and references therein). The existence of ice-related sediments of Late Ordovician age was established in northern (Beuf *et al.*, 1971), western (Deynoux and Trompette, 1981) and southernmost Africa (Hiller, 1992), in western Europe (review in Robardet and Doré, 1988), in Saudi Arabia (Vaslet, 1990) and more recently in Jordan (Abed *et al.*, 1993). In Turkey, however, the presence of Ordovician glacial deposits, although suspected (e.g. Göncüoglu and Kozlu, 2000), had not been demonstrated, but a new examination of several Lower Palaeozoic sections in the Central and Eastern Taurus has now provided evidence of ice-related, upper Ashgill sediments. Similar observations were also made in the Border Folds region (Derik–Mardin area). The purpose of this paper is to present the evidence for a late Ordovician glaciomarine episode in southern Turkey, and a reappraisal of the Ordovician–Silurian relationships there.

Correspondence: Olivier Monod, ISTO-CNRS, Université d'Orléans, 45067-Orléans, France. E-mail: olivier.monod@univ-orleans.fr

Upper Ordovician deposits in the Eastern Taurus

In the Taurus Range (Fig. 1), Upper Ordovician deposits have been recognized only intermittently, following their initial discovery in south-easternmost Turkey (Sort Tepe Formation, Dean *et al.*, 1981). By contrast, Silurian black shales were recognized long ago, thanks to their conspicuous, well-documented graptolite fauna (Özgül *et al.*, 1973), and their 'basal conglomerate' was considered to mark the beginning of a 'Silurian transgression' (Özgül *et al.*, 1973; Demirtasli, 1984; Dean and Monod, 1990; Kozur and Göncüoglu, 1998). These coarse-grained deposits are now dated as late Ashgill (Fig. 2), and reflect the proximity of an ice sheet, as shown below. In order to separate the ice-related deposits from non-glacial marine Ordovician and Silurian strata, the new term 'Halevikdere Formation' has been introduced (Ghienne *et al.*, 2001), with stratotype along the Halevikdere stream in the eastern Taurus, 2.5 km ESE of Degirmentas village (Sariz area) (Fig. 3), where the glacial record is best represented.

Ashgill preglacial deposits

The Halevikdere Formation rests upon the preglacial, shallow-marine Sort Tepe Fm. (100 m), which consists of finely laminated, siltstones and sandstones that grade upwards into red or green silty shales. The contact of the Sort Tepe Fm. with the overlying Halevikdere Fm. at its type section is transitional (Fig. 4a); in the uppermost 5 m of the Sort Tepe Fm., thin manganese-rich horizons are interstratified with green silty shales, and are followed by thin (< 5 cm) levels of sandy diamictite containing isolated quartz gravels.

In Sardinia, in the same stratigraphic position, Mn-rich deposits reflecting more oxidizing conditions occur just before the onset of the Hirnantian glaciation (Leone *et al.*, 1995; Ghienne *et al.*, 2000). The base of the Halevikdere Fm. is defined by the first deposition of thick sandstone beds.

Ice-related sediments and depositional environments (Halevikdere Fm.)

Eight sections of the Halevikdere Fm. were logged between the Sariz and Saimbeyli areas (Eastern Taurus, Fig. 3), showing only minor lateral facies changes (Fig. 5). The ice-related deposits are subdivided into lower, middle and upper sedimentary units.

Lower unit

The lower unit comprises a chaotic succession of irregular beds of massive, poorly sorted sandstone (Fig. 4a) that are in erosional or transitional contact with clast-bearing, structureless muddy sandstones. Fine- to coarse-grained, cross- to horizontally laminated sandstones form isolated beds, channel structures or large-scale (up to 3 m in diameter) ball-and-pillow structures. Channel structures are erosion-based, E–W-orientated

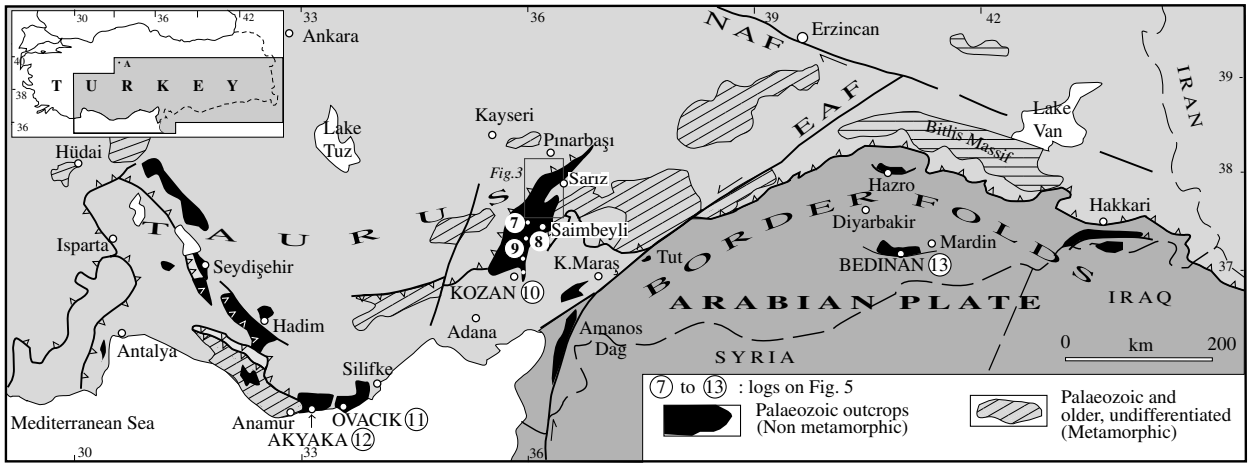

Fig. 1 Map of southern and south-eastern Turkey showing Palaeozoic outcrops.

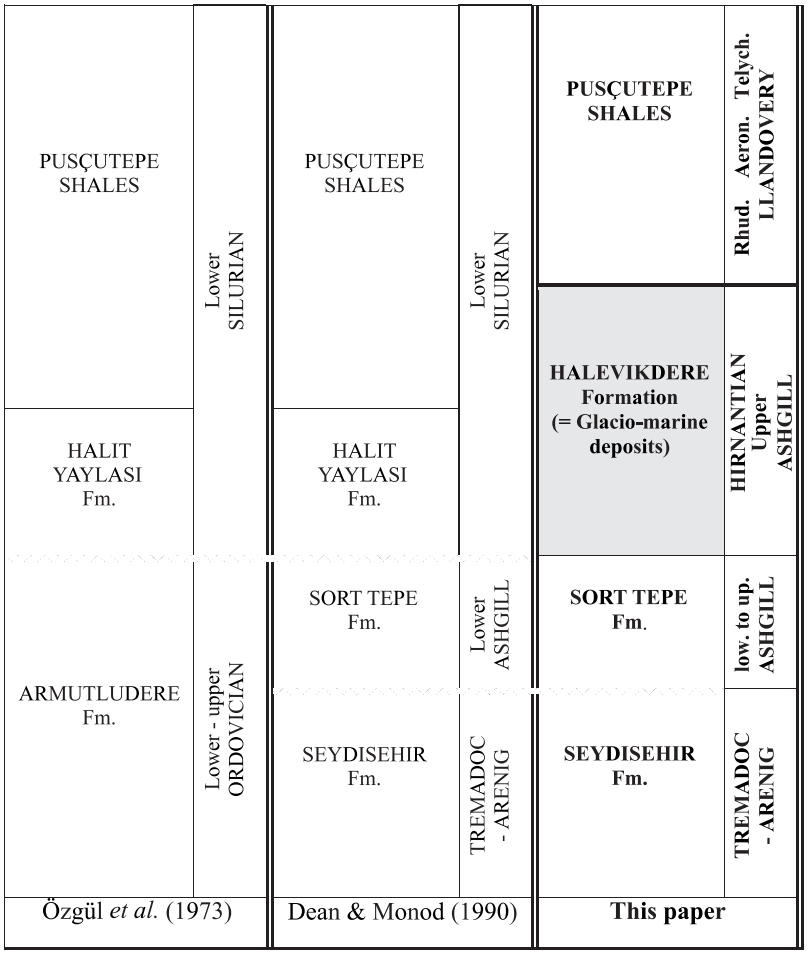

Fig. 2 Previous and new stratigraphic interpretations of the Lower Palaeozoic succession in the Eastern Taurus and the position of the Halevikdere Fm.

sandstone bodies, 0.5–10 m thick and 3–50 m wide. Larger channel structures are present within the upper part of the lower unit, along with well-sorted, quartz gravel conglomerate lenses.

The transitional contact with the underlying marine Sort Tepe Fm. demonstrates a submarine depositional setting. High rates of deposition, close to the sediment source, are suggested by: (1) the unsorted, chaotic character of the deposits; (2) numerous sandstone channels indicating stream-flow deposits in rapidly shifting channels; and (3) muddy sandstones, reflecting highly concentrated or cohesive debris flow deposits. The lateral continuity of the lower unit (Fig. 5) and the orientation of channels suggest a N–S- to NE–SW-orientated line source for the clastic material. Scattered striated pebbles (mainly vein quartz and granite, metamorphic rocks) indicate a nearby glacial source. In the higher horizons, better-sorted sands in larger channels, and gravel conglomerates that suggest winnowing by waves, reflect more ice-distal conditions.

Middle unit

The middle unit lies above a striated surface in the type section (Fig. 4b), where parallel striae and small-scale grooves, orientated N310, are preserved on a sandstone surface. The latter contains scattered pebbles (inset to Fig. 4c) with flattened upper surfaces exhibiting striae parallel to those preserved on the sandstone. A stiff, muddy sandstone horizon, 10 cm thick, directly overlies the striated surface. Above, the middle unit is made up of dark, structureless sandstones, which grade upwards into

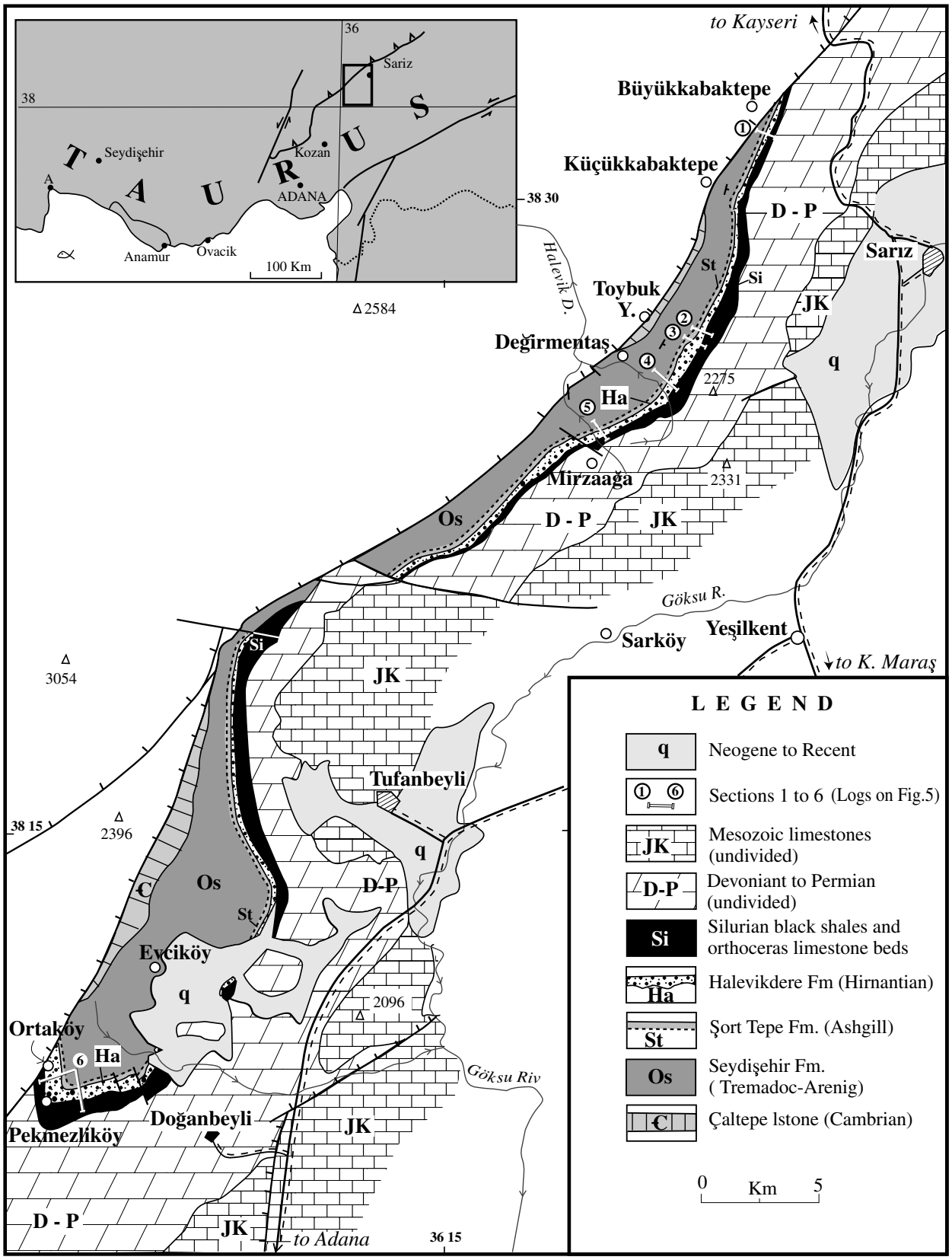

Fig. 3 Geological sketch-map of the Sariz–Tufanbeyli area, showing the lower Palaeozoic succession and the location of sections 1 to 6 (after TPAO map 1992, modified).

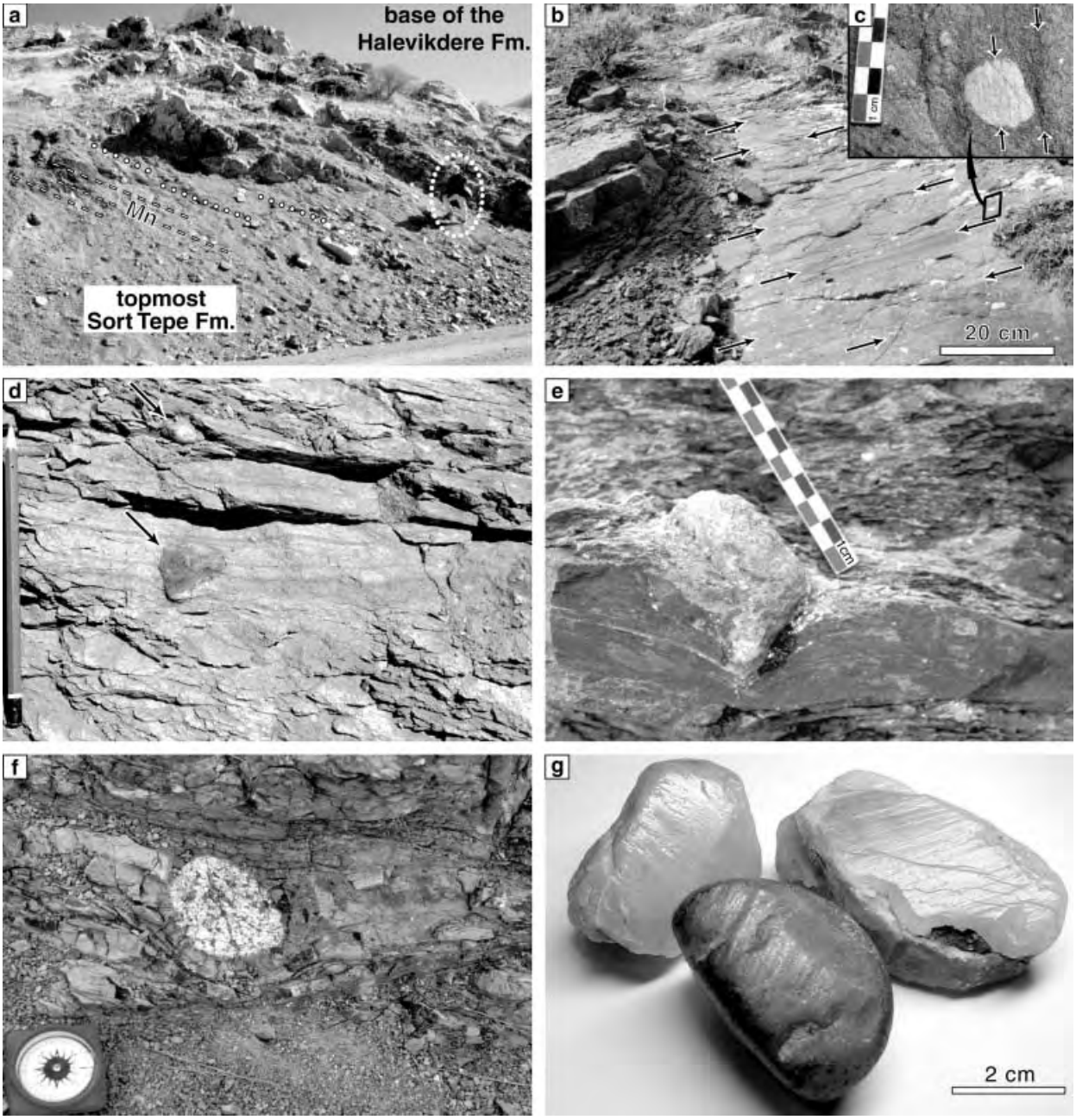

Fig. 4 Photographs of typical glacial features. (a) The Sort Tepe–Halevikdere Fm. transitional boundary showing the Mn-rich horizons (dashed lines) and the first input of ice-rafted debris (dotted lines) in the highest Sort Tepe Fm., and channels in the lower glacial unit (type section) (encircled person for scale). (b) Fragment of striated pavement (arrows) including (inset c) a striated pebble (type section). (d) Crudely laminated sandstones of the middle glacial unit with striated lonestones (type section). (e) *In-situ* dropstone (type section). (f) Granitic dropstone (Ovacik section, middle unit). (g) Striated pebbles from the glacial deposits overlying the Bedinan formation (Mardin region, northern Arabian plate).

stratified deposits with coarsening- and thickening-upwards, laterally discontinuous sequences, 1–3 m thick. Faintly laminated sandy siltstones in the lower part of each sequence grade upwards into sharp-based, non-graded sandstone beds (1–5 cm thick) alternating with mica-rich siltstone layers (<1 mm–2 cm thick). Sharp-based, well-sorted, fine-grained sandstone beds, made up internally of horizontal, low-angle or hummocky cross-stratification (HCS), are interstratified within the succession. In some places, striated, exotic dropstones can be seen in place, deforming sandstone beds (Fig. 4e). The middle unit forms an overall fining-upwards succession that ends with a thin (*c*. 15 cm) horizon of laminated silty shales.

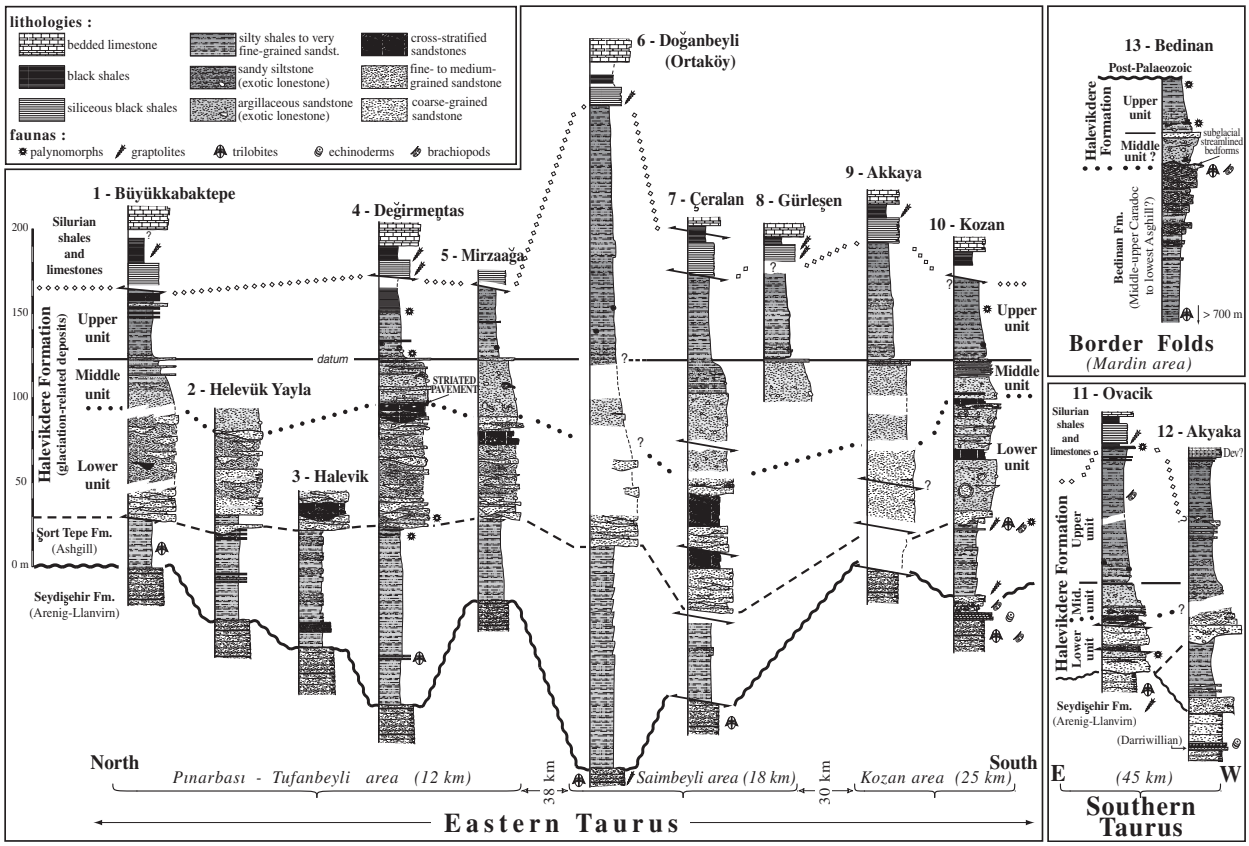

Fig. 5 Stratigraphic logs from the Eastern Taurus (1–10), the Southern Taurus (11, Ovacik; 12, Akyaka) and the Border Folds (13, Bedinan).

The striated surface represents a subglacial pavement upon which abrasion by in-ice debris has grooved unlithified sands, and striated the embedded pebbles. The overlying thin horizon may be considered as a subglacial tillite. Structureless sandstones are interpreted as disorganized muddy sands, deposited by ice-proximal, sand–mud debris-flows. Stratified sandstones reflect sandy gravity flow deposits, and their high sand-to-silt ratio and erosional contacts suggest deposition relatively close to the source, with intervening siltstone horizons indicating relatively ice-distal conditions. Coarsening-upwards sequences reflect the progradation of sandy lobes, punctuated by HCS-bearing storm deposits. The fall-out of ice-rafted dropstones indicates drifting icebergs.

Upper unit

In the type section, a rapid transition exists between the middle and upper units. The upper unit comprises an overall sandstone–siltstone–shale succession. Basal muddy sandstones, 0.5–2 m thick, are overlain by yellow to green, fining-upwards, sandy siltstones, with rare lonestones (granules to cobbles). This succession comprises intercalations of laminated, wavy bedded, black siltstones to very fine-grained, rippled sandstones. The upper boundary of the upper unit is generally mechanically disrupted in the black shales that underlie the siliceous beds of lower Silurian age. However, 200 m SW of the type-section, the first 2 m of the latter yielded index graptolites of the lowermost Llandovery (Kozlu *et al.*, 2002).

Sandstone deposition in the basal upper unit records an approaching sediment source. Within the siltstone succession, lonestones interpreted as dropstones suggest distal glaciomarine conditions. A deeper-water environment, mostly below storm-wave base (lower offshore?), characterizes the bulk of the upper unit.

Interpretation of the glaciomarine succession in the Eastern Taurus (Fig. 6)

As shown above, the onset of glaciation appears in the highest beds of the Sort Tepe Fm. Lower unit deposits reflect ice-proximal, subaquatic fan environments, which record the fluctuations of an ice-sheet margin of temperate type, as suggested by the permanence of meltwater and sand-dominated discharges. A proglacial outwash braid-plain delta environment in front of a terrestrial ice margin is suggested by the absence of ice-rafted debris. Better-sorted deposits in the upper part of the lower unit indicate a retreat of the glacial line source.

Succeeding a major glacial advance across the shelf, middle unit deposits suggest a submarine, ice-contact, grounding line-fan system (Powell, 1990). The recession of the ice-sheet margin is shown by the evolution from subglacial conditions (striated pavement) to ice-distal environments. The final

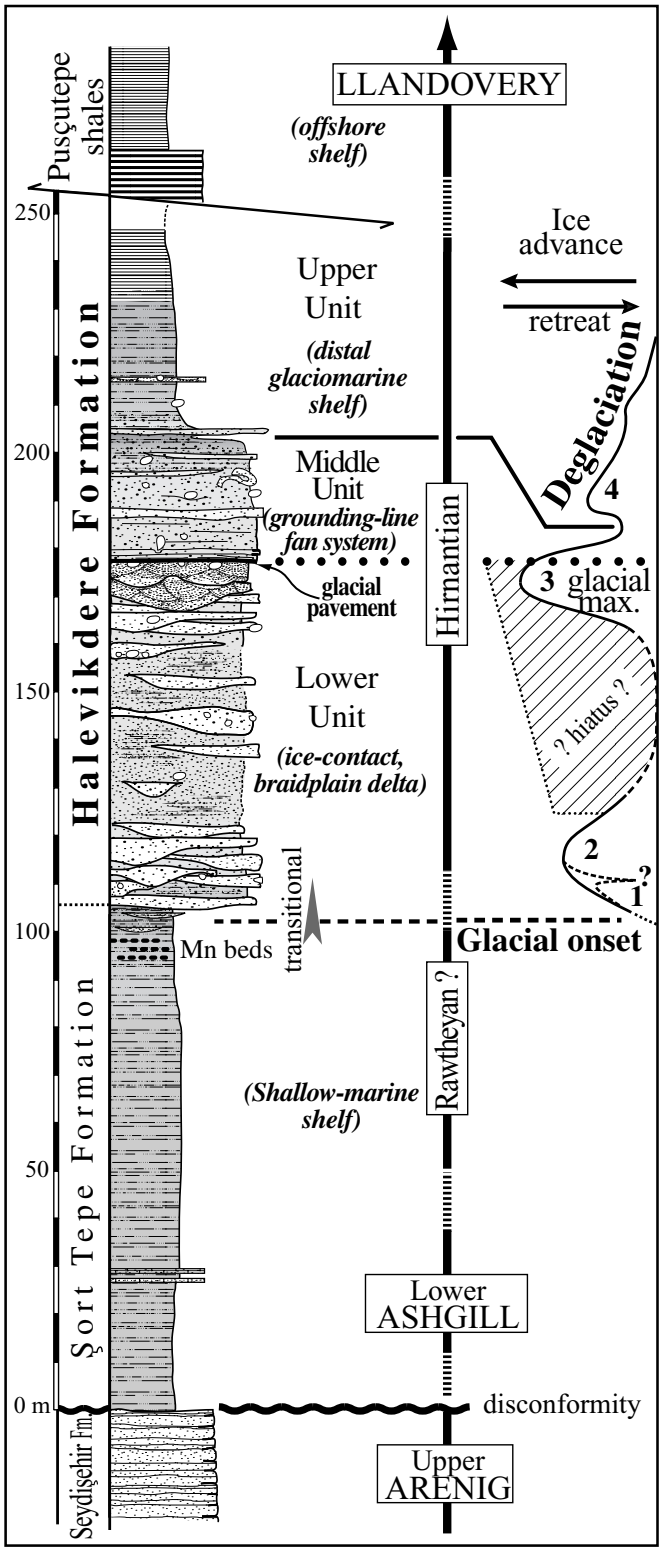

Fig. 6 Interpretation of glacial fluctuations along the Halevikdere Fm. stratotype.

deposition of silty shales records the disappearance of the glacial input and the onset of condensed sedimentation.

Finally, the fining-upwards, distal glaciomarine sediments of the upper unit reflect a late, but less extensive, glacial advance and subsequent retreat. The final marine flooding of the shelf marks the collapse of the Late Ordovician ice sheet. This deeper environment results in a transitional contact between the Halevikdere Fm. and inner-shelf black shales at the base of the Silurian strata.

Extent of the Halevikdere Fm. in southern and south-eastern Turkey

The three units defined in the Degirmentas area are readily recognizable at numerous sections in the Taurus range, from Anamur to Sariz. Some changes are noted in the lower unit which, north of Kozan (Fig. 5), comprises two sandstone-dominated subunits (cross-bedded channels in the lower, but wave-ripples and sorted gravel conglomerates in the upper) separated by a muddy interval containing large sand balls and numerous exotic, striated pebbles. This succession suggests that, at Kozan, the lower unit records two glacial fluctuations.

Near Akyaka village, 30 km east of Anamur (Figs 1 and 5), ice-related deposits rest disconformably along an irregular erosional surface above siliciclastic Ordovician strata that have not yet yielded macrofossils. The latter strata unconformably overlie limestone horizons in the highest Seydisehir Formation, from which conodonts of upper Darriwilian age have been reported (Sarmiento *et al.*, 1999). The lower unit there consists of coarse-grained, fining-upwards sandstones of fluvial to shallow-marine origin. The upper unit is followed by black, siliceous shales with middle Llandovery (Aeronian Stage, *convolutus* Zone) graptolites (Kozlu *et al.*, 2002).

West of Ovacik village, 30 km SW of Silifke (Figs 1 and 5), the lower unit rests upon sandstones and shales of the Seydisehir Fm. containing Arenig graptolites and trilobites (Dean and Monod, 1990). In the lower unit, clast-bearing argillaceous sandstones are overlain by well-sorted, coarse-grained, cross-bedded sandstones to fine-grained wave-rippled sandstones. This succession suggests wave reworking of glaciomarine deposits in a coastal environment. The overlying middle unit

contains abundant exotic dropstones (Fig. 4f), and the top of the upper unit is a conspicuous, erosion-based, psammitic sandstone bed, 0.4–2 m thick, underlying the Silurian shales. It is followed by black siliceous shales containing, 4 m from the base, Middle Llandovery graptolites of lower Aeronian age (*triangulatus* and *leptotheca* Zones, Kozlu *et al*., 2002).

The presence of ice-related sediments in the Border Folds of SE Turkey was unexpected. A Palaeozoic inlier, 15 km west of Mardin (Figs 1 and 5), contains the type-section of the Bedinan Fm., mainly Caradoc shales ending with storm-dominated sandstones. Directly above lie discontinuous patches of conglomeratic, coarse-grained sandstones, with extensional step fractures of glacial origin (Biju-Duval *et al*., 1974) and probable subglacial streamlined bedforms. Above are coarsening-upwards, fine- to coarse-grained, argillaceous sandstones that contain abundant faceted and striated pebbles (Fig. 4g) of quartz, rhyolite and granite. They are overlain by a fining-upwards succession ranging from argillaceous sandstones to silty shales, with occasional deformed sandstone masses. Clearly, the lowermost horizons of this glacial succession, situated in the northernmost part of the Arabian platform, differ from those in the Eastern Taurus. The upper deposits, however, similarly reflect the end-glacial flooding of the shelf in Late Ordovician times.

Review of biostratigraphic data

Degirmentas–Mirzaaga section

In the Sort Tepe Fm., rare trilobites (Dean and Monod, 1990) include *Nankinolithus*? (lowest Ashgill in China), *Hammatocnemis* of lower Ashgill type, *Cyclopyge* sp., and illaenids originally assigned to the closely similar genus *Zdicella* but better referred to *Ulugtella*, as noted by Hammann and Leone (1997, p. 95). The faunule suggests a level probably in the lower half of the Ashgill. Sampling of the Lower Silurian (Llandovery) black shales provided graptolites indicating the Rhuddanian (*acuminatus* Zone, det. Sachanski, in Kozlu *et al*., 2002) to Telychian stages.

Kozan area

Below the ice-related deposits, *c*. 30 m of grey–green mudstones are referred provisionally to the Sort Tepe Fm. They contain the blind illaenid *Ulugtella*, noted earlier from the Ashgill of Degirmentas and Kemer (Dean and Monod, 1990; Dean *et al*., 1999), where some cranidia are broadly comparable with specimens from Sardinia said to be of 'late Caradoc/early Ashgill' age (Hammann and Leone, 1997).

Ovacik area

At the coastal section west of Ovacik village (Fig. 5; review in Dean and Monod, 1990), the lower glacial unit overlies the Seydisehir Fm., dated here as lower Arenig by didymograptid graptolites and asaphid trilobites. The upper unit is of Ashgill and more precisely Hirnantian (*Tanuchitina elongata* zone, Paris *et al*., 1995) age, as indicated by chitinozoans (*Armoricochitina nigerica*, *Belonechitina* sp., *Desmochitina* and *Tanuchitina*), and poorly diversified acritarch assemblages, including tolerant forms (Netromorphs: *Leiofusa* spp., *Veryhachium* spp.) that are typical of stressed conditions during glaciomarine and deglaciation periods in the latest Ordovician (Paris *et al*., 2000). The assemblages also contain reworked elements (e.g. middle Ordovician *Stelliferidium* spp., or some acanthomorphs such as *Baltisphaeridium* spp.). Macrofossils are very rare but include the brachiopod *Mirorthis* sp. (det. L. R. M. Cocks), indicative of a Hirnantian age, as recorded in southern Sardinia (Hammann and Leone, 1997), and in other areas of Gondwanaland (review in Cocks, 1988).

Derik–Mardin area

The Bedinan inlier (Fig. 1) contains the type-section of the Bedinan Fm. (Kellogg, 1960; Dean, 1967), mostly middle to upper Caradoc shales with trilobites and brachiopods. The formation ends with a ferruginous sandstone horizon containing heterorthid brachiopods and a trilobite assemblage (*Calymenella boisseli*, *Dreyfussina*? sp.; Dean, 1983; Dean and Monod, 1990) that are generally considered as highest Caradoc or lowest Ashgill. At the base of the upper glacial unit, structureless muddy sandstones contain an acritarch assemblage that includes typical Ordovician forms together with some *Evittia* sp. and *Multiplicisphaeridium* spp., which, although of Silurian aspect, are generally considered to appear in the Caradoc/Ashgill and lower Ashgill, as already noted from wells in the Diyarbakir region (Steemans *et al*., 1996). At the top, chitinozoan assemblages include *Eisenochitina* gr. *lepta*, *Acanthochitina barbata* and *Armoricochitina nigerica*, which are good markers for the Ashgill in Northern Gondwana.

Conclusions and implications

The glaciomarine succession in the eastern Taurus records the fluctuations of a Late Ordovician ice sheet, most probably of Hirnantian age (Brenchley *et al*., 1994), in agreement with the fossil record. Three glacial events are recognized with confidence, the second of which corresponds to the glacial maximum during which southern Turkey was partly covered by ice. It is suggested that most of the succession in the eastern Taurus represents glacial retreat conditions. Southern Turkey thus appears in an intermediate position between the ice-proximal continental deposits of North Africa (Ghienne, 2003), and more ice-distal areas (e.g. Sardinia) where the glacial events are recorded within a continuously marine succession.

Implications concern the maximum extent of the Late Ordovician ice sheet, the position of the former Taurus platform along the northern Gondwana margin, and possible Silurian oil targets. In the Late Ordovician, southern Turkey lay in front of Egypt (e.g. Keeley, 1989), as a continuous ice front may now be drawn (Fig. 7) from northern Libya to the Border Folds of SE Turkey. This suggests that the Arabian platform was almost totally covered by ice, and consequently the granitic pebbles found in the Halevikdere Fm. must have come from the Proterozoic Arabian–Nubian shield, or from further south. From the petroleum exploration point of view, the Late Ordovician ice-proximal glacial

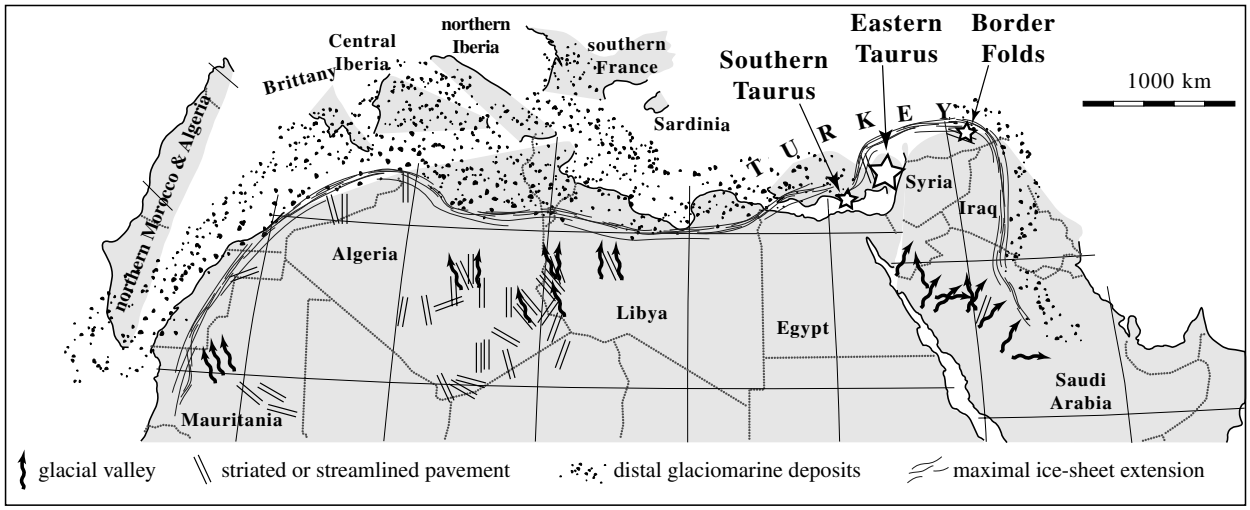

Fig. 7 Area covered by the Ashgill (Hirnantian) ice sheet, from North Africa to southern Turkey.

deposits in southern Turkey also suggest a potential extension of the lower Silurian source rocks (the 'hot shales', e.g. Lüning *et al.*, 2000) both in the Taurus range and in the Border Folds.

Acknowledgements

We are grateful to the following colleagues for interim determinations: Dr L. R. M. Cocks, Prof. R. B. Rickards, Dr V. Sachanski and Dr T. Tolmacheva. The useful comments of A. Okay and M. de Wit are acknowledged. This work was supported by CNRS-University units (ISTO, EOST) and the National Museum of Wales, and benefited from field work facilities provided by TPAO.

References

Abed, A.M., Makhlouf, I.M., Amireh, B.S. and Khalil, B., 1993. Upper Ordovician glacial deposits in southern Jordan. *Episodes*, **16**, 316–328.

Beuf, S., Biju-Duval, B., De Charpal, O., Rognon, P., Gariel, O. and Bennacef, F., 1971. Les grès du Paléozo inférieur au Sahara, Sédimentation et discontinuités, évolution d'un craton. *Publications de l'Institut français du Pétrole*, **18**, 464 pp.

Biju-Duval, B., Deynoux, M. and Rognon, P., 1974. Essai d'interprétation des "fractures en gradins" observées dans les formations glaciaires précambriennes et ordoviciennes du Sahara. *Rev. Géogr. Phys. Géol. Dyn.*, **16**, 503–512.

Brenchley, P.J., Marshall, J.D., Carden, G.A.F., Robertson, D.B.R., Long, D.G.F., Meidla, T., Hints, L. and Anderson, T.F., 1994. Bathymetric and isotopic evidence for a short-lived Late Ordovician glaciation in a greenhouse period. *Geology*, **22**, 295–298.

Cocks, L.R.M., 1988. Brachiopods across the Ordovician–Silurian boundary. *Bull. Br. Museum (Natural History), Geology*, **43**, 311–315.

Dean, W.T., 1967. The correlation and trilobite fauna of the Bedinan Formation (Ordovician) in south-eastern Turkey. *Bull. Br. Museum (Natural History), Geology*, **15**, 81–123.

Dean, W.T., 1983. Additional faunal data for the Bedinan Formation (Ordovician) of south-eastern Turkey. *Special Papers Palaeontol.*, **30**, 89–105.

Dean, W.T. and Monod, O., 1990. Revised stratigraphy and relationships of Lower Palaeozoic rocks, eastern Taurus Mountains, south central Turkey. *Geol Mag.*, **127**, 333–347.

Dean, W.T., Monod, O. and Perinçek, D., 1981. Correlation of Cambrian and Ordovician rocks in southeastern Turkey. Petroleum Activities at the 100th Year. *Türkiye Cumhuriyet Petrol. Isleri Müdürlügü Dergisi, Ankara*, **25**, 269–291 (English), 292–300 (Turkish).

Dean, W.T., Uyeno, T.T. and Rickards, R.B., 1999. Ordovician and Silurian stratigraphy and trilobites, Taurus Mountains near Kemer, southwestern Turkey. *Geol. Mag.*, **136**, 373–393.

Demirtasli, E., 1984. Stratigraphy and tectonics of the area between Silifke and Anamur, Central Taurus Mountain. In: *Geology of the Taurus Belt* (O. Tekeli and M. C. Göncüoglu, eds), pp. 101–118. MTA, Ankara.

Deynoux, M. and Trompette, R., 1981. Late Ordovician tillites of the Taoudeni Basin, West Africa. In: *Earth's Pre-Pleistocene Glacial Record* (M. J. Hambrey and W. B. Harland, eds), pp. 89–96. Cambridge University Press, Cambridge

Ghienne, J.-F., 2003. Late Ordovician sedimentary environments, glacial cycles, and post-glacial transgression in the Taoudeni Basin, West Africa. *Palaeogeogr. Palaeoclim. Palaeoecol.*, **189**, 117–145.

Ghienne, J.-F., Bartier, D., Leone, F. and Loi, A., 2000. Caractérisation des horizons manganifères de l'Ordovicien supérieur de Sardaigne: relation avec la glaciation fini-ordovicienne. *C.R. Acad. Sci. Paris*, **331**, 257–264.

Ghienne, J.-F., Kozlu, H., Dean, W.T., Günay, Y. and Monod, O., 2001. Discovery of the northernmost Gondwanan evidence of an upper Ordovician glacier: Southern Turkey. *EUG XI, Strasbourg April 2001*, Abstract, p. 103. *J. Conf. Abs.* **6**. (Cambridge Publications).

Göncüoglu, M.C. and Kozlu, H., 2000. Early Palaeozoic evolution of the NW Gondwanaland: data from southern Turkey and surrounding regions. *Gondwana Res.*, **3**, 315–324.

Hammann, W. and Leone, F., 1997. Trilobites of the post-Sardic (Upper Ordovician) sequences of the Iglesiente, Arburese and Sarrabus regions, southern Sardinia, Italy. Part 1. *Beringeria*, **20**, 1–217.

Hiller, N., 1992. The Ordovician System in South Africa: a review. In: *Global Perspectives on Ordovician Geology* (L. Webby, ed.), pp. 473–485. Balkema, Rotterdam.

Keeley, M.L., 1989. The Palaeozoic history of the Western Desert of Egypt. *Basin Res.*, **2**, 35–48.

Kellogg, H.E., 1960. *Stratigraphic Report, Derik–Mardin area, Petroleum District VI, Southeast Turkey*. Report of the Exploration Division, American Petroleum Ltd, Ankara.

Kozlu, H., Günay, Y. and Sachanski, V., 2002. *Stratigraphy and graptolite biostratigraphy of the Lower Silurian succession in SE Anatolia and the Taurus Belt*. TPAO Exploration Group, Ankara.

Kozur, H. and Göncüoglu, C., 1998. Main features of the pre-Variscan development in Turkey. *Acta Universitatis Carolinae-Geologica*, **42**, 459–464.

Leone, F., Loi, A. and Pillola, G.L., 1995. The post Sardic Ordovician sequence in SW Sardinia. In: *6th Palaeobenthos International Symposium* (A. Cherchi, ed.), Guide book, pp. 81–108. Cagliari University.

Lüning, S., Craig. J., Loydell, D.K., Störch, P. and Fitches, B., 2000. Lower Silurian 'hot shales' in North Africa and Arabia: regional distribution and depositional model. *Earth-Sci. Rev*., **49**, 121–200.

Özgül, N., Metin, S., Erdogan, B., Göger, E. and Bingöl, O., 1973. Cambrian–Tertiary rocks of the Tufanbeyli region, eastern Taurus, Turkey. *Bull. Geol. Soc. Turkey*, **16**, 82–100 (in Turkish).

Paris, F., Bourahrouh, A. and Le Hérissé, A., 2000. The effects of the final stages of the Late Ordovician glaciation on marine palynomorphs (chitinozoans, acritarchs, leiospheres) in well NL-2 (NE Algerian Sahara). *Rev. Paleobot. Palynol*., **113**, 87–104.

Paris, F., Elaouad-Debbaj, Z., Jaglin, J.C., Massa, D. and Oulebsir, L., 1995. Chitinozoans and Late Ordovician glacial events on Gondwana. In: *Ordovician Odyssey: Short Papers for the 7th ISOS, Las Vegas* (J. C. Cooper, M. L. Droser and S. Finney, eds). *Society for Sedimentary Geology, Pacific Section*, **77**, 171–176.

Powell, R.D., 1990. Glacimarine processes at grounding-line fans and their growth to ice-contact deltas. In: *Glacimarine Environments: Processes and Sediments* (J. A. Dowdeswell and J. D Scourse, eds). *Geol. Soc. Spec. Publ*., **53**, 53–73.

Robardet, M. and Doré, F., 1988. The Late Ordovician formations from SW Europe: North-Gondwana glaciomarine deposits. *Palaeogeogr. Palaeoclimatol. Palaeoecol*., **66**, 19–31.

Sarmiento, G.N., Gül, M.A., Kozlu, H. and Göncüoglu, M.C., 1999. Darriwilian conodonts from the Taurus Mountains, southern Turkey. *Acta Universitatis Carolinae, Geologica*, **43**, 37–40.

Steemans, P., Le Hérissé, A. and Bozdogan, N., 1996. Ordovician and Silurian cryptospores and miospores from southeastern Turkey. *Rev. Palaeobot. Palynol*., **93**, 35–76.

Vaslet, D., 1990. Upper Ordovician glacial deposits in Saudi Arabia. *Episodes*, **13**, 147–161.

Received 2 October 2002; revised version accepted 21 May 2003

Available online at www.sciencedirect.com
ScienceDirect
ELSEVIER
Palaeogeography, Palaeoclimatology, Palaeoecology 245 (2007) 200–226
PALAEO
www.elsevier.com/locate/palaeo

Maximum extent of ice sheets in Morocco during the Late Ordovician glaciation

Daniel Paul Le Heron [a,b,*], Jean-François Ghienne [a], Mohamed El Houicha [c], Yahya Khoukhi [d], Jean-Loup Rubino [e]

[a] *École et Observatoire des Sciences de la Terre, 1 rue Blessig, 67084 Strasbourg Cedex, France*
[b] *CASP, Department of Earth Sciences, University of Cambridge, West Building, 181a Huntingdon Road, Cambridge, CB3 ODH, United Kingdom*
[c] *Université Chouaib Doukkali, El Jadida, Morocco*
[d] *Faculté des Sciences, Université Mohamed Ier, Oujda, Morocco*
[e] *CSTJF, Total, Avenue Laribeau 64018 Pau, France*

Received 14 February 2005; accepted 2 February 2006

Abstract

New field data demonstrate that during the Late Ordovician (Hirnantian) glaciation, an ice sheet expanding northwestwards over the Anti-Atlas range reached into the southern Meseta of northern Morocco. Its growth to a glacial maximum position resulted in extensive subglacial erosion and deformation including the development of soft-sediment striated surfaces and streamlined subglacial bedforms preserved between the High Atlas of Marrakech and Rehamna. These features imply that this ice mass extended >200 km further than previously thought, and increase its size by at least ca. 190, 000 km^2 (comparable in area to the UK). Correlation between a measured section in the High Atlas of Marrakech and that of the southern Meseta identifies sedimentary evolution within an ice-contact system common to both. These findings imply that the West African Craton and northern Morocco were in full glaciological communication during the latest Ordovician. Palaeogeographic reconstruction shows that beyond the ice sheet, south and southeastward palaeoslopes persisted on the shelf. A palaeohigh beyond the main ice sheet was a major source for sand, feeding delta systems that grew along the shelf as far as the shelf break. This palaeohigh probably formed as a result of rift shoulder uplift and supported a satellite ice mass. In the eastern Meseta, a thick (350 m) underflow-dominated deep-marine fan was fed both from this shelf delta system and from glaciogenic debris derived from the main ice sheet. The occurrence of this unexpected deep-marine area in northern Morocco implies that continued northward advance of the ice sheet was hampered by a dramatic break in bathymetry. Two depositional units are recognised across the Meseta, containing four distinct sedimentary cycles, each recognised as a glacioeustatic response to the waxing and waning of ice masses elsewhere in West Gondwana.

Keywords: Glaciation; Ordovician; Morocco; Ice sheet; Gondwana

1. Introduction

During the latest Ordovician glaciation, an ice sheet grew and decayed over West Gondwana in <1 my (Brenchley et al., 1994). During the Hirnantian (Destombes et al., 1985), a stage coeval with the *elongata* and

* Corresponding author. CASP, Department of Earth Sciences, University of Cambridge, West Building, 181a Huntingdon Road, Cambridge, CB3 ODH, United Kingdom. Tel.: +44 1223 277586; fax: +44 1223 276604.
E-mail address: daniel.leheron@casp.cam.ac.uk (D.P. Le Heron).

0031-0182/$ - see front matter © 2006 Elsevier B.V. All rights reserved.
doi:10.1016/j.palaeo.2006.02.031

following *oulebsiri* chitinozoan biozones (Bourahrouh et al., 2004), this glacier covered the main part of northern and western Africa (e.g., Beuf et al., 1971; Deynoux, 1985; Ghienne, 2003). The ice was complex and dynamic and characterised by migrating ice fronts during successive phases of ice advance and recession (Ghienne, 2003). The number of glacial cycles preserved in West Gondwana is controversial and varies between 2 and 5; see additional reviews in Rust (1981), Sutcliffe et al. (2000, 2001) and Le Heron et al. (2005).

The record of Hirnantian ice sheet growth is largely preserved in the form of glaciotectonic deformation structures within unconsolidated glacial sediments. They include complex subglacial shear zones, decametre-scale sediment diapirs, load-structures and pluri-kilometric composite thrust and fold systems (Beuf et al., 1971; Biju-Duval, 1974; Ghienne, 2003; Deynoux and Ghienne, 2004; Le Heron et al., 2005). Phases of ice-sheet decay were accompanied by the incision of ca. 100–200 m deep, 2–5 km wide anastomosing tunnel valleys from Mauritania to Libya (Ghienne and Deynoux, 1998; Hirst et al., 2002; Ghienne et al., 2003; Le Heron et al., 2004). It is clear that repeated cannibalisation of these areas during successive phases of glaciation has made reconstructing a proximal–distal shelf profile somewhat difficult.

In Morocco (Fig. 1), Destombes (1968) showed that the ice sheet grew over the Tindouf Basin as far as the Anti-Atlas in the south of the country. Extension further northward, over the Southern Atlas Thrust and into the

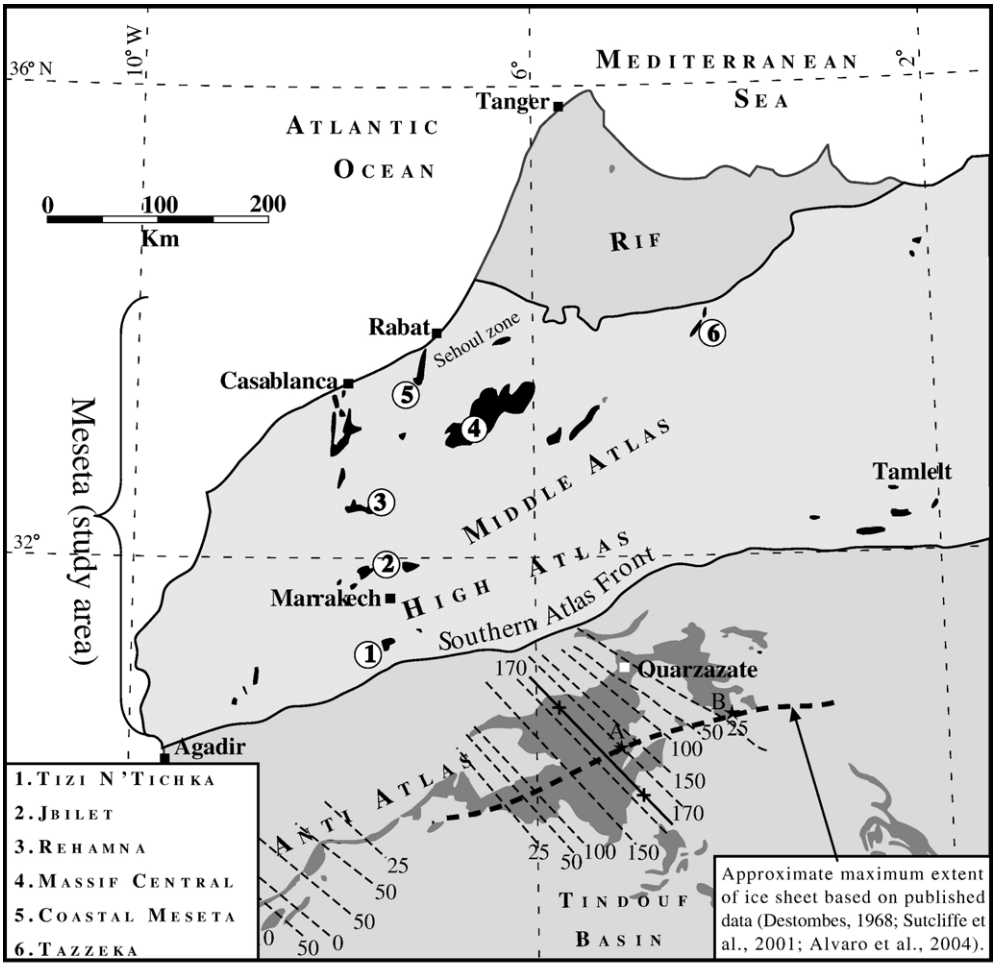

Fig. 1. Location map of Morocco. Lower Palaeozoic inliers in the Meseta and High Atlas regions are shown in black, whereas those in the Anti-Atlas are shown in grey. Numbers indicate inliers examined during the course of this study. Contours are isopachs drawn for the pre-glacial upper Ordovician (Ashgill) Upper Ktaoua Formation in the Anti-Atlas (from Destombes et al., 1985). These data give a good impression of topography on the pre-glacial substrate (axis of depositional trough is marked). Previous estimation of the Late Ordovician glacial maximum in this region put the ice front in the Anti Atlas (stippled line; Destombes, 1968). Control data points in the Anti Atlas are the Zagora/Tagounite areas (A) and the Erfoud area (B).

Meseta (Moroccan Hercynides) has never been demonstrated, partly because the tectonic relationship between the Meseta and the West Gondwana cratonic shelf remains highly controversial. It is debated whether these areas were in full palaeogeographic communication (e.g., Piqué and Michard, 1989; Paris et al., 1995; Sutcliffe et al., 2001). Solving these palaeogeographic problems will provide constraints on both the maximum size of the Late Ordovican ice sheet and the reconstruction of the Hercynides.

This paper attempts to define the Late Ordovician ice maximum in Morocco, and presents sedimentological evidence that the Moroccan Hercynides (Meseta) were connected to the West Gondwana cratonic shelf during the Lower Palaeozoic. The Late Ordovician glacial record in Morocco is unique in that it is one of the only regions in North Africa where the ancient glacial maximum can be determined at outcrop and not from unpublished well data (cf. Beuf et al., 1971). In addition, in a manner analogous to the analysis of Pleistocene glaciated shelves, it is the first attempt to describe, at a basin scale, the architectural linkage between proglacial shallow shelf through shelf edge to slope systems and the direct response of these systems to this polyphased glaciation.

2. Regional geological setting

Throughout the Phanerozoic, central parts of North Africa were characterised by tectonic stability with only relatively minor, intraplate deformation (Selley, 1997). In contrast, the evolution of the West Gondwana margin (e.g., Spain, Turkey, Morocco) was complex and characterised by phases of rifting, basin development, inversion and orogenesis during the Phanerozoic (e.g., Piqué and Michard, 1989; Piqué, 2001).

From north to south, four distinct tectonostratigraphic domains are recognised in Morocco, namely, the Rif, Meseta, High Atlas and Anti-Atlas (Piqué, 2001) (Fig. 1). The Meseta comprises a belt of Hercynian deformation that runs between the alpine Rif and High Atlas domains (Piqué and Michard, 1989). In the south of the country, a major structural discontinuity (the Tizi N′ Test fault and its associated splay) separate the High Atlas from the Anti-Atlas domain, which comprises a large antiform corresponding to a thick-skinned inversion belt related to the Hercynian uplift of the Precambrian basement of the West African craton (Fabre, 1971; Soulaimani, 1998; Caritg et al., 2004) (Fig. 1).

Some regional palaeogeographic reconstructions have shown northern Morocco as an allochthonous terrane (e.g., Sutcliffe et al., 2001; Monod et al., 2003), despite its Lower Palaeozoic stratigraphic similarity with the Anti-Atlas (Destombes, 1971; Destombes et al., 1985), and the common NE–SW-striking Hercynian grain that these regions share (Piqué and Michard, 1989). Intense controversy remains, and compromise models depicting rift margins have also been developed. Extensive Cambrian graben formation in the western part of Meseta (Bernardin et al., 1988; El Attari et al., 1997) and in the western High Atlas (Cornée et al., 1987) was mirrored in the Anti-Atlas (Piqué et al., 1990; Piqué et al., 1995), lending support for failed rifting in NW Africa during the earliest Palaeozoic. For the Late Ordovician, sedimentary models show a large NE–SW-oriented trough or basinal depression in the Meseta (Hamoumi, 1988; Khoukhi and Hamoumi, 2001) subsequently amplified during the Devonian (Piqué, 2001). In addition, during the mid-Late Ordovician, around 455–445 Ma, a thermal event (Clauer et al., 1995) is identified and the eruption of Silurian alkali basalts occurred in the coastal (north-western) Meseta (El Kamel et al., 1998). These data led Stampfli and Borel (2002) to interpret a renewed phase of rifting by the beginning of the Silurian.

A clear evaluation of the tectonic setting of the northern Morocco is vital for the reconstruction of Late Ordovician ice sheets because it could reasonably be expected to have had a controlling influence on the distribution of grounded ice. If northern Morocco was an allochthonous terrane, evidence for Late Ordovician grounded ice sheets should not be present. Conversely, evidence for the presence of ice sheets could present a strong case for its palaeogeographic continuity with Gondwana.

3. Structural evolution

In northern Morocco, upper Ordovician rocks crop out within large but disconnected Lower Palaeozoic inliers (Fig. 1). During the course of this study, data were collected from the Tazzeka Massif (Middle Atlas, eastern Meseta), the coastal Meseta, from three major Palaeozoic massifs (Massif Central, Rehamna, and Jbilet areas), and from the High Atlas of Marrakech (central High Atlas) (Fig. 1). The inliers were significantly deformed during the Hercynian Orogeny (Devonian to Carboniferous), which is partly concealed by post-orogenic Mesozoic cover. The Meseta was then subject to Alpine tectonism (Piqué and Michard, 1989; Piqué et al., 1993). Therefore, a brief synopsis of its Hercynian tectonic history is necessary to explain the present distribution of Lower Palaeozoic inliers.

In the Meseta, pre-Hercynian deformation is locally intense but probably had little influence on the distribution of upper Ordovician rocks. Caledonian folding and metamorphism occurred at its northern margin in the

Table 1
Simplified stratigraphic comparison of formation names for pre-glacial, syn-glacial and post-glacial strata in Morocco

	Anti-Atlas	Rehamna	Massif Central	Coastal Meseta	Tazzeka
Post-glacial	Ain Delouine Formation	El Mesrane Formation	Sidi M'Bellej Formation	Unnamed shale formation	Unnamed shale formation
Syn-glacial	Upper Second Bani Formation	Goulibet Formation	Ezzhiliga Formation	Informal "Douar–Zrahna formation" of Sutcliffe et al. (2001)	Tifarouine Formation
Pre-glacial	Lower Second Bani Formation	El Mechech Formation	Ould Akra Formation	Unnamed	Tehar El Brehl Formation

Formalised stratigraphies exist in the Anti Atlas (Destombes et al., 1985), Massif Central (e.g., Razin et al., 2001) and Tazzeka Massif (Destombes et al., 1985; Khoukhi and Hamoumi, 2001). A stratigraphic scheme awaits formalisation in the Rehamna where an active mapping programme is currently underway (P. Razin, personal communication). An informal formation name (Douar–Zrahna formation) for syn-glacial strata was suggested for the Coastal Meseta region by Sutcliffe et al. (2001). No formalised stratigraphy exists for either the High Atlas of Marrakech or Jbilet regions.

Sehoul zone (Piqué et al., 1993), and was followed by the emplacement of small granitoids at 430±2 Ma (El Hassani et al., 1991). In contrast, Hercynian deformation, associated with the closure of the Proto-Tethys in the "middle" Palaeozoic and collision of Gondwana with Laurussia (Badalini et al., 2002) was severe. This orogeny was the primary control on the distribution of upper Ordovician strata (Piqué and Michard, 1989). Deformation was polyphase and heterogeneous, propagating westward during the Devonian to the Carboniferous. On the basis of the timing of Hercynian deformation (Piqué and Michard, 1989; Laville and Piqué, 1991), two major tectonic zones can be distinguished within Lower Palaeozoic basement of the High Atlas and Meseta.

Zone 1 includes the eastern Massif Central, the eastern Jbilet, Tazzeka Massif, as well as those outcrops in the eastern Meseta not considered here (Midelt, Debdou, Mekam). Deformation in this zone was characterised by an early phase of westward-directed folding and/or thrusting, during the late Devonian to late Visean (Eovariscan, Breton or Sudete phases: Allary et al., 1976; Hoepffner, 1987; Bouabdelli, 1989). This deformation resulted in significant stratigraphic repetition of the Cambro-Ordovician succession, most clearly demonstrated in the western Tazzeka Massif (Hoepffner, 1987), but also in the eastern Massif Central, eastern Jbilet and Ait Tamlil (Jenny, 1983; Bamoumen, 1988; Bouabdelli, 1989; El Houicha, 1994). Zone 1 was then affected by transtension, whereby a basin bounded by NE–SW-trending dextral faults, accompanied by andesitic volcanism, formed at the western margin of the Eastern Meseta (Bouabdelli, 1989). Renewed compression formed syn-sedimentary and gravitational nappes in Ordovician to Devonian rocks (Allary et al., 1972; Huvelin, 1977; Hollard et al., 1977; Jenny, 1983; Bouabdelli, 1989), thrust west or northwest during the late Visean–Namurian (Bouabdelli, 1989).

Zone 2 lacks Eovariscan structures and deformation was restricted to the late Carboniferous. The western part of this zone, including the extreme west of the Massif Central, western Rehamna, western Jbilet and Isk N'Tazzoult in the High Atlas of Marrakech, was weakly deformed, except at its eastern extremity near the NE–SW-oriented Western Meseta Shear Zone (Piqué et al., 1980). Deformation in this zone is characterised by upright, pluri-kilometric open folds associated with nearly vertical wrench faults or reverse faults (El Attari, 2001), variously dipping shear zones and syn- to late kinematic granites (Piqué, 1979; Lagarde and Michard, 1986). In the westernmost Massif Central, the fold structures consist of NE–SW-oriented anticlinoria cored by Lower Palaeozoic strata, whereas southward, in the central Rehamna, central Jbilet and High Atlas of Marrakech, NNE–SSW-striking thrusts formed during 3–4 phases of deformation (Piqué and Michard, 1989). This was followed by extension and gravity collapse in the Rehamna (Aghzer and Arenas, 1995; Razin et al., 2001; Baudin et al., 2001), western High Atlas (Cornée et al., 1987), and probably in the western Massif Central (Baudin et al., 2001). Within this zone, the relative absence of deformation in the Lower Palaeozoic block of the High Atlas of Marrakech compares to the Anti-Atlas against which it is juxtaposed (Piqué and Michard, 1989). Structurally, it is thus considered to belong to the Anti-Atlas domain (Ouanami and Petit, 1992).

Despite the overall intensity of deformation, the consistent orientation of metamorphic isograds, cleavage, and thrust faults between the Coastal Meseta, Massif Central, Rehamna and Jbilet massifs implies that the Lower Palaeozoic inliers are, at a regional scale, mainly autochthonous (Piqué and Michard, 1989). However, it should be emphasised that regional thrusting involving the basement may result in an underestimation of the pre-tectonic distances between

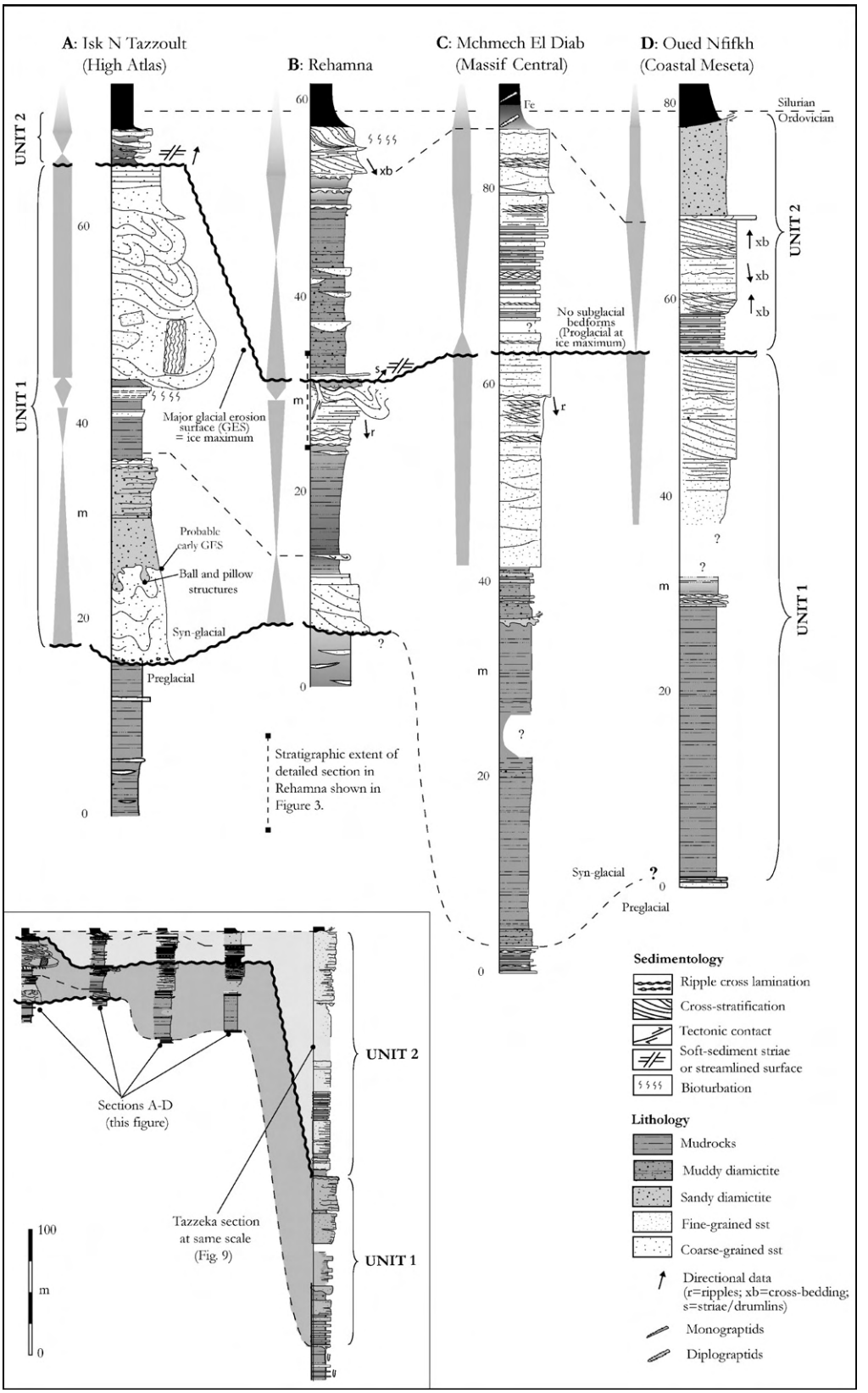
A: Isk N Tazzoult
(High Atlas)
B: Rehamna
C: Mchmech El Diab
(Massif Central)
D: Oued Nfifkh
(Coastal Meseta)
UNIT 2
UNIT 1
Major glacial erosion surface (GES) = ice maximum
Probable early GES
Ball and pillow structures
Syn-glacial
Preglacial
Stratigraphic extent of detailed section in Rehamna shown in Figure 3.
No subglacial bedforms (Proglacial at ice maximum)
Silurian
Ordovician
Sections A-D (this figure)
Tazzeka section at same scale (Fig. 9)
Sedimentology
Ripple cross lamination
Cross-stratification
Tectonic contact
Soft-sediment striae or streamlined surface
Bioturbation
Lithology
Mudrocks
Muddy diamictite
Sandy diamictite
Fine-grained sst
Coarse-grained sst
Directional data (r=ripples; xb=cross-bedding; s=striae/drumlins)
Monograptids
Diplograptids

the localities described in this paper (particularly in the Jbilet; Huvelin, 1977). These problems must be borne in mind during palaeogeographic reconstruction.

Following the Hercynian orogeny, a period of WSW–ENE-oriented crustal extension ensued with the onset of mid-Atlantic rifting in the Triassic (Piqué et al., 2002). Rift basins were infilled from the early Liassic, then inverted by transpressional deformation during the Middle Jurassic. This deformation was then overprinted during the Atlas Orogeny in the Cenozoic (Piqué et al., 2002). These post-Hercynian deformation events did not influence the distribution of Lower Palaeozoic inliers (Piqué and Michard, 1989).

4. Late Ordovician glaciation in northern Morocco

Hirnantian (syn-glacial) strata are generally devoid of macrofossils in northern Morocco. However, Ashgill fauna are identified in the underlying strata (Razin et al., 2001 and references therein) and a lowermost Silurian graptolite-bearing shale is generally found above the syn-glacial strata (Destombes and Willefert, 1988) (Table 1). This shale is therefore a useful lithostratigraphic guide, and correlation with the syn-glacial Upper Second Bani Formation of the Anti-Atlas is thus readily facilitated (Table 1; Destombes et al., 1985). Formal formation names have so far only been given to the syn-glacial succession in the Rehamna, Massif Central and Tazzeka sections in northern Morocco (Table 1). In the Massif Central, transitional uppermost Ordovician–lowermost Silurian beds (*persculptus?* and *ascensus–acuminatus* biozones, determination by P. Storch, Prague) have been found by us directly above the glacially related succession. Similar fauna have been found in the Jbilet (Destombes and Willefert, 1988), suggesting that syn-glacial sedimentation ended before the Silurian in the Meseta.

Below, a detailed stratigraphic description and interpretation of the Rehamna inlier is provided. Because this locality contains the best evidence for the presence of Hirnantian ice sheets, together with a readily interpretable stratigraphy, it is used as a benchmark section for the rest of the paper, in which basin-scale stratigraphic architecture is evaluated from outcrops in the High Atlas of Marrakech, Jbilet, Massif Central, Coastal Meseta and Tazzeka inliers (Fig. 1). These data allow palaeogeographic changes over >400 km to be assessed. A correlation scheme is presented, the maximum extent of ice sheets determined, and the temporal relationship between syn-glacial rocks in each inlier is evaluated. All directional data (palaeocurrents, ice flows) has been corrected for tectonic tilt.

4.1. Rehamna

In the Rehamna Massif, upper Ordovician pre-glacial strata form the El Mechach Formation, syn-glacial strata form the Goulibet Formation, and those of the Silurian belong to the El Mesrane Formation (according to the ongoing regional geological mapping programme, P. Razin, personal communication). Exposures were studied near the village of Amar Ben Nouti, beneath the Jbel Kharrou, ca. 25 km east of the town of Skour des Rehamna. Here, the Goulibet Formation is vertical to overturned and crops out along ridges that mark the crests of stacked, westward-transported and refolded thrust sheets (Hoepffner, 1974). Pre-glacial sediments are characterised by poorly exposed, green-weathering interstratified siltstone and fine-grained sandstone (storm-dominated deposits) of at least 400 m in thickness.

4.1.1. Description

Syn-glacial strata are divisible into two units that are bounded by a zone of soft-sediment deformation. Both units are characterised by 20–25 m thick fining- then coarsening-up motifs (Fig. 2B).

Unit 1 rests unconformably on the pre-glacial storm-dominated succession. Its lowermost strata comprise channel fills (up to 6 m thick), showing crudely developed cross-stratification, and fining up from coarse- to medium-grained sandstone. The latter passes upward into silty shales, containing one isolated bioclastic (*Lingula*-bearing) bed. These are overlain by a coarsening-upward motif, characterised by the progressive appearance in laminated mudrock of tabular, 5–15 cm thick, well-bedded, current-rippled sandstone beds with occasional load casts. A sharp-based, coarse-grained sandstone bed (20–40 cm thick), and overlying thick-bedded (20–40 cm), fine- to medium-grained, climbing-rippled sandstone with southward-directed palaeocurrents forms the upper part of unit 1 in the study section. The latter sediments are involved in the zone of soft-sediment

Fig. 2. Correlation panel between sedimentary logs for (A) the High Atlas of Marrakech (Isk N'Tazzoult; GPS 31°18.299′N 07°20.729′W), (B) Rehamna (Amar Ben Nouti; GPS 32°25.577′N 07°31.072′W), (C) Massif Central (Mchmech El Diab; 33°16.045′N 06°26.01′W) and (D) Coastal Meseta (Oued Nfifkh; 33°33.703′N 07°11.474′W) areas. Inset shows, to the same scale, the dramatic increase in the thickness of Hirnantian sediment off-shelf toward the NE into the Tazzeka Massif (Zerarda section; Fig. 9). These thickness changes are interpreted as a major increase in sediment accommodation space basinward, indicative of a major bathymetric break.

deformation. However, laterally, a more complete record has been preserved (Fig. 3). Above the rippled sandstones, a several metre-thick mudstone succession is cut by thick channelised sandstone bodies with pervasive parallel lamination or trough cross-stratification. They are in turn truncated and capped by a distinctive sandy diamictite corresponding to the base of unit 2 (Figs. 3 and 4A–C).

The clast-poor, red-brown, sandy diamictite is widespread and traceable over several kilometres. It is intimately associated with the zone of soft-sediment deformation affecting up to 15 m of sediment. Detailed sections (Fig. 3) reveal that this deformation zone contains from base to top (1) chaotic and north to northwestward-verging, decametre-scale folds affecting the underlying sandstones, (2) soft-sediment striae preserved along intrastratal detachments within the diamictite (Fig. 4C), and (3) downward-tapering sedimentary dykes, penetrating the diamictite and sourced from an overlying coarse-grained rippled sandstone (Fig. 4B). This sandstone, of several decimetres thickness, contains a pervasive shear fabric (Fig. 4D) and locally rests angularly on the diamictite, which is undeformed.

Above the deformation zone and associated sediments, the lower half of unit 2 differs from that of unit 1 in the importance of poorly sorted sediments (clast-poor, muddy to sandy diamictites), punctuated by minor sand-filled channels. The middle to upper coarsening-upward part comprises from base to top (1) laminated very fine-grained sandstones, (2) thin and tabular-bedded sandstones with occasional ball-and-pillow structures, load casts and flute casts in the lower beds, hummocky cross-stratification in the upper beds, (3) a sharp-based, crudely cross-stratified, coarse- to very coarse-grained sandstone bed, (4) fine-grained pure-quartz sandstone beds, bearing south-eastward-dipping sigmoidal cross-beds with cyclic thickness variations (Fig. 4E). The latter are capped by a final bioturbated horizon. The contact with the overlying Silurian shale is tectonic.

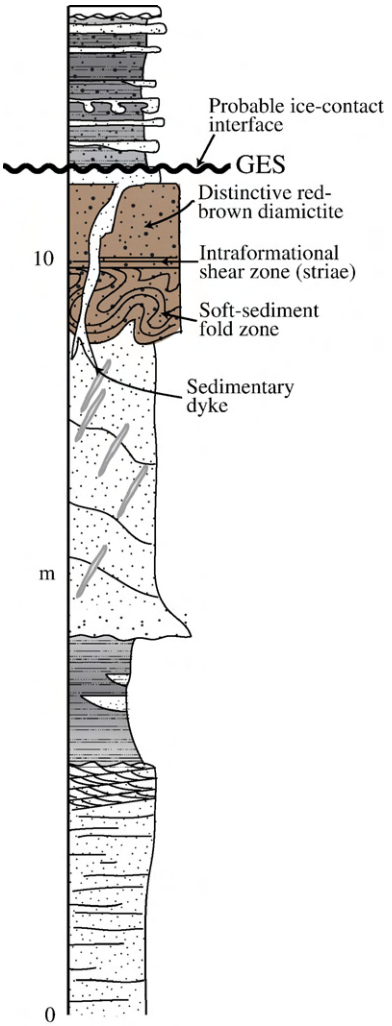

Fig. 3. Detailed section of syn-glacial deposits in the Rehamna inlier, approximately 1 km north-west of the log shown in Fig. 2B, to highlight stratigraphic position of soft-sediment deformation structures and their relationship to the distinctive red-brown diamictite. This section corresponds to the interval indicated in Fig. 2B.

4.1.2. Interpretation

The key point in the Rehamna section is the preservation of a restricted zone of soft-sediment deformation. In a manner consistent with similar deformation structures in the Late Ordovician record of Libya (Le Heron et al., 2005), the folded zone is interpreted as a suite of gravitational deformation structures induced by the weight and/or shear of an overriding ice sheet. The truncation of these folds by the distinctive red-brown diamictite and the occurrence of a soft-sediment striated surface (Deynoux and Ghienne, 2004) add further credence to this interpretation. The structures thus formed within a subglacial shear zone (Hart and Boulton, 1991; Van der Wateren et al., 2000). Downward-injection of sedimentary dykes is not unusual in subglacial settings (e.g., Hyam et al., 1997). In the Rehamna, a mechanism involving ice sheet-induced intrusion of the dykes is favoured by (a) their downward tapering nature and (b) the position of the source bed above them. The pervasive shear fabric in the coarse-grained topmost bed suggests a glacial outwash deposit directly overridden by flowing ice. Therefore, its upper surface probably formed at the ice–sediment interface.

The presence of a subglacial deformation zone in the Rehamna implies that sediment supply and depositional facies are at least partly related to the waxing and

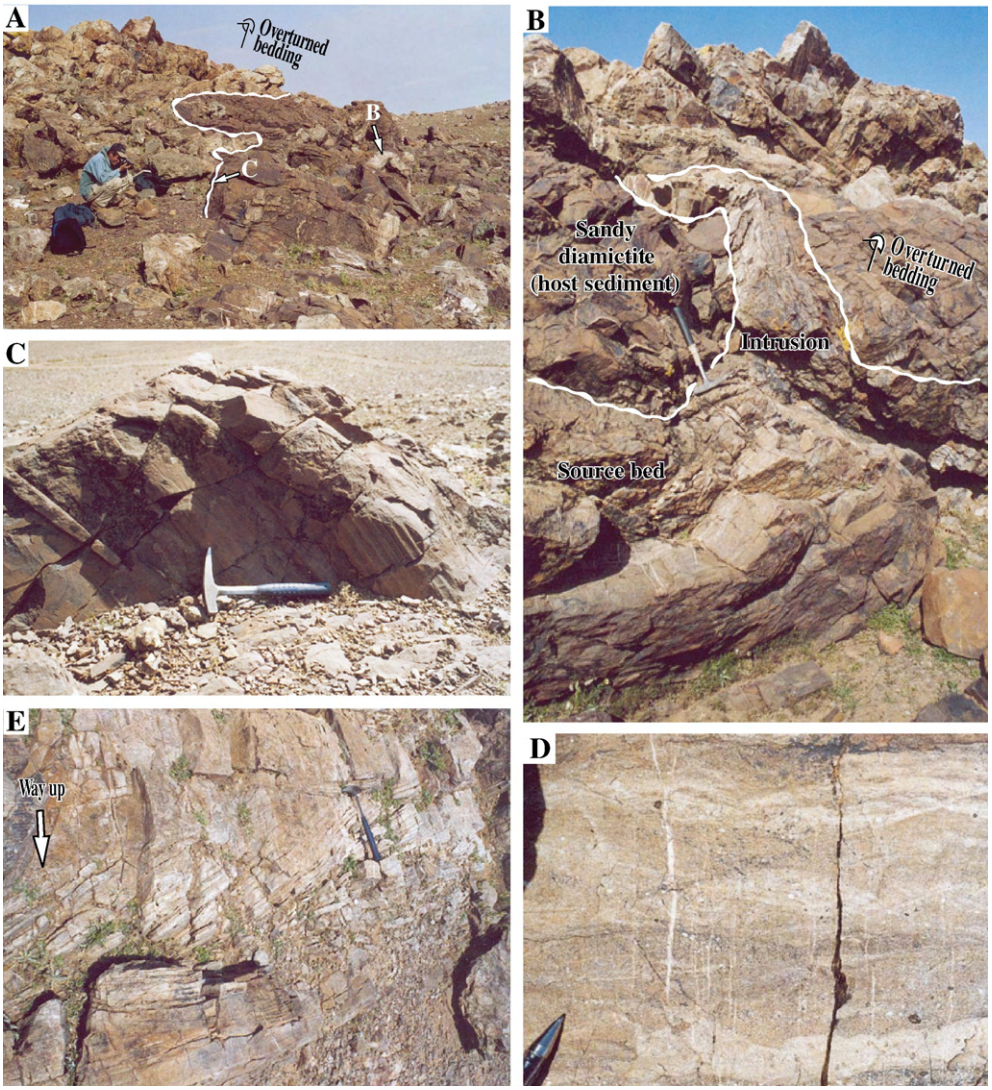

Fig. 4. Glaciogenic facies at the top of unit 1 in the Rehamna inlier at Amar Ben Nouti (taken from one-kilometre radius centred on 32°25.577′N 07°31.072′W). (A) Distinctive brown-red clast-poor sandy diamictite, preserving the counterpart to a pair of soft-sediment striae (C). (B) Complex and irregular white sandstone dykes sourced from directly above the diamictite and intruded down into it. (D) Detail of centimetre-scale shear zones developed within the white sandstone bed that sources the dykes. Together, the soft-sediment striae, downward-injected sedimentary dykes, and massive diamictite provide strong evidence of a subglacial erosion surface (GES) in the Rehamna; see text for details. (E) Sigmoidal cross-bedding in tidal sandstones at the top of unit 2.

waning of this ice mass in the Meseta. These structures reflect a glacial erosion surface (GES). This provides guidelines for the interpretation of the sedimentary record in the Rehamna.

The sharp-based and coarse-grained lithofacies at the base of unit 1 are interpreted as an ice-proximal outwash deposit, in the form of glaciofluvial or glaciomarine bars on the formerly storm-dominated shelf. They imply a first significant ice advance, with well-developed fining-up of overlying sediments indicating rapid retreat. The concentration of *Lingula* at a discrete interval above these sediments could correspond to opportunist colonization within the marine setting of an interglacial. Above, the succession of rippled sandstone beds with finer grained interbeds, sharp-based coarse-grained sandstone beds and overlying climbing rippled lithofacies corresponds to regressive–transgressive fluctuation reflected successively by shoreface, fluvial and tidal flat deposits. A glacio-eustatic cycle is inferred for these deposits since they bear no evidence of glacially fed depositional environments.

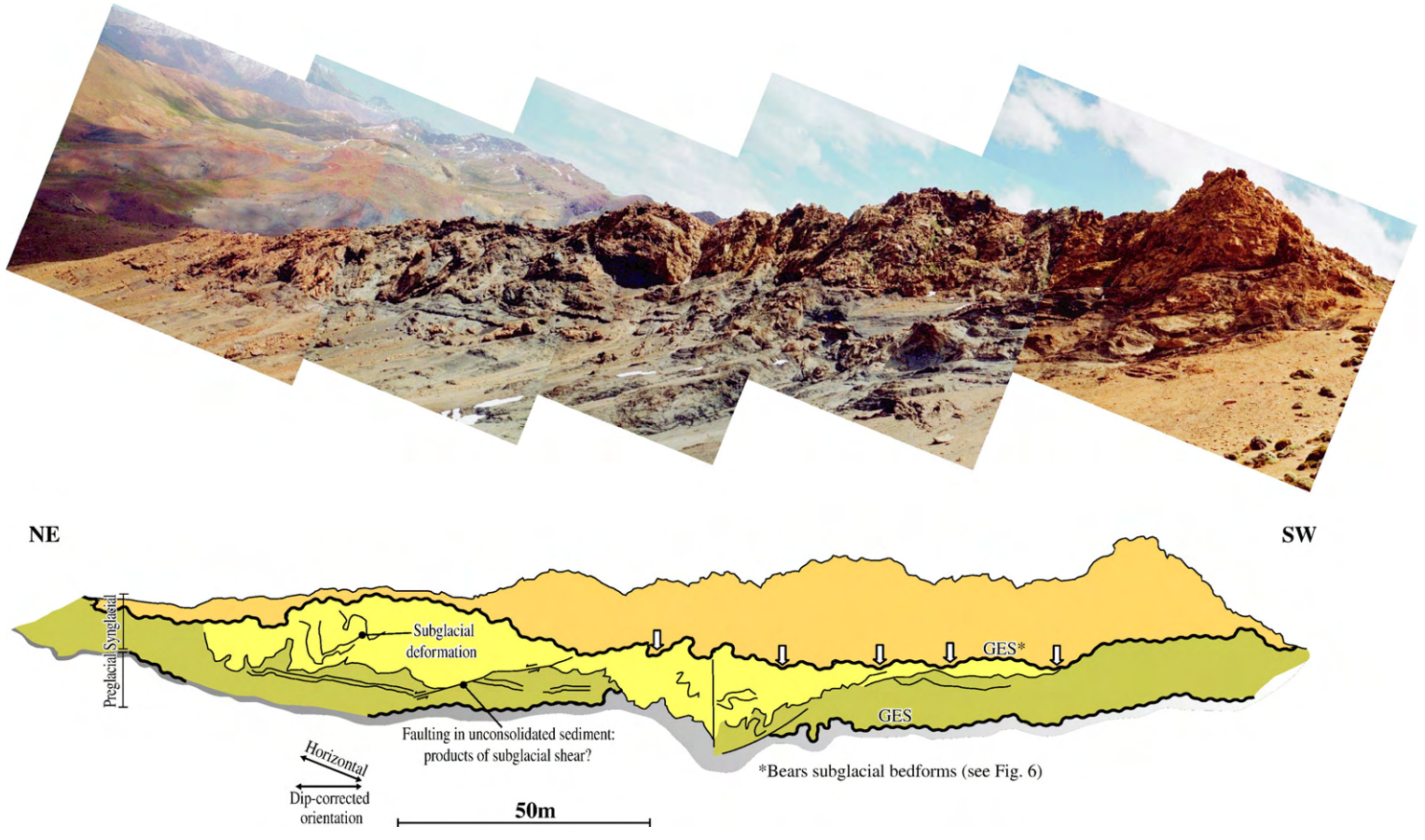

Fig. 5. Large-scale channel systems and soft-sediment deformation at Isk N'Tazzoult, High Atlas of Marrakech. Two glacial erosion surfaces (GES) can be recognised in this section. The subglacial bedforms (Fig. 6) occur along the second, higher, surface. Note chaotic internal organisation of lithofacies. Significant lateral facies variations occur over short distances.

Therefore, mudstones that cap these sediments were probably deposited during renewed interglacial conditions. Overlying rocks of the uppermost part of unit 1 were thus deformed during a second, significant glacial advance. The lower part of unit 2 is considered to reflect (1) erosion and deposition of high-energy sandstones reflecting ice-proximal outwash deposits, (2) diamictite deposition (either glaciomarine or subglacial?), (3) subglacial deformation and glacio-fluvial deposition. The overlying clast-poor, muddy to sandy diamictites and sand-filled channels reflects glaciomarine sedimentation in an underflow-fed submarine outwash fan system during ice sheet recession.

Overlying shoreface sediments, punctuated first by turbiditic (load and flute casts) and then storm (Hummocky cross-stratification) events, may have been deposited in a prodelta setting. As in the upper part of unit 1, the succession of shoreface deposits, a thin fluvial horizon and overlying well developed, tidally bundled, migrating bedforms (Nio and Yang, 1991) reflects an additional regressive–transgressive fluctuation. The tidal sediments may represent transgressive facies below the overlying Silurian shales. However, comparison between the upper part of unit 2 with that of unit 1 identifies a further glacio-eustatic cycle operational prior to post-glacial flooding in the earliest Silurian.

4.1.3. Regional implications

Vergence of fold structures in the subglacial deformation zone indicate a top to the north sense of shear, indicating the growth of ice sheets from ice centres in the Anti-Atlas and further southward (Algeria, Mauritania). The presence of this subglacial deformation zone in the Rehamna implies that the Hirnantian glaciers extended into the Meseta at least 200 km over the Southern Atlas Thrust.

Depositional units correspond to two first-order glacial cycles (e.g., Sutcliffe et al., 2000), each of them subdivided into two second-order cycles. Thus, event stratigraphy identifies four sedimentary cycles in total, each potentially controlled by regional advance and retreat cycles of the Hirnantian ice sheet (Ghienne, 2003). In each unit, the first (lower) second-order cycle records ice-proximal to subglacial deposition, and subsequent retreat following a major ice sheet advance into the basin. In contrast, the second (upper) second-order cycle only records a glacio-eustatic fluctuation, lacking any evidence for even local glaciers in the basin. An alternative is that the uppermost cycle in each unit was driven by glacioisostacy (isostatic rebound) following glacial retreat as suggested by Sutcliffe et al. (2000) elsewhere in North Africa. However, this explanation is not considered appropriate because no evidence of uplift, hardground development or erosion is preserved at the base of these cycles in Rehamna. These conclusions are fully supported by the record of the Hirnantian glaciation in the other Palaeozoic inliers of Northern Morocco.

4.2. High atlas of Marrakech

Exposures at Isk N′ Tazzoult, 2.5 km west of the Tizi N′ Tichka pass (Fig. 1), occur in a Lower Palaeozoic inlier that preserves a thick succession of Cambrian to Silurian strata (Ouanami, 1989, 1998). This locality belongs to the Anti-Atlas tectonostratigraphic domain rather than to the Meseta (Allary et al., 1972; Ouanami and Petit, 1992). Therefore, comparison between upper Ordovician deposits in this locality with those in the Meseta will yield affirmative data on the palaeo-tectonic relationship of these two regions.

4.2.1. Sedimentary succession

The syn-glacial strata rest with sharp disconformity upon pre-glacial, bioturbated, storm-dominated fine-grained deposits. Large (100 m wide) crosscutting channels (Fig. 5), filled with sand-grade sediment are interstratified with heterolithic lithofacies including well-stratified shale, siltstone, and fine sandstone or massive sandy clast-poor diamictite. Although complex lateral and vertical substitutions occur between these lithofacies, the basal part of the succession comprises coarse-grained sand-filled channels (Fig. 2A, 17–25 m) overlain sharply by sandy diamictite that bears large (1–5 m) ball-and-pillow structures (Fig. 2A, 25–37 m). The diamictite is capped by a well-bedded, coarsening- and thickening-upward rippled siltstone and sandstone succession, with bioturbation (Fig. 2A, 37–43 m), passing upward into shale (Fig. 2A, 45 m). Coarse-grained sand-filled channels with scattered boulder-sized clasts (Fig. 6A) (Fig. 2A, 45–65 m) cut down into these sediments. These sediments, which show flute casts, tool marks and conglomerate lenses at their base, are reworked upsection into a soft-sediment deformation zone comprising large, polished, streamlined bedforms (Fig. 6B) with superimposed hairpin structures (Fig. 6C) (Fig. 2A, 65 m). This zone, which is sealed by a thin and discontinuous diamictite horizon, is in turn overlain by a thin coarsening-then-fining upward succession with lenticular coarse-grained sandstone beds in the middle part (Fig. 2A, 66–70 m). The topmost part of the succession comprises finely laminated siltstone and black shale (the so-called Silurian shale), which attains at least 30 m thick. Rare lonestones occur within the lowermost part of this shale.

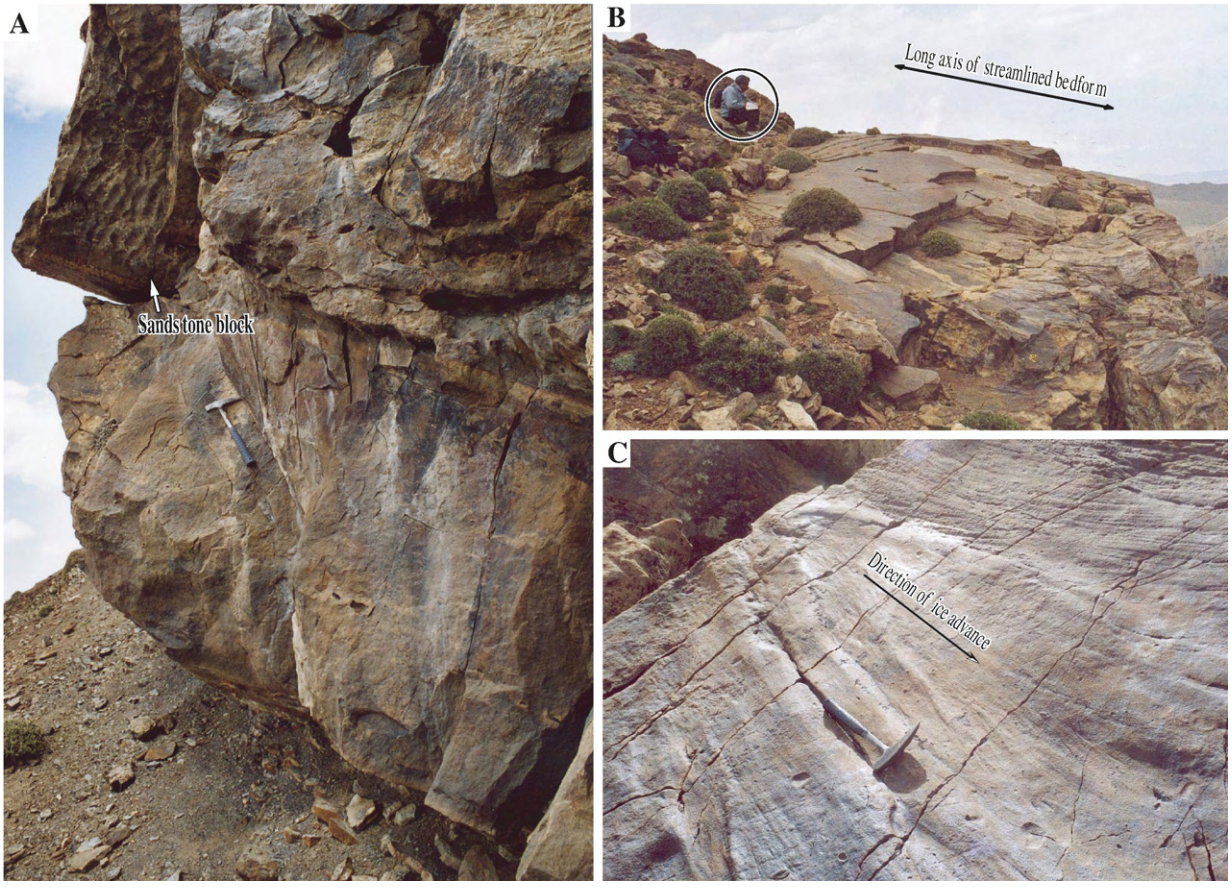

Fig. 6. (A) Large boulder of rippled sandstone within a pro- or subglacial channel at Isk N'Tazzoult, High Atlas of Marrakech. (B) Polished drumlin-like bedform. (C) Large "hairpin-like" structure on the polished surface of a folded drumlin. These structures are interpreted to have formed subglacially, with the last structure characteristic of the hydroplastic deformation of unconsolidated sediment.

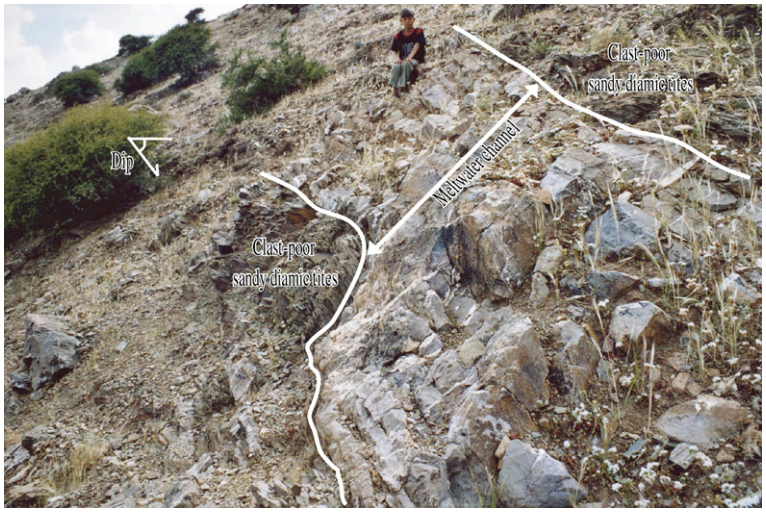

Fig. 7. Large sandstone channels within clast-poor sandy diamictites at Larissa (31°56.194′N 07°39.980′W), Jbilet inlier, constituting the thickest uninterrupted example of these facies (150 m) observed in Morocco.

The large channels were cut and filled in a high-energy setting, most probably in a sub- or proglacial environment during the rapid release of glacial meltwater (e.g., by "jökulhlaup" outburst floods). The heterolithic lithofacies variably indicate suspension settling (shale), traction (well bedded siltstone and fine sandstone) and slurry/mass-flow processes (diamictites). Bioturbation implies colonisation of the substrate by opportunistic fauna in environments far from the glacial sediment input points. Polished streamlined bedforms result from glacial fluting, and hairpin structures resemble spindle flutes found on Pleistocene deglaciated surfaces (e.g., Kor et al., 1991). These structures, interpreted as subglacial bedforms and attributed to a grounded ice sheet, indicate a subglacial deformation zone in the upper part of the succession in the High Atlas of Marrakech.

4.2.2. Event stratigraphy and correlation

The following sequence of events is interpreted from the syn-glacial succession: (1) incision of channels into pre-glacial substrate and deposition of ice proximal lithofacies, (2) glacial retreat (diamictite fining up to non-glacial mudrock), (3) a distinct regressive–transgressive cycle remote from an ice front, (4) following a second phase of channel incision, truncation of ice proximal lithofacies by a GES, (5) glacial retreat (thin diamictite drape), (6) a regressive–transgressive cycle deposited under a glaciomarine influence (channels with coarse-grained sand fill, occasional dropstones). Comparison to the Rehamna section suggests that most of the succession belongs to unit 1 in the High Atlas (below the major subglacial surface); topmost sediments, bearing the uppermost glacially related facies, therefore, correspond to unit 2. As in other parts of northwest Africa such as the Taoudeni Basin (Underwood et al., 1998; Paris et al., 1998), these sediments are transitional into postglacial (probably late Hirnantian and earliest Silurian) shale with no hiatus inferred.

4.3. Jbilet

Lying between the High Atlas and the Rehamna (Fig. 1), the Jbilet inlier probably occupied an intermediate palaeogeographic position. Like the Rehamna, it consists of westward-directed imbricate thrust slices (Huvelin, 1977). Recognition of syn-glacial deposits includes the disappearance of the ubiquitous bioturbation present in pre-glacial mudrocks, or the sudden appearance of diamictites. Uppermost sandstones of the succession have yielded a terminal Ordovician graptolite fauna (*persculptus* biozone, Destombes and Willefert, 1988).

Syn-glacial deposits attain >160 m thickness and comprise structureless, homogeneous, unstratified clast-poor sandy diamictites. Two poorly defined coarsening-up cycles are recognised, the lower of which is punctuated by >10 m wide, sandstone-filled channels (Fig. 7), whilst the upper one is capped by current rippled and cross-bedded (northeastward-directed palaeocurrents) siltstones and fine-grained sandstones.

The homogeneity and thickness of the sandy diamictites implies that the Jbilet lay close to an ice front during deposition. Their unstratified nature, coarsening-up profile and interruption by channelised sandstone implies the rapid progradation of a thick, subaqueous diamicton fan whose poorly expressed foresets were dominated by glaciogenic debris flows and topsets by tractive processes, rather than an ice-rafting mechanism.

4.4. Massif Central

Detailed study was undertaken in the western part of the Massif Central at Mchmech El Diab, 10 km SE of the village of Ezziligha (Fig. 2C) and additional outcrops were examined in the central, northern and eastern Massif Central. A synthetic overview is given below. Syn-glacial strata of the mud-dominated Ould Akra (early-late Ashgill) and overlying sand-dominated Ezzhiliga formations (late Ashgill), are overlain by shales of the lower Silurian Sidi M'Bellej Formation (Baudin et al., 2001; Chèvremont et al., 2001; Razin et al., 2001).

4.4.1. Sedimentary succession

The lower contact of the syn-glacial strata (upper Ould Akra Formation) is placed at the first appearance of clast-poor muddy diamictites above bioturbated siltstones and fine-grained, current rippled to hummocky cross-stratified sandstones. Diamictites, either massive or crudely stratified, make up the lower part of unit 1 (Fig. 8A). These become thicker and coarser grained upsection at Mchmech El Diab (Fig. 2C, 3–40 m), but in the eastern Massif Central (Khenifra area) fine upwards. Lonestones are pebble- to cobble-sized, and comprise quartzite or sandstone (Fig. 8B). Discontinuous, cross-stratified sandstone horizons are locally interstratified within the diamictites. Above, sand-dominated lithofacies (Ezzhiliga Formation) are widespread and traceable over the whole Massif Central (Figs. 8C–E and 2C, 40–85 m). Locally, they rest on the underlying diamictites with a sharp and loaded contact. This sandstone comprises two conspicuous coarsening- and thickening-upward motifs, comprising moderately to well-sorted, fine- to coarse-grained sandstone (Fig. 8E). Wave ripples and rare amalgamated hummocky cross-stratification (HCS) occurs in the

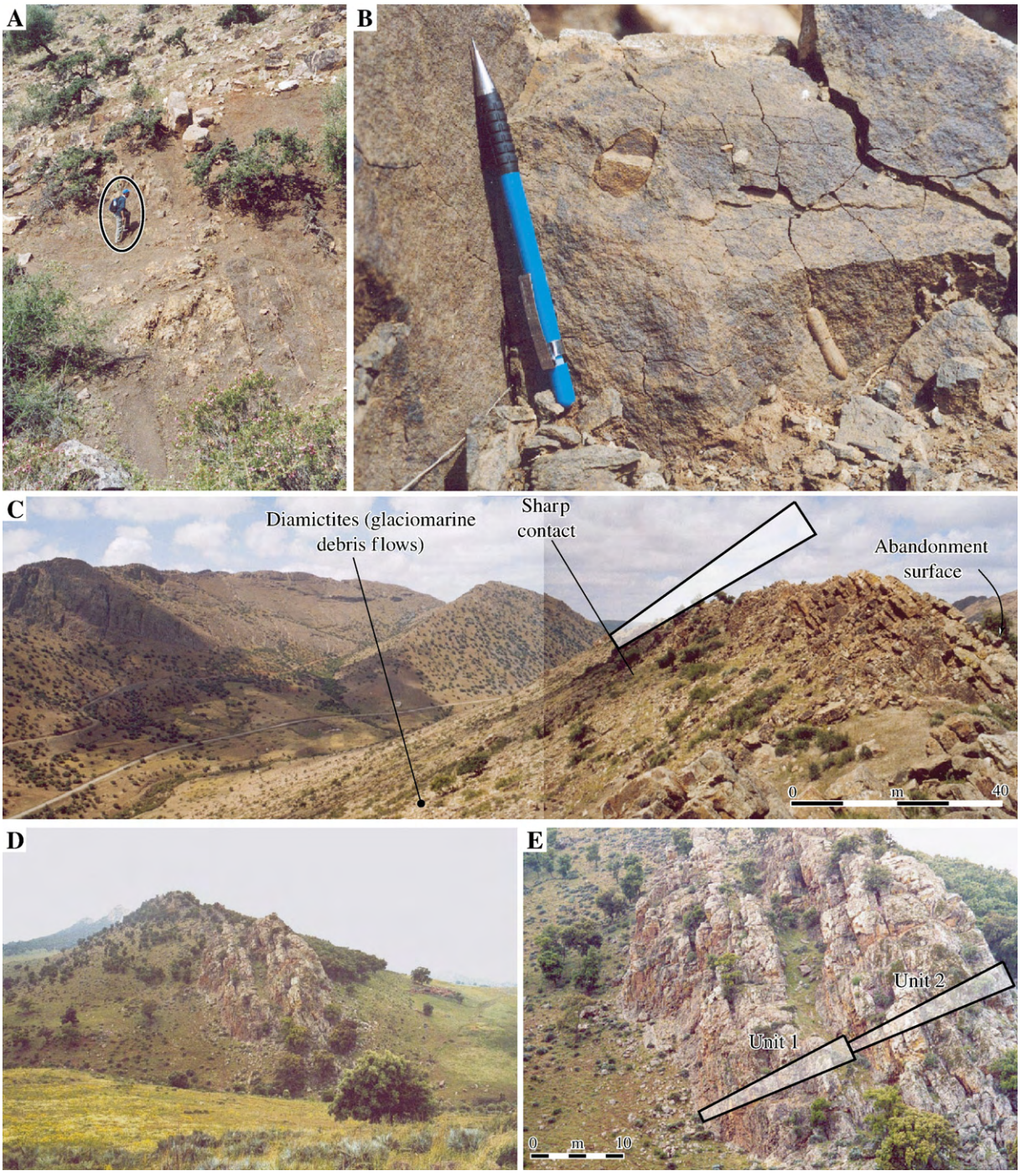

Fig. 8. Syn-glacial lithofacies in the Massif Central. (A) Diamictites in depositional unit 1 at Mchmech El Diab (see Fig. 2 C for GPS co-ordinates), showing interbedding of massive and thinly bedded variants of this lithofacies. (B) Examples of lonestones within massive, clast-poor sandy diamictites considered to have been deposited by glaciogenic debris flows. (C) Section view at Mchmech El Diab from poorly exposed diamictite to overlying sandstone. (D) (and (E), close-up) Well defined subdivision of the Ezzhiliga Formation (top of depositional unit 1 to unit 2) into two coarsening-up motifs developed exclusively in sandstone at El Harcha. This subdivision and the sharp surface separating these motifs are developed widely in the Massif Central. The sharp contact between the Ezzhiliga Formation and underlying diamictite implies that the former does not simply cap a coarsening-upward unit. GPS co-ordinates for El Harcha: 33°30.830′N 06°08.690′W.

lowermost sandstone beds of the lower thickening-upward motifs with metre-scale megaripples becoming more common upward. The sharp surface bounding the two thickening-upward motifs is regionally developed dividing unit 1 from unit 2 (Figs. 2C and 8E). Poorly exposed sediments at the base of unit 2 comprise interstratified siltstones and fine-grained sandstones. Its upper part compares closely to that of unit 1, but characterised by more abundant climbing ripple cross-stratification (Fig. 2C). At Mchmech El Diab, a green siltstone unit, several metres thick, caps the sandstone (Ezzhiliga Formation) and fines up into graptolite-bearing shale with a thin, ferruginous horizon. In the eastern Massif Central, graptolite-bearing shale directly overlies the sandstone.

Fluid escape structures are locally abundant in the sandstone lithofacies (Razin et al., 2001). However, no deformation structures related to soft-sediment subglacial deformation were found. Regionally, the sand-dominated Ezzhiliga Formation tends to be finer grained and thinner southward and eastward, an observation consistent with south-eastward-directed palaeocurrents in rippled or cross-stratified facies.

HCS-bearing and current rippled sandstones in the latest pre-glacial deposits imply storm-deposition in a dominantly lower shoreface setting. The diamictites are interpreted as glaciomarine facies, deposited from glaciogenic debris flows with gravity re-sedimentation. However, their variable motif (variably coarsening and fining up depending on the locality), coarse grain size and sharp upper contact with the overlying sandstones suggest that they do not belong to the lower part of a coarsening-upward succession to which the Ezzhiliga Formation forms the upper part. The two regionally extensive overlying coarsening- and thickening-up motifs comprising relatively well-sorted sandstones formed through efficient mud winnowing on delta mouth bars. The predominance of the sharp to irregular-based sandstone beds implies low accommodation and extensive, high-energy re-distribution. Storms contributed to mouth bar reworking, as evidenced by HCS, but the predominance of cross-strata highlights the importance of traction currents upsection. The sharp surface separating the two motifs is interpreted as a major abandonment surface. A second phase of delta mouth bar build-out is interpreted on the basis of a renewed coarsening-up profile following abandonment of the former delta and the occurrence of similar lithofacies to those in the lower part of the Ezzhiliga Formation. The overlying green siltstones most probably represent prodelta deposits, grading up into shale reflecting offshore conditions. As siltstones and then shale overlie abruptly delta sandstones, a rapid backstepping of the delta system is envisaged.

4.4.2. Event stratigraphy and correlation

Compared with the High Atlas and Rehamna domains, the sedimentary record in the Massif Central is correlated in the following way: diamictites (uppermost Ould Akra Formation) are correlative to the first ice-proximal deposits (Fig. 2). Coarsening-upward sand-dominated motifs (delta mouth bars) most likely represent proximal counterparts of the two regressive–transgressive, glacio-eustatically driven second order cycles (Fig. 2). Under this model, the subglacial erosion surface (GES) identified in the High Atlas and Rehamna domains, probably synchronous with a major sea-level fall, corresponds to the abandonment surface between the two delta systems. The ferruginous horizon in graptolite-bearing shale above the delta should thus be correlated with the postglacial maximum flooding surface within Silurian hot shales elsewhere on the Gondwana platform (Lüning et al., 2000).

4.5. Coastal Meseta

Syn-glacial strata of Ben Slimane (Oued Nfifkh), which await formal stratigraphic recognition, are affected by 3–4 stages of Hercynian deformation, and large-scale conjugate faulting (El Attari, 2001). They comprise two well-defined coarsening- and thickening-upward motifs, overlain by a diamictite succession (Fig. 2D). The lower motif (unit 1) comprises mudstones with thin current-rippled sandstones (>30 m) overlain by coarsening-up, well-sorted, siltstone to medium-grained sandstone that bears eastward-directed, decametre-scale cross-beds and linguoid ripples. A decimetre-thick, erosionally based pebbly conglomerate caps this succession (Fig. 2D). The upper coarsening-upward motif (unit 2) sharply overlies the lower one and comprises an identical, coarsening-up lithofacies evolution capped by a second conglomerate. In contrast with the Massif Central, topmost deposits are abruptly overlain by 10 m of clast-poor sandy diamictites, passing transitionally into graptolite-bearing shale (Fig. 2D). No striated surfaces or other glaciotectonic structures are preserved in this area.

The coarsening-up motifs and progressive upward appearance of large bedforms implies two phases of deltaic progradation. The sharp surface bounding the two motifs is interpreted as an abandonment surface prior to a renewed phase of build-out. The thin, sharp-based pebble beds capping each unit suggests scour on the upper surface of the mouth bar, potentially by fluvial processes. These data would imply that the delta topsets were

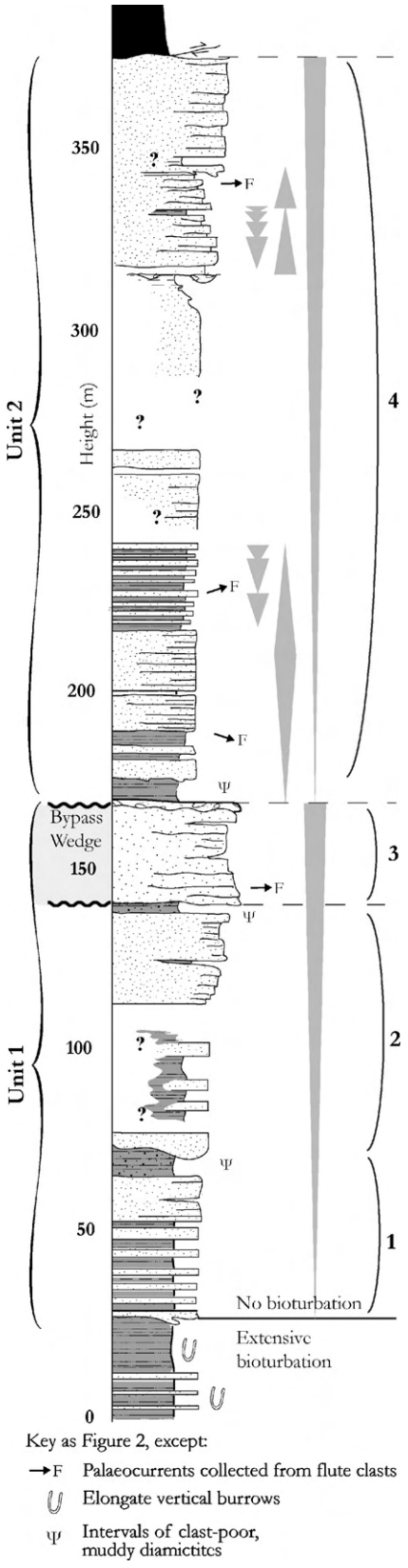

Fig. 9. Measured section of latest Ordovician strata at Zerarda, Tazzeka Massif (Eastern Meseta; 34° 01. 545′N 04°20.148′W). As in other parts of the Meseta, two units are recognised. Numbers on the log correspond to major phases in the evolution of the Tazzeka fan, which are directly attributed to ice sheet waxing and waning on the shelf. Minor coarsening and fining-upward motifs are probably autocyclic in nature. The package marked "bypass wedge" is thought to be coeval with glacial erosion next to the ice sheet, resulting from bypass of the shelf margin (see Fig. 13).

extremely thin and characterised by bypass rather than deposition. However, a 20 m thick succession of pebbly sandstone with large-scale cross-bedding occurs northward (40 km west of Settat, Sutcliffe et al., 2001) and may suggest a thickening of the pebbly facies, either locally (channel, incised valley?) or regionally (in a more proximal setting). Textural characteristics of the overlying diamictite suggest direct glacial derivation. The two successive coarsening-up motifs in both the Coastal Meseta and Massif Central are clearly correlative. Reasons for the occurrence of a diamictite in the upper synglacial succession are discussed below.

4.6. Eastern Meseta

In the Tazzeka Massif, pre-glacial strata (Tehar El Brehl Formation), syn-glacial strata (Tifarouine Formation) and the overlying Silurian shales crop out immediately south of the Rif within a 15 km radius of Tahala, with the best exposure at Zerarda (Fig. 9) (Destombes et al., 1985; Khoukhi, 1993; Khoukhi and Hamoumi, 2001). These exposures are presently located ~200 km north-east of those in the Massif Central (Fig. 1) but prior to Hercynian deformation may have been more distant during the Ordovician.

4.6.1. Sedimentary succession

Pre-glacial rocks mainly comprise rhythmically bedded, bioturbated, silty shale and siltstone. In the upper levels of pre-glacial strata, within which Ashgill palynomorphs have been identified (determination F. Paris, Rennes), fine-grained lithofacies interbedded with current-rippled sandstone beds prevail. Bioturbation becomes more subtle upward. The first stratigraphic occurrence of syn-glacial strata is considered to be defined by a sharp-based sandstone bed with flute casts (Fig. 9; 25 m).

Syn-glacial strata are organised into two well-defined stratigraphic units (Figs. 9 and 10), traceable over 20 km. Subordinate smaller scale coarsening-up cycles on two smaller orders of magnitude are also expressed (Fig. 11A). Syn-glacial strata are made up of extremely well-differentiated shale, siltstone, sandstone and rare clast-

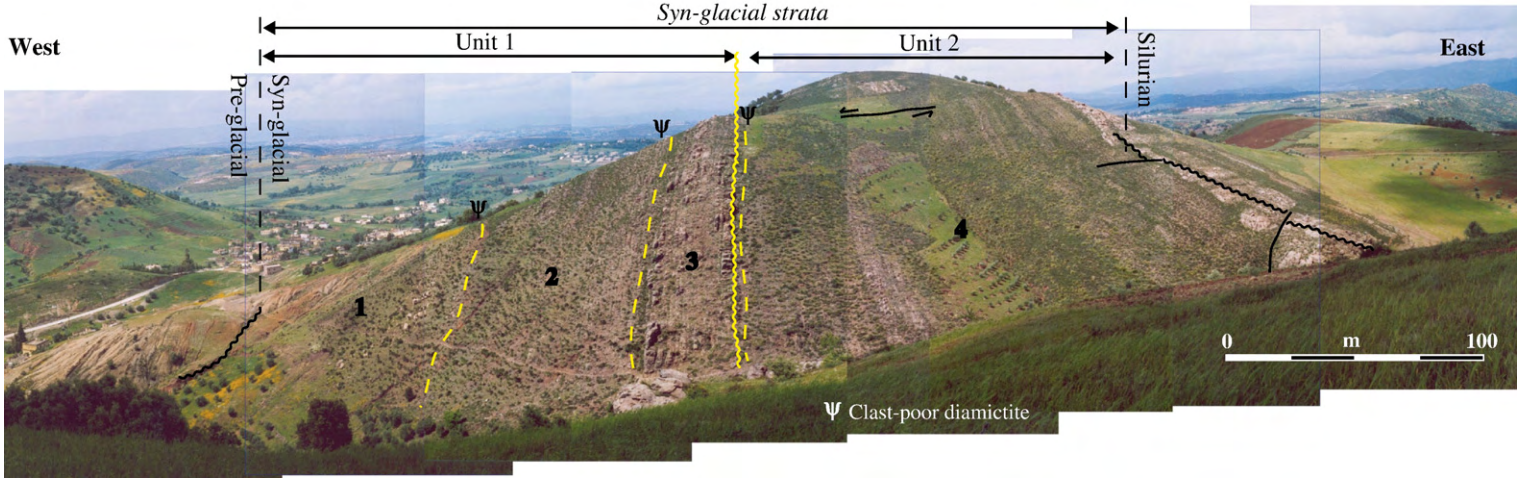

Fig. 10. Panoramic photograph of the logged Zerarda section showing generally high quality of exposure and stratigraphic continuity, annotated for direct comparison with Fig. 9. The interpreted pre-glacial to syn-glacial transition is shown, together with transition of these rocks into lowermost Silurian shale.

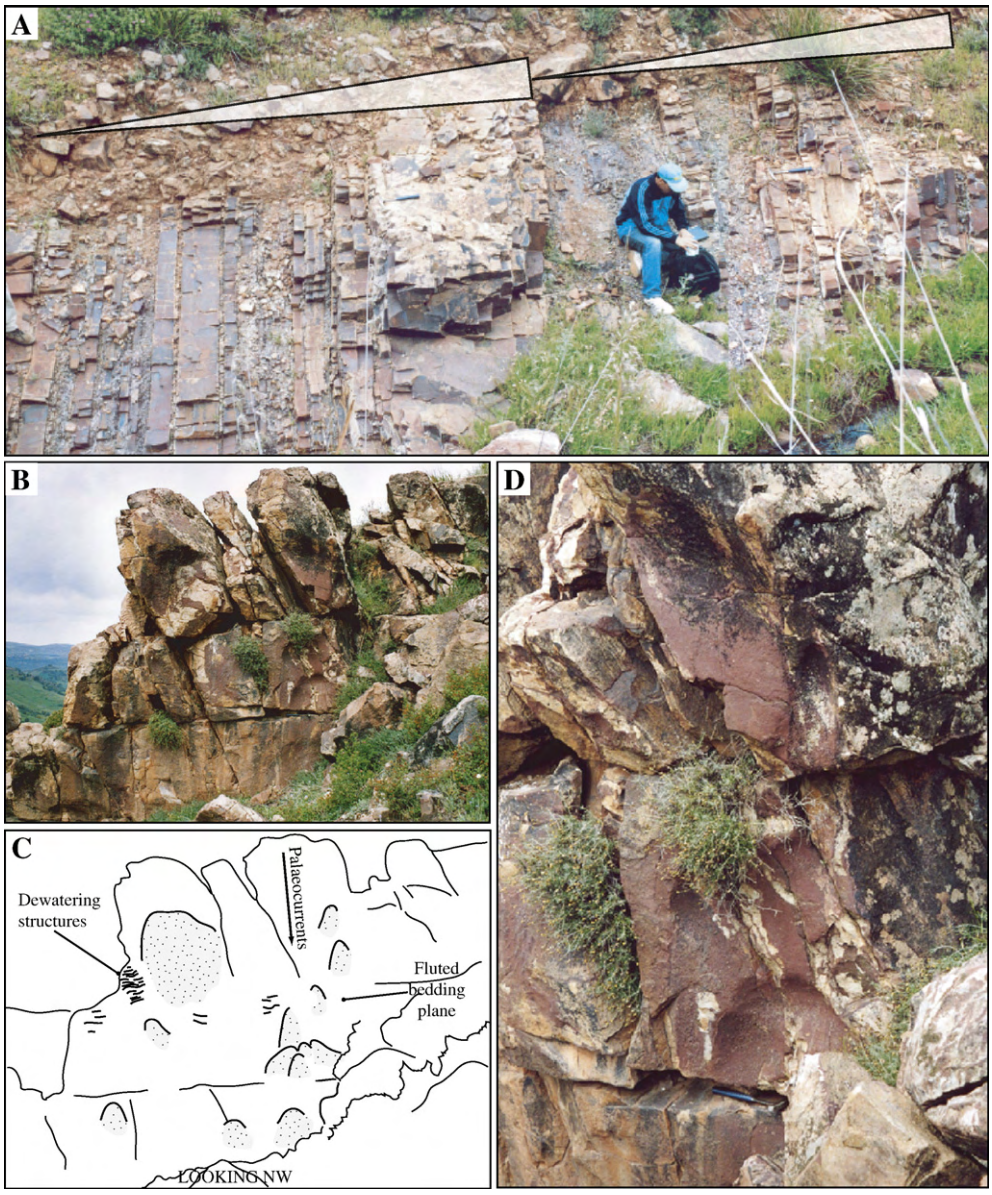

Fig. 11. Sedimentary facies at Zerarda, Tazzeka Massif. (A) Well-defined, sharp-based sandstones interbedded with mudrocks form metre to tens of metre-scale coarsening upward motifs. These are probably due to allocyclic phases of fan lobe growth and abandonment. (B) View looking down onto the top of unit 1, represented by an amalgamated package of sandstone (Fig. 9, 172 m). Clearly visible on this surface (illustrated in C) are large flutes. (D) Close-up of these features, with hammer for scale, showing gravel lag in the central depressed part of a flute.

poor, sandy diamictite. Each coarsening-up cycle attains 100–150 m thick, with an unexpected total section thickness (approaching 350 m; Figs. 9 and 10). The diamictite facies are preserved intermittently in unit 1 (attaining several metres thick at ca. 70 m, Fig. 9) but rare in unit 2.

Two types of fine- to medium-grained sandstone lithofacies co-occur with mudstone, namely, (1) thin, isolated, SE-directed current-rippled horizons that predominate at the base of each unit and (2) well-defined, structureless, sometimes graded, crudely horizontally laminated or rippled tabular beds prevailing mid-way up each unit (Fig. 11A). These latter sandstone beds occur toward the top of metre-scale coarsening-up motifs (Fig. 11A). They are sharp-based, irregular, or channelised with S- to SE-directed (and rarely NW-directed) flute casts or small channels occasionally filled by coarse-grained sandstone. Aside from centimetre-

scale load casts at the base of these beds, no soft-sediment deformation occurs in the Tazzeka Massif.

The upper part of both units comprises stacked, erosionally based, horizontally laminated sandstone beds, forming amalgamated packages up to 10 m in thickness (Figs. 9 and 10). They rest directly on clast-poor muddy diamictite. At the top of unit 1 (135–170 m, Fig. 9), they are coarse-grained and contain abundant sheet dewatering structures. Metre-scale flute-like structures of consistent long-axis orientation toward the SE (Fig. 11B–D) containing gravel lags are overlain by a single fining-upward sandstone bed, 40–80 cm thick, with a wave-rippled top. A sharp contact with overlying shale and sandstone occurs.

Sandstones capping unit 2 are fine- to medium (and rarely coarse)-grained (320–375 m, Fig. 9). Diffuse horizontal lamination and small flute casts occur. The transition into Silurian shale and well-bedded phtanite (diatomite) is sharp and tectonic. Scattered quartz grains (<1 mm) are preserved in the lowermost exposures of shale below phtanitic beds.

4.6.2. Interpretation

Together, the lithofacies described above characterise the cyclic progradation of a turbiditic deep-marine fan (e.g., Stow and Mayall, 2000). Significant water depths during deposition are indicated by the great (and presently compacted) thickness of these sediments, by the absence of angular unconformities supporting continuous sedimentation and by the almost total absence of wave- or storm-induced sedimentary facies.

The three main types of sandstone lithofacies, i.e., isolated and current rippled, the tabular beds within mudrock, and the amalgamated, stacked examples, are interpreted to belong to distal, medial and proximal portions of the fan system, respectively. The first lithofacies were probably deposited by distal, low-density turbidity currents; the SE-oriented palaeocurrents obtained from these rocks thus provide a palaeoslope indicator. The second and third sandstone lithofacies are interpreted as sandy gravity flows, with the diffuse, horizontal lamination within the amalgamated sandstone beds testifying to non-Newtonian rheology, internal shearing, and to the emplacement of stacked debris flows (Shanmugam, 2000). The emplacement of these last flows as discrete "event beds" is supported by the frequent occurrence of fluted and gravely surfaces within these strata. Their lateral extent over at least 20 km, together with their position at the top of the first-order coarsening up cycles, indicates that they occupied an extensive upper part of this fan system. The surface with large-scale flutes is thought to reflect high-energy underflows, possibly linked with abrupt meltwater discharge during jökulhlaup glacial outburst events (e.g., Carrivick et al., 2004). A rapid end to sand sedimentation above this surface implies avulsion of the depositional lobe.

4.6.3. Event stratigraphy and correlation

Syn-glacial rocks in the Tazzeka Massif are notable for their significantly greater thickness (350 m) than anywhere else in the Meseta and, in common with the Massif Central and Coastal Meseta areas, the absence of glacially related soft-sediment deformation structures. These observations suggest high sediment accommodation within a basin untouched by an ice sheet. Four cycles corresponding to coarsening- and thickening-upward succession bounded by diamictite horizons are recognized (Fig. 9). The proposed correlation, developed further below, suggests that these four cycles reflect the four glacial cycles identified in the Rehamna and High Atlas domains, the major glacial advance being reflected by the coarse-grained lithofacies of the upper third of unit 1 and its conspicuous fluted erosion surface.

5. Hirnantian sedimentary systems in northern Morocco

Our data demonstrate the presence of the Late Ordovician ice sheet in the Meseta that reached as far north as the Rehamna Massif. Unequivocal evidence for subglacial deformation is restricted to the surface separating depositional units 1 and 2 (Figs. 2 and 12). This surface formed during the third glacially related cycle and is considered to reflect the maximum extent reached by the Gondwanan ice sheet during glaciation of Morocco (i.e., the glacial maximum). However, the coarse-grained and erosionally based nature of sandstones at the base of unit 1 in both the Rehamna and High Atlas probably imply deposition during an earlier glacial advance prior to advance of the ice sheet toward its ice maximum position. No direct evidence for subglacial erosion (e.g., soft sediment striation) was found in or above these channel deposits, but in the High Atlas, the abundance of sandy diamictites above them strongly suggests the presence of a nearby ice front. Therefore, these data imply two advances of the Gondwanan ice sheet into northern Morocco.

This section investigates why the ice did not extend further north into the Massif Central or Coastal Meseta. It unravels complex stratal geometries (Fig. 12), proposing a palaeogeographic reconstruction (Fig. 13A) and depositional model (Fig. 13B).

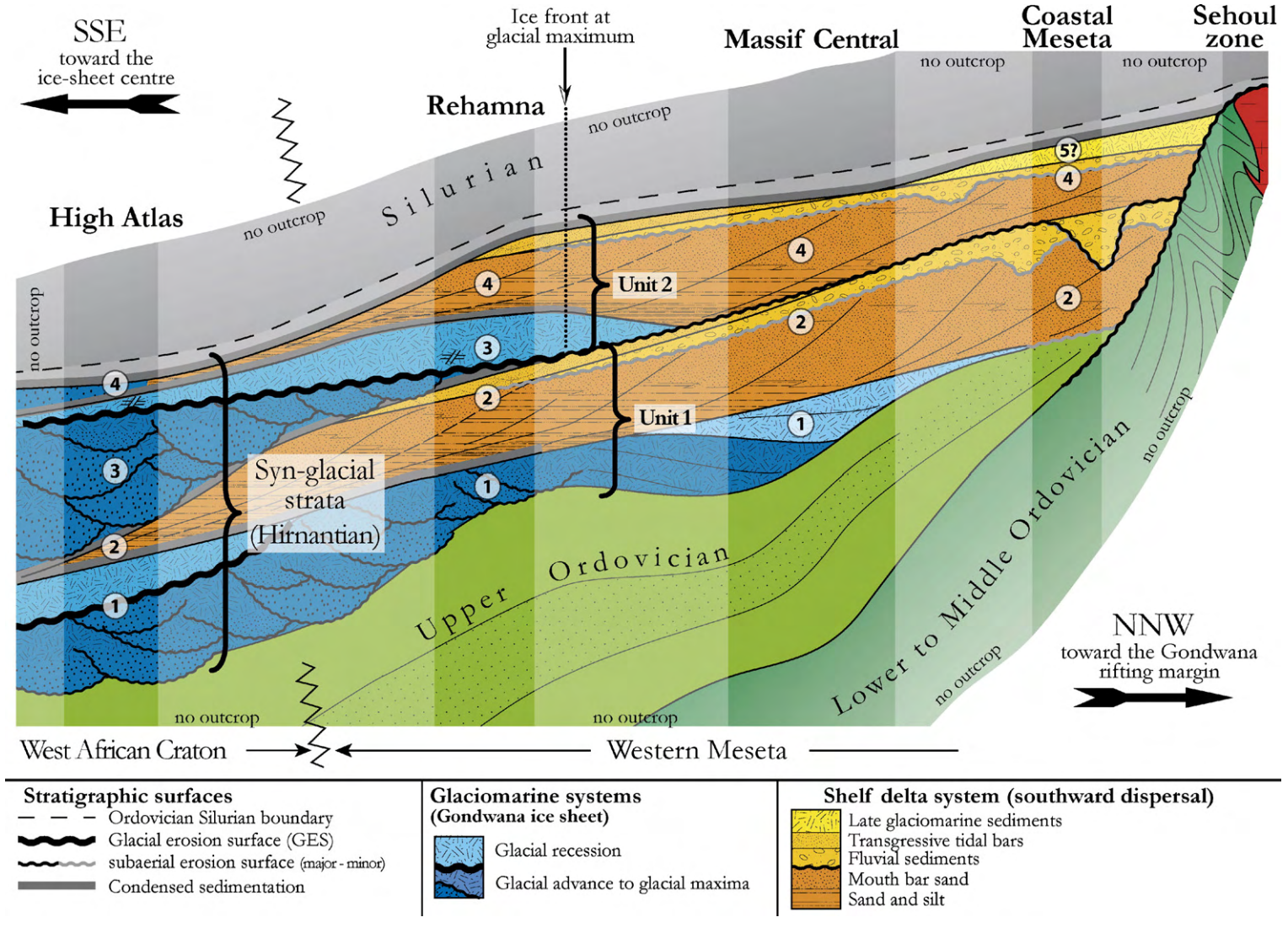

Fig. 12. Synthesis of stratigraphic architecture shown on correlation panel (Fig. 2), emphasising the occurrence of four glacially related cycles in northern Morocco. The ice maximum is represented by the GES at the top of unit 1.

5.1. Regional correlation

A correlation is proposed between the glacial record of four of the Palaeozoic inliers (High Atlas of Marrakech, Rehamna, Massif Central and Coastal Meseta), which are approximately aligned in a palaeogeographic profile (Figs. 2, 12 and 13) A). Four chronostratigraphic boundaries are identified; the first and third corresponding to glacial erosion surfaces (GES).

Limited but consistent palaeocurrent data, palaeo-ice flow indicators and regional trends identify three palaeogeographic domains. The "ice-contact system" was characterised by a south–north proximal-distal trend in glacially related sedimentary systems identified in the Rehamna and High Atlas (Fig. 12, blue colour). The second, a "shelf-delta system", shows that a north–south (to NE–SW) proximal-distal trend persisted in the delta systems of the Massif Central and Coastal Meseta (Fig. 12, orange colour). Therefore, ice contact and shelf delta sediments were shed from different sources. The linkage and relationship between these systems is further investigated below.

The Jbilet and Tazzeka inliers are more difficult to place on the High Atlas–Coastal Meseta profile because the former, comprising only glacially derived material and lacking delta deposits, is regarded as a distal glaciomarine equivalent of the High Atlas section (Fig. 13). The Tazzeka succession represents a third palaeogeographic domain ("deep-marine system") and the buildout of a submarine fan in the eastern, deeper portion of the platform connected to and fed by both the shelf-delta and ice-contact systems (Fig. 13).

Below, the linkage between ice-contact, shelf-delta and deep-marine systems is investigated, with emphasis on palaeogeographic setting at the glacial maximum (Fig. 13A).

5.2. Ice-contact system

At the glacial maximum, the upward transition from outwash facies (diamictites and large sand-filled channels), into a conspicuous subglacial deformation zone, and finally distal glaciomarine facies (diamicton deltas?) is characteristic. These changes imply proximal proglacial deposition during ice-sheet advance, full glacial conditions, and rapid retreat of the grounded ice sheet. Lateral and vertical lithofacies substitution is common in the ice-contact system. However, since ice-contact systems are recognised in both the High Atlas and Rehamna sections, palaeogeographic linkage between these areas at the glacial maximum was likely. Sediment was probably transported onto the proglacial shelf by a combination of subglacial and proglacial channels (Fig. 13). The transition toward shelf delta systems is less certain because of the lack of continuous exposure between the Rehamna and Massif Central, but it is suggested that these systems interdigitated at their depositional termini (Fig. 12).

5.3. Shelf-delta system

The lack of subglacial soft-sediment deformation structures north of the Rehamna inlier suggests that syn-glacial sediments north of it were deposited in a paraglacial setting untouched by an ice sheet (Fig. 13A). The growth of deltas in this area is consistent with earlier interpretations (e.g., Khoukhi and Hamoumi, 2001; Baudin et al., 2001; Razin et al., 2001). The similarity in the vertical lithofacies successions in both the Massif Central and Coastal Meseta, and lateral extent of mouth bar sands over at least 100 km between them, implies delta formation over a vast, topographically subdued shelf area. Growth of these deltas during a significant phase of sea-level fall is supported by the sand-prone nature of mouth bar facies and evidence for their extensive reworking. Syn-glacial sediments of the Massif Central and Coastal Meseta are comparable to shelf margin deltas perched at or near a break in slope on the continental shelf (Porebski and Steel, 2003). During glacio-eustatic sea level fall, bypassing of sediment onto the shelf edge is promoted, and sandy mouth-barred deltas offlap inner shelf sand and mud (Porebski and Steel, 2003). Such a palaeogeographic position is supported by the lateral extent and tabular geometry of their mouth bar sands. Thin fluvial sediments (pebbly horizons) were deposited either as delta topsets or during late lowstand conditions. As tidal facies interpreted as transgressive deposits occur directly above the mouth bars, the second hypothesis is preferred.

Shelf margin deltas probably merged landward (northward) into a network of fluvial channels (Fig. 13B). The local occurrence of clast poor, sandy diamictites in the Coastal Meseta could suggest that at least some sediment was ice-derived from a local ice cap (see below). Basinward (southward), deltas merged into inner shelf environments (High Atlas, Rehamna) (Fig. 12), dominated by storm deposition, with subordinate turbiditic deposition.

At the glacial maximum, accommodation space was minimal. The disconformity separating the two coarsening-upward motifs in the Massif Central and Coastal Meseta is considered to be time-equivalent to subglacial erosion southward, forming as the ice advanced to its glacial maximum position (Fig. 12). It resulted in erosion

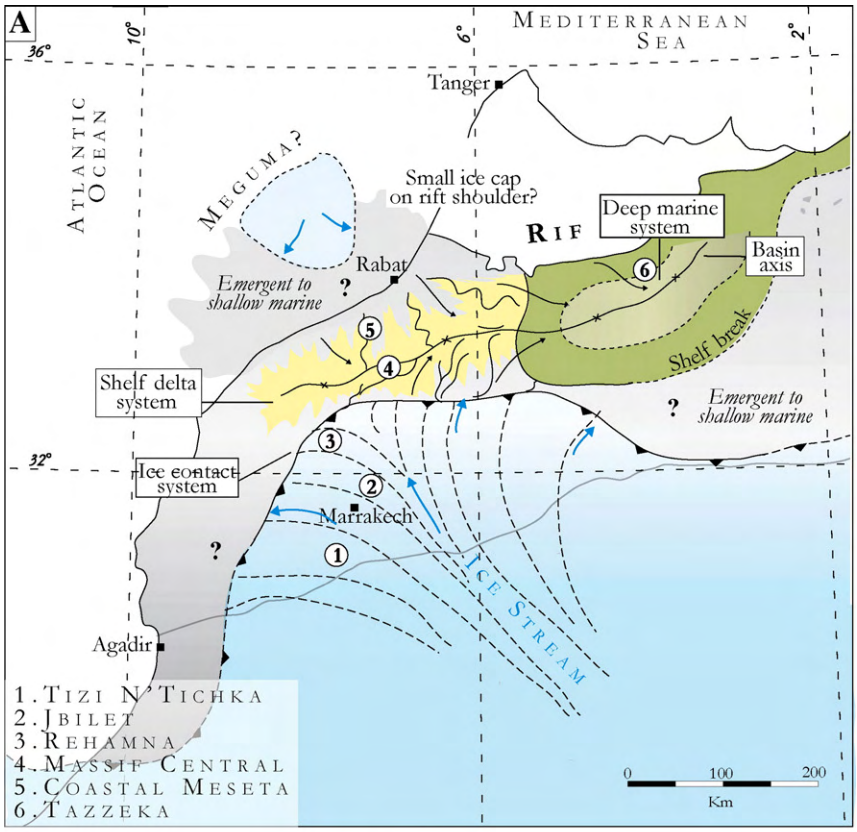
A
MEDITERRANEAN SEA
ATLANTIC OCEAN
36°
10°
6°
2°
32°
Tanger
Rabat
Marrakech
Agadir
MEGUMA?
Small ice cap on rift shoulder?
RIF
Deep marine system
Basin axis
Shelf break
Emergent to shallow marine
Shelf delta system
Ice contact system
ICE STREAM
1. TIZI N'TICHKA
2. JBILET
3. REHAMNA
4. MASSIF CENTRAL
5. COASTAL MESETA
6. TAZZEKA
0 100 200
Km

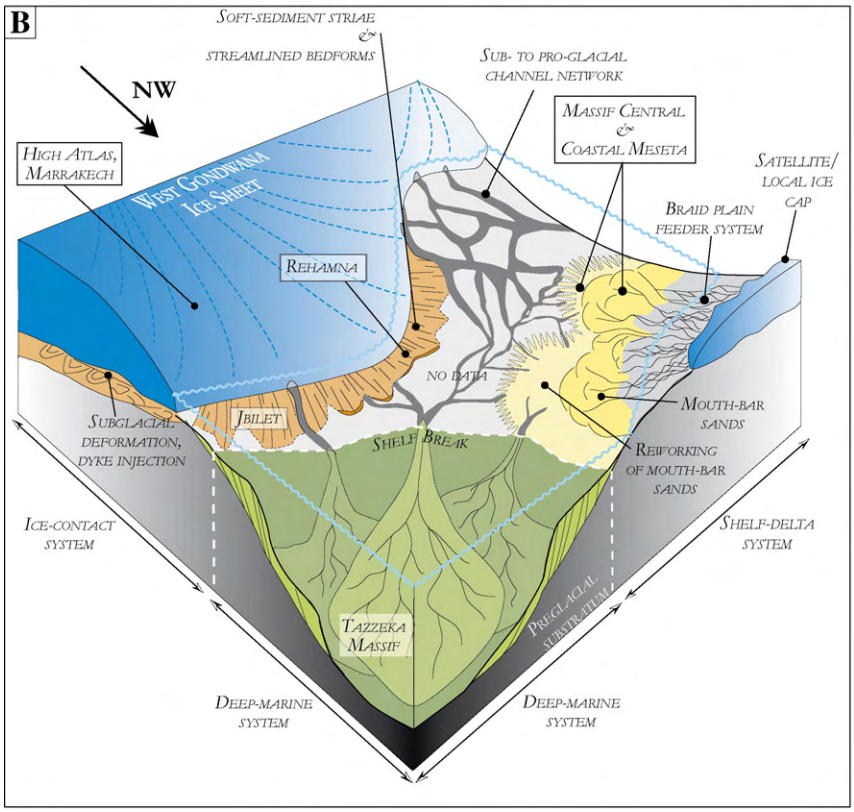
B
NW
SOFT-SEDIMENT STRIAE & STREAMLINED BEDFORMS
SUB- TO PRO-GLACIAL CHANNEL NETWORK
MASSIF CENTRAL & COASTAL MESETA
SATELLITE/ LOCAL ICE CAP
HIGH ATLAS, MARRAKECH
WEST GONDWANA ICE SHEET
BRAID PLAIN FEEDER SYSTEM
REHAMNA
NO DATA
MOUTH-BAR SANDS
SUBGLACIAL DEFORMATION, DYKE INJECTION
JBILET
SHELF BREAK
REWORKING OF MOUTH-BAR SANDS
ICE-CONTACT SYSTEM
SHELF-DELTA SYSTEM
TAZZEKA MASSIF
PREGLACIAL SUBSTRATUM
DEEP-MARINE SYSTEM
DEEP-MARINE SYSTEM

of the mouth bar as a result of sea-level fall during ice sheet expansion. At that time, the fluvial system would have connected directly with an underflow-dominated deep-marine system (Tazzeka domain). Though we observed no canyon systems in the course of this study, probably as a result of their very limited lateral extent, they are likely to exist and probably formed an integral sediment pathway to the deep-marine system (Fig. 13B).

5.4. Deep-marine system

During the late Quaternary glacial maximum, large trough–mouth fan-systems formed beyond the shelf break in the Barents Sea (e.g., Taylor et al., 2002). However, these deposits are a poor analogue to those of the Tazzeka Massif because they are built largely of unevolved glaciogenic debris flows. In contrast, the Wilkes Land turbidite systems fed by palaeo-ice streams in Antarctica are a better analogue (e.g., Escutia et al., 2000). Whereas the main part of the Tazzeka succession represent deposition on distal to medial part of a deep-marine fan, the stacked, amalgamated packages of sandstone towards the top of unit 1, interpreted as stacked debris flows, are best developed in the proximal part of the turbidite fan and imply heightened rates of sediment supply, sediment remobilisation, and fan-lobe growth in the deep basin. These conditions prevailed at the glacial maximum.

Knowledge of the causes of sediment remobilisation is essential to understand the linkage between ice-contact, shallow and deep-marine settings. In modern settings, mobilisation of shelf-margin sediments to the deep-marine system occurs via mass-movement/slope instability (Stow and Johansson, 2000), "seafloor polishing" from wave and tide agitation (Armishaw et al., 2000; Stow and Mayall, 2000), or direct throughput by fluvial floods (Mutti et al., 1996, 1999). These processes generate gravity flows (Shanmugam, 2000).

In the Tazzeka Massif, turbidites evolved downdip from mouth bar sands at the foot of a south to south-eastward slope from the Massif Central and Coastal Meseta. These conditions are thought to have persisted during the first, second and fourth glacially related cycles. It is thus suggested that bypass wedges resulted from periodic instability of the shelf-margin delta mouth bars, in combination with direct throughput by fluvial floods. Distal glaciomarine facies were deposited during ice retreat episodes and correlative sea-level rise.

This deep-water area lay beyond both the shelf-delta and ice-contact systems (Fig. 13A, B). It was the final repository for glacially derived sediments, sourced from the NNW advancing ice sheet that covered the Tindouf Basin (Destombes et al., 1985). The latter interpretation is supported by earlier work (Sutcliffe et al., 2001), raising the possibility that sediments in the deeper parts of the basin were derived from two sediment sources, one from the ice sheet, and the other from an upland area/palaeohigh beyond the ice front (Fig. 12). Such a mixed sediment source is envisaged for the amalgamated sandstones at the top of unit 1 (deposited during the glacial maximum), both by their coarse-grained nature and their depositional processes (stacked debris flows, high-energy underflows). The dramatic increase in sediment thickness between the Massif Central/Coastal Meseta and the Tazzeka Massif (Fig. 2, inset) may thus indicate the first description of a Late Ordovician trough-mouth fan in North Africa, though further work is required to confirm this interpretation.

6. Palaeogeographic implications

6.1. Gondwana ice-sheet extent

The lateral extent of subglacial bedforms is a powerful means of constraining the dimensions of former ice sheets (e.g., Jansson and Glasser, 2005). The occurrence of subglacial deformation structures in the High Atlas of Marrakech and the Rehamna inliers extends the ice sheet at least 200 km beyond the northernmost occurrences of striated surfaces reported by previous authors (Central Anti-Atlas, Destombes, 1969; Hamoumi, 1988), or 150 km north of the most distal glaciotectonic folds and thrusts (Alnif, Sutcliffe et al., 2001) or glacial valleys (Destombes et al., 1985; Alvaro et al., 2004). Taking into account directional data in the Anti-Atlas, and assuming a lobate ice front geometry, similar to that of the late Pleistocene in Fennoscandia (e.g., Punkari, 1997), then the ice covered a semi-elliptical area of at least 200 km×

Fig. 13. (A) Palaeogeographic reconstruction of the northwestern fringe of Africa during the Late Ordovician glacial maximum, showing extension of the ice front across the Anti-Atlas and into the Moroccan Meseta. A shallow-marine area occupied by shelf margin deltas occurred just in front of the ice sheet. Limited palaeocurrent data imply a palaeohigh towards the northwest, potentially an extension of Nova Scotian upland. These two sediment sources probably commingled in the deep basin, which received a thick succession of underflow deposits. (B) Block diagram/depositional model for northern Morocco at the Late Ordovician glacial maximum. The linkage and inter-relationship of both the ice-contact and shelf delta environments and the deep-marine system is emphasised in the text.

400 km. The area of this hitherto unknown ice cover is approximately 0.2 million km^2, of comparable size to the UK (Fig. 13A).

The new data presented in this article give a lucid illustration of the palaeogeographic changes that occur at and beyond the terminus of an ancient ice sheet at its glacial maximum. Both the geometry of this ice front and the character of sediments derived from it were probably closely dependent on the character of ice sheet flow and processes of erosion further up-glacier, south into the Anti-Atlas of Morocco and the Algerian Sahara. Recent work on the Pleistocene glacial record has focussed on the location of palaeo-ice streams, fast-flowing corridors of ice up to hundreds of kilometres long and tens of kilometres wide (e.g., Stokes and Clark, 2001). Their description as the arteries of ice sheets reflects their phenomenal drainage capacity and ability to substantially modify their topographic profile and lateral extent (Bennett, 2003). In the Anti-Atlas and the Tindouf Basin, isopach maps show (1) a pre-glacial depocentre dominated by clay-prone sediment that is centred over the Central Anti-Atlas (Fig. 1) and (2) a syn-glacial depocentre oriented SSE–NNW (Destombes et al., 1985). As the axis of both the pre-glacial and synglacial depocentres are aligned, these may preferentially have been occupied by a palaeo-ice stream at the glacial maximum (Fig. 13A). For these reasons, a palaeo-ice stream is tentatively placed over the Anti-Atlas at the height of the glaciation (Fig. 13). New data are needed to support this hypothesis, which for the moment can only be regarded as speculative.

6.2. Location of the Meseta relative to the West African Craton

Close correlation between the High Atlas and Rehamna is extremely significant because, structurally, the former area belongs to the West African Craton (Allary et al., 1972). Therefore, as the ice-sheet straddling the Meseta originated from the south, our data not only show the presence of ice in the Meseta (Rehamna) but demonstrate that it was in full palaeogeographic communication with the Anti-Atlas. These data imply that during the Late Ordovician, no large oceanic domain existed between the Meseta and Gondwana, supporting the conclusions of Piqué and Michard (1989). However, lateral displacement along the South Atlas Thrust may have occurred since the Ordovician, and the Late Ordovician location of the Meseta relative to the Anti-Atlas may have been shifted to some extent eastward or westward.

6.3. Palaeohighs on the West Gondwana margin

As discussed above, shelf margin deltas prograding south- or southeastward developed beyond the NW margin of the Gondwana ice-sheet. Deep-marine systems occurred eastward in the Tazzeka domain, supporting the existence of an eastward deepening basin/embayment between the Anti-Atlas and the northern Meseta, as proposed by previous workers (Hamoumi, 1988; Khoukhi and Hamoumi, 2001). To the west and/or north of the Coastal Meseta lay an upland area (Fig. 13). Addition data to support the occurrence of such a palaeohigh includes Middle to Late Ordovician hiatus accompanied by magmatic activity (Charlot et al., 1973; El Hassani et al., 1991; El Kamel et al., 1998). In the Sehoul zone, Silurian strata rest directly on deformed Cambrian strata that are intruded by Middle Ordovician granite (Piqué et al., 1993). In addition, in Nova Scotia, which was a part of the West Gondwana margin in the Late Ordovician (the Meguma zone; e.g., Schenk, 1997), up to 10 km of volcanogenic deposits dated at 438+3/−2 Ma were deposited on lower Ordovician clastics after a 60 Ma hiatus (MacDonald et al., 2001). The alkaline affinity of these rocks implies an intraplate rift (MacDonald et al., 2001) and of comparable geochemistry to rarely occurring ash horizons in the Coastal Meseta (El Kamel et al., 1998). It is possible that the thermal event known in the Meseta (Clauer et al., 1995) could account for palaeo-highs to the west of this area. Taken together, these observations suggest that upland areas in the westernmost and/or northern Meseta might relate to rift shoulder uplift. However, the thickness of underflow deposits in the Tazzeka Massif aside, no evidence is found for a rift propagating directly into the Meseta is identified as suggested previously (e.g., Stampfli and Borel, 2002). Instead, the locus for rifting probably lay beyond the present-day Meseta.

6.4. Satellite ice caps

In the context of uplands beyond the ice sheet, the occurrence of relatively proximal glaciomarine deposits in the uppermost part of the Late Ordovician succession in the Coastal Meseta is noteworthy. Here, glaciogenic lithofacies were not deposited during the main part of the glaciation because glacio-eustatic sea-level fall exposed the shelf leading to the development of a fluvial network that fed the shelf margin deltas (see above). However, following melting of the Hirnantian ice sheet, high sea levels were restored and backstepping shorelines may have allowed a marine ice front to form from individual ice caps centred on upland area that

were probably more stable and long-lived than the huge, low-lying Gondwana ice sheet.

In Western Europe (Portugal, Spain, France), which lay at the fringes of Gondwana, widespread glaciomarine lithofacies are recognised (Robardet and Doré, 1988). To analyse these successions in detail is beyond the scope of this paper. However, the prevalence of sandy diamictite facies merits consideration because of their similarity to the topmost diamictites of the Coastal Meseta (Fig. 2). Earlier workers suggested glacier-ice or sea-ice rafting for the deposition of these rocks (Fortuin, 1984; Robardet and Doré, 1988). An alternative explanation could be the existence of several ice caps sited on upland areas during the Hirnantian. The recognition of widespread subglacial structures in these areas is unlikely as glaciers would have populated palaeohighs, leaving no sedimentary record on the uplands. However, marine ice fronts imply that valley glaciers or glacial lobes reached sea level. Localised subglacial deformation may have been preserved, but while striated pavements have been reported by previous workers (Arbey and Tamain, 1971), later authors prefer a tectonic interpretation for these structures (Robardet and Doré, 1988). Nevertheless, the existence of small ice caps is also inferred from the Late Ordovician glacial record in Newfoundland, an area that was located at notably lower palaeolatitudes but corresponding to island arcs in the Iapetus Ocean (MacNiocaill et al., 1997).

7. Conclusions

1. Firm evidence that the Moroccan Meseta was in palaeogeographic communication with the Anti-Atlas during the Late Ordovician is provided by the discovery of glaciogenic deposits north of the Southern Atlas Thrust. Correlation between the Rehamna and the High Atlas of Marrakech demonstrates that the Anti-Atlas and Meseta were subject to a mutual phase of glaciation during the glacial maximum.
2. Evidence for the presence of former ice sheets includes soft-sediment striations, streamlined bedforms, downward-injected sedimentary dykes, shear zones and chaotic fold zones, capped, at least in the Rehamna inlier, by a distinctive diamictite. High-energy meltwater channels (jökulhlaup outburst channels) occur in the High Atlas.
3. A palaeogeographic transect over >400 km recognises ice-contact, shelf-margin and deep-marine proglacial depositional environments. The transition between these zones is not defined by a simple proximal-distal profile because an upland area persisted beyond the Coastal Meseta, potentially occupied by a satellite ice cap and possibly caused by rift-shoulder uplift.
4. A deep-marine system, represented by the Tazzeka Massif, lay in the eastern Meseta beyond the ice front. It was not overridden by an ice sheet as a result of the significant break in bathymetry that would have occurred in a north-eastward direction, and was probably fed from two sediment sources—namely, the ice-contact and shelf-delta systems.
5. Two depositional units contain the record of four glacioeustatic sea level variations, thought to relate to the waxing and waning of other parts of the Gondwana ice sheet.

Acknowledgements

Dan Le Heron was supported by TOTAL during his tenure as a research scientist. He was employed by the CNRS, France, and based at École et Observatoire des Sciences de la Terre, Université Louis Pasteur, Strasbourg (UMR CNRS 7517). Age determinations and analyses of fossil material were kindly undertaken by Petr Storch (graptolites) of the Institute of Geology, Academy of Sciences, Czech Republic, and Florentin Paris (chitinozoa) of Géosciences Rennes. We are especially grateful to Dr Philippe Razin for providing basemaps and key information on the best localities in the Massif Central and Rehamna, and to Professor Hassan El Chellai for his generous spirit and warm hospitality in Marrakech. The comments of two reviewers (Professor Pat Brenchley and Anonymous) allowed us to improve this work considerably. Dr Dom Strogen is acknowledged for his comments on the final version. This paper is a contribution to IGCP 503.

References

Aghzer, A.M., Arenas, R., 1995. Détachement et tectonique extensive dans le massif hercynien des Rehamna, (Maroc). Journal of African Earth Sciences 21 (3), 383–393.

Allary, A., Andrieux, J., Lavenu, A., Ribeyrolles, M., 1972. Les nappes hercyniennes de la Meseta sud-orientale (Maroc central). Comptes Rendus de l'Academie des Sciences, Paris. Serie D. Sciences Naturelles 274, 2284–2287.

Allary, A., Lavenu, A., Ribeyrolles, M., 1976. Etude tectonique et microtectonique d'un segment de chaîne hercynienne dans la partie sud-orientale du Maroc central. Notes et Mémoires de la Service Géologique du Maroc, vol. 276. 169 pp.

Alvaro, J.-J., Vennin, E., Villas, E., Destombes, J., Vizcaïno, D., 2004. Hirnantian valley–glacier sedimentation in the eastern Anti-Atlas, Morocco. Erlanger Geologische Abhandlungen. Sonderband 5, 18–19.

Arbey, F., Tamain, G., 1971. Existence d'une glaciation siluro-ordovicienne en Sierra Morena (Espagne). Comptes Rendus de

l'Academie des Sciences, Paris. Serie D. Sciences Naturelles 272, 1721–1723.
Armishaw, J., Holmes, R., Stow, D.A.V., 2000. The Barra Fan: a bottom-current reworked, glacially-fed submarine fan system. Marine and Petroleum Geology 17, 219–238.
Badalini, G., Redfern, J., Carr, I., 2002. Introduction: a synthesis of current understanding of the structural evolution of North Africa. Journal of Petroleum Geology 25, 1–15.
Baudin, T., Chevremont, P., Razin, P., Theiblemont, D., Rachdi, H., Roger, J., Benhaourch, R., Winckel, A., 2001. Carte Géologique du Maroc au 1: 50,000 Feuille d'Oulmès-Mémoire Explicatif. Éditions du service géologique du Maroc, Rabat.
Bamoumen, H., 1988. Géométrie et cinématique de la déformation dans les nappes hercyniennes des Jebilet centre-orientales, Maroc. Thèse de 3ème Cycle, Université de Marrakech, 189p.
Bennett, M.R., 2003. Ice streams as the arteries of an ice sheet: their mechanics, stability and significance. Earth-Science Reviews 61 (3–4), 309–339.
Biju-Duval, B., 1974. Exemples de depots fluvioglaciares dans l'Ordovicien superieur du Sahara central. Bulletin Centre de Recherches de Pau 8, 209–236.
Bernardin, C., Cornée, J-J., Corsini, M., Mayol, S., Muller, J., Tayebi, M., 1988. Les variations d'épaisseurs du Cambrien moyen en Meseta occidentale. Données de surface et de subsurfaces. Signification géodynamique. Canadian Journal of Earth Sciences 25, 2104–2117.
Beuf, S., Biju-Duval, B., de Charpal, O., Rognon, P., Gariel, O., Bennacef, A., 1971. Les Grés du Paléozoïque inférieur au Sahara. Paris, Editions Technip. 464 pp.
Bouabdelli, M., 1989. Tectonique et sédimentation dans un bassin orogénique, le sillon viséen d'Azrou-Khénifra (Est du Massif hercynien central du Maroc). Thèse d'Etat, Université Louis-Pasteur, Strasbourg, 262p.
Bourahrouh, A., Paris, F., Elaouad-Debbaj, Z., 2004. Biostratigraphy, biodiversity and palaeoenvironments of the chitinozoans and associated palynomorphs from the Upper Ordovician of the Central Anti-Atlas, Morocco. Review of Palaeobotany and Palynology 130, 17–40.
Brenchley, P.J., Marshall, J.D., Carden, G.A.F., Robertson, D.B.R., Long, D.G.F., Meidla, T., Hints, L., Anderson, T.F., 1994. Bathymetric and isotopic evidence for a short-lived Ordovician glaciation in a greenhouse period. Geology 22, 295–298.
Caritg, S., Burkhard, M., Ducommun, R., Helg, U., Kopp, L., Sue, C., 2004. Fold interference patterns in the Late Palaeozoic Anti-Atlas belt of Morocco. Terra Nova 16, 27–37.
Carrivick, J.L., Russell, A.J., Tweed, F.S., 2004. Sedimentology and palaeohydrology of jökulhlaups from Kverkfjöll, Iceland. Sedimentary Geology 172, 19–40.
Charlot, R., Rhalib, M., Tisserant, D., 1973. Étude géochronologique préliminaire des granites de la region du Rabat-Tiflet (Maroc occidental). Notes et Mémoires du Service Géologique du Maroc 249, 55–58.
Chèvremont, P., Cailleux, Y., Baudin, T., Razin, P., Thiéblemont, D., Hoepffner, C., Bensahal, A., Benhaourch, R., 2001. Carte Géologique du Maroc au 1: 50,000 Feuille de d'Ezzhiliga-Mémoire Explicatif. Éditions du service géologique du Maroc, Rabat.
Clauer, N., Rais, N., Schaltegger, U., Piqué, A., 1995. K–Ar systematics of clay-to-mica minerals in a multi-stage low-grade metamorphic evolution. Chemical Geology 124, 305–316.
Cornée, J.-J., Destombes, J., Willefert, S., 1987. Stratigraphie du Paléozoïque de l'extrémité nord-ouest du Haut-Atlas occidental (Maroc hercynien); interprétation du cadre sédimentaire du Maroc occidental. Bulletin de la Societé Geologique de France 8, 327–335.
Destombes, J., 1968. Sur la presence d'une discordance generale de ravinement d'age Ashgill superieur dans l'Ordovicien terminal de l'Anti-Atlas (Maroc). Comptes Rendus de l'Academie des Sciences, Paris. Serie D. Sciences Naturelles 267, 565–567.
Destombes, J., 1971. L'Ordovicien au Maroc. Essai de synthèse stratigraphique. Mémoires de la B.R.G.M. Paris, vol. 73, pp. 237–263.
Destombes, J., Holland, H., Willefert, S., 1985. Lower Paleozoic rocks of Morocco. In: Holland, C.H. (Ed.), Lower Palaeozoic Rocks of the World. Wiley, London, pp. 91–336.
Destombes, J., Willefert, S., 1988. The Ordovician–Silurian boundary in Morocco. Bulletin of the British Museum, Natural History. Geology 43, 165–170.
Deynoux, M., 1985. Terrestrial or waterlain glacial diamictites? Three case studies from the Late Precambrian and Late Ordovician glacial drifts in West Africa. Palaeogeography, Palaeoclimatology, Palaeoecology 51, 97–141.
Deynoux, M., Ghienne, J.-F., 2004. Late Ordovician glacial pavements revisited: a reappraisal of the origin of striated surfaces. Terra Nova 16, 95–101.
El Attari, A., 2001. Etude lithostratigraphique et tectonique des terrains paléozoïques du Môle Côtier (Meseta Orientale, Maroc). Thèse d'Etat, Université Mohammed V Agdal, Rabat, 394p.
El Attari, A., Hoepffner, C., Jouhari, A., 1997. Nouvelles données magmatiques et structurales en relation avec la cinématique de l'ouverture du bassin cambrien de la Meseta occidentale (Maroc). Gaia 14, 11–21.
El Hassani, A., Huon, S., Hoepffner, C., Whitechurch, H., Piqué, A., 1991. Une déformation d'âge ordovicien moyen dans la zone des Sehoul (Meseta marocaine septentrionale). Regard sur les segments "calédoniens" au NW de l'Afrique. Comptes Rendus de l'Academie des Sciences, Paris. Serie 2. Sciences de la Terre 312, 1027–1032.
El Houicha, M., 1994. Dynamique d'un bassin orogénique et processus gravitaires syn-à-tadi-sédimentaires: Le sillon viséo-namurien de Khénifra (SE du Massif hercynien central du Maroc). Thèse de 3ème Cycle, Université de Marrakech, 170p.
El Kamel, F., Remmal, T., Mohsine, A., 1998. Evidence of a post Caledonian withinplate alkaline magmatism in the Ouled Abbou Silurian basin (coastal Meseta, Morocco). Comptes Rendus de l'Academie des Sciences, Paris. Series II. Sciences de la Terre et des Planetes 327, 309–314.
Escutia, C., Eittreim, A.K., Cooper, A.K., Nelson, C.H., 2000. Morphology and acoustic character of the Antarctic Wilkes Land turbidite systems: ice-sheet-sourced versus river-sourced fans. Journal of Sedimentary Research 70, 84–93.
Fabre, J., 1971. Structure de l'Algérie saharienne. Eléments pour une carte tectonique. Bulletin du Service géologique de l'Algérie 41, 161–185.
Fortuin, A.P., 1984. Late Ordovician glaciomarine deposits (Orea Shale) in the Sierra de Albarracin, Spain. Palaeogeography, Palaeoclimatology, Palaeoecology 48, 245–261.
Ghienne, J.-F., 2003. Late Ordovician sedimentary environments, glacial cycles, and post-glacial transgression in the Taoudeni Basin, West Africa. Palaeogeography, Palaeoclimatology, Palaeoecology 189, 117–145.
Ghienne, J.-F., Deynoux, M., 1998. Large-scale channel fill structures in Late Ordovician glacial deposits in Mauritania, western Sahara. Sedimentary Geology 119, 141–159.
Ghienne, J.-F., Deynoux, M., Manatschal, G., Rubino, J.-L., 2003. Palaeovalleys and fault-controlled depocentres in the Late Ordovician glacial record of the Murzuq Basin (central Libya). Comptes Rendus Geosciences 335, 1091–1100.

Hamoumi, N., 1988. La plate-forme ordovicienne du Maroc: Dynamique des ensembles sédimentaires. Thèse de 3ème Cycle, Université Louis Pasteur, Strasbourg, 237p.

Hart, J.K., Boulton, G.S., 1991. The interrelation of glaciotectonic and glaciodepositional processes within the glacial environment. Quaternary Science Reviews 10, 335–350.

Hirst, J.P.P., Benbakir, A., Payne, D.F., Westlake, I.R., 2002. Tunnel valleys and density flow processes in the upper Ordovician glacial succession, Illizi Basin, Algeria: influence on reservoir quality. Journal of Petroleum Geology 25, 297–324.

Hoepffner, C., 1974. Contribution a la géologie structurale des Rehamna (Meseta marocaine méridionale): Le matériel Paléozoïque et son évolution Hercynienne dans l'est du massif. Thèse de 3ème Cycle, Université Louis Pasteur, Strasbourg, 91p.

Hoepffner, C., 1987. La tectonique hercynienne dans l'Est du Maroc. Thèse d'Etat, Université Louis Pasteur, Strasbourg, 280p.

Hollard, H., Huvelin, P., Mamet, B., 1977. Stratigraphie du Viséen supérieur des Jebilets et âge de la mise en place de la nappe des Jebilets orientales (Maroc). Notes et Mémoires du Service Géologique du Maroc 37 (267), 7–22.

Huvelin, P., 1977. Etude Geologique et Gitologique du Massif Hercynien des Jebilet (Maroc Occidental), vol. 232. Editions du service géologique du Maroc, Rabat. 307 pp.

Hyam, D.M., Marshall, J.E.A., Sanderson, D.J., 1997. Carboniferous dykes in the Falkland Islands. Journal of African Earth Sciences 25, 505–517.

Jansson, K.N., Glasser, N., 2005. Palaeoglaciology of the Welsh sector of the British–Irish ice sheet. Journal of the Geological Society (London) 162, 25–37.

Jenny, J., 1983. L'avant-pays présaharien (Anti-Atlas central) et la partie méridionale de la chaîne hercynienne du Maroc. In: Caledonian Orogeny IGCP n°27, Rabat symposium. Excursion guide B5, 82-99. Service Géologique du Maroc.

Khoukhi, Y., 1993. L'Ordovicien et le Cambro-ordovicien de la Meseta orientale, Maroc: Pétrologie, dynamique sédimentaire et stratigraphie séquentielle. Thèse de 3ème Cycle, Faculté des Sciences d'Oujda, Morocco.

Khoukhi, Y., Hamoumi, N., 2001. L'Ordovicien de la Meseta orientale (Maroc): Stratigraphie génétique- contrôle géodynamique, climatique et eustatique. African Geoscience Review 8, 289–302.

Kor, P.S.G., Shaw, J., Sharpe, D.R., 1991. Erosion of bedrock by subglacial meltwater, Georgian Bay, Ontario: a regional view. Canadian Journal of Earth Sciences 28, 623–642.

Lagarde, J.-L., Michard, A., 1986. Stretching normal to the regional thrust displacement in a thrust wrench shear zone, Rehamna massif, Morocco. Journal of Structural Geology 8 (3/4), 483–492.

Laville, E., Piqué, A., 1991. La distension crustale atlantique et atlasique au Maroc au début du Mésozoïque: Le rejeu des structures hercyniennes. Bulletin de la Société géologique de France 162, 1161–1171.

Le Heron, D., Sutcliffe, O., Bourgig, K., Craig, J., Visentin, C., Whittington, R., 2004. Sedimentary architecture of Upper Ordovician tunnel valleys, Gargaf Arch, Libya: implications for the genesis of a hydrocarbon reservoir. GeoArabia 9, 137–160.

Le Heron, D.P., Sutcliffe, O.E., Whittington, R.J., Craig, J., 2005. The origins of glacially related soft-sediment deformation structures in Upper Ordovician glaciogenic rocks: implication for ice sheet dynamics. Palaeogeography, Palaeoclimatology, Palaeoecology 218, 75–103.

Lüning, S., Craig, J., Loydell, D.K., Storch, P., Fitches, W., 2000. Lowermost Silurian "hot shales" in north Africa and Arabia: regional distribution and depositional model. Earth-Science Reviews 49, 121–200.

MacDonald, L.A., Barr, S.M., White, C.E., Ketchum, J.W.F., 2001. Petrology, age, and tectonic setting of the White Rock Formation, Meguma terrane, Nova Scotia: evidence for Silurian continental rifting. Canadian Journal of Earth Sciences 39, 259–277.

MacNiocaill, C., van der Pluijm, B.A., van der Voo, R., 1997. Ordovician paleogeography and the evolution of the Iapetus Ocean. Geology 25, 159–162.

Monod, O., Kozlu, H., Ghienne, J-F., Dean, W.T., Günay, Y., Le Hérissé, A., Paris, F., Robardet, M., 2003. Late Ordovician glaciation in southern Turkey. Terra Nova 15 (4), 249–257.

Mutti, E., Davoli, G., Tinterri, R., Zavala, C., 1996. The importance of ancient fluvio-deltaic systems dominated by catastrophic flooding in tectonically active basins. Memorie di Scienze Geologiche Padova 48, 233–291.

Mutti, E., Tinterri, R., Remacha, E., Mavilla, N., Angella, S., Fava, L., 1999. An introduction to the analysis of ancient turbidite basins from an outcrop perspective. American Association of Petroleum Geologists Continuing Education Course Notes Series, vol. 39. Oklahoma, USA.

Nio, S.-D., Yang, C.-S., 1991. Diagnostic attributes of clastic tidal deposits: a review. In: Smith, D.G., Reinson, B., Zaitlin, B.A., Rahmani, R.A. (Eds.), Clastic Tidal Sedimentology. Canadian Society of Petroleum Geologists Memoir, vol. 16, pp. 3–28.

Ouanami, H., 1989. Évolution sédimentaire et tectonique de la partie orientale du Massif Ancien du Haut Atlas (Maroc). Thèse de 3ème Cycle, Université de Montpelier-II.

Ouanami, H., 1998. Le passage Ordovicien–Silurien à Tizi n'Tichka (Haut-Atlas, Maroc): Variations du niveau marin. Comptes Rendus de l'Académie des Sciences, Paris. Series II. Sciences de la Terre et des Planetes 326, 65–70.

Ouanami, H., Petit, J.-P., 1992. La limite sud de la chaîne hercynienne dans le Haut Atlas marocain: Reconstitution d'un saillant non déforme. Bulletin de la Société géologique de France 162, 63–72.

Paris, F., Elaouad-Debbaj, Z., Jaglin, J.C., Massa, D., Oulebsir, L., 1995. Chitinozoans and Late Ordovician glacial events on Gondwana. In: Cooper, J.D., Droser, M.L., Finney, S.C. (Eds.), Ordovician Odyssey: Short Papers for the Seventh International Symposium on the Ordovician System. The Pacific Section Society for Sedimentary Geology (SEPM), Fullerton, California, pp. 171–177.

Paris, F., Deynoux, M., Ghienne, J.F., 1998. Découverte de chitinozoaires à la limite Ordovicien–Silurien en Mauritanie; implications paléogéographiques. Comptes Rendus de l'Académie des Sciences, Paris. Series II. Sciences de la Terre et des Planetes 326, 499–504.

Piqué, A., 1979. Evolution structurale d'un segment de la chaîne hercynienne: La Meseta marocaine nord-occidentale. Thèse d'Etat, Université Louis Pasteur, Strasbourg, 253p.

Piqué, A., 2001. Gebrueder Borntraeger Verlagsbuchhandlung. Geology of Northwest Africa. Federal Republic of Germany, Berlin-Stuttgart. 324 pp.

Piqué, A., Michard, A., 1989. Moroccan Hercynides: a synopsis. The Paleozoic sedimentary and tectonic evolution at the northern margin of West Africa. American Journal of Science 289, 286–330.

Piqué, A., Jeannette, D., Michard, A., 1980. The western Meseta shear zone, a major and permanent feature of the Hercynian belt in Morocco. Journal of Structural Geology 2 (1/2), 55–61.

Piqué, A., O'Brien, S., King, A.F., Schenk, P.E., Skehan, J.W., Hon, R., 1990. La marge nord-occidentale du Paleo-Gondwana (Maroc occidental et zones orientales des Appalaches); Rifting au Précambrien terminal et au Paléozoïque inférieur, et compression hercynienne et alleghanienne au Paléozoique supérieur. Comptes Rendus de l'Académie des Sciences,

Paris. Series II. Sciences de la Terre et des Planetes 310, 411–416.
Piqué, A., El Hassani, A., Hoepffner, C., 1993. Les déformations ordoviciennes dans la zone des Sehoul (Maroc septentrional): Une orogenèse calédonienne en Afrique du Nord. Canadian Journal of Earth Sciences 30, 1332–1337.
Piqué, A., Bouabdelli, M., Darboux, R., 1995. Le rift cambrien du Maroc occidental. Comptes Rendus de l'Académie des Sciences, Paris 320, 1017–1024.
Piqué, A., Tricart, P., Guiraud, R., Laville, E., Bouaziz, S., Amrhar, M., Aït Ouali, R., 2002. The Mesozoic–Cenozoic Atlas belt (North Africa): an overview. Geodinamica Acta 15, 185–208.
Porebski, S.J., Steel, R., 2003. Shelf-margin deltas: their stratigraphic significance and relation to deepwater sands. Earth-Science Reviews 62, 283–326.
Punkari, M., 1997. Glacial and glaciofluvial deposits in the interlobate areas of the Scandinavian ice sheet. Quaternary Science Reviews, Special Issue 16, 12–26.
Razin, P., Janjou, D., Baudin., T., Benschal., A., Hoepffner, C., Thiéblemont, D., Chèvremont, P., Benhaourch, R., 2001. Carte Géologique du Maroc au 1: 50, 000 Feuille de Sidi Matla' Ech Chams-Mémoire Explicatif. Éditions du service géologique du Maroc, Rabat.
Robardet, M., Doré, F., 1988. The Late Ordovician diamictic formations from southwestern Europe: north-Gondwana glaciomarine deposits. Palaeogeography, Palaeoclimatology, Palaeoecology 66, 19–31.
Schenk, P.E., 1997. Sequence stratigraphy and provenance on Gondwana's margin: the Meguma Zone (Cambrian to Devonian) of Nova Scotia, Canada. Geological Society of America Bulletin 109 (4), 395–409.
Selley, R.C., 1997. In: Selley, R.C. (Ed.), The basins of NW Africa: structural evolution. African Basins: Sedimentary Basins of the World, vol. 3. Elsevier, Amsterdam, pp. 17–26.
Shanmugam, G., 2000. 50 years of the turbidite paradigm (1950s–1990s): Deep-water processes and facies models—a critical perspective. Marine and Petroleum Geology 17, 285–342.
Soulaimani, A., 1998. Interactions socle/couverture dans l'Anti-Atlas occidental (Maroc): Rifting fini-protérozoïque et orogenèse hercynienne. Thèse d'Etat, Université de Marrakech, Morocco, 189p.
Stampfli, G.M., Borel, G.D., 2002. A plate tectonic model for the Palaeozoic and Mesozoic constrained by dynamic plate boundaries and restored synthetic oceanic isochrons. Earth and Planetary Science Letters 196, 17–33.
Stokes, C.R., Clark, C.D., 2001. Palaeo-ice streams. Quaternary Science Reviews 20, 1437–1457.
Stow, D.A.V., Johansson, M., 2000. Deep-water massive sands: nature, origin and hydrocarbon implications. Marine and Petroleum Geology 17, 145–174.
Stow, D.A.V., Mayall, M., 2000. Deep-water sedimentary systems: new models for the 21st century. Marine and Petroleum Geology 17, 125–135.
Sutcliffe, O.E., Theron, J.A., Whittington, R.J., Theron, J.N., Craig, J., 2000. Calibrating the Late Ordovician glaciation and mass extinction by the eccentricity cycles of the Earth's orbit. Geology 23, 967–970.
Sutcliffe, O.E., Harper, D.A.T., Aït Salem, A., Whittington, R.J., Craig, J., 2001. The development of an atypical Hirnantia-brachiopod Fauna and the onset of glaciation in the Late Ordovician of Gondwana. Transactions of the Royal Society of Edinburgh. Earth Sciences 92, 1–14.
Taylor, J., Dowdeswell, J.A., Kenyon, N.H., O'Cofaigh, C., 2002. Late Quaternary architecture of trough-mouth fans: debris flows and suspended sediments on the Norwegian margin. In: Dowdeswell, J.A., O'Cofaigh, C. (Eds.), Glacier-Influenced Sedimentation on High-Latitude Continental Margins. Special Publication, vol. 203. Geological Society, London, pp. 55–71.
Underwood, C.J., Deynoux, M., Ghienne, J.-F., 1998. High palaeo-latitude (Hodh, Mauritania) recovery of graptolite fauna after the Hirnantian (end Ordovician) extinction event. Palaeogeography, Palaeoclimatology, Palaeoecology 142, 91–105.
Van der Wateren, F.M., Kluiving, S.J., Bartek, L.R., 2000. Kinematic indicators of subglacial shearing. In: Maltman, A.J., Hubbard, B., Hambrey, M.J. (Eds.), Deformation of Glacial Materials. Special Publication, vol. 176. Geological Society, London, pp. 259–278.

Did the Late Ordovician African ice sheet reach Europe?

Juan C. Gutiérrez-Marco[1]*, Jean-François Ghienne[2], Enrique Bernárdez[3], and Manuel P. Hacar[4]
[1]Instituto de Geología Económica (CSIC-UCM), Facultad de Ciencias Geológicas, Universidad Complutense de Madrid, José Antonio Novais 2, E-28040 Madrid, Spain
[2]Institut de Physique du Globe de Strasbourg (EOST), UMR 7516 CNRS/ Université de Strasbourg, 1 rue Blessig, F-67084 Strasbourg Cedex, France
[3]Departamento de Paleontología, Facultad de Ciencias Geológicas, Universidad Complutense de Madrid, E-28040 Madrid, Spain
[4]Ferrovial Agromán S.A., 434 Irakleiou Avenue and Thermopylon 6, G-14122 N Iraklio Attikis, Greece

ABSTRACT

Paleovalleys and their infilling successions are described from outcrops and drill cores of the Cantabrian Range (northern Spain). A *Hirnantia* fauna and associated diamictites with striated lonestones indicate that the paleovalleys are related to the Hirnantian (latest Ordovician) glacial event. Based on overall geometry, depositional facies, and associated deformation structures, the paleovalleys are interpreted as subglacial tunnel valleys. They were most likely related to the North Gondwana ice sheet. The ice sheet therefore reached the Ibero-Armorican domain that was still attached to the Gondwana landmass at least until the latest Ordovician.

INTRODUCTION

The Hirnantian glacial record documents one or several ice sheets throughout Africa, Arabia, and South America, the extents of which are still controversial (Ghienne et al., 2007; Schönian and Egenhoff, 2007). Although glaciomarine strata are widespread in European peri-Gondwanan terranes (Robardet and Doré, 1988; Brenchley et al., 1991), they do not precisely indicate the presence of glaciers at those localities. Because a number of these terranes would have been attached to the Gondwana landmass during the Late Ordovician (e.g., Robardet, 2003), the Gondwanan ice sheet may have reached some of them. The Hirnantian paleovalleys of the Cantabrian Range (northwest Spain) are the first glacial valleys to be recognized outside the Gondwana landmass. They may be related to a Gondwanan ice sheet lobe or to a peri-Gondwana satellite ice cap.

GEOLOGICAL SETTING AND STRATIGRAPHIC OVERVIEW

The Cantabrian Zone belongs to the northern part of the Iberian Massif of western Spain and Portugal (Fig. 1). It exhibits a Variscan thin-skinned structure complicated by the arcuate shape of the Ibero-Armorican Arc. It includes a relatively thin Cambrian–Ordovician succession in comparison with other parts of the Iberian Massif (Gutiérrez-Marco et al., 2002, and references therein). The late Cambrian–Early Ordovician Barrios Formation is a quartzite partially correlated to the Armorican Quartzite of southwestern Europe (Gutiérrez-Alonso et al., 2007). In most areas, the Barrios Formation is directly overlain by Silurian or Late Devonian strata (Aramburu and García-Ramos, 1993). Although the unconformity usually involves Middle Ordovician to Early Silurian rocks, outcrops of Darriwilian–Rhuddanian fossiliferous strata, including in places a late Katian limestone horizon (Del Moral, 2003), are locally preserved within the Somiedo, Bodón, and Correcilla nappes of the Cantabrian Zone (Fig. 1). Hirnantian diamictites, interbedded sandstones, and an overlying sharp-based sandstone horizon (Luna quartzite, named here from the location for the Luna dam; Fig. 1) have been identified (Bernárdez et al., 2006). This suggests that the regional unconformity between the Silurian black shales and the Early Ordovician quartzites may be, at least in part, related to the Hirnantian glacioeustatic sea-level fall rather than previously interpreted rift-related uplifts (Aramburu and García-Ramos, 1993; García-Alcalde, 1995).

Diamictites were initially identified by Bernárdez et al. (2006) in three localities (loc. 1, 3, and 7 in Fig. 1). These, together with five additional localities, have since been studied. The Hirnantian age of the diamictites is given by a low diversity *Hirnantia* fauna of brachiopods (*Plectothyrella crassicosta chauveli* Havlíček and *Arenorthis*, a.o.) both beneath (loc. 3; Bernárdez et al., 2006) and above the diamictites (loc. 8, in the Luna quartzite). Above the Luna quartzite or directly above the diamictites, the Silurian Formigoso Formation normally begins with a glauconitic sandstone (Getino Bed). Overlying graptolitic shales correlate with the upper Aeronian–lowest Telychian, with a possible hiatus of the earliest Silurian. Rhuddanian–Aeronian strata are, however, locally identified by rare limestone horizons (Sarmiento et al., 1994), suggesting that lowest Silurian rocks may compose the topmost beds of the Luna quartzite and the Getino Bed.

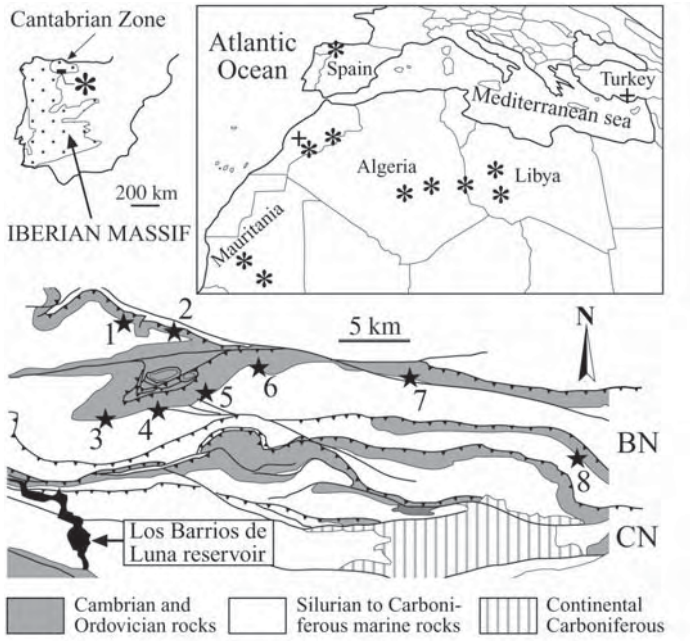

Figure 1. Location of studied area with reference to Iberian Massif (upper left) and to North Africa and southern Europe (upper right). Asterisks indicate locations of tunnel valleys related to Late Ordovician glaciation. Black crosses indicate northernmost occurrences of subglacial shear zones (Monod et al., 2003; Le Heron et al., 2007). Black stars in lower map indicate occurrences of Hirnantian rocks in southern Cantabrian Zone (BN—Bodón nappe; CN—Correcilla nappe). Localities: 1—Telledo paleovalley and drill core ST-5; 2—Pajares paleovalley; 3—Caldas de Luna intervalley zone and fossil locality; 4—Casares de Arbás diamictites; 5—Viadangos de Arbás paleovalley and drill core ST-16bis; 6—Busdongo; 7—Pontedo paleovalley; 8—Valdeteja fossil locality in Luna quartzite.

GEOMETRY OF HIRNANTIAN PALEOVALLEYS

Incisions that truncate Early Ordovician strata (Barrios Formation) are 200–250 m deep and 1–3 km wide, and have relatively flat bottoms. Valley margins have slopes of 5°–15°. The basal erosional surface is poorly recognized in outcrop, but sharp contacts are observed in drill cores where fine-grained strata directly overlie the Barrios Formation (Fig. 2A).

*E-mail: jcgrapto@geo.ucm.es.

Essentially two-dimensional profiles do not allow the orientation or the sinuosity of the paleovalleys to be determined. East-west–oriented cross sections through the outcrops, however, suggest a submeridian orientation. Several-kilometer-wide zones of lesser erosion are identified between two adjacent incisions. The sedimentary infill is mainly confined within the incisions and the uppermost beds rarely overstep intervalley zones.

PALEOVALLEY INFILL

Basal Sandstones

Most often, a basal depositional unit, as thick as 25 m, can be differentiated (loc. 5 and 7). It essentially comprises fine- to medium-grained, erosion-based, decimeter- to meter-thick sandstone beds. Horizontal lamination prevails, but ripple lamination or ripple morphologies on bed tops are also identified. Thin (<2 m) heterolithic intervals (see following) constitute a subordinate facies. This unit locally molds the erosion surface and is onlapped by the main infill (Fig. 2C). Basal sandstones include a variety of soft-sediment deformation structures, i.e., vertical sheet dewatering, load casts, undifferentiated liquefaction structures, extensional microfaults locally involved in boudinage structures (Fig. 2D), and sheath folds. A single outcrop yields small-scale intraformational grooves (Fig. 2E) (in the sense of Deynoux and Ghienne, 2004).

Main Infill

The paleovalley infill comprises three distinct lithofacies: sandstones, heterolithics, and diamictites. A sandstone-dominated lower part can be generally differentiated from a finer-grained upper part essentially containing heterolithic deposits and diamictites (Figs. 2A and 2B). In places (loc. 7), the lower sandstones are absent and the whole infill comprises a mixed heterolithic-diamictite succession that includes discontinuous sandstone bodies.

Sandstones constitute fine- to medium-grained units, several meters or tens of meters thick, that are amalgamated or interstratified with meter-thick heterolithic intervals. Discontinuous sandstone bodies (channel 5–50 m in width, 3–15 m in thickness) that are encased in finer-grained successions are locally associated with downward-tapering sand dikes. Sandstone beds, decimenters to meters thick, show horizontal laminae and load casts, but quartzification usually hampers identification of primary sedimentary structures.

Heterolithic deposits comprise siltstones to very fine-grained sandstones, which include more or less deformed centimeter-thick beds or millimeter-thick laminae (Figs. 2F and 2G). A varve-like, virtually undeformed subfacies is made up of alternating millimeter-thick siltstone and sandstone laminae.

The diamictite facies essentially comprises argillaceous sandstones to clast-poor (<10 per m^2) sandy diamictites. At outcrop, the facies appears massive, with onion-skin weathering (Fig. 2I). In drill cores, equivalent strata are either structureless or show an irregular alternation of discontinuous, centimeter-scale, sand-rich and/or silt-rich stringers. Gravel- to pebble-sized angular to subrounded lonestones are sometimes faceted and/or striated (Figs. 2I and 2J); cobbles are rare. Clast lithologies are sandy limestone, micaceous sandstone, siltstone, ignimbritic tuffite, lava, sideritic crust, and quartz. The sand-sized matrix has the same composition.

Luna Quartzite

The sharp-based and discontinuous Luna quartzite locally seals the main infill. However, in places (loc. 7), Silurian strata directly overlie the infill succession, indicating a pinchout of the Luna quartzite. The Luna quartzite is made up of well-stratified, well-sorted, medium- to coarse-grained sandstone. Pebble- to cobble-sized rip-up clasts of mudstone are locally embedded. Beds are 0.2–1.5 m thick, horizontally to subhorizontally laminated, with subordinate cross-stratification. Upper horizons are bioturbated. The Luna quartzite can be subdivided into two superimposed successions. The *Hirnantia* fauna occur at the base of the second one at locality 8.

INTERPRETATION

North Gondwanan successions underlying Silurian strata and including diamictites are attributed to the Late Ordovician glacial event, as confirmed by biostratigraphic data and faceted and striated pebbles. As the tectonic context was stable, great incision depths rule out fluvial downcuttings. Two alternative interpretations for paleovalley formation are thus considered: subglacial tunnel valleys, and canyons at a shelf to slope transition. The former hypothesis is supported by the comparable geometry, size, and spacing of the Cantabrian paleovalleys with Late Ordovician tunnel valleys in Africa (Ghienne and Deynoux, 1998; Le Heron et al., 2004) and with Quaternary analogues related to marginal segments of ice sheets overriding shallow-marine sedimentary platforms (Huuse and Lykke-Andersen, 2000). It is also supported by the occurrence of the atypical basal sandstone and associated synsedimentary shear deformation structures (vertical sheet dewatering structures, step fractures, sheath folds, and intraformational grooves). Such structures typify subglacial soft-sediment shear zones in coeval African strata (Deynoux and Ghienne, 2004; Le Heron et al., 2005; Denis et al., 2009), which are in places recognized within the sediments at the bases of tunnel valleys (Le Heron et al., 2004). Therefore, it is argued that paleovalleys in the Cantabrian Range most likely represent tunnel valleys cut by subglacial meltwaters. Certain aspects of regional tectonics suggest that the initiation of some of these tunnel valleys may have been controlled by the development of synsedimentary extensional faults.

After ice-front recession, the main paleovalley infills represent proglacial delta-slope depositional environments, as shown by (1) the association of alternating sand-rich layers (turbidity currents) and mud layers (muddy turbidity current and/or deposition from turbid surface plumes), (2) abundant liquefaction and deformation structures suggesting high rates of sedimentation over unstable slopes, and (3) isolated sandbodies interpreted as channels along fan slopes and associated with dikes representing sand injections, a feature typical of turbiditic channels (Parize and Friès, 2003). A marginal glacial setting is evidenced by diamictite deposition, including unreworked glacially shaped lonestones. Clasts of volcanic rocks, early diagenetic crusts, and carbonates were likely derived from the neighboring areas. Whether they were emplaced as ice-rafted debris dropped in a layered, turbiditic sediment pile or as floating clasts within cohesive debris flows (structureless subfacies) has not been determined. Note that incisions may belong to successive generations of tunnel valleys resulting from distinct glacial events.

The overlying Luna quartzite is interpreted as a late Hirnantian–earliest Silurian, shallow-marine, late glacial to postglacial transgressive wedge. It was deposited in shallow water by processes that redistributed glacial sediments across the platform. These shallow-water strata are overlain by Early Silurian condensed deposits (Getino Bed) and offshore shales.

CONCLUSION

Tunnel valleys in the Cantabrian Range, and consequently the development of Late Ordovician glaciers in northern Spain, indicate that either the North Gondwana ice sheet (Ghienne et al., 2007) reached the Cantabrian Zone of Spain or a satellite ice sheet grew from localized uplifts in relation with a fragmenting North Gondwana margin (e.g., Von Raumer and Stampfli, 2008). In the former case, the Cantabrian Range must have been juxtaposed with the Gondwana landmass. In the latter case, the Cantabrian Zone may have been located anywhere in the European peri-Gondwana domain and not necessarily adjacent to Gondwana. However, the preservation in intervalley zones of a thin pre-Hirnantian (<100 m) Upper Ordovician succession suggests a slowly subsiding platform domain that

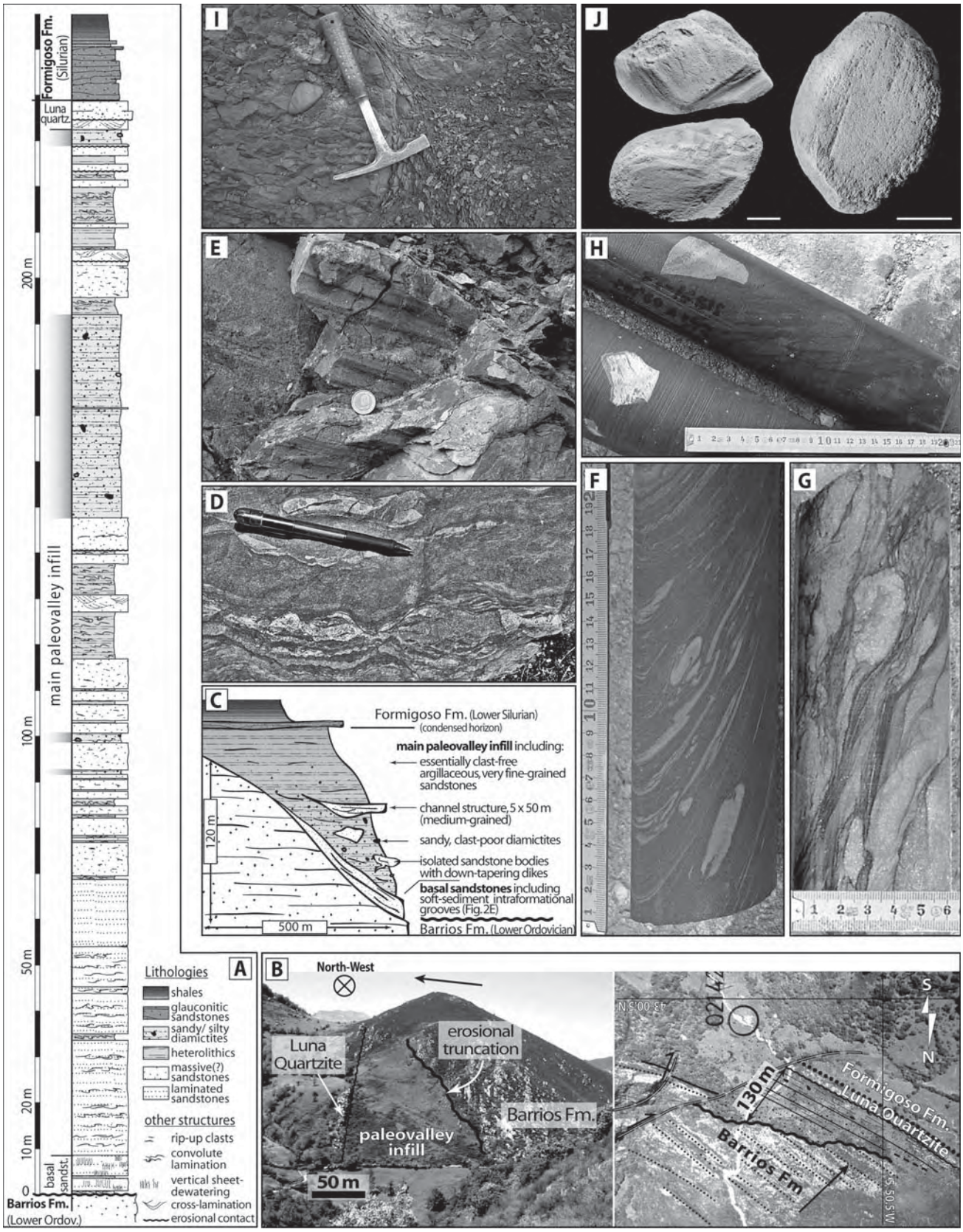

Figure 2. Facies and stratigraphic architecture. A: Log from the ST-16bis drill core, locality (loc.) 5. B: Field and interpreted aerial photographs of Telledo paleovalley margin, loc. 1 (dips are near vertical; arrow points toward stratigraphic top). C: Schematic architecture along paleovalley margin (loc. 7), highlighting geometry related to basal sandstone unit. D: Soft-sediment fractures involved in boudinage structure (point 5). E: Intraformational grooves (loc. 7) from basal sandstones. Coin diameter = 23 mm. F and G: Heterolithic facies in drill cores, loc. 5. Scale in cm. H: Diamictite with lonestones from drill cores, loc. 5. Scale in cm. I: Diamictite with onion splitting, loc. 4. Length of hammer = 28 cm. J: Striated pebbles from diamictites (loc. 4); scale bars = 1 cm.

did not point toward the development of adjacent topographic features on which a satellite ice sheet would have been able to initiate. As the tunnel valleys are comparable in size and infill to Quaternary analogues related to continental-scale ice sheets, we conclude that the Spanish glaciers originated from the North Gondwana ice sheet.

Our conclusion, that ice fronts of the North Gondwana ice sheet reached Europe, conforms to the widespread occurrence of relatively coarse-grained glaciomarine strata, and may explain some prominent erosional unconformities (Robardet and Doré, 1988; Gutiérrez-Marco et al., 2002) for which local tectonics would otherwise have been inferred, in addition to the major coeval sea-level fall across all of southern and central Europe. It also supports the interpretation of an Armorican domain still attached to the Gondwana landmass, at least until the latest Ordovician (e.g., Robardet, 2003).

ACKNOWLEDGMENTS

We thank Enrique Villas (University of Zaragoza, Spain) for the kind identification of the brachiopods from the Valdeteja locality, Julien Moreau (Aberdeen) and two anonymous reviewers for their detailed and constructive criticism of this paper, and the Administrator of Railway Infrastructures (ADIF, Ministry of Development) that facilitated the access to some of the drill cores related to the Pajares tunnel (high-speed rail line, Asturias-Madrid). This work was supported by the Spanish Ministry of Science and Innovation (project CGL2006-07628/BTE) and the French Centre National de la Recherche Scientifique (CNRS).

APPENDIX: LOCALITIES STUDIED

Localities shown in Figure 1 and their grid references in geographic coordinates.

1. Telledo paleovalley and drill core ST-5 (lat 43°0′41″N, long 5°50′16″W; Greenwich Meridian)
2. Pajares paleovalley (lat 43°0′5″N, long 5°47′12″W)
3. Caldas de Luna intervalley zone and fossil locality (lat 42°56′44″N, long 5°51′19″W)
4. Casares de Arbás diamictites (lat 42°57′21″N, long 5°47′26″W)
5. Viadangos de Arbás paleovalley and drill core ST-16bis (lat 42°57′41″N, long 5°45′40″W)
6. Busdongo (lat 42°59′1″N, long 5°43′16″W)
7. Pontedo paleovalley (lat 42°58′25″N, long 5°33′44″W)
8. Valdeteja fossil locality in the Luna quartzite (lat 42°54′52″N, long 5°25’31”W).

REFERENCES CITED

Aramburu, C., and García-Ramos, J.C., 1993, La sedimentación Cambro-Ordovícica en la Zona Cantábrica (NO de España): Trabajos de Geología, Oviedo, v. 19, p. 45–73.

Bernárdez, E., Gutiérrez-Marco, J.C., and Hacar, M., 2006, Sedimentos glaciomarinos del Ordovícico terminal en la Zona Cantábrica (NO de España): Geogaceta, v. 40, p. 239–242.

Brenchley, P.J., Romano, M., Young, T.P., and Storch, P., 1991, Hirnantian glaciomarine diamictites—Evidence for the spread of glaciation and its effect on Upper Ordovician faunas, *in* Barnes, C.R., and Williams, S.H., eds., Advances in Ordovician geology: Geological Survey of Canada Paper 90–9, p. 325–336.

Del Moral, B., 2003, Primeros conodontos kralodvorienses (Ordovícico Superior) de la Zona Cantábrica, Portilla de Luna, León (España): Revista Española de Micropaleontología, v. 35, p. 275–283.

Denis, M., Guiraud, M., Konaté, M., and Buoncristiani, J.-F., 2009, Subglacial deformation and water-pressure cycles as a key for understanding ice stream dynamics: Evidence from the Late Ordovician succession of the Djado Basin (Niger): International Journal of Earth Sciences, doi: 10.1007/s00531-009-0455-z (in press).

Deynoux, M., and Ghienne, J.-F., 2004, Late Ordovician glacial pavements revisited—A reappraisal of the origin of striated surfaces: Terra Nova, v. 16, p. 95–101, doi: 10.1111/j.1365-3121.2004.00536.x.

García-Alcalde, J.L., 1995, L’évolution paléogeographique pré-varisque de la Zone Cantabrique (Espagne): Revista Española de Paleontología, v. 10, p. 9–29.

Ghienne, J.-F., and Deynoux, M., 1998, Large-scale channel fill structures in Late Ordovician glacial deposits in Mauritania, western Sahara: Sedimentary Geology, v. 119, p. 141–159, doi: 10.1016/S0037-0738(98)00045-1.

Ghienne, J.-F., Le Heron, D., Moreau, J., Denis, M., and Deynoux, M., 2007, The Late Ordovician glacial sedimentary system of the North Gondwana platform, *in* Hambrey, M., et al., eds., Glacial sedimentary processes and products: International Association of Sedimentologists Special Publication 39, p. 295–319.

Gutiérrez-Alonso, G., Fernández-Suárez, J., Gutiérrez-Marco, J.C., Corfu, F., Murphy, J.B., and Suárez, M., 2007, U-Pb depositional age for the upper Barrios Formation (Armorican Quartzite facies) in the Cantabrian zone of Iberia: Implications for stratigraphic correlation and paleogeography, *in* Linnemann, U., et al., eds., The evolution of the Rheic Ocean: From Avalonian-Cadomian active margin to Alleghenian-Variscan collision: Geological Society of America Special Paper 423, p. 287–296.

Gutiérrez-Marco, J.C., Robardet, M., Rábano, I., Sarmiento, G.N., San José Lancha, M.A., Herranz Araújo, P., and Pieren Pidal, A.P., 2002, Ordovician, *in* Gibbons, W., and Moreno, T., eds., The geology of Spain: London, Geological Society of London, p. 31–49.

Huuse, M., and Lykke-Andersen, H., 2000, Overdeepened Quaternary valleys in the eastern Danish North Sea: Morphology and origin: Quaternary Science Reviews, v. 19, p. 1233–1253, doi: 10.1016/S0277-3791(99)00103-1.

Le Heron, D., Sutcliffe, O., Bourgig, K., Craig, J., Visentin, C., and Whittington, R., 2004, Sedimentary architecture of Upper Ordovician tunnel valleys, Gargaf Arch, Libya: Implications for the genesis of a hydrocarbon reservoir: GeoArabia, v. 9, p. 137–160.

Le Heron, D.P., Sutcliffe, O.E., Whittington, R.J., and Craig, J., 2005, The origins of glacially related soft-sediment deformation structures in Upper Ordovician glaciogenic rocks: Implication for ice sheet dynamics: Palaeogeography, Palaeoclimatology, Palaeoecology, v. 218, p. 75–103.

Le Heron, D.P., Ghienne, J.-F., El Houicha, M., Khoukhi, Y., and Rubino, J.-L., 2007, Maximum extent of ice sheets in Morocco during the Late Ordovician glaciation: Palaeogeography, Palaeoclimatology, Palaeoecology, v. 245, p. 200–226, doi: 10.1016/j.palaeo.2006.02.031.

Monod, O., Kozlu, H., Ghienne, J.-F., Dean, W.T., Günay, Y., Le Hérissé, A., Paris, F., and Robardet, M., 2003, Late Ordovician glaciation in southern Turkey: Terra Nova, v. 15, p. 249–257, doi: 10.1046/j.1365-3121.2003.00495.x.

Parize, O., and Friès, G., 2003, The Vocontian clastic dykes and sills: A geometric model, *in* Hillis, P et al., eds., Subsurface sediment mobilization: Geological Society of London Special Publication 216, p. 51–71.

Robardet, M., 2003, The Armorica ‘microplate’: Fact or fiction? Critical review of the concept and contradictory palaeobiogeographical data: Palaeogeography, Palaeoclimatology, Palaeoecology, v. 195, p. 125–148, doi: 10.1016/S0031-0182(03)00305-5.

Robardet, M., and Doré, F., 1988, The Late Ordovician diamictic formations from southwestern Europe: North Gondwana glaciomarine deposits: Palaeogeography, Palaeoclimatology, Palaeoecology, v. 66, p. 19–31, doi: 10.1016/0031-0182(88)90078-8.

Sarmiento, G., Méndez-Bedia, I., Aramburu, C., Arbizu, M., and Truyols, J., 1994, Early Silurian conodonts from the Cantabrian Zone, NW Spain: Geobios, v. 27, p. 507–522.

Schönian, F., and Egenhoff, S.O., 2007, A Late Ordovician ice sheet in South America: Evidence from the Cancañiri tillites, southern Bolivia, *in* Linnemann, U., et al., eds., The evolution of the Rheic Ocean: From Avalonian-Cadomian active margin to Alleghenian-Variscan collision: Geological Society of America Special Paper 423, p. 525–548.

Von Raumer, J.F., and Stampfli, G.M., 2008, The birth of the Rheic ocean—Early Palaeozoic patterns and subsequent tectonic plate scenarios: Tectonophysics, v. 461, p. 9–20, doi: 10.1016/j.tecto.2008.04.012.

Manuscript received 1 June 2009
Revised manuscript received 14 October 2009
Manuscript accepted 23 October 2009

Printed in USA

Chapitre 5

5- L'enregistrement de la glaciation sur la plate-forme distale

Le sud de la Sardaigne (Iglesiente) offre un enregistrement distal de la glaciation fini-ordovicienne (Leone et al., 2002). Ici, les cycles glaciaires sont enregistrés par une succession de régressions forcées superposant brutalement des faciès peu profond (partie médiane à fine stratification) à des faciès profond (partie inférieure, argileuse). Les grès dans la partie supérieure enregistrent une tendance transgressive synchrone d'un retrait glaciaire. La surface à leur base marque un maximum d'avancée glaciaire dans les domaines plus internes du Gondwana.

Publications associées

Le Heron D.P., Khoukhi Y., Paris F., Ghienne J.-F., Le Herissé A. (2008) Black shale, grey shale, fossils and glaciers : anatomy of the Upper Ordovician-Silurian succession in the Tazzeka Massif of eastern Morocco. Gondwana Research, 14, 483-496.

Ghienne J.-F., Bartier D., Leone F., Loi Alfredo (2000) Caractérisation des horizons manganésifères de l'Ordovicien supérieur de Sardaigne : relation avec la glaciation fini-Ordovicienne. Comptes Rendus de l'Académie des Sciences, Paris, 331, 257-264.

➔ Voir aussi

Ghienne et al., 2010b (Chapitre 1)

L'enregistrement sédimentaire de la glaciation sur la plate-forme distale jamais englacée permet d'étudier une succession stratigraphique potentiellement complète au sein de laquelle les érosions auront été minimales. Par rapport à des enregistrements situés loin des centres de glaciation, par exemple ceux des plates-formes carbonatées inter-tropicales (Kaljo et al., 2008 ; Long, 2007 ; Desrochers et al., 2010) ces successions intègrent un ou plusieurs horizons glaciomarins permettant de positionner l'évolution stratigraphique dans le calendrier glaciaire. Malheureusement localisées à proximité de l'ancienne marge continentale, ces successions ont été impliquées dans les collisions varisques ou alpines. La continuité latérale des affleurements a le plus souvent été perdue. Cet enregistrement distal de la glaciation a été étudié au Maroc, en Espagne, en France (massif armoricain, Corse) et en Turquie. Trois successions-types peuvent être différentiées en fonction de leur position sur la marge continentale et par rapport aux fronts glaciaires :

- Successions dominées par les turbidites. Les zones à bathymétrie élevée (quelques centaines de mètres, plate-forme externe), approchées par les fronts glaciaires à leur maximum d'extension, sont le siège d'une sédimentation turbiditique active. Elles ont été identifiées en différents points de la Meseta marocaine (*Le Heron et al., 2007, §4,* et *2008*). Des épisodes interglaciaires se marquent par une sédimentation glaciomarine distale plus ou moins condensée. Les dépôts contemporains du maximum glaciaire correspondent essentiellement à faciès sableux relativement triés de type écoulements turbiditiques de haute densité. Des surfaces érosives à méga-flûtes pourraient être la signature de crues proglaciaires. L'épaisseur cumulée des dépôts peut atteindre 400 m. Ces caractéristiques suggèrent un système de transit sur la plate-forme, connectant les sources glaciaires et les dépôt-centres turbiditiques. Bien que très probablement connectés à des sources issues des fronts de fleuves de glaces, de tels systèmes turbiditiques ne sont pas les analogues des grands éventails proglaciaires turbiditiques du Quaternaire, qui sont eux dominés par des écoulements de débris plus ou moins directement issus des fronts glaciaires atteignant le rebord du talus continental (Dowdeswell et al., 2002 ; Taylor et al., 2002).

- Successions à dominante glaciomarine. Les secteurs de la plate-forme externe restées à l'écart — au-devant, ou latéralement ? — des dépôt-centres turbiditiques ont enregistré l'épisode hirnantien sous la forme d'une double séquence glaciomarine dominée par des faciès de diamictites sableuses à galets lâchés (Nappes d'Antalya en Turquie, *Ghienne et al., 2010b, §1*; Corse). Ces faciès, d'apparence massive à l'affleurement, sont en fait laminés *(Guttierez-Marco et al., 2010, §4* et correspondent en partie à des accumulations de turbidites de basse densité (hyperpycnites). La base de cette double séquence, correspondant aux deux cycles glaciaires hirnantiens, est érosive, parfois soulignée par des grès (faciès turbiditiques ?), constitutant une possible signature de la régression forcée correspondant à la montée en charge de l'inlandsis. L'épisode interglaciaire voit le retour des conditions de plate-forme externe qui prévalaient avant l'Hirnantien alors que la sédimentation postglaciaire voit l'installation de conditions originales qui conduisent à l'accumulation de lydites, faciès siliceux riches en matière organiques dont l'âge est variable selon le secteur considéré (Chalonnes-sur-Loire près d'Angers, Bourahrouh, 2002 ; Piccarra et al., 2009 ; Corse, Barca et al., 1996; Bulgarie, Yanev, 2000 ; Turquie). Il s'agit de bancs d'épaisseurs centimétriques à décimétriques, avec interbancs silto-argileux riches en matière organique (jusqu'à 7%). Les bancs siliceux présentent une fine lamination traduisant l'existence de courants ; quelques radiolaires préservées sont encore reconnaissables. Les interbancs sont parfois associés à de la pyrite en lits millimétriques ou framboïde. Ces successions à lydites sont interprétées comme les dépôts de courants de contour sur la plate-forme externe. La contribution biogénique attestée par des concentrations significatives en baryum et phosphore est à mettre en relation avec des

processus upwellings. Elle s'exprime à la faveur d'une condensation sédimentaire drastique par suite du déport des sources sédimentaires loin (> 2000 km) vers le sud.

- Successions dominées par les tempêtes. Sur la plate-forme distale, les secteurs à faible bathymétrie sont soit déconnectés, soit indirectement connectés aux sources clastiques d'origine glaciaire. Ils enregistrent les phases de chutes de niveau marin au sein de faciès littoraux (Iglesiente en Sardaigne, bassin de Prague en Tchéquie). Des enregistrements très complets peuvent y être préservés, sous la forme de successions pluridécamétriques dans lesquelles dominent les litages en mamelons (HCS) traduisant les prédominance des processus de tempête. La succession sarde est particulièrement intéressante (Leone et al., 2002). Les chutes de niveau marin et les récurrences de sédimentation glaciomarine distale permettent de subdiviser cette succession en deux cycles distincts. Le second cycle comprend lui-même deux sous-cycles. L'ensemble avait été initialement considéré comme Hirnantien. Cependant, la biostratigraphie et la corrélation avec les successions marocaines (*Loi et al., 2010, §2*) aboutit maintenant à la conclusion que seul le deuxième cycle est hirnantien. Le premier correspondrait à l'événement glaciaire anté-Hirnantien. Lors de ce premier cycle, des conditions originales ont permis la concentration et la formation d'un gisement à manganèse sous la forme d'encroûtements à oxydes ou à carbonates manganésifères (*Ghienne et al., 2000*). La physiographie de la plate-forme était contrôlée par les reliefs ou au moins les topographies sous-marines issues des événements tectoniques affectant la marge continentale (Martini et al., 1991 ; cf. chapitre 1). La chute glacioeustatique a conduit à l'individualisation de seuils isolant des aires de dépôt particulières comparables à la Mer Baltique actuelle (Ingri, 1993 ; Zhamoida et al., 1996). Lors des bas niveaux marins, la prédominance d'eau douce issue du drainage continental a induit un système oxydant, avec formation d'oxydes à manganèse. Lors de niveaux marins relativement plus hauts, le retour de conditions plus franchement marines a permis une stratification des eaux, un fonctionnement réducteur et la formation des carbonates de manganèse. La géochimie permet d'envisager une source hydrothermale de manganèse liée à un processus de *rifting* en cours sur la marge.

C. R. Acad. Sci. Paris, Sciences de la Terre et des planètes / Earth and Planetary Sciences 331 (2000) 257–264

S1251805000014051/FLA

Géomatériaux / Geomaterials
(Sédimentologie / Sedimentology)

Caractérisation des horizons manganésifères de l'Ordovicien supérieur de Sardaigne : relation avec la glaciation fini-ordovicienne

Jean-François Ghienne[a], Danièle Bartier[a]*, Francesco Leone[b], Alfredo Loi[b]

[a] Centre de géochimie de la surface, UMR 7517, EOST, 1, rue Blessig, 67084 Strasbourg cedex, France
[b] Dipartimento di Scienze della Terra, Università di Cagliari, via Trentino 51, 09127 Cagliari, Italie

Reçu le 20 mars 2000 ; accepté le 26 juin 2000

Présenté par Jean Dercourt

Abstract – Characterization of Upper Ordovician Mn-layers of Sardinia: relationships with the Late Ordovician glaciation. Mn-rich crusts interbedded within glacially-related Hirnantian deposits of Sardinia result from starved sedimentation in isolated sub-basins. These latter result from low glacio-eustatic sea-levels on the North-Gondwanian platform. During very low sea-levels, large supplies of fresh water are responsible for oxidizing conditions allowing Mn-oxides concretions to form. During relatively higher sea-levels, sea water inflows result in water stratification, reducing conditions and Mn-carbonate concretions. A hydrothermal origin associated with a rifting event is suggested for the manganese. © 2000 Académie des sciences / Éditions scientifiques et médicales Elsevier SAS

Sardinia / Mn-carbonates / Mn-oxides / glaciation / eustasy

Résumé – Des encroûtements manganésifères, intercalés dans les dépôts sardes contemporains de la glaciation hirnantienne, sont la signature d'épisodes à sédimentation déficitaire, au sein de sous-bassins isolés du reste de la plate-forme nord-gondwanienne par le bas niveau marin glacio-eustatique. Lors de bas niveaux marins très prononcés, la prédominance d'eau douce issue du drainage continental induit un système oxydant, avec formation d'oxydes à Mn. Lors de niveaux marins relativement plus hauts, les apports d'eau salée permettent une stratification des eaux, un fonctionnement réducteur et la formation de carbonates de Mn. Une source hydrothermale de Mn liée à un processus de *rifting* est envisagée. © 2000 Académie des sciences / Éditions scientifiques et médicales Elsevier SAS

Sardaigne / Mn-carbonates / Mn-oxydes / glaciation / eustatisme

Abridged version

1. Introduction and sedimentary description

The Upper Ordovician sequence in the Iglesiente area (Southwest Sardinia) was deposited upon the North Gondwanian platform. After a rifting event probably occurring during the Caradoc, this sequence records (*figure 1*) a large sea-level drop, which took place during the Hirnantian [7, 10, 12]. This event is correlated to the Late Ordovician glaciation [5]. The siliciclastic sedimentary assemblages correspond to coastal and platform facies environments. Succeeded by a high sea-level episode (lower offshore facies, Cyclopygidea fauna), deposits contemporaneous with the glacial event comprise (*figure 1*): (*i*) 0–80 m (the Punta Areans member) of a pelitic facies succession within which occur Mn-rich carbonates and oxides concretions; several sandstone beds, occasionally conglomeratic (sandstones and volcanic clasts from local origin) can be

* Correspondence and reprints dbartier@illite.u-strasbg.fr

observed; (*ii*) 20–80 m of upper offshore deposits made up of an alternation of hummochy cross-stratified sandstones and pelitic interbeds; (*iii*) 0–5 m of a condensed deposit and (*iv*) 80–200 m of offshore facies, characterized by micaceous siltstones including scattered quartz granules which are interpreted as glaciomarine-related deposits. Deposits 2 to 4 record the deglaciation phase when abundant sediments are supplied by ice melting. The condensed deposit (**3**) represents the peak post-glacial sea-level rise. Deposition of pelitic deposits (**1**), which comprise the studied Mn-rich concretions, therefore took place during a glacio-eustatically controlled sea-level fall or during a low glacial sea level.

2. Mn-oxides and Mn-carbonates description and origin

The black to ochre manganiferous beds (Mn-oxides and Mn-carbonates), 1–15 cm thick, have a total cumulated thickness up to 10 m. Mn-oxides comprise a matrix including relictual pelitic aggregates (*figure 2*). The matrix is subdivided into two distinct facies which may each comprise microlaminations formed by the alternation of Mn-oxides layers and silty-clayish layers with quartz, mica, illite and chlorite compounds (*figure 2*). The former (a few mm thick) surrounds the aggregates. Its base is subplane while the top presents a convoluted geometry. This facies and aggregates are surrounded by a flashy facies. The continuity of primary sedimentary laminations between aggregates indicates that these latter do not correspond to transported fragments. The aggregate geometry is determined by fine vertical fractures. These fractures present a different filling on either side of a Mn-enriched horizontal band (*figure 2*) which is identified across the entire width of the sample. The lower part of the filling is composed of Mn-oxides, siliceous zones and authigeneous chlorites. The upper part is comprised of a massive Mn-oxide and less numerous siliceous zones with observed net corrosion. These structures suggest that Mn-oxide concretions were formed by impregnation and further substitution of a primary siliciclastic horizon by early diagenetic fluids drained through fractures. This submarine process, which took place when starved sedimentation occurred on the platform, resulted in the formation of sedimentary condensed horizons. Major and trace element analysis (*table*) shows low Co and Ni contents, distinguishing these concretions from deep oceanic nodules and crusts [14, 15]. Higher values for P, Mg, Co, Ni, Cu, Zn are correlated to high Mn contents. The Fe/Ti-Al/(Al+Fe+Mn) diagram [2] suggests the participation of a hydrothermal source for the Mn (*figure 3*), as confirmed by the Co/Zn ratio, being lower than 0.25 [16].

The Mn-carbonates, without evidence of sedimentary structure, are composed of calcite, dolomite and different types of Mn-carbonates that differ in the proportion of Mn. The cementation phase around quartz, illites, detrital and authigenic Fe–Mg–chlorites and phosphates is generally $Mn_{60–80}Ca_{30–18}Fe_{0–1}Mg_{0–1}$ or calcite. The REE pattern of Mn-carbonates presents a negative Eu anomaly suggesting very early diagenetic reducing processes [8].

3. Depositional model

The development of Mn-bearing sediments necessitates a concentration process and a secondary process driving the training and the preservation of Mn concentrations. In Sardinia, Mn-bearing sediments are only present during the glaciation. Physiographic modifications on the platform can thus be supposed, such as the individualisation of small isolated sub-basins after a rapid glacio-eustatic fall. During a globally low glacio-eustatic sea level episode, glacio-eustatically driven fluctuations control the basinal redox dynamic. During very low sea-levels, large supplies of fresh water are responsible for oxidizing conditions allowing Mn-oxides concretions to form (*figure 4a*). During relatively higher sea-levels, sea water inflows result in water stratification and reducing conditions. Mn-carbonate can form by the reduction of Mn-oxides and dissolved Mn in water can concentrate in sea water (*figure 4b*). A hydrothermal origin associated with a rifting event is suggested for the manganese.

The Late Ordovician–Sardinian Mn-concretions are very close to modern Fe–Mn-concretions collected in the Baltic Sea [6, 18], as shown by their morphology, geochemistry and geological setting.

4. Conclusion

Mn-rich concretions of Sardinia correspond to condensed levels. These latter result from episodes of starved sedimentation that occur in restricted sub-basins relatively isolated from the open ocean during the low glacio-eustatic sea level. These glacially-driven conditions favour the concentration of Mn during reducing periods and the formation of Mn-oxides concretions during oxidizing periods. The source of Mn is probably related to the rifting event. As already noted elsewhere [3], the resultant close time and space relationship between a potent oceanic source and a suitable continental-shelf depositional setting optimised accumulation and preservation of Mn-rich deposits.

1. Introduction et contexte géologique

Les processus sédimentaires de concentration du manganèse, et spécialement ceux concernant les plates-formes protérozoïques ou cénozoïques, ont fait l'objet de nombreuses études [14]. Sur la plate-forme ordovicienne de l'Iglesiente (Sud-Ouest de la Sardaigne), des concentrations stratiformes manganésifères (jusqu'à 25 % de MnO) sont contemporaines de la période glaciaire fini-ordovicienne [10]. Cette étude a pour objectif de déterminer s'il existe une relation entre la glaciation et la présence de ces concentrations, puis de préciser la signification de ces encroûtements.

Après une phase de *rifting* au Caradoc, l'Iglesiente (*figure 1*) est le siège, à l'Ordovicien supérieur, d'une sédimentation silicoclastique de type marge passive, évoluant depuis des faciès continentaux jusqu'à des faciès marins [7, 9, 10, 12] (*figure 1*). Ce secteur de la plate-forme nord-gondwanienne, structuré mais relativement subsident, a enregistré de façon continue l'épisode glaciaire hirnantien, qui correspond au développement d'un inlandsis sur l'actuelle Afrique [5].

La formation hirnantienne de Rio San Marco fait suite à un épisode de haut niveau marin représenté par des dépôts d'offshore supérieur, puis d'offshore inférieur (Membre de Punta s'Argiola, *figure 1*). Elle débute par le membre de Punta Arenas (0–80 m), qui contient les encroûtements stratiformes à Mn, et se poursuit avec une succession de séquences à dépôts d'offshore (150–300 m). Ceux-ci correspondent à la phase de déglaciation, pendant laquelle des flux sédimentaires importants sont libérés par la fonte des glaciers nord-gondwaniens. Ces dépôts (membre de Cuccuruneddu) présentent à la base un horizon métrique de « diamictites » et sont ensuite essentiellement constitués d'alternances de pélites et de grès à litage oblique en mamelons, et se terminent, après une succession à sédimentation condensée (membre de Serra Corroga), par un faciès pélitique à clastes quartzeux ou lithiques dispersés (membre de Girisi). La succession condensée du membre de Serra Corroga est interprétée comme la signature (du pic) du maximum de vitesse de remontée du niveau marin [10].

Le membre de *Punta Arenas* (*figure 1*) est composé à la base de pélites, peu différentes de celles du membre de *Punta s'Argiola*, et passe vers le sommet à des argilites silteuses verdâtres à cassure conchoïdale. En plus des encroûtements à Mn, le membre de Punta Arenas se caractérise par la présence de bancs gréso-argileux à gréso-conglomératiques, à galets de grès et de volcanites. Les encroûtements à Mn forment des horizons stratiformes d'épaisseur pluridécimétrique, de couleur noire à ocre, dans lesquels s'intercalent parfois de minces lits argileux; certains niveaux sont perturbés par la bioturbation. Ces niveaux sont principalement constitués d'oxydes de Mn ; d'autres, moins nombreux, contiennent des carbonates manganésifères [10].

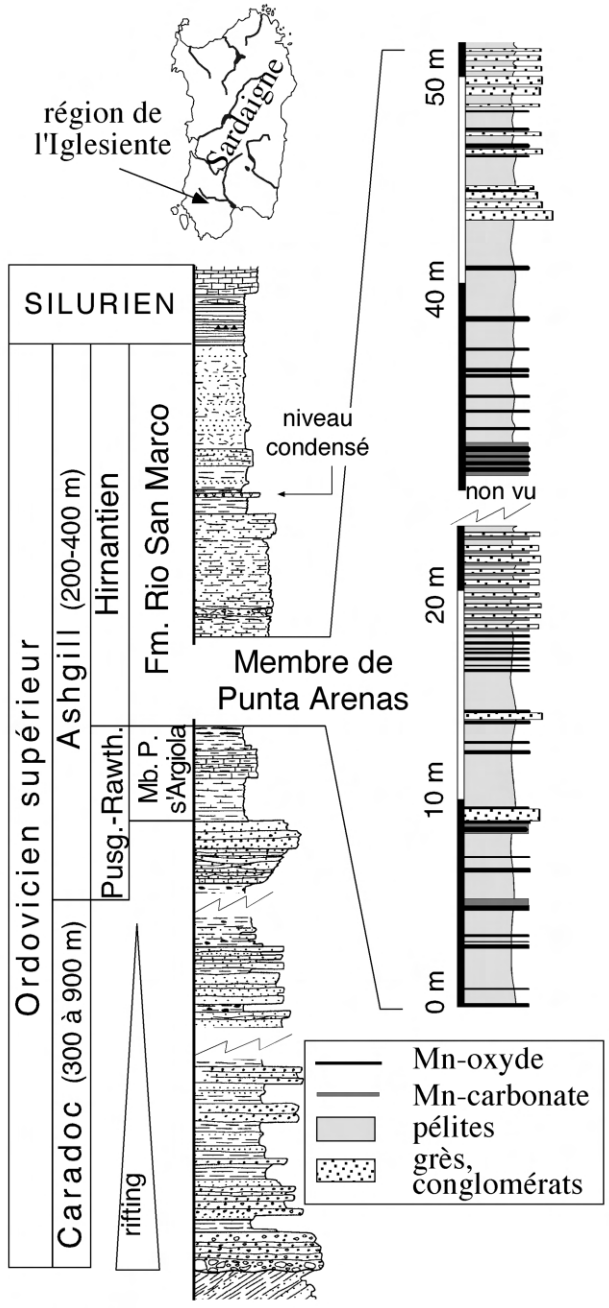

Figure 1. Contexte géologique des encroûtements manganésifères étudiés. Ceux-ci sont préservés dans le membre de Punta Arenas, au sein d'une séquence silicoclastique de plate-forme consécutive à un épisode de *rifting*. Le membre de Punta Arenas forme la base de la formation de Rio San Marco, contemporaine de la glaciation fini-ordovicienne.

Figure 1. Geological setting. Studied Mn-concretions are located within the Punta Arenas member which is comprised of a siliciclastic shelf succession, with rift-related sedimentation in its basal part. The Punta Arenas member forms the basal part of the Rio San Marco formation, which is contemporaneous with the Late Ordovician glaciation.

2. Nature des encroûtements manganésifères

Macroscopiquement (*figure 2a*), les encroûtements d'oxydes de Mn sont constitués d'une matrice noire, qui englobe des plages centimétriques silto-argileuses beiges (p.s.a.). La continuité des laminations sédimentaires entre ces plages et leur horizontalité indiquent que ces dernières ne correspondent pas à des fragments remaniés. Leur forme est déterminée par de fines fractures verticales (f.r.), sécantes à l'ensemble de l'encroûtement. Les plages silto-argileuses sont entourées par un faciès noir mat (f.m.) de quelques millimètres d'épaisseur. La limite inférieure de ce faciès mat est subhorizontale, alors que sa limite supérieure présente une géométrie très contournée. Enfin, le tout est enveloppé par un faciès noir à éclat métallique (f.e.m.), localement laminé.

L'observation en microscopie électronique à balayage couplée à une sonde EDS a permis de préciser la nature des faciès à oxydes de Mn (*figure 2b*). Le faciès mat révèle de très fines laminations (10–50 µm), qui drapent la surface irrégulière des plages argileuses. Ces laminations sont déformées au contact des fractures verticales. Le faciès à éclat métallique, plus riche en Mn que le faciès mat, présente des lamines épaisses (100–300 µm) à l'aplomb des plages argileuses, alors qu'il apparaît sans structure interne de part et d'autre. Une discordance entre les deux types de lamines apparaît souvent au contact des deux faciès. Les lamines des deux faciès à oxydes de Mn montrent une alternance d'oxydes de Mn et de silts argilo-quartzeux, au sein desquels peut apparaître de la silice amorphe. Les analyses (EDS, DRX) montrent l'existence des minéraux du groupe de la psilomélane et de différents silicates alumineux manganifères. Les fractures verticales présentent un remplissage différent de part et d'autre d'une bande horizontale, enrichie en Mn et identifiée sur toute la largeur de l'échantillon (*figure 2a*). La partie inférieure du remplissage est constituée par un mélange d'oxyde de Mn de type todorokite à structure colloïdale, de silice amorphe (Si) en plages et de grandes (jusqu'à 40 µm) chlorites (Chl) automorphes aux épontes (*figure 2c*). La partie supérieure des fractures (au-dessus de la bande horizontale enrichie en Mn) montre un remplissage principalement composé d'un oxyde à Mn beaucoup plus massif ; les plages siliceuses, moins nombreuses, témoignent d'une nette corrosion ; aucune chlorite n'y est observée.

Les encroûtements à carbonates de Mn ne montrent pas en microscopie optique de structure interne particulière. Les analyses attestent la présence de calcite et de dolomite, ainsi que de plusieurs types de carbonates aux teneurs variées en Mn, Ca, Mg et Fe. Ces échantillons présentent une cimentation mangano-carbonatée ($Mn_{60–80}Ca_{30–18}Fe_{0–1}Mg_{0–1}$), dont la partie centrale est majoritairement constituée de calcite. Le reste de l'encroûtement se compose de quartz, d'illite, de chlorites ferro-magnésiennes et de phosphates.

Des analyses chimiques ont été effectuées sur les deux types d'encroûtement, ainsi que sur les pélites (*tableau*). Comparativement aux faciès pélitiques, la présence de manganèse contrôle des enrichissements relatifs en Co (jusqu'à 55 ppm), Ni (jusqu'à 280 ppm), Cu (plus de 2 000 ppm) et Zn (jusqu'à 250 ppm). Par ailleurs, le diagramme Fe/Ti–Al/(Al + Fe + Mn) [2] (*figure 3*), ainsi que le rapport Co/Zn, inférieur à 0,25, inclinent également à supposer une source hydrothermale pour le Mn [16]. Le spectre des terres rares (REE) des horizons à Mn montre un enrichissement prononcé en REE intermédiaires et une très légère anomalie positive en Ce. Une anomalie négative en Eu est spécifiquement observée pour les horizons à carbonates de Mn. Les pélites encaissantes qui sont directement au contact des encroûtements manganésifères montrent, quant à elles, un enrichissement en REE lourdes, corrélé à de fortes teneurs en Zr, U et Th.

3. Signification des concentrations de Mn

Les dépôts manganésifères sont reconnus dans les environnements marins de la zone littorale, jusqu'aux zones abyssales. Comparativement aux nodules des grands fonds [15], les encroûtements manganésifères sardes se distinguent par leurs teneurs en Co, Ni et Cu relativement faibles, une forte proportion d'argiles et leur structure ; celle-ci présente, en effet, une architecture qui semble déterminée, de la base au sommet, par des fractures verticales précoces dans un niveau pélitique ; elle est incompatible avec l'organisation en lamines concentriques, identifiée dans la plupart des nodules océaniques.

L'association des encroûtements manganésifères sardes avec des dépôts peu profonds, leur organisation stratiforme et la présence de minces lits argileux permettent d'avancer l'hypothèse de précipitations liées aux conditions redox. Ces processus ont été décrits par de nombreux auteurs dans des environnements peu profonds, où ils semblent contrôlés par une stratification des eaux et le déplacement de l'interface redox au cours des cycles transgression–régression [4, 13] ; en fonction des conditions redox, la précipitation du Mn dissous va s'effectuer sous forme d'oxydes ou de carbonates [13]. Dans les environnements agités de plateforme ouverte, le Mn peut se présenter sous forme d'oolithes ou de pisolithes [1, 4, 14], alors que dans les environnements plus protégés il peut constituer des encroûtements stratiformes. Un faciès similaire a par ailleurs déjà été décrit en Chine, dans des sédiments mis en place durant des périodes glaciaires [17].

La disposition successive au sein des oxydes de Mn suivant le schéma observé (masses résiduelles–faciès à éclat mat–faciès à éclat métallique) semble suggérer le remplacement d'un horizon détritique silto-argileux primaire. Ce remplacement s'effectuerait progressivement

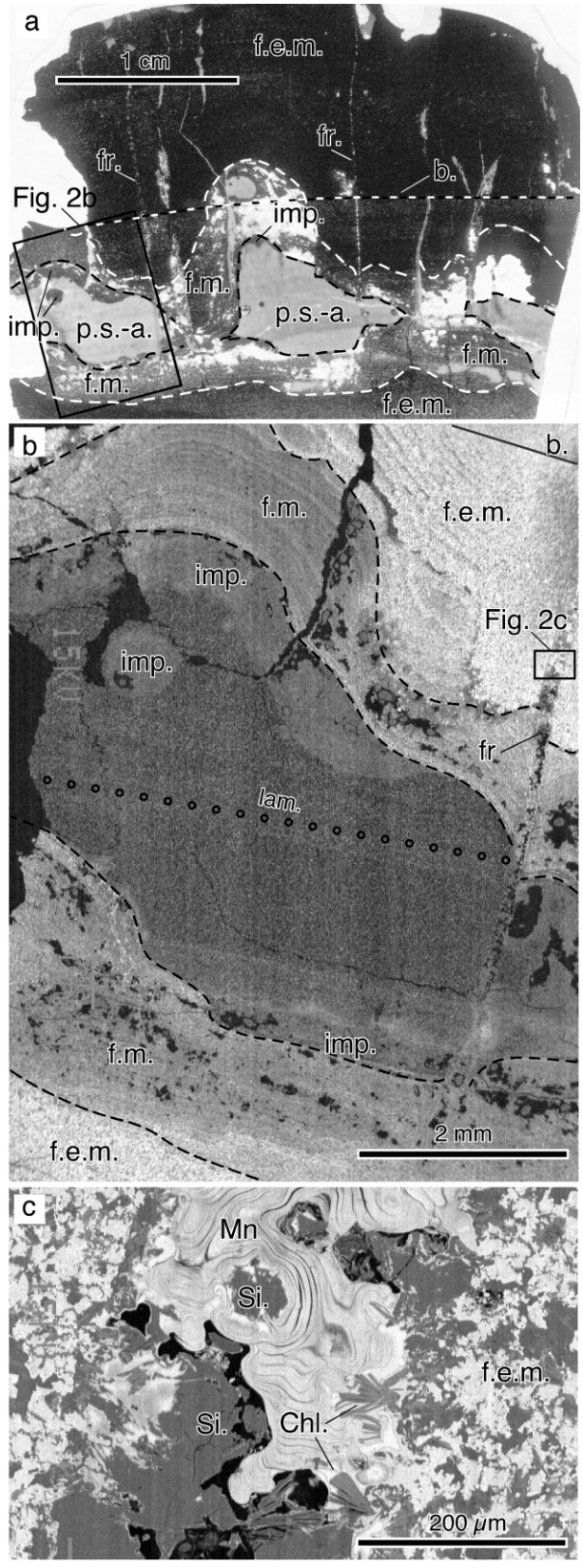

Figure 2. Encroûtement à oxydes de manganèse. **a.** Vue générale d'une lame mince en lumière naturelle. Noter le changement de couleur au sein des fractures minéralisées (fr.), de part et d'autre d'une bande (b.) enrichie en Mn et interprétée comme la trace d'un front d'oxydo-réduction. Ces fractures contrôlent la morphologie des plages claires silto-argileuses (p.s.-a.). On distingue, en sombre, les faciès à oxydes de Mn mat (f.m.) et à éclat métallique (f.e.m.). Des oxydes de Mn imprègnent la porosité des bordures des plages silto-argileuses (imp.). **b.** Vue au MEB montrant les microlaminations, discordantes entre elles, des faciès d'oxydes de Mn f.m. et f.e.m., les laminations sédimentaires (lam.) dans les plages silto-argileuses apparaissant en sombre, et les imprégnations de la porosité en bordure de ces dernières par des oxydes de Mn en gris clair (mp.). **c.** Détail de la minéralisation d'une fracture verticale (partie basse), avec chlorites aux épontes (Chl.), silice (Si.) et précipitation collomorphe d'oxydes de Mn riches en K.

Figure 2. Mn-oxides petrography. **a.** Optical microscopy observation. General view displays a change of color occurring in mineralized fractures (fr.) on both sides of the Mn-rich band (b.) which is interpreted as a redox front. Fractures control the morphology of silty-clayish aggregates (p.s.-a). Matt Mn-oxides facies (f.m.) and metallic Mn-oxides facies (f.e.m.) can be observed. Mn-oxides impregnate the porosity of silty-clayish aggregate rims (imp.). **b.** MEB observations showing discordance between f.m. and f.e.m. sedimentary laminations (lam.). Laminations look dark in aggregates, and porosity impregnation in light gray (imp.). **c.** Lower part of a mineralized vertical fracture with K-rich Mn-oxides, siliceous zones (Si.) and chlorites (Chl.) in fracture walls.

et de manière centripète, par le jeu de processus d'oxydo-réduction associant des fluides drainés dans les fractures verticales. Débutant par une imprégnation de la porosité, observée aux bordures des plages silto-argileuses (*figure 2*), ce remplacement oblitère ensuite totalement la texture primaire. La bande horizontale

Tableau. Analyses chimiques sur roche totale.
Table. Bulk rock chemical data.

	Éléments majeurs (%)								Éléments en traces (ppm)								
	SiO_2	Al_2O_3	MgO	CaO	Fe_2O_3	MnO	TiO_2	P_2O_5	Ba	V	Ni	Co	Zn	Cu	Zr	Th	U
Pélites	66,6	18,0	1,61	0,15	5,2	0,07	0,68	0,09	778	114	48	10	46	226	256	15,23	1,8
	57,3	22,1	2,15	0,10	7,2	0,17	0,84	0,06	831	130	122	18	109	523	109	13,93	1,7
	56,2	20,3	2,38	0,58	8,5	0,68	0,76	0,29	1 045	132	48	26	163	72	302	19,05	2,3
	51,7	20,1	2,5	0,33	14,8	0,24	1	0,2	966	174	96	28	165	0	152	13,73	1,7
Pélites manganésifères (encaissantes)	61,6	16,4	2,06	3,18	4,6	1,73	0,65	0,22	845	90	38	21	118	260	470	26,18	6,7
	52,6	23,1	2,52	0,67	6,6	2,46	1,24	0,38	1 164	115	51	36	179	101	555	30,95	5,9
	54,0	19,7	2,1	3,7	5,3	2,12	0,5	0,1	956	73	45	21	112	280	655	32,91	6,1
Oxydes de Mn	36,5	14,6	2,38	0,79	8,7	21,24	0,66	0,83	413	155	129	50	255	2 170	179	8,205	2,9
	45,0	17,5	3,09	1,17	9,7	11,12	0,86	1,26	730	186	140	55	257	1 270	217	10,45	3,8
	49,8	17,8	2,11	1,65	10,8	3,24	0,98	1,02	465	59	118	20	106	50	292	14	6,4
	43,5	14,2	3,85	2,09	11,5	13,25	0,45	1,14	986	175	279	40	170	174	166	5,397	1
Carbonates manganésifères	37,2	13,7	3,6	10,3	9,7	7,94	0,3	0,4	491	44	89	36	222	400	265	12,87	4
	25,6	7,90	5,01	13,71	10,5	14,35	0,22	0,18	3 387	156	171	52	254	38	65	2,9	0,4
	32,7	12,7	4,32	11,17	10,5	9,31	0,36	0,48	402	51	95	48	323	1 100	276	13,75	4,6

pourrait être interprétée comme la trace d'un front d'oxydo-réduction, et le remplissage des fractures comme le témoin de processus de précipitation précoce. Les faibles concentrations en Co, Ni et Cu, ainsi que l'absence d'anomalie marquée en Ce, s'expliquent par un cadre redox particulier lié à une diagenèse précoce oxydante [8]. Les encroûtements à carbonates manganésifères se formeraient en conditions plus réductrices, directement ou par transformation diagénétique précoce des niveaux à oxydes de Mn. Cette deuxième hypothèse pourrait expliquer l'anomalie négative en Eu des carbonates manganésifères.

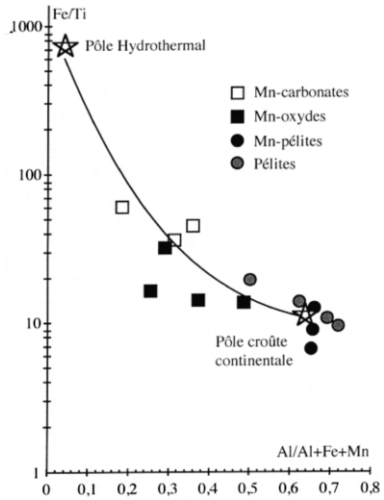

Figure 3. Localisation des faciès à Mn et des pélites encaissantes dans le diagramme de Boström [2], montrant comment ceux-ci se répartissent entre un pôle hydrothermal et un pôle de croûte continentale.

Figure 3. Plot of Mn-facies and pelites analyses in Boström diagram [2]. Data are located between hydrothermal and continental crust poles.

Les sources de Mn sont probablement multiples. Les données chimiques suggèrent la contribution d'une source hydrothermale et d'une source terrigène. Cette double contribution pourrait s'expliquer par la participation de manganèse provenant de l'altération de volcanites. Ces volcanites sont inconnues à l'affleurement, mais l'existence originelle d'un volcanisme d'âge présumé Rawtheyien a pu être mise en évidence par la présence de galets de lave basique remaniés dans les sédiments du membre de Punta Arenas [9] et par l'apparition soudaine, dans ce membre, d'une population de zircons volcaniques d'origine mantellique [11]. Les concentrations en Zr, U et Th des pélites directement au contact de ces encroûtements, qui mettent en évidence la présence de minéraux lourds, marquent dans un tel contexte la concentration de minéraux lourds résultant du vannage des particules fines par des courants de fond.

4. Modèle de dépôt

La formation d'encroûtements riches en Mn nécessite, d'une part, des processus de concentration et, d'autre part, des processus conduisant à la formation, puis à la préservation de concentrations stratiformes. En Sardaigne, les encroûtements manganésifères ne se forment que pendant la période glaciaire de l'Ordovicien supérieur. Cela suggère que la concentration sédimentaire du Mn a donc été spécialement favorisée à cette période. Il est proposé ici que les modifications physiographiques du domaine de plate-forme induite par la glaciation soient à l'origine de la concentration du manganèse et de la formation des encroûtements manganésifères. La structure compartimentée de la plate-forme nord-gondwanienne, héritée de la tectonique extensive à l'Ordovicien supérieur, suggère l'existence de bassins à seuil, relativement isolés de l'océan ouvert, et fonction-

Figure 4. Modèle de dépôt synthétique montrant les relations entre niveau marin glacio-eustatique et dynamique redox de bassins à seuil sur la plate-forme. **a.** Les minima eustatiques et l'abondance d'eau douce continentale favorisent un fonctionnement oxydant et la formation d'oxydes de Mn. **b.** Un niveau marin légèrement plus élevé favorise par l'adjonction d'eau salée une stratification des eaux, un fonctionnement réducteur, la recharge en Mn dissous et la formation de carbonates manganésifères.

Figure 4. Synthetic deposition model showing relationships between glacio-eustatic sea level and basin redox dynamics. **a.** Eustatic minima and fresh water abundance favor a oxidizing environment and Mn-oxides development. **b.** Water stratification is favoured by a higher sea level and sea water addition, a non-oxidizing environment, a dissolved Mn recharge, induced Mn-carbonates formation.

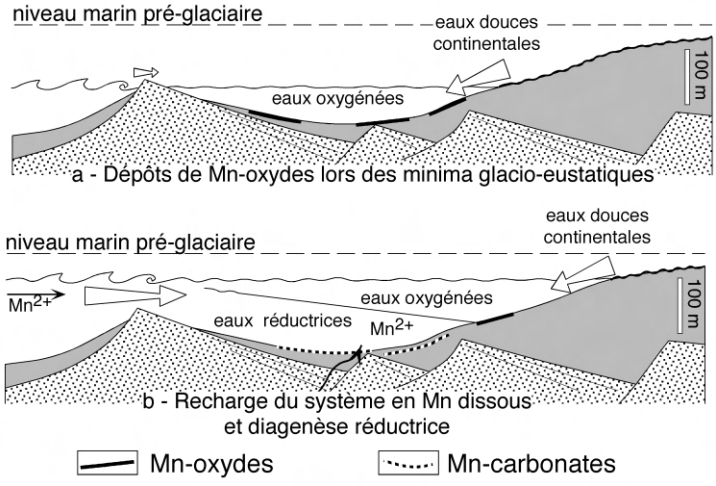

nant comme tels, dès que la baisse glacio-eustatique rapide du niveau marin est suffisante. Dans le membre de Punta Arenas, l'hypothèse de bassin confiné est argumentée, entre autres, par l'absence de remaniement des faciès grossiers par les tempêtes, alors que l'ensemble de la série ordovicienne est dominé par les tempêtes [10]. Dans ce type de sous-bassin situé à de relativement hautes latitudes, le bilan des flux hydriques excédentaires en eaux douces permet le développement d'une surface halocline à faible profondeur séparant des eaux « profondes » salées et réductrices, issues de l'océan ouvert, d'eaux superficielles saumâtres et oxygénées provenant du drainage continental (*figure 4*). Ce dispositif, à l'inverse de celui qui prédomine dans les régions où l'évaporation est forte, favorise la concentration de Mn dissous, lorsque le sous-bassin est largement connecté à l'océan ouvert. Pendant un épisode global de bas niveau marin, conséquence de la glaciation, les fluctuations glacio-eustatiques à plus haute fréquence contrôlent la dynamique redox du bassin. Lors de bas niveaux marins très prononcés (minima glacio-eustatiques, *figure 4a*), l'abondance relative des eaux douces oxygénées par rapport aux eaux salées fragilise les surfaces haloclines, entraînant plus fréquemment un fonctionnement oxydant du bassin et la possibilité de former des encroûtements à oxydes de Mn. Inversement, lors de niveaux marins relativement plus hauts (*figure 4b*), des apports d'eau salée plus abondants, le rétablissement de la stratification et le développement de sous-bassins présentant des eaux réductrices favorisent la recharge du système en Mn dissous et la formation de concrétions de carbonates authigènes à Mn.

Les nombreux encroûtements indiquent de fréquentes périodes de ralentissement de la sédimentation. Celles-ci sont très nombreuses et ne s'accompagnent pas de modifications de faciès de dépôt ; elles ne correspondent donc vraisemblablement pas à des périodes transgressives du cycle à haute fréquence. Ces ralentissements sont interprétés ici comme contrôlés par les déplacements des courants de fond. Un encroûtement à Mn se forme alors, par concentration et remobilisation hydrogénétiques. Le déplacement autocyclique au cours du temps de ces courants permet localement le retour de la sédimentation pélitique, qui enfouit et préserve les horizons à Mn.

Les encroûtements manganésifères de Sardaigne s'apparentent, par leur environnement sédimentaire, leur morphologie et leur chimie, aux concrétions ferro-manganésifères modernes de la mer Baltique [6]. Dans ce bassin à seuil (détroit du Danemark), le Mn est mobilisé dans les secteurs les plus réducteurs, généralement sous la halocline. Les nodules, disques ou croûtes, sont présents entre 20 et 50 m de fond (profondeur de la halocline–redoxcline). Pour Zhamoida, Glasby et Popova [18], la morphologie des concrétions dépend des taux d'érosion/sédimentation. Les encroûtements stratiformes de Mn se forment ainsi dans les zones soumises à de très faibles taux d'érosion par la présence de courants lors d'oxygénations saisonnières ou décennales de la mer Baltique.

5. Conclusion

Les encroûtements manganésifères de Sardaigne représentent un type particulier de niveaux condensés. Ils sont les témoins d'épisodes à sédimentation déficitaire, qui affectent des sous-bassins relativement confinés de la plate-forme nord-gondwanienne pendant une période de bas niveau marin glacio-eustatique. Ils peuvent ainsi être considérés comme une conséquence directe de la glaciation fini-ordovienne. Cependant, le contexte régional de *rifting* qui, au Caradoc supérieur, a structuré la marge nord-gondwanienne, a pu favoriser à l'Hirnantien l'individualisation de sous-bassins. D'autre part, le volcanisme d'âge présumé Rawtheyien a probablement pu constituer une source importante de manganèse. La conjonction de ces différents facteurs apparaît être à l'origine du développement de ces encroûtements. Comme à d'autres époques de l'histoire de la

Terre [3], le rapprochement, dans le temps et dans l'espace, d'une source de Mn et d'un environnement sédimentaire approprié, favorise le dépôt et la préservation de concentrations manganésifères.

Références

[1] Bolton B.R., Frakes L.A., Geology and genesis of manganese oolite, Chiatura, Georgia, USSR, Geol. Soc. Am. Bull. 96 (1985) 1398–1406.

[2] Boström K., Submarine volcanism as a source of iron, Earth Planet. Sci. Lett. 9 (1970) 348–354.

[3] Bühn B., Stanistreet I.G., Insight into the enigma of Neoproterozoic manganese and iron formations from the perspective of supercontinental break-up and glaciation, in : Nicholson K., Hein J.R., Bühn B., Dasgupta S. (Eds.), Manganese mineralization: geochemistry and mineralogy of terrestrial and marine deposits, Geol. Soc. Spec. Publs., 119, 1997, pp. 81–90.

[4] Frakes L.A., Bolton B.R., Origin of manganese giants: sea-level change and anoxic-oxic history, Geology 12 (1984) 83–86.

[5] Ghienne J.-F., Modalités d'enregistrement d'une glaciation ancienne ; exemple de la glaciation fini-ordovicienne sur la plateforme nord-gondwanienne en Afrique de l'Ouest, thèse, université Louis-Pasteur, Strasbourg, 1998.

[6] Glasby G.P., Emelyanov E.M., Zhamoida V.A., Baturin G.N., Leipe T., Bahlo R., Bonacker P., Environments of formation of ferromanganese concretions in the Baltic Sea: a critical review, in : Nicholson K., Hein J.R., Bühn B., Dasgupta S. (Eds.), Manganese mineralization: geochemistry and mineralogy of terrestrial and marine deposits, Geol. Soc. Spec. Publs., 119, 1997, pp. 213–237.

[7] Hammann W., Leone F., Trilobites of the post-sardic (Upper Ordovician) sequence of southern Sardinia. Part 1, Beringeria 20 (1998) 3–217.

[8] Ingri J., Redox potential, a significant factor in regulating the uptake of Cu, Ni, and Zn in Mn-oxyhydroxide at the sediment-water interface in the northern Baltic Sea, EOS Trans. Am. Geophys, Union 74 (16) (1993) 326–327.

[9] Leone F., Hammann W., Laske R., Serpagli E., Villas E., Lithostratigraphic units and biostratigraphy of the post-sardic Ordovician sequence in south-west Sardinia, Bull. Soc. Paleont. Ital. 30 (2) (1991) 201–235.

[10] Studio sedimentologico-petrografico e considerazioni paleogeografiche dell'Ordoviciano superiore della Sardegna centro meridionale, thèse, Università degli Studi di Cagliari, 1993.

[11] Loi A., Dabard M.-P., Zircon typology and geochemistry in the palaeogeographic reconstruction of the Late Ordovician of Sardinia (Italy), Sediment. Geol. 112 (1997) 263–279.

[12] Martini I.P., Tongiorgi M., Oggiano G., Cocozza T., Ordovician alluvial fan to marine shelf transition in SW Sardiania, Western Mediterranean Sea: tectonically (" Sardic phase ") influenced clastic sedimentation, Sediment. Geol. 72 (1991) 97–115.

[13] Roy S., Environments and processes of manganese deposition, Econ. Geol. Bull. Soc. 87 (1992) 1218–1236.

[14] Roy S., Genetic diversity of manganese deposition in the terrestrial geological record, in : Nicholson K., Hein J.R., Bühn B., Dasgupta S. (Eds.), Manganese mineralization : geochemistry and mineralogy of terrestrial and marine deposits, Geol. Soc. Spec. Publs., 119, 1997, pp. 5–27.

[15] Tooms J.S., Summerhayes C.P., Geochemistry of marine phosphate and manganese deposits, Oceanogr. Mar. Biol. Ann. Rev. 7 (1969) 49–100.

[16] Toth J.R., Deposition of submarine crusts rich in manganese and iron, Geol. Soc. Am. Bull. 91 (1980) 44–54.

[17] Ye L., Fan D., Yang P., Characteristics of manganese ore deposits in China, Ore Geol. Rev. 4 (1988) 99–113.

[18] Zhamoida V.A., Glasby G.P., Popova I.A., Ferromanganese concretions of the Gulf of Finland, Baltic Sea, Mar. Georesour. Geotec. 14 (1996) 161–176.

Available online at www.sciencedirect.com
ScienceDirect
Gondwana Research 14 (2008) 483–496
www.elsevier.com/locate/gr

Black shale, grey shale, fossils and glaciers: Anatomy of the Upper Ordovician–Silurian succession in the Tazzeka Massif of eastern Morocco

Daniel Paul Le Heron [a,*], Yahya Khoukhi [b], Florentin Paris [c], Jean-François Ghienne [d], Alain Le Herissé [e]

[a] Department of Earth Sciences, Royal Holloway University of London, Egham, Surrey, TW20 0EX, United Kingdom
[b] Faculté des Sciences, Université Mohamed Ier, Oujda, Morocco
[c] UMR 6118 Geosciences Rennes, Université de Rennes I, 35042 Rennes cedex, France
[d] École et Observatoire des Sciences de la Terre, Centre de Géochimie de la Surface, 1 rue Blessig, 67084 Strasbourg Cedex, France
[e] Université de Bretagne Occidentale, Domaines Oceaniques, Brest, France

Received 2 September 2007; received in revised form 25 February 2008; accepted 25 February 2008
Available online 6 March 2008

Abstract

A 400 m thick clastic succession of Late Ordovician through Silurian age crops out in the Tazzeka Massif, eastern Morocco. Biostratigraphic data (chitinozoa, acritarchs) constrain these rocks to the Late Katian through Hirnantian (coeval with glaciation in Gondwana), with a ~8 Myr hiatus at the Ordovician–Silurian boundary. Sedimentological analysis reveals six facies associations, including interbedded black and grey shale couplets (poorly oxygenated shelf sediments), a bioturbated shale with wave rippled sandstone (inner shelf deposits), several occurrences of diamictite (of probable glaciogenic origin), interbedded sandstone and mudstone (storm and fair-weather wave agitated shoreface), rippled sandstone (storm return flow deposits) and amalgamated sandstone deposits (delta-front debris flows). Direct evidence for glaciation in the Hirnantian deposits is poor. Third order sequence stratigraphic analysis reveals two transgressive systems tracts (Late Katian and intra-Hirnantian), two highstand systems tracts (both intra-Hirnantian), lowstand wedges probably corresponding to two principal glacial lowstands, two maximum flooding surfaces (Late Katian and intra-Hirnantian), and a major ravinement surface (Hirnantian–Silurian contact). Remote from the centre of glaciation, the Tazzeka succession is suggested to be an excellent reference section with which to understand glacially-moderated sea-level changes in the Late Ordovician. Silurian (Late Llandovery or younger) shale geochemistry indicates organic enrichment (TOC >4.5%). This organic enrichment greatly increases the known extent of the upper of two Silurian organic shales across North Africa (potential hydrocarbon source rocks) across the region.

Keywords: Katian; Hirnantian; Sequence stratigraphy; Ordovician; Silurian; Morocco

1. Introduction

In recent years, aspects of ancient glaciation on Earth have been the subject of intense study. Much effort has been devoted to unravelling the nature of Neoproterozoic glaciations (e.g. Maruyama and Santosh, 2008), and their stratigraphy, but Early Palaeozoic Ice House periods are also becoming a major interest amongst the academic community (Page et al., 2007). The Late Ordovician–Early Silurian interval belongs to this latter Ice House period and in the North Africa region, it is of interest for four principal reasons. The first is directly economic: more than 50 oil and gas fields produce from terminal Ordovician sandstones across Libya and Algeria, some of which are classified as "giants" (>500 million barrels of oil in place) (Hallett, 2002). The second is biogeographic: the Late Ordovician glaciation is coincident with the second largest mass extinction in Earth's history (e.g. Brenchley et al., 2003). The third tangent is palaeogeographic: excellent exposures are available in the Saharan region to reconstruct the flow and recessional pattern of Late

* Corresponding author.
E-mail address: d.leheron@es.rhul.ac.uk (D.P. Le Heron).

1342-937X/$ - see front matter © 2008 Inertnational Association for Gondwana Research. Published by Elsevier B.V. All rights reserved.
doi:10.1016/j.gr.2008.02.006

Ordovician ice sheets (e.g. Ghienne et al., 2007; Le Heron and Craig, 2008). The fourth justification comes in the form of understanding the origins of one of the great second order transgressions that affect the stratigraphic record from NW Africa (Lüning et al., 2000) to Arabia (Armstrong et al., 2005) and South Africa (Young et al., 2004), namely patterns of Early Silurian shale deposition and organically enriched horizons within this interval.

Outcrops of Late Ordovician glacially-related deposits in northern Morocco were the subject of a recent paper by Le Heron et al. (2007). In recent years, a major research programme in France (ECLIPSE Project) has been focusing specifically on the Lower Palaeozoic (Cambrian–Ordovician) stratigraphy of the Anti-Atlas region, with 3 field seasons from 2005–2007. These results will be forthcoming in future publications; specifically, the record of the Late Ordovician glaciation in the Moroccan Anti-Atlas was covered recently by Le Heron (2007).

In contrast to recent research papers on related topics by the authors, the current work has a more restricted geographical remit, presenting a detailed description and interpretation of Upper Ordovician through Lower Silurian clastic sedimentary rocks in the Tazzeka Massif, northern Morocco (Fig. 1), from sedimentological, biostratigraphic, geochemical and sequence stratigraphic datasets. The reason for focusing on this single study region is that this area lay beyond the reach of Late Ordovician ice sheets (Le Heron et al., 2007), and hence it may serve as an excellent stratigraphic reference section for other Upper Ordovician–Lower Silurian sections north of the Atlas range (Fig. 1). Given this paleogeographic setting (Le Heron et al., 2007), it may be possible to extract information on glacioeustacy that is not possible in more ice-proximal locations. A new biostratigraphic framework for Upper Ordovician through Lower Silurian rocks is presented, which is based on chitinozoa and acritarch assemblages (Table 1), and a re-assessment of the environmental processes at work prior to Hirnantian glaciation is attempted that is based on our field observations. Our final aim is to present new data on the thermal maturity and total organic carbon (TOC) content of shales with implications for petroleum exploration in NW Africa, as the hunt for suitable source rocks in this region continues.

2. Geological setting and previous research

Transitional Ordovician–Silurian stratigraphic sections are exposed in the Tazzeka Massif, which lies immediately south of the Rif (Fig. 1). These rocks were deposited along the NW corner of a passive continental margin that dipped toward the present day north into the Tethys Sea and extended from Morocco to Egypt (e.g. Selley, 1997). They were then subject to up to 4 phases of compressional deformation during the Hercynian Orogeny, culminating in a Late Devonian tectonometamorphic event, before undergoing Late Palaeozoic–Early Mesozoic extension during rift basin development (Piqué, 2001). The tectonic setting of the Tazzeka Massif is poorly understood, although it has been described as “para-autochthonous” with respect to the Hercynides of the Middle Atlas (Piqué and Michard, 1989). Consequently, the precise Early Palaeozoic palaeogeographic position of the Tazzeka Massif relative to other Moroccan inliers is quite uncertain.

In the Tazzeka Massif, the Ordovician through Silurian stratigraphy was established by Hoepffner (1987). He recognised 1) the Bouchfaâ Formation, comprising olive green pelites

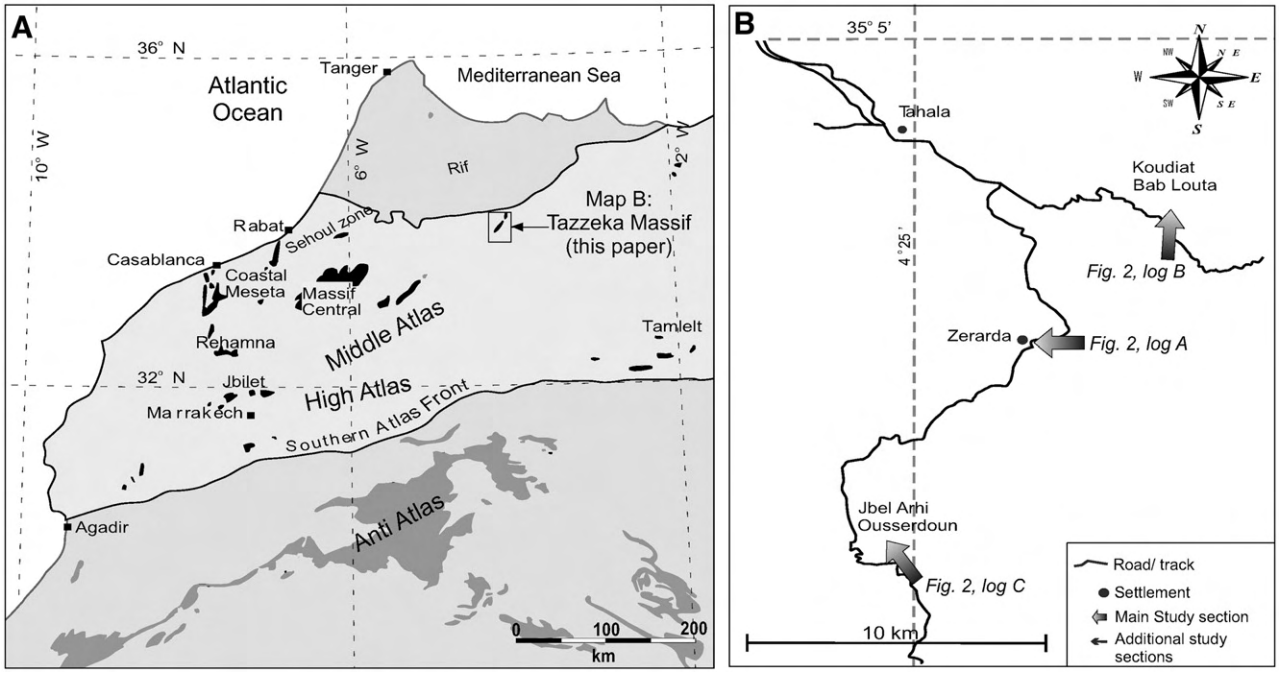

Fig. 1. Sketch map of Morocco, emphasising the location of the Tazzeka Massif within the Middle Atlas. Inset shows position of Zerarda, Bab Louta and Jbel Arhi Ousserdoun sections in the vicinity of Tahala town.

and dated by graptolites in its upper part as basal Llanvirn, 2) the overlying arenaceous Tehar el Brehl Formation and 3) the Tifarouine Formation. These latter two formations are the subject of the present study. Un-named shales overlying the Tifarouine Formation were dated by graptolite fauna as Early Silurian (Destombes, 1971) and thus the Tifarouine Formation has traditionally been assigned an Ashgill age (Khoukhi and Hamoumi, 2001).

Khoukhi (1993) piloted a detailed palynological study in conjunction with the Institut Algérian du Pétrole. This study included the analysis of 40 mudstone samples. However, as a result of poor preservation of microfossil material, only two samples yielded sufficient acritarchs and rare chitinozoa of biostratigraphic value. Terminal Arenig ages were assigned to the Bouchfaâ Formation. Prior to the present study, however, the Upper Ordovician through Lower Silurian succession has never been subject to detailed (or successful) biostratigraphic investigation. Previous work on Ordovician clastic deposits in the Tazzeka Massif has included extensive petrographic research on the composition of sandstones (Khoukhi, 1993). From a stratigraphic perspective, more recent research focused on attempts to decouple climatic and eustatic processes from the sedimentary record of Upper Ordovician deposits (Khoukhi and Hamoumi, 2001), concluding that the sediments were deposited in a prograding delta system.

A "glacial" influence in the Upper Ordovician succession has long been suspected on the basis of petrographic findings (Khoukhi and Hamoumi, 2001). For example, it has been shown that "microconglomerates" of the Tifarouine Formation (essentially clast-poor diamictites) are greatly enriched with feldspathic detritus, chlorites and biotite grains by comparison to the underlying strata and some of the quartz grains are sharply etched suggesting an ultimate glacial source (Khoukhi, 1993). Most recently, Le Heron et al. (2007) visited the main Lower Palaeozoic outcrops of northern Morocco, demonstrating that there is evidence for Late Ordovician grounded ice sheets in the High Atlas of Marrakech, Jbilet and Rehamna, but not in the Massif Central, the Coastal Meseta, or in the Tazzeka Massif. These authors thus concluded that ice sheets in the Late Ordovician did not reach the Tazzeka Massif, which they suggested lay beyond the ice sheet maximum.

In the Tazzeka Massif, transitional Ordovician–Silurian sedimentary rocks crop out in the vicinity of Tahala (Fig. 1). In this paper, data are presented from three exposures at Jbel Arhi Ousserdoun, Koudiat Bab Louta and Zerarda (Fig. 2). The Zerarda locality offers the best exposure quality and hence serves as a reference logged section (Fig. 2, log A). However, a comparable stratigraphic succession is recognised at Jbel Arhi Ousserdoun and Koudiat Bab Louta from which partial logs are presented (Fig. 2, logs B, C). Accurate correlation between these successions is possible on the basis of 1) a "triad" of sandstone beds encountered toward the base of the succession that can be correlated across the region, 2) thick sandstones with characteristic dewatering structures that can also be traced laterally, and 3) a sharp discontinuity characterises the contact between Ordovician sandstone and Silurian shale (Fig. 2, logs A, C). The sedimentological similarities and differences between these three stratigraphic sections are assessed in this contribution to build up a detailed depositional and sequence stratigraphic model for Upper Ordovician and Lower Silurian rocks.

3. Biostratigraphy

The biostratigraphy of the Upper Ordovician through Silurian succession in the Tazzeka Massif is shown in Table 1; the sample intervals are shown alongside each of the sedimentary logs (Fig. 2). Over recent years, the global chronostratigraphic subdivisions of the Ordovician have been subject to considerable revision, to the extent that the International Commission on Stratigraphy recently replaced most epochs with a numbering system (Webby et al., 2004). The Late Ordovician now comprises three epochs, including the Sandbian, the Katian and the Hirnantian. At the time of writing (August 2007), these epochs await ratification. In the British regional terminology, these epochs respectively correspond to the early Caradoc, the middle and upper part of the Caradoc plus the main part of the Ashgill, and the Upper Ashgill.

Shale intervals were extensively sampled from each of the three localities (Ousserdoun, Bab Louta and Zerarda) in the Tazzeka Massif, enabling us to recover both chitinozoa and acritarch assemblages. In common with earlier attempts (e.g. Khoukhi, 1993), microfossil recovery was generally poor, despite the relatively undeformed character of Ordovician and Silurian sediments and the high outcrop quality.

3.1. Late Katian

The Tehar El Brehl Formation (samples TZ1 and TZ17) yields *Belonchitina* sp., *Cyathochitina gr. kuckersiana*, *Euconochitina gr. lepta*, *Desmo. minor*, *Calpichitina lenticularis*, *Tanu fistulosa*, *Conochitina* and possibly *A. nigerica*. Overlying shales (TZ20) bear very abundant chitinozoa dominated by *C. lenticularis*, together with *D. minor*, *Euconochitina* and an atypical *Lagenochitina* (*Lagenochitina.* sp. aff. *nuayyimensis*). A diverse assemblage comprising *D. minor*, *Euconochitina gr. lepta*, *C. lenticularis*, *T. fistulosa*, *B. micracantha*, *L. prussica*, and large *Conochitina* fossils characterise TZ5. A sample from the topmost shale of the Tehar El Brehl Formation (TZ 28) contains *C. lenticularis*, *Lagenochitina baltica*, *Euconochitina lepta*, *Tanuchitina ontariensis*, *T. fistulosa*, and one small atypical *Lagenochitina*.

The lowermost chitinozoa assemblages (TZ1, TZ17) are compatible with a Late Katian age (c.f. Bourahrouh et al., 2004), whereas overlying samples (TZ20, TZ5, TZ28) favour age assignment to the *barbata*/*fistulosa* biozone. With reference to a well studied section in the Bou Ingarf area, Moroccan Anti-Atlas (Bourahrouh et al., 2004), this biozone corresponds to the Late Katian (Fig. 2).

3.2. Late Katian to Hirnantian

Shale sample TZ2 was collected from basal shales of the Tifarouine Formation (4 m above sample TZ28) and yields

Table 1
Biostratigraphic data collected from the Tazzeka Massif, documenting both chitinozoa and acritarch microfossils recovered and the stratigraphic extent of the taxa

Tazzeka samples	*Desmo. minor*	*Eucono. gr. lepta*	*Cyatho. gr. kuckersiana*	*Tanu. fistulosa*	*Belonechitina* ssp.	*Euconochitina* ssp.	*Tanuchitina* sp.	*Lageno. n.* sp. aff. *nuayyimensis*	*Calpi. lenticularis*
TZ 37									
TZ 4									
TZ 42									
TZ 35	X	X			X				
TZ 32									
TZ 31									
TZ 3					X				
TZ 41									
TZ 10									
TZ 2	X	X			X				X
TZ 29	X	X						X	X
TZ 28	X	X		X		X	X	X	X
TZ 25	X	X			X	X		X	XX
TZ 5	X	X		?				X	XX
TZ 20	X	X	X					X	X
TZ 1	X	X			X	X		x	X
TZ 17	X	X	X	X	X	X	?		

Desmo. minor, *Euconochitina gr. Lepta*, *Belonechitina* ssp., *C. lenticularis*, *Armorochitina nigerica*, *Spinachitina* sp. and *Conochitinidae indet*. By comparison to the Bou Ingarf section, this assemblage is referable to the *nigerica* biozone of the Late Katian (Bourahrouh et al., 2004). Fragmentary chitinozoa were also present in sample TZ41, and acritarchs identified within this sample were *Veryhachium* and *Aremoricanium*. In wells sunk in northeast Libya, the latter taxon is referable to the Late Katian (formerly Ashgill: Hill and Molyneux, 1988).

3.3. Hirnantian

Samples collected from shales in the overlying 340 m of the formation yield abundant but fragmentary chitinozoa (TZ31, TZ32, TZ35) (Table 1). In TZ3 the following chitinozoa were noted: *Belonechitina* ssp., *Conochitinidae indet.*, *Armorichitina nigerica*, *Ancyrochitina prima*, *Spina. gr. oulebsiri*, *L. baltica* in addition to an acritarch assemblage consisting of *Orthosphaeridium* and *Veryhachium*.

In none of the above samples were *T. elongata* identified, with which reference to the *elongata* biozone could be made for certain. Again, however, comparison to the Bou Ingarf section in the Anti-Atlas (Bourahrouh et al., 2004) for the assemblage in TZ3 strongly suggests that reference to the *elongata* and/or *oulebsiri* biozones (i.e. to the Hirnantian) is appropriate for this interval. We consider, therefore, that Hirnantian strata begin just beneath the first occurrence of the chitinozoan assemblage described above (Fig. 2). This stratigraphic position for the Katian–Hirnantian boundary is also considered appropriate beneath the first diamictite horizon to be observed up-section.

The chitinozoan biostratigraphy is potentially of a higher resolution than that possible from the acritarch assemblages. For example, acritarchs in sample TZ3 span the Ashgill (*Orthosphaeridium*) and Late Ordovician–Silurian (*Veryhachium*) and do not, therefore, permit further biostratigraphic subdivision (Vecoli and Le Hérissé, 2004). Additional fossils throughout the Tifarouine Formation include scattered graptolite fragments and scolecodonts.

3.4. Silurian (Late Llandovery or younger)

Samples TZ4 and TZ37 were collected from shale a few decimetres above the uppermost sandstone of the Tifarouine Formation. Fragmentary graptolites and chitinozoa were recorded from TZ4, and TZ37 bears *Angochitina* sp., *Fungochitina* sp., *Linochitina* sp., *Cingulochitina* sp., *Ancyrochitina. gr. primitiva* and *Calpichitina* cf. *accolare*. In this sample, none of the taxa indicate an earliest Silurian (Rhuddanian) age. Instead, the assemblage indicates that the shale probably has a Late Llandovery (Telychian) or even younger age (Paris et al., 1995).

4. Sedimentology

A cursory account of the sedimentology of the Zerarda succession was provided by Le Heron et al. (2007). Below, a more detailed facies analysis is presented for the Tehar El Brehl Formation, the overlying Tifarouine Formation and un-named Silurian shale that caps the succession. The analysis draws on sedimentological data from three outcrops, mainly from Zerarda, but also from Bab Louta and Jbel Arhi Ousserdoun (Fig. 1). Six facies associations are recognised that are described and interpreted below. Each of the facies associations are marked up against the measured sections (Fig. 2). A sequence stratigraphic treatment of sediment stacking patterns follows in the Discussion section.

4.1. Black and grey shale facies association (FA1)

These deposits comprise paper-laminated shales that are characterised by intercalation of black and grey shale laminae (Fig. 3A). The black laminae are enriched in organic matter compared to the grey laminae, with total organic carbon (TOC)

Conochitinidae indet.	*Armoricochitina nigerica*	*Angochitina* sp.	*Tanu. ontariensis* (short forms)	Tanu. *ontariensis* (long forms)	*Lageno. prussica*	*Spinachitina* sp.	*Eisenackitina* sp.	*Angochitina* n. sp. *A*	*Acantho. barbata*
X									
X	X								
X									
X									
X	X								
X	X				X	X			
X	?							X	
X	?		X	X		X		X	?
X				X			?		
	?		X	X		X	X		?
X		?	X	X	?	X	X		
X	?	?							

(continued on next page)

values fetching 0.61–0.85%. The laminae are devoid of bioturbation. This facies association is restricted to one stratigraphic occurrence at the very top of the Tehar El Brehl Formation (Fig. 2).

Paper-laminated black and grey shales record quiescent suspension settling of mud. Two possibilities exist for the origin of interlaminated grey and black shale. Firstly, these facies can be interpreted as switching between oxic and dysoxic conditions at or below the sediment–water interface, accounting for heightened preservation potential of organic material within the black shale laminae. Alternatively, the laminae could record subtle changes in terrestrial weathering processes. Kennedy et al. (2002) argued that up to 85% of TOC variation within shale can be attributed to changes in the surface area of clay mineral crystals, with adsorption capacity for organic material being more dependent on crystal size than sea water chemistry or biological productivity. Regardless of which interpretation is favoured, the absence of bioturbation implies that oxygen levels at the sea floor were below the threshold required for infaunal burrowers to survive.

4.2. Bioturbated shale and wave rippled sandstone facies association (FA2)

This facies association is characterised by the presence of metre-long, single vertical tube burrows within shale (Fig. 3B). Less distinct bioturbation (mottling) affects interbedded sandstones, which are commonly medium bedded (10–25 cm) and tabular. They contain delicately interwoven, upbuilding wave ripples and hummocky cross-stratification (Fig. 3C). Thicker (1 m), sharp-based sandstone beds also occur, most notably three distinct beds toward the base of the measured section at Zerarda where they form the regionally developed "triad" described above.

The presence of bioturbation implies an oxygenated substrate and low rates of sediment accumulation. Furthermore, the length of the burrows indicates that oxic conditions persisted to a depth of at least one metre below the sea floor. The interwoven wave ripples and interwoven hummocky cross-stratification indicate the action of combined flows associated with storm agitation on the lower shoreface (e.g. Cheel and Leckie, 1993). The bioturbated shale and wave rippled sandstone can therefore be regarded as the deposits of an oxygenated shoreface that was affected by storm agitation.

4.3. Diamictite facies association (FA3)

These sediments comprise structureless to diffusely laminated sandy diamictites. Preserved at four discrete intervals within the Tifarouine Formation on the measured section (Fig. 2, log A), the sandy diamictites are light brown to olive green in colour. They are poorly exposed but easily distinguished from regular sandstones by their relatively high mud content and the occasional preservation of granule sized quartz grains "floating" within a finer-grained matrix. As outlined earlier, thin section analysis of these diamictites reveals their significant textural and compositional differences from sandstones of the Tehar el Brehl Formation (more angular grains, higher proportion of feldspar, chlorite and biotite: Khoukhi, 1993). No pebbles are observed in diamictites of the Tazzeka Massif, unlike those found in the Central Anti-Atlas (Destombes et al., 1985) and in the Massif Central (Le Heron et al., 2007).

The textural distinction between the diamictites and true sandstones observed throughout the succession indicates that they are best interpreted as sediments derived from a glacial source. The absence of well developed stratification coupled with the relatively fine grain size of these deposits makes it impossible to identify evidence of direct glacial processes within this facies association. It is worth emphasising that structureless diamictites may acquire their textural characteristics by debris flow processes, including those that remobilise pre-existing glacial deposits (Eyles, 1993).

Table 1 (*continued*)

Tazzeka samples	*Saharo. fungiformis*	*Desmo. n.* sp. *A*	*Cyatho. latipatagium*	*Calpichitina* sp.	*Ancyrochitina prima*	*Tanu. elongate*	*Spina. gr. oulebsiri*	*Lageno. baltica*	*Spina.* cf. *taugourdeaui*	*Angochitina* sp.
TZ 37										X
TZ 4										
TZ 42										
TZ 35					X		X		X	
TZ 32										
TZ 31										
TZ 3					X	?	X	X		
TZ 41										
TZ 10										
TZ 2			X		?					
TZ 29				X						
TZ 28	X	X	X							
TZ 25	X									
TZ 5										
TZ 20										
TZ 1										
TZ 17										

4.4. Interbedded sandstone and mudrock facies association (FA4)

These sediments comprise interbedded sandstone, siltstone, silty shale and shale. Sandstones are well sorted, fine grained and occur both as discrete, tabular beds 30–40 cm thickness (and rarely up to 1.5 m) and thin, isolated, current-rippled horizons within the mudrocks. Sandstone beds are sharp-based (Fig. 3D), locally channelised, and preserve load and flute casts. The latter structures are filled with coarse-grained sandstone and indicate a range of S to SE-directed and NW-directed palaeocurrents. The tabular sandstones are parallel laminated or preserve an upward transition from massive to parallel laminated facies and capped by SE-directed current ripples. This facies association is characterised by stacked coarsening up cycles (parasequences) up to several metres thick. The topmost sandstone of each parasequence is characterised by a sharp contact with overlying shale.

This facies association is interpreted to result largely from wave agitation. The discrete, tabular sandstones are interpreted as event beds deposited by storm wave activity on the lower shoreface. An alternative explanation for these beds would be proximal turbidites: however, the absence of significant channelisation at their bases, or well-defined Bouma cycles (e.g. Browne and Slatt, 2002), tends to discount this possibility. Furthermore, although palaeocurrent data are few, the spread of orientation of flute casts to the S/SE and to the NW is comparable to that reported previously from storm-deposited successions of the Mesoproterozoic of India (Sarkar et al., 2002). The thin, isolated sandstone beds with current ripples are interpreted as the products of low intensity, fair-weather agitation of the sea floor, which deposited fine-grained sandstone under lower energy conditions (Ashley, 1990). The intercalation of sandstone and mudstone within this facies association indicates a clear compositional bimodality in the depositional environment: the mudstones and shales record fallout from suspension in calm water conditions when wave activity was minimal.

4.5. Rippled sandstone facies association (FA5)

This facies association is best developed at the Bab Louta outcrop. It comprises thinly bedded, fine-grained quartzitic sandstones and siltstones. This facies association is organised into ~2 m thick fining-upward packages (Fig. 3E). The sandstone bed at the base of each fining-upward package bears flute casts. The sandstones contain stacked ripple cross-laminae. Accurate palaeocurrent measurements are extremely difficult from low quality two dimensional exposures but ripple foresets show an apparent dip toward the southeast. The siltstones are unstructured but thinly laminated.

The organisation of fine-grained sandstones and siltstones into 2 m thick fining-upward packages bound at their bases by flute casts potentially indicates a genetic relationship between beds in a waning flow succession. In the marine realm, such waning flow deposits are typical of both tempestite/storm depositional processes and turbidites (Nichols, 1999). The presence of stacked ripple cross-laminae in fined grained sandstones is indicative of low energy transport along a slope that was at least locally oriented southeastwards. The siltstones are interpreted to record quiescent interludes.

4.6. Amalgamated sandstone facies association (FA6)

Stacked, sharp-based sandstones of variable grain size characterise this facies association, which attains up to 25 m thick. Both the basal surface and upper contact of the facies association bear very large (1 m long, 0.3 m wide) flute casts that may contain pebble lags (Fig. 4A, B). Sandstones are moderately to well sorted, of fine to coarse grain size, and are characterised by vertical dewatering structures that crosscut diffuse, horizontal lamination. Beds are >1 m thick, laterally extensive (>25 m), with no obvious channel/scour geometries observed. This facies association rests in sharp contact upon underlying rocks and is bounded above by an abrupt

Fungochitina sp.	*Linochitina* sp.	*Cingulochitina* sp.	*Ancyro. gr. primitive*	*Calpi.* cf. *accolare*	Chitinozoan fragments	Graptolites remains	Acritarchs	Chitinozoan assemblages	Chronostratigraphy
X	X	X	X	X					Mid Silurian
					X	X		?	?
						X	X	*oulebsiri/elongate*	Hirnantian
							X		
							X		
					X		X	?	Late Katian
					X				
								nigerica	
							X	*fungiformis*	
								fistulosa	
						X			

contact with shale. It is laterally extensive and forms the top of coarsening upward successions in Zerarda, Bab Louta and Jbel Arhi Ousserdoun, indicating that is characterised as a regionally extensive, tabular depositional unit.

The thickly bedded, stacked sandstones with diffuse lamination and dewatering structures are interpreted as debris flow deposits that underwent fluid expulsion during sediment consolidation (e.g. Major, 2000). Whilst the presence of flute casts could also be explained by turbidity current erosion, the presence of diffuse lamination may suggest a shearing process within the flow, which is consistent with delamination of a non-Newtonian fluid (Leeder, 1999). The pervasive vertical dewatering structures indicate rapid expulsion of fluid in a high-sand supply setting. The predominance of tabular beds, as opposed to obvious channel scours, is striking. These observations may suggest that this facies association was deposited in an overbank sedimentary environment. Alternatively, the tabular sandstone beds may also record a system of amalgamated, very low relief (shallow and wide channels) beyond the scale of outcrop observation. It is suggested that the amalgamated sandstone facies association records delta-front sedimentation.

4.7. Summary

The six facies associations record deposition in a range of sedimentary environments under variable energy conditions. Evidence for sedimentation in a lower shoreface setting is provided by the presence of large burrows in the bioturbated shale and wave rippled sandstone facies association. It is suggested that the black and grey shale facies association records the deepest water (or least agitated) sedimentary environment in the sections studied in the Tazzeka Massif, with low oxygen levels suppressing the ability of infaunal organisms to survive. The interbedded sandstone and mudrock facies association was deposited in shallower water (possibly in a lower to upper shoreface environment) under the influence of both storm and fair-weather waves (wave ripples and hummocky cross-stratification).

The rippled sandstone facies association, which provides evidence for unidirectional current activity in an otherwise wave-dominated sedimentary environment, may record the seaward return of rip currents following coastal set-up during storms. The amalgamated sandstone facies association, on the other hand, which preserves evidence of debris flow deposition, records the most proximal sedimentary processes in the Tazzeka Massif. These processes are compatible with delta-front sedimentation. The presence of diamictite in a succession otherwise poor in evidence for true glacial activity provides an interesting problem, and makes it possible to speculate that these deposits were introduced by iceberg rafting (e.g. Dowdeswell et al., 1994). Our previous search for direct indications of grounded ice sheets in the Tazzeka Massif failed to unveil any convincing evidence (Le Heron et al., 2007) but, given the context, it is plausible that these diamictites ultimately originated from a grounded ice sheet situated some distance to the south.

In earlier work (Le Heron et al., 2007), we suggested that sediments of the Tifarouine Formation recorded deposition as a series of turbidite deposits. However, detailed examination indicates that sedimentary facies more closely resemble the deposits of a periodically abandoned, wave-dominated delta. These general interpretations are in accordance with the earlier conclusions of Khoukhi (1993) and Khoukhi and Hamoumi (2001).

5. Lower Silurian shale

5.1. Description

Strata of Early Silurian age rest disconformably above the Tafarouine Formation in both Zerarda and Jbel Arhi Ousserdoun sections of the Tazzeka Massif (Figs. 2 and 4C). However, faults crosscut both the topmost Tafarouine Formation and

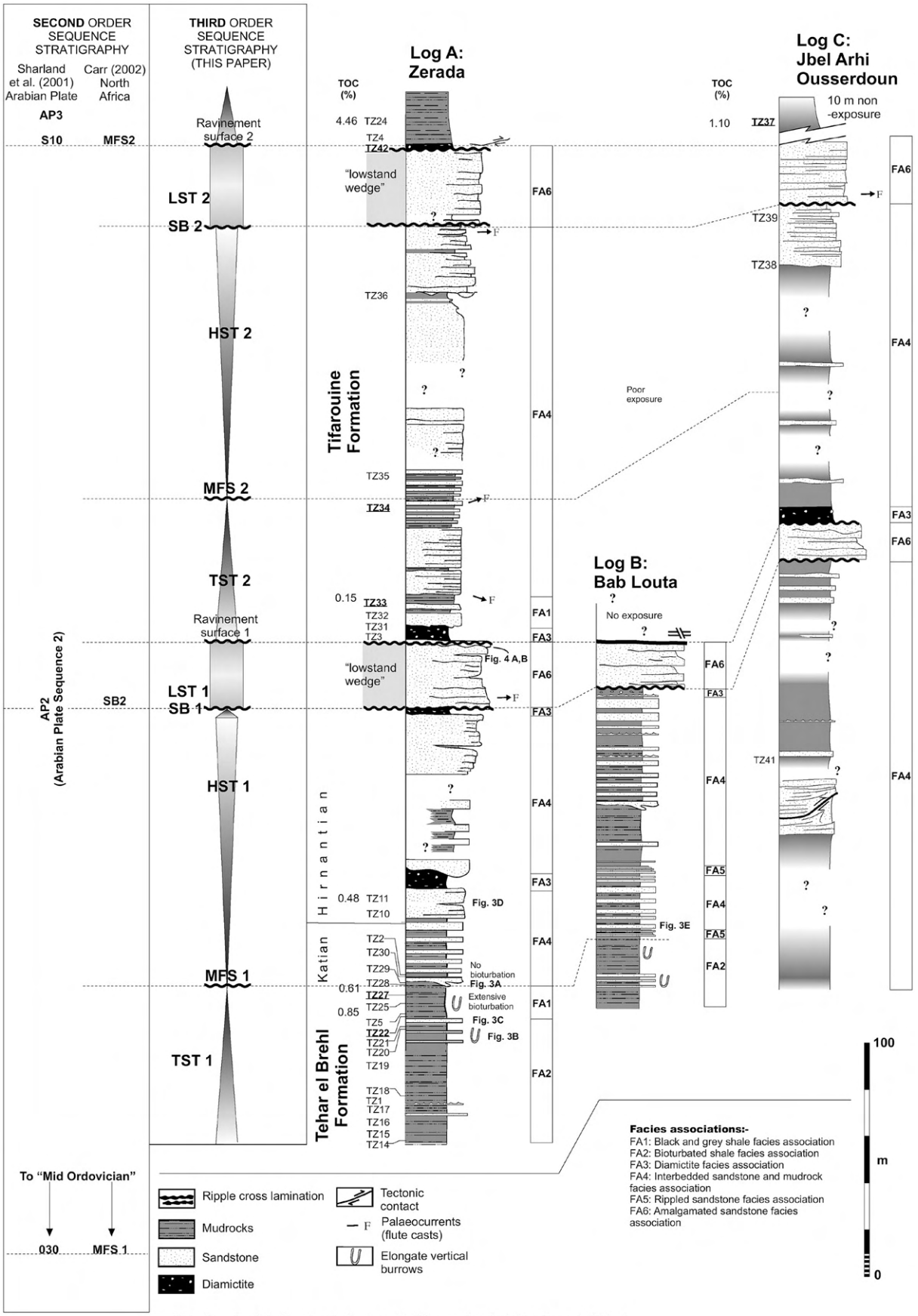

Note: Samples in bold and underlined provided the geochemical data shown in Table 1.

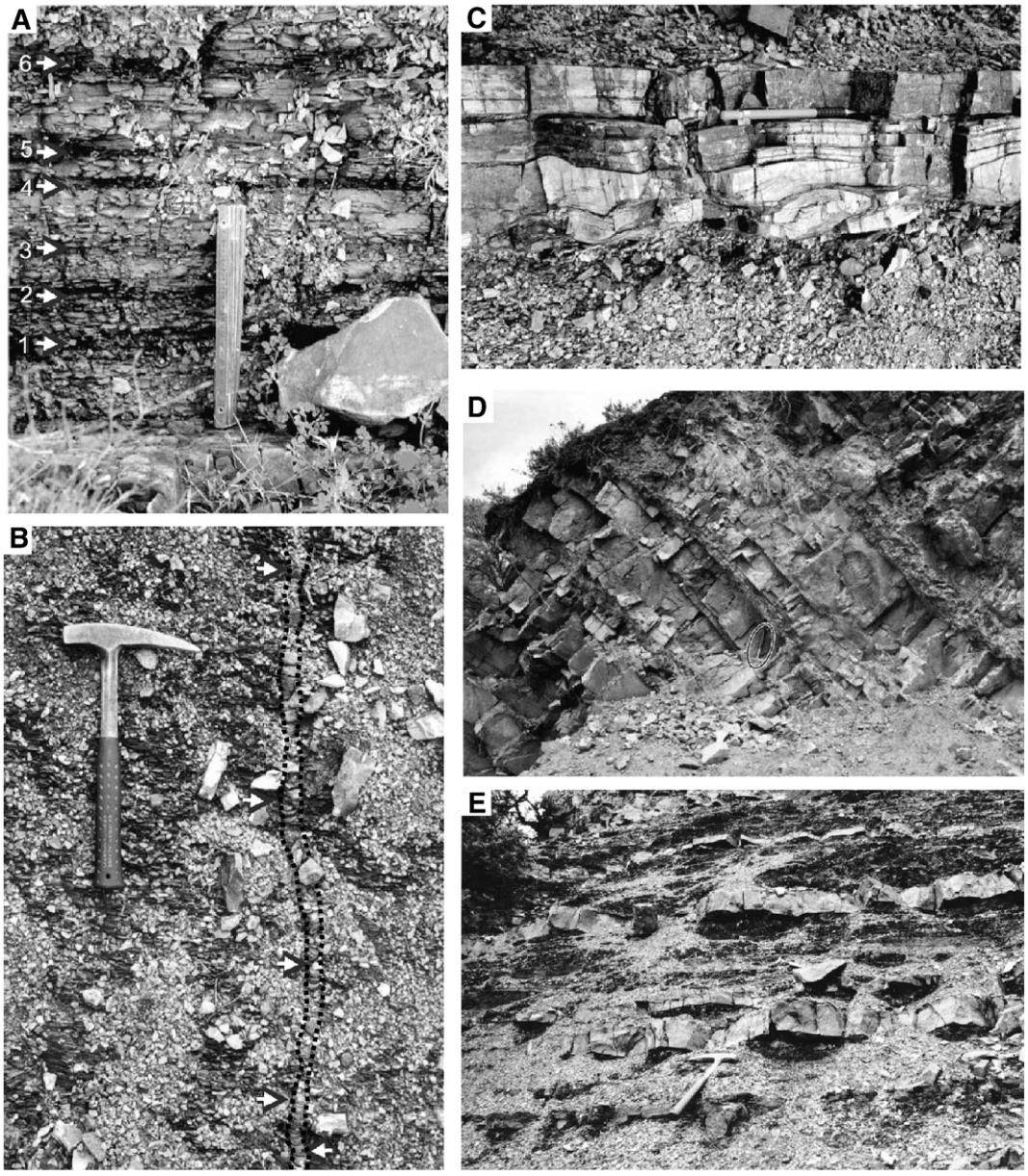

Fig. 3. Sedimentary facies of the Tehar El Brehl and Tifarouine formations of the Tazzeka Massif. A: Centimetre-thick black shale laminae interstratified with grey shales at Zerarda. Six black shales are identified in total: note the sharp base and top of black shale 4. The sharp definition of the shale indicates a primary depositional origin and hence rapid switching between anoxic and more oxygenated conditions at or near the sea floor. B: Single vertical burrow crosscutting laminated grey shale and reaching 1 m in length at Zerarda. C: 10 cm thick fine-grained sandstone bed comprising stacked, symmetrically rippled sandstone, protruding from an otherwise shale-rich section at Zerarda. These sandstones are interpreted as offshore storm beds. D: Sharp-based, tabular sandstones at Zerarda organised into a 10 m thick coarsening up package. Thin shale deposits are preserved between the sandstones (fissile deposit above the circled geological hammer). These deposits are interpreted as tempestites. E: Thin (2 m thick) fining-upward cycles comprising sharp-based, rippled sandstones passing up into rippled siltstones at Bab Louta (rippled sandstone facies association).

Early Silurian deposits (Fig. 4C), and thus a seamless stratigraphic contact between these rocks cannot be demonstrated. As our biostratigraphic analysis has shown, the oldest recovered chitinozoa are Late Llandovery (i.e. Telychian) or younger in age (TZ37) and were collected only a few decimetres above the topmost sandstone of the Tifarouine Formation (Fig. 2, log A). Lower Silurian sediments comprise shale passing upward over several metres into thinly bedded silicytes.

Fig. 2. The main sedimentary dataset from the three study sections in the Tazzeka Massif. The interval of interests spans the Late Katian, the entire Hirnantian, and part of the Silurian. The main (most complete) section is in Zerarda. Sampling points are shown to the left of each log. Those samples which are bold and underlined were processed for geochemical analysis. The sedimentary facies associations documented in the text are shown to the right of each log. The third order sequence stratigraphic interpretation of these sedimentary rocks is shown to the left of the figure, with earlier published second order sequence stratigraphic frameworks for both North Africa and Arabia shown for comparative purposes.

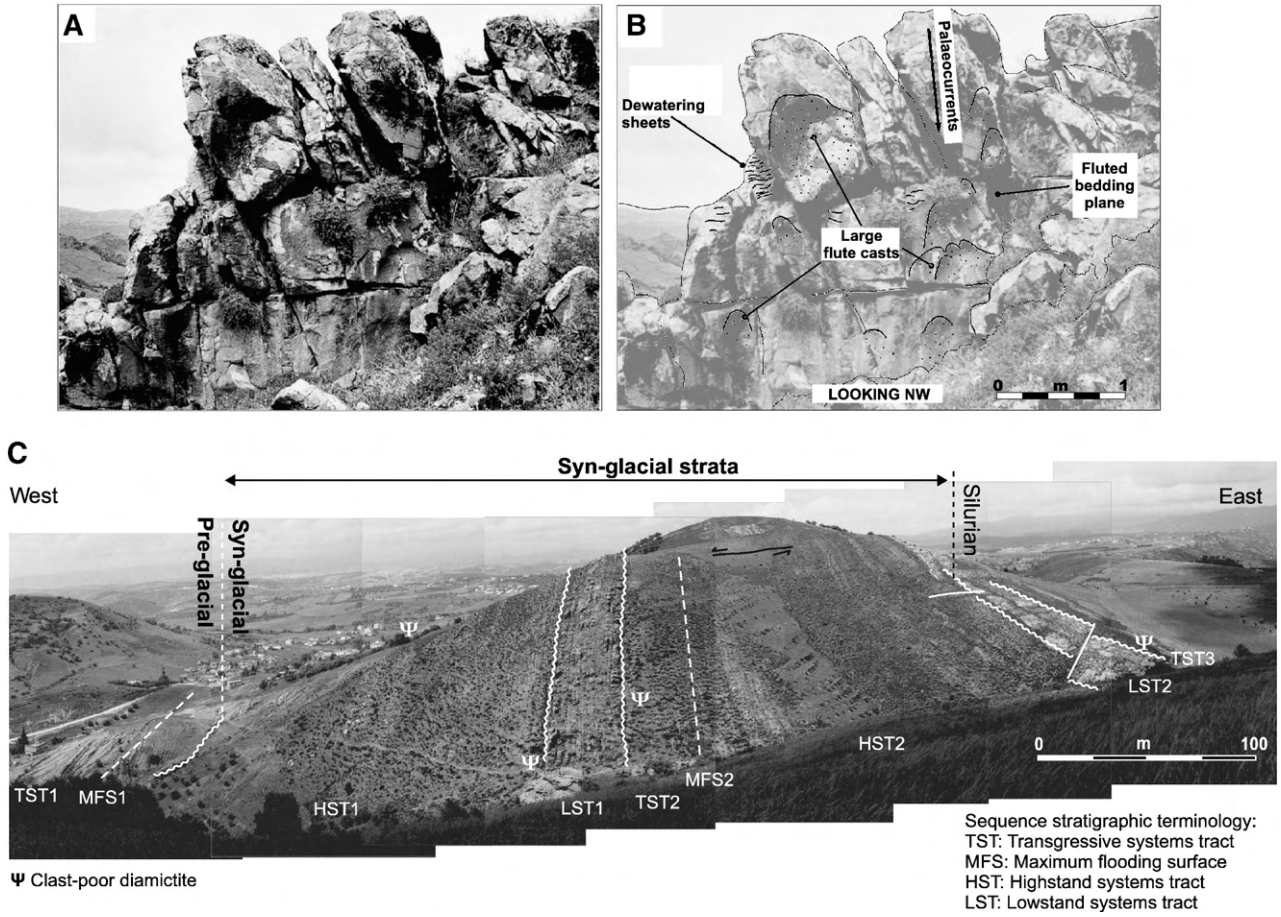

Fig. 4. A: Photograph and B interpretative overlay of large flute casts within the amalgamated sandstone facies association at Zerarda (the first "lowstand wedge" in Fig. 2). Beds are dippining vertically, and hence view is looking down on a bedding plane. The amalgamated sandstone facies association shows very different sedimentological characteristics (grain size, large flute casts, dewatering structures, amalgamated beds) from the interbedded sandstone and mudstone facies association that comprises the majority of the Tifarouine Formation, and is interpreted as a turbidite deposit that was probably sourced from a Late Ordovician ice sheet situated to the south. C: Panoramic photo of the representative Zerarda section (c.f. Fig. 3, log A), showing sequence stratigraphic interpretation of the Upper Ordovician through Silurian succession.

5.2. Interpretation

The potential fault contact between makes it more difficult to assess the genetic relationship between shale and silicytes of the Lower Silurian and sandstones of the uppermost Tifarouine Formation. However, any dislocation associated with faulting at this level is likely to have exploited the rheological contrast between sandstone and shale, suggesting that this contact is largely sedimentological. Lower Silurian shale records a sharp loss of sandstone from the underlying Tifarouine Formation and thus, potentially, transgressive flooding. The age of chitinozoa from TZ37 suggest, however, a significant hiatus between latest Ordovician and the Late Llandovery (i.e. Telychian). The most recent stratigraphic timescale indicates that at least 8 Myr separate the early and Late Llandovery (Gradstein et al., 2004), and our data therefore record a hiatus of at least the same duration.

6. Organic enrichment of shale

Across North Africa, Lower Silurian shale includes organically enriched intervals that have been argued to be the source of 90% of the regions' Lower Palaeozoic oil (Lüning et al., 2000). Samples of shale from all three intervals of interest– the Tehar el Brehl Formation, the Tifarouine Formation and the un-named Silurian shale– were therefore processed using Rock-Eval pyrolysis to establish their total organic content (TOC). The TOC values in Table 2 provide a measure of the organic richness of the sample (% weight of the dry rock sample). The relatively high TMax temperatures for all samples in the set (~500 °C or greater) suggests that any organic material in Ordovician–Silurian shales of northern Morocco is post-mature and unable to generate hydrocarbons.

The table shows that the two samples analysed from the uppermost Tehar el Brehl Formation have low TOC values of 0.61–0.85%, and that samples TZ33 and TZ34 from within the Tifarouine Formation are similarly depleted in organic matter. In contrast, those collected from the un-named Silurian shale are relatively enriched in TOC (1.10%: TZ37; 4.46%: TZ24). These values compare favourably to values in Early Silurian oil shales elsewhere in North Africa such as in the northern Murzuq Basin of southwest Libya (Lüning et al., 2000).

Across North Africa and into Jordan, two Early Silurian "hot shales" are identified, characterised by elevated TOC values that give a pronounced "kick" on gamma ray logging tools (Lüning

Table 2
Geochemical data table of seven samples processed using RockEval pyrolysis to determine total organic carbon (TOC) and thermal maturity of shales in the Tazzeka Massif

Formation	Sample	TMax	TOC (%)	HI	S1	S2
Un-named Silurian shale	TZ37	518	1.10	4	0.01	0.05
	TZ42	517	0.12	16	0.01	0.02
	TZ24	489	4.46	1	0.00	0.04
Tifarouine Formation	TZ33	535	0.15	5	0.00	0.01
	TZ34	542	0.57	7	0.02	0.04
Tehar el Brehl Formation	TZ22	590	0.85	0	0.01	0.00
	TZ27	565	0.61	0	0.00	0.00

Three populations of samples are shown, namely from the Tehar el Brehl and Tifarouine formations, and from the un-named Silurian shale that overlies them.

et al., 2000). The age of these organically enriched horizons, which are referred to as lower and upper hot shales, is Rhuddanian and Telychian–Wenlockian respectively (e.g. Lüning et al., 2005). These ages indicate that the lower hot shale is absent in the Tazzeka Massif but that high TOC values in TZ 24 and TZ 37 may potentially be associated with the younger of the two Gondwana-wide anoxic events. The origin of the lower hot shale, which is unevenly distributed across Saharan cratonic basins, may be related to topography left behind by retreating Late Ordovician ice sheets (Lüning et al., 2000). The upper hot shale is more evenly distributed but remains poorly understood and ill defined in terms of its lateral extent. Prior to the present paper, the presence of this organically enriched horizon had not been established in northern Morocco. Given that the most reliable documentation of Telychian hot shale comes from the Berkine Basin of eastern Algeria (Lüning et al., 2000), our results appear to considerably increase the known lateral extent of the upper "hot shale" interval across the region.

7. Discussion

7.1. Third order sequence stratigraphy

The majority of the Tifarouine Formation is referred to the Hirnantian, an interpretation much supported by the occurrence of diamictites: lithofacies which appear to be exclusively restricted to Hirnantian glacial deposits across the North Africa region (e.g. Ghienne, 2003; Ghienne et al., 2007; Le Heron et al., 2004, 2005, 2006; Le Heron, 2007). Therefore, the sedimentary model developed for Hirnantian sedimentary rocks in the Tazzeka Massif also describes the evolution of a basin prior to glaciation, at the glacial maximum, and during glacial retreat. In this section, a third order sequence stratigraphic analysis of the Tehar El Brehl Formation and overlying Tifarouine Formation is attempted which takes account of the vertical stacking pattern of parasequences, our biostratigraphic data and sedimentological observations on the depositional system. The second order sequence stratigraphic framework of the Arabian Plate (Sharland et al., 2001) and North Africa (Carr, 2002) provides a within which the sequence stratigraphic development of the succession in the Tazzeka Massif can be considered.

The development of high frequency anoxic events in the uppermost Tehar El Brehl Formation is suggested to relate to reduced sediment supply. In the Upper Cretaceous of the Gulf of Mexico, Liu (2005) considered that anoxic depositional events may occur in two phases of a rising sea-level cycle: the first, at the onset of transgression (early transgressive systems tract), and the second at the maximum sea-level high (maximum flooding surface). Owing to the occurrence of large vertical burrows beneath the thin black–grey shale interbeds, which imply the existence of an oxygenated sea floor, the uppermost Tehar El Brehl Formation is interpreted as a transgressive systems tract (TST 1) culminating up-section in a maximum flooding surface (the black shale–grey shale couplets: MFS 1). Our biostratigraphic data suggest that this maximum flooding surface may have occurred toward the end of the Katian. This MFS is likely to have occurred later than the well recognised Mid Ordovician flooding event across the region (i.e. second order MFS1 of Carr, 2002, across North Africa; O30 of Sharland et al., 2001, in the Arabian Plate). Following maximum flooding, progradation of the shoreface as a forestepping parasequence set occurred (highstand systems tract: HST 1). This phase of deposition was characterised by normal shelf progradation, although the stratigraphic evolution was complicated by at least two higher frequency pulses of glaciation, explaining the occurrence of diamictites within the lower part of the Tifarouine Formation (Fig. 2, log A).

A lowstand systems tract is proposed toward the middle of the Tifarouine Formation (LST 1; Fig. 2). The sharp base of the amalgamated sandstone facies association at this level, coupled with the abundant occurrence of dewatering structures and large flute casts, may indicate that delta-front debris flows may be glacially-derived. Comparison to the Late Ordovician glacial record in the Rehamna region, central Morocco (Le Heron et al., 2007) identifies a suite of subglacial soft-sediment deformation structures, including soft-sediment striated surfaces, at about the same level. These observations suggest that the lowstand systems tract pinches out landward, with both its basal and upper surface converging into a subglacially produced unconformity. Thus, it is suggested that the lowstand systems tract is a detached wedge of sediment (hence "lowstand wedge": Fig. 2).

The upper surface of LST 1 is sharp and abrupt into shale (ravinement surface 1). As argued above, the chitinozoan assemblage from this level is referable to the *elongata* biozone of the Hirnantian (e.g. Bourahrouh et al., 2004). The first shale above this ravinement surface is interpreted as the base of a series of backstepping parasequences belonging to a second transgressive systems tract (TST 2), and culminating in a maximum flooding surface (MFS 2). Above this surface, another series of forestepping parasequences is recognised (HST 2), truncated by a second lowstand systems tract (LST 2) at the top of the Tifarouine Formation (Fig. 2). Silurian shale, capping the topmost sandstones, heralds another transgressive systems tract (TST 3) at the top of the succession. This last transgressive sedimentary system is also regionally developed, and associated with a major, regional flooding surface (second order MFS 2 of Carr, 2002; base of AP2 in Sharland et al., 2001).

In the above analysis, it has been assumed that controls on sediment stacking patterns were mainly extrabasinal. This

assumption is justified by 1) the absence of slumps and soft-sediment deformation features that might otherwise point to more local controls on accommodation space creation and destruction, and 2) the lack of evidence for Late Ordovician grounded ice sheets in the Tazzeka Massif. An extrabasinal control on sediment architecture– i.e. relative sea level moderated by the behaviour (growth and decay) of Hirnantian ice sheets– indicates that the Tazzeka stratigraphy should be directly referable to the global eustatic curve.

Published global sea-level curves for the Late Ordovician are particularly detailed (e.g. Brenchley and Storch, 1989), and show the following features: 1) gradual sea-level fall during the *complexus* and *pacificus* graptolite biozones (during the Katian: formerly Rawtheyan), 2) a sharp fall during the Hirnantian (*extraordinarius* graptolite biozone), 3) an intra-Hirnantian sea-level high, then 4) a further sea-level fall before 5) major deepening at the end of the *extraordinarius* biozone/beginning of the *persculptus* bizone in the Late Hirnantian (e.g. Brenchley et al., 1994, 2003). The *extraordinarius* and *persculptus* biozones in the graptolites correspond approximately to the *elongata* and *oulebsiri* biozones in the chitinozoa. However, it is emphasised that interpretation of our data favours a maximum flooding surface– rather than a gradual sea-level fall– in pre-Hirnantian rocks. For comparison, Kaljo et al. (2004) constructed a relative sea-level curve for Katian through Hirnantian carbonates on the Baltic margin in which they interpreted a maximum flooding surface beneath Hirnantian limestones.

7.2. Limitations of the sea-level interpolation

Unlike other areas where pre-glacial transgression has been interpreted (e.g. Mauritania: Ghienne, 2003), the Tazzeka Massif appears to have been remote from the effects of grounded ice sheets (and hence glacio-isostatic downwarping), and thus our findings should be a reliable indication of eustatic sea-level change. Our study has found no evidence for soft-sediment deformation related to gravitational collapse (e.g. Alonso et al., 2008), which might otherwise point to a tectonic influence on sediment accommodation space through the Katian and Hirnantian in the Tazzeka Massif.

7.3. Condensed sedimentation and the onset of glaciation

The sedimentological and biostratigraphic data presented in this paper enable us to propose that deposition occurred uninterrupted in the Tazzeka Massif from the Late Katian through to the Hirnantian. It is now thought that Late Ordovician ice sheets grew to their maximum extent across North Africa during the Hirnantian (e.g. Ghienne et al., 2007), but the timing of onset of glaciation has remained extremely controversial. On the basis of inflexions observed in the stable oxygen isotope curve derived from Laurentian carbonates, Saltzmann and Young (2005) argue for an early onset of Late Ordovician glaciation some 10 Myr prior to the Hirnantian, whereas Brenchley et al. (2003) suggest that the glaciation was short and sharp-based on a rapid increase in δO_{18} in carbonates of Scandinavia. In this latter area, the drawdown of δO_{18} is exactly coincident with the beginning of the Hirnantian and the major initial phase of ice sheet growth (Brenchley et al., 2003).

Unfortunately, the data presented in the current paper do not allow us to resolve this controversy. The black and grey shale couplets recorded at Zerarda occur just below the first appearance of *nigerica* chitinozoans. As *A. nigerica* has its first appearance datum in the Late Katian (i.e. in the early Ashgill, close to the Caradoc–Ashgill boundary), this species cannot be used to document the base of the Hirnantian. Instead, it is suggested that the black and grey shale couplets correspond to the *fistulosa* transgressive event already recognised in the Anti-Atlas of Morocco (Bourahrouh et al., 2004). The couplets (Fig. 3A) indicate extremely low rates of sedimentation prior to the onset of glaciation in the Hirnantian. Given the restriction of this facies association to this interval, it is suggested that each of the black shale intervals may potentially correspond to an early phase of sea ice growth and seasonal cooling. Sea ice growth would have reduced the terrestrial nutrient supply by cutting off the wind-transported dust, hence drastically reducing marine productivity. Within the Central Anti-Atlas of Morocco stratigraphic continuity occurs between these two stages although, surprisingly, recent palynological studies (Bourahrouh et al., 2004) record no dramatic changes in biodiversity across this boundary. In this area, the boundary is, however, characterised by Fe and Ph-rich horizons and a bloom in phytoplankton productivity (Bourahrouh et al., 2004).

In North Africa, a two-phased glaciation was proposed by Sutcliffe et al. (2000), but it is now known that the associated glaciogenic sediments preserve a more complex history with up to four (Ghienne, 2003; Le Heron et al., 2007) or locally five (Moreau et al., 2005,) cycles of ice sheet waxing and waning across the region. Furthermore, biostratigraphic data are frequently of insufficient resolution to discriminate between different glacial cycles across the region, which may also record evidence for migrating or diachronous ice centres (Ghienne et al., 2007). Despite these complexities, a very well-defined transgressive systems tract (TST 2) culminating in a maximum flooding surface (MFS 2) has been shown to occur within the Tifarouine formations. As these sediments were deposited at some distance from an ice front, these two units are interpreted as the clear signal of glacioeustatic sea-level change, recording two principal cycles of ice sheet growth separated by a major interglacial. Oxygen isotope data of both Brenchley et al. (2003) and Kaljo et al. (2004) show a short-lived increase in δO_{16} within Scandinavian carbonates that could correspond to such an interglacial— and to the resultant glacioeustatic sea-level rise that could explain TST 2. Similar isotopic responses are also reported from Arctic Canada (Melchin and Holmden, 2006).

8. Conclusions

- Based on extensive mudstone sampling, a biostratigraphic framework of Upper Ordovician through Silurian clastic sedimentary rocks for the Tahar El Brehl and Tifarouine formations in the Tazzeka Massif, eastern Moroccan Hercynides, is proposed for the first time. The biostratigraphic framework, which is based on chitinozoa and acritarch assemblages,

provides vital age constraints for an internationally important stratigraphic section.

- Detailed sedimentological analysis of Hirnantian (syn-glacial) deposits reveals the architecture of a shallow marine sedimentary system that lay beyond the influence of Late Ordovician ice sheets. Sedimentological analysis reveals the influence of wave-dominated (both storm and fair weather) sedimentary processes, although relatively poor evidence for Hirnantian glacial is recorded.
- Newly available data on organic richness of samples collected from shales indicate that Upper Ordovician mudstones are organically depleted whereas Silurian shales are organically enriched to >4.5%. These represent the first discovery of Early to Mid Silurian (?Telychian) "hot shales" in northern Morocco, greatly extending the known lateral extent of this organically enriched interval across North Africa and raising the prospect that a suitable hydrocarbon source rock may be found in the surrounding region.
- Detailed sequence stratigraphic analysis of Upper Ordovician through Lower Silurian deposits identifies transgressive, highstand, and lowstand systems tracts. The second transgressive systems tract in the succession, culminating in a maximum flooding surface, is tentatively linked to a major interglacial in the Hirnantian. The lowstand systems tracts are reckoned to be detached, with lower and upper bounding surfaces converging landward into a subglacial unconformity.

Acknowledgements

This paper was reviewed by Drs Julien Moreau and Gary Nichols. The authors are very grateful to them for their comments which greatly enhanced the paper. The data in this paper were mostly collected when DPLeH was a postdoctoral research associate in Strasbourg, France. TOTAL provided the funding to do the fieldwork. The authors wish to express thanks to Jean-Loup Rubino of TOTAL, Pau, who processed the mudstone/shale samples for TOC and thermal maturity purposes. Dr Jutta Winsemann is thanked for providing expert advice on the interpretation of turbidite vs wave-dominated shoreface deposits, and whose sedimentological opinions helped to shape latter drafts of the manuscript. Dan Le Heron would like to express his personal thanks to his long-suffering fiancée for tolerating seemingly endless evenings of manuscript redrafting. He hopes that she will become more geologically inclined in their future married life.

References

Alonso, J.L., Gallastegui, J., Garcia-Sansegundo, J., Farias, P., Rodriguez Fernandez, L.R., Ramos, V.A., 2008. Extensional tectonics and gravitational collapse in an Ordovician passive margin: the Western Argentine Precordillera. Gondwana Research 13, 204–215.

Armstrong, H.A., Turner, B.R., Makhlouf, I.M., Weedon, G.P., Williams, M., Al Smadi, A., Abu Salah, A., 2005. Origin, sequence stratigraphy and depositional environment of an Upper Ordovician (Hirnantian) deglacial black shale, Jordan. Palaeogeography, Palaeoclimatology, Palaeoecology 220 (3–4), 273–289.

Ashley, G.M., 1990. Classification of large-scale subaqueous bedforms; a new look at an old problem. Journal of Sedimentary Research 60, 161–172.

Brenchley, P.J., Storch, P., 1989. Environmental changes in the Hirnantian (upper Ordovician) of the Prague Basin, Czechoslovakia. Geological Journal 24, 165–182.

Brenchley, P.J., Marshall, J.D., Carden, G.A.F., Robertson, D.B.R., Long, D.G.F., Meidla, T., Hints, L., Anderson, T.F., 1994. Bathymetric and isotopic evidence for a short-lived Ordovician glaciation in a greenhouse period. Geology 22, 295–298.

Brenchley, P.J., Carden, G.A., Hints, L., Kaljo, D., Marshall, J.D., Martma, T., Meidla, T., Nölvak, J., 2003. High-resolution stable isotope stratigraphy of Upper Ordovician sequences: constraints on the timing of bioevents and environmental changes associated with mass extinction and glaciation. GSA Bulletin 115 (1), 89–104.

Browne, G.H., Slatt, R.M., 2002. Outcrop and behind-outcrop characterization of a late Miocene slope fan system, Mt. Messenger Formation, New Zealand. AAPG Bulletin 86 (5), 841–862.

Bourahrouh, A., Paris, F., Elaouad-Debbaj, Z., 2004. Biostratigraphy, biodiversity and palaeoenvironments of the chitinozoans and associated palynomorphs from the Upper Ordovician of the Central Anti-Atlas, Morocco. Review of Palaeobotany and Palynology 130, 17–40.

Carr, I.D., 2002. Second-order sequence stratigraphy of the Palaeozoic of North Africa. Journal of Petroleum Geology 25, 259–280.

Cheel, R.J., Leckie, D.A., 1993. Hummocky cross-stratification. Sedimentology Review 103–122.

Destombes, J., 1971. L'Ordovicien au Maroc. Essai de synthèse stratigraphique. Mémoires de la B.R.G.M, vol. 73. Paris, pp. 237–263.

Destombes, J., Holland, H., Willefert, S., 1985. Lower palaeozoic rocks of Morocco. In: Holland, C.H. (Ed.), Lower Palaeozoic rocks of the World. Wiley, London, pp. 91–336.

Dowdeswell, J.A., Whittington, R.J., Marienfeld, P., 1994. The origin of massive diamicton facies by iceberg rafting and scouring, Scoresby Sund, East Greenland. Sedimentology 41 (1), 21–35.

Eyles, N., 1993. Earth's glacial record and its tectonic setting. Earth Science Reviews 35 (1–2), 1–248.

Ghienne, J.-F., 2003. Late Ordovician sedimentary environments, glacial cycles, and postglacial transgression in the Taoudeni Basin, West Africa. Palaeogeography, Palaeoclimatology, Palaeoecology 189, 117–145.

Ghienne, J.-F., Le Heron, D.P., Moreau, J., Deynoux, M., 2007. The Late Ordovician glacial sedimentary system of the West Gondwana platform. In: Hambrey, A., Christoffersen, M.J., Glasser, N.F., Hubbard, B. (Eds.), Glacial Sedimentary Processes and Products, vol. 39. International Association of Sedimentologists, Special Publications. pp. 295–319.

Gradstein, F., Ogg, J., Smith, A., 2004. A Geologic Time Scale 2004. Cambridge University Press. 610p.

Hallett, D., 2002. Petroleum Geology of Libya. the Netherlands, Elsevier. 503p.

Hill, P.J., Molyneux, S.G., 1988. Biostratigraphy, palynofacies and provincialism of Late Ordovician–Early Silurian acritarchs from northeastern Libya. In: El-Arnauti, A., Owens, B., Thusu, B. (Eds.), Subsurface palynostratigraphy of northeast Libya. Garyounis University Publications, Benghazi, pp. 27–43.

Hoepffner, C., 1987. La tectonique hercynienne dans l'Est du Maroc. Thèse d'Etat, Université Louis Pasteur, Strasbourg, 280p.

Kaljo, D., Hints, L., Martma, T., Nölvak, J., Oraspöld, A., 2004. Late Ordovician carbon isotope trend in Estonia, its significance in stratigraphy and environmental analysis. Palaeogeography, Palaeoclimatology, Palaeoecology 210, 165–185.

Kennedy, M.J., Pevear, D.R., Hill, R.J., 2002. Mineral surface control of organic carbon in black shale. Science 295, 657–660.

Khoukhi, Y., 1993. L'Ordovicien et le Cambro-ordovicien de la Meseta orientale, Maroc: Pétrologie, dynamique sédimentaire et stratigraphie séquentielle. Thèse de 3ème Cycle, Faculté des Sciences d'Oujda, Morocco.

Khoukhi, Y., Hamoumi, N., 2001. L'Ordovicien de la Meseta orientale (Maroc): Stratigraphie génétique-contrôle géodynamique, climatique et eustatique. African Geoscience Review 8, 289–302.

Leeder, M., 1999. Sedimentology and Sedimentary Basins: From Turbulence to Tectonics. Blackwell. 592p.

Le Heron, D.P., 2007. Late Ordovician glacial record of the Anti Atlas, Morocco. Sedimentary Geology 201 (1–2), 93–110.

Le Heron, D.P., Craig, J., 2008. First order reconstructions of a Late Ordovician Saharan ice sheet. Journal of the Geological Society 165, 19–29 (London).

Le Heron, D., Sutcliffe, O., Bourgig, K., Craig, J., Visentin, C., Whittington, R., 2004. Sedimentary architecture of Upper Ordovician tunnel valleys, Gargaf Arch, Libya: implications for the genesis of a hydrocarbon reservoir. GeoArabia 9, 137–160.

Le Heron, D.P., Sutcliffe, O.E., Whittington, R.J., Craig, J., 2005. The origins of glacially related soft-sediment deformation structures in Upper Ordovician glaciogenic rocks: implication for ice sheet dynamics. Palaeogeography, Palaeoclimatology, Palaeoecology 218, 75–103.

Le Heron, D.P., Ghienne, J.-F., El Houicha, M., Khoukhi, Y., Rubino, J.-L., 2007. Maximum extent of ice sheets in Morocco during the Late Ordovician glaciation. Palaeogeography, Palaeoclimatology, Palaeoecology 245, 200–226.

Liu, K., 2005. Upper Cretaceous sequence stratigraphy, sea-level fluctuations and oceanic anoxic events 2 and 3, northeastern Gulf of Mexico. Stratigraphy 2 (2), 147–166.

Lüning, S., Craig, J., Loydell, D.K., Storch, P., Fitches, W., 2000. Lowermost Silurian “hot shales” in North Africa and Arabia: regional distribution and depositional model. Earth-Science Reviews 49, 121–200.

Lüning, S., Shahin, Y.M., Loydell, D., Al-Rabi, H.Y., Masri, A., Tarawneh, B., Kolonic, S., 2005. Anatomy of a world-class source rock: distribution and depositional model of Silurian organic-rich shales in Jordan and implications for hydrocarbon potential. AAPG Bulletin 89, 1397–1427.

Major, J., 2000. Gravity-driven consolidation of granular slurries— implications for debris-flow deposition and deposit characteristics. Journal of Sedimentary Research 70 (1), 64–83.

Maruyama, S., Santosh, M., 2008. Models on snowball Earth and Cambrian explosion: a synopsis. Gondwana Research 14, 22–32. doi:10.1016/j.gr.2008.01.004.

Melchin, M.J., Holmden, C., 2006. Carbon isotope chemostratigraphy in Arctic Canada: sea-level forcing of carbonate platform weathering and implications for Hirnantian global correlation. Palaeogeography, Palaeoclimatology, Palaeoecology 234, 186–200.

Moreau, J., Ghienne, J.-F., Le Heron, D.P., Rubino, J.-L., Deynoux, M., 2005. 440 Ma ice stream in North Africa. Geology 33 (9), 753–756.

Nichols, G., 1999. Sedimentology and Stratigraphy. Blackwell, United Kigdom. 355p.

Page, A., Zalasiewicz, J.A., Williams, M., Popov, L.E., 2007. Were transgressive black shales a negative feedback modulating glacioeustacy in the Early Palaeozoic Icehouse? Geological Society Special Publication 123–156.

Paris, F., Elaouad-Debbaj, Z., Jaglin, J.C., Massa, D., Oulebsir, L., 1995. Chitinozoans and Late Ordovician glacial events on Gondwana. In: Cooper, J.D., Droser, M.L., Finney, S.C. (Eds.), Ordovician Odyssey: Short Papers for the Seventh International Symposium on the Ordovician System. The Pacific Section Society for Sedimentary Geology (SEPM), Fullerton, California, pp. 171–177.

Piqué, A., 2001. Gebrueder Borntraeger Verlagsbuchhandlung. Geology of Northwest Africa. Federal Republic of Germany, Berlin-Stuttgart. 324 pp.

Piqué, A., Michard, A., 1989. Moroccan Hercynides: a synopsis. The Paleozoic sedimentary and tectonic evolution at the northern margin of West Africa. American Journal of Science 289, 286–330.

Saltzmann, M.R., Young, S.A., 2005. Long-lived glaciation in the Late Ordovician? Isotopic and sequence— stratigraphic evidence from western Laurentia. Geology 33 (2), 109–112.

Sarkar, S., Banerjee, S., Chakraborty, S., Bose, P.K., 2002. Shelf storm flow dynamics: insight from the Mesoproterozoic Rampur Shale, central India. Sedimentary Geology 147 (1–2), 89–104.

Selley, R.C., 1997. The basins of NW Africa: structural evolution. In: Selley, R.C. (Ed.), African Basins: Sedimentary Basins of the World 3. Elsevier, Amsterdam, pp. 17–26.

Sharland, P.R., Archer, R., Casey, D.M., Davies, R.B., Hall, S.H., Heward, A.P., Horbury, A.D., Simmons, M.D., 2001. Arabian plate sequence stratigraphy. GeoArabia Special Publications 2 371 pp.

Sutcliffe, O.E., Dowdeswell, J.A., Whittington, R.J., Theron, J.N., Craig, J., 2000. Calibrating the Late Ordovician glaciation and mass extinction by the eccentricity cycles of the Earth’s orbit. Geology 23, 967–970.

Vecoli, M., Le Hérissé, A., 2004. Biostratigraphy, taxonomic diversity and patterns of morphological evolution of Ordovician acritarchs (organic-walled microphytoplankton) from the northern Gondwana margin in relation to palaeoclimatic and palaeogeographic changes. Earth-Science Reviews 67, 267–311.

Webby, B.D., Cooper, R.A., Bergström, S.M., Paris, F., 2004. Stratigraphic framework and time slices. In: Webby, B.D., Paris, F., Droser, M., Percival, I. (Eds.), The Great Ordovician Diversification Event. Columbia University Press, pp. 41–47. 496pp.

Young, G.M., Minter, W.E.L., Theron, J.N., 2004. Geochemistry and palaeogeography of Upper Ordovician glaciogenic sedimentary rocks in the Table Mountain Group, South Africa. Palaeogeography, Palaeoclimatology, Palaeoecology 214 (4), 323–345.

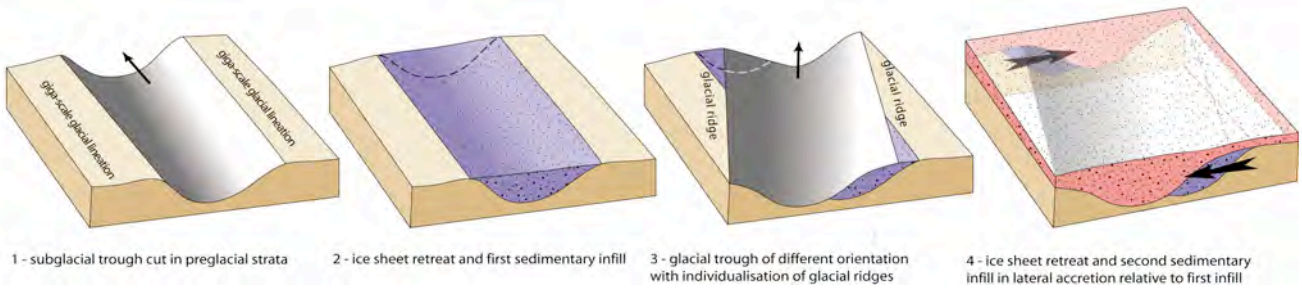

6- Stratigraphie séquentielle en contexte glaciaire

L'architecture stratigraphique des successions glaciaires est constitutée de séquences latéralement juxtaposées. On voit ici une surface d'érosion glaciaire entaillant un premier ensemble ((plutôt noir, en bas à droite) et surmonté en biseau d'aggradation par une nouvelle séquence de remplissage (couleur crème, à gauche). Le géologue au centre de l'image donne l'échelle. L'axe des incisions n'étant pas nécessairement parallèle d'une phase glaciaire à l'autre, un phénomène d'accrétion latérale à grande échelle intervient (croquis A. Bouzeghaia).

Publications associées

Ghienne J.-F. (2003) Late Ordovician sedimentary environments, glacial cycles, and post-glacial transgression in the Taoudeni Basin, West Africa. Palaeogeogr. Palaeoclimat. Palaeoecol., 189, 117-145.

Ghienne J.-F., LeHeron D., Moreau J., Denis M., Deynoux M. (2007b) The Late Ordovician glacial sedimentary system of the North Gondwana platform. In : Hambrey, M., Christoffersen, P., Glasser, N., Janssen, P., Hubbard, B. and Siegert, M. (eds.) Glacial Sedimentary Processes and Products. Special Publication n°39, International Association of Sedimentologists, Blackwells, Oxford, pp. 295-319.

➔ Voir aussi

Ghienne et al., 2003 (Chapitre 3)

Loi et al., 2010 (Chapitre 2)

A la différence des successions glaciaires néoprotérozoïques et permo-carbonifères (Eyles, 1993, 2008), l'enregistrement sédimentaire de la glaciation Ordovicien supérieur sur le domaine nord-gondwanien est préservé au sein de bassins de plate-forme intracratonique en contexte tectonique stable. Il en résulte un enregistrement stratigraphique peu épais (typiquement, 50 à 200 m) ainsi qu'une communauté de faciès et d'architecture sédimentaires reconnaissables de la Mauritanie à l'Arabie Saoudite, et de l'Espagne à la Turquie. La migration des fronts glaciaires depuis les domaines internes à subsidence faible ou nulle vers ce domaine de plate-forme peu (< 5 m/Ma) à fortement (>50 m/Ma) subsident a conditionné le style sédimentaire de l'enregistrement glaciaire Ordovicien supérieur. En dehors des zones marginales à externes, l'essentiel de l'accommodation ayant permis la préservation d'archives glaciaires (planchers glaciaires, glaciotectonique, faciès glaciomarins…) résulte d'érosions localisées (< 5 km, ex. : vallée en tunnel) à généralisées (> 100 km, ex. : fleuve de glace).

Le système sédimentaire sous contrôle glaciaire peut être appréhendé selon deux perspectives. Dans la première, on considère une pulsation glaciaire en particulier mais à l'échelle de la plate-forme nord-gondwanienne ; c'est la méthode retenue lorsque l'on étudie spécifiquement l'un ou l'autre des deux grands cycles glaciaires hirnantiens (*Ghienne et al., 2007b*). La seconde perspective consiste à caractériser pour un secteur restreint de la plate-forme la signature sédimentaire de chacun des événements glaciaires successifs, sachant que la nature de cette signature dépend au premier ordre de la distance au front glaciaire (*Ghienne, 2003* ; *Loi et al., 2010, §2*); c'est la méthode retenue lorsque que l'on étudie une succession stratigraphique dans son ensemble (ex. : l'Anti-Atlas marocain ou le Bassin de Murzuq en Libye). Croiser ces deux types d'approche permet de construire un modèle sédimentaire explicitant les architectures stratigraphiques de séquences de dépôt sous contrôle glaciaire depuis les domaines distaux (atteignant le rebord de plate-forme et jamais atteints par la glace) jusqu'aux domaines les plus internes (vers le centre du Gondwana, et englacés sur le long terme). Les contrastes de subsidence et la présence ou l'absence d'un fleuve de glace sur une zone considérée semblent être responsables des variabilités latérales observables entre différents bassins sédimentaires.

6.1. Origine de l'accommodation en contexte glaciaire

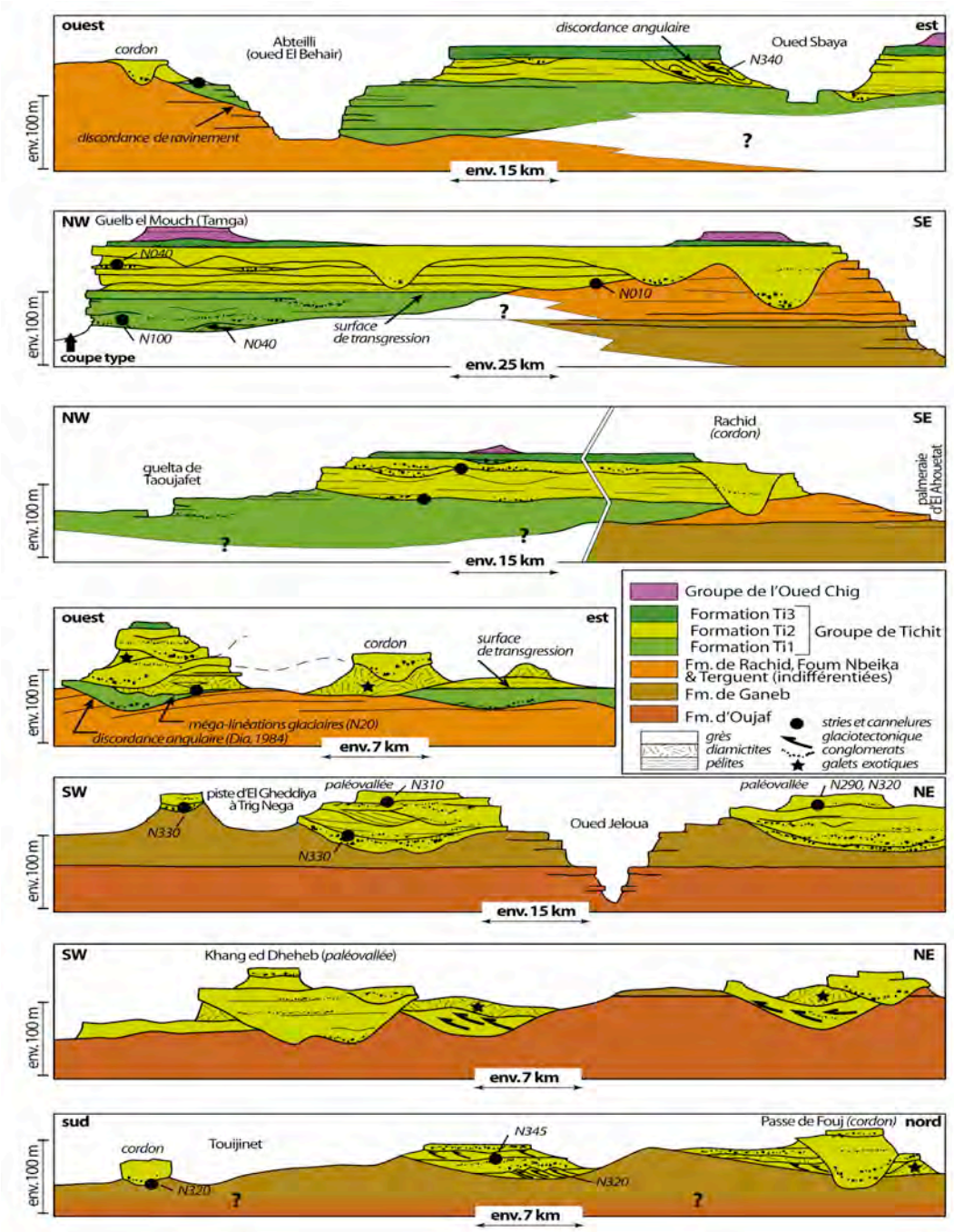

Sélection de profils géologiques illustrant l'architecture sédimentaire du Groupe de Tichit, correspondant au « glaciaire fini-ordovicien » dans le Bassin de Taoudéni en Mauritanie (les profils sont répartis de bas en haut sur environs 400 km du plus proximal, vers le SE, au plus distal, vers le NW). Les surfaces d'érosion (sous-glaciaire, fluviatile, ravinements transgressifs) sont nombreuses mais l'épaisseur du Groupe de Tichit, dépendant au premier ordre de l'importance des érosions successives, est finalement assez peu variable latéralement.

Sur un domaine de plate-forme stable, la relative brièveté des épisodes glaciaires à l'Ordovicien fait que l'enregistrement sédimentaire est au premier ordre indépendant des taux de subsidence. La préservation à long terme du message sédimentaire est permise dans ce cas particulier par l'une ou l'autre, ou la combinaison des situations suivantes : (i) comblement d'une accommodation — espace disponible pour l'accumulation des sédiments — créée antérieurement à l'épisode glaciaire ; (ii) comblement d'une dépression créée par érosion glaciaire ; (iii) accommodation dégagée pendant la transgression postglaciaire, pour peu que cette dernière ait une amplitude supérieure à la chute glacioeustatique correspondant à l'événement considéré. Au court d'une phase glaciaire, le taux de variation de l'accommodation est contrôlé essentiellement par le glacioeustatisme. Sur les domaines internes plusieurs fois englacés, la répétition des érosions glaciaires aboutit à une imbrication des dépôts de chacune des phases d'avancée/ retrait glaciaire. La cannibalisation des dépôts glaciaires est la règle sur ce domaine de plate-forme cratonique.

Le fonctionnement de fleuves de glace sur la plate-forme nord-gondwanienne est potentiellement le processus de contrôle de la localisation à grande échelle (>100 km) des zones à érosion glaciaire significatives. La présence au Quaternaire d'une topographie accentuée a favorisé la formation de fleuves de glace confinés par les reliefs, dont l'exemple type est le glacier Lambert (Bennett, 2003). En revanche, à l'Ordovicien, l'absence de topographie sur la plate-forme laisse imaginer des fleuves de glaces non confinés, avec des transition fleuve de glace/ interfluve qui peuvent avoir été assez peu marquées (O'Cofaigh et al., 2010). La distribution cartographique des fleuves de glaces à l'échelle de la plate-forme reste assez floue. Des répartitions spatiales de fleuves de glaces peu nombreux mais larges (jusqu'à 250 km ; *Ghienne et al., 2007a*) ou au contraire étroit (<100 km) mais plus nombreux ont été proposées (Le Heron et Craig, 2008). En plus de processus spécifiques d'érosion et d'écoulement glaciaire, les fleuves de glaces sont classiquement associés à la présence de dépôt-centres lorsque des cônes d'épandage volumineux soulignent leur front, ou au contraire à la présence de dépression restées sous-remplies et qui seront les lieux privilégiés du dépôts et de la préservation de faciès riches en matière organique (cf. section 3.4).

6.2. Modèles de séquences glaciaires

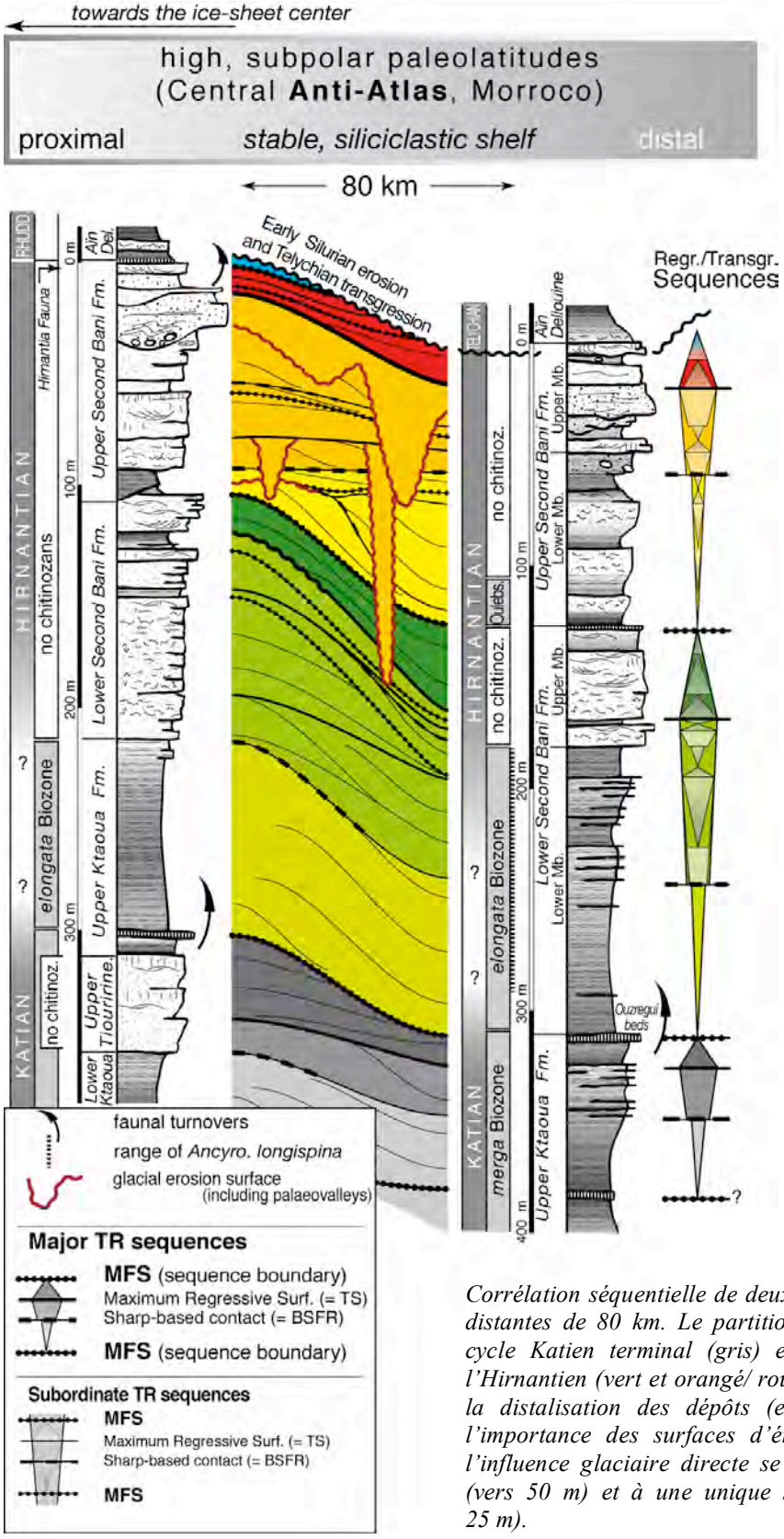

Corrélation séquentielle de deux coupes de l'Anti-Atlas marocain distantes de 80 km. Le partitionnement des dépôts au cours du cycle Katien terminal (gris) et des deux cycles glaciaires de l'Hirnantien (vert et orangé/ rouge) est bien visible, de même que la distalisation des dépôts (environnement, granulométrie) et l'importance des surfaces d'érosion. Sur la coupe de droite, l'influence glaciaire directe se limite à un horizon glaciomarin (vers 50 m) et à une unique surface d'érosion glaciaire (vers 25 m).

La subdivision d'une succession sédimentaire en séquences de dépôt permet une approche chronologique du message sédimentaire, par la corrélation à grande échelle de marqueurs stratigraphiques telles que des surfaces ou des géométries traduisant les interactions entre apports sédimentaires et accommodation. Une séquence de dépôt est correctement caractérisée dès lors que les relations génétiques entre faciès et architectures stratigraphiques sont établies. La stratigraphie séquentielle s'est typiquement attachée à caractériser des séquences de dépôts contrôlées par les variations de niveau marin relatif, considérant, pour simplifier, constants d'autre paramètres tels que les taux d'apport sédimentaire, les régimes hydrodyamiques… (Posamentier et Vail, 1988 ; Zecchin, 2007 ; Catuneanu et al., 2009 ; Embry, 2009). Peu de modèles ont été proposés pour des séquences à contrôle glaciaire (par exemple, Proust et Deynoux, 1993, Dunbar et al., 2008 ; Fielding et al., 2008). Deux paramètres ne peuvent plus être considérés comme secondaires dans un système glaciaire: d'une part la variation des apports sédimentaires, en quantité et en localisation des sources avec la migration des points d'injection sur des distances de 500 à 2000 km (Brookfield et Martini, 1999 ; Powell et Cooper, 2002), d'autre part le découplage de l'accommodation vis-à-vis des seules variations de niveau marin relatif par suite de la géométrie accusée des surfaces d'érosion glaciaire à l'origine de topographie antécédentes. En effet, la présence d'un glacier impose à la plate-forme des niveaux de base au comportement inédit : érosions de profondeurs hectométriques bien en-dessous des niveaux de base non- ou inter-glaciaires ; ou encore capacité d'aggradation fluviale bien au-dessus de ces mêmes niveaux, en particulier pendant des périodes de chutes de niveau marin correspondant à des avancées glaciaires. Le niveau de base sous contrôle glaciaire est donc relativement indépendant du niveau de base couplé aux variations glacioeustatiques, ce dernier restant prédominant dans les domaines sédimentaires côtiers de la plate-forme distale isolés des fronts glaciaires.

En contexte glaciaire, il est à priori logique d'imaginer que la surface d'émersion des modèles standard est, selon les cas, remplacée (front glaciaire glaciomarin) ou prolongée (front continental) vers le continent par la surface d'érosion glaciaire. Un modèle de séquence glaciaire a été proposé (*Ghienne, 2003*) qui considère qu'en domaine proximal les dépôts encadrés par deux surfaces glaciaires représentent essentiellement des faciès de retrait glaciaire suivi de faciès fluvio-deltaïques en progradation dans un contexte de haut niveau marin interglaciaire (voir aussi Dunbard et al., 2008). Le maximum d'avancée glaciaire correspond à la surface d'érosion glaciaire, remaniant les éventuels dépôts contemporains de la phase d'avancée glaciaire et créant une accommodation initiale. Ce modèle a par la suite était complété, en considérant deux types de dynamique glaciaire à l'origine de la surface d'érosion basale (*Ghienne et al., 2007b*). Dans les zones de fleuves de glace, les processus érosifs sont significatifs mais, en parallèle, les taux de sédimentation au front du glacier sont amplifiés. L'avancée glaciaire produit la surface érosive de base de la séquence glaciaire tandis que s'édifient au front du fleuve de glace des cônes d'épandage glaciomarins ou turbiditiques. Le retrait glaciaire en domaine glaciomarin est rapide, voire catastrophique, par suite de l'instabilité intrinsèque de ce système dans lequel la base du glacier se situe sous le niveau de la mer. La surface d'érosion glaciaire — ou surface de retrait glaciaire de Powell et Cooper, 2002 — s'amalgame alors avec une surface transgressive, comme proposé par Dunbar et al. (2008) sur la plate-forme antarctique à l'Oligocène. Les périodes de stabilisation du front sont associées à l'édification de grands systèmes fluvio-deltaïques dont les accumulations résultantes peuvent atteindre la centaine de mètres (cf. section 4.3). En revanche, hors des fleuves de glaces, le retrait s'effectue de manière plus échelonnée, en domaine continental, et avec des faciès à dominante fluvioglaciaire. Des progradations deltaïques de faible envergure interviennent pendant les interglaciaires. Avec les avancées/ retraits glaciaires successifs, ce modèle aboutit à une architecture dans laquelle les séquences glaciaires apparaissent en partie verticalement superposée mais surtout latéralement juxtaposée, et spécialement dans les zones

de fleuve de glaces caractérisées par des surfaces d'érosion glaciaires présentant des linéations glaciaires plurikilométriques.

Ce schéma est dorénavant remis en question. En effet, l'analyse de détail de l'architecture interne d'une séquence glaciaire (thèse F. Girard, en cours) montre qu'en fait les grandes progradations fluvio-deltaïques pourraient plutôt caractériser les périodes d'avancée glaciaire et seraient ainsi synchrones des phases d'érosion glaciaire dans les domaines plus internes. Les faciès de retrait n'occuperaient qu'un volume limité correspondant à des cônes juxtaglaciaires peu développés voire absent et le plus souvent remaniés par l'avancée suivante ou les processus transgressifs. On aboutit alors à une inversion complète de la logique séquentielle, en considérant que l'essentiel d'une séquence glaciaire est assimilable à un cortège de bas niveau (relativement tardif), plutôt qu'à un cortège de haut niveau.

Cette attribution en termes de cortège de dépôt des séquences glaciaires prend tout son sens lorsque l'on tente une corrélation entre un domaine interne englacé et un domaine externe libre de glace enregistrant essentiellement un signal glacioeustatique. Les faciès distaux, typiquement les dépôts dominés par des processus de tempêtes, sont alors contemporains de la phase d'avancée glaciaire. Les faciès les plus régressifs sont synchrones des systèmes fluvio-glaciaires qui se mettent en place en fin de période de chute de niveau marin. La période de maximum glaciaire est peu différentiée dans le domaine distal si ce dernier n'est pas atteint par les fronts glaciaires. Sur la plate-forme externe et dans les secteurs à fronts glaciaires marins, les faciès glaciomarins distaux représentent le début de la déglaciation qui est marqué par la déstabilisation des fronts glaciaires (Katz et Worster, 2010) et une forte production d'icebergs (Eyles et McCabe, 1989 ; Siegert et Dowdeswell, 2004). Une aggradation tidale intervient en parallèle dans les domaines intermédiaires alimentés par des systèmes fluvio-glaciaires connectés à des fronts glaciaires continentaux en récession. Enfin, une condensation sédimentaire prend le relais, pendant la phase finale de déglaciation et l'interglaciaire, déportant un éventuel cortège de haut niveau vers les domaines les plus internes, où la probabilité de préservation est faible. Dans ce nouveau schéma, une séquence glaciaire comble une accommodation initiale antécédente laissée libre par le retrait de l'épisode glaciaire antérieur, alors que dans le premier schéma, elle comblait l'accommodation résultant de l'érosion glaciaire de l'épisode correspondant. De plus, par suite des aggradations fluvio-glaciaires forcées par les apports sédimentaires, la surface d'émersion des domaines externes peut ne plus être connectée physiquement à la surface glaciaire qui prend la signification d'une surface de maximum de régression (ou surface de transgression).

Une séquence glaciaire devient un volume de sédiment représentant un cycle complet d'avancée/ retrait glaciaire. Elle se connecte vers le bassin sur une séquence de type génétique délimitée par les surfaces d'inondation maximale correspondant aux épisodes interglaciaires qui l'encadrent. Dans les domaines internes où l'érosion glaciaire se sera surimposée à la surface d'inondation maximale, c'est la surface glaciaire qui prend valeur de limite de séquence.

ELSEVIER

Palaeogeography, Palaeoclimatology, Palaeoecology 189 (2003) 117–145

PALAEO

www.elsevier.com/locate/palaeo

Late Ordovician sedimentary environments, glacial cycles, and post-glacial transgression in the Taoudeni Basin, West Africa

Jean-François Ghienne

Ecole et Observatoire des Sciences de la Terre, Centre de Géochimie de la Surface (CNRS – Université Louis Pasteur), 1 rue Blessig, 67084 Strasbourg, France

Received 5 April 2002; received in revised form 25 September 2002; accepted 25 October 2002

Abstract

The sedimentary record and worldwide palaeontological and isotopic data support the existence of short-lived, latest Ordovician (Hirnantian) ice sheets over western Gondwanaland. Located in the cratonic Taoudeni Basin (West Africa), the study areas are distributed across a 500-km-long profile ranging from ice-proximal to ice-distal depositional conditions (Hodh and Adrar areas, respectively; central and northwestern Mauritania). Glaciation-related but mainly non-glacial deposits form the Tichitt Group, which rests upon Cambrian–Ordovician rocks on top of a basin-wide erosional surface. The glacial record consists of depositional successions bound by unconformities of glacial origin in ice-proximal areas, or of sub-aerial origin in ice-distal areas. Facies associations reflect a variety of environments (braided streams, flood-dominated alluvial plains, delta plain to delta slope, tidal or storm-wave influenced shallow-marine settings). The upper bounding surface of the Tichitt Group generally corresponds to a wave–ravinement surface, overlain by uppermost Ordovician to lower Silurian shales. Four, inter-regionally distributed units are vertically superimposed and laterally juxtaposed. A unit is a hundreds of kilometres long sedimentary body, up to 100 m thick, which is laterally discontinuous as it typically infills palaeodepressions or palaeovalleys. In ice-proximal areas, aggrading fluvial deposits are identified. Coarse-grained braided stream deposits, including glacial surfaces related to minor glacial advances, predominate upstream. Downstream, finer-grained flood-dominated fluvial deposits are identified. In ice-distal areas, thick fluvial-dominated delta sediments are deposited. Each of the four units, of climatic significance, and built under high accommodation conditions, records a recession stage of the northern Gondwana ice sheet following a major glacial advance. The overall backstepping of the glacial units characterises the large-scale depositional architecture. The fourth unit, characterised by glaciomarine deposits in ice-proximal areas, and non-glacial, bioturbated storm-dominated deposits in ice-distal areas, records the final retreat of the northern Gondwana ice sheet. The lower bounding surface of this later glacial unit marks a Late Hirnantian major transgressive surface of a Late Ordovician–Silurian relative sea-level rise starting before the glaciation.

Keywords: glaciation; Ordovician; Silurian; West Africa; Gondwana; Mauritania

1. Introduction;

Sedimentary records from pre-Pleistocene glaciations are dominated by glaciomarine deposits

E-mail address: ghienne@illite.u-strasbg.fr (J.-F. Ghienne).

0031-0182/02/$ – see front matter © 2002 Elsevier Science B.V. All rights reserved.
PII: S0031-0182(02)00635-1

(94% according to Eyles, 1993), mainly identified in rapidly subsiding foreland and rift settings with thin deposits preserved in continental shelf areas (Nystuen, 1985; Bjørlykke, 1985; Eyles, 1993). In contrast, the glacial upper Ordovician sediments throughout northern Gondwanaland are preserved over a slowly subsiding cratonic platform and are dominated by glaciofluvial to fluvial-dominated deltaic facies. To date, emphasis in published works dealing with the Late Ordovician glaciation has been on biostratigraphy (e.g. Paris et al., 1995a) and stratigraphic relationships with pre- and post-glacial deposits, large-scale sedimentary architecture, and glaciogenic features such as palaeovalleys, diamictite facies, glacio–tectonic deformation structures, glaciated pavements and various palaeo-ice-flow indicators (e.g. Beuf et al., 1971; Deynoux, 1980, 1985; Vaslet, 1990; Crowell, 1999). However, much less work has been undertaken on the non-glacial but glaciation-related deposits that form the bulk of the sedimentary record of the Late Ordovician glaciation in northern Gondwanaland.

During the Ordovician, western Gondwanaland (Africa and South America) was located in southern high latitudes whereas its eastern part (Antarctica, Australia and India) was in tropical to equatorial latitudes. Palaeomagnetic evidence indicates that what is now West Africa was located over the South Pole (Kent and Van Der Voo, 1990; Bachtadse and Briden, 1990; Smith, 1997), in agreement with palaeo-environmental reconstructions (Scotese and Barett, 1990; Fig. 1). Since the discovery of the Late Ordovician glaciation (Sougy and Lécorché, 1963), correlative ice-proximal deposits have been reported mainly from Mauritania (Deynoux et al., 1985), Morocco (Destombes et al., 1985; Ouanaimi, 1998), Algeria and Niger (Beuf et al., 1971; Biju-Duval et al., 1981; Legrand, 1985), Libya (Massa, 1988; McDougall and Martin, 2000), Jordan (Abed et al., 1993), Saudi Arabia (Vaslet, 1990; McGillivray and Husseini, 1992), South Africa (Hiller, 1992) and South America (Caputo, 1998). Some possible tillites have been identified in Argentina (Martinez, 1998). These studies suggest extensive

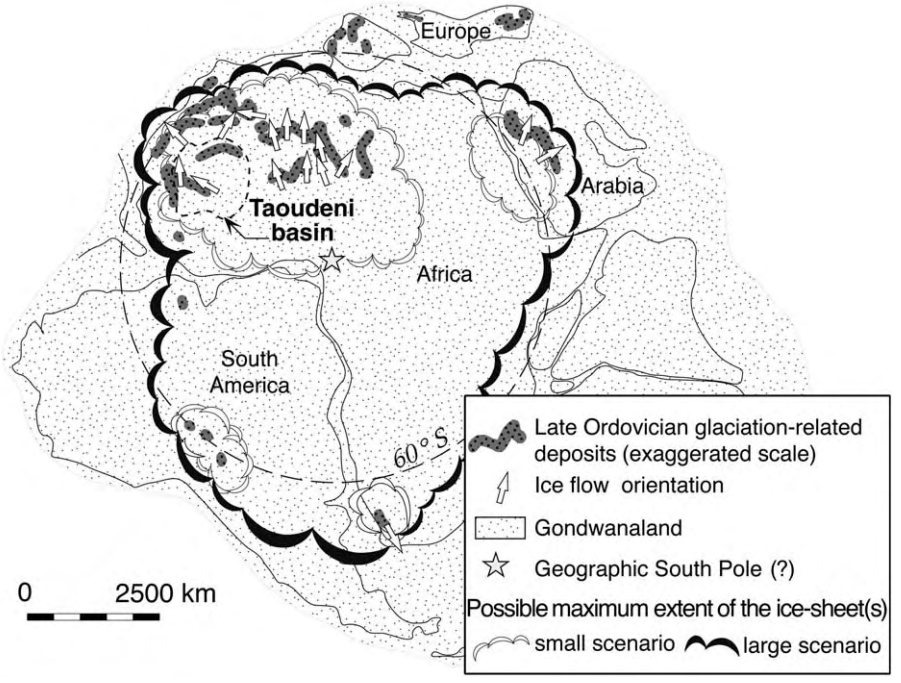

Fig. 1. Palaeogeographic reconstructions showing ice extent during the Late Ordovician glaciation. Ice-flow directions are from Deynoux (1980), Beuf et al. (1971) and Vaslet (1990), respectively for Mauritania, Algeria and Arabia.

glaciers over western Gondwanaland. This is confirmed by widespread ice-distal glaciomarine deposits in lower palaeolatitudes (Robardet and Doré, 1988; Brenchley et al., 1991), as well as by a high-amplitude global regressive–transgressive event (Brenchley, 1988; Finney et al., 1999). A significant positive stable carbon and oxygen isotope excursion is also recorded (Brenchley et al., 1994; Wang et al., 1997; Underwood et al., 1997), whilst basinal deposits provide evidence for the turnover of the oceanic thermohaline patterns (Armstrong and Coe, 1997).

Palaeogeographic reconstructions of the Late Ordovician glacial period typically show an ice sheet centre located near central Africa (Beuf et al., 1971; Deynoux, 1980; Vaslet, 1990) with a peripheral extension of the ice front remaining poorly known (Fig. 1). The timing of the glaciation is still a matter of debate (Hambrey, 1985). However, several studies suggest that glacial sedimentation in northern Gondwanaland was restricted to the Hirnantian (latest Ordovician), in agreement with palaeontological data from ice-distal sedimentary successions (Storch, 1990; Brenchley et al., 1991; Leone et al., 1995; Zhang et al., 2000; Sutcliffe et al., 2000). Non-glacial conditions existed during the lower part of the Ashgill (Destombes et al., 1985; Legrand, 1993; Ghienne et al., 2002), and, in agreement with the work of Deynoux (1980), biostratigraphers have demonstrated that the main ice sheet(s) disappeared during the Late Hirnantian (*persculptus* graptolite zone: Paris et al., 1995a,b, 2000; Underwood et al., 1998), as in South Africa (e.g. Hiller, 1992). Nevertheless, other subsequent Early Silurian glacial events have been recorded when South America drifted over the South Pole (Caputo and Crowell, 1985; Grahn and Paris, 1992; Crowell, 1999).

The aim of the present paper is to reassess the Late Ordovician glacial record, highlighting the significance of the non-glacial deposits. The latter, which comprise facies associations related to a spectrum of environments ranging from continental to shallow-marine, shed new light on the significance and timing of the upper Ordovician glacial drift, which records ice recessions and late- to post-glacial environmental changes rather than full glacial conditions. This paper, based on fieldwork in Mauritania, includes an overview of the Late Ordovician glacial record preserved within the Taoudeni Basin (West Africa). Four unconformity-bound depositional successions, which are correlated along a 500-km-long profile ranging from ice-proximal to more ice-distal areas, are interpreted as four glacial units of climatic origin. Relationships between the Late Ordovician glaciation and the so-called post-glacial Silurian transgression are then discussed.

2. The Late Ordovician glacial record in the Taoudeni Basin

2.1. Geological setting

The investigated upper Ordovician sediments are located in the Taoudeni Basin, which makes up the 2–4 km thick sedimentary cover of the West African Craton (Fig. 2). Since the Cambrian, the northern Gondwana platform, which extended from South America to the Middle East including the Taoudeni Basin, was characterised by continental to shallow-marine clastic sediments, without any significant facies change over long distances. Four supergroups, which are separated by basin-wide slightly angular disconformities, have been identified throughout the Taoudeni Basin (Trompette, 1973; Deynoux et al., 1985; Bertand-Sarfati et al., 1990). From bottom to top, they are: (1) Neoproterozoic siliciclastics and stromatolite-bearing carbonates (1000–1500 m thick); (2) thin glacial deposits of the lowermost Cambrian, overlain by thick Cambrian–Ordovician sandstones and shales (up to 1000 m thick); (3) upper Ordovician glacial deposits (0–200 m thick), here referred to as the Tichitt Group (Deynoux and Trompette, 1981), and overlying latest Ordovician–Silurian shales (generally less than 100 m thick); (4) Devonian–Carboniferous siliciclastics and carbonates (up to 300 m thick) (Fig. 2). The present-day basinal structure is a result of a combination of a variety of Phanerozoic deformation events and does not reflect the depositional basin that developed during Cambrian–Ordovician times.

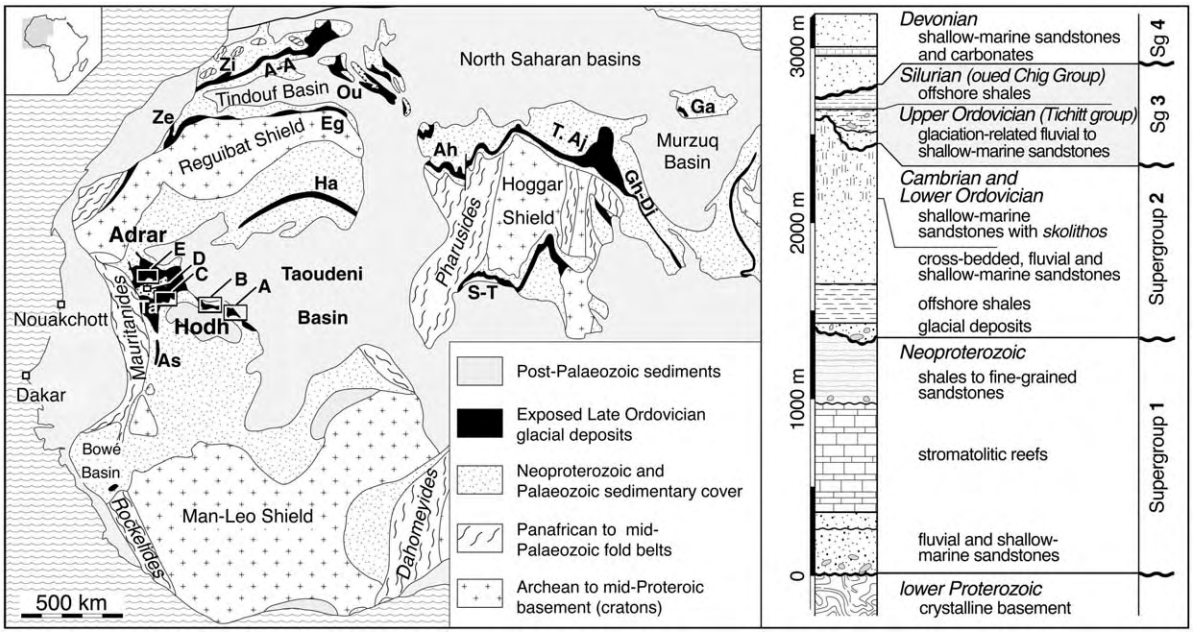

Fig. 2. General lithostratigraphic column (Adrar, modified from Trompette, 1973) and geological sketch map of West Africa with the distribution of the upper Ordovician glacial deposits (modified from Deynoux, 1980). The eastern (A) and western (B) Hodh, and central (E) Adrar are the main studied areas. Additional field work has been carried out in the Tagant area (C) and in the Southern Adrar (D). Abbreviations of names of other areas: A-A, Anti-Atlas, Morocco; Ah, Ahnet, Algeria; As, Assaba, Mauritania; Eg, Eglab, Algeria; Ga, Gargaf, Libya; Gh–Dj, Ghat–Djado area, Algeria, Libya and Niger; Ha, Hank, Mauritania; Ou, Ougarta, Algeria; S-T, southern Tassili, Algeria and Niger; T. Aj, Ajjers Tassili, Algeria; Ze, Zemmour, Mauritania and Western Sahara; Zi, Zini, Morocco.

2.2. Depositional features

In the Taoudeni Basin, upper Ordovician strata have been interpreted mainly on the basis of their deeply erosional lower bounding surface, their relatively coarse-grained character, with occasional glaciogenic features, and their stratigraphic position underlying Silurian successions. The interpretation of primary sedimentary structures in terms of depositional environments indicates that several glaciation-related facies associations representing shallow-marine to glaciofluvial environments are preserved in the Taoudeni Basin (Table 1). upper Ordovician deposits are characterised by: (1) the presence of numerous erosional surfaces of various scale, e.g. tidal channels, eskers, anastomosing distributary channels, tunnel valleys, subglacial erosion surfaces, sub-aerial unconformities; (2) the sand-dominated character of the deposits; (3) very rapid lateral changes in facies and thickness at outcrop scale; (4) high-energy fluvial deposits showing abundant signs of upper flow regime conditions; and (5) a high rate of sedimentation as indicated by very common climbing ripples and megaripples, abundant slide- or slump-induced deformation structures and conspicuous liquefaction and fluidisation structures (Ghienne, 1998).

In the cratonic, slowly subsiding setting, the space available for the preservation of the sediments of successive glacial cycles was most probably limited. Thus, a single, vertical, detailed sedimentary log is incomplete because significant hiatuses are likely to occur as the result of deep and irregular erosion surfaces and the subsequent entire or partial reworking of one or several depositional units. Moreover, above an erosion surface, the subsequent depositional onlap geometry leads to a longer hiatus in the highest areas. Therefore, only synthetic logs are shown in this

Table 1
Glaciation-related associations of depositional environments

Main lithologies	Large-scale depositional features	Sedimentary structures	Interpreted depositional processes	Association of depositional environments
	Infilling in large depressions			(1) *glaciofluvial*
coarse-grained to conglomeratic sandstones	several kilometres wide, 5–20 m thick sandstone sheet, pinching out laterally and limited by erosional bounding surfaces (Fig. 5b,c), mainly of glacial origin (Fig. 6c)	mostly trough and planar, 0.1–5 m high, cross-laminated bed sets (Fig. 6a); structureless sandstones; low-angle lamination with parting lineation; unidirectional palaeocurrents at the kilometre scale, mainly westwards; abundant synsedimentary deformation: overturned cross-strata, sheet-dewatering structures, extensional step-fractures (Fig. 5); basement-derived clasts may still display glacial striae	mainly lower flow regime conditions, in-channel aggradation of migrating small to giant dunes and low-lying submergent sand flat accretion, within deep, perennial, sand-bed braided streams in an outwash plain	(a) braided streams
sand-rich, clast-poor diamictites, subordinate sandstones	5–20 km wide, 5–40 m thick lenses, interfingering with braided stream deposits (association 1a)	faint lamination with 5–40° dips, parallel to the preferred orientation of granules and gravels; clasts from granules (mostly quartz) to cobbles (mostly metamorphic rocks and granites, generally striated); sandstone lenses; some 5–50 cm thick, vertically laminated, randomly oriented sandstone dykes cutting through diamictites	debris flows initiated by the destabilisation and mixing of fluvial and subglacial deposits; subordinate waterlaid deposits	(b) proglacial debris flows
medium- to coarse-grained sandstones	regionally extensive, erosionally-based, fining-upwards sheets or large-scale, flat-bottomed channels (0.3–1 km wide, 50–100 m thick, 2–20 km long), incised in glaciofluvial deposits	several-metres-thick, fining-upwards, low-angle to trough cross-laminated sequences with parting lineation, mud clasts and synsedimentary deformation (mainly folding within channel form and dewatering); common subcritically to critically, climbing, 0.1–1.5 m high, sinuous-crested megaripples (Fig. 6d)	concentrated, decelerating, stream- or sheet-flow deposits; climbing mega-ripples imply high velocity and coarse sand as suspended load; channel incision by sediment-deficient meltwaters	(2) *outburst-dominated outwash plain*
	overall coarsening-up sediment pile			(3) *glaciomarine shallow shelf*
shales with lonestones, conglomerates	discontinuous soft outcrops above a regionally extensive erosional glacial surface	reddish shales succession including striated clasts (1–100 cm in diameter; quartzite, granite, greenstone; Fig. 6e), massive or cross-laminated conglomeratic beds, slump structures, small-scale channels	proglacial gravity-flow and channel deposits, iceberg-derived dropstones	(a) ice-contact subaquatic fans
sand-rich, clast-poor diamictites	regionally extensive sheet (up to 200 km across) (Fig. 8)	massive, green to reddish deposits; crude foliation emphasised by coloured joints; 'onion splitting'; some striated cobbles	deposition dominated by melting sea-ice floes or icebergs, and winnowing of fines by weak currents	(b) glaciomarine shelf

Table 1 (*Continued*).

Main lithologies	Large-scale depositional features	Sedimentary structures	Interpreted depositional processes	Association of depositional environments
well-sorted sandstones	well-stratified, laterally extensive, 5–30 m thick sandstone sheet, truncating underlying glaciomarine deposits (Fig. 8)	sharp-based beds, with occasional furrows, low-angle, hummocky and trough cross-lamination; straight-crested or polygonal ripples; loading and dewatering structures; rarely isolated striated cobbles and soft-sediment scour marks (Fig. 6f)	storm- and waves processes, reworking previously deposited glaciomarine sediments; scours and transport of lonestones by floating ice	(c) wave-dominated nearshore
	onlap onto glacially-related deposits			(4) *siliciclastic shelf*
sandy shales and some diamictites	extensive, fining-upwards, several-metres-thick, soft talus	massive to weakly stratified sandy shales with rare striated lonestones; diamictites form structureless, discontinuous, thin beds	deposition below the storm wave-base; some occasional fall-out events from floating ice	(a) distal glaciomarine shelf
shales and muddy fine-grained sandstones	regionally extensive soft talus, transitionally overlying distal glaciomarine deposits; sharp-based, 0.1–2 m thick sandstone beds (Fig. 8)	finely laminated grey shales, bearing abundant fauna (graptolites, chitinozoa); intense bioturbation and mottling in thinly bedded ferruginous sandstones, containing phosphatic and chloritic ooids	transgressive–regressive cycles in offshore to shoreface deposits	(b) post-glacial shelf
medium-grained sandstones	tabular beds, or laterally amalgamated, up to 100 m wide, 5–15 m thick, erosionnally-based bodies (Fig. 10b); lowermost part of palaeovalleys (Fig. 9)	lateral accretion surfaces and vertical sequences with low-angle, cross- and ripple-lamination; 0.5–2 m high, cross-laminated beds with inverted bottomset ripples; 10–50 cm thick beds with ripple-lamination (rib-and-furrow pattern, rythmically aggrading to climbing ripples)	lower to upper flow regime conditions in tidal sand flats with occasionally migrating, possibly meandering channels and tidal sand waves	(5) *tidal flats*
medium-grained sandstones	vertically stacked, 5–20 m thick, laterally extensive sandstone sheets (Fig. 10b); lower part of palaeovalleys	mostly sheet-like beds, thin horizontal lamination with parting lineation; gutter casts, climbing ripples, rare graded beds, small-scale channels (Fig. 10c) filled by low-angle lamination or climbing megaripples	upper flow regime conditions in wide, shallow, flat-bottomed, low-sinusoity channel; occasionally concentrated to hyperconcentrated streamflow	(6) *flood-dominated fluvial*
	coarsening-up successions, in the upper part of palaeovalleys (Fig. 9)			(7) *fluvial-dominated delta*
micaceous siltstones to sandstones	coarsening-up soft outcrops	massive or thinly laminated, incipient ripple cross-bedding, disoriented mica flakes; intercalated sandstone beds, 1–50 cm thick, with flutes, structureless or with low-angle lamination; slump fold (0.1–2 m)	delta-fed low- to high-density currents	(a) prodelta to delta front

Table 1 (*Continued*).

Main lithologies	Large-scale depositional features	Sedimentary structures	Interpreted depositional processes	Association of depositional environments
fine to medium, micaceous, and/or silty sandstones	well-stratified, laterally-extensive, 5–30 m thick sheets	ripple or small megaripple cross-laminated beds with sinuous to straight crests preserved on bed tops, wave ripples locally superimposed in trough (Fig. 10d); very abundant critically climbing ripples; rare bundles of sigmoidal laminae with ripples on reactivation surfaces, small-scale channels filled by well-sorted low-angle to cross-laminated sandstones, with opposing palaeocurrent directions	deceleration in shallow friction-dominated river mouth of sediment-laden, mixed-load streams, with high rates of deposition and with subordinate sediment dispersal by waves and tides	(b) delta front to distal delta plain, tidal influence
medium- to coarse-grained sandstones	monotonous, 20–100 m thick successions, including well-defined several kilometres long, 0.1–0.5 km wide, 30–70 m thick, fining-upwards channels	sheet-like beds, thin horizontal lamination with parting lineation; within channels, superimposed erosion-based, few-metres-thick, fining-upwards sequences of low-angle to cross-laminated sandstones	upper flow regime conditions in sand- and flood-dominated overbank environments, between sinuous, distributary, anastomosing channels	(c) proximal delta plain
fine- to coarse-grained sandstones	a single regionally-extensive, 10–25 m thick, erosion-based, fining-up sheet, truncating underlying glacial deposits or Cambrian–Ordovician palaeorelief forms	trough cross-stratified sandstone beds, with occasional burrows, symmetrical megaripples (Fig. 10e) on bed tops; erosionally-based, low-angle to trough cross-laminated sandstones, with parting lineation, and gravel as lags or clustered in cut-and-fill structures; in the upper levels, abundant wave ripples	coarse-grained storm deposition and fair-weather reworking and burrowing; migrating rip channel/longshore bar systems on a non-barred, high-energy shoreline	(8) *wave- to storm-dominated coast*

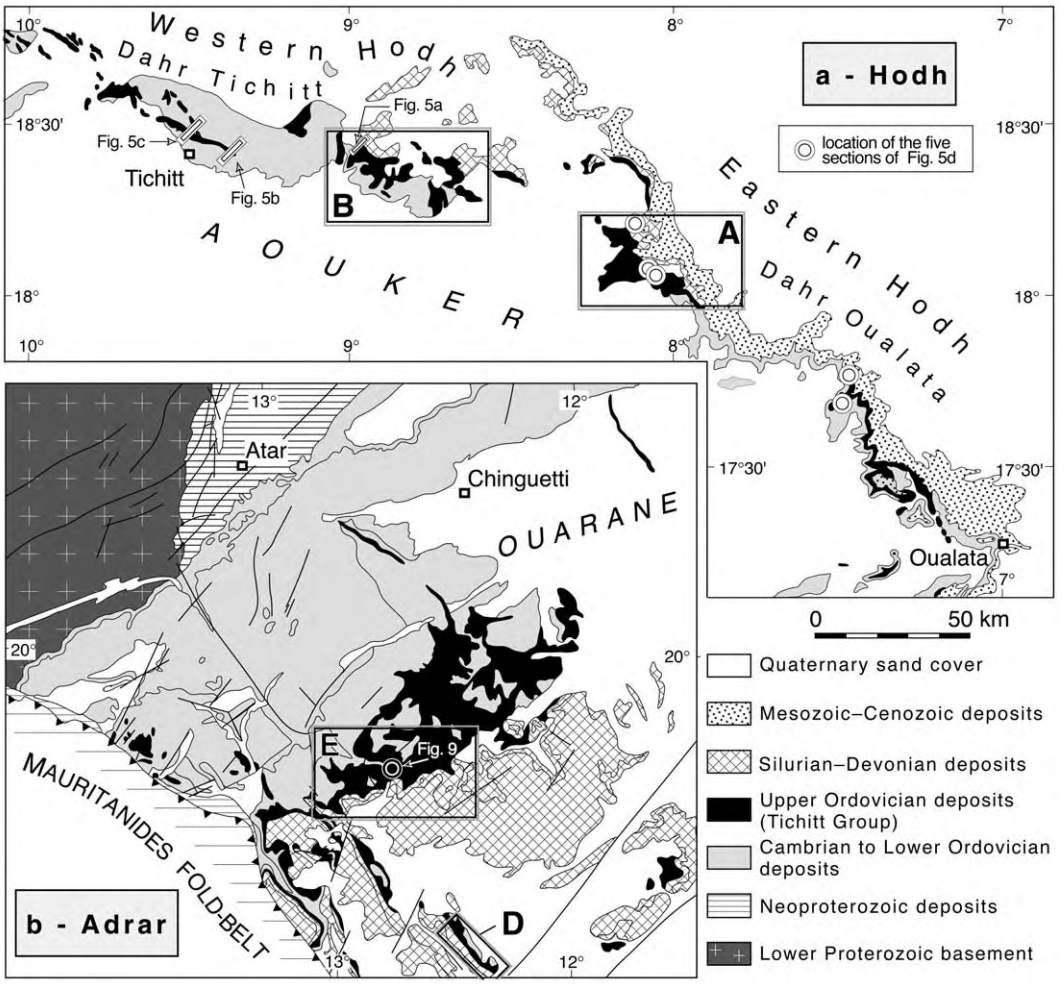

Fig. 3. Geological sketch map of (a) the Hodh (modified from Deynoux, 1980) and (b) the Adrar (modified from Trompette, 1973). Rectangles and letters refer to the areas for which a synthetic section is given in Fig. 4.

paper. They provide an overall picture of the sedimentary succession and sequence of events characterising a large area.

2.3. Study areas

Upper Ordovician deposits are particularly well-exposed in the Adrar, Tagant and Hodh areas, which are located in northwestern, western, and southeastern Mauritania, respectively (Figs. 2 and 3). In the palaeogeographic reconstruction of Deynoux (1980, 1985), the Hodh, and particularly its eastern part, appears more ice-proximal than the Adrar and Tagant, with respect to an ice sheet centre located in central Africa (Figs. 1 and 2). Outcrop data of these three vast and well outcropping areas are described below. Five synthetic sedimentary logs are illustrated, corresponding to the eastern Hodh, western Hodh, Tagant, southern Adrar and central Adrar (Fig. 4). These five selected areas are roughly aligned along a profile perpendicular to the inferred ice front.

Upper Ordovician glaciation-related deposits are also exposed in the Hank (Marchand et al., 1972), and in the Assaba (LePage, 1986) (Fig. 2). Here, they comprise fine- to coarse-grained, cross-

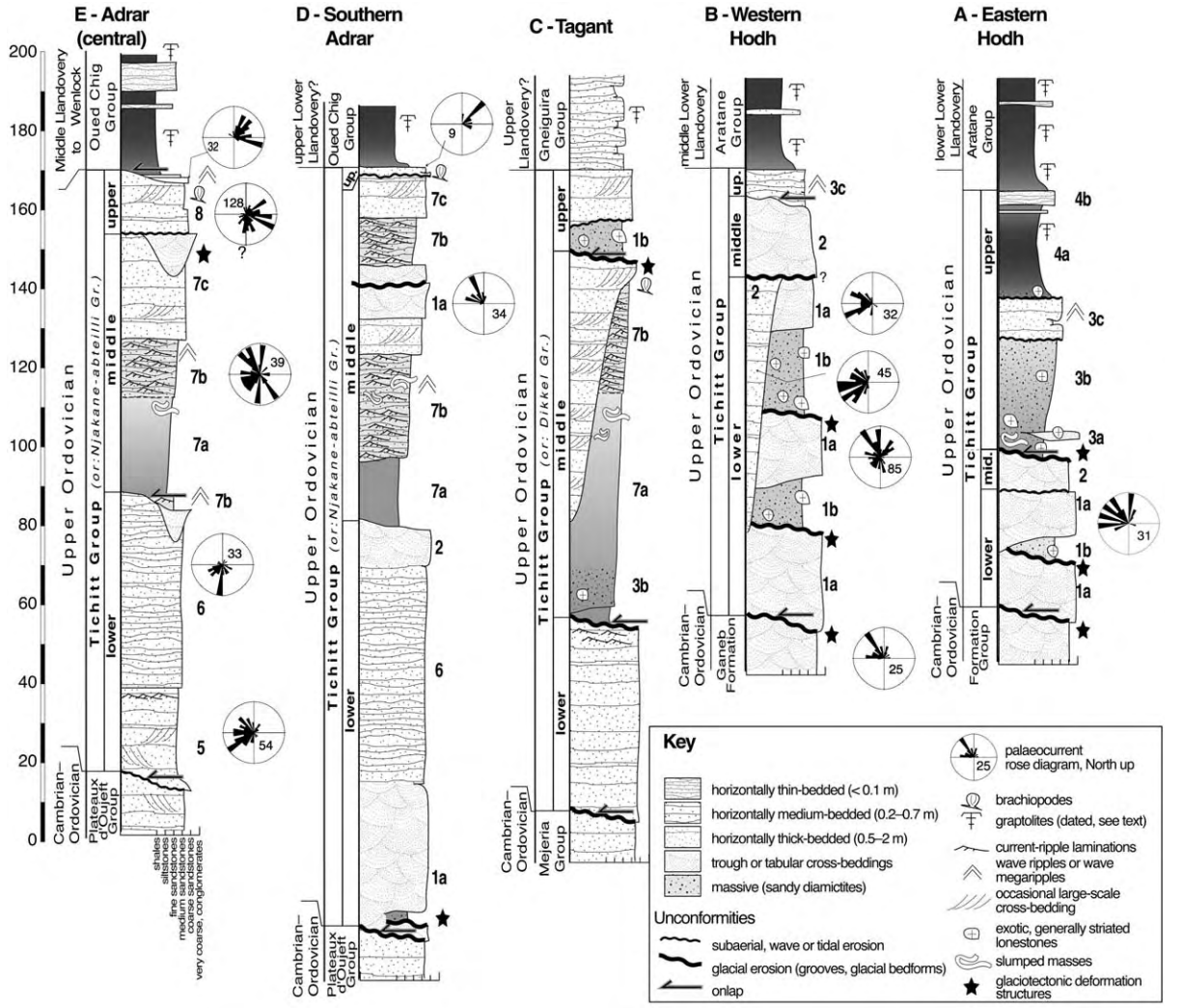

Fig. 4. Synthetic glacial record for five selected areas. Section (C) is modified from Dia (1984). Stratigraphic ages in (A) from Underwood et al. (1998) and Paris et al. (1998), in (B) from Deynoux (1980) and Willefert (1988), in (C) from Dia (1984), in (D) and (E) from Trompette (1973) and Willefert (1988). Numbers refer to facies associations defined in the Hodh and central Adrar (see Table 1). Deposits in the Tagant (C) and southern Adrar (D) display facies associations present in both the Hodh and central Adrar. Vertical scale is only an approximation.

laminated sandstones of probable fluvial origin with dips of laminae indicating palaeocurrents oriented toward the NW and NNE. Outcrops of the two latter areas were not revisited for this study.

2.4. The glacial record in the Hodh

Deynoux (1980, 1985; Deynoux et al., 1985) presented lithostratigaphic logs for the upper Ordovician deposits and underlying or overlying rocks, studied the large-scale depositional architecture and gave evidence for glacial deformation structures in the Hodh area. Only the most instructive glacial deformation structures will be briefly reported in the present paper.

In the Hodh, three depositional successions (lower, middle and upper) have been characterised

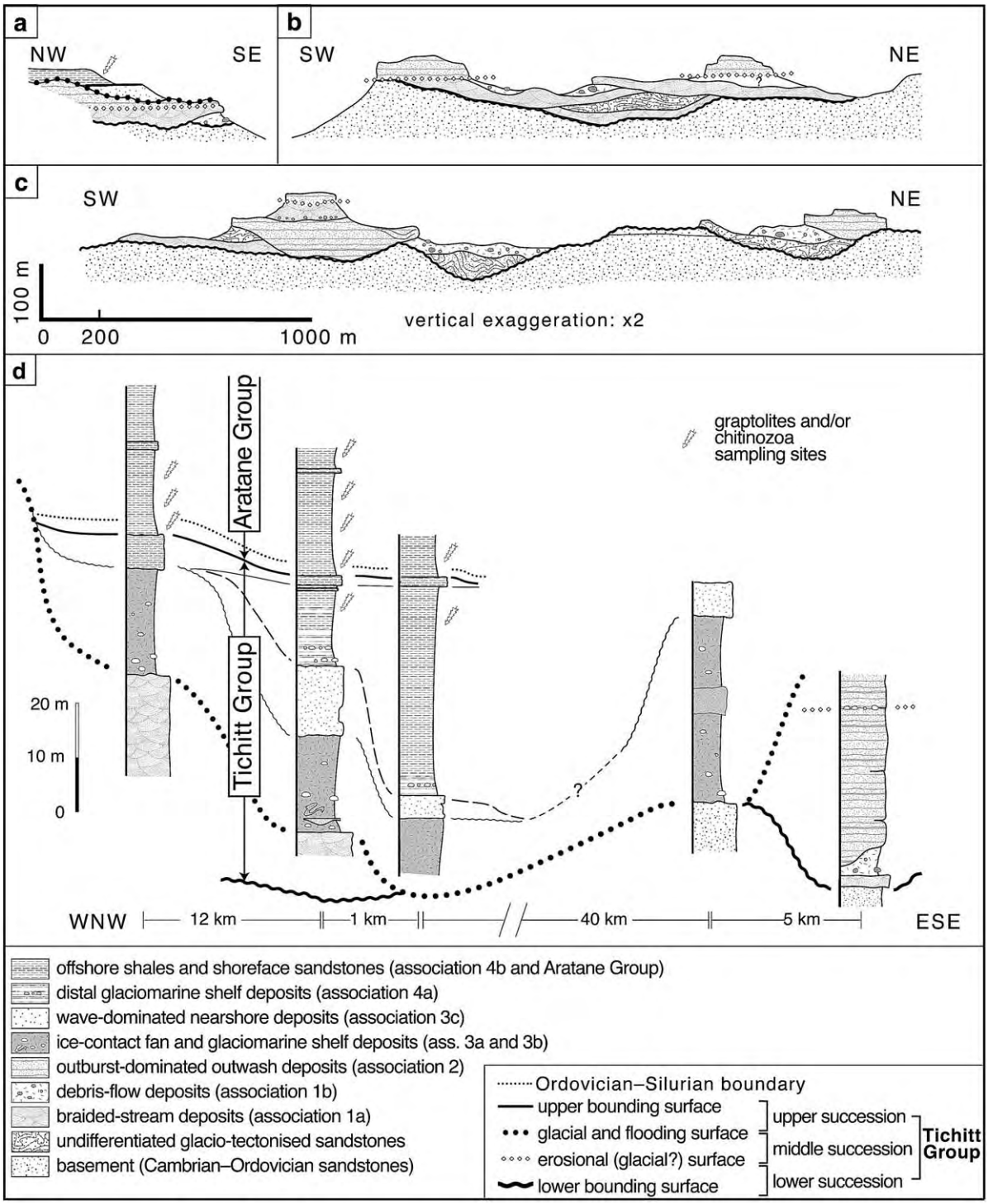

Fig. 5. Sedimentary architecture (modified from Deynoux, 1980) and subdivision in unconformity-bound successions within the Tichitt Group in the Hodh area. Locations are in Fig. 3.

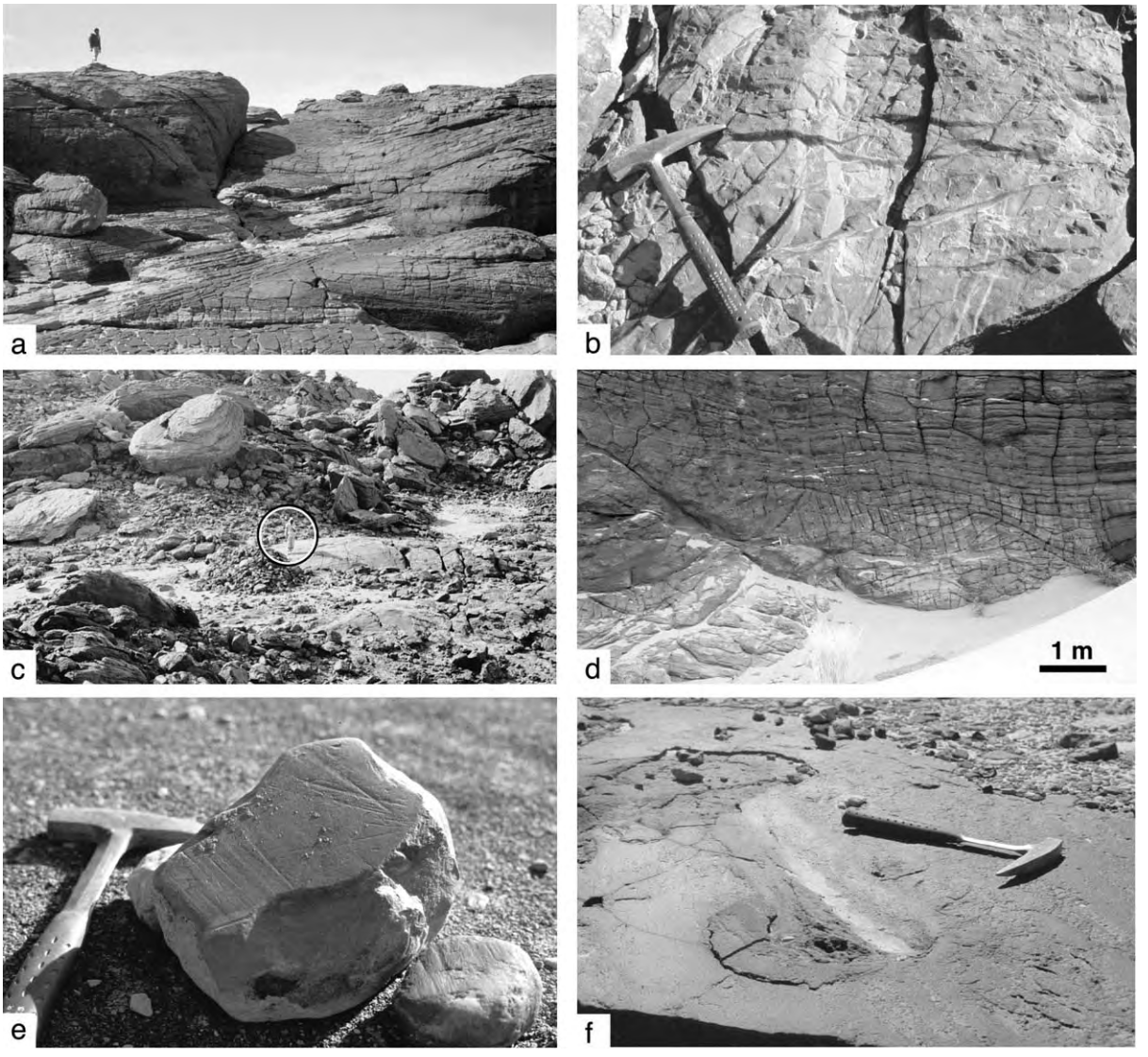

Fig. 6. Upper Ordovician deposits and glacial deformation structures in the Hodh. (a) Large-scale trough cross-bedded sandstones (association 1a) (person for scale). (b) Small-scale anastomosing extensional step-fractures in braided stream deposits (association 1a). (c) Subglacially formed streamlined features (circled person for scale). (d) Climbing megaripple grading up into vertically aggrading undulatory laminae in coarse-grained sands (association 2) (circled hammer for scale). (e) Subglacially striated quartzite cobble and granite pebbles found in diamictites (association 3a). (f) Ice-keel scour mark in shallow-marine sandstones (association 3c).

on the basis of regionally extensive, erosional, bounding unconformities (Ghienne, 1998; Fig. 4, logs A and B; Fig. 5). The lower and middle depositional successions form the lower Tichitt Group of Deynoux (1980), whereas the upper depositional succession corresponds to the upper Tichitt Group.

Throughout the Taoudeni Basin, the Tichitt Group rests upon an erosional surface truncating Cambrian–Ordovician sandstones, which were likely to have been lithified at the time of the glaciation (Deynoux, 1980). In the Hodh, the lower bounding surface of the Tichitt Group is planar on a regional scale, with overdeepened, wide,

shallow depressions within which Deynoux (1980) described ridges of glacio–tectonic origin.

2.4.1. Lower depositional succession

The lower depositional succession, mainly exposed in the western Hodh (Dahr Tichitt; Fig. 3), is mostly made up of cross-laminated fluvial sandstones. It is truncated upward by the erosional lower bounding surface of either the middle or upper depositional succession.

This succession, 0–100 m thick, consists of coarse-grained braided stream sandstone sheets (association 1a; Fig. 6a), typically with abundant synsedimentary deformation structures (Fig. 6b), and interfingering proglacial debris flow diamictites (association 1b; Fig. 5). Cross-laminae indicate W- to NW-oriented palaeocurrents (Fig. 4). In places, along internal bounding surfaces, extensive glacial deformation is responsible for elongated (>10 m) asymmetrical structures similar to roches moutonnées, displaying a smooth southeastern stoss side and a fractured northwestern lee side (Fig. 6c). Arcuate sandstone ridges, with internal shear indicated by the deformation of the primary bedding, are occasionally present. They are several hundred metres in radius and convex toward the NW or WNW. The last event recorded within the lower unit is the incision of large-scale channels, cut into bodies of braided stream and debris flow deposits, subsequently filled by flood-dominated sandstones (association 2; Fig. 5c).

In the eastern Hodh, the lower succession is laterally discontinuous on a regional scale, suggesting preservation in scoured areas. As proglacial debris flows are generally lacking, the sedimentary record is dominated by glaciofluvial braided stream deposits (association 1a).

Depositional and glacial features suggest sedimentation in an aggrading braided outwash plain affected by episodic glacial re-advances (Fig. 7a,b). At the scale of a single sandstone sheet (association 1a), the aggradation probably occurred during ice stagnation with high sediment supply and relatively low meltwater discharge. Proglacial outwash sediments are glacio–tectonised during ice re-advances (Boulton, 1986; Van Der Wateren, 1995; Hambrey and Huddart, 1995). When ice retreats, till and part of the glaciofluvial material are reworked by gravity processes and re-deposited in subglacial overdeepened zones (association 1b; Collinson et al., 1989; Zielinski and Van Loon, 1996). The incision of large-scale channels (association 2) suggests highly turbulent, relatively sediment-deficient meltwater streams (Fig. 7c; Kehew and Lord, 1986). At last, they are filled by concentrated sediment-laden stream flows related to progressively reduced discharges which are interpreted as reflecting a coeval ice front recession (Fig. 7d).

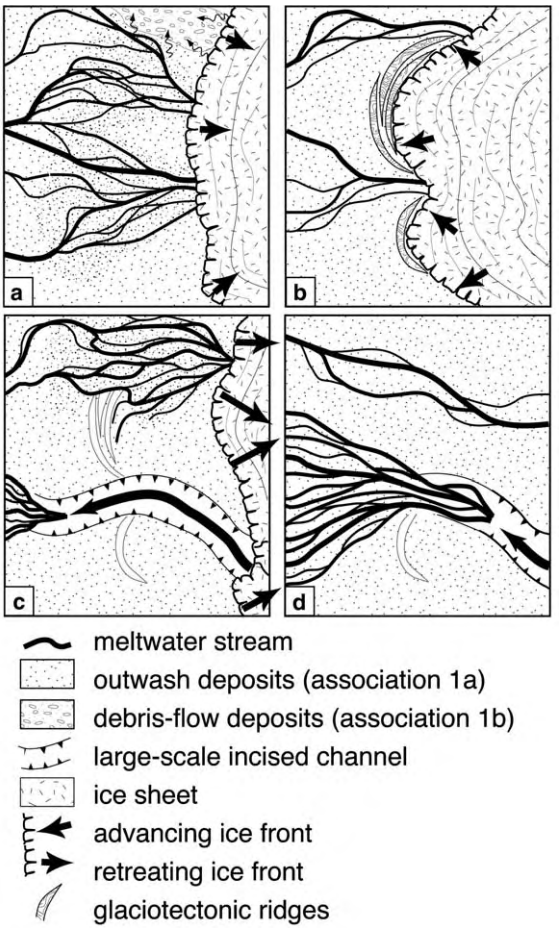

Fig. 7. Temporal evolution of glaciofluvial environments within the lower succession in the Hodh. (a) and (b) Episodic minor retreats and re-advances of the ice front. (c) and (d) Incision and infilling of meltwater channels coeval with a major ice front recession.

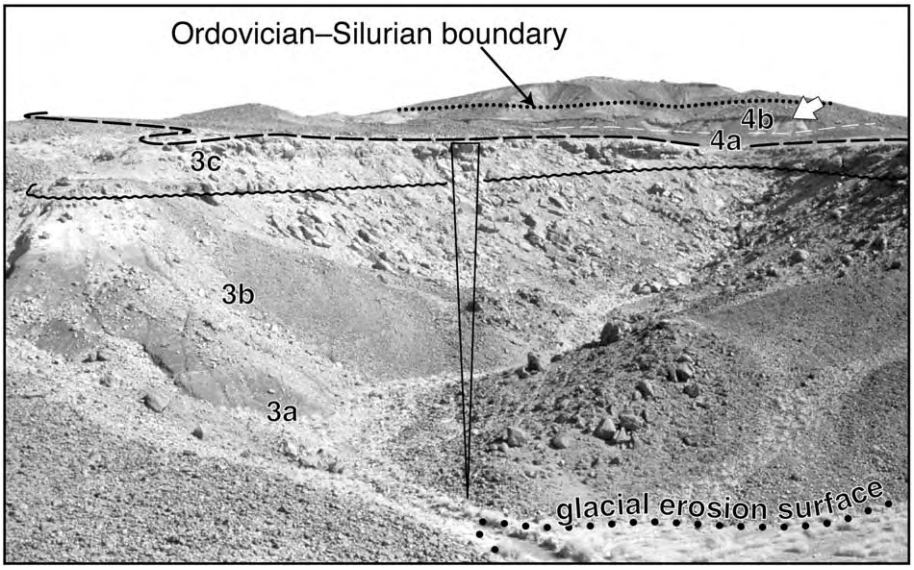

Fig. 8. The upper sucession (association 3) and the Ordovician–Silurian boundary in the eastern Hodh. Non-glacial offshore conditions (association 4b) were established before the end of the Ordovician. The sandstone bed (white arrow), a few metres below the Ordovician–Silurian boundary, is related to an additional, latest Ordovician–earliest Silurian sea-level oscillation, which occurred after the northern Gondwana ice sheet disappeared from the Taoudeni Basin.

2.4.2. Middle depositional succession

The middle depositional succession rests along an erosional surface, roughly planar on a regional scale (Fig. 5a–c), which is characterised by abundant gravel to pebble lags. A glacial striated pavement has been found, suggesting, at least locally, a possible glacial origin.

The middle succession forms a regionally extensive, 10–40 m thick, fining-upwards sandstone sheet, which typically shows climbing megaripples. It is made up of high-energy, concentrated, decelerating sheet-flow deposits (association 2; Fig. 6d). In the proglacial overall setting, these deposits are interpreted as the result of meltwater floods, possibly corresponding to outburst events (Rudoy and Baker, 1993; Russell and Knudsen, 1999). The overall fining-up trend suggests a retreating sediment source. Few exposures of the middle succession have been identified in the eastern Hodh. Here, this unit has not been deposited or eroded before the deposition of the upper depositional succession.

2.4.3. Upper depositional succession

The upper depositional succession, which is well-developed in the eastern Hodh (Figs. 5d and 8), is characterised by a regionally extensive glaciomarine diamictite sheet. It rests along an erosional, glacial surface, truncating sandstones of either the lower succession or the Cambrian–Ordovician basement (Deynoux, 1980). The style of glacial deformation, which associates streamlined ridges, flutes and hummocky surfaces on top of glaciofluvial sands, suggests that glacier ice more likely moved across poorly drained, deformable subglacial sediments (Rose, 1987; Visser, 1990; Boulton, 1996).

The region-wide succession from basal ice-contact subaquatic fan deposits (association 3a; Fig. 6e; Lønne, 1995), to shelf diamictites dominated by sand-sized rafted debris (association 3b; Gilbert, 1990), and then to overlying wave-dominated nearshore sandstones (association 3c; Fig. 6f), suggests a retreating, grounded, marine ice margin (Fig. 8). The erosional base of nearshore deposits indicates a significant relative sea-level fall. In this glaciomarine setting, a short-lived post-glacial isostatic rebound is inferred.

In a restricted area, offshore shelf deposits (association 4) overlie the glaciomarine deposits

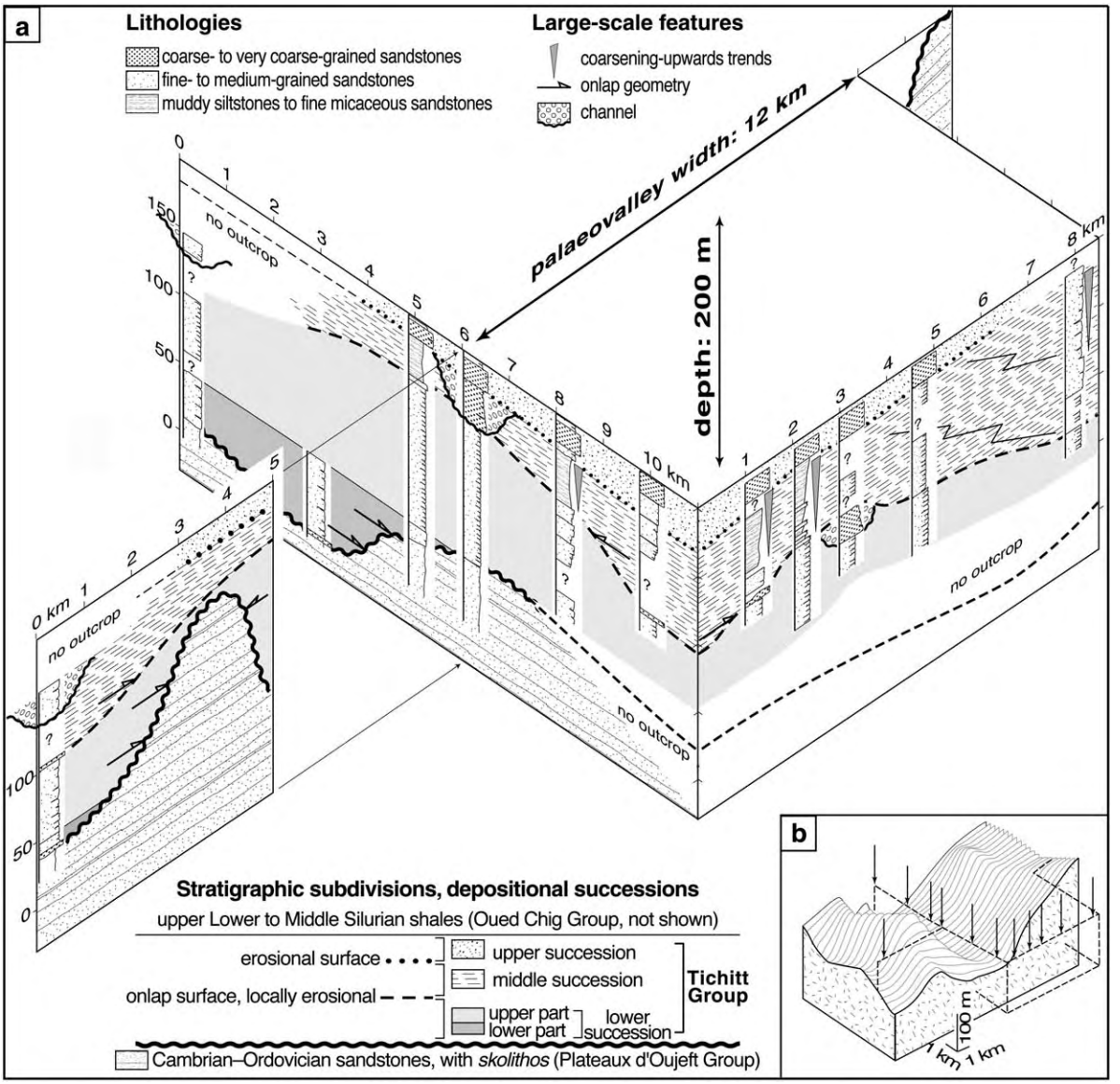

Fig. 9. 3-D architecture of the Tichitt Group in the Adrar. (a) Field sections and outcrop correlations, showing three unconformity-bound successions, corresponding to glacial units 1, 2 and 4 (investigated area located in Fig. 3). (b) Schematic 3-D view of the erosional lower bounding surface of the Tichitt Group.

(Figs. 5d and 8). Sandy siltstones with thin sandstone beds and occasional pebble-sized dropstones (association 4a), grading up into graptolite-bearing shales (association 4b), show the progressive disappearance of glacial influence (Deynoux, 1980) and colonisation by graptolites and chitinozoans before the end of the Ordovician (Underwood et al., 1998; Paris et al., 1998). A ferruginous, partly oolitic, sandstone horizon records an additional regressive–transgressive fluctuation during the latest Hirnantian. Upward, Hirnantian to Llandovery deposits are truncated by the Devonian unconformity.

In the western Hodh, only the higher levels of

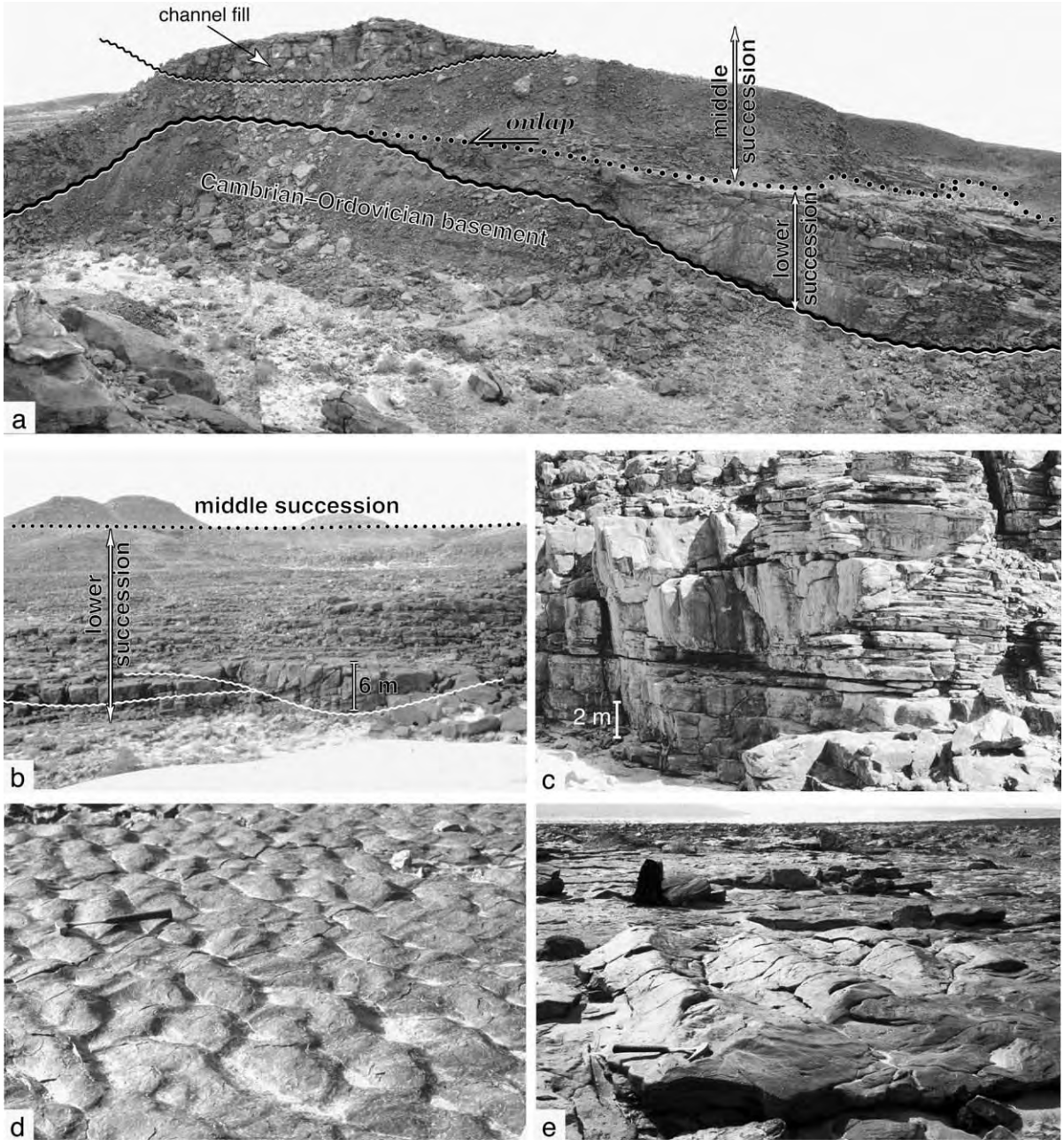

Fig. 10. Upper Ordovician deposits from the Adrar. (a) Panoramic view showing the erosional lower bounding surface, the infilling of the palaeotopography and the onlap of the middle succession onto the lower one. Cliff is about 75 m high. (b) Lower succession sandstones, with amalgamated tidal channels at the base (association 5), overlain by thick, horizontally bedded fluvial deposits (70 m) (association 6). (c) Flood-dominated sandstones (association 6). (d) Wave-reworked current ripples in tidal sand flat deposits (association 7b). (e) Wave megaripples (association 8).

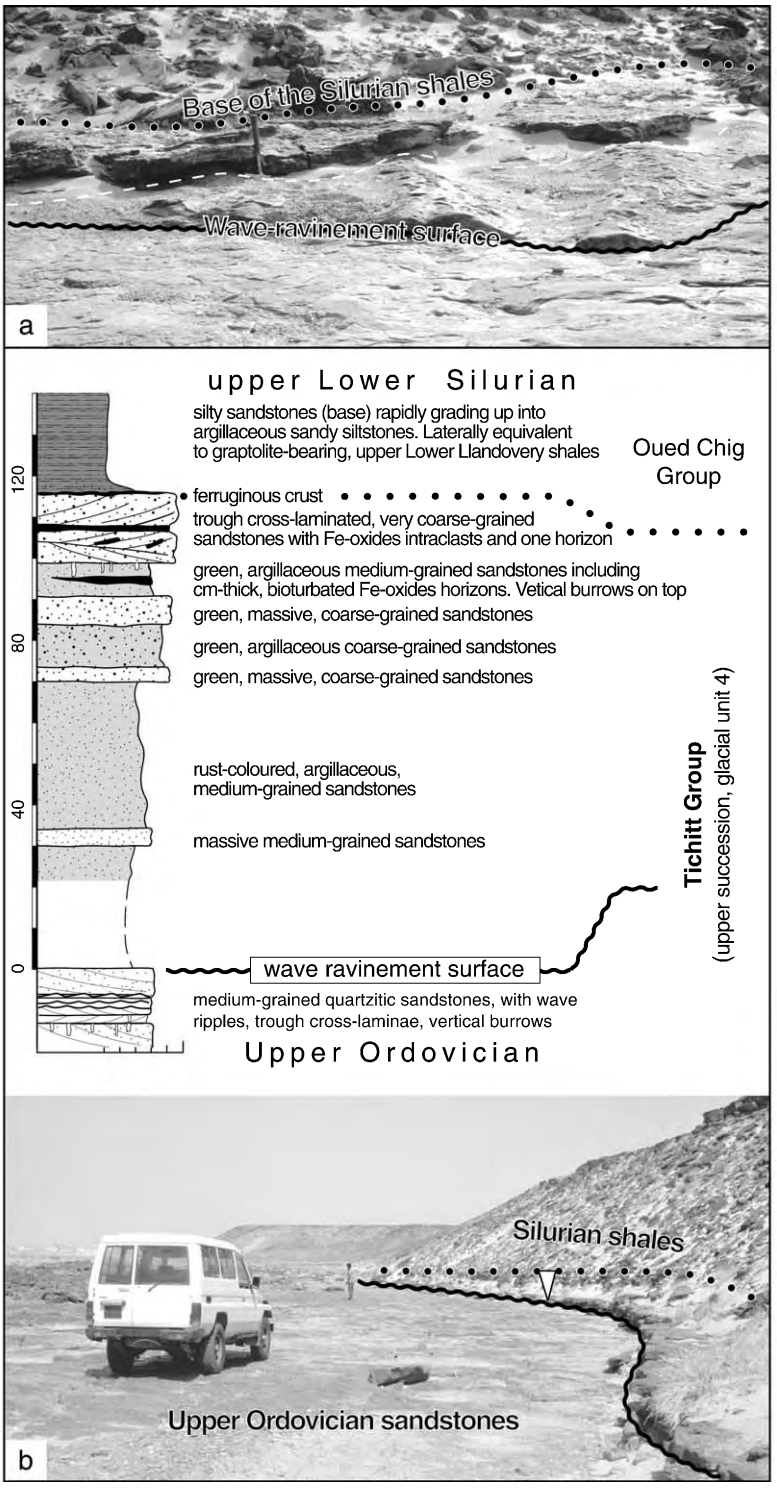
Base of the Silurian shales
Wave-ravinement surface
a
upper Lower Silurian
silty sandstones (base) rapidly grading up into argillaceous sandy siltstones. Laterally equivalent to graptolite-bearing, upper Lower Llandovery shales
Oued Chig Group
ferruginous crust
trough cross-laminated, very coarse-grained sandstones with Fe-oxides intraclasts and one horizon
green, argillaceous medium-grained sandstones including cm-thick, bioturbated Fe-oxides horizons. Vetical burrows on top
green, massive, coarse-grained sandstones
green, argillaceous coarse-grained sandstones
green, massive, coarse-grained sandstones
rust-coloured, argillaceous, medium-grained sandstones
massive medium-grained sandstones
Tichitt Group
(upper succession, glacial unit 4)
wave ravinement surface
medium-grained quartzitic sandstones, with wave ripples, trough cross-laminae, vertical burrows
Upper Ordovician
120
80
40
0
Silurian shales
Upper Ordovician sandstones
b

the upper succession have been identified eastward. They comprise wave-dominated, glaciomarine-influenced nearshore deposits (association 3c), which onlap onto the middle depositional succession and are overlain by lowermost Silurian shales excluding the latest Ordovician *persculptus* graptolite zone (Fig. 5a).

2.5. The glacial record in the Adrar

In the central Adrar, the depositional architecture of the glacial deposits (former Njakane–Abteilli Group) was first described by Trompette (1973), Deynoux (1980) and Deynoux et al. (1985) (Fig. 3; Fig. 4, log E). Deynoux (1980) identified three sandstone bodies with two intercalated soft, siltstone-dominated horizons. However, the identification of two regionally extensive internal erosional unconformities indicates that, in the central Adrar, the upper Ordovician glacial deposits are more simply subdivided in three depositional successions (lower, middle and upper), conforming to the stratigraphic scheme of Trompette (1973) (Fig. 4, log E). However, in the southern Adrar, four successions are distinguished (Fig. 4, log D).

In the central Adrar, the glacial deposits rest above Cambrian–Ordovician sandstones upon an erosional surface with large (>10 km) and deep (>150 m), NW–SE to WNW–ESE oriented palaeovalleys (Fig. 9). The three successions successively onlap onto the palaeovalley margins or onto isolated palaeorelief forms (Fig. 10a). In places, thin, discontinuous coarse-grained deposits, including cobbles of Cambrian–Ordovician sandstones, are present along the lower bounding surface of the Tichitt Group. In the southern part of the Adrar (Fig. 3, section D; Fig. 4), a subglacially formed streamlined and grooved structure was discovered 5 m above the lower bounding surface.

2.5.1. Lower depositional succession

The lower depositional succession is made up of two conformable packages (Fig. 9a). The lower one (5–50 m thick), preserved in the lowermost part of the palaeovalleys, comprises tidal deposits including large sand waves and multistorey, generally laterally amalgamated, sandstone channel fills (association 5; Table 1). The upper package forms thick sandstone tabular bodies comprising high-energy sand flat deposits with occasional channel fills, interpreted as sheet-flood-dominated fluvial environments (association 6; Fig. 9b,c). Westward to southwestward palaeocurrents do not necessarily conform to small-scale palaeovalley orientations (Fig. 9b), suggesting that the passive upstreamward infilling of the tributary abandoned palaeovalleys may have occurred.

The nature and thickness of the lower succession, and the vertical evolution from tidal-dominated, laterally amalgamated sandstone channel fills in the lowermost part, to vertically superimposed sheet-like fluvial sandstone beds in the upper part, suggests transition from a low to a high accommodation system in an overall aggrading, sand-rich system in combination with high sediment supply (Shanley and McCabe, 1994). Relatively fine-grained flood-dominated facies and the absence of glacial structures suggest that deposition occurred away from the ice front in the central Adrar.

2.5.2. Middle depositional succession

The middle depositional succession, up to 100 m thick, is typically coarsening-upwards (association 7). It onlaps onto either the upper part of palaeovalley margins or onto the lower succession deposits along a topographically irregular contact, without evidence of glacial deformation. The middle succession is occasionally underlined by thin or channelised coarse-grained, cross-laminated fluvial sandstones (Figs. 9 and 10a).

Fig. 11. The Ordovician–Silurian boundary in the central Adrar. (a) A wave–ravinement surface generally separates the glaciation-related sandstones from the overlying lower to middle Silurian shales. (b) Locally, a coarse-grained sandstone intercalation suggests that a condensed sedimentation occurred close to the Ordovician–Silurian boundary.

In places, the lowermost part of the succession shows thin sandy tidal flat deposits, up to 5 m, including small-scale channel fills (association 5; Fig. 10d). The bulk of the middle succession comprises coarsening-upwards deltaic sediments (associations 7a to 7c). Fine- to coarse-grained sandstone channel fills, interpreted as distributary features, are preserved in the upper part of the succession (Fig. 9). Evidence of a subsequent extensive glacial advance is given by glacio–tectonic deformation structures (tight folds and thrust faults) or the incision of deep and narrow palaeovalleys interpreted as subglacial tunnel valleys (Ghienne and Deynoux, 1998). They suggest that the topmost part of the middle succession is eroded in the central Adrar. This region-wide glacial advance is supported by the existence of an additional coarsening-upwards deltaic succession that is preserved in the southern Adrar, and which is separated from the underlying one by ice-proximal glaciofluvial sandstones (Fig. 4, log D).

Channelised fluvial deposits at its base suggest that the middle succession rests along a sub-aerial unconformity. The overlying coarsening-upwards deposits, at the scale of the whole depositional succession, record the evolution of a delta system that comprises fluvial-dominated, prograding, bar finger sand systems (Wood and Ethridge, 1988). Following the deposition of the lower succession, the middle one filled the residual palaeotopography up to the level of the higher palaeorelief forms.

2.5.3. Upper depositional succession

The upper depositional succession forms an erosionally based, 1–30 m thick, fining-upwards sandstone sheet resting on either the middle succession or the higher palaeorelief forms (Fig. 9). In detail, it is subdivided in smaller-scale, erosionally based, sandstone sheets comprising high-energy, torm-dominated, slightly bioturbated coastal deposits (association 8), including well-developed wave megaripples (Fig. 9e; e.g. Leckie, 1988). Palaeocurrents indicate the reversal of the sediment dispersal pattern, resulting from either shallow-marine dispersal processes or an inverted drainage network (Fig. 4, log E). No glacial feature has been identified within this succession.

A well-defined erosional surface in the uppermost part of the succession is underlined by storm-generated, coarse-grained wave megaripples concentrating pebbles within their troughs (Fig. 11a). These features suggest a wave–ravinement surface (Nummedal and Swift, 1987). The latter is overlain by thin and discontinuous coarsening-upwards sandstones (0.5–2 m) (Fig. 11b). As the overlying Silurian shales of the Oued Chig Group starts in the middle lower Silurian according to Trompette (1973) and Willefert (1988), these sandstones are thought to reflect a condensed sedimentation above the upper Ordovician glaciation-related deposits.

2.6. The glacial record in the Tagant

The upper Ordovician deposits of the Tagant (Dikkel Group) have been described by Dia et al. (1969) and Dia (1984). In this area, located in between the Hodh and the Adrar, a re-examination of the main field sections of Dia (1984) has shown that the depositional facies and architecture of the glacial deposits share characteristics identified in both areas. Above an angular unconformity, the succession is subdivided into three depositional successions (Fig. 4, log C).

The lower depositional succession (0–55 m thick) infills palaeovalleys cut in Cambrian–Ordovician sandstones. It is made up of sandstones, the character of which is similar to the glaciofluvial facies association 1 in the lower part of the succession, and similar to the fluvial facies association 6 in its upper part. Hence, the lower succession is likely to record the evolution of fluvial depositional environments associated with the retreat of an ice front.

The lower depositional succession is truncated by a well-defined streamlined subglacial pavement, which is overlain by the middle depositional succession, up to 100 m thick, which is characterised by an overall coarsening-upwards pattern. The lower bounding surface of glacial origin is overlain by a glaciomarine succession in its lower part (association 3b), passing upward to coarsening-upwards deltaic deposits (association 7b). In

the upper part of the middle succession, erosionally-based, fining-upwards sandstone bodies, which truncate deltaic deposits, are similar to the distributary channel fills observed in the Adrar (association 7c). However, in the topmost part of the middle succession, bioturbations and brachiopods are already occasionally present. The middle succession is truncated by an erosional surface of glacial origin, which is characterised by glacio–tectonic deformation structures. In places, the whole of the middle depositional succession is eroded.

Above the underlying erosional surface, the upper succession (20–40 m thick) onlaps onto either the lower or the middle depositional succession. Relatively thin glaciomarine deposits (facies associations 3a or 3b) are overlain by coarse-grained, locally highly deformed, cross-laminated sandstones suggesting the glaciofluvial facies association 1a. The upper succession is directly over-

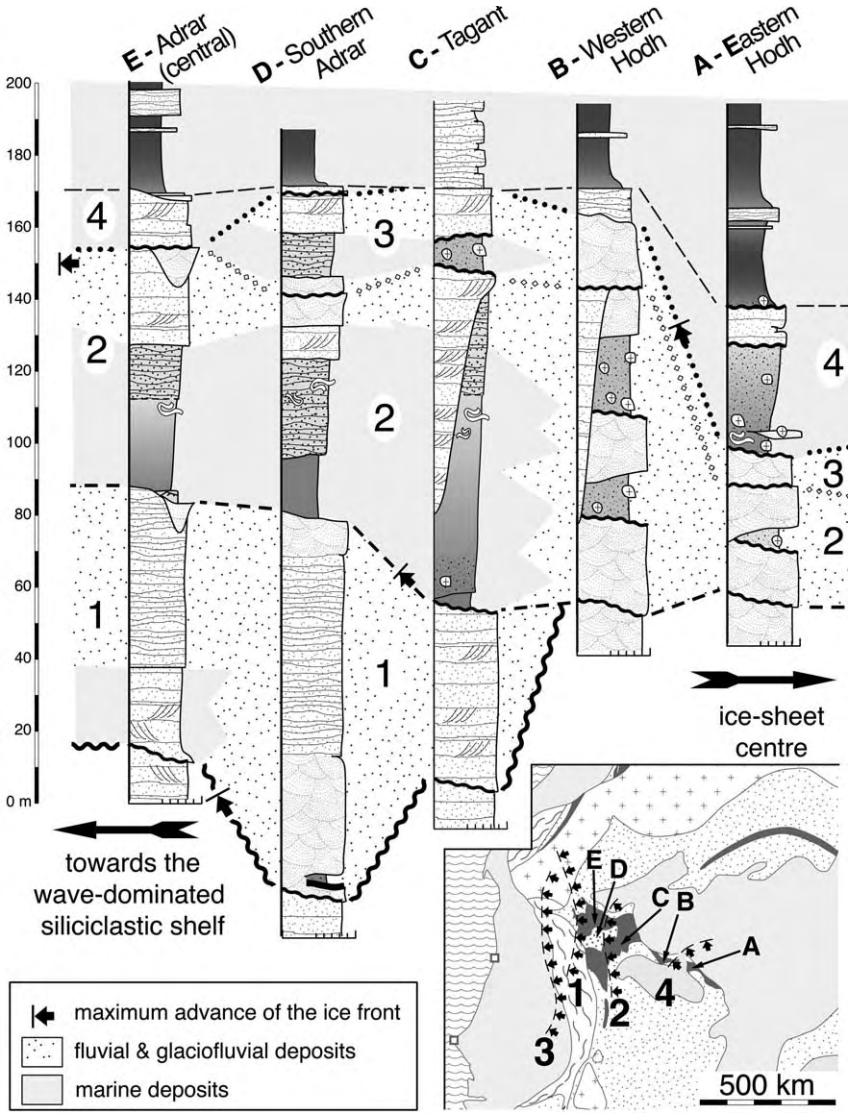

Fig. 12. Correlation of unconformity-bound regional-wide successions (for patterns and horizontal scale, see Fig. 4). Four glacial units are delineated. Ice front extents shown on the index map are only approximated.

lain by Silurian sandstones and shales including reworked phosphatic clasts Fe-rich ooids, brachiopods, crinoids, and a graptolite fauna that is possibly Late Llandovery in age (Dia, 1984).

2.7. Synthesis of sedimentary data

Successive glaciation-related deposits and post-glacial offshore shales of Hirnantian and then Llandovery age onlap onto a palaeotopography cut in Cambrian–Ordovician rocks. The erosional bounding surfaces between depositional successions are most often of glacial origin. Glacial sedimentation (ice-contact fans, glacial dropstones, very coarse-grained to conglomeratic glaciofluvial facies) and synsedimentary glacio–tectonic deformation structures are generally restricted to the lower part of the depositional successions. Glacial deformation in the upper part of a depositional succession is associated with the formation of the lower bounding surface of the overlying succession. A variety of types of depositional succession have been identified in the Taoudeni Basin: (1) aggrading, fluvial-dominated successions, with tidal deposits in the lower part of ice-distal ones, or glaciofluvial deposits and synsedimentary glacial deformation structures within ice-proximal successions; (2) deltaic deposits overlying either thin shallow-marine transgressive facies in the lower part of ice-distal successions, or glaciomar-

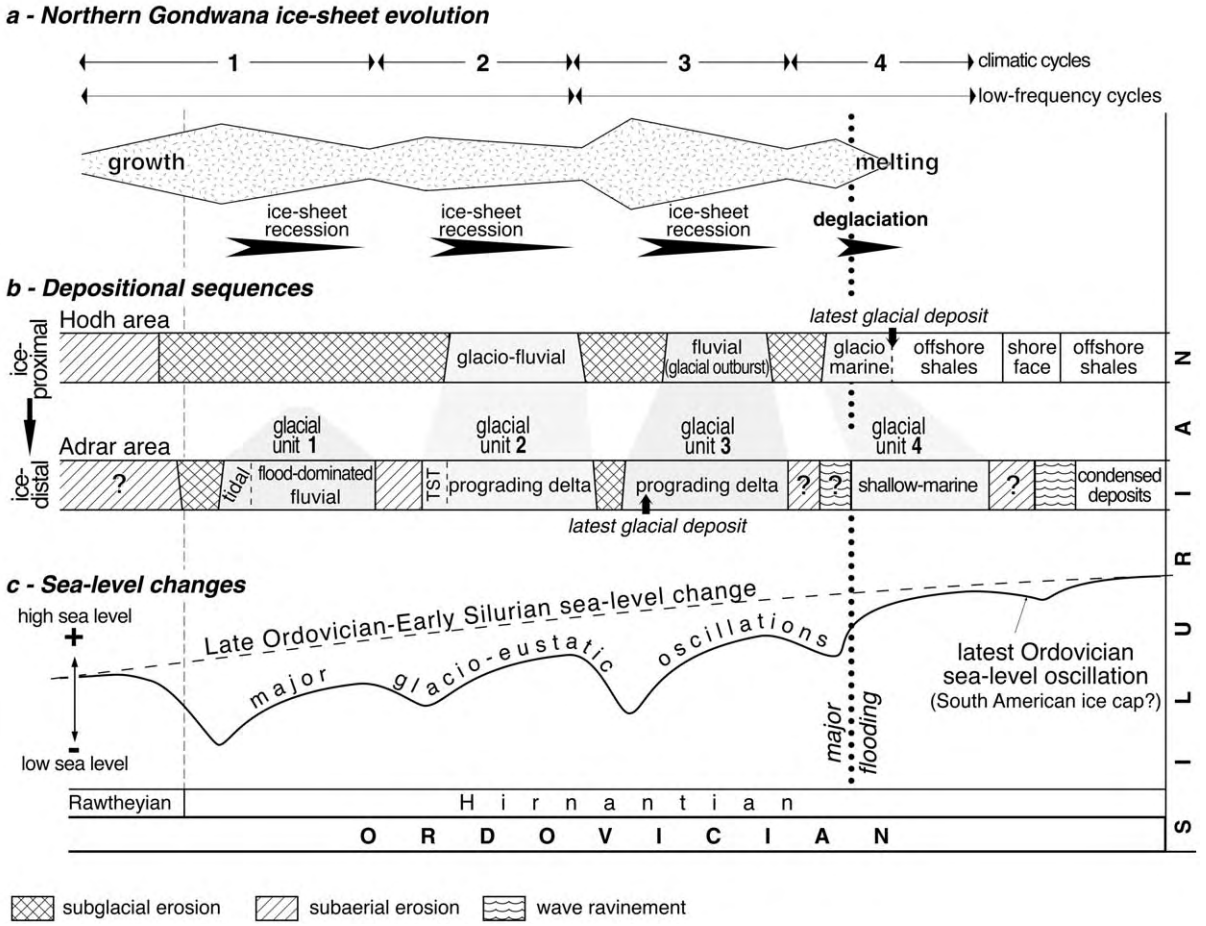

Fig. 13. Late Ordovician ice sheet evolution, glacial units and inferred sea-level changes in the hypothesis of glacio–eustatic cycles driven by the northern Gondwana ice sheet growth and melting.

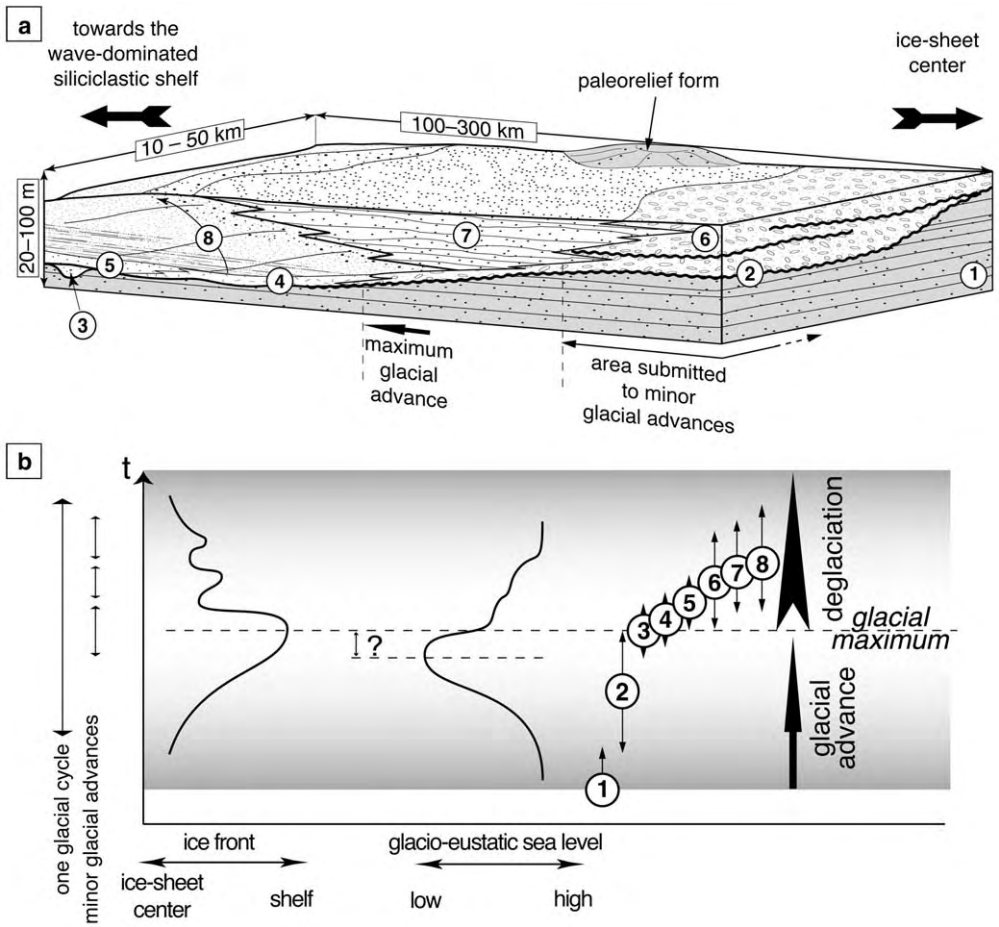

Fig. 14. Architecture of a glacial unit. (a) Key: (1) Cambrian–Ordovician or underlying glacial deposits; (2) incision of a palaeovalley; (3) fluvial channel fills corresponding to lowstand system tract deposits; (4) glaciomarine deposits, may be absent; (5) thin tidally-influenced transgressive system tract deposits; (6) and (7) aggrading glaciofluvial and fluvial sediments; (8) deltaic succession. Sediments 6–8 correspond to highsteand system tract deposits. (b) Relationships, during the deposition of an individual glacial unit, between the ice front location, the ice-distal glacio–eustatic sea-level and the sedimentary record (events 1–8). A time lag may exist between the time of maximal glacial advance and the time of lowest sea-level.

ine influence within ice-proximal ones; (3) fully glaciomarine successions, recording the later marine ice front recession in ice-proximal areas; and (4) shallow-marine, mainly wave- or storm-dominated deposits in the ice-distal, uppermost Ordovician deposits, which do not bear any glacial characteristics. Each of the depositional succession records an ice sheet recession regime following a glacial advance, either in a continental or in a marine setting.

No information is available for the thermal regime of Late Ordovician glaciers during glacial advances and maxima as the upper Ordovician glacial record corresponds to ice sheet recession stages. Conversely, during deglaciation phases, the abundant fluvial to glaciofluvial or fluvial-dominated deltaic deposits, rare true glaciogenic facies, low organic carbon content in distal marine successions, as well as relatively few dropstones in glaciomarine deposits, together suggest the dominance of temperate warm-based glacier ice and the release of large quantities of sub- to

supraglacial meltwater (Anderson and Ashley, 1991; Matsch and Ojakangas, 1991).

3. Glacial units, climatic cycles and post-glacial evolution

The upper Ordovician glacial record throughout the Taoudeni Basin shows a great variety of depositional facies ranging from ice-proximal to ice-distal deposits. Correlation of the depositional successions and their bounding surfaces, across five areas relatively close to each other, offers an insight into the depositional architecture at the platform scale (Fig. 4).

3.1. Glacial units and climatic cycles

Depositional successions described in a particular area are defined between regionally extensive unconformities. Correlation of the depositional successions and their bounding unconformities defines a set of basin-wide, glacial units. Within a glacial unit, the proposed correlations try to take into account: (1) the longitudinal organisation of depositional environments, from a more ice-proximal setting toward the east, to more ice-distal environments toward the northwest, in agreement with palaeocurrent data; (2) the relative thickness of age-equivalent depositional units; (3) the onlap relationships identified on a regional scale; and finally, for the uppermost glacial deposits, (4) the temporal relationships between the uppermost glaciation related Ordovician deposits and the overlying firstly deposited offshore deposits, which display either an uppermost Ordovician or a lower Silurian age.

The preferred correlation outlines four unconformity-bound glacial units (Fig. 12). Each of the four units records an ice sheet recession regime (Fig. 13a). The distribution of subglacial features (glacial pavements and bedforms, glacio–tectonic deformation structures), and the distribution of ice-proximal deposits suggest that the maximum ice front limits are different for each of the four units. The first (unit 1) and, in particular, the third glacial advances (unit 3), would correspond to the greater Late Ordovician ice sheet extents in the Taoudeni Basin. Paradoxically, these two units are not associated with well-preserved proglacial sediments. Conversely, during deposition of the second unit, which followed a somewhat less extensive glacial advance, ice-proximal glaciofluvial sediments were largely preserved in the Hodh. The fourth glacial unit records the ice sheet recession following the last glacial advance. The upper succession in the Hodh, reflecting proximal to distal glaciomarine conditions, is interpreted as coeval with the upper succession in the Adrar that comprises ice-distal, erosionally based, shallow-marine sandstones devoid of glacial influence. Idealised spatial and temporal relationships between the depositional units, from ice-proximal to ice-distal areas, are depicted in Fig. 13b.

Considering the maximum extent of ice across the basin, units 1 and 3 following major glacial advances are interfingered with units 2 and 4 related to less extensive glacial advances (Fig. 12). As the units are bounded by erosional surfaces related to glacial advances, they most probably provide a record of climatically controlled oscillations of the Late Ordovician ice sheet.

3.2. Architecture of a glacial unit

Based on units 1 and 3, the depositional architecture of a glacial unit is tentatively reconstructed (Fig. 14). With the exception of the fourth, a unit forms a sedimentary wedge bounded at both its base and its top by erosional unconformities. In ice-proximal areas, erosion mainly results from subglacial scouring associated with an ice sheet advance. Here, wide palaeovalleys or depressions are typically cut (2 in Fig. 14) within Cambrian–Ordovician or previously deposited glaciation-related deposits (1 in Fig. 14). In more ice-distal areas, the contact between two successive units may locally appear conformable, although the lower bounding surface is occasionally associated with incised channels (3 in Fig. 14).

Sediments of a glacial unit onlap laterally and upstreamward onto their substratum. In relatively ice-distal areas, the coarse-grained channel fills associated with the lower erosional bounding surface of a glacial unit represent lowstand deposits (3 in Fig. 14). Only minor deposition of transgres-

sive deposits are locally reported, such as the tidally influenced sandstones in the lowermost part of a unit (5 in Fig. 14). The glaciomarine influence that is recorded in places only within the lower and more proximal part of the deltaic deposits (4 in Fig. 14), indicates that the initial influence of marine ice fronts rapidly disappears upwards. The bulk of a glacial unit is made up of aggrading glaciofluvial or fluvial sediments (respectively 6 and 7 in Fig. 14), which grade downstream, toward relatively more ice-distal areas, into deltaic, prograding deposits (8 in Fig. 14). Although the latter display a noticeable aggrading component as they onlap laterally and upstreamward, most of a glacial unit is similar to highstand system tract deposits characterised by a high aggradation rate. Glacio–eustatically-dominated relative sea-level rises, coeval with ice front retreats, maintained a high rate of accommodation coeval with a high rate of sediment supply.

3.3. The end of the glaciation and the related flooding

In the Taoudeni Basin, sediments related to the final melting of the ice sheet that covered the northern Gondwanaland form the fourth unit. An overall onlap geometry of glaciomarine deposits and overlying Hirnantian and Llandovery offshore shales has been identified above the Cambrian–Ordovician basement and sediments of the underlying glacial units (Fig. 5d). This geometry, and the nature of the sediments, together indicate an overall long-term transgressive dynamic regime coeval with the ice sheet recession.

In the ice-proximal areas, the fourth unit is characterised by an extensive glaciomarine diamictite sheet, indicative of extensive marine flooding (Figs. 4, 8 and 12). In its upper part, the unit comprises nearshore deposits resting on a marine erosional surface above deeper glaciomarine shelf deposits, most probably resulting from a glacio–isostatically-driven regression. Within the Taoudeni Basin, the subsequent latest Ordovician–earliest Silurian sea-level oscillation is no longer associated with glacial or even distal glaciomarine sediments, attesting to the absence of glaciers from that time. However, this later sea-level oscillation might still be related to the evolution of remote ice caps in the continental interior or in South America. In ice-proximal areas, the lack of a significant hiatus between the latest glaciomarine diamictites and non-glacial, latest Hirnantian to lowermost Llandovery shales is demonstrated.

In the ice-distal Adrar area, the fourth unit is barren of any glacial feature. The post-glacial evolution in such a relatively ice-distal, but formerly ice-covered area is dominated by a condensed sedimentation or erosion in shallow-marine environments (Fig. 11). Wave–ravinement surfaces or undifferentiated erosion surfaces are related either to marine erosion (wave–ravinement and retreating shorelines) or to sub-aerial erosion, both resulting from one or several minor relative sea-level oscillations. Here, graptolite-bearing offshore shales, which onlap onto an irregular surface (Fig. 5a), were deposited later in the Llandovery, leading to an apparent Silurian transgression (Adrar, western Hodh). In ice-distal, formerly ice-covered, areas the flooding is not related to the melting of the northern Gondwana ice sheet, which was complete before the end of the Ordovician. However, the marine invasion occurred before the shales-dominated sedimentation, as shown by the shallow-marine nature of the fourth-unit deposits. The overlying condensed sandstone-dominated sediment may range from the latest Hirnantian to lower Llandovery (Fig. 11).

Therefore, in the more ice-proximal areas, the early flooding and the deposition of relatively thick latest Ordovician–lowermost Silurian offshore deposits most probably occurred simultaneously with the post-glacial flooding in the low latitude areas and with nearshore depositional conditions prevailing in the ice-distal, formerly ice-covered areas. The same is true in southern areas of Algeria and Libya (Legrand, 1988; Klitzsch, 1981). It suggests the existence of relatively deep interior epicratonic seaways (eastern Hodh), established as soon as the latest Ordovician, and separated from the northern or northwestern open ocean by discontinuous shoaling areas (western Hodh, Adrar). As the thickness of glacial sediments underlying these relatively deeper areas is rather thin, it is proposed that the southern post-glacial successions were depos-

ited either in areas of starved glacial sedimentation dominated by erosional processes or in basins overdeepened by ice during the latest (fourth) glacial advance. After the glaciation, the palaeogeography of northern Gondwanaland was notably more intricate than a simple low-gradient platform deepening regularly toward the north or northwest.

4. Discussion

4.1. Glacial cycles

The correlation leads to the identification of four glacial units corresponding to four inferred climatic cycles (Figs. 12 and 13). The four glacial cycles (units 1–4), and their association in two lower-frequency cycles (units 1–2 and units 3–4) may represent two orders of cyclicity, which make sense with the sequential data of an evaporite succession in Australia showing cycles of 100 ± 12 k.y. and subordinate additional cycles of 206–233 k.y. (Williams, 1991).

Beuf et al. (1971) and Deynoux and Trompette (1981) already identified in Algeria and Mauritania 2–4 glacial cycles. However, the latter correspond to small retreat–advance oscillations of the ice fronts during the deposition of a single glacial unit. Conversely, several recent studies have identified two major glacial cycles both in glaciated areas (Ouanaimi, 1998; Sutcliffe et al., 2000) and in low latitude non-glaciated areas (Brenchley and Storch, 1989; Brenchley et al., 1994). The first of these two cycles most likely corresponds to the glacial units 1 and 2, the second cycle comprises the glacial units 3 and 4 starting with a major glacial advance.

Several upper Ordovician successions indicate more than two glacial cycles. In the Zini (western Morocco), an area where the glacial record is the thickest within the Tindouf Basin, three superimposed glaciomarine horizons have been identified (J. Destombes, pers. commun.). Field work in Libya, either in progress by the author or recently published (McDougall and Martin, 2000), and in Turkey (Ghienne et al., 2002), have recognised three to four glacial units associated with significant ice sheet advances. The number of four glacial cycles is in better agreement with the data from the low latitude carbonate shelf succession of Anticosti Island (Canada), which provides evidence for five glacio–eustatic cycles (Long, 1993). The fifth and later cycle could possibly correspond to the short-term, latest Ordovician–earliest Silurian sea-level oscillation that is preserved in the eastern Hodh (Figs. 5 and 8). This additional, but restricted, oscillation was not associated with glacial deposits in the Taoudeni Basin because the ice sheet has probably retreated further south at that time.

4.2. Significance of the Hirnantian glacial event

Palaeontological data suggest that the Late Ordovician glaciation was restricted to the lower part of the Hirnantian (*Extraordinarius* zone), which was estimated to have lasted 0.5–1 m.y. (Harland et al., 1990; Brenchley et al., 1994). This time-slice would conform to the time represented by the Late Ordovician glacial record in the Taoudeni Basin, which comprises four cycles of possibly 100 k.y. This is a minimal value for the duration of the glaciation of the northern Gondwanaland as other, non-recorded, glacial cycles may have occurred.

Even if non-glacial conditions prevailed in West Africa as early as the Late Hirnantian, a longer glaciation cannot be excluded. Smaller ice sheets limited to the continental interior or to South America could have existed from pre-Hirnantian to Silurian times (Crowell, 1999). Glacial cycles have been postulated for the Early Silurian on the basis of several diamictite horizons (Grahn and Caputo, 1992) and high-amplitude eustatic cycles (Johnson, 1996). Then, the glaciation of the northern Gondwanaland during the Hirnantian would correspond only to the glacial maximum. This time period is characterised by: (1) the full glaciation of continental shelves, ice sheets covering northern Gondwanaland as well as southern Africa; (2) repetitive and extensive advance–retreat glacial cycles; and (3) significant marine ice fronts. Before the Hirnantian and during the upper Hirnantian, these features are not recognised.

4.3. The Late Ordovician glaciation and the Silurian transgression

In the Taoudeni Basin, the upper Ordovician glacial deposits, usually resting along an unconformity above Cambrian–lower Ordovician rocks, are overlain by marine deposits ranging from the latest Ordovician to the upper Silurian, without any significant sedimentary hiatus. Thus, the Late Ordovician glaciation coincides with the first stages of a lasting flooding of the platform, which continues during the lower Silurian. The Silurian transgression does not correspond to the post-glacial flooding related to the melting of the ice sheet covering northern Gondwanaland.

The erosional lower bounding surface of the glacial succession corresponds to a climatically controlled unconformity. Deposits associated with the initial glacio–eustatic sea-level fall are not identified in the Taoudeni Basin. They are probably preserved in more ice-distal areas such as the Anti-Atlas (Morocco), where a Hirnantian shelf sandstone succession underlies the glacial deposits (Destombes et al., 1985). Above, the superposition of glacial units, with a shoreline migrating toward the continent from the first lower unit to the fourth upper unit (Fig. 14), suggests an overall retrogradation of the depositional environments. Whereas the succession of the first, second and third glacial units progressively overlaps onto the Cambrian–Ordovician rocks, corresponding to either backstepping lowstand deposits or an early, retrograding transgressive wedge, the fourth glacial unit marks the definitive flooding of the cratonic platform. Despite temporary effects of the glacial rebound in the isostatic zone, the lower bounding surface of the fourth glacial unit is considered as a major transgressive surface at the scale of a Late Ordovician–Silurian transgression (Fig. 13c). In the Taoudeni Basin, the maximum flooding may correspond to the maximum flooding of the higher-frequency latest Ordovician–earliest Silurian sea-level oscillation that is associated with the deeper-water palynomorph assemblages (Paris et al., 1998). The subsequent further relative sea-level rise, and reduced sediment supply during Early Silurian times led to an eustatic sea-level maximum in the Late Llandovery (Lüning et al., 2000), several million years after the melting of the ice sheet which covered northern Gondwanaland.

4.4. Accommodation and glacial record

The preserved thickness of a glacial unit, which ranges laterally from 0 to 100 m, is controlled by the original thickness of sediments deposited during a glacial cycle, which is itself related to the amplitude of the coeval glacio–eustatic sea-level rise and the depth of previous as well as subsequent glacial erosion. In contrast to the glacial units, which are individually high accommodation sedimentary wedges, the overall Late Ordovician glaciation-related sedimentary record, which comprises both vertically superimposed and laterally juxtaposed glacial units, represents low accommodation conditions throughout the depositional area.

The maximum thickness of the upper Ordovician deposits, observed in depressions bounded by palaeorelief forms, evenly ranges from 100 to 200 m, with the exception of some deep and narrow glacial valleys. A part of the net accommodation probably resulted from glacially incised depressions or valleys and their subsequent post-glacial flooding (e.g. Nystuen, 1985). However, additional accommodation may arise considering that the Taoudeni Basin and adjacent areas would have been already flooded before the onset of glaciation. Transgressive pre-glacial upper Ordovician facies overlying Cambrian to lower Ordovician rocks in several peri-Gondwana areas (e.g. Dean and Monod, 1990), in South America (Grahn and Caputo, 1994) and the existence of Ashgill graptolites as far as the Djado in northern Niger (Legrand, 1993), support this idea. Thin, pre-glacial (lower Ashgill, Caradoc?) deposits were totally reworked during the glaciation in the Taoudeni Basin. According to this hypothesis, the glaciation-related deposits filled the cumulative accommodation space resulting from the pre-glacial to end-glacial relative sea-level rise. The preservation of the upper Ordovician glacial deposits would be enhanced by the coincidence of the glaciation with a relative sea-level rise corresponding to a Late Ordovician–Silurian cycle, possibly related to re-

mote rifting events known at the end of the Ordovician throughout the northern Gondwana realm.

5. Conclusion

In the Taoudeni Basin, the upper Ordovician glacial deposits are subdivided into four units, bounded by subglacial or sub-aerial erosional surfaces. Each glacial unit records the recession of a continental-wide ice sheet, succeeding to a major glacial advance in response to climate forcing.

The position of the shoreline, relative to the ice front, controlled the distribution and the nature of depositional facies. Glacio–eustatic sea-level variations controlled the internal architecture of a unit, which is built under high accommodation conditions. Low accommodation rates during the whole glaciation resulted in significant reworking of previously deposited glacial units.

The glaciation of northern Gondwanaland is the glacial maximum of a longer glaciation. The long-term preservation of the glacial drift is interpreted as the combination of the infilling of glacially cut depressions, mainly palaeovalleys, and the temporal coincidence of the Late Ordovician glaciation with a large-scale Late Ordovician–Silurian relative sea-level rise.

Acknowledgements

I am grateful for stimulating discussions with M. Deynoux and M. Hambrey. The manuscript benefited from constructive reviews by F. Surlyk and N. Eyles. Part of this work was made possible through research grants provided by the TOTAL Oil Company. This is EOST contribution no. 2002.501-UMR7517.

References

Abed, M.A., Makhlouf, I.M., Amireh, B.S., Khalil, B., 1993. Upper Ordovician glacial deposits in southern Jordan. Episodes 16, 316–328.

Anderson, J.B., Ashley, G.A., 1991. Glacial marine sedimentation; Paleoclimatic significance; A discussion. Geol. Soc. Am. Spec. Pap. 261, 223–226.

Armstrong, H.A., Coe, A.L., 1997. Deep-sea sediments record the geophysiology of the late Ordovician glaciation. J. Geol. Soc. Lond. 154, 929–934.

Bachtadse, V., Briden, J.C., 1990. Palaeomagnetic constraints on the position of Gondwanaland during Ordovician to Devonian times. In: McKerrow, W.S., Scotese, C.R. (Eds.), Paleozoic Palaeography and Biogeography. Geol. Soc. Lond. Mem. 12, pp. 43–48.

Bertand-Sarfati, J., Moussine-Pouchkine, A., Affaton, P., Trompette, R., Bellion, Y., 1990. Cover sequences of the West African Craton. In: Dallmeyer, R.D., Lécorché, J.P. (Eds.), The West African Orogens and Circum-Atlantic Correlatives. Springer, Berlin, pp. 65–82.

Beuf, S., Biju-Duval, B., De Charpal, O., Rognon, P., Gariel, O., Bennacef, A., 1971. Les grès du Paléozoïque inférieur au Sahara. Institut Français du Pétrole, Technip, Paris.

Biju-Duval, B., Deynoux, M., Rognon, P., 1981. Late Ordovician tillites of the Central Sahara. In: Hambrey, M.J., Harland, W.B. (Eds.), Earth's Pre-Pleistocene Glacial Record. Cambridge Univ. Press, Cambridge. pp. 99–107.

Bjørlykke, K., 1985. Glaciations, preservation of their sedimentary record and sea-level changes – A discussion based on the Late Precambrian and Lower Palaeozoic sequence in Norway. Palaeogeogr. Palaeoclimatol. Palaeoecol. 51, 197–207.

Boulton, G.S, 1986. Push-moraines and glacier-contact fans in marine and terrestrial environments. Sedimentology 33, 677–698.

Boulton, G.S, 1996. Theory of glacial erosion, transport and deposition as a consequence of subglacial sediment deformation. J. Glaciol. 42, 43–62.

Brenchley, P.J., 1988. Environmental changes close to the Ordovician–Silurian boundary. Bull. Br. Mus. Nat. Hist. (Geol.) 43, 377–385.

Brenchley, P.J., Storch, P., 1989. Environmental changes in the Hirnantian (upper Ordovician) of the Prague Basin, Czechoslovakia. Geol. J. 24, 165–181.

Brenchley, P.J., Romano, M., Young, T.P., Storch, P., 1991. Hirnantian glaciomarine diamictites – evidence for the spread of glaciation and its effect on Upper Ordovician faunas. In: Barnes, C.R., Williams, S.H. (Eds.), Advances in Ordovician Geology. Geol. Surv. Can. Pap. 90-9, pp. 325–336.

Brenchley, P.J., Marshall, J.D., Carden, G.A.F., Robertson, D.B.R., Long, D.G.F., Meidla, T., Hints, L., Anderson, T.F., 1994. Bathymetric and isotopic evidence for a short-lived Late Ordovician glaciation in a greenhouse period. Geology 22, 295–298.

Caputo, M.V., 1998. Ordovician–Silurian glaciations and global sea-level changes. Bull. N.Y. State Mus. 491, 15–25.

Caputo, M.V., Crowell, J.C., 1985. Migration of glacial centers across Gondwanaland during Paleozoic Era. Geol. Soc. Am. Bull. 96, 1020–1036.

Collinson, J.D., Bevins, R.E., Clemmensen, L.B., 1989. Post-glacial mass flow and associated deposits preserved in pa-

laeovalleys: the Late Precambrian Morænesø Formation, North Greenland. Medd. Grønland Geosci. 21, 3–26.
Crowell, J.C., 1999. Pre-Mesozoic Ice Ages: Their Bearing on Understanding the Climate System. Mem. Geol. Soc. Am. 192, 106 pp.
Dean, W.T., Monod, O., 1990. Revised stratigraphy and relationships of Lower Palaeozoic rocks, eastern Taurus Mountains, south central Turkey. Geol. Mag. 127, 333–347.
Destombes, J., Hollard, H., Willefert, S., 1985. Lower Palaeozoic rocks of Morocco. In: Holland, C.H (Ed.), Lower Paleozoic Rocks of Northwest and West-Central Africa. Wiley, New York, pp. 91–336.
Deynoux, M., 1980. Les formations glaciaires du Précambrien terminal et de la fin de l'Ordovicien en Afrique de l'Ouest. Deux exemples de glaciation d'inlandsis sur une plate-forme stable. Trav. Lab. Sci. Terre St.Jérome, Marseille, 17.
Deynoux, M., 1985. Terrestrial or waterlain glacial diamictites? Three case studies from the Late Precambrian and Late Ordovician glacial drifts in West Africa. Palaeogeogr. Palaeoclimatol. Palaeoecol. 51, 97–141.
Deynoux, M., Trompette, R., 1981. Late Ordovician tillites of the Taoudeni Basin, West Africa. In: Hambrey, M.J., Harland, W.B. (Eds.), Earth's Pre-Pleistocene Glacial Record. Cambridge Univ. Press, Cambridge, pp. 89–96.
Deynoux, M., Sougy, J., Trompette, R., 1985. Lower Paleozoic rocks of West Africa and the western part of Central Africa. In: Holland, C.H. (Ed.), Lower Paleozoic Rocks of Northwest and West-Central Africa. Wiley, New York, pp. 337–495.
Dia, O., 1984. La chaîne panafricaine et hercynienne des Mauritanides face au bassin Protérozoïque à Dévonien de Taoudéni dans le secteur clef de Mejeria (Taganet, sud RIM). Lithostratigraphie et tectonique. Un exemple de tectonique tangentielle superposée. Thesis, Marseille.
Dia, O., Sougy, J., Trompette, R., 1969. Discordance de ravinement et discordance angulaire dans le Cambro–Ordovicien de la région de Mejeria (Taganet occidental, Mauritanie). Bull. Soc. Géol. Fr. 11, 207–221.
Eyles, N., 1993. Earth's glacial record and its tectonic setting. Earth-Sci. Rev. 35, 1–248.
Finney, S.C., Berry, W.B.N., Cooper, J.D., Ripperdan, R.L., Sweet, W.C., Jacobson, S.R., Soufiane, A., Achab, A., Noble, P.J., 1999. Late Ordovician mass extinction: A new perspective from stratigraphic sections in central Nevada. Geology 27, 215–218.
Ghienne, J.-F., 1998. Modalités d'enregistrement d'une glaciation ancienne; exemple de la glaciation fini-ordovicienne sur la plate-forme nord-gondwanienne en Afrique de l'Ouest. Ph.D. Thesis, Université L. Pasteur, Strasbourg.
Ghienne, J.-F., Deynoux, M., 1998. Large-scale channel fill structures in Late Ordovician glacial deposits in Mauritania, Western Africa. Sediment. Geol. 119, 141–159.
Ghienne, J.-F., Monod, O., Dean, W., Kozlu, H., Gûnay, Y., 2002. The Late Ordovician glaciomarine succession in Southern Turkey. Abstracts 16th International Sedimentological Congress, Rand University, Johannesburg, pp. 114–115.
Gilbert, R., 1990. Rafting in glaciomarine environments. In: Dowdeswell, J.A., Scourse, J.D. (Eds.), Glaciomarine Environments: Processes and Sediments. Geol. Soc. Spec. Publ. 53, pp. 105–120.
Grahn, Y., Caputo, M.V., 1992. Early silurian glaciations in Brazil. Palaeogeogr. Palaeoclimatol. Palaeoecol. 99, 9–15.
Grahn, Y., Caputo, M.V., 1994. Late Ordovician evolution of the intracratonic basins in north-west Gondwanaland. Geol. Rundsch. 83, 665–668.
Grahn, Y., Paris, F., 1992. Age and correlation of the Trombetas group, Amazonian basin, Brasil. Rev. Micropaleontol. 35, 20–32.
Hambrey, M.J., 1985. The Late Ordovician–Early Silurian glacial period. Palaeogeogr. Palaeoclimatol. Palaeoecol. 51, 273–289.
Hambrey, M.J., Huddart, D., 1995. Englacial and proglacial glaciotectonic processes at the snout of a thermally complex glacier in Svalbard. J. Quat. Sci. 10, 313–326.
Harland, W.B., Amstrong, R.L., Cox, A.V., Craig, L.E., Smith, A.G., Smith, D.G., 1990. A Geological Time Scale. Cambridge Univ. Press, Cambridge.
Hiller, N., 1992. The Ordovician System in South Africa: a review. In: Webby, L. (Ed.), Global Perspectives on Ordovician Geology. Balkema, Rotterdam, pp. 473–485.
Johnson, M.E., 1996. Stable cratonic sequences and a standard for Silurian eustasy. Geol. Soc. Am. Spec. Pap. 306, 203–211.
Kehew, A.H., Lord, M.L., 1986. Origin and large-scale erosional features of glacial-lake spillways in the northern Great Plains. Geol. Soc. Am. Bull. 97, 162–177.
Kent, D.V., Van Der Voo, R., 1990. Palaeozoic palaeogeography from palaeomagnetism of the Atlantic-bordering continents. In: McKerrow, W.S., Scotese, C.R. (Eds.), Paleozoic Palaeography and Biogeography. Geol. Soc. Lond. Mem. 12, pp. 49–56.
Klitzsch, E., 1981. Lower Palaeozoic rocks of Libya, Egypt, and Sudan. In: Holland, C.H. (Ed.), Lower Palaeozoic of the Middle East, Eastern and Southern Africa, and Antarctica. Wiley, New York, pp. 131–163.
Leckie, D.A., 1988. Wave-formed, coarse-grained ripples and their relationship to hummocky cross-stratification. J. Sediment. Petrol. 58, 607–622.
Legrand, P., 1985. Lower Palaeozoic rocks of Algeria. In: Holland, C.H (Ed.), Lower Paleozoic Rocks of Northwest and West-Central Africa. Wiley, New York, pp. 5–89.
Legrand, P., 1988. The Ordovician–Silurian boundary in the Algerian Sahara. Bull. Br. Mus. Nat. Hist. (Geol.) 43, 139–143.
Legrand, P., 1993. Graptolites d'âge ashgillien dans la région de Chirfa (Djado, République du Niger). Bull. Centre Rech. Explor.-Prod. Elf Aquitaine 17, 435–442.
Leone, F., Loi, A., Pillola, G.L., 1995. The post-sardic Ordovician sequence in south-western Sardinia. Guide Book, 6th Paleobenthos International Symposium, Cagliari University.
LePage, A., 1986. La lithostratigraphie des grandes zones structurales des Mauritanides, entre le 14e et le 16e parallèle

Nord (Sénégal Oriental et Rép, Isl. de Mauritanie). J. Afr. Earth Sci. 5, 119–134.

Long, D.G.F, 1993. Limits on late Ordovician eustatic sea-level change from carbonate shelf sequences: an example from Anticosti Island, Quebec. Spec. Publ. Int. Assoc. Sediment. 18, 487–499.

Lønne, I., 1995. Sedimentary facies and depositional architecture of ice-contact glaciomarine systems. Sediment. Geol. 98, 13–43.

Lüning, S., Craig, J., Loydell, D.K., Storch, P., Fitches, B., 2000. Lower Silurian 'hot shales' in North Africa and Arabia: regional distribution and depositional model. Earth-Sci. Rev. 49, 121–200.

Marchand, J., Trompette, R., Sougy, J., 1972. Etude photogéologique de la région El Mreiti – Mejahouda – Agaraktem (Mauritanie). Trav. Lab. Sci. Terre, St Jérome, Marseille, 21.

Martinez, M., 1998. Late Ordovician glacial deposits of northwest Argentina: new evidence from the Mecoyita Formation, Santa Victoria Range. J. Afr. Earth Sci. 27, 136–137.

Massa, D., 1988. Paléozoïque de Libye occidentale. Stratigraphie et Paléogéographie. Thesis, Université de Nice.

Matsch, C.L., Ojakangas, R.W., 1991. Comparisons in depositional style of 'polar' and 'temperate' glacial ice; Late Paleozoic Whiteout Conglomerate (West Antarctica) and late Proterozoic Mineral Fork Formation (Utah). Geol. Soc. Am. Spec. Pap. 261, 191–206.

McDougall, N., Martin, M., 2000. Facies models and sequence stratigraphy of Upper Ordovician outcrops in the Murzuq Basin, SW Libya. In: Sola, M.A., Worsley, D. (Eds.), Geological Exploration in Murzuq Basin. Elsevier, pp. 223–236.

McGillivray, G.J., Husseini, M., 1992. The Paleozoic petroleum geology of Central Saudi Arabia. Am. Assoc. Pet. Geol. Bull. 76, 1473–1490.

Nummedal, D., Swift, D.P.J., 1987. Transgressive stratigraphy at sequence bounding conformities – some principles derived from Holocene and Cretaceous examples. In: Nummedal, D. (Ed.), Sea-level Fluctuation and Coastal Evolution. Soc. Econ. Paleontol. Miner., Spec. Publ. 41, pp. 241–260.

Nystuen, J.P., 1985. Facies and preservation of glacigenic sequences from the Varanger Ice Age in Scandinavia and others parts of the North Atlantic region. Palaeogeogr. Palaeoclimatol. Palaeoecol. 51, 209–229.

Ouanaimi, H., 1998. Le passage Ordovicien–Silurien à Tizi n'Tichka (Haut-Atlas, Maroc): variations du niveau marin. C.R. Acad. Sci. Paris 326, 65–70.

Paris, F., Elaouad-Debbaj, Z., Jaglin, J.C., Massa, D., Oulebsir, L., 1995a. Chitinozoans and Late Ordovician glacial events on Gondwanaland. In: Cooper, J.D, Droser, M.L., Finney, S. (Eds.), Ordovician Odyssey. Short papers Seventh International Symposium on the Ordovician System, SEPM, Fullerton, CA, pp. 171–176.

Paris, F., Verniers, J., Al-Hajri, S., Al-Tayyar, H., 1995b. Biostratigraphy and palaeogeographic affinities of early Silurian chitinozoans from Saudi Arabia. Rev. Palaeobot. Palynol. 89, 75–90.

Paris, F., Deynoux, M., Ghienne, J.-F., 1998. Chitinozoaires de la limite Ordovicien–Silurien en Mauritanie. C.R. Acad. Sci. Paris 326, 499–504.

Paris, F., Bourahrouh, A., Hérissé, A.L., 2000. The effects of the final stages of the Late Ordovician glaciation on marine palynomorhps (chitinozoans, acritarchs, leiospheres) in well Nl-2 (NE Algerian Sahara). Rev. Palaeobot. Palynol. 113, 87–104.

Robardet, M., Doré, F., 1988. The Late Ordovician diamictic formations from southwestern Europe: North-Gondwanaland glaciomarine deposits. Palaeogeogr. Palaeoclimatol. Palaeoecol. 66, 19–31.

Rose, J., 1987. Drumlins as part of a glacier continuum. In: Menzies, J., Rose, J. (Eds.), Drumlin Symposium. Balkema, Rotterdam, pp. 103–116.

Rudoy, A.N., Baker, V.R., 1993. Sedimentary effects of cataclasmic late Pleistocene glacial outburst flooding, Altay Mountains, Siberia. Sediment. Geol. 85, 53–62.

Russell, A.J., Knudsen, O., 1999. An ice-contact rhythmite succession deposited during the November 1996 catastrophic outburst flood (jökulhlaup), Skeiðarárjökull, Iceland. Sediment. Geol. 127, 1–10.

Shanley, K.W., McCabe, P.J., 1994. Perspectives on the sequence stratigraphy of continental strata. Am. Assoc. Pet. Geol. Bull. 78, 544–568.

Scotese, C.R., Barett, S.F., 1990. Gondwanaland's movement over the South Pole during the Paleozoic: Evidence from lithological indicators of climate. In: McKerrow, W.S., Scotese, C.R. (Eds.), Paleozoic Palaeography and Biogeography. Geol. Soc. Lond. Mem. 12, pp. 65–85.

Smith, A.G., 1997. Estimates of the Earth's spin (geographic) axis relative to Gondwanaland from glacial sediments and palaeomagnetism. Earth-Sci. Rev. 42, 161–169.

Sougy, J., Lécorché, J.-P., 1963. Sur la nature glaciaire de la base de la série de Garat el Hamoueïd (Zemmour, Mauritanie septentrionale). C.R. Acad. Sci. Paris 256, 4471–4474.

Storch, P., 1990. Upper Ordovician–lower Silurian sequences of the Bohemian Massif, central Europe. Geol. Mag. 127, 225–239.

Sutcliffe, O.E., Dowdeswell, J.A., Whittington, R.J., Theron, J.N., Craig, J., 2000. Calibrating the Late Ordovician glaciation and mass extinction by the eccentricity cycles of Earth's orbit. Geology 28, 967–970.

Trompette, R., 1973. Le Précambrien supérieur et le Paléozoïque inférieur de l' Adrar de Mauritanie (bordure occidentale du bassin de Taoudeni, Afrique de l'Ouest). Un exemple de sédimentation de craton. Etude stratigraphique et sédimentologique. Thesis, Université Aix-Marseille.

Underwood, C.J., Crowley, S.F., Marshall, J.D., Brenchley, P.J., 1997. High resolution carbon isotope stratigraphy of the basal Silurian stratotype (Dob's Linn, Scotland) and its global correlation. J. Geol. Soc. Lond. 154, 709–718.

Underwood, C.J., Deynoux, M., Ghienne, J.-F., 1998. High palaeolatitude recovery of graptolites faunas after the Hirnantian (top Ordovician) extinction event. Palaeogeogr. Palaeoclimatol. Palaeoecol. 142, 91–105.

Van Der Wateren, F.M., 1995. Structural geology and sedi-

mentology of push moraines. Processes of soft sediment deformation on a glacial environment and the distribution of glaciotectonic styles. Meded. Rijks Geol. Dienst, Geol. Survey of The Netherlands, Haarlem.

Vaslet, D., 1990. Upper Ordovician glacial deposits in Saudi Arabia. Episodes 13, 147–161.

Visser, J.N.J., 1990. Glacial bedforms at the base of the Permo–Carboniferous Dwyka Formation along the western margin of the Karoo Basin, South Africa. Sedimentology 37, 231–245.

Wang, K., Chatterton, B.D.E., Wang, Y., 1997. An organic carbon isotope record of Late Ordovician to Early Silurian marine sedimentary rocks, Yangtze Sea, South China: Implications for CO_2 changes during the Hirnantian glaciation. Palaeogeogr. Palaeoclimatol. Palaeoecol. 132, 147–158.

Willefert, S., 1988. The Ordovician–Silurian boundary in Mauritania. Bull. Br. Mus. Nat. Hist. (Geol.) 43, 177–182.

Williams, G.E., 1991. Milankovitch-band cyclicity in bedded halite deposits contemporaneous with Late Ordovician–Early Silurian glaciation, Canning Basin, Western Australia. Earth Planet. Sci. Lett. 103, 143–155.

Wood, M.L., Ethridge, F.G., 1988. Sedimentology and architecture of Gilbert and mouth bar-type fan deltas, Paradox Basin, Colorado. In: Nemec, W., Steel, R.J. (Eds.), Fan Deltas; Sedimentology and Tectonic Setting. Blackie, Glasgow, pp. 251–263.

Zhang, T., Kershaw, S., Wan, Y., Lan, G., 2000. Geochimical and facies evidence for palaeoenvironmental change during the Late Ordovician Hirnantian glaciation in South Sichuan Province, China. Glob. Planet. Change 24, 133–152.

Zielinski, T., Van Loon, A.J., 1996. Characteristics and genesis of moraine-derived flowtill varieties. Sediment. Geol. 101, 119–143.

The Late Ordovician glacial sedimentary system of the North Gondwana platform

JEAN-FRANCOIS GHIENNE*, DANIEL PAUL LE HERON*†, JULIEN MOREAU*, MICHAEL DENIS‡ *and* MAX DEYNOUX*

**Ecole et Observatoire des Sciences de la Terre, Centre de Géochimie de la surface, CNRS-UMR 7517, 1 rue Blessig, 67084 Strasbourg, France (e-mail: ghienne@illite.u-strasbg.fr)*
†Institut für Geologie, Leibniz Universität Hannover, Callinstrasse 30, D-30167, Germany
‡UMR 5561, Biogéosciences, Université de Bourgogne, 6 Bd Gabriel, 21 000 Dijon, France

ABSTRACT

The Late Ordovician (Hirnantian) glaciation is examined through the North Gondwana record. This domain extended from southern high palaeo-latitudes (southeastern Mauritania, Niger) to northern lower palaeo-latitudes (Morocco, Turkey) and covered a more than 4000 km-wide section perpendicular to ice-flow lines. A major mid-Hirnantian deglaciation event subdividing the Hirnantian glaciation in two first-order cycles is recognised. As best illustrated by the glacial record in western Libya, each cycle comprises 2–3 glacial phases separated by ice-front retreats several hundreds kilometres to the south. From ice-proximal to ice-distal regions, the number of glacial surfaces differentiates (i) a continental interior with post-glacial reworking of the glacial surfaces), (ii) a glaciated continental shelf that is subdivided into inner (1–2 surfaces), middle (2–5 surfaces) and outer (a single surface related to the glacial maximum) glaciated shelves, and (iii) the non-glaciated shelf. Ice-stream-generated glacial troughs, 50–200 km in width, cross-cut these domains. These troughs are zones of preferential glacial erosion and subsequent sediment accumulation. A glacial depositional sequence, bounded by two glacial erosion surfaces, records one glacial phase. The position either within or outside a glacial trough controls the stratigraphic architecture of a glacial sequence. Glaciomarine outwash diamictites are developed at or near the maximum position of the ice-front. During ice-sheet recession, and in an ice-stream-generated trough, a relatively thin sediment cover blankets the foredeepened erosion surface. An initial rapid ice-sheet withdrawal is inferred. Marine-terminating ice fronts then evolve later into more slowly retreating, land-terminating ice fronts. In adjacent inter-stream areas where a more gradual ice-sheet recession occurred, fluvio-glacial deposits prevailed. The progradation of a delta-shelf system, coeval with fluvial aggradation, that may be locally interrupted by a period of isostatic rebound, characterises the late glacial retreat to interglacial conditions. This model should facilitate the sequence stratigraphic interpretation of Late Ordovician glacial deposits and other ancient glacial successions.

Keywords Glacial record, Hirnantian, North Africa, ice stream, sequence stratigraphy.

INTRODUCTION

The Late Ordovician glacial record comprises extensive exposures distributed over the former North Gondwana cratonic platform. The size of this domain is >1500 km from south to north (in present-day coordinates), and extended from Mauritania to Arabia. Southern regions were positioned near the ice centres while the northern part of the platform was located at lower palaeo-latitudes (Fig. 1). During the 1960s–1980s, studies in Morocco (Destombes, 1968a, Hamoumi, 1988), Algeria (Beuf *et al.*, 1971), Libya (Klitzsch, 1981; Massa, 1988), Mauritania (Deynoux, 1980; 1985; Deynoux and Trompette, 1981) and Arabia (McLure, 1978; Vaslet, 1990; McGillivray and Husseini, 1992)

In : Hambrey, M., Christoffersen, P., Glasser, N., Janssen, P., Hubbard, B. and Siegert, M. (eds.) Glacial Sedimentary Processes and Products. Special Publication n°39 (2007), International Association of Sedimentologists, Blackwells, Oxford, pp. 295-319.

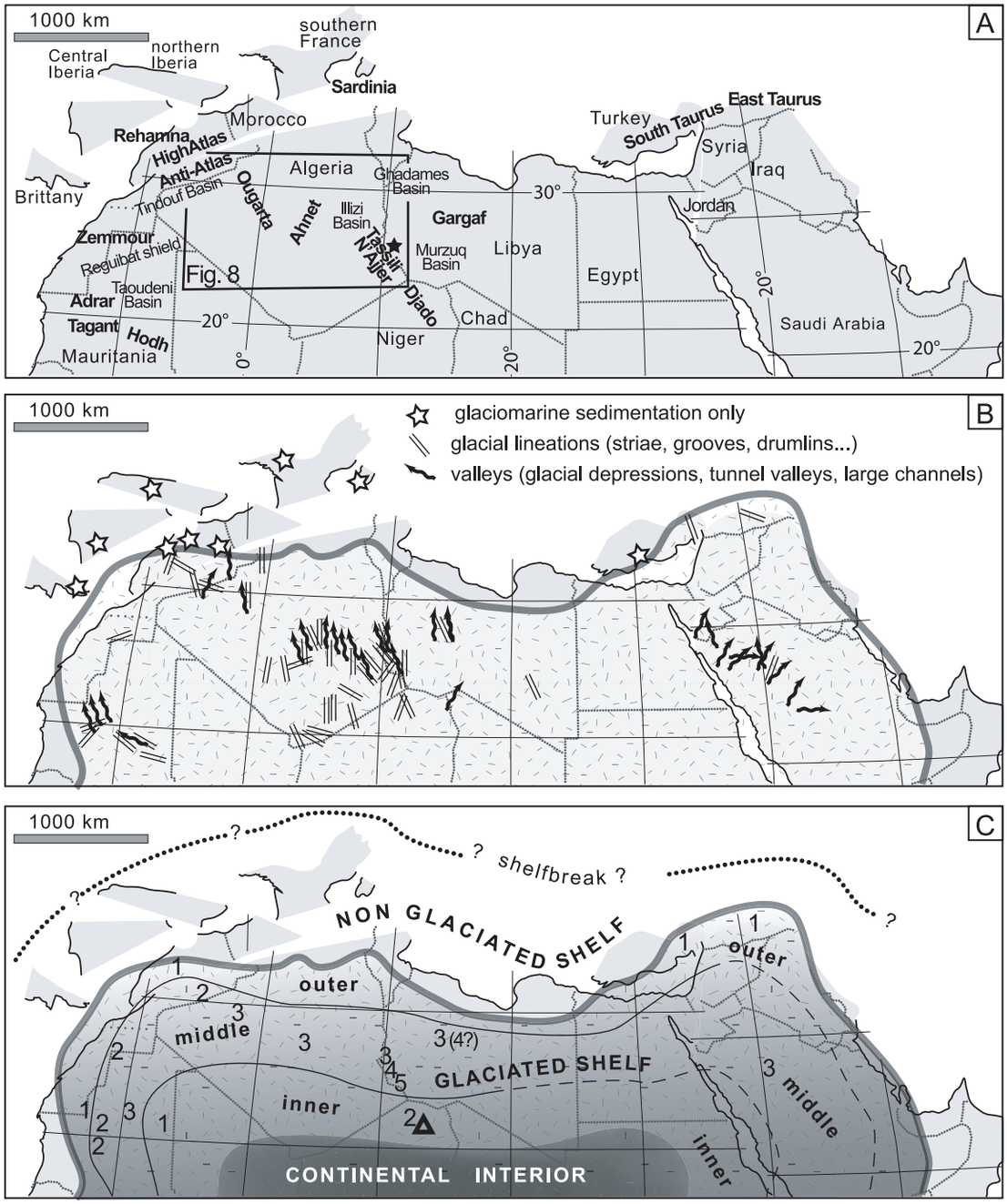

Fig. 1 The North Gondwana platform during the Hirnantian glacial event. (A) Main names cited in the text (see also Fig. 8). Names in bold indicates study areas comprising the data base. The black star locates the pre-glacial (Late Ordovician) trilobite-bearing lonestone found within the syn-glacial strata. (B) Location of areas that experienced grounded ice (glacial lineations and palaeovalleys) and those that have never been glaciated (glaciomarine sediments only). The outlined surface corresponds to the envelope of the ice fronts during the Hirnantian glacial maximum (modified from Deynoux and Ghienne, 2004). (C) Subdivisions of the glaciated platform in five domains (name in bold) based on the number of glacial surfaces preserved. The location of the shelfbreak (continental margin) is not known but was located to the north of the study area, beyond the maximum ice fronts. The Δ locates mid-Hirnantian graptolite-bearing marine facies in the Djado area, suggesting the marine limit of the associated deglaciation was located to the south of this point.

showed the extent, diversity and complexity of the syn-glacial strata. Renewed interest arose in the 1990s, when oil companies recognised the association of syn-glacial strata (reservoir rocks) with lower Silurian shales (source rocks) as one of the most significant plays in the North African Lower Palaeozoic succession (Lüning *et al.*, 2000). Recent work has included detailed field and subsurface studies conducted in Mauritania (Ghienne, 1998; Ghienne and Deynoux, 1998; Ghienne, 2003), Morocco (Ouanaimi, 1998; Sutcliffe *et al.*, 2000, 2001; Le Heron *et al.*, 2007), Algeria (Hirst *et al.*, 2002; Eschard *et al.*, 2005), Niger (Denis *et al.*, 2007), Libya (McDougall and Martin, 2000; Smart, 2000; Ghienne *et al.*, 2003; Le Heron *et al.*, 2004; El-ghali, 2005; Moreau, 2005), Jordan (Abed *et al.*, 1993; Powell *et al.*, 1994; Turner *et al.*, 2005), Saudi Arabia (Senalp and Al-Laboun, 2000) and the Horn of Africa (Ethiopia and Eritrea, Kumpulainen, 2005). In addition to these areas, studies have also been undertaken around the northern Gondwana periphery to better provide an overall understanding of the glacial record as a whole, e.g. in Sardinia (Leone *et al.*, 1995; Ghienne *et al.*, 2000) and in Turkey (Monod *et al.*, 2003).

This paper proposes a large-scale reconstruction of the North Gondwana platform in present-day North and West Africa during the Late Ordovician glaciation. The number of glacial advance-retreat events recorded from the near-polar ice centre to lower palaeo-latitudes, and the presence or absence of ice-stream tracks, are used to subdivide the platform into a number of domains characterised by a specific palaeo-glaciological evolution, particularly subglacial processes, stratigraphic architecture and depositional environments. Finally, a conceptual glacial depositional sequence that could be expected within a typical glacial advance-retreat event is depicted. Such a sequence will form the basis for a more robust stratigraphic analysis of the Late Ordovician glacial record and more generally for ancient glacial successions.

PRE-GLACIAL SETTING

No evidence for Late Ordovician glacial sediments older than Hirnantian (Fig. 2) has thus far been found in North or West Africa. However, this does not preclude the possibility that glaciers grew

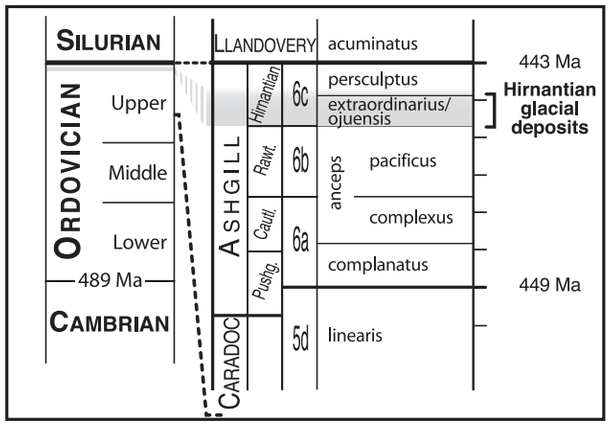

Fig. 2 Late Ordovician stratigraphic chart modified from Webby *et al.* (2004) showing the time range corresponding to Hirnantian glacial event.

elsewhere on Gondwana both before and after the Hirnantian. Saltzman and Young (2005) proposed a glacio-eustatic lowstand during the early Late Ordovician (Fig. 2) and, in South America, glacial deposits are recognized in the Silurian (Grahn and Caputo, 1992; Caputo, 1998). Ghienne (2003) suggested that the Hirnantian simply reflected a continent-wide ice maximum, during which ice sheets reached the North and West African sedimentary basins where their glacial sedimentary record could be preserved. In this paper, pre-glacial time is defined as the period preceding the Hirnantian, i.e. the Cambrian and Ordovician, including the main part of the Ashgill with the exception of the Hirnantian (Fig. 2). Le Heron *et al.* (2005) published a schematic lithostratigraphic summary of Hirnantian glaciogenic rocks across Africa and Arabia. A regional correlation scheme, including the names of the main pre-glacial and glacial formations in this huge region, is contained therein.

Geological setting

Late Ordovician glacial deposits rest on a Cambrian to Ordovician, clastic-dominated succession that has an off-shelf gradient towards the NNW (Boote *et al.*, 1998; Carr, 2002). These sediments progressively buried palaeorelief forms associated with both the late Neoproterozoic Panafrican Orogeny and Cambrian post-orogenic collapse/strike-slip basins. Early Ordovician tectonic activity uplifted

large areas such as the Taoudeni Basin and Reguibat shield, Central Algeria, Ahnet, Eastern Tassili and southern Taurus (e.g. Beuf *et al.*, 1971; Crossley and McDougall, 1998) (for location names, see Fig. 1A), resulting in deep erosion of earlier strata or reduced sedimentation on the highs during the Middle to Late Ordovician. Continuous sedimentation occurred in subsiding areas, e.g. the Tindouf Basin and Ougarta in Algeria, Ghadames Basin in Libya, eastern Taurus in Turkey. Here, a complete Ordovician succession is preserved (e.g. Boote *et al.*, 1998). High eustatic sea level in the Late Ordovician (Ross and Ross, 1992) resulted in the flooding of previously uplifted areas (e.g. easternmost Turkey, Dean & Monod, 1990). In Algeria, shallow-marine Ashgill facies are known in the south of the Ougarta Range (Legrand, 1985) and Ashgill carbonates are identified in drill holes as far south as the Illizi Basin (e.g. *Oued Ahara* borehole, unpublished data). In SW Libya, some dropstones in glaciomarine facies include trilobites (located in Fig. 1A), yielding an age close to the Caradoc-Ashgill boundary (W.T. Dean, pers. comm., 2003). These fauna, which probably derived from higher southern polar palaeolatitudes, imply a southwards-directed Late Ordovician transgression, which penetrated far south onto the platform. Transgressive deposits have been difficult to recognise owing to glacially related erosion, but are herein considered as key evidence for the flooding of the main part of the North Gondwana platform prior to the Hirnantian glacial event.

Subglacial substrate

As a consequence of this pre-glacial flooding, it is clear that a large part of the glaciated areas should have been characterised by subglacial soft-sediment conditions. If Ashgill siliciclastics were not lithified in Hirnantian time, it is surprising that much older deposits were also very poorly lithified at that time, as suggested by three sets of observations: sand injections, cross-sections of palaeovalleys and a sand-dominated glacial record. Firstly, sand injections in the form of pipes or undulating dykes occur beneath glacial erosion surfaces cut in sediments as old as Early Ordovician (>30 Ma before the Hirnantian glacial event) in the western Murzuq Basin. Secondly, cross-sections of palaeovalleys, either subglacially or fluvially formed, show low-angle margins, with slopes typically in the 1–10° range. These gradients are more compatible with erosion in soft material than in consolidated sediments. In addition, in the Ahnet area (south Algeria, Fig. 1A), palaeovalleys have a flat bottom coinciding with the basal unconformity of the Cambrian-Ordovician succession above the slightly metamorphosed late Neoproterozoic shales and sandstones. This suggests a clear contrast between the underlying metamorphosed basement and the overlying non- to poorly lithified sandy succession. Thirdly, the Late Ordovician glacial record is sand-dominated, with subordinate finer-grained, silt-dominated units. Glacial conglomerates contain clasts from Precambrian basement lithologies (granites, metasediments e.g. quartzite), but not from the underlying Cambro-Ordovician sandstones (Oujeft sandstones in Mauritania, Hamra Formation in Algeria, Ash Shabiyat or Haouaz formations in Libya), which can be recognised by abundant *Scolithos* burrows. Notwithstanding small inliers of crystalline basement or rare carbonate-cemented Ordovician strata, the evidence presented above suggests that Late Ordovician ice sheets grew and decayed on largely unconsolidated substrates.

RECOGNITION OF GLACIAL EROSION SURFACES

In the sand-dominated setting of the Late Ordovician glacial record, depths of glacial erosion range from 10 to 500 m (maximum erosion depths in Saudi Arabia, e.g. McGillivray and Husseini, 1992), and widths of glacially-cut depressions range from 10 m to >100 km. Erosional features form lineations, ovoid to elongated spoon-shaped depressions, straight to slightly sinuous channels and palaeovalleys, or basin-scale incisions. Criteria used to distinguish glacial erosion surfaces from fluvial or transgressive wave-ravinement surfaces include: large-scale morphologies, glaciotectonic structures and specific depositional features such as esker structures.

Depths of erosion greater than 100 m normally point towards subglacial processes (Fig. 3). If the erosion feature is relatively narrow (<5 km), tunnel valleys are inferred (Ghienne and Deynoux, 1998; Hirst *et al.*, 2002; Le Heron *et al.*, 2004)

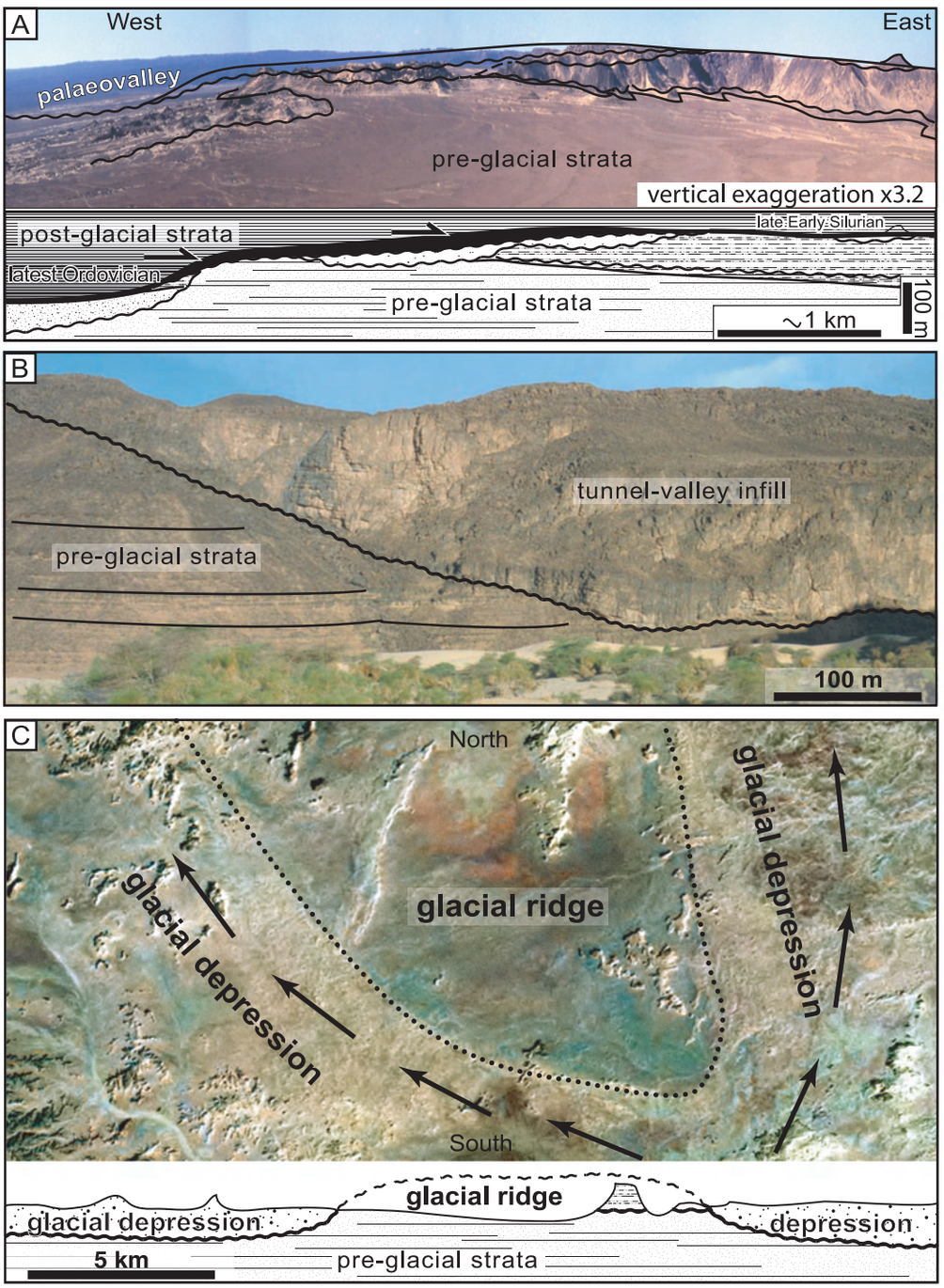

Fig. 3 Diversity in glacial erosion surfaces. (A) A wide palaeodepression within the Eastern Tassili n'Ajjer glacial trough (Ghat area, western Murzuq Basin, Libya) (view with vertical exaggeration, interpretation from field sections). Bounding surfaces of syn-glacial depositional units are gently dipping glacial erosion surfaces (wavy lines). The upper unit (in black) mainly represents a late to post glacial transgressive wedge, that reworked the latest glacial erosion surface (see also Fig. 5). The latest glacial palaeodepression was underfilled and post-glacial sediments progressively onlapped on the residual palaeotopography from the latest Ordovician to the Silurian (see also Fig. 9B). (B) An overfilled tunnel valley characterised by a narrow, steep-sided erosion surface (Adrar, Mauritania, modified from Ghienne and Deynoux, 1998). (C) Landsat image showing a glacial ridge (inverted topography, present-day lower area) with two adjacent palaeovalley-like depressions into a glacial trough (Tihemboka Arch, western Murzuq Basin).

(Fig. 3B). Conversely, basin-scale subglacial scours are inferred if the width is >50 km. In other circumstances, overdeepenings or the occurrence of erosional troughs that narrow in planform also suggest subglacial processes (Beuf *et al.*, 1971). However, the most reliable subglacial erosion surfaces are those associated with subglacial lineations. Subglacial lineations (mega-scale glacial lineations, flow-parallel and attenuated drumlins) are characterised by parallel bedforms, <100 m to >10 km in length, 1–30 m in height, with high elongation ratios (>10) (Moreau *et al.*, 2005) (Fig. 4 A, B and C). Most of them are erosional features cored by older sediments. Only the sediments directly beneath the sediment-ice interface are affected by intense glaciotectonic deformation (Deynoux and Ghienne, 2004, 2005).

The best outcrop-scale evidence for glacially cut erosion surfaces is preserved in the record of deformation structures formed beneath them as a combination of shear-induced and gravitational deformation structures within the sediment column. Glaciotectonic deformation includes all the deformation that can be linked with the subglacial shear zone. Structures or deposits resulting from processes at the ice-sediment interface (striae, grooves, lodgement till) are generally poorly preserved in the Late Ordovician glacial record (Deynoux and Ghienne, 2005; Le Heron *et al.*, 2005). Intraformational deformation structures are more readily preserved and are therefore most commonly observed. Soft-sediment intraformational striated surfaces (Fig. 4F) were formed at several metres in depth beneath the ice-sediment interface (Deynoux and Ghienne, 2004; Le Heron *et al.*, 2005). They are typically associated with intraformational grooves (Fig. 4D), drag and sheath folds (Fig. 4E), Riedel shears and water-escape structures. Intraformational striated surfaces are particularly well developed beneath mega-scale glacial lineations with which they are parallel. Deformation associated with glacial surfaces includes chaotic sandstone units ('grès bousculés' of Deynoux, 1980 and Deynoux and Ghienne, 2004), large-scale loading structures such as domes, cylindrical folds and sediment diapirs (Le Heron *et al.*, 2005), overturned fold and thrust-and-fold belts, 5–50 m high. However, the last may also occur in association with proglacial glaciotectonic processes, such as broadly arcuate belts, or with slide-generated structures.

HIRNANTIAN GLACIES CYCLES AND PHASES

It is established that the so-called Upper Ordovician syn-glacial strata in West and North Africa are, in fact, strictly Hirnantian in age (Destombes, 1968b; Destombes *et al.*, 1985; Paris *et al.*, 1995, 1998; Underwood *et al.*, 1998; Sutcliffe *et al.*, 2000). They are also time-equivalent with a significant isotopic excursion of global extent (Brenchley *et al.*, 2003). The Hirnantian is generally considered to have lasted less than 1 Ma, but the new Ordovician timescale suggests that it could have been as long as 2 Ma (Webby *et al.*, 2004) (Fig. 2). Within this time-slice, a number of glacial advances and subsequent retreats occurred (Ghienne, 2003). At present, the number, as well as the significance and extent, of each of these Hirnantian glacial events is not known, but is the subject of ongoing work. However, the comparison of the stratigraphic architecture of syn-glacial successions from distinct areas gives noteworthy temporal relationships.

Areas closest to the ice centre

Glacial erosion in the areas closest to the ice centre has resulted in reworking of pre-glacial sediments, and during later glacial phases, cannibalisation of the earlier glacial sequences. In these regions, geological mapping covering a minimum representative area of about 1000 km^2 has revealed several, laterally juxtaposed glacial erosion surfaces (Fig. 5) that generate a complex stratigraphic architecture (Ghienne, 2003; Ghienne *et al.*, 2003; Moreau, 2005).

Depositional sequences are bounded by subglacially-cut unconformities or correlative subaerial unconformities. These surfaces were formed regionally during major phases of glacial advance. Subaerial exposure commonly occurred beyond the ice front. Glacial depositional sequences, comprising a range of alluvial plain to shelf sediments (see below), were deposited on top of these surfaces during ice recession towards the south, and during ensuing interglacials. Four to five depositional sequences occur in Mauritania (Ghienne, 2003), Libya (Gargaf Uplift: Deynoux *et al.*, 2000; Le Heron, 2004; Ghienne *et al.*, 2003; western Murzuq Basin: Moreau, 2005; Moreau *et al.*, 2005; Le Heron *et al.*, 2006) and Jordan (Turner *et al.*, 2005).

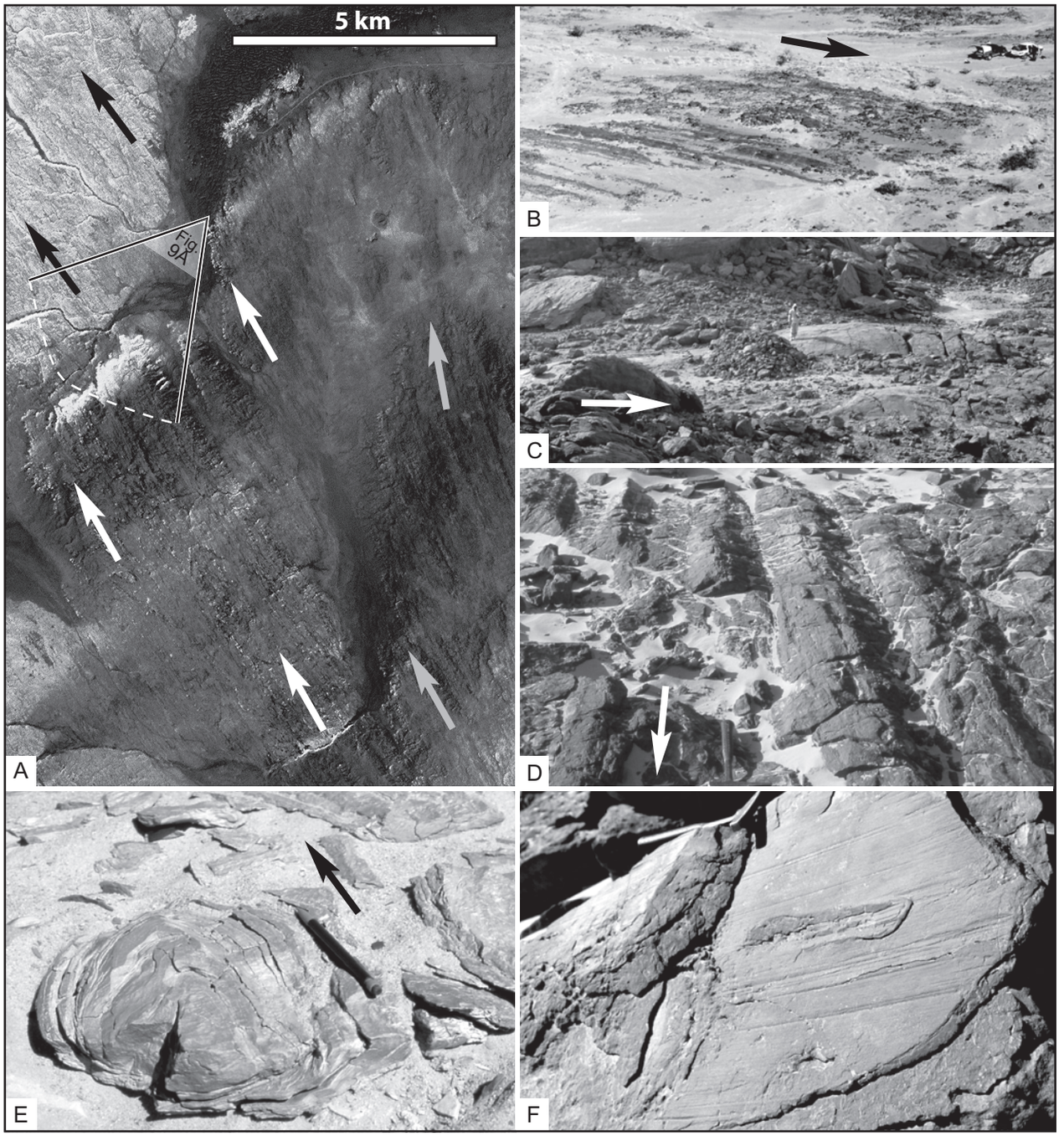

Fig. 4 Multi-scale glacial lineations associated with glacial erosion surfaces; all structures are in syn-glacial sands. Arrows show ice-flow orientation. (A) Landsat image showing three sets of ice-stream-generated mega-scale glacial lineations (Eastern Tassili n'Ajjer, Ghat area, western Murzuq Basin, Libya). (B) Glacial lineations (Tagant, Mauritania, cars for scale). (C) Asymmetrical glacial alignments shaped as a roche moutonnée (western Hodh, Mauritania, person for scale). (D) Grooves preserved within an intraformational subglacial shear zone (Ghat area, western Murzuq Basin, hammer for scale). (E) Sheath folds, the elongation of which is parallel to the shear orientation (Djado, Niger, pencil for scale). (F) Intraformational striae and ploughing structure in sandstones (Tihemboka Arch, western Murzuq Basin).

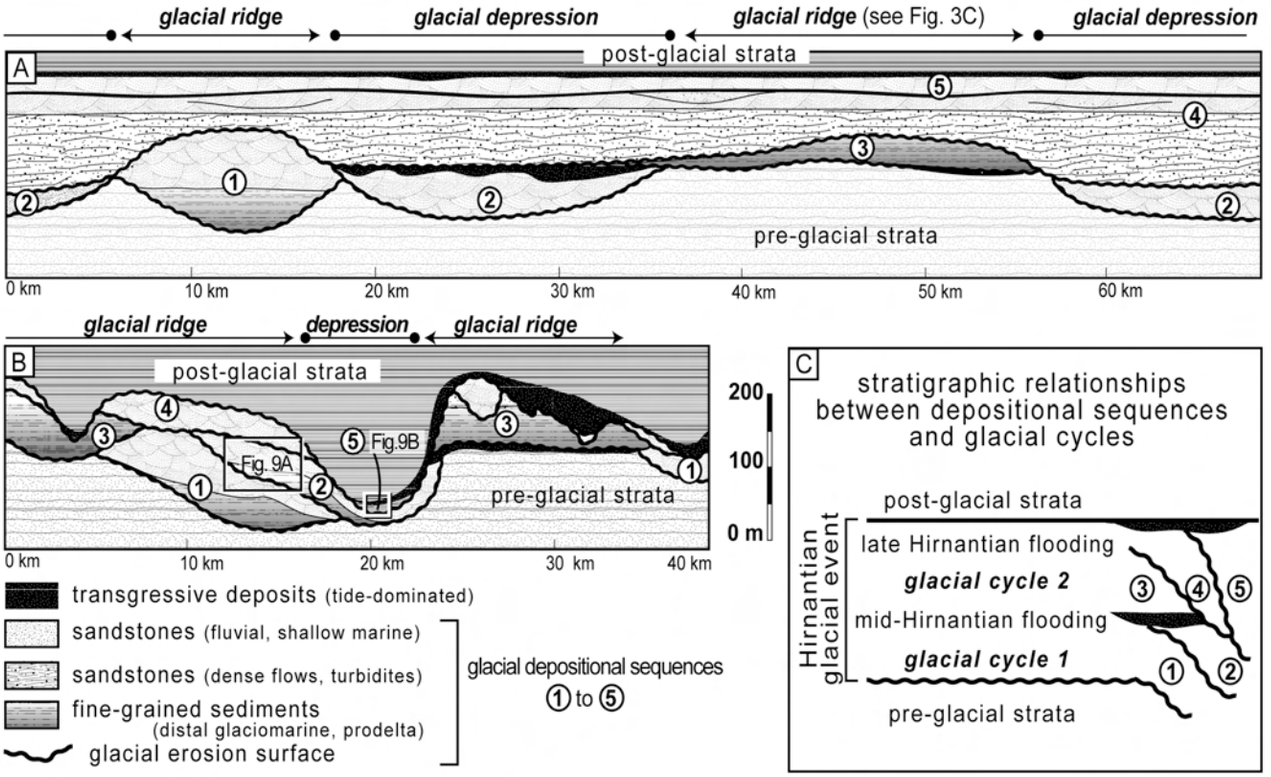

Fig. 5 Stratigraphic architecture of the syn-glacial strata in the western Murzuq Basin, Libya (profile location in Fig. 8A). Syn-glacial strata fill in palaeovalley-like depressions separated by glacial ridges. Indicated depressions and ridges were formed during the glacial maximum (fourth glacial phase). See text for more details about depositional facies. (A) Tihemboka Arch (26°10′N). (B) Eastern Tassili n'Ajjer, Ghat area (25°N). (C) Stratigraphic relationships and subdivision of the Hirnantian succession in two glacial cycles separated by the mid-Hirnantian deglaciation event, and five glacial phases of glacial advance and subsequent retreat.

In Mauritania and Libya, the most extensive ice sheet (e.g. phase 3 of Ghienne, 2003 in Mauritania; phase 4 of Moreau *et al.*, 2005 in western Libya) occurred after a major transgressive event characterised by the deposition of a tide-dominated succession (Fig. 5). This transgression is interpreted as a major phase of deglaciation within the Hirnantian.

Ice sheet margins

In ice-marginal areas, the effects of glacial erosion are less pronounced. Bounding surfaces of successive glacial depositional sequences are frequently preserved within a single vertical section (e.g. Monod *et al.*, 2003). A number of regressive-transgressive cycles are observed and interpreted in terms of glacioeustatically-driven rhythms (Leone *et al.*, 1995). These areas also preserve evidence of three to five glacial events, as best exemplified by the glacial record of Morocco (e.g. Le Heron *et al.*, 2007) where the Hirnantian strata can be divided into two glacial successions separated by a major transgression (Fig. 6). This major transgression is interpreted to correlate with the deglaciation event associated with tidal deposits in areas closest to the ice centres. Furthermore, in Turkey, evidence for subglacial processes is found at only one stratigraphic interval (Monod *et al.*, 2003) above well-developed transgressive deposits. These regionally correlatable features indicate that a key interglacial transgression was followed by the most widespread and significant phase of ice sheet advance across North Gondwana.

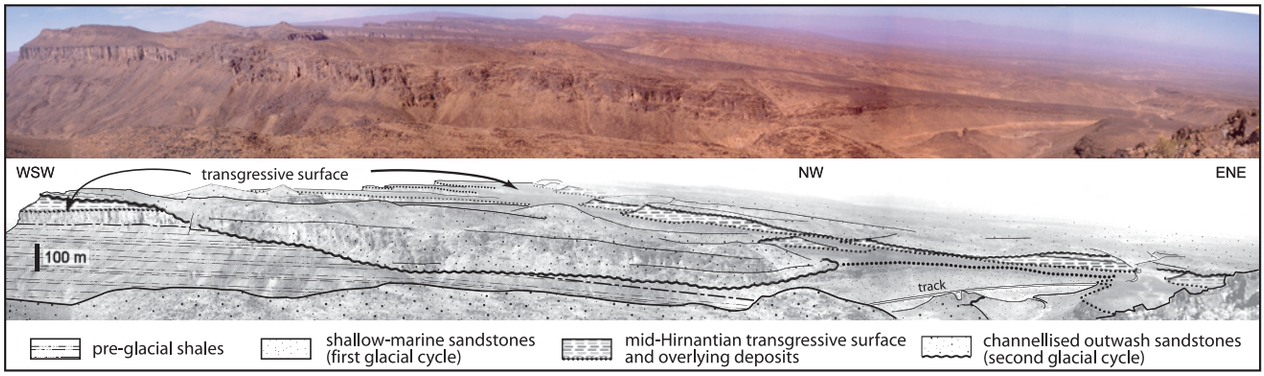

Fig. 6 The mid-Hirnantian deglaciation event in the Anti-Atlas (southern Morocco, northeast of Zagora). The glacially-related succession that mainly comprises shallow-marine and channellised outwash sandstones in contrast with pre-glacial shale-dominated sediments, is divided into two sedimentary wedges, separated by a major transgressive surface related to the mid-Hirnantian event. The panoramic view is c. 4 km in width in the foreground.

The Hirnantian glacial event: a multiphase glaciation

As glacial depositional sequences record major ice advances and retreats, they provide excellent potential for regional allostratigraphic correlation. The present understanding is that successive Hirnantian glacial events occurred within a single graptolite or chitinozoa biozone (*extraordinarius* and *elongata* Biozones respectively) (Paris *et al.*, 1995). Because no biostratigraphic subdivision is currently available, the best chronostratigraphic marker is probably the mid-Hirnantian transgression detailed above. This event of great amplitude is recorded as far south as the Djado area (northern Niger, location in Fig. 1C). Here, fauna-rich marine shales, originally considered as pre-Hirnantian strata (Legrand, 1993), and now attributed to the *extraordinarius* Biozone (P. Storch, pers. comm., 2004) were deposited between two major glacial erosion surfaces (Denis *et al.*, 2007). These data imply that the transgression advanced deep into North Africa at least within erosional troughs. This transgression is also recognised in non-glaciated area such as Sardinia (e.g. Storch & Leone, 2003).

This transgressive interval, coeval with a major deglaciation event, subdivides the Hirnantian into two first-order glacial cycles (Sutcliffe *et al.*, 2000) (Fig. 5C). Each cycle includes a limited number of glacial phases, the correlation of which throughout the North Gondwana is at present more controversial. At least two glacial phases are recognised within both the first (early Hirnantian) and the second (late Hirnantian) glacial cycles. Major ice recessions (~500 km) occurred between two successive phases, to compare with the mid-Hirnantian deglaciation associated with ice-front retreats >1000 km, possibly much more (Moreau, 2005).

Ice sheet size: the glacial maximum

Accurate reconstruction of pre-Pleistocene ice sheets, and the demonstration of synchronous, continent-wide ice fronts, is not straightforward. The size of both Permo-Carboniferous (Eyles *et al.*, 2003) and Neoproterozoic (Eyles and Januszack, 2004) ice sheets has recently been challenged, because their size may have been affected by enhanced polar wander or rates of rift propagation. Even assuming a maximum duration for the Hirnantian of 2 Ma (Webby *et al.*, 2004), and although the opening of the Palaeotethys (rifting of the Hun superterrane of Stampfli and Borel, 2002) occurred in Late Ordovician time, we argue here that these processes have not had a substantial impact on Hirnantian ice-sheet reconstructions. Synchronous growth of ice sheets, at least during the most protracted phase of glaciation, was likely from Mauritania to Turkey. This stands in contrast to Permo-Carboniferous centres of glaciation, which waxed and waned asynchronously over an interval of c. 55 Ma (Eyles *et al.*, 2003).

A reconstruction of the maximum size of the West Gondwana ice sheets, based on the occurrence of a regionally correlatable glacial erosion surface

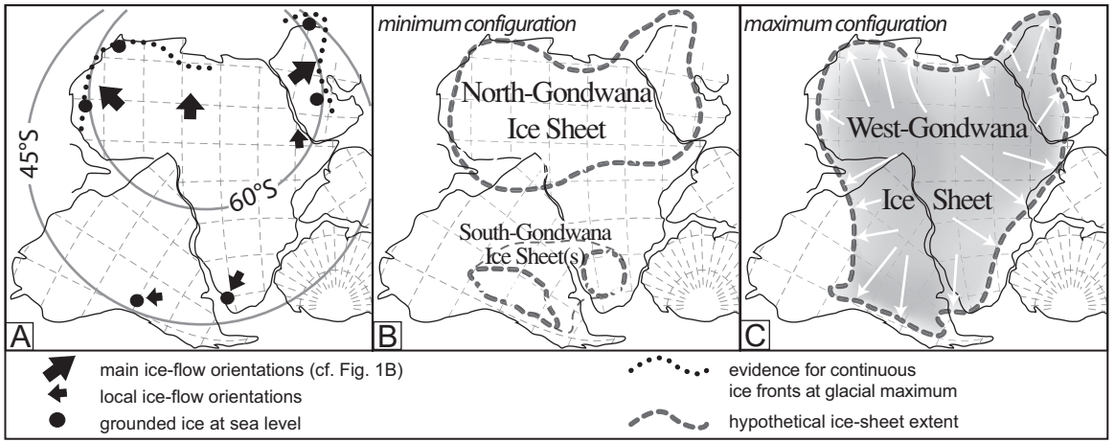

Fig. 7 The extent of the Late Ordovician glaciation. (A) Locations of identified subglacial deformation zones in the more distant areas from the ice centres. On the North Gondwana platform, these are from west to east: Tagant (western Mauritania), Rehamna (northern Morocco), Eastern Taurus (south-eastern Turkey) and Central Arabia. These four locations were glacierised at the Hirnantian glacial maximum, implying that grounded ice occurred at sea level close to the 60°S parallel. To include glacial successions from South America and South Africa (potentially of Hirnantian age) implies grounded ice occurring at sea level within the 45°S parallel. (B) The minimum-sized Hirnantian ice sheets, with a large North Gondwana Ice Sheet, and possibly penecontemporaneous subordinate ice centres in South America (linked with a pre-cordilleran setting) and South Africa, which may have coalesced together. (C) The maximum-sized Hirnantian West-Gondwana Ice Sheet, assuming fully coalescent synchronous glaciers.

following the major mid-Hirnantian interglacial, is presented in Fig. 7A. Ice-front migrations from place-to-place during the same glacial event (e.g. Boulton and Clark, 1990; Boulton *et al.*, 2001) means that ice fronts at the glacial maximum would have been best represented as an envelope rather than a continuous line. Late Ordovician ice fronts were continuous from Mauritania to western Libya. The existence of a continuous ice front between western Libya and Arabia is controversial, but likely at least during the most protracted phase of glaciation, which also affected southern Turkey (Monod *et al.*, 2003). Although Upper Ordovician glacial successions are also known in South Africa (e.g. Hiller, 1992) and South America (Caputo, 1998; Diaz-Martinez *et al.*, 2001), dating uncertainty still exists for the related glacial successions (e.g. Boucot *et al.*, 2003 for the South African example).

At the Hirnantian glacial maximum, the sedimentary record supports the concept of a continuous ice sheet across North Africa that possibly extended into Arabia, with WNW-to-NE oriented ice flow directions (Figs. 1B & 7A). A minimum-sized ice sheet at the glacial maximum had to incorporate a roughly symmetrical ice-front line, depicting a North Gondwana Ice Sheet (the Saharan Ice Sheet of Young *et al.*, 2004), characterised by southward-flowing ice in sub-Saharan Africa (Fig. 7B). As ice flowed from south to north in Eritrea and Ethiopia (Kumpulainen, 2005; Fig. 7A), this minimum-sized ice sheet must have reached Central Africa. A maximum-sized Hirnantian ice sheet may, in addition, have overridden South America and South Africa where subglacial deformation zones have been also identified (Blignault, 1981; Martinez, 1998; Le Heron *et al.*, 2004; Deynoux and Ghienne, 2005) (Fig. 7C). The maximum-sized ice-sheet scenario envisages a huge West Gondwana Ice Sheet (Vaslet, 1990; Sutcliffe *et al.*, 2000; Ghienne, 2003) centred above Central Africa where no Upper Ordovician sediments crop out.

THE NORTH GONDWANA PLATFORM DURING THE HIRNANTIAN

This section proposes the subdivision of the North Gondwana platform, from the ice centre to lower palaeolatitudes, into several palaeogeographic domains based on the number of glacial erosion surfaces preserved. A second palaeogeographical

scheme is then presented, providing a subdivision of the ice sheet perpendicular to ice-flow lines based on the occurrence of ice-stream-generated glacial troughs.

Palaeogeographic domains of the glaciated shelf

The number of glacial erosion surfaces distributed regionally define five proximal-to-distal palaeogeographic domains in North Gondwana (Fig. 1C). The continental interior corresponds to a domain that was not deglaciated until the close of the Hirnantian. The dominance of subglacial and postglacial erosion in these areas means that the glacial record in this domain is limited and restricted to small-scale, fault-bounded intracontinental basins (Konaté *et al.*, 2003). It is conceivable that the continental interior may have been glacierised both prior and after the Hirnantian glaciation.

The inner, middle and outer domains of the glaciated continental shelf were subject to multiple phases of ice-sheet growth and decay. On the inner glaciated shelf, typified by the Niger succession (Denis *et al.*, 2007), two glacial erosion surfaces and associated overlying sequences are recorded, and, are separated by the mid-Hirnantian graptolitic shales (see above). This domain was deglaciated during the mid-Hirnantian, but remained glacierised during phases of ice-front retreat within each of the two first-order glacial cycles. Glacio-isostacy should have played a significant role in developing the stratigraphic architecture. The middle glaciated shelf corresponds to the area subjected to from 2 to 5, possibly more, phases of subglacial erosion. In this zone, encompassing the well-known successions in Mauritania, Algeria and Libya, both glacio-eustatic and glacio-isostatic processes were operative, and the most complete record of multiple advance and retreat events of the Hirnantian ice sheets is preserved. The outer glaciated shelf, including northern Morocco and Turkey, was glacierised only during the most protracted advance phase of the Hirnantian glacial maximum (Figs. 1C and 7A). Glacio-eustacy was probably more important than glacio-isostacy in these regions (e.g. Boulton, 1990). The shelf areas beyond the outer ice-sheet limit comprise a sedimentary record controlled solely by glacio-eustacy. In these areas, distal glaciomarine sediments are locally preserved (Fig. 1B; e.g. Sardinia, Brittany, Bohemia: Robardet and Doré, 1988 and references therein; western Taurus, Turkey: Monod *et al.*, 2003; northernmost Morocco: Le Heron *et al.*, 2007).

Ice sheet configuration: the case study of Algeria

Legrand (1974, 1985) published a map of Algeria showing well-defined, 50–200 km wide, so-called sediment 'thicks' of 'upper Caradoc-Ashgill-lower Silurian' strata, separated by 150 to 300 km wide sediment 'thins'. This map is reproduced in Fig. 8A including data collected by the authors from Morocco (Anti-Atlas, Tamlelt area), Ougarta (NW Algeria) and Tassili n'Ajjer (western Murzuq Basin, Libya). It excludes smaller-scale variations, such as steep contour gradients over <10 km that could be attributed to tunnel valley incisions or fluvial incised valleys. Recent biostratigraphic work confirms that the strata outlined by Legrand (1985) are well constrained to Hirnantian syn-glacial strata (Paris *et al.*, 1995; Oulebsir and Paris, 1995; Vecoli and Le Hérissé, 2004).

It seems likely that areas with thick Hirnantian successions outline depositional lows and areas typified by thin successions designate palaeo-highs. North of the Hoggar, the data reviewed above are interpreted as a series of Late Ordovician glacially formed erosional troughs separated by plateaux or 'interfluves'. Four glacial troughs are identified across the Algerian middle glaciated shelf, from Ahnet to Tassili n'Ajjer, where the glaciogenic sediments reach >300 m in thickness. It is stressed that the isopach maps may mask the amalgamation of multiple glacial cycles in the stratigraphic record. In the interfluves, with the exception of deep but narrow palaeovalleys, the contact between pre-glacial and syn-glacial strata is stratigraphically higher.

The glacial troughs are very difficult to identify in the field as they are comparable in scale to tectonic structures (e.g. zones of preferential subsidence or post-depositional lithospheric bending). However, the easternmost glacial trough on Fig. 7A is the northward extension of a glacial trough already described in western Libya (Moreau *et al.*, 2005). This well-defined trough is >200 km in length and >80 km in width, and the depth of glacial erosion is up to 300 m, despite residual relief forms occurring on the upper surface of pre-glacial strata (Fig. 5). This trough contains several glacial surfaces

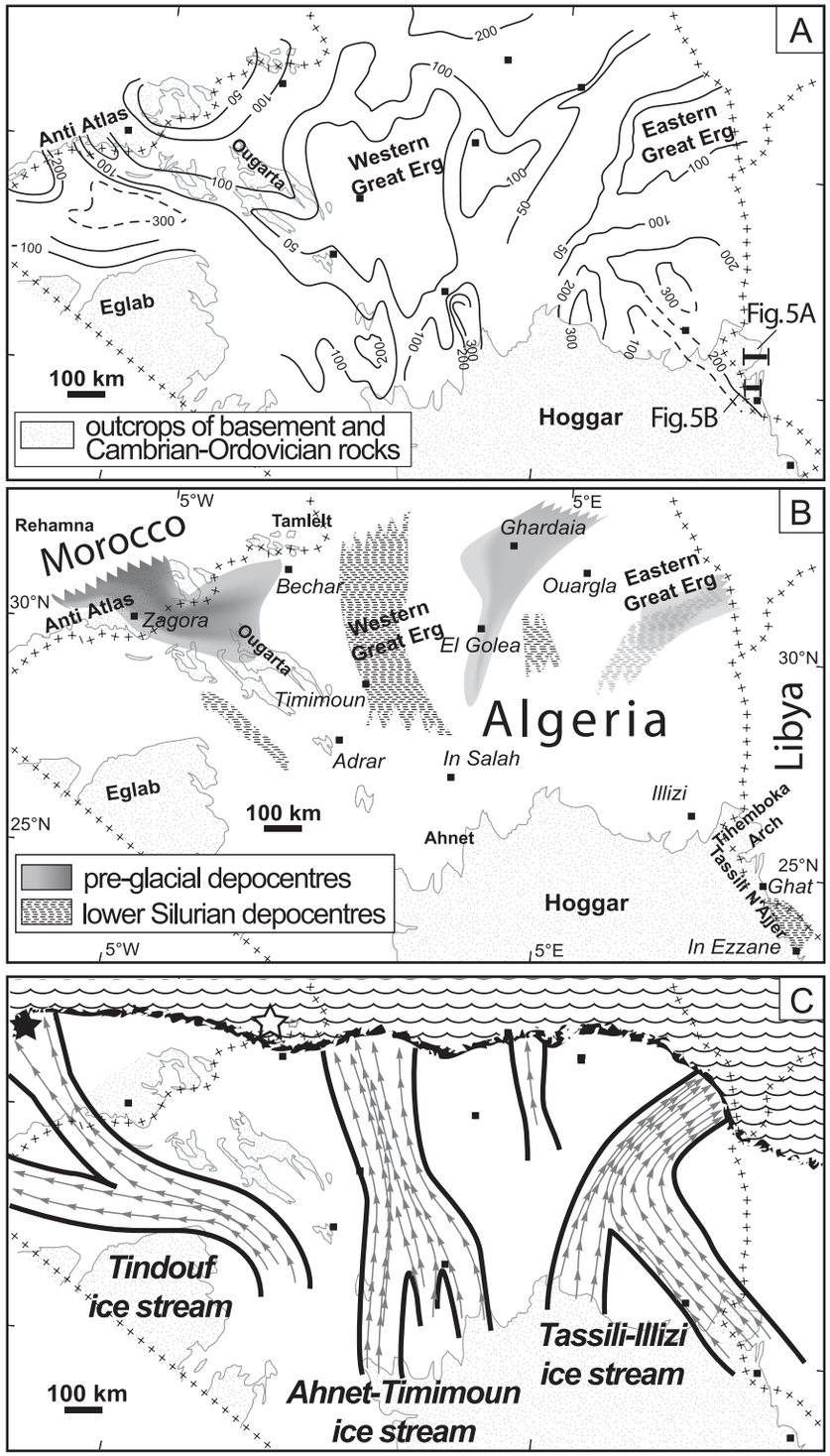

Fig. 8 Glacial troughs and ice streams in Algeria. (A) Isopach map corresponding to the syn-glacial Hirnantian strata (modified from Legrand, 1974). Erosional troughs are identified at the northern edge of the Hoggar Massif. (B) Pre-Hirnantian preferential depocentres (from Legrand, 1974 and Destombes *et al.*, 1985) and earliest to Early Silurian depocentres corresponding to depositional lows (from Klitsczh, 1981; Legrand, 1985; Lüning *et al.*, 2000). (C) Potential locations of major ice streams in Algeria as inferred from the locations of glacial erosional troughs and ice-flow orientations (cf. Fig. 1B). The black star is the northernmost glacierised area (Le Heron *et al.*, 2007); the white star indicates an area that was not glaciated (Tamlelt area, southeastern Morocco, unpublished data). Ice-stream fronts correspond to the Hirnantian glacial maximum. They are tentatively figured as shallow-marine ice fronts with no ice shelves.

characterised by mega-scale glacial lineations (Fig. 4A) (Clark, 1993; Stokes and Clark, 2001). These lineations have elongation ratios ranging from 5 to >20 and are 1–30 m in height. The lineations make up a large-scale undulating morphology on the glacial erosion surface, which is superimposed on wide elongated ridges separated by straight valley-like depressions (Figs 3C and 5). The morphology, comparable to the landforms produced by former Antarctic (e.g. Canals *et al.*, 2000; Anderson *et al.*, 2002; Evans *et al.*, 2004) or Scandinavian (Ottesen *et al.*, 2005) ice streams, defines a Late Ordovician ice-stream pathway (Moreau *et al.*, 2005). As a working hypothesis, the other glacial troughs of Algeria are interpreted as palaeo ice-stream pathways.

North of the glacial troughs, the general thinning of the sediment wedge is interpreted either as a decrease in the depth of erosion, or a decrease of sediment thickness in glacial troughs that are gradually underfilled. The latter scheme makes sense with the occurrence of elongate areas that Legrand (1985, 2003) and Lüning *et al.* (2000) have mapped, where lower Silurian organic-rich shales preferentially occur (Fig. 7B). These elongate areas are interpreted as depositional lows within which postglacial lower Silurian deposits may have accumulated, in contrast to highs that were not covered by sediments until middle Silurian time. Those depositional lows are interpreted as reflecting glacial troughs that remained underfilled after the ice-sheet retreat.

Connecting the overfilled glacial troughs of the Hoggar Massif (Fig. 8A) with underfilled depressions containing lower Silurian deposits to the north (Fig. 8B), a network of ice streams is reconstructed at regional scale (Fig. 8C). Hence, the Late Ordovician ice sheet over Algeria and western Libya was drained by a number of north-flowing ice streams separated by more stagnant ice in inter-stream areas. The shelfbreak extended a long distance from the ice fronts (Fig. 8C) and the existence of a shallow shelf (<200 m deep) may have restricted the formation of extensive frontal ice shelves.

More subtle depocentres are found northward in the Algerian outer glaciated shelf. However, they coincide spatially with pre-glacial depocentres (Fig. 8B) and are therefore not interpreted as erosional features. They cannot be considered as proxies for distal ice-stream pathways.

STRATIGRAPHIC ARCHITECTURES IN THE LATE ORDOVICIAN GLACIAL RECORD

Distinctive stratigraphic architectures faithfully reflect the position of each area on the shelf. For instance, low accommodation space and repeated 'cannibalisation' characterised the middle glaciated shelf, while restricted glacial erosion and greater accommodation space prevail on the outer glaciated shelf. This palaeogeographic subdivision of the glaciated shelf, parallel to ice flow, is coupled with a flow-transverse subdivision of the ice sheet into ice-stream troughs and inter-stream areas. That means a great deal of lateral variability should exist in the Late Ordovician glacial record. In the following section, the stratigraphic architectures of ice-stream pathways and inter-stream areas are compared for the middle and outer glaciated shelf.

Ice-stream-related depositional systems

The middle glaciated shelf: western Libya

In the Murzuq Basin (Libya), the depositional succession of the Hirnantian glacial record has been studied extensively (McDougall and Martin, 2000; Deynoux *et al.*, 2000; Sutcliffe *et al.*, 2000; Ghienne *et al.*, 2003; Le Heron, 2004; Le Heron *et al.*, 2004; El-ghali, 2005; Le Heron *et al.*, 2006). Most of the interpretations are based on field studies conducted in the Gargaf area, in the northern Murzuq Basin. In the following, we developed to some extent the glacial record of the western Murzuq Basin (Eastern Tassili n'Ajjer and Tihemboka Arch, see location in Fig. 8B). It characterises the stratigraphic architecture in ice-stream pathways on the middle glaciated shelf.

Despite partial reworking during later glacial cycles, 4–5 glacial depositional sequences are recognised, each separated by subglacial unconformities (Deynoux and Ghienne, 2004; Moreau *et al.*, 2005). The erosion depth of an individual unconformity is up to 200 m. The total thickness of the syn-glacial succession approaches 250–300 m. These sequences record the progressive infilling of glacially cut palaeovalley-like depressions. The long axis of younger depressions deviates from older examples (e.g. Smart, 2000), resulting in a complex depositional architecture (Figs 4A and 5) akin to Late Cenozoic alluvial terraces (e.g. Blum & Törnqvist, 2000).

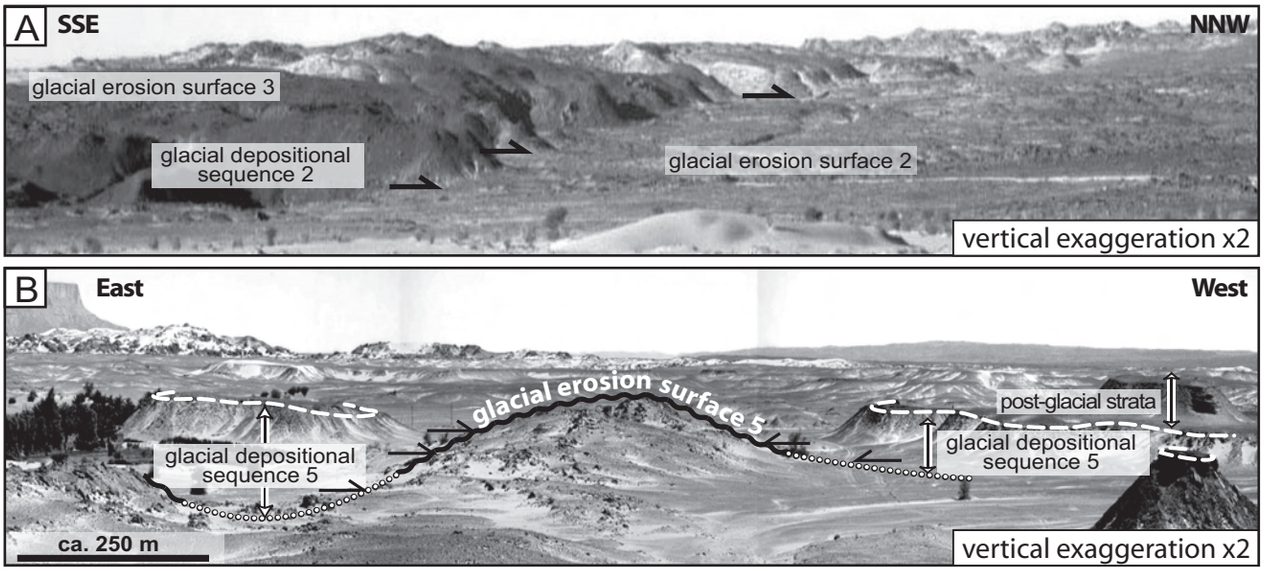

Fig. 9 Onlap relationships (black arrows) in the syn-glacial strata of the Eastern Tassili n'Ajjer (Ghat area, western Murzuq Basin). (A) A glacial depositional sequence onlaps on a glacial erosional surface with mega-scale glacial lineations (see location Fig. 4A). It is made up of fine-grained deposits at the base (distal glaciomarine, prodelta), truncated by fluvial sandstones at the top (depositional sequence 2 in Fig. 5B). (B) Glaciomarine and shelf deposits onlapping on a surface with mega-scale glacial lineations (depositional sequence 5 in Fig. 5B).

Depositional sequences 1–3. In the Eastern Tassili n'Ajjer (Ghat area), sequences 1–3 comprise coarsening upward successions, each 30–100 m thick, bounded above and below by a glacial erosion surface (Figs 5B and 9A). Sequences 1 and 2 belong to the first glacial cycle, and sequence 3 to the second glacial cycle (Fig. 5C). The lowermost 20–75 m of each sequence comprises crudely laminated micaceous sandstones and shales with occasional lonestone-bearing diamictite horizons. These are interpreted as distal glaciomarine (plume) deposits or prodelta sediments. The middle section, 5–20 m thick, rests with a sharp or rapid transitional contact with the underlying section, and comprises well sorted medium-grained to poorly sorted coarse-grained sandstones. These deposits contain current and wave ripples, trough or tabular cross-laminae and plane beds with parting lineations. They are interpreted as shallow-marine to distal alluvial plain deposits. The upper part of each sequence includes sharp-based, coarse- to very coarse-grained sandstones bearing numerous internal erosional surfaces. Cross-laminated sandstones grade laterally into fine- to medium grained sandstones bearing horizontal to low-angle lamination with parting lineations and climbing ripple cross-lamination. These are interpreted as a series of amalgamated fluvial channels and associated overbank sediments, deposited on a flood-dominated aggrading braid-plain.

Each depositional sequence is considered to record (i) rapid retreat of a marine-terminating ice front, followed by (ii) flooding of the glacial erosion surface, then (iii) progradation of a fluvial-delta-shelf system. A braid-plain separated the retreating, land-terminating ice margin from the shoreline. An abrupt facies change occurs within the prograding succession, either pointed out by sharp-based shallow marine deposits or by erosionally based fluvial deposits. In each of these sequences, a sea-level fall or a fluvial incision may be attributable to the effect of glacio-isostacy. Fluvial aggradation is concomitant with renewed progradation.

Depositional sequence 4. This sequence is associated with the Hirnantian glacial maximum that occurred during the second glacial cycle (see above) (Fig. 5C). In the Tihemboka Arch, a thick sandstone wedge has been deposited on the glacial erosion surface (Fig. 5A). It is overlain by a sandstone

sheet, which can be followed to the south into the Eastern Tassili n'Ajjer, resting here directly on the basal glacial erosion surface (Figs 5A and B).

The sandstone wedge, 75–150 m thick, displays a coarsening and thickening-upward succession. The sandstones pass upwards from fine-grained massive sandy deposits, through a poorly stratified, medium-grained section characterised by sharp-based, horizontally laminated, graded, and de-watered sandstones, to low-angle or horizontally laminated deposits at the top. This succession is overlain by a channel-overbank system comprising cross-bedded medium- to coarse-grained sandstones. Channel fill structures, 10–40 m in thickness, 0.2–1 km in width, have transitional contact with overbank facies and any levée structures have been identified. These sandstones contain abundant subcritical climbing megaripples in 2–20 m thick beds (Figs 10A and B), associated with deep-sided cut-and-fill structures and undulating bedforms that show a steep climbing (40°) to aggradational (90°) superposition (Fig. 10C). Large glaciotectonic structures in the form of thrusted fold belts (20–40 m in height) are also preserved within these strata.

The coarsening sandstone wedge described above is capped by a medium-grained sandstone sheet, extending from the Eastern Tassili n'Ajjer

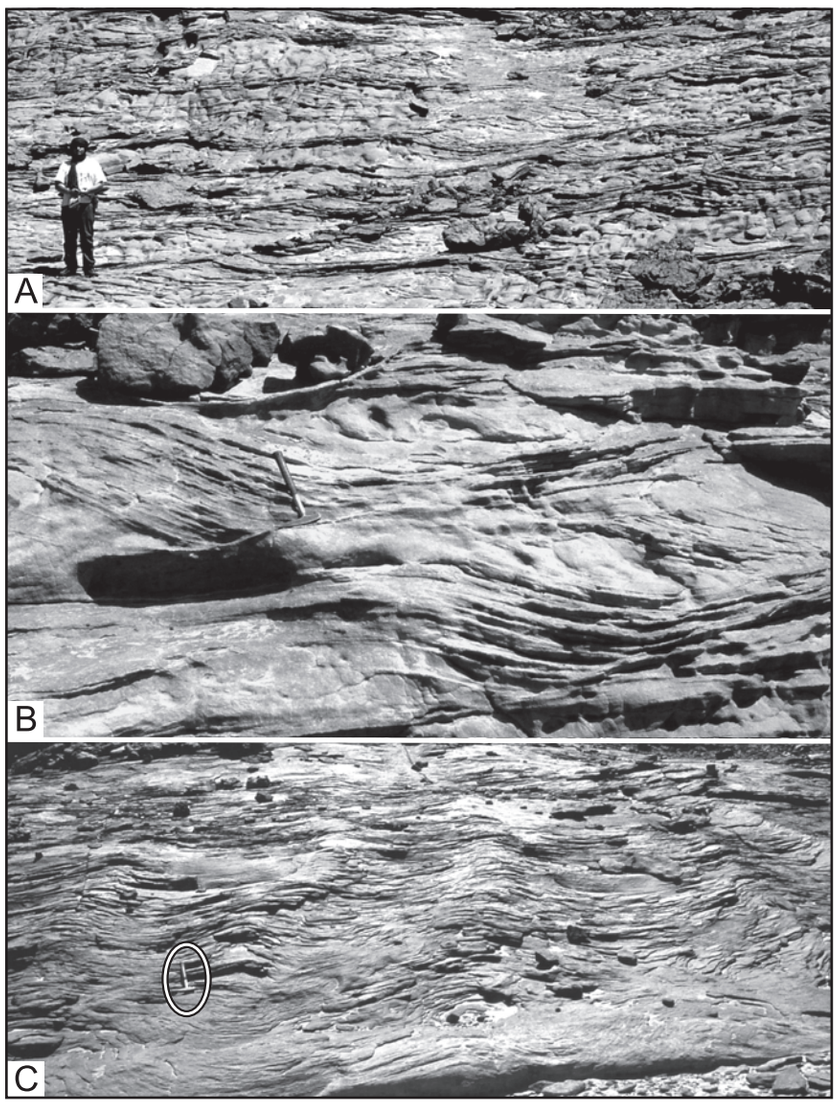

Fig. 10 Flood (possibly outburst)-dominated facies in an ice-stream-related outwash fan (glacial depositional sequence 4, Tihemboka Arch, western Murzuq Basin). (A) 2D climbing dunes composed of medium- to coarse-grained sandstones forming a 10 m-thick depositional package. (B) Close up view of facies illustrated in (A). (C) Nearly symmetrical, vertically climbing, large-scale bedforms interpreted as oversupplied climbing dunes or alternatively antidunes (encircled hammer for scale).

to the Tihemboka Arch. Its internal architecture is characterised by channel-fill structures and epsilon cross-stratification. The size of these structures increases towards the north. Horizontal lamination, climbing ripples and megaripples are ubiquitous.

Within the sandstone wedge, the climbing megaripples suggest deposition from highly concentrated sediment-laden streamflows with high rates of sediment fall-out. Such highly concentrated flows are most probably achievable by long-lived, turbulent glacial outburst floods (Russell and Arnott, 2003; Russell *et al.*, 2003). The origin of undulating climbing to aggradational bedforms (Fig. 10C) is enigmatic, and could reflect over-supplied climbing megaripples or alternatively antidunes. This last interpretation has been proposed for correlative deposits near Djanet, Algeria (Hirst *et al.*, 2002). Distal counterparts of this flood-dominated environment comprise poorly stratified to massive, largely dewatered sandstones deposited in environments dominated by high-density sandy turbidites. The overall sandstone wedge is interpreted as an ice-contact, flood-dominated outwash fan. The channel structures form the distributary system, which was directly linked with the subglacial drainage system. It is uncertain whether the sandstone wedge was deposited on a large submarine outwash related to a marine ice front or as part of a fan delta system related to an ice front terminating on land. In either case, its scale exceeds comparable depositional systems in the literature (Powell, 1990; Lønne, 1995; Lønne *et al.*, 2001) by one to two orders of magnitude. The size and thickness of the sand wedge suggests that the ice-sheet retreat occurred in the study area much more slowly than for sequences 1–3. This suggests that deposition occurred during a phase of stabilisation of the ice sheet. The overlying sandstone sheet was deposited by a regional-wide sinuous to meandering, sand-dominated fluvial system when ice-front position retreated further to the south and a delta most probably developed to the north.

Depositional sequence 5. This sequence is restricted to the Ghat area (Eastern Tassili n'Ajjer) and is considered as compelling evidence for a locally developed, fifth phase of ice-sheet advance. To the north of a boundary zone corresponding to the maximum ice advance, a sandstone wedge that is similar to but thinner than that of sequence 4, contains a channel-fill network and associated overbank deposits. To the south of the boundary zone, a glacial erosion surface bears fan-shaped drumlins with associated subglacial channel fills, both of which cross-cut older glacial lineations (Moreau *et al.*, 2005). A thin veneer (5–20 m) of distal glaciomarine deposits caps this surface in the axis of glacially cut depressions that remained essentially underfilled after the ice sheet retreated (Figs 3A, 5B and 9B).

This depositional sequence had preserved the spatial relationship between a subglacial drainage network to the north and the proglacial outwash system to the south. The thin glaciomarine deposits that blanket the glacial surface suggest a rapid ice-sheet withdrawal. Post glacial evolution in a very last phase of Ordovician sedimentation was characterised by tide-dominated reworking processes and the deposition of a transgressive wedge on the flanks of underfilled palaeovalleys (Figs 3A and 5B).

The outer glaciated shelf: High Atlas and Meseta (Morocco)

Glacial troughs have not been found at outcrop on the outer glaciated shelf. However, a large depocentre of marine sediments has been identified in northeastern Morocco (Tazzeka Massif, Khoukhi and Hamoumi, 2001) beyond the maximum ice-front position on the non-glaciated shelf. Here, a relatively deep (200–400 m) marine fan was deposited at the continental margin (Le Heron *et al.*, 2007). This fan system is not an analogue to the trough-mouth fans identified in front of Quaternary ice streams beyond the shelfbreak (Vorren and Laberg, 1997), within which sedimentation is dominated by very thick, poorly evolved diamictite facies. However, focused and massive sand-dominated deposition is interpreted as the signature of a sediment delivery system fed by an ice stream.

To the south, on the outer glaciated shelf, the two major Hirnantian glacial cycles are recorded, with sediments related to the first (lower) glacial cycle being somewhat more ice-distal than those of the second (upper) glacial cycle. Only the latter is discussed below. Further details are given in Le Heron *et al.* (2007).

In the Rehamna inlier, a thin sandy diamictite interpreted as a till is observed in close association with subglacial features such as glaciofluvial

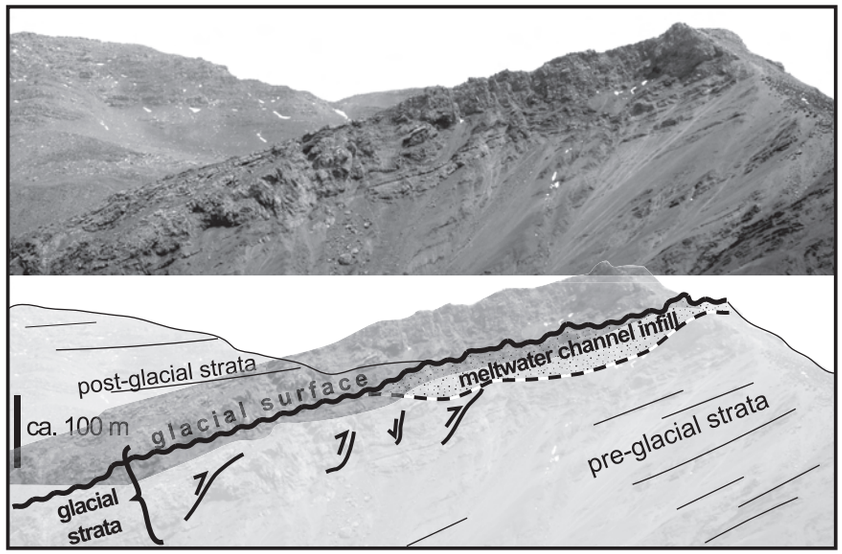

Fig. 11 The glacial succession in the High Atlas (Morocco). The following events are illustrated: (i) glaciotectonic deformation involving glaciomarine outwash fan facies, deposits of the first glacial cycle and subordinate pre-glacial strata, (ii) incision of a subglacial channel and sandy diamictite infill, (iii) truncation by a glacial erosion surface comprising streamlined bedforms (not illustrated, see Le Heron *et al.*, 2007).

sandstones, sand intrusions and a striated surface. This till horizon rest above thin outwash facies and is overlain by well developed glaciomarine diamictite facies, up to 20 m thick. In the High Atlas, c. 100 km further to the south, the sedimentary succession of the second glacial cycle begins with thick outwash facies comprising sandstones interstratified with massive to poorly stratified, sandy, clast-poor diamictites (Ouanaimi, 1998). These sediments are deformed by glaciotectonic thrusts and gravitational loads, and are truncated by 20–40 m thick, 100–300 m wide channel structures (Fig. 10). The latter are filled with stratified coarse-grained sandstones, sandy diamictites and subordinate conglomerate lenses, including boulder-sized clasts of local origin. These deposits are capped by a glacial erosion surface with subglacial streamlined bedforms overlain by a thin (<2 m) diamictite.

The Rehamna succession, probably in close proximity to the maximum ice-front position, reflects more ice-marginal conditions than the High Atlas succession (Le Heron *et al.*, 2007). Glaciomarine diamictites overlying the glacial surface in the Rehamna were probably deposited during an earlier phase of ice-front recession. This stage has immediately preceded an ice-sheet collapse that prevented further glacial sedimentation over the area, as suggested by the thin 'post-glacial' glaciomarine sediment blanket above the underlying glacial erosion surface in the High Atlas.

Combining observations from the three study areas (Tazzeka, Rehamna and High Atlas), the Moroccan succession related to the Hirnantian glacial maximum records: (i) deposition in a submarine, ice-contact outwash fan dominated by mass-flow diamictites and sandy turbidites, (ii) glaciotectonic deformation and incision by channels suggesting subglacial, focused, sediment input points, (iii) subglacial conditions characterised by fast-flowing ice indicated by streamlined bedforms on the outer glaciated shelf, whereas an ice-stream-related 'deep' marine fan developed on the non-glaciated shelf, and (iv) a rapid ice-sheet withdrawal. A depositional succession related to a glacial advance on a shallow-marine shelf, followed by the development of an ice stream and a subsequent ice-stream collapse is then apparent.

Depositional systems in inter-stream areas

The middle glaciated platform: Mauritania

Syn-glacial strata in eastern and western Mauritania (Hodh and Adrar, Fig. 1) are organised into four laterally juxtaposed and vertically superimposed depositional units (Ghienne, 2003). As in Libya, each depositional sequence rests on a glacial erosion surface and records essentially an ice-sheet recession with the influence of glacial processes rapidly disappearing up-section. Key differences with the

record in western Libya include (i) a markedly thinner succession (c. 40–100 m), thickening only within palaeovalleys or subglacial depressions, (ii) widespread palaeorelief forms on the upper surface of pre-glacial strata, (iii) better developed fluvio-glacial, fluvial and delta facies, and (iv) poorly developed offshore marine facies.

In the Hodh area, syn-glacial strata of the first Hirnantian glacial cycle record the recession of a land-terminating ice margin characterised by episodic, high-frequency retreats and re-advances of the ice front, resulting in a complex depositional architecture (Deynoux, 1985; Ghienne, 2003). This architecture includes aggrading outwash sediments deposited near a stagnating ice front that is partly glaciotectonised by minor re-advances. Both tills and some glaciofluvial material were reworked by gravity processes and re-deposited in subglacially overdeepened zones (Ghienne, 1998). The final phase of ice retreat was accompanied by the incision and subsequent infilling of large subglacial or proglacial meltwater channels (Ghienne, 2003).

During the second glacial cycle, a rather thin (<50 m) succession was deposited, with the exception of tunnel-valley infills (Ghienne and Deynoux, 1998; Fig. 3B). The last depositional sequence lacks any glacial features in western Mauritania where erosion prevailed in shallow-marine environments. In the east, in the Hodh area, the sequence comprises a fining-up glaciomarine succession, characterised by thin (<10 m) submarine outwash-fan deposits at its base, truncated by nearshore sediments. This sequence indicates a significant relative sea-level fall ascribed to a late post-glacial isostatic rebound (Ghienne, 1998, 2003). It occurred, nevertheless, before the end of the Hirnantian (Paris *et al.*, 1998; Underwood *et al.*, 1998).

The outer glaciated shelf: Turkey (Taurus Mountains)

This area is characterised by laterally extensive (up to 100 km), superimposed depositional units (Monod *et al.*, 2003). Relatively clast-rich sandy diamictites, representing mass-flow or low- to high-density sandy turbidites, characterise glaciomarine outwash environments in front of a marine-terminating ice margin. The absence of large-scale channel structures suggest a limited availability of meltwater and line, rather than point, sources (e.g. grounding-line fans). Non-glacial shelf processes, e.g. storm deposits, are also present. A rather condensed shelf sedimentation regime not influenced by glacial processes, occurred during interglacial periods.

The glacial maximum is characterised by the deposition of a thin (<0.2 m) till horizon overlying a striated pavement. Upwards, a progressively fining-up, lonestone bearing glaciomarine succession records a gradual ice-front retreat. Therefore, in contrast to Moroccan successions, no evidence for a rapid ice-sheet withdrawal is identified in Turkey.

PLATFORM-SCALE FACIES MODEL

Only rarely have sequence stratigraphic methodologies have been applied successfully in glacial settings (e.g. Proust and Deynoux, 1993; Brookfield and Martini, 1999; Powell and Cooper, 2002; Elghali, 2005). Large-scale facies models for glacial sedimentary systems are thus still needed. When developed, they will form the basis of a more robust sequence stratigraphic approach to ancient glacial successions.

The database presented herein is regionally comprehensive (Fig. 1A) and should facilitate correlation of Late Ordovician depositional sequences across the North Gondwana platform. This correlation is complicated both by the number of palaeogeographic domains (e.g. inner, middle, outer glaciated shelves) and whether each study area lies within an ice-stream pathway or an inter-stream area. Based on the glacier dynamics inferred for each study area, a facies model illustrating the stratigraphic architecture of a glacial sequence is now proposed for two parallel S-N profiles (Fig. 12). The first set of diagrams on the left illustrates the stratigraphy within an ice-stream pathway, whereas the set on the right depicts an adjacent co-evally evolving inter-stream area. The model captures four phases in the temporal evolution of a glacial sequence, namely the glacial advance, the glacial maximum, the ice-margin recession and the interglacial minimum. The two points of maximum ice advance and ice retreat, as well as the marine limit, are not fixed palaeogeographically. They are located at different positions across the platform according to the amplitude of both the maximum and minimum ice extent associated with each glacial phase.

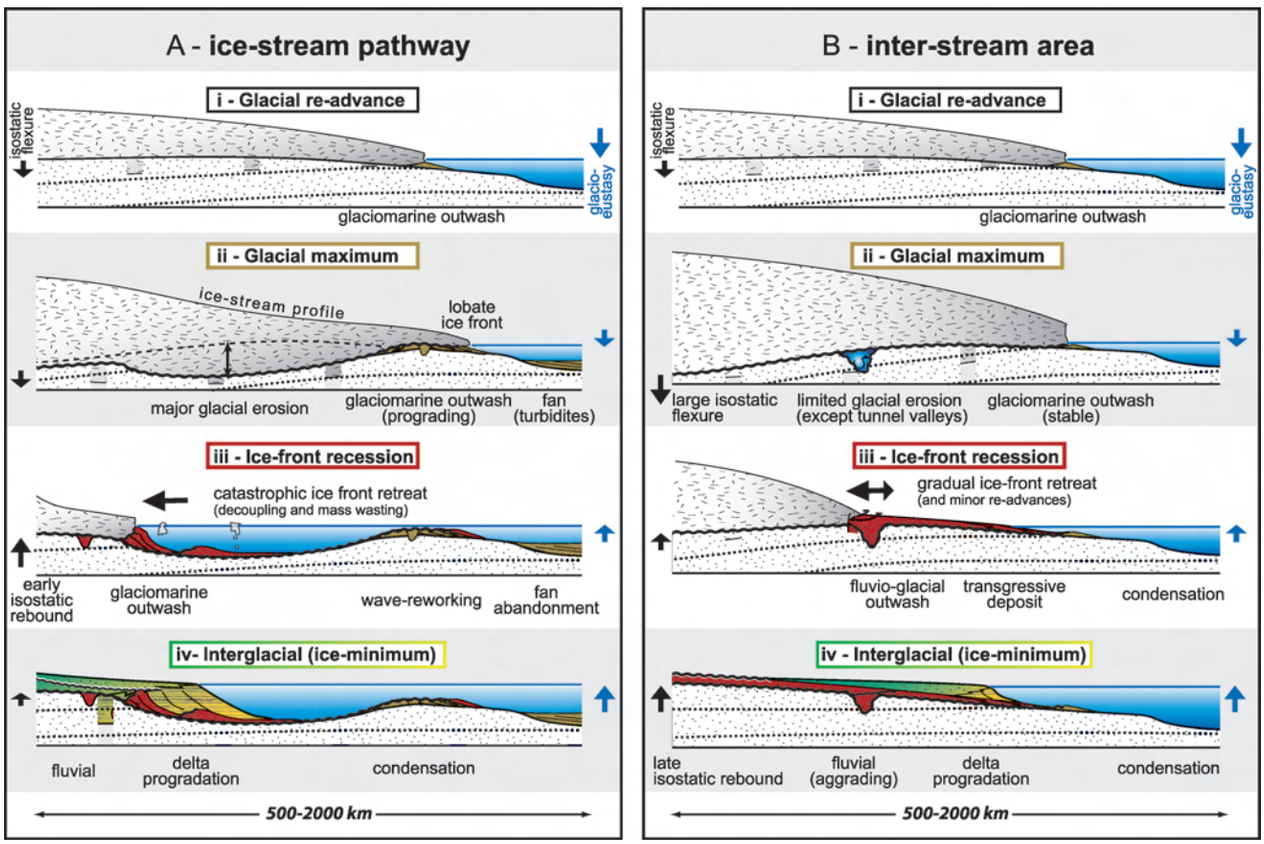

Fig. 12 An idealised glacial depositional sequence corresponding to a single glacial phase (glacial advance and subsequent retreat) in (A) ice-stream-related depositional environments (left, mainly based on the Libyan case study), and (B) inter-stream areas (right, mainly based on the Mauritanian case study, Ghienne *et al.*, 2003). (i) Glacial re-advance. (ii) Glacial maximum and initial retreat. (iii) Ice-front recession. (iv) interglacial (ice-minimum). The stratigraphic superposition of several glacial sequences (2–5), and the potential lateral migration of ice streams result in an intricate glacial record (e.g. Fig. 5). Post-glacial transgressive deposits are not figured. Vertical exaggeration: ~1000.

Glacial advance

This stage is generally poorly recorded on the glaciated platform where regressive successions are poorly developed possibly due to a rapid sea-level fall. Immediately prior to the ice maximum, glaciomarine outwash sediments are deposited in some areas such as northern Morocco. This infilling of accommodation space probably supported the ice sheet as it advanced northward on the shallow-marine platform, and was affected by concomitant fall in sea-level (e.g. Dahlgren *et al.*, 2002). It is not possible to ascertain whether ice streams had developed at this stage.

Glacial maximum and initial glacial retreat

While glaciomarine deposition occurred at the ice margin, subglacial erosion surfaces developed to the south. They are characterised by foredeepened depressions, glaciotectonic thrusts and folds, mega-scale glacial lineations and meltwater channels.

Focused sediment input-points located in front of ice-stream systems, may have been locally connected to some deeper turbiditic fans beyond a shelf edge inherited from the pre-glacial shelf architecture (e.g. in northern Morocco). This shelf edge may have controlled the maximum ice-stream advance (Le Heron *et al.*, 2007), which does not

appear to have reached the shelf-break, unlike ice sheets in Antarctica or Scandinavia during the Pleistocene Late Glacial Maximum (e.g. Ottesen *et al.*, 2005).

In contrast, linear and distributed sediment-input points built small-scale, diamictite-dominated outwash systems in front of inter-stream areas (e.g. in Turkey). Initial glacial retreat was generally associated with the deposition of relatively thick glaciomarine succession above a thin till. It is at this stage that large tunnel valleys began forming up-glacier in the inter-stream areas (e.g. Le Heron *et al.*, 2004).

Ice-front recession

As ice stream retreat, only a thin sediment cover remains, comprising fine-grained distal glaciomarine deposits that rest directly on top of each glacial erosion surface as in the eastern Tassili n'Ajjer. The preservation of fine-grained sediment above glacial erosion surfaces implies the sudden withdrawal of the ice sheet from the outer glaciated shelf. These processes strongly suggest decoupling at the ice/bed interface, mass-wasting, rapid retreat of marine-terminating ice fronts to a new set of pinning-points, and flooding of the deglaciated area (Eyles and McCabe, 1989; Anderson and Thomas, 1991). This suite of processes is in agreement with the interpretation of a glacial trough as a former ice-stream pathway, characterised by foredeepened topography where intense calving may have occurred. After initial rapid retreat, a more stable and slow retreat of ice fronts produced a renewed and voluminous ice-contact, flood-dominated, outwash system such as a submarine fan or fan delta (sequence 4, Tihemboka Arch). The latter system then evolves into a delta system once a flood-dominated fluvial plain becomes established in front of the land-terminating ice margin.

In inter-stream areas, the sediments from the ice-sheet recession stage comprise the tunnel-valley basal infill (Ghienne and Deynoux, 1998; Le Heron *et al.*, 2004). Glacial recession was more gradual as no sudden glacial withdrawal is observed (Turkey). With slow continuous retreat, a land-terminating ice margin deposited braided outwash sediments grading seaward into transgressive, shallow-marine deposits such as in Mauritania. During this time, a land-terminating ice margin may have persisted locally in inter-stream areas in a position to the north of some marine ice fronts that were established to the south in the axis of adjacent glacial troughs. Such a complex configuration may explain some peculiar fluvio-glacial drainage patterns. A source in a higher inter-stream area and a depocentre located within an adjacent glacial trough may be inferred when delta systems show evidence of progradation perpendicular to the regional palaeoslope

Interglacial (ice-minimum)

In both ice-stream and inter-stream areas, interglacial conditions resulted in high sea levels and the progradation of fluvial-delta-shelf systems as in western Libya and Mauritania. Fluvial aggradation occurs, locally temporarily interrupted by glacio-isostatic rebound. This aggradational-progradational pattern infilled any remaining accommodation space in glacially cut glacial troughs and tunnel valleys. In the proximal (southern) parts of the shelf, these sediments may actually form the bulk of syn-glacial strata preserved within each glacial depositional sequence. In northern parts of the platform, more restricted or condensed sedimentation occurs, although this may also have been fed by local highlands providing an additional sediment source (Le Heron *et al.*, 2007).

CONCLUSIONS

The model given above should be regarded as a first attempt to merge numerous observations and interpretations in various parts of Northern Gondwana. The architecture of Late Ordovician glacial depositional sequences is mainly controlled by their location within or outside an ice-stream-generated trough. Ice-stream-dominated systems are characterised by up to 300 m deep incisions, a greater sediment supply typified by flood-dominated outwash-fan sedimentation, and a sedimentary record indicating rapid ice-sheet collapse. In inter-stream areas, shallower erosion surfaces are observed and sediment as well as meltwater supply are less vigorous. The general depositional features that can be portrayed for a complete cycle of glacial advance and subsequent retreat include:

1 Ice-proximal, coarse-grained glaciomarine successions are best developed at or near the maximum ice-front position and characterise the outer glaciated shelf in both ice-stream and inter-stream-dominated areas. Relatively deep marine fans occurred beyond the shelf edge in the axis of ice streams;
2 During ice-sheet recession, ice-sheet collapse in ice-stream-generated troughs resulted in a relatively thin ice-distal glaciomarine sediment cover blanketing the glacial erosion surface. Gradual ice-front recession in adjacent inter-stream areas resulted in well developed fluvio-glacial to fluvial facies;
3 Outwash systems preserved in ice-proximal segments of ice-stream troughs mark transitional conditions showing an evolution from marine-terminating to land-terminating ice fronts in association with a slowing down in the rate of ice-sheet recession;
4 Much of the Hirnantian strata in the middle glaciated shelf essentially record late glacial retreat to interglacial phases. In general, they are finer-grained than strata deposited several hundreds kilometres to the north when the ice-front position was at its maximum.

Several factors have resulted in a complicated glacial record: the stratigraphic superimposition of several, erosionally based, glacial sequences (e.g. Fig. 5B); the possibility that ice streams of successive glacial phases do not necessarily coincide spatially; and Hirnantian glacially induced reactivation of pre-existing basement faults (Ghienne *et al.*, 2003; Turner *et al.*, 2005; Denis *et al.*, 2007). The model presented herein should facilitate a better integration of outcrop and subsurface data, guiding the sequence stratigraphic interpretation of Late Ordovician glacial deposits and other ancient glacial successions. Future research looks forward to the development of a detailed chronostratigraphic framework, which will be the subject of a forthcoming paper.

ACKNOWLEDGEMENTS

This regional scale study would not have been possible without the combined support of TOTAL, ENI, NOC, REMSA, SONATRACH and TPAO for financial and logistical support necessary for both the fieldwork and writing-up phases of this work. This research was also made possible by the Centre National de la Recherche (CNRS, programme Eclipse). Daniel Paul Le Heron publishes with the support of the CASP Libya Project Consortium. The manuscript benefited from considerable improvements following the thoughtful reviews of Dag Ottesen and Risto Kumpulainen, and from the editorial support of Mike Hambrey. This is a contribution of EOST (Ecole et Observatoire des Science de la Terre), number 2006.501 – UMR 7517.

REFERENCES

Abed, M.A., Makhlouf, I.M., Amireh, B.S. and Khalil, B. (1993) Upper Ordovician glacial deposits in southern Jordan. *Episodes*, **16**, 316–328.

Anderson, J.B. and Thomas, M.A. (1991) Marine ice-sheet decoupling as a mechanism for rapid, episodic sea-level change: the record of such events and their influence on sedimentation. *Sed. Geol.*, **70**, 87–104.

Anderson, J.B., Shipp, S.S., Lowe, A.L., Wellner, J.S. and Mosola, A.B. (2002) The Antarctic Ice Sheet during the Last Glacial Maximum and its subsequent retreat history: a review. *Quatern. Sci. Rev.*, **21**, 49–70.

Beuf, S., Biju-Duval, B., De Charpal, O., Rognon P., Gariel, O. and Bennacef, A. (1971) *Les grès du Paléozoïque inférieur au Sahara.* 'Science et Technique du pétrole', **18**, Paris, 464 pp.

Blignault, H.J. (1981) Ice sheet deformation in the Table Mountain Group, Western Cape. *Annale Universiteit van Stellenbosch. Series A1 (Geology)*, **3**, 1–66.

Blum, M.D. and Törnqvist, T.E. (2000) Fluvial responses to climate and sea-level change: a review and look forward. *Sedimentology*, **47** (suppl.), 2–48.

Boote, D.R.D., Clark-Lowes, D.D. and Traut M.W. (1998) Paleozoic petroleum systems of North Africa. In: *Petroleum Geology of North Africa* (Eds D.S. Macgregor, R.T.J. Moody and D.D. Clark-Lowes), *Geol. Soc. London Spec. Publ.*, **132**, 7–68.

Boucot, A.J., Jia-Yu, R., Xu, C. and Scotese, C.R. (2003) Pre-Hirnantian Ashgill climatically warm event in the Mediterranean region. *Lethaia*, **36**, 119–131.

Boulton, G.S. (1990) Sedimentary and sea level changes during glacial cycles and their control on glaciomarine facies architecture. In: *Glacimarine environments: processes and sediments* (Eds J.A. Dowdeswell and J.D. Scourse), *Geol. Soc. London Spec. Publ.*, **53**, 15–52.

Boulton, G.S. and Clark, C.D. (1990) A highly mobile Laurentide Ice Sheet revealed by satellie images of glacial lineations. *Nature*, **346**, 613–817.

Boulton, G.S., Dongelmans, P., Punkari, M. and Broadgate M. (2001) Palaeoglaciology of an ice sheet through a glacial cycle: the European ice sheet through the Weichselian. *Quater. Sci. Rev.*, **20**, 591–625.

Brenchley, P.J., Carden, G.A., Hints, L., Kaljo, D., Marshall, J.D., Martma, T., Meidla, T. and Nolvak, J. (2003) High-resolution stable isotope stratigraphy of Upper Ordovician sequences: Constraints on the timing of bioevents and environmental changes associated with mass extinction and glaciation. *Geol. Soc. Am. Bull.*, **115**, 89–104.

Brookfield, M.E. and Martini, I.P. (1999) Facies architecture and sequence stratigraphy in glacially influenced basins: basic problems and water level/glacier input-point controls (with an example from the Quaternary of Ontario, Canada). *Sed. Geol.*, **123**, 183–197.

Canals, M., Urgeles, R. and Calafat, A.M. (2000) Deep sea-floor evidence of past ice streams off the Antarctic Peninsula. *Geology*, **28**, 31–34.

Caputo, M.V. (1998) Ordovician-Silurian glaciations and global sea-level changes. *Bull. New York State Mus.*, **491**, 15–25.

Carr, I.D. (2002) Second-order sequence stratigraphy of the Palaeozoic of North Africa. *Mar. Petrol. Geol.*, **25**, 259–280.

Clark, C.D. (1993) Mega-scale glacial lineations and cross-cutting ice flow landforms. *Earth Surf. Proc. Land.*, **18**, 1–29.

Crossley, R. and McDougall, N. (1998) Lower Palaeozoic reservoirs of North Africa. In: *Petroleum Geology of North Africa* (Eds D.S. Macgregor, R.T.J. Moody and D.D. Clark-Lowes), *Geol. Soc. London Spec. Publ.*, **132**, 157–166.

Dahlgren, K.I.T., Vorren, T.O. and Laberg, J.S. (2002) The role of grounding-line sediment supply in ice-sheet advances and growth on continental shelves: an example from the mid-Norwegian sector of the Fennoscandian ice sheet during the Saalian and Weichselian. *Quatern. Int.*, **95–96**, 25–33.

Dean, W.T. and Monod, O. 1990. Revised stratigraphy and relationships of Lower Palaeozoic rocks, eastern Taurus Mountains, south central Turkey. *Geol. Mag.*, **127**, 333–347.

Denis, M., Buoncristiani, J.-F., Konaté, M., Ghienne, J.-F. and M. Guiraud. Hirnantian glacial and deglacial record in SW Djado Basin (NE Niger) (2007). *Geodynamica Acta*, **20**, 177–195.

Destombes, J. (1968a) Sur la présence d'une discordance générale de ravinement d'âge Ashgill supérieur dans l'Ordovicien terminal de l'Anti-Atlas (Maroc). *CR Acad. Sci. Paris*, **267**, 565–567.

Destombes, J. (1968b) Sur la nature glaciaire des sédiments du groupe du 2^{e} Bani, Ashgill supérieur de l'Anti-Atlas, Maroc. *CR Acad. Sci. Paris*, **267**, *D*, 684–686.

Destombes, J., Hollart, H. and Willefert, S. (1985) Lower Paleozoic rocks of Morocco. In: *Lower Paleozoic Rocks of northwest and west Central Africa* (Ed. C.H. Holland), pp. 291–325, John Wiley, New-York.

Deynoux, M. (1980) Les formations glaciaires du Précambrien terminal et de la fin de l'Ordovicien en Afrique de l'ouest. Deux exemples de glaciation d'inlandsis sur une plate-forme stable. *Travaux des Laboratoires des Sciences de la Terre, St.Jérome, Marseille*, **B17**, 554 pp.

Deynoux, M. (1985) Terrestrial or waterlain glacial diamictites? Three case studies from the Late Precambrian and Late Ordovician glacial drifts in West Africa. *Palaeogeogr. Palaeoclimatol. Palaeoecol.*, **51**, 97–141.

Deynoux, M. and Ghienne, J.-F. (2004) Late Ordovician glacial pavements revisited – a reappraisal of the origin of striated surfaces.*Terra Nova*, **16**, 95–101.

Deynoux, M. and Ghienne, J.-F. (2005) Late Ordovician glacial pavements revisited – a reappraisal of the origin of striated surfaces. Discussion. *Terra Nova*, **17**, 488–491.

Deynoux, M. and Trompette, R. (1981) Late Ordovician tillites of the Taoudeni Basin, West Africa. In: *Earth's pre-Pleistocene glacial record* (Eds M.J. Hambrey, W.B. Harland), pp. 89–96, Cambridge University Press. Available on-line via www.aber.ac.uk/glaciology.

Deynoux, M., Ghienne, J.-F. and Manatschal, G. (2000) Stratigraphy and sedimentology of the Upper Ordovician glacially-related deposits of the western Gargaf High, Fezzan, Northern Libya. Unpublished explanatory booklet of the geological map, CNRS-EOST, Ecole et Observatoire des Sciences de la Terre, Université L. Pasteur, Strasbourg, 41 pp.

Diaz-Martinez, E., Acosta, H., Cardenas J., Carlotta, V. and Rodriguez, R. (2001) Paleozoic diamictites in the Peruvian Altiplano: evidence and tectonic implications. *J. S. Am. Earth Sci.*, **14**, 587–592.

Eschard, R., Abdallah, H., Braik, F. and Desaubliaux, G. (2005) The Lower Paleozoic succession in the Tasilli outcrops, Algeria: sedimentology and sequence Stratigraphy. *First Break*, **23**, 27–36

El-ghali, M.A.K. (2005) Depositional environments and sequence stratigraphy of paralic glacial, paraglacial and postglacial Upper Ordovician siliciclastic deposits in the Murzuq Basin, SW Libya. *Sed. Geol.*, **177**, 145–173.

Evans, J., Dowdeswell, J.A. and O'Cofaigh, C. (2004) Late Quaternary submarine bedforms and ice-sheet flow in Gerlache Strait and on the adjacent continental shelf, Antartica Peninsula. *J. Quatern. Sci.*, **19**, 397–407.

Eyles, C.H., Mory, A.J. and Eyles, N. (2003) Carboniferous–Permian facies and tectonostratigraphic successions of the glacially influenced and rifted Carnarvon Basin, western Australia. *Sed. Geol.*, **155**, 63–86.

Eyles, N. and Januszczak, N. (2004) 'Zipper-rift': a tectonic model for Neoproterozoic glaciations during the breakup of Rodinia after 750 Ma, *Earth-Sci. Rev.*, **65**, 1–73.

Eyles, N. and McCabe, A.M. (1989) The Late Devensian (<22000 BP) Irish Sea Basin: the sedimentary record of a collapsed ice sheet margin. *Quatern. Sci. Rev.*, **8**, 307–351.

Ghienne, J.-F. (1998) Modalités d'enregistrement d'une glaciation ancienne; exemple de la glaciation fini-ordovicienne sur la plate-forme nord-gondwanienne en Afrique de l'Ouest. Unpubl. PhD thesis, Université Louis Pasteur, Strasbourg, 407 pp.

Ghienne, J.-F. (2003) Late Ordovician sedimentary environments, glacial cycles, and post-glacial transgression in the Taoudeni Basin, West Africa. *Palaeogeogr., Palaeoclimatol., Palaeoecol.*, **189**, 117–145.

Ghienne, J.-F. and Deynoux, M. (1998) Large-scale channel fill structures in Late Ordovician glacial deposits in Mauritania, western Sahara. *Sed. Geol.*, **119**, 141–159.

Ghienne, J.-F., Bartier, D., Leone, F. and Loi, A. (2000) Caractérisation des horizons manganésifères de l'Ordovicien supérieur de Sardaigne: relation avec la glaciation fini-Ordovicienne. *CR Acad. Sci. Paris*, **331**, 257–264.

Ghienne, J.F., Deynoux, M., Manatschal, G. and Rubino J.L. (2003) Palaeovalleys and fault-controlled depocenters in the Late Ordovician glacial record of the Murzuq Basin (Central Libya), *CR Geosciences*, **335**, 1091–1100.

Grahn, Y. and Caputo, M.V. (1992) Early Silurian glaciations in Brazil. *Palaeogeogr. Palaeoclimatol. Palaeoecol.*, **99**, 9–15.

Hamoumi, N. (1988) La plate-forme ordovicienne du Maroc: dynamique des ensembles sédimentaires. Unpubl. PhD thesis, Université Louis Pasteur, Strasbourg, 237p.

Hiller, N. (1992) The Ordovician System in South Africa: a review. In: *Global perspectives on Ordovician geology* (Eds Webby, Laurie), 473–485 pp, Balkema, Rotterdam.

Hirst, J.P.P., Benbakir, A., Payne, D.F. and Westlake, I.R. (2002) Tunnel Valleys and Density Flow Processes in the upper Ordovician glacial succession, Illizi Basin, Algeria: influence on reservoir quality. *Mar. Petrol. Geol.*, **25**, 297–324.

Khoukhi, Y. and Hamoumi, N. (2001) L'Ordovicien de la Méséta orientale (Maroc): stratigraphie génétique-contrôle géodynamique, climatique et eustatique. *Africa Geosci. Rev.*, **8**, 289–302.

Klitzsch, E. (1981) Lower Palaeozoic rocks of Libya, Egypt, and Sudan. In: *Lower Palaeozoic of the Middle East, Eastern ans Southern Africa, and Antarctica* (Ed. C.H. Holland), pp. 131–163, John Wiley, New York.

Konaté, M, Guiraud, M., Lang, J. and Yahaya, M. (2003) Sedimentation in the Kandi extensional basin (Benin and Niger): fluvial and marine deposits related to the Late Ordovician deglaciation in West Africa. *J. Afr. Earth Sci.*, **36**, 185–206.

Kumpulainen, R.A. (2005) Ordovician glaciation in Eritrea and Ethiopia. International Conference on *Glacial Sedimentary Processes and Products*, University of Wales, Aberystwyth (22–27 august), abstract volume.

Le Heron D. (2004) The development of the Murzuq Basin, SW Libya, during the late Ordovician. Unpubl. PhD thesis, University of Wales, Aberystwyth.

Le Heron, D., Sutcliffe, O.E., Bourgig, K., Craig, J., Visentin, C. and Whittington, R. (2004) Sedimentary Architecture of Upper Ordovician Tunnel Valleys, Gargaf Arch, Libya: Implications for the Genesis of a Hydrocarbon Reservoir. *GeoArabia*, **9**, 137–160.

Le Heron, D.P., Sutcliffe, O.E., Whittington, R.J. and Craig, J. (2005) The origins of glacially related soft-sediment deformation structures in Upper Ordovician glaciogenic rocks: implication for ice sheet dynamics. *Palaeogeogr., Palaeoclimatol., Palaeoecol.*, **218**, 75–103.

Le Heron, D., Craig, J., Sutcliffe, O. and Whittington, R. (2006) Ordovician glaciogenic reservoir heterogeneity: an example from the Murzuq Basin Libya. *Mar. Petrol. Geol*, **23**, 655–677.

Le Heron, D., Ghienne, J.-F., El Houicha, M., Khoukhi, Y. and Rubino, J.-L. (2007) Maximum extent of ice sheets in Morocco during the Late Ordovician glaciation. In: *Lower Palaeozoic Palaeogeography and Palaeoclimate* (Eds Munnecke, A. and Servais, T.), *Palaeogeogr. Palaeoclimatol. Palaeoecol*, **245**, 200–226.

Legrand, P. (1974) Essai sur la paléogéographie de l'Ordovicien du sahara algérien. *Compagnie Française des Pétroles, Notes et Mémoires*, **11**, 121–138.

Legrand, P. (1985) Lower Palaeozoic rocks of Algeria. In: *Lower Palaeozoic of north-western and west-central Africa* (Ed. C.H. Holland), pp. 5–89, John Wiley, New-York.

Legrand, P. (1993) Graptolites d'âge ashgillien dans la région de Chirfa (Djado, République du Niger). *Bull. Centres Rech. Explor.-Prod. Elf Aquitaine*, **17**, 435–442.

Legrand, P. (2003) Paléogeographie du Sahara algérien à l'Ordovicien terminal et au Silurien inférieur. *Bull. Soc. Geol. Fr.*, **174**, 19–32.

Leone, F., Loi, A. and Pillola G.L. (1995) The post Sardic Ordovician sequence in SW Sardinia. In: *6th Palaeobenthos International Symposium* (Ed. A. Cherchi), *Guide book*, pp. 81–108, Cagliari University.

Lønne, I. (1995) Sedimentary facies and depositional architecture of ice-contact glaciomarine systems. *Sed. Geol.*, **98**, 13–43.

Lønne, I., Nemec, W., Blikra, L.H. and Lauritsen, T. (2001) Sedimentary architecture and dynamic stratigraphy of a marine ice-contact system. *J. Sed. Petrol.*, **71**, 922–943.

Lüning, S., Craig. J., Loydell, D.K., Storch, P. and Fitches, B. (2000) Lower Silurian 'hot shales' in North Africa and Arabia: regional distribution and depositional model. *Earth-Sci. Rev.*, **49**, 121–200.

Martinez, M. (1998) Late Ordovician glacial deposits of northwest Argentina: new evidence from the Mecoyita Formation, Santa Victoria Range. *J. Afr. Earth Sci.*, **27**, supplement 1, 136–137.

Massa, D. (1988) *Paléozoïque de Libye occidentale. Stratigraphie et Paléogéographie*. Unpublish. Thèse d'Etat, Université de Nice, 514 pp.

McDougall, N. and Martin, M. (2000) Facies models and sequence stratigraphy of Upper Ordovician outcrops in the Murzuq Basin, SW Libya. In: *Geological Exploration in Murzuq Basin* (Eds M.A. Sola and D. Worsley), pp. 223–236, Elsevier Science.

McGillivray, G.J. and Husseini, M. (1992) The Paleozoic petroleum geology of Central Saudi Arabia. *AAPG Bull.*, **76**, 1473–1490.

McLure, H.A. (1978) Early Paleozoic glaciation in Arabia. *Palaeogeogr., Palaeoclimatol., Palaeoecol.*, **25**, 315–326.

Monod, O., Kozlu, H., Ghienne, J-F., Dean, W.T., Günay, Y., Le Hérissé, A., Paris, F. and Robardet, M. (2003) Late Ordovician glaciation in southern Turkey. *Terra Nova*, **15**, 249–257.

Moreau, J. (2005) Architecture stratigraphique et dynamique des dépôts glaciaires ordoviciens du Bassin de Murzuk (Libye). Unpubl. PhD thesis, Université Louis Pasteur, Strasbourg.

Moreau, J., Ghienne, J.-F., Le Heron, D., Rubino, J.-L. and Deynoux, M. (2005) A 440 Ma old ice stream in North Africa. *Geology*, **33**, 753–756.

Ottesen, D., Dowdeswell, J.A. and Rise, L. (2005) Submarine landforms and the reconstruction of fast-flowing ice streams within a large Quaternary ice sheet: The 2500-km-long Norwegian-Svalbard margin (57°–80°N). *Geol. Soc. Am. Bull.*, **117**, 1033–1050.

Ouanaimi, H. (1998) Le passage Ordovicien-Silurien à Tizi n'Tichka (Haut-Atlas, Maroc): variations du niveau marin, *CR Acad. Sci. Paris*, **326**, 65–70.

Oulebsir, L. and Paris, F. (1995) Chitinozoaires ordoviciens du Sahara algérien: biostratigraphie et affinités paléogéographiques. *Rev. Palaeobot. Palynol.*, **86**, 49–68.

Paris, F., Elaouad-Debbaj, Z., Jaglin, J.C., Massa, D. and Oulebsir, L. (1995) Chitinozoans and Late Ordovician glacial events on Gondwana. In: *Ordovician Odyssey* (Eds J.D. Cooper, M.L. Droser and S. Finney), pp. 171–176, Short papers for the seventh international symposium on the Ordovician System, SEPM, Fullerton, California.

Paris, F., Deynoux, M. and Ghienne, J.-F. (1998) Chitinozoaires de la limite Ordovicien-Silurien en Mauritanie. *CR Acad. Sci. Paris*, **326**, 499–504.

Powell, R.D. (1990) Sedimentary processes at grounding line fans and their growth to ice-contact deltas. In: *Glacimarine environments: processes and sediments* (Eds J.A. Dowdeswell and J.D. Scourse), *Geol. Soc. London Spec. Publ.*, **53**, 53–77.

Powell, R.D., Khalil Moh'd, B. and Masri, A. (1994) Late Ordovician-Early Silurian glaciofluvial deposits preserved in palaeovalleys in South Jordan. *Sed. Geol.*, **89**, 303–314.

Proust, J.-N. and Deynoux, M. (1993) Marine to non marine sequence architecture of an intracratonic glacially related basin. Late Proterozoic of the West African platform in western Mali. In: *Earth's Glacial Record* (Eds M. Deynoux, J.MG. Miller, E.W. Domack, N. Eyles, I.J. Fairchild and G.M. Young), pp. 241–259, Cambridge University Press.

Powell, R.D. and Cooper, J.M. (2002) A glacial sequence stratigraphic model for temperate, glaciated continental shelves. In: *Glacier-Influenced Sedimentation on High-Latitude Continental Margin* (Eds J.A. Dowdeswell and C. Cofaigh), pp. 215–244, *Geol. Soc. London Spec. Publ.*, **203**.

Robardet, M. and Doré, F. (1988) The Late Ordovician diamictic formations from southwestern Europe: North-Gondwana glaciomarine deposits. *Palaeogeogr. Palaeoclimatol. Palaeoecol.*, **66**, 19–31.

Ross, J.R.P. and Ross C.A. (1992) Ordovician sea-level fluctuations. In: *Global perspectives on Ordovician geology* (Eds B.D. Webby and J.R. Laurie), pp. 327–336, Balkema, Rotterdam.

Russell, H.A.J. and Arnott, R.W.C. (2003) Hydraulic-jump and hyperconcentrated-flow deposits of a glacigenic subaqueous fan: Oak Ridges Moraines, southern Ontario, Canada. *J. Sed. Res.*, **73**, 887–905.

Russell, H.A.J., Arnott, R.W.C. and Sharpe, D.R. (2003) Evidence for rapid sedimentation in a tunnel channel, Oak Ridges Moraine, southern Ontario, Canada. *Sed. Geol.*, **160**, 33–55.

Saltzman, M.R. and Young, S.A. (2005) Long-lived glaciation in the Late Ordovician? Isotopic and sequence-stratigraphic evidence from western Laurentia. *Geology*, **33**, 109–112.

Senalp M. and Al-Laboun A. (2000) New evidence on the Late Ordovician Glaciation in Central Saudi Arabia. *Saudi Aramco Journal of Technology*, 1–40 (Spring).

Smart, J. (2000) Seismic expressions of depositional processes in the upper Ordovician succession of the Murzuq Basin, SW Libya. In: *Symposium on Geological Exploration in Murzuq Basin* (Eds M.A. Sola and D. Worsley), pp. 397–415, Elsevier, Amsterdam.

Stampfli, G.M. and Borel G.D. (2002) A tectonic model for the Paleozoic and Mesozoic constrained by dynamic plate boundaries and restored synthetic oceanic isochrones. *Earth Planet. Sci. Lett*., 196, 17–33.

Stokes, C.R. and Clark, C.D. (2001). Palaeo-ice streams. *Quatern. Sci. Rev.*, **20**, 1437–1457.

Storch, P. and Leone, F. (2003) Occurrence of the late Ordovician (Hirnantian) graptolite Normalograptus ojuensis (Koren & Mikhaylova, 1980) in south-western Sardinia, Italy. *Bol. Della Soc. Paleont. Ital.*, **42**, 31–38.

Sutcliffe, O.E., Dowdeswell, J.A., Whittington, R.J., Theron, J.N. and Craig, J. (2000) Calibrating the Late Ordovician glaciation and mass extinction by the eccentricity cycles of Earth's orbit. *Geology*, **28**, 967–970.

Sutcliffe, O.E., Harper, D.A.T., Aït Salem, A., Whittington, R.J. and Craig, J. (2001) The development of an atypical Hirnantia-brachiopod Fauna and the onset of glaciation in the late Ordovician of Gondwana. *Trans. Roy. Soc. Edinb. Earth Sci.*, **92**, 1–14.

Underwood, C.J., Deynoux, M. and Ghienne, J.-F. (1998) High palaeolatitude recovery of graptolite faunas after the Hirnantian (top Ordovician) extinction event. *Palaeogeogr. Palaeoclimatol. Palaeoecol*., **142**, 91–105.

Turner, B.R., Makhlouf, I.M. and Armstrong, H.A. (2005) Late Ordovician (Ashgillian) glacial deposits in southern Jordan. *Sed. Geol.*, **181**, 73–91.

Vaslet, D. (1990) Upper Ordovician glacial deposits in Saudi Arabia. *Episodes*, **13**, 147–161.

Vecoli, M. and Le Hérissé, A. (2004) Biostratigraphy, taxonomic diversity and patterns of morphological evolution of Ordovician acritarchs (organic-walled microphytoplankton) from the northern Gondwana margin in relation to palaeoclimatic and palaeo-geographic changes. *Earth-Sci. Rev*., **67**, 267–311.

Vorren, T.O. and Laberg, J.S. (1997) Trough mouth fans – Palaeoclimate and ice-sheet monitors. *Quatern. Sci. Rev.*, **16**, 865–881.

Webby, B.D., Cooper, R.A., Bergström, S.M. and Paris, F. (2004) Stratigraphic framework and time slices. In: *The Great Ordovician Diversification Event* (Eds B.D. Webby, F. Paris, M. Droser and I. Percival), pp. 41–47, Columbia University Press, New York.

Young, G.M., Minter W.E.L. and Theron, J.N. (2004) Geochemistry and palaeogeography of upper Ordovician glaciogenic sedimentary rocks in the Table Mountain Group, South Africa, *Palaeogeogr., Palaeoclimatol., Palaeoecol*., **214**, 323–345.

6.3. Rebonds postglaciaires

Dans le Hodh (sud-est mauritanien), la séquence de déglaciation au toit de la dernière surface d'érosion glaciaire (à la base de la photographie) comprend des diamictites glaciomarines à la base (partie inférieur, violines et vertes), des faciès d'offshore à graptolite au sommet (vert sombre, Ordovicien terminal, puis gris, Silurien). Elle est temporairement interrompue par l'apparition de faciès littoraux sableux (grès de couleur ocre) interprétés comme la signature du rebond post-glaciaire consécutif à la dernière phase d'avancée glaciaire dans le bassin. Le hauteur de la section est d'environ 80 m.

Un mot s'impose quant à la caractérisation de la signature de rebonds isostatiques postglaciaires dans l'enregistrement statigraphique (Boulton, 1990 ; Eyles et Eyles, 1992). Les éléments de ces réajustements postglaciaires de la lithosphère apparaissent clairement aujourd'hui dans les paysages des régions englacées au Pléistocène (Svensson, 1991 ; Rayburn et Teller, 2007). Cependant, il s'agit là de domaines déjà à l'émersion avant la glaciation, et pour lesquels la séquence d'émersion d'origine isostatique (McCabe et al., 1994 ; Dethier et al., 1995) ne sera pas préservée. Ils ne sont en aucun cas comparables au système ordovicien, dans lequel les glaciers s'avancent sur un domaine sédimentaire à taux de subsidence faible mais effectif. La comparaison avec des analogues quaternaires (Mer du Nord ou marge NE américaine) suggère que le rebond isostatique puisse se marquer dans l'enregistrement sédimentaire par un bref épisode de bas niveau marin interrompant temporairement la dynamique transgressive postglaciaire. Plus qu'une surface d'émersion, un rebond isostatique peut être idendifié par la mise en place diachrone de faciès deltaïques ou littoraux (Forbes et al., 1993 ; Barnhardt et al., 1995) et/ou d'horizons de vannage par les vagues (Barrie et Conway, 2002) au sein d'une séquence de retrait initialement glaciomarine et terminant en domaine d'offshore (*Ghienne, 2003*). Pour l'Ordovicien, plusieurs surfaces d'érosion ont cependant été interprétées comme la signature d'un rebond isostatique (Blanpied et al., 2000 ; McDougal et Martin, 2000 ; El-ghali, 2005). Si de telles surfaces d'émersion ont localement existé, elles ont été surimposées le plus souvent par les surfaces de ravinement transgressif, d'origine tidale ou en domaine de *shoreface* (cf. section 3.4).

Les processus de réajustement postglaciaire à l'échelle lithosphérique induisent la réactivation d'accidents du socle (Johnston, 1989). En modifiant le régime des contraintes, ces réajustements semblent à l'origine d'anomalies locales se présentant sous la forme de dépôt-centres d'extension kilométrique associés à la succession glaciaire (*Ghienne et al., 2003, §3*) ou fini- à post-glaciaire (Denis et al., 2007).

6.4. Corrélations inter-régionales

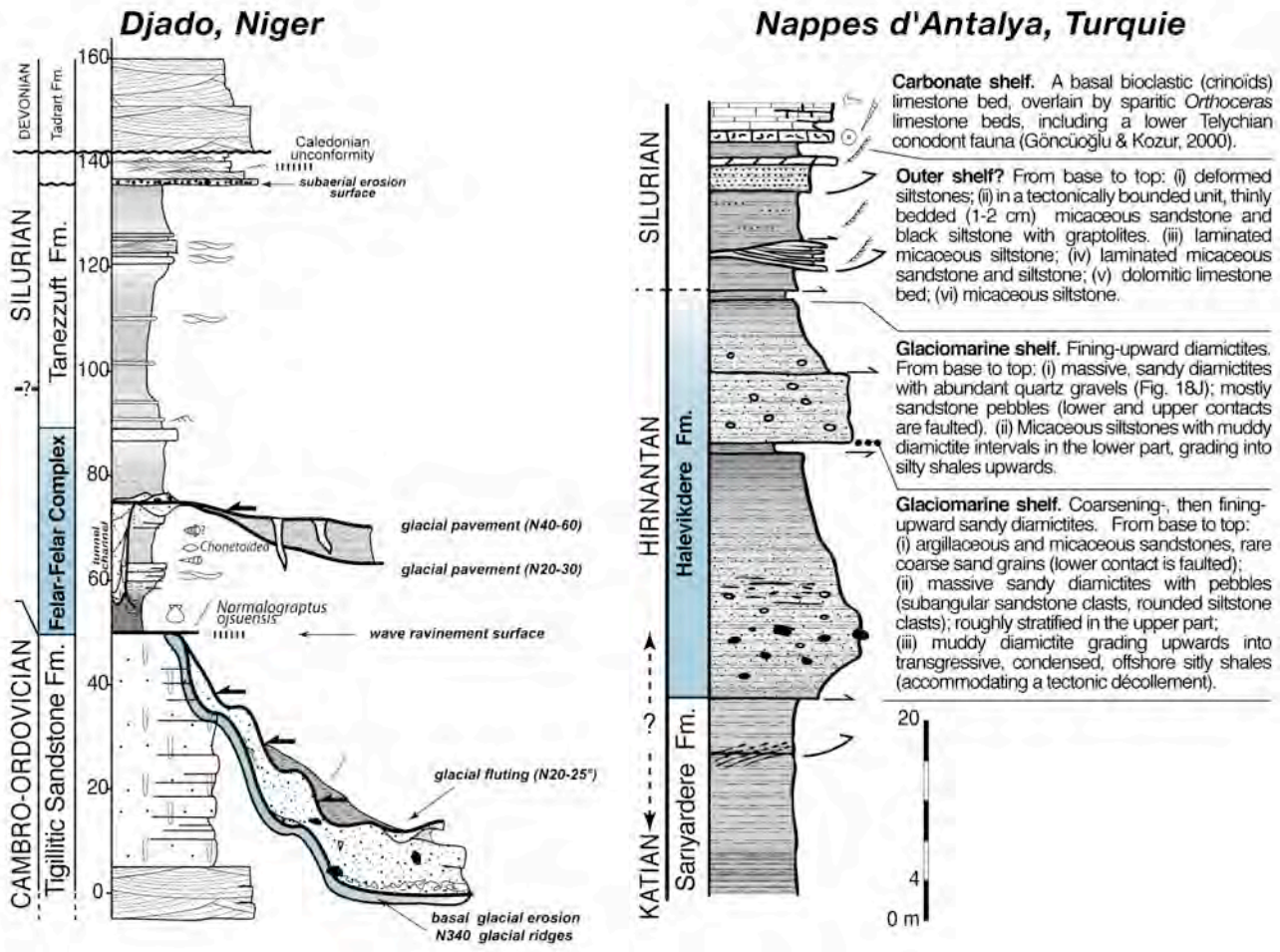

Comment corréler ces deux sections distantes de plus de près de 2000 km ? La couleur bleue souligne la sédimentation sous influence glaciaire, au sein de laquelle apparaît dans les deux cas un « doublet glaciaire ». Au Niger, l'enregistrement de la glaciation est dominé par des surfaces d'érosion glaciaires (d'après Denis et al., 2007*, modifié). En Turquie, il s'agit d'une succession distale entièrement glaciomarine (Ghienne et al., 2010b, §1). A titre d'hypothèse, l'événement glaciaire initial du Niger n'est pas enregistré en Turquie et les deux cycles glaciomarins de Turquie, séparés par la transgression « intra-Hirnantien », ne correspondent qu'à la surface glaciaire marquée au Niger par des orientations N20-N30. La dernière surface (N40-N60) correspondrait à une réavancée de l'inlandsis nouveau sans signature reconnaissable en Turquie.*

Ma manière de construire des corrélations inter-régionales à l'aide de séquences glaciaires a connu 3 phases de développement. Initialement, les géométries de dépôts et les surfaces entraient dans un modèle s'appuyant sur une unique phase d'avancée et de retrait glaciaire, avec des spécificités locales d'ordre autocyclique (Ghienne, 1998 ; Blanpied et al., 2000). Dans un second temps, par la généralisation d'une approche cartographique des successions glaciaires, il est apparu que plusieurs cycles glaciaires (jusqu'à 5) pouvaient être proposés au cours de l'Hirnantien (*Ghienne, 2003* ; *Moreau et al., 2005, §3* ; *Ghienne et al., 2007b*). Avec la prise en compte de régressions forcées pré-hirnantiennes, il apparaît que des séquences inférieures des successions glaciaires les plus internes peuvent également être plus anciennes que l'Hirnantien, et que leur signature sur la plate-forme distale est à rechercher plus bas dans l'enregistrement sédimentaire (Katien, voir figure en Introduction).

Un problème fondamental en stratigraphie séquentielle est celui de la hiérarchisation des séquences, qui s'emboîtent les unes dans les autres en fonction de leur fréquence (Homewood et al., 1992 ; Catuneanu et al., 2009 ; *Loi et al., 2010, §2*, Neal et Abreu, 2009). Si l'on dispose d'un enregistrement fiable et complet, une analyse du signal peut faire ressortir les cyclicités de type Milankovitch. Dans le cas de la glaciation Ordovicien supérieur, il apparaît que les enregistrements sédimentaires sur une même verticale englobent préférentiellement 2 séquences glaciaires. Ainsi, Sutcliffe et al. (2000) avaient été amenés à proposer que l'enregistrement glaciaire hirnantien comprenait deux cycles contrôlés par les paramètres orbitaux. Cependant, ces deux cycles n'ont pas la même valeur partout sur la plate-forme. Les multiples répétitions d'érosions et de dépôts glaciaires se traduisent au final statistiquement le plus souvent par deux séquences glaciaires, des séquences antérieures, intermédiaires ou postérieures n'apparaissant préservées que latéralement suite à la juxtaposition des séquences, ou n'incluant pas de signature glaciogénique. Ce « doublet glaciaire » n'est pas partout restreint à l'Hirnantien, et finalement, la compilation des enregistrements sédimentaires préservés sur les domaines proximaux, intermédiaires et distaux de la plate-forme nord-gondwanienne montre qu'il est nécessaire de « jouer » avec les éléments suivants : (1) l'Ordovicien terminal connaît deux séquences glaciaires de premier ordre, la première Katien terminal, la seconde Hirnantien supérieur (Ghienne et al., 2008 ; *Loi et al., 2010, §2*) ; la séquence de premier ordre Hirnantien supérieur est subdivisée en deux séquences glaciaires de second ordre, entre lesquelles est intercalé un interglaciaire — ou maximun d'inondation — dit « intra-Hirnantien » (*Ghienne et al., 2007b*) ; (3) chacune des deux séquences de second ordre englobe 2 à 4 séquences de troisième ordre. La nature allocyclique, à contrôle climatique, des séquences glaciaires de premier et second ordres est très probable. La contribution d'un signal autocyclique dans le contrôle des séquences de troisième ordre ne peut pas être exclue.

Les extensions glaciaires associées à ces différents cycles sont variables. On a vu que l'extension maximale des glaciers intervenait au cours du second cycle de second ordre (Hirnantien supérieur), avec des surfaces glaciaires préservées jusque dans des domaines distaux de la plate-forme (cf. chapitre 4). L'épisode du Katien terminal n'a en revanche laissé sur la plate-forme externe ni dépôt glaciomarin, ni même la signature d'une régression forcée par suite de l'éloignement des sources. Parfois, il correspond simplement à la disparition de la bioturbation dans les environnements *d'offshore*. Inversement, la transgression intra-hirnantienne, si évidente au Maroc (*Loi et al., 2010, §2*), ne possède pas de signature stratigraphique propre au Niger. Ce dernier secteur n'a pas été déglacé et c'est possiblement une simple ré-orientation des écoulements glaciaires qui peut en être la signature. Cette même transgression est également très discrète sur la plate-forme distale, où elle peut prendre la forme d'un simple niveau condensé. Attribuer une signification en termes d'ordre à une séquence glaciaire nécessite la prise en compte du signal stratigraphique complet offert par la totalité de la pile sédimentaire, et pas seulement de celui inclu dans la succession à caractère glaciogénique.

Chapitre 7

7. Perspectives

- **Construire un modèle de séquence de dépôt en contexte glaciaire.** Etablir un tel modèle est nécessaire pour le développement des corrélations inter-régionales, pour une meilleure caractérisation et prédiction des architectures de réservoirs glaciaires, et pour une meilleure compréhension de la dynamique glaciaire sous l'angle de vue d'une succession sédimentaire, quelle soit ordovicienne ou associée à une glaciation néoprotérozoïque, permo-carbonifère ou cénozoïque.

- **Caractériser la réponse de la bio-géosphère aux fluctuations glaciaires**. Le signal climatique extrait du message sédimentaire glaciaire doit maintenant être confronté à celui issu des des plates-formes carbonatées intertropicales (Desrochers et al., 2010), aux signaux bio-géochimiques, et aux sorties de modélisations paléoclimatiques. La glaciation fini-ordovicienne fournit dorénavant un cadre de mieux en mieux contraint permettant de comprendre, illustrer et modéliser les interactions et rétroactions à l'échelle des temps géologiques entre paléoclimat, biodiversité et signaux biogéochimiques. L'analyse des enregistrements glaciaires des hautes (paléo-)latitudes agit comme une loupe pour qui cherche à comprendre la signification des dérives isotopiques qui apparaissent faussement comme de brusques excursions dans l'enregistrement des basses (paléo-)latitudes (quelques cm sur le stratotype chinois de l'Ordovicien, Xu Chen et al., 2006). Les résultats acquis pour l'Ordovicien terminal permettront de mieux décrypter la période pré-hirnantienne qui connaît des fluctuations climatiques mais ne possède qu'un enregistrement glaciaire très parcellaire ; ils seront également à confronter à des intervalles de temps plus récents du Phanérozoïque (ex. : le Jurassique) qui pourraient constituer des analogues aux événements glaciaires du Paléozoïque inférieur.

- **Contribuer aux reconstructions paléogéographiques anté-varisques.** Si la configuration de la Pangée (A ou B ?) post-varique est encore controversée, les reconstructions anté-varisques n'en sont qu'à leurs prémices (Cocks et Torsvik, 2002 ; Von Raumer et Stampfli, 2008). La glaciation fini-ordovicienne, au tout au moins la période correspondant au maximum glaciaire, a imprimé sur la marge continentale gondwanienne une paléogéographie inédite que les déformations dévoniennes à carbonifères (rifts, rotations de blocs, translations, métamorphisme) ont bouleversée. La prise en compte de la logique interne à la paléogéographie glaciaire permet de confirmer, infirmer ou proposer des reconstructions (*Ghienne et al., 2010b, §1*). La présence des vallées glaciaires au nord de l'Espagne *(Guttiérez-Marco et al., 2010, §3)* confirme les schémas indiquant une rotation à 180° du domaine ibérique au sein duquel l'enregistrement glaciaire se distalise vers le sud. De même, la présence en Corse d'une succession glaciaire caractéristique de la marge continentale et radicalement différente de la succession sarde, va dans le sens de grands décrochements dextres tardi-hercyniens mis en évidence par la géologie structurale (Rossi et al., 2009).

Initialement envisagée comme une glaciation longue (>10 Ma), la glaciation de l'Ordovicien supérieur a ensuite été considérée comme un événement climatique court, bien que polyphasé, correspondant à une partie seulement de l'étage Hirnantien (445,6-443,7 Ma). Cependant, un nouveau consensus émerge, considérant une multiplicité d'événements glaciaires au cours de l'Ordovicien supérieur et du Silurien inférieur. Si l'essentiel des archives glaciaires *s.s.* est d'âge Hirnantien, les régressions forcées antérieures et postérieures sont à considérer elles-aussi comme la signature d'événements glaciaires. L'événement hirnantien n'en serait que le climax, tout comme le Pléistocène supérieur ne représente qu'un des épisodes marquant du Cénozoïque, ou l'événement Permien Inférieur pour la glaciation du Paléozoïque supérieur (Fielding et al. 2008b). Cette glaciation et la transgression postglaciaire corrélative ont généré un système pétrolier très prolifique. Si la nécessité de la caractérisation de ce système a abouti à une meilleure connaissance des archives glaciaires, il existe encore de nombreuses zones d'ombre que le champ de recherche académique doit encore éclaircir, en particulier celles qui concernent les relations entre glaciation, signaux biologiques et indicateurs géochimiques.

Références

Achab A., Paris F. (2007) The Ordovician chitinozoan biodiversification and its leading factors. Palaeogeography, Palaeoclimatology, Palaeoecology 245, 5-19.

Ainsaar L., Kaljo D., Martma T., Meidla T., Männik P., Nolvak J., Tinn O. (2010) Middle and Upper Ordovician carbon isotope chemostratigraphy in Baltoscandia : A correlation standart and clues to environmental history. Palaeogeography Palaeoclimatology Palaeoecology, 294, 189-201.

Alvaro J.J., Vliet Lanoe, B.V. (2010) Late Ordovician carbonate productivity and glaciomarine record under quiescent and active extensional tectonics in NE Spain. In: Bassett (ed.) Early Palaeozoic Peri-Gondwana Terranes: New insights from Tectonics and Biogeography. Geological Society, London, Special Publications, 325, 141-155.

Amireh B.S., Schneider W. & Abed A.M. (2001) Fluvial-shallow marine-glaciofluvial depositional environments of the Ordovician system in Jordan. Journal of Asian Earth Sciences, 19, 45-60.

Andreassen C., Ødegaard C.M., Rafaelsen B. (2007) Imprints of former ice streams, imaged and interpreted using industry three-dimensional seismic data from the south-western Barents Sea. In: Davies R.J., Posamentier H.W., Wood L.J., Cartwright J.A. (eds) Seismic Geomorphology: Applications to Hydrocarbon Exploration and Production. Geological Society, London, Special Publications, 277, 151-169.

Armstrong H.A., Baldini J., Challands T.J., Gröcke D.R., Owen A.W. (2009) Response of the Inter-tropical Convergence Zone to Southern Hemisphere cooling during Upper Ordovician glaciation. Palaeogeography, Palaeoclimatology, Palaeoecology 284, 227-236.

Barnhardt W. A., Gehrels W. R., Belknap D. F., Kelley J. T. (1995) Late Quaternary relative sea-level change in the western Gulf of Maine: Evidence for a migrating glacial forebulge. Geology, 23, 4, 317-320.

Barca S., Durand-Delga M., Rossi P., Storch P. (1996) Les micaschistes panafricains de Corse et leur couverture paléozoïque : leur interprétation au sein de l'orogène varisque sud-européen, Comptes Rendus Académie des Sciences Paris, 322, 981-989.

Barrie J.V., Conway K.W. (2002) Contrasting glacial sedimentation processes ad sea-level changes in two adjacent basins on the Pacific margin of Canada. Geological Society Spec. Publs., 203, 181-194.

Bellini E., Massa D. (1980) A stratigraphic contribution to the Paleozoic of the southern basins of Libya. In: Salem, M.J., Busrewil, M.T. (Eds), The Geology of Libya. Academic Press, London, pp. 3–56.

Benn D.I., Evans D.J.A. (1998) Glaciers and glaciations. Arnold, London, 734 p.

Bennett M.R. (2003) Ice streams as the arteries of an ice sheet: Their mechanics, stability and significance: Earth-Science Reviews, 61, 309–339.

Beuf S., De Charpal O., Debyser J., Gariel O. and Montadert L. (1962) Recherche sédimentologique; Le Cambro-Ordovicien du Tassili des Ajjers (Résultats de la mission 1961-1962). Institut Français du Pétrole, unpublished report 7700-A.

Beuf S., Biju-Duval B., De Charpal O., Rognon P., Gariel O., Bennacef A. (1971) Les grès du Paleozoïque inférieur au Sahara. Science et Technique du pétrole 18, Paris, 464 pp.

Blanpied C., Deynoux M., Ghienne J.-F. et Rubino J.-L. (2000) Late Ordovician glacially related depositional systems of the Gargaf Uplift (Libya) and comparisons with correlative deposits in the Taoudeni Basin (Mauritania). Geological Exploration in Murzuq Basin (M.A. Sola et D. Worsley Eds), Elsevier, 485-507.

Boote D.R.D., Clark-Lowes D.D., Traut M.W. (1998) Palaeozoic petroleum systems of North Africa. In: MacGregor, D.S. Moody, R.T.J., Clark-Lowes, D.D. (Eds.), Petroleum Geology of North Africa, Geological Society of London, Special Publication 132, pp. 7–68.

Borroco J., Nyssen R. (1959) Nouvelles observations sur les « grès inférieurs » cambro-ordoviciens du Tassili interne (Nord-Hoggar). Bulletin de la Société Géologique de France, 7, 197-206.

Boulton G. S. (1990) Sedimentary and sea level changes during glacial cycles and their control on glaciomarine facies architecture. In : Glacimarine Environments: processes and sediments, Dowdeswell J. A., Scourse J. D. (Eds), Geol. Soc. Spec. Pub., 53, 15-52.

Boulton G. S. (1996) Theory of glacial erosion, transport and deposition as a consequence of subglacial sediment deformation. Journal of Glaciology, 42, 43-62.

Bourahrouh (2002) Chitinozoaires & palynomorphes de l'Ordovicien Supérieur Nord-Gondwanien: impact de la glaciation ashgillienne. Thèse de l'Université de Rennes 1, 271 pp.

Bourahrouh A., Paris F., Elaouad-Debbaj Z. (2004) Biostratigraphy, bodiversity and palaeoenvironments of the chitinozoans and associated palynomorphs from the Upper Ordovician of the Central Anti-Atlas, Morocco. Review of Palaeobotany and Palynology 130, 17–40.

Brenchley P.J., Marshall J.D., Carden C.A.F., Robertson D.B.R., Long D.G.F., Leidla T., Hints L., Anderson T.F. (1994) Bathymetric and isotope evidence for a short-lived late Ordovician glaciation in a greenhouse period. Geology 22, 295–298.

Brenchley, P.J., Carden, G.A., Hints, L., Kaljo, D., Marshall, J.D., Martma, T., Meidla, T., Nolvak, J. (2003) High-resolution stable isotope stratigraphy of Upper Ordovician sequences: constrains on the timing of bioevents and environmental changes associated with mass extinction and glaciation. Bulletin of the Geological Society of America, 115, 89–104.

Brookfield M.E., Martini I.P. (1999) Facies architecture and sequence stratigraphy in glacially influenced basins: basic problems and water-level/glacier input-point controls (with an example from the Quaternary of Ontario, Canada). Sediment. Geol., 123, 183-193.

Calner, M., Lehnert, O., Joachimski, M. (2009) Carbonate mud mounds, conglomerates, and sea-level history in the Katian (Upper Ordovician) of central Sweden. Facies. 56, 167-172.

Canals, M., Urgeles, R., and Calafat, A.M. (2000) Deep sea-floor evidence of past ice streams off the Antarctic Peninsula: Geology, v. 28, p. 31–34.

Catuneanu O., Abreu, V., Bhattachary, J.P., Blum, M., Dalrymple, R.W., Eriksson, P.G., Fielding, C.R., Fisher, W.L., Galloway, W.E., Gibling, M.R., Giles, K.A., Holbrook, J.M., Jordan, R., Kendall, C.G.St.C., Macurda, B., Martinsen, O.J., Miall, A.D., Neal, J.E., Nummedal, D., Pomar, L., Posamentier, H.W., Pratt, B.R., Sarg, J.F., Shanley, K.W., Steel, R.J., Strasser, A., Tucker, M.E., Winker, C. (2008) Towards the standardization of sequence stratigraphy. Earth-Science Reviews 92, 1–33.

Chen, X., Rong. J., Fan, J., Zhan, R., Mitxhell, C.E., Harper, A.T., Melchin, M.J., Peng, P., Finney, S.C., Wang, X. (2006) The Global Boundary Stratotype Section and Point (GSSP) for the base of the Hirnantian Stage (the uppermost of the Ordovician System). Episodes 29, 183–196.

Cocks L.R.M., Fortey R.A. (2010) Avalonia: a long-lived terrane in the Lower Palaeozoic? In: Bassett (ed.) Early Palaeozoic Peri-Gondwana Terranes: New insights from Tectonics and Biogeography. Geological Society, London, Special Publications, 325, 141-155.

Cocks L.R.M., Torsvik T.H. (2005) Earth geography from 500 to 400 million year ago: a faunal and palaeomagnetic review. Journal of the Geological Society, London, 159, 631-644.

Collomb G.R. (1962) Etude géologique du Jebel Fezzan et de sa bordure paléozoïque. Notes et Mémoires, Compagnie Française des Pétroles, Paris, 36 pp.

Dars R., Sougy J. et Tessier F. (1957) Nouvelle stratigraphie des series paléozoïques de Kayes (Soudan français). Comptes Rendus de l'Académie des Sciences, 244, 2312-2314.

Davidson L., Beswetherick S., Craig J., Eales M., Fisher A., Himmali A., Jho J., Mejrab B., Smart J. (2000) The structure, stratigraphy and petroleum geology of the Murzuq Basin, southwest Libya, 295-320. In SOLA, M.A. & WORSLEY, D. (eds) Geological Exploration in Murzuq Basin, Elsevier Science, Amsterdam.

Debyser J., de Charpal O., Merabet O. (1965) Sur le caractère glaciaire de la sedimentation de l'Unité IV au Sahara central. Comptes Rendus de l'Académie des Sciences, Paris, 261, 5575-5576.

Delabroye A., Vecoli, M. (2010) The end-Ordovician glaciation and the Hirnantian Stage: A global review and questions about Late Ordovician event stratigraphy. Earth Science Reviews, 98, 269-282.

Denis M., Buoncristiani J.-F., Konaté M., Ghienne J.-F. et Guiraud M. (2007) Hirnantian glacial and deglacial record in SW Djado Basin (NE Niger). Geodinamica Acta, 20-3, 177-194.

Denis, M., Buoncristiani, J.-F., Konaté, M., Guiraud, M. (2007b) The origin and glaciodynamic significance of sandstone ridge networks from the Hirnantian glaciation of the Djado Basin (Niger). Sedimentology 54, 1225–1243.

Denis M., Guiraud M., Konaté M., Buoncristiani J.F. (2010) Subglacial deformation and water-pressure cycles as a key for understanding ice stream dynamics: evidence from the Late Ordovician succession of the Djado Basin (Niger). International Journal of Earth Science, 99, 1399-1425.

Desrochers A., Farley C., Achab, A., Asselin E., Riva J. (2010) A far-field record of the end Ordovician glaciation : The Ellis Bay Formation, Anticoti Island, eastern Canada. Palaeogeography Palaeoclimatology Palaeoecology, 296, 248-263.

Destombes, J. (1968a) Sur la présence d'une discordance générale de ravinement d'âge Ashgill supérieur dans l'Ordovicien terminal de l'Anti-Atlas (Maroc). Comptes Rendus Académie des Sciences Paris 267, 565–567.

Destombes, J. (1968b) Sur la nature glaciaire des sédiments du groupe du 2^{e} Bani, Ashgill supérieur de l'Anti-Atlas, Maroc. Comptes Rendus Académie des Sciences Paris 267, 684–686.

Destombes, J., Hollard, H., Willefert, S. (1985) Lower Palaeozoic rocks of Morocco. In: Holland, C.H. (Ed.), Lower Palaeozoic of North-western and West Central Africa. John Wiley, New-York., pp. 91–336.

Dethier D. P., Pessl F., Keuler R. F., Balzarini M. A., Pevear D. R. (1995) Late Wisconsinan glaciomarine deposition and isostatic rebound, northern Puget Lowland, Washington. Geol. Soc. Am. Bull., 107, 1288-1303.

Deynoux, M. (1980) Les formations glaciaires du Précambrien terminal et de la fin de l'Ordovicien en Afrique de l'ouest. Deux exemples de glaciation d'inlandsis sur une plate-forme stable. Trav. Lab. Sci. Terre St.Jérome, Marseille, 17, 554 pp.

Deynoux, M., Sougy J., Trompette R. (1985) Lower Paleozoic rocks of West Africa and the western part of Central Africa. In: Lower Paleozoic rocks of NW and W Central Africa, C.H. Holland (Ed.), John Wiley, New-York., pp. 337–495.

Deynoux M., Ghienne J.F. (2004) Late Ordovician glacial pavements revisited – a reappraisal of the origin of striated surfaces. Terra Nova, 16, 95-101.

Deynoux M., Ghienne J.F. (2005) Late Ordovician glacial pavements revisited – a reappraisal of the origin of striated surfaces. Reply. Terra Nova, 17, 488-491.

Dia O., Sougy J.and Trompette R. (1969) Discordance de ravinement et discordance angulaire dans le Cambro-Ordovicien de la région de Mejeria (Taganet occidental, Mauritanie). Bull. Soc. Géol. Fr., 11, 207-221.

Díaz-Martínez, E., Grahn, Y. (2007) Early Silurian glaciation along the western margin of Gondwana (Peru, Bolivia and northern Argentina): Palaeogeographic and geodynamic setting. Palaeogeography, Palaeoclimatology, Palaeoecology 245, 62–81.

Dowdeswell J.A., O Cofaigh C., Taylor J., Kenyon N.H., Mienert J., Wilken M. (2002) On the architecture of high-latitude continental margins: the influence of ice-sheet and sea-ice processes in the Polar North Atlantic. In: Dowdeswell J.A. & O Cofaigh C. (eds) Geological Society, London, Special Publications, 203, 33-54.

Dronkers J. (2005) Dynamics of Coastal Systems. World Scientific Pub Co Inc., 540 pp.

Duller, R.A., Mountney, N.P., Russell, A.J., Cassidy, N.C. (2008) Architectural analysis of a volcaniclastic jökulhlaup deposit, southern Iceland: sedimentary evidence for supercritical flow. Sedimentology, 55, 939-964.

Dunbar, G. B., Naish, T.R., Barrett, P.J., Fielding, C.R., Powell, R.D. (2008) Contrasting the amplitude of late Oligocene bathymetric changes in Western Ross Sea during orbitally-induced oscillations in the East antarctic Ice Sheet : (1) Implication for glaciomarine sequence stratigraphic models. Palaeogeography, Palaeoclimatology, Palaeoecology 260, 50–65.

El-ghali, M.A.K. (2005) Depositional environments and sequence stratigraphy of paralic glacial, paraglacial and postglacial Upper Ordovician siliciclastic deposits in the Murzuq Basin, SW Libya. Sedimentaty Geology, 177, 145-173.

Embry, A.F. (2009) Practical Sequence Stratigraphy. Canadian Society of Petroleum Geologists, Online at www.cspg.org, 79 p.

Eschard, R., Abdallah, H., Braik, F. and Desaubliaux, G. (2005) The Lower Paleozoic succession in the Tasilli outcrops, Algeria: sedimentology and sequence Stratigraphy. First Break, 23, 27-36.

Evans DJA, Phillips ER, Hiemstra JF, Auton CA (2006) Subglacial till: formation, sedimentary characteristics and classification. Earth Sci Rev 78:115–176.Eyles, N. (1993) Earth's glacial record and its tectonic setting. Earth-Sciences Reviews, 35, 1-248.

Eyles N (2006) The role of meltwater in glacial processes. Sedimentary Geology, 190, 257-268.

Eyles N (2008) Glacio-epochs and the supercontient cycle after ~ 3.0 Ga:Tectonic boundary conditions for glaciation. Palaeogeography, Palaeoclimatology, Palaeoecology, 258, 89-129

Eyles N., Boyce J. L. (1998) Kinematic indicators in fault gouge: tectonic analog for soft-bedded ice sheets. Sediment. Geol., 116, 1-12.

Eyles N. & de Broekert P (2001) Glacial tunnel valleys in the Eastern Goldfields of Western Australia cut below the Late Paleozoic Pilbara ice sheet. Palaeogeography, Palaeoclimatology, Palaeoecology, 171, 29-40.

Eyles N., Eyles C.H. (1992) Glacial depositional system s. In: Walker R.G. & James N.P. (eds) Facies Models, response to sea-level change. Geological Association of Canada, Toronto, 73-100.

Eyles N., McCabe A.M. (1989) The late Devensian (<22 000 BP) Irish Sea Basin: the sedimentary record of a collapsed ice sheet margin. Quaternary Science Rev., 8, 307-351.

Fabre, J. (1988) Les séries paléozoïques d'Afrique : une approche. Journal of African Earth Science 7, 1-40.

Fabre, J. & Kazi-Tani, N. (2005) Ordovicien, Silurien, Devonien, Permo-Carbonifère, 147-360. In Fabre, J. (ed.) Géologie du Sahara occidental et central (ed.), Tervuren African Geoscience Collection, 18, Musée Royal de l'Afrique Centrale, Tervuren, Belgique.

Fello N., Lüning S., Storch P. and Redfern J. (2006) Identification of early Llandovery (Silurian) anoxic palaeo-depressions at the western margin of the Murzuq Basin (southwest Libya), based on gamma ray spectrometry in surface exposures. Geoarabia, 11, 101-117.

Fielding C.R., Frank T.D., Birgenheier L.P., Rygel M.C., Jones A.T., Roberts J. (2008) Stratigraphic record and facies associations of the late Paleozoic ice age in eastern Australia (New Soth Wales and Queensland). In : Fielding C.R., Frank T.D., Isbell J.L (eds) Resolving the Late Paleozoic Ice Age in Time and Space. The Geological Society of America, Special Paer 441, 41-57.

Fielding C.R., Frank T.D.,Isbell J.L (2008) The late Paleozoic ice age—A review of current understanding and synthesis of global climate patterns. In : Fielding C.R., Frank T.D., Isbell J.L (eds) Resolving the Late Paleozoic Ice Age in Time and Space. The Geological Society of America, Special Paer 441, 343-354.

Forbes D. L., Shaw J., Eddy B. G. (1993) Late Quaternary sedimentation and the postglacial sea-level minimum in Port au Port Bay and vicinity, west Newfoundland. Atlantic Geology, 29, 1-26.

Frakes L. A., Francis J. E., Syktus J. I. (1992) Climate Modes of the Phanerozoic. The history of the Earth's climate over the past 600 million years. Cambridge University Press, 274p.

Freulon J.-M.(1959, 1964) Etude géologique des series Primaires du Sahara central (Tassili n'Ajjer et Fezzan). Thèse de doctorat des Sciences, CNRS Mém., C.R.Z.A., série géologie, 2, 198p.

Ghienne, J.-F. (1998) Modalités d'enregistrement d'une glaciation ancienne; exemple de la glaciation fini-ordovicienne sur la plate-forme nord-gondwanienne en Afrique de l'Ouest. Thèse de l'Université L. Pasteur, Strasbourg, 407 pp.

Ghienne J.-F. (2003) Late Ordovician sedimentary environments, glacial cycles, and post-glacial transgression in the Taoudeni Basin, West Africa. Palaeogeography Palaeoclimatology Palaeoecology, 189, 117-145.

Ghienne J.-F. et Deynoux M. (1998) Large-scale channel fill structures in Late Ordovician glacial deposits in Mauritania, Western Africa. Sedimentary Geology, 119, 141-159.

Ghienne J.-F., Bartier D., Leone F. et Loi Alfredo (2000) Caractérisation des horizons manganésifères de l'Ordovicien supérieur de Sardaigne : relation avec la glaciation fini-Ordovicienne. Comptes Rendus de l'Académie des Sciences, Paris, 331, 257-264.

Ghienne J.-F., Boumendjel K., Paris F., Videt B., Racheboeuf P. et Ait Salem H. (2007a) The Cambrian-Ordovician succession in the Ougarta Range (western Algeria, North Africa) and interference of the Late Ordovician glaciation on the development of the Lower Palaeozoic transgression on northern Gondwana. Bulletin of Geosciences, 82(3), 183-214. Doi 10.3140/bull.geosci.2007.03.183

Ghienne J.-F., Le Heron D., Moreau J., Denis M. et Deynoux M. (2007b) The Late Ordovician glacial sedimentary system of the North Gondwana platform. In : Hambrey, M., Christoffersen, P., Glasser, N., Janssen, P., Hubbard, B. and Siegert, M. (eds.) Glacial Sedimentary Processes and Products. Special Publication n°39, International Association of Sedimentologists, Blackwells, Oxford, pp. 295-319.

Ghienne J.-F., Loi A., Paris, F. et Rubino J.-L. (2008) Platform-scale correlation of North Gondwanan, Late Ordovician glacial cycles. Rend. Online Soc. Geol. Italia, 3, 429-430.

Ghienne J.-F., Girard F., Moreau J. et Rubino J.-L. (2010a) Late Ordovician climbing-dune cross-stratification: a signature of outburst floods in proglacial outwash environments? Sedimentology, 57, 1175-1198.

Ghienne J.-F., Monod, O., Kozlu, H., Dean, W.T. (2010b) Cambrian-Ordovician depositional sequences in the Middle East : a perspective from Turkey. Earth Science Reviews, 101, 101-146.

Gibling, M.R. (2006) Width and thickness of fluvial channel bodies and valley fills in the geological record: a literature compilation and classification. Journal of Sedimentary Research, 76, 731-770.

Grahn Y., Caputo M.V., 1992. Early Silurian glaciations in Brazil. Palaeogeography, Palaeoclimatology, Palaeoecology 99, 9–15.

Gutiérrez-Marco J.C., Robardet M., Rábano I., Sarmiento G.N., San José Lancha M.A., Herranz Araújo P., and Pieren Pidal A.P. (2002) Ordovician, in Gibbons, W. and Moreno, T., eds., The Geology of Spain: London, The Geological Society, p. 31–49.

Gutiérrez-Marco J.-C., Ghienne J.-F., Bernárdez E. et Hacar M.P. (2010) Did the Late Ordovician African ice sheet reach Europe? Geology, 38, 279-282.

Hambrey M.J. (1985) The Late Ordovician-Early Silurian glacial period. Palaeogeo. Palaeoclim. Palaeoeco., 51, 273-289.

Herrmann A.D., Haupt B.J., Patzkowsky M.E., Seidov D., Slingerland R.L. (2004) Response of Late Ordovician paleoceanography to changes in sea level, continental drift, and atmospheric pCO2: potential causes for long-term cooling and glaciation. Palaeogeography Palaeoclimatology Palaeoecology 210, 385–401.

Hirst J.P.P., Benbakir A., Payne D.F. and Westlake I.R. (2002) Tunnel Valleys and Density Flow Processes in the upper Ordovician glacial succession, Illizi Basin, Algeria: influence on reservoir quality. Mar. Petrol. Geol. 25, 297-324

Homewood P.W., Guillocheau F., Eschard R., Cross T.A. (1992) Corrélation Haute Résolution et Stratigraphie Génétique: une approche intégrée. Bulletin des Centres de Recherches Exploration-Production Elf-Aquitaine 16, 357–381.

Huuse M., Lykke-Andersen H., 2000. Overdeepened Quaternary valleys in the eastern Danish North Sea: morphology and origin. Quaternary Science Reviews 19, 1233–1253.

Huvelin P. (1977) Etude géologique et gîtologique du massif hercynien des Jebilet (Maroc occidental). Notes Mém. Serv. géol. Maroc, Rabat, 232 bis, 307 p.

Hwang I-G., Heller P.L. (2002) Anatomy of a transgressive lag : Panther Tongue Sandstone, Star Point Formation, central Utah. Sedimentology, 49, 977-999.

Ingri J. (1993) Redox potential, a significant factor in regulating the uptake of Cu, Ni, and Zn in Mn-oxyhydroxide at the sediment-water interface in the northern Baltic Sea, EOS Transactions of the American Geophys. Union,

74, 16, 326-327.

Isbell J.L., Cole D.I., Catuneanu O. (2010) Carboniferous-Permian glaciation in the main Karoo Basin, South Africa/ Stratigraphy, depostional controls, and glacial dynamics. In : Fielding C.R., Frank T.D., Isbell J.L (eds) Resolving the Late Paleozoic Ice Age in Time and Space. The Geological Society of America, Special Paer 441, 71-82

Johnston A.C. (1989) The effect of large ice sheets on earthquake genesis, in: S. Gregersen, P.W. Basham (Eds.), Earthquakes at North-Atlantic Passive Margins: Neotectonics and Postglacial Rebound, in: NATO ASI Series, Series C, v. 266, pp. 581–600.

Joubert J.-B., Moreau J., Ghienne J.-F. et Rubino J.-L. (2007) FMI characterisation of Late Ordovician glacial facies and surfaces. 3rd North African/ Mediterranean Petroleum and Geosciences Conference & Exhibition (EAGE), 26 to 28 February 2007, Tripoli (Libya).

Joulia F. (1959) Les séries primaires au N et NW de l'Aïr (Sahara central). Discordances observées. Bulletin de la Société Géologique de France, 7, 192-196.

Jørgensen, F., Sandersen, P.B.E. (2006) Buried and open tunnel valleys in Denmark – erosion beneath multiple ice sheets. Quaternary Science Reviews, 25, 1339-1363.

Kaljo, D., Hints, L., Männik, P., Nõlvak, J. (2008) The succession of Hirnantian events based on data from Baltica: brachiopods, chitinozoans, conodonts, and carbon isotopes. Estonian Journal of Earth Sciences 57, 197-218.

Katz, R.F., Worster, M.G. (2010) Stability of ice-sheet grounding lines. Proceedings of the Royal Society A, doi: 10.1098/rspa.2009.0434.

Kilian C. (1922) Aperçu général de la structure des Tassilis des Ajjers. Comptes Rendus de l'Académie des Sciences, 175, 825-827.

Klitzsch, E. (1981) Lower Palaeozoic rocks of Libya, Egypt, and Sudan, 131-163. In C.H. Holland (ed.) Lower Palaeozoic of the Middle East, Eastern and Southern Africa, and Antarctica, John Wiley, New York.

Kump L.R., Arthur M.A., Patzkowsky M.E., Gibbs M.T., Pinkus D.S., Sheehan P.M. (1999) A weathering hypothesis for glaciation at high pCO2 during the Late Ordovician. Palaeogeography Palaeoclimatology Palaeoecology, 152, 173-187.

Lahondère D., Le Metour J., Callec Y., Roger J., Ghienne J.-F., Gourvennec R. (2008) Notice explicative des cartes géologiques à 1/200 000 de la zone Centre de la Mauritanie. DMG, Ministère des Mines et de l'Industrie, Nouakchott, Rapport BRGM/RC-56742-FR, 398 pages.

Lang J., Yahaya M., El Hamet M.O., Besombes J.C., Cazoulat M. (1991) Dépôts glaciaires du Carbonifère inférieur à l'Ouest de l'Aïr (Niger). Geological Rundschau, 80, 611-622.

Le Heron, D.P., Thusu, B. (2007) Prospects in Libya's mature and frontier basins. First Break 25, 73-79.

Le Heron, D.P., Craig, J. (2008) First-order reconstructions of a Late Ordovician Saharan ice sheet. Journal of the Geological Society 165, 19–29.

Le Heron, D., Dowdeswell, J.A. (2009) Calculating ice volumes and ice flux to constrain the dimensions of a 440 Ma North African ice sheet. Journal of the Geological Society, London 166, 277-281.

Le Heron, D., Sutcliffe, O., Bourgig, K., Craig, J., Visentin, C., Whittington, R. (2004) Sedimentary architecture of Upper Ordovician tunnel valleys, Gargaf Arch, Libya: implications for the genesis of a hydrocarbon reservoir. GeoArabia 9, 137–160.

Le Heron D.P., Sutcliffe O.E., Whittington R.J., Craig J. (2005) The origins of glacially related soft-sediment deformation structures in Upper Ordovician glaciogenic rocks: implication for ice sheet dynamics. Palaeogeography, Palaeoclimatology, Palaeoecology 218, 75–103.

Le Heron D.P., Craig J., Sutcliffe O.E., Whittington R. (2006) Glaciogenic reservoir heterogeneity: an example from the Late Ordovician of the Murzuq Basin, SW Libya. Marine and Petroleum Geology 23, 655–677.

Le Heron D., Ghienne J.-F., El Houicha M., Khoukhi Y., Rubino J.-L. (2007) Maximum extent of ice sheets in Morocco during the Late Ordovician glaciation. Palaeogeography Palaeoclimatology Palaeoecology, 245, 200-226. doi:10.1016/j.palaeo.2006.02.031

Le Heron D.P., Khoukhi Y., Paris F., Ghienne J.-F. et Le Herissé A. (2008) Black shale, grey shale, fossils and glaciers : anatomy of the Upper Ordovician-Silurian succession in the Tazzeka Massif of eastern Morocco. Gondwana Research, 14, 483-496.

Le Heron, D.P., Craig, J., Etienne, J.L. (2009) Ancient glaciations and hydrocarbon accumulations in North Africa and theMiddle East. Earth Science Reviews 93, 47–76.

Legrand, P. (1985) Lower Palaeozoic rocks of Algeria, 5-89. In C.H. HOLLAND (ed.) Lower Paleozoic Rocks of northwest and west Central Africa (ed.), John Wiley, NewYork.

Legrand, P. (2003) Paléogeographie du Sahara algérien à l'Ordovicien terminal et au Silurien inférieur. Bulletin de la Société géologique de France 174, 19-32.

Leone, F., Ferretti, A., Hammann, W., Loi, A., Pillola, G.L., Serpagli, E. (2002) A general view on the post-Sardic Ordovician sequence from SW Sardinia. Rendiconti della Società Paleontologica Italiana, vol. 1, pp. 51–68.

Lehnert, O., Männik, P., Joachimski, M.M., Calner, M., Fryda, J. (2010) Palaeoclimate perturbations before the Sheinwoodian glaciation : a trigger for extinctions during the 'Ireveken Event'. Palaeogeography Palaeoclimatology Palaeoecology, 296, 320-331.

Loi A., Ghienne J.-F., Dabard M.P., Paris F., Botquelen A., Christ N., Elaouad-Debbaj Z., Gorini A., Vidal M., Videt B., Destombes J. (2010) The Late Ordovician glacio-eustatic record from a high-latitude storm-dominated shelf succession: the Bou Ingarf section (Anti-Atlas, Southern Morocco). Palaeogeography Palaeoclimatology Palaeoecology, 296, 332-358.

Lonergan, L., Maidment, S. C. R. et Collier, J. S. (2006) Pleistocene subglacial tunnel valleys in the central North Sea basin: 3-D morphology and evolution. Journal of Quaternary Science, 21, 891-903.

Long, D.G.F. (2007) Tempestite frequency curves: a key to Late Ordovician and Early Silurian subsidence, sea-level change, and orbital forcing in the Anticosti foreland basin, Quebec, Canada. Canadian Journal of Earth Sciences 44, 413–431.

Lüning, S., Craig. J., Loydell, D.K., Štorch, P. & Fitches, B. (2000) Lower Silurian 'hot shales' in North Africa and Arabia: regional distribution and depositional model. Earth-Science Reviews 49, 121-200.

Lüning, S., Shahin, Y. M., Loydell, D., Al-Rabi, H. T., Masri, A., Tarawneh, B. & Kolonic S (2005) Anatomy of a world class source rock: Distribution and depositional model of Silurian organic-rich shales in Jordan and implications for hydrocarbon potential. American Association of Petroleum Geologists, Bulletin, 89, 1397-1427.

Lutz, R., Kalka, S., Gaedicke, C. Reinhardt, L., Winsemann, J. (2009) Pleistocene tunnel valleys in the German North Sea : spatial distribution and morphology. Zeitschrift der Deutschen Gesellschaft für Geowissen-schaften, Stuttgart, 160, 225-235.

Massa, D. 1988. Paléozoïque de Libye occidentale. Stratigraphie et Paléogéographie, 514 pp. Thèse d'Etat, Université de Nice, France (unpublished).

McGillivray, G.J. & Husseini, M. (1992) The Paleozoic petroleum geology of Central Saudi Arabia. AAPG 76, 1473-1490.

Marren, P.M. (2005) Magnitude and frequency in proglacial rivers: a geomorphological and sedimentological perspective. Earth-Sc. Rev., 70, 203-251.

Martini I.P., Tongiorgi M., Oggiano G. et Cocozza T. (1991) Ordovician alluvial fan to marine shelf transition in SW Sardiania, Western Mediterranean Sea: tectonically (« Sardic phase ») influenced clastic sedimentation, Sedimentary Geology, 72, 97-115.

McCabe A. M, Carter R. W. G., Haynes J. R. (1994) A shallow marine emergent sequence from the northwestern sector of the last Britih ice sheet, Portballintrae, Northern Ireland. Marine Geology, 117, 19-34.

McDougall N., Martin M. (2000) Facies models and sequence stratigraphy of Upper Ordovician outcrops in the Murzuq Basin, SW Libya, in : M.A. Sola et D. Worsley (Eds), Geological Exploration in Murzuq Basin, Elsevier Science, 223-236.

Melchin, M.J., Holmden, C. (2006). Carbon isotope chemostratigraphy in Arctic Canada: Sea-level forcing of carbonate platform weathering and implications for Hirnantian global correlation. Palaeogeography, Palaeoclimatology, Palaeoecology 234, 186–200.

Michard, A., Hoepffner, C., Soulaimani, A., Baidder, L. (2008) The variscan belt. In: Continental evolution: the Geology of Morocco (Eds. A. Michard, O. Saddiqi, A. Chalouan, D. Frizon de Lamotte), Lecture Notes in Earth Sciences 126, pp. 65–132, Springer.

Michoud, P., Desmit, P., Gramont, M. (1963) Reconnaissance de la partie centrale du bassin de Taoudéni (novembre 1961-avril 1962). Unpublished Rapport. Soc. Afr. Petr. (S.A.P.), 139 pp.

Moix, P., Beccaletto, L., Kozur, H.W., Hochard, C., Rosselet, F., Stampfli, G.M. (2008) A new classification of the Turkish terranes and sutures and its implication for the paleotectonic history of the region. Tectonophysics 451: 7-39.

Monod T. (1962) Observations nouvelles sur la série gréseuse infra-gothlandienne de l'Adrar mauritanien. Bull. Inst. fr. Afr. noire, Dakar, 47 p.

Monod O., Kozlu H., Ghienne J-F., Dean W.T., Günay Y., Le Hérissé A., Paris F. et Robardet M. (2003) Late Ordovician glaciation in Southern Turkey. Terra Nova, 15, 249-257.

Moreau J., Ghienne J.-F., Le Heron D., Rubino J.-L. et Deynoux M. (2005) 440 Ma old ice stream in North Africa. Geology, 33, 753-756.

Moreau J., Degermann L., Ghienne J.-F. et Rubino J.-L. (2007) Large-scale physiography of the Murzuq Basin shelf during Hirnantian ice-sheet final retreat and Silurian transgression: outcrops and seismic interpretations. 3rd North African/ Mediterranean Petroleum and Geosciences Conference & Exhibition (EAGE), 26 to 28 February 2007, Tripoli (Libya).

Neal J., Abreu V. (2009) Sequence stratigraphy hierarchy and the accommodation succession method. Geology, 37, 779-782.

O Cofaigh C., Evans D.J.A., Smith I.R. (2010) Large-scale reorganization and sedimentation of terrestrial ice streams during late Wisconsinian Laurentide Ice Sheet deglaciation. Geological Society of America, Bulletin, 122, 743-756.

Ottesen D., Stokes C.R., Rise L., Olsen L. (2008) Ice-sheet dynamics and ice streaming along the coastal parts of northern Norway. Quaternary Science Reviews, 27, 922-940.

Ouanaimi, H. (1998) Le passage Ordovicien-Silurien à Tizi n'Tichka (Haut-Atlas, Maroc): variations du niveau marin, C. R. Acad. Sc. Paris, 326, II, 65-70.

Page A.A., Zalasiewicz J.A., Williams M., Popov L.E. (2007) Were transgressive black shaels a negative feedback modulating glacioeustasy in the Early Palaeozoic Icehouse? In: Williams M., Haywood A.M., Gregory F.J., Schmidt D.N.(eds) Deep-time Perspectives on climate Change: Marrying the Signal from computer Models and biological Proxies. The Micropallaeontological Society, Special Publications. The Geological Society London, 123-156.

Paris, F., Elaouad-Debbaj, Z., Jaglin, J.C., Massa, D., Oulebsir, L., 1995. In: Cooper, C., Droser, M., Finney, S. (Eds.), Chitinozoans and Late Ordovician Glacial Events on Gondwana. 7th, ISOS, Society of Economic Paleontologists and Mineralogists (SEPM) publication, Las Vegas, pp. 171–176.

Paris F., Deynoux M. et Ghienne J.-F. (1998) Chitinozoaires de la limite Ordovicien-Silurien en Mauritanie. Comptes Rendus de l'Académie des Sciences, Paris, 326,499-504.

Paris F., Le Hérissé A., Monod O., Kozlu H., Ghienne J.F., Dean W.T., Vecoli M. et Günay Y. (2007) Ordovician chitinozoans and acritarchs from southern and southeastern Turkey/Chitinozoaires et acritarches ordoviciens du sud et du sud-est de la Turquie. Revue de Micropaléontologie, 50, 81-107.

Piçarra J.M., Robardet M., Oliveira T., Paris F., Lardeux H. (2009) Graptolites faunas of the Llandovery « phtanites » at Les Fresnaies (Chalonnes-sur-Loire, southeasternArmorican Massif): Palaeontology and biostratigraphy, Bulletin of Geosciences 84, 41-50.

Piotrowski JA, Larsen NK, Menzies J, Wysota W (2006) Formation of subglacial till under transient bed conditions: deposition, deformation, and basal decoupling under a Weichselian ice sheet lobe, central Poland. Sedimentology 53:83–106.

Posamentier, H.W., Vail, P.R. (1988) Eustatic controls on clastic deposition II — sequence and systems tract models. In: Wilgus, C.K., Hastings, B.S., Kendall, C.G.St.C., Posamentier, H.W., Ross, C.A., Van Wagoner, J.C. (Eds.), Sea Level Changes — An Integrated Approach. Special Publication, vol. 42. Society of Economic Paleontologists and Mineralogists (SEPM), pp. 125–154.

Pope, M.C., Steffen, J.B. (2003) Widespread, prolongated late Middle to Late Ordovician upwelling in North America: a proxy record of glaciation? Geology 31, 63–66.

Powell R.D., Cooper, J.M (2002) A glacial sequence stratigraphic model for temperate, glaciated continental shelves. In: Dowdeswell J.A. & O Cofaigh C. (eds) Geological Society, London, Special Publications, 203, 215-244.

Powell J. H., Khalil M.B., Masri A. (1994) Late Ordovician-Early Silurian glaciofluvial deposits preserved in palaeovalleys in South Jordan. Sedimentary Geology, 89, 303-314.

Proust J. N., Deynoux M. (1994) - Marine to non-marine sequence architecture of intracratonic glacially related basin. Late Proterozoic of the West African platform in western Mali. In : Earth's Glacial Record, M. Deynoux et al. (Eds.), Int. Geol. Correl. Project 260, World and Regional Geology, Cambridge University Press. 121-145.

Rayburn, J.A., Teller J.T. (2007) Isostatic rebound in the northwestern part of the Lake Agassiz basin: Isobase changes and overflow. Palaeogeography Palaeoclimatology Palaeoecology, 246, 23-30.

Robardet M., Doré F. (1988) - The Late Ordovician diamictic formations from southwestern Europe: North-Gondwana glaciomarine deposits. Palaeogeography Palaeoclimatology Palaeoecology, 66, 19-31.

Roberts, M.J. (2005) Jökulhlaups: a reassessment of floodwater flow through glaciers. Rev. Geophys., 43, 1-21.

Rognon P. (1971) Interprétation des principales discontinuités dans la sédimentation du Paéozoïque saharien. Thèse, Faculté des Sciences de l'Université de Strasbourg, 36pp.

Rossi P., Oggiano G., Cocherie A. (2009) A restored section of the « southern Variscan realm » across the Corsica—Sardinia microcontient. Comptes Rendus Géoscience, 341, 224-238

Rubino J.-L., Anfray R., Blanpied C., Ghienne J.-F. et Manatschal G. (2003) Meander belt complex within the lower Mamuniyat Formation in western Al Qarqaf area, Libya. In: The geology of northwest Libya; Volume II, Sedimentary basins of Libya, second symposium (Salem M.J. & Oun Khaled M. eds), Symposium on the Sedimentary Basins of Libya. 2, 3-18. 2003.

Russell, A.J., Fay, H., Marren P.M., Tweed, F.S. and Knudsen, Ó. (2005) Icelandic jökulhlaup impacts. In: Iceland—Modern Processes and past environments (C. Caseldine, A. Russell, Hardardóttir, J. and Ó. Knudsen Eds), Developments in Quaternary Science, 5, pp. 153-203.

Sanchez M.T., Benedetto J.L., Brussa E. (1991) Late Ordovician stratigraphy, paleoecology, and sea level changes in the Argentine Precordillera. In : Advances in Ordovician geology, Barnes C. R. & Williams S. H. (Eds.), Geol. Survey of Canada, Paper 90-9, 245-258.

Saltzman, M.R., Young, S.A. (2005) Long-lived glaciation in the Late Ordovician? Isotopic and sequence-stratigraphic evidence from western Laurentia. Bulletin of the Geological Society of America 33, 109–112.

Sepkoski Jr, J.J. (1995) The Ordovician Radiations: diversification and extinction shown by global genus-level taxonomic data. In: Cooper, C., Droser, M., Finney, S. (Eds.), 7th International Symposiumon the Ordovician System, Las Vegas, SEPMPublication, 77, pp. 75–80.

Servais T., Owen A.W., Harper D.A.T., Kröger B., Munnecke A. (2010) The Great Ordovician Biodiversification Event (GOBE): The palaeoecological dimension. Palaeogeography Palaeoclimatology Palaeoecology, 294, 99-119.

Sharland, P.R., Archer, R., Casey, D.M., Davies, R.B., Hall, S.H., Heward, A.P., Horbury, A.D., Simmons, M.D. (2001) Arabian Plate Sequence Stratigraphy. GeoArabia Spec. Publ. 2, 371 p.

Sheehan, P. M. (2001) The Late Ordovician Mass Extinction, Annual Review of Earth and Planetary Sciences, 29, 331-364.

Siegert M.J., Dowdeswell J.A. (2004) Numerical reconstructions of the Eurasian Ice Sheet and climate during the Late Weichselian. Quaternary Science Reviews, 23, 1273-1283.

Snorrason, Á., Jónsson, P., Sigurdsson, O., Pálsson, S., Árnasson, S., Vikingsson, S. and Kaldal, I. (2002) November 1996 jökulhlaup on Skeidarársandur outwash plain, Iceland. In: Flood and megaflood processes and deposits: recent and ancient examples (Eds I.P. Martini, V.R. Baker and G. Garzón), Spec. Publs. Int. Ass. Sediment., 32, 55-65.

Sougy J. (1957) Division en deux series distinctes de la série de l(Oumat-el-Ham. (Mauritanie occidentale). Comptes Rendus sommaires de la Société Géologique de France, 180-181.

Sougy, J., Lécorché, J.-P. (1963) Sur la nature glaciaire de la base de la série de Garat el Hamoueïd (Zemmour, Mauritanie septentrionale). C. R. Acad. Sc. Paris, 256, 4471-4474.

Spjeldnæs, N. (1961) Ordovician climatic zones. Norsk Geologisk Tidsskrift 41, 45–77.

Stampfli G.M. & Borel, G.D. (2002) A tectonic model for the Paleozoic and Mesozoic constrained by dynamic plate boundaries and restored synthetic oceanic isochrones. Earth Planetary Science Letters 196, 17-33.

Sutcliffe, O.E., Dowdeswell, J.A., Whittington, R.J., Theron, J.N., Craig, J. (2000) Calibrating the Late Ordovician glaciation and mass extinction by the eccentricity cycles of the Earth's orbit. Geology 23, 967–970.

Sutcliffe, O.E., Harper, D.A.T., Aït Salem, A., Whittington, R.J., Craig, J. (2001) The development of an atypical Hirnantian brachiopod fauna and the onset of glaciation in the Late Ordovician of Gondwana. Transactions of the Royal Society of Edinburgh: Earth Sciences 92, 1–14.

Stokes C.R., Clark C.D. (2001) Quaternary Science Reviews, 20, 1347-1457.

Stokes, C.R., Clark, C.D., Lian, O.B., Tulaczyk, S. (2007) Ice stream sticky spots: A review of their identification and influence beneath contemporary and palaeo-ice streams. Earth Science Reviews, 81, 217-249.

Storch, P. (1990) Upper Ordovician-lower Silurian sequences of the Bohemian Massif, central Europe. Geological Magazine 127, 225–239.

Storch, P., Massa D. (2006) Middle Llandovery (Aeronian) graptolites of the western Murzuq Basin and Al Qarqaf Arch region, south-west Libya. Palaeontology, 49, 83-112.

Svensson N.-O. (1991) Postglacial land uplift patterns of south Sweden and the Baltic Sea region. Terra Nova, 3, 369-378.

Taylor J., Dowdeswell J.A., Kenyon N.H., O Cofaigh C. (2002) Late Quaternary architecture of trough-mouth fans : debris flows and suspended sediments on the Norwegian margin. In: Dowdeswell J.A. & O Cofaigh C. (eds) Geological Society, London, Special Publications, 203, 55-71.

Trompette R. (1973) Le Précambrien supérieur et le Paléozoïque inférieur de l' Adrar de Mauritanie (bordure occidentale du bassin de Taoudeni, Afrique de l'Ouest). Un exemple de sédimentation de craton. Etude stratigraphique et sédimentologique. Thèse d'Etat, Université Aix-Marseille, 702 p.

Trotter JA, Williams IS, Barnes CR, Lecuyer C, Nicoll RS (2008) Did cooling oceans trigger Ordovician biodiversification? Evidence from conodont thermometry. Science, 321:550–554.

Underwood C., Deynoux M. et Ghienne J.-F. (1998) High palaeolatitude recovery of graptolites faunas after the Hirnantian (top Ordovician) extinction event. Palaeogeography Palaeoclimatology Palaeoecology, 142, 91-105.

Vaslet, D. (1990) Le Paléozoïque (Anté-Permien supérieur) d'Arabie Saoudite. Histoire géologique de la bordure occidentale de la plate-forme arabe. Document du BRGM, 191, 209p.

Vaslet, D. (1990) Upper Ordovician glacial deposits in Saudi Arabia. Episodes 13, 147–167.

Vandenbroucke, T.R.A., Gabbott, S.E., Paris, F., Aldridge, R.J., Theron, J.N. (2009) Chitinozoans and the age of the Soom Shale, an Ordovician black shale Lagerstätte, South Africa. Journal of Micropalaeontology 28, 53-66.

Vandenbroucke T.J.A., Armstrong H.A., Williams, M., Paris F., Zalasiewicz J.A., Sabbe K., Nolvak J., Challands T.J., Verniers J., Servais T. (2010) Polar front shift and atmospheric CO2 during the glacial maximum of the Early Paleozoic Icehouse. Proceedings of the National Academy of Sciences of the United States of America 34, 14983-14896.

Vecoli, M. (2008) Fossil microphytoplankton dynamics across the Ordovician–Silurian boundary. Review of Palaeobotany and Palynology 148, 91–107.

Videt B., Paris F., Rubino J.-L., Boumendjel K., Dabard, M.-P., Loi A., Ghienne J.-F., Marante A., Gorini, A. (2010) Biostratigraphical calibration of the third-order Ordovician sequences on the northern Gondwana platform. Palaeogeography Palaeoclimatology Palaeoecology, 298, 359-375.

Villas, E., Vizcaïno, D., Álvaro, J.J., Destombes, J., Vennin, E. (2006) Biostratigraphic control of the latest-Ordovician glaciogenic unconformity in Alnif (Eastern Anti-Atlas, Morocco), based on brachiopods. Geobios 39, 727–737.

Von Raumer, J.F., and Stampfli, G.M. (2008) The birth of the Rheic ocean – Early Palaeozoic patterns and subsequent tectonic plate scenarios: Tectonophysics, v. 461, p. 9–20.

Winsemann J., Brandes C., Polom U. (2010) Response of a proglacial delta to rapid high-amplitude lake-level change : an integration of outcrop data and high-resolution shear wave seismics. Basin Research, in press

Woodworth-Lynas, C.M.T., and Dowdeswell, J.A. (1994) Soft-sediment striated surfaces and massive diamicton facies produced by floating ice: In: Earth's Glacial Record (M. Deynoux et al., eds.), pp. 241-259, Cambridge University Press.

Yanev S. (2000) Palaeozoic terranes of the Balkan Peninsula in the framework of Pangea assembly, Palaeogeography, Palaeoclimatology, Palaeoecology, 161, 151-177

Young, G.M., Minter W.E.L., Theron, J.N. (2004) Geochemistry and palaeogeography of upper Ordovician glaciogenic sedimentary rocks in the Table Mountain Group, South Africa. Palaeogeography, Palaeoclimatology, Palaeoecology 214, 323–345.

Zhamoida V.A., Glasby G.P., Popova I.A. (1996) Ferromanganese concretions of the Gulf of Finland, Baltic Sea, Marine Georesources and Geotechnology, 14, 161-176.

Zecchin, M. (2007) The architectural variability of small-scale cycles in shelf and ramp clastic systems: The controlling factorsEarth-Science Reviews, 84, 21–55.